IMMUNOPARASITOLOGY: A UNIQUE INTERPLAY BETWEEN HOST AND PATHOGEN

EDITED BY: Xun Suo, Hyun Soon Lillehoj, Wenbin Tuo and Zhiguang Wu
PUBLISHED IN: Frontiers in Immunology and Frontiers in Microbiology

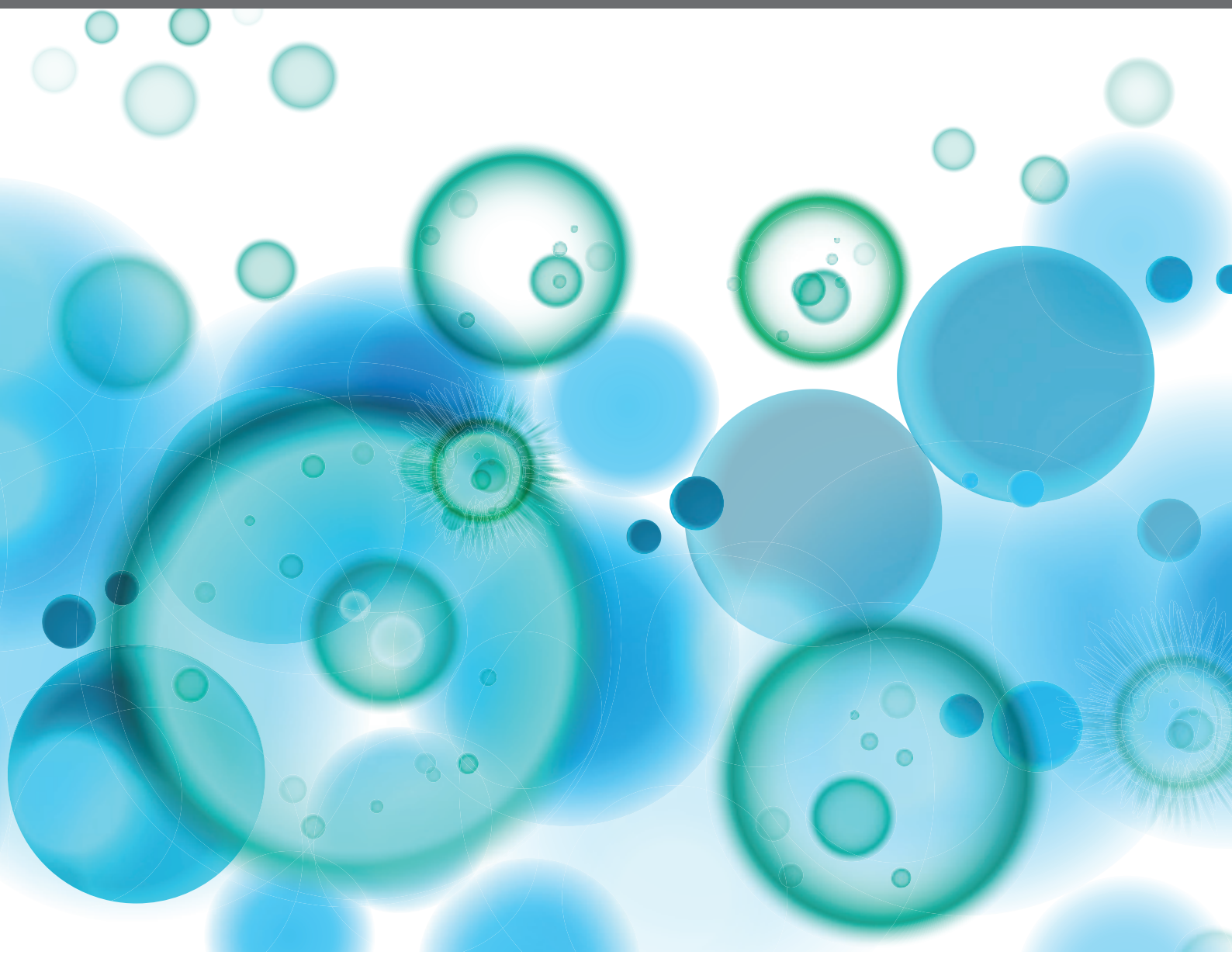

frontiers Research Topics

frontiers

ISSN 1664-8714
ISBN 978-2-88963-801-7
DOI 10.3389/978-2-88963-801-7

About Frontiers

Frontiers is more than just an open-access publisher of scholarly articles: it is a pioneering approach to the world of academia, radically improving the way scholarly research is managed. The grand vision of Frontiers is a world where all people have an equal opportunity to seek, share and generate knowledge. Frontiers provides immediate and permanent online open access to all its publications, but this alone is not enough to realize our grand goals.

Frontiers Journal Series

The Frontiers Journal Series is a multi-tier and interdisciplinary set of open-access, online journals, promising a paradigm shift from the current review, selection and dissemination processes in academic publishing. All Frontiers journals are driven by researchers for researchers; therefore, they constitute a service to the scholarly community. At the same time, the Frontiers Journal Series operates on a revolutionary invention, the tiered publishing system, initially addressing specific communities of scholars, and gradually climbing up to broader public understanding, thus serving the interests of the lay society, too.

Dedication to Quality

Each Frontiers article is a landmark of the highest quality, thanks to genuinely collaborative interactions between authors and review editors, who include some of the world's best academicians. Research must be certified by peers before entering a stream of knowledge that may eventually reach the public - and shape society; therefore, Frontiers only applies the most rigorous and unbiased reviews.
Frontiers revolutionizes research publishing by freely delivering the most outstanding research, evaluated with no bias from both the academic and social point of view. By applying the most advanced information technologies, Frontiers is catapulting scholarly publishing into a new generation.

What are Frontiers Research Topics?

Frontiers Research Topics are very popular trademarks of the Frontiers Journals Series: they are collections of at least ten articles, all centered on a particular subject. With their unique mix of varied contributions from Original Research to Review Articles, Frontiers Research Topics unify the most influential researchers, the latest key findings and historical advances in a hot research area! Find out more on how to host your own Frontiers Research Topic or contribute to one as an author by contacting the Frontiers Editorial Office: researchtopics@frontiersin.org

IMMUNOPARASITOLOGY: A UNIQUE INTERPLAY BETWEEN HOST AND PATHOGEN

Topic Editors:
Xun Suo, China Agricultural University, China
Hyun Soon Lillehoj, United States Department of Agriculture (USDA), United States
Wenbin Tuo, Beltsville Agricultural Research Center, Agricultural Research Service (USDA), United States
Zhiguang Wu, University of Edinburgh, United Kingdom

Citation: Suo, X., Lillehoj, H. S., Tuo, W., Wu, Z., eds. (2020). Immunoparasitology: A Unique Interplay Between Host and Pathogen. Lausanne: Frontiers Media SA.
doi: 10.3389/978-2-88963-801-7

Table of Contents

frontiers in Immunology

EDITORIAL
published: 07 May 2020
doi: 10.3389/fimmu.2020.00880

Editorial: Immunoparasitology: A Unique Interplay Between Host and Pathogen

Xun Suo[1,2], *Zhiguang Wu*[3], *Hyun Lillehoj*[4] *and Wenbin Tuo*[5*]

[1] National Animal Protozoa Laboratory & College of Veterinary Medicine, China Agricultural University, Beijing, China, [2] Key Laboratory of Animal Epidemiology of the Ministry of Agriculture, China Agricultural University, Beijing, China, [3] The Roslin Institute, University of Edinburgh, Easter Bush, Midlothian, United Kingdom, [4] Animal Biosciences and Biotechnology Laboratory, Agricultural Research Service, United States Department of Agriculture (USDA), Beltsville, MD, United States, [5] Animal Parasitic Diseases Laboratory, Agricultural Research Service, United States Department of Agriculture (USDA), Beltsville, MD, United States

Keywords: parasite, helminth, protozoa, Apicomplexa, flagellate, co-infection, immunity, vaccines

Editorial on the Research Topic

Immunoparasitology: A Unique Interplay Between Host and Pathogen

This Research Topic, "Immunoparasitology: A unique interplay between host and pathogen," was intended to emphasize broadly the latest advances in immunoparasitology and has been concluded with more than 30 high quality papers encompassing aspects of parasite biology, host-parasite responses and interactions, and up-to-date control measures. Such an accomplishment is unattainable without the enthusiastic involvement of all contributing authors and participating reviewers, and the day-to-day assistance from the staff of Frontiers in Immunology editorial office.

Approximately one third of the articles in this collection are reviews and the rest are original research papers, covering multiple parasitic species and their hosts. As expected, two thirds of the papers are focused on protozoan parasites, 50% of which use *Toxoplasma gondii* as a model pathogen. The next-most covered group is parasitic helminths with eight papers. At the time this Editorial was submitted for publication, this Research Topic achieved well over 75,000 online views, with average views per article of >2,000 since publication.

The most viewed article covers the popular and important subject of co-infection (Mabbott). The author emphasizes the fact that co-infection is a common occurrence in the field, where malarial parasites, soil-transmitted helminths, bacteria and viruses, are the causes for chronic infections in a large proportion of the population. Ample examples of co-infection are described, where existing infections by parasites can have a dramatic influence on host susceptibility and/or disease pathogenesis. The impact of co-infection on disease diagnosis, vaccine development, and host resistance, clearly warrants further investigation. The findings of Djokic et al. demonstrate specifically how co-infection by *Babesia microti* and *Borrelia burgdorferi*, both tick-borne pathogens, influences age-dependent immune responses and disease outcomes. Additional review articles cover protozoa and helminths, representing up-to-date advances in research. Maurya et al. present an excellent review on the functions of leptin in infectious diseases. Leptin, primarily secreted by adipose tissue, is important in resistance to diseases as it is emerging as a key regulator in both immunity and nutrition.

While malaria and trypanosomiasis are not extensively covered in this issue, in terms of original research, research progress for these two diseases is nonetheless summarized by several in-depth reviews. Lee et al. give an expert account of recent advances in the complex cytoadhesive interactions between *Plasmodium falciparum*-infected erythrocytes and other host cells, providing insight into how such cytoadherence may contribute to malaria pathogenesis. In malaria, B

OPEN ACCESS

Edited and reviewed by:
Ian Marriott,
University of North Carolina at Charlotte, United States

***Correspondence:**
Wenbin Tuo
wenbin.tuo@usda.gov

Specialty section:
This article was submitted to Microbial Immunology, a section of the journal Frontiers in Immunology

Received: *08 March 2020*
Accepted: *16 April 2020*
Published: *07 May 2020*

Citation:
Suo X, Wu Z, Lillehoj H and Tuo W (2020) Editorial: Immunoparasitology: A Unique Interplay Between Host and Pathogen. Front. Immunol. 11:880. doi: 10.3389/fimmu.2020.00880

cell-mediated, parasite-specific, antibody-dependent protection may depend on, and be achieved by, appropriate activation in the lymph nodes and optimal interactions among antigen-specific and antibody-secreting B cells with T helper cells and cytokines. This process is described in depth in a review article written by Silveira et al..

Several major species of trypanosomes are the pathogenic agents of trypanosomiasis worldwide, profoundly affecting the well-being and immunocompetency of both humans and animals. To date, there is no vaccine against trypanosomiasis, although the parasite can elicit strong immune responses in the host. The difficulty in developing protective vaccines stems from the ability of parasites to evolve and evade host immune surveillance by genetic exchange among the parasites, acquisition of resistant genotypes in the insect vector, and plasticity in adaptation in new environments (Radwanska et al.). One of the approaches to understanding differential host responses is by investigating routes of transmission. Berreto de Albuquerque et al. summarize their recent findings and those of others in comparing host responses and disease outcomes following *Trypanosoma cruzi* infection through oral or gastrointestinal routes. In Latin American countries, oral transmission of resultant Chagas disease is predominant. In animal models, the oral route of infection can give rise to higher rates of mortality and morbidity when compared to vector-mediated transmission. These authors indicate that oral transmission, in fact, consists of intraoral cavity and intragastric transmissions, with increased parasitemia and mortality through the intraoral cavity route (Berreto de Albuquerque et al.). *T. cruzi* appears to enhance its replication in macrophages by exploiting the cell's Wnt signaling system based upon the ability of Wnt/β-Catenin signaling inhibition *in vitro* and *in vivo* to restrict *T. cruzi* replication, thereby promoting host resistance (Volpini et al.). Similarly, *Leishmania amazonensis,* a close relative of the trypanosome, also promotes its own infectivity using a host cell protein, CD100, through a macrophage surface receptor, CD72 (Galuppo et al.). *Histomonas meleagridis* is a flagellated protozoan parasite, causing histomonosis in turkeys and chickens, with the latter being more resistant to infection (Mitra et al.). Recent studies by Kidane et al. show that, unlike turkeys, resistance in chickens relies on the presence of higher percentage of interferon-gamma (IFN-γ) positive cells early in infection.

Infections caused by parasitic protozoa are very common in humans and animals, and the clinical symptoms may be transient or asymptomatic; but infected, apparently healthy individuals may remain infected throughout life, e.g., toxoplasmosis. Many years of research on *T. gondii* as a model zoonotic pathogen has advanced the field tremendously. Important discoveries continue to be made using this model and provide the basis for translational research. Indeed, findings of articles in this Research Topic show that *Toxoplasma* infection in the cat, the definitive host for *T. gondii*, elicits multi-tissue transcriptional changes mostly associated with immune functions (Cong et al.). Findings by Liu et al. demonstrate that galectin-3 and galectin-9 differentially regulate the expression of microglial M1/M2 macrophage markers and T helper 1/2 (Th1/2) cytokines in the brain of genetically susceptible (C57Bl/6) or resistant (Balb/c) mice, following peroral infection with *T. gondii*. Further, acute infection with *T. gondii* induces M1 polarization in the mouse brain, while chronic infection with the same strain inhibits the harmful Th1-associated inflammatory responses while M1 phenotype is maintained, indicating the complexity of the immune initiation stage upon infection (Hwang et al.). Admittedly, description of macrophage phenotypes and associated functions is rapidly expanding, thereby the intricate role of macrophage lineages in response to *T. gondii* infection warrants extensive investigation.

In North America and Europe, the strains of types I, II, and III *T. gondii* predominate, while in China, type Chinese 1 for *T. gondii* is prevalent. The type Chinese 1 is unique in that it carries a type II GRA15 protein (GRA15II) and a type I ROP16 protein (ROP16I), and known to polarize the host macrophages toward both M1 and M2 phenotypes at the early stage of infection. Using the type Chinese 1 strain deficient of $ROP16_{I/III}$, WH3Δ*rop16*, created with CRISPR/Cas9 technology, it is evident that pregnant mice infected with WH3Δ*rop16* have elevated Th1, but repressed Th2 and Treg responses, leading to pregnancy failure (Wang et al.). This suggests that disturbance of host immunotolerance during pregnancy by *T. gondii* or its sister parasite *Neospora caninum* can contribute to pregnancy failure.

T. gondii ROP18 is an essential virulence factor but its interaction with host targets has not been studied extensively. In an effort to identify ROP18 binding partners in human cells, Xia et al. use a high-throughput bimolecular fluorescence complementation (BiFC) approach to reveal numerous human protein partners for the type I and II strain ROP18, most of which are related to immune responses and apoptosis. Future studies will be needed to analyze the physiological significance of such host-parasite protein-based interactions. Further, IFN-γ-induced degradation of tryptophan by indoleamine 2, 3-dioxygenase (IDO) is a crucial anti-*Toxoplasma* mechanism. Recent investigations by Bando et al. show that, of the two IDO isoforms in humans, IDO1 is required for IFN-γ-induced immunity against toxoplasmosis.

Toxoplasmosis is one of the leading foodborne causes of deaths. The disease can be transmitted by oocysts in cat feces and contaminated undercooked meats. While there is a need for an effective vaccine against toxoplasmosis in humans and animals, most vaccines studied thus far are low in protective efficacy and remain at the experimental stage. *Toxoplasma* DNA vaccines containing a single antigen (TgDOC2) and multiple antigens (TgPF, TgROP18, TgROP18, TgMIC6 and TgCDPK3) are reported (Zhang, Elsheikha et al.; Zhang, Hou et al.). Both vaccines achieved considerable protection against challenge in the mouse model of infection. Development of vaccines, particularly efficacious and cost-effective subunit vaccines, is challenging for all parasites. Thus, far, the best protection is still achieved by live attenuated vaccines. Research by Xia et al. reveals that a *T.* gondii mutant (Δldh) lacking lactate dehydrogenases 1 and 2 propagates *in vitro*, but not *in vivo*. Mice vaccinated with this mutant are protected from lethal challenges with wild-type strains of *T. gondii* (Xia et al.). It is very promising that such mutants can provide protection but are unable to replicate in animals, as this may lead to development of live

attenuated vaccines and identification of candidate antigens for subunit vaccines. Translational research will be required to assess protective efficacy in target species.

Avian coccidiosis caused by *Eimeria* spp. results in production losses to the poultry industry. Kim, Chaudhari et al. review the literature encompassing many years of research on the complex host responses to this infection that include typical Th1 inflammatory responses and those mediated by Treg cells, highlighting the importance of Th17 T cell subsets in host resistance/susceptibility to coccidiosis. In addition, studies by the same group show that the dietary indoles, ligands for the aryl hydrocarbon receptor, upregulate Treg responses while downregulate Th17 responses, leading to reduced host intestinal lesions caused by coccidiosis (Kim, Lillehoj et al.). This suggests that effective dietary treatments can alleviate coccidiosis-elicited pathogenesis and/or reduce or prevent subsequent opportunistic infections (Kim, Lillehoj et al.).

There are numerous important animal and human pathogens in the phylum Apicomplexa, such as *Plasmodium* spp., *Toxoplasma gondii*, *Eimeria* spp., *Babesia* spp., and *Cryptosporidium* spp. Natural killer (NK) cells are potent first line effector cells in control of apicomplexan infections by producing IL-12-dependent IFN-γ and direct killing of the parasites and infected cells (Ivanova et al.). However, functions attributed to NK cells may be functions of one of the innate lymphoid cell (ILCs) lineages based on extensive and vigorous research performed since the discovery of ILCs; as such, intensive research is justified to understand the functions of these emerging and important ILCs in the interaction between Apicomplexa parasites and their hosts (Ivanova et al.).

Parasitic helminths are multicellular, eukaryotic, invertebrates of medical and veterinary importance. In the past decades, animal and human parasitic helminth control has relied almost entirely on anthelmintic drugs. However, drug-resistant parasites are emerging, illustrating the need for intense research on the parasitic worms and development of alternative control measures. In addition, prior or existing exposure to, and infection by, helminths can result in polarized immune responses in the host. Such a preexisting immunologic background can unavoidably affect the host immune responses and outcome of infections caused by bacterial, viral or fungal pathogens (Mabbott). Eight articles in this issue, most of which describe original research, emphasize helminths infecting humans and animals. The review article in this Research Topic is focused on helminth-mediated immunoregulation through host pattern recognition receptor (PRR)-dependent and -independent mechanisms (Zakeri et al.), involving host-parasite interactions via parasitic excretory/secretory products and extracellular vesicles. The outcome of such a cross-regulation is two-fold, in general. On the one hand, the worms have evolved to acquire the ability to manipulate the host immune responses in favor of their own survival and parasitism. On the other hand, the host requires exposure to helminth infections for establishing a bystander immunity essential for downregulating deleterious host responses due to allergies and autoimmune diseases. Indeed, the results of recent studies by Ebner et al. indicate that, using a cell line in combination with the infective *Ascaris suum* larvae *in vitro* and analysis by dual-species RNA-Seq, worm exposure elevates host metabolic activities and suppresses some of the chemotactic genes, but does not affect overall immune responsive genes or immune signaling pathways. However, upon contact with the host cell, *Ascaris* larval genes responsible for motor function development and invasion are upregulated, an example of parasitic evasion and promotion of self-development, migration and survival.

Trichinella spiralis, an important food-borne pathogen, attenuates collagen-induced arthritis through programmed death 1 (PD1) by downregulating Th1/Th17 responses, an instance of a therapeutic effect exerted by helminth infections (Cheng et al.). Results of the recent studies by these investigators illustrate that infection by *T. spiralis* elevates PD1 in CD4 T cells, and mice infected with the parasite have reduced pathology of collagen-induced arthritis. Moreover, the infection-induced therapeutic effect can be abolished by anti-PD1 antibodies. Lack of such a therapeutic effect is shown in PD1-deficient mice, further demonstrating the importance of PD1 (Cheng et al.). Using a bioinformatics systems approach, Homan et al. further demonstrate the importance of co-infection by epitope networking. In this study, predicted T cell epitopes of multiple helminth species and the associated host responses are analyzed for their ability to bind with MHC molecules, as well as for the presence of T cell-exposed motifs, which are comprised of amino acids in a peptide bound to MHC molecules that engage the T cell receptor. Interestingly, T cell-exposed motifs identified in the study are shared among the helminth species and with the taxonomically unrelated pathogens commonly seen in co-infections. The results indicate that a systems approach must be taken when investigating an infection against a backdrop of co-infection and the potential presence of preexisting immune response bias. In the highly complex process of host-gastrointestinal (GI) parasite interactions, the interrelationship between the parasite and the host GI microbiota should also be considered. *Heligmosomoides polygyrus*, a nematode that infects the small intestine of mice, produces excretory/secretory products with antimicrobial activities (Rausch et al.). Using the germ-free rodent model, research conducted by Rausch et al. shows that the parasite may sense and modulate enteric microbiota, in their favor, by controlled release of nematode-derived antimicrobial excretory/secretory products.

Anti-worm vaccines are considered an important alternative to anthelmintics in the face of rapid emergence of drug resistance in the worm; thus, it is crucial to identify protective vaccine candidates in parasitic worms of interest. The *Haemonchus contortus* serine/threonine-protein phosphatase, an excretory/secretory protein, is identified and characterized for its potential to be a vaccine candidate, based on the protein's ability to modulate cytokine production, immune cell migration, and apoptosis, and to downregulate cell proliferation and MHC protein expression (Ehsan et al.). Immunodominant structural proteins and a wide range of moonlighting proteins are identified using combined 2-dimensional electrophoresis and LS-MS/MS in worm extract as well as surface preparations from the adult tapeworm *Hymenolepis diminuta* (Mlocicki et al.). Some of the proteins may be excellent vaccine candidates. It

has been known that granulocytes play a key role in bridging the innate and acquired immunities and mediating clearance of helminth infections. The study by Rajamanickam et al. illustrates that *Strongyloides stercoralis* infection promotes the level of eosinophil, neutrophil, and mast cell granule proteins present in peripheral blood, while anthelmintic drug treatment suppresses them, indicating a direct involvement of activated granulocytes during helminth infection.

Taken together, this Editorial gives a brief overview of the findings presented by all articles in this Research Topic, and we hope that these articles provide readers a cross-sectional view of status of current research on some of the parasites of medical and veterinary importance. This collection of articles provides valuable and timely insights into the need for, and recent developments in, parasite research, the mechanisms underlying infection and pathogenesis, and potential therapeutic and prophylactic interventions. Humans and animals in their life times are confronted with constant threat of infections by, or exposure to, several types of parasites, in addition to a whole battery of other pathogens. Parasitic infections may result in protective immunity for life, biased/compromised immune functions, and/or loss of productivity. As stated earlier, the underlying conditions, such as biased immune status by previous parasitic infection or exposure, can be determining factors influencing potential immunities against pathogens which are irrelevant to those of prior exposure. In the laboratory setting, experiments must be designed in such a way as to yield definitive results. However, in the field, we must appreciate that co-infection of individuals is often inevitable. Again, this Research Topic is focused on host-parasite interactions, and those who contributed to this special issue have addressed the importance and significantly advanced the research in each field. We eagerly look forward to advances in parasitology research in the coming years, and to a greater understanding of the interplay between parasites, the host, and other infections in particular.

AUTHOR CONTRIBUTIONS

All authors listed have made a substantial, direct and intellectual contributions to the writing, and approved its publication.

ACKNOWLEDGMENTS

We wish to thank all authors who have participated in this Research Topic and the reviewers for their insightful comments and suggestions. XS was supported by the National Natural Science Foundation of China (31572507).

Conflict of Interest: The authors declare that the research was conducted in the absence of any commercial or financial relationships that could be construed as a potential conflict of interest.

frontiers in Immunology

ORIGINAL RESEARCH
published: 07 December 2018
doi: 10.3389/fimmu.2018.02891

Age-Related Differential Stimulation of Immune Response by *Babesia microti* and *Borrelia burgdorferi* During Acute Phase of Infection Affects Disease Severity

Vitomir Djokic†, *Shekerah Primus*†, *Lavoisier Akoolo*†, *Monideep Chakraborti and Nikhat Parveen**

Department of Microbiology, Biochemistry and Molecular Genetics, Rutgers New Jersey Medical School, Newark, NJ, United States

Lyme disease is the most prominent tick-borne disease with 300,000 cases estimated by CDC every year while ∼2,000 cases of babesiosis occur per year in the United States. Simultaneous infection with *Babesia microti* and *Borrelia burgdorferi* are now the most common tick-transmitted coinfections in the U.S.A., and they are a serious health problem because coinfected patients show more intense and persisting disease symptoms. *B. burgdorferi* is an extracellular spirochete responsible for systemic Lyme disease while *B. microti* is a protozoan that infects erythrocytes and causes babesiosis. Immune status and spleen health are important for resolution of babesiosis, which is more severe and even fatal in the elderly and splenectomized patients. Therefore, we investigated the effect of each pathogen on host immune response and consequently on severity of disease manifestations in both young, and 30 weeks old C3H mice. At the acute stage of infection, Th1 polarization in young mice spleen was associated with increased IFN-γ and TNF-α producing T cells and a high Tregs/Th17 ratio. Together, these changes could help in the resolution of both infections in young mice and also prevent fatality by *B. microti* infection as observed with WA-1 strain of *Babesia*. In older mature mice, Th2 polarization at acute phase of *B. burgdorferi* infection could play a more effective role in preventing Lyme disease symptoms. As a result, enhanced *B. burgdorferi* survival and increased tissue colonization results in severe Lyme arthritis only in young coinfected mice. At 3 weeks post-infection, diminished pathogen-specific antibody production in coinfected young, but not older mice, as compared to mice infected with each pathogen individually may also contribute to increased inflammation observed due to *B. burgdorferi* infection, thus causing persistent Lyme disease observed in coinfected mice and reported in patients. Thus, higher combined proinflammatory response to *B. burgdorferi* due to Th1 and Th17 cells likely reduced *B. microti* parasitemia significantly only in young mice later in infection, while the presence of *B. microti* reduced humoral immunity later in infection and enhanced tissue colonization by Lyme spirochetes in these mice even at the acute stage, thereby increasing inflammatory arthritis.

Keywords: *Babesia microti*, age-related immunity, babesiosis, *Borrelia burgdorferi*, Lyme disease, immunity to tick-borne coinfections

OPEN ACCESS

Edited by:
Xun Suo,
China Agricultural University, China

Reviewed by:
Dean T. Nardelli,
University of Wisconsin–Milwaukee, United States
Yi-Pin Lin,
Wadsworth Center, United States

***Correspondence:**
Nikhat Parveen
Parveeni@njms.rutgers.edu

†*These authors have contributed equally to this work*

Specialty section:
This article was submitted to Microbial Immunology, a section of the journal Frontiers in Immunology

Received: *14 August 2018*
Accepted: *26 November 2018*
Published: *07 December 2018*

Citation:
Djokic V, Primus S, Akoolo L, Chakraborti M and Parveen N (2018) Age-Related Differential Stimulation of Immune Response by Babesia microti and Borrelia burgdorferi During Acute Phase of Infection Affects Disease Severity. Front. Immunol. 9:2891. doi: 10.3389/fimmu.2018.02891

INTRODUCTION

Concomitant coinfections with parasites and bacteria in humans are common in the developing world (1); however, reports of such coinfections in the developed world are rare. In contrast, coinfections with tick-borne protozoan parasite of *Babesia* species and *Borrelia burgdorferi* sensu lato group of spirochetes have been emerging more recently (2–5). The CDC estimates that ∼300,000 cases of Lyme disease and ∼2,000 cases of babesiosis occur in the U.S.A. every year. Lyme disease is caused by *B. burgdorferi* spirochetes while the Apicomplexan protozoan parasite *Babesia microti* is the major causative agent of babesiosis in the United States and *B. divergence* is prevalent in Europe. Coinfections of *Ixodes* species ticks with *B. burgdorferi* and *B. microti* have been increasing steadily over the years (6–10). Reservoir hosts and tick-feeding habits determine the spread of these pathogens to humans. The most commonly recognized tick-borne coinfection in most of the Eastern United States is Lyme spirochetes and *B. microti* with detection levels of concurrent infections by these pathogens in New York as high as 67% (11).

B. burgdorferi is responsible for systemic Lyme disease that affects the skin, musculoskeletal system, heart, joints, and nervous system. Babesiosis remains asymptomatic in healthy individuals such that donation of blood by these infected persons can often lead to transfusion-transmitted babesiosis, raising serious health care problems for already sick recipients of this tainted blood or blood products (12–14). Severe babesiosis in splenectomized patients result in high morbidity and even mortality indicating that the spleen plays a critical role in resolution of *Babesia* infection (15–19). Several immunological deficiencies emerge with age, resulting in an increased susceptibility of the elderly to various infections. Innate immune response in both humans and mice affect clearance of infections that changes with age (20–23). For example, declines in function of neutrophils and defect in macrophage (mφ) response with in aged humans in responses to infection have been described previously (24, 25). Therefore, it is not surprising that severe babesiosis is most common in people >40 years of age, especially in the elderly individuals (2, 26). Severe disease requires patient hospitalization, and can even cause death due to multi-organ failure (27). In contrast, Lyme disease severity has not been reported to be age dependent in humans but older mice are somewhat resistant to inflammatory Lyme disease. These observations underscore the need for a comprehensive evaluation of the effect of coinfections on overall disease severity using the susceptible mouse model of infection.

The lack of symptoms in patients and unavailability of cost-effective and sensitive diagnostic tests often results in underestimation of babesiosis prevalence. Epidemiological studies demonstrated that *B. microti-B. burgdorferi* coinfected patients suffer from significantly more diverse and intense symptoms, which persist longer than those in patients infected with each pathogen individually (28–30). Symptoms, such as chronic fatigue and headache have been reported to persist in coinfected patients for months and were significantly higher than patients with Lyme disease alone (28). In the United States, 10% of patients with initial erythema migrans show persistent flu-like symptoms, joint and muscular pain, and fatigue even after completion of antibiotic treatment regimen (31). Physicians in the endemic regions are encouraged to recommend additional blood tests for concurrent infection with *B. microti* because the treatment approach for this parasitic disease is different from bacterial infections and testing for babesiosis is not often conducted to determine coinfection (11).

Susceptible C3H mouse strain infection system has provided significant information about immune responses against *B. burgdorferi* and *B. microti* and the impact of these infections on respective disease manifestations. Splenic cells of *B. burgdorferi* infected C3H mice showed an increase in B and CD4+ lymphocytes, increase in IFN-γ levels and diminished levels of IL-4 production (32–36). IFN-γ production together with increase in IL-17 producing Th17 cells, which produce TNF-α simultaneously, were shown to contribute to Lyme arthritis severity, while primarily antibodies against *B. burgdorferi* facilitated clearance of the spirochetes, reducing their burden in tissues (32, 36–38). Both Th1 and Th2 responses are indicative of the development of the adaptive immune response including their contribution to humoral immunity. Innate immune response, involving macrophage and NK cells, has been found to be critical for control of protozoan infections, including intracellular pathogen *B. microti* during acute phase (39–44). Cytokines IFN-γ and TNF-α contribute to infection-associated inflammatory complications; however, they also help in elimination of protozoan pathogens with the help of Nitric oxide (NO) produced during infection (39–44). Increase in IL-10 levels was found to exacerbate *Plasmodium* parasitemia but this cytokine suppressed hepatic pathology (45). Thus, balance between these 3 cytokines; IFN-γ, TNF-α, and IL-10 levels are critical for moderating parasitic disease severity, and establishment of long-term, non-fatal diseases (43, 46). Macrophage and NK cells were also shown to play critical roles in conferring resistance in C57BL/6 mice to highly infectious WA-1 strain of *Babesia* species (21), while both CD4+ cells and IFN-γ contributed to resolution of parasitemia of *B. microti,* which causes milder disease in mice (47).

Only limited murine studies have been conducted to study tick-borne coinfections until now. Two previous investigations reported contradictory outcomes of coinfections particularly as demonstrated by Lyme disease severity (48, 49). We decided to conduct a comprehensive study to understand the effect of simultaneous *B. burgdorferi* and *B. microti* infections on acute immune responses of inbred mice during parasitemia upward incline phase, and consequentially, on survival and persistence of each pathogen later as affected by the age of mice. We selected C3H mice for our coinfection studies because young mice of this strain exhibit Lyme arthritis and carditis (50, 51), as well as *B. microti* parasitemia and anemia (48, 49) similar to humans. We hypothesized that using a mouse model of Borrelia-Babesia coinfection, we will be able to understand why patients with these coinfections show more persistent subjective symptoms. We describe here the impact of coinfection on the splenic immune response in C3H young and mature, older mice at acute phase of infection and its effect on parasitemia and Lyme disease due

to modulation of immune response by *B. microti* particularly in coinfected mice.

MATERIALS AND METHODS

Ethical Statement

This study was carried out in accordance with the guidelines of the Animal Welfare Act and the Institute of Laboratory Animal Resources Guide for the Care and Use of Laboratory Animals, and Public Health Service Policy with the recommendations of Newark Institutional Animal Care and Use Committee (IACUC) designated members. The protocol number D-14011-A1 of the corresponding author was approved by the Newark IACUC and study was conducted at Rutgers-New Jersey Medical School following this approved protocol.

Culture and Maintenance of *B. burgdorferi* and *B. microti* and Injection of Mice

C3H/SCID female mice were first injected with *B. microti* infected RBCs stock to obtain inoculum for subsequent experiments. Parasitemia was determined daily using the approved guidelines as described previously (52, 53). *B. burgdorferi* N40 strain carrying a firefly luciferase gene (Bbluc) (54), which is a derivative of the N40D10/E9 clone (55), was used in this study and is labeled as N40 throughout. N40 was cultured at 33°C in Barbour-Stoenner-Kelly-II (BSK-II) medium supplemented with 6% rabbit serum (BSK-RS). The spirochetes were harvested and count adjusted to 10^4 N40 per ml of medium. Only female mice were used in all experiments to avoid the effect of testosterone on parasitemia and innate immune response reported for parasitic diseases (56).

To assess the mechanistic details of coinfections, we conducted experiments in susceptible C3H mice. Young mice were used because they display both Lyme disease and babesiosis disease manifestations while middle age, mature 30 weeks old mice (referred as old mice throughout) were included to determine if they show different immune response in acute phase and display higher parasitemia as observed in humans. Three weeks or Twenty-Nine weeks old female C3H mice were purchased from Rutgers approved reputable vendor(s) and were used in the experiments after acclimatization for one week. The mice were randomly divided into 4 experimental groups in each set with each group containing 5 mice, thus a total of 40 mice were used, 20 young mice at 4 weeks of age and 20 mice that were 30 weeks old. The first group of mice in each age category remained uninfected, second group were injected with *B. burgdorferi* (N40) alone, third group received both N40 strain and *B. microti* and fourth group was inoculated with *B. microti* alone. Mice were injected with 1×10^4 gray strain of *B. microti* (ATCC30221 strain) infected RBCs/mouse diluted in Phosphate Buffered Saline (PBS) intraperitoneally (ip), or injected with 10^3 *B. burgdorferi* diluted in 100 µl BSK-RS subcutaneously (sc) in each mouse on the lateral aspect of the right thigh, or injected with both pathogens at the respective sites. Naïve mice received BSK-RS and PBS, sc and ip, respectively. BSK-RS does not interfere in live imaging of mice and allows light emission to occur *in vivo* for 10 min. Based upon our experience, we do not expect any impact of the vehicles, if any, beyond a few days post-infection. Due to different vehicles suitable for each microbe survival and dissemination in host after injection, both pathogens were injected at different sites using the established protocols for each pathogen.

We determined the effect of coinfections during the acute phase of infection before the development of peak parasitemia and adaptive immune response. Our goal was to analyze the effect of *B. burgdorferi* impact on *B. microti* parasitemia and consequently on splenic immunity during pre-convalescence period. Mice were euthanized when *B. microti* parasitemia was ∼20%, i.e., before reaching the peak parasitemia. Thus, for determination of immune response at early stage of infection, young mice were euthanized at 11 days post-infection and old mice at 17th day of infection because parasitemia and Lyme spirochetes colonization was slower in the older as compared to the young mice. Dose and mode of injection for each pathogen is described above.

Monitoring of Infected Mice

Infected mice were monitored closely for both N40 and *B. microti* infection progression for up to 21 days post infection in the initial experiment to determine the acute phase of infection before peak parasitemia develops. Based upon the parasitemia profile, a thorough investigation of acute phase of infection on immune response and evaluation of disease severity is presented here. Plasma was also recovered for antibody response determination at 3 weeks of infection. Samples collected from mice at acute phase were then evaluated further for splenic immune response, tissue colonization, and disease pathology. Mice infected with *B. microti* were monitored for parasitemia every day by examination of Giemsa stained blood smears.

Assessment of Tissue Colonization Levels by *B. burgdorferi* and Disease Pathology

To eliminate microbiome on skin surface after euthanasia, mice were soaked in Betadine for 30–40 min followed by soaking in 70% ethyl alcohol for 30 min and then dissected in biosafety hood to aseptically remove organs to recover live spirochetes. The skin at the injection site, ear, blood and urinary bladder were transferred to tubes containing BSK-II+RS medium and antibiotic mixture for Borreliae with 100x stock containing 2 mg Phosphomycin, 5 mg Rifampicin and 250 µg of Amphotericin B in 20% DMSO (HI-MEDIA Laboratories, PA) and grown at 33°C to recover live *B. burgdorferi* from each tissue. In each experiment, right joint and heart were fixed in neutral buffered formalin, processed by routine histological methods, sectioned and scored in a blinded manner for carditis and arthritis severity caused by *B. burgdorferi*. DNA was isolated from the left joint and brain of mice in each experiment to use for qPCR. The qPCR was carried out using *B. burgdorferi recA* amplicon and the specific molecular beacon probes tagged with FAM fluorophore in the duplex assay developed in our laboratory (57). To determine spirochete burden in each organ, nidogen amplicon copy number using the specific molecular beacon tagged with TET fluorophore was used for normalization of *B. burgdorferi* copy number. After

euthanasia, aseptically removed liver and spleens were weighed, and splenocytes collected for flow cytometry as described below.

HISTOPATHOLOGY

Two graduates of veterinary medicine (LA and VD) evaluated sections of joints and hearts independently in a blinded manner and scored for inflammation. Briefly, severity of arthritic manifestation was measured by assessing (i) synovial hyperplasia and (ii) erosion of cartilage, (iii) increase in lymphocytic infiltration and (iv) change in synovial space as observed in N40-infected and coinfected mice compared to the naïve or mice infected with *B. microti* alone. Scoring of joint inflammation ranged from "–" (for naïve mice) to "+ + +" in *B. burgdorferi* infected/coinfected mice based upon display of all four criteria. Carditis is considered severe (+) in mice if mixed leukocyte infiltration (primarily macrophage) and fibroblastic proliferation of the connective tissue around the aortic valve and origin of the coronary artery are observed. Infiltration of macrophages and lymphoid cells may also appear around the aorta or in focal areas of the auricular or ventricular epicardium to the apex of the heart (50). These manifestations are usually observed between 2 and 3 weeks of infection with our N40 strain. Manifestations (+/-) are considered milder if consistently reduced distribution of these features is observed. The lack of these characteristics is indicative of no (-) carditis.

Analyses of Splenic Cells by Flow Cytometry

Single cell suspensions of the splenocytes was obtained by slicing the organ into small pieces and straining it into 50 ml conical tube using a 70 μm nylon sterile cell strainer. The cells were then washed with PBS by centrifugation at 350 xg and RBCs lysed by Ammonium-Chloride–Potassium (ACK) lysis buffer (Thermo Fisher # A10492201). The cells were then resuspended in fluorescence-activated cell sorting (FACS) buffer (PBS +5%FBS), and stained with specific antibodies diluted 1:50. Using hemocytometer cell number was adjusted to 10^8 for each individual sample in 2 separate tubes. In the first tube, B cells were detected with Brilliant violet 421 conjugated anti-mouse CD19 antibodies (BioLegend, #115537) and macrophages with PE conjugated anti-mouse F4/80 antibodies (BioLegend, # 123110) followed by FACS. In the second tube, splenocytes were incubated with APC-Cy7 conjugated anti-NK1.1 mouse monoclonal (PK136) antibodies (Bilegend # 108724), T cells with PE/Cy7 conjugated anti-mouse CD3 antibodies (BioLegend #100220), T helper cells with FITC conjugated anti-mouse CD4 antibodies (BioLegend #100406) and cytotoxic T cells with Alexafluor-700 conjugated anti-mouse CD8a antibodies (BioLegend #1000730) by incubation for 30 min in the dark on ice. The cells were washed three time with PBS containing 5% FBS (FACS Buffer) by centrifugation and resuspended in Fixation buffer (BioLegend # 420801) for 20 min at room temperature, and then permeabilized twice in 1x Intracellular Staining Permeabilization Wash Buffer (BioLegend # 421002). After centrifugation, for intracellular cytokines staining, cells were incubated with anti-mouse IFN-γ antibodies conjugated with Pacific Blue (BioLegend #505818), anti-mouse TNF-α antibodies conjugated with PE (BioLegend #506306), anti-mouse IL-4 antibodies conjugated with BV605 (BioLegend #504126), anti-mouse IL-10 antibodies conjugated with PerCP-Cy5.5 (BioLegend #505028), anti-mouse IL-21 antibodies conjugated with eFluor 660 (ThermoFisher #50-7211-82) all used at 1:50 dilution, for 20 min on RT in dark. The samples were then washed twice with Intracellular Staining Permeabilization Wash Buffer and centrifuged at 350 xg for 5 min. Fixed and labeled cells were then resuspended in 0.5 ml of FACS Buffer and analyzed using BD LSRFortessa™ X-20 (BD Biosciences) driven by software FACS DiVa (BD Biosciences). For each fluorophore, appropriate compensation was made using one of the naïve mice splenocytes. Acquired data was analyzed using FlowJo, Version 10.3 software. After analysis of samples, ratio between CD19+ and F4/80+ was determined from the first tube while FcR+ cells were distinguished from CD3+ cells in the second tube. Furthermore, subpopulation of CD4+ and CD8+ were quantified among these CD3+ cells. Intracellular cytokine profile was used to quantify Th1 cells by identifying IFN-γ+ label only, Th2 cells marked with IL-4+, IL-10+, Th17 with IL-21+ only and Tregs labeled for only IL-10+.

In vitro Stimulation of Splenic T Cells

Splenic cells separated as described above were suspended in 5 ml cell staining buffer (BioLegend #420201). All further treatments were done in this buffer. After counting live cells, splenocytes from each mouse were labeled with 1:50 dilutions of APC.Cy7 anti-NK1.1 mouse antibodies (BioLegend #108724), and anti-mouse CD45 coupled with PE (BioLegend #103106). Anti-NK1.1 mouse monoclonal IgGa2 antibodies (PK136 clone), binds to mouse FcR+ cells such as high affinity FcγRI possessing macrophages and neutrophils, and cells that are primarily involved in inflammatory response and display low affinity FcγRII and FcγRIII on myeloid cells and platelets (58). Since NK1.1 marker is lacking in C3H mice, anti-NK1.1 mouse monoclonal antibodies helped us quantify splenic FcR+ cells because Fc rather than Fab region of antibodies bound to the cells. DAPI (1 mg/ml) was also included in the buffer at 1:50 dilution to separate dead cells. Cell suspensions were incubated on ice in dark for 30 min for staining. After washing three times with the buffer by centrifugation at 350 xg for 5 min each, cell pellets were suspended in 1 ml buffer and 5 samples from each mouse group pooled. Cell sorting was done using BD AREA II (BD Biosciences) by first gating for appropriate cell size, then for DAPI negative, live cells followed for APC.Cy7 positive in first tube, and PE positive cells for the second tube.

For *in vitro* stimulation, six aliquots of 50,000 cells suspended in 200 μl of RPMI with 10% FBS and 5% penicillin-streptomycin (cell suspension medium) were prepared for pooled cells from spleens from each mouse group in 96-well plate. Three wells served as untreated control and the other three replicates treated with 100 ng/ml phorbol 12 myristate 13-acetate (PMA) for stimulation, 1 μg/ml ionomycin to increase intracellular levels of calcium, 5 μg/ml monestin as protein transport blocker that helps retention of intracellular cytokines in stimulated lymphoid

cells in the Golgi complex and 5 μg/ml brefeldin A, a lactone antiviral that inhibits protein transport from the endoplasmic reticulum to the Golgi apparatus, i.e., in the presence of the mixture of ionomycin-monestin-brefeldin A or IMB. The plates were incubated at 37°C with 5% CO_2 for 10 h. Cells from each well were transferred to 4 ml tube and wells washed twice to recover all untreated/treated cells. After centrifugation at 350 xg for 5 min, supernatant was removed and cells washed twice with cell staining buffer. Cell pellets were then resuspended in 1 ml buffer and then stained for surface markers using 1:50 dilution of anti-mouse CD4 antibodies labeled with FITC (BioLegend #100406) and anti-mouse CD8a antibodies labeled with AlexaFluor 647 (BioLegend #100724) by incubation on ice in dark for 30 min. After three washings, cells were fixed using BioLegend Intracellular Flow Cytometry Staining protocol. Briefly, after two incubations of cells in 0.5 ml of fixation buffer at room temperature for 20 min in dark, cells were recovered by centrifugation, washed twice in 1 × Intracellular Staining and Permeabilization Wash Buffer (BioLegend #421002). Cocktail of 1:50 dilution of anti-mouse IFN-γ antibodies labeled with Pacific Blue (BioLegend #505818), anti-TNF-α antibodies labeled with APC.Cy7 (BioLegend #506344), anti-IL-21 antibodies labeled with e-Fluor 711 (ThermoFisher #50-7211-82), anti-IL-10 antibodies labeled with PerCP/Cy5.5 (BioLegend #505028) and IL-4 coupled with Brilliant Violet 605 (BioLegend #504125) was prepared and after adding to cells in each tube, incubated at room temperature in dark for 20 min to mark intracellular cytokines present in each cell type. Cells were then washed twice using 2 ml buffer to remove unbound antibodies and then resuspended in 0.5 ml of cell staining buffer for Flow cytometry. Cell identifications were carried out on BD LSRFortessa™ X-20 (BD Biosciences) driven by software FACS DiVa (BD Biosciences). Acquired data was analyzed using FloxJo, software Version 10.3.

B. microti Protein Extract Preparation

When parasitemia in infected C3H/SCID mice reached to approximately 30%, blood was collected and centrifuged at 2,000 ×g at 4°C for 5 min. Free parasites that were released were recovered from the supernatant by centrifugation at 10,000 ×g for 5 min. The remaining RBC pellet was treated with 0.15% saponin on ice for 30 min and centrifuged at 2,900 ×g for 25 min to recover the parasite pellet. The pellet was washed three times with ice cold PBS by centrifugation at 10,000 ×g for 5 min and resuspended in 1.5 ml of 5 mM MgCl2 solution in PBS in an Eppendorf tube. Parasites were treated with detergent to lyse and incubated with 10 μl DNAse at 37 C for 30 min. The antigen preparation was kept frozen at −20°C and was thawed to use in ELISA.

Humoral Response

ELISA was used to determine antibody response against each pathogen. Plates were coated with either 50 μL *B. burgdorferi* N40 lysate or with *B. microti* total protein extract (concentration adjusted to 0.3 mg/ml) and incubated at 37°C overnight. Wells without protein coating (buffer only) were included as controls. Plates were then blocked with 1% BSA containing PBS for 1 h and then incubated for 1 h with plasma recovered from all mice diluted at 1:5,000 for *B. burgdorferi* or 1:200 for *B. microti*. After washing three times with PBS containing 5% Tween-20 (PBST), bound mouse antibodies were reacted with 1:2,500 anti-mouse-IgG HRP-conjugated secondary antibody. After washing with PBST, 50 μL of TMB substrate (KPL SureBlue, #520001) was added to each well to detect antibody reactivity. Absorbance was measured at OD_{620} using a SpectraMax M2 plate reader.

Statistical Analysis

All data collected was analyzed by Prism version 8.0 for Mac, GraphPad Software (La Jolla, CA). Data is presented as mean ± standard deviation (s.d.). Comparisons were made between groups using one-way ANOVA with binomial 95% confidence interval. In *post-hoc* analysis, when ANOVA *P*-value was below 0.05, unpaired, two-tailed student *t*-tests with Welch's correction for unequal s.d. was conducted to determine significant differences between respective groups. Thus, values below 0.05 were considered statistically significant for a paired group comparison at 95% confidence interval. Two tailed unpaired parametric student *t*-test was used to compare two variables between groups, and *P*-values bellow 0.05 were found to be statistically significant.

RESULTS

Effect of Coinfections on *B. microti* Parasitemia in C3H Mice

In our initial experiment, young mice infected with *B. microti* alone, or coinfected with *B. microti* and N40 exhibited similar temporal patterns of parasitemia such that peak parasitemia was reached on 13th day post infection. In that experiment, peak parasitemia levels were significantly higher by ∼10% in mice infected with *B. microti* as compared to coinfected mice while difference was not significant in old mice (data not shown). Based upon this data, we selected time points here for euthanasia at acute phase before peak parasitemia was obtained. We show here that on 11th day post infection, there was no statistically significant difference in parasitemia levels between single and coinfected young mice (**Figure 1A**). Older mice previously showed delay in development of parasitemia after *B. microti* infection (59). We conducted experiments here to determine age-related differences in the host immune response at acute phase of both infections to find reason for differences between young and old mice later in infection. In our experiment with 30-week old mice, parasitemia developed slightly slower as compared to young infected mice because 20%parasitemia was obtained on 17th day compared to on 11th day in young mice (**Figure 1B**). These results agree with previous finding of delayed peak parasitemia in old *B. microti* infected mice (60). Therefore, we euthanized mice when the parasitemia reached ∼20% in young and old mice, i.e., on 11th and 17th day post-infection, respectively (**Figures 1A,B**).

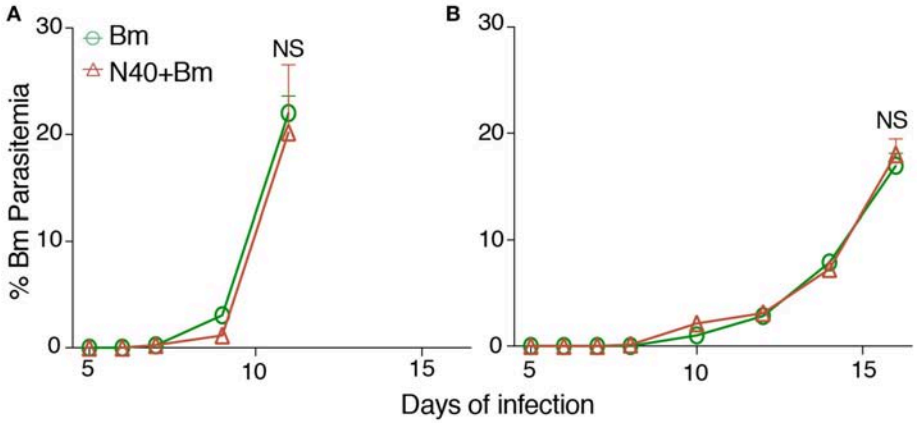

FIGURE 1 | *B. microti* (Bm) and *B. burgdorferi* (N40) coinfection and their impact on the host. **(A)** Bm parasitemia in young female C3H mice at different time points until euthanasia at 11th day post-infection. Each point represents average parasitemia in each group of mice (mean ± s.d.) **(B)** Determination of parasitemia in *B. microti* infected and coinfected old female mice until euthanasia on 17th day post-infection. In each case **(A,B)**, mice were euthanized when parasitemia was ∼20%.

B. microti-Mediated Splenomegaly and Hepatomegaly During Acute Phase of Infection

We examined the effect of *B. microti* infection on liver and spleen of mice during acute phase because these organs of the reticuloendothelial system are also involved in clearance of blood-borne pathogens and help in disease resolution (61, 62). Damaged or parasitized erythrocytes are also removed from circulation by macrophages located primarily within these organs. Although spleen size was slightly larger in N40 infected vs. naïve young mice at 11 days post-infection (**Figure 2A**), size of spleen was not significantly different in old N40 infected mice (**Figure 2B**). In young mice, moderate but significant splenomegaly was observed in *B. microti* infected and coinfected mice (**Figure 2A**) while pronounced splenomegaly was apparent in the old mice (**Figure 2B**). Surprisingly, we did not see a change in the size of liver in any infected mouse group at this stage of infection (data not shown).

We previously showed that marginal zone disappears 3 weeks after infection with *B. microti* (53). Our results here show that disruption of marginal zone starts during the acute phase of *B. microti* infection (**Figures 2C,E**) and erosion of marginal zone is more pronounced during coinfection of both in young and old C3H mice (**Figures 2D,F**). Both young and old mice infected with *B. burgdorferi* alone show normal splenic architecture (data not shown). These results suggest that changes in splenic immunity modulation also begin at the acute stage of infection, particularly in response to protozoan infection. Therefore, we further examined the splenic innate and adaptive immune response more in detail at this stage.

Effect of *B. burgdorferi* and *B. microti* on Splenic Leukocytes at Acute Phase of Infection

To determine the effect of each infection on splenic cells that affects parasitemia development and Lyme spirochetes colonization before adaptive immune response establishment, total splenocytes were analyzed by flow cytometry during pre-peak parasitemia (upward incline phase of parasitemia) and acute phase of Lyme disease (**Table 1**). To understand the impact of innate immune response during infections, we first analyzed numbers of macrophages. A significant increase in myeloid cell numbers in infected as compared to naïve mice was noticed in young mice with total macrophage numbers increased at higher levels in *B. microti* infected or coinfected young mice (27.6 and 28.9%) relative to N40 infected and naïve mice (18.1 and 7.79%) while increase in macrophage numbers in old infected mice (7–9%) was not as pronounced (**Figure 3B**). Moreover, in both single and coinfection macrophage numbers were significantly higher in young compared to old mice (N40 infection p-value = 0.0286; *B. microti* infection p-value = 0.0008; coinfection p-value < 0.0001). A significant proliferation in FcR+, representing primarily phagocytic cell total numbers and their percent in young and old infected mice suggests that these cells are potentially involved in clearance of both *B. burgdorferi* and *B. microti* at acute phase of infection in young and old mice (**Table 1**). Only N40 infection of young mice resulted in production of significantly higher FcR+ cells compared to old mice (p value = 0.0407). Statistically significant increase in CD3+ T cells was observed in all infected young but not old mice with highest change in total T cells observed in *B. microti* infected and coinfected young mice relative to naïve mice (**Table 1**). In contrast, there was almost no change in CD19+ B cells in young mice compared to controls, and greatest change in B cells were observed in N40 and *B. microti* infected old mice individually (approximately 3-fold and 2-fold increase, respectfully) relative to naïve mice that reduced significantly (from 14.3 and 11.2% to 8.32%) during coinfection with these pathogens (**Table 1**). Although the CD19+ proliferation varied greatly among old single and coinfected mice, still these numbers are statistically higher than in young infected mice with the same pathogens (N40 infection p-value < 0.0001; *B. microti* infection p-value < 0.0001; coinfection p-value $= 0.0063$). Not surprising, the numbers of CD4+ and CD8+ cells remained similar to naïve

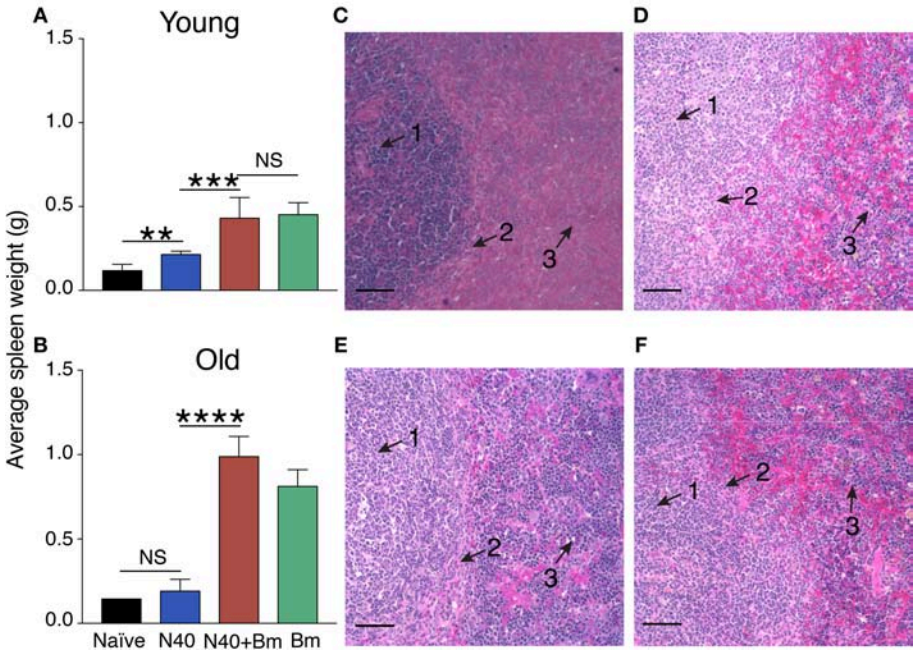

FIGURE 2 | *B. microti* (Bm) infection causes enlargement of the spleen in both young and old C3H mice at acute phase of infection. **(A)** Spleen weights of Bm infected and coinfected mice showed a significant increase over spleens of N40 infected mice on 11th day of infection in young mice, and **(B)** on 17th (pre-peak parasitemia) day of infection in 30 weeks old mice. Each bar represents the mean ± s.d. (*p <0.01, ***p < 0.001, ****p < 0.001). **(C–F)** H & E stained spleen sections showed erosion of marginal zone (arrow 2) between white (arrow 1) and red pulp (arrow 3) regions in *B. microti* infected **(C)** young, and **(E)** old mice. Disruption of marginal zone was found to have progressed more significantly in coinfected **(D)** young, and **(F)** old mice at this stage of infection, resulting in the absence of clear demarcation between red and white pulp in these **(D,F)** mice. Bar in microscopic images represents 100 μm.

mice, without any statistically significant difference between young and old mice at this stage of infections. These results suggest differential splenic T and B cell response to infection with *B. microti* and *B. burgdorferi* in young vs. old mice at acute phase of infection.

The pattern observed with total splenic cells was also reflected in the percentage of each cell type. One representative infected mouse from each group with data normalized to 5,000 cells is shown in **Figure 3A**. In sets of old mice, infection with N40 caused a significant and most pronounced increase in $CD19^+$ B cells likely because it was a little later in infection (17th day post-infection) as compared to young mice (11th day of infection). B cells percentage also increased in *B. microti* infected old mice (11.2%) but not as high as that after N40 infection (14.3%). Increase in total $CD3^+$ T cell percentage was moderately but significantly higher in N40 infected as compared to the naïve young mice with p-values of 0.021 (**Figure 3B**). A significantly higher stimulation of CD3+ cells in *B. microti* infected and coinfected young mice (with $p < 0.0001$ for both) indicates that T cells could play a prominent role in elimination of the intracellular protozoan pathogens. Although the previous reports showed that CD4+ cells are critical for clearance of *B. microti* infected erythrocytes (47, 63), the change in total CD4+ T cell percentage was neither significantly different in infected young nor old mice as compared to the uninfected controls (**Figures 3A,B**) suggesting that during pre-adaptive immune response development period at which point this experiment was concluded, CD4+ T cells were not yet fully stimulated.

Response of Splenic T-Helper (TH), CD4+ Cells During Acute Phase of Infection

The experimental scheme for determining different cytokines production after *in vitro* stimulation by PMA+IMB, and identification of different types of CD4+ cells is shown in **Figure 4**. Briefly, to understand the priming and T-cell mediated immune mechanism involved during acute phase of infection, we stained splenocytes with anti-CD45 antibodies to label all leukocytes and NK1.1 for FcR+ cells, and cells sorted by FACS. The remaining leukocytes mixtures containing macrophages, CD4+ and CD8+ cells were used for *in vitro* stimulation with PMA+IMB. After stimulation, cells were marked with individual cell-type markers, then fixed, permeabilized and stained for different intracellular cytokines. **Figure 4** shows the example of CD4+ cells producing each cytokine, data for which is shown in **Figure 5A**, and outline for identification of each category of CD4+ cell type based upon specific or combination of cytokines production with results shown in **Figure 5B**. Furthermore, various cytokines production by the sorted and stimulated CD8+ cells from infected and naïve, young and old, mice were also determined (top right of **Figure 4**) and results are shown in **Figure 6**.

CD4+ cell numbers that produced IL-10 were not significantly different between uninfected naïve and various

TABLE 1 | Analyses of splenocytes and determination of lymphocytes and myeloid cells by flow cytometry at parasitemia between 15 and 20%.

Young (Average values)				Old (Average values)			
	Cells	**Total No**	**Percentage**	**Cells**	**Total No**	**Percentage**	***t*-test Young vs. Old, *p*-values**
N40	Splenocytes	89446.8	89.4	Splenocytes	89891.0	89.9	
	F4/80	16187.0	18.1	F4/80	7832.3	8.71	0.0286(*)
	Nk1.1/FcR+	38793.6	43.4	Nk1.1/FcR+	36438.8	40.5	0.0407(*)
	CD19	2548.6	2.83	CD19	12855.7	14.3	<0.0001(****)
	CD3	6299.6	7.04	CD3	4073.3	4.53	0.0117(*)
	CD8a	1311.2	1.46	CD8a	1661.3	1.85	0.7278(NS)
	CD4	2333.4	2.59	CD4	3780.0	4.20	0.2127(NS)
N40+Bm	Splenocytes	90755.6	90.8	Splenocytes	92252.6	92.3	
	F4/80	26300.0	28.9	F4/80	6901.3	7.48	<0.0001(****)
	Nk1.1/FcR+	37486.8	41.3	Nk1.1/FcR+	38820.0	42.1	0.2876(NS)
	CD19	2742.0	3.02	CD19	7679.0	8.32	0.0063(**)
	CD3	10599.0	11.7	CD3	3091.3	3.35	<0.0001(****)
	CD8a	2225.8	2.45	CD8a	1750.3	1.89	0.4594(NS)
	CD4	4459.4	4.91	CD4	3062.5	3.32	0.5896(NS)
Bm	Splenocytes	90480.2	90.5	Splenocytes	98637.2	98.6	
	F4/80	25000.6	27.6	F4/80	9461.5	9.59	0.0008(***)
	Nk1.1/FcR+	37720.8	41.7	Nk1.1/FcR+	41822.2	42.4	0.1853(NS)
	CD19	3107.8	3.44	CD19	11047.4	11.2	0.0130(*)
	CD3	9758.7	10.8	CD3	3915.9	3.97	0.0001(***)
	CD8a	2104.0	2.32	CD8a	1361.2	1.38	0.0716(NS)
	CD4	4192.4	4.64	CD4	3166.3	3.21	0.1251(NS)
Naïve	Splenocytes	82605.6	82.6	Splenocytes	85431	85.4	
	F4/80	6436.7	7.79	F4/80	5007	5.86	
	Nk1.1/FcR+	30209.4	36.5	Nk1.1/FcR+	15922	28.7	
	CD19	1876.0	2.26	CD19	4268	4.99	
	CD3	3507.7	4.24	CD3	4678	5.47	
	CD8a	837.3	1.01	CD8a	1364	1.59	
	CD4	3319.2	4.02	CD4	2857	3.34	

*Statistical analyses: (*p < 0.05, **p <0.01, ***p <0.001, ****p <0.0001, NS-Not significant).*

infected old mice. Whereas, young coinfected mice have significantly higher number of CD4+ cells produced IL-10 as compared to naïve mice. At the same time the level of cells producing IL-10 was significantly lower in mice infected with N40 and *B. microti* individually (**Figure 5A**). Even untreated CD4+ cells from uninfected and infected mice produced IL-10 but increase in numbers of these IL-10 producing cells was higher in young N40 infected and coinfected mice as compared to *B. microti* infected mice. IL-10 producing cell numbers were indistinguishable in uninfected and infected old mice. After *in vitro* stimulation, a significantly higher number of CD4+ T cells obtained from all infected mice irrespective of age showed production of TNF-α, IFN-γ, IL-4, and IL-21 as compared to the cells from naïve uninfected mice demonstrating high proliferation of T cells as a response on infection with N40 and *B. microti* individually or together. Surprisingly, increase in stimulated CD4+ cells producing IL-4 and IL-21 cytokines was higher in young as compared to all respective old infected mice. IFN-γ producing CD4+ cells representing Th1 cells were particularly higher in response to infection of young mice with *B. microti* after *in vitro* stimulation. This response is likely due to the high levels of *B. burgdorferi* lipoproteins presence, thus offering a potent proinflammatory ligand to induce Th1 polarization and also potentially by yet to be identified Pathogen Associated Membrane Patterns (PAMPs) of *B. microti* (**Figure 5A**).

Th1 cellular proliferation and response (**Figure 5B**) demonstrated by intracellular IFN-γ production was most pronounced in both young and old mice infected with *B. microti* early in infection indicating that these cells likely play important role in resolution of parasitemia. Increase in Th1 cells was also significant in N40 infected and coinfected mice suggesting contribution of these cells in potential clearance of both pathogens during acute phase of infection. Interestingly, Th2 cells increase in response to both infections was higher in old mice compared to naïve mice, suggesting a faster activation by more mature and fully developed immune system in these mice. Th2 response was highest in response to N40 infection followed by that in *B. microti* infected old mice; however, IL-4

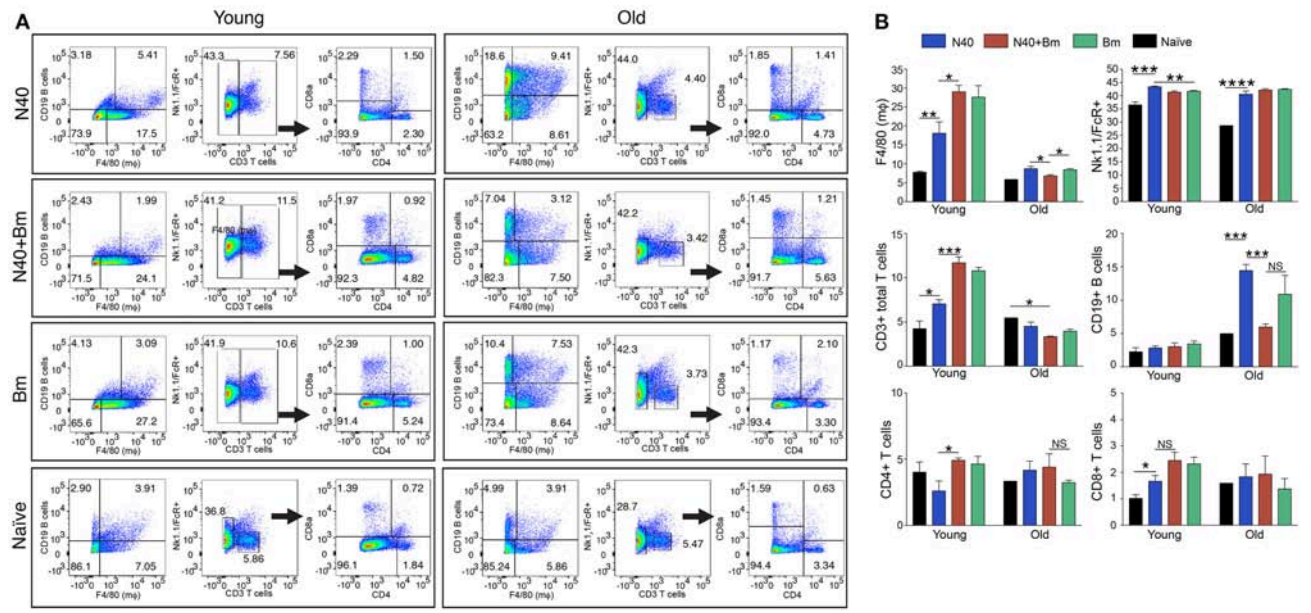

FIGURE 3 | N40 and *B. microti* infection affects splenic leukocytes of young and old mice differently. **(A)** Analyses of one young and one old representative mouse spleen cells from each infection group is shown at 11th and 17th day post-infection, respectively. **(B)** Although percentage of all splenic leukocytes increased in infected mice, growth was highest in B cells in N40 infected old mice, CD3+ T cells in young *B. microti* and coinfected mice, and CD8+ T cells in all young infected mice. Macrophage increased most prominently in *B. microti* infected and coinfected young mice while total FcR+ cells increased in all young and old infected mice. Each bar represents the mean ± s.d. (*$p < 0.05$, **$p < 0.01$, ***$p < 0.001$, ****$p < 0.0001$).

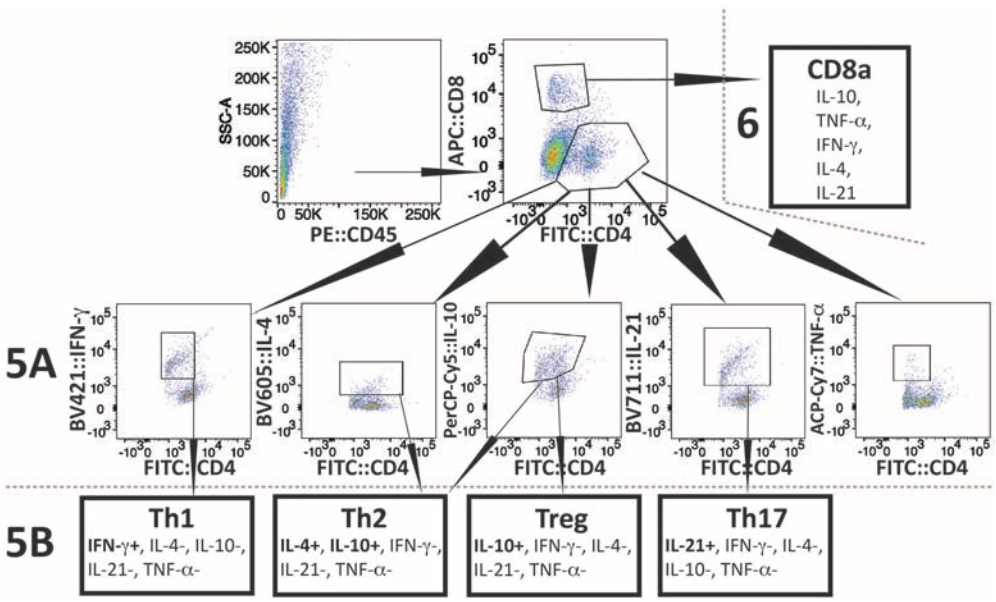

FIGURE 4 | Scheme of Flow-based quantification of various intracellular cytokines production, and of different types of CD4+ cell, and different cytokine producing CD8+ cells in infected mice after *in vitro* stimulation with PMA+IMB. After cell sorting for CD45+ cells (top left), cells were stimulated and then marked with antibodies against mouse CD4 (FITC), and CD8 (AF 647) cells (top center). Cells were then fixed, permeabilized, and stained for intracellular cytokines: IFN-γ-PB, TNF-α-APC.Cy7, IL-21-e-Fluor 711, IL-10-PerCP/Cy5.5, and IL-4-BV605 (2nd row). Then CD4+ cells producing different cytokines were quantified (results presented in **Figure 5A**). In CD4+ subpopulation, cells that were positive for IFN-γ, but negative for other four cytokines were identified as Th1 cells (bottom left). CD4+ cells that had IL-10 but no other cytokines were defined as Tregs, whereas cells producing both IL-4 and IL-10 cytokines, but not IL-21, IFN-γ, and TNF-α were identified as Th2 (bottom center two boxes). CD4+ cells that produced only IL-21 were identified as Th17 (bottom right) and results are presented in **Figure 5B**). CD8 cells producing different cytokines are presented in **Figure 6**.

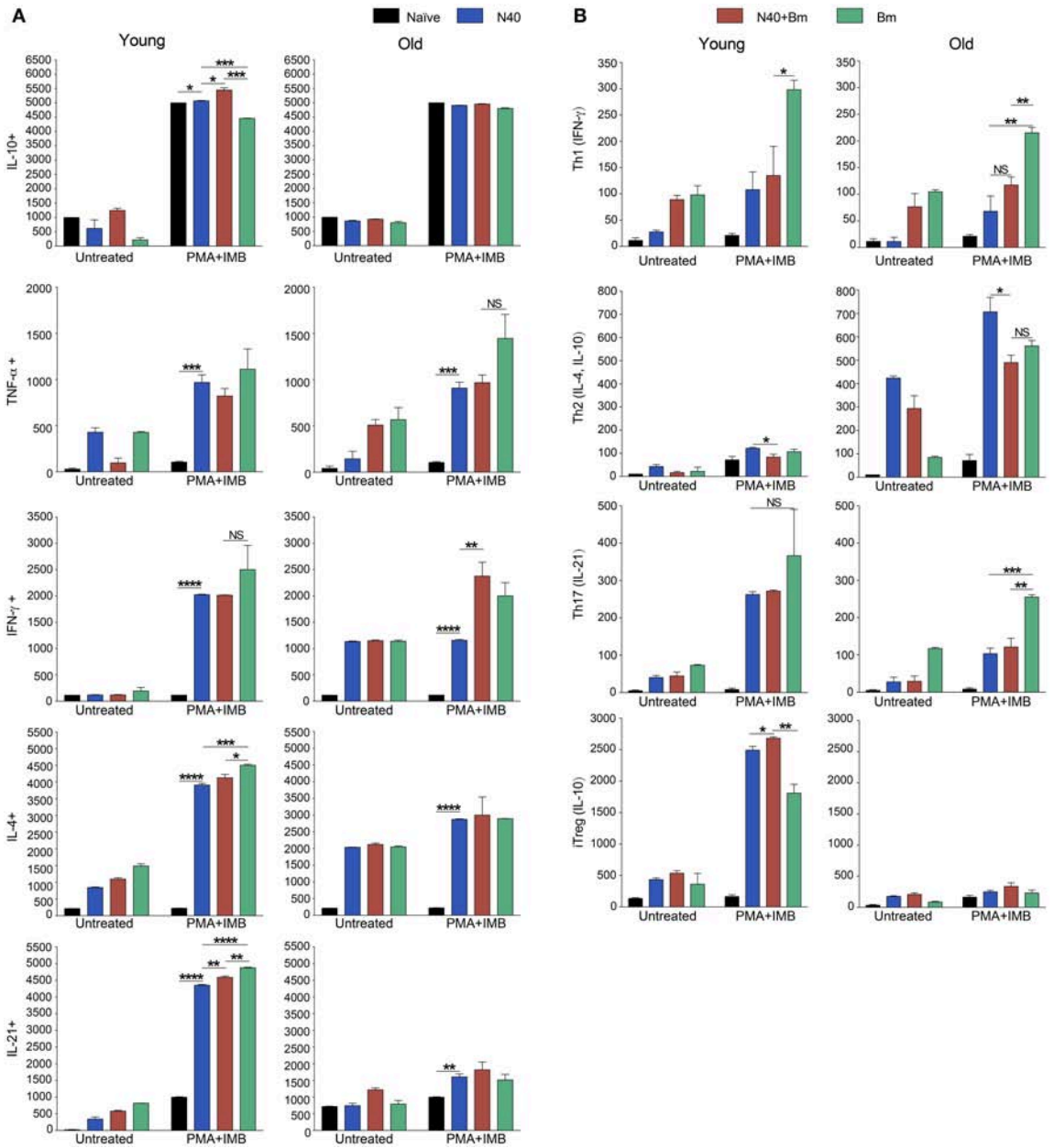

FIGURE 5 | Delineation and quantification of different types of CD4+ T cells based upon their cytokines production by FACS after *ex-vivo* stimulation of splenic leukocytes by PMA. Intracellular cytokines transport blockers IMB were included during stimulation. **(A)** Various cytokines, IL-10, TNF-α, IFN-γ, IL-4, and IL-21 producing CD4+ T cells increased significantly in young mice after PMA stimulation while high levels of IFN-γ and IL-4 cytokine producing CD4+ T cells are observed in old mice even without PMA stimulation. High numbers of IL-10 cytokine producing CD4+ cells were observed in all young and old mice irrespective of infection. **(B)** Th1 response was stimulated in all infected mice with most pronounced change in T cells of *B. microti* infected mice after PMA stimulation. Th2 response was most pronounced in all infected old C3H mice. High Th17 cells stimulation in young infected mice could indicate inflammatory response; however, a much higher Tregs response in these mice appears to maintain splenic immune cells homeostasis preventing fatal disease. Lowest ratio of Tregs/Th17 cells was observed in old *B. microti* infected mice but mice did not appear sick or lethargic at this stage of infection. Each bar represents the mean ± s.d. (*$p < 0.05$, **$p < 0.01$, ***$p < 0.001$, ****$p < 0.0001$).

production only occurred after *in vitro* stimulation. Analysis of CD4+ cells after PMA stimulation showed highest Th1 response by *B. microti* infected mice cells as seen in other intracellular protozoa in both young and old mice (**Figure 5B**) that could not be detected in the unstimulated fresh splenocytes (**Table 2**). More pronounced Th2 response was observed in spleens of old mice with and without PMA stimulation (**Figure 5B**, **Table 2**).

We analyzed splenic leukocytes based upon surface markers and respective cytokines production to further determine the specific T helper cell types that increase in numbers during

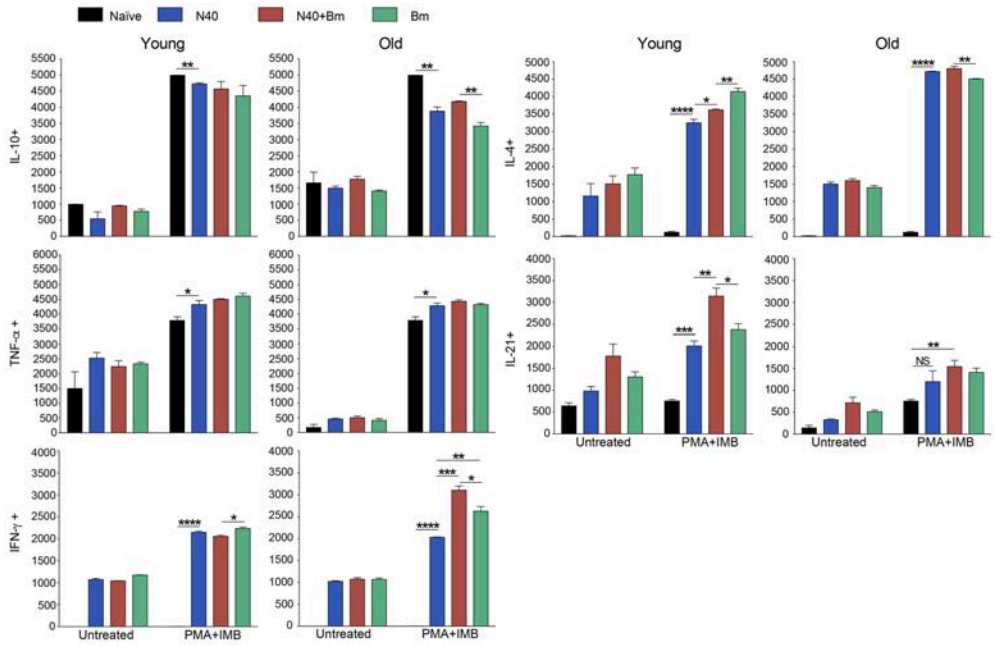

FIGURE 6 | Analysis of splenic CD8+ cells from young and old mice collected at acute phase and stimulated *ex-vivo* by PMA. Intracellular cytokines transport blockers IMB were included during stimulation. Response of CD8+ T cells observed in young mice infected with *B. microti*, N40 or both was comparable to respective infected old mice except IL-21 producing cells numbers were higher in young infected mice. Each bar represents the mean ± s.d. (*p <0.05, **p <0.01, ***p <0.001, ****p <0.0001).

infection with N40 and *B. microti*. Increase in Th17 and T-regulatory (Treg) cells were observed in all young infected mice as compared to the naïve mice. Interestingly, Th17 cells proliferation was most pronounced in *B. microti* infected old mice and was more than double in numbers of those observed in old mice infected with either N40 or *B. microti* alone. Increase in Th17 cells in N40 infected and coinfected mice were significantly higher as compared to naïve mice after stimulation with PMA (**Figure 5B**). High ratio of Tregs/Th17 fresh splenocytes in N40 infected and coinfected young mice, 9.5 ± 0.53 and 9.84 ± 0.04, respectively at acute phase of infection suggests maintenance of immune homeostasis in spleen of these mice that prevents excessive inflammation by these infections (**Table 2**). Even though ratio of Tregs/Th17 was not as high (6.19 ± 0.63) in *B. microti* infected young mice, it was sufficient to prevent excessive inflammation by Th17 cells. Increase in Tregs was substantially lower in all infected old mice with Tregs/Th17 ratio of 2.44 ± 0.25, 2.88 ± 0.73, and 0.89 ± 0.29 in N40 infected, coinfected and *B. microti* infected mice, respectively. Th17 stimulation was highest in old *B. microti* infected mice suggesting possible occurrence of a more severe splenic pathology at later day of infection.

Cytokines Production by CD8+ Cells During Acute Phase of N40 and *B. microti* Infection

PMA stimulated CD8+ cells producing IL-10 and TNF-α between uninfected naïve and various infected young or old mice were similar in numbers (**Figure 6**); however, higher cell numbers producing IL-10 and TNF-α were detected after PMA stimulation. More of CD8+ T cells obtained from all infected mice irrespective of age showed production of IFN-γ, and IL-4 after PMA stimulation as compared to the cells from naïve uninfected mice demonstrating that infection with N40 and *B. microti* individually or together caused priming and proliferation of these T cells in mice that increased further on *in vitro* stimulation. Interestingly, IL-21 producing CD8+ cells were significantly higher in numbers in young as compared to old infected mice even without PMA treatment.

Lyme Disease at Acute Phase of Infection

We were able to recover live spirochetes by culture into BSK-RS from all tissues examined from mice infected with N40 alone, or with *B. microti* from the skin at the injection site, ear, blood, and urinary bladder. We observed light emission due to the presence of bioluminescent spirochetes in joints and head region of N40 infected and coinfected mice on the day of euthanasia (**Figure 7A**). Brain colonization by *B. burgdorferi* N40 strain has been reported in mice in studies conducted in early nineties (64–66); however thorough investigation of brain colonization has not been conducted until now. Therefore, to further assess the burden of *B. burgdorferi* in joints and potentially brain, we isolated DNA from these organs and conducted duplex qPCR (**Figure 7B**). Spirochete copy number normalized to 10^5 mouse nidogen copies indicated high *B. burgdorferi* burden in joints and brain of all mice infected with N40 alone or coinfected with *B. microti*, likely because mice have not yet fully developed adaptive immune response that is critical for clearance

of extracellular spirochetes. N40 quantities were slightly higher in young as compared to old mice. Interestingly, young coinfected mice showed significantly higher *B. burgdorferi* burden in joints relative to those in the N40 infected mice.

Although we found high burden of spirochetes in joints, inflammation in tibiotarsus was not yet fully developed in N40 infected young or old mice (**Table 3**, **Figure 7C**). Coinfected young mice showed more pronounced inflammation with 2/5 mice showing maximum (+++) arthritic severity and 3/5 with moderate (++) inflammatory arthritis (**Table 3**). Neither N40 infected, nor coinfected old mice showed joints swelling visually and exhibited only moderate arthritis in some mice such that all criteria demonstrating fully developed arthritis were not detected. Lymphocytes infiltration was observed in the tibiotarsus of old N40 infected mice, but they did not show as pronounced synovial hyperplasia, erosion of cartilage, and change in synovial space as observed in 2/5 young coinfected mice despite euthanasia of old mice at 17th day post-infection as compared to the 11th day of infection of young mice (**Figure 7C** top vs. bottom, and **Table 3**). Carditis was not observed in either young or old mice either infected with N40 alone, or coinfected with *B. microti*.

Immunomodulation of Humoral Response by *B. microti*

At 3 weeks of infection, antibody response against both pathogens could be detected. Antibody production by B cells is facilitated by CD4+ T helper cells. To determine the effect of significant and consistent reduction in splenic B and T cells caused by *B. microti* infection on *B. burgdorferi* and to determine association of the pathogen specific antibodies production with the change in percentage of B cells, we used ELISA to determine reactivity of mouse antibodies to total protein extract of N40 strain or *B. microti* coated on plates as antigenic cocktail. There was a significant reduction in absorbance when plasma from coinfected young mice were used as compared to plasma from young mice infected with *B. burgdorferi* alone, indicating apparent subversion of the humoral immune response against *B. burgdorferi* by *B. microti* only in young mice (**Figure 8**). A moderate but significant decrease in antibody production against *B. microti* was also observed in coinfected as compared to *B. microti* infected young mice. The specific antibody reactivity against each pathogen was comparable among old mice infected by each pathogen individually and coinfected. However, Overall antibody production against each pathogen was lower in the older mice. Although slightly higher burden of spirochetes was observed in young N40 infected and coinfected mice as compared to old mice, this data is not sufficient to explain the reason for the lack of inflammatory Lyme disease manifestations observed here or was previously reported in old C3H mice (51).

TABLE 2 | Specific splenic CD4+ cells response in Naïve and infected young and old mice.

	Average ± SD			
Young	**Naïve**	**N40**	**N40 + Bm**	**Bm**
Treg	164.7 ± 48.4	2492.0 ± 103.2	2681.0 ± 37.5	1809.0 ± 243.7
Th17	8.33 ± 2.08	262.7 ± 12.4	271.7 ± 5.03	366.3 ± 41.5
Treg/Th17	31.7 ± 9.77	9.50 ± 0.53	9.84 ± 0.04	6.19 ± 0.63
Th1	21.0 ± 6.08	108.0 ± 9.54	168.3 ± 19.7	298.3 ± 31.0
Th2	71.3 ± 25.7	121.7 ± 7.51	83.7 ± 12.1	106.7 ± 18.8
Th1/Th2	0.30 ± 0.03	0.87 ± 0.43	2.03 ± 0.47	2.82 ± 0.23
Old				
Treg	164.7 ± 48.4	248.7 ± 46.4	336.3 ± 97.6	229.7 ± 82.6
Th17	15.0 ± 3.61	103.3 ± 15.9	121.3 ± 14.5	255.3 ± 10.5
Treg/Th17	10.9 ± 0.56	2.44 ± 0.25	2.88 ± 0.73	0.89 ± 0.29
Th1	21.0 ± 6.08	68.0 ± 20.2	117.3 ± 25.7	215.3 ± 17.01
Th2	71.33 ± 19.0	706.7 ± 107.8	490.0 ± 55.05	560.7 ± 41.8
Th1/Th2	0.39 ± 0.22	0.09 ± 0.06	0.24 ± 0.03	0.38 ± 0.006

DISCUSSION

Our studies here demonstrate the age-related immune response against two tick-borne pathogens in the susceptible C3H mice. Reduction in erythrocytes population observed in blood of *B. microti* infected mice agree with that previously reported in gerbils infected with *B. divergens* (67). Hematologic abnormalities, such as anemia and thrombocytopenia are also associated with babesiosis in humans, often requiring blood transfusion and even hospitalization (19, 68, 69). To evaluate differences between old and young mice, we determined host response to each infection at acute phase. Immune response at this stage affects peak parasitemia and inflammatory Lyme disease later in infection. For example, a lower peak *B. microti* parasitemia was observed later in infection in coinfected as compared to *B. microti* young infected mice and not in old mice suggesting that innate immune response at early phase of infection against *B. burgdorferi* in young susceptible mice, likely induced by abundance of spirochetal lipoproteins and TLR2 signaling, contributes to decrease in erythrocytic infection cycles by this protozoan only in these mice (data not shown).

Splenic immunity plays an important role in resolution of parasitic diseases. For example, splenomegaly shown here irrespective of age of mice and reported previously during infection with *B. microti* has also been observed on infection with other vector-borne, blood protozoan pathogens, such as *Trypanosoma congolense*, *Plasmodium falciparum*, and *Plasmodium yoeli* and can even lead to rupture of spleen in humans (49, 70–76) demonstrating consistent splenic involvement in response to various parasitic diseases (67, 77–79). In humans, babesiosis can be a life-threatening disease particularly in the elderly, immunodeficient or immunosuppressed and in asplenic patients, further emphasizing the importance of the spleen in babesiosis resolution (13, 80). In acute phase, we observed moderate but significant splenomegaly in *B. microti* infected and coinfected young mice (**Figure 2A**) while pronounced splenomegaly was apparent in the old mice (**Figure 2B**). This is likely because it took longer to reach the same level of parasitemia in these mice (euthanasia at 17th day post-infection rather than 11th day), allowing spleen to clear parasitized and damaged blood cells for slightly longer

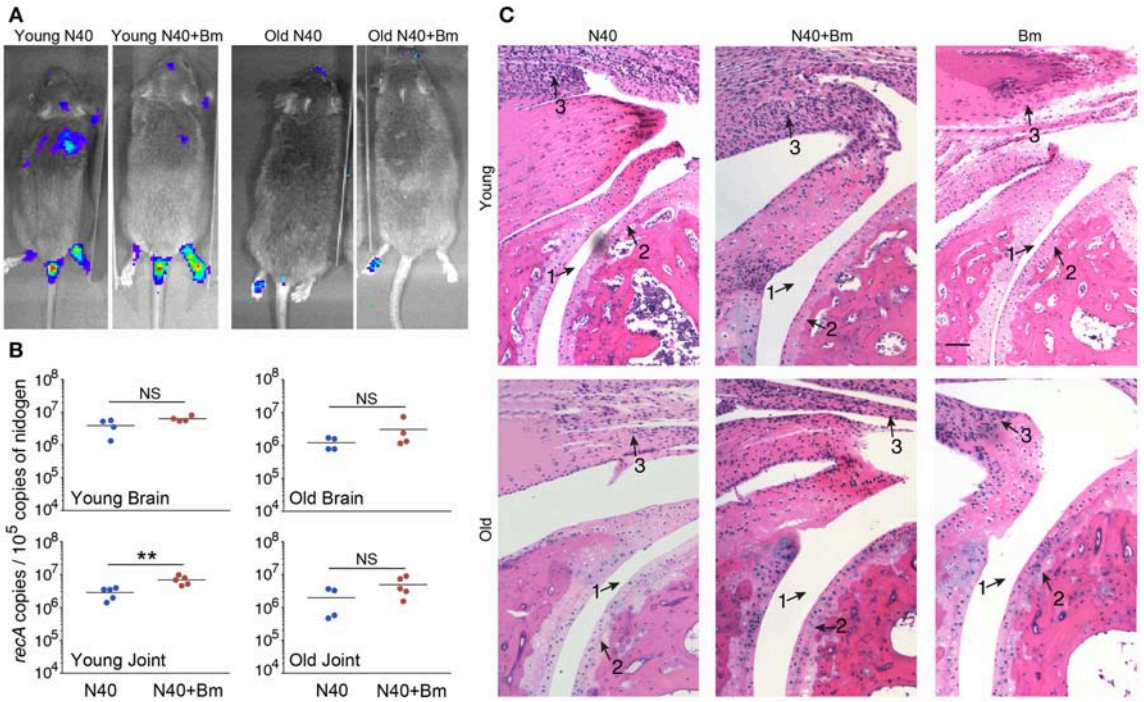

FIGURE 7 | *B. microti* (Bm) and N40 coinfection increases colonization of joints by *B. burgdorferi* causing joint inflammation during acute phase only in young mice. **(A)** Although significant spirochetes-associated bioluminescence was observed in joints and brains of both young and old infected mice, **(B)** burden of N40 was significantly (**$p < 0.01$) higher in joint of coinfected compared to N40 infected young mice. **(C)** *B. burgdorferi* infection causes only mild inflammation of the joints at acute phase of disease as indicated by synovial hyperplasia and erosion of cartilage (arrow 2), lymphocytic infiltration (arrow 3) and change in synovial space (arrow 1) while respective markers show higher inflammation in coinfected young mice. Although lymphocytes infiltration is observed in old mice, cartilage erosion and change in synovial space was not noticeable in joints of different mice. Bar represents 100 μm in all panels.

period and thus, causing a significant enlargement of spleen. The inflammation of liver in response to *B. divergens* infection has been reported to occur due to hemorrhage, hyperplasia of Kupffer cells and infiltration of lymphocytes (67, 81). Our observation of the absence of hepatomegaly in C3H mice infected with *B. microti* alone or with N40 (data not shown) agrees with that reported in rats (82). We did not visually observe any difference in vitality of these two sets of young or old mice suggesting that either the effect of age on babesiosis is minimum in mice or the difference becomes more obvious only in very old mice (≥18 months).

Innate immune response is critical to curb various infectious diseases. Aguilar-Delfin showed that innate immunity is crucial for determining the fate of *Babesia* infection and development of resistance to babesiosis in mice (83). Since the spleen is a major reservoir of undifferentiated, immature monocytes in mice that can mature into macrophages and dendritic cells *in vitro* (84), it is conceivable that infection of mice with *B. microti* could result in development of these cells *in vivo* into macrophages, which then facilitate clearance of the infected erythrocytes. Indeed, IFN-γ stimulated macrophages have been considered critical for inhibiting growth of *B. microti* and for offering cross-protection against *B. rodhaini* in mice (85, 86). Depletion of macrophages at different stages of infection using drugs resulted in a significant increase in *B. microti* parasitemia and even led to mortality in mice (87). Furthermore, *in vivo* depletion of NK cells did not significantly impair protection against *Babesia* species in mice, indicting their minor role in conferring resistance to this protozoan (86) further emphasizing the importance of splenic macrophages in clearance of *Babesia* infected erythrocytes.

TABLE 3 | Histopathological scoring of joints of mice at acute phase of infection.

Experimental groups	Knee			Tibiotarsus				
Score	–	±	+	–	±	+	++	+++
Young–N40	1	2	2	0	0	1	4	0
Old–N40	0	3	1	0	1	1	2	0
Young–N40+Bm	1	0	4	0	0	0	3	2
Old–N40+Bm	2	1	2	0	0	3	2	0
Young–Bm	5	0	0	5	0	0	0	0

To better understand the immunological responses during acute phase of infection, we conducted both FACS analyses and *in vitro* stimulation of splenic leukocytes (CD45 labeled) mixture excluding FcR+ cells (**Figures 3**, **5**, **6**). An increase in levels of innate and Th1-associated cytokines and chemokines, IFN-γ, IL-8, IL-6, and TNF-α has recently been reported in Lyme disease patients (88, 89). A positive association of type I, and III IFN with Lyme arthritis in humans and production of IFN-γ and IL-23 in response to *B. burgdorferi* infection in animal model

systems has also been reported previously (90, 91). IFN-γ is also produced in response to *B. microti* infection by activated T cells that help in killing ingested pathogens by activated macrophage (92). Our results support the reported critical role of cell-mediated immunity and Type 1 cytokine response, although it may not always be sufficient in generating protective immunity for controlling intracellular protozoan pathogens (93–98). A comparison of persisting symptoms reported in humans with coinfections, such as fatigue, in which Th1 response may contribute, cannot be determined in mice to fully appreciate the consequence of concurrent infection on overall disease manifestations. We observed more prominent Th2 response in older mice. Th2 response has been known to exacerbate diseases by some protozoan pathogens and could contribute to sustenance of *B. microti* in old hosts reported previously (59, 99). Higher levels of IL-4 production in the young mice at acute phase could lead to significant stimulation of B cells and antibody production later in infection that is critical for *B. burgdorferi* clearance.

Th17 cells play an important role in inflammation as well as clearance of extracellular pathogens, including Borreliae, while they counteract the action of Tregs that prevent excessive inflammatory response caused by Th17 cells (100). Although a high level of regulatory cytokine IL-10 producing CD4+ cells were detected in both young and old mice, the cytokine was associated with Th2 cells in old and Tregs in young mice. A significant Tregs/Th17 ratio was observed during the acute phase of infection by both *B. burgdorferi* and *B. microti* individually or together in young mice. No death associated with babesiosis was observed unlike that by highly infectious WA-1 strain of *Babesia* during acute phase of infection in mice and hamsters (101–103). Mice fatality by WA-1 infection was reported to be associated with prolific pro-inflammatory response including intravascular aggregation of large mononuclear inflammatory cells and multifocal coagulative necrosis in various organs (101–103). Although we cannot determine the molecular mechanism involved, a higher Tregs/Th17 ratio in coinfected mice as compared to *B. microti* infected young mice at acute phase of infection (**Table 2**) could play a role in significantly lower peak parasitemia observed in coinfected young mice (data not shown). High levels of Tregs were also found to be associated with milder, nonlethal malaria with *Plasmodium yoelii* infection in mice, as compared to low levels of Treg cells observed during disease by the lethal strain of *P. berghei* ANKA strain (104). Higher numbers of IL-10 producing CD4+ cells (**Figure 4**) together with increased Treg cell numbers supports participation of these immune responses in suppression of excessive inflammation during simultaneous infection by *B. burgdorferi* and *B. microti* in C3H mice. Thus, despite development of high parasitemia levels by *B. microti*, combined anti-inflammatory response promoted by IL-10 and Tregs could partially explain why this infection does not result in death of mice unlike infection with *Babesia* strain WA-1, which displays fatal outcomes that showed association with the high levels of IFN-γ and TNF-α production in spleen and lungs, heavy intravascular hemolysis, and multiorgan failure (101–103).

Our results here agree with the previous report that mainly young C3H mice, but not old, show more pronounced

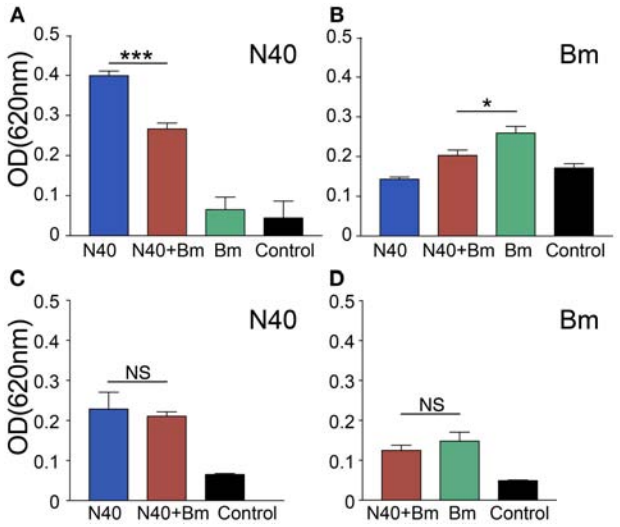

FIGURE 8 | Determination of the specific antibody response in young and old mice at 3 weeks of infection. **(A–C)** N40 protein extract probed with pooled plasma of either young **(A)**, or old **(C)** from each group of infected mice by ELISA indicated a significant reduction in the specific antibodies in plasma of only young coinfected mice with no reactivity observed with plasma from *B. microti* (Bm) infected mice. **(B–D)** Bm protein extract probed with pooled mice plasma from young **(B)**, or old **(D)** mice by ELISA showed that Bm-specific antibodies reduced significantly but moderately in coinfected mice only in young mice. Each bar represents the mean ± s.d. (*$p < 0.05$, ***$p < 0.001$).

inflammatory Lyme arthritis manifestations (51) indicating inherent development of resistance to Lyme disease in older mice. Unlike previously reported independent courses of infection by *B. burgdorferi* and *B. microti* in young C3H mice (49), we observed a major influence of *B. microti* infection on increased survival and tissue colonization by *B. burgdorferi*. Significant increase in joint colonization by *B. burgdorferi* in coinfected mice resulting in inflammatory Lyme arthritis even at acute phase indicates consequence of *B. microti* infection on increased *B. burgdorferi* survival and adverse effect on severity of inflammatory Lyme disease. B cells play a role as professional antigen presenting cells, display regulatory function through cytokine production and play a critical role in humoral immunity by producing protective antibodies. Based upon the infecting pathogen, subversion of different B-cell subsets during parasitic and viral infections has been summarized recently (105). In many protozoan diseases, specific B-cell responses against parasites were delayed or abrogated due to B cell apoptosis and their depletion in spleen (72, 106). Antibodies play an important role in clearance of *B. burgdorferi* by encompassing different effector mechanisms, such as complement activation, neutralization and opsonization that results in phagocytosis facilitated by interaction of the Fc-region of antibodies and Fc-receptors on the professional phagocytes (107). Immunoglobulin levels are elevated in response to *B. burgdorferi* infection and after antibodies maturation, they persist for long periods of time (108). We found reduction in antibody response against both *B. burgdorferi* and *B. microti* only in young coinfected

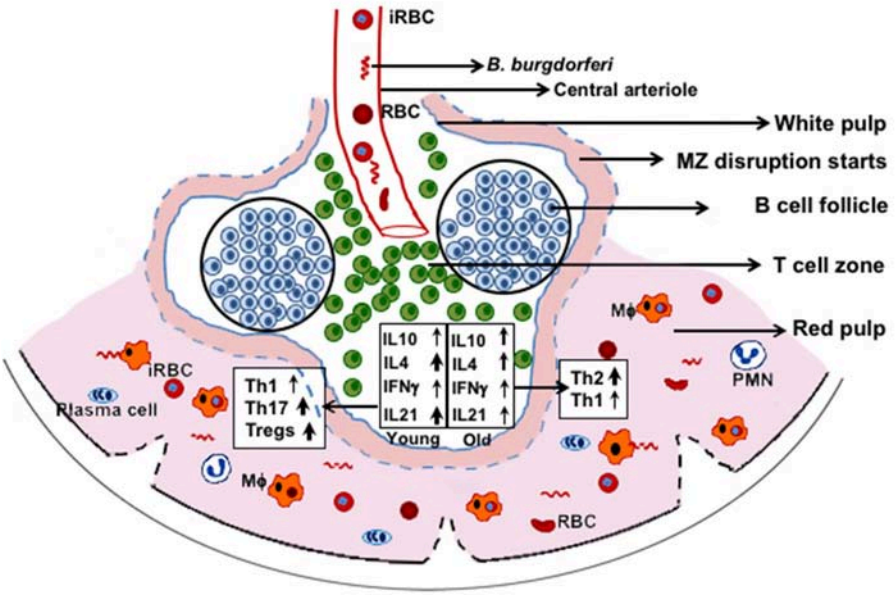

FIGURE 9 | C3H mice splenic immune response at acute phase of coinfection with *B. microti* and *B. burgdorferi*. RBCs and *B. microti* infected RBCs (iRBC) together with *B. burgdorferi* from blood are released in spleen. These pathogens then trigger a differential immune response with more pronounced induction of Th17 cells and Tregs in young mice and significantly higher Th2 cells in the older mice. Disruption of marginal zone (MZ) and atrophy of B cells are also stimulated by *B. microti* such that fewer B cells develop into plasma cells resulting in lower antibody production against both pathogens. Splenic macrophages (Mϕ) are the major player in clearance of both pathogens but because of hematopoiesis and phagocytosis of iRBCs, fewer of them are available for clearance of *B. burgdorferi*, causing better survival of these spirochetes.

mice relative to those infected with each pathogen separately. Antibody reduction was most pronounced in coinfected young mice relative to N40 infected mice (**Figure 8**). This reduction could result in better survival of *B. burgdorferi* even at later stages of infection causing increase in inflammatory Lyme disease.

CONCLUSIONS

In our studies, the adverse effect of infection with N40 on *B. microti* was subtle, but we consistently observed diminished parasitemia in coinfected young C3H mice. Th2 polarization at acute phase of infection could play a more effective role in preventing Lyme disease symptoms in coinfected older mice, even at the acute phase of infection. Conversely, despite high Tregs/Th17 ratio and moderate Th1 response in spleens of coinfected young mice, inflammatory arthritis is observed, suggesting that tissue specific colonization by *B. burgdorferi* triggers different immune responses. Based upon these results and our observation of complete disruption of marginal zone of spleen after parasitemia resolution (53), we propose that both marginal zone disruption and B cell atrophy starts at the acute phase of coinfection (**Figure 9**) while *B. microti* infection ultimately results in reduction in splenic B cells and pathogens specific antibody production. Furthermore, phagocytosis of infected RBCs and hematopoiesis in the red pulp region may overwhelm macrophages, making them less available for Lyme spirochetes phagocytosis. Thus, each pathogen affects disease severity by the other microbe directly, or indirectly by influencing the host immune response with a more pronounced effect seen in the young mice. Despite some differences observed in severity of diseases in mice and humans during coinfection with *B. burgdorferi* and *B. microti,* our results indicate that a thorough understanding of these coinfections can be obtained by study of pathogenesis and immunity at different stages of infection using the susceptible animal model system(s).

DATA AVAILABILITY STATEMENT

All data are fully available without restriction.

AUTHOR CONTRIBUTIONS

The first 3 authors contributed equally to this work. NP conceived the study while VD and SP designed and carried out all animal experiments. VD analyzed and interpreted FACS data, LA carried out all parasitemia determinations and ELISA and SP and MC prepared and analyzed samples as relevant to Lyme spirochetes. All authors read and approved the manuscript before submission.

FUNDING

National Institutes of Health (R01AI089921) and New Jersey Health Foundation grants to NP supported this study.

ACKNOWLEDGMENTS

We acknowledge valuable assistance provided by the technical Director, Sukhwinder Singh of Flow cytometry core laboratory of Rutgers New Jersey Medical School. We also greatly appreciate assistance by Luke Fritzky and Joel Pierre in organ samples preparation, sectioning, and H & E staining for the histopathological examination.

REFERENCES

1. Cox FE. Concomitant infections, parasites and immune responses. *Parasitology* (2001) 122:S23–38. doi: 10.1017/S003118200001698X
2. Diuk-Wasser MA,Vannier E, Krause PJ. Coinfection by *Ixodes* tick-borne pathogens: ecological, epidemiological, and clinical consequences. *Trends Parasitol.* (2016) 32l:30–42. doi: 10.1016/j.pt.2015.09.008
3. Knapp KL, Rice NA. Human coinfection with *Borrelia burgdorferi* and *Babesia microti* in the United States. *J Parasitol Res.* (2015) 2015:587131. doi: 10.1155/2015/587131
4. Rizzoli A, Silaghi C, Obiegala A, Rudolf I, Hubalek Z, Foldvari G, et al. *Ixodes ricinus* and Its transmitted pathogens in urban and peri-urban areas in Europe: new hazards and relevance for public health. *Front Public Health* (2014) 2:251. doi: 10.3389/fpubh.2014.00251
5. Dunn JM, Krause PJ, Davis S, Vannier EG, Fitzpatrick MC, Rollend L, et al. *Borrelia burgdorferi* promotes the establishment of *Babesia microti* in the northeastern United States. *PLoS ONE* (2014) 9:e115494. doi: 10.1371/journal.pone.0115494
6. Moutailler S, Valiente Moro C, Vaumourin E, Michelet L, Tran FH,Devillers E, et al. Co-infection of ticks: the rule rather than the exception. *PLoS Negl Trop Dis.* (2016) 10:e0004539. doi: 10.1371/journal.pntd.0004539
7. Lommano E, Bertaiola L, Dupasquier C, Gern L. Infections and coinfections of questing *Ixodes ricinus* ticks by emerging zoonotic pathogens in Western Switzerland. *Appl Environ Microbiol.* (2012) 78:4606–12. doi: 10.1128/AEM.07961-11
8. Piesman J, Mather TN,Donahue JG,Levine J, Campbell JD,Karakashian SJ, et al. Comparative prevalence of *Babesia microti* and *Borrelia burgdorferi* in four populations of *Ixodes dammini* in eastern Massachusetts. *Acta Trop.* (1986) 43:263–70.
9. Hersh MH,Ostfeld RS,McHenry DJ,Tibbetts M, Brunner JL,Killilea ME,et al. Co-infection of blacklegged ticks with *Babesia microti* and *Borrelia burgdorferi* is higher than expected and acquired from small mammal hosts. *PLoS ONE* (2014) 9:e99348. doi: 10.1371/journal.pone.0099348
10. Schulze TL,Jordan RA,Healy SP, Roegner VE. Detection of *Babesia microti* and *Borrelia burgdorferi* in host-seeking *Ixodes scapularis* (Acari: Ixodidae) in Monmouth County, New Jersey. *J Med Entomol.* (2013) 50:379–83. doi: 10.1603/ME12088
11. Swanson SJ,Neitzel D, Reed KD, Belongia EA. Coinfections acquired from Ixodes ticks. *Clin Microbiol Rev.* (2006) 19:708–27. doi: 10.1128/CMR.00011-06
12. Krause PJ, Spielman A, Telford SR 3rd, Sikand VK, McKay K, Christianson D, et al. Persistent parasitemia after acute babesiosis. *N Engl J Med.* (1998) 339:160–5. doi: 10.1056/NEJM199807163390304
13. Krause PJ, Gewurz BE, Hill D, Marty FM, Vannier E, Foppa IM, et al. Persistent and relapsing babesiosis in immunocompromised patients. *Clin Infect Dis.* (2008) 46:370–6. doi: 10.1086/525852
14. Herwaldt BL, Linden JV, Bosserman E, Young C, Olkowska D, Wilson M. Transfusion-associated babesiosis in the United States: a description of cases. *Ann Int Med.* (2011) 155:509–19. doi: 10.7326/0003-4819-155-8-201110180-00362
15. Ruebush TK 2nd, Collins WE, Warren M. Experimental *Babesia microti* infections in *Macaca mulatta*: recurrent parasitemia before and after splenectomy. *Am J Trop Med Hyg.* (1981) 30:304–7. doi: 10.4269/ajtmh.1981.30.304
16. Wormser GP, Lombardo G, Silverblatt F, El Khoury MY, Prasad A, Yelon JA, et al. Babesiosis as a cause of fever in patients undergoing a splenectomy. *Am Surg.* (2011) 77:345–7.
17. Wudhikarn K, Perry EH, Kemperman M, Jensen KA, Kline SE. Transfusion-transmitted babesiosis in an immunocompromised patient: a case report and review. *Am J Med.* (2011) 124:800–5. doi: 10.1016/j.amjmed.2011.03.009
18. Homer MJ,Aguilar-Delfin I, Telford SR 3rd, Krause PJ, Persing DH. Babesiosis. *Clin Microbiol Rev.* (2000) 13:451–69. doi: 10.1128/CMR.13.3.451
19. White DJ, Talarico J, Chang HG, Birkhead GS, Heimberger T, Morse DL. Human babesiosis in New York State: review of 139 hospitalized cases and analysis of prognostic factors. *Arch Intern Med.* (1998) 158:2149–54. doi: 10.1001/archinte.158.19.2149
20. Shaw AC, Joshi S, Greenwood H, Panda A, Lord JM. Aging of the innate immune system. *Curr Opin Immunol.* (2010) 22:507–13. doi: 10.1016/j.coi.2010.05.003
21. Aguilar-Delfin I, Wettstein PJ, Persing DH. Resistance to acute babesiosis is associated with interleukin-12- and gamma interferon-mediated responses and requires macrophages and natural killer cells. *Infect Immun.* (2003) 71:2002–8. doi: 10.1128/IAI.71.4.2002-2008.2003
22. Beerman I, Bhattacharya D, Zandi S, Sigvardsson M, Weissman IL,Bryder D, et al. Functionally distinct hematopoietic stem cells modulate hematopoietic lineage potential during aging by a mechanism of clonal expansion. *Proc Natl Acad Sci USA.* (2010) 107:5465–70. doi: 10.1073/pnas.1000834107
23. Beerman I, Maloney WJ,Weissmann IL, Rossi DJ. Stem cells and the aging hematopoietic system. *Curr Opin Immunol.* (2010) 22:500–6. doi: 10.1016/j.coi.2010.06.007
24. Wenisch C, Patruta S, Daxbock F, Krause R, Horl W. Effect of age on human neutrophil function. *J Leukoc Biol.* (2000) 67:40–5. doi: 10.1002/jlb.67.1.40
25. Agius E, Lacy KE,Vukmanovic-Stejic M, Jagger AL, Papageorgiou AP, Hall S, et al. Decreased TNF-alpha synthesis by macrophages restricts cutaneous immunosurveillance by memory CD4+ T cells during aging. *J Exp Med.* (2009) 206:1929–40. doi: 10.1084/jem.20090896
26. Akoolo L, Schlachter S, Khan R, Alter L, Rojtman AD, Gedroic K, et al. A novel quantitative PCR detects *Babesia* infection in patients not identified by currently available non-nucleic acid amplification tests. *BMC Microbiol.* (2017) 17:16. doi: 10.1186/s12866-017-0929-2
27. Martinez-Balzano C, Hess M, Malhotra A, Lenox R. Severe babesiosis and *Borrelia burgdorferi* co-infection. *QJM* (2015) 108:141–3. doi: 10.1093/qjmed/hcs100
28. Krause PJ, Telford SR 3rd, Spielman A, Sikand V, Ryan R, Christianson D, et al. Concurrent Lyme disease and babesiosis. Evidence for increased severity and duration of illness. *JAMA* (1996) 275:1657–60. doi: 10.1001/jama.1996.03530450047031
29. Krause PJ, McKay K, Gadbaw J, Christianson D, Closter L, Lepore T, et al. Increasing health burden of human babesiosis in endemic sites. *Am J Trop Med Hygiene* (2003) 68:431–6. doi: 10.4269/ajtmh.2003.68.431
30. Krause PJ, McKay K, Thompson CA, Sikand VK, Lentz R, Lepore T, et al. Disease-specific diagnosis of coinfecting tickborne zoonoses: babesiosis, human granulocytic ehrlichiosis, and Lyme disease. *Clin Infect Dis.* (2002) 34:1184–91. doi: 10.1086/339813
31. Shapiro ED, Baker PJ, Wormser GP. False and misleading information about Lyme disease. *Am J Med.* (2017) 130:771–2. doi: 10.1016/j.amjmed.2017.01.030
32. Keane-Myers A, Nickell SP. Role of IL-4 and IFN-gamma in modulation of immunity to *Borrelia burgdorferi* in mice. *J Immunol.* (1995) 155:2020–8.
33. Anguita J, Persing DH, Rincon M, Barthold SW, Fikrig E. Effect of anti-interleukin 12 treatment on murine lyme borreliosis. *J Clin Invest.* (1996) 97:1028–34. doi: 10.1172/JCI118494
34. Zeidner N, Mbow ML, Dolan M, Massung R, Baca E, Piesman J. Effects of *Ixodes scapularis* and *Borrelia burgdorferi* on modulation of the host immune response: induction of a TH2 cytokine response in Lyme disease-susceptible (C3H/HeJ) mice but not in disease-resistant (BALB/c) mice. *Infect Immun.* (1997) 65:3100–6.
35. Kang I, Barthold SW, Persing DH, Bockenstedt LK. T-helper-cell cytokines in the early evolution of murine Lyme arthritis. *Infect Immun.* (1997) 65:3107–11.

36. Glickstein L, Edelstein M, Dong JZ. Gamma interferon is not required for arthritis resistance in the murine Lyme disease model. *Infect Immun.* (2001) 69:3737–43. doi: 10.1128/IAI.69.6.3737-3743.2001
37. Infante-Duarte C, Horton HF, Byrne MC, Kamradt T. Microbial lipopeptides induce the production of IL-17 in Th cells. *J Immunol.* (2000) 165:6107–15. doi: 10.4049/jimmunol.165.11.6107
38. Hu LT, Klempner MS. Host-pathogen interactions in the immunopathogenesis of Lyme disease. *J Clin Immunol.* (1997) 17:354–65. doi: 10.1023/A:1027308122565
39. Basso B. Modulation of immune response in experimental Chagas disease. *World J Exp Med.* (2013) 3:1–10. doi: 10.5493/wjem.v3.i1.1
40. Dunay IR, Damatta RA, Fux B, Presti R, Greco S, Colonna M, et al. Gr1(+) inflammatory monocytes are required for mucosal resistance to the pathogen *Toxoplasma gondii*. *Immunity* (2008) 29:306–17. doi: 10.1016/j.immuni.2008.05.019
41. Hunter CA, Sibley LD. Modulation of innate immunity by *Toxoplasma gondii* virulence effectors. *Nat Rev Microbiol.* (2012) 10:766–78. doi: 10.1038/nrmicro2858
42. Pifer R, Yarovinsky F. Innate responses to *Toxoplasma gondii* in mice and humans. *Trends Parasitol.* (2011) 27:388–93. doi: 10.1016/j.pt.2011.03.009
43. Magez S, Caljon G. Mouse models for pathogenic African trypanosomes: unravelling the immunology of host-parasite-vector interactions. *Parasite Immunol.* (2011) 33:423–9. doi: 10.1111/j.1365-3024.2011.01293.x
44. Liese J, Schleicher U, Bogdan C. The innate immune response against *Leishmania* parasites. *Immunobiology* (2008) 213:377–87. doi: 10.1016/j.imbio.2007.12.005
45. Niikura M, Inoue S, Kobayashi F. Role of interleukin-10 in malaria: focusing on coinfection with lethal and nonlethal murine malaria parasites. *J Biomed Biotechnol.* (2011) 2011:383962. doi: 10.1155/2011/383962
46. Stevenson MM, Tam MF, Wolf SF, Sher A. IL-12-induced protection against blood-stage *Plasmodium chabaudi* AS requires IFN-gamma and TNF-alpha and occurs via a nitric oxide-dependent mechanism. *J Immunol.* (1995) 155:2545–56.
47. Skariah S, Arnaboldi P, Dattwyler RJ, Sultan AA, Gaylets C, Walwyn O, et al. Elimination of *Babesia microti* is dependent on intraerythrocytic killing and CD4+ T cells. *J Immunol.* (2017) 199:633–42. doi: 10.4049/jimmunol.1601193
48. Moro MH, Zegarra-Moro OL, Bjornsson J, Hofmeister EK, Bruinsma E, Germer JJ, et al. Increased arthritis severity in mice coinfected with *Borrelia burgdorferi* and *Babesia microti*. *J Infect Dis.* (2002) 186:428–31. doi: 10.1086/341452
49. Coleman JL, LeVine D, Thill C, Kuhlow C, Benach JL. *Babesia microti* and *Borrelia burgdorferi* follow independent courses of infection in mice. *J Infect Dis.* (2005) 192:1634–41. doi: 10.1086/496891
50. Armstrong AL, Barthold SW, Persing DH, Beck DS. Carditis in Lyme disease susceptible and resistant strains of laboratory mice infected with *Borrelia burgdorferi*. *Am J Trop Med Hyg.* (1992) 47:249–58. doi: 10.4269/ajtmh.1992.47.249
51. Barthold SW, Beck DS, Hansen GM, Terwilliger GA, Moody KD. Lyme borreliosis in selected strains and ages of laboratory mice. *J Infect Dis.* (1990) 162:133–8. doi: 10.1093/infdis/162.1.133
52. Garcia LS, Bullock-Iacullo SL, Fritsche TR, Grady KK, Healy GR, Palmer J, et al. *Laboratory Diagnosis of Blood-borne Parasitic Diseases; Approved Guideline*. Clinical and Laboratory Standards Institute (2000) p. 1–36.
53. Djokic V, Akoolo L, Parveen N. *Babesia microti* infection changes host spleen architecture and is cleared by a Th1 immune response. *Front Microbiol.* (2018) 9:85. doi: 10.3389/fmicb.2018.00085
54. Chan K, Alter L, Barthold SW, Parveen N. Disruption of *bbe02* by insertion of a luciferase gene increases transformation efficiency of *Borrelia burgdorferi* and allows live imaging in Lyme disease susceptible C3H mice *PLoS ONE* (2015) 10:e0129532. doi: 10.1371/journal.pone.0129532
55. Chan K, Casjens S, Parveen N. Detection of established virulence genes and plasmids to differentiate *Borrelia burgdorferi* strains. *Infection Immunity* (2012) 80:1519–29. doi: 10.1128/IAI.06326-11
56. Sasaki M, Fujii Y, Iwamoto M, Ikadai H. Effect of sex steroids on *Babesia microti* infection in mice. *Am J Trop Med Hyg.* (2013) 88:367–75. doi: 10.4269/ajtmh.2012.12-0338
57. Chan K, Marras SA, Parveen N. Sensitive multiplex PCR assay to differentiate Lyme spirochetes and emerging pathogens *Anaplasma phagocytophilum* and *Babesia microti*. *BMC Microbiol.* (2013) 13:295. doi: 10.1186/1471-2180-13-295
58. Takai T, Li M, Sylvestre D, Clynes R, Ravetch JV. FcR gamma chain deletion results in pleiotrophic effector cell defects. *Cell* (1994) 76:519–29. doi: 10.1016/0092-8674(94)90115-5
59. Vannier E, Borggraefe I, Telford SR 3rd, Menon S, Brauns T, Spielman A, et al. Age-associated decline in resistance to *Babesia microti* is genetically determined. *J Infect Dis.* (2004) 189:1721–8. doi: 10.1086/382965
60. Habicht GS, Benach JL, Leichtling KD, Gocinski BL, Coleman JL. The effect of age on the infection and immunoresponsiveness of mice to *Babesia microti*. *Mech Ageing Dev.* (1983) 23:357–69. doi: 10.1016/0047-6374(83)90036-2
61. Wong CH, Jenne CN, Petri B, Chrobok NL, Kubes P. Nucleation of platelets with blood-borne pathogens on Kupffer cells precedes other innate immunity and contributes to bacterial clearance. *Nat Immunol.* (2013) 14:785–92. doi: 10.1038/ni.2631
62. Cousens LP, Wing EJ. Innate defenses in the liver during Listeria infection. *Immunol Rev.* (2000) 174:150–9. doi: 10.1034/j.1600-0528.2002.017407.x
63. Igarashi I, Suzuki R, Waki S, Tagawa Y, Seng S, Tum S, et al. Roles of CD4(+) T cells and gamma interferon in protective immunity against *Babesia microti* infection in mice. *Infect Immun.* (1999) 67:4143–8.
64. Pachner AR, Itano A. *Borrelia burgdorferi* infection of the brain: characterization of the organism and response to antibiotics and immune sera in the mouse model. *Neurology* (1990) 40:1535–40. doi: 10.1212/WNL.40.10.1535
65. Pachner AR, Ricalton N, Delaney E. Comparison of polymerase chain reaction with culture and serology for diagnosis of murine experimental Lyme borreliosis. *J Clin Microbiol.* (1993) 31:208–14.
66. Barthold SW, Sidman CL, Smith AL. Lyme borreliosis in genetically resistant and susceptible mice with severe combined immunodeficiency. *Am J Trop Med Hygiene* (1992) 47:605–13. doi: 10.4269/ajtmh.1992.47.605
67. Dkhil MA, Al-Quraishy S, Abdel-Baki AS. Hepatic tissue damage induced in *Meriones ungliculatus* due to infection with *Babesia divergens*-infected erythrocytes. *Saudi J Biol Sci.* (2010) 17:129–32. doi: 10.1016/j.sjbs.2010.02.005
68. Hatcher JC, Greenberg PD, Antique J, Jimenez-Lucho VE. Severe babesiosis in Long Island: review of 34 cases and their complications. *Clin Infect Dis.* (2001) 32:1117–25. doi: 10.1086/319742
69. Joseph JT, Roy SS, Shams N, Visintainer P, Nadelman RB, Hosur S, et al. Babesiosis in lower hudson valley, New york, USA. *Emerg Infect Dis.* (2011) 17:843–7. doi: 10.3201/eid1705.101334
70. Oz HS, Hughes WT. Acute fulminating babesiosis in hamsters infected with Babesia microti. *Int J Parasitol.* (1996) 26:667–70. doi: 10.1016/0020-7519(96)00022-7
71. Semel ME, Tavakkolizadeh A, Gates JD. Babesiosis in the immediate postoperative period after splenectomy for trauma. *Surg Infect.* (2009) 10:553–6. doi: 10.1089/sur.2008.001
72. Obishakin E, de Trez C, Magez S. Chronic *Trypanosoma congolense* infections in mice cause a sustained disruption of the B-cell homeostasis in the bone marrow and spleen. *Parasite Immunol.* (2014) 36:187–98. doi: 10.1111/pim.12099
73. Buffet PA, Safeukui I, Deplaine G, Brousse V, Prendki V, Thellier M, Turner GD,and Mercereau-Puijalon O. The pathogenesis of *Plasmodium falciparum* malaria in humans: insights from splenic physiology. *Blood* (2011) 117:381–92. doi: 10.1182/blood-2010-04-202911
74. Weiss L, Geduldig U, Weidanz W. Mechanisms of splenic control of murine malaria: reticular cell activation and the development of a blood-spleen barrier. *Am J Anat.* (1986) 176:251–85. doi: 10.1002/aja.1001760303
75. Dumic I, Patel J, Hart M, Niendorf ER, Martin S, Ramanan P. Splenic rupture as the first manifestation of *Babesia Microti* infection: report of a case and review of literature. *Am J Case Rep.* (2018) 19:335–41. doi: 10.12659/AJCR.908453
76. Imbert P, Rapp C, Buffet PA. Pathological rupture of the spleen in malaria: analysis of 55 cases (1958-2008). (2009) *Travel Med Infect Dis.* 7:147–59. doi: 10.1016/j.tmaid.2009.01.002

77. Wilson S, Vennervald BJ, Dunne DW. Chronic hepatosplenomegaly in African school children: a common but neglected morbidity associated with schistosomiasis and malaria. *PLoS Negl Trop Dis.* (2011) 5:e1149. doi: 10.1371/journal.pntd.0001149
78. Kuna A, Gajewski M, Szostakowska B, Nahorski WL,Myjak P, Stanczak J. Imported malaria in the material of the institute of maritime and tropical medicine: a review of 82 patients in the years 2002-2014. *Biomed Res Int.* (2015) 2015:941647. doi: 10.1155/2015/941647
79. Kafetzis DA. An overview of paediatric leishmaniasis. *J Postgrad Med.* (2003) 49:31–8. doi: 10.4103/0022-3859.930
80. Raffalli J, Wormser GP. Persistence of babesiosis for >2 years in a patient on rituximab for rheumatoid arthritis. *Diagn Microbiol Infect Dis.* (2016) 85:231–2. doi: 10.1016/j.diagmicrobio.2016.02.016
81. Dkhil MA, Abdel-Baki AS, Al-Quraishy S, Abdel-Moneim AE. Hepatic oxidative stress in Mongolian gerbils experimentally infected with *Babesia divergens*. *Ticks Tick Borne Dis.* (2013) 4:346–51. doi: 10.1016/j.ttbdis.2013.01.002
82. Okla H, Jasik KP, Slodki J, Rozwadowska B, Slodki A, Jurzak M, et al. Hepatic tissue changes in rats due to chronic invasion of *Babesia microti*. *Folia Biol.* (2014) 62:353–9. doi: 10.3409/fb62_4.353
83. Aguilar-Delfin I, Homer MJ, Wettstein PJ, Persing DH. Innate resistance to *Babesia* infection is influenced by genetic background and gender. *Infect Immun.* (2001) 69:7955–8. doi: 10.1128/IAI.69.12.7955-7958.2001
84. Swirski FK, Nahrendorf M, Etzrodt M, Wildgruber M, Cortez-Retamozo V, Panizzi P, et al. Identification of splenic reservoir monocytes and their deployment to inflammatory sites. *Science* (2009) 325:612–6. doi: 10.1126/science.1175202
85. Chen D, Copeman DB, Hutchinson GW, Burnell J. Inhibition of growth of cultured *Babesia microti* by serum and macrophages in the presence or absence of T cells. *Parasitol Int.* (2000) 48:223–31. doi: 10.1016/S1383-5769(99)00022-7
86. Li Y, Terkawi MA, Nishikawa Y, Aboge GO, Luo Y, Ooka H, et al. Macrophages are critical for cross-protective immunity conferred by *Babesia microti* against *Babesia rodhaini* infection in mice. *Infect Immun.* (2012) 80:311–20. doi: 10.1128/IAI.05900-11
87. Terkawi MA, Cao S, Herbas MS, Nishimura M, Li Y, Moumouni PF, et al. Macrophages are the determinant of resistance to and outcome of nonlethal *Babesia microti* infection in mice. *Infect Immun.* (2015) 83:8–16. doi: 10.1128/IAI.02128-14
88. Strle K, Sulka KB, Pianta A, Crowley JT, Arvikar SL, Anselmo A, et al. T-Helper 17 cell cytokine responses in Lyme disease correlate with *Borrelia burgdorferi* antibodies during early infection and with autoantibodies late in the illness in patients with antibiotic-refractory Lyme arthritis. *Clin Infect Dis.* (2017) 64:930–8. doi: 10.1093/cid/cix002
89. Fallahi P, Elia G, Bonatti A. Interferon-gamma-induced protein 10 in Lyme disease. *Clin Ter.* (2017) 168:e146–50. doi: 10.7417/CT.2017.1997
90. Bachmann M, Horn K, Rudloff I, Goren I, Holdener M, Christen U, et al. Early production of IL-22 but not IL-17 by peripheral blood mononuclear cells exposed to live *Borrelia burgdorferi*: the role of monocytes and interleukin-1. *PLoS Pathog.* (2010) 6:e1001144. doi: 10.1371/journal.ppat.1001144
91. Love AC, Schwartz I, Petzke MM. *Borrelia burgdorferi* RNA induces type I and III interferons via Toll-like receptor 7 and contributes to production of NF-kappaB-dependent cytokines. *Infect Immun.* (2014) 82:2405–16. doi: 10.1128/IAI.01617-14
92. Vannier E, Krause PJ. Human babesiosis. *N Engl J Med.* (2012) 366:2397–407. doi: 10.1056/NEJMra1202018
93. Sher A, Reis e Sousa C. Ignition of the type 1 response to intracellular infection by dendritic cell-derived interleukin-12. *Eur Cytokine Netw.* (1998) 9(3 Suppl):65–8.
94. Park AY, Scott P. Il-12: keeping cell-mediated immunity alive. *Scand J Immunol.* (2001) 53:529–32. doi: 10.1046/j.1365-3083.2001.00917.x
95. Moll H, Berberich C. Dendritic cell-based vaccination strategies: induction of protective immunity against leishmaniasis. *Immunobiology* (2001) 204:659–66. doi: 10.1078/0171-2985-00105
96. Rogers KA, DeKrey GK, Mbow ML, Gillespie RD, Brodskyn CI, Titus RG. Type 1 and type 2 responses to *Leishmania major*. *FEMS Microbiol Lett.* (2002) 209:1–7. doi: 10.1111/j.1574-6968.2002.tb11101.x
97. Rogers WO, Weiss WR, Kumar A, Aguiar JC, Tine JA, Gwadz R, et al. Protection of rhesus macaques against lethal *Plasmodium knowlesi* malaria by a heterologous DNA priming and poxvirus boosting immunization regimen. *Infect Immun.* (2002) 70:4329–35. doi: 10.1128/IAI.70.8.4329-4335.2002
98. Scott P. Development and regulation of cell-mediated immunity in experimental leishmaniasis. *Immunol Res.* (2003) 27:489–98. doi: 10.1385/IR:27:2-3:489
99. Ruebush TK 2nd, Juranek DD, Spielman A, Piesman J, Healy GR. Epidemiology of human babesiosis on Nantucket Island. *Am J Trop Med Hyg.* (1981) 30:937–41. doi: 10.4269/ajtmh.1981.30.937
100. Bettelli E, Korn T, Oukka M, Kuchroo VK. Induction and effector functions of T(H)17 cells. *Nature* (2008) 453:1051–7. doi: 10.1038/nature 07036
101. Dao AH, Eberhard ML. Pathology of acute fatal babesiosis in hamsters experimentally infected with the WA-1 strain of Babesia. *Lab Invest.* (1996) 74:853–9.
102. Hemmer RM, Ferrick DA, Conrad PA. Up-regulation of tumor necrosis factor-alpha and interferon-gamma expression in the spleen and lungs of mice infected with the human Babesia isolate WA1. *Parasitol Res.* (2000) 86:121–8. doi: 10.1007/s004360050021
103. Wozniak EJ, Lowenstine LJ, Hemmer R, Robinson T, Conrad PA. Comparative pathogenesis of human WA1 and *Babesia microti* isolates in a Syrian hamster model. *Lab Anim Sci.* (1996) 46:507–15.
104. Keswani T, Bhattacharyya A. Differential role of T regulatory and Th17 in Swiss mice infected with *Plasmodium berghei* ANKA and *Plasmodium yoelii*. *Exp Parasitol.* (2014) 141:82–92. doi: 10.1016/j.exppara.2014.03.003
105. Borhis G, Richard Y. Subversion of the B-cell compartment during parasitic, bacterial, and viral infections. *BMC Immunol.* (2015) 16:15. doi: 10.1186/s12865-015-0079-y
106. Radwanska M, Guirnalda P, De Trez C, Ryffel B, Black S, Magez S. Trypanosomiasis-induced B cell apoptosis results in loss of protective anti-parasite antibody responses and abolishment of vaccine-induced memory responses. *PLoS Pathog.* (2008) 4:e1000078. doi: 10.1371/journal.ppat.1000078
107. Connolly SE, Benach JL. The versatile roles of antibodies in Borrelia infections. *Nat Rev Microbiol.* (2005) 3:411–20. doi: 10.1038/nrmicro1149
108. Kalish RA, Kaplan RF, Taylor E, Jones-Woodward L, Workman K, Steere AC. Evaluation of study patients with Lyme disease 10-20-year follow-up. *J Infect Dis.* (2001) 183:453–60. doi: 10.1086/318082

Conflict of Interest Statement: The authors declare that the research was conducted in the absence of any commercial or financial relationships that could be construed as a potential conflict of interest.

frontiers in Immunology

ORIGINAL RESEARCH
published: 26 March 2019
doi: 10.3389/fimmu.2019.00560

Indole Treatment Alleviates Intestinal Tissue Damage Induced by Chicken Coccidiosis Through Activation of the Aryl Hydrocarbon Receptor

Woo H. Kim[1], *Hyun S. Lillehoj*[1]* *and Wongi Min*[2]

[1] *Animal Biosciences and Biotechnology Laboratory, U. S. Department of Agriculture, Beltsville Agricultural Research Center, ARS, Beltsville, MD, United States,* [2] *College of Veterinary Medicine and Institute of Animal Medicine, Gyeongsang National University, Jinju, South Korea*

Indoles, as the ligands of aryl hydrocarbon receptor (AhR), have been shown to possess immune-modulating property in terms of the balancing between regulatory T cells (Treg) and T helper 17 cells (Th17) activities. In the present study, we examined the effects of dietary indoles, 3,3′-diindolylmethane (DIM) and indole-3-carbinol (I3C), on $CD4^+$T cell population and functions in chickens. Furthermore, the effects of dietary DIM treatment on chicken coccidiosis caused by an apicomplexan parasite were investigated. Dietary treatment of healthy chickens with DIM and I3C induced increased $CD4^+CD25^+$ (Treg) cells and the mRNA expression of IL-10, while decreasing number of $CD4^+$IL-$17A^+$ (Th17) cells and Th17-related cytokines transcripts expression in the intestine. In addition, we explored the role of AhR in indole-treated splenic lymphocytes by using AhR antagonist and our results suggested that DIM is a ligand for chicken AhR. In chicken coccidiosis, treatment of DIM increased the ratio of Treg/Th17 cells and significantly reduced intestinal lesion although no significant changes in body weight and fecal oocyst production were noted compared to non-treated control group. These results indicate that DIM is likely to affect the ratios of Treg/Th17 reducing the level of local inflammatory response induced by *Eimeria* or facilitate repairing process of inflamed gut following *Eimeria* infection. The results described herein are thus consistent with the concept that AhR ligand modulates the T cell immunity through the alteration of Treg/Th17 cells with Treg dominance. To our knowledge, present study is the first scientific report showing the effects of dietary indole on T cell immunity in poultry species.

Keywords: indole, $CD4^+$ T cells, Treg cells, Th17 cells, chicken, coccidiosis

OPEN ACCESS

Edited by:
Jason Paul Gigley,
University of Wyoming, United States

Reviewed by:
Sharvan Sehrawat,
Indian Institute of Science Education and Research Mohali, India
Xinming Tang,
China Agricultural University, China
Berit Bangoura,
University of Wyoming, United States

***Correspondence:**
Hyun S. Lillehoj
hyun.lillehoj@ars.usda.gov

Specialty section:
This article was submitted to Microbial Immunology, a section of the journal Frontiers in Immunology

Received: *13 August 2018*
Accepted: *04 March 2019*
Published: *26 March 2019*

Citation:
Kim WH, Lillehoj HS and Min W (2019) Indole Treatment Alleviates Intestinal Tissue Damage Induced by Chicken Coccidiosis Through Activation of the Aryl Hydrocarbon Receptor. Front. Immunol. 10:560. doi: 10.3389/fimmu.2019.00560

INTRODUCTION

Coccidiosis which is caused by apicomplexan protozoan parasites of *Eimeria* spp. is one of the most economically important diseases affecting poultry production (1). After chickens ingest sporulated oocysts, sporozoites are released in the intestinal tract, invading intestinal epithelial cells for intracellular development. Invasion and egress of sporozoites and merozoites, which are, two major invasive form of *Eimeria* lead to the destruction of the intestinal mucosa, thus resulting in local inflammation in the intestine (2). In *E. tenella*-infected chickens, the number of $CD4^+$ lymphocytes in the intestine significantly increases (3). Early studies have shown that T lymphocytes and their cytokines are essential for immunity against *Eimeria* infection in chickens

(4, 5). *Eimeria* infection elicits strong IFN-γ-driven immune responses by T cells, and it plays a crucial role in control of coccidiosis (6). However, a growing body of literature implicates Th17- and Treg-related cytokines in host defense by the intestinal lymphocytes during *Eimeria* infection in chickens (7–10).

Indoles are phytochemicals that are very common in the body and diet and are abundant in Brassica (cruciferous) vegetables, including broccoli, Brussels sprouts, cabbage, and cauliflower (11). After ingestion, indole compounds such as 3,3′-diindolymethane (DIM) and indole-3-carbinol (I3C) are converted from glucosinolates, which are abundant in cruciferous vegetables (11). Both DIM and I3C are ligands for the aryl hydrocarbon receptor (AhR) and have been found to exhibit anti-inflammatory and anticancer properties through AhR activation (12, 13). AhR is a ligand-activated transcription factor recognizing a consensus xenobiotic responsive element binding site located in the upstream regulatory regions of target genes including cytochrome P450 family 1 members such as CYP1A1 and CYP1A2 (14–16). Recently, several studies have focused on activation of AhR by indoles in $CD4^+$ T cell immunity; interestingly, the findings have indicated different effects on the differentiation of T cell subsets, particularly regulatory T (Treg) and T helper 17 (Th17) cells, depending on the type of indole, although the underlying mechanism is not fully established (17–21). For example, 6-formylindolo[3,2-b]carbazole (FICZ), the tryptophan photoproduct containing two indole rings, specifically induces the differentiation of Th17 cells (21–23), whereas DIM and I3C promote the generation of Treg cells and the suppression of Th17 cells (17, 18). Treg and Th17 cells are relatively newly described lineages of $CD4^+$ T helper cells. Although Treg and Th17 cells share a common precursor cell (the naïve CD4 T cell) and require a common tumor growth factor (TGF)-β signal for initial differentiation, Treg cells play a role in the maintenance of T cell homeostasis and regulation of self-tolerance, whereas Th17 cells are involved in the inflammatory response by producing proinflammatory cytokines such as interleukin (IL)-17. The interplay or balance between Treg and Th17 cells is a major factor in inflammation (24).

The effects of indole compounds in chickens and the roles of Treg and Th17 cells in chicken coccidiosis have not been extensively studied. Given the ability of indoles to regulate the T cell immune response and the importance of T cell immunity in coccidiosis, in the present study, we investigated whether dietary indoles might regulate $CD4^+$ T cell immunity in chicken coccidiosis. We hypothesized that DIM and I3C administered orally would activate AhR in chicken and lead to Treg-dominance, thereby decreasing the intestinal inflammatory response and preventing tissue damage.

MATERIALS AND METHODS

Reagents and Antibodies

DIM (D9568, CAS no. 1968-05-04) and I3C (I7256, CAS no. 700-06-1) were purchased from Sigma (St. Louis, MO). Both DIM and I3C were suspended in DMSO (D2650, Sigma) for *in vitro* studies and diluted with corn oil purchased from a local market for *in vivo* studies. Concanavalin A (Con A, C5275), phorbol-12-myristate-13-acetate (PMA, P8139) ionomycin (I9657), and CH223191 (C8124) were purchased from Sigma. Antibodies (Abs) with the following specificities were used for flow cytometry: CD4-PE (CT-4), CD8-Alexa Fluor 700 (CT-8), CD3-Pacific blue (CT-3), and CD45-APC (LT40) (Southern Biotech, Birmingham, AL). The following antibodies were purified and conjugated in-house: CD25-FITC (#32) and IL-17A-FITC (1G8) (25, 26).

Chickens

Newly hatched broiler chickens (Ross/Ross) were purchased from Longnecker's Hatchery (Elizabethtown, PA) and housed in electrically heated battery starter cages (Petersime, Gettysburg, OH). All chickens were raised in starter cages until 14 days of age and transferred to finisher cages, where they were kept until they are sacrificed. Feed and water were provided *ad libitum* under coccidian-free conditions. We used 150 birds for *in vivo E. tenella* infection study and another 12 healthy birds were used for preparation of lymphocytes from spleen and cecal tonsil. Animal husbandry followed the guidelines for the care and use of animals in agricultural research. All experiments were approved and followed by the United States Department of Agriculture (USDA)-Agricultural Research Service Beltsville Institutional Animal Care and Use Committee (protocol number: 18-019).

Cell Culture

Chicken primary lymphocytes from cecal tonsils or spleen were isolated as previously described with modifications (8). Briefly, spleen and cecal tonsils were collected aseptically from healthy chicken and homogenized using gentleMACS Dissociator (Miltenyi Biotec, Gaithersburg, USA). The lymphocytes were purified by a Histopaque-1077(Sigma) density gradient method. Freshly purified primary lymphocytes from cecal tonsils or spleen were cultured in complete RPMI-1640 (GE Healthcare, Pittsburgh, PA) supplemented with 10% FBS (GE Healthcare), penicillin/streptomycin (10,000 unit/ml, Invitrogen, Carlsbad, CA), 50 μg/ml gentamycin (Sigma), 25 mM HEPES (Gibco, Gaithersburg, MD), and 55 μM 2-Mercaptoethanol (Gibco). For sporozoite viability test, chicken epithelial cell line (MM-CHiC clone, 8E11) was purchased and cultured in DMEM/F-12 (1:1, Sigma) supplemented with 2 mM L-glutamine (Sigma), 10 % FBS, and 10,000 unit/ml penicillin/streptomycin.

Parasite Propagation and Preparation of Sporozoite Antigen

To obtain sporulated *E. tenella* oocysts (ARS strain) for *in vivo* study, unsporulated were purified from the feces of infected chickens, and sporulation was conducted with incubation in 2.5% potassium dichromate solution for 48 h. Sporozoites of *E. tenella* were obtained by excystation of sporulated oocysts (27). Briefly, freshly sporulated oocysts were disrupted with 0.5-mm glass beads for 5–7 s by using a Mini-beadbeater (BioSpec Products, Bartlesville, OK). The released sporocysts were purified by isopycnic centrifugation in a Percoll gradient and washed in ice-cold Hank's balanced salt solution (HBSS, Sigma), and the excystation of sporozoites was induced by treatment with 0.25%

trypsin and 0.014 M taurocholic acid (Sigma) at 41°C for 90 min. The excysted sporozoites were collected, washed three times with HBSS at 3,000 × g for 10 min at 4°C and resuspended to 1.0 × 10^7/ml in HBSS. *E. tenella* sporozoite antigen (EtSzAg) was obtained through a series of sonication and freeze and thaw cycles followed by filtration with a 0.22 μm filter. The concentration was measured with a Pierce BCA Protein Assay kit (Thermo Fisher Scientific, Frederick, MD), and samples were stored at −80°C until use.

Intracellular Staining and Flow Cytometry

For the intracellular staining of IL-17A, lymphocytes were stimulated with PMA (10 ng/ml) and ionomycin (500 μg/ml) in complete RPMI-1640 for 4 h in the presence of golgiplug (1 μl/1 × 10^6 cells, BD, Franklin Lakes, NJ). Cells were analyzed with a Cytoflex flow cytometer (Beckman Coulter, Brea, CA). Lymphocytes from single-cell suspensions were identified according to their light scattering properties and the $CD45^+$ population. Potential doublet cells were discriminated by FSC-H/FSC-W, and dead cells were excluded by using Fixable Viability Stain 780 (BD). Treg cells and Th17 cells were designated as $CD45^+CD3^+CD4^+CD25^+$ and $CD45^+CD3^+CD4^+$IL-$17A^+$ cells, respectively. Unfortunately, foxp3, a signature transcription factor for Treg, has not been cloned in chickens; thus, we had to consider the $CD4^+CD25^+$ phenotype as being indicative of Treg cells (28, 29).

Quantitative Real-Time PCR

RNA was isolated from primary lymphocytes from the cecal tonsils or spleen by using an RNeasy Isolation Kit (Qiagen, Germantown, MD), per the manufacturer's instructions, then treated with RNase-free DNase (Qiagen) and eluted in RNase-free water (Qiagen). The concentration and purity of the RNA were measured using a NanoDrop spectrophotometer (Thermo Fisher Scientific). cDNA was synthesized using random hexamer primers and a QuantiTect Reverse Transcription Kit (Qiagen). Real-time RT-PCR was performed using a Stratagene Mx3000P thermocycler (Agilent Technologies, USA) with a QuantiTect SYBR Green PCR Kit (Qiagen) and the various chicken chemokine and cytokine primers listed in **Table 1**. A melting curve was obtained at the end of each run to verify the presence of a single amplification product without primer dimers. Standard curves were generated using serial five-fold dilutions of cDNA to validate the amplification efficiency. The fold changes in each transcript were normalized to β-actin and are reported relative to the transcript expression in the vehicle control group or non-infected group (normalized to 1), on the basis of the comparative ΔΔCt method, as previously described (27).

TABLE 1 | List of quantitative real-time RT-PCR primers used in this study.

Target	Primer and sequence	References
IL-10	(For) 5′-ACATCCAACTGCTCAGCTCT-3′	(30)
	(Rev) 5′-ATGCTCTGCTGATGACTGGT-3′	
IL-17A	(For) 5′-GAGAAGAGTGGTGGGAAAG-3′	(31)
	(Rev) 5′-TCTACAAACTTGTTTATCAGCAT-3′	
IL-17F	(For) 5′-TGAAGACTGCCTGAACCA-3-3′	(31)
	(Rev) 5′-AGAGACCGATTCCTGATGT-3′	
IL-21	(For) 5′-CAACTTCACCAAAAGCAATGAAAT-3′	(32)
	(Rev) 5′-ATCCATCCCCAGGGTTTTCT-3′	
IL-22	(For) 5′-TGTTGTTGCTGTTTCCCTCTTC-3′	(33)
	(Rev) 5′-CACCCCTGTCCCTTTTGGA-3′	
CYP1A4	(For) 5′-CCGTGACAACCGCCCTGTCC-3′	(34)
	(Rev) 5′-GAGTTCGGTGCCGGCTGCAT-3′	
CYP1A5	(For) 5′-GGACCGTTGCGTGTTTAT-3′	(35)
	(Rev) 5′-CTCCCACTTGCCTATGTTTT-3′	
IL-1β	(For) 5′-TGGGCATCAAGGGCTACA-3′	(31)
	(Rev) 5′-CGGCCCACGTAGTAAATGAT-3′	
IL-6	(For) 5′-CAAGGTGACGGAGGAGGAC-3′	(31)
	(Rev) 5′-TGGCGAGGAGGGATTTCT-3′	
CXCLi2	(For) 5′-GGCTTGCTAGGGGAAATGA-3′	(31)
	(Rev) 5′-AGCTGACTCTGACTAGGAAACTGT-3′	
TL1A	(For) 5′-CCTGAGTTATTCCAGCAACGCA-3′	(36)
	(Rev) 5′-ATCCACCAGCTTGATGTCACTAAC-3′	
JAM2	(For) 5′-AGCCTCAAATGGGATTGGATT-3′	(37)
	(Rev) 5′-CATCAACTTGCATTCGCTTCA-3′	
ZO1	(For) 5′-CCGCAGTCGTTCACGATCT-3′	(37)
	(Rev) 5′-GGAGAATGTCTGGAATGGTCTGA-3′	
β-actin	(For) 5′-CACAGATCATGTTTGAGACCTT-3′	(38)
	(Rev) 5′-CATCACAATACCAGTGGTACG-3′	

Eimeria tenella Infection Model

For *in vivo* study, One-hundred-fifty 1-day-old birds were randomly distributed into five groups ($n = 30$): non-infected control (NI), non-infected, DIM treated (NIDIM), *E. tenella*-infected (ET), *E. tenella*-infected, vehicle treated (ETVH), and *E. tenella*-infected, DIM treated (ETDIM). The schematic outline of *in vivo* study is shown in **Figure 4A**. The chickens in ET, ETVH and ETDIM groups were orally infected with *E. tenella* sporulated oocysts (1 × 10^4/bird) at 7 days old and the other groups were given HBSS as a control. The chickens in the NIDIM and ETDIM groups were treated every other day (starting at 5 days old) with DIM (200 mg/kg) and the other groups were given corn oil as a vehicle control by oral gavage until the end of experimental period (20 days old). Body weight gain (BWG) was measured at 0 and 13 days post infection (DPI) ($n = 15$). Cecal tissues were collected from four chickens of each group at 1, 4, 7, 10, and 13 days post infection (DPI) to extract RNA, and the expression of Treg- and Th17-related mRNAs was analyzed ($n = 4$). Five chickens from each group were randomly selected for gut lesion scoring in the cecum at 7 DPI ($n = 5$). Lesion scores were evaluated by three independent observers based on scoring techniques previously described (39). Each chicken received a numerical value from 0 to 4. Same cecal samples were used for histological examination ($n = 5$). Briefly, the tissues were fixed in 4% paraformaldehyde (Sigma), and paraffin blocks were prepared, microtome sections were made, and sections were stained using hematoxylin and eosin. The sections were examined for intestinal structure, parasites and infiltration of inflammatory cells using an Eclipse 80i microscope (Nikon, Japan). To count fecal *Eimeria* oocyst shedding, collection of feces from three cages of each group was started at 5 DPI until

9 DPI ($n = 3$), and the number of *E. tenella* oocyst in the feces was calculated, as previously described, by using a McMaster counting chamber (Marienfeld-Superior, Germany) (40). The total number of oocysts was calculated according to the following formula: total oocysts = oocysts counted × dilution factor × fecal sample volume/counting chamber volume. The values were converted as oocyst per gram of feces.

Sporozoite Viability Test

To assess the viability of sporozoites, purified sporozoites were incubated with DIM (0–500 μM) for 24 h, the viability was measured using CyQuant direct cell proliferation assay (41). To infect sporozoites into chicken epithelial cell line (8E11), purified sporozoites were stained with carboxyfluorescein succinimidyl ester (CFSE, Thermo Fisher Scientific) according to manufacturer's instructions. 8E11 was cultured in DMEM/F12 supplemented with 10% FBS, penicillin/streptomycin, and 25 mM HEPES and the sporozoites was infected at a multiplicity of infection of 1.0 (sporozoite/cell ratio of 1:1). Free sporozoites were washed after 3 h incubation and new media was replaced. After further incubation for 21 h, the number of sporozoites was measured at 485/528 nm.

Statistical Analysis

The data were analyzed using Prism Version 5.01 (GraphPad Software, La Jolla, CA). The normality of each data was tested by Kolmogorov–Smirnov test. Parametric tests were used to compare between groups with one-way ANOVA and Dunnett's multiple comparison test and non-parametric tests were conducted with Kruskal–Wallis test and Dunn's multiple comparison test. The data are expressed as the mean ± standard error for parametric analysis and median with interquartile range for non-parametric analysis and the differences were considered significant at $p < 0.05$ or $p < 0.01$.

RESULTS

Increased Treg Cells and Th17/Treg Ratio in Indole-Treated Chickens

To determine the dietary effects of indole treatment on $CD4^+$ T cells in healthy chickens, we firstly investigated the frequencies of $CD4^+CD25^+$ (Treg) and $CD4^+IL\text{-}17A^+$ (Th17) cells from the spleen and intestine after oral treatment of either DIM or I3C. In the indole-treated groups compared with the vehicle control group, Treg cells were significantly higher, whereas the treatment with indoles induced a decrease in Th17 cells in both the spleen and cecal tonsils (**Figures 1A,B**). The ratio of Th17/Treg cells decreased in both indole-treated groups (**Figure 1C**). There was no significant difference in the frequencies of Treg or Th17 cells between the treatments with DIM and I3C. Furthermore, the real-time qPCR results showed that indoles increased the mRNA expression of the Treg-related cytokine IL-10 and decreased Th17-related cytokines such as IL-17F, IL-21, and IL-22 in cecal tonsils (**Figure 1D**).

The *in vitro* Effects of Indoles on Treg Cells and Aryl Hydrocarbon Receptor

To validate *in vivo* findings on the role of indoles on CD4+ T cell subsets, we performed *in vitro* experiments to investigate the effects of indole treatment on Treg cells in chicken lymphocytes. Chicken splenic lymphocytes were purified and stimulated with Con A or EtSzAg in the presence or absence of both indoles for 72 h. The data indicated that cell proliferation induced by Con A was inhibited by both DIM or I3C, as compared with the results for Con A-stimulated cells. Interestingly, indole treatment also inhibited the proliferation induced by EtSzAg, thus suggesting a role in coccidiosis in chickens (**Figure 2A**). We further investigated the mRNA expression of Treg-related (IL-10) or Th17-related (IL-17A) cytokine mRNAs in those cells. Both indole treatments significantly up-regulated expression of IL-10 while down-regulating IL-17A (**Figures 2B,C**). In agreement with data from *in vivo* experiments, the proportion of Treg cells in *in vitro* assays was increased in splenic lymphocytes incubated with DIM or I3C (**Figure 2D**). To test the hypothesis that indoles are ligands for AhR and can cause AhR activation in chickens as in mammals (42), we determined the mRNA expression levels of the chicken cytochrome P-450 enzymes CYP1A4 and CYP1A5, which are orthologous to mammalian CYP1A1 and CYP1A2, in indole-treated cecal tonsil lymphocytes. Both are AhR-regulated genes and markers of AhR activation (43). As shown in **Figure 3A**, the expression of CYP1A4 and CYP1A5 increased after treatment with DIM or I3C, and normal expression was restored in the presence of the AhR-specific antagonist CH223191 (**Figure 3A**). Furthermore, the frequency of Treg cells was higher in DIM-treated cecal tonsil lymphocytes than in non-treated cells in the presence of CH223191 (**Figure 3B**).

Effects of DIM on Treg and Th17 Cells in *E. tenella* Infection

Because our findings indicated that indoles induced Treg cells while suppressing Th17 cells in chickens, and Th17 is known to play a pathological role in coccidiosis (7, 44), we designed the *in vivo* experiment to determine the effect of DIM on the regulation of $CD4^+$ T cells in *E. tenella* infection in chickens (**Figure 4A**). Treatment of chickens with DIM, compared with vehicle control, induced a significant increase in intestinal Treg cells while decreasing Th17 cells. Compared with the ET group, the ETDIM group showed an increase in Treg cells at from 4 DPI, and Treg cells remained elevated until the end of experiment, whereas the decrease in Th17 cells was seen only early in infection, such as at 4 DPI (**Figures 4B,C**). The ratio of Th17/Treg cells exhibited significant decrease at 1, 4, and 7 DPI (**Figure 4D**). We also found that DIM inhibited the proliferation of lymphocytes. As shown in **Figure 4E**, the ETDIM group showed lower proliferation than the other groups during the re-activation of the lymphocytes with DIM *in vitro*. Notably, the NIDIM group did not show any significant inhibition of proliferation, thus suggesting that the inhibitory effect of DIM is much stronger when the lymphocytes are pre-activated with *Eimeria* antigen.

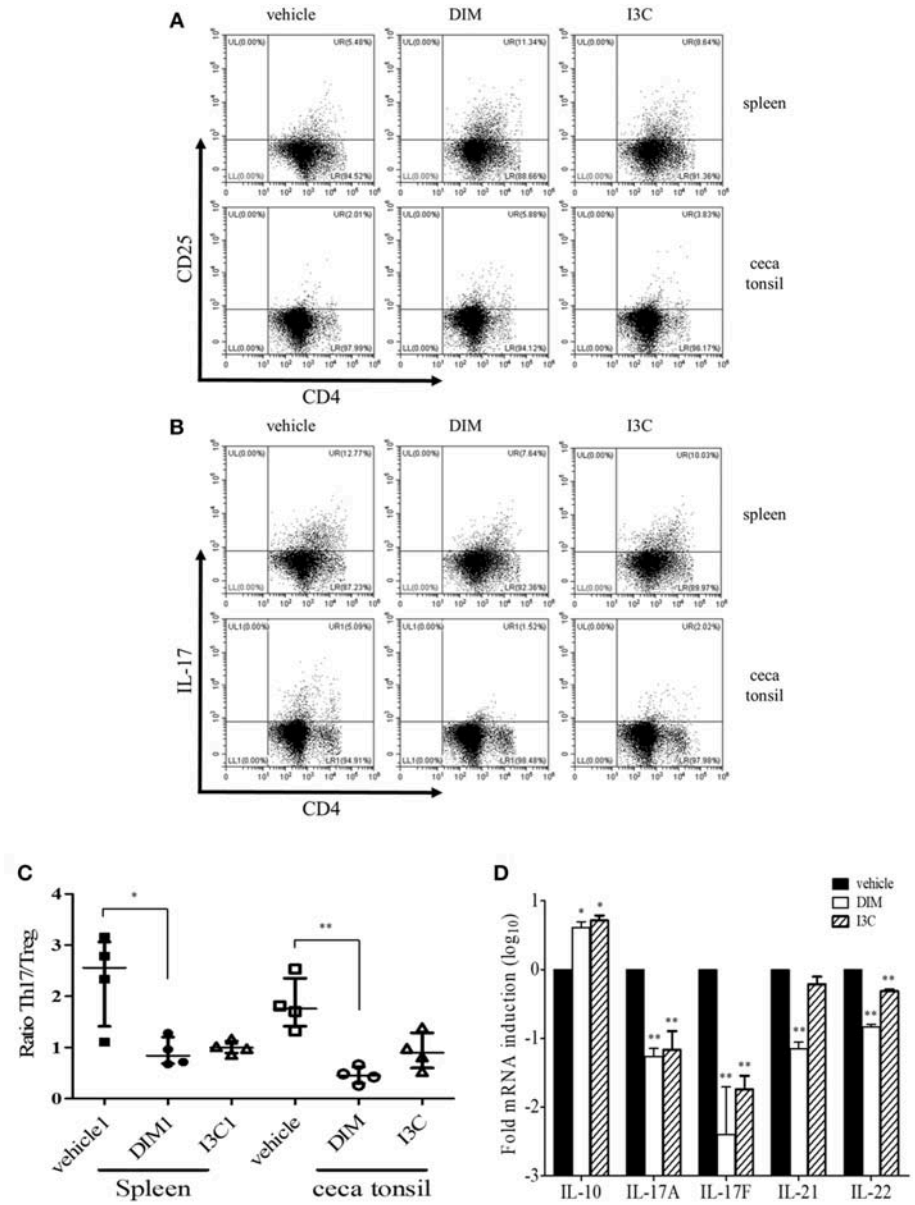

FIGURE 1 | Effects of indoles to induce Treg cells in indole-treated chickens**.** Two-weeks-old chickens were given orally corn oil as a vehicle control, DIM (200 mg/kg), or I3C (200 mg/kg) for 14 days on a daily basis. Lymphocytes were isolated from the spleen and cecal tonsils, and stained with CD3, CD45, CD4, and CD25, or CD3, CD45, CD4, and IL-17A for analyzing Treg **(A)** and Th17 **(B)** populations, respectively, and gated CD4+ T cells. Cells were stimulated with PMA and ionomycin for the determination of Th17 cells. Data show the representative staining from two independent experiments. **(C)** The ratio of Th17/Treg cells in the spleen and cecal tonsils. The data represent median with interquartile range after Kruskal-Wallis test with Dunn's multiple comparison test. **(D)** RNA was isolated from cecal tonsils and used for real-time qPCR to measure Treg- (IL-10) and Th17-related (IL-17A, IL-17F, IL-21, and IL-22) mRNA expression. The data represent the mean ± SE from two independent experiments. $^{*}p < 0.05$ and $^{**}p < 0.01$ were considered statistically significant compared to the vehicle control in each sample or target.

mRNA Expression of Treg- and Th17-Related Genes in DIM-Treated Chickens

To determine the cytokines involved in T cell regulation by DIM, we carried out real-time qPCR to measure the mRNA expression of Treg- and Th17-related genes in T cells. In agreement with our *in vitro* findings, the expression of IL-10 increased after treatment of DIM. Following *E. tenella* infection, IL-10 expression increased in the ET group and the increased IL-10 expression in the ET groups persisted until the end of the experiment. Compared with DIM, ETDIM induced greater IL-10 expression after 1 DPI, thus suggesting that DIM induces more Treg cells in coccidiosis (**Figure 5A**). However, the expression of Th17-related cytokines was generally down-regulated in the DIM and ETDIM

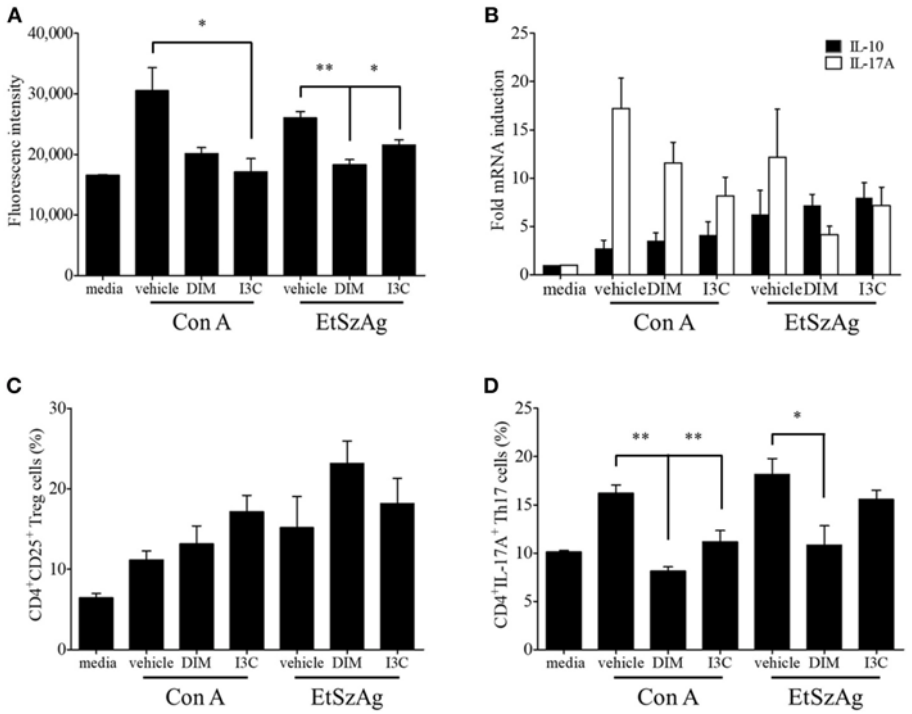

FIGURE 2 | Effects of indoles to induce Treg cells *in vitro*. **(A)** Lymphocytes from spleen of healthy chickens were isolated and stimulated with DMSO as a vehicle control, DIM (100 μM), or I3C (100 μM) in the presence of Con A (10 μg/ml) or EtSzAg for 24 h and the proliferation was measured by CyQuant direct cell proliferation assay. **(B)** The mRNA expressions of Treg- and Th17-related cytokine were measured after 24 h by real-time qPCR. The frequency of Treg **(C)** and Th17 cells **(D)** were analyzed by flow cytometry. The data represent the mean ± SE from two independent experiments. $^{*}p < 0.05$ and $^{**}p < 0.01$ were considered statistically significant compared to the vehicle control of each treatment.

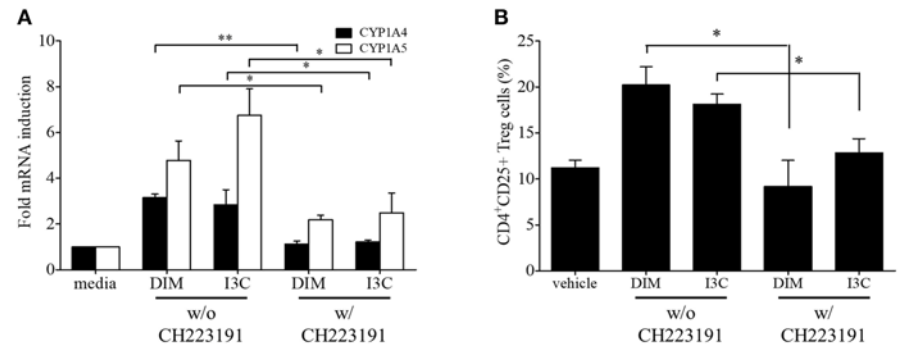

FIGURE 3 | Regulation of indoles by AhR**.** Lymphocytes from cecal tonsils were isolated and stimulated with DMSO as a vehicle control, DIM (100 M/ml), or I3C (100 M/ml) in the absence of presence of specific AhR antagonist, CH223191 for 24 h. **(A)** The mRNA expressions of CYP1A4 and CYP1A5 were measure by real-time qPCR. **(B)** The frequency of Treg cells were analyzed by flow cytometry. The data represent the mean ± SE from two independent experiments. $^{*}p < 0.05$ and $^{**}p < 0.01$ were considered statistically significant compared to the samples.

groups (**Figure 5B**). Interestingly, we found high expression of IL-17A in the ET group between 7 and 13 DPI, but the increases in expression of these cytokines were diminished in the ETDIM group (**Figure 5B**). These results suggest that *E. tenella* infection induces Th17 cells at a later stage of infection, and the suppression of Th17 cells by DIM seems to depend on the level of Th17 cytokine.

Effects of DIM on Growth Performance, Oocyst Production, and Intestinal Lesions

Next, we examined the effects of dietary DIM on BWG, oocyst production, and intestinal lesions in *E. tenella*-infected chickens. The NIDIM group showed no difference in BWG compared with the NI group, thus indicating that DIM has no effect on growth performance. Furthermore, the ETDIM and ET groups

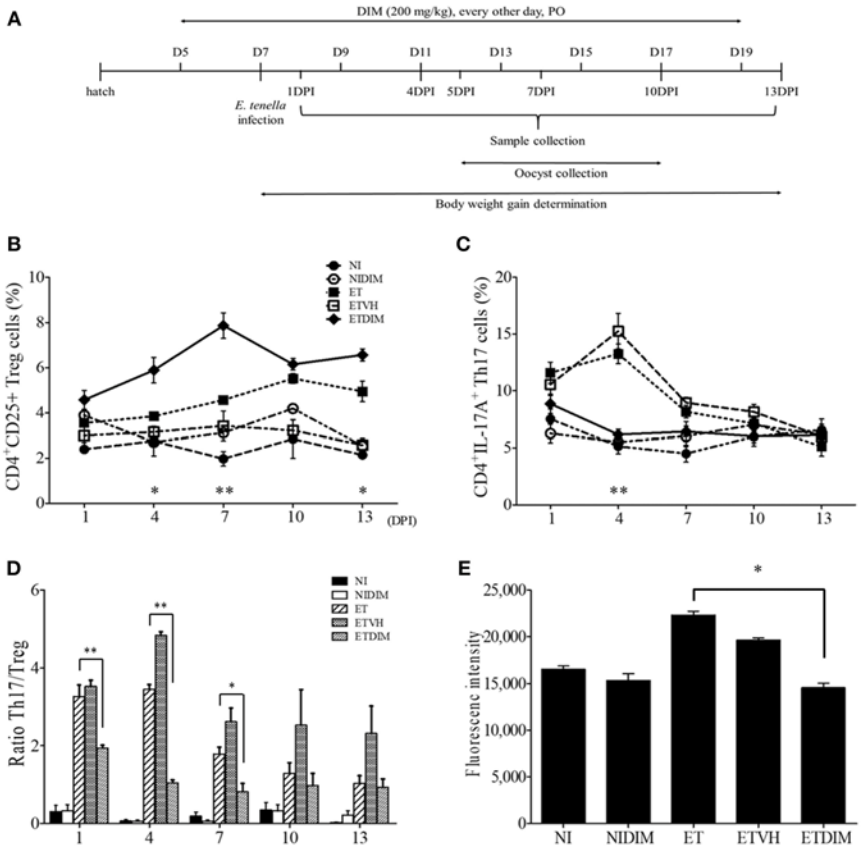

FIGURE 4 | Effect of dietary DIM on intestinal T cells in *E. tenella* infection. **(A)** Schematic outline of the *in vivo* experimental design. The frequencies of Treg **(B)** and Th17 cells **(C)** of cecal tonsil lymphocytes were analyzed at indicated DPIs by flow cytometry. *$p < 0.05$ and **$p < 0.01$ were considered statistically significant compared between the ET and ETDIM groups at each time point. **(D)** The ratio of Th17/Treg cells in and cecal tonsils. **(E)** Lymphocytes were stimulated with Con A (10 μg/ml) and the proliferation of cecal tonsil lymphocytes was measured by CyQuant direct cell proliferation assay in EtSzAg-activated cells. *$p < 0.05$ and **$p < 0.01$ were considered statistically significant compared to the samples.

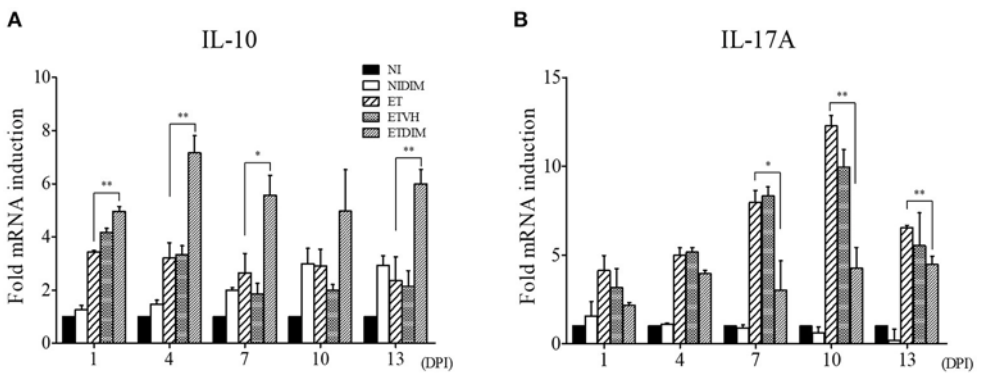

FIGURE 5 | Effect of dietary DIM on mRNA expressions of Treg- and Th17-related genes in *E. tenella* infection**.** The mRNA expressions of IL-10 **(A)** and IL-17A **(B)** were measure in cecal tonsils by real-time qPCR. The data represent the mean ± SE from two independent experiments. *$p < 0.05$ and **$p < 0.01$ were considered statistically significant compared to the samples.

showed comparable BWG (**Figure 6A**). In agreement with the BWG data, the ETDIM group, compared with the ET group, did not exhibit significantly less oocyst shedding from feces (**Figure 6B**). Interestingly, however, the severity of intestinal lesions was significantly lower in the ETDIM group than the ET group (**Figure 6C**). In H&E staining, the NI and NIDIM groups displayed a normal structure and no visible changes. In all ET groups, there was structural disorder, epithelial loss, and inflammatory cell infiltration; however, the ETDIM group showed less severity in terms of abnormality of villi structure and inflammatory cell number (**Figure 6D**). These has been validated by our histological finding that showed the gross morphological changes in the cecum of ETDIM group showed less hemorrhage in the mucosa and less watery ingesta mixed with mucus than did the ET group (data not shown).

mRNA Expression of Proinflammatory Genes in DIM-Treated Chickens

From the findings from our *in vivo* experiments, we hypothesized that DIM treatment decreases inflammation in the intestine through the regulation of Treg and Th17 cells. To this end, we determined the mRNA expression profiles of proinflammatory genes in intestinal tissues by using real-time qPCR. As expected, *E. tenella* infection induced robust expression of proinflammatory genes such as IL-1β, IL-6, and CXCLi2 (a homolog of mammalian CXCL8) but not TNFSF15 (TL1A, a functional homolog of mammalian TNF-α) (36). Compared with the ET group, the ETDIM group showed lower expression of those genes (**Figure 7A**). Next, we measured the expression of tight junction proteins such as JAM2, and ZO1 to determine whether DIM treatment is involved in intestinal barrier function. Following *E. tenella* infection, mRNA expression of JAM2, and ZO1 significantly decreased, but their expression was restored to a much greater extent in the ETDIM group than the ET or ETVEH groups (**Figure 7B**). Together, these results suggest that treatment of DIM in coccidiosis may be beneficial to reduce intestinal inflammation and to help to restore the damage from coccidiosis.

Direct Effect of DIM on *E. tenella*

Finally, we determined whether DIM has any direct activity against *Eimeria* sporozoites, an invasive form of parasites. First, we incubated *E. tenella* sporozoites with various concentrations of DIM. **Figure 8A** shows that DIM had no effect on sporozoites viability. Second, we infected sporozoites to the chicken epithelial cell line 8E11, then treated DIM to the cells harboring sporozoites. DIM treatment did not alter the viability of sporozoites inside of cells (**Figure 8B**). It suggests that the beneficial effects of DIM on *E. tenella* infection are not associated with its activity against parasite itself.

DISCUSSION

I3C is derived from cruciferous vegetables, which contain abundant indoles. When digested, it produces several biologically active I3C oligomers such as DIM. Earlier studies of dietary indole derivatives have focused on their anti-cancer effect, given that they have been shown to reduce the risk of cancer (45–47). Indoles have been shown to induce antioxidant activity and apoptosis of cancer cells, and to regulate hormone metabolism (48–51). Recently, several studies have reported that indoles also have immunoregulatory properties, especially on T cells. For example, Singh et al. (17) have reported that dietary indoles suppress the delayed-type hypersensitivity (DTH) response through the regulation of Treg and Th17 cells in mice. Dietary supplementation of indoles also has been shown to suppress neuroinflammation by induction of reciprocal differentiation of Treg and Th17 cells in experimental autoimmune encephalomyelitis (EAE) mice (18). These abilities of indoles to modulate the immune response are related to AhR signaling (21). AhR was first discovered as a transcription factor mediating the toxicity of chemicals such as 2,3,7,8-tetrachlorodibenzo-*p*-dioxin (TCDD) (52). Recent studies have suggested that AhR activation plays diverse roles in cellular function including the regulation of the immune system (53, 54). Interestingly, there are two types of AhR found in chickens, AhR1 and AhR2, and AhR1 is the dominant form in cormorants (*Phalacrocorax carbo*) (55). In the chicken intestine, both mRNA were expressed; however further studies will be required to elucidate their role in T cell regulation (56). Moreover, there is a distinct set of cytochrome P450 family members in chickens: CYP1A4 and CYP1A5. On the basis of their amino acid sequences, they can be classified in the CYP1A family, but both are more like CYP1A1 than CYP1A2 (57). Because they are induced by AhR activation in chickens (34, 58), we identified their expression levels after DIM treatment in cecal tonsil lymphocytes. Inhibition assays using AhR-specific inhibitor confirmed that DIM and its precursor I3C induce AhR activation in chickens. Unfortunately, we did not find any evidence of an effect of chicken CYP1As on T cell regulation, thus suggesting that the mechanism of AhR activation in modulating Treg and Th17 cells may differ from the one that mediating the toxicity of environmental toxins. Quintana et al. (21) have identified an evolutionarily conserved binding site for AhR in the foxp3 gene and three non-evolutionarily conserved AhR-binding sites in the promoter regions of foxp3 genes in zebrafish, mice, and humans. Their subsequence studies proved that AhR controls foxp3 expression, which induces the generation of Treg cells. Another report has explained the possible AhR activation mechanism. Singh et al. (17) have investigated microRNA profiles in DTH mice treated with several AhR ligands and found that several microRNAs targeting foxp3 and IL-17 mRNA are important in regulating Treg and Th17 cells. The activation of AhR to regulate T cells is dependent on the type of AhR ligands. For example, TCDD induces Treg cells in EAE mice to reduce the EAE score, whereas FICZ increases Th17 cell differentiation and the severity of EAE (21, 59). DIM, an AhR ligand that we used in this study, has therapeutic effects in oxazolone-induced colitis and mBSA-induced DTH in mice through Treg cell induction and suppression of Th2 or Th17 cells (17, 60). In chickens, compared to mammals, very little is known about the effect of dietary indoles as AhR ligands on the immune response. In this study, we provide the first demonstration in chickens of

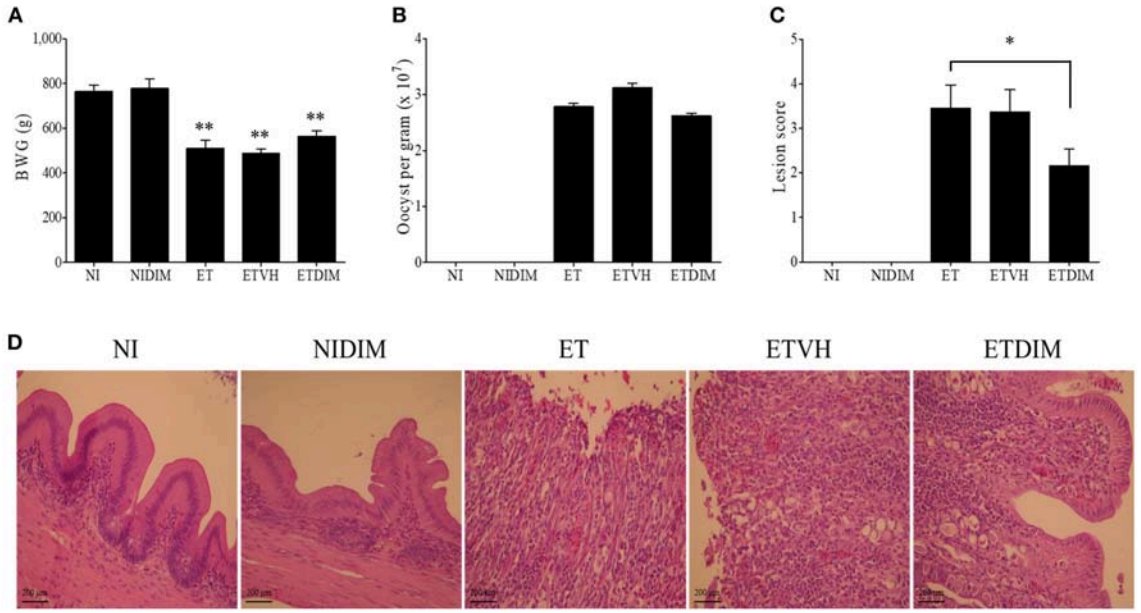

FIGURE 6 | Effect of dietary DIM on growth performance, oocyst production and intestinal lesions in *E. tenella* infection**. (A)** Body weight gain was measured from 0 to 13 DPI ($n = 15$). **(B)** Fecal oocysts were collected and pooled from 5 to 9 DPI and counted using McMaster counting chamber ($n = 15$). *$p < 0.05$ and **$p < 0.01$ were considered statistically significant compared to the samples. **(C)** Lesion score was determined from cecum at 7 DPI ($n = 5$). **(D)** Histological sections prepared from the cecum (X400).

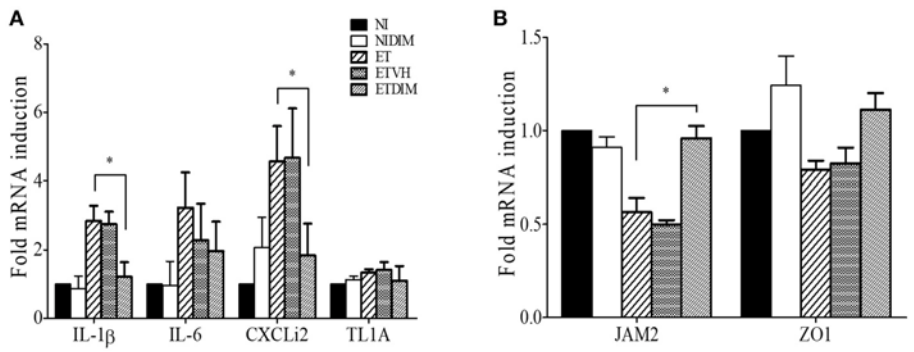

FIGURE 7 | Effect of dietary DIM on mRNA expressions of proinflammatory and tight junction protein genes in *E. tenella* infection. The mRNA expressions of proinflammatory genes; IL-1β, IL-6, CXCLi2, and TL1A **(A)** and tight junction protein gene; JAM2 and ZO1 **(B)** were measure in cecum by real-time qPCR. *$p < 0.05$ and was considered statistically significant compared to the samples.

how AhR ligand modulates T cells in terms of Treg and Th17 cells. As we expected, DIM and I3C increased the number of $CD4^+CD25^+$ cells in chicken lymphocytes *in vivo* as well as *in vitro*, thus suggesting that they have comparable effects to those in mammals. Regarding the Th17 cells, the data showed a decrease in $CD4^+$IL-$17A^+$ cells, but to a lesser extent than the increase in intestinal Treg cells. Moreover, the expression of each lineage of Th cell-related cytokines was consistent with data obtained from flow cytometry. The anti-inflammatory cytokine IL-10 showed increased expression in DIM-treated groups, whereas the expression of the IL-17A, IL-17F, IL-21, and IL-22 was downregulated in the DIM-treated groups. These data suggest that the cytokine profile for each Th lineage is likely to overlap in chickens and mammals.

We further investigated the effects of indole in regulating Treg and Th17 cells in coccidiosis. Coccidiosis caused by *Eimeria* spp. induces an inflammatory response in parasitized intestinal tissues (61). Profiling of cytokines in coccidiosis revealed that most T cell cytokines are increased along with the inflammation in the intestine (62, 63). Moreover, our previous studies have indicated that Th17-related cytokines such as IL-17A and IL-17F, and IL-17 receptor signaling are involved in inflammation induced by coccidiosis, although the predominant protective response in coccidiosis is considered to be an IFN-γ-related

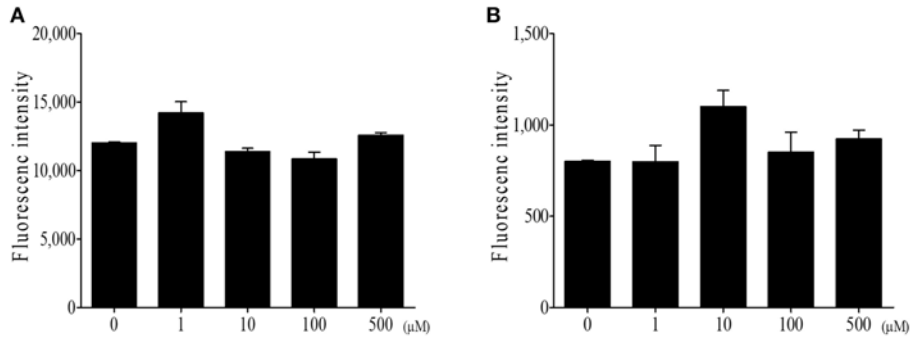

FIGURE 8 | Direct effect of DIM on *E. tenella* parasite**. (A)** DIM was incubated with *E. tenella* sporozoites for 24 h and measured viability using CyQuant direct cell proliferation assay. **(B)** *E. tenella* sporozoites were stained with CFSE and infected to intestinal epithelial cells (8E11). Following infection, DIM was treated and fluorescence was measured. The data represent the mean ± SE from two independent experiments.

Th1 response (6, 8, 31, 64). We investigated the changes in Th1 cells as $CD4^{+}IFN\text{-}\gamma^{+}$ cells in *E. tenella* infection. Initially, we expected that DIM would also affect the Th1 response, because several studies have shown that AhR agonists can also modulate the differentiation of Th1 cells (65, 66). As shown in **Figure S1**, Th1 cells were highly induced at 1 and 4 DPI following *E. tenella* infection although they did not change as much as Treg and Th17 cells in the DIM-treated groups. Therefore, Th1 response may play a role during the early phase of coccidiosis by initiating local inflammatory response started by the host cell invasion of sporozoites of *Eimeria* with subsequent intracellular development in early to intermediate phase. Compared to the NI group, Treg and Th17 cells in the ET groups were induced in a later phase, thus suggesting that they might be involved in tissue recovery from the damage induced by Th17 responses or have an important function in gut homeostasis. Several studies have reported that chicken IL-17A plays a pathogenic role in *Eimeria* infection (7, 44). Likewise, in the ETDIM group, which showed a lower degree of intestinal lesions, Th17 cells were downregulated compared with their levels in the NI or DIM group, and it is likely Th17 cells are involved in pathogenicity or inhibiting recovery from inflammation. At the same time points, Treg cells showed increased populations in the ETDIM group, thus indicating that DIM increased the Treg populations and decreased the inflammation in the parasitized intestine. IL-10 has been considered to play an important role to evade host immune response in coccidiosis. One possible mechanism is that coccidial parasites have evolved to stimulate Treg cells to express IL-10 and it helps parasites to facilitate invasion and survival in chickens through the suppression of protective response mediating IFN-γ-expressing Th1 cells. Using two inbred lines of chicken differing in their resistance or susceptibility to *Eimeria* infection, it is revealed that the expression of IL-10 was the major difference between those two lines. The expression of IL-10 was highly induced in susceptible line of chickens among the genes related to different helper T cell lineages such as IFN-γ for Th1, IL-4 for Th2, and IL-10 and TGF-β for Treg cells while it is suppressed in age-matched resistant line (10). The administration of IL-10 antibody in *Eimeria*-infected chicken showed improved growth rate compared to control antibody group but it did not influence fecal oocyst production (67, 68). These results are indicating that the regulation of protective immune response to *Eimeria* spp. by Treg cells is critical and IL-10 contributes to pathogenesis in coccidiosis. In the current study, on the other aspect of Treg cells, we found another role of Treg cells that involves in anti-inflammatory response through suppress inflammatory Th17 cells. It is thought that the anti-inflammatory Treg cells could be participate in the self-limiting mechanism of *Eimeria* spp. that prevents the collateral intestinal damage caused by exaggerated inflammation. Other evidences of reduced intestinal inflammation we found in this study was the expression of proinflammatory genes and tight junction protein. Chicken IL-17A and IL-17F have known to induce proinflammatory cytokines such as IL-1β, IL-6, and CXCLi2 as in mammals (31) thus decrease of Th17 cytokines might involve the anti-inflammatory process in the intestine. As a marker of intestinal integrity, tight junction protein play an important role in the regulation of intestinal permeability by sealing the paracellular space between intestinal epithelial cells (69). The recovery of tight junction protein expressions was induced by dietary treatment of DIM and it might be associated with that mammalian IL-17A and IL-17F reported to disrupt the distribution of tight junction protein (70).

As the main source of indoles in cruciferous vegetables, Glucosinolates (GLS) have been used to measure the biologically active constituent. McNaughton and Mark reported GLS content of various cruciferous vegetables (71). It varies depending on the species (e.g., cress for the highest GLS content as 389 mg/100 g while the lowest content for Pe-tsai chinese cabbage; 20 mg/100 g) and there is large variation in the values reported for the same vegetable by different studies (71, 72). Since the US Food and Drug Administration permitted the use of claims acknowledging the relationship between increased vegetable consumption and decreased cancer risk in 1993, there has been a growing literature reporting human health benefits of cruciferous vegetables, more specifically, indoles (73, 74). In poultry research, however, there is a lack of information of the effects of any forms of indole supplementation. In

addition, the production of indoles, especially food-grade indole naturally derived is very highly priced, due to an expensive chemical conversion process which makes commercial chicken supplementation unfeasible at this phase. Nonetheless, the present study could support the scientific evidences for beneficial effects of indole supplementation in human as well as animal. From the present study, DIM treatment exhibited significantly upregulated Treg cells and IL-10 expression in *Eimeria*-infected chicken while DIM-treated chickens with no *Eimeria* infection did not increase as much as the group infected indicating that DIM likely displays of better effectiveness in *Eimeira*-infected gut rather than those of healthy ones. In the approach to such a drug to prevent/treat chicken gut inflamed by coccidiosis, indoles might have potentials since coccidiosis is considered one of most problematic disease in the poultry industry.

In summary, this is the first evidence to show the effect of dietary indole in reducing intestinal damage induced by coccidiosis in chickens occurs through the regulation of Treg and Th17 cells in the intestine. Because of the lack of immune reagents to detect chicken cytokines related to the T cell response, the study of T cell immunology in chickens has been lagging far behind that in mammals. In this study, we validated that monoclonal antibodies which we previously developed (6, 26) for flow cytometry application could be easily applied to study T cell immune response by determining specific cytokine-expressing T cell phenotypes and in our knowledge, this is the first report to stain chicken lymphocytes with four different fluorescent dyes.

AUTHOR CONTRIBUTIONS

WK designed the project, performed the experiments, analyzed the data, and wrote the manuscript. HL supervised the research. WM and HL revised the manuscript.

FUNDING

This research was supported, in part, by Development of Poultry Immune Reagent program (award number: 2017-67015-26793) funded by USDA/NIFA and ARS CRIS project (8042-32000-106-00D).

SUPPLEMENTARY MATERIAL

The Supplementary Material for this article can be found online at: https://www.frontiersin.org/articles/10.3389/fimmu.2019.00560/full#supplementary-material

REFERENCES

1. Shirley MW, Lillehoj HS. The long view: a selective review of 40 years of coccidiosis research. *Avian Pathol*. (2012) 41:111–21. doi: 10.1080/03079457.2012.666338
2. Dong X, Abdelnabi GH, Lee SH, Li G, Jin H, Lillehoj HS, et al. Enhanced Egress of Intracellular *Eimeria tenella* Sporozoites by splenic lymphocytes from coccidian-infected chickens. *Infect Immun*. (2011) 79:3465–70. doi: 10.1128/IAI.01334-10
3. Vervelde L, Vermeulen AN, Jeurissen SH. *In situ* characterization of leucocyte subpopulations after infection with *Eimeria tenella* in chickens. *Parasite Immunol*. (1996) 18:247–56.
4. Wakelin D, Rose ME, Hesketh P, Else KJ, Grencis RK. Immunity to coccidiosis: genetic influences on lymphocyte and cytokine responses to infection with *Eimeria vermiformis* in inbred mice. *Parasite Immunol*. (1993) 15:11–9.
5. Lillehoj HS, Trout JM. CD8+ T cell-coccidia interactions. *Parasitol Today*. (1994) 10:10–4.
6. Yun CH, Lillehoj HS, Choi KD. *Eimeria tenella* infection induces local gamma interferon production and intestinal lymphocyte subpopulation changes. *Infect Immun*. (2000) 68:1282–8. doi: 10.1128/IAI.68.3.1282-1288.2000
7. Zhang L, Liu R, Song M, Hu Y, Pan B, Cai J, Wang M. *Eimeria tenella*: interleukin 17 contributes to host immunopathology in the gut during experimental infection. *Exp Parasitol*. (2013) 133:121–30. doi: 10.1016/j.exppara.2012.11.009
8. Kim WH, Jeong J, Park AR, Yim D, Kim S, Chang HH, et al. Downregulation of chicken interleukin-17 receptor A during *Eimeria* infection. *Infect Immun*. (2014) 82:3845–54. doi: 10.1128/IAI.02141-14
9. Min W, Kim WH, Lillehoj EP, Lillehoj HS. Recent progress in host immunity to avian coccidiosis: IL-17 family cytokines as sentinels of the intestinal mucosa. *Dev Comp Immunol*. (2013) 41:418–428. doi: 10.1016/j.dci.2013.04.003
10. Rothwell L, Young JR, Zoorob R, Whittaker CA, Hesketh P, Archer A, et al. Cloning and characterization of chicken IL-10 and its role in the immune response to *Eimeria maxima*. *J Immunol*. (2004) 173:2675–82. doi: 10.4049/jimmunol.173.4.2675
11. Verhoeven DT, Verhagen H, Goldbohm RA, van den Brandt PA, van Poppel G. A review of mechanisms underlying anticarcinogenicity by brassica vegetables. *Chem Biol Interact*. (1997) 103:79–129.
12. Ribaux P, Irion O, Cohen M. An active product of cruciferous vegetables, 3,3′-diindolylmethane, inhibits invasive properties of extravillous cytotrophoblastic cells. *Neuro Endocrinol Lett*. (2012) 33:133–7. Available online at: http://www.nel.edu/an-active-product-of-cruciferous-vegetables-3-3-diindolylmethane-inhibits-invasive-properties-of-extravillous-cytotrophoblastic-cells-752/
13. Taylor-Harding B, Agadjanian H, Nassanian H, Kwon S, Guo X, Miller C, et al. Indole-3-carbinol synergistically sensitises ovarian cancer cells to bortezomib treatment. *Br J Cancer*. (2012) 106:333–43. doi: 10.1038/bjc.2011.546
14. Schmidt J V, Su GH, Reddy JK, Simon MC, Bradfield CA. Characterization of a murine Ahr null allele: involvement of the Ah receptor in hepatic growth and development. *Proc Natl Acad Sci USA*. (1996) 93:6731–6.
15. Hankinson O. The aryl hydrocarbon receptor complex. *Annu Rev Pharmacol Toxicol*. (1995) 35:307–40. doi: 10.1146/annurev.pa.35.040195.001515
16. Whitlock JP. Induction of cytochrome P4501A1. *Annu Rev Pharmacol Toxicol*. (1999) 39:103–25. doi: 10.1146/annurev.pharmtox.39.1.103
17. Singh NP, Singh UP, Rouse M, Zhang J, Chatterjee S, Nagarkatti PS, et al. Dietary indoles suppress delayed-type hypersensitivity by inducing a switch from proinflammatory Th17 cells to anti-inflammatory regulatory T cells through regulation of MicroRNA. *J Immunol*. (2016) 196:1108–22. doi: 10.4049/jimmunol.1501727
18. Rouse M, Singh NP, Nagarkatti PS, Nagarkatti M. Indoles mitigate the development of experimental autoimmune encephalomyelitis by induction of reciprocal differentiation of regulatory T cells and Th17 cells. *Br J Pharmacol*. (2013) 169:1305–21. doi: 10.1111/bph.12205
19. Funatake CJ, Marshall NB, Steppan LB, Mourich DV, Kerkvliet NI. Cutting edge: activation of the aryl hydrocarbon receptor by 2,3,7,8-tetrachlorodibenzo-p-dioxin generates a population of CD4+ CD25+ cells with characteristics of regulatory T cells. *J Immunol*. (2005) 175:4184–8. doi: 10.4049/jimmunol.175.7.4184
20. Esser C, Rannug A, Stockinger B. The aryl hydrocarbon receptor in immunity. *Trends Immunol*. (2009) 30:447–54. doi: 10.1016/j.it.2009.06.005

21. Quintana FJ, Basso AS, Iglesias AH, Korn T, Farez MF, Bettelli E, et al. Control of Treg and TH17 cell differentiation by the aryl hydrocarbon receptor. *Nature*. (2008) 453:65–71. doi: 10.1038/nature06880
22. Veldhoen M, Hirota K, Christensen J, O'Garra A, Stockinger B. Natural agonists for aryl hydrocarbon receptor in culture medium are essential for optimal differentiation of Th17 T cells. *J Exp Med*. (2009) 206:43–49. doi: 10.1084/jem.20081438
23. Kimura A, Naka T, Nohara K, Fujii-Kuriyama Y, Kishimoto T. Aryl hydrocarbon receptor regulates Stat1 activation and participates in the development of Th17 cells. *Proc Natl Acad Sci USA*. (2008) 105:9721–6. doi: 10.1073/pnas.0804231105
24. Diller ML, Kudchadkar RR, Delman KA, Lawson DH, Ford ML. Balancing inflammation: the link between Th17 and regulatory T cells. *Mediators Inflamm*. (2016) 2016:1–8. doi: 10.1155/2016/6309219
25. Lee SH, Lillehoj HS, Jang SI, Baldwin C, Tompkins D, Wagner B, et al. Development and characterization of mouse monoclonal antibodies reactive with chicken interleukin-2 receptor αlpha chain (CD25). *Vet Immunol Immunopathol*. (2011) 144:396–404. doi: 10.1016/j.vetimm.2011.08.001
26. Yoo J, Chang HH, Bae YH, Seong C-N, Choe N-H, Lillehoj HS, et al. Monoclonal antibodies reactive with chicken interleukin-17. *Vet Immunol Immunopathol*. (2008) 121:359–63. doi: 10.1016/j.vetimm.2007.10.004
27. Kim WH, Lillehoj HS, Min W. Evaluation of the immunomodulatory activity of the chicken NK-lysin-derived peptide cNK-2. *Sci Rep*. (2017) 7:45099. doi: 10.1038/srep45099
28. Shanmugasundaram R, Selvaraj RK. Regulatory T cell properties of chicken $CD4^+CD25^+$ Cells. *J Immunol*. (2011) 186:1997–2002. doi: 10.4049/jimmunol.1002040
29. Denyer MP, Pinheiro DY, Garden OA, Shepherd AJ. Missed, not missing: phylogenomic evidence for the existence of Avian FoxP3. *PLoS ONE*. (2016) 11:e0150988. doi: 10.1371/journal.pone.0150988
30. John DA, Williams LK, Kanamarlapudi V, Humphrey TJ, Wilkinson TS. The bacterial species *Campylobacter jejuni* induce diverse innate immune responses in human and avian intestinal epithelial cells. *Front Microbiol*. (2017) 8:1840. doi: 10.3389/fmicb.2017.01840
31. Kim WH, Jeong J, Park AR, Yim D, Kim Y-H, Kim KD, et al. Chicken IL-17F: Identification and comparative expression analysis in *Eimeria*-infected chickens. *Dev Comp Immunol*. (2012) 38:401–9. doi: 10.1016/j.dci.2012.08.002
32. Shaughnessy RG, Meade KG, McGivney BA, Allan B, O'Farrelly C. Global gene expression analysis of chicken caecal response to *Campylobacter jejuni*. *Vet Immunol Immunopathol*. (2011) 142:64–71. doi: 10.1016/j.vetimm.2011.04.010
33. Kim S, Faris L, Cox CM, Sumners LH, Jenkins MC, Fetterer RH, et al. Molecular characterization and immunological roles of avian IL-22 and its soluble receptor IL-22 binding protein. *Cytokine*. (2012) 60:815–27. doi: 10.1016/j.cyto.2012.08.005
34. Bussmann UA, Pérez Sáez JM, Bussmann LE, Barañao JL. Aryl hydrocarbon receptor activation leads to impairment of estrogen-driven chicken vitellogenin promoter activity in LMH cells. *Comp Biochem Physiol Part C Toxicol Pharmacol*. (2013) 157:111–18. doi: 10.1016/j.cbpc.2012.10.006
35. Shang S, Jiang J, Deng Y. Chicken cytochrome P450 1A5 is the key enzyme for metabolizing T-2 toxin to 3′OH-T-2. *Int J Mol Sci*. (2013) 14:10809–18. doi: 10.3390/ijms140610809
36. Takimoto T, Sato K, Akiba Y, Takahashi K. Role of chicken TL1A on inflammatory responses and partial characterization of its receptor. *J Immunol*. (2008) 180:8327–32. doi: 10.4049/jimmunol.180.12.8327
37. Gadde UD, Oh S, Lee Y, Davis E, Zimmerman N, Rehberger T, et al. Dietary Bacillus subtilis- based direct-fed microbials alleviate LPS-induced intestinal immunological stress and improve intestinal barrier gene expression in commercial broiler chickens. *Res Vet Sci*. (2017) 114:236–43. doi: 10.1016/j.rvsc.2017.05.004
38. De Boever S, Vangestel C, De Backer P, Croubels S, Sys SU. Identification and validation of housekeeping genes as internal control for gene expression in an intravenous LPS inflammation model in chickens. *Vet Immunol Immunopathol*. (2008) 122:312–7. doi: 10.1016/J.VETIMM.2007.12.002
39. Johnson J, Reid WM. Anticoccidial drugs: lesion scoring techniques in battery and floor-pen experiments with chickens. *Exp Parasitol*. (1970) 28:30–6.
40. Lee SH, Lillehoj HS, Jang SI, Lillehoj EP, Min W, Bravo DM. Dietary supplementation of young broiler chickens with Capsicum and turmeric oleoresins increases resistance to necrotic enteritis. *Br J Nutr*. (2013) 110:840–7. doi: 10.1017/S0007114512006083
41. Jones LJ, Gray M, Yue ST, Haugland RP, Singer VL. Sensitive determination of cell number using the CyQUANT cell proliferation assay. *J Immunol Methods*. (2001) 254:85–98. doi: 10.1016/S0022-1759(01)00404-5
42. Hu J, Chang H, Wang L, Wu S, Shao B, Zhou J, et al. Detection, occurrence and fate of indirubin in municipal sewage treatment plants. *Environ Sci Technol*. (2008) 42:8339–44. doi: 10.1021/es801038y
43. Hu W, Sorrentino C, Denison MS, Kolaja K, Fielden MR. Induction of Cyp1a1 is a nonspecific biomarker of aryl hydrocarbon receptor activation: results of large scale screening of pharmaceuticals and toxicants *in vivo* and *in vitro*. *Mol Pharmacol*. (2007) 71:1475–86. doi: 10.1124/mol.106.032748
44. Del Cacho E, Gallego M, Lillehoj HS, Quílez J, Lillehoj EP, Ramo A, et al. IL-17A regulates *Eimeria tenella* schizont maturation and migration in avian coccidiosis. *Vet Res*. (2014) 45:25. doi: 10.1186/1297-9716-45-25
45. Traka MH. Health benefits of glucosinolates. *Adv Bot Res*. (2016) 80:247–79. doi: 10.1016/BS.ABR.2016.06.004
46. Higdon J, Delage B, Williams D, Dashwood R. Cruciferous vegetables and human cancer risk: epidemiologic evidence and mechanistic basis. *Pharmacol Res*. (2007) 55:224–36. doi: 10.1016/j.phrs.2007.01.009
47. Tang L, Zirpoli GR, Guru K, Moysich KB, Zhang Y, Ambrosone CB, et al. xConsumption of raw cruciferous vegetables is inversely associated with bladder. *Cancer Epidemiol Biomarkers Prev*. (2008) 17:938–44. doi: 10.1158/1055-9965.EPI-07-2502
48. Aggarwal BB, Ichikawa H. Molecular targets and anticancer potential of indole-3-carbinol and its derivatives. *Cell Cycle*. (2005) 4:1201–15. doi: 10.4161/cc.4.9.1993
49. Weng J-R, Bai L-Y, Chiu C-F, Wang Y-C, Tsai M-H. The dietary phytochemical 3,3′-diindolylmethane induces G2/M arrest and apoptosis in oral squamous cell carcinoma by modulating Akt-NF-κB, MAPK, and p53 signaling. *Chem Biol Interact*. (2012) 195:224–30. doi: 10.1016/j.cbi.2012.01.0031
50. Khwaja FS, Wynne S, Posey I, Djakiew D. 3,3′-Diindolylmethane Induction of p75NTR-dependent cell death via the p38 mitogen-activated protein kinase pathway in prostate cancer cells. *Cancer Prev Res*. (2009) 2:566–71. doi: 10.1158/1940-6207.CAPR-08-0202
51. Nachshon-Kedmi M, Yannai S, Haj A, Fares FA. Indole-3-carbinol and 3,3′-diindolylmethane induce apoptosis in human prostate cancer cells. *Food Chem Toxicol*. (2003) 41:745–52. doi: 10.1016/S0278-6915(03)00004-8
52. Fernandez-Salguero P, Pineau T, Hilbert DM, McPhail T, Lee SS, Kimura S, et al. Immune system impairment and hepatic fibrosis in mice lacking the dioxin-binding Ah receptor. *Science*. (1995) 268:722–6.
53. Singh NP, Hegde VL, Hofseth LJ, Nagarkatti M, Nagarkatti P. Resveratrol (trans-3,5,4′-trihydroxystilbene) ameliorates experimental allergic encephalomyelitis, primarily via induction of apoptosis in T cells involving activation of aryl hydrocarbon receptor and estrogen receptor. *Mol Pharmacol*. (2007) 72:1508–21. doi: 10.1124/mol.107.038984
54. Singh NP, Nagarkatti M, Nagarkatti P. Primary peripheral T cells become susceptible to 2,3,7,8-tetrachlorodibenzo-p-dioxin-mediated apoptosis *in vitro* upon activation and in the presence of dendritic cells. *Mol Pharmacol*. (2008) 73:1722–35. doi: 10.1124/mol.107.043406
55. Yasui T, Kim E-Y, Iwata H, Franks DG, Karchner SI, Hahn ME, et al. Functional characterization and evolutionary history of two aryl hydrocarbon receptor isoforms (AhR1 and AhR2) from avian species. *Toxicol Sci*. (2007) 99:101–17. doi: 10.1093/toxsci/kfm139
56. Lee J-S, Iwabuchi K, Nomaru K, Nagahama N, Kim E-Y, Iwata H. Molecular and functional characterization of a novel aryl hydrocarbon receptor isoform, AHR1β, in the Chicken (Gallus gallus). *Toxicol Sci*. (2013) 136:450–466. doi: 10.1093/toxsci/kft192
57. Gilday D, Gannon M, Yutzey K, Bader D, Rifkind AB. Molecular cloning and expression of two novel avian cytochrome P450 1A enzymes induced by 2,3,7,8-tetrachlorodibenzo-p-dioxin. *J Biol Chem*. (1996) 271:33054–9.
58. Sinclair PR, Gorman N, Walton HS, Sinclair JF, Lee CA, Rifkind AB. Identification of CYP1A5 as the CYP1A enzyme mainly responsible for uroporphyrinogen oxidation induced by AH receptor ligands in chicken liver and kidney. *Drug Metab Dispos*. (1997) 25:779–83.

59. Veldhoen M, Hirota K, Westendorf AM, Buer J, Dumoutier L, Renauld J-C, et al. The aryl hydrocarbon receptor links TH17-cell-mediated autoimmunity to environmental toxins. *Nature*. (2008) 453:106–9. doi: 10.1038/nature06881
60. Huang Z, Jiang Y, Yang Y, Shao J, Sun X, Chen J, et al. 3,3′-Diindolylmethane alleviates oxazolone-induced colitis through Th2/Th17 suppression and Treg induction. *Mol Immunol*. (2013) 53:335–44. doi: 10.1016/j.molimm.2012.09.007
61. Lillehoj HS, Trout JM. Coccidia: a review of recent advances on immunity and vaccine development. *Avian Pathol*. (1993) 22:3–31. doi: 10.1080/03079459308418897
62. Hong YH, Lillehoj HS, Lee SH, Dalloul RA, Lillehoj EP. Analysis of chicken cytokine and chemokine gene expression following *Eimeria acervulina* and *Eimeria tenella* infections. *Vet Immunol Immunopathol*. (2006) 114:209–23. doi: 10.1016/j.vetimm.2006.07.007
63. Hong YH, Lillehoj HS, Lillehoj EP, Lee SH. Changes in immune-related gene expression and intestinal lymphocyte subpopulations following *Eimeria maxima* infection of chickens. *Vet Immunol Immunopathol*. (2006) 114:259–72. doi: 10.1016/j.vetimm.2006.08.006
64. Min W, Lillehoj HS. Isolation and Characterization of Chicken Interleukin-17 cDNA. *J Interf Cytokine Res*. (2002) 22:1123–8. doi: 10.1089/10799900260442548
65. Negishi T, Kato Y, Ooneda O, Mimura J, Takada T, Mochizuki H, et al. Effects of aryl hydrocarbon receptor signaling on the modulation of TH1/TH2 balance. *J Immunol*. (2005) 175:7348–56. doi: 10.4049/jimmunol.175.11.7348
66. Beamer CA, Shepherd DM. Role of the aryl hydrocarbon receptor (AhR) in lung inflammation. *Semin Immunopathol*. (2013) 35:693–704. doi: 10.1007/s00281-013-0391-7
67. Sand JM, Arendt MK, Repasy A, Deniz G, Cook ME. Oral antibody to interleukin-10 reduces growth rate depression due to *Eimeria* spp. infection in broiler chickens. *Poult Sci*. (2016) 95:439–46. doi: 10.3382/ps/pev352
68. Arendt MK, Sand JM, Marcone TM, Cook ME. Interleukin-10 neutralizing antibody for detection of intestinal luminal levels and as a dietary additive in *Eimeria* challenged broiler chicks. *Poult Sci*. (2016) 95:430–438. doi: 10.3382/ps/pev365
69. Anderson JM. Molecular structure of tight junctions and their role in epithelial transport. *News Physiol Sci*. (2001) 16:126–30. doi: 10.1152/physiologyonline.2001.16.3.126
70. Chen Y, Yang P, Li F, Kijlstra A. The effects of Th17 cytokines on the inflammatory mediator production and barrier function of ARPE-19 cells. *PLoS ONE*. (2011) 6:e18139. doi: 10.1371/journal.pone.0018139
71. McNaughton SA, Marks GC. Development of a food composition database for the estimation of dietary intakes of glucosinolates, the biologically active constituents of cruciferous vegetables. *Br J Nut*. (2003) 90:687–97. doi: 10.1079/BJN2003917
72. Ciska E, Martyniak-Przybyszewska B, Kozlowska H. Content of glucosinolates in cruciferous vegetables grown at the same site for two years under different climatic conditions. *J Agric Food Chem*. (2000) 48:2862–7. doi: 10.1021/jf981373a
73. *FDA Specific Requirements for Health Claims*, 21 C.F.R § 101.78 (1993).
74. Minich DM, Bland JS. A review of the clinical efficacy and safety of cruciferous vegetable phytochemicals. *Nutr Rev*. (2007) 65:259–67. doi: 10.1111/j.1753-4887.2007.tb00303.x

Conflict of Interest Statement: The authors declare that the research was conducted in the absence of any commercial or financial relationships that could be construed as a potential conflict of interest.

frontiers in Immunology

MINI REVIEW
published: 22 November 2019
doi: 10.3389/fimmu.2019.02732

Involvement of T Cell Immunity in Avian Coccidiosis

*Woo H. Kim†, Atul A. Chaudhari† and Hyun S. Lillehoj**

Animal Biosciences and Biotechnology Laboratory, U.S. Department of Agriculture, Beltsville Agricultural Research Center, ARS, Beltsville, MD, United States

Avian coccidiosis is caused by *Eimeria*, which is an intracellular apicomplexan parasite that invades through the intestinal tract to cause devastating disease. Upon invasion through the intestinal epithelial cells, a strong inflammatory response is induced that results in complete villous destruction, diarrhea, hemorrhage, and in severe cases, death. Since the life cycle of *Eimeria* parasites is complex and comprises several intra- and extracellular developmental stages, the host immune responses are diverse and complex. Interferon-γ-mediated T helper (Th)1 response was originally considered to be the predominant immune response in avian coccidiosis. However, recent studies on other avian T cell lineages such as Th17 and T regulatory cells have implicated their significant involvement in maintaining gut homeostasis in normal and disease states including coccidiosis. Therefore, there is a need to understand better their role in coccidiosis. This review focuses on research findings concerning the host immune response induced by avian coccidiosis in the context of T cell immunity, including expression of T-cell-related cytokines and surface molecules that determine the phenotype of T lymphocytes.

Keywords: chicken, coccidiosis, T cells, avian immunology, host immunity

OPEN ACCESS

Edited by:
Armin Saalmueller, University of Veterinary Medicine Vienna, Austria

Reviewed by:
Renato Augusto DaMatta, Universidade Estadual Do Norte Fluminense Darcy Ribeiro, Brazil
Guangwen Yin, Fujian Agriculture and Forestry University, China

***Correspondence:**
Hyun S. Lillehoj
Hyun.Lillehoj@ars.usda.gov

†These authors have contributed equally to this work

Specialty section:
This article was submitted to Comparative Immunology, a section of the journal Frontiers in Immunology

Received: *31 July 2018*
Accepted: *07 November 2019*
Published: *22 November 2019*

Citation:
Kim WH, Chaudhari AA and Lillehoj HS (2019) Involvement of T Cell Immunity in Avian Coccidiosis. Front. Immunol. 10:2732. doi: 10.3389/fimmu.2019.02732

INTRODUCTION

Avian coccidiosis is caused by intracellular protozoan parasites that belong to several different species of *Eimeria* (1, 2). This apicomplexan parasite invades intestinal epithelial tissues and causes severe damage in birds, resulting in enormous economic losses in the poultry industry. The major challenge in coccidiosis control is the diversity among several *Eimeria* species that target different specific regions of the intestine.

The coccidia exhibit a complex life cycle comprising both intracellular and extracellular stages as well as asexual and sexual reproduction (3, 4). The life cycle mainly consists of an exogenous stage, characterized by excretion of unsporulated oocysts, and endogenous stage of schizogony (asexual reproduction) and gametogony (sexual differentiation) (5, 6). During the exogenous stage, the unsporulated oocysts become sporulated (with four sporocysts, each containing two sporozoites) under the influence of external environmental factors such as moisture, oxygen, and warmth. The endogenous stage occurs inside the host, which involves several stages of asexual reproduction followed by sexual reproduction, fertilization, and shedding of the unsporulated oocysts. In general, two to four generations of asexual reproduction are followed by the sexual phase, in which zygote formation takes place that eventually matures into oocysts that are released in the intestinal mucosa and finally shed into feces (7). The coccidia life cycle is usually short (4–6 days depending on several different species) and production of sporulating oocysts can easily increase the infectivity of the parasites in a large population of chickens. After ingesting the sporulated oocysts, excystation of

oocysts occurs in the gizzard and the sporozoites are released, invade the intestinal cells, and cause severe damage as the reproductive cycle of the parasite begins. As a result, symptoms such as bloody diarrhea and reduced body weight and feed intake are observed in the birds.

Upon exposure to developing schizonts, anti-*Eimeria* immunity develops and is subsequently boosted by multiple re-exposures to oocysts (7). The immunity to avian coccidiosis can be categorized as innate and adaptive (8). As a first line of defense, the innate immune response is activated in response to the conserved antigens. Innate immune responses include recognition of conserved pathogen-associated molecular patterns (PAMPs) by pattern recognition receptors (PRRs) such as Toll-like receptors (TLRs) (5, 9, 10). A major TLR ligand, profilin, is expressed in all the developmental stages of the life cycle of several *Eimeria* parasites and is conserved (11). Such ligands induce a robust innate response such as immune cell proliferation and cytokine production. The cells involved in innate immune responses to *Eimeria* parasites at different phases are natural killer (NK) cells, dendritic cells, epithelial cells, heterophils, and macrophages. In particular, macrophage migration inhibitory factor plays a crucial role in mediating innate immunity in coccidiosis (12).

On the other hand, adaptive immunity is specific and regulates the antigen-specific immune responses to prevent colonization and growth of the pathogen inside the host. Like mammals, two major lymphocyte types, B cells (producing surface immunoglobulins) and T cells (T cell receptors), are the major components of adaptive immune responses in birds (13). Anticoccidial antibodies in serum and mucosal secretions have been reported in avian coccidiosis (13). Although B cell depletion studies (14) have revealed that antibodies do not play a specific role in anticoccidial protective immunity, other studies have emphasized the importance of passively transferred humoral immunity in *Eimeria* infection in chickens (15–18). Cell-mediated immunity in avian coccidiosis is characterized by antigen-specific or non-specific activation of several immune cells such as T cells, NK cells, and macrophages. The $CD4^+$ T helper (Th) cells and $CD8^+$ cytotoxic T lymphocytes (CTLs) are the two major T-cell subsets that are involved in anticoccidial immunity (19–22). Although the role of several T-cell subpopulations in avian coccidiosis remains to be elucidated, T cells are the most important for protection against *Eimeria* infections in birds.

In this article, we reviewed the historical progress of immunological studies on the host immune response to avian coccidiosis, with an emphasis on recent findings in the understanding of the complexity of T-cell immune responses in avian coccidiosis, especially those mediated by Th17 and T regulatory (Treg) cells.

DEVELOPMENT OF IMMUNOLOGY IN AVIAN COCCIDIOSIS

Since the first report of chicken coccidiosis in the cecum in the late eighteenth century (1), immunity to several *Eimeria* parasites has been investigated thoroughly. An important contribution from Rose and colleagues (23) defined the basic principles of avian immunity to coccidial parasites in terms of specificity, wherein one species of *Eimeria* offers little protection against heterologous challenge with other species. Over the past few decades, studies focusing on investigating the role of avian immunity in response to various coccidial parasites has shown promising developments toward better understanding of avian immunity to coccidiosis (20, 24, 25). From all these studies, it was apparent that out of the two types of immunity, cellular immunity was more important than humoral immunity in coccidiosis, as the later offered little protection against the infection. Early investigations in both mammalian and avian species have revealed that the cellular immune responses through T cells and their associated cytokines play an important role in anticoccidial immunity (2, 26, 27). Acquired immunity to murine coccidiosis is attributed more to T cells than B cells (26). Several immune cell types including NK cells, dendritic cells, and macrophages are involved in innate immune responses to avian coccidiosis (8, 27). B-cell-deficient chickens have shown increased oocyst production after primary infection with *Eimeria* species. However, secondary infection does not yield clinical coccidiosis in the bursectomized chickens due to the protective immunity acquired by the primary infection (8). This indicates that the anticoccidial immunity acquired after primary infection is B cell independent. It is also apparent that chicken coccidiosis can be prevented by adaptive transfer of peripheral blood lymphocytes and splenocytes from *Eimeria*-infected chickens in the syngeneic recipients (28). Subsequently, the T-cell immunosuppressant cyclosporin A abolished the protective immunity offered by *Eimeria* re-infection, thus further emphasizing the integral role of cellular immune mechanisms in chicken coccidiosis (14).

The early findings indicated that T cells serve as a key factor to mediate anticoccidial immunity in chickens (8, 14). Greater numbers of CTLs expressing CD8 cell surface antigen were predominantly observed in chickens after primary infection (29–31). Furthermore, the differential role of $CD4^+$ and $CD8^+$ T lymphocytes in offering resistance to primary and secondary coccidial infection was also reported (32, 33). Increased populations of T cells are linked to elevated production of proinflammatory cytokine interferon (IFN)-γ, which has an immunoregulatory effect (34), as well as inhibiting intracellular development of the parasite (35, 36). The role of T cells in mediating host immunity to coccidiosis became more evident when flow cytometric analysis of intestinal epithelial lymphocytes (IELs), using lymphocyte-specific immune reagents, revealed their significance in innate immunity in naïve chickens and adaptive immunity in previously infected chickens (19, 37, 38). More studies showed that different IEL subtypes are involved in anti-*Eimeria* defense in the gut (39, 40). Research over the past several years has shown that, as a part of protective immunity against avian coccidiosis, T cells produce numerous secretions besides IFN-γ, such as cytokines interleukin (IL)-1, IL-2, IL-4–6, IL-8, IL-10, IL-12, IL-13, and IL-15–18, tumor necrosis factor (TNF)-α, lipopolysaccharide-induced TNF-α factor (LITAF), TNF-α superfamily 15 (TNFSF15), transforming growth factor

(TGF)-β1–4, and granulocyte–macrophage colony-stimulatory factor (GM-CSF). All these findings are based on research oriented toward investigating the immunoregulatory responses of these molecules after primary and/or secondary coccidiosis (40–60). More recent work has indicated the involvement of TLR4 and TLR15 as a part of the innate immune response to *Eimeria* infection (61). IL-17 also contributes to host immunopathology in response to experimental infection (62). The immunoproteomics analysis of three *Eimeria* species has identified several immunodominant antigens from these three species that could provide a useful breakthrough in exploring anticoccidial immunity, as some of these molecules cause profuse inflammatory and cellular immune response that contribute to pathogenesis and severity of infection (3, 63). Additionally, research on anticoccidial vaccines and natural alternatives has explored the immunobiology of coccidiosis in poultry (7). All these findings show the immunoregulatory effect of vaccines or several naturally occurring anti-inflammatory products such as curcumin and *Allium hookeri*. These findings also provide a useful insight into immunoregulation in avian coccidiosis, however, this is outside the scope of this review and has been reviewed previously (7). Much of this work has focused on immunomodulation by dietary ingredients in experimental *Eimeria* infections (64, 65).

Besides the above information, immunological variation among the different strains of the same *Eimeria* species has also been reported in chickens (66, 67). These findings show the characteristic intraspecific variations attributed to the biological features of *Eimeria*, such as morphology of oocysts, pathogenicity, and sensitivity to drugs (68). This inter- and intraspecies variation has been recently defined with the help of more advanced molecular approaches such as random amplification of polymorphic DNA–PCR, and restricted or amplified fragment length polymorphism (69). Analysis of these variations has led to the identification of several strain-specific immunoprotective antigens (70, 71). Similarly, more recent findings have also highlighted the variation in immune responses to *Eimeria tenella* infection in genetically distinct chicken lineages (72).

ROLE OF IFN-γ-MEDIATED IMMUNITY IN AVIAN COCCIDIOSIS

Among all the cytokines mentioned above, IFN-γ is a major cytokine that has anticoccidial effects (73). In mammals, parasitic infections are often characterized by increased levels of IFN-γ. Similarly, the functional role of this cytokine in *Eimeria* infections has been studied thoroughly (34, 74, 75). Until the cDNA cloning of chicken IFNs revealed the independent existence of type I (76) (IFN-α) and type II (77) (IFN-γ) IFNs, most of the findings on the role of IFN-like activity in *Eimeria* infections were believed to be associated with IFN-γ. All these IFN-dependent activities inhibit the invasion or development of *Eimeria* in cultured cells *in vitro* (73, 78). *In vivo* studies have also revealed the anticoccidial IFN-like activity in *Eimeria*-infected birds (79, 80). The specific involvement of IFN-γ in anti-*Eimeria* immunity was later described by Breed et al. who showed that IFN-γ was produced specifically after stimulation of peripheral blood lymphocytes from *Eimeria*-infected birds (31). It was then discovered that mitogen- or antigen-stimulated specific T cells circulating in the blood of *Eimeria*-infected chickens specifically produced IFN-γ (81). Based on these findings, it was proposed that T-cell priming might occur at the site of infection, resulting in production of IFN-γ at the infection site, thus regulating anticoccidial immunity (81). It was also hypothesized that $CD8^+$ cells produce IFN-γ, which is involved in immunoregulation in primary coccidiosis (81). These findings were extended by Rothwell et al. who showed that IFN-γ-producing cells were present in blood and the spleen and may migrate from the spleen after secondary infection (82). *In situ* hybridization has shown that, following *Eimeria* challenge, IFN-γ is produced by the cells (predominantly T cells) at the site of infection (cecum) and by splenocytes (82). Several studies have shown the potential application of IFN-γ in protecting against *Eimeria* infections (36, 83, 84). Birds immunized with recombinant IFN-γ show increased body weight gain during infection with *Eimeria acevirulina* (36, 83). Also, the development of *E. tenella* is inhibited by IFN-γ *in vitro* (36, 84). When chicken cells are treated with recombinant IFN-γ, intracellular development of *E. tenella* is inhibited, with no significant effect on sporozoite invasion of the cells (36). Similarly, *in vivo* administration of recombinant IFN-γ protects against *E. acevirulina* characterized by reduced oocyst production and increased body weight gain (36, 83).

Besides its immunoregulatory or immunoprotective effect against chicken coccidiosis, IFN-γ has also been shown to have an adjuvant effect on coccidial vaccine in *Eimeria*-infected chickens (85). The adjuvant effect of IFN-γ is characterized by enhanced immune response to the vaccine antigen that induces a microbicidal effect to resolve the parasitic infection, thus increasing vaccine efficacy (85). Some DNA vaccines administered with IFN-γ increased the immunity at intestinal level and protected against avian coccidiosis (36, 86, 87). Recent studies have also indicated the beneficial effect of IFN-γ on anticoccidial DNA vaccine (88, 89). A chimeric vaccine constructed by fusion of genes encoding the *E. tenella* surface antigen, and IFN-γ alleviated the cecal lesions and improved the anticoccidial index in experimentally infected chickens, further suggesting the adjuvant effect of IFN-γ (89). Thus, all these efforts indicate the anticoccidial role of IFN-γ, direct, or as an adjuvant, and underline the significance of IFN-γ in anticoccidial immunity.

Th17 CELLS AND THEIR CYTOKINES IN AVIAN COCCIDIOSIS

Besides the response elicited by IFN-γ-mediated Th1 cells against avian coccidiosis, the other CD4 T-cell subsets have also been studied since the discovery of their homologs in mammals (42). A lineage of IL-17-producing $CD4^+$ T helper (Th)17 cells

that are distinct from the previously well-characterized Th1/Th2 paradigm, has emerged and is involved in proinflammatory responses in various autoimmune diseases and infections (90). The biological activities of IL-17 as a signature cytokine of Th17 cells include recruitment of neutrophils, stimulation of antimicrobial peptide production, such as β-defensins and mucins, as well as induction of cytokines and chemokines, in particular IL-6, CXCL8 and GM-CSF (91). Chicken IL-17 isolated from *Eimeria*-infected IELs exerts a proinflammatory role in coccidiosis (8). The exact role of Th17 cells in chicken is poorly understood due to the lack of immunological reagents. This section describes studies that focused on the role of IL-17 as a signature cytokine in Th17 cells in chicken coccidiosis. Following infection by *E. acervulina* or *E. maxima*, IL-17 mRNA levels were increased in IELs compared to uninfected controls (40). In *E. tenella* infection, IL-17 expression in IELs was downregulated, except in the latter stage of infection (39). Similarly, Kim et al. reported that chicken IL-17 expression was downregulated in inflamed intestinal tissue following *E. tenella* infection, and treatment with IL-17 or IL-17F induced expression of proinflammatory cytokines in chicken fibroblasts (92). These results suggest that chicken coccidiosis induces IL-17 expression in the gut and is dependent on the species of *Eimeria*. Th17 response can play both protective and pathological roles in protozoan infections. The cloning of IL-17 receptor A (IL-17RA), which binds IL-17A and IL-17F in chickens, has revealed that *Eimeria* infection downregulates expression of IL-17RA, and modulation of this receptor facilitates the host to reduce intestinal pathogenesis amplified by IL-17/IL-17RA signaling. Several authors have proposed that Th17 cells or IL-17 promote pathogenesis in leishmaniasis, toxoplasmosis, and *Eimeria falciformis* infection (93–95), whereas others have demonstrated that they are involved in protective immunity against trypanosomiasis, toxoplasmosis and *Pneumocystis carinii* infection (96, 97). Recent evidence seems to support a role for Th17 cytokines in host immunopathology in coccidiosis in chickens. Treatment with IL-17 neutralizing antibody in *E. tenella* infection induces lower heterophil recruitment, inflammatory cytokine expression, and parasite burden in the intestinal tract, resulting in enhanced body weight gain, reduced oocyst production in feces, and intestinal lesions (62). IL-17 is also involved in the initiation and migratory response of epithelial cells during intracellular development, and maturation of parasites, contributing to pathogenesis in the intestinal tract. Following *E. tenella* infection, chickens treated with IL-17 neutralizing antibody have a reduced number of second-generation schizonts and cecal lesions (98).

ANTI-INFLAMMATORY IL-10 AND Treg CELLS IN AVIAN COCCIDIOSIS

Treg cells are a subset of T cells involved in immunosuppression. Mammalian Treg cells have the phenotype $CD4^+CD25^+FoxP3^+$ (99). In chickens, the ortholog of mammalian FoxP3 has yet to be identified, although there is a report of an avian *foxp3* gene (100, 101). Thus, $CD4^+CD25^+$ T cells in chickens have been characterized as Treg cells showing suppression of activated immune cells (102). These cells produce high amounts of IL-10, TGF-β, CTLA-4, and LAG-3, as in mammals (103). IL-10 showed 29-fold higher expression in $CD4^+CD25^+$ cells compared to $CD4^+CD25^-$ cells and its immunosuppression in chickens has been extensively studied (102). In coccidiosis, IL-10 is considered to play an important role in evasion of the host immune response. One possible mechanism to explain its role in coccidiosis is that coccidial parasites have evolved to stimulate Treg cells to express IL-10, and it helps parasites to facilitate invasion and survival in chickens through suppression of the IFN-γ-related Th1 response that is critical for protective immunity against coccidial parasites. Two inbred lines of chickens that differ in their resistance or susceptibility to *Eimeria* infection have revealed that expression of IL-10 is the major difference between the two lines. Expression of IL-10 is highly induced in susceptible chickens among the genes related to different Th lineages, such as IFN-γ for Th1, IL-4 for Th2, and IL-10 and TGF-β for Treg cells, while IL-10 is suppressed in the age-matched resistant line (46). *Eimeria*-infected chickens treated with IL-10 neutralizing antibody show improved growth rate compared to those with control antibody but it has no effect on fecal oocyst production (104, 105). Morris et al. reported that supplementation of vitamin D induced IL-10 expression as well as Treg cells and showed decreased production losses associated with coccidial infection (106). These results indicate that regulation of the protective immune response to *Eimeria* infection by Treg cells is critical, and IL-10 plays a role in pathogenesis in chicken coccidiosis. We recently identified that Treg cells could help to reduce pathology in *Eimeria*-infected intestine by suppression of Th17 cells that induce tissue inflammation. Increased expression of $CD4^+CD25^+$ Treg cells has been found in *E. tenella*-infected chickens with increased IL-10 expression. After treatment with aryl hydrocarbon receptor such as 3,3′-diindolylmethane, Treg cells are increased in the intestine, whereas $CD4^+IL\text{-}17^+$ Th17 cells are suppressed. We have also found that generation of Th17 cells is suppressed by Treg cells, which leads to reduced pathogenicity in chicken coccidiosis (107).

CONCLUDING REMARKS

It is the consensus that the Th1 response is the most efficient host response in avian coccidiosis. However, studies on other aspects like Th17 and Treg responses are also important because the immune responses are not independent, but rather they are connected and work together in an integrated immune system. It is becoming clear that the outcome of an inflammatory process caused by infection depends on the balance of responses by several components of the immune system of particular relevance is the interplay between Treg and Th17 cells during immunoinflammatory events (108). Compared to mammalian immunology, little is known about the role of T cells in chickens, although the number of reports on

coccidiosis is steadily growing. To understand better immunity against chicken coccidiosis, it is necessary to know how T cells are modulated and how they interplay since this intracellular pathogen predominantly induces a T-cell-associated immune response that involves several types of T cells. In regard to controlling coccidiosis, the best way might be development of alternatives to antibiotics because most effective anticoccidial drugs that produce resistance or residues will be banned from the market in the future. Understanding the mechanism of how chickens respond to *Eimeria* will lead to new approaches to control coccidiosis.

AUTHOR CONTRIBUTIONS

All authors listed have made a substantial, direct and intellectual contribution to the work, and approved it for publication.

FUNDING

This research was supported, in part, by an ARS CRIS project 8042-32000-106-00D and by Development of Poultry Immune Reagent program (Award No: 2017-67015-26793) funded by USDA/NIFA.

REFERENCES

1. Railliet ALA. Developpement experimental des coccidies de l'epithelium intestinal du lapin et de la poule. *C R Soc Biol Paris*. (1891) 36:820–3.
2. Rose ME, Hesketh P. Immunity to coccidiosis : t-lymphocyte- deficient animals B-lymphocyte-. *Immunology*. (1979) 26:630–7.
3. Lal K, Bromley E, Oakes R, Prieto JH, Sanderson SJ, Kurian D, et al. Proteomic comparison of four *Eimeria tenella* life-cycle stages: Unsporulated oocyst, sporulated oocyst, sporozoite and second-generation merozoite. *Proteomics*. (2009) 9:4566–76. doi: 10.1002/pmic.200900305
4. Norton CC, Chard MJ. The oocyst sporulation time of *Eimeria* species from the fowl. *Parasitology*. (1983) 86:193–8. doi: 10.1017/S0031182000050368
5. Dalloul RA, Lillehoj HS. Recent advances in immunomodulation and vaccination strategies against coccidiosis. *Avian Dis*. (2005) 49:1–8. doi: 10.1637/7306-11150R
6. Gilbert ER, Cox CM, Williams PM, McElroy AP, Dalloul RA, Keith Ray W, et al. *Eimeria* species and genetic background influence the serum protein profile of broilers with coccidiosis. *PLoS ONE*. (2011) 6:e14636. doi: 10.1371/journal.pone.0014636
7. Quiroz-Castañeda RE, Dantán-González E. Control of avian coccidiosis: future and present natural alternatives. *BioMed Res Int*. (2015) 2015:430610. doi: 10.1155/2015/430610
8. Min W, Kim WH, Lillehoj EP, Lillehoj HS. Recent progress in host immunity to avian coccidiosis: IL-17 family cytokines as sentinels of the intestinal mucosa. *Dev Compar Immunol*. (2013) 41:418–28. doi: 10.1016/j.dci.2013.04.003
9. Kumar H, Kawai T, Akira S. Pathogen recognition by the innate immune system. *Int Rev Immunol*. (2011) 30:16–34. doi: 10.3109/08830185.2010.529976
10. Brownlie R, Allan B. Avian toll-like receptors. *Cell Tissue Res*. (2011) 343:121–30. doi: 10.1007/s00441-010-1026-0
11. Fetterer RH, Miska KB, Jenkins MC, Barfield RC. A conserved 19-kDa *Eimeria tenella* antigen is a profilin-like protein. *J Parasitol*. (2004) 90:1321–8. doi: 10.1645/GE-307R
12. Sun H-W, Bernhagentt J, Bucalat R, Lolis E. Crystal structure at 2.6-A resolution of human macrophage migration inhibitory factor. *Proc Natl Acad Sci USA*. (1996) 93:5191–6. doi: 10.1073/pnas.93.11.5191
13. Girard F, Fort G, Yvore P, Quere P. Kinetics of specific immunoglobulin A, M and G production in the duodenal and caecal mucosa of chickens infected with *Eimeria acervulina* or *Eimeria tenella*. *Int J Parasitol*. (1997) 27:803–9. doi: 10.1016/S0020-7519(97)00044-1
14. Lillehoj HS. Effects of immunosuppression on avian coccidiosis: cyclosporin A but not hormonal bursectomy abrogates host protective immunity. *Infect Immun*. (1987) 55:1616–21.
15. Wallach M, Halabi A, Pillemer G, Sar-Shalom O, Mencher D, Gilad M, et al. Maternal immunization with gametocyte antigens as a means of providing protective immunity against *Eimeria maxima* in chickens. *Infect Immun*. (1992) 60:2036–9.
16. Wallach M. Role of antibody in immunity and control of chicken coccidiosis. *Trends Parasitol*. (2010) 26:382–7. doi: 10.1016/j.pt.2010.04.004
17. Lee SH, Lillehoj HS, Park DW, Jang SI, Morales A, García D, et al. Induction of passive immunity in broiler chickens against *Eimeria acervulina* by hyperimmune egg yolk immunoglobulin Y. *Poultry Science*. (2009) 88:562–6. doi: 10.3382/ps.2008-00340
18. Lee SH, Lillehoj HS, Park DW, Jang SI, Morales A, García D, et al. Protective effect of hyperimmune egg yolk IgY antibodies against *Eimeria tenella* and *Eimeria maxima* infections. *Vet Parasitol*. (2009) 163:123–6. doi: 10.1016/j.vetpar.2009.04.020
19. Lillehoj HS. Role of T lymphocytes and cytokines in coccidiosis. *Int J Parasitol*. (1998) 28:1071–81. doi: 10.1016/S0020-7519(98)00075-7
20. Lillehoj HS, Lillehoj EP. Avian coccidiosis. A review of acquired intestinal immunity and vaccination strategies. *Avian Dis*. (2000) 44:408–25. doi: 10.2307/1592556
21. Trout JM, Lillehoj HS. T lymphocyte roles during *Eimeria acervulina* and *Eimeria tenella* infections. *Vet Immunol Immunopathol*. (1996) 53:163–72. doi: 10.1016/0165-2427(95)05544-4
22. Yun CH, Lillehoj HS, Lillehoj EP. Intestinal immune responses to coccidiosis. *Dev Compar Immunol*. (2000) 24:303–24. doi: 10.1016/S0145-305X(99)00080-4
23. Rose ME, Long PL. Immunity to four species of *Eimeria* in fowls. *Immunology*. (1962) 5:79–92.
24. Allen PC, Fetterer RH. Recent advances in biology and immunobiology of *Eimeria* species and in diagnosis and control of infection with these coccidian parasites of poultry. *Clin Microbiol Rev*. (2002) 15:58–65. doi: 10.1128/CMR.15.1.58-65.2002
25. Shirley MW, Lillehoj HS. The long view: a selective review of 40 years of coccidiosis research. *Avian Pathol*. (2012) 41:111–21. doi: 10.1080/03079457.2012.666338
26. Rose ME, Ogilvie BM, Hesketh P, Festing MFW. Failure of nude. (athymic) rats to become resistant to reinfection with the intestinal coccidian parasite *Eimeria nieschulzi* or the nematode *Nippostrongylus brasiliensis*. *Parasite Immunol*. (1979) 1:125–32. doi: 10.1111/j.1365-3024.1979.tb00700.x
27. Wakelin D, Rose ME, Hesketh P, Else KJ, Grencis RK. Immunity to coccidiosis: genetic influences on lymphocyte and cytokine responses to infection with *Eimeria vermiformis* in inbred mice. *Parasite Immunol*. (1993) 15:11–9. doi: 10.1111/j.1365-3024.1993.tb00567.x
28. Rose ME, Hesketh P, Ogilvie BM. Peripheral blood leucocyte response to coccidial infection: a comparison of the response in rats and chickens and its correlation with resistance to reinfection. *Immunology*. (1979) 36:71–9.
29. Lillehoj HS, Bacon LD. Increase of intestinal intraepithelial lymphocytes expressing CD8 antigen following challenge infection with *Eimeria acervulina*. *Avian Dis*. (1991) 35:294–301. doi: 10.2307/1591179
30. Breed DGJ, Dorrestein J, Vermeulen AN. Immunity to *Eimeria tenella* in chickens: phenotypical and functional changes in peripheral blood T-cell subsets. *Avian Dis*. (1996) 40:37–48. doi: 10.2307/1592369
31. Breed DGJ, Dorrestein J, Schetters TPM, Waart LVD, Rijke E, Vermeulen AN. Peripheral blood lymphocytes from *Eimeria tenella* infected chickens produce gamma-interferon after stimulation *in vitro*. *Parasite Immunol*. (1997) 19:127–35. doi: 10.1046/j.1365-3024.1997.d01-191.x
32. Rose ME, Hesketh P, Wakelin D. Immune control of murine coccidiosis: CD4+ and CD8+ T lymphocytes contribute differentially in resistance

to primary and secondary infections. *Parasitology*. (1992) 105:349–354. doi: 10.1017/S0031182000074515
33. Rothwell L, Gramzinski RA, Rose ME, Kaiser P. Avian coccidiosis: changes in intestinal lymphocyte populations associated with the development of immunity to *Eimeria maxima*. *Parasite Immunol*. (1995) 17:525–33. doi: 10.1111/j.1365-3024.1995.tb00883.x
34. Rose ME, Wakelin D, Hesketh P. Interferon-gamma-mediated effects upon immunity to coccidial infections in the mouse. *Parasite Immunol*. (1991) 13:63–74. doi: 10.1111/j.1365-3024.1991.tb00263.x
35. Choi KD, Lillehoj HS, Song KD, Han JY. Molecular and functional characterization of chicken IL-15. *Dev Compar Immunol*. (1999) 23:165–77. doi: 10.1016/S0145-305X(98)00046-9
36. Lillehoj HS, Choi KD. Recombinant chicken interferon-gamma-mediated inhibition of Eimeria tenella development *in vitro* and reduction of oocyst production and body weight loss following *Eimeria acervulina* challenge infection. *Avian Dis*. (1998) 42:307–14. doi: 10.2307/1592481
37. Lillehoj HS. Lymphocytes involved in cell-mediated immune responses and methods to assess cell-mediated immunity. *Poultry Sci*. (1991) 70:1154–64. doi: 10.3382/ps.0701154
38. Lillehoj HS. Analysis of *Eimeria acervulina*-induced changes in the intestinal T lymphocyte subpopulations in two chicken strains showing different levels of susceptibility to coccidiosis. *Res Vet Sci*. (1994) 56:1–7. doi: 10.1016/0034-5288(94)90188-0
39. Hong YH, Lillehoj HS, Lillehoj EP, Lee SH. Changes in immune-related gene expression and intestinal lymphocyte subpopulations following *Eimeria maxima* infection of chickens. *Vet Immunol Immunopathol*. (2006) 114:259–72. doi: 10.1016/j.vetimm.2006.08.006
40. Hong YH, Lillehoj HS, Lee SH, Dalloul RA, Lillehoj EP. Analysis of chicken cytokine and chemokine gene expression following *Eimeria acervulina* and *Eimeria tenella* infections. *Vet Immunol Immunopathol*. (2006) 114:209–23. doi: 10.1016/j.vetimm.2006.07.007
41. Avery S, Rothwell L, Degen WDJ, Schijns VEJC, Young J, Kaufman J, et al. Characterization of the first nonmammalian T2 cytokine gene cluster: the cluster contains functional single-copy genes for IL-3, IL-4, IL-13, and GM-CSF, a gene for IL-5 that appears to be a pseudogene, and a gene encoding another cytokinelike transcript. *J Interf Cytokine Res*. (2004) 24:600–10. doi: 10.1089/jir.2004.24.600
42. Min W, Lillehoj HS. Isolation and characterization of chicken interleukin-17 cDNA. *J Interf Cytokine Res*. (2002) 22:1123–8. doi: 10.1089/10799900260442548
43. Min W, Lillehoj HS. Identification and characterization of chicken interleukin-16 cDNA. *Dev Compar Immunol*. (2004) 28:153–62. doi: 10.1016/S0145-305X(03)00133-2
44. Min W, Lillehoj HS, Fetterer RH. Identification of an alternatively spliced isoform of the common cytokine receptor γ chain in chickens. *Biochem Biophys Res Commun*. (2002) 299:321–7. doi: 10.1016/S0006-291X(02)02636-0
45. Pan H, Halper J. Cloning, expression, and characterization of chicken transforming growth factor β4. *Biochem Biophys Res Commun*. (2003) 303:24–30. doi: 10.1016/S0006-291X(03)00300-0
46. Rothwell L, Young JR, Zoorob R, Whittaker CA, Hesketh P, Archer A, et al. Cloning and characterization of chicken IL-10 and its role in the immune response to *Eimeria maxima*. *J Immunol*. (2004) 173:2675–82. doi: 10.4049/jimmunol.173.4.2675
47. Schneider K, Puehler F, Baeuerle D, Elvers S, Staeheli P, Kaspers B, et al. cDNA cloning of biologically active chicken interleukin-18. *J Interf Cytokine Res*. (2000) 20:879–83. doi: 10.1089/107999000501 63244
48. Schneider K, Klaas R, Kaspers B, Staeheli P. Chicken interleukin-6: cDNA structure and biological properties. *Eur J Biochem*. (2001) 268:4200–6. doi: 10.1046/j.1432-1327.2001.02334.x
49. Song KD, Lillehoj HS, Choi KD, Zarlenga D, Han JY. Expression and functional characterization of recombinant chicken interferon-gamma. *Vet Immunol Immunopathol*. (1997) 58:321–33. doi: 10.1016/S0165-2427(97)00034-2
50. Yoo J, Jang SI, Kim S, Cho JH, Lee HJ, Rhee MH, et al. Molecular characterization of duck interleukin-17. *Vet Immunol Immunopathol*. (2009) 132:318–22. doi: 10.1016/j.vetimm.2009.06.003
51. Zhang S, Lillehoj HS, Ruff MD. Chicken tumor necrosis-like factor. I. *In vitro* production by macrophages stimulated with *Eimeria tenella* or bacterial lipopolysaccharide. *Poultry Sci*. (1995) 74:1304–10. doi: 10.3382/ps.0741304
52. Degen WGJ, van Daal N, van Zuilekom HI, Burnside J, Schijns VEJC. Identification and molecular cloning of functional chicken IL-12. *J Immunol*. (2004) 172:4371–80. doi: 10.4049/jimmunol.172.7.4371
53. Hong YH, Lillehoj HS, Hyen Lee S, Woon Park D, Lillehoj EP. Molecular cloning and characterization of chicken lipopolysaccharide-induced TNF-A factor. (LITAF). *Dev Compar Immunol*. (2006) 30:919–29. doi: 10.1016/j.dci.2005.12.007
54. Jakowlew SB, Dillard PJ, Winokur TS, Flanders KC, Sporn MB, Roberts AB. Expression of transforming growth factor-βs 1-4 in chicken embryo chondrocytes and myocytes. *Dev Biol*. (1991) 143:135–48. doi: 10.1016/0012-1606(91)90061-7
55. Jeong J, Lee C, Yoo J, Koh PO, Kim YH, Chang HH, et al. Molecular identification of duck and quail common cytokine receptor γ chain genes. *Vet Immunol Immunopathol*. (2011) 140:159–65. doi: 10.1016/j.vetimm.2010.11.023
56. Jeong J, Kim WH, Yoo J, Lee C, Kim S, Cho J-H, et al. Identification and comparative expression analysis of interleukin 2/15 receptor β chain in chickens infected with *E. tenella*. *PLoS ONE*. (2012) 7:e37704. doi: 10.1371/journal.pone.0037704
57. Koskela K, Kohonen P, Salminen H, Uchida T, Buerstedde JM, Lassila O. Identification of a novel cytokine-like transcript differentially expressed in avian γδ T cells. *Immunogenetics*. (2004) 55:845–54. doi: 10.1007/s00251-004-0643-8
58. Kaiser P, Poh TY, Rothwell L, Avery S, Balu S, Pathania US, et al. A genomic analysis of chicken cytokines and chemokines. *J Interf Cytokine Res*. (2005) 25:467–84. doi: 10.1089/jir.2005.25.467
59. Lillehoj HS, Min W, Dalloul RA. Recent progress on the cytokine regulation of intestinal immune responses to *Eimeria*. *Poultry Sci*. (2004) 83:611–23. doi: 10.1093/ps/83.4.611
60. Gadde U, Rathinam T, Erf GF, Chapman HD. Acquisition of immunity to the protozoan parasite *Eimeria adenoeides* in turkey poults and cellular responses to infection. *Poultry Sci*. (2013) 92:3149–57. doi: 10.3382/ps.2013-03406
61. Zhou Z, Wang Z, Cao L, Hu S, Zhang Z, Qin B, et al. Upregulation of chicken TLR4, TLR15 and MyD88 in heterophils and monocyte-derived macrophages stimulated with *Eimeria tenella in vitro*. *Exp Parasitol*. (2013) 133:417–33. doi: 10.1016/j.exppara.2013.01.002
62. Zhang L, Liu R, Song M, Hu Y, Pan B, Cai J, et al. *Eimeria tenella*: interleukin 17 contributes to host immunopathology in the gut during experimental infection. *Exp Parasitol*. (2013) 133:121–30. doi: 10.1016/j.exppara.2012.11.009
63. Liu L, Huang X, Liu J, Li W, Ji Y, Tian D, et al. Identification of common immunodominant antigens of *Eimeria tenella*, *Eimeria acervulina* and *Eimeria maxima* by immunoproteomic analysis. *Oncotarget*. (2017) 8:34935–45. doi: 10.18632/oncotarget.16824
64. Allen PC. Dietary supplementation with *Echinacea* and development of immunity to challenge infection with coccidia. *Parasitol Res*. (2003) 91:74–8. doi: 10.1007/s00436-003-0938-y
65. Lee SH, Lillehoj HS, Jang SI, Lee KW, Bravo D, Lillehoj EP. Effects of dietary supplementation with phytonutrients on vaccine-stimulated immunity against infection with *Eimeria tenella*. *Vet Parasitol*. (2011) 181:97–105. doi: 10.1016/j.vetpar.2011.05.003
66. Joyner LP. Immunological variation between two strains of *Eimeria acervulina*. *Parasitology*. (1969) 59L725–732. doi: 10.1017/S0031182000031243
67. Norton CC, Hein EH. *Eimeria maxima*: a comparison of two laboratory strains with a fresh isolate. *Parasitology*. (1976) 72:345–54. doi: 10.1017/S0031182000049544
68. Jeffers TK. Genetic transfer of anticoccidial drug resistance in *Eimeria tenella*. *J Parasitol*. (1974) 60:900–4. doi: 10.2307/3278505
69. Chapman HD, Barta JR, Blake D, Gruber A, Jenkins M, Smith NC, et al. A selective review of advances in coccidiosis research. *Adv Parasitol*. (2013) 83:93–171. doi: 10.1016/B978-0-12-407705-8.00002-1

70. Blake DP, Oakes R, Smith AL. A genetic linkage map for the apicomplexan protozoan parasite *Eimeria maxima* and comparison with *Eimeria tenella*. *Int J Parasitol*. (2011) 41:263–70. doi: 10.1016/j.ijpara.2010.09.004
71. Blake DP, Billington KJ, Copestake SL, Oakes RD, Quail MA, Wan KL, et al. Genetic mapping identifies novel highly protective antigens for an apicomplexan parasite. *PLoS Pathog*. (2011) 7:e1001279. doi: 10.1371/journal.ppat.1001279
72. Lee SH, Dong X, Lillehoj HS, Lamont SJ, Suo X, Kim DK, et al. Comparing the immune responses of two genetically B-complex disparate Fayoumi chicken lines to *Eimeria tenella*. *British Poultry Sci*. (2016) 57:165–71. doi: 10.1080/00071668.2016.1141172
73. Kogut M, Lange C. Interferon-g-mediated inhibition of the development of *Eimeria tenella* in cultured cells. *J Parasitol*. (1989) 75:313–7. doi: 10.2307/3282782
74. Rose ME, Wakelin D, Hesketh P. Gamma imerferon controls *Eimeria vermiformis* primary infection in BALB/c mice. *Infect Immun*. (1989) 57:1599–603.
75. Smith AL, Hayday AC. Genetic analysis of the essential components of the immunoprotective response to infection with *Eimeria vermiformis*. *Int J Parasitol*. (1998) 28:1061–9. doi: 10.1016/S0020-7519(98)00081-2
76. Sekellick MJ, Ferrandino AF, Hopkins DA, Marcus PI. Chicken interferon gene: cloning, expression, and analysis. *J Interf Res*. (1994) 14:71–9. doi: 10.1089/jir.1994.14.71
77. Digby M, Lowenthal J. Cloning and expression of the chicken interferon-gamma gene. *J Interf Cytokine Res*. (1995) 15:939–45. doi: 10.1089/jir.1995.15.939
78. Kogut MH, Lange C. Recombinant interferon-γ inhibits cell invasion by *Eimeria tenella*. *J Interf Res*. (1989) 9:67–77. doi: 10.1089/jir.1989.9.67
79. Prowse SJ, Pallister J. Interferon release as a measure of the T-cell response to coccidial antigens in chickens. *Avian Pathol*. (1989) 18:619–30. doi: 10.1080/03079458908418637
80. Byrnes S, Emerson K, Kogut M. Dynamics of cytokine production during coccidial infections in chickens: colony-stimulating factors and interferon. *FEMS Immunol Med Microbiol*. (1993) 6:45–52. doi: 10.1111/j.1574-695X.1993.tb00302.x
81. Breed DGJ, Schetters TPM, Verhoeven NAP, Vermeulen AN. Characterization of phenotype related responsiveness of peripheral blood lymphocytes from *Eimeria tenella* infected chickens. *Parasite Immunol*. (1997) 19:536–69. doi: 10.1046/j.1365-3024.1997.d01-174.x
82. Rothwell L, Muir W, Kaiser P. Interferon-γ is expressed in both gut and spleen during *Eimeria tenella* infection. *Avian Pathol*. (2000) 29:333–42. doi: 10.1080/03079450050118467
83. Lowenthal JW, York JJ, O'Neil TE, Rhodes S. Prowse SJ, Strom DG, et al. *In vivo* effects of chicken interferon-γ during infection with *Eimeria*. *J Interf Cytokine Res.* (1997) 17:551–8. doi: 10.1089/jir.1997.17.551
84. Dimier IH, Quéré P, Naciri M, Bout DT. Inhibition of *Eimeria tenella* development *in vitro* mediated by chicken macrophages and fibroblasts treated with chicken cell supernatants with IFN-gamma activity. *Avian Dis*. (1998) 42:239–47. doi: 10.2307/1592473
85. Takehara K, Kobayashi K, Ruttanapumma R, Kamikawa M, Nagata T, Yokomizo Y, et al. Adjuvant effect of chicken interferon-gamma for inactivated *Salmonella Enteritidis* antigen. *J Vet Med Sci*. (2003) 65:1337–41. doi: 10.1292/jvms.65.1337
86. Lillehoj HS, Ding X, Quiroz MA, Bevensee E, Lillehoj EP. Resistance to intestinal coccidiosis following DNA immunization with the cloned 3-1E *Eimeria* gene plus IL-2, IL-15, and IFN-gamma. *Avian Dis*. (2005) 49:112–7. doi: 10.1637/7249-073004R
87. Min W, Lillehoj HS, Burnside J, Weining KC, Staeheli P, Zhu JJ. Adjuvant effects of IL-1β, IL-2, IL-8, IL-15, IFN-α, IFN-γ TGF-β4 and lymphotactin on DNA vaccination against *Eimeria acervulina*. *Vaccine*. (2001) 20:267–74. doi: 10.1016/S0264-410X(01)00270-5
88. Shah MAA, Song X, Xu L, Yan R, Song H, Ruirui Z, et al. The DNA-induced protective immunity with chicken interferon gamma against poultry coccidiosis. *Parasitol Res*. (2010) 107:747–50. doi: 10.1007/s00436-010-1940-9
89. Song X, Huang X, Yan R, Xu L, Li X. Efficacy of chimeric DNA vaccines encoding Eimeria tenella 5401 and chicken IFN-γ or IL-2 against coccidiosis in chickens. *Exp Parasitol*. (2015) 156:19–25. doi: 10.1016/j.exppara.2015.05.003
90. Martinez GJ, Nurieva RI, Yang XO, Dong C. Regulation and function of proinflammatory TH17 cells. *Annals N Y Acad Sci*. (2008) 1143:188–211. doi: 10.1196/annals.1443.021
91. Pappu R, Rutz S, Ouyang W. Regulation of epithelial immunity by IL-17 family cytokines. *Trends Immunol*. (2012) 33:343–9. doi: 10.1016/j.it.2012.02.008
92. Kim WH, Jeong J, Park AR, Yim D, Kim Y-H, Kim KD, et al. Chicken IL-17F: Identification and comparative expression analysis in *Eimeria*-infected chickens. *Dev Compar Immunol*. (2012) 38:401–9. doi: 10.1016/j.dci.2012.08.002
93. Bacellar O, Faria D, Nascimento M, Cardoso TM, Gollob KJ, Dutra WO, et al. Interleukin 17 production among patients with american cutaneous leishmaniasis. *J Infect Dis*. (2009) 200:75–8. doi: 10.1086/599380
94. Guiton R, Vasseur V, Charron S, Arias MT, Van Langendonck N, Buzoni-Gatel D, et al. Interleukin 17 receptor signaling is deleterious during *Toxoplasma gondii* infection in susceptible BL6 mice. *J Infect Dis*. (2010) 202:427–35. doi: 10.1086/653738
95. Stange J, Hepworth MR, Rausch S, Zajic L, Kühl AA, Uyttenhove C, et al. IL-22 mediates host defense against an intestinal intracellular parasite in the absence of IFN-γ at the cost of Th17-driven immunopathology. *J Immunol*. (2012) 188:2410–8. doi: 10.4049/jimmunol.1102062
96. Miyazaki Y, Hamano S, Wang S, Shimanoe Y, Iwakura Y, Yoshida H. IL-17 is necessary for host protection against acute-phase *Trypanosoma cruzi* infection. *J Immunol*. (2010) 185:1150–7. doi: 10.4049/jimmunol.0900047
97. Kelly MN, Kolls JK, Happel K, Schwartzman JD, Schwarzenberger P, Combe C, et al. Interleukin-17/interleukin-17 receptor-mediated signaling is important for generation of an optimal polymorphonuclear response against *Toxoplasma gondii* infection. *Infect Immun*. (2005) 73:617–21. doi: 10.1128/IAI.73.1.617-621.2005
98. Del Cacho E, Gallego M, Lillehoj HS, Quílez J, Lillehoj EP, Ramo A, et al. IL-17A regulates *Eimeria tenella* schizont maturation and migration in avian coccidiosis. *Vet Res*. (2014) 45:1–9. doi: 10.1186/1297-9716-45-25
99. Tiemessen MM, Jagger AL, Evans HG, van Herwijnen MJC, John S, Taams LS. $CD4^+CD25^+Foxp3^+$ regulatory T cells induce alternative activation of human monocytes/macrophages. *Proc Natl Acad Sci USA*. (2007) 104:19446–51. doi: 10.1073/pnas.0706832104
100. Shack LA, Buza JJ, Burgess SC. The neoplastically transformed. (CD30hi) Marek's disease lymphoma cell phenotype most closely resembles T-regulatory cells. *Cancer Immunol Immunother*. (2008) 57:1253–62. doi: 10.1007/s00262-008-0460-2
101. Denyer MP, Pinheiro DY, Garden OA, Shepherd AJ. Missed, not missing: phylogenomic evidence for the existence of avian foxP3. *PLoS ONE*. (2016) 11:e0150988. doi: 10.1371/journal.pone.0150988
102. Shanmugasundaram R, Selvaraj RK. Regulatory T cell properties of chicken $CD4^+CD25^+$ cells. *J Immunol*. (2011) 186:1997–2002. doi: 10.4049/jimmunol.1002040
103. Selvaraj RK. Avian $CD4^+CD25^+$ regulatory T cells: properties and therapeutic applications. *Dev Compar Immunol*. (2013) 41:397–402. doi: 10.1016/j.dci.2013.04.018
104. Sand JM, Arendt MK, Repasy A, Deniz G, Cook ME. Oral antibody to interleukin-10 reduces growth rate depression due to *Eimeria* spp. infection in broiler chickens. *Poultry Sci*. (2016) 95:439–46. doi: 10.3382/ps/pev352
105. Arendt MK, Sand JM, Marcone TM, Cook ME. Interleukin-10 neutralizing antibody for detection of intestinal luminal levels and as a dietary additive in *Eimeria* challenged broiler chicks. *Poultry Sci*. (2016) 95:430–8. doi: 10.3382/ps/pev365

106. Morris A, Shanmugasundaram R, McDonald J, Selvaraj RK. Effect of *in vitro* and *in vivo* 25-hydroxyvitamin D treatment on macrophages, T cells, and layer chickens during a coccidia challenge. *J Anim Sci*. (2015) 93:2894–903. doi: 10.2527/jas.2014-8866
107. Kim WH, Lillehoj HS, Min W. Indole treatment alleviates intestinal tissue damage induced by chicken coccidiosis through activation of the aryl hydrocarbon receptor. *Front Immunol*. (2019) 10:560. doi: 10.3389/fimmu.2019.00560
108. Sehrawat S, Rouse BT. Interplay of regulatory T cell and Th17 cells during infectious diseases in humans and animals. *Front Immunol*. (2017) 8:341. doi: 10.3389/fimmu.2017.00341

Conflict of Interest: The authors declare that the research was conducted in the absence of any commercial or financial relationships that could be construed as a potential conflict of interest.

frontiers in Immunology

REVIEW
published: 12 October 2018
doi: 10.3389/fimmu.2018.02349

Immunomodulation by Helminths: Intracellular Pathways and Extracellular Vesicles

Amin Zakeri[1]*, *Eline P. Hansen*[2], *Sidsel D. Andersen*[1], *Andrew R. Williams*[2] and *Peter Nejsum*[1]*

[1] Department of Clinical Medicine, Faculty of Health, Aarhus University, Aarhus, Denmark, [2] Department of Veterinary and Animal Sciences, Faculty of Health and Medical Sciences, University of Copenhagen, Frederiksberg, Denmark

Helminth parasites are masters at manipulating host immune responses, using an array of sophisticated mechanisms. One of the major mechanisms enabling helminths to establish chronic infections is the targeting of pattern recognition receptors (PRRs) including toll-like receptors, C-type lectin receptors, and the inflammasome. Given the critical role of these receptors and their intracellular pathways in regulating innate inflammatory responses, and also directing adaptive immunity toward Th1 and Th2 responses, recognition of the pathways triggered and/or modulated by helminths and their products will provide detailed insights about how helminths are able to establish an immunoregulatory environment. However, helminths also target PRRs-independent mechanisms (and most likely other yet unknown mechanisms and pathways) underpinning the battery of different molecules helminths produce. Herein, the current knowledge on intracellular pathways in antigen presenting cells activated by helminth-derived biomolecules is reviewed. Furthermore, we discuss the importance of helminth-derived vesicles as a less-appreciated components released during infection, their role in activating these host intracellular pathways, and their implication in the development of new therapeutic approaches for inflammatory diseases and the possibility of designing a new generation of vaccines.

Keywords: extracellular vesicle, helminths, immunosuppression, intracellular pathways, pattern recognition receptors

OPEN ACCESS

Edited by:
Zhiguang Wu,
University of Edinburgh,
United Kingdom

Reviewed by:
William Horsnell,
University of Cape Town, South Africa
Alan L. Scott,
Johns Hopkins University,
United States

***Correspondence:**
Amin Zakeri
amin.zakeri@clin.au.dk
Peter Nejsum
pn@clin.au.dk

Specialty section:
This article was submitted to Microbial Immunology, a section of the journal Frontiers in Immunology

Received: *28 July 2018*
Accepted: *21 September 2018*
Published: *12 October 2018*

Citation:
Zakeri A, Hansen EP, Andersen SD, Williams AR and Nejsum P (2018) Immunomodulation by Helminths: Intracellular Pathways and Extracellular Vesicles. Front. Immunol. 9:2349. doi: 10.3389/fimmu.2018.02349

INTRODUCTION

Host-Parasite Interactions (Live Infection, Excretory Secretory Molecules, and Extracellular Vesicle)

Parasitic worms (helminths) constitute a very successful group of pathogens that have evolved a number of unique host adaptations (1). Despite their large size, and local or systemic migration throughout the host body, the worms only elicit limited inflammation in invaded tissues and install an immunoregulatory environment which ensures their survival (1). Such a masterful adaption is ascribed to their long coevolution with the hosts enabling them to perform an effective modulation of the immune system (2). Of note, this mutual relationship between worm and host evolves to reciprocal beneficial outcomes, as deworming can result in the emergence of immune-related disorders along with clinical manifestations (3). Various mechanisms have been identified by which helminths restrain host immune responses including expansion of regulatory cells (4),

induction of apoptosis in immune cells (5), manipulation of pattern recognition receptors (PRRs) and downstream signaling (6), and suppression of Th1/Th2 cells and associated cytokines (7). However, there are likely to still be complex and unknown aspects of the strategies underpinning this sophisticated interface which are yet to be investigated (8).

In recent years, the regulatory functions of helminths and their potential ability to ameliorate inflammatory diseases have received much interest (8). Seminal research in this area mostly derives from the hypothesis of Strachan et al. who suggested an inverse relationship between sanitation and prevalence of allergy in different societies, the so-called "hygiene hypothesis" (9, 10). Based on this hypothesis, changes in or eradication of infections can lead to dysregulation of host immune responses, paving the way for allergic and autoimmune disorders (11).

A number of animal models along with some human pilot studies have evaluated the effects of live helminth infections on various inflammatory and autoimmune diseases, such as experimental autoimmune encephalomyelitis (12), asthma (13, 14), anaphylaxis (15) and inflammatory bowel disease (IBD) (16, 17). These experimental studies provided promising results concerning the beneficial effects of helminth infections on allergic and autoimmune diseases through stimulation of Treg cells, activation of toll-like receptor (TLRs), and induction of anti-inflammatory cytokines, such as TGFβ and IL-10 (18). Promising results obtained in both human and animal studies prompted clinical evaluations (16), but due to potential deleterious consequences and side effects which live worms may cause for humans, investigations have also focused on characterizing and recognition of helminth-derived products (HDPs) via exploiting high-throughput assays and omics-based techniques, such as proteomics (19, 20).

There are a number of studies indicating that many HDPs possess immunoregulatory properties. For example, the tapeworm, *Echinococcus granulosus* is able to bypass host immunosurveillance and polarize immune response toward the regulatory state (21). Antigen B (AgB) and sheep hydatid fluid (SHF) are two major components by which *E. granulosus* suppresses dendritic cell (DC) maturation and monocyte differentiation, resulting in reduced anti-parasite responses (21). Likewise, a well-known compound with remarkable regulatory functions is the phosphorylcholine-containing glycoprotein, ES-62 released by the filarial worm, *Acanthocheilonema viteae,* which has widely been investigated by Harnett and collogues (22). In addition, glycan-based compounds, such as Lacto-N-fucopentaose III /LewisX from helminths have been found to be central molecules eliciting Th2 responses and orchestration of immunoregulation through the involvement of C-type lectin receptors (23). Interestingly, some worms, such as the whipworm, *Trichuris suis* can forestall pro-inflammatory responses in human DCs (24). *T. suis* has been found to possess a high level of lipid-based biomolecules, such as prostaglandin (PGE2) which impairs TLR4-associated myeloid differentiation primary response protein 88 (MyD88) and the TIR-domain-containing adaptor-inducing interferon-β (TRIF) signaling (25, 26). Similarly, there is evidence showing that helminth defense molecules contribute to immunomodulatory outcomes of parasitic infections via targeting innate immunity (27). However, the study of HDPs is still a major research area and fractionating HDPs and subsequent detailed studies have opened a new avenue for ongoing investigations.

Recently, extracellular vesicles (EVs) have emerged as a previously unappreciated entity of HDPs which may play a crucial role in parasite immunomodulation. These "magic bullets" have encouraged investigators to unravel their role in pathogenicity, invasion, and longevity of parasitic infections (28). Currently, EVs have shown that may be central in the host-parasite interplay and intracellular communication (29). During infection, the immune system is constantly interacting with a wide range of helminth-derived products including EVs which eventually results in either immune stimulation or immunoregulation. For example, it has recently been documented that parasite EVs can manipulate macrophage activation and regulate inflammatory responses (30, 31). The intercellular delivery of EV-associated RNAs, such as microRNAs, has identified them as important means for inducing epigenetic modifications in intracellular signaling and post-transcriptional regulation of gene expression (30, 32).

In this review, we aim to elaborate modulation of intracellular pathways, mainly in antigen presenting cells (APCs), by which HDPs polarize and suppress host immunity. Moreover, we suggest that understanding the intracellular outcomes upon interaction with HDPs will provide a broad insight into the possible interactions between EVs (as an important component of HDPs) and host intracellular machinery. The putative pathways enabling EVs to impose immunomodulatory effects on host immunity are highlighted. Furthermore, the implication of these vehicles in the development of new therapeutic approaches against inflammatory responses and possibilities of designing a new generation of vaccines based on EVs are discussed.

HELMINTH-DERIVED PRODUCTS (HDPS) AS POTENT IMMUNOMODULATORS

How HDPs Polarize Immune Responses by Targeting Intracellular Pathways

Helminths have evolved sophisticated mechanisms to target intracellular machinery in host cells (33). They have shown a remarkable ability to induce a tolerogenic immune microenvironment by releasing an array of bioactive materials (33). A large body of literature has identified HDPs as powerful modulators of inflammatory signals comprising an impressive range of molecular pathways elicited against parasites (33). HDPs, in total and as individual compounds, play a central role establishing a beneficial niche for the parasite via an effective manipulation of the host immunity to engage a receptor, degrade intracellular molecules, and interfering with essential signals (34). However, the majority of intracellular pathways targeted by these biomolecules are poorly described, but in the following, we focus on innate receptors as important sensors which are targeted by HDPs.

Pattern recognition receptors (PRRs) are one of the most important immune receptors, and their signaling is now

becoming more apparent in regulation of immune responses (35). PRRs are a family of highly sensitive extra and intracellular sensors including Toll-like receptors (TLRs), nucleotide-binding oligomerization domain (NODs)-like receptors (NLRs), retinoic acid-inducible gene-like receptors (RIG-like receptors), and C-type lectin receptors (CLRs) (35). They are widely expressed by immune cells, in particular, those responsible for immunosurveillance, such as DCs and macrophages. PRRs are able to trigger a complex of intracellular crosstalk resulting in DC maturation and T cell priming (36).

Since HDPs are mostly rich in glycan-based products, such as glycoprotein along with lipid structures, TLRs and CLRs have been found to be predominantly targeted by these antigens during immunomodulation and hyporesponsiveness (37). HDPs not only alter the expression of TLRs but also masterfully manipulate their intracellular signaling, reflecting a strict control over host immunity by helminths (6). Interfering with these intracellular pathways, which are main drivers for priming inflammatory responses, suggests that these extracellular parasites can release substances modulating early responding cells in innate immunity (38). Despite the general view that microbial components can engage PRRs and thereby activate DCs, it is well-known that DCs exposed concurrently to HDPs and TLR agonists, such as viral or bacterial products do often not express markers associated with classical maturation (39, 40). For instance, murine DCs treated with soluble SEA fail to express MHC-II, costimulatory molecules, and proinflammatory cytokines in response to LPS (40). In the same way, the release of antigen B (AgB) (a hydatid cyst-derived antigen) by *E. granulosus* prevents upregulation of LPS-induced CD80, CD86, and TNFα in DCs (21), monocytes, and macrophages via an IL-10 independent manner (41).

Intriguingly, HDPs can also modulate TLRs signaling to prime a tolerogenic phenotype of DCs that produce anti-inflammatory cytokines (42). *Schistosoma mansoni* and released eggs can produce bioactive antigens, such as lysophosphatidylserine, lacto-N-fucopentaose III (LNFPIII), and double-stranded RNA (dsRNA) which attenuate inflammatory responses by targeting TLRs. LNFPIII has also been reported to induce DCs maturation and Th2 response polarization through CLRs (23). Another biomolecule that interacts with TLRs is ES-62 released by *A. viteae* which targets TLR4 on host immune cells. ES-62 is able to interfere with the downstream signalings mediated by TLR4, and through which diminishes the production of inflammatory mediators (22).

Likewise, many other HDPs, such as body fluid from adult *Ascaris suum,* have also been documented to induce hyporesponsiveness in human APCs treated with LPS and modulate different human macrophage phenotypes (43, 44). Although HDPs mainly seem to impair TLR4-associated inflammatory responses, it appears that these components tend to target manifold pathways in TLRs and CLRs signaling. Recent bioinformatics-based data has suggested that HDPs constitute a myriad of molecules with complex structures (20). Thus, recognition of a target on DCs would be essential to dissect and identify the major immunosuppressive functions. Here we focus on the main PRR-associated intracellular machinery that is altered by HDPs to favor helminth survival and persistence in the host (**Figure 1**).

TLR Signaling (Map Kinases and Nf-κ B Cascade)

Mitogen-activated protein kinases (MAPKs) are a group of highly important molecules orchestrating the production of different cytokines via involving various downstream accessory proteins in DCs (45). The MAPK pathway is one of the main signaling cascades induced as a result of TLRs stimulation (45). Different kinases contribute to MAPK signaling including the extracellular signal-related kinases 1 and 2 (ERK 1/2), c-jun NH2-terminal kinase (JNK), and p38 MAPK. Activation of these molecules results in DC maturation, cytokine production, and gene expression via stimulation of transcription factors, such as activating protein 1 (AP-1), nuclear factor-κB (NF-κB), and IFN regulatory factors (IRFs) (45). ERK1/2 signaling mostly mediates Th2 response and DCs hyporesponsiveness due to stabilization of the c-fos transcription factor which suppresses IL-12 production (46, 47), whereas JNK and p38 are mostly associated with Th1 responses and DCs activation (47). In support of this, blocking ERK1/2 pathway by the specific inhibitor U0126 up-regulates IL-12 and suppresses TLR2-induced IL-10 production (47). Furthermore, it has been reported that ERK1 knockout mice spontaneously develop autoimmunity (48). On the other hand, two important adaptor molecules associated with TLRs signaling are MyD88 and TRIF, and TLR-induced activation of these molecules is responsible for the expression of genes encoding inflammatory mediators, such as IL-12 and TNFα (36). A number of helminths release molecules that are capable of triggering anti-inflammatory responses via interference with these downstream pathways (38, 49, 50). For example, soluble products of *T. suis* not only suppress transcription of essential molecules orchestrating both MyD88 and TRIF pathways in LPS-treated DCs, but also restrain TLR4 expression preventing DC maturation (26). The precise mechanisms by which HDPs influence these intracellular events are currently the subject of intense investigation. However, interesting data is becoming available regarding inhibitory effects of some HDPs, such as ES-62 and LNFPIII on key molecules involved in these inflammatory pathways.

One of the most important molecules that is targeted by HDPs to subvert TLRs signaling is ERK1/2. This intracellular component plays an essential role in mediation of anti-inflammatory functions of ES-62 and LNFPIII. In fact, both LNFP-III and ES-62, through engagement of TLR4 on DCs, induce Th2 responses (38, 49, 50). Although the capacity of TLR4 in skewing immune response toward Th2 seems surprising, various mechanisms might be at play and might explain the strikingly different response to LPS and some HDPs (51). The main explanations for this phenomenon are selective stimulation of ERK1/2 signaling and involvement of different co-receptors by HDPs which eventually interfere with TLR4-induced inflammatory signals in DCs (38, 51). In addition, it should be noted that TLR4 signaling can be conducted by two distinct of adaptor molecule pathways (TRIF and MyD88), however, it is still obscure which adaptor molecule is responsible for induction of immunoregulatory signals and how it is selectively activated by HDPs (38).

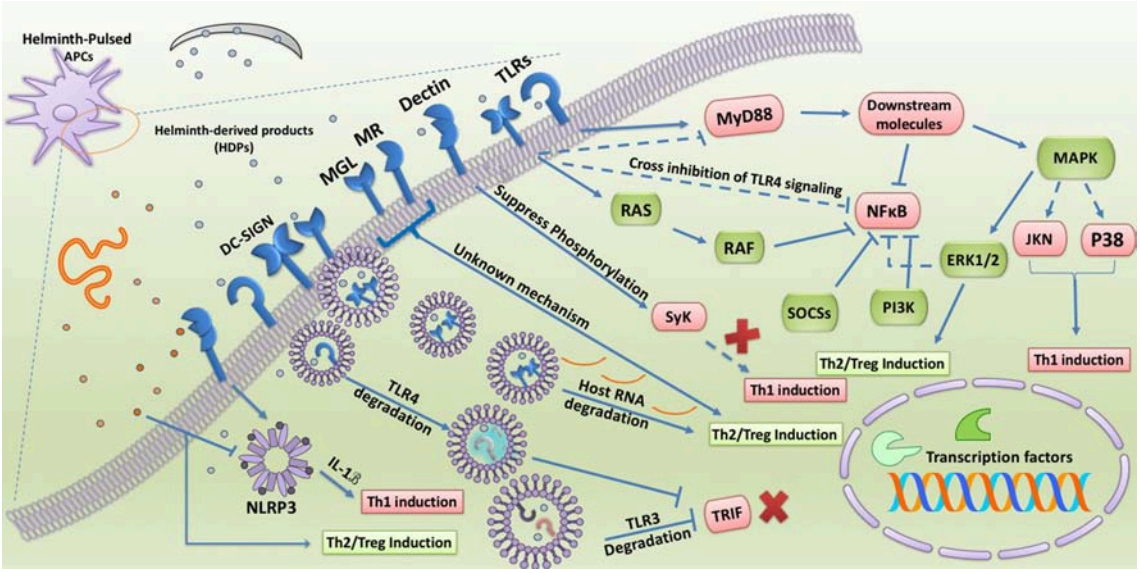

FIGURE 1 | Involvement of TLRs and CLRs during interaction with HDPs. TLRs and CLRs are widely targeted by HDPs during induction of immunomodulation and hyporesponsiveness in APCs. HDPs not only alter the expression of TLRs and CLRs in APCs but also masterfully manipulate their intracellular signaling. Some HDPs are able to redirect TLR4 signaling toward MAPK pathway and ERK1/2 activation supporting Treg/Th2 induction. In addition, co-engagement of DC-SIGN along with TLR4 enables HDPs to trigger unknown intracellular pathways which cross-inhibit MyD88 and NFκB activation. HDPs can further restrain NFκB activity via DC-SIGN-mediated RAF signaling along with upregulation of negative regulators of TLRs signaling, such as SOCSs and PI3K. Obviously, strict inhibition of NFκB as the main transcription factor supporting inflammation results in prevention of priming Th1 cells. Other CLRs have been reported to participate in priming Treg/Th2 cells upon stimulation by HDPs. For example, some HDPs suppress phosphorylation of Dectin1/2-induced Syk molecule and through which inhibit deviation of immune response toward Th1. On the other hand, MR and MGL upon activation by HDPs through an unknown mechanism support Treg/Th2 differentiation. Degrading host key intracellular molecules is another strategy that HDPs exploit to reprogram host immunity. Omega-1, ES-62, and FheCL1 by degrading host mRNA, endosomal TLR4, and TLR3, respectively, not only strengthen Treg/Th2 responses but also forestall anti-parasite immunity. NLRP3 also has been revealed to be targeted by some HDPs to modulate inflammatory responses. However, there has been reported that some HDPs are able to fight anti-worm immunity by stimulation of NLRP3 leading to release of IL-1B and Th1 amplification.

There is strong evidence that activation of ERK1/2 signaling inhibits a Th1 response and instead polarizes immune responses toward anti-inflammatory and Th2 response both *in vivo* and *in vitro* (45, 52). LNF-PIII is one the most powerful HDPs in supporting ERK signaling which significantly induces phosphorylation of ERK and TLR4-dependent differentiation of naive DCs to a DC2 phenotype (50). It seems that such a dysregulation of TLR signaling with a bias toward ERK1/2 is an effective strategy employed by the parasite to suppress Th1 responses and polarization of host immunity. In addition, *Trichinella spiralis* muscle larvae secrete bioactive components which strongly induce transient ERK1/2 signaling, thereby priming Th2/Treg-inducing DCs (53). However, different stages of this nematode have also been shown to arrest NF-κB translocation and the phosphorylation of p38 and ERK1/2 in LPS-treated J774A.1 murine macrophage cell line (54).

To further explore the mechanism of these biomolecules on immune cells, it is necessary to compare the signaling pathway(s) triggered by these antigens and LPS (38). First, stimulation of TLR4 by LPS results in triggering three different aforementioned MAPK cascades (ERK1/2, JNK, and p38 MAP kinases) along with NF-κB pathway activation which ultimately leads to the release of pro-inflammatory mediators (55). In contrast to the response to LPS, it has been shown that LNFPIII and ES-62 are able to induce mainly ERK1/2 signaling without significant stimulation of p38 and JNK. Second, further molecular dissection revealed that these HDPs not only slightly activate NF-κB signaling relative to LPS, but also shorten NF-κB longevity by stabilizing its inhibitor (50, 56). Third, the suppressive functions of ES-62 have been ascribed to inhibition of p38 and JNK, which play a central role in the production of Th1-associated cytokines, such as IL-12, IL-6, and TNFα (56, 57). Fourth, it should be noted that another explanation for such a difference in signal transduction between LPS and ES-62 might be due to the discrepancy in ubiquitylation of TLR4 and/or downstream signaling complexes (57). These data support the notion that some HDPs can elicit Th2 response by TLR4 stimulation in a manner distinct from customary agonists like LPS, which is a strong Th1 inducer.

The modulatory effects of ES-62 are not restricted only to the skewing of TLR4 signaling toward ERK1/2. Melendez et al. showed that ES-62 can also degrade key molecules involved in FcεRI signaling on mast cells via TLR4 engagement (58). Multiple downstream molecules are activated upon binding IgE to FcεRI, such as protein kinase Cα (PKCα), phospholipase D-coupled, and sphingosine kinase 1 (SPHK1) which subsequently trigger NF-κB signaling. In comparison to LPS, which strengthens (FcεRI)-mediated signaling, ES-62 directs PKCα toward degradation via a TLR4-dependent and proteasome-independent manner, suppressing mast cell activation in response to IgE stimulation (58). Importantly, other members of the PKC family (PKCβ,

PKCδ, PKCι, and PKCζ) can also be degraded by ES-62 (58, 59). Among them, PKCδ is regarded as a TLR4-mediated pathway molecule, which plays an important role in full activation of LPS-induced inflammation (60). Eason et al. have recently reported that despite LPS, ES-62 can exert downregulation and autophagolysosomal degradation of PKCδ in DCs to undergo autophagy (60).

Finally, a significant discrepancy between LPS and ES-62 stimulation of TLR4 relates to intracellular trafficking of this receptor. It has been shown that ES-62 can trigger TLR4 trafficking to a distinct caveolae lipid raft route leading to TLR4 degradation, whereas the route through which LPS induces TLR4 trafficking is associated with the promotion of Th1 and inflammatory responses (58) . Owing to promising results achieved from ES-62, analog molecules of ES-62 termed 11a, 11e, 11i, and 12b have been synthesized by Harnett and colleagues. These synthetic structures could experimentally suppress collagen-induced arthritis (CIA) by downregulation of key adaptor molecules in TLRs signaling, such as MyD88 and NF-κB (61–63).

Of note, other helminthes, such as *S. mansoni* and *Ascaris lumbricoides* can induce an imbalance in the intracellular signaling of LPS-treated human DCs via engagement of TLR2 and high stimulation of the ERK pathway. Given the fact that ERK1/2 signaling can increase c-Fos stabilization and IL-12 inhibition (47), it has been demonstrated that *S. mansoni* and *A. lumbricoides*-derived phospholipids support Th2 polarization via induction of imbalance in TLR2 signaling by strengthening ERK pathway in human monocyte-derived DCs (64). Interestingly, soluble SEA through TLR2 signaling induces a crosslink manipulation on the expression of co-inhibitory-associated genes, such as programmed death-ligand 1 (PD-1) and PD-L2 on murine BMDCs and $CD4^+$ T cells, respectively. Upregulation of PD-1 and PD-L2 expression by egg antigens is a TLR2-dependent mechanism leading to anergy and hyporesponsiveness during interaction between macrophages and $CD4^+$ T cells (65).

In addition, Correale et al. have suggested that SEA can activate several genes associated with retinoic acid synthesis, such as SOCS3 and IL-10R in DCs, via engagement of TLR2 and activation of ERK1/2 signaling (66). Importantly, egg antigen-treated DCs have been shown to strongly prime Tregs and suppress production of inflammatory cytokines, indicating a clear polarization by targeting TLR signaling. Mechanistically, Agrawal et al. suggested that immunoregulatory function of egg antigen is mediated via ERK1/2-induced c-Fos phosphorylation, as in the absence of c-Fos immune response were redirected toward Th1 (47).

Moreover, some HDPs, such as egg antigens condition DCs to prime Foxp3 Tregs via TLR2-dependent ERK1/2 signaling. This effect can also be observed with the antigen SJMHE1 from *S. japonicum* which increases proliferation and suppressive functions of Tregs by activating TLR2 (67–69). However, it is unknown how HDPs modify TLRs on Tregs to optimize their lifespan and suppressive activity, so further research is required to document the underlying molecular mechanism. Generally, TLRs signaling is mediated through two distinct pathways known as MAPK and NF-κB cascade. NF-κB signaling also plays an essential role in priming Th2 response, since the lack of NF-κB in DCs has been shown to result in Th2 impairment in the presence of egg antigens and LNFPIII (70, 71).

SOCSs, JAK/STAT, and PI3K

There is evidence suggesting that some HDPs can directly manipulate molecules controlling TLRs signaling, such as suppressor of cytokine signaling 3 (SOCS3) (66, 72). In this regard, it has been shown that *F. hepatica* produces biomolecules, such as tegumental coat antigens (FhTeg) and cathepsin L1 cysteine protease (FheCL1) which are capable of interfering with both the NF-κB and ERK/MAPK pathways in a manner distinct from other HDPs (72, 73). For instance, FhTeg can diminish the expression of inflammatory mediators in LPS-treated DCs via upregulation of a negative regulator of the TLRs pathway known as SOCS3 (72). On the other hand, FheCL1 is involved in neutralizing TLR3 signaling, as a TLR utilizing TRIF adaptor as an activator of downstream molecules. In fact, Donnelly et al. indicated that TRIF-dependent MyD88-independent signaling pathway is impaired by FheCL1 via degradation of TLR3 (73). Similar to FheCL1, SmCB-1 from *S. mansoni* has been found to enter the endosome and degrade TLR3. The protective effects of these antigens (FheCL1 and SmCB-1) against LPS-induced lethality were found to be mediated through MyD88-independent and TRIF-dependent pathways shared by both TLR4 and TLR3, suggesting the potential of HDPs as druggable targets due to their ability to disrupt intracellular pathways activated during inflammation (73). The TRIF-dependent pathway of TLR4 signaling can also be inhibited by *T. spiralis*-derived antigens as a mechanism to orchestrate regulatory responses (74). *Brugia malayi* has also been shown to produce a component known as abundant larval transcript (ALT-2) which promotes type 2 immune response and attenuates IFN-dependent signals via activation of GATA-3 and SOCS-1 in macrophages (75). SOCS-1 has also been reported to be upregulated by SEA in human DCs exposed to LPS which was associated with inhibition of pro-inflammatory cytokines (76).

Apart from ES-62, another well-known and highly bioactive component from *A. viteae* with significant intracellular activity is AvCystatin (77). Generally, cystatins are regarded as protease inhibitors which have been detected in excretory-secretory products of most filarial nematodes (78). Macrophages and IL-10 have been found to be central in the immunoregulatory effects of AvCystatin on experimental models of colitis and asthma (77, 79). AvCystatin is able to induce regulatory macrophages (Mreg) representing remarkable suppressive effects on DCs via IL-10 dependent and cell-contact independent mechanism (79). Klotz et al. identified the molecular mechanism by which AvCystatin can reprogram the macrophage phenotype and suppresses inflammation. They suggest that AvCystatin is taken up by macrophages and through stimulation of dual specificity phosphatases (DUSPs), which are negative regulators of MAPK signaling and IL-10 expression, targets ERK1/2 and p38 to modulate downstream signals inducing regulatory responses (77). Through this mechanism, the immunoregulatory effects of AvCystatin are mediated via the phosphorylation of the CREB and STAT3 (77). In addition, some HDPs, such as dsRNA

derived from *S. mansoni* egg can also modulate STAT1 signaling (80). This dsRNA is able to engage TLR3 and phosphorylate STAT1 in DCs supporting signaling pathway associated with type I IFN expression (80). Yang et al. have recently provided evidence suggesting that the immunomodulatory activity of *S. mansoni* egg antigens (SEA) and *S. japonicum* worm antigen (SWA) in myeloid-derived suppressor cells (MDSCs) is mediated through the Janus kinase/signal transducers and activators of transcription 3 (JAK/STAT3) pathway (81). They corroborated their findings by application of a JAK inhibitor (JSI-124) which abrogated immunomodulatory functions of SEA and SWA (81). Besides STAT1 and 3, STAT6 signaling has also been found to be manipulated by some HDPs, such as *T. spiralis*-derived cathepsin B-like protein (82). Liu et al. indicated that the recombinant form of this antigen (rTsCPB) can significantly restrain intestinal ischemia/reperfusion injury in mice by active reprogramming macrophages from an inflammatory (M1) to an alternative phenotype (M2) (82). One of the main intracellular signalings for such a phenotypic alteration is activation of STAT6 in M1 macrophages (82). Mechanistically, rTsCPB was shown to support upregulation of M2-associated markers and subsequently transition of M1 to M2 macrophage via STAT6-dependent manner, as inhibition of STAT6 restored disease severity and M1 domination (82).

Some parasites tend to target another pathway in TLR signaling known as phosphoinositide 3-kinase (PI3K) which is a strong inhibitor of TLR-induced IL-12 production and DCs maturation (77, 83, 84). Accordingly, this pathway has been revealed to shape immune response toward Th2 and IL-10 production. For instance, some protozoan parasites, such as *Giardia lamblia* and *Leshmania major,* along with *A. vitae,* are able to interfere with TLR-mediated DCmaturation via stimulation of PI3K signaling maturation (77, 83, 84). Importantly, both CLRs and TLRs can share ERK and PI3K signaling to redirect immune response toward Th2 during infection with helminths (85).

These data show how HDPs may impact TLR signaling, thereby bypassing inflammatory responses. The predominant pathway triggered by HDPs is ERK1/2 signaling which supports phosphorylation of the transcription factor c-Fos inducing modified Th2 and/or anti-inflammatory responses (46, 50, 56). Generally, it seems that one of the main mechanisms by which helminths minimize host tissue injury is suppression of innate immunity via modification of TLR signaling (6, 85).

C-Type Lectins Receptor (CLRs) Signaling

There is evidence suggesting the commencement of Th2 response can be initiated independent of the two adaptor proteins MyD88 and TRIF (86). In this case, it is expected that other PRRs beside TLRs also can initiate the Th2 response (37). As mentioned above, APCs express an array of receptors known as CLRs specialized in the recognition of glycans (87). CLRs can mediate different immunological processes including antigen uptake, intracellular trafficking, and priming innate immunity (87). Various types of CLRs are expressed by APCs including DC-specific ICAM-3 grabbing nonintegrin (DC-SIGN), macrophage galactose binding lectin receptor (MGL), mannose receptor (MR), and Dectin-1. DC-SIGN is involved in recognition of high mannose glycans and is able to stimulate TLR signaling (87). MGL and MR detect pathogens-associated mannose-containing glycans with high sensitivity (87). Recently, surfactant protein (SP)-D, collectin related to the family of C-type lectins, has also been reported to interact with carbohydrate-based compartments of worms, such as *Nippostrongylus brasiliensis* in the lung (88). Thawer et al. demonstrated that SP-D KO mice are unable to control *N. brasiliensis* in the lung, as this protein plays a key role in stimulation of Th2 responses and alternative activation of alveolar macrophages (alvM) which is essential for binding to and killing L4 parasites (88).

Importantly, CLRs play an important role in host-parasite interaction through recognition of glycan-based components in helminth-derived antigens (89). These parasite-derived glycans constitute versatile glycoconjugates with highly various structures targeting CLRs, and in turn skew adaptive immunity (90). For instance, N-linked glycoconjugates from *A. suum* extract engage DC-SIGN and MR to suppress LPS-induced DCs maturation and triggering inflammatory signals (89). Similarly, it has been shown that DC-SIGN, MR, and MGL can be involved in capturing and internalization of SEA (91–93). Also, some HDPs are quite similar to host glycans which, during interplay with CLRs of DCs, induce both Th2 suppression and Treg proliferation, establishing a tolerogenic state in host immune function (94). In this way, this mechanism can create a balance between Th1 and Th2 responses through the involvement of CLRs on DCs (37, 95). Unfortunately, limited data are available on the parasite components inducing immunological bias via the involvement of CLRs.

One of the main pathways shared by most CLRs to trigger downstream signaling is the spleen tyrosine kinase (Syk) pathway, which has been shown to contribute to DC priming and elicitation of inflammatory responses (96). Interestingly, *Heligmosomoides polygyrus* and its products elicit a strong downregulation of different CLRs including CLEC7A, 9A, 12A, and 4N along with suppression of Syk phosphorylation (96). In fact, it is suggested that the inhibitory effects of this worm on CLRs and Syk expression leading to induction of regulatory DCs in intestine and mitigation of colitis in infected mice (96). In another way, excretory-secretory products of *Taenia crassiceps* (TcES) have been found to inhibit DCs maturation in response to TLR4 and TLR9 agonist (97). Molecular dissections revealed that TcES are able to interfere with TLR signaling and induce tolerogenic DCs. Terrazas et al. delineated that TcES support Th2 response by activation of MGL, MR, and TLR2 (97). The reported that the major intracellular mechanism by which TcES prevent TLR4-mediate DCs maturation is by targeting c-RAF, which is a MAP3K acting on downstream pathways of the Ras family (97). Indeed, TcES significantly suppress downstream molecules, such as p38 and NF-κB by phosphorylation of c-RAF and consequently polarize immune responses toward a Th2 phenotype (97). It has also recently been observed that *T. crassiceps*-induced Ly6C^{hi} monocyte-derived alternatively activated macrophages (AAMs) express a high level of MR (CD206), PD-L2, and CCR2/CX3CR1 enabling

them to prime Tregs and suppress experimental autoimmune encephalomyelitis in mice (98).

CLRs have also been suggested to associate with induction of Th2 responses by *Toxocara*-derived antigens (99). Among them, DC-SIGN is one of the most important receptors in recognition of *T. canis*, *F. hepatica*, and *B. malayi*-derived glycan products shaping the immune response toward a Th2/regulatory state (100–102). Rodríguez and colleagues have recently found that DC-SIGN plays a central role in priming Treg upon interaction with *F. hepatica*-derived glycans (102). The presence of mannose and fucose residues in *F. hepatica*-glycoconjugates can facilitate DC-SIGN stimulation and trigger intracellular pathway enabling DCs to prime Treg and inhibit proliferation of allogeneic T cells (102). Surprisingly, stimulation of DC-SIGN with *F. hepatica*-glycoconjugates activates a pathway in DCs which, during intracellular crosstalk with TLR-mediated signaling, induces IL-10 and IL-27 secretion in support of Treg expansion (102). A similar mechanism has been reported for immunoregulatory effects of *F. hepatica*-derived glycans upon engagement of MGL on both human monocyte-derived DCs (mo-DCs) and $mMgl2^+$ $CD11^+$ cells in mice (103). In this study, the authors suggest that a cross regulation between pathways due to co-stimulation of MGL and TLR4 with *F. hepatica*-derived glycans and LPS, respectively, which enables DCs to produce immunoregulatory cytokines and support Th2/Treg proliferation (103). MR can recognize *F. hepatica* tegumental antigens (FhTeg) and condition DCs to induce anergy in $CD4^+$ T cells (104). In addition, this receptor is able to suppress DCs maturation or Th2 induction in response to *F. hepatica* total extract (105, 106). However, it is believed that MR is not solely involved in conduction of immunosuppressive function of FhTeg and other CLRs most likely also contribute to these interactions (107). In support of this, *F. hepatica* excretory-secretory products (FhESP) have been demonstrated to suppress T cell activation via Dectin-1 dependent upregulation of PD-L2 and IL-10 in macrophages (108). Also, the strong suppressive activity of FhESP has been ascribed to co-activation of MR and Dectine-1 in macrophages underpinned by high levels of TGF-β and IL-10 production (109).

SEA possesses an array of complex glycan-based products which are predominantly recognized and taken up by surface CLRs on DC including MR, MGL, DC-SIGN, and Dectin1, triggering SYK-mediated intracellular pathways (91–93, 110). Endocytosis of egg-derived antigens results in interference with TLR signaling in DCs (93). The most well-known antigens of *schistosoma* egg which stimulate CLRs are LEX-containing glycans, omega-1, lacto-N-fucopentaose III and lacto-N-neotetraose. LEX-containing glycans involve DC-SIGN on DCs and trigger intracellular signaling, thereby promoting Th2 responses (111). Moreover, plant-based reconstruction of omega-1 has recently been reported to provoke Th2 responses by engaging DC-SIGN (51). Omega-1 is a Lex-containing glycoprotein structure representing T2 ribonuclease (RNase) activity. The MR has also been displayed to capture and internalize omega-1 leading to Th2 polarization along with interfering protein synthesis via degrading host cell RNAs (112, 113). LNFPIII and lacto-N-neotetraose are potent suppressors of T cell proliferation and DCs activation through stimulation of IL-10 production (114). Interestingly, it has been indicated that the immunoregulatory functions of these glycan-based biomolecules are mediated via the MR and DC-SIGN (38, 49, 115). Of interest is a recent study by Kooij et al. which highlighted a critical role of MR in polarization of human classical monocytes toward regulatory phenotype (expressing SOCS1, IL-10, and TGFβ) upon interaction with soluble products of *T. suis* (TsSP) (116). In this study, MR was found to respond to TsSP and triggers a PKC-mediated signaling (mainly PKCδ) responsible for induction of anti-inflammatory monocytes (116). Also, glycan compounds in *T. spiralis* muscle larvae excretory-secretory antigens (ES L1) have been reported to be able to polarize host immunity toward Th2/Treg via corroboration of ERK1/2 signaling in DCs and production of IL-10 and TGFβ (117). However, the major receptor responsible for such modulation is obscure and possible candidates need to be investigated (117).

These data suggest that CLRs can strongly react to HDPs and condition DCs to redirect immune response toward Th2 immunity and/or an anti-inflammatory response (118). However, the precise shared pathway by TLRs and CLRs upon simultaneous activation leading to release of regulatory cytokines remains enigmatic. In the following, we discuss this topic, to which less attention has been given.

Co-involvement of TLRs and CLRs by HDPs

Interestingly, recent data suggest that the immunomodulatory functions of some HDPs are mediated via simultaneous involvement of TLRs and CLRs. In fact, signaling pathways of CLRs have shown to co-operate with TLRs which strengthen effective immunomodulation. For example, *S. mansoni* secretes glycolipids which co-involve DC-SIGN and TLR4 in human DCs (119). Regarding intracellular crosstalk, Meyer-Wentrup et al. suggested that TLR8-mediated production of inflammatory cytokines, such as IL-12 and TNFα can be forestalled by dendritic cell immunoreceptor (DCIR) as a C-type lectin receptor (120).

This complex mechanism suggests an intricate intracellular crosstalk between two distinct receptors which results in hyporesponsiveness and immunosuppression. Activation of CLR signaling can modify inflammatory responses via manipulation of TLRs signaling (121, 122). For instance, SEA and LNFPIII are among the well-known schistosome-associated antigens which have been reported to co-involve TLRs and CLRs in host DCs. Egg antigens can regulate TLR2, TLR3, and TLR4 signaling through stimulation of β-galactoside-binding lectin galectin 3 (40, 80, 123–125), while LNFPIII via interaction with DC-SIGN and MGL1(23, 126), cross-inhibits the TLR4 pathway (101). DC-SIGN also strongly directs the immune response toward Th2, Treg, and modulation of inflammatory reactions. In this regard, Geijtenbeek et al. showed that mannosylated components of Mycobacterial cell walls diminish TLR4-associated inflammation via DC-SIGN (122). Similarly, other pathogens seem to modify TLR-mediated inflammatory consequences through stimulating DC-SIGN-associated Raf-1 signaling (127).

Likewise, other glycan-based compounds released by *S. mansoni* are expected to modify inflammatory responses via co-involvement (128). The immunoregulatory activity of

schistosome-derived lysoPS may be similar to zymosan, which co-engages TLR2 and Dectin-1 (a type of CLRs) on DCs and induces Treg priming along with IL-10 production (129). Stimulation of Dectin-2 by whole extracts of *S. mansoni* eggs was reported to trigger Syk and inflammasome signaling and thereby enable inhibition of TLR signaling (110). Apart from intracellular crosstalk, physical interaction between CLRs and other surface receptors is believed to affect their intracellular signaling leading to a significant modification in immune response (128). Generally, it seems that glycan-based materials released by helminths can modulate host immunity through manifold signaling stemming from different receptors, such as TLRs, CLRs, and likely other PRRs provoking both Th2 and regulatory responses (23, 130). Tracking the mechanisms through which HDPs induce Th2 and/or regulatory responses will provide new insight into recognition of molecules and targets that selectively stimulate ERK signaling, which may be beneficial in development of new generations of vaccines and therapeutics against inflammatory diseases.

Inflammasome

Inflammasomes constitute an intracellular platform possessing NOD-like receptor (NLR) family proteins which are highly sensitive to various PAMPs and DAMPs (131). These cytosolic sensors include different family of NLRPs and absent in melanoma 2 (AIM2) which play a key role in triggering inflammatory signals in most immune cells, but mainly in APCs (131). Stimulation of inflammasomes results in activation of a cascade signaling supporting active release of IL-1β and IL-18 (131). However, limited data is available on the interaction of helminths with inflammasome, but some studies have provided interesting results in this regard. For example, Rzepecka et al. reported that a synthetic analog of ES-62 known as SMA-12b is able to suppress arthritis in mice by prevention of inflammasome activation (132). Further in-depth molecular dissection on murine macrophages revealed the underlying mechanisms are mediated through downregulation of IL-1β and inflammasome-associated signals which strongly counters inflammasome-induced responses supporting arthritis (132). Some helminth infections and their products are able to activate inflammasome in order to restrict production of early released innate cytokines, such as IL-25 and IL-33 (133). For example, *H. polygyrus* has been found to instigate NLRP3 in intestinal lamina propria cells inducing IL-1β secretion and by this mechanism prevents Th2 response initiation, ILC2 expansion, and eventually helminth expulsion (133). The same scenario has recently been reported for *T. muris* as Alhallaf et al. unraveled a novel mechanism by which *T. muris* exosomes and ESP suppress anti-parasite immunity by targeting NLRP3 (134). This study showed that this worm and its released compounds actively counter Th2 response and worm expulsion by increasing NLRP3-mediated IL-18 both *in vivo* and *in vitro* (134). Thus, this intracellular sensor may be targeted by helminths to suppress Th2 responses via IL-1β and IL-18 (133, 134).

Likewise, a well-known component from *S. mansoni* called omega-1 has also shown to be able to activate NLRP3 via co-involvement of Dectin-1 in macrophages (135). However, it is unknown how modulating the inflammasome can facilitate infection. In the same line, Ritter et al. studied the inflammasome-associated activity of SEA (110). They suggested that egg antigens can simultaneously suppress TLR signaling and activate NLRP3. Mechanistically, egg antigens were found to require co-activation of Dectin-1/FcγR and downstream signaling (Syk kinase signaling) to irritate NLRP3 via activation of reactive oxygen species and potassium efflux leading to IL-1β secretion in BMDCs (100).

Targeting Non-PRR Signaling

Generally, no precise pattern of intra- and extracellular sensors along with downstream signaling has been fully recognized by which HDPs exert immunomodulation. Indeed, helminths have shown to be able to exploit an array of highly complex strategies beyond the manipulation of canonical PRRs signaling to restore aberrant immune responses (136). In the following section, immunosuppressive functions of some HDPs through a PRR-independent manner will be discussed (**Figure 2**).

Impairment in antigen presentation, T cell receptor (TCR), and B cell receptor (BCR) signaling

Given the myriad biomolecules released by helminths, it is not surprising that some HDPs manipulate host immune cells via receptor-independent manner, such as enzymatic activity. For instance, *B. malayi* cystatins, such as Bm-CPI-1 (produced by the L2 and L3 stage of *B. malayi*) and Bm-CPI-2 are able to impede antigen presentation in APCs via interference with host cysteine protease function, reducing T cell priming (136, 137). In this way, Bm-CPI-2 was reported to inhibit human B cells to present tetanus toxoid associated peptide. Bm-CPI-2 was shown to possess two inhibitory sites enabling it to hinder host cysteine proteases and asparaginyl endopeptidase (AEP) (136–138). Likewise, *Onchocerca volvulus* was shown to diminish HLA-DR expression by release of onchocystatin (139, 140). Other worms, such as *Nippostrongylus brasiliensis* and *Litomosoides sigmodontis* produce cystatins enabling these worms to block B cell-associated endosomal proteases and T cell proliferation via IL-10 induction, respectively (140–143). However, the main mechanism through which helminth-derived cystatins affect host cells is unknown, but there is evidence suggesting the involvement of scavenger receptors and the transforming growth factor-β receptor (TGFβ R) pathways in particular by Avcystatin (*A. viteae*-derived recombinant cystatin) and calreticulin (a protein secreted by *H. polygyrus*), thereby polarizing Th2 responses (144, 145). In support of the critical role of helminth cystatins in promoting worm longevity, it has been suggested that presence of anti-cystatin circulating antibodies in mice can confine infection, suggesting that cystatins restrict the process of antigen loading and presentation by MHCII in APCs (141).

TCR signaling can also be affected by some HDPs in favor of shaping immune response toward immunoregulation (146–148). A well-known component of SEA known as omega-1 is the best example of HDPs which directs host immunity toward Th2 response through an intriguing mechanism. Mechanistically, omega-1 has been found to target cytoskeletal compartments to

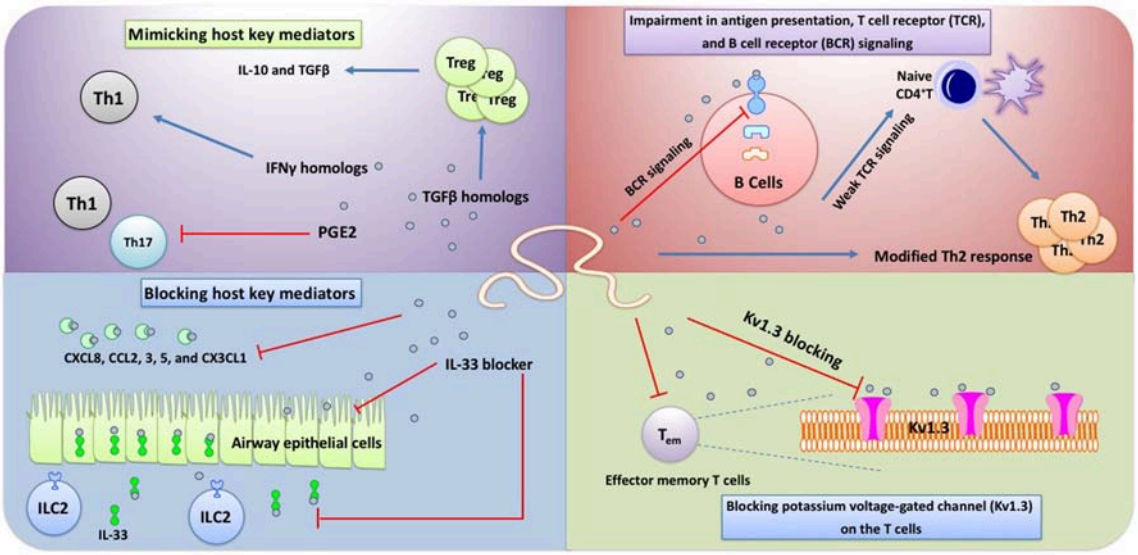

FIGURE 2 | Some HDPs has been shown to target non-PRRs sensors including Kv1.3 and TCRs on T cells. Blocking Kv1.3 can significantly decrease Th1 cell activity and proliferation. Also, presenting HDPs on the MHCII leads to induction a weak TCR signaling in naïve CD4 T cells which corroborates Th2 differentiation. Of note, the main phenotype of Th2 response elicited by helminths and their products is "modified Th2" immunity in which IL-5, IL-13, eosinophlilia, and IgE are all downregulated, while IL-4, TGFβ, and IL-10 are increased. BCR signaling has also been shown to be impaired by some HDPs which prevent B cell activation. HDPs have recently been more considered as magic components which are able to mimic or block several host key mediators which play an important role in immunosuppression and Th2 amplification, respectively.

confine the formation of a stable DC-CD4$^+$ T cell interplay, leading to suppression of TCR signaling strength and eventually Th2 cell differentiation. Since it has been documented that low dose antigens, which induce a weak TCR signaling, can prime Th2 response, the Th2-inducing property of omega-1 has also been ascribed to this hypothesis (149). Although omega-1 is able to inhibit TLR4-mediated DC stimulation independent of TLR-, MyD88- and TRIF, the main receptor targeted by omega-1 is still unknown, and it is thought that its enzymatic activity (T2 ribonuclease) likely contributes to such effects (86, 146). More investigations are required to identify whether other *S. mansoni* egg-derived antigens deviate immune responses toward Th2 by targeting TCR signaling (147). In support of helminth-mediated TCR signaling manipulation, Appleby et al. recently reported that in schistosome-endemic area of rural Zimbabwe, patients infected with *S. haematobium* had lower expression of CD3ζ (an integral part of TCR signaling) on peripheral blood mononuclear cells (PBMCs) than non-infected individuals, suggesting a possible TCR-targeted mechanism for hyporesponsiveness and immunosuppression (150).

In comparison to omega-1, the precise interruptive effects of ES-62 on TCR and BCR signaling have widely been determined (148). In fact, ES-62 by degradation of key components of downstream TCR and BCR signaling induces desensitization and in turn restrains cell proliferation and antibody production (151). Protein kinase C (PKC) and its different isoforms are one group of the major molecules that play a central role in orchestration of downstream cascade in TCR and BCR signaling for activation of transcription factors (152). It has been documented that ES-62 not only targets PKCs to be degraded/down-regulated in B and T cells but also up-regulates negative regulators of MAPKs signaling, such as RasGAP to suppress this pathway in Jurkat T cells (153). In addition, exposure of activated Th17 cells to LPS in the presence of ES-62 resulted in down-regulation of MyD88 and inhibition of LPS-mediated IL-17 production (154).

IgE signaling

Some HDPs, such as *Dirofilaria immitis*-derived antigen (DiAg) and *Clonorchis sinensis*-derived components called venom allergen-like proteins (CsVAL) are able to impair IgE-mediated degranulation followed by downstream signaling (155, 156). In this way, DiAg has been demonstrated to suppress type 1 diabetes in non-obese diabetic mice via Th1 inhibition and IL-10 induction (157). Interestingly, application of recombinant DiAg was associated with induction of nonspecific IgE by involving CD40 on B cells and saturation of FcεRI on mast cells, representing protective function against passive cutaneous anaphylaxis in rats (155). CsVAL has also displayed inhibitory activity on IgE-mediated degranulation of mast cells via targeting downstream pathways (156). Prevention of IgE receptor signaling has also been observed during exposure of human PBMCs to *S. mansoni* (158). It was revealed that the worm is able to secrete a component termed as schistosome-generated (SG) sCD23 which not only functions as a soluble decoy for the IgE receptor but also decreases the expression of this receptor (158). In addition, one of the well-characterized HDPs with interruptive effects on IgE signaling is ES-62. Collectively, these molecules might be considered as a potential therapeutic candidate in allergic disorders.

Mimicking and blocking host key mediators

TGFβ is one of the most powerful cytokines with immunoregulatory activity, which stimulates naïve T cells into regulatory T and B cells inducing immunobalance and tolerance in mucosal tissues, such as the intestine (159). This immunosuppressive cytokine and its receptor pathway have been reported to be mimicked and manipulated by helminths (159). Up to now, various components from nematodes like *A. caninum*, *B. malayi*, *H. polygyrus*, and trematodes, such as *F. hepatica* and the *Schistosoma* species have shown to produce TGFβ homologs (159). Bm-tgh-1 and Bm-tgh-2 from Brugia species and SmRK-1, 2, a TGF-β receptor homolog, from *S. mansoni* are well-known examples of HDPs with immunoregulatory activity due to mimicking TGFβ-induced mechanism (159). *H. polygyrus* is also able to stimulate naive T cells to express Treg-associated markers, such as Foxp3 amplifying immunoregulation via an unknown mechanism (160). Recently, Johnston et al. have characterized an important component from this worm known as *H. polygyrus* TGF-β mimic (Hp-TGM) which is structurally similar to a member of the complement control protein superfamily (161). Interestingly, Hp-TGM is functionally able to ligand mammalian TGFβR and mimic properties of TGFβ in induction of both mouse and human Foxp3$^+$ Treg cells (161).

Furthermore, Sulaiman et al. have recently suggested that juvenile stages of *F. hepatica* release a TGF-like molecule known as FhTLM, engaging host TGF-β receptors and triggers Smad2/3 signaling in leukocytes (162). They showed that TGF-β RII is the main target of this component through which FhTLM increases the production of IL-10 and PD-L1 and the mannose receptor expression which eventually facilitate the early evasion of juvenile by suppression host immune activation (162).

Another class of host mediators which are masterfully mimicked by some helminths, such as *S. mansoni* (163), *Taenia taeniaeformis*, and *B. malayi* are prostaglandins (PGs) (164). Among various PGs, the immunoregulatory properties of PGE2 have widely been documented (165), and it is known that it can modulate DC function to polarize immune response from Th1 toward Th2 (166). Laan et al. have recently found that *T. suis* releases high levels of PGE2 in its excretory-secretory products which are likely responsible for inhibition of LPS-induced production of inflammatory cytokines from human DCs (25). By contrast, *T. muris* may expedite Th1 response by production of IFNγ homologs to engage IFNγ receptors leading to Th1 amplification and suppression of IL-4 mediated responses against the worm (167, 168). Of note, the immune response depends on the host genotype and the infection levels, for example, resistant genotypes display Th2 response while susceptible hosts represent Th1 response. Also, low infection levels of *T. muris* elicit a Th1 and high infection induces a Th2 response (168).

Another strategy whereby helminths attenuate inflammatory signals is production of bioactive blockers to occupy receptors and entrap mediators triggering inflammatory responses, such as chemokines (169). For instance, a well-known chemokine blocker is a chemokine-binding protein which is released by SEA called smCKBP (169). This component has been found to be able to bind several chemokine ligands including CXCL8, CCL2, 3, 5, and CX3CL1 resulting in suppression of both inflammatory signals and recruitment of inflammatory cells at the site of insult (169). Relevant to helminth-derived blocking compounds, a very recent study by Osbourn et al. recognized a potent IL-33 blocking component called *H. polygyrus* Alarmin Release Inhibitor (HpARI) (170). Mechanistically, HpARI binds to both nuclear DNA and mature IL-33, preventing its release and interaction with IL-33R on airway epithelial cells and ILC2. Further experiments in mice confirmed the suppression ability of HpARI on IL-33 and subsequent airway allergic responses, involving eosinophilia and IL-5 and−13 (170). These authors revealed a novel mechanism of suppressing Th2 response onset via inhibition of IL-33 released from necrotic epithelial cells which are insulted during helminth infection and exposure to airway allergens (170).

Blocking potassium voltage-gated channel (Kv1.3) on the T cells

It has recently been shown that some HDPs can control the function of T cells by blocking potassium voltage-gated channel (Kv1.3) (171). AcK1 and BmK1 are a large family of Stichodactyla helianthus toxin (ShK) composed of peptide structures secreted by *A. ceylanicum* and *B. malayi*, respectively. These compounds are able to block Kv1.3 channels on T cells by engaging the outer vestibule of the channel (171). Kv1.3 channels have been proved to widely be expressed and involved in activation of human T cells (172). Since there are an immense number of myelin-reactive T cells (autoreactive) resembling Kv1.3^{high} phenotype in multiple sclerosis (MS) forestalling these cells by targeting Kv1.3 channels would be of great interest (173, 174). In accordance with this, some clinical trial studies have been launched to evaluate the efficacy of AcK1 and BmK1 in attenuation of inflammation (NCT02446340; NCT02435342).

Taken together, these data show that a complex of diverse intracellular pathways is triggered by HDPs which ultimately converge host immunity toward hyporesponsiveness and immunological tolerance via manipulation of PRR-dependent and independent strategies. Up to now, we have briefly reviewed the intracellular interferences of HDPs as a foundation to provide novel insights into the possible mechanisms of extracellular vesicles (EVs) as an important component of HDPs. In the following section, we aim to discuss the recognized pathways utilized by EVs released during helminth infections to bypass host immunity with the aim of proposing other unknown mechanisms.

EXTRACELLULAR VESICLES

Biogenesis, Content, and Morphological Properties

Various types of extracellular vesicles exist, but the structures that are most often referred to are called exosomes, which are 30–100 nm in diameter, or microvesicles, which measure about 100–1,000 nm in diameter (175). In terms of morphological properties and contents, exosomes are endocytic vesicles with a spherical shape surrounded by a bilamellar membrane. Their

contents constitute a wide variety of biomolecules including glycans, proteins, lipids, and nucleic acids (176). Exosomes are originally derived from endosomes via budding from their wall, and then aggregated in a large body known as the multivesicular body (MVB). Exosomes are unleashed in extracellular environment upon exocytosis of MVB through fusion with the plasma membrane (176). Apart from exosomes, other distinct vesicles with similar function and properties can be detected in extracellular space including microvesicles (plasma membrane-derived microparticle) and apoptotic bodies, which can be distinguished from exosomes in terms of biogenesis, size, protein contents, density, and isolation technique (176). Also, the formation of microvesicles is simpler and happens through an outward budding of the plasma membrane (177). Generally, all of them are considered as EV and exosomes are the smallest EV with the lowest density (176). Apoptotic bodies are not the subjects of this review and beyond our discussion.

Uptake in Recipient Cells

EVs have been acknowledged as important elements of cell-cell communication due to their role as vehicles for molecules and biological signals to be shuttled from one cell to another (178). Transfer of molecules, such as protein and miRNA can completely change the physiology of the receiving target cell and can in this way control both normal biological processes as well as distinct pathological processes (178).

EVs recognize and attach to their target cells through surface proteins, such as integrins, tetraspannins, proteoglycans, lectins, and immunoglobulins (179). The transfer of the EV content occurs as the EVs fuse with the target cells, which can be facilitated by various endocytic internalization pathways and the fusion can appear as rapidly as 15 min after exposure (180). Macropinocytosis is one such mechanism where EVs are captured and enclosed during the invagination of ruffled extensions from the plasma membrane (179). Another mechanism is phagocytosis, which is exploited by bacteria and viruses as well as DCs and macrophages and is facilitated by absorbing EVs by extended pseudopodia (180). Alternatively, EVs can be taken up by clathrin-mediated endocytosis, which involves the deformation of the target cell membrane by clathrin on the EV surface creating an inward bud that encloses the EVs, which can then pinch off and fuse with the endosome (181). Calveolin-dependent endocytosis is yet another mechanism for EV uptake where EVs oligomerize calveolin proteins on the membrane of the target cells facilitating the formation of intracellular calveolin-rich vesicles which then transports the EV contents to the target site (182). Finally, under specific conditions, EVs can fuse directly with the cell surface membrane (183).

Parasites use this remarkable ability of EVs to communicate with other parasite cells (parasite-parasite communication) (184) and host cells (host-parasite communication) (185). Strong evidence of the uptake of EVs by host cells has been obtained for a range of parasite species, including *Giardia duodenalis* (186), *Leishmania major* (187), *Plasmodium falciparum* (184), *Trichomonas vaginalis* (188), *Trypanosoma brucei* (189), *T. cruzi* (190), *Echinostoma caproni* (191), *F. hepatica* (28), *H. polygyrus* (30), *S. mansoni* (192), *A. suum*, *O. Dentatum*, and *T. suis* (Hansen et al., unpublished). Interestingly, Eichenberger et al. have recently employed organoids from murine colonic crypts to explore uptake of *T. muris*-derived EVs (193). These authors showed that when labeled EVs are delivered into the central lumen of organoids, they are internalized within 3 h and this process can be inhibited upon prevention of endocytosis (193). Furthermore, in this study transcriptomic and proteomic profile of *T. muris* EVs were characterized in which a number of miRNA with potential immunoregulatory effects on host immunity were identified (193). Upon fusion, specifically loaded compounds and biological signals in the EVs are transferred, which then can exert its function in the target cell. These events are responsible for the EV-related host immune manipulation (30, 194, 195), pathogenesis (196, 197) and parasite development (198), that have been reported for many parasitological diseases as described previously.

EVs FOR THE HOST IMMUNE SYSTEM

EV-Mediated Delivery of Message by Helminths

A number of parasites have shown to release EVs and they have received great interest due to their remarkable immunomodulatory properties including suppression of IL-6, TNFα, and IL-17A in mice (191, 199, 200). Various potential mechanisms have been suggested through which these vesicles might affect host cells (201). In fact, they have unique biological properties mediating cell-cell interaction both via direct contact and/or delivering biomaterial contents affecting intracellular crosstalk (202). However, the specific intracellular mechanisms that are targeted remain unknown or only partially characterized.

In recent years, helminth-associated EVs have shown to be essential mediators that contain bioactive cargo that contribute to establishing a permissive infection (30, 202). Apart from helminths, other microbes including fungi, bacteria, and protozoa are able to produce EVs and mediate active interaction with their host immunity to achieve a suitable niche (203). The release of such a protected package can undoubtedly optimize the integrity of contents, which in turn improve their efficacy in genetic exchange and secure delivery to modulate host immunity (203). Indeed, several studies have shown that powerful biomolecules are present in the helminth-derived EVs, which can offer potential and druggable candidates against inflammatory diseases (204). In addition, omics-based approaches, such as proteomics and transcriptomics have provided a plethora of valuable data facilitating recognition of major components mediating host immunosuppression. Such explorations provide novel insight into previously unknown strategies by which worms send messages to host cells to manipulate the host immune system and may therefore also pave the way to new ways to control infections (204–206).

Given interesting results achieved from EVs investigation, a surge of interest has been paid to focus on their contents. In the following, the most important biomolecules represented by helminth EVs along with their potential implications are discussed.

miRNAs as an Important Player for Intracellular Communication

One important component of EVs is miRNA, which is an evolutionary conserved class of short non-coding RNA, of 19–24 nucleotides in length, which plays an essential role in post-transcriptional gene regulation and is involved in the fine-tuning of a range of cellular processes. miRNA has been discovered in all types of human body fluids (207) and in various different species (208), including parasitic organisms (209, 210).

miRNA has been shown to take part in the regulation of any kind of biological process, here among embryonic development (211), cell differentiation and apoptosis (212–214) but also various immunological processes (215). In fact, miRNA seems to be involved in basically all aspects of immunological events of both innate and adaptive character. That being differential and activation of macrophages (216), dendritic cells (217), granulocytes (218), NK cells (219), and other innate immune cells (220) as well as development and function of B cells (221, 222) and T cells (223, 224).

Recent investigations suggest that helminth EVs also contain various RNA molecules including miRNA which may participate to the manipulating signaling pathways which orchestrating inflammatory responses (193). This mechanism may enable worms to directly interfere with host gene translation and thereby immunity to facilitate parasite survive (29, 30, 225). In support of this, an *in vitro* study showed that *E. multilocularis* produces a type of miRNA (emu-miR-71) which is able to suppress NO production and inflammation-associated miRNAs in LPS/IFN-treated murine macrophage RAW264.7 (29). By contrast, the effects of *S. japonicum*-derived exosomes on the same cell line of macrophages showed an increase of iNOS and TNF-α, supporting M1-type macrophage development (226). The steadily growing body of literature is supporting the critical role of exosome-associated miRNA as an important player involved in suppression or stimulation of target cells (30). One of this miRNA-mediated mechanism which has been recently suggested by Buck et al. is genetically blocking or targeting host mRNA for degradation, causing a severe defect in host immune response to confine worm expulsion. Molecular digestion showed that this miRNA is able to target 3′ untranslated region of the mRNA encoding Th2-associated cytokines, such as IL-33 which in turn prevents the ILC2 expansion and eliciting a strong Th2 response (30). Thus, it seems that helminths possess EVs with bioactive compounds, such as miRNAs that are able to effectively neutralize host immunity and polarize immune responses toward the way supporting their survival.

Gu et al. also suggest that some helminth miRNAs only might target host genes and that their release is a selective process as the profile of released miRNAs in the excretory-secretory products differed from that of adult extracts of *Haemonchus contortus* (227).

In addition to miRNA, other RNA molecules have been identified within helminth EVs, such as mRNA and tsRNA (193, 228) but their potential function and role in host-parasite interaction still need to be elucidated.

Proteins and Lipids in EVs

In addition to nucleic acid, EVs do also contain a diverse collection of molecules including lipids and proteins (229, 230). The protein composition has been characterized in excretory-secretory products from several parasite species using proteomic approaches based on mass spectrometry and has shown that it contains a suite of immunomodulatory proteins with immune suppressive effects e.g., on type 1 and type 2 effector molecules (30, 231–233).

Proteins identified in EVs comprise several peptidases, proteases, cytoskeletal proteins, nuclear proteins, calcium-binding proteins as well as stress-related proteins (28, 234, 235). Importantly, Coakley et al. demonstrated that *H. polygyrus* secretes EVs containing Argonaute protein, which is a central protein in the RNA-induced silencing complex (RISC) and is a powerful mechanism of gene silencing (229, 236). Furthermore, EVs are expected to be an important part of the secretome and it has been shown that the secreotomes of many helminths contain a variety of highly-abundant leaderless proteins, which is homolog to damage-associated molecular pattern molecules (DAMPs) in the host (28, 197). These DAMPs can, just like the host's DAMPs, modulate the host innate cells, such as stimulation of cytokine secretion in macrophages and lymphocytes. This could indicate that helminths have evolved mechanisms that are similar to their hosts in order to avoid elimination by the immune response of the hosts (182, 237).

Interestingly, besides parasite proteins, EVs have also been shown to contain host-derived proteins. Marcilla et al. identified 36 different host proteins in vesicles from the trematode *E. caproni*, which mainly corresponded to histones, partial sequences of mucins, metabolic enzymes, and immunoglobulins (28). Their study suggests that EVs might be an important part of the host-parasite communication as host proteins were identified in the parasite EVs and as the vesicles were taken up by host cells. These findings are interesting, however further studies are needed to confirm the role of the vesicles for the establishment of the infection (28). Very recently a similar study has been conducted by Eichenberger et al. in which proteomic profile of *T. muris*-derived EVs also identified a number of proteins of importance in host-parasite interaction. Of interest, among the common most proteins were predicted not to have a signal peptide supporting the idea that EVs constitute an important mechanism by which molecules are transferred to the host (193).

Surprisingly, several studies have shown that a significant proportion of the EV proteins are lacking an N-terminal presequence, also referred to as transit peptide. The transit peptide is required for protein transport across relevant membranes and indicates a protein transport through a classical sorting pathway via ER/Golgi pathway (238). Since a significant proportion of the parasite proteins are lacking the transit peptide, this suggests that EVs may be an important mechanism for transport of proteins host cells (28, 185, 239).

Lipids are a major component of EVs and play an important role in the function, stability, rigidity, and uptake of EVs, as they are directly exposed to the environment. Most of the lipidomic studies have been performed in cancer cells and these studies have indicated that EVs may have a function as lipid carriers where

they carry bioactive lipids to recipient cells. In the context of the tumor microenvironment, this transport may have an effect on the enrichment of tumor progression and immunosuppressive lipids, such as prostaglandins that enhance tumor growth (240, 241). Even though lipids are central to EV trafficking, only a few studies have yet explored the lipid content of EVs in parasites and their specific role remain to be elucidated (242, 243).

EVs AS NOVEL VACCINES

Even though helminth parasites infect over 25% of the world's population and are highly prevalent in livestock worldwide, these infections are one of the most "neglected" tropical diseases with no effective vaccines available for humans and only a few for animals (244, 245). The use of EVs as vaccines is an area of growing interest due to their immunomodulation role and EVs ability to generate specific antibodies (30, 191, 202).

Using EVs purified from *Echinostoma caproni*, Trelis et al. found that subcutaneous injection could reduce symptom severity and mortality of subsequent experimental infection in mice (191). Likewise, EV vaccination in mice generates specific antibodies and was sufficient to confer protective immunity against *H. polygyrus* challenge (202). *T. muris*-derived EVs has also recently been found to confer protection against subsequent infection (246). Several proteins were identified in the *T. muris* EVs and some proposed to be potential candidates for vaccine (246).

However, further studies are needed to further explore the potential of parasite-derived EVs as novel vaccine candidates (206). In another approach, DCs have been stimulated or infected with protozoan parasites following isolation of EVs, which then have been tested as vaccines. In this way, DC-derived EVs have shown to confer protective immunity against *Toxoplasma gondii* (247), *Leishmania major* (248).

Sotillo et al. observed that 31% of the identified proteins in EVs secreted from *S. mansoni* are homolog to previous describes vaccine candidates, where several of these proteins are common throughout the life cycle of the parasite. This indicates that a vaccine based on EVs could target different life stages of the parasite and may be effective against *S. mansoni* infection (249). However, EVs are biological complex and virtually nothing is known about their specific mechanisms and how they engage with the immune system. However, it was recently demonstrated that EVs from *H. polygyrus* are able to suppress both the activation of macrophages and target the Il-33 pathway, which is known to be essential for worm expulsion (202). Taken together, all these observations indicate that EVs hold a great potential for future vaccine development, and thereby pave the way for novel treatment options against parasite infection (206).

EVs AS NOVEL GENERATION OF BIOMARKERS: POSSIBILITIES AND POTENTIALS FOR EARLY DIAGNOSIS OF PARASITIC INFECTIONS

EVs have shown to contain a rich source of molecules and as these are protected from the environment by a membrane they are stable over time (250). In addition, as EVs are distributed in various body fluids and organs, they have received great interest for biomarker-based diagnosis (250). Indeed, the potential of EVs as a biomarker has widely been investigated in the field of cancers and the contents of exosomes derived from ovarian cancer patients have shown to differ from that of healthy individuals (250). Interestingly, some cancer types are associated with specific miRNA signatures in the exosomes and may, therefore, serve as a novel way of diagnosis and monitoring progression of treatment (251, 252). In infectious diseases, EVs isolated from serum samples have also shown potential in diagnostics (253). However, the physical location of the pathogen may affect the applicability of this method or at least the way samples should be collected. Buck et al. found that miRNA of *Litomosoides sigmodontis*, which is located in the pleural cavity, could be identified in the host serum whereas no miRNA of *H. polygyrus*, which resides in the gut lumen could be detected (30).

With the advent of high throughput assays, which now also includes EV array (254), a profound understanding is being established regarding host-parasite interplay and the main pathway by which EVs target host immune cells. Proteomics analysis on the HDPs concentrated in EVs has provided invaluable data to identify and purify the central candidate components for biomarkers, diagnostic tools, and vaccine development (255, 256). Likewise, HDPs merely have shown an acceptable potential to be considered as an approach to early infection diagnosis (257). For instance, cathepsin B1 from *Opisthorchis viverrini* has shown a potential candidate for further consideration as a biomarker in sera (258).

Altogether, the release of EVs might be a reciprocal beneficial interaction for both host and helminths. Eliciting an effective immune response against EVs is an obvious reason for the presence of highly immunogenic components which may offer possible biomarker candidate. On the other hand, helminths constantly explore a way to defeat host immunity and set up a permissive infection which production of EVs containing various types of material is might be a strong strategy (**Figure 3**).

PERSPECTIVES

Until now, many different and highly complex mechanisms have been suggested for immunosuppressive functions of HDPs. But, given the advances in recognition of EVs and their importance as an effective tool in manipulation of host immune cells, it makes sense to suppose the possible involvement of EVs in most HDPs-mediated immunomodulation.

Main intracellular pathways manipulated by HDPs were reviewed, but limited information has been provided regarding interaction between helminth-derived EVs and immune cells. Although several investigations have recently reported the potential intracellular functions of EVs, they are only partially characterized. Given the different mechanisms by which EVs are taken up by recipient cells (discussed in EV section), future investigations should focus on the intracellular mechanisms and pathways responsible for immunosuppression.

We believe that most mechanistic pathways which have been reported for HDPs can be tracked for EVs and their contents. Most biomolecules form contents of EVs require to reach into

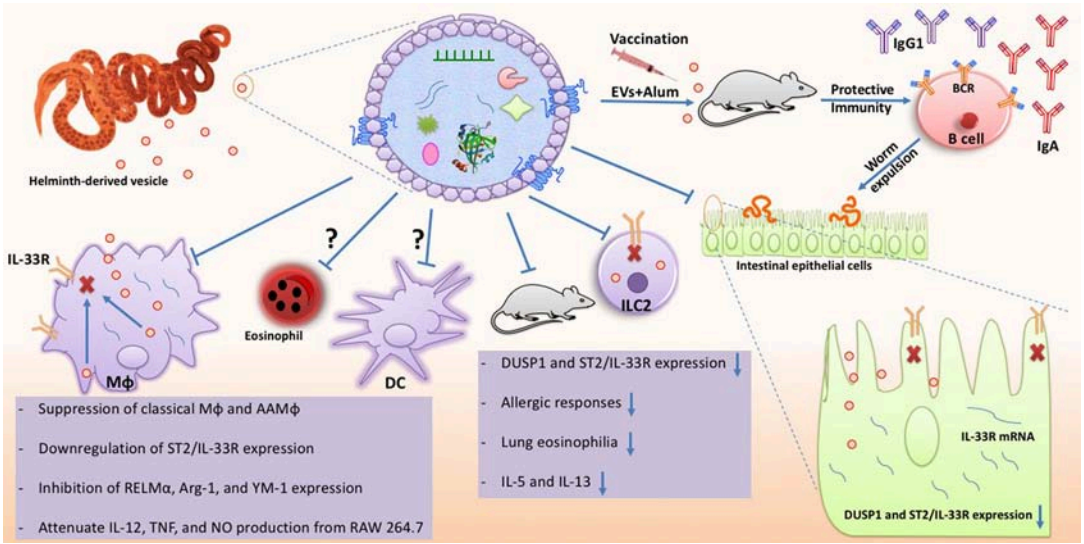

FIGURE 3 | Schematic illustration of known effects imposed by helminth-derived EVs during interaction with host immunity. As illustrated here, EVs can affect different host cells including immune cells and intestinal epithelial cells (IECs). Also, they can potentially be used to develop new vaccines against helminths. EVs deliver cargo containing various biomolecules to host cells which can interfere with host cell gene transcription. EVs are internalized by macrophages and IECs via unknown mechanism and target IL-33R and DUSP1 expression reducing signal transmission and leads to inhibition of helminth expulsion. EVs have also shown great potential in priming host immunity along with Alum as a vaccine complex against helminth infections. Effective suppression of both classical Mϕ and AAMϕ have also been reported, implying EVs are well-equipped with a wide range of active components. In addition to *in vitro* studies, immunomodulatory functions of EVs have also been monitored in *in vivo* model in which allergic responses, associated cytokines, ILC2, and eosinophilia are down-regulated in Alternaria-exposed mice.

the recipient cells to show their functions. The intracellular and PRR-targeting mechanisms of HDPs which were discussed in this review provide a framework to explore the possible interaction between EVs contents and intracellular components. In this regard, study on the PRRs-EV interplay would be of great interest to address some of the intracellular effects mediated by EVs. Release of EVs cargo in host immune cells can be associated with various outcomes, so determining the potential interaction between EVs cargo and PRRs downstream signaling would be valuable. For instance, Kojima et al. (259) showed that mesenteric lymph is able to exacerbate inflammatory responses via activation of TLR4 on macrophages without uptake through this receptor. They also showed that TLR4 signaling pathway is essential for exosome-induced macrophage activation (259).

EVs have recently been considered as a promising option to tune immune responses, as well as reprogram aberrant reactions to innocuous antigens. With respect to this, unraveling the main components of helminth-derived EVs, which are responsible for host immunomodulation may offer personalized therapeutic approaches in translational medicine.

Also, from a diagnostic point of view, EVs released by helminths may pave the way for developing a rapid diagnostic test that also can detect early parasitic infection. In addition, recognition and targeting main players in the biogenesis of helminth-derived EVs will be associated with novel insights into control of parasitic infections. Obviously, suppression of EVs synthesis containing a wide array of bioactive components will neutralize one of the central mechanism of helminths to overcome host immunity. Interestingly, interfering with EVs biogenesis with exploiting selective inhibitors has provided promising results in the field of cancer therapy (260), but the applicability of this approach to combat helminth infections remains elusive. However, several investigations have been conducted to assess the potential of protozoan EVs for vaccine development against toxoplasmosis and leishmaniasis (248, 261). In these studies, exosomes derived from DCs exposed to parasite antigens have shown to be able to protect against infection in experimental models. Collectively, it seems that the importance of EVs and their relevance in establishment of a chronic infection are less-known and eagerly awaited to precisely be unraveled in the near future.

AUTHOR CONTRIBUTIONS

AZ was the major contributor in conception, design, illustrations, and writing of the manuscript. EH and SA wrote the EV section. PN and AW edited the manuscript and provided critical comments, suggestions, and insightful revisions. This work was supervised by PN.

FUNDING

AZ was supported by the Lundbeck Foundation (Grant R249-2017-763). PN was supported by the Danish Council for Independent Research (DFF-6111-00521).

ACKNOWLEDGMENTS

All the authors thank their respective Institutes and Universities.

REFERENCES

1. Allen JE, Maizels RM. Diversity and dialogue in immunity to helminths. *Nat Rev Immunol*. (2011) 11:375–88. doi: 10.1038/nri2992
2. Jackson JA, Friberg IM, Little S, Bradley JE. Review series on helminths, immune modulation and the hygiene hypothesis: immunity against helminths and immunological phenomena in modern human populations: coevolutionary legacies? *Immunology* (2009) 126:18–27. doi: 10.1111/j.1365-2567.2008.03010.x
3. Wammes LJ, Mpairwe H, Elliott AM, Yazdanbakhsh M. Helminth therapy or elimination: epidemiological, immunological, and clinical considerations. *Lancet Infect Dis.* (2014) 14:1150–62. doi: 10.1016/S1473-3099(14)70771-6
4. Finlay CM, Walsh KP, Mills KH. Induction of regulatory cells by helminth parasites: exploitation for the treatment of inflammatory diseases. *Immunol Rev.* (2014) 259:206–30. doi: 10.1111/imr.12164
5. Zakeri A. Helminth-induced apoptosis: a silent strategy for immunosuppression. *Parasitology* (2017) 144:1663–76. doi: 10.1017/S0031182017000841
6. Zakeri A, Borji H, Haghparast A. Interaction between helminths and toll-like receptors: possibilities and potentials for asthma therapy. *Int Rev Immunol*. (2016) 35:219–48. doi: 10.3109/08830185.2015.1096936
7. Oliveira SC, Figueiredo BC, Cardoso LS, Carvalho EM. A double edged sword: *Schistosoma mansoni* Sm29 regulates both Th1 and Th2 responses in inflammatory mucosal diseases. *Mucosal Immunol*. (2016) 9:1366–71. doi: 10.1038/mi.2016.69
8. Harris NL, Loke P. Recent advances in Type-2-cell-mediated immunity: insights from helminth infection. *Immunity* (2017) 47:1024–36. doi: 10.1016/j.immuni.2017.11.015
9. Yazdanbakhsh M, Kremsner PG, van Ree R. Allergy, parasites, and the hygiene hypothesis. *Science* (2002) 296:490–4. doi: 10.1126/science.296.5567.490
10. Strachan DP. Hay fever, hygiene, and household size. *BMJ* (1989) 299:1259–60. doi: 10.1136/bmj.299.6710.1259
11. Bach JF. The hygiene hypothesis in autoimmunity: the role of pathogens and commensals. *Nat Rev Immunol*. (2018) 18:105–20. doi: 10.1038/nri.2017.111
12. La Flamme AC, Ruddenklau K, Backstrom BT. Schistosomiasis decreases central nervous system inflammation and alters the progression of experimental autoimmune encephalomyelitis. *Infect Immun*. (2003) 71:4996–004. doi: 10.1128/IAI.71.9.4996-5004.2003
13. Wilson MS, Taylor MD, Balic A, Finney CA, Lamb JR, Maizels RM. Suppression of allergic airway inflammation by helminth-induced regulatory T cells. *J Exp Med.* (2005) 202:1199–212. doi: 10.1084/jem.20042572
14. Schwartz C, Hams E, Fallon PG. Helminth modulation of lung inflammation. *Trends Parasitol*. (2018) 34:388–403. doi: 10.1016/j.pt.2017.12.007
15. Mangan NE, Fallon RE, Smith P, van Rooijen N, McKenzie AN, Fallon PG. Helminth infection protects mice from anaphylaxis via IL-10-producing B cells. *J Immunol*. (2004) 173:6346–56. doi: 10.4049/jimmunol.173.10.6346
16. Summers RW, Elliott DE, Urban JF, Jr., Thompson R, Weinstock JV. *Trichuris suis* therapy in Crohn's disease. *Gut* (2005) 54:87–90. doi: 10.1136/gut.2004.041749
17. Smith P, Mangan NE, Walsh CM, Fallon RE, McKenzie AN, van Rooijen N, et al. Infection with a helminth parasite prevents experimental colitis via a macrophage-mediated mechanism. *J Immunol*. (2007) 178:4557–66. doi: 10.4049/jimmunol.178.7.4557
18. Weinstock JV, Elliott DE. Helminth infections decrease host susceptibility to immune-mediated diseases. *J Immunol*. (2014) 193:3239–47. doi: 10.4049/jimmunol.1400927
19. Hepworth MR, Hartmann S. Worming our way closer to the clinic. *Int J Parasitol Drugs Drug Resist*. (2012) 2:187–90. doi: 10.1016/j.ijpddr.2012.07.001
20. Sotillo J, Toledo R, Mulvenna J, Loukas A. Exploiting helminth-host interactomes through big data. *Trends Parasitol*. (2017) 33:875–88. doi: 10.1016/j.pt.2017.06.011
21. Rigano R, Buttari B, Profumo E, Ortona E, Delunardo F, Margutti P, et al. *Echinococcus granulosus* antigen B impairs human dendritic cell differentiation and polarizes immature dendritic cell maturation towards a Th2 cell response. *Infect Immun.* (2007) 75:1667–78. doi: 10.1128/IAI.01156-06
22. Pineda MA, Eason RJ, Harnett MM, Harnett W. From the worm to the pill, the parasitic worm product ES-62 raises new horizons in the treatment of rheumatoid arthritis. *Lupus* (2015) 24:400–11. doi: 10.1177/0961203314560004
23. Harn DA, McDonald J, Atochina O, Da'dara AA. Modulation of host immune responses by helminth glycans. *Immunol Rev*. (2009) 230:247–57. doi: 10.1111/j.1600-065X.2009.00799.x
24. Summan A, Nejsum P, Williams AR. Modulation of human dendritic cell activity by Giardia and helminth antigens. *Parasite Immunol*. (2018) 40:e12525. doi: 10.1111/pim.12525
25. Laan LC, Williams AR, Stavenhagen K, Giera M, Kooij G, Vlasakov I, et al. The whipworm (*Trichuris suis*) secretes prostaglandin E2 to suppress proinflammatory properties in human dendritic cells. *FASEB J*. (2017) 31:719–31. doi: 10.1096/fj.201600841R
26. Klaver EJ, van der Pouw Kraan TC, Laan LC, Kringel H, Cummings RD, Bouma G, et al. *Trichuris suis* soluble products induce Rab7b expression and limit TLR4 responses in human dendritic cells. *Genes Immun.* (2015) 16:378–87. doi: 10.1038/gene.2015.18
27. Robinson MW, Donnelly S, Dalton JP. Helminth defence molecules-immunomodulators designed by parasites! *Front Microbiol*. (2013) 4:296. doi: 10.3389/fmicb.2013.00296
28. Marcilla A, Trelis M, Cortes A, Sotillo J, Cantalapiedra F, Minguez MT, et al. Extracellular vesicles from parasitic helminths contain specific excretory/secretory proteins and are internalized in intestinal host cells. *PLoS ONE* (2012) 7:e45974. doi: 10.1371/journal.pone.0045974
29. Zheng Y, Guo X, He W, Shao Z, Zhang X, Yang J, et al. Effects of *Echinococcus multilocularis* miR-71 mimics on murine macrophage RAW264.7 cells. *Int Immunopharmacol*. (2016) 34:259–62. doi: 10.1016/j.intimp.2016.03.015
30. Buck AH, Coakley G, Simbari F, McSorley HJ, Quintana JF, Le Bihan T, et al. Exosomes secreted by nematode parasites transfer small RNAs to mammalian cells and modulate innate immunity. *Nat Commun*. (2014) 5:5488. doi: 10.1038/ncomms6488
31. Nazimek K, Bryniarski K, Askenase PW. Functions of exosomes and microbial extracellular vesicles in allergy and contact and delayed-type hypersensitivity. *Int Arch Allergy Immunol*. (2016) 171:1–26. doi: 10.1159/000449249
32. Ung TH, Madsen HJ, Hellwinkel JE, Lencioni AM, Graner MW. Exosome proteomics reveals transcriptional regulator proteins with potential to mediate downstream pathways. *Cancer Sci*. (2014) 105:1384–92. doi: 10.1111/cas.12534
33. Loukas A, Hotez PJ, Diemert D, Yazdanbakhsh M, McCarthy JS, Correa-Oliveira R, et al. Hookworm infection. *Nat Rev Dis Primers*. (2016) 2:16088. doi: 10.1038/nrdp.2016.88
34. Shepherd C, Navarro S, Wangchuk P, Wilson D, Daly NL, Loukas A. Identifying the immunomodulatory components of helminths. *Parasite Immunol*. (2015) 37:293–303. doi: 10.1111/pim.12192
35. Lee MS, Kim YJ. Signaling pathways downstream of pattern-recognition receptors and their cross talk. *Annu Rev Biochem*. (2007) 76:447–80. doi: 10.1146/annurev.biochem.76.060605.122847
36. De Nardo D. Toll-like receptors: activation, signalling and transcriptional modulation. *Cytokine* (2015) 74:181–9. doi: 10.1016/j.cyto.2015.02.025
37. Maizels RM, Hewitson JP. "Immune Recognition of Parasite Glycans," In: Kosma P, Müller-Loennies S. editors *Anticarbohydrate Antibodies*. Vienna: Springer (2012).
38. Harnett W, Harnett MM. Helminth-derived immunomodulators: can understanding the worm produce the pill? *Nat Rev Immunol*. (2010) 10:278–84. doi: 10.1038/nri2730
39. Falcon C, Carranza F, Martinez FF, Knubel CP, Masih DT, Motran CC, et al. Excretory-secretory products (ESP) from *Fasciola hepatica* induce tolerogenic properties in myeloid dendritic cells. *Vet Immunol Immunopathol*. (2010) 137:36–46. doi: 10.1016/j.vetimm.2010.04.007
40. Kane CM, Cervi L, Sun J, McKee AS, Masek KS, Shapira S, et al. Helminth antigens modulate TLR-initiated dendritic cell activation. *J Immunol*. (2004) 173:7454–61. doi: 10.4049/jimmunol.173.12.7454
41. Silva-Alvarez V, Folle AM, Ramos AL, Kitano ES, Iwai LK, Corraliza I, et al. *Echinococcus granulosus* Antigen B binds to monocytes and macrophages modulating cell response to inflammation. *Parasit Vectors* (2016) 9:69. doi: 10.1186/s13071-016-1350-7

42. Nono JK, Pletinckx K, Lutz MB, Brehm K. Excretory/secretory-products of *Echinococcus multilocularis* larvae induce apoptosis and tolerogenic properties in dendritic cells *in vitro*. *PLoS Negl Trop Dis*. (2012) 6:e1516. doi: 10.1371/journal.pntd.0001516
43. Midttun HLE, Acevedo N, Skallerup P, Almeida S, Skovgaard K, Andresen L, et al. *Ascaris Suum* infection downregulates inflammatory pathways in the pig intestine *in vivo* and in human dendritic cells *in vitro*. *J Infect Dis*. (2018) 217:310–19. doi: 10.1093/infdis/jix585
44. Almeida S, Nejsum P, Williams AR. Modulation of human macrophage activity by Ascaris antigens is dependent on macrophage polarization state. *Immunobiology* (2018) 223:405–12. doi: 10.1016/j.imbio.2017.11.003
45. Arthur JS, Ley SC. Mitogen-activated protein kinases in innate immunity. *Nat Rev Immunol*. (2013) 13:679–92. doi: 10.1038/nri3495
46. Dunand-Sauthier I, Santiago-Raber ML, Capponi L, Vejnar CE, Schaad O, Irla M, et al. Silencing of c-Fos expression by microRNA-155 is critical for dendritic cell maturation and function. *Blood* (2011) 117:4490–500. doi: 10.1182/blood-2010-09-308064
47. Agrawal S, Agrawal A, Doughty B, Gerwitz A, Blenis J, Van Dyke T, et al. Cutting edge: different Toll-like receptor agonists instruct dendritic cells to induce distinct Th responses via differential modulation of extracellular signal-regulated kinase-mitogen-activated protein kinase and c-Fos. *J Immunol*. (2003) 171:4984–9. doi: 10.4049/jimmunol.171.10.4984
48. Nekrasova T, Shive C, Gao Y, Kawamura K, Guardia R, Landreth G, et al. ERK1-deficient mice show normal T cell effector function and are highly susceptible to experimental autoimmune encephalomyelitis. *J Immunol*. (2005) 175:2374–80. doi: 10.4049/jimmunol.175.4.2374
49. White RR, Artavanis-Tsakonas K. How helminths use excretory secretory fractions to modulate dendritic cells. *Virulence* (2012) 3:668–77. doi: 10.4161/viru.22832
50. Thomas PG, Carter MR, Atochina O, Da'Dara AA, Piskorska D, McGuire E, et al. Maturation of dendritic cell 2 phenotype by a helminth glycan uses a Toll-like receptor 4-dependent mechanism. *J Immunol*. (2003) 171:5837–41. doi: 10.4049/jimmunol.171.11.5837
51. Wilbers RH, Westerhof LB, van Noort K, Obieglo K, Driessen NN, Everts B, et al. Production and glyco-engineering of immunomodulatory helminth glycoproteins in plants. *Sci Rep*. (2017) 7:45910. doi: 10.1038/srep45910
52. Tripathi P, Sahoo N, Ullah U, Kallionpaa H, Suneja A, Lahesmaa R, et al. A novel mechanism for ERK-dependent regulation of IL4 transcription during human Th2-cell differentiation. *Immunol Cell Biol*. (2012) 90:676–87. doi: 10.1038/icb.2011.87
53. Cvetkovic J, Sofronic-Milosavljevic L, Ilic N, Gnjatovic M, Nagano I, Gruden-Movsesijan A. Immunomodulatory potential of particular Trichinella spiralis muscle larvae excretory-secretory components. *Int J Parasitol*. (2016) 46:833–42. doi: 10.1016/j.ijpara.2016.07.008
54. Bai X, Wu X, Wang X, Guan Z, Gao F, Yu J, et al. Regulation of cytokine expression in murine macrophages stimulated by excretory/secretory products from *Trichinella spiralis in vitro*. *Mol Cell Biochem*. (2012) 360:79–88. doi: 10.1007/s11010-011-1046-4
55. Rosadini CV, Kagan JC. Early innate immune responses to bacterial LPS. *Curr Opin Immunol*. (2017) 44:14–9. doi: 10.1016/j.coi.2016.10.005
56. Goodridge HS, Marshall FA, Else KJ, Houston KM, Egan C, Al-Riyami L, et al. Immunomodulation via novel use of TLR4 by the filarial nematode phosphorylcholine-containing secreted product, ES-62. *J Immunol*. (2005) 174:284–93. doi: 10.4049/jimmunol.174.1.284
57. Goodridge HS, Deehan MR, Harnett W, Harnett MM. Subversion of immunological signalling by a filarial nematode phosphorylcholine-containing secreted product. *Cell Signal*. (2005) 17:11–6. doi: 10.1016/j.cellsig.2004.05.014
58. Melendez AJ, Harnett MM, Pushparaj PN, Wong WS, Tay HK, McSharry CP, et al. Inhibition of Fc epsilon RI-mediated mast cell responses by ES-62, a product of parasitic filarial nematodes. *Nat Med*. (2007) 13:1375–81. doi: 10.1038/nm1654
59. Bell KS, Al-Riyami L, Lumb FE, Britton GJ, Poole AW, Williams CM, et al. The role of individual protein kinase C isoforms in mouse mast cell function and their targeting by the immunomodulatory parasitic worm product, ES-62. *Immunol Lett*. (2015) 168:31–40. doi: 10.1016/j.imlet.2015.09.001
60. Eason RJ, Bell KS, Marshall FA, Rodgers DT, Pineda MA, Steiger CN, et al. The helminth product, ES-62 modulates dendritic cell responses by inducing the selective autophagolysosomal degradation of TLR-transducers, as exemplified by PKCdelta. *Sci Rep*. (2016) 6:37276. doi: 10.1038/srep37276
61. Al-Riyami L, Pineda MA, Rzepecka J, Huggan JK, Khalaf AI, Suckling CJ, et al. Designing anti-inflammatory drugs from parasitic worms: a synthetic small molecule analogue of the Acanthocheilonema viteae product ES-62 prevents development of collagen-induced arthritis. *J Med Chem*. (2013) 56:9982–10002. doi: 10.1021/jm401251p
62. Lumb FE, Doonan J, Bell KS, Pineda MA, Corbet M, Suckling CJ, et al. Dendritic cells provide a therapeutic target for synthetic small molecule analogues of the parasitic worm product, ES-62. *Sci Rep*. (2017) 7:1704. doi: 10.1038/s41598-017-01651-1
63. Doonan J, Lumb FE, Pineda MA, Tarafdar A, Crowe J, Khan AM, et al. Protection against arthritis by the parasitic worm product ES-62, and its drug-like small molecule analogues, is associated with inhibition of osteoclastogenesis. *Front Immunol*. (2018) 9:1016. doi: 10.3389/fimmu.2018.01016
64. van Riet E, Everts B, Retra K, Phylipsen M, van Hellemond JJ, Tielens AG, et al. Combined TLR2 and TLR4 ligation in the context of bacterial or helminth extracts in human monocyte derived dendritic cells: molecular correlates for Th1/Th2 polarization. *BMC Immunol*. (2009) 10:9. doi: 10.1186/1471-2172-10-9
65. Gao Y, Chen L, Hou M, Chen Y, Ji M, Wu H, et al. TLR2 directing PD-L2 expression inhibit T cells response in Schistosoma japonicum infection. *PLoS ONE* (2013) 8:e82480 doi: 10.1371/journal.pone.0082480
66. Correale J, Farez MF. Parasite infections in multiple sclerosis modulate immune responses through a retinoic acid-dependent pathway. *J Immunol*. (2013) 191:3827–37. doi: 10.4049/jimmunol.1301110
67. van der Kleij D, Latz E, Brouwers JF, Kruize YC, Schmitz M, Kurt-Jones EA, et al. A novel host-parasite lipid cross-talk. Schistosomal lyso-phosphatidylserine activates toll-like receptor 2 and affects immune polarization. *J Biol Chem*. (2002) 277:48122–9. doi: 10.1074/jbc.M206941200
68. Layland LE, Rad R, Wagner H, da Costa CU. Immunopathology in schistosomiasis is controlled by antigen-specific regulatory T cells primed in the presence of TLR2. *Eur J Immunol*. (2007) 37:2174–84. doi: 10.1002/eji.200737063
69. Wang X, Zhou S, Chi Y, Wen X, Hoellwarth J, He L, et al. $CD4^+CD25^+$ Treg induction by an HSP60-derived peptide SJMHE1 from *Schistosoma japonicum* is TLR2 dependent. *Eur J Immunol*. (2009) 39:3052–65. doi:10.1002/eji.200939335
70. Thomas PG, Carter MR, Da'dara AA, DeSimone TM, Harn DA. A helminth glycan induces APC maturation via alternative NF-kappa B activation independent of I kappa B alpha degradation. *J Immunol*. (2005) 175:2082–90. doi: 10.4049/jimmunol.175.4.2082
71. Artis D, Kane CM, Fiore J, Zaph C, Shapira S, Joyce K, et al. Dendritic cell-intrinsic expression of NF-kappa B1 is required to promote optimal Th2 cell differentiation. *J Immunol*. (2005) 174:7154–9. doi: 10.4049/jimmunol.174.11.7154
72. Vukman KV, Adams PN, O'Neill SM. Fasciola hepatica tegumental coat antigen suppresses MAPK signalling in dendritic cells and up-regulates the expression of SOCS3. *Parasite Immunol*. (2013) 35:234–8. doi: 10.1111/pim.12033
73. Donnelly S, O'Neill SM, Stack CM, Robinson MW, Turnbull L, Whitchurch C, et al. Helminth cysteine proteases inhibit TRIF-dependent activation of macrophages via degradation of TLR3. *J Biol Chem*. (2010) 285:3383–92. doi: 10.1074/jbc.M109.060368
74. Yu YR, Deng MJ, Lu WW, Jia MZ, Wu W, Qi YF. Systemic cytokine profiles and splenic toll-like receptor expression during *Trichinella spiralis* infection. *Exp Parasitol*. (2013) 134:92–101. doi: 10.1016/j.exppara.2013.02.014
75. Gomez-Escobar N, Bennett C, Prieto-Lafuente L, Aebischer T, Blackburn CC, Maizels RM. Heterologous expression of the filarial nematode alt gene products reveals their potential to inhibit immune function. *BMC Biol*. (2005) 3:8. doi: 10.1186/1741-7007-3-8
76. Klaver EJ, Kuijk LM, Lindhorst TK, Cummings RD, van Die I. *Schistosoma mansoni* soluble egg antigens induce expression of the negative regulators SOCS1 and SHP1 in human dendritic cells via interaction with the mannose receptor. *PLoS ONE* (2015) 10:e0124089. doi: 10.1371/journal.pone.0124089
77. Klotz C, Ziegler T, Figueiredo AS, Rausch S, Hepworth MR, Obsivac N, et al. A helminth immunomodulator exploits host signaling events to regulate

cytokine production in macrophages. *PLoS Pathog.* (2011) 7:e1001248. doi: 10.1371/journal.ppat.1001248
78. Schierack P, Lucius R, Sonnenburg B, Schilling K, Hartmann S. Parasite-specific immunomodulatory functions of filarial cystatin. *Infect Immun.* (2003) 71:2422–9. doi: 10.1128/IAI.71.5.2422-2429.2003
79. Ziegler T, Rausch S, Steinfelder S, Klotz C, Hepworth MR, Kuhl AA, et al. A novel regulatory macrophage induced by a helminth molecule instructs IL-10 in $CD4^+$ T cells and protects against mucosal inflammation. *J Immunol.* (2015) 194:1555–64. doi: 10.4049/jimmunol.1401217
80. Aksoy E, Zouain CS, Vanhoutte F, Fontaine J, Pavelka N, Thieblemont N, et al. Double-stranded RNAs from the helminth parasite Schistosoma activate TLR3 in dendritic cells. *J Biol Chem.* (2005) 280:277–83. doi: 10.1074/jbc.M411223200
81. Yang Q, Qiu H, Xie H, Qi Y, Cha H, Qu J, et al. A *Schistosoma japonicum* infection promotes the expansion of myeloid-derived suppressor cells by activating the JAK/STAT3 Pathway. *J Immunol.* (2017) 198:4716–27. doi: 10.4049/jimmunol.1601860
82. Liu WF, Wen SH, Zhan JH, Li YS, Shen JT, Yang WJ, et al. Treatment with recombinant *Trichinella spiralis* cathepsin B-like protein ameliorates intestinal ischemia/reperfusion injury in mice by promoting a switch from M1 to M2 macrophages. *J Immunol.* (2015) 195:317–28. doi: 10.4049/jimmunol.1401864
83. Fukao T, Tanabe M, Terauchi Y, Ota T, Matsuda S, Asano T, et al. PI3K-mediated negative feedback regulation of IL-12 production in DCs. *Nat Immunol.* (2002) 3:875–81. doi: 10.1038/ni825
84. Kamda JD, Singer SM. Phosphoinositide 3-kinase-dependent inhibition of dendritic cell interleukin-12 production by *Giardia lamblia*. *Infect Immun.* (2009) 77:685–93. doi: 10.1128/IAI.00718-08
85. Motran CC, Ambrosio LF, Volpini X, Celias DP, Cervi L. Dendritic cells and parasites: from recognition and activation to immune response instruction. *Semin Immunopathol.* (2017) 39:199–213. doi: 10.1007/s00281-016-0588-7
86. Steinfelder S, Andersen JF, Cannons JL, Feng CG, Joshi M, Dwyer D, et al. The major component in schistosome eggs responsible for conditioning dendritic cells for Th2 polarization is a T2 ribonuclease (omega-1). *J Exp Med.* (2009) 206:1681–90. doi: 10.1084/jem.20082462
87. Brown GD, Willment JA, Whitehead L. C-type lectins in immunity and homeostasis. *Nat Rev Immunol.* (2018) 18:374–89. doi: 10.1038/s41577-018-0004-8
88. Thawer S, Auret J, Schnoeller C, Chetty A, Smith K, Darby M, et al. Surfactant protein-D is essential for immunity to helminth infection. *PLoS Pathog.* (2016) 2:e1005461. doi: 10.1371/journal.ppat.1005461
89. Favoretto BC, Casabuono AAC, Portes-Junior JA, Jacysyn JF, Couto AS, Faquim-Mauro EL. High molecular weight components containing N-linked oligosaccharides of *Ascaris suum* extract inhibit the dendritic cells activation through DC-SIGN and MR. *Mol Immunol.* (2017) 87:33–46. doi: 10.1016/j.molimm.2017.03.015
90. Tundup S, Srivastava L, Harn DA, Jr. Polarization of host immune responses by helminth-expressed glycans. *Ann NY Acad Sci.* (2012) 1253:1–13. doi: 10.1111/j.1749-6632.2012.06618.x
91. van Liempt E, Bank CM, Mehta P, Garcia-Vallejo JJ, Kawar ZS, Geyer R, et al. Specificity of DC-SIGN for mannose- and fucose-containing glycans. *FEBS Lett.* (2006) 580:6123–31. doi: 10.1016/j.febslet.2006.10.009
92. van Die I, van Vliet SJ, Nyame AK, Cummings RD, Bank CM, Appelmelk B, et al. The dendritic cell-specific C-type lectin DC-SIGN is a receptor for Schistosoma mansoni egg antigens and recognizes the glycan antigen Lewis x. *Glycobiology* (2003) 13:471–8. doi: 10.1093/glycob/cwg052
93. van Liempt E, van Vliet SJ, Engering A, Garcia Vallejo JJ, Bank CM, Sanchez-Hernandez M, et al. *Schistosoma mansoni* soluble egg antigens are internalized by human dendritic cells through multiple C-type lectins and suppress TLR-induced dendritic cell activation. *Mol Immunol.* (2007) 44:2605–15. doi: 10.1016/j.molimm.2006.12.012
94. van Die I, Cummings RD. Glycan gimmickry by parasitic helminths: a strategy for modulating the host immune response? *Glycobiology* (2010) 20:2–12. doi: 10.1093/glycob/cwp140
95. Paveley RA, Aynsley SA, Turner JD, Bourke CD, Jenkins SJ, Cook PC, et al. The Mannose Receptor (CD206) is an important pattern recognition receptor (PRR) in the detection of the infective stage of the helminth Schistosoma mansoni and modulates IFNgamma production. *Int J Parasitol.* (2011) 41:1335–45. doi: 10.1016/j.ijpara.2011.08.005
96. Hang L, Blum AM, Kumar S, Urban JF, Jr., Mitreva M, Geary TG, et al. Downregulation of the syk signaling pathway in intestinal dendritic cells is sufficient to induce dendritic cells that inhibit colitis. *J Immunol.* (2016) 197:2948–57. doi: 10.4049/jimmunol.1600063
97. Terrazas CA, Alcantara-Hernandez M, Bonifaz L, Terrazas LI, Satoskar AR Helminth-excreted/secreted products are recognized by multiple receptors on DCs to block the TLR response and bias Th2 polarization in a cRAF dependent pathway. *FASEB J.* (2013) 27:4547–60. doi: 10.1096/fj.13-228932
98. Terrazas C, de Dios Ruiz-Rosado J, Amici SA, Jablonski KA, Martinez-Saucedo D, Webb LM, et al. Helminth-induced Ly6C(hi) monocyte-derived alternatively activated macrophages suppress experimental autoimmune encephalomyelitis. *Sci Rep.* (2017) 7:40814. doi: 10.1038/srep40814
99. Loukas A, Maizels RM. Helminth C-type lectins and host-parasite interactions. *Parasitol Today* (2000) 16:333–9. doi: 10.1016/S0169-4758(00)01704-X
100. Schabussova I, Amer H, van Die I, Kosma P, Maizels RM. O-methylated glycans from toxocara are specific targets for antibody binding in human and animal infections. *Int J Parasitol.* (2007) 37:97–109. doi: 10.1016/j.ijpara.2006.09.006
101. Tawill S, Le Goff L, Ali F, Blaxter M, Allen JE. Both free-living and parasitic nematodes induce a characteristic Th2 response that is dependent on the presence of intact glycans. *Infect Immun.* (2004) 72:398–407. doi: 10.1128/IAI.72.1.398-407.2004
102. Rodriguez E, Kalay H, Noya V, Brossard N, Giacomini C, van Kooyk Y, et al. *Fasciola hepatica* glycoconjugates immuneregulate dendritic cells through the dendritic cell-specific intercellular adhesion molecule-3-Grabbing Non-integrin inducing T cell anergy. *Sci Rep.* (2017) 7:46748 doi: 10.1038/srep46748
103. Rodriguez E, Carasi P, Frigerio S, da Costa V, van Vliet S, Noya V, et al. *Fasciola hepatica* immune regulates CD11c(+) cells by interacting with the macrophage Gal/GalNAc Lectin. *Front Immunol.* (2017) 8:264. doi: 10.3389/fimmu.2017.00264
104. Ravida A, Cwiklinski K, Aldridge AM, Clarke P, Thompson R, Gerlach JQ, et al. *Fasciola hepatica* surface tegument: glycoproteins at the interface of parasite and host. *Mol Cell Proteomics* (2016) 15:3139–53. doi: 10.1074/mcp.M116.059774
105. Aldridge A, O'Neill SM. *Fasciola hepatica* tegumental antigens induce anergic-like T cells via dendritic cells in a mannose receptor-dependent manner. *Eur J Immunol.* (2016) 46:1180–92. doi: 10.1002/eji.201545905
106. Rodriguez E, Noya V, Cervi L, Chiribao ML, Brossard N, Chiale C, et al. Glycans from *Fasciola hepatica* modulate the host immune response and TLR-induced maturation of dendritic cells. *PLoS Negl Trop Dis.* (2015) 9:e0004234. doi: 10.1371/journal.pntd.0004234
107. Ravida A, Aldridge AM, Driessen NN, Heus FA, Hokke CH, O'Neill SM. *Fasciola hepatica* surface coat glycoproteins contain mannosylated and phosphorylated N-glycans and exhibit immune modulatory properties independent of the mannose receptor. *PLoS Negl Trop Dis.* (2016) 10:e0004601. doi: 10.1371/journal.pntd.0004601
108. Guasconi L, Chiapello LS, Masih DT. *Fasciola hepatica* excretory-secretory products induce $CD4^+$T cell anergy via selective up-regulation of PD-L2 expression on macrophages in a Dectin-1 dependent way. *Immunobiology* (2015) 220:934–9. doi: 10.1016/j.imbio.2015.02.001
109. Guasconi L, Serradell MC, Garro AP, Iacobelli L, Masih DT. C-type lectins on macrophages participate in the immunomodulatory response to *Fasciola hepatica* products. *Immunology* (2011) 133:386–96. doi: 10.1111/j.1365-2567.2011.03449.x
110. Ritter M, Gross O, Kays S, Ruland J, Nimmerjahn F, Saijo S, et al. *Schistosoma mansoni* triggers Dectin-2, which activates the Nlrp3 inflammasome and alters adaptive immune responses. *Proc Natl Acad Sci USA.* (2010) 107:20459–64. doi: 10.1073/pnas.1010337107
111. Aranzamendi C, Tefsen B, Jansen M, Chiumiento L, Bruschi F, Kortbeek T, et al. Glycan microarray profiling of parasite infection sera identifies the LDNF glycan as a potential antigen for serodiagnosis of trichinellosis. *Exp Parasitol.* (2011) 129:221–6. doi: 10.1016/j.exppara.2011.08.015
112. Everts B, Hussaarts L, Driessen NN, Meevissen MH, Schramm G, van der Ham AJ, et al. Schistosome-derived omega-1 drives Th2 polarization

by suppressing protein synthesis following internalization by the mannose receptor. *J Exp Med*. (2012) 209:1753–67. doi: 10.1084/jem.20111381
113. Meevissen MH, Wuhrer M, Doenhoff MJ, Schramm G, Haas H, Deelder AM, et al. Structural characterization of glycans on omega-1, a major *Schistosoma mansoni* egg glycoprotein that drives Th2 responses. *J Proteome Res*. (2010) 9:2630–42. doi: 10.1021/pr100081c
114. Bhargava P, Li C, Stanya KJ, Jacobi D, Dai L, Liu S, et al. Immunomodulatory glycan LNFPIII alleviates hepatosteatosis and insulin resistance through direct and indirect control of metabolic pathways. *Nat Med.* (2012) 18:1665–72. doi: 10.1038/nm.2962
115. Velupillai P, Harn DA. Oligosaccharide-specific induction of interleukin 10 production by $B220^+$ cells from schistosome-infected mice: a mechanism for regulation of $CD4^+$ T-cell subsets. *Proc Natl Acad Sci USA*. (1994) 91:18–22. doi: 10.1073/pnas.91.1.18
116. Kooij G, Braster R, Koning JJ, Laan LC, van Vliet SJ, Los T, et al. *Trichuris suis* induces human non-classical patrolling monocytes via the mannose receptor and PKC: implications for multiple sclerosis. *Acta Neuropathol Commun*. (2015) 3:45. doi: 10.1186/s40478-015-0223-1
117. Cvetkovic J, Ilic N, Sofronic-Milosavljevic L, Gruden-Movsesijan A. Glycans expressed on *Trichinella spiralis* excretory-secretory antigens are important for anti-inflamatory immune response polarization. *Comp Immunol Microbiol Infect Dis*. (2014) 37:355–67. doi: 10.1016/j.cimid.2014.10.004
118. van Die I, Cummings RD. The mannose receptor in regulation of helminth-mediated host immunity. *Front Immunol*. (2017) 8:1677. doi: 10.3389/fimmu.2017.01677
119. van Stijn CM, Meyer S, van den Broek M, Bruijns SC, van Kooyk Y, Geyer R, et al. *Schistosoma mansoni* worm glycolipids induce an inflammatory phenotype in human dendritic cells by cooperation of TLR4 and DC-SIGN. *Mol Immunol*. (2010) 47:1544–52. doi: 10.1016/j.molimm.2010.01.014
120. Meyer-Wentrup F, Cambi A, Joosten B, Looman MW, de Vries IJ, Figdor CG, et al. DCIR is endocytosed into human dendritic cells and inhibits TLR8-mediated cytokine production. *J Leukoc Biol*. (2009) 85:518–25. doi: 10.1189/jlb.0608352
121. Trinchieri G, Sher A. Cooperation of Toll-like receptor signals in innate immune defence. *Nat Rev Immunol*. (2007) 7:179–90. doi: 10.1038/nri2038
122. Geijtenbeek TB, Van Vliet SJ, Koppel EA, Sanchez-Hernandez M, Vandenbroucke-Grauls CM, Appelmelk B, et al. Mycobacteria target DC-SIGN to suppress dendritic cell function. *J Exp Med.* (2003) 197:7–17. doi: 10.1084/jem.20021229
123. Vanhoutte F, Breuilh L, Fontaine J, Zouain CS, Mallevaey T, Vasseur V, et al. Toll-like receptor (TLR)2 and TLR3 sensing is required for dendritic cell activation, but dispensable to control *Schistosoma mansoni* infection and pathology. *Microbes Infect*. (2007) 9:1606–13. doi: 10.1016/j.micinf.2007.09.013
124. Kane CM, Jung E, Pearce EJ. *Schistosoma mansoni* egg antigen-mediated modulation of Toll-like receptor (TLR)-induced activation occurs independently of TLR2, TLR4, and MyD88. *Infect Immun*. (2008) 76:5754–9. doi: 10.1128/IAI.00497-08
125. Breuilh L, Vanhoutte F, Fontaine J, van Stijn CM, Tillie-Leblond I, Capron M, et al. Galectin-3 modulates immune and inflammatory responses during helminthic infection: impact of galectin-3 deficiency on the functions of dendritic cells. *Infect Immun*. (2007) 75:5148–57. doi: 10.1128/IAI.02006-06
126. Van Liempt E, Imberty A, Bank CM, Van Vliet SJ, Van Kooyk Y, Geijtenbeek TB, et al. Molecular basis of the differences in binding properties of the highly related C-type lectins DC-SIGN and L-SIGN to Lewis X trisaccharide and *Schistosoma mansoni* egg antigens. *J Biol Chem.* (2004) 279:33161–7. doi: 10.1074/jbc.M404988200
127. Gringhuis SI, den Dunnen J, Litjens M, van Het Hof B, van Kooyk Y, Geijtenbeek TB. C-type lectin DC-SIGN modulates Toll-like receptor signaling via Raf-1 kinase-dependent acetylation of transcription factor NF-kappaB. *Immunity*. (2007) 26:605–16. doi: 10.1016/j.immuni.2007.03.012
128. Kuijk LM, van Die I. Worms to the rescue: can worm glycans protect from autoimmune diseases? *IUBMB Life* (2010) 62:303–12. doi: 10.1002/iub.304
129. Dillon S, Agrawal S, Banerjee K, Letterio J, Denning TL, Oswald-Richter K, et al. Yeast zymosan, a stimulus for TLR2 and dectin-1, induces regulatory antigen-presenting cells and immunological tolerance. *J Clin Invest*. (2006) 116:916–28. doi: 10.1172/JCI27203
130. Motran CC, Silvane L, Chiapello LS, Theumer MG, Ambrosio LF, Volpini X, et al. Helminth infections: recognition and modulation of the immune response by innate immune cells. *Front Immunol*. (2018) 9:664. doi: 10.3389/fimmu.2018.00664
131. Awad F, Assrawi E, Louvrier C, Jumeau C, Georgin-Lavialle S, Grateau G, et al. Inflammasome biology, molecular pathology and therapeutic implications. *Pharmacol Ther*. (2018) 187:133–49. doi: 10.1016/j.pharmthera.2018.02.011
132. Rzepecka J, Pineda MA, Al-Riyami L, Rodgers DT, Huggan JK, Lumb FE, et al. Prophylactic and therapeutic treatment with a synthetic analogue of a parasitic worm product prevents experimental arthritis and inhibits IL-1beta production via NRF2-mediated counter-regulation of the inflammasome. *J Autoimmun*. (2015) 60:59–73. doi: 10.1016/j.jaut.2015.04.005
133. Zaiss MM, Maslowski KM, Mosconi I, Guenat N, Marsland BJ, Harris NL. IL-1beta suppresses innate IL-25 and IL-33 production and maintains helminth chronicity. *PLoS Pathog.* (2013) 9:e1003531. doi: 10.1371/journal.ppat.1003531
134. Alhallaf R, Agha Z, Miller CM, Robertson AAB, Sotillo J, Croese J, et al. The NLRP3 inflammasome suppresses protective immunity to gastrointestinal helminth infection. *Cell Rep*. (2018) 23:1085–1098. doi: 10.1016/j.celrep.2018.03.097
135. Ferguson BJ, Newland SA, Gibbs SE, Tourlomousis P, Fernandes dos Santos P, Patel MN, et al. The *Schistosoma mansoni* T2 ribonuclease omega-1 modulates inflammasome-dependent IL-1beta secretion in macrophages. *Int J Parasitol*. (2015) 45:809–13. doi: 10.1016/j.ijpara.2015.08.005
136. Klotz C, Ziegler T, Danilowicz-Luebert E, Hartmann S. Cystatins of parasitic organisms. *Adv Exp Med Biol*. (2011) 712:208–21. doi: 10.1007/978-1-4419-8414-2_13
137. Manoury B, Gregory WF, Maizels RM, Watts C. Bm-CPI-2, a cystatin homolog secreted by the filarial parasite *Brugia malayi*, inhibits class II MHC-restricted antigen processing. *Curr Biol.* (2001) 11:447–51. doi: 10.1016/S0960-9822(01)00118-X
138. Hartmann S, Lucius R. Modulation of host immune responses by nematode cystatins. *Int J Parasitol*. (2003) 33:1291–302. doi: 10.1016/S0020-7519(03)00163-2
139. Lustigman S, Brotman B, Huima T, Prince AM, McKerrow JH. Molecular cloning and characterization of onchocystatin, a cysteine proteinase inhibitor of *Onchocerca volvulus*. *J Biol Chem.* (1992) 267:17339–46.
140. Hartmann S, Kyewski B, Sonnenburg B, Lucius R. A filarial cysteine protease inhibitor down-regulates T cell proliferation and enhances interleukin-10 production. *Eur J Immunol*. (1997) 27:2253–60. doi: 10.1002/eji.1830270920
141. Dainichi T, Maekawa Y, Ishii K, Zhang T, Nashed BF, Sakai T, et al. Nippocystatin, a cysteine protease inhibitor from Nippostrongylus brasiliensis, inhibits antigen processing and modulates antigen-specific immune response. *Infect Immun*. (2001) 69:7380–6. doi: 10.1128/IAI.69.12.7380-7386.2001
142. Pfaff AW, Schulz-Key H, Soboslay PT, Taylor DW, MacLennan K, Hoffmann WH. Litomosoides sigmodontis cystatin acts as an immunomodulator during experimental filariasis. *Int J Parasitol*. (2002) 32:171–8. doi: 10.1016/S0020-7519(01)00350-2
143. Schonemeyer A, Lucius R, Sonnenburg B, Brattig N, Sabat R, Schilling K, et al. Modulation of human T cell responses and macrophage functions by onchocystatin, a secreted protein of the filarial nematode *Onchocerca volvulus*. *J Immunol*. (2001) 167:3207–15. doi: 10.4049/jimmunol.167.6.3207
144. Schnoeller C, Rausch S, Pillai S, Avagyan A, Wittig BM, Loddenkemper C, et al. A helminth immunomodulator reduces allergic and inflammatory responses by induction of IL-10-producing macrophages. *J Immunol*. (2008) 180:4265–72. doi: 10.4049/jimmunol.180.6.4265
145. Rzepecka J, Rausch S, Klotz C, Schnoller C, Kornprobst T, Hagen J, et al. Calreticulin from the intestinal nematode *Heligmosomoides polygyrus* is a Th2-skewing protein and interacts with murine scavenger receptor-A. *Mol Immunol*. (2009) 46:1109–19. doi: 10.1016/j.molimm.2008.10.032
146. Everts B, Perona-Wright G, Smits HH, Hokke CH, van der Ham AJ, Fitzsimmons CM, et al. Omega-1, a glycoprotein secreted by Schistosoma mansoni eggs, drives Th2 responses. *J Exp Med*. (2009) 206:1673–80. doi: 10.1084/jem.20082460
147. Paul WE, Zhu J. How are T(H)2-type immune responses initiated and amplified? *Nat Rev Immunol*. (2010) 10:225–35. doi: 10.1038/nri2735

148. Pineda MA, Lumb F, Harnett MM, Harnett W. ES-62, a therapeutic anti-inflammatory agent evolved by the filarial nematode *Acanthocheilonema viteae*. *Mol Biochem Parasitol*. (2014) 194:1–8. doi: 10.1016/j.molbiopara.2014.03.003
149. Hosken NA, Shibuya K, Heath AW, Murphy KM, O'Garra A. The effect of antigen dose on CD4$^+$ T helper cell phenotype development in a T cell receptor-alpha beta-transgenic model. *J Exp Med*. (1995) 182:1579–84. doi: 10.1084/jem.182.5.1579
150. Appleby LJ, Nausch N, Heard F, Erskine L, Bourke CD, Midzi N, et al. Down regulation of the TCR Complex CD3zeta-Chain on CD3$^+$ T Cells: a potential mechanism for helminth-mediated immune modulation. *Front Immunol*. (2015) 6:51. doi: 10.3389/fimmu.2015.00051
151. Harnett W, Harnett MM. What causes lymphocyte hyporesponsiveness during filarial nematode infection? *Trends Parasitol*. (2006) 22:105–10. doi: 10.1016/j.pt.2006.01.010
152. Deehan MR, Harnett W, Harnett MM. A filarial nematode-secreted phosphorylcholine-containing glycoprotein uncouples the B cell antigen receptor from extracellular signal-regulated kinase-mitogen-activated protein kinase by promoting the surface Ig-mediated recruitment of Src homology 2 domain-containing tyrosine phosphatase-1 and Pac-1 mitogen-activated kinase-phosphatase. *J Immunol*. (2001) 166:7462–8. doi: 10.4049/jimmunol.166.12.7462
153. Harnett MM, Deehan MR, Williams DM, Harnett W. Induction of signalling anergy via the T-cell receptor in cultured Jurkat T cells by pre-exposure to a filarial nematode secreted product. *Parasite Immunol*. (1998) 20:551–63. doi: 10.1046/j.1365-3024.1998.00181.x
154. Pineda MA, McGrath MA, Smith PC, Al-Riyami L, Rzepecka J, Gracie JA, et al. The parasitic helminth product ES-62 suppresses pathogenesis in collagen-induced arthritis by targeting the interleukin-17-producing cellular network at multiple sites. *Arthritis Rheum*. (2012) 64:3168–78. doi: 10.1002/art.34581
155. Furuhashi Y, Imai S, Tezuka H, Fujita K. Recombinant dirofilaria immitis-derived antigen can suppress passive cutaneous anaphylaxis reactions. *Int Arch Allergy Immunol*. (2001) 125:144–51. doi: 10.1159/000053808
156. Jeong YI, Kim YJ, Ju JW, Hong SH, Lee MR, Cho SH, et al. Identification of anti-allergic effect of Clonorchis sinensis-derived protein venom allergen-like proteins (CsVAL). *Biochem Biophys Res Commun*. (2014) 445:549–55. doi: 10.1016/j.bbrc.2014.01.189
157. Imai S, Tezuka H, Fujita K. A factor of inducing IgE from a filarial parasite prevents insulin-dependent diabetes mellitus in nonobese diabetic mice. *Biochem Biophys Res Commun*. (2001) 286:1051–8. doi: 10.1006/bbrc.2001.5471
158. Griffith Q, Liang Y, Whitworth P, Rodriguez-Russo C, Gul A, Siddiqui AA, et al. Immuno-evasive tactics by schistosomes identify an effective allergy preventative. *Exp Parasitol*. (2015) 153:139–50. doi: 10.1016/j.exppara.2015.03.012
159. Johnston CJ, Smyth DJ, Dresser DW, Maizels RM. TGF-beta in tolerance, development and regulation of immunity. *Cell Immunol*. (2016) 299:14–22. doi: 10.1016/j.cellimm.2015.10.006
160. McSorley HJ, Grainger JR, Harcus Y, Murray J, Nisbet AJ, Knox DP, et al. daf-7-related TGF-beta homologues from Trichostrongyloid nematodes show contrasting life-cycle expression patterns. *Parasitology* (2010) 137:159–71. doi:10.1017/S0031182009990321
161. Johnston CJC, Smyth DJ, Kodali RB, White MPJ, Harcus Y, Filbey KJ, et al. A structurally distinct TGF-beta mimic from an intestinal helminth parasite potently induces regulatory T cells. *Nat Commun*. (2017) 8:1741. doi:10.1038/s41467-017-01886-6
162. Sulaiman AA, Zolnierczyk K, Japa O, Owen JP, Maddison BC, Emes RD, et al. A trematode parasite derived growth factor binds and exerts influences on host immune functions via host cytokine receptor complexes. *PLoS Pathog*. (2016) 12:e1005991. doi: 10.1371/journal.ppat.1005991
163. Fusco AC, Salafsky B, Kevin MB. *Schistosoma mansoni*: eicosanoid production by cercariae. *Exp Parasitol*. (1985) 59:44–50. doi: 10.1016/0014-4894(85)90055-4
164. Szkudlinski J. Occurrence of prostaglandins and other eicosanoids in parasites and their role in host-parasite interaction. *Wiad Parazytol*. (2000) 46:439–46.
165. Nakanishi M, Rosenberg DW. Multifaceted roles of PGE2 in inflammation and cancer. *Semin Immunopathol*. (2013) 35:123–37. doi: 10.1007/s00281-012-0342-8
166. Kalinski P. Regulation of immune responses by prostaglandin E2. *J Immunol*. (2012) 188:21–8. doi: 10.4049/jimmunol.1101029
167. Grencis RK, Entwistle GM. Production of an interferon-gamma homologue by an intestinal nematode: functionally significant or interesting artefact? *Parasitology* (1997) 115:S101–6.
168. Cliffe LJ, Grencis RK. The *Trichuris muris* system: a paradigm of resistance and susceptibility to intestinal nematode infection. *Adv Parasitol*. (2004) 57:255–307. doi: 10.1016/S0065-308X(04)57004-5
169. Smith P, Fallon RE, Mangan NE, Walsh CM, Saraiva M, Sayers JR, et al. *Schistosoma mansoni* secretes a chemokine binding protein with antiinflammatory activity. *J Exp Med*. (2005) 202:1319–25. doi: 10.1084/jem.20050955
170. Osbourn M, Soares DC, Vacca F, Cohen ES, Scott IC, Gregory WF, et al. HpARI protein secreted by a helminth parasite suppresses interleukin-33. *Immunity* (2017) 47:739–51. doi: 10.1016/j.immuni.2017.09.015
171. Chhabra S, Chang SC, Nguyen HM, Huq R, Tanner MR, Londono LM, et al. Kv1.3 channel-blocking immunomodulatory peptides from parasitic worms: implications for autoimmune diseases. *FASEB J*. (2014) 28:3952–64. doi: 10.1096/fj.14-251967
172. Chandy KG, DeCoursey TE, Cahalan MD, McLaughlin C, Gupta S. Voltage-gated potassium channels are required for human T lymphocyte activation. *J Exp Med*. (1984) 160:369–85. doi: 10.1084/jem.160.2.369
173. Wulff H, Calabresi PA, Allie R, Yun S, Pennington M, Beeton C, et al. The voltage-gated Kv1.3 K(+) channel in effector memory T cells as new target for MS. *J Clin Invest*. (2003) 111:1703–13. doi: 10.1172/JCI16921
174. Beeton C, Wulff H, Standifer NE, Azam P, Mullen KM, Pennington MW, et al. Kv1.3 channels are a therapeutic target for T cell-mediated autoimmune diseases. *Proc Natl Acad Sci USA*. (2006) 103:17414–9. doi: 10.1073/pnas.0605136103
175. Raposo G, Stoorvogel W. Extracellular vesicles: exosomes, microvesicles, and friends. *J Cell Biol*. (2013) 200:373–83. doi: 10.1083/jcb.201211138
176. Buzas EI, Gyorgy B, Nagy G, Falus A, Gay S. Emerging role of extracellular vesicles in inflammatory diseases. *Nat Rev Rheumatol*. (2014) 10:356–64. doi: 10.1038/nrrheum.2014.19
177. Kanada M, Bachmann MH, Contag CH. Signaling by extracellular vesicles advances cancer hallmarks. *Trends Cancer* (2016) 2:84–94. doi: 10.1016/j.trecan.2015.12.005
178. Robbins PD, Morelli AE. Regulation of immune responses by extracellular vesicles. *Nat Rev Immunol*. (2014) 14:195–208. doi: 10.1038/nri3622
179. Mulcahy LA, Pink RC, Carter DR. Routes and mechanisms of extracellular vesicle uptake. *J Extracell Vesicles* (2014) 3. doi: 10.3402/jev.v3.24641
180. Feng D, Zhao WL, Ye YY, Bai XC, Liu RQ, Chang LF, et al. Cellular internalization of exosomes occurs through phagocytosis. *Traffic* (2010) 11:675–87. doi: 10.1111/j.1600-0854.2010.01041.x
181. Kirchhausen T. Clathrin. *Annu Rev Biochem*. (2000) 69:699–727. doi: 10.1146/annurev.biochem.69.1.699
182. Doherty GJ, McMahon HT. Mechanisms of endocytosis. *Annu Rev Biochem*. (2009) 78:857–902. doi: 10.1146/annurev.biochem.78.081307.110540
183. Parolini I, Federici C, Raggi C, Lugini L, Palleschi S, De Milito A, et al. Sargiacomo and *S. fais*: microenvironmental pH is a key factor for exosome traffic in tumor cells. *J Biol Chem*. (2009) 284:34211–22. doi: 10.1074/jbc.M109.041152
184. Regev-Rudzki N, Wilson DW, Carvalho TG, Sisquella X, Coleman BM, Rug M, et al. Cell-cell communication between malaria-infected red blood cells via exosome-like vesicles. *Cell* (2013) 153:1120–33. doi: 10.1016/j.cell.2013.04.029
185. Marcilla A, Martin-Jaular L, Trelis M, de Menezes-Neto A, Osuna A, Bernal D, et al. Extracellular vesicles in parasitic diseases. *J Extracell Vesicles* (2014) 3:25040. doi: 10.3402/jev.v3.25040
186. Benchimol M. The release of secretory vesicle in encysting Giardia lamblia. *FEMS Microbiol Lett*. (2004) 235:81–7. doi: 10.1016/j.femsle.2004.04.014
187. Silverman JM, Clos J, de'Oliveira CC, Shirvani O, Fang Y, Wang C, et al. An exosome-based secretion pathway is responsible for protein export from Leishmania and communication with macrophages. *J Cell Sci*. (2010) 123:842–52. doi: 10.1242/jcs.056465

188. Twu O, de Miguel N, Lustig G, Stevens GC, Vashisht AA, Wohlschlegel JA, et al. *Trichomonas vaginalis* exosomes deliver cargo to host cells and mediate hostratioparasite interactions. *PLoS Pathog.* (2013) 9:e1003482. doi: 10.1371/journal.ppat.1003482
189. Szempruch AJ, Sykes SE, Kieft R, Dennison L, Becker AC, Gartrell A, et al. Extracellular vesicles from *Trypanosoma brucei* mediate virulence factor transfer and cause host anemia. *Cell* (2016) 164:246–57. doi: 10.1016/j.cell.2015.11.051
190. Garcia-Silva MR, Cabrera-Cabrera F, das Neves RF, Souto-Padron T, de Souza W, Cayota A. Gene expression changes induced by Trypanosoma cruzi shed microvesicles in mammalian host cells: relevance of tRNA-derived halves. *Biomed Res Int*. (2014) 305239 doi: 10.1155/2014/305239
191. Trelis M, Galiano A, Bolado A, Toledo R, Marcilla A, Bernal D. Subcutaneous injection of exosomes reduces symptom severity and mortality induced by Echinostoma caproni infection in BALB/c mice. *Int J Parasitol.* (2016) 46:799–808. doi: 10.1016/j.ijpara.2016.07.003
192. Samoil V, Dagenais M, Ganapathy V, Aldridge J, Glebov A, Jardim A, et al. Vesicle-based secretion in schistosomes: analysis of protein and microRNA (miRNA) content of exosome-like vesicles derived from *Schistosoma mansoni*. *Sci Rep*. (2018) 8:3286. doi: 10.1038/s41598-018-21587-4
193. Eichenberger RM, Talukder MH, Field MA, Wangchuk P, Giacomin P, Loukas A, et al. Characterization of *Trichuris muris* secreted proteins and extracellular vesicles provides new insights into host-parasite communication. *J Extracell Vesicles* (2018) 7:1428004. doi: 10.1080/20013078.2018.1428004
194. Kifle DW, Sotillo J, Pearson MS, Loukas A. Extracellular vesicles as a target for the development of anti-helminth vaccines. *Emerg Topics Life Sci.* (2017) 1:659–65. doi: 10.1042/ETLS20170095
195. Silverman JM, Clos J, Horakova E, Wang AY, Wiesgigl M, Kelly I, et al. Leishmania exosomes modulate innate and adaptive immune responses through effects on monocytes and dendritic cells. *J Immunol*. (2010) 185:5011–22. doi: 10.4049/jimmunol.1000541
196. Combes V, Coltel N, Alibert M, van Eck M, Raymond C, Juhan-Vague I, et al. ABCA1 gene deletion protects against cerebral malaria: potential pathogenic role of microparticles in neuropathology. *Am J Pathol*. (2005) 166:295–302. doi: 10.1016/S0002-9440(10)62253-5
197. Cwiklinski K, de la Torre-Escudero E, Trelis M, Bernal D, Dufresne PJ, Brennan GP, et al. Biogenesis pathways and cargo molecules involved in parasite pathogenesis. *Mol Cell Proteomics* (2015) 14:3258–73. doi: 10.1074/mcp.M115.053934
198. Simoes MC, Lee J, Djikeng A, Cerqueira GC, Zerlotini A, da Silva-Pereira RA, et al. Identification of *Schistosoma mansoni* microRNAs. *BMC Genomics* (2011) 12:47. doi: 10.1186/1471-2164-12-47
199. Roig J, Saiz ML, Galiano A, Trelis M, Cantalapiedra F, Monteagudo C, et al. Extracellular vesicles from the *Helminth Fasciola* hepatica prevent DSS-induced acute ulcerative colitis in a T-lymphocyte independent mode. *Front Microbiol.* (2018) 9:1036. doi: 10.3389/fmicb.2018.01036
200. Eichenberger RM, Ryan S, Jones L, Buitrago G, Polster R, Montes de Oca M, et al. Hookworm secreted extracellular vesicles interact with host cells and prevent inducible colitis in mice. *Front Immunol*. (2018) 9:850. doi: 10.3389/fimmu.2018.00850
201. Eichenberger RM, Sotillo J, Loukas A. Immunobiology of parasitic worm extracellular vesicles. *Immunol Cell Biol*. (2018) 96:704–13. doi: 10.1111/imcb.12171
202. Coakley G, McCaskill JL, Borger JG, Simbari F, Robertson E, Millar M, et al. Extracellular vesicles from a helminth parasite suppress macrophage activation and constitute an effective vaccine for protective immunity. *Cell Rep*. (2017) 19:1545–57. doi: 10.1016/j.celrep.2017.05.001
203. Schorey JS, Cheng Y, Singh PP, Smith VL. Smith: Exosomes and other extracellular vesicles in host-pathogen interactions. *EMBO Rep*. (2015) 16:24–43. doi: 10.15252/embr.201439363
204. Lustigman S, Grote A, Ghedin E. Ghedin: The role of 'omics' in the quest to eliminate human filariasis. *PLoS Negl Trop Dis*. (2017) 11:e005464. doi: 10.1371/journal.pntd.0005464
205. Zhu L, Liu J, Dao J, Lu K, Li H, Gu H, et al. Molecular characterization of *S. japonicum* exosome-like vesicles reveals their regulatory roles in parasite-host interactions. *Sci Rep*. (2016) 6:5885. doi: 10.1038/srep25885
206. Mekonnen GG, Pearson M, Loukas A, Sotillo J. Extracellular vesicles from parasitic helminths and their potential utility as vaccines. *Expert Rev Vaccines* (2018) 17:197–205. doi: 10.1080/14760584.2018.1431125
207. Weber JA, Baxter DH, Zhang S, Huang DY, Huang KH, Lee MJ, et al. The microRNA spectrum in 12 body fluids. *Clin Chem.* (2010) 56:1733–41. doi: 10.1373/clinchem.2010.147405
208. Berezikov E. Evolution of microRNA diversity and regulation in animals. *Nat Rev Genet*. (2011) 12:846–60. doi: 10.1038/nrg3079
209. Zheng Y, Cai X, Bradley JE. microRNAs in parasites and parasite infection. *RNA Biol*. (2013) 10:371–9. doi: 10.4161/rna.23716
210. Gutierrez-Loli R, Orrego MA, Sevillano-Quispe OG, Herrera-Arrasco L, Guerra-Giraldez C. MicroRNAs in *Taenia solium* neurocysticercosis: insights as promising agents in host-parasite interaction and their potential as biomarkers. *Front Microbiol*. (2017) 8:1905. doi: 10.3389/fmicb.2017.01905
211. Darnell DK, Kaur S, Stanislaw S, Konieczka JH, Yatskievych TA, Antin PB. MicroRNA expression during chick embryo development. *Dev Dyn*. (2006) 235:3156–65. doi: 10.1002/dvdy.20956
212. Aranha MM, Santos DM, Xavier JM, Low WC, Steer CJ, Sola S, et al. Apoptosis-associated microRNAs are modulated in mouse, rat and human neural differentiation. *BMC Genomics* (2010) 11:514. doi: 10.1186/1471-2164-11-514
213. Le MT, Xie H, Zhou B, Chia PH, Rizk P, Um M, et al. MicroRNA-125b promotes neuronal differentiation in human cells by repressing multiple targets. *Mol Cell Biol*. (2009) 29:5290–305. doi: 10.1128/MCB.01694-08
214. Nguyen HT, Dalmasso G, Yan Y, Laroui H, Dahan S, Mayer L, et al. MicroRNA-7 modulates CD98 expression during intestinal epithelial cell differentiation. *J Biol Chem*. (2010) 285:1479–89. doi: 10.1074/jbc.M109.057141
215. Tsitsiou E, Lindsay MA. microRNAs and the immune response. *Curr Opin Pharmacol*. (2009) 9:514–20. doi: 10.1016/j.coph.2009.05.003
216. O'Connell RM, Taganov KD, Boldin MP, Cheng G, Baltimore D. MicroRNA-155 is induced during the macrophage inflammatory response. *Proc Natl Acad Sci USA*. (2007) 104:1604–9. doi: 10.1073/pnas.0610731104
217. Turner ML, Schnorfeil FM, Brocker T. MicroRNAs regulate dendritic cell differentiation and function. *J Immunol*. (2011) 187:3911–7. doi: 10.4049/jimmunol.1101137
218. Johnnidis JB, Harris MH, Wheeler RT, Stehling-Sun S, Lam MH, Kirak O, et al. Regulation of progenitor cell proliferation and granulocyte function by microRNA-223. *Nature* (2008) 451:1125–9. doi: 10.1038/nature06607
219. Pobezinsky LA, Etzensperger R, Jeurling S, Alag A, Kadakia T, McCaughtry TM, et al. Let-7 microRNAs target the lineage-specific transcription factor PLZF to regulate terminal NKT cell differentiation and effector function. *Nat Immunol*. (2015) 16:517–24. doi: 10.1038/ni.3146
220. Lu J, Guo S, Ebert BL, Zhang H, Peng X, Bosco J, et al. MicroRNA-mediated control of cell fate in megakaryocyte-erythrocyte progenitors. *Dev Cell*. (2008) 14:843–53. doi: 10.1016/j.devcel.2008.03.012
221. Nutt SL, Kee BL. The transcriptional regulation of B cell lineage commitment. *Immunity* (2007) 26:715–25. doi: 10.1016/j.immuni.2007.05.010
222. Vigorito E, Perks KL, Abreu-Goodger C, Bunting S, Xiang Z, Kohlhaas S, et al. microRNA-155 regulates the generation of immunoglobulin class-switched plasma cells. *Immunity* (2007) 27:847–59. doi: 10.1016/j.immuni.2007.10.009
223. Cobb BS, Nesterova TB, Thompson E, Hertweck A, O'Connor E, Godwin J, et al. T cell lineage choice and differentiation in the absence of the RNase III enzyme dicer. *J Exp Med*. (2005) 201:1367–73. doi:10.1084/jem.20050572
224. Li QJ, Chau J, Ebert PJ, Sylvester G, Min H, Liu G, et al. miR-181a is an intrinsic modulator of T cell sensitivity and selection. *Cell* (2007) 129:147–61. doi: 10.1016/j.cell.2007.03.008
225. Hansen EP, Kringel H, Williams AR, Nejsum P. Secretion of RNA-containing extracellular vesicles by the porcine whipworm, *Trichuris suis*. *J Parasitol*. (2015) 101:336–40. doi: 10.1645/14-714.1
226. Wang L, Li Z, Shen J, Liu Z, Liang J, Wu X, et al. Exosome-like vesicles derived by *Schistosoma japonicum* adult worms mediates M1 type immune- activity of macrophage. *Parasitol Res*. (2015) 114:1865–73. doi: 10.1007/s00436-015-4373-7
227. Gu HY, Marks ND, Winter AD, Weir W, Tzelos T, McNeilly TN, et al. Conservation of a microRNA cluster in parasitic nematodes and

profiling of miRNAs in excretory-secretory products and microvesicles of *Haemonchus contortus*. *PLoS Negl Trop Dis*. (2017) 11:e0006056. doi: 10.1371/journal.pntd.0006056
228. Nowacki FC, Swain MT, Klychnikov OI, Niazi U, Ivens A, Quintana JF, et al. Protein and small non-coding RNA-enriched extracellular vesicles are released by the pathogenic blood fluke Schistosoma mansoni. *J Extracell Vesicles* (2015) 4:28665. doi:10.3402/jev.v4.28665
229. Coakley G, Maizels RM, Buck AH. Exosomes and other extracellular vesicles: the new communicators in parasite infections. *Trends Parasitol*. (2015) 31:477–89. doi: 10.1016/j.pt.2015.06.009
230. Subra C, Grand D, Laulagnier K, Stella A, Lambeau G, Paillasse M, et al. Exosomes account for vesicle-mediated transcellular transport of activatable phospholipases and prostaglandins. *J Lipid Res*. (2010) 51:2105–20. doi: 10.1194/jlr.M003657
231. Grainger JR, Smith KA, Hewitson JP, McSorley HJ, Harcus Y, Filbey KJ, et al.Helminth secretions induce *de novo* T cell Foxp3 expression and regulatory function through the TGF-beta pathway. *J Exp Med*. (2010) 207:2331–41. doi: 10.1084/jem.20101074
232. Moreno Y, Geary TG. Stage- and gender-specific proteomic analysis of *Brugia malayi* excretory-secretory products. *PLoS Negl Trop Dis*. (2008) 2:e326. doi: 10.1371/journal.pntd.0000326
233. Chehayeb JF, Robertson AP, Martin RJ, Geary TG. Proteomic analysis of adult *Ascaris suum* fluid compartments and secretory products. *PLoS Negl Trop Dis*. (2014) 8:e2939. doi: 10.1371/journal.pntd.0002939
234. de la Torre-Escudero E, Bennett APS, Clarke A, Brennan GP, Robinson MW. Extracellular vesicle biogenesis in helminths: more than one route to the surface? *Trends Parasitol*. (2016) 32:921–9. doi: 10.1016/j.pt.2016.09.001
235. Bernal D, Carpena I, Espert AM, De la Rubia JE, Esteban JG, Toledo R, et al. Identification of proteins in excretory/secretory extracts of Echinostoma friedi (Trematoda) from chronic and acute infections. *Proteomics* (2006) 6:2835–43. doi: 10.1002/pmic.200500571
236. Pratt AJ, MacRae IJ. The RNA-induced silencing complex: a versatile gene-silencing machine. *J Biol Chem*. (2009) 284:17897–901. doi: 10.1074/jbc.R900012200
237. Robinson MW, Hutchinson AT, Donnelly S, Dalton JP. Worm secretory molecules are causing alarm. *Trends Parasitol*. (2010) 26:371–2. doi: 10.1016/j.pt.2010.05.004
238. Robinson MW, Menon R, Donnelly SM, Dalton JP, Ranganathan S. An integrated transcriptomics and proteomics analysis of the secretome of the helminth pathogen *Fasciola hepatica*: proteins associated with invasion and infection of the mammalian host. *Mol Cell Proteomics* (2009) 8:1891–907. doi: 10.1074/mcp.M900045-MCP200
239. Geiger A, Hirtz C, Becue T, Bellard E, Centeno D, Gargani D, et al. Exocytosis and protein secretion in Trypanosoma. *BMC Microbiol*. (2010) 10:20. doi: 10.1186/1471-2180-10-20
240. Roma-Rodrigues C, Fernandes AR, Baptista PV. Exosome in tumour microenvironment: overview of the crosstalk between normal and cancer cells. *BioMed Res. Int*. (2014) 2014: 179486. doi: 10.1155/2014/179486
241. Xiang X, Poliakov A, Liu C, Liu Y, Deng ZB, Wang J, et al. Induction of myeloid-derived suppressor cells by tumor exosomes. *Int J Cancer* (2009) 124:2621–33. doi: 10.1002/ijc.24249
242. Yoon YJ, Kim OY, Gho YS. Extracellular vesicles as emerging intercellular communicasomes. *BMB Rep*. (2014) 47:531–9. doi: 10.5483/BMBRep.2014.47.10.164
243. Simbari F, McCaskill J, Coakley G, Millar M, Maizels RM, Fabrias G, et al. Plasmalogen enrichment in exosomes secreted by a nematode parasite versus those derived from its mouse host: implications for exosome stability and biology. *J Extracell Vesicles* (2016) 5:30741. doi: 10.3402/jev.v5.30741
244. Hotez PJ, Brindley PJ, Bethony JM, King CH, Pearce EJ, Jacobson J. Helminth infections: the great neglected tropical diseases. *J Clin Invest*. (2008) 118:1311–21. doi: 10.1172/JCI34261
245. Hewitson JP, Maizels RM. Vaccination against helminth parasite infections. *Expert Rev Vaccines* (2014) 13:473–87. doi: 10.1586/14760584.2014.893195
246. Shears RK, Bancroft AJ, Hughes GW, Grencis RK, Thornton DJ. Extracellular vesicles induce protective immunity against *Trichuris muris*. *Parasite Immunol*. (2018) 40:e12536. doi: 10.1111/pim.12536
247. Beauvillain C, Juste MO, Dion S, Pierre J, Dimier-Poisson I. Exosomes are an effective vaccine against congenital toxoplasmosis in mice. *Vaccine* (2009) 27:1750–7. doi: 10.1016/j.vaccine.2009.01.022
248. Schnitzer JK, Berzel S, Fajardo-Moser M, Remer KA, Moll H. Fragments of antigen-loaded dendritic cells (DC) and DC-derived exosomes induce protective immunity against *Leishmania* major. *Vaccine* (2010) 28:5785–93. doi: 10.1016/j.vaccine.2010.06.077
249. Sotillo J, Pearson M, Potriquet J, Becker L, Pickering D, Mulvenna J, et al. Extracellular vesicles secreted by *Schistosoma mansoni* contain protein vaccine candidates. *Int J Parasitol*. (2016) 46:1–5. doi: 10.1016/j.ijpara.2015.09.002
250. Carriere J, Barnich N, Nguyen HT. Exosomes: from functions in host-pathogen interactions and immunity to diagnostic and therapeutic opportunities. *Rev Physiol Biochem Pharmacol*. (2016) 172:39–75. doi: 10.1007/112_2016_7
251. Hu G, Drescher KM, Chen XM. Exosomal miRNAs: biological properties and therapeutic potential. *Front Genet*. (2012) 3:56. doi: 10.3389/fgene.2012.00056
252. Tokuhisa M, Ichikawa Y, Kosaka N, Ochiya T, Yashiro M, Hirakawa K, et al. Exosomal miRNAs from peritoneum lavage fluid as potential prognostic biomarkers of peritoneal metastasis in gastric cancer. *PLoS ONE* (2015) 10:e0130472. doi: 10.1371/journal.pone.0130472
253. Singh PP, Smith VL, Karakousis PC, Schorey JS. Exosomes isolated from mycobacteria-infected mice or cultured macrophages can recruit and activate immune cells *in vitro* and *in vivo*. *J Immunol*. (2012) 189:777–85. doi: 10.4049/jimmunol.1103638
254. Jorgensen M, Baek R, Pedersen S, Sondergaard EK, Kristensen SR, Varming K. Extracellular Vesicle (EV) array: microarray capturing of exosomes and other extracellular vesicles for multiplexed phenotyping. *J Extracell Vesicles* (2013) 2:1–9. doi: 10.3402/jev.v2i0.20920
255. Wang Y, Cheng Z, Lu X, Tang C. *Echinococcus multilocularis*: proteomic analysis of the protoscoleces by two-dimensional electrophoresis and mass spectrometry. *Exp Parasitol*. (2009) 123:162–7. doi: 10.1016/j.exppara.2009.06.014
256. Knudsen GM, Medzihradszky KF, Lim KC, Hansell E, McKerrow JH. Proteomic analysis of *Schistosoma mansoni* cercarial secretions. *Mol Cell Proteomics* (2005) 4:1862–75. doi: 10.1074/mcp.M500097-MCP200
257. Harnett W. Secretory products of helminth parasites as immunomodulators. *Mol Biochem Parasitol*. (2014) 195:130–6. doi: 10.1016/j.molbiopara.2014.03.007
258. Sripa J, Brindley PJ, Sripa B, Loukas A, Kaewkes S, Laha T. Evaluation of liver fluke recombinant cathepsin B-1 protease as a serodiagnostic antigen for human opisthorchiasis. *Parasitol Int*. (2012) 61:191–5. doi: 10.1016/j.parint.2011.05.009
259. Kojima M, Gimenes-Junior JA, Chan TW, Eliceiri BP, Baird A, Costantini TW, et al. Exosomes in postshock mesenteric lymph are key mediators of acute lung injury triggering the macrophage activation via Toll-like receptor 4. *FASEB J*. (2018) 32:97–110. doi: 10.1096/fj.201700488R
260. S ELA, Mager I, Breakefield XO, Wood MJ. Extracellular vesicles: biology and emerging therapeutic opportunities. *Nat Rev Drug Discov*. (2013) 12:347–57. doi: 10.1038/nrd3978
261. Aline F, Bout D, Amigorena S, Roingeard P, Dimier-Poisson I. *Toxoplasma gondii* antigen-pulsed-dendritic cell-derived exosomes induce a protective immune response against *T. gondii* infection. *Infect Immun*. (2004) 72:4127–37. doi: 10.1128/IAI.72.7.4127-4137.2004

Conflict of Interest Statement: The authors declare that the research was conducted in the absence of any commercial or financial relationships that could be construed as a potential conflict of interest.

frontiers in Immunology

REVIEW
published: 27 June 2019
doi: 10.3389/fimmu.2019.01444

Sticking for a Cause: The Falciparum Malaria Parasites Cytoadherence Paradigm

Wenn-Chyau Lee[1], *Bruce Russell*[2] *and Laurent Rénia*[1]*

[1] Singapore Immunology Network (SIgN), Agency for Science, Technology and Research (A*STAR), Singapore, Singapore,
[2] Department of Microbiology and Immunology, University of Otago, Dunedin, New Zealand

After a successful invasion, malaria parasite *Plasmodium falciparum* extensively remodels the infected erythrocyte cellular architecture, conferring cytoadhesive properties to the infected erythrocytes. Cytoadherence plays a central role in the parasite's immune-escape mechanism, at the same time contributing to the pathogenesis of severe falciparum malaria. In this review, we discuss the cytoadhesive interactions between *P. falciparum* infected erythrocytes and various host cell types, and how these events are linked to malaria pathogenesis. We also highlight the limitations faced by studies attempting to correlate diversity in parasite ligands and host receptors with the development of severe malaria.

Keywords: malaria, *Plasmodium*, cytoadherence, pathogenesis, host immune responses

OPEN ACCESS

Edited by:
Xun Suo,
China Agricultural University, China

Reviewed by:
Alister Craig,
Liverpool School of Tropical Medicine, United Kingdom
James G. Beeson,
Burnet Institute, Australia

***Correspondence:**
Laurent Rénia
renia_laurent@immunol.a-star.edu.sg

Specialty section:
This article was submitted to Microbial Immunology, a section of the journal Frontiers in Immunology

Received: *12 July 2018*
Accepted: *10 June 2019*
Published: *27 June 2019*

Citation:
Lee WC, Russell B and Rénia L (2019) Sticking for a Cause: The Falciparum Malaria Parasites Cytoadherence Paradigm. Front. Immunol. 10:1444. doi: 10.3389/fimmu.2019.01444

INTRODUCTION

Malaria continues to be a significant healthcare problem to many human populations, despite efforts to eliminate this debilitating and potentially fatal tropical disease. While the malaria mortality did not significantly change between 2015 and 2016, the number of malaria cases increased by five millions within the same period (1). Among the medically important malaria parasites (2, 3), *Plasmodium falciparum* is the primary cause of severe disease and death (4, 5).

As with other malaria parasites, *P. falciparum* has a complex life cycle involving humans as the intermediate host and *Anopheles* mosquitoes as the definitive host (where sexual reproductive forms of the parasites establish) (**Figure 1**). During its blood meal, the infected female *Anopheles* mosquito releases *Plasmodium* sporozoites from its salivary glands into the dermis of human host. A proportion of sporozoites migrate rapidly to the blood capillaries, then to the liver and invade the parenchymal hepatocytes after traversing the Kupffer cells (6). Inside the invaded parenchymal cells, parasites asexually multiply, producing numerous (∼20,000–40,000) liver merozoites. Subsequently, these merozoites are released into the blood circulation, where they target and invade the erythrocytes (RBCs). It is the erythrocytic life cycle that is responsible for the manifestation of signs and symptoms in malaria. Within the infected erythrocytes (IRBCs), the blood stage-parasites develop from the early ring forms into trophozoites, subsequently form schizonts, which upon maturation will rupture and release blood stage merozoites to invade other uninfected erythrocytes (URBCs). Meanwhile, a fraction of the parasites are driven into the formation of sexual forms (gametocytes), which will be taken up by mosquitoes during feeding. Inside the mosquito, fertilization of male and female gametocytes leads to zygote formation. Subsequent developments lead to formation of salivary gland sporozoites, which are infective to the human host.

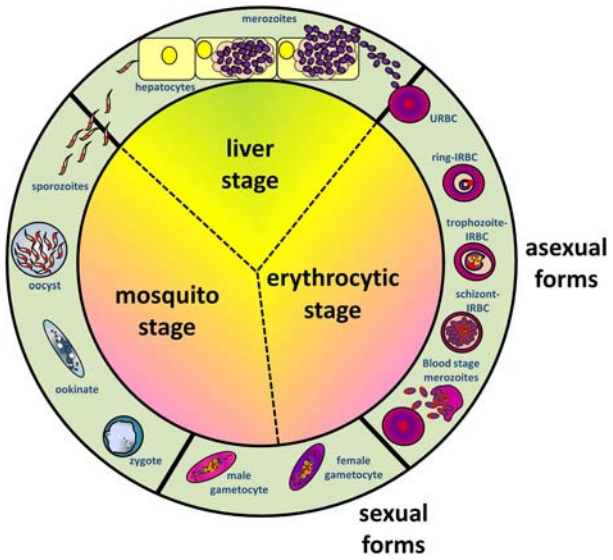

FIGURE 1 | Schematic diagram depicting life cycles of *Plasmodium falciparum*, involving *Anopheles* mosquito and human hosts, where the stages in humans can be furthered divided into liver (exoerythrocytic) and erythrocytic stages.

One fascinating aspect of *P. falciparum* infection is the cytoadherence phenomenon associated with the late stage-IRBC (7), which is considered to be a major contributor to the pathogenesis of falciparum malaria (8). As the parasite develops and matures within the host RBC, it causes substantial alteration to the IRBC membrane architecture, which changes various rheological properties of the IRBC, including its cytoadhesive characteristics (9–11). Here, we review the different types of cytoadhesive interactions of the IRBCs, how they are linked to each other, the molecular and cellular mechanisms behind these phenomena and their proposed involvement in malaria pathology. We also discuss knowledge gap, controversies and diverging views on the role of cytoadherence in *P. falciparum* immunopathogenesis.

COMPLEX PROFILE OF *P. falciparum*-IRBC CYTOADHERENCE

The cytoadherence of IRBCs to host cells in falciparum malaria is highly complex, involving at least three distinct groups of parasite-derived variant surface antigens (VSAs) encoded by multigene families, namely; *P. falciparum* Erythrocyte Membrane Protein 1 (PfEMP1) (12, 13), Subtelomeric Variable Open Reading frame (STEVOR) proteins (14), and repetitive interspersed family (RIFIN) proteins (15). The temporal expression of these ligands also differs, with PfEMP1 being expressed the earliest (transcription starts at ring forms and protein surface expression happens when parasites mature into trophozoites) (16, 17), followed by RIFIN (17, 18), then STEVOR (17, 19–21). In addition, only few members of VSA are expressed by a single IRBC. Members of these VSA families bind to a wide range of different host-derived proteins, proteoglycans, and glycosaminoglycans (as summarized in **Table 1**). The role of RIFINs and STEVORs in the cytoadhesion of *P. falciparum* IRBCs is undoubtedly of significance. Apart from forming rosettes (a cytoadherence phenomenon by the late stage-IRBCs, which is elaborated in latter section) via interactions with the A antigens on the URBCs (15), some RIFINs can interact with leukocyte immunoglobulin-like receptor B1 (LILRB1), which inhibits the activation of B cells and natural killer (NK) cells expressing LILRB1 (51). This discovery suggests the involvement of RIFIN in the parasite's immune-evasion mechanisms. STEVOR proteins interact with the RBCs, and current evidence suggests their involvement in immune evasion, rosette formation and merozoite invasion (14, 21). By comparison, PfEMP1 binds to diverse array of host receptors on different host cells, leading to suggestions of its involvement in immune evasion (52) and immune modulation (53). Hence, it is generally accepted that the PfEMP1 is the most important of the VSAs. A detailed description of PfEMP1 variant domains and their binding targets, as well as the switching of expressions, have been elegantly reviewed elsewhere (54–56). In general, the extracellular domain of PfEMP1 can be classified into four major regions, which are the N-terminal segment (NTS), the C2 region, the Cysteine-rich inter-domain region (CIDR), and the Duffy binding-like region (DBL). These regions are responsible for the diverse cytoadherence phenomena attributed to PfEMP1, and difference in these regions gives rise to different cytoadherence properties, hence different tissue tropism for different strains of parasites (57, 58). Importantly, the various parasite-derived antigens that are expressed on IRBC surface make IRBCs an obvious target for host's immune system (59).

The IRBC-cytoadherence events are usually classified based on their binding sites, i.e., endothelial cytoadhesion, cytoadhesion to placental syncytiotrophoblasts, platelets, URBCs (rosetting phenomenon) and leukocytes (monocytes, macrophages, and dendritic cells) (23, 60–62). *P. falciparum* IRBCs can adhere to each other through platelet bridges, forming aggregates of IRBCs, a mechanism defined as autoagglutination (63–65). This phenomenon has been shown to be uncorrelated to rosetting and parasitemia, but significantly associated with severe malaria (63). These different interactions between the parasites and the host described above have been proposed to shape the immunopathobiology of malaria.

WHY DO *P. falciparum* IRBC CYTOADHERE?

Within hours after the *P. falciparum* merozoite invading the RBCs, the relatively low intra-erythrocytic viscosity of liquid hemoglobin is transformed into viscous gel-like cytoplasm of a developing IRBC (66). Besides, the parasite also remodels the IRBC by building a trafficking network with its parasite-derived proteins and organelles (such as Maurer's cleft) to bring in nutrients essential for its survival (67). The net consequence of these modifications (∼10 h post-invasion) is a host cell with a compromised rheological profile (68). Such biomechanical

TABLE 1 | Host-derived receptors for *P. falciparum* cytoadherence ligands.

Ligands	Receptors	Expression sites	References
PfEMP1	Complement receptor 1 (CR1/CD35)	RBCs, leukocytes, splenic follicular dendritic cells	(22)
	Chondroitin sulfate A (CSA)	Endothelial cells, placental syncytiotrophoblasts	(23, 24)
	Hyaluronic acid (HA)	Placenta, and other connective, epithelial and neural tissues	(25)
	Heparan sulfate (HS)	All tissues	(26, 27)
	Platelet glycoprotein 4 (CD36)	Platelets, RBCs, monocytes, differentiated adipocytes, microdermal endothelial cells, skeletal muscles	(28–33)
	Intercellular adhesion molecule 1 (ICAM1/CD54)	Endothelial cells, leukocytes	(29, 31, 33–36)
	Vascular cell adhesion protein molecule 1 (VCAM1/CD106)	Endothelial cells	(31, 33, 35)
	RBC group A/B antigens	RBCs	(37, 38)
	Platelet endothelial cell adhesion molecule 1 (PECAM-1/CD31)	Platelets, monocytes, neutrophils, T-cells, endothelial cell (intercellular junctions)	(39, 40)
	Ig M	Circulation	(41–43)
	P-selectin (CD62P)	Activated platelets, activated endothelial cells	(31, 33, 44)
	E-selectin (CD62E)	Activated endothelial cells	(29, 35)
	Endothelial protein C receptor (EPCR/CD201)	Endothelial cells	(45–47)
	Hyaluronan-binding protein 1 (HABP1/gC1qR/P32)	Extracellular matrix, endothelial cells, platelets	(48, 49)
	Neural cell adhesion molecule (NCAM)	Endothelial cells	(50)
STEVOR	Glycophorin C (Gly C)	RBC	(14)
RIFIN	RBC group A antigen	RBC, B cells, NK cells	(15, 51)

changes render the IRBCs highly susceptible to splenic filtration. Within a spleen, the sinusoids of the red pulps act as a mechanical filter of the circulation. All entities in circulation have to move through the narrow (4 μm at its widest point) inter-endothelial slits (IES) of the red pulps (69). These are the smallest passage space for the blood circulation (69, 70). Healthy erythrocytes with normal morphology and rheology will be able to move through these IES whereas the abnormal cells will be retained and engulfed by the macrophages. As the red pulp of spleen is very effective in destroying rheologically impaired and less deformable erythrocytes, the developing malaria parasite has developed mechanisms that alters the host cell in some ways to escape splenic clearance (71). To this end, *P. falciparum* IRBCs avoid splenic clearance by cytoadhering to the vascular endothelium and sequestering in capillary beds of organs that are less dangerous than the spleen (72).

The central role of the spleen as a selective pressure for the evolution of cytoadhesive IRBCs is supported by the fact that in falciparum malaria patients and *P. falciparum*-infected monkeys whose spleens were removed prior to the infection, late stage-IRBCs that do not sequester are readily detected in peripheral blood (73–75). These circulating late-stage IRBCs have lost the capacity to cytoadhere to endothelial cells (74). These observations form the basis for the development of an anti-sequestration vaccine against *P. falciparum* (76). Theoretically, under spleen-intact conditions, the blockade of late stage-IRBCs to cytoadhere to endothelial cells will render these forms highly susceptible to splenic filtration. Thus, IRBC-cytoadherence plays critical roles in the immune-escape strategies by *P. falciparum*.

Besides endothelial cells, late stage-IRBCs can also adhere to URBC, forming flower-like structures known as "rosettes" (61). To date, *P. falciparum* rosetting has been attributed to three ligands, namely PfEMP1, STEVOR, and RIFIN (11, 13–15). Various host-derived receptors on RBCs have been found to be rosetting receptors (**Table 1**), the majority of these interact with the variant extracellular domains of PfEMP1. The binding affinity of these variants to the various receptors depends on the sequences coded for these regions, which has been described in detail elsewhere (55, 57, 77). Various roles have been proposed for rosetting; firstly, to facilitate merozoite invasion by bringing URBCs closer to the intracellular parasite. However, this "invasion facilitation" hypothesis for rosettes has been ruled out (78). The second proposed role for rosetting is that URBCs mask parasite-derived antigens (VSAs) expressed on the surface of IRBCs, allowing them to escape immune-recognition by antibodies or phagocytes. Practically, this masking strategy is similar to those applied by other parasites such as the blood flukes *Schistosoma* spp., where the flukes adsorb host-derived antigens (such as the blood surface A, B, H, Lewis b+ antigens) onto its surface (79–81). During the course of malaria infection, phagocytosis of IRBC plays a critical role in the clearance of parasites, especially in the spleen as mentioned earlier (82, 83). Opsonization of IRBCs leads to phagocytosis by the host phagocytes. The opsonization of IRBCs happens via antibody-mediated recognition and complement deposition (84–87). For instance, complement-decorated IRBCs are opsonized through the complement receptor 1 (CR1/CD35) (86, 88). Interestingly, CR1 on URBC is a receptor used by PfEMP1 on the surface of *P.*

falciparum-IRBC in rosetting (22). Formation of rosette via CR1 may block this phagocytosis pathway. Meanwhile, phagocytosis can also be mediated in a complement-independent, CD36-dependent manner (89, 90). Likewise, CD36 is also one of the receptors that bind with PfEMP1 for rosette formation (28) (**Table 1**). Although direct evidence of rosette hampering phagocytosis has yet to be reported, a previous study has demonstrated an inverse relationship between the amount of group A antigens (another rosetting receptor) being expressed on IRBC and its susceptibility to phagocytosis (91), and this may be linked to the better ability of blood group A-IRBCs to form rosettes (92). In addition, the larger size of a rosette relative to individual IRBCs may be more difficult to be engulfed by individual phagocytes as well. Previously, it has been demonstrated that opsonized targets larger than 3 μm and non-opsonized targets larger than 2 μm negatively affect the attachment step of phagocytosis (93). Of note, the thickest point of a RBC is 2–2.5 μm whereas the thinnest point of this cell is ∼1 μm. Thus, size wise, a rosette will affect at least this critical step of phagocytosis. Furthermore, adherence of an IRBC to a URBC significantly reduces the deformability of the whole rosetting structure further, as compared to a non-rosetting IRBC harboring parasite of similar stage (68, 94). Such larger, more rigid yet stable structures are likely to be "mechanically" sequestered in microvasculature and may not even be able to reach the spleen.

Apart from endothelial cytoadhesion and rosetting as described above, some strains of *P. falciparum* can sequester within the placental intervillous space of pregnant patients (95), particularly the first-time-pregnant mothers (96). This enables the parasite to escape maternal immune responses (97). Interestingly, parasites that can sequester in placenta usually do not form rosettes well (98). On top of these evasion mechanisms, there are reports showing ability of PfEMP1 and RIFIN to modulate or suppress the host's immune responses as mentioned earlier (51, 53). Thus, it seems that *P. falciparum* uses various cytoadherence phenomena as an immune-escape mechanism.

HOST IMMUNE RESPONSES AND ANTIGENIC VARIATION OF THE CYTOADHERENCE LIGANDS

Since the cytoadherence of IRBCs relies on the IRBC-surface expression of parasite-derived cytoadherence ligands, these ligands would be easily recognized and hence destroyed by the host's immune system (59, 99). For instance, antibodies against PfEMP1 have been shown to inhibit rosette formation and induce phagocytosis in experiments using a laboratory-adapted *P. falciparum* strain (100). Antibodies raised against STEVOR expressed by different stages of *P. falciparum* can also inhibit either rosetting or merozoite reinvasion (14). Furthermore, the level of antibodies specific for RIFINs in pediatric malaria patients was reported to be positively correlated with the speed of parasite clearance (101). In fact, antibodies targeting the VSA have been shown to confer protection against malaria (101–106). For an extra level of survival advantage to the parasites, these critical cytoadhesion ligands are VSA coded by multigene families as mentioned earlier (107). During multiplication, VSA expression changes, with a fraction of the progeny expressing a different set of VSAs. Such switching of VSA expression hampers the successful development of an immune response against all IRBCs (108–110). Taking PfEMP1 as an example, DBL and CIDR are the two regions of its extracellular domain responsible for the most of its cytoadherence activities (55, 111). Following the expression switching, the extracellular domains of PfEMP1, hence the binding receptors (targets) are different (112). Nevertheless, many binding receptors targeted by various PfEMP1 extracellular domains are available on endothelial cells. This also partly explains the diverse cytoadhesion receptors for PfEMP1, where the sequestration of IRBCs continues even with altered PfEMP1 variant expression.

SIDE EFFECTS OF THE PARASITE SEQUESTRATION ESCAPE STRATEGY

While the evolution of cytoadhesive IRBCs by *P. falciparum* has proven to be a potent immune-evasion strategy, the sequestration of IRBCs has an important side effect, which is the development of severe malaria (113). The manifestation of severe malaria largely depends on the site of sequestration. For instance, cytoadhesion of the IRBCs to syncytiotrophoblasts causes placental malaria, which is characterized by the inflammation of placental tissues, occlusion of nutrient supply to the fetus by the mother, resulting in higher risk of premature delivery, low birth weight of the neonates and subsequent negative impacts on future growth and development (114, 115).

Cytoadhesion of IRBCs to endothelial cells directly activates the endothelial cells, as shown *in vivo* (116) and *in vitro* (117), which in part may lead to endothelial injuries and vascular leakage (118). Various studies have implicated PfEMP1 [particularly its interaction with endothelial protein C receptor (EPCR)] in the pathogenesis of cerebral malaria, one of the most important forms of malaria-induced complications (45, 119–121). Nevertheless, the definitive *in vivo* demonstration of its involvement remains to be performed. There are apparent differences between the *in vitro* and *in vivo* conditions, encompassing content of nutrients, waste products, hormones, cytokines, oxygen level and shear force to name a few, as highlighted elsewhere (122). These differences may become the confounding factors in *in vitro* studies. However, the advancement of technology in the *in vivo* vascular imaging may provide a platform for the relevant *in vivo* works in future (123).

Based on the available information, a simplified sequential development of PfEMP1-mediated cerebral malaria has been suggested (7). The series of parasite-host interactive events start with the IRBCs binding to the endothelial cells via EPCR (119). EPCR plays protective role in maintaining the integrity of circulation through its ability to activate protein C, which is anti-coagulative and anti-inflammatory. The binding of IRBC-PfEMP1 to EPCR may hamper the protein C activation by EPCR, hence reducing the level of activated protein C in the microvasculature affected, which facilitates thrombin formation

(112). Such pro-coagulative environment further contributes to compromising microvasculature integrity. Following this, endothelial activation and inflammation may happen (124). The early onset of endothelial inflammation is characterized by the release of Weibel-Palade bodies and subsequent endothelial surface expression of P-selectin and von Willebrand factor (vWF) (113, 125, 126), which in turn mediate leukocyte and platelet rolling on inflamed endothelial cells (127).

Weibel-Palade bodies are the storage granules of endothelial cells (128). This structure contains of a number of components (P-selectin, VWF, angiopoietin 2, IL-8) that have been associated with endothelial injuries and vasculature leakage in malaria pathogenesis (113, 125, 126, 129–134). Other reported components of Weibel-Palade bodies include eotaxin 3, CD63, tissue plasminogen activator (TPA), factor VIII, endothelin 1, osteoprotegerin (OPG), alpha-(1,3)-fucosyltransferase (FUT6), endothelin-converting enzyme, calcitonin gene-related peptide, and insulin-like growth factor-binding protein 7 (IGFBP7). These components are involved in various homeostasis and inflammation related functions encompassing vasculature toning, inflammation and repair, regulating blood coagulation and angiogenesis (135–143). Remarkably, the release of different components within Weibel-Palade bodies is tightly regulated according to the microenvironment of the vasculature (140, 144, 145). This enables the endothelial cells to respond to changes of its microenvironment such as injuries, inflammation or shear stress changes. For instance, the release of VWF from Weibel-Palade bodies by endothelial cells can be triggered by interruption of blood flow (146). In such pro-coagulation environment, platelets can also serve as the bridge between IRBCs and endothelial cells, allowing cytoadhesion to happen even on endothelial cells devoid of principal cytoadhesion receptors (147). Additionally, platelet-mediated autoagglutination of IRBCs may happen in parallel (63), which further disrupts blood flow and activates the endothelial cells (148). Furthermore, angiopoietin-2 released from Weibel-Palade bodies can disrupt the integrity of endothelial junctions, which drives vasculature leakage (149). Following the "first bout" of endothelial inflammation, the expression of EPCR and thrombomodulin by host endothelial cells is downregulated (150), aggravating the pro-coagulation situation. The subsequent release of cytokines triggers expression upregulation of endothelial cell adhesion molecules (CAMs) such as ICAM1, E-selectin, and VCAM (151, 152). ICAM1 is used by other IRBCs to remain sequestering in the microvasculature, possibly with an expression switch of PfEMP1 variants (7). Notably, the disrupted blood flow can cause metabolic acidosis, which further facilitates the acidic pH-dependent binding of IRBCs to receptors like ICAM1 and CD36 (153). The vicious cycle continues, and the integrity of blood brain barrier is altered, leading to hemorrhages and possibly death if left without proper medical intervention.

The hypothesized sequences of pathological events described above remain to be validated fully. Of note, the dual EPCR/ICAM1 binding ability by certain PfEMP1 variants has been demonstrated (154), which may confound the hypothesized sequences of vascular pathogenesis events. Nevertheless, the critical role of EPCR in severe malaria pathogenesis has been highlighted by recent studies. The EPCR-binding *P. falciparum* isolates have been shown to be associated with severe malaria in both adults and children, with different clinical presentations including cerebral malaria, retinopathy and severe malaria-induced anemia (45–47, 155–159). On the other hand, falciparum malaria cases with predominantly CD36-binding parasites have been correlated with uncomplicated clinical presentations (159). Succinctly, the complex IRBC cytoadherence events trigger biological cascade reactions that lead to severe malaria pathologies.

P. falciparum ROSETTING AND SEVERE DISEASE

Rosetting was first reported in the simian malaria parasite *P. fragile,* and subsequently in *P. falciparum* and all other human malaria parasites (61, 160, 161). While it has been suggested that rosetting may aggravate the vasculature occlusion initiated by endothelial-cytoadhered IRBCs (162–164), its importance to pathogenesis of falciparum malaria is still debated. Associations between rosetting rates and malaria severity have been confounded with locality. African cohorts showed positive correlation between rosetting and malaria severity, where association of rosetting rates with parasitemia and different clinical parameters of severe malaria, as well as correlation between malaria severity and impairment of rosette formation due to availability of anti-rosette antibodies in serum and genetic blood disorders with abnormal erythrocytes have been reported (165–169). On the other hand, those conducted in Asia could not find such correlation (170, 171). Although correlation-based findings help to generate hypotheses, it is also important not to overlook the availability of confounding factors in many correlation studies, and the difference between a correlation and a causation.

As mentioned earlier, PfEMP1 is one of the key rosetting ligands for *P. falciparum*. The PfEMP1-mediated rosetting and endothelial cytoadhesion are two distinct biological phenomena, as demonstrated by previous studies (61, 162, 163). Nevertheless, dual cytoadhesion of rosetting IRBCs to endothelial cells have been demonstrated (164, 172), and distinct domain of PfEMP1 variant that possesses dual cytoadhesive (to endothelial cells and URBCs) properties has been described, albeit with very weak affinity to endothelia (the rosetting IRBCs were seen rolling instead of stably adhering to endothelial cells) under flow conditions mimicking microvasculature shear stress (164). Therefore, it remains to be investigated if such dual-binding phenomenon by IRBCs exists *in vivo*.

Importantly, all rosetting studies have been conducted under *in vitro* or *ex vivo* conditions using blood samples collected from peripheral circulation of patients, or clones of parasites derived from such sampling methods. The conundrum lies in the fact that the IRBCs that stably cytoadhere to microvasculature endothelium are responsible for parasite sequestration and may be the major contributor to the manifestation of severe malaria. However, the subpopulation of IRBCs collected from peripheral blood may be phenotypically different from those sequestering in

the microvasculature when it comes to propensity of the IRBCs to cytoadhere. From another viewpoint, if the cytoadhesive phenotypes of IRBCs (usually the early stages) collected from the peripheral circulation are essentially similar to the sequestering late stage-IRBCs, the findings from *in vitro* rosetting studies (conducted on these parasites after *ex vivo* maturation) may not imply the actual situation *in vivo* since the recruited IRBCs are not given an equal exposure to URBCs and endothelial cells in rosetting assays, which raises doubts if rosetting ever happens *in vivo*. If this were the case, the rosetting phenomenon seen *in vitro* is merely an indication of "IRBC's stickiness," where the IRBCs would probably adhere to the microvasculature wall *in vivo*. Such situation makes it difficult to extrapolate the importance of rosetting in contributing to pathogenesis of severe malaria.

Malaria pathogenesis develops with time and often takes days to occur. One of the important shortcomings of studies correlating severe malaria with cytoadhesive IRBCs is that these studies are essentially snapshots of a multi-step process, which may be difficult to capture the complete chronology of an infection's pathogenesis. For cases with low parasite density, IRBCs have plenty of endothelial cells to cytoadhere to, leaving the non-endothelial cytoadhering IRBCs available in peripheral circulation. To avoid splenic clearance, these IRBCs may default to form rosettes over IRBC-endothelial cytoadhesion. Hence, it would be difficult to draw any correlation between rosetting phenomenon by this IRBC subpopulation and the pathology development that is happening in the deep microvasculature. On the other hand, parasite density in certain patients from certain localities may become too high (depending on parasite's virulence, genetic background and immunity status of the host, or lack of accessibility to timely treatment) and over-saturated relative to the total surface area of deep vasculature endothelial cells available for IRBC cytoadhesion. Thus, the IRBCs that do not get to cytoadhere to endothelia will be available in peripheral circulation. Of note, the availability of late stage *P. falciparum*-IRBCs in peripheral blood of a patient suffering hyperparasitemia has been reported (173). When these IRBCs are collected for rosetting assay, they are provided with only URBCs. Without their preferred cytoadhesive target (endothelial cells), these IRBCs may form rosette with the URBCs. Such alternative binding may happen as host-derived receptors like heparan sulfate (HS) (26, 164, 174–176), and CD36 (28, 177) have been reported as the receptor for endothelial cytoadhesion and rosette formation by the IRBCs. Rosetting rates obtained from such samples may reflect the relative endothelial cytoadhesion propensity of the IRBCs, which is associated with the severe malaria development. This may explain the positive correlation between rosetting and parasitemia in African clinical isolates previously reported (168). This hypothesis may also partly explain the discrepancies in correlation studies of rosetting rates and malaria severity conducted in different parts of the world. Notably, earlier studies have shown that the parasite clones in peripheral circulation and those sequestering in deep vasculature are similar (178, 179). Nevertheless, these molecular findings were based only on MSP-1 and MSP-2 alleles, and the tissue tropisms of the parasite subpopulations in a patient may not be revealed without specifically analyzing genes related to cytoadherence, as highlighted by the study (179).

So, the question remains: does the rosetting phenomenon contribute to severe malaria apart from its role as an immune-evasion strategy? To date, there is still a lack of solid evidence demonstrating stable, direct binding of rosetting IRBCs to endothelial cells under flow conditions. Nevertheless, such event may still be possible if the site of occurrence (microvasculature) has its blood flow hampered significantly in advance by the IRBC-endothelial cytoadhesion. Alternately, the rosetting IRBCs may be adhered securely to the endothelial cells via platelet as elaborated earlier (147). Regardless of how the rosette-endothelial binding interactions are, the contribution by rosetting to vasculature occlusion may not even require direct cytoadherence of rosetting IRBC to the endothelial cells. As mentioned earlier, it was shown that rosettes are less deformable and takes longer time to flow through a capillary-mimicking micropipette (68). In addition, Kaul et al. (180) demonstrated in an *ex vivo* system using rat isolated mesocecum that rosetting IRBCs contributed to microvasculature occlusion under flow condition. In this system, rosette-forming *P. falciparum* IRBC formed aggregates at venule junction, which restricted the flow. These aggregates were eventually dissociated slowly by the induced upstream force mimicking blood flow, leaving some IRBCs still attached to the endothelial cells afterwards. Here, rosetting was seen as an event that "widens the zone of vasculature occlusion." With merely IRBC-endothelial cytoadhesion, blockade may only happen at fine capillaries with lumen size ($\sim$5–10 μm) close to the size of a normal RBC. However, sites of IRBC sequestration encompass capillaries and venules (lumen size of $\sim$ 7 μm to 1 mm) (73, 181). As pointed out by Nash et al. (68), even with a monolayer of IRBCs cytoadhering to its endothelial wall, venules should has lumen wide enough to allow circulation flow, albeit with higher resistance. Following this theory, rosetting may occlude microvasculature distal to the endothelial-cytoadhered IRBC-obstructed fine capillaries. Nevertheless, it is important to note that another species of human malaria parasite, *P. vivax*, also readily forms rosettes (182, 183). Besides, the rigidity of *P. vivax* rosettes also increases (94). However, *P. vivax*-related cerebral malaria cases are not as common, with majority of such cases being reported from India (184–190), suggesting involvement of the human host-derived factors in this relatively geography-restricted pathology. Importantly, the endothelial cytoadhesion phenomenon by *P. vivax* IRBCs has been demonstrated, which is of similar binding strength but ten times lower in frequency than that of *P. falciparum* IRBCs (191). Therefore, this suggests that the key player that drives vasculature occlusion is IRBC-endothelial cytoadhesion. In this context, rosette formation is likely to play a subsidiary role.

Genetic polymorphisms influencing rosetting receptor expression is another factor to consider when assessing the roles of rosetting in malaria pathogenesis. For example, low level expression of CR1 on the surface of URBC (receptor for both rosette formation and IRBC clearance by the host) was reported to be a risk factor for severe malaria in Thai population (192). Another polymorphism that increases RBC surface

expression of CR1 was reported to confer protection against cerebral malaria development in Thai population (193). On the other hand, studies conducted in India yielded complex picture, where low CR1 expression was found to be correlated with severe malaria susceptibility in non-endemic regions whereas high CR1 levels were associated with disease development in the malaria-endemic areas (194). Another study conducted in eastern part of India reported that extremely high and extremely low expression level of CR1 can lead to the higher risk of cerebral malaria development (195). Likewise, studies from Africa and Papua New Guinea yielded conflicting outcomes (196–198). Recently, two distinct CR1 polymorphisms commonly seen in African populations were found to demonstrate opposing correlation with the development of cerebral malaria in Kenya (199). The *Sl2* allele was reported to confer protection against cerebral malaria, possibly due partly to its reduced rosetting phenomenon in addition to other factors, as suggested by the authors; whereas McC^b allele served as a risk factor to develop cerebral malaria, but arises from selection probably due to survival advantage against other infections (199). Based on the example above, it is not easy to draw clear conclusions based on the correlations between genetic polymorphisms in a population and the outcome of a *P. falciparum* infection. More downstream experiments with carefully controlled longitudinal studies are needed to validate the significance of these findings.

ROSETTING AGAINST ENDOTHELIAL CYTOADHESION?

Parasitism is a relationship between two organisms where one party (the parasite) causes harms to the other party (the host) while living in/on the host. Evolution, through selection process, tends to drive this relationship toward a relatively "peaceful" one, where the selected parasites cause as little harm as possible to the host while the host is evolved and adapted to accommodate the parasite, without eliciting much immune response against the parasites. Following this evolutionary point of view, it would make more sense that *P. falciparum* that do not kill its human host while trying to survive within its host would be selected over time. As elaborated earlier, the *P. falciparum* late stage-IRBCs require sequestration to escape host's immune system. However, the endothelial cytoadhesion-mediated sequestration causes potentially fatal outcomes to the host, which is disadvantageous to the parasite as well.

Importantly, in areas with seasonal malaria transmission, asymptomatic carriers of *P. falciparum* serve as the parasite reservoirs during dry seasons, when the *Anopheline* mosquito number is low (200–203). Parasites persist within the hosts for months without causing clinical symptoms. In addition, the severity of clinical presentations for falciparum malaria covers a broad spectrum. This suggests that sequestration of late stage-IRBCs away from peripheral circulation can still happen without inducing grave outcomes to the host. Is endothelial cytoadhesion the only way for the parasites to sequester and escape splenic clearance?

Interestingly, cytoadhesive events such as rosetting, autoagglutination, and endothelial cytoadhesion use PfEMP1 as their ligand. Is there any form of competition between these events *in vivo*? In fact, the whorl of URBCs around a rosetting IRBCs can serve as a mechanical barrier against IRBC-endothelial cytoadhesion (164, 204, 205) and autoagglutination (206). Does rosetting carry any merit in reducing or preventing the endothelial injuries? Such theory has been raised no long after the discovery of rosetting phenomenon, where the role of rosetting either as a friend or foe to human host relies on the location or timing of rosette formation (68). IRBC-endothelial cytoadhesion occurs at capillaries and venules. If rosettes are formed ahead of these sites, rosettes can prevent IRBC-endothelial cytoadhesion. If rosettes can only be formed at similar vasculature sites as the IRBC-endothelial cytoadhesion, rosettes formed by the already endothelial-cytoadhered IRBCs can worsen the vasculature occlusion.

The manifestation of rosetting relies on the stability of rosetting complex under flow conditions. Rosettes are stable under sheared conditions, from very low shear forces to shear stress of about 1.5 Pa (68, 207), which is applicable to shear stress generated by blood flowing through arteries (208). This suggests that rosettes are available throughout the systemic circulation and that the *in vivo* rosettes may prevent IRBC-endothelial cytoadhesion. One concern was raised by an earlier study based on observation from its micropipette assay (68), where a rosetting IRBC that is forced into a capillary by blood flow will eventually have direct contact with the capillary wall (endothelial cells), hence IRBC-endothelial cytoadhesion may still happen even with rosetting. It is important to note that the force applied by that study to maneuver the rosetting IRBC into the micropipette was much higher (30 Pa) than the *in vivo* arterial shear force. Assuming that rosettes cannot move into capillaries *in vivo*, they may block the flow of blood into the capillary bed. If this were the case, the brain tissues covered by the affected capillary bed would suffer hypoxia and irreversible damages. However, cerebral malaria cases with irreversible hypoxia-induced brain tissue damages (as in stroke patients) following microvasculature occlusion by the IRBCs are rarely seen (209). Interestingly, via microvasculature-mimicking microfluidics channels, it was observed that the more rigid *P. vivax* rosettes that blocked the channel openings did not occlude the flow of normal URBCs through the channels (94). Although the experiment was conducted with *P. vivax*, we believe that it is applicable to *P. falciparum* as well, since both species preferably rosette with normocytes (matured RBCs) with similar binding strength (94, 183), and the rosettes formed by both species show enhanced rigidity (68, 94).

Another interesting evidence that suggests rosetting as "counter-endothelial cytoadhesion" stems from studies that investigated effects of sulfated glycoconjugates on rosetting and IRBC-endothelial adhesion. A number of sulfated glycoconjugates such as fucoidan, dextran sulfate, and heparin can disrupt rosettes (174, 210, 211). However, these molecules were found to enhance cytoadherence of IRBCs to CD36-bearing endothelial cells (177). An earlier study also reported the need of rosette disruption to allow IRBC adherence to CD36

(205). These findings suggest the need of cautious approach in considering heparin-derived molecules as malaria adjunctive treatment on the ground that they can disrupt rosette formation, as such adjunctive therapy may worsen the clinical situation by promoting IRBC-endothelial cytoadhesion (177). Is rosetting by the IRBCs purely a risk factor to human host, or an attempt by the parasites to minimize damages to the host without compromising its own survival? Various host- and parasite-derived confounding factors complicate the role characterization of rosetting.

INVOLVEMENT OF HUMAN-DERIVED FACTORS IN SHAPING THE DIRECTION OF IRBC-CYTOADHERENCE?

To date, most of the studies on human host-malaria parasite interactions in the context of IRBC cytoadherence focus on injuries sustained by the host from the parasites. Whether there is any "damage control" approach by either party in this parasitism relationship remains unknown. This is rather bizarre for a parasitism relationship with such a long evolutionary history. Importantly, as mentioned earlier, the parasites can persist in some human hosts for a very long time without causing signs and symptoms. This suggests that the survival-essential phenomena of the parasites, such as deep vasculature sequestration to avoid splenic clearance, can be tolerated by the host, and these phenomena may be the result of host-parasite interactions. Interestingly, the host-derived complement factor D, albumin, and anti-band 3 IgG have been reported as the rosette-promoting factors for *P. falciparum* (212). On top of that, a recent study reported "something" other than IgG from pooled human sera inhibited cytoadhesion of PfEMP1 to EPCR (213). Such serum-mediated IRBC-cytoadherence inhibition suggests intervention attempts by the host to control damages. According to this study, the inhibitors are available in circulation even under non-malaria infected conditions (usage of pooled donor sera) (213). Nevertheless, it is not known if there is any underlying medical condition among the donors. This is important since the serum component profiles of individual with cardiovascular problems, diabetes or chronic subclinical inflammation may be different from those of optimal health condition (214, 215). In addition, the components of serum from peripheral blood maybe different from that of the microenvironment within deep vasculature suffering endothelial injuries following IRBC-endothelial cytoadhesion. Nevertheless, this study sheds lights on potential host-parasite interactions in malaria pathogenesis.

As stated earlier, the adherence of IRBCs to endothelial cells trigger endothelial activation and inflammation. Subsequently, the level of various cytokines at the inflamed site is increased. Weibel-Palade body is one of the components being released by endothelial cells upon the onset of endothelial activation. As elaborated earlier, of the various components found within Weibel-Palade bodies, some have been associated with severe malaria pathogenesis and some have important role in regulating homeostasis in vasculature. It would be interesting to examine the effects of all key components in Weibel-Palade bodies on the dynamics of IRBC cytoadherence, as well as other interplays between the host and the parasite.

Based on the currently available literature, it is likely that the malaria-related cytoadherence phenomena may give rise to

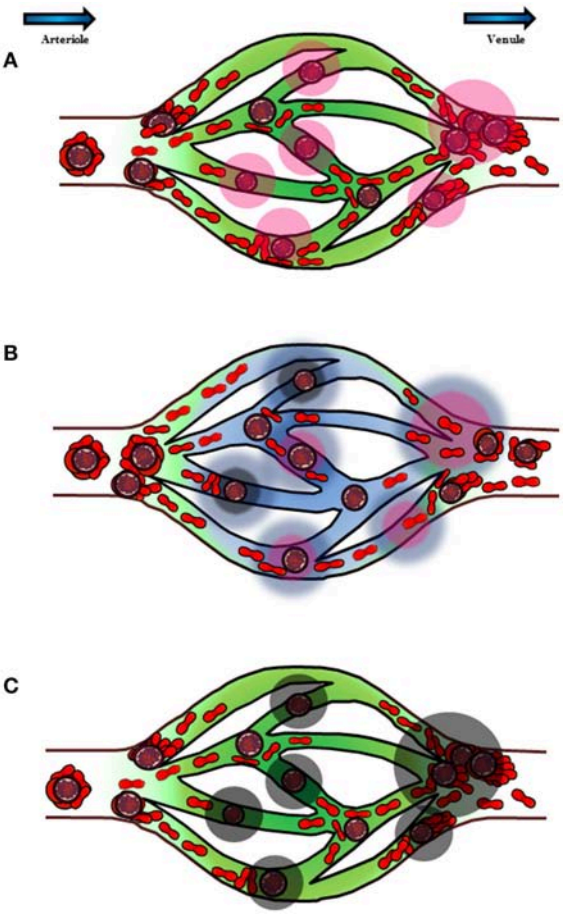

FIGURE 2 | Schematic diagram to illustrate the postulated chronology and mechanism of *P. falciparum* sequestration and pathogenesis in deep vasculature. The blue arrows on top of the diagram represent the direction of blood flow from arteriole to venule. **(A)** Cytoadhesion of IRBCs on endothelial cells causes endothelial inflammation. In addition, rosette formation at the capillary junctions opening into venules also contributes to the hampering of blood flow within the vasculature. The endothelial inflammation by direct IRBC-cytoadherence, coupled with hampering of blood flood stimulate the affected endothelial cells (pink halo) to release various substances in response to the changes in its environment. **(B)** Some of the components released by the endothelial cells (blue halo) may reverse and prevent IRBC-endothelial cytoadhesion, at the same time stimulate rosette formation. Rosetting mechanically prevents IRBCs from binding to endothelial cells while enabling the IRBCs to sequester in larger microvasculature. This will enable the parasite to escape splenic clearance. This switch of cytoadhesive characteristics also prevents complete occlusion of blood flow, thus minimizing, if not preventing irreversible tissue damages from tissue hypoxia. **(C)** However, for hosts with endothelial cells that are not as well-responsive to IRBC-endothelial cytoadhesion and slowing down of blood flow, the components that can reverse and prevent IRBC-endothelial cytoadhesion may be inadequate to exert such effect. As a result, vasculature occlusion ensures. At the same time, endothelial injury and vasculature leakage worsen (black halo), which may lead to fatal outcome.

complex host-parasite immunopathological interactions, starting from IRBC-endothelial cytoadhesion at the microvasculature (**Figure 2**). This results in endothelial activation and vasculature inflammation. Blood flow slows down due to the IRBC sequestration, which enables some immediately reformed rosettes with dual cytoadhesive capability to adhere at the venular junction. In fact, vasculature areas subjected to complex shear stresses such as the vascular branching junctions have abundant VWF-containing Weibel-Palade bodies (144), which may facilitate IRBC-endothelial binding. This further aggravates vasculature occlusion. On the other hand, stable rosettes that are formed before entering capillary bed will stay at the arteriole due to the higher rigidity of the whole rosetting structure. This form of rosettes prevents the rosetting IRBCs from having direct contact with the capillary endothelial, hence preventing endothelial cytoadhesion. Meanwhile, the reduction in shear stress of the microvasculature (capillaries and venules), coupled with endothelial inflammation trigger the affected endothelial cells to alter their expression, releasing unknown factors that may reverse IRBC-endothelial cytoadhesion. The endothelial cells may also secrete some other components to shield the endothelia from cytoadherence by incoming IRBCs, or the aforementioned unknown factors may be capable of reversing and preventing IRBC-endothelial cytoadhesion. The IRBCs detached from endothelial cells will flow out of the capillary bed into the venule, and form rosettes. The rigid structure of rosettes enables the IRBCs to escape splenic clearance by mechanically sequester in larger-size microvasculature. This may avoid further damaging of host's vasculature, minimize complete occlusion of blood flow hence hypoxia and tissue necrosis. Finally, the ability of the host to respond to IRBC-induced endothelial activation by secreting and releasing these anti-endothelial cytoadhesion mediators will determine his survival in battling malaria.

CONCLUDING REMARKS

Undeniably, IRBC cytoadhesion is an important aspect in the pathogenesis of malaria, and a key interplay between the malaria parasite and its host. However, there are many "unresolved issues," such as the role of rosetting and feedback responses by the host following malaria-induced vascular injury, which deserve further research attention. A better understanding on these issues will enable us to understand malaria pathogenesis better, and design a reliable and safe clinical intervention strategies to improve the clinical management of malaria patients.

AUTHOR CONTRIBUTIONS

All authors listed have made a substantial, direct and intellectual contribution to the work, and approved it for publication.

FUNDING

WL was supported by funding from SIgN and Open Fund-Young Individual Research Grant (NMRC/OFYIRG/0070/2018) by the National Medical Research Council, Ministry of Health, Singapore. LR was supported by core funding to SIgN from A*STAR and the Horizontal Programme on Infectious Diseases under A*STAR. BR was supported by University of Otago start-up grant.

REFERENCES

1. Alonso P, Noor AM. The global fight against malaria is at crossroads. *Lancet*. (2017) 390:2532–4. doi: 10.1016/S0140-6736(17)33080-5
2. White NJ. *Plasmodium knowlesi*: the fifth human malaria parasite. *Clin Infect Dis*. (2008) 46:172–3. doi: 10.1086/524889
3. Ta TH, Hisam S, Lanza M, Jiram AI, Ismail N, Rubio JM. First case of a naturally acquired human infection with *Plasmodium cynomolgi*. *Malar J*. (2014) 13:68. doi: 10.1186/1475-2875-13-68
4. Olliaro P. Editorial commentary: mortality associated with severe *Plasmodium falciparum* malaria increases with age. *Clin Infect Dis*. (2008) 47:158–60. doi: 10.1086/589288
5. Baird JK. Evidence and implications of mortality associated with acute *Plasmodium vivax* malaria. *Clin Microbiol Rev*. (2013) 26:36–57. doi: 10.1128/CMR.00074-12
6. Frevert U. Sneaking in through the back entrance: the biology of malaria liver stages. *Trends Parasitol*. (2004) 20:417–24. doi: 10.1016/j.pt.2004.07.007
7. Hviid L, Jensen AT. PfEMP1—A parasite protein family of key importance in *Plasmodium falciparum* malaria immunity and pathogenesis. *Adv Parasitol*. (2015) 88:51–84. doi: 10.1016/bs.apar.2015.02.004
8. Smith JD, Rowe JA, Higgins MK, Lavstsen T. Malaria's deadly grip: cytoadhesion of *Plasmodium falciparum*-infected erythrocytes. *Cell Microbiol*. (2013) 15:1976–83. doi: 10.1111/cmi.12183
9. Boddey JA, Cowman AF. *Plasmodium* nesting: remaking the erythrocyte from the inside out. *Annu Rev Microbiol*. (2013) 67:243–69. doi: 10.1146/annurev-micro-092412-155730
10. Elsworth B, Crabb BS, Gilson PR. Protein export in malaria parasites: an update. *Cell Microbiol*. (2014) 16:355–63. doi: 10.1111/cmi.12261
11. Yam XY, Niang M, Madnani KG, Preiser PR. Three is a crowd—new insights into rosetting in *Plasmodium falciparum*. *Trends Parasitol*. (2017) 33:309–20. doi: 10.1016/j.pt.2016.12.012
12. Howard RJ, Barnwell JW, Rock EP, Neequaye J, Ofori-Adjei D, Maloy WL, et al. Two approximately 300 kilodalton *Plasmodium falciparum* proteins at the surface membrane of infected erythrocytes. *Mol Biochem Parasitol*. (1988) 27:207–23. doi: 10.1016/0166-6851(88)90040-0
13. Chen Q, Barragan A, Fernandez V, Sundstrom A, Schlichtherle M, Sahlen A, et al. Identification of *Plasmodium falciparum* erythrocyte membrane protein 1 (PfEMP1) as the rosetting ligand of the malaria parasite *P. falciparum*. *J Exp Med*. (1998) 187:15–23. doi: 10.1084/jem.187.1.15
14. Niang M, Bei AK, Madnani KG, Pelly S, Dankwa S, Kanjee U, et al. STEVOR is a *Plasmodium falciparum* erythrocyte binding protein that mediates merozoite invasion and rosetting. *Cell Host Microbe*. (2014) 16:81–93. doi: 10.1016/j.chom.2014.06.004
15. Goel S, Palmkvist M, Moll K, Joannin N, Lara P, Akhouri RR, et al. RIFINs are adhesins implicated in severe *Plasmodium falciparum* malaria. *Nat Med*. (2015) 21:314–7. doi: 10.1038/nm.3812
16. Kyes S, Pinches R, Newbold C. A simple RNA analysis method shows var and rif multigene family expression patterns in *Plasmodium falciparum*. *Mol Biochem Parasitol*. (2000) 105:311–5. doi: 10.1016/S0166-6851(99)00193-0
17. Bachmann A, Petter M, Tilly AK, Biller L, Uliczka KA, Duffy MF, et al. Temporal expression and localization patterns of variant surface antigens in clinical *Plasmodium falciparum* isolates during erythrocyte schizogony. *PLoS ONE*. (2012) 7:e49540. doi: 10.1371/journal.pone.0049540
18. Kyes SA, Rowe JA, Kriek N, Newbold CI. Rifins: a second family of clonally variant proteins expressed on the surface of red cells infected with *Plasmodium falciparum*. *Proc Natl Acad Sci USA*. (1999) 96:9333–8. doi: 10.1073/pnas.96.16.9333

19. Kaviratne M, Khan SM, Jarra W, Preiser PR. Small variant STEVOR antigen is uniquely located within Maurer's clefts in *Plasmodium falciparum*-infected red blood cells. *Eukaryot Cell.* (2002) 1:926–35. doi: 10.1128/EC.1.6.926-935.2002
20. Lavazec C, Sanyal S, Templeton TJ. Expression switching in the stevor and Pfmc-2TM superfamilies in *Plasmodium falciparum*. *Mol Microbiol.* (2007) 64:1621–34. doi: 10.1111/j.1365-2958.2007.05767.x
21. Niang M, Yan Yam X, Preiser PR. The *Plasmodium falciparum* STEVOR multigene family mediates antigenic variation of the infected erythrocyte. *PLoS Pathog.* (2009) 5:e1000307. doi: 10.1371/journal.ppat.1000307
22. Rowe JA, Moulds JM, Newbold CI, Miller LH. *P. falciparum* rosetting mediated by a parasite-variant erythrocyte membrane protein and complement-receptor 1. *Nature.* (1997) 388:292–5. doi: 10.1038/40888
23. Fried M, Duffy PE. Adherence of *Plasmodium falciparum* to chondroitin sulfate A in the human placenta. *Science.* (1996) 272:1502–4. doi: 10.1126/science.272.5267.1502
24. Khattab A, Kun J, Deloron P, Kremsner PG, Klinkert MQ. Variants of *Plasmodium falciparum* erythrocyte membrane protein 1 expressed by different placental parasites are closely related and adhere to chondroitin sulfate A. *J Infect Dis.* (2001) 183:1165–9. doi: 10.1086/319288
25. Beeson JG, Rogerson SJ, Cooke BM, Reeder JC, Chai W, Lawson AM, et al. Adhesion of *Plasmodium falciparum*-infected erythrocytes to hyaluronic acid in placental malaria. *Nat Med.* (2000) 6:86–90. doi: 10.1038/71582
26. Vogt AM, Barragan A, Chen Q, Kironde F, Spillmann D, Wahlgren M. Heparan sulfate on endothelial cells mediates the binding of *Plasmodium falciparum*-infected erythrocytes via the DBL1alpha domain of PfEMP1. *Blood.* (2003) 101:2405–11. doi: 10.1182/blood-2002-07-2016
27. Barragan A, Fernandez V, Chen Q, Von Euler A, Wahlgren M, Spillmann D. The duffy-binding-like domain 1 of *Plasmodium falciparum* erythrocyte membrane protein 1 (PfEMP1) is a heparan sulfate ligand that requires 12 mers for binding. *Blood.* (2000) 95:3594–9.
28. Handunnetti SM, Van Schravendijk MR, Hasler T, Barnwell JW, Greenwalt DE, Howard RJ. Involvement of CD36 on erythrocytes as a rosetting receptor for *Plasmodium falciparum*-infected erythrocytes. *Blood.* (1992) 80:2097–104.
29. Turner GD, Morrison H, Jones M, Davis TM, Looareesuwan S, Buley ID, et al. An immunohistochemical study of the pathology of fatal malaria. Evidence for widespread endothelial activation and a potential role for intercellular adhesion molecule-1 in cerebral sequestration. *Am J Pathol.* (1994) 145:1057–69.
30. Baruch DI, Ma XC, Singh HB, Bi X, Pasloske BL, Howard RJ. Identification of a region of PfEMP1 that mediates adherence of Plasmodium falciparum infected erythrocytes to CD36: conserved function with variant sequence. *Blood.* (1997) 90:3766–75.
31. Udomsangpetch R, Reinhardt PH, Schollaardt T, Elliott JF, Kubes P, Ho M. Promiscuity of clinical *Plasmodium falciparum* isolates for multiple adhesion molecules under flow conditions. *J Immunol.* (1997) 158:4358–64.
32. Baruch DI, Ma XC, Pasloske B, Howard RJ, Miller LH. CD36 peptides that block cytoadherence define the CD36 binding region for *Plasmodium falciparum*-infected erythrocytes. *Blood.* (1999) 94:2121–7.
33. Yipp BG, Anand S, Schollaardt T, Patel KD, Looareesuwan S, Ho M. Synergism of multiple adhesion molecules in mediating cytoadherence of *Plasmodium falciparum*-infected erythrocytes to microvascular endothelial cells under flow. *Blood.* (2000) 96:2292–8.
34. Smith JD, Craig AG, Kriek N, Hudson-Taylor D, Kyes S, Fagan T, et al. Identification of a *Plasmodium falciparum* intercellular adhesion molecule-1 binding domain: a parasite adhesion trait implicated in cerebral malaria. *Proc Natl Acad Sci USA.* (2000) 97:1766–71. doi: 10.1073/pnas.040545897
35. Armah H, Dodoo AK, Wiredu EK, Stiles JK, Adjei AA, Gyasi RK, et al. High-level cerebellar expression of cytokines and adhesion molecules in fatal, paediatric, cerebral malaria. *Ann Trop Med Parasitol.* (2005) 99:629–47. doi: 10.1179/136485905X51508
36. Gullingsrud J, Saveria T, Amos E, Duffy PE, Oleinikov AV. Structure-function-immunogenicity studies of PfEMP1 domain DBL2betaPF11_0521, a malaria parasite ligand for ICAM-1. *PLoS ONE.* (2013) 8:e61323. doi: 10.1371/journal.pone.0061323
37. Barragan A, Kremsner PG, Wahlgren M, Carlson J. Blood group A antigen is a coreceptor in *Plasmodium falciparum* rosetting. *Infect Immun.* (2000) 68:2971–5. doi: 10.1128/IAI.68.5.2971-2975.2000
38. Vigan-Womas I, Guillotte M, Juillerat A, Hessel A, Raynal B, England P, et al. Structural basis for the ABO blood-group dependence of *Plasmodium falciparum* rosetting. *PLoS Pathog.* (2012) 8:e1002781. doi: 10.1371/journal.ppat.1002781
39. Treutiger CJ, Heddini A, Fernandez V, Muller WA, Wahlgren M. PECAM-1/CD31, an endothelial receptor for binding *Plasmodium falciparum*-infected erythrocytes. *Nat Med.* (1997) 3:1405–8. doi: 10.1038/nm1297-1405
40. Berger SS, Turner L, Wang CW, Petersen JE, Kraft M, Lusingu JP, et al. *Plasmodium falciparum* expressing domain cassette 5 type PfEMP1 (DC5-PfEMP1) bind PECAM1. *PLoS ONE.* (2013) 8:e69117. doi: 10.1371/journal.pone.0069117
41. Rowe JA, Shafi J, Kai OK, Marsh K, Raza A. Nonimmune IgM, but not IgG binds to the surface of Plasmodium falciparum-infected erythrocytes and correlates with rosetting and severe malaria. *Am J Trop Med Hyg.* (2002) 66:692–9. doi: 10.4269/ajtmh.2002.66.692
42. Creasey AM, Staalsoe T, Raza A, Arnot DE, Rowe JA. Nonspecific immunoglobulin M binding and chondroitin sulfate A binding are linked phenotypes of *Plasmodium falciparum* isolates implicated in malaria during pregnancy. *Infect Immun.* (2003) 71:4767–71. doi: 10.1128/IAI.71.8.4767-4771.2003
43. Akhouri RR, Goel S, Furusho H, Skoglund U, Wahlgren M. Architecture of human IgM in complex with *P. falciparum* erythrocyte membrane protein 1. *Cell Rep.* (2016) 14:723–36. doi: 10.1016/j.celrep.2015.12.067
44. Senczuk AM, Reeder JC, Kosmala MM, Ho M. *Plasmodium falciparum* erythrocyte membrane protein 1 functions as a ligand for P-selectin. *Blood.* (2001) 98:3132–5. doi: 10.1182/blood.V98.10.3132
45. Kessler A, Dankwa S, Bernabeu M, Harawa V, Danziger SA, Duffy F, et al. Linking EPCR-binding PfEMP1 to brain swelling in pediatric cerebral malaria. *Cell Host Microbe.* (2017) 22:601–14.e605. doi: 10.1016/j.chom.2017.09.009
46. Bernabeu M, Danziger SA, Avril M, Vaz M, Babar PH, Brazier AJ, et al. Severe adult malaria is associated with specific PfEMP1 adhesion types and high parasite biomass. *Proc Natl Acad Sci USA.* (2016) 113:E3270–9. doi: 10.1073/pnas.1524294113
47. Shabani E, Hanisch B, Opoka RO, Lavstsen T, John CC. *Plasmodium falciparum* EPCR-binding PfEMP1 expression increases with malaria disease severity and is elevated in retinopathy negative cerebral malaria. *BMC Med.* (2017) 15:183. doi: 10.1186/s12916-017-0945-y
48. Biswas AK, Hafiz A, Banerjee B, Kim KS, Datta K, Chitnis CE. *Plasmodium falciparum* uses gC1qR/HABP1/p32 as a receptor to bind to vascular endothelium and for platelet-mediated clumping. *PLoS Pathog.* (2007) 3:1271–80. doi: 10.1371/journal.ppat.0030130
49. Magallon-Tejada A, Machevo S, Cistero P, Lavstsen T, Aide P, Rubio M, et al. Cytoadhesion to gC1qR through *Plasmodium falciparum* erythrocyte membrane protein 1 in severe malaria. *PLoS Pathog.* (2016) 12:e1006011. doi: 10.1371/journal.ppat.1006011
50. Pouvelle B, Matarazzo V, Jurzynski C, Nemeth J, Ramharter M, Rougon G, et al. Neural cell adhesion molecule, a new cytoadhesion receptor for *Plasmodium falciparum*-infected erythrocytes capable of aggregation. *Infect Immun.* (2007) 75:3516–22. doi: 10.1128/IAI.01852-06
51. Saito F, Hirayasu K, Satoh T, Wang CW, Lusingu J, Arimori T, et al. Immune evasion of *Plasmodium falciparum* by RIFIN via inhibitory receptors. *Nature.* (2017) 552:101–5. doi: 10.1038/nature24994
52. Gomes PS, Bhardwaj J, Rivera-Correa J, Freire-De-Lima CG, Morrot A. Immune escape strategies of malaria parasites. *Front Microbiol.* (2016) 7:1617. doi: 10.3389/fmicb.2016.01617
53. Sampaio NG, Eriksson EM, Schofield L. *Plasmodium falciparum* PfEMP1 modulates monocyte/macrophage transcription factor activation and cytokine and chemokine responses. *Infect Immun.* (2018) 86:e00447–17. doi: 10.1128/IAI.00447-17
54. Flick K, Chen Q. var genes, PfEMP1 and the human host. *Mol Biochem Parasitol.* (2004) 134:3–9. doi: 10.1016/j.molbiopara.2003.09.010
55. Kraemer SM, Smith JD. A family affair: var genes, PfEMP1 binding, and malaria disease. *Curr Opin Microbiol.* (2006) 9:374–80. doi: 10.1016/j.mib.2006.06.006

56. Smith JD. The role of PfEMP1 adhesion domain classification in *Plasmodium falciparum* pathogenesis research. *Mol Biochem Parasitol.* (2014) 195:82–7. doi: 10.1016/j.molbiopara.2014.07.006
57. Smith JD, Subramanian G, Gamain B, Baruch DI, Miller LH. Classification of adhesive domains in the *Plasmodium falciparum* erythrocyte membrane protein 1 family. *Mol Biochem Parasitol.* (2000) 110:293–310. doi: 10.1016/S0166-6851(00)00279-6
58. Juillerat A, Lewit-Bentley A, Guillotte M, Gangnard S, Hessel A, Baron B, et al. Structure of a *Plasmodium falciparum* PfEMP1 rosetting domain reveals a role for the N-terminal segment in heparin-mediated rosette inhibition. *Proc Natl Acad Sci USA.* (2011) 108:5243–8. doi: 10.1073/pnas.1018692108
59. Beeson JG, Chan JA, Fowkes FJ. PfEMP1 as a target of human immunity and a vaccine candidate against malaria. *Expert Rev Vaccines.* (2013) 12:105–8. doi: 10.1586/erv.12.144
60. Barnwell JW, Ockenhouse CF, Knowles DM II. Monoclonal antibody OKM5 inhibits the *in vitro* binding of *Plasmodium falciparum*-infected erythrocytes to monocytes, endothelial, and C32 melanoma cells. *J Immunol.* (1985) 135:3494–7.
61. Udomsangpetch R, Wahlin B, Carlson J, Berzins K, Torii M, Aikawa M, et al. *Plasmodium falciparum*-infected erythrocytes form spontaneous erythrocyte rosettes. *J Exp Med.* (1989) 169:1835–40. doi: 10.1084/jem.169.5.1835
62. Wassmer SC, Lepolard C, Traore B, Pouvelle B, Gysin J, Grau GE. Platelets reorient *Plasmodium falciparum*-infected erythrocyte cytoadhesion to activated endothelial cells. *J Infect Dis.* (2004) 189:180–9. doi: 10.1086/380761
63. Roberts DJ, Pain A, Kai O, Kortok M, Marsh K. Autoagglutination of malaria-infected red blood cells and malaria severity. *Lancet.* (2000) 355:1427–8. doi: 10.1016/S0140-6736(00)02143-7
64. Pain A, Ferguson DJ, Kai O, Urban BC, Lowe B, Marsh K, et al. Platelet-mediated clumping of *Plasmodium falciparum*-infected erythrocytes is a common adhesive phenotype and is associated with severe malaria. *Proc Natl Acad Sci USA.* (2001) 98:1805–10. doi: 10.1073/pnas.98.4.1805
65. Chotivanich K, Sritabal J, Udomsangpetch R, Newton P, Stepniewska KA, Ruangveerayuth R, et al. Platelet-induced autoagglutination of *Plasmodium falciparum*-infected red blood cells and disease severity in Thailand. *J Infect Dis.* (2004) 189:1052–5. doi: 10.1086/381900
66. Russell BM, Cooke BM. The rheopathobiology of *Plasmodium vivax* and other important primate malaria parasites. *Trends Parasitol.* (2017) 33:321–34. doi: 10.1016/j.pt.2016.11.009
67. Mbengue A, Yam XY, Braun-Breton C. Human erythrocyte remodelling during *Plasmodium falciparum* malaria parasite growth and egress. *Br J Haematol.* (2012) 157:171–9. doi: 10.1111/j.1365-2141.2012.09044.x
68. Nash GB, Cooke BM, Carlson J, Wahlgren M. Rheological properties of rosettes formed by red blood cells parasitized by *Plasmodium falciparum*. *Br J Haematol.* (1992) 82:757–63. doi: 10.1111/j.1365-2141.1992.tb06955.x
69. Pivkin IV, Peng Z, Karniadakis GE, Buffet PA, Dao M, Suresh S. Biomechanics of red blood cells in human spleen and consequences for physiology and disease. *Proc Natl Acad Sci USA.* (2016) 113:7804–9. doi: 10.1073/pnas.1606751113
70. Mebius RE, Kraal G. Structure and function of the spleen. *Nat Rev Immunol.* (2005) 5:606–16. doi: 10.1038/nri1669
71. Sosale NG, Rouhiparkouhi T, Bradshaw AM, Dimova R, Lipowsky R, Discher DE. Cell rigidity and shape override CD47's "self"-signaling in phagocytosis by hyperactivating myosin-II. *Blood.* (2015) 125:542–52. doi: 10.1182/blood-2014-06-585299
72. Suwanarusk R, Cooke BM, Dondorp AM, Silamut K, Sattabongkot J, White NJ, et al. The deformability of red blood cells parasitized by *Plasmodium falciparum* and *P. vivax J Infect Dis.* (2004) 189:190–4. doi: 10.1086/380468
73. David PH, Hommel M, Miller LH, Udeinya IJ, Oligino LD. Parasite sequestration in Plasmodium falciparum malaria: spleen and antibody modulation of cytoadherence of infected erythrocytes. *Proc Natl Acad Sci USA.* (1983) 80:5075–9. doi: 10.1073/pnas.80.16.5075
74. Bachmann A, Esser C, Petter M, Predehl S, Von Kalckreuth V, Schmiedel S, et al. Absence of erythrocyte sequestration and lack of multicopy gene family expression in *Plasmodium falciparum* from a splenectomized malaria patient. *PLoS ONE.* (2009) 4:e7459. doi: 10.1371/journal.pone.0007459
75. Buffet PA, Safeukui I, Deplaine G, Brousse V, Prendki V, Thellier M, et al. The pathogenesis of *Plasmodium falciparum* malaria in humans: insights from splenic physiology. *Blood.* (2011) 117:381–92. doi: 10.1182/blood-2010-04-202911
76. Franke-Fayard B, Fonager J, Braks A, Khan SM, Janse CJ. Sequestration and tissue accumulation of human malaria parasites: can we learn anything from rodent models of malaria? *PLoS Pathog.* (2010) 6:e1001032. doi: 10.1371/journal.ppat.1001032
77. Rowe JA, Claessens A, Corrigan RA, Arman M. Adhesion of *Plasmodium falciparum*-infected erythrocytes to human cells: molecular mechanisms and therapeutic implications. *Expert Rev Mol Med.* (2009) 11:e16. doi: 10.1017/S1462399409001082
78. Clough B, Atilola FA, Pasvoi G. The role of rosetting in the multiplication of *Plasmodium falciparum*: rosette formation neither enhances nor targets parasite invasion into uninfected red cells. *Br J Haematol.* (1998) 100:99–104. doi: 10.1046/j.1365-2141.1998.00534.x
79. Smithers SR, Terry RJ, Hockley DJ. Host antigens in schistosomiasis. *Proc R Soc Lond B Biol Sci.* (1969) 171:483–94. doi: 10.1098/rspb.1969.0007
80. Goldring OL, Clegg JA, Smithers SR, Terry RJ. Acquisition of human blood group antigens by *Schistosoma mansoni*. *Clin Exp Immunol.* (1976) 26:181–7.
81. Loukas A, Jones MK, King LT, Brindley PJ, Mcmanus DP. Receptor for Fc on the surfaces of schistosomes. *Infect Immun.* (2001) 69:3646–51. doi: 10.1128/IAI.69.6.3646-3651.2001
82. Chotivanich K, Udomsangpetch R, Mcgready R, Proux S, Newton P, Pukrittayakamee S, et al. Central role of the spleen in malaria parasite clearance. *J Infect Dis.* (2002) 185:1538–41. doi: 10.1086/340213
83. Chua CL, Brown G, Hamilton JA, Rogerson S, Boeuf P. Monocytes and macrophages in malaria: protection or pathology? *Trends Parasitol.* (2013) 29:26–34. doi: 10.1016/j.pt.2012.10.002
84. Groux H, Gysin J. Opsonization as an effector mechanism in human protection against asexual blood stages of *Plasmodium falciparum*: functional role of IgG subclasses. *Res Immunol.* (1990) 141:529–42. doi: 10.1016/0923-2494(90)90021-P
85. Mota MM, Brown KN, Holder AA, Jarra W. Acute *Plasmodium chabaudi chabaudi* malaria infection induces antibodies which bind to the surfaces of parasitized erythrocytes and promote their phagocytosis by macrophages *in vitro*. *Infect Immun.* (1998) 66:4080–6.
86. Turrini F, Giribaldi G, Carta F, Mannu F, Arese P. Mechanisms of band 3 oxidation and clustering in the phagocytosis of *Plasmodium falciparum*-infected erythrocytes. *Redox Rep.* (2003) 8:300–3. doi: 10.1179/135100003225002943
87. Dasari P, Fries A, Heber SD, Salama A, Blau IW, Lingelbach K, et al. Malarial anemia: digestive vacuole of *Plasmodium falciparum* mediates complement deposition on bystander cells to provoke hemophagocytosis. *Med Microbiol Immunol.* (2014) 203:383–93. doi: 10.1007/s00430-014-0347-0
88. Silver KL, Higgins SJ, Mcdonald CR, Kain KC. Complement driven innate immune response to malaria: fuelling severe malarial diseases. *Cell Microbiol.* (2010) 12:1036–45. doi: 10.1111/j.1462-5822.2010.01492.x
89. Smith TG, Serghides L, Patel SN, Febbraio M, Silverstein RL, Kain KC. CD36-mediated nonopsonic phagocytosis of erythrocytes infected with stage I and IIA gametocytes of *Plasmodium falciparum*. *Infect Immun.* (2003) 71:393–400. doi: 10.1128/IAI.71.1.393-400.2003
90. Patel SN, Serghides L, Smith TG, Febbraio M, Silverstein RL, Kurtz TW, et al. CD36 mediates the phagocytosis of *Plasmodium falciparum*-infected erythrocytes by rodent macrophages. *J Infect Dis.* (2004) 189:204–13. doi: 10.1086/380764
91. Wolofsky KT, Ayi K, Branch DR, Hult AK, Olsson ML, Liles WC, et al. ABO blood groups influence macrophage-mediated phagocytosis of *Plasmodium falciparum*-infected erythrocytes. *PLoS Pathog.* (2012) 8:e1002942. doi: 10.1371/journal.ppat.1002942
92. Moll K, Palmkvist M, Ch'ng J, Kiwuwa MS, Wahlgren M. Evasion of immunity to *Plasmodium falciparum*: rosettes of blood group A impair recognition of PfEMP1. *PLoS ONE.* (2015) 10:e0145120. doi: 10.1371/journal.pone.0145120
93. Champion JA, Walker A, Mitragotri S. Role of particle size in phagocytosis of polymeric microspheres. *Pharm Res.* (2008) 25:1815–21. doi: 10.1007/s11095-008-9562-y
94. Zhang R, Lee WC, Lau YL, Albrecht L, Lopes SC, Costa FT, et al. Rheopathologic consequence of *Plasmodium vivax* rosette formation. *PLoS Negl Trop Dis.* (2016) 10:e0004912. doi: 10.1371/journal.pntd.0004912

95. Sharma L, Shukla G. Placental malaria: a new insight into the pathophysiology. *Front Med.* (2017) 4:117. doi: 10.3389/fmed.2017.00117
96. Rogerson SJ, Hviid L, Duffy PE, Leke RF, Taylor DW. Malaria in pregnancy: pathogenesis and immunity. *Lancet Infect Dis.* (2007) 7:105–17. doi: 10.1016/S1473-3099(07)70022-1
97. Reeder JC. Malaria in pregnancy: getting to grips with a sticky problem. *P N G Med J.* (1999) 42:73–6.
98. Maubert B, Fievet N, Tami G, Boudin C, Deloron P. *Plasmodium falciparum*-isolates from Cameroonian pregnant women do not rosette. *Parasite.* (1998) 5:281–3. doi: 10.1051/parasite/1998053281
99. Bull PC, Abdi AI. The role of PfEMP1 as targets of naturally acquired immunity to childhood malaria: prospects for a vaccine. *Parasitology.* (2016) 143:171–86. doi: 10.1017/S0031182015001274
100. Ghumra A, Khunrae P, Ataide R, Raza A, Rogerson SJ, Higgins MK, et al. Immunisation with recombinant PfEMP1 domains elicits functional rosette-inhibiting and phagocytosis-inducing antibodies to *Plasmodium falciparum*. *PLoS ONE.* (2011) 6:e16414. doi: 10.1371/journal.pone.0016414
101. Abdel-Latif MS, Dietz K, Issifou S, Kremsner PG, Klinkert MQ. Antibodies to *Plasmodium falciparum* rifin proteins are associated with rapid parasite clearance and asymptomatic infections. *Infect Immun.* (2003) 71:6229–33. doi: 10.1128/IAI.71.11.6229-6233.2003
102. Marsh K, Howard RJ. Antigens induced on erythrocytes by *P. falciparum*: expression of diverse and conserved determinants. *Science.* (1986) 231:150–3. doi: 10.1126/science.2417315
103. Marsh K, Otoo L, Hayes RJ, Carson DC, Greenwood BM. Antibodies to blood stage antigens of *Plasmodium falciparum* in rural Gambians and their relation to protection against infection. *Trans R Soc Trop Med Hyg.* (1989) 83:293–303. doi: 10.1016/0035-9203(89)90478-1
104. Bull PC, Lowe BS, Kortok M, Molyneux CS, Newbold CI, Marsh K. Parasite antigens on the infected red cell surface are targets for naturally acquired immunity to malaria. *Nat Med.* (1998) 4:358–60. doi: 10.1038/nm0398-358
105. Fried M, Nosten F, Brockman A, Brabin BJ, Duffy PE. Maternal antibodies block malaria. *Nature.* (1998) 395:851–2. doi: 10.1038/27570
106. Baruch DI, Gamain B, Barnwell JW, Sullivan JS, Stowers A, Galland GG, et al. Immunization of *Aotus* monkeys with a functional domain of the *Plasmodium falciparum* variant antigen induces protection against a lethal parasite line. *Proc Natl Acad Sci USA.* (2002) 99:3860–5. doi: 10.1073/pnas.022018399
107. Wahlgren M, Goel S, Akhouri RR. Variant surface antigens of *Plasmodium falciparum* and their roles in severe malaria. *Nat Rev Microbiol.* (2017) 15:479–91. doi: 10.1038/nrmicro.2017.47
108. Hommel M, David PH, Oligino LD. Surface alterations of erythrocytes in *Plasmodium falciparum* malaria. *Antigenic variation, antigenic diversity, and the role of the spleen J Exp Med.* (1983) 157:1137–48. doi: 10.1084/jem.157.4.1137
109. Fandeur T, Le Scanf C, Bonnemains B, Slomianny C, Mercereau-Puijalon O. Immune pressure selects for *Plasmodium falciparum* parasites presenting distinct red blood cell surface antigens and inducing strain-specific protection in *Saimiri sciureus* monkeys. *J Exp Med.* (1995) 181:283–95. doi: 10.1084/jem.181.1.283
110. Scherf A, Lopez-Rubio JJ, Riviere L. Antigenic variation in *Plasmodium falciparum*. *Annu Rev Microbiol.* (2008) 62:445–70. doi: 10.1146/annurev.micro.61.080706.093134
111. Smith JD, Gamain B, Baruch DI, Kyes S. Decoding the language of var genes and *Plasmodium falciparum* sequestration. *Trends Parasitol.* (2001) 17:538–45. doi: 10.1016/S1471-4922(01)02079-7
112. Bernabeu M, Smith JD. EPCR and malaria severity: the center of a perfect storm. *Trends Parasitol.* (2017) 33:295–308. doi: 10.1016/j.pt.2016.11.004
113. Craig AG, Khairul MF, Patil PR. Cytoadherence and severe malaria. *Malays J Med Sci.* (2012) 19:5–18.
114. Menendez C, Ordi J, Ismail MR, Ventura PJ, Aponte JJ, Kahigwa E, et al. The impact of placental malaria on gestational age and birth weight. *J Infect Dis.* (2000) 181:1740–5. doi: 10.1086/315449
115. Walther B, Miles DJ, Crozier S, Waight P, Palmero MS, Ojuola O, et al. Placental malaria is associated with reduced early life weight development of affected children independent of low birth weight. *Malar J.* (2010) 9:16. doi: 10.1186/1475-2875-9-16
116. Elhassan IM, Hviid L, Satti G, Akerstrom B, Jakobsen PH, Jensen JB, et al. Evidence of endothelial inflammation, T cell activation, and T cell reallocation in uncomplicated *Plasmodium falciparum* malaria. *Am J Trop Med Hyg.* (1994) 51:372–9. doi: 10.4269/ajtmh.1994.51.372
117. Tripathi AK, Sha W, Shulaev V, Stins MF, Sullivan DJ Jr. *Plasmodium falciparum*-infected erythrocytes induce NF-kappaB regulated inflammatory pathways in human cerebral endothelium. *Blood.* (2009) 114:4243–52. doi: 10.1182/blood-2009-06-226415
118. Gillrie MR, Ho M. Dynamic interactions of *Plasmodium* spp. with vascular endothelium. *Tissue Barriers.* (2017) 5:e1268667. doi: 10.1080/21688370.2016.1268667
119. Turner L, Lavstsen T, Berger SS, Wang CW, Petersen JE, Avril M, et al. Severe malaria is associated with parasite binding to endothelial protein C receptor. *Nature.* (2013) 498:502–5. doi: 10.1038/nature12216
120. Mosnier LO, Lavstsen T. The role of EPCR in the pathogenesis of severe malaria. *Thromb Res.* (2016) 141(Suppl. 2):S46–9. doi: 10.1016/S0049-3848(16)30364-4
121. Mkumbaye SI, Wang CW, Lyimo E, Jespersen JS, Manjurano A, Mosha J, et al. The severity of *Plasmodium falciparum* infection Is associated with transcript levels of var genes encoding endothelial protein C receptor-binding *P. falciparum* erythrocyte membrane protein 1. *Infect Immun.* (2017) 85:e00841-16. doi: 10.1128/IAI.00841-16
122. Leroux M, Lakshmanan V, Daily JP. *Plasmodium falciparum* biology: analysis of *in vitro* versus *in vivo* growth conditions. *Trends Parasitol.* (2009) 25:474–81. doi: 10.1016/j.pt.2009.07.005
123. Hong G, Lee JC, Robinson JT, Raaz U, Xie L, Huang NF, et al. Multifunctional *in vivo* vascular imaging using near-infrared II fluorescence. *Nat Med.* (2012) 18:1841–6. doi: 10.1038/nm.2995
124. Viebig NK, Wulbrand U, Forster R, Andrews KT, Lanzer M, Knolle PA. Direct activation of human endothelial cells by *Plasmodium falciparum*-infected erythrocytes. *Infect Immun.* (2005) 73:3271–7. doi: 10.1128/IAI.73.6.3271-3277.2005
125. Van Mourik JA, Romani De Wit T, Voorberg J. Biogenesis and exocytosis of Weibel-Palade bodies. *Histochem Cell Biol.* (2002) 117:113–22. doi: 10.1007/s00418-001-0368-9
126. Dole VS, Bergmeier W, Mitchell HA, Eichenberger SC, Wagner DD. Activated platelets induce Weibel-Palade-body secretion and leukocyte rolling *in vivo*: role of P-selectin. *Blood.* (2005) 106:2334–9. doi: 10.1182/blood-2005-04-1530
127. Cambien B, Wagner DD. A new role in hemostasis for the adhesion receptor P-selectin. *Trends Mol Med.* (2004) 10:179–86. doi: 10.1016/j.molmed.2004.02.007
128. Valentijn KM, Sadler JE, Valentijn JA, Voorberg J, Eikenboom J. Functional architecture of Weibel-Palade bodies. *Blood.* (2011) 117:5033–43. doi: 10.1182/blood-2010-09-267492
129. Hermsen CC, Konijnenberg Y, Mulder L, Loe C, Van Deuren M, Van Der Meer JW, et al. Circulating concentrations of soluble granzyme A and B increase during natural and experimental *Plasmodium falciparum* infections. *Clin Exp Immunol.* (2003) 132:467–72. doi: 10.1046/j.1365-2249.2003.02160.x
130. Yeo TW, Lampah DA, Gitawati R, Tjitra E, Kenangalem E, Piera K, et al. Angiopoietin-2 is associated with decreased endothelial nitric oxide and poor clinical outcome in severe falciparum malaria. *Proc Natl Acad Sci USA.* (2008) 105:17097–102. doi: 10.1073/pnas.0805782105
131. Lovegrove FE, Tangpukdee N, Opoka RO, Lafferty EI, Rajwans N, Hawkes M, et al. Serum angiopoietin-1 and−2 levels discriminate cerebral malaria from uncomplicated malaria and predict clinical outcome in African children. *PLoS ONE.* (2009) 4:e4912. doi: 10.1371/journal.pone.0004912
132. Conroy AL, Phiri H, Hawkes M, Glover S, Mallewa M, Seydel KB, et al. Endothelium-based biomarkers are associated with cerebral malaria in Malawian children: a retrospective case-control study. *PLoS ONE.* (2010) 5:e15291. doi: 10.1371/journal.pone.0015291
133. Conroy AL, Glover SJ, Hawkes M, Erdman LK, Seydel KB, Taylor TE, et al. Angiopoietin-2 levels are associated with retinopathy and predict mortality in Malawian children with cerebral malaria: a retrospective case-control study. *Crit Care Med.* (2012) 40:952–9. doi: 10.1097/CCM.0b013e3182373157

134. O'Regan N, Gegenbauer K, O'sullivan JM, Maleki S, Brophy TM, Dalton N, et al. A novel role for von Willebrand factor in the pathogenesis of experimental cerebral malaria. *Blood.* (2016) 127:1192–201. doi: 10.1182/blood-2015-07-654921
135. Vischer UM, Wagner DD. CD63 is a component of Weibel-Palade bodies of human endothelial cells. *Blood.* (1993) 82:1184–91.
136. Galbusera M, Zoja C, Donadelli R, Paris S, Morigi M, Benigni A, et al. Fluid shear stress modulates von Willebrand factor release from human vascular endothelium. *Blood.* (1997) 90:1558–64.
137. Rosnoblet C, Vischer UM, Gerard RD, Irminger JC, Halban PA, Kruithof EK. Storage of tissue-type plasminogen activator in Weibel-Palade bodies of human endothelial cells. *Arterioscler Thromb Vasc Biol.* (1999) 19:1796–803. doi: 10.1161/01.ATV.19.7.1796
138. Schnyder-Candrian S, Borsig L, Moser R, Berger EG. Localization of α1,3-fucosyltransferase VI in Weibel-Palade bodies of human endothelial cells. *Proc Natl Acad Sci USA.* (2000) 97:8369–74. doi: 10.1073/pnas.97.15.8369
139. Zannettino AC, Holding CA, Diamond P, Atkins GJ, Kostakis P, Farrugia A, et al. Osteoprotegerin (OPG) is localized to the Weibel-Palade bodies of human vascular endothelial cells and is physically associated with von Willebrand factor. *J Cell Physiol.* (2005) 204:714–23. doi: 10.1002/jcp.20354
140. Rondaij MG, Bierings R, Kragt A, Van Mourik JA, Voorberg J. Dynamics and plasticity of Weibel-Palade bodies in endothelial cells. *Arterioscler Thromb Vasc Biol.* (2006) 26:1002–7. doi: 10.1161/01.ATV.0000209501.56852.6c
141. Van Breevoort D, Van Agtmaal EL, Dragt BS, Gebbinck JK, Dienava-Verdoold I, Kragt A, et al. Proteomic screen identifies IGFBP7 as a novel component of endothelial cell-specific Weibel-Palade bodies. *J Proteome Res.* (2012) 11:2925–36. doi: 10.1021/pr300010r
142. Turner NA, Moake JL. Factor VIII Is synthesized in human endothelial cells, packaged in Weibel-Palade bodies and secreted bound to ULVWF strings. *PLoS ONE.* (2015) 10:e0140740. doi: 10.1371/journal.pone.0140740
143. Maleszewski JJ, Lai CK, Veinot JP. Chapter 1—anatomic considerations and examination of cardiovascular specimens (excluding devices) A2 - Buja, L. Maximilian. In: Butany J, editor. *Cardiovascular Pathology, 4th ed*. San Diego: Academic Press (2016). p. 1–56. doi: 10.1016/B978-0-12-420219-1.00001-X
144. Babich V, Meli A, Knipe L, Dempster JE, Skehel P, Hannah MJ, et al. Selective release of molecules from Weibel-Palade bodies during a lingering kiss. *Blood.* (2008) 111:5282–90. doi: 10.1182/blood-2007-09-113746
145. Kiskin NI, Babich V, Knipe L, Hannah MJ, Carter T. Differential cargo mobilisation within Weibel-Palade bodies after transient fusion with the plasma membrane. *PLoS ONE.* (2014) 9:e108093. doi: 10.1371/journal.pone.0108093
146. Dekker RJ, Boon RA, Rondaij MG, Kragt A, Volger OL, Elderkamp YW, et al. KLF2 provokes a gene expression pattern that establishes functional quiescent differentiation of the endothelium. *Blood.* (2006) 107:4354–63. doi: 10.1182/blood-2005-08-3465
147. Combes V, Coltel N, Faille D, Wassmer SC, Grau GE. Cerebral malaria: role of microparticles and platelets in alterations of the blood-brain barrier. *Int J Parasitol.* (2006) 36:541–6. doi: 10.1016/j.ijpara.2006.02.005
148. Jenkins NT, Padilla J, Boyle LJ, Credeur DP, Laughlin MH, Fadel PJ. Disturbed blood flow acutely induces activation and apoptosis of the human vascular endothelium. *Hypertension.* (2013) 61:615–21. doi: 10.1161/HYPERTENSIONAHA.111.00561
149. Scholz A, Plate KH, Reiss Y. Angiopoietin-2: a multifaceted cytokine that functions in both angiogenesis and inflammation. *Ann N Y Acad Sci.* (2015) 1347:45–51. doi: 10.1111/nyas.12726
150. Moxon CA, Wassmer SC, Milner DA Jr, Chisala NV, Taylor TE, Seydel KB, et al. Loss of endothelial protein C receptors links coagulation and inflammation to parasite sequestration in cerebral malaria in African children. *Blood.* (2013) 122:842–51. doi: 10.1182/blood-2013-03-490219
151. Turner GD, Ly VC, Nguyen TH, Tran TH, Nguyen HP, Bethell D, et al. Systemic endothelial activation occurs in both mild and severe malaria. Correlating dermal microvascular endothelial cell phenotype and soluble cell adhesion molecules with disease severity. *Am J Pathol.* (1998) 152:1477–87.
152. Tripathi AK, Sullivan DJ, Stins MF. *Plasmodium falciparum*-infected erythrocytes increase intercellular adhesion molecule 1 expression on brain endothelium through NF-κB. *Infect Immun.* (2006) 74:3262–70. doi: 10.1128/IAI.01625-05
153. Pouvelle B, Fusai T, Lepolard C, Gysin J. Biological and biochemical characteristics of cytoadhesion of *Plasmodium falciparum*-infected erythrocytes to chondroitin-4-sulfate. *Infect Immun.* (1998) 66:4950–6.
154. Avril M, Bernabeu M, Benjamin M, Brazier AJ, Smith JD. Interaction between endothelial protein C receptor and intercellular adhesion molecule 1 to mediate binding of *Plasmodium falciparum*-infected erythrocytes to endothelial cells. *mBio.* (2016) 7:e00615–16. doi: 10.1128/mBio.00615-16
155. Lavstsen T, Turner L, Saguti F, Magistrado P, Rask TS, Jespersen JS, et al. *Plasmodium falciparum* erythrocyte membrane protein 1 domain cassettes 8 and 13 are associated with severe malaria in children. *Proc Natl Acad Sci USA.* (2012) 109:E1791–800. doi: 10.1073/pnas.1120455109
156. Bertin GI, Lavstsen T, Guillonneau F, Doritchamou J, Wang CW, Jespersen JS, et al. Expression of the domain cassette 8 *Plasmodium falciparum* erythrocyte membrane protein 1 is associated with cerebral malaria in Benin. *PLoS ONE.* (2013) 8:e68368. doi: 10.1371/journal.pone.0068368
157. Abdi AI, Kariuki SM, Muthui MK, Kivisi CA, Fegan G, Gitau E, et al. Differential *Plasmodium falciparum* surface antigen expression among children with Malarial Retinopathy. *Sci Rep.* (2015) 5:18034. doi: 10.1038/srep18034
158. Seydel KB, Kampondeni SD, Valim C, Potchen MJ, Milner DA, Muwalo FW, et al. Brain swelling and death in children with cerebral malaria. *N Engl J Med.* (2015) 372:1126–37. doi: 10.1056/NEJMoa1400116
159. Jespersen JS, Wang CW, Mkumbaye SI, Minja DT, Petersen B, Turner L, et al. *Plasmodium falciparum* var genes expressed in children with severe malaria encode CIDRalpha1 domains. *EMBO Mol Med.* (2016) 8:839–50. doi: 10.15252/emmm.201606188
160. David PH, Handunnetti SM, Leech JH, Gamage P, Mendis KN. Rosetting: a new cytoadherence property of malaria-infected erythrocytes. *Am J Trop Med Hyg.* (1988) 38:289–97. doi: 10.4269/ajtmh.1988.38.289
161. Lowe BS, Mosobo M, Bull PC. All four species of human malaria parasites form rosettes. *Trans R Soc Trop Med Hyg.* (1998) 92:526. doi: 10.1016/S0035-9203(98)90901-4
162. Wahlgren M, Carlson J, Udomsangpetch R, Perlmann P. Why do *Plasmodium falciparumm*-infected erythrocytes form spontaneous erythrocyte rosettes? *Parasitol Today.* (1989) 5:183–5. doi: 10.1016/0169-4758(89)90141-5
163. Carlson J, Holmquist G, Taylor DW, Perlmann P, Wahlgren M. Antibodies to a histidine-rich protein (PfHRP1) disrupt spontaneously formed *Plasmodium falciparum* erythrocyte rosettes. *Proc Natl Acad Sci USA.* (1990) 87:2511–5. doi: 10.1073/pnas.87.7.2511
164. Adams Y, Kuhnrae P, Higgins MK, Ghumra A, Rowe JA. Rosetting *Plasmodium falciparum*-infected erythrocytes bind to human brain microvascular endothelial cells *in vitro*, demonstrating a dual adhesion phenotype mediated by distinct *P. falciparum* erythrocyte membrane protein 1 domains. *Infect Immun.* (2014) 82:949–59. doi: 10.1128/IAI.01233-13
165. Treutiger CJ, Hedlund I, Helmby H, Carlson J, Jepson A, Twumasi P, et al. Rosette formation in *Plasmodium falciparum* isolates and anti-rosette activity of sera from Gambians with cerebral or uncomplicated malaria. *Am J Trop Med Hyg.* (1992) 46:503–10. doi: 10.4269/ajtmh.1992.46.503
166. Carlson J, Nash GB, Gabutti V, Al-Yaman F, Wahlgren M. Natural protection against severe *Plasmodium falciparum* malaria due to impaired rosette formation. *Blood.* (1994) 84:3909–14.
167. Rowe A, Obeiro J, Newbold CI, Marsh K. *Plasmodium falciparum* rosetting is associated with malaria severity in Kenya. *Infect Immun.* (1995) 63:2323–6.
168. Rowe JA, Obiero J, Marsh K, Raza A. Short report: positive correlation between rosetting and parasitemia in Plasmodium falciparum clinical isolates. *Am J Trop Med Hyg.* (2002) 66:458–60. doi: 10.4269/ajtmh.2002.66.458
169. Doumbo OK, Thera MA, Kone AK, Raza A, Tempest LJ, Lyke KE, et al. High levels of *Plasmodium falciparum* rosetting in all clinical forms of severe malaria in African children. *Am J Trop Med Hyg.* (2009) 81:987–93. doi: 10.4269/ajtmh.2009.09-0406
170. Ho M, Davis TM, Silamut K, Bunnag D, White NJ. Rosette formation of *Plasmodium falciparum*-infected erythrocytes from patients with acute malaria. *Infect Immun.* (1991) 59:2135–9.
171. Al-Yaman F, Genton B, Mokela D, Raiko A, Kati S, Rogerson S, et al. Human cerebral malaria: lack of significant association between erythrocyte

rosetting and disease severity. *Trans R Soc Trop Med Hyg.* (1995) 89:55–8. doi: 10.1016/0035-9203(95)90658-4
172. Udomsangpetch R, Webster HK, Pattanapanyasat K, Pitchayangkul S, Thaithong S. Cytoadherence characteristics of rosette-forming *Plasmodium falciparum*. *Infect Immun.* (1992) 60:4483–90.
173. Branco A, Melo-Cristino J. Extreme parasitemia in *P. falciparum malaria Blood.* (2018) 132:868. doi: 10.1182/blood-2018-07-861880
174. Carlson J, Ekre HP, Helmby H, Gysin J, Greenwood BM, Wahlgren M. Disruption of *Plasmodium falciparum* erythrocyte rosettes by standard heparin and heparin devoid of anticoagulant activity. *Am J Trop Med Hyg.* (1992) 46:595–602. doi: 10.4269/ajtmh.1992.46.595
175. Vogt AM, Winter G, Wahlgren M, Spillmann D. Heparan sulphate identified on human erythrocytes: a *Plasmodium falciparum* receptor. *Biochem J.* (2004) 381:593–7. doi: 10.1042/BJ20040762
176. Angeletti D, Sandalova T, Wahlgren M, Achour A. Binding of subdomains 1/2 of PfEMP1-DBL1alpha to heparan sulfate or heparin mediates *Plasmodium falciparum* rosetting. *PLoS ONE.* (2015) 10:e0118898. doi: 10.1371/journal.pone.0118898
177. McCormick CJ, Newbold CI, Berendt AR. Sulfated glycoconjugates enhance CD36-dependent adhesion of *Plasmodium falciparum*-infected erythrocytes to human microvascular endothelial cells. *Blood.* (2000) 96:327–33.
178. Dembo EG, Phiri HT, Montgomery J, Molyneux ME, Rogerson SJ. Are *Plasmodium falciparum* parasites present in peripheral blood genetically the same as those sequestered in the tissues? *Am J Trop Med Hyg.* (2006) 74:730–2. doi: 10.4269/ajtmh.2006.74.730
179. Montgomery J, Milner DA Jr, Tse MT, Njobvu A, Kayira K, Dzamalala CP, et al. Genetic analysis of circulating and sequestered populations of *Plasmodium falciparum* in fatal pediatric malaria. *J Infect Dis.* (2006) 194:115–22. doi: 10.1086/504689
180. Kaul DK, Roth EF Jr, Nagel RL, Howard RJ, Handunnetti SM. Rosetting of *Plasmodium falciparum*-infected red blood cells with uninfected red blood cells enhances microvascular obstruction under flow conditions. *Blood.* (1991) 78:812–9.
181. Berendt AR, Ferguson DJ, Newbold CI. Sequestration in *Plasmodium falciparum* malaria: sticky cells and sticky problems. *Parasitol Today.* (1990) 6:247–54. doi: 10.1016/0169-4758(90)90184-6
182. Chotivanich KT, Pukrittayakamee S, Simpson JA, White NJ, Udomsangpetch R. Characteristics of *Plasmodium vivax*-infected erythrocyte rosettes. *Am J Trop Med Hyg.* (1998) 59:73–6. doi: 10.4269/ajtmh.1998.59.73
183. Lee WC, Malleret B, Lau YL, Mauduit M, Fong MY, Cho JS, et al. Glycophorin C (CD236R) mediates vivax malaria parasite rosetting to normocytes. *Blood.* (2014) 123:e100–9. doi: 10.1182/blood-2013-12-541698
184. Ozen M, Gungor S, Atambay M, Daldal N. Cerebral malaria owing to *Plasmodium vivax*: case report. *Ann Trop Paediatr.* (2006) 26:141–4. doi: 10.1179/146532806X107494
185. Thapa R, Patra V, Kundu R. *Plasmodium vivax* cerebral malaria. *Indian Pediatr.* (2007) 44:433–4.
186. Sarkar S, Bhattacharya P. Cerebral malaria caused by *Plasmodium vivax* in adult subjects. *Indian J Crit Care Med.* (2008) 12:204–5. doi: 10.4103/0972-5229.45084
187. Mahgoub H, Gasim GI, Musa IR, Adam I. Severe *Plasmodium vivax* malaria among sudanese children at New Halfa Hospital, Eastern Sudan. *Parasit Vectors.* (2012) 5:154. doi: 10.1186/1756-3305-5-154
188. Pinzon MA, Pineda JC, Rosso F, Shinchi M, Bonilla-Abadia F. *Plasmodium vivax* cerebral malaria complicated with venous sinus thrombosis in Colombia. *Asian Pac J Trop Med.* (2013) 6:413–5. doi: 10.1016/S1995-7645(13)60050-4
189. Karanth SS, Marupudi KC, Gupta A. Intracerebral bleed, right haemiparesis and seizures: an atypical presentation of vivax malaria. *BMJ Case Rep.* (2014) 2014:bcr2014204833. doi: 10.1136/bcr-2014-204833
190. Gupta H, Dhunputh P, Bhatt AN, Satyamoorthy K, Umakanth S. Cerebral malaria in a man with *Plasmodium vivax* mono-infection: a case report. *Trop Doct.* (2016) 46:241–5. doi: 10.1177/0049475515624857
191. Carvalho BO, Lopes SC, Nogueira PA, Orlandi PP, Bargieri DY, Blanco YC, et al. On the cytoadhesion of *Plasmodium vivax*-infected erythrocytes. *J Infect Dis.* (2010) 202:638–47. doi: 10.1086/654815
192. Nagayasu E, Ito M, Akaki M, Nakano Y, Kimura M, Looareesuwan S, et al. CR1 density polymorphism on erythrocytes of falciparum malaria patients in Thailand. *Am J Trop Med Hyg.* (2001) 64:1–5. doi: 10.4269/ajtmh.2001.64.1.11425154
193. Teeranaipong P, Ohashi J, Patarapotikul J, Kimura R, Nuchnoi P, Hananantachai H, et al. A functional single-nucleotide polymorphism in the CR1 promoter region contributes to protection against cerebral malaria. *J Infect Dis.* (2008) 198:1880–91. doi: 10.1086/593338
194. Sinha S, Jha GN, Anand P, Qidwai T, Pati SS, Mohanty S, et al. CR1 levels and gene polymorphisms exhibit differential association with falciparum malaria in regions of varying disease endemicity. *Hum Immunol.* (2009) 70:244–50. doi: 10.1016/j.humimm.2009.02.001
195. Rout R, Dhangadamajhi G, Mohapatra BN, Kar SK, Ranjit M. High CR1 level and related polymorphic variants are associated with cerebral malaria in eastern-India. *Infect Genet Evol.* (2011) 11:139–44. doi: 10.1016/j.meegid.2010.09.009
196. Zimmerman PA, Fitness J, Moulds JM, Mcnamara DT, Kasehagen LJ, Rowe JA, et al. CR1 Knops blood group alleles are not associated with severe malaria in the Gambia. *Genes Immun.* (2003) 4:368–73. doi: 10.1038/sj.gene.6363980
197. Cockburn IA, Mackinnon MJ, O'donnell A, Allen SJ, Moulds JM, Baisor M, et al. A human complement receptor 1 polymorphism that reduces *Plasmodium falciparum* rosetting confers protection against severe malaria. *Proc Natl Acad Sci USA.* (2004) 101:272–7. doi: 10.1073/pnas.0305306101
198. Thathy V, Moulds JM, Guyah B, Otieno W, Stoute JA. Complement receptor 1 polymorphisms associated with resistance to severe malaria in Kenya. *Malar J.* (2005) 4:54. doi: 10.1186/1475-2875-4-54
199. Opi DH, Swann O, Macharia A, Uyoga S, Band G, Ndila CM, et al. Two complement receptor one alleles have opposing associations with cerebral malaria and interact with alpha(+)thalassaemia. *Elife.* (2018) 7:e31579. doi: 10.7554/eLife.31579
200. Babiker HA, Abdel-Muhsin AM, Ranford-Cartwright LC, Satti G, Walliker D. Characteristics of *Plasmodium falciparum* parasites that survive the lengthy dry season in eastern Sudan where malaria transmission is markedly seasonal. *Am J Trop Med Hyg.* (1998) 59:582–90. doi: 10.4269/ajtmh.1998.59.582
201. Zwetyenga J, Rogier C, Spiegel A, Fontenille D, Trape JF, Mercereau-Puijalon O. A cohort study of *Plasmodium falciparum* diversity during the dry season in Ndiop, a Senegalese village with seasonal, mesoendemic malaria. *Trans R Soc Trop Med Hyg.* (1999) 93:375–80. doi: 10.1016/S0035-9203(99)90122-0
202. Baliraine FN, Afrane YA, Amenya DA, Bonizzoni M, Menge DM, Zhou G, et al. High prevalence of asymptomatic Plasmodium falciparum infections in a highland area of western Kenya: a cohort study. *J Infect Dis.* (2009) 200:66–74. doi: 10.1086/599317
203. Sagna AB, Gaayeb L, Sarr JB, Senghor S, Poinsignon A, Boutouaba-Combe S, et al. *Plasmodium falciparum* infection during dry season: IgG responses to *Anopheles gambiae* salivary gSG6-P1 peptide as sensitive biomarker for malaria risk in Northern Senegal. *Malar J.* (2013) 12:301. doi: 10.1186/1475-2875-12-301
204. Howard RJ, Gilladoga AD. Molecular studies related to the pathogenesis of cerebral malaria. *Blood.* (1989) 74:2603–18.
205. Handunnetti SM, Hasler TH, Howard RJ. *Plasmodium falciparum*-infected erythrocytes do not adhere well to C32 melanoma cells or CD36 unless rosettes with uninfected erythrocytes are first disrupted. *Infect Immun.* (1992) 60:928–32.
206. Rogerson SJ, Beck HP, Al-Yaman F, Currie B, Alpers MP, Brown GV. Disruption of erythrocyte rosettes and agglutination of erythrocytes infected with *Plasmodium falciparum* by the sera of Papua New Guineans. *Trans R Soc Trop Med Hyg.* (1996) 90:80–4. doi: 10.1016/S0035-9203(96)90487-3
207. Chotivanich KT, Dondorp AM, White NJ, Peters K, Vreeken J, Kager PA, et al. The resistance to physiological shear stresses of the erythrocytic rosettes formed by cells infected with *Plasmodium falciparum*. *Ann Trop Med Parasitol.* (2000) 94:219–26. doi: 10.1080/00034983.2000.11813532
208. Saxer T, Zumbuehl A, Muller B. The use of shear stress for targeted drug delivery. *Cardiovasc Res.* (2013) 99:328–33. doi: 10.1093/cvr/cvt102
209. Idro R, Marsh K, John CC, Newton CR. Cerebral malaria: mechanisms of brain injury and strategies for improved neurocognitive outcome. *Pediatr Res.* (2010) 68:267–74. doi: 10.1203/PDR.0b013e3181eee738

210. Rogerson SJ, Reeder JC, Al-Yaman F, Brown GV. Sulfated glycoconjugates as disrupters of *Plasmodium falciparum* erythrocyte rosettes. *Am J Trop Med Hyg.* (1994) 51:198–203. doi: 10.4269/ajtmh.1994.51.198
211. Rowe A, Berendt AR, Marsh K, Newbold CI. *Plasmodium falciparum*: a family of sulphated glycoconjugates disrupts erythrocyte rosettes. *Exp Parasitol.* (1994) 79:506–16. doi: 10.1006/expr.1994.1111
212. Luginbuhl A, Nikolic M, Beck HP, Wahlgren M, Lutz HU. Complement factor D, albumin, and immunoglobulin G anti-band 3 protein antibodies mimic serum in promoting rosetting of malaria-infected red blood cells. *Infect Immun.* (2007) 75:1771–7. doi: 10.1128/IAI.01514-06
213. Azasi Y, Lindergard G, Ghumra A, Mu J, Miller LH, Rowe JA. Infected erythrocytes expressing DC13 PfEMP1 differ from recombinant proteins in EPCR-binding function. *Proc Natl Acad Sci USA*. (2018) 115:1063–8. doi: 10.1073/pnas.1712879115
214. Haffner SM. Pre-diabetes, insulin resistance, inflammation and CVD risk. *Diabetes Res Clin Pract.* (2003) 61(Suppl. 1):S9–18. doi: 10.1016/S0168-8227(03)00122-0
215. Movva LR, Ho DKL, Corbet EF, Leung WK. Type-2 diabetes mellitus, metabolic control, serum inflammatory factors, lifestyle, and periodontal status. *J Dent Sci.* (2014) 9:1–9. doi: 10.1016/j.jds.2013.10.006

Conflict of Interest Statement: The authors declare that the research was conducted in the absence of any commercial or financial relationships that could be construed as a potential conflict of interest.

frontiers in Immunology

REVIEW
published: 02 November 2018
doi: 10.3389/fimmu.2018.02518

Unravelling the Immunity of Poultry Against the Extracellular Protozoan Parasite *Histomonas meleagridis* Is a Cornerstone for Vaccine Development: A Review

Taniya Mitra[1], *Fana Alem Kidane*[1], *Michael Hess*[1,2] *and Dieter Liebhart*[1]*

[1] Clinic for Poultry and Fish Medicine, Department for Farm Animals and Veterinary Public Health, University of Veterinary Medicine Vienna, Vienna, Austria, [2] Christian Doppler Laboratory for Innovative Poultry Vaccines (IPOV), University of Veterinary Medicine Vienna, Vienna, Austria

OPEN ACCESS

Edited by:
Zhiguang Wu,
University of Edinburgh,
United Kingdom

Reviewed by:
Ruediger Hauck,
Auburn University, United States
Bruno Maria Goddeeris,
KU Leuven, Belgium
Robert Byron Beckstead,
North Carolina State University,
United States

***Correspondence:**
Dieter Liebhart
dieter.liebhart@vetmeduni.ac.at

Specialty section:
This article was submitted to Microbial Immunology, a section of the journal Frontiers in Immunology

Received: *02 July 2018*
Accepted: *12 October 2018*
Published: *02 November 2018*

Citation:
Mitra T, Kidane FA, Hess M and Liebhart D (2018) Unravelling the Immunity of Poultry Against the Extracellular Protozoan Parasite Histomonas meleagridis Is a Cornerstone for Vaccine Development: A Review. Front. Immunol. 9:2518. doi: 10.3389/fimmu.2018.02518

The protozoan parasite *Histomonas meleagridis* is the causative agent of histomonosis in gallinaceous birds, predominantly in turkeys and chickens. Depending on the host species the outcome of the disease can be very severe with high mortality as observed in turkeys, whereas in chickens the mortality rates are generally lower. The disease is known for more than 100 years when *in vitro* and *in vivo* investigations started to understand histomonosis and the causative pathogen. For decades histomonosis could be well-controlled by effective drugs for prevention and therapy until the withdrawal of such chemicals for reasons of consumer protection in Europe, the USA and additional countries worldwide. Consequently, research efforts also focused to find new strategies against the disease, resulting in the development of an efficacious live-attenuated vaccine. In addition to efficacy and safety several studies were performed to obtain a deeper understanding of the immune response of the host against *H. meleagridis*. It could be demonstrated that antibodies accumulate in different parts of the intestine of chickens following infection with *H. meleagridis* which was much pronounced in the ceca. Furthermore, expression profiles of various cytokines revealed that chickens mounted an effective cecal innate immune response during histomonosis compared to turkeys. Studying the cellular immune response following infection and/or vaccination of host birds showed a limitation of pronounced changes of B cells and T-cell subsets in vaccinated birds in comparison to non-protected birds. Additionally, numbers of lymphocytes including cytotoxic T cells increased in the ceca of diseased turkeys compared to infected chickens suggesting an immunopathological impact on disease pathogenesis. The identification of type 1 and type 2 T-helper (Th) cells in infected and lymphoid organs by *in situ* hybridization did not show a clear separation of Th cells during infection but revealed a coherence of an increase of interferon (IFN)-γ mRNA positive cells

in ceca and protection. The present review not only summarizes the research performed on the immune response of host birds in the course of histomonosis but also highlights the specific features of *H. meleagridis* as a model organism to study immunological principles of an extracellular organism in birds.

Keywords: *Histomonas meleagridis*, histomonosis, immunity, vaccination, immune response, extracellular parasite, poultry

INTRODUCTION

Histomonas meleagridis is an important flagellated parasite of poultry causing the disease histomonosis (syn. blackhead disease, histomoniasis, or infectious typhlohepatitis) (1). Historically, the disease was extensively investigated in the first half of the last century and thereby effective chemotherapeutics were identified to prevent and treat birds from infection. This success neglects that for a long time the true etiology of the disease was questioned and under debate. Difficulties to determine the real cause of histomonosis in earlier studies are comprehensively recapitulated elsewhere (2). However, to date the disease is of high relevance in poultry flocks as effective prophylactic and therapeutic options are not available anymore in many countries for reasons of food safety. As a consequence research was intensified in recent years and with it several reviews were published addressing different features of the parasite or the disease. This includes a general overview on the disease (3), updated findings of the recent years (4), a summary of experimental infections (5), a recapitulation on previous and current strategies for prevention and therapy (6), and assumptions how the disease might be controlled in the future (7).

The purpose of this review is to emphasize on studies investigating mechanisms of the immune response of host birds against the disease. This includes early studies describing inflammatory reactions of birds' up to recent investigations on specific immune cells and signaling proteins involved in host defense. Furthermore, the host reaction due to vaccination and its functional aspects are reviewed. Finally, *H. meleagridis* might be a model to unravel peculiar immune mechanisms of extracellular pathogens considering that the avian immune response against these organisms is not as investigated in depth compared to viral or bacterial infections.

Histomonosis, an Important Poultry Disease

Histomonosis was firstly described in turkeys by Cushman (8) more than a century ago. Infection with *H. meleagridis* can occur directly or via embryonated eggs of the nematode *Heterakis gallinarum* which was already described by Graybill and Smith (9). Horizontal transmission was hypothesized to occur by active uptake via the cloaca (10) or orally, based on successful oral application of cultured histomonads (11).The first signs of histomonosis are reflected by clinical changes such as reduced appetite, depression, drowsiness, droopy wings, and ruffled feathers. Infected birds might suffer from yellowish diarrhea and succumb to death (4). The pathogenesis generally varies between species of gallinaceous birds: in turkeys (*Meleagris gallopavo*) the disease can cause high mortality due to severe necrotic inflammation of the ceca and the liver, while in chickens (*Gallus gallus*) clinical signs are milder and pathological manifestations are often restricted to the ceca of infected birds.

Following infection, *H. meleagridis* migrates into the mucosa and deeper layers of the cecal wall leading to inflammation and ulceration, resulting in a thickening of the cecal tissue and formation of fibrin. Occasionally, ulcers erode throughout the cecal wall leading to peritonitis. Following destruction of cecal tissue, the parasite is able to infiltrate into blood vessels and to reach the liver via the portal vein. As a consequence, areas of inflammation and necrosis can occur in the liver. Liver lesions are highly variable in appearance: they may be up to 4 cm in diameter and can involve parts or the entire organ. Liver and cecal lesions together are a strong hint during post mortem investigations. The disease causes generally less severe lesions in chickens. Especially changes in the liver occur less frequently in chickens as compared to turkeys. In the final stage, the disease may become systemic when DNA of histomonads can be found in the blood and in the tissues of many organs, whether lesions are present or not (12). Lesions can be observed in different organs beside cecum and liver, such as kidneys, bursa of Fabricius, spleen, and pancreas (13–15). Apart from turkeys and chickens, other members of the galliformes, including pheasants, partridges, and farm-reared bobwhite quails can serve as hosts (16–19). In contrary, other avian species like ostriches and ducks show a high resistance to disease even though they may contribute to the transmission of the parasite (20, 21).

Histomonas meleagridis, a Unique Protozoan Parasite

H. meleagridis is a member of the family *Dientamoebidae*, order Tritrichomonadida (22). The parasite mainly possesses cell organelles that are typical for trichomonads (3). It is pleomorphic and generally two forms of the parasite are known: (i) the tissue form and (ii) the cecal lumen dwelling form. The tissue form is almost round with 6–20 μm in size and capable of forming pseudopodia (23, 24). Unlike the tissue form the cecal lumen form (3–16 μm) has a single flagellum although early during cell division, two may be observed (25). It was observed that the flagellum is getting lost during the invasion in the host tissue (26). In culture, *H. meleagridis* exhibits the morphology of the lumen-dwelling form. More recently, the occurrence of a cyst-like stage was reported (27). Later on, this resistant stage of *H. meleagridis* was investigated *in vitro* and it could be

observed independent of the passage level and pathogenicity *in vivo* indicating an early adaption to *in vitro* conditions (28).

H. meleagridis is antigenetically (29) closely related to the intestinal parasite *Dientamoeba fragilis*, a trichomonad with a wider host range in mammals which is suspected to be associated with gastrointestinal disorders in humans. *Dientamoeba fragilis* is a protozoan parasite often described as "neglected parasite" (30). Recently, several major advances have been made with respect to this organism's life cycle and molecular biology, although knowledge on immune response against the pathogen is scant. The pathogenic potential of *D. fragilis* is still debatable. However, because of the close relativity to histomonads, the immunological research on *H. meleagridis* can give an indication to the immunological responsiveness of host against *D. fragilis*.

Hyperimmune antisera raised in rabbits against the two flagellates cross-reacted in an indirect fluorescent antibody test (31), although in agar gel immune-diffusion test (32) species-specific precipitin lines were seen. Both, antigenic differences and some cross-reactivity could also be demonstrated by immunoelectrophoresis (33). The nucleotide sequence analysis of a small subunit rRNA of the organism showed a close relationship between *D. fragilis* and *H. meleagridis* (34). First investigations on specific proteins of *H. meleagridis* were performed by Mazet et al. (35). The authors characterized genes encoding three proteins involved in hydrogenosomal carbon metabolism: a nicotinamide adenine dinucleotide phosphate-dependent hydrogenosomal malic enzyme, an α-subunit of a succinyl coenzyme-A synthetase and an iron-only hydrogenase. Afterwards, Bilic et al. (36) identified a broad spectrum of partial protein-coding sequences with homology to both intracellular and surface proteins. The antigenic potential of α-actinins of the parasite in host animals was later on demonstrated (37). Lynn and Beckstead, (38) applied splinkerette PCR to identify new genes. Their sequence analysis identified the 5′ coding portions of the β-tubulin genes, the intergenic regions, and two different open reading frames encoding for a putative serine/threonine phosphatase and a putative ras-related protein, racG. They predicted that these intergenic regions contain polyadenylation and cleavage signals for the two open reading frames and initiator elements for the β-tubulin genes. These regulatory elements are necessary for gene transcription in *H. meleagridis*. Most recently, sequencing of a cDNA library reported sequences of 3425 *H. meleagridis* genes (39). These analyses identified 81 genes coding for putative hydrogenosomal proteins and determined the codon usage frequency. That study also suggested that *H. meleagridis* α-actinins strongly contribute to the immune-reaction of host birds. Recently, *de novo* transcriptome sequencing of a virulent and an attenuated *H. meleagridis* strain provided novel insights into the parasite's biological processes, such as metabolism, locomotion, cell signaling and its ability to adapt to dynamic environmental changes (40). In addition, the study elucidated potential pathogenic mechanisms in respect to cytoadherence and host cell membrane disruption, together with the possible regulation of such processes. Monoyios et al. (41) addressed differences between *in vivo* cultivated virulent and attenuated *H. meleagridis* parasites on protein expression level. Based on mass spectrometry data it could be shown that eight different proteins, with the majority related to cellular stress management, have been found up-regulated in virulent histomonads compared to the attenuated strain which potentially affect the host-pathogen interaction between the two strains. Additionally, a virulence factor named legumain cysteine peptidase was detected. Applying two-dimensional electrophoresis in combination with mass spectrometric analysis 32 spots were identified as specific for the attenuated strain. These spots were described to correspond to the increased metabolism due to *in vitro* adaptation of the parasite and the amoeboid morphology.

IMMUNOLOGICAL RESPONSES AGAINST HISTOMONOSIS

Modulations of the innate and adaptive immune responses of the host by pathogens are known to be major determinants in the outcome of certain infectious diseases. Histomonosis causes severe disease in turkeys whereas less clinical signs occur in chickens as described above. This outcome can be linked with the host defense, indicating substantial differences between these two phylogenetically closely related species against *H. meleagridis*. Elucidating these differences in host response does not only unravel a certain host reaction it is also useful to understand protection and susceptibility in a broader context. Important studies investigating distinct parameter of the immune response against *H. meleagridis* are listed in **Table 1**.

Innate Immune Response

The first arm of the innate immune system against histomonosis is the anatomical barrier in the gastrointestinal tract. The parasite can infect its host via cloacal or oral route. However, oral inoculation was not always successful probably due to the acidity of the gizzard (10, 11, 54–56). The acid environment in the gizzard is a physiological barrier against pathogens and it was reported earlier that an effective infection depends upon the pH of the gizzard and the upper intestine (55). In the last mentioned work it was observed that the severity of lesions increased in chickens that have starved or were fed with an alkali mixture before the oral infection. Feed restriction after the application of live histomonads was shown to be an additional parameter which should be considered in the context of a successful oral infection (11).

Concerning the innate cellular response, first observations were made by histopathology in birds infected with *H. gallinarum* and *H. meleagridis* (57). Thereby, larvae of the cecal worm and an influx of heterophilic granulocytes were visible already from day 1 post infection (p.i.), even though first histomonads were only visualized after 5 days p.i.. First lesions in the liver, characterized by lymphocytic infiltration with few heterophils at the portal area, were observed at the same time point (13). Specific detection of the parasite in tissue sections was described to be accompanied with infiltrations of mononuclear and polymorphonuclear cells in the infected organs cecum and liver (58, 59). In recent studies, quantitative analyses using specific

TABLE 1 | Year wise experimental studies in turkeys and/or chickens investigating important immunological parameters of histomonosis.

Parameter	Components	Technique	Tissue	Host	Strain or antigenic preparation	Year of publication (reference)
Serum antibodies	Precipitating antibodies	Agar gel immunodiffusion (Ouchterlony test)	Serum	Turkeys (Beltsville White) and chicken (Light Sussex cockerels)	Homogenate of cecum and liver tissues harvested from an infected turkey or ceca contents of an infected chicken	1963 (42)
Serum antibodies	IgG	Indirect immunofluorescence assay	Serum	Turkeys (breed BIG 6)	Virulent *H. meleagridis* (strain mdc), and a lysed (by sonication) preparation of the same strain	2009 (43)
Serum antibodies	IgG	indirect sandwich ELISA	Serum	Turkeys and chickens	Virulent *H. meleagridis*Turkey/Austria/2922-C6/04 or the same clones passaged for 95, 215 or 295 times	2009 (44)
Chemokine and cytokine mRNA	IL-1β, IL-6, CXCLi2, IL-10, TGF-β4, IFN-γ, IL-4, and IL-13	RT-qPCR	Cecal tonsil, liver and spleen	Turkeys and chickens (broilers and breeder cockerels)	A suspension of severely affected cecum and liver tissue homogenate harvested from chickens orally inoculated with embryonated eggs of *H. gallinarum*	2009 (45)
β-defensin mRNA	AvBD2		Cecal tonsil and liver			
Immune cells	$CD4^+$, $CD8\alpha^+$, $CD28^+$ and $CD44^+$ cells	Immunohistochemistry	Liver and spleen			
Serum & mucosal antibodies	IgA, IgG, IgM	Indirect sandwich ELISA	Serum, duodenum, jejunum & cecum	Chickens	Clonal cultures of virulent (passaged for 21 times) *H. meleagridis* / Turkey/Austria/2922-C6/04	2010 (46)
Serum antibodies	IgG	Blocking ELISA	Serum	Turkeys (BUT 6) and chickens (Isa Brown layers)	A Dutch field strain (strain /Deventer/NL/AL327-type I/03)	2010 (47)
Serum antibodies	IgG	Indirect sandwich ELISA	Serum	Turkeys (BUT 9)	Clonal cultures of virulent (passaged for 21 times) and/or attenuated (passaged for 295 times) *H. meleagridis* / Turkey/Austria/2922-C6/04	2010 (48)
Serum antibodies	IgG	Indirect sandwich ELISA	Serum	Chickens (layer type)	Clonal cultures of virulent (passaged for 21 times) and/or attenuated (passaged for 295 times) *H. meleagridis* / Turkey/Austria/2922-C6/04	2013 (49)
Serum antibodies	IgG	indirect sandwich ELISA	Serum	Turkeys	Clonal cultures of attenuated (passaged for 295) *H. meleagridis* / Turkey/Austria/2922-C6/04 or the same strain back passaged *in vivo*	2013 (50)
Serum antibodies	IgG	Indirect sandwich ELISA	Serum	Chickens (layer and meat-type)	*H. meleagridis* strain Turkey/Germany/GB551/04 from an outbreak in a commercial meat turkey flock in Germany	2014 (51)
Immune cells	$CD4^+$, $CD8\alpha^+$, B cells, heterophils, macrophages	Flow cytometry	cecum, liver, spleen, PBMC	Turkeys and chickens	Clonal cultures of virulent (passaged for 21 times) and/or attenuated (passaged for 295 times) *H. meleagridis*/Turkey/Austria/2922-C6/04	2017 (52)
	Heterophils, macrophages		Whole blood	Chickens		
Immune cells	T cells, B cells and monocytes/macrophages	Immunofluorescence	Cecum, liver, and spleen	Chickens	Clonal cultures of virulent (passaged for 21 times) and/or attenuated (passaged for 295 times) *H. meleagridis* / Turkey/Austria/2922-C6/04	2018 (53)
Type1/type2 signature cytokines	IFN-γ or IL-13 mRNA positive cells	*In situ* hybridization		Turkeys and chickens		

markers against chicken macrophages/monocytes revealed that significantly higher amounts of this cell population were present in the blood (52) and the cecum (53) of infected chickens from the early stage of infection until the time period when most severe lesions were observed. The ability of macrophages to incorporate cells by phagocytosis indicates efforts to contain the parasite during the initial stage of infection in chickens. Furthermore, a lower presence of heterophils in the infected chickens' blood can be explained by the infiltration of these granulocytes to the local site of infection (52). Due to the lack of specific or cross-reactive antibodies for innate immune cells of turkeys it was so far not possible to generate comparative data in this more affected host species.

To investigate the innate cell signaling following infection, mRNA expression of the pro-inflammatory innate cytokines IL-1beta, IL-6, and CXCLi2 were measured in chickens and in turkeys after infection with histomonads (45). It was found that the immune response in the chicken was initiated in the cecal tonsils already after 1 day p.i. Interestingly, mRNA expression levels of these pro-inflammatory cytokines in turkeys were not up-regulated locally during the initial phase of infection even until the protozoa were already detectable in the liver. This depicts that an initial induced innate inflammatory response in the cecal tonsils may be critical to limit the dissemination of the parasite to the liver, with consequences on the clinical outcome within the different poultry species.

Adaptive Immune Response

Pathogen-Specific Antibodies

The first study on specific antibodies against *H. meleagridis* was reported by Clarkson (42), who detected serum precipitins 7 days after infection. The attempt to transfer protective immunity by injections of serum from infected turkeys to naïve birds failed in the last mentioned study. Several years later, Powell et al. (45), observed increased antibody levels in sera of infected chickens compared to infected turkeys, but no further information on the methodology was given. More recently, vaccination against histomonosis using killed vaccines which elicit a dominantly antibody-mediated immune response was shown to be ineffective in providing protection (60). Similarly, Bleyen et al. (43) confirmed the inadequacy of serum antibodies in protecting turkeys from histomonosis, although the same immune component was shown to induce complement-mediated lysis of *H. meleagridis in vitro*. In recent years, an indirect sandwich ELISA (44), as well as a blocking ELISA using monoclonal antibodies (47) for the detection of antibodies against histomonads have been established. In these studies, an increase of antibodies in sera could be demonstrated in experimentally infected chickens and turkeys. Field studies on the prevalence of histomonads-specific antibodies in chicken flocks revealed a wide dissemination of the parasite in European countries (61, 62). In experimental studies, it was demonstrated that pathogen-specific serum antibodies increased already 2 weeks p.i. (44) and 3 weeks post vaccination with attenuated parasites above the cut off value until the following 13 weeks when the experiment was finished (48).

In a single study, the occurrence of different types of systemic and intestinal antibodies of chickens following infection with *H. meleagridis* was investigated by ELISA (46). Thereby, first optical density values for IgG above the cut-off in the serum were detected at 14 days p.i., whereas IgA and IgM levels remained low. Furthermore, it could be revealed that the intestinal tissue showed an intense humoral response in the parasitized ceca with an initial peak of IgM, high levels of IgG as well as a continuous increase of IgA and similar high levels of IgG together with IgA in the small intestine. Unfortunately, comparative results to the last mentioned studies in turkeys are not available which might be due to the lack of suitable reagents. However, along with an elevated level of antibodies the numbers of B cells increased in infected organs and systemically during infection were also reported recently in chickens and turkeys (52), which is outlined in the following chapter.

Another study, involving different lines of chickens, reported that antibody production differ due to the genetic background of the host (51). The study reported that the humoral immune response against actinin 1 started sooner and was significantly more pronounced in layer-type chickens than in meat-type chickens.

Cell-Mediated Immune Response

First investigations on leukocytes were based on histopathology and indicated an influx of different populations of immune cells including lymphocytes in the infected organs cecum and liver (57). However, until recently there was no detailed information on the phenotype of immune cells that are involved in an adapted immune response and the link with the appearance following infection. In the last few years different studies were performed to investigate the mechanisms of the cellular modulation by detailed characterization of the involved leukocytes as well as cytokines triggering specific changes in the cellular response.

In general, the polarization of $CD4^+$ T-helper (Th) and $CD8^+$ T-cytotoxic (Tc) cells plays a major role in host-pathogen interaction. $CD3^+CD4^+CD8\alpha^-$ T cells are predominantly of helper phenotype, act as coordinators of the immune response by producing a variety of cytokines and secrete soluble molecules to the extracellular space which affects other cells of the immune system. In contrast, $CD3^+CD4^-CD8\alpha^+$ T cells are cytotoxic cells, promoting the cytolytic pathway. A protective immune response may rely on the ability of $CD4^+$ T cells to accumulate high numbers of effector cells in order to activate a response against an invading pathogen. They can promote B cell-immunity with antibody production or, on the opposite, directly modulate, respectively control, the activity of different types of T cells. Secreted cytokines can activate macrophages and other cells through cell to cell signal communication. Powell et al. (45) used immunohistochemical stainings to specifically detect $CD4^+$, $CD8\alpha^+$, $CD28^+$, and $CD44^+$ cells in the spleen as well as liver of chickens and turkeys infected with *H. meleagridis*. With this, they noticed an influx of the mentioned T cell-subpopulations into the liver of turkeys and chickens in coincidence with parasite infiltration. These cellular changes were more pronounced in turkeys and correlated with a decrease in numbers of such cells in

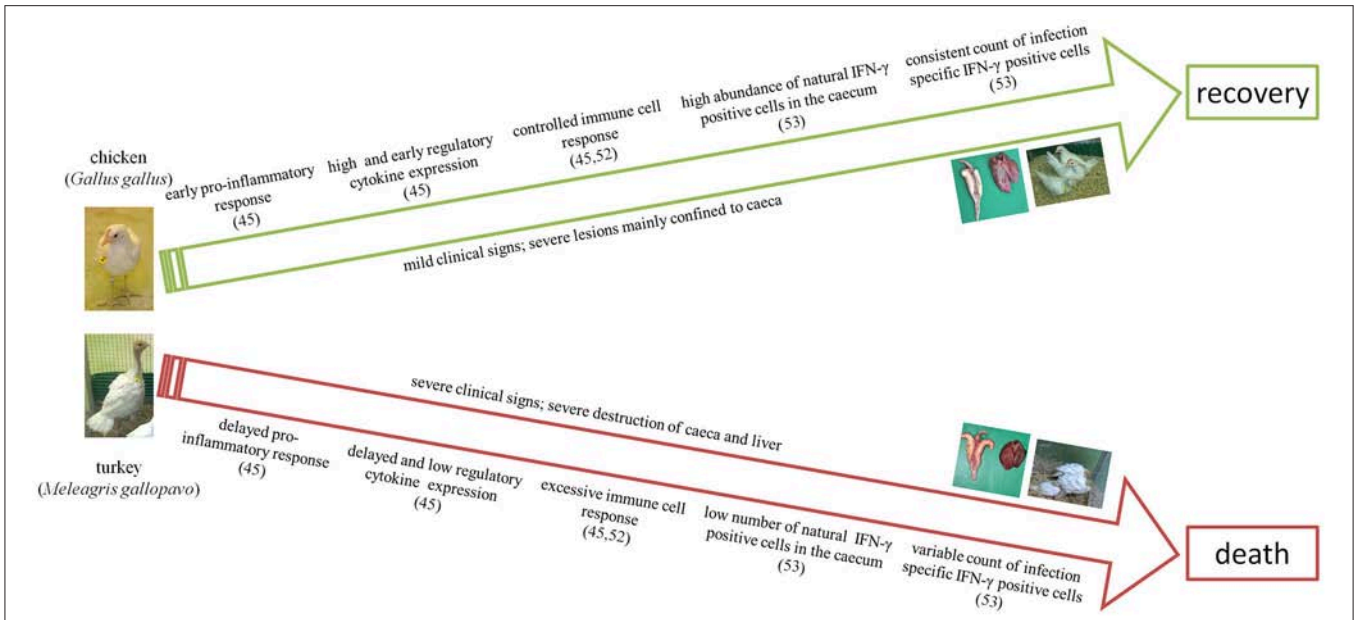

FIGURE 1 | Key differences in the disease and immune response of the two main avian host species during infection with *H. meleagridis*. The numbers refer to the respective references.

spleens whereas no obvious changes were observed in the spleen of chickens.

By investigating T-cell subsets of chickens co-infected with *H. gallinarum* and *H. meleagridis*, a decrease of splenic $CD4^+$ T cells together with a destruction of the cecal mucosa in association with a severe T cell infiltration in the cecal lamina propria was described (63).

In a more recent work, different populations of lymphocytes of host birds were analyzed by flow cytometry after vaccination with attenuated histomonads and/or infection using virulent parasites (52). Thereby, a detailed investigation on the adaptive immune system by investigating quantitative changes of $CD4^+$, $CD8\alpha^+$ T cells and B cells in different organs and blood of turkeys and chickens was performed. In that study, all infected turkeys died by 14 days p.i. due to severe histomonosis whereas infected chickens or vaccinated birds were not clinically affected. It was hypothesized that the excessive necrosis of caecum and liver in infected tissues of turkeys might be an effect of cytotoxic activity of effector $CD8^+$ T cells which still needs to be verified. The predominance of $CD8\alpha^+$ T cells might contribute to the destruction of the host tissue and the local suppression of other immune responses including the inhibition of $CD4^+$ T-cell proliferation (52). This is supported by the finding that $CD4^+$ T cells were significantly decreased in the cecum of infected turkeys. On the other hand, the challenge of vaccinated turkeys led to a significant increase of $CD4^+$, $CD8\alpha^+$, and B cells in the blood already at 4 days post inoculation, indicating an effective and fast recall response of the primed immune system. In infected chickens the analyzed immune cells in cecum and liver were mostly in the range of values of non-infected birds matching with the lower lesion scores. However, a continuing recruitment of $CD4^+$ and $CD8\alpha^+$ T cells was observed in the blood of infected chickens. Beside the translocation of these cells to the target organs of infection, this finding might also be explained by the presence of the parasite in the blood of infected host birds (14, 64, 65). In vaccinated as well as vaccinated and challenged chickens, changes of cecal B cells, $CD4^+$ and $CD8\alpha^+$ T cells were in general even lower compared to infected chickens (52). Overall, such findings demonstrated that vaccination of turkeys and chickens using clonal cultures of *H. meleagridis* limits severe changes of B cells and T cell-subsets as compared to the exacerbated influx observed in non-protected animals. Additionally, a more intense cellular immune response in infected organs of turkeys in comparison to chickens was concluded to contribute to the fatal clinical outcome of the infection in turkeys.

Immunofluorescence and quantification of lymphocyte populations by image analyses, confirmed an influx of B cells and T cells in the infected chicken's cecum from 4 days p.i. until 10 days p.i. (53). In contrast, chickens that were vaccinated showed a similar range of the above mentioned cell population in the cecum compared to control birds even after challenge. Comparative data on turkey ceca obtained by immunofluorescence have so far not been reported due to the lack of cross-reactivity of those antibodies for this host species (52).

Investigations on cytokines in context of an immune response against *H. meleagridis* were performed in different studies by gene expression analyses and *in situ* hybridization for the detection of cells that contain transcripts of specific cytokines. Along with innate pro-inflammatory cytokines mentioned above, Powell et al. (45) investigated adaptive response-signature cytokines IFN-γ, IL-13, and IL-4 and the regulatory cytokines IL-10 and

TGF-β4 by RT-qPCR in different organs of infected chickens and turkeys. Most important, in chickens, IFN-γ and IL-13 mRNA expression was up-regulated while IL-4 mRNA expression remained unaltered during infection. Expression of the regulatory cytokine IL-10 was up-regulated very early during infection in this host species while TGF-β4 mRNA expression levels were unchanged during the experiment. In turkeys, IFN-γ mRNA expression levels were down-regulated in the cecal tonsils soon after infection but up-regulated during later stages. IL-4 mRNA expression levels were variable while IL-13 again showed a sustained up-regulation. As in chickens, IL-10 did not appear to play a significant role during infection in turkeys, but TGF-β4 mRNA expression levels were increased.

Later on, Schwarz et al. (63) found a significant increase in mRNA expression of IFN-γ in chicken cecal tissue infected with *H. gallinarum* harboring histomonads in contrast to an elevated expression of IL-13 when chickens were infected only with *H. gallinarum*. The authors hypothesized that the IFN-γ over-expression in the co-infection was modulated by the presence of *H. meleagridis*. Nevertheless, based on the experimental setting it is difficult to determine if both parasites together cause a variant immune response.

Recently, Kidane et al. (53) investigated the abundance of Th1 and Th2 cytokines, IFN-γ, respectively IL-13 mRNA positive cells by *in situ* hybridization in vaccinated and/or infected chickens and turkeys. It was demonstrated that changes in the abundance of positive cells following infection or vaccination were less pronounced in chickens compared to turkeys. Infected turkeys showed an early decrease of cytokine mRNA positive cells in cecum which later increased together with a severe destruction of the mucosa and infiltration of cytokine expressing cells up to the muscularis layer. A similar destruction and cytokine distribution was observed in the liver of these birds. In comparison, an increased percentage of IFN-γ mRNA positive cells were noticed in vaccinated and challenged turkeys already 4 days post challenge confirming the priming of an immune response by vaccination. An interesting finding was that IFN-γ mRNA positive cells in the cecum of naïve chickens were distinctly higher than in naïve turkeys. These findings led to the conclusion that IFN-γ positive cells may act as a protective trait against histomonosis. However, no distinct Th1/Th2 separation in the immune response was noticed, indicating a more balanced activation of the Th pathways during infection with an extracellular protozoan parasite in birds. Moreover, it could be demonstrated that the fatal clinical outcome of turkeys due to histomonosis is in coherence with a more intense adaptive immune response in infected organs compared to chickens.

CONCLUSION AND OUTLOOK

The reviewed studies are fundamental in devising prospective immunoprophylactic strategies against histomonosis. Results on different types of vaccine either killed or live, revealed a possible direction into how a vaccine could successfully mount a protective immune response. Furthermore, it is crucial to understand relevant protective traits as well as the failure of the immune system against an infection with *H. meleagridis*.

The most peculiar and differing changes in the immune response in chickens and turkeys against histomonosis are drafted in **Figure 1**. From the experimental studies on the immune response during histomonosis we can clearly elicited that differing profiles of cytokine expression and abundances of specific immune cells resulted in a varying disease progression and outcome in the two main avian host species, chickens and turkeys. At the early infection phase chickens show an expeditious immune response against the parasite which triggers the immune cascade to restrict the parasite progression. In comparison, the turkey's immune responsiveness is delayed, which obviously allows the parasite to disseminate systematically to the liver and other organs. After the initial phase, the effectiveness of the adaptive immune response is based on the accessibility of natural IFN-γ positive cells and a controlled expression of adaptive immune cells which seem to be further key factors to minimize clinical signs and to induce the recovery of chickens. In contrast, a predominance of the cellular response toward the cytolytic pathway may be involved in aggravating tissue destruction in turkeys. Thus, un-controlled immune response and excessive destruction of the tissue can be understood as a further failure of the immune system with consequences on the fatal outcome of the disease in turkeys. Conclusions on the different immune response in chickens and turkeys are supported by the fact that vaccination triggered a similar enhanced allocation of IFN-γ cells and controlled adaptive cell response for both host species. Overall, it can be concluded that an early and locally induced immune response is the crucial factor behind the survival of chickens and immunoprophylaxis induced by vaccination independent of the host.

Further studies on the immune response of poultry against *Histomonas meleagridis* should consider both host and pathogen factors. Given the fact that turkeys and chickens display a different involvement of the immune response to *H. meleagridis*, it could be beneficial to use these contrasting host features in further exploring traits of the immune response. So far, there is hardly any information on the innate immune response against histomonosis. Especially the role of toll-like receptors (TLRs), with possible consequences on modulation of the immune response following vaccination and/or infection, needs to be understood. Furthermore, mechanisms on the function of innate immunity, particularly pro-inflammatory cytokines and antigen-presenting cells, could be useful to link the transition from the innate to the adaptive stage of the immune response. This can unveil essential features such as the quality and persistence of the acquired immune response which is helpful in establishing vaccination schedules. Data collected in experimental studies investigating histomonosis or following vaccination against the disease revealed important changes in the immune response but further identification on pathogen-specific mechanisms would be valuable. Hence, determining specific immunological correlates of protection e.g., the role and function of pathogen-specific T cells would

contribute in pin-pointing features that mediate protection. Consequently, unraveling selective mechanisms that induce protection would be useful to promote such effector functions for facilitating new prospects in research on vaccination against histomonosis. Finally, along with studies on screening virulence factors of the protozoa, further explorations on the molecular plethora for potential immunogenic components are necessary to explain pathogen-directed immune reactions of the host.

AUTHOR CONTRIBUTIONS

TM, FK, MH, and DL conceived and designed the review. All authors read and approved the final manuscript.

REFERENCES

1. Smith T. An infectious disease among turkeys caused by protozoa (infectious entero-hepatitis). *USDA Bur Anim Ind Bull.* (1895) 8:3–27.
2. Hess M. Commensal or pathogen—A challenge to fulfil Koch's Postulates. *Br Poult Sci.* (2017) 58:1–12. doi: 10.1080/00071668.2016.1245849
3. McDougald LR. Blackhead disease (histomoniasis) in poultry: a critical review. *Avian Dis.* (2005) 49:462–76. doi: 10.1637/7420-081005R.1
4. Hess M, Liebhart D, Bilic I, Ganas P. *Histomonas meleagridis*—New insights into an old pathogen. *Vet Parasitol.* (2015) 208:67–76. doi: 10.1016/j.vetpar.2014.12.018
5. Hauck R, Hafez HM. Experimental infections with the protozoan parasite *Histomonas meleagridis*: a review. *Parasitol Res.* (2013) 112:19–34. doi: 10.1007/s00436-012-3190-5
6. Liebhart D, Ganas P, Sulejmanovic T, Hess M. Histomonosis in poultry: previous and current strategies for prevention and therapy. *Avian Pathol.* (2017) 46:1–18. doi: 10.1080/03079457.2016.1229458
7. Clark S, Kimminau E. Critical review: future control of blackhead disease (histomoniasis) in poultry. *Avian Dis.* (2017) 61:281–8. doi: 10.1637/11593-012517-ReviewR
8. Cushman S. *The Production of Turkeys*. Kingston, RI: Bulletin 25, Agricultural Experiment Station, Rhode Island College of Agriculture and Mechanical Arts (1893). 89–123.
9. Graybill HW, Smith T. Production of fatal blackhead in turkeys by feeding embryonated eggs of *Heterakis papillosa*. *J Exp Med.* (1920) 31:647–55. doi: 10.1084/jem.31.5.647
10. Hu J, Fuller L, McDougald LR. Infection of turkeys with *Histomonas meleagridis* by the cloacal drop method. *Avian Dis.* (2004) 48:746–50. doi: 10.1637/7152
11. Liebhart D, Hess M. Oral infection of turkeys with *in vitro*-cultured *Histomonas meleagridis* results in high mortality. *Avian Pathol.* (2009) 38:223–7. doi: 10.1080/03079450902912192
12. Huber K, Reynaud M-C, Callait MP, Zenner L. *Histomonas meleagridis* in turkeys: dissemination kinetics in host tissues after cloacal infection. *Poult Sci.* (2006) 85:1008–14. doi: 10.1093/ps/85.6.1008
13. Malewitz TD. The pathology of experimentally produced histomoniasis in turkeys. *Am J Vet Res.* (1958) 19:181–5.
14. McGuire WC, Morehouse NF. Blood-induced blackhead. *J Parasitol.* (1958) 44:292–6.
15. Peardon DL, Ware JE. Atypical foci of histomoniasis lesions in a study of direct oral transmission. *Avian Dis.* (1969) 13:340–4. doi: 10.2307/1588502
16. Potts GR. Long-term changes in the prevalences of caecal nematodes and histomonosis in gamebirds in the UK and the interaction with poultry. *Vet Rec.* (2009) 164:715–8. doi: 10.1136/vr.164.23.715
17. Reis Jr JL, Beckstead RB, Brown CC, Gerhold RW. *Histomonas meleagridis* and capillarid infection in a captive chukar (*Alectoris chukar*). *Avian Dis.* (2009) 53:637–9. doi: 10.1637/8678-030409-Case.1
18. McDougald LR, Abraham M, Beckstead RB. An outbreak of blackhead disease (*Histomonas meleagridis*) in farm-reared bobwhite quail (*Colinus virginianus*). *Avian Dis.* (2012) 56:754–6. doi: 10.1637/10140-032212-Case.1
19. Liebhart D, Neale S, Garcia-Rueda C, Wood AM, Bilic I, Wernsdorf P, et al. A single strain of *Tetratrichomonas gallinarum* causes fatal typhlohepatitis in red-legged partridges (*Alectoris rufa*) to be distinguished from histomonosis. *Avian Pathol.* (2014) 43:473–80. doi: 10.1080/03079457.2014.959435
20. Gordo FP, Herrera S, Castro AT, Durán BG, Diaz RAM. Parasites from farmed ostriches (*Struthio camelus*) and rheas (*Rhea americana*) in Europe. *Vet Parasitol.* (2002) 107:137–60. doi: 10.1016/S0304-4017(02)00104-8
21. Callait-Cardinal MP, Chauve C, Reynaud MC, Alogninouwa T, Zenner L. Infectivity of *Histomonas meleagridis* in ducks. *Avian Pathol.* (2006) 35:109–16. doi: 10.1080/03079450600597626
22. Cepicka I, Hampl V, Kulda J. Critical taxonomic revision of parabasalids with description of one new genus and three new species. *Protist* (2010) 161:400–33. doi: 10.1016/j.protis.2009.11.005
23. Tyzzer EE. Developmental phases of the protozoon of "Blackhead" in turkeys. *J Med Res.* (1919) 40:1–30.
24. Tyzzer EE. The flagellate character and reclassification of the parasite producing "Blackhead" in turkeys: *Histomonas* (gen. nov.) *meleagridis* (Smith). *J Parasitol.* (1920) 6:124–31. doi: 10.2307/3271065
25. Honigberg BM, Benett CJ. Lightmicroscopic observations on structure and division of *Histomonas meleagridis* (Smith). *J Eukaryot Microbiol.* (1971) 18:687–97.
26. Bishop A. Histomonas meleagridis in domestic fowls (*Gallus gallus*). Cultivation and experimental infection. *Parasitology* (1938) 30:181–94. doi: 10.1017/S0031182000025749
27. Zaragatzki E, Hess M, Grabensteiner E, Abdel-Ghaffar F, Al-Rasheid KAS, Mehlhorn H. Light and transmission electron microscopic studies on the encystation of *Histomonas meleagridis*. *Parasitol Res.* (2010) 106:977–83. doi: 10.1007/s00436-010-1777-2
28. Gruber J, Ganas P, Hess M. Long-term *in vitro* cultivation of *Histomonas meleagridis* coincides with the dominance of a very distinct phenotype of the parasite exhibiting increased tenacity and improved cell yields. *Parasitology* (2017) 144:1253–63. doi: 10.1017/S0031182017000646
29. Dwyer DM. Analysis of the antigenic relationships among *Trichomonas, Histomonas, Dientamoeba*, and *Entamoeba*. I. Quantitative fluorescent antibody methods. *J Eukaryot Microbiol.* (1972) 19:316–25. doi: 10.1111/j.1550-7408.1972.tb03467.x
30. Stark D, Barratt J, Chan D, Ellis JT. *Dientamoeba fragilis*, the neglected trichomonad of the human bowel. *Clin Microbiol.* (2016) 29(3):553–80. doi: 10.1128/CMR.00076-15
31. Dwyer DM, Honigberg BM. Immunologic analysis by quantitative fluorescent antibody methods of effects of prolonged cultivation on *Histomonas meleagridis* (Smith). *Z Parasitenkd* (1972) 39:39–52.
32. Dwyer DM. Analysis of the antigenic relationships among *Trichomonas, Histomonas, Dientamoeba*, and *Entamoeba*. II. Gel diffusion methods. *J Eukaryot Microbiol.* (1972) 19:326–32. doi: 10.1111/j.1550-7408.1972.tb03468.x
33. Dwyer DM. Analysis of the antigenic relationships among *Trichomonas, Histomonas, Dientamoeba*, and *Entamoeba* III. immunoelectrophoresis technics. *J Eukaryot Microbiol.* (1974) 21:139–45. doi: 10.1111/j.1550-7408.1974.tb03628.x
34. Gerbod D, Edgcomb VP, Noël C, Zenner L, Wintjens R, Delgado-Viscogliosi P, et al. Phylogenetic position of the trichomonad parasite of turkeys, *Histomonas meleagridis* (smith) tyzzer, inferred from small subunit rRNA sequence1. *J Eukaryot Microbiol.* (2005) 48:498–504. doi: 10.1111/j.1550-7408.2001.tb00185.x
35. Mazet M, Diogon M, Alderete JF, Vivares CP, Delbac F. First molecular characterisation of hydrogenosomes in the protozoan parasite *Histomonas meleagridis*. *Int J Parasitol.* (2008) 38:177–90. doi: 10.1016/j.ijpara.2007.06.006

36. Bilic I, Leberl M, Hess M. Identification and molecular characterization of numerous *Histomonas meleagridis* proteins using a cDNA library. *Parasitology* (2009) 136:379–91. doi: 10.1017/S0031182008005477
37. Leberl M, Hess M, Bilic I. *Histomonas meleagridis* possesses three alpha-actinins immunogenic to its hosts. *Mol Biochem Parasitol.* (2010) 169:101–7. doi: 10.1016/j.molbiopara.2009.10.007
38. Lynn EC, Beckstead RB. Identification of gene expression elements in *Histomonas meleagridis* using splinkerette PCR, a variation of ligated adaptor PCR. *J Parasitol.* (2012) 98:135–41. doi: 10.1645/GE-2916.1
39. Klodnicki ME, McDougald LR, Beckstead RB. A genomic analysis of *Histomonas meleagridis* through sequencing of a cDNA library. *J Parasitol.* (2013) 99:264–9. doi: 10.1645/GE-3256.1
40. Mazumdar R, Endler L, Monoyios A, Hess M, Bilic I. Establishment of a *de novo* reference transcriptome of *Histomonas meleagridis* reveals basic insights about biological functions and potential pathogenic mechanisms of the parasite. *Protist* (2017) 168:663–85. doi: 10.1016/j.protis.2017.09.004
41. Monoyios A, Patzl M, Schlosser S, Hess M, Bilic I. Unravelling the differences: comparative proteomic analysis of a clonal virulent and an attenuated *Histomonas meleagridis* strain. *Int J Parasitol.* (2018) 48:145–57. doi: 10.1016/j.ijpara.2017.08.017
42. Clarkson MJ. Immunological responses to *Histomonas meleagridis* in the turkey and fowl. *Immunology* (1963) 6:156–68.
43. Bleyen N, Ons E, De Gussem M, Goddeeris BM. Passive immunization against *Histomonas meleagridis* does not protect turkeys from an experimental infection. *Avian Pathol.* (2009) 38:71–6. doi: 10.1080/03079450802641255
44. Windisch M, Hess M. Establishing an indirect sandwich enzyme-linked-immunosorbent-assay (ELISA) for the detection of antibodies against *Histomonas meleagridis* from experimentally infected specific pathogen-free chickens and turkeys. *Vet Parasitol.* (2009) 161:25–30. doi: 10.1016/j.vetpar.2008.12.014
45. Powell FL, Rothwell L, Clarkson MJ, Kaiser P. The turkey, compared to the chicken, fails to mount an effective early immune response to *Histomonas meleagridis* in the gut. *Parasite Immunol.* (2009) 31:312–27. doi: 10.1111/j.1365-3024.2009.01113.x
46. Windisch M, Hess M. Experimental infection of chickens with *Histomonas meleagridis* confirms the presence of antibodies in different parts of the intestine. *Parasite Immunol.* (2010) 32:29–35. doi: 10.1111/j.1365-3024.2009.01159.x
47. van der Heijden HMJF, Stegeman A, Landman WJM. Development of a blocking-ELISA for the detection of antibodies against *Histomonas meleagridis* in chickens and turkeys. *Vet Parasitol.* (2010) 171:216–22. doi: 10.1016/j.vetpar.2010.03.028
48. Liebhart D, Windisch M, Hess M. Oral vaccination of 1-day-old turkeys with *in vitro* attenuated *Histomonas meleagridis* protects against histomonosis and has no negative effect on performance. *Avian Pathol.* (2010) 39:399–403. doi: 10.1080/03079457.2010.506906
49. Liebhart D, Sulejmanovic T, Grafl B, Tichy A, Hess M. Vaccination against histomonosis prevents a drop in egg production in layers following challenge. *Avian Pathol.* (2013) 42:79–84. doi: 10.1080/03079457.2012.760841
50. Sulejmanovic T, Liebhart D, Hess M. *In vitro* attenuated *Histomonas meleagridis* does not revert to virulence, following serial *in vivo* passages in turkeys or chickens. *Vaccine* (2013) 31:5443–50. doi: 10.1016/j.vaccine.2013.08.098
51. Lotfi A, Hauck R, Olias P, Hafez HM. Pathogenesis of histomonosis in experimentally infected specific-pathogen-free (SPF) layer-type chickens and SPF meat-type chickens. *Avian Dis.* (2014) 58:427–32. doi: 10.1637/10782-012814-Reg.1
52. Mitra T, Gerner W, Kidane FA, Wernsdorf P, Hess M, Saalmüller A, et al. Vaccination against histomonosis limits pronounced changes of B cells and T-cell subsets in turkeys and chickens. *Vaccine* (2017) 35:4184–96. doi: 10.1016/j.vaccine.2017.06.035
53. Kidane FA, Mitra T, Wernsdorf P, Hess M, Liebhart D. Allocation of interferon (IFN)-gamma mRNA positive cells in caecum hallmarks a protective trait against histomonosis. *Front Immunol.* (2018) 9:1164. doi: 10.3389/fimmu.2018.01164
54. Farmer RK, Stephenson J. Infectious enterohepatitis (blackhead) in turkeys; a comparative study of methods of infection. *J Comp Pathol Ther.* (1949) 59:119–26.
55. Horton-Smith C, Long PL. Studies in histomoniasis: I. The infection of chickens (*Gallus gallus*) with histomonad suspensions. *Parasitology* (1956) 46:79–90. doi: 10.1017/S0031182000026354
56. Lund EE. Oral transmission of Histomonas in turkeys. *Poult Sci.* (1956) 35:900–4.
57. Tyzzer EE. A study of immunity produced by infection with attenuated culture-strains of *Histomonas meleagridis*. *J Comp Pathol Ther.* (1936) 49:285–303. doi: 10.1016/S0368-1742(36)80025-3
58. Liebhart D, Grabensteiner E, Hess M. A virulent mono-eukaryotic culture of *Histomonas meleagridis* is capable of inducing fatal histomonosis in different aged turkeys of both sexes, regardless of the infective dose. *Avian Dis.* (2008) 52:168–72. doi: 10.1637/8107-090707-ResNote
59. Singh A, Weissenböck H, Hess M. *Histomonas meleagridis*: immunohistochemical localization of parasitic cells in formalin-fixed, paraffin-embedded tissue sections of experimentally infected turkeys demonstrates the wide spread of the parasite in its host. *Exp Parasitol.* (2008) 118:505–13. doi: 10.1016/j.exppara.2007.11.004
60. Hess M, Liebhart D, Grabensteiner E, Singh A. Cloned *Histomonas meleagridis* passaged *in vitro* resulted in reduced pathogenicity and is capable of protecting turkeys from histomonosis. *Vaccine* (2008) 26:4187–93. doi: 10.1016/j.vaccine.2008.05.071
61. Grafl B, Liebhart D, Windisch M, Ibesich C, Hess M. Seroprevalence of *Histomonas meleagridis* in pullets and laying hens determined by ELISA. *Vet Rec.* (2011) 168:160. doi: 10.1136/vr.c6479
62. van der Heijden HMJF, Landman WJM. High seroprevalence of *Histomonas meleagridis* in Dutch layer chickens. *Avian Dis.* (2011) 55:324–7. doi: 10.1637/9609-120610-ResNote.1
63. Schwarz A, Gauly M, Abel H, Daş G, Humburg J, Weiss ATA, et al. Pathobiology of *Heterakis gallinarum* mono-infection and co-infection with *Histomonas meleagridis* in layer chickens. *Avian Pathol.* (2011) 40:277–87. doi: 10.1080/03079457.2011.561280
64. Clarkson MJ. The progressive pathology of Heterakis-produced histomoniasis in turkeys. *Res Vet Sci.* (1962) 3:443–8.
65. Farmer RK, Hughes DL, Whiting G. Infectious enterohepatitis (blackhead) in turkeys: a study of the pathology of the artificially induced disease. *J Comp Pathol Ther.* (1951) 61:251–62. doi: 10.1016/S0368-1742(51)80025-0

Conflict of Interest Statement: The authors declare that the research was conducted in the absence of any commercial or financial relationships that could be construed as a potential conflict of interest.

frontiers in Immunology

REVIEW
published: 14 December 2018
doi: 10.3389/fimmu.2018.02961

To B or Not to B: Understanding B Cell Responses in the Development of Malaria Infection

Eduardo L. V. Silveira, Mariana R. Dominguez and Irene S. Soares*

Department of Clinical and Toxicological Analyses, School of Pharmaceutical Sciences, University of São Paulo, São Paulo, Brazil

Malaria is a widespread disease caused mainly by the *Plasmodium falciparum* (Pf) and *Plasmodium vivax* (Pv) protozoan parasites. Depending on the parasite responsible for the infection, high morbidity and mortality can be triggered. To escape the host immune responses, *Plasmodium* parasites disturb the functionality of B cell subsets among other cell types. However, some antibodies elicited during a malaria infection have the potential to block pathogen invasion and dissemination into the host. Thus, the question remains, why is protection not developed and maintained after the primary parasite exposure? In this review, we discuss different aspects of B cell responses against *Plasmodium* antigens during malaria infection. Since most studies have focused on the quantification of serum antibody titers, those B cell responses have not been fully characterized. However, to secrete antibodies, a complex cellular response is set up, including not only the activation and differentiation of B cells into antibody-secreting cells, but also the participation of other cell subsets in the germinal center reactions. Therefore, a better understanding of how B cell subsets are stimulated during malaria infection will provide essential insights toward the design of potent interventions.

Keywords: B cell biology, malaria, antibodies, effective mechanism, protective immunity

OPEN ACCESS

Edited by:
Xun Suo,
China Agricultural University, China

Reviewed by:
Sunil Joshi,
Leonard M. Miller School of Medicine, United States
Britta Christina Urban,
Liverpool School of Tropical Medicine, United Kingdom

****Correspondence:***
Eduardo L. V. Silveira
eduardosilveira@usp.br

Specialty section:
This article was submitted to Microbial Immunology, a section of the journal Frontiers in Immunology

Received: *30 June 2018*
Accepted: *03 December 2018*
Published: *14 December 2018*

Citation:
Silveira ELV, Dominguez MR and Soares IS (2018) To B or Not to B: Understanding B Cell Responses in the Development of Malaria Infection. Front. Immunol. 9:2961. doi: 10.3389/fimmu.2018.02961

MALARIA INFECTION AND IMMUNITY

Malaria is a widespread disease mainly caused by the *Plasmodium falciparum* (Pf) and *Plasmodium vivax* (Pv) parasites in tropical countries. Currently, half of the world population lives in areas at risk of a malaria infection. In 2016, a global estimative enumerated 216 million clinical cases and 445,000 deaths associated with this disease (1), portraying the real magnitude of this public health problem. Most cases of malaria morbidity and mortality have been attributed to Pf infections, prevalent in sub-Saharan Africa and characterized by high parasitemias and severe complications, especially in children (2). Contrarily, Pv infections are more disseminated in American and Asian countries and induce lower parasitemia levels and milder symptoms. Rarely, Pv infections can elicit severe symptoms and kill like Pf infections (2–4).

Plasmodium parasites have a complex life cycle, with sporozoites transmitted from the *Anopheles* mosquito salivary glands to the human skin dermis during mosquito blood meals. These motile parasites cross layers of the skin and enter the bloodstream, reaching the liver within hours upon infection. Then, they invade the hepatocytes, replicating and differentiating into schizonts. In the case of a Pv infection, part of the sporozoites are transformed into dormant forms called hypnozoites, which can be activated even after a long term of parasite infection. As a result of

the hepatocyte burst, the merozoites are released in the bloodstream and invade the erythrocytes (Pf parasites) or the reticulocytes (Pv parasites), initiating the asexual blood stage of the cycle. These parasitic forms undergo several rounds of multiplication and differentiation, increasing the parasitemia levels in the host. Those forms found in infected red blood cells (iRBCs) have been identified as rings, trophozoites, schizonts, and gametocytes. Whereas the newly-released merozoites can keep re-invading the erythrocytes, a small fraction of them differentiate directly into gametocytes, giving rise to the sexual blood stage. Gametocytes are ingested during the mosquito blood meal and fuse to each other within the digestive tract, forming a zygote. The zygote differentiates into an ookinete, followed by oocyst forms, previously to the generation of infectious sporozoites that can be found in a mosquito's salivary glands (5, 6). Interestingly, the bone marrow has been described as the major parasite reservoir for early blood stage (asexual and sexual) and gametocytes in Pv infections (7, 8).

Regarding the mechanisms of immunity naturally induced by malaria, the humoral response has been described as the most important for the establishment of protection. This concept has been solidified after the finding that a passive transfer of serum samples from malaria-immune adults controlled the Pf parasitemia levels and ameliorated symptoms in acutely infected children (9). Although the elicitation of the humoral response is critical to reduce malaria morbidity and mortality, antibody-dependent protective immunity usually takes multiple parasitic exposures and may take even years to be established. The extensive genetic diversity of clinical Pf and Pv malaria episodes (10, 11) and the low frequency of malaria-specific memory B cells (MBCs) detected in residents of high endemic areas (12, 13) corroborate this statement. Considering that antibodies represent a snapshot of B cell responses at a single cell level (14), it is fundamental to understand how this cellular component is stimulated upon *Plasmodium* infection to improve vaccine formulations and consequently generate more effective antibodies against human malaria. In this review, we present the distinct aspects of B cell immunity derived from a malaria infection, ranging from the activation of naive B cells to the generation of antibody-secreting cells and the mechanisms of action by protective antibodies.

MALARIA-SPECIFIC B CELL RESPONSES

During malaria infection, thousands of parasitic antigens are expressed in each stage of the parasite life cycle (15). However, the anti-malarial humoral responses are preferentially headed to blood stage antigens rather than the liver counterparts. Besides the differences on the antigen density, a malaria murine model has shown that the blood stage of infection weakens the humoral immunity against the liver stage antigens through the modification of lymphoid structures and the expression of cytokines and chemokines (16). Overall, these responses are mainly characterized by the generation of the antibody-secreting cells (ASCs), memory B cells (MBCs), and antibody titers. Whereas, the MBCs and antibody titers have been found with steady levels for years in individuals living in low Pf and Pv malaria-endemic areas without the evidence of reinfection (17), these parameters are not sustained for longer periods, especially in younger individuals from high Pf-endemic areas (12, 13).

The question arises, disregarding the timing that antibodies can be detected in serum samples, how is their secretion triggered upon malaria infection? Usually, the antigen-specific antibodies are expected to be detected in the serum in <2 weeks upon any pathogen exposure. During this period, the naive B cells are activated upon B cell receptor (BCR) interaction with a parasitic antigen in the periphery, eliciting cell proliferation and differentiation into multiple subsets such as the MBCs, follicular B cells (FoBs), major players of the germinal center (GC) reactions, or marginal zone B cells (MZBs). Although all these B cell subsets express immunoglobulin (Ig) genes, only the ASCs secrete antibodies. Regarding FoBs, they form and maintain structures called the germinal centers (GCs) together with the follicular T helper cells (TFh), dendritic cells (FDCs), cytokines [IL-21, IL-6, and B cell activating factor (BAFF)], and the critical participation of co-stimulatory molecules (CD40L and ICOS). During the germinal center reactions, the GC B cells are activated and undergo several rounds of antigen selection, acquiring a mature status through the somatic hypermutations and class-switch in Ig genes. Thus, it prompts the production of high-affinity, class-switched antibodies. Models of human and murine malaria infections point to higher numbers of GC B cells and lower for MZB-like cells (18, 19). Terminal signaling triggered by activation guides the FoB cells to exit the follicles and differentiate into high-affinity, atypical, or classical MBCs (20) or short-lived, class-switched ASCs. However, there is evidence from a malaria murine model that high affinity, somatic hypermutated IgM+ MBCs dominate a recall response, being differentiated either into IgM+ or IgG+ ASCs and MBCs (21). The higher the frequency of the antigen-specific MBCs during that second encounter with the antigen, the higher will be the frequency of the antigen-specific ASCs generated. It is still controversial whether the unswitched or switched MBCs enter the GCs or form the ASCs: [reviewed by (22)]. Once generated, the ASCs migrate through circulation to the bone marrow or secondary lymphoid organs. More specifically, their physical contact with bone marrow stroma cells and the recognition of cytokines described above lead to modifications in their transcriptome profile, upregulating preferentially the expression of anti-apoptotic genes. This process culminates in their transformation from short-lived to long-lived ASCs, whose function results in the increased titers of serum antibodies (23).

On the other hand, malaria infection affects the generation of some critical cell subsets for humoral responses. Repeated parasitic exposures drive the expansion and accumulation of atypical MBCs in individuals from Pf malaria-endemic areas (24, 25). Although these cells have been mostly associated with the impaired B cell responses in this infection context, some groups have stated that atypical MBCs present a similar function as classical MBCs (26). Furthermore, this was demonstrated in an impaired GC response in a murine model of severe malaria due to the inhibition of TFh cell differentiation (27).

In addition, the murine conventional DCs presented lower BAFF expression, culminating in a reduced ASC number in the spleen (28). Noteworthily, the bone marrow ASCs have serious restrictions for sampling due to their location, being avoided in malaria clinical trials. This issue has impaired our complete understanding around the immune response triggered by malaria infection in humans.

ACTIVATION OF B CELLS

Similar to pathogenic infections such as *Trypanosoma cruzi* (the etiologic agent of Chagas disease) or HIV, malaria infection elicits the polyclonal activation of B cells. Among the major factors contributing to this condition are the parasite-specific antigens and cytokines. Consequently, malaria patients present hypergammaglobulinemia, i.e., the increased serologic IgG titers. Furthermore, asymptomatic individuals with high parasitemia usually display broader antibody responses than the asymptomatic individuals with low parasitemia or symptomatic individuals (29). Thus, the malarial parasite load derived from the acute phase of infection seems to drive the ASC response as described for HIV and SIV (30) and Silveira et al., manuscript in preparation. A primary parasite exposure elicits the activation and differentiation of naive B cells into *Plasmodium*-specific MBCs and ASCs. These antigen-specific MBCs, activated through engagement of BCR or Toll-like receptors (31), can also be differentiated into ASCs, enhancing the antibody secretion upon Pf infection (32–35). Alternatively, MBCs induced by *S. mansion* worms may cross-react with Pf antigens and become activated in an malarial-specific manner (36, 37). However, this humoral response does not reach enough concentration in the serum to provide protection. As already mentioned, the individuals from malaria-endemic areas develop an antibody-derived natural immunity only after multiple parasite exposures.

Among the several potential parasite antigens that could induce hypergammaglobulinemia under infection, the domain C1DR1a of EMP1 from a cloned strain (FCR3S1.2), a blood-stage antigen, has been identified in Pf (38). It remains elusive whether the same antigen derived from Pf isolates can also trigger hypergammaglobulinaemia. Interestingly, the domain C1DR1a of PfEMP1 preferentially promotes the MBC activation and proliferation (39). Another *Plasmodium* variant antigen (MSP-1) has been described to activate antigen-specific IgM+ MBCs as the earlier responders upon a malaria re-challenge in mice. Both IgM- and IgG-secreting cells can be generated from the differentiation of those IgM+ MBCs (21). It is still obscure whether the domain C1DR1a is capable of eliciting a similar response during malaria infection in humans. Considering that autoimmunity has been commonly detected during malaria infection as a result of hypergammaglobulinemia, molecular mimicking cannot be ruled out for parasite antigens. In fact, the serum samples of systemic lupus erythematosus (SLE) patients displayed the ability to recognize the Pf malarial antigens (40). Cardiolipin, histones, and DNA are among the auto-antigens usually targeted by the anti-*Plasmodium* antibodies (41).

Another important piece of the polyclonal B cell activation puzzle is related to the modifications in the cytokine profile during malaria infection. BAFF is known to support B cell differentiation into ASCs and potentially elicit hypergammaglobulinemia. Increased levels of this cytokine have been found in the plasma of volunteers upon the Pf challenge (42), in acute Pf-infected children (43), in pregnant women (44), and in Pv infection (45). Moreover, the IL-10 has shown increased levels detected upon the Pf or Pv infections (46) and can influence the serological BAFF levels (47).

B Cell Subsets

Strikingly, human and murine malaria infections strongly alter the composition of B cell subsets. A murine malaria model showed severe reductions in the bone marrow-derived B cell progenitor numbers (48). Alternately, the infection enhances the numbers of atypical hematopoietic stem and progenitor cells (HSPCs) in the murine spleen. Considering their potential to differentiate into B cells and generate the GC B cells, MBCs, and antigen-specific ASCs *in vivo* (49), the HSPCs could repopulate the immune cell repertoire by counteracting the deficiency in B cell progenitors. Besides progenitor B cells, the Pf and Pv infections also affect the frequency of the peripheral B cells. Whereas the kinetics of classical MBCs and ASCs seem paradoxical in infected individuals living in endemic or non-endemic areas, the transitional B cells (TBCs) and atypical MBCs consistently have shown increased numbers in the blood of all individuals (42, 50).

In terms of TBCs, their frequency has been directly correlated to high parasitemias and an impaired immunity to Pf infection (50). Interestingly, the BAFF receptor signaling has been connected to the control of the immature B cell differentiation to TBCs (51). Considering that BAFF levels are significantly higher during the acute phase of Pf and Pv malaria (43, 45), this cytokine could indeed stimulate a stronger TBC proliferation. Regarding the atypical MBCs in malaria, these cells have been mainly characterized as exhausted cells with a decreased capability to differentiate into ASCs and secrete antibodies (24, 25), as for HIV infection (52). However, the monoclonal antibodies cloned out from those cells majorly recognized the Pf-infected RBCs and neutralized Pf parasites. Furthermore, it has been speculated that their contribution for the neutralizing IgG titers would be similar to the classical MBCs (26). Although total atypical MBCs significantly expand upon Pf or Pv malaria infections, parasitic-specific atypical MBCs still present similar frequencies to classical counterparts (26). In terms of longevity, it remains undetermined whether atypical MBCs represent the majority of the malarial-specific MBCs detected years after parasite exposure in primed individuals without reinfection (17). In infected mice, malarial-specific atypical MBCs were recently associated to short-lived responses that were dependent on the presence of the parasite (53). It would be plausible that the atypical MBCs are high-affinity, somatic hypermutated MBCs in human malaria. Indeed, these cells have been described as the first cells to expand during a recall malaria challenge in mice (21) and both cell subsets

can differentiate into IgG+ ASCs, strongly related to malaria immunity.

Follicular T Helper Cells

To clear microbial infections, the immune system simultaneously triggers cellular and humoral responses that converge to the onset of a long-lasting, protective response. Although it correlates with the titers of high-affinity, class-switched antibodies, B cells are not the unique players in this scenario. In fact, the generation of these antibodies relies on assistance from a particular CD4+ T cell subset called the follicular T helper (TFh) cells. More specifically, the germinal center (GC) B cells physically interact with the activated CD4+ T cells in structures of lymphoid organs called follicles. Within the GCs, B-T cell talk leads to B cell activation, which mature through somatic hypermutations in V(D)J Ig genes as well as the Ig isotype switch, and differentiation into ASCs. Importantly, some TFh cytokines have shown to be critical in this process, such as the IL-6 and IL-21 that regulate B cell survival and cell differentiation.

It has been demonstrated that Pv malaria stimulates the expansion of the TFh cells and secretion of the TFh cytokines (54). Interestingly, Pf infection stimulates a less-functional Th1-like Tfh cell subset, whose function does not correlate to ASC differentiation and antibody secretion. Due to the increased secretion of IFNγ and TNFα during the Pf acute malaria, TFh cell precursors increase the T-bet expression and hinder their differentiation into mature TFh cells (55). Moreover, B cells are also affected by that IFNγ secretion, expressing high levels of T-bet and mainly expanding IgG3 class-switched cells that have the phenotype of atypical MBCs (20). Similarly, this issue is also seen in murine malaria models, implicating lower frequencies of the GC B cells and ASCs as well as the decreased antibody titers. Noteworthily, the murine bone marrow reconstituted with T-bet KO $CD4^+$ T cells had the TFh cell functionality restored, followed by the elicitation of GC formation and higher antibody titers (27). Alternately, IL-10 signaling restricts the T-bet expression and rescues the GC formation and antibody responses upon malaria infection in mice (56). Hence, the IL-21 has also demonstrated an important role during this process since the IL-21 KO mice showed decreased numbers of splenic GC B cells and ASCs in the bone marrow, lower antibody titers, and, consequently, a failure to control the parasitemia levels upon challenge (57).

Moreover, other factors can disturb the TFh cell differentiation and influence the effectiveness of humoral responses, such as the expression of particular MHC class II molecules by B cells or co-infections. Regarding the MHC class II expression, humanized mice expressing only HLA-DR0401 as the only MHC class II molecules had impaired antibody responses and could not clear parasitemia after a challenge with a strain causing murine malaria. An expanded subset of the regulatory T cells (Tregs) was found to interact with B cells in those mice, rather than the TFh cells. However, the Treg depletion or HLA-DR0401 co-expression with murine MHC class II molecules boosted the antibody titers and, consequently, the parasitemia dropped to undetectable levels in these mice (58). The expression of T-bet and the influence of Th1 cytokines, such as IFNγ, have been associated with that Treg expansion which impairs the Tfh cell differentiation and survival as well as wanes the secretion of malaria-specific antibodies (59, 60). In terms of co-infections, an acute gammaherpesvirus (MHV68) infection decreased the resistance against a non-lethal malaria in mice. This co-infection diminished the frequencies of the Tfh cells, GC B cells, and ASCs, suppressing the humoral response to malaria (61).

Antibody-dependent Protective Immunity

The malarial-specific antibody responses derived from Pf exposure are usually transient since their titers decrease by the next parasitic transmission season. After their contraction, the antibody levels are still maintained in a higher magnitude than the respective titers detected in the previous parasite exposure (62). For the Pv infection, it follows an opposite pattern (17, 54). However, once secreted at a certain level in the serum, the antibodies can provide protection against human malaria. Serology data against blood stage antigens have determined an inverse correlation between the antibody titers specific for Pf MSP-2-, MSP-3-, and AMA-1 and Pf morbidity in the infected individuals. Thus, an increased breadth of antibody specificity would be associated with a lower chance to experience a clinical episode or be admitted to hospital with severe Pf malaria (63).

To provide antibody-dependent protection, the immune system launches different mechanisms of action upon malaria infection. Considering that the blood stage of infection breaks humoral immunity against the liver stage antigens in murine malaria models (16), malaria-specific antibodies would preferentially opsonize the merozoites. Subsequently, they could trigger effector functions, such as inhibition of cell invasion, phagocytosis, activation of respiratory burst, or complement-derived parasite death [reviewed by (64)]. In the context of the inhibition of cell invasion, it has been challenging to study the breadth of antibody responses which could block sporozoite or merozoite invasion into the hepatocytes or erythrocytes (Pf) / reticulocytes (Pv), respectively. To assess the antigens linked to protective humoral responses against Pf malaria, the high-throughput technologies have been utilized. Among the identified antigens were liver and blood-stage antigens (65). Regarding the reactivity against the *Plasmodium* liver stage antigens, most of such response is driven to the circumsporozoite protein (CSP). The most immunogenic region of Pf CSP for antibodies consists of the central repeat-region. Recently, a Pf CSP-specific mAb (CIS43) displayed a high capacity of parasite neutralization, with its binding region identified in the junction between the N-terminal and central repeat regions of CSP (66). Another anti-Pf CSP repeat-region mAb (2A10) has been shown to elicit protection in mice challenged with chimeric Pb-Pf sporozoites. After being cloned into a adeno-associated virus vector, 2A10 was expressed for long-term and reduced parasite burden, providing protection in mice either by sporozoite injection or mosquito bites (67). The N-terminal region flanking those Pf CSP repeat-regions also possess a linear protective B cell epitope recognized by the mAb 5D5. The antibody-binding inhibits the CSP proteolytic cleavage,

neutralizing the hepatocyte invasion. Whenever administrated in combination with mAb 2A10, these mAbs enhanced the sporozoite neutralization *in vivo* (68). Contrarily, the antibody reactivity had multiple targets against the blood stage antigens. Anti-EBA-175 mAbs (R217 and R218) have been described as inhibitory for Pf invasion in RBCs. Whereas R217, the more inhibitory mAb, engages fundamental antigen residues for RBC binding, R218 interacts with F1 region residues, irrelevant for RBC binding (69). The subdomains I and II of Duffy binding protein (DBP) have also been targeted by the neutralizing antibodies detected in high concentration in the serum of individuals from Pv malaria-endemic areas. Mutations in those antibody sequences accumulate over parasitic exposures, enhancing their breadth and potency (70). Furthermore, although barely recognized during infection even in residents of Pf malaria-endemic areas (71), the anti-RH5 antibodies have demonstrated a great capacity of inhibiting invasion of the Pf merozoites in erythrocytes (72–76). Due to a subcellular location, the RH5 antigen has been detected around the moving junction that is assembled just before the erythrocyte invasion. Thus, RH5 would be accessible to antibodies only during the short contact between Pf merozoites and erythrocytes. Crystallography data showed that anti-RH5 bNabs bind at or close to the basigin-binding site, blocking the interaction between RH5 and basigin (77) that is critical for Pf merozoite invasion. However, this protein interaction does not seem to be the unique spot for the anti-RH5 mAb neutralizing activity. Considering that distinct RH5-derived B cell epitopes have been described with those bNAbs, it suggests that the RH5 sequences may suffer some immunological pressure (78). Other Pf antigens have been described as stimulators of malaria bNAbs, such as EXP1, MSP-3, GLURP, RAMA, SEA, and EBA-181. Those antigens were discovered after an investigation of serum samples from the cured Pf malaria patients and individuals with subsequent recrudescent infection. The cured patient samples had higher antibody titers against all those antigens and consequently, a higher capacity to inhibit the erythrocytes invasion by Pf merozoites (79). Recently, a mechanism based on interchromosomal DNA transposition was described as the contributor to the antibody diversity in the context of Pf malaria infection. A DNA insertion from a sequence of a collagen-binding inhibitory receptor (LAIR1) into V(D)J Ig genes was described to generate broad reactive antibodies against the Pf-infected erythrocytes (80). Although these LAIR1-containing antibodies were found in 5-10% of residents of Pf malaria-endemic areas and recognized distinct members of the RIFIN family, they did not confer protection against the disease (80, 81).

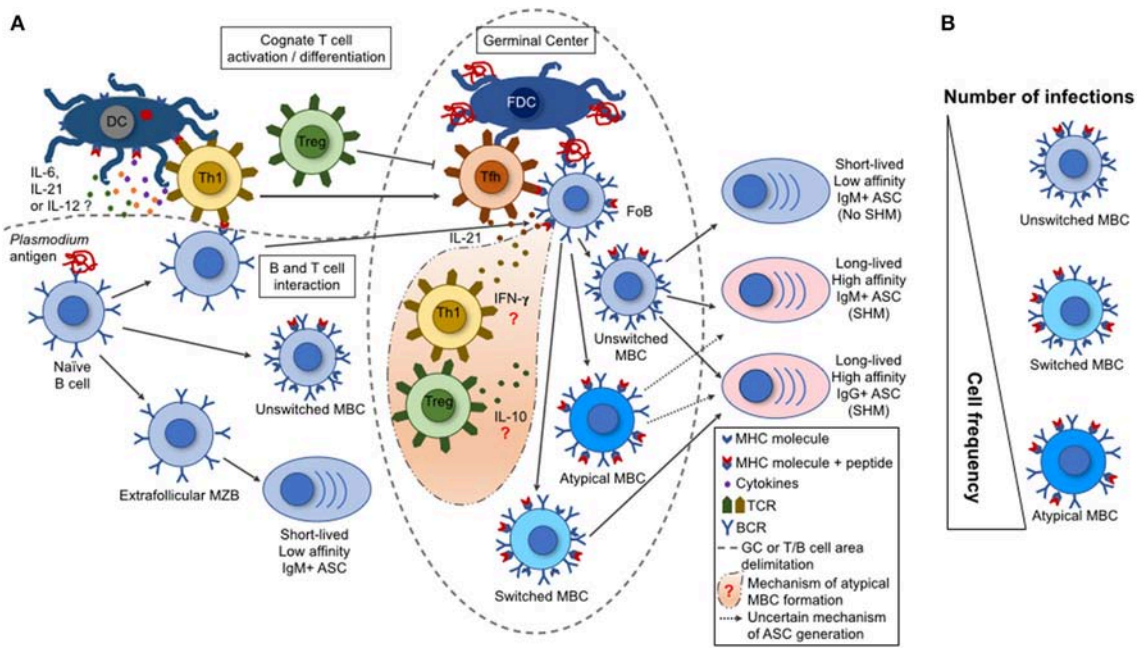

FIGURE 1 | B cell response triggered by malaria infection. **(A)** During a malaria infection, the naive B cells are activated by a *Plasmodium* antigen through the interaction with B cell receptors (BCR), leading to their differentiation into marginal zone B cells (MZB), follicular B cells (FoB), or unswitched memory B cell (MBCs). The switched and atypical MBCs are derived from the activation of FoBs within the germinal centers (GCs). Either the MZBs, or the unswitched, switched, or atypical MBCs can differentiate into antibody-secreting cells (ASCs). These ASCs range from short-lived, low-affinity, IgM+ to long-lived, high-affinity, IgM+ or IgG+. This variation depends on the type of interaction between a particular B cell with a T cell subset. The activated Th1 T cells migrate to the GCs, becoming follicular T helper cells (TFh) that help the GC reactions (acquisition of somatic hypermutations in V(D)J Ig genes and class switch by activated FoBs). Contrarily, the regulatory T cells (Tregs) have the potential to inhibit TFh cell differentiation and GC reactions. **(B)** A single parasite infection can induce the differentiation of multiple *Plasmodium*-specific B cell clones. However, the repeated parasite exposures shift the MBC frequencies with an increase for an atypical MBC over the unswitched or switched MBCs. This shift in cell frequency may interfere on the function of the secreted antibodies and, consequently, on the development of protective immunity.

Similar to the importance of immunoglobulin variable regions for effective humoral responses, Fc regions also have a fundamental role in mediating protection against infectious diseases. Receptors for immunoglobulin Fc regions have been described to be involved in cellular processes such as phagocytosis, antibody-dependent cellular cytotoxicity, and inflammation, among others (82). In the context of Pf malaria infection, the inoculations of human anti-$MSP1_{19}$ IgG protected transgenic mice for human Fc gamma receptor after challenge with chimeric Pb-Pf sporozoites. Contrarily, protection was not obtained when the same mAb was tested in non-transgenic mice, suggesting that the antibody interaction with $MSP1_{19}$ is not sufficient, while the presence of the Fc region is critical for parasite clearance (83). Few studies about human single nucleotide polymorphisms (SNPs) of the Fc gamma receptor have already validated the relevance of this opsonizing antibody-dependent phagocytosis for Pf malaria immunity [reviewed by (64)]. Noteworthily, the merozoite opsonisation has been associated with several conserved antigens and induces immunity against multiple Pf parasite strains (84).

Among the cells that can phagocyte and eliminate an opsonised Pf merozoite are neutrophils through the activation of respiratory burst [reviewed by (64)]. A SNP study has associated the increased levels of nitric oxide (NO) to Pf malaria protection (85). Furthermore, ROS levels have been correlated to natural acquired Pf malaria immunity (86). Once secreted to the extracellular medium, NO and ROS can both dampen the growth of Pf parasites *in vitro* (64, 87).

In terms of antibody-dependent complement activation, complement C1q proteins have shown to be deposited on the merozoite surface after the antibody-antigen interaction, allowing the further formation of the membrane attack complex (MAC) for parasite destruction. MSP-1 and MSP-2 have been identified as the main Pf merozoite targets involved in this protective mechanism. The higher is the C1q deposition, the higher is the protection. Interestingly, older children from Pf endemic areas presented higher C1q deposition than the younger children (88).

CONCLUDING REMARKS

After decades of suffering with malaria morbidity and mortality in several tropical areas, the at risk-populations are long overdue for effective strategies to contain this epidemic. The development of *Plasmodium*-specific vaccines already tested in clinical trials has not presented a considerable degree of protection yet. Hence, it has been strongly demonstrated that *Plasmodium* parasites have an enhanced resistance against the anti-malarial drugs on a daily basis. Thus, other alternatives of preventative or therapeutic treatments for malaria should be considered. Following all the characteristics presented in this manuscript about malaria-derived B cell immunity (**Figure 1**), those formulations must prioritize the best conditions for optimal B cell activation and development of the GC, TFh, and ASC responses. In terms of antibodies which are the final and effector products of the potential formulations, there are several reports of neutralizing antibodies identified for human malaria. However, their mechanisms of action have not been elucidated yet. Overall, it has been widely seen that antibody-based prophylaxis or therapeutical approaches possess a great efficacy against multiple pathogens. Therefore, strategies that properly stimulate malarial B cell responses may be beneficial not only in inhibiting infection, but also in reducing the morbidity and mortality numbers and disease transmission.

AUTHOR CONTRIBUTIONS

ELVS and MRD wrote the draft of this manuscript. ISS reviewed the manuscript and contributed significantly to the final draft. All authors read and approved the final manuscript.

ACKNOWLEDGMENTS

The authors thank Feda Masseoud (Centers for Disease Control and Prevention) for the critical reading of this manuscript and Fapesp grants 2012/13032-5 and 2017/11931-6 for the financial support. ELVS and ISS received fellowships from CNPq. MRD is currently receiving CAPES (Coordenação de Aperfeiçoamento de Pessoal de Nível Superior) fellowship.

REFERENCES

1. World Health Organization. *World Malaria Report 2016*. (2016). Available from: http://www.who.int/malaria/publications/world-malaria-report-2016/report/en/ (Accessed February 14, 2017).
2. World Health Organization. *Management of Severe Malaria: A Practical Handbook*. Geneva (2012). p. 1–83.
3. Lacerda MV, Mourão MP, Alexandre MA, Siqueira AM, Magalhães BM, Martinez-Espinosa FE, et al. Understanding the clinical spectrum of complicated *Plasmodium vivax* malaria: a systematic review on the contributions of the Brazilian literature. *Malar J.* (2012) 11:12. doi: 10.1186/1475-2875-11-12
4. Murray CJ, Rosenfeld LC, Lim SS, Andrews KG, Foreman KJ, Haring D, et al. Global malaria mortality between 1980 and 2010: a systematic analysis. *Lancet* (2012) 379:413–31. doi: 10.1016/S0140-6736(12)60034-8
5. Ménard R, Tavares J, Cockburn I, Markus M, Zavala F, Amino R. Looking under the skin: the first steps in malarial infection and immunity. *Nat Rev Microbiol.* (2013) 11:701–12. doi: 10.1038/nrmicro3111
6. Absalon S, Robbins JA, Dvorin JD. An essential malaria protein defines the architecture of blood-stage and transmission-stage parasites. *Nat Commun.* (2016) 7:11449. doi: 10.1038/ncomms11449
7. Obaldia N, Meibalan E, Sa JM, Ma S, Clark MA, Mejia P, et al. Bone marrow is a major parasite reservoir in *Plasmodium vivax* infection. *MBio* (2018) 9:e00625-18. doi: 10.1128/mBio.00625-18
8. Joice R, Nilsson SK, Montgomery J, Dankwa S, Egan E, Morahan B, et al. Plasmodium falciparum transmission stages accumulate in the human bone marrow. *Sci Transl Med.* (2014) 6:244re5. doi: 10.1126/scitranslmed.3008882
9. Cohen S, McGregor IA, Carrington S. Gamma-globulin and acquired immunity to human malaria. *Nature* (1961) 192:733–7. doi: 10.1038/192733a0
10. Ferreira MU, da Silva Nunes M, Wunderlich G. Antigenic diversity and immune evasion by malaria parasites. *Clin Diagn Lab Immunol.* (2004) 11:987–95. doi: 10.1128/CDLI.11.6.987-995.2004

11. Neafsey DE, Galinsky K, Jiang RH, Young L, Sykes SM, Saif S, et al. The malaria parasite *Plasmodium vivax* exhibits greater genetic diversity than *Plasmodium falciparum*. *Nat Genet.* (2012) 44:1046–50. doi: 10.1038/ng.2373
12. Weiss GE, Traore B, Kayentao K, Ongoiba A, Doumbo S, Doumtabe D, et al. The Plasmodium falciparum-specific human memory B cell compartment expands gradually with repeated malaria infections. *PLoS Pathog.* (2010) 6:e1000912. doi: 10.1371/journal.ppat.1000912
13. Nogaro SI, Hafalla JC, Walther B, Remarque EJ, Tetteh KK, Conway DJ, et al. The breadth, but not the magnitude, of circulating memory B cell responses to *P. falciparum* increases with age/exposure in an area of low transmission. *PLoS ONE* (2011) 6:e25582. doi: 10.1371/journal.pone.0025582
14. Wrammert J, Smith K, Miller J, Langley WA, Kokko K, Larsen C, et al. Rapid cloning of high-affinity human monoclonal antibodies against influenza virus. *Nature* (2008) 453:667–71. doi: 10.1038/nature06890
15. Le Roch KG, Johnson JR, Florens L, Zhou Y, Santrosyan A, Grainger M, et al. Global analysis of transcript and protein levels across the *Plasmodium falciparum* life cycle. *Genome Res.* (2004) 14:2308–18. doi: 10.1101/gr.2523904
16. Keitany GJ, Kim KS, Krishnamurty AT, Hondowicz BD, Hahn WO, Dambrauskas N, et al. Blood stage malaria disrupts humoral immunity to the pre-erythrocytic stage circumsporozoite protein. *Cell Rep*. (2016) 17:3193–205. doi: 10.1016/j.celrep.2016.11.060
17. Wipasa J, Suphavilai C, Okell LC, Cook J, Corran PH, Thaikla K, et al. Long-lived antibody and B Cell memory responses to the human malaria parasites, *Plasmodium falciparum* and *Plasmodium vivax*. *PLoS Pathog*. (2010) 6:e1000770. doi: 10.1371/journal.ppat.1000770
18. Ubillos I, Campo JJ, Requena P, Ome-Kaius M, Hanieh S, Rose H, et al. Chronic exposure to malaria is associated with inhibitory and activation markers on atypical memory B cells and marginal zone-like B cells. *Front Immunol.* (2017) 8:966. doi: 10.3389/fimmu.2017.00966
19. Stephens R, Ndungu FM, Langhorne J. Germinal centre and marginal zone B cells expand quickly in a second *Plasmodium chabaudi* malaria infection producing mature plasma cells. *Parasite Immunol.* (2009) 31:20–31. doi: 10.1111/j.1365-3024.2008.01066.x
20. Obeng-Adjei N, Portugal S, Holla P, Li S, Sohn H, Ambegaonkar A, et al. Malaria-induced interferon-γ drives the expansion of Tbethi atypical memory B cells. *PLoS Pathog.* (2017) 13:e1006576. doi: 10.1371/journal.ppat.1006576
21. Krishnamurty AT, Thouvenel CD, Portugal S, Keitany GJ, Kim KS, Holder A, et al. Somatically hypermutated plasmodium-specific IgM(+) memory B cells are rapid, plastic, early responders upon malaria rechallenge. *Immunity* (2016) 45:402–14. doi: 10.1016/j.immuni.2016.06.014
22. Harms Pritchard G, Pepper M. Memory B cell heterogeneity: remembrance of things past. *J Leukoc Biol.* (2018) 103:269–74. doi: 10.1002/JLB.4MR0517-215R
23. Radbruch A, Muehlinghaus G, Luger EO, Inamine A, Smith KG, Dörner T, et al. Competence and competition: the challenge of becoming a long-lived plasma cell. *Nat Rev Immunol.* (2006) 6:741–50. doi: 10.1038/nri1886
24. Weiss GE, Crompton PD, Li S, Walsh LA, Moir S, Traore B, et al. Atypical memory B cells are greatly expanded in individuals living in a malaria-endemic area. *J Immunol.* (2009) 183:2176–82. doi: 10.4049/jimmunol.0901297
25. Portugal S, Tipton CM, Sohn H, Kone Y, Wang J, Li S, et al. Malaria-associated atypical memory B cells exhibit markedly reduced B cell receptor signaling and effector function. *Elife* (2015) 4:e07218. doi: 10.7554/eLife.07218
26. Muellenbeck MF, Ueberheide B, Amulic B, Epp A, Fenyo D, Busse CE, et al. Atypical and classical memory B cells produce *Plasmodium falciparum* neutralizing antibodies. *J Exp Med.* (2013) 210:389–99. doi: 10.1084/jem.20121970
27. Ryg-Cornejo V, Ioannidis LJ, Ly A, Chiu CY, Tellier J, Hill DL, et al. Severe malaria infections impair germinal center responses by inhibiting T follicular helper cell differentiation. *Cell Rep.* (2016) 14:68–81. doi: 10.1016/j.celrep.2015.12.006
28. Xue J, Zhan B, Guo J, He N, Qiang HQ, Hotez P, et al. Acquired hookworm immunity in the golden hamster (*Mesocricetus auratus*) elicited by living *Necator americanus* third-stage infective larvae. *Exp Parasitol.* (2012) 130:6–12. doi: 10.1016/j.exppara.2011.10.007
29. Finney OC, Danziger SA, Molina DM, Vignali M, Takagi A, Ji M, et al. Predicting antidisease immunity using proteome arrays and sera from children naturally exposed to malaria. *Mol Cell Proteomics* (2014) 13:2646–60. doi: 10.1074/mcp.M113.036632
30. Cepok S, von Geldern G, Nolting T, Grummel V, Srivastava R, Zhou D, et al. Viral load determines the B-cell response in the cerebrospinal fluid during human immunodeficiency virus infection. *Ann Neurol.* (2007) 62:458–67. doi: 10.1002/ana.21195
31. Crompton PD, Mircetic M, Weiss G, Baughman A, Huang CY, Topham DJ, et al. The TLR9 ligand CpG promotes the acquisition of *Plasmodium falciparum*-specific memory B cells in malaria-naive individuals. *J Immunol.* (2009) 182:3318–26. doi: 10.4049/jimmunol.0803596
32. Elias SC, Choudhary P, de Cassan SC, Biswas S, Collins KA, Halstead FD, et al. Analysis of human B-cell responses following ChAd63-MVA MSP1 and AMA1 immunization and controlled malaria infection. *Immunology* (2014) 141:628–44. doi: 10.1111/imm.12226
33. Turner L, Wang CW, Lavstsen T, Mwakalinga SB, Sauerwein RW, Hermsen CC, et al. Antibodies against PfEMP1, RIFIN, MSP3 and GLURP are acquired during controlled Plasmodium falciparum malaria infections in naïve volunteers. *PLoS ONE*. (2011) 6:e29025. doi: 10.1371/journal.pone.0029025
34. Walker DM, Oghumu S, Gupta G, McGwire BS, Drew ME, Satoskar AR. Mechanisms of cellular invasion by intracellular parasites. *Cell Mol Life Sci.* (2014) 71:1245–63. doi: 10.1007/s00018-013-1491-1
35. Walker KM, Okitsu S, Porter DW, Duncan C, Amacker M, Pluschke G, et al. Antibody and T-cell responses associated with experimental human malaria infection or vaccination show limited relationships. *Immunology* (2015) 145:71–81. doi: 10.1111/imm.12428
36. Naus CW, Jones FM, Satti MZ, Joseph S, Riley EM, Kimani G, et al. Serological responses among individuals in areas where both schistosomiasis and malaria are endemic: cross-reactivity between *Schistosoma mansoni* and *Plasmodium falciparum*. *J Infect Dis.* (2003) 187:1272–82. doi: 10.1086/368361
37. Pierrot C, Wilson S, Lallet H, Lafitte S, Jones FM, Daher W, et al. Identification of a novel antigen of *Schistosoma mansoni* shared with *Plasmodium falciparum* and evaluation of different cross-reactive antibody subclasses induced by human schistosomiasis and malaria. *Infect Immun.* (2006) 74:3347–54. doi: 10.1128/IAI.01724-05
38. Donati D, Zhang LP, Chêne A, Chen Q, Flick K, Nyström M, et al. Identification of a polyclonal B-cell activator in *Plasmodium falciparum*. *Infect Immun.* (2004) 72:5412–8. doi: 10.1128/IAI.72.9.5412-5418.2004
39. Donati D, Mok B, Chêne A, Xu H, Thangarajh M, Glas R, et al. Increased B cell survival and preferential activation of the memory compartment by a malaria polyclonal B cell activator. *J Immunol.* (2006) 177:3035–44. doi: 10.4049/jimmunol.177.5.3035
40. Zanini GM, De Moura Carvalho LJ, Brahimi K, De Souza-Passos LF, Guimarães SJ, Da Silva Machado E, et al. Sera of patients with systemic lupus erythematosus react with plasmodial antigens and can inhibit the *in vitro* growth of *Plasmodium falciparum*. *Autoimmunity* (2009) 42:545–52. doi: 10.1080/08916930903039810
41. Brahimi K, Martins YC, Zanini GM, Ferreira-da-Cruz MeF, Daniel-Ribeiro CT. Monoclonal auto-antibodies and sera of autoimmune patients react with *Plasmodium falciparum* and inhibit its *in vitro* growth. *Mem Inst Oswaldo Cruz.* (2011) 106(Suppl. 1):44–51. doi: 10.1590/S0074-02762011000900006
42. Scholzen A, Teirlinck AC, Bijker EM, Roestenberg M, Hermsen CC, Hoffman SL, et al. BAFF and BAFF receptor levels correlate with B cell subset activation and redistribution in controlled human malaria infection. *J Immunol.* (2014) 192:3719–29. doi: 10.4049/jimmunol.1302960
43. Nduati E, Gwela A, Karanja H, Mugyenyi C, Langhorne J, Marsh K, et al. The plasma concentration of the B cell activating factor is increased in children with acute malaria. *J Infect Dis.* (2011) 204:962–70. doi: 10.1093/infdis/jir438
44. Muehlenbachs A, Fried M, Lachowitzer J, Mutabingwa TK, Duffy PE. Genome-wide expression analysis of placental malaria reveals features of lymphoid neogenesis during chronic infection. *J Immunol.* (2007) 179:557–65. doi: 10.4049/jimmunol.179.1.557
45. Patgaonkar M, Herbert F, Powale K, Gandhe P, Gogtay N, Thatte U, et al. Vivax infection alters peripheral B-cell profile and induces persistent serum IgM. *Parasite Immunol.* (2018) 40:e12580. doi: 10.1111/pim.12580
46. Rodrigues-da-Silva RN, Lima-Junior JaC, Fonseca BeP, Antas PR, Baldez A, Storer FL, et al. Alterations in cytokines and haematological parameters during the acute and convalescent phases of *Plasmodium falciparum* and

Plasmodium vivax infections. *Mem Inst Oswaldo Cruz.* (2014) 109:154–62. doi: 10.1590/0074-0276140275
47. Craxton A, Magaletti D, Ryan EJ, Clark EA. Macrophage- and dendritic cell–dependent regulation of human B-cell proliferation requires the TNF family ligand BAFF. *Blood* (2003) 101:4464–71. doi: 10.1182/blood-2002-10-3123
48. Bockstal V, Geurts N, Magez S. Acute Disruption of Bone Marrow B Lymphopoiesis and apoptosis of transitional and marginal zone B cells in the spleen following a blood-stage *Plasmodium chabaudi* infection in mice. *J Parasitol Res*. (2011) 2011:534697. doi: 10.1155/2011/534697
49. Ghosh D, Wikenheiser DJ, Kennedy B, McGovern KE, Stuart JD, Wilson EH, et al. An atypical splenic B cell progenitor population supports antibody production during plasmodium infection in mice. *J Immunol.* (2016) 197:1788–800. doi: 10.4049/jimmunol.1502199
50. Sullivan RT, Ssewanyana I, Wamala S, Nankya F, Jagannathan P, Tappero JW, et al. B cell sub-types following acute malaria and associations with clinical immunity. *Malar J.* (2016) 15:139. doi: 10.1186/s12936-016-1190-0
51. Rowland SL, Leahy KF, Halverson R, Torres RM, Pelanda R. BAFF receptor signaling aids the differentiation of immature B cells into transitional B cells following tonic BCR signaling. *J Immunol.* (2010) 185:4570–81. doi: 10.4049/jimmunol.1001708
52. Moir S, Ho J, Malaspina A, Wang W, DiPoto AC, O'Shea MA, et al. Evidence for HIV-associated B cell exhaustion in a dysfunctional memory B cell compartment in HIV-infected viremic individuals. *J Exp Med*. (2008) 205:1797–805. doi: 10.1084/jem.20072683
53. Pérez-Mazliah D, Gardner PJ, Schweighoffer E, McLaughlin S, Hosking C, Tumwine I, et al. Plasmodium-specific atypical memory B cells are short-lived activated B cells. *Elife* (2018) 7:e39800. doi: 10.7554/eLife.39800
54. Figueiredo MM, Costa PAC, Diniz SQ, Henriques PM, Kano FS, Tada MS, et al. T follicular helper cells regulate the activation of B lymphocytes and antibody production during *Plasmodium vivax* infection. *PLoS Pathog*. (2017) 13:e1006484. doi: 10.1371/journal.ppat.1006484
55. Obeng-Adjei N, Portugal S, Tran TM, Yazew TB, Skinner J, Li S, et al. Circulating Th1-cell-type Tfh cells that exhibit impaired B cell help are preferentially activated during acute malaria in children. *Cell Rep*. (2015) 13:425–39. doi: 10.1016/j.celrep.2015.09.004
56. Guthmiller JJ, Graham AC, Zander RA, Pope RL, Butler NS. Cutting Edge: IL-10 is essential for the generation of germinal center B cell responses and anti-plasmodium humoral immunity. *J Immunol.* (2017) 198:617–22. doi: 10.4049/jimmunol.1601762
57. Pérez-Mazliah D, Ng DH, Freitas do Rosário AP, McLaughlin S, Mastelic-Gavillet B, Sodenkamp J, et al. Disruption of IL-21 signaling affects T cell-B cell interactions and abrogates protective humoral immunity to malaria. *PLoS Pathog*. (2015) 11:e1004715. doi: 10.1371/journal.ppat.1004715
58. Wijayalath W, Danner R, Kleschenko Y, Majji S, Villasante EF, Richie TL, et al. HLA class II (DR0401) molecules induce Foxp3+ regulatory T cell suppression of B cells in *Plasmodium yoelii* strain 17XNL malaria. *Infect Immun.* (2014) 82:286–97. doi: 10.1128/IAI.00272-13
59. Zander RA, Obeng-Adjei N, Guthmiller JJ, Kulu DI, Li J, Ongoiba A, et al. PD-1 co-inhibitory and OX40 co-stimulatory crosstalk regulates helper T cell differentiation and anti-plasmodium humoral immunity. *Cell Host Microbe* (2015) 17:628–41. doi: 10.1016/j.chom.2015.03.007
60. Zander RA, Guthmiller JJ, Graham AC, Pope RL, Burke BE, Carr DJ, et al. Type I interferons induce T regulatory 1 responses and restrict humoral immunity during experimental malaria. *PLoS Pathog*. (2016) 12:e1005945. doi: 10.1371/journal.ppat.1005945
61. Matar CG, Anthony NR, O'Flaherty BM, Jacobs NT, Priyamvada L, Engwerda CR, et al. Gammaherpesvirus co-infection with malaria suppresses anti-parasitic humoral immunity. *PLoS Pathog*. (2015) 11:e1004858. doi: 10.1371/journal.ppat.1004858
62. Hviid L, Barfod L, Fowkes FJ. Trying to remember: immunological B cell memory to malaria. *Trends Parasitol.* (2015) 31:89–94. doi: 10.1016/j.pt.2014.12.009
63. Osier FH, Fegan G, Polley SD, Murungi L, Verra F, Tetteh KK, et al. Breadth and magnitude of antibody responses to multiple *Plasmodium falciparum* merozoite antigens are associated with protection from clinical malaria. *Infect Immun.* (2008) 76:2240–8. doi: 10.1128/IAI.01585-07
64. Hill DL, Schofield L, Wilson DW. IgG opsonization of merozoites: multiple immune mechanisms for malaria vaccine development. *Int J Parasitol.* (2017) 47:585–95. doi: 10.1016/j.ijpara.2017.05.004
65. Dent AE, Nakajima R, Liang L, Baum E, Moormann AM, Sumba PO, et al. *Plasmodium falciparum* protein microarray antibody profiles correlate with protection from symptomatic malaria in Kenya. *J Infect Dis.* (2015) 212:1429–38. doi: 10.1093/infdis/jiv224
66. Kisalu NK, Idris AH, Weidle C, Flores-Garcia Y, Flynn BJ, Sack BK, et al. A human monoclonal antibody prevents malaria infection by targeting a new site of vulnerability on the parasite. *Nat Med.* (2018) 24:408–16. doi: 10.1038/nm.4512
67. Deal C, Balazs AB, Espinosa DA, Zavala F, Baltimore D, Ketner G. Vectored antibody gene delivery protects against *Plasmodium falciparum* sporozoite challenge in mice. *Proc Natl Acad Sci USA*. (2014) 111:12528–32. doi: 10.1073/pnas.1407362111
68. Espinosa DA, Gutierrez GM, Rojas-López M, Noe AR, Shi L, Tse SW, et al. Proteolytic cleavage of the *Plasmodium falciparum* circumsporozoite protein is a target of protective antibodies. *J Infect Dis.* (2015) 212:1111–9. doi: 10.1093/infdis/jiv154
69. Chen E, Paing MM, Salinas N, Sim BK, Tolia NH. Structural and functional basis for inhibition of erythrocyte invasion by antibodies that target *Plasmodium falciparum* EBA-175. *PLoS Pathog*. (2013) 9:e1003390. doi: 10.1371/journal.ppat.1003390
70. Chootong P, Ntumngia FB, VanBuskirk KM, Xainli J, Cole-Tobian JL, Campbell CO, et al. Mapping epitopes of the *Plasmodium vivax* Duffy binding protein with naturally acquired inhibitory antibodies. *Infect Immun.* (2010) 78:1089–95. doi: 10.1128/IAI.01036-09
71. Partey FD, Castberg FC, Sarbah EW, Silk SE, Awandare GA, Draper SJ, et al. Kinetics of antibody responses to PfRH5-complex antigens in Ghanaian children with *Plasmodium falciparum* malaria. *PLoS ONE* (2018) 13:e0198371. doi: 10.1371/journal.pone.0198371
72. Douglas AD, Williams AR, Illingworth JJ, Kamuyu G, Biswas S, Goodman AL, et al. The blood-stage malaria antigen PfRH5 is susceptible to vaccine-inducible cross-strain neutralizing antibody. *Nat Commun.* (2011) 2:601. doi: 10.1038/ncomms1615
73. Douglas AD, Baldeviano GC, Lucas CM, Lugo-Roman LA, Crosnier C, Bartholdson SJ, et al. A PfRH5-based vaccine is efficacious against heterologous strain blood-stage Plasmodium falciparum infection in aotus monkeys. *Cell Host Microbe* (2015) 17:130–9. doi: 10.1016/j.chom.2014.11.017
74. Weaver R, Reiling L, Feng G, Drew DR, Mueller I, Siba PM, et al. The association between naturally acquired IgG subclass specific antibodies to the PfRH5 invasion complex and protection from *Plasmodium falciparum malaria*. *Sci Rep.* (2016) 6:33094. doi: 10.1038/srep33094
75. Kapulu MC, Da DF, Miura K, Li Y, Blagborough AM, Churcher TS, et al. Comparative assessment of transmission-blocking vaccine candidates against *Plasmodium falciparum*. *Sci Rep.* (2015) 5:11193. doi: 10.1038/srep11193
76. Payne RO, Silk SE, Elias SC, Miura K, Diouf A, Galaway F, et al. Human vaccination against RH5 induces neutralizing antimalarial antibodies that inhibit RH5 invasion complex interactions. *JCI Insight.* (2017) 2:96381. doi: 10.1172/jci.insight.96381
77. Wright KE, Hjerrild KA, Bartlett J, Douglas AD, Jin J, Brown RE, et al. Structure of malaria invasion protein RH5 with erythrocyte basigin and blocking antibodies. *Nature* (2014) 515:427–30. doi: 10.1038/nature13715
78. Douglas AD, Williams AR, Knuepfer E, Illingworth JJ, Furze JM, Crosnier C, et al. Neutralization of *Plasmodium falciparum* merozoites by antibodies against PfRH5. *J Immunol.* (2014) 192:245–58. doi: 10.4049/jimmunol.1302045
79. Goh YS, Peng K, Chia WN, Siau A, Chotivanich K, Gruner AC, et al. Neutralizing antibodies against *Plasmodium falciparum* associated with successful cure after drug therapy. *PLoS ONE* (2016) 11:e0159347. doi: 10.1371/journal.pone.0159347
80. Tan J, Pieper K, Piccoli L, Abdi A, Perez MF, Geiger R, et al. A LAIR1 insertion generates broadly reactive antibodies against malaria variant antigens. *Nature* (2016) 529:105–9. doi: 10.1038/nature16450
81. Pieper K, Tan J, Piccoli L, Foglierini M, Barbieri S, Chen Y, et al. Public antibodies to malaria antigens generated by two LAIR1 insertion modalities. *Nature* (2017) 548:597–601. doi: 10.1038/nature23670

82. Pleass RJ, Holder AA. Opinion: antibody-based therapies for malaria. *Nat Rev Microbiol*. (2005) 3:893–9. doi: 10.1038/nrmicro1267
83. McIntosh RS, Shi J, Jennings RM, Chappel JC, de Koning-Ward TF, Smith T, et al. The importance of human FcgammaRI in mediating protection to malaria. *PLoS Pathog*. (2007) 3:e72. doi: 10.1371/journal.ppat.0030072
84. Hill DL, Wilson DW, Sampaio NG, Eriksson EM, Ryg-Cornejo V, Harrison GLA, et al. Merozoite antigens of *Plasmodium falciparum* elicit strain-transcending opsonizing immunity. *Infect Immun*. (2016) 84:2175–84. doi: 10.1128/IAI.00145-16
85. Kun JF, Mordmüller B, Perkins DJ, May J, Mercereau-Puijalon O, Alpers M, et al. Nitric oxide synthase 2(Lambaréné) (G-954C), increased nitric oxide production, and protection against malaria. *J Infect Dis.* (2001) 184:330–6. doi: 10.1086/322037
86. Joos C, Marrama L, Polson HE, Corre S, Diatta AM, Diouf B, et al. Clinical protection from falciparum malaria correlates with neutrophil respiratory bursts induced by merozoites opsonized with human serum antibodies. *PLoS ONE* (2010) 5:e9871. doi: 10.1371/journal.pone.0009871
87. Hodgson SH, Llewellyn D, Silk SE, Milne KH, Elias SC, Miura K, et al. Changes in serological immunology measures in UK and Kenyan adults post-controlled human malaria infection. *Front Microbiol.* (2016) 7:1604. doi: 10.3389/fmicb.2016.01604
88. Boyle MJ, Reiling L, Feng G, Langer C, Osier FH, Aspeling-Jones H, et al. Human antibodies fix complement to inhibit *Plasmodium falciparum* invasion of erythrocytes and are associated with protection against malaria. *Immunity* (2015) 42:580–90. doi: 10.1016/j.immuni.2015.02.012

Conflict of Interest Statement: The authors declare that the research was conducted in the absence of any commercial or financial relationships that could be construed as a potential conflict of interest.

frontiers in Immunology

REVIEW
published: 08 November 2018
doi: 10.3389/fimmu.2018.02579

The Influence of Parasite Infections on Host Immunity to Co-infection With Other Pathogens

*Neil A. Mabbott**

The Roslin Institute & Royal (Dick) School of Veterinary Studies, University of Edinburgh, Edinburgh, United Kingdom

Parasites have evolved a wide range of mechanisms that they use to evade or manipulate the host's immune response and establish infection. The majority of the *in vivo* studies that have investigated these host-parasite interactions have been undertaken in experimental animals, especially rodents, which were housed and maintained to a high microbiological status. However, in the field situation it is increasingly apparent that pathogen co-infections within the same host are a common occurrence. For example, chronic infection with pathogens including malarial parasites, soil-transmitted helminths, *Mycobacterium tuberculosis* and viruses such as HIV may affect a third of the human population of some developing countries. Increasing evidence shows that co-infection with these pathogens may alter susceptibility to other important pathogens, and/or influence vaccine efficacy through their effects on host immune responsiveness. Co-infection with certain pathogens may also hinder accurate disease diagnosis. This review summarizes our current understanding of how the host's immune response to infection with different types of parasites can influence susceptibility to infection with other pathogenic microorganisms. A greater understanding of how infectious disease susceptibility and pathogenesis can be influenced by parasite co-infections will enhance disease diagnosis and the design of novel vaccines or therapeutics to more effectively control the spread of infectious diseases.

Keywords: parasite, helminth, co-infection, pathogenesis, susceptibility, immunity

OPEN ACCESS

Edited by:
Hyun Soon Lillehoj, United States Department of Agriculture, United States

Reviewed by:
Robin James Flynn, University of Liverpool, United Kingdom
Mark Wilson, Genentech, Inc., United States

***Correspondence:**
Neil A. Mabbott
neil.mabbott@roslin.ed.ac.uk

Specialty section:
This article was submitted to Microbial Immunology, a section of the journal Frontiers in Immunology

Received: *29 June 2018*
Accepted: *19 October 2018*
Published: *08 November 2018*

Citation:
Mabbott NA (2018) The Influence of Parasite Infections on Host Immunity to Co-infection With Other Pathogens. Front. Immunol. 9:2579. doi: 10.3389/fimmu.2018.02579

INTRODUCTION

The important host-parasite interactions that influence the progression and control of infection to individual pathogenic microorganisms have been studied in much detail, especially in laboratory mice. However, since many pathogens are acquired through similar routes of exposure (e.g., orally following ingestion of contaminated water, food, or pasture) infection of natural host species in field situations and humans with multiple pathogens is common, especially in regions with poor sanitation and/or limited access to clean drinking water. In order to sustain chronic infections, the parasitic microorgansisms have evolved a diverse range of mechanisms to enable them to evade or manipulate the host's immune response. As a consequence, by-stander effects due to infection with certain parasite species can significantly alter susceptibility to other important pathogens, and/or influence the development of pathology. Discussed throughout this review are examples of the many studies that have investigated the effects of parasitic helminth infections on host susceptibility to co-infection with a diverse range other pathogenic microorganisms.

Helminths are large, multicellular parasitic microorganisms. Estimates suggest that approximately a third of the global human population may be infected with helminth parasites, causing important public health concerns, especially in regions with poor sanitation or limited access to clean drinking water. Helminths are commonly referred to as parasitic worms and can include the following groupings: roundworms (nematodes), such as *Ascaris lumbricoides*; whipworms, such as *Trichuris trichiura* in humans and *T. muris* in mice; hookworms, such as *Necator americanus*; flukes (trematodes), such as *Facsiola hepatica* and *Schistosoma mansoni*; and cestodes (tapeworms). Many of these helminth parasites are soil-transmitted and cause gastrointestinal infections following ingestion of pasture or water contaminated with their eggs. The schistosomes, in contrast, can establish chronic infection within the host's bloodstream. Infections with helminth parasites often cause significant pathology, for example as they migrate through host tissues following infection via the skin (e.g., schistosomes), or feed on the gut epithelium (e.g., *Trichuris* spp.) (1). These chronic infections are often associated with the development of systemic and mucosal $CD4^+$ T helper cell type 2 (Th2) polarized immune responses. These are typically characterized by increased expression of cytokines such as interleukin-4 (IL-4), IL-13, eosinophilia, production of immunoglobulin E (IgE), and stimulation of alternatively activated (M2) macrophages and type 2 innate lymphoid cells (ILC2) (2, 3). The alternatively activated macrophages are considered to play an important role in repairing the tissue damage caused by the helminth infection.

However, the characteristics of the immune response to infection with other types of parasites can differ substantially. Trypanosomes and malaria parasites are important vector-borne unicellular protozoan parasites, and are the causative agents of trypanosomiasis and malaria, respectively, in humans and animals. Each of these parasite species can establish chronic infections in the host's bloodstream: the trypanosomes living extracellularly, whereas the malaria parasites establish cyclical rounds of intracellular infection within erythrocytes. Host immune responses to infection with these protozoan parasites are usually fundamentally distinct from the predominantly Th2-polarized responses induced by helminth infections. Malaria infections, for example, are associated with elevated levels of pro-inflammatory cytokines such as interferon-γ (IFNγ), IL-12, increased levels of $CD4^+$ Th1 cells, $CD8^+$ T cells, and NK cells and the stimulation of pro-inflammatory classically activated (M1) macrophages (4, 5).

An increasing body of data indicates that alterations to these responses due to co-infection with other pathogens can dramatically influence disease susceptibility. Many of the examples presented below suggest links between parasite-induced disturbances to the Th1/Th2 balance and/or macrophage phenotype (alternatively activated vs. classically activated) and altered susceptibility or pathogenesis following subsequent co-infection with other pathogens. The effects of the parasite infection on the host's immune response may also have serious implications for the accurate diagnosis of other infections within the same individual. Bovine tuberculosis is an important infectious disease of cattle caused by the pathogenic bacterium *Mycobacterium bovis*. Current measures to control this disease include the regular testing of cattle and removal of infected stock from herds. A widely used diagnostic test for this disease is based on the detection of *M. bovis*-specific IFNγ production by peripheral blood lymphocytes. However, as helminth infections can modulate host IFNγ responses, co-infections with these parasites could have serious consequences for the reliable detection of other important pathogens (see section *Mycobacterium tuberculosis*).

This review therefore discusses how the induction of an immune response to infection with distinct types of parasites may modulate the development of effective immunity and/or disease pathogenesis to co-infections with other important pathogenic microorganisms. Many of the data obtained in the studies described below was derived from experimental mouse models, but studies from humans and natural host species are included where data were available.

MALARIA

Malaria, caused by infection with unicellular protozoan *Plasmodium* parasites, is an important infectious disease of humans and animals that inflicts significant morbidity and mortality in tropical and sub-tropical regions throughout the world. Infections are transmitted through the deposition of sporozoite parasite stages into the skin via the bite of infected mosquito vectors. These then travel via the bloodstream to the liver, where they infect hepatocytes and undergo morphological change and replication before subsequently infecting erythrocytes. The parasites then undergo extensive cycles of replication and infection in erythrocytes leading to anemia. During the erythrocytic stage of malaria infection, IFNγ production from $CD4^+$ Th1-cells and $CD4^+$ T-cell help for the B-cell response are each required for effective control and elimination of the parasitaemia. The actions of $CD4^+$ T cells are also important for controlling the pre-erythrocytic stages of infection through the activation of parasite-specific $CD8^+$ T cells [for in-depth review see (5)]. However, excessive inflammatory responses in response to malaria infection can also lead to significant immunopathology.

Effects of Malaria on Helminth Co-infection

Malaria patients in endemic regions are often co-infected with soil-transmitted helminths. Following infection of the mammalian host the larval stages of certain parasitic helminth species migrate to the lungs of the host where they cause pathology. The larvae typically induce strong pulmonary Th2 immune responses and are accompanied by the induction of alternatively activated macrophages. The combined actions of these immune responses are considered to help mediate parasite clearance and the repair of host tissues. In BALB/c mice infected with hookworms parasites such as *Nippostrongylus brasiliensis*, the development of a Th2-polarized immune response to the hookworm infection was impaired in those co-infected with *P. chabaudi chabaudi* malaria parasites. This effect also coincided with the reduced expression of alternatively activated macrophage-derived factors in the lung such as chitinase and

resistin family members (6). Similarly, in a separate study the incidence of lung granulomas induced by infection with *Litomosoides sigmodontis* microfilariae was reduced in mice co-infected with either *P. chabaudi* or *P. yoelii* malaria parasites (7). These experimental mouse studies suggest that malaria infection can negatively impact on the ability of the host to induce a Th2-polarized specific immune response to co-infection with helminths. How malaria infection mediates these effects is not known. Further experiments are clearly necessary to determine whether they are a consequence of direct effects of the malaria parasites themselves or are an indirect consequence of the induction of a strong Th1-polarized immune response/cytokine milieu in response to the malaria infection.

Effects of Helminth Co-infection on Malaria

Co-infections with parasites such as helminths may also have a significant impact on malaria pathogenesis and susceptibility (8). In mice infected with *N. brasiliensis* 2 weeks before subsequent infection with *P. berghei* malaria parasites, the induction of a malaria-driven Th1 cytokine response was impeded, affecting the activation phenotype of the macrophages in the lung (8). Helminth infections can promote the secretion of IL-10 by regulatory T cells (9, 10), and this can downregulate the expression of pro-inflammatory cytokines such as IL-12p70 and IFNγ. Since IFNγ plays an important role in protective immunity to *P. falciparum* infection, it is plausible that expression of an anti-inflammatory cytokine milieu during helminth infection might exacerbate malaria pathogenesis and susceptibility. In support of this hypothesis, co-infection of mice with the hookworm parasite *N. brasiliensis* was reported to impede the induction of a pro-inflammatory classically activated macrophage phenotype in the lungs of mice subsequently infected with malaria parasites (8). The induction of an effective Th1 response to *P. berghei* infection was similarly reduced in mice co-infected with schistosomes (*S. mansoni*). As a consequence, the co-infected mice were less able to control the malaria infection, displaying increased parasitemias during the early phase of *P. berghei* infection and increased fatality (11). Mice chronically infected with the gastrointestinal helminth pathogen *Heligmosomoides polygyrus* before a subsequent *P. chabaudi* AS infection likewise displayed reduced immunity to the bloodstream stage of malaria infection, including decreased production of IFNγ and malaria-specific Th1-associated IgG2a antibody production (12).

Parasite co-infections may also affect the magnitude of the pathology that develops in host tissues. For example, an exacerbation of immunopathology during *P. chabaudi* infection was observed in mice co-infected with *L. sigmodontis* microfilariae (13). The incidence of pathology in the co-infected mice was found to be associated with the absence of microfilaraemia. This implies that the presence of the microfilariae stimulates an immunomodulatory response in the host that can partially protect against severe malaria (13). However, helminth co-infections may differentially regulate murine malarial infections in a malaria strain-dependent way. For example, co-infection of mice with *L. sigmodontis* impaired the development of lesions in the kidneys caused by infection with either *P. chabaudi* or *P. yoelii*. However, the peak of malaria parasitaemia was decreased in mice co-infected *P. yoelii*, but not in those co-infected with *P. chabaudi* (7). Conversely, the growth of *P. yoelii* in the liver was inhibited in mice co-infected with *S. mansoni*, and malaria parasite gametocyte infectivity was much reduced (14).

Whether co-infections with helminths such as schistosomes can modulate susceptibility to malaria in humans is uncertain, but an experimental study in baboons (*Papio anubis*) suggests that this also plausible. This study showed that the baboons that were chronically infected with *S. mansoni* had significantly lower *P. knowlesi* malaria parasite burdens and were protected from anemia (15). A study of Senegalese children similarly showed that those with light *S. haematobium* infection had lower burdens of *P. falciparum* when compared to those that weren't co-infected with schistosomes (16). The mechanisms responsible for mediating these effects are not known. It is possible that the reduced levels of regulatory T cells or a Th2-polarized cytokine milieu in *S. haematobium* infected children may provide protection against falciparum malaria by modulating systemic expression of Th1 cytokines (17).

Effects of Parasite Co-infection on Experimental Cerebral Malaria

Severe forms of malaria are leading causes of mortality in infected children and pregnant mothers, presenting as cerebral malaria, severe anemia, or acidosis (18). The sequestration of malaria parasites across the blood-brain barrier leads to the influx of immune lymphocytes and leukocytes into the brain, particularly parasite-specific $CD8^+$ T cells, which ultimately leads to the development of neuropathology. Studies using a murine experimental cerebral malaria (ECM) model show that co-infection with Chikungunya virus can impede the sequestration of malaria parasites into the brain and provide some protection against ECM (19). In this model co-infection system, the malaria parasite-specific pathogenic $CD8^+$ T cells appeared to be retained in the spleens of mice co-infected with Chikungunya virus due to their reduced expression of the CXCR3 chemokine receptor (19). This implied that the reduced early migration of pathogenic $CD8^+$ T cells into the brains of the virus co-infected mice may have impeded the development of ECM and brain pathology.

Systemic co-infection of mice with the schistosomes (*S. mansoni*) seven weeks before infection with *P. berghei* malaria parasites was similarly shown to reduce the severity of ECM (11, 20). In this study, protection from ECM was dependent on the relative doses of the parasites used in the co-infections. Here, infection with a high dose of schistosome cercariae resulted in higher protection against ECM when co-infected with a low dose of *P. berghei* malaria paratites. Conversely, when the mice were co-infected with *S. mansoni* and a higher dose of *P. berghei*, the development of ECM was unaffected when compared to mice infected with malaria parasites alone (21). Development of ECM in mice is considered to be Th1-associated. The switch

toward a Th2-polarized cytokine profile in the *S. mansoni* co-infected mice suggests a mechanism by which the effects on ECM pathogenesis may have been mediated. Clearly further experiments are required to specifically confirm the identify of the cellular and molecular factors responsible for these effects. A predominantly Th1-polarized cytokine profile is observed in mice by 4 weeks after *S. mansoni* infection (before significant egg production occurs). When mice were co-infected with malaria parasites 4 weeks after *S. mansoni* infection (prior to the onset of the Th1/Th2 switch), no improvements to ECM pathogenesis were observed (20), supporting the hypothesis that a Th2-polarized cytokine response may have a protective role.

Co-infections with the helminth parasites *A. lumbricoides* and *T. trichiura* have also been associated with reductions in risk of cerebral malaria in humans (22). However, it is interesting to note that the beneficial effects of *T. trichiura* were reduced when the individuals were also co-infected with hookworms (22). This study reveals an additional layer of complexity in naturally affected host-species where the outcome on the host of interactions between two parasite species can be modified by the presence of a third. These data emphasize how the relationships between multiple parasite communities in an individual host can significantly affect disease outcomes.

TREMATODES (FLUKES)

Liver Fluke

The liver fluke *Fasciola hepatica* is highly prevalent in ruminant livestock species, but can also establish infection in a wide range of other mammalian species including humans. Infection of livestock with *F. hepatica* occurs through the ingestion of pasture contaminated with encysted cercariae. The parasites then migrate through the gut wall and peritoneal cavity to the liver and bile ducts, where they mature and produce large numbers of eggs that are excreted into the environment. In common with many helminth infections, the migrating juvenile parasite stages induce a strong Th2-polarized immune response in the mammalian host. Infection of mice with *F. hepatica* can down-regulate Th1-responses *in vivo*, even in IL-4-deficient mice (23) suggesting this is not simply due to the actions of Th2 cells or cytokines. Indeed, the parasites produce a large range of excretory/secretory (ES) molecules that help them to mediate tissue invasion, feeding and immunomodulation (24) including the suppression of IFNγ responses (25).

Bovine tuberculosis (BTB), caused by infection with the bacterium *M. bovis* is an important pathogen of cattle worldwide and has zoonotic potential. Although some countries have reduced or eliminated BTB, wildlife *M. bovis* reservoirs and the limitations of diagnostic tests have hindered successful eradication in other regions. The single intradermal comparative cervical tuberculin test (SICCT) and the *in vitro* IFNγ assay are commonly used to identify *M. bovis* infected cattle. However, certain parasite co-infections can reduce the sensitivity of these assays. A large-scale epidemiological study in England and Wales showed that in dairy herds with a high incidence of *F. hepatica* fewer animals were detected as positive reactors against BTB (26). Experiments in cattle confirmed that infection with *F. hepatica* reduces the sensitivity of the standard BTB tests (SICCT test and IFNγ test) through reduced *M. bovis*-specific Th1 immune responses (27). However, *F. hepatica* co-infection did not influence the detection of visible lesions in BTB infected cows (28). These data clearly show how the immunomodulatory effects of *F. hepatica* on the bovine host can reduce the sensitivity of current pre-mortem BTB tests. This may significantly influence the ability of practical measures to eliminate BTB infections in regions with high prevalence of *F. hepatica*.

Despite the reduced *M. bovis*-specific Th1 immunity in cows co-infected with *F. hepatica*, mycobacterial burdens were shown to be reduced (29). The mechanisms responsible for this are uncertain, but the authors proposed that the actions of alternatively-activated macrophages induced in response to *F. hepatica* infection may act to limit the proliferation of *M. bovis*.

In sheep, infections with the liver flukes *Dicrocoelium dentriticum* or *F. hepatica* can predispose the ewes to mastitis in the immediate *post-partum* period (30). Abnormal metabolism of carbohydrates during the later stages of pregnancy in ewes can cause pregnancy toxemia. This disease is associated with hyperketonaeimia, and blood concentrations of the ketone body β-hydroxybutyrate can help detect ewes at risk of developing pregnancy toxemia. Higher concentrations of β-hydroxybutyrate were recorded in trematode-infected ewes (30). Since β-hydroxybutyrate may have immunomodulatory effects, the authors hypothesized that its increased levels in infected ewes may suppress immunity in the udder enhancing the risk of infection at this site (30). This has raised the hypothesis that the use of anthelmintic drugs may also help reduce the incidence of mastitis in trematode-affected flocks.

Finally, infection with the human liver fluke *Opisthorchis viverrini* is endemic in the Greater Mekong sub-region. This fluke is classified as a group 1 carcinogen by the International Agency for Research on Cancer because chronic infections with *O. viverrini* can lead to the development of cholangiocarcinoma, a malignant cancer of the bile ducts. In areas of Thailand where flukes are endemic, the Gram-negative bacterium *Helicobacter pylori* was found in 66.7% of the patients studied that had cholangiocarcinoma (31). This raised the hypothesis that co-infections with *H. pylori* and with *O. viverrini* synergistically increases the severity of hepatobiliary abnormalities. Indeed, in an experimental hamster model the severity of the hepatobiliary abnormalities was increased in those that were co-infected with *O. viverrini* (32).

Effects on Schistosome (Blood Fluke) Infections

Infections with schistosomes cause chronic inflammatory disease in humans and animals. The diseases they cause can lead to the development of severe pathology, significant morbidity, and economic loss. Schistosomes are transmitted through the skin via contact with infected water sources inhabited by the snail vector. The parasites establish chronic infections in the mammalian

host's bloodstream where they mature, mate, and produce substantial quantities of eggs. The eggs enter the intestines and bladder where they are excreted via feces and urine. Deposition of the eggs in host tissues can cause chronic inflammation, tissue damage and fibrosis. Schistosomes typically induce a Th2-polarized immune response in the mammalian host that enables them to establish chronic infections where they can persist for years (33).

Experiments in mice have shown that a gastrointestinal nematode infection can influence the pathogenesis of a subsequent schistosome infection. A chronic *Trichuris muris* infection within the large intestine enhanced the survival and migration of *S. mansoni* schistosomula to the portal system. Consequently, schistosome worm and egg burdens and associated pathology were enhanced when compared to mice infected with *S. mansoni* alone (34). This suggests that the immunomodulatory effects elicited in the mucosa of the large intestine to enable the gastrointestinal helminth to establish chronic infection can extend to other host tissues. This may exacerbate host susceptibility to subsequent co-infection with other helminth parasites. A similar effect has been reported to occur in a naturally-affected livestock species. A longitudinal study of free-ranging African buffalo reported that animals infected with *Cooperia fuelleborni* had greater burdens of schistosomes (*Schistosoma mattheei*) than those where this nematode species was not detected (35). The mechanisms that mediate these effects in the co-infected animals remain to be determined. This could simply represent host variation in susceptibility to gastrointestinal nematodes. However, since infection of cattle with the related gastrointestinal nematode species *C. oncophora* enhanced their susceptibility to lungworm (*Dictyocaulus viviparus*) infection (36), it is plausible that nematode-mediated effects on the buffalo immune response may similarly impede the establishment of immunity to schistosomes.

However, it is important to note that data from mouse studies show that differences in the species of the co-infecting parasite may have contrasting effects on schistosome infections (34, 37). The gastrointestinal helminth *H. polygyrus* establishes infection specifically within the murine duodenum. In mice infected with *H. polygyrus* a marked reduction in schistosome egg-induced hepatic pathology was observed. This effect appeared to correlate with significant decreases in the expression of pro-inflammatory cytokines responsible for the induction of the egg-induced immunopathology (37). Thus, although co-infection with gastrointestinal helminths may significantly impact on schistosomiasis, the currently available data do not help us to reliably predict whether they are likely to exacerbate or reduce the disease pathogenesis.

TRYPANOSOMES

African Trypanosomes

African trypanosomes are single-cell extracellular hemoflagellate protozoan parasites and are transmitted between mammalian hosts via blood-feeding tsetse flies of the genus *Glossina*. The *Trypanosoma brucei rhodesiense* and *T. b. gambiense* subspecies cause human African trypanosomiasis in endemic regions within the tsetse fly belt across sub-Saharan Africa. Animal African trypanosomiasis is caused by *T. congolense*, *T. vivax,* and *T. brucei* and inflicts substantial economic strains on the African livestock industry. The parasitic life cycle within the mammalian host is initiated by the intradermal injection of metacyclic trypomastigotes by the tsetse fly vector. The extracellular parasites then reach the draining lymph nodes, presumably via invasion of the afferent lymphatics and then disseminate systemically (38, 39). During this process the metacyclic trypanosome forms differentiate into long slender bloodstream forms that are adapted for survival within the mammalian host. When C57BL/6 mice are infected with *T. brucei* the initial parasitaemic wave coincides with the expression of high levels of IFNγ by the host in an attempt to control the infection. However, the trypanosomes also cause significant immunosuppression enabling them to establish chronic infections in the hostile environment of the host's bloodstream.

A study has shown that the severity of malaria and trypanosomiasis was exacerbated in mice co-infected with *P. berghei* and *T. brucei* (40). In the co-infected mice survival rates were reduced and the parasitaemias were greater, with more severe anemia and hypoglycaemia. Each of these infections induces a strong pro-inflammatory response with high levels of IFNγ. Further studies are necessary to determine whether additive/synergistic effects of each infection on IFNγ expression are responsible for the increased disease severity observed in the co-infected mice.

Trypanosome infections may also modulate host susceptibility to infection with some pathogenic bacteria. For example, in mice chronically-infected with either *Brucella melitensis*, *B. abortus,* or *B. suis*, the burden of bacteria in the spleen was reduced if the mice were also co-infected with *T. brucei* (41). The effects of *T. brucei* infection on *Brucella* burdens in co-infected mice were impeded in the absence of functional IL-12p35/IFNγ signaling. This suggests that the strong pro-inflammatory IFNγ-mediated immune response induced by the *T. brucei* infection aided the clearance of *Brucella*. Thus, although infections with *T. brucei* can induce significant levels of immunosuppression and immunopathology, this study shows that under some circumstances the host's response to *T. brucei* infection may provide protection against co-infection with other pathogens (41). However, this not true for all pathogenic bacteria. Although Th1 responses are essential for protection against *Mycobacterium tuberculosis*, *T. brucei* infection did not ameliorate the susceptibility of mice to co-infection with this pathogenic bacterium (41).

T. cruzi

Infection with the obligate intracellular parasite *T. cruzi* causes Chagas' disease and is an important cause of morbidity and mortality in humans in Central and South America (42). Concurrent infection of mice with *S. mansoni* can significantly affect disease pathogenesis and susceptibility following infection with *T. cruzi* (43). The co-infected mice were shown to be unable to effectively control the *T. cruzi* infection, and the increased parasitic load was accompanied by substantial inflammation in their livers. Infections with *T. cruzi* are associated with

the establishment of a Th1-polarized immune response, and the production of macrophage-derived NO from arginine by inducible NO synthetase (iNOS) is important for parasite clearance. However, during the chronic phase of schistosomiasis high levels of arginase-1 are instead expressed by alternatively activated macrophages. In the *S. mansoni* co-infected mice, the reduced protection against *T. cruzi* coincided with the reduced production of IFN-γ and NO (43). This study illustrates how macrophage polarity and the relative expression levels of iNOS and arginase-1 in response to infection with one parasite could influence the host's ability to co-infection with other parasites.

APICOMPLEXAN PARASITES

Toxoplasma gondii

T. gondii is an orally-acquired obligate intracellular protozoan parasite affecting ∼30% of the human population. Following oral infection, the parasites typically disseminate systemically and convert into dormant stages in muscle tissues and the brain. Infection with *T. gondii* elicits a strong Th1-polarized immune response characterized by production of IFNγ, IL-12, and parasite specific IgG2a antibodies. Studies in mice suggest these responses are important for host protection. Infections are typically asymptomatic in immunocompetent humans, but can reactivate in immunocompromised individuals and result in the development of a life-threatening encephalitis.

Although a study has shown that gastrointestinal helminth (*H. polygyrus*) co-infection did not affect the induction of a protective Th1 response to *T. gondii* infection (44), the Th2-response to the *H. polygyrus* infection was impeded. Co-infection with *T. gondii* in these mice was instead accompanied by a shift toward a non-protective helminth-specific Th1 response (44). Conversely, separate studies have shown that *H. polygyrus* co-infection can negatively impact upon $CD8^+$ T cell differentiation and cytokine production in response to *T. gondii* infection (45, 46). Conventional dendritic cells from the *H. polygyrus* co-infected mice also had reduced expression of IL-12 (46). The reasons for the contrasting outcomes in these two studies are not immediately apparent, but are perhaps explained by important differences in their experiment design. In the first study (44), the mice were first infected with *T. gondii* and 14 days later orally co-infected with *H. polygyrus*. However, in the other studies (45, 46), the mice were first infected with *H. polygyrus* and subsequently co-infected with *T. gondii* parasites.

Although further experiments are necessary to confirm the cellular and molecular mechanisms that underpin these effects, these studies suggest that differences in the order and timing of the infections with two distinct oral pathogens, can significantly influence the host's response to the second. In particular these data imply that the presence of a strong Th1-polarized immune response to an ongoing *T. gondii* infection can impede the development of Th2-polarized immune responses to a subsequent helminth co-infection (44). However, the induction of CD8+ T-cell responses against *T. gondii* co-infection is impeded in the presence of an existing Th2-polarized immune response to a gastrointestinal helminth infection.

Eimeria

Eimeria tenella is a major pathogen of chickens causing intestinal coccidiosis. Infection with *E. tenella* is restricted to the caecum and causes significant morbidity and mortality, including diarrhea, mucosal lesions and weight loss. The prevalence of *E. tenella* and *T. gondii* is widespread, suggesting co-infections with these two pathogens may be common. The effect of co-infection of chickens with *Eimeria* and *T. gondii* has been addressed in an experimental study (47). However, the pathology and immune response following co-infection with these parasites did not differ significantly from that observed in chickens infected with *Eimeria* alone. Co-infection with *Eimeria* also did not affect the abundance of *T. gondii*-positive tissue samples or the clinical course of *T. gondii* infection. Distinct *T. gondii* strain types have been characterized in Europe and North America (type I, II, and III) and these can significantly influence the virulence and severity of the disease in different host species (48). For example, chickens are generally considered refractory to infection with type I or II oocysts (49, 50), but they may cause severe disease in other host species such as mice (51). Whereas, co-infection of chickens with two common apicomplexan parasites did not reveal any significant mutual effects on disease pathogenesis (47), a study of wild rabbits in Scotland suggested a link between *T. gondii* infection and higher burdens of *E. stiedae* (52). Whether differences in the virulence of *T. gondii* infection in different host species could have a significant impact on their susceptibility to co-infection with other pathogens remains to be determined. Of course, the possibility also cannot be excluded that the rabbits with high *Eimeria* burdens had high susceptibility to orally-acquired parasite infections.

Giardia

Infection with *Giardia duodenalis* (syn. *G. intestinalis*, or *G. lamblia*) is a leading cause of waterborne diarrhoeal disease. The characteristic signs of Giardiasis include diarrhea, abdominal pain, nausea, vomiting, and anorexia, with some individuals also developing extra-intestinal and post-infectious complications. Little is currently known of the effects of parasite co-infections on susceptibility to giardiasis. A study of 3 year old children in the Quininde district of Ecuador has shown that those co-infected with the gastrointestinal helminth *A. lumbricoides* had plasma cytokine profiles indicative of an increased Th2/Th1 cytokine bias, and significantly lower plasma levels of IL-2 and TNF-α when compared to those infected with *G. lamblia* alone (53). Studies from mouse models have shown that expression of TNF-α is essential for resistance to *G. lamblia* infection (54). Little is known of the mechanisms that are essential for protection of humans against *Giardia* infections. However, it is plausible that the effects of *Ascaris* infection on TNF-α expression may have negatively affected the ability of the children to eradicate *Giardia*.

EFFECTS ON BACTERIAL INFECTIONS

Effects on *Salmonella* Pathogenesis

Oral infections with the Gram negative bacterium *Salmonella*, through consumption of contaminated food such as meat, eggs, or milk are amongst the most common causes of diarrhea.

Co-infections with distinct parasites, helminths, and malaria parasites, have each been shown to exacerbate susceptibility to, or the pathogenesis of, salmonellosis.

Many of the examples discussed above have suggested a link between the induction of a Th2-polarized immune response to helminth infection and the reduced development of Th1-polarized immunity to co-infection with other pathogens. However, co-infection of mice with the gastrointestinal helminth *H. polygyrus* has also been shown to enhance the pathogenesis of infection with *Salmonella enterica* serovar Typhimurium independently of the actions of Th2 cells and regulatory T cells (55). Here, co-infection with *H. polygyrus* has been reported to disrupt the metabolic profile within the small intestine, and by doing so, directly affect the invasive capacity of *S. typhimurium*. This helminth infection was shown to mediate this effect through the enhancement of bacterial expression of *Salmonella* pathogenicity island 1 (SPI-1) genes (55). This study reveals a novel immune system-independent mechanism by which a helminth-modified metabolome in the host's intestine can promote susceptibility to bacterial co-infection.

Invasive nontyphoid *Salmonella* (NTS) bacteraemia is a common cause of community-acquired bacteraemia in the human populations of several regions of sub-Saharan Africa (56). Associations between NTS co-infection and high malaria mortality have been reported (57), and a study of hospitalized children in north-eastern Tanzania showed that a decline in malaria cases was associated with a similar decline in the incidence of NTS and other forms of bacteraemia (58).

Since malaria parasites establish infection within erythrocytes, the daily rounds of parasite replication within these cells can cause high levels of erythrocyte lysis and haemolysis, resulting in anemia. The association of NTS infection with haemolysis is well-established in humans with malaria, especially in patients with severe malarial anemia (59). This haemolysis releases large quantities of cell-free haeme which is toxic to the host. To counter this cytotoxicity, haeme oxygenase 1 (HO-1) expression is induced to degrade the haeme and provide tolerance toward some of the pathological consequences of malaria infection. The actions of HO-1 also provide an additional cytoprotective role by limiting the production of reactive oxygen species (60). However, data from mice (61) and from the analysis of neutrophils from malaria-infected children (62) show that the actions of HO-1 in granulocytes in response to haemolysis during malaria infection impedes their oxidative burst activity and production of reactive oxygen species. This leads to dysfunctional granulocyte mobilization and long-term neutrophil dysfunction. As a consequence, *Salmonella* are able to survive and proliferate within neutrophils during malaria infection due to their decreased oxidative burst activity, leading to increased NTS susceptibility (61, 62). These data clearly show how a host-induced cytoprotective response to one of the pathological consequences of malaria infection (haemolysis) can significantly impair neutrophil-mediated resistance to co-infection with another pathogen.

Mycobacterium tuberculosis

Infection with the obligate intracellular bacterium *M. tuberculosis* causes tuberculosis (TB), a chronic disease affecting ∼2 billion people worldwide. This infection typically affects the lungs, and the majority of individuals infected with *M. tuberculosis* have latent infections and are asymptomatic. However, data from various clinical studies in humans have raised the hypothesis that helminth co-infections may affect TB susceptibility and the risk of developing latent *M. tuberculosis* infection, as co-infected patients often displayed more advanced disease (63, 64). Gastrointestinal helminth infections may also modulate susceptibility and/or disease pathogenesis to co-infection with other pathogenic *Mycobacteria* spp. Infection with *M. leprae* or *M. lepromatis* causes leprosy, a chronic granulomatous infectious disease. A study of Indonesian patients infected with *M. lepromatis* reported that those with gastrointestinal helminth infections (e.g., *T. trichiura*, *Stongyloides sterocalis*) similarly presented with more severe types of leprosy (65).

Studies from animal models, especially mice, indicate that protection against TB infection is dependent upon the induction of a strong pro-inflammatory Th1-polarized immune response and production of IFNγ, IL-12, and TNF-α, as well as contribution from Th17 cells and IL-17 and IL-23 (66, 67). The immune response induced by co-infection with gastrointestinal helminths may affect immunity to *M. tuberculosis* through a range of distinct mechanisms, including the induction of regulatory T cell responses (68), modulation of Th1 and Th17 responses to the bacterial infection and reduced expression of effector cytokines (69–71). The increased expression of Th2 cytokines, especially IL-4, in mice co-infected with helminths also promotes the induction of alternatively activated macrophages. These cells have been shown to be less effective than pro-inflammatory IFNγ-stimulated macrophages in controlling *M. tuberculosis* (72, 73). Indeed, antigens from helminths such as *T. muris* and *Hymenolepis diminuta* (tapeworms) can induce an alternatively activated phenotype in human macrophages, reducing their ability to control *M. tuberculosis* infection *in vitro* (74). However, mouse studies show that under some circumstances the acute host response to helminth infection might enhance the early control of *M. tuberculosis* infection by alveolar macrophages (75).

Although the induction of T cell responses is considered essential for protective immunity against TB infection, B cells, and the production of mycobacterial-specific antibodies have also been proposed to play an important role (76). However, helminth infections can also influence B cell responses to *M. tuberculosis* infection. Co-infection of humans with *Strongyloides stercoralis* has been shown to affect B cell responses during latent tuberculosis infection, significantly reducing B cell numbers, the induction of mycobacterial-specific IgM and IgG resopnses and expression levels of the B-cell growth factors APRIL and BAFF (77). These helminth-associated impairments to mycobacteria-specific B cell responses could have significant implications for the efficacy of vaccine-induced immune responses to TB in affected regions. However, a clinical trial study in healthy, previously BCG vaccinated adolescents reported that helminth

co-infection (*S. mansoni* did not impact on the efficacy of a candidate viral vector-based TB vaccine (78).

Pneumonia

A study of goats in Nigeria revealed that the incidence of pneumonia corresponded with the presence of gastrointestinal parasitism in the same animals (79). Furthermore, a strong association was observed between the occurrence of helminth infections and granulomatous pneumonia. In this study the affected goats were often hydrated, implying that the gastrointestinal helminth infections may have caused pulmonary oedema due to increased fluid accumulation in the lung. The authors suggested that may this have reduced the efficacy of immunity in the lung, enabling other pathogenic microorganisms (bacteria and/or viruses) to establish infection and the subsequent development of pneumonia (79).

Pathogenic *Escherichia coli*

The zoonotic bacterium *E. coli* O157 is a worldwide problem for public health causing haemorrhagic diarrhea in infected humans. Cattle are considered the major reservoir for human infection, and infection in these animals is usually asymptomatic. A study of 14 British farms suggested that co-infection with the liver fluke *F. hepatica* may increase the risk of *E. coli* O157 shedding (80). This implies that strategies aimed at controlling *F. hepatica* infection may have additional benefit by reducing the shedding of *E. coli* O157.

Giardia lamblia and enteroaggregative *E. coli* are two of the most commonly isolated pathogens in malnourished children. Mice fed on a protein-deficient diet were used to model the pathogenesis of co-infection with these pathogens in malnourished individuals (81). The malnourished mice fed a protein-deficient diet exhibited significantly greater weight loss following co-infection with *G. lamblia* and enteroaggregative *E. coli* when compared to co-infected mice that received a normal diet. This study reveals how the combined effects of the composition of the host's diet and pathogen infection can affect disease pathogenicity. Studies using a laboratory biofilm system to mimic the human gut microbiota have revealed that *G. duodenalis* can cause significant dysbiosis. These effects were mediated in part through the actions of secretory-excretory *Giardia* cysteine proteases, and these could promote gut epithelial cell apoptosis, tight junction disruption, and bacterial translocation across the gut epithelium (82).

Despite the ability of *Giardia* infection to cause intestinal dysbiosis, in countries with poor standards of sanitation *Giardia* infection has been associated with decreased incidence of diarrhoeal disease. This raised the hypothesis that infection with *Giardia* spp. might modulate host responses to co-infection with attaching and effacing enteropathogens. Weight loss, pathological signs of colitis and bacterial colonization and translocation were significantly attenuated in mice co-infected with *G. muris* and the attaching and effacing enteropathogen *Citrobacter rodentium* (83). These effects coincided with enhanced secretion of the antimicrobial factors β-defensin 2 and trefoil factor 3 by gut epithelial cells during co-infection (83). This suggests that components of the host response to infection with *Giardia* spp. (e.g., production of antimicrobial factors) may reduce susceptibility to gastrointestinal co-infection with certain pathogenic bacteria. These studies also highlight how differences in the anatomical niches that the parasites inhabit may also have a significant influence on the disease pathogenesis of a bacterial co-infection. When pathogens infect the same niche such as the gastrointestinal tract, infection with *Giardia* spp. may provide protection against bacterial co-infection (83). Conversely, infection with *F. hepatica* in the liver was associated with the enhanced pathogenesis of a bacterial co-infection in the intestine (80).

EFFECTS ON VIRAL INFECTIONS

Several studies have revealed how parasite co-infections, especially helminths, can reduce immunity to important viral pathogens. In many of these instances the induction of a Th2-polarized immune response to the parasite infection appears to impede the development of effective antiviral immunity. For example, mice co-infected with the gastrointestinal helminths *Trichinella spiralis* or *H. polygyrus* and mouse norovirus (MNV) had increased viral loads and reduced levels of virus-specific CD4+ T cells expressing IFNγ and TNF-α when compared to mice infected with norovirus alone (84). The production of Th2 cytokines during helminth infection is associated with the expression of the transcription factor signal transducer and activator of transcription 6 (STAT6) by alternatively activated macrophages. In mice deficient in STAT6, viral loads were reduced when compared to wild-type controls indicating that the induction of STAT6-dependent alternatively activated macrophages during helminth infection can impede the induction of antiviral innate and adaptive immunity (85). As well as impeding the efficacy of anti-viral immunity, the expression of IL-4 and activation of the transcription factor STAT6 during helminth infection in mice can also promote the reactivation of a latent γ-herpesvirus infection (85). The sections below describe how parasite co-infections may impede immunity to certain viral pathogens, but examples are also provided where potential host-protective effects have been proposed.

Impeding Viral Immunity

Hepatitis C Virus (HCV)

Infections with HCV can cause liver fibrosis and cirrhosis and are major causes of chronic liver disease throughout the world. A study of Egyptian HCV patients co-infected with *S. mansoni* showed that these individuals had significantly higher concentrations of HCV proteins in distinct stages of the virus-mediated hepatic fibrosis (86). Co-infected individuals may also have an increased rate of progressing through the different pathological stages of HCV-mediated hepatic fibrosis than those infected with HCV alone. The authors suggested that the immune response induced in response to *S. mansoni* infection may have led to enhanced HCV propagation and increased concentration of HCV proteins. This implies that that components of the immune response to the schistosome infection may have suppressed the HCV-induced Th1 cytokine

production, reducing antiviral immunity. Treatment of co-infected patients with anti-schistosome therapy may therefore help to decrease the progression rate of the HCV-induced hepatic fibrosis.

Human Immunodeficiency Virus (HIV)

African adults infected with HIV are often co-infected with gastrointestinal parasites. A study of HIV-infected Ugandans showed a high prevalence of parasitic infections (especially *Necator americanus*), and co-infection with hookworms correlated with much lower peripheral blood $CD4^+$ T cell levels than those infected with HIV alone (87). This raises the suggestion that individuals co-infected with hookworms and HIV are at a distinct immunologic disadvantage when compared to those infected with HIV alone. This hypothesis has been experimentally tested in mice using a helminth/retrovirus co-infection model (88). Although the ability of the mice to control the *L. sigmodontis* infection was not affected in the co-infected mice, helminth infection did interfere with the host's ability to the control of the viral infection. Levels of virus-specific $CD8^+$ T cells, $FoxP3^+$ regulatory T cells, and cytokines were similar in co-infected mice and those infected with Friend virus alone. The increased viral loads in co-infected mice were instead associated with reduced titres of neutralizing virus-specific IgG2b and IgG2c antibodies. However, earlier studies in humans have reported no beneficial effect of antihelminthic treatment on HIV viral loads [plasma HIV-1 RNA concentrations; (89)], and other studies have suggested that helminth co-infections do not exacerbate HIV infection (90). On face value, the prospective studies undertaken in humans suggest that antihelmitic treatments or helminth-specific vaccines are unlikely to have any beneficial effects in regions with high incidence of helminth and HIV infections. However, further studies are necessary to determine whether additional factors such as host age, the intensity of the helminth infection or magnitude of the viral load affect the efficacy of such approaches.

Human T-Cell Lymphotropic Virus-1 (HTLV-1)

Strongyloides stercoralis is a soil-transmitted intestinal helminth parasite of humans. Infection occurs following penetration of the skin by filiform larvae. The majority of *S. stercoralis* infections are asymptomatic to mild, but a life-threatening hyper-infection syndrome can develop in immunosuppressed hosts. This is accompanied by the massive dissemination of the filariform larvae from the colon to the lungs, liver, central nervous system, or kidneys. Co-infection with HTLV-1 can impede the induction of Th2-polarized immunity (91, 92), and patients infected with HTLV-1 have more frequent and more severe forms of strongyloidiasis. Patients co-infected with HTLV-1 and *S. stercoralis* were shown to have higher parasite burdens than those with strongyloidiasis alone (93). Mouse models have shown that IL-5-mediated eosinophil production and activation is important for protection against infection with *S. stercoralis* (94). In patients co-infected with HTLV-1 and *S. stercoralis* both parasite antigen-specific IL-5 responses and eosinophil levels were significantly decreased, suggesting an additional means by which the virus infection may impede immunity to helminths. However, rare incidences of acute respiratory distress syndrome have been encountered in HTLV-1-infected patients following treatment with antihelminthics (95). The mechanisms responsible for the development of this pathology are unknown, but it is plausible that acute immune reactions to the intrapulmonary destruction of the large parasite burden following antihelminthic treatment may play a role in triggering this response (95).

Vaccinia Virus

A study in BALB/c mice has shown that co-infection with *Ascaris* in *Vaccinia* virus-infected hosts enhances the virus-associated pathology due to impaired *Vaccinia* virus-specific immunity (96). The levels of splenic CD8+ T cells in the co-infected mice were significantly reduced, as was the frequency of IFN-γ-producing virus-specific $CD4^+$ and $CD8^+$ T cells. Similar effects have also been reported in mice co-infected with *S. mansoni* (97). In this study *Vaccinia* virus-specific $CD8^+$ cytotoxic T-cell responses were reduced in the mice co-infected with *S. mansoni*, suggesting a mechanistic link between the increased viral loads and reduced viral clearance. Since many chronic helminth infections induce a strong Th2-polarized immune response, the above examples suggest that the presence of this cytokine milieu at the time of virus co-infection may play an important role in impeding the induction of the IFNγ-mediated control of virus replication.

Respiratory Syncytial Virus (RSV)

In contrast to the above reports, it is plausible that in some circumstances that co-infection with helminths may enhance protection against viruses. Respiratory syncytial virus (RSV) is a major respiratory pathogen, and nearly all infants are infected with this virus by the age of 2 years old. However, because the virus does not induce lasting immunity recurrent RSV infections can occur throughout life. A study has shown how a gastrointestinal helminth infection can promote protective antiviral effects in the lung (98). Mice infected with *H. polygyrus* had reduced viral loads after co-infection with RSV and developed significantly less disease and pulmonary inflammation. These effects were not a considered to be a consequence of the induction of a Th2-polarized immune response to the worm infection. Instead, *H. polygyrus* infection coincided with the upregulated expression of type I IFN in the gut and the lung in a microbiota-dependent manner. Furthermore, the protective effects of helminth infection on RSV co-infection were impeded in mice lacking type I IFN receptor signaling (*Ifnar1*-deficient mice).

Virus Infection in Amphibians

All the above studies have described parasite virus co-infections in mammals or birds, but similar interactions have been reported in experimental amphibians. Prior infection of the larval stages (tadpole) of four distinct amphibian species with trematode parasites (*Echinoparyphium* spp.) significantly reduced viral loads following co-infection with ranavirus (99). Furthermore, *Echinoparyphium* co-infection coincided with reduced ranavirus transmission within a community of larval wood frogs (*Lithobates sylvaticus*). The cellular

and molecular mechanisms by which helminth co-infection mediated these effects on ranavirus pathogenesis remain to be determined.

INFECTIONS WITH PRIONS (TRANSMISSIBLE SPONGIFORM ENCEPHALOPATHIES)

Prions are a unique group of pathogens that can cause infectious, chronic, neurodegenerative diseases in humans and some domesticated and free-ranging animal species. The precise nature of the infectious prion is uncertain, but an abnormal, relatively proteinase-resistant isoform (PrP^{Sc}) of the host cellular prion protein (PrP^{C}), co-purifies with prion infectivity in diseased tissues (100). Many natural prion diseases are acquired by oral consumption of contaminated food or pasture. The gut-associated lymphoid tissues (GALT) within the lining of the intestine such as the tonsils, Peyer's patches, appendix, colonic, and caecal patches, together with the mesenteric lymph nodes, help to provide protection against intestinal pathogens. However, the early replication of prions within the Peyer's patches in the small intestine is essential for their efficient spread of from the gut to the brain (a process termed *neuroinvasion*) (101–104).

Natural prion disease susceptible hosts such as sheep, deer, and cattle are regularly exposed to helminths but it is uncertain whether co-infections with these pathogens can influence oral prion disease pathogenesis, for example by causing damage to the gut epithelium and enhancing the uptake of prions into the GALT. In one study, lambs with high genetic susceptibility to natural sheep scrapie were experimentally co-infected with *Teladorsagia circumcincta* at monthly intervals from 6 to 11 months old and effects on prion disease determined (105). Although no mechanistic insights were reported, the authors suggested that the onset of prion disease was shortened in the co-infected lambs. However, the significance of data reported in this study is unclear as the animals were co-infected with *T. circumcincta* long after prion neuroinvasion from the intestine had occurred (106, 107). Conversely, when mice were co-infected with the large intestine-restricted helminth pathogen *T. muris* around the time of oral prion exposure, no effects on prion disease duration were observed (104). This is most likely because the large intestinal GALT are not important early sites of prion accumulation and neuroinvasion (104). Clearly additional studies are required to determine whether the pathology specifically in small intestine caused by a helminth infection may influence the prion neuroinvasion from the gut to the brain.

CONCLUDING REMARKS

Infectious diseases are commonly studied in experimental animals exposed to individual pathogenic microorganisms. However, this review described many examples of how infection with certain parasites can have a dramatic influence on host susceptibility or disease pathogenesis to co-infection with other pathogens. Many of these studies have reported correlations between alterations to specific immune parameters (T cell polarity etc.) and pathogen susceptibility, raising the hypothesis that many of the effects of co-infection are immune mediated. For example, alterations to the polarity of the T-cell response or macrophage phenotype induced by the parasite infection could affect the induction of protective immunity to co-infection with another pathogen. Further scrutiny of these studies shows that in many instances definitive demonstrations that the effects are indeed immune-mediated are lacking. Addressing these issues in natural host species is technically challenging. However, a large array of murine *in vivo* tractable systems are now available that enable the contributions of specific cellular and molecular immune components to be determined.

Laboratory mice housed to high microbiological status in specific-pathogen free conditions have proved to be highly tractable model systems in which to study the pathogenesis of many infectious diseases. How representative these mice are to natural host species in field conditions is questionable, since wild mice are typically infected with numerous micro- and macro-parasite species. The immune status of laboratory mice and wild mice differs significantly (108). Wild mice are markedly more antigen-experienced than laboratory mice, displaying on-going immune activation and the presence of an inflammatory myeloid cell subset that has not been detected in laboratory mice. Wild mice also express cytokine responses to microbial ligands that are similar or lower when compared to laboratory mice, and have highly heterogeneous gut microbiomes (108, 109). This suggests that the high level of pathogen exposure is a major driver of the enhanced immune activation in wild mice.

Many of the above examples suggest links between alterations to Th2/Th1 polarity or the nature of the innate immune response and susceptibility to pathogen co-infection. However, the underlying rules that dictate whether these interactions are likely to confer increased susceptibility or protection are not always apparent and are likely influenced by multiple factors. For example, susceptibility to these co-infections may be dependent on the individual niches that each pathogen inhabits in the host e.g., the same niche, or mucosal (gastrointestinal) vs. systemic. In other situations, the induction of a strong pro-inflammatory response to a parasite infection may exacerbate susceptibility and/or pathology following co-infection with another pathogen that induces a similar pro-inflammatory response. Chronic helminth infection in mice also promoted the reactivation of a latent virus infection. But not all the effects on co-infection appear to be directly immune mediated, as disruptions to the metabolic profile within the gastrointestinal tract following helminth infection promoted susceptibility to co-infection with certain pathogenic bacteria. As well as influencing host susceptibility to pathogen co-infection, the immune response to certain parasite infections may have other important health issues by negatively affecting the induction of antigen-specific immunity to vaccine antigens, reducing vaccine efficacy.

A greater understanding of how infectious disease susceptibility and pathogenesis are influenced by concurrent parasite infections will help the design of more effective treatments to control the spread of infectious diseases. For example, some helminth-derived ES products possess potent immunoregulatory properties, and these could be sufficient to suppress allograft rejection (110). Whether similar parasite-derived molecules can suppress host-responses to other pathogens, or conversely can be used therapeutically to enhance their clearance, remains to be determined.

AUTHOR CONTRIBUTIONS

The author confirms being the sole contributor of this work and has approved it for publication.

FUNDING

This work was supported by project and Institute Strategic Programme Grant funding from the Biotechnology and Biological Sciences Research Council (grant numbers BB/G003947/1 and BBS/E/D/20002174).

REFERENCES

1. Inclan-Rico JM, Siracusa MC. First responders: innate immunity to helminths. *Trends Parasitol.* (2018) 34:861–80. doi: 10.1016/j.pt.2018.08.007
2. Allen JE, Maizels RM. Diversity and dialogue in immunity to helminths. *Nat Rev Immunol.* (2011) 11:375–88. doi: 10.1038/nri2992
3. Gerbe F, Sidot E, Smyth DJ, Ohmoto M, Matsumoto I, Dardalhon V, et al. Intestinal epithelial tuft cells initiate type 2 mucosal immunity to helminth parasites. *Nature* (2016) 529:226–30. doi: 10.1038/nature16527
4. Langhorne J, Ndungu FM, Sponaas AM, Marsh K. Immunity to malaria: more questions than answers. *Nat Immunol.* (2008) 9:725–32. doi: 10.1038/ni.f.205
5. Perez-Mazliah D, Langhorne J. CD4 T-cell subsets in malaria: TH1/TH2 revisited. *Front Immunol.* (2015) 5:671. doi: 10.3389/fimmu.2014.00671
6. Hoeve MA, Mylonas KJ, Fairlie-Clarke KJ, Mahajan SM, Allen JE, Graham AL. *Plasmodium chabaudi* limits early *Nippostrongylus brasiliensis*-induced pulmonary immune activation and Th2 polarization in co-infected mice. *BMC Immunol.* (2009) 10:60. doi: 10.1186/1471-2172-10-60
7. Karadjian G, Berrebi D, Dogna N, Vallarino-Lhermitte N, Bain O, Landau I, et al. Co-infection restrains *Litomosoides sigmodontis* filarial load and plasmodial *P. yoelii* but not *P. chabaudi parasitaemia* in mice. *Parasite* (2014) 21:16. doi: 10.1051/parasite/2014017
8. Craig JM, Scott AL. Antecedent *Nippostrongylus* infection alters the lung immune response to *Plasmodium berghei*. *Parasite Immunol.* (2016) 39:e12441. doi: 10.1111/pim.12441
9. Hartmann W, Haben I, Fleischer B, Breloer M. Pathogenic nematodes suppress humoral responses to third-party antigens *in vivo* by IL-10-mediated interference with Th cell function. *J Immunol.* (2011) 187:4088–99. doi: 10.4049/jimmunol.1004136
10. Metenou S, Dembele B, Konate S, Dolo H, Coulibaly YI, Diallo AA, et al. Filarial infection suppresses malaria-specific multifunctional Th1 and Th17 responses in malaria and filarial coinfections. *J Immunol.* (2011) 186:4725–33. doi: 10.4049/jimmunol.1003778
11. Bucher K, Dietz K, Lackner P, Pasche B, Fendel R, Mordmüller B, et al. Schistosoma co-infection protects against brain pathology but does not prevent severe disease and death in a murine model of cerebral malaria. *Int J Parasitol.* (2011) 41:21–31. doi: 10.1016/j.ijpara.2010.06.008
12. Su Z, Segura M, Morgan K, Loredo-Osti JC, Stevenson MM. Impairment of protective immunity to blood-stage malaria by concurrent nematode infection. *Infect Immun.* (2005) 73:3531–9. doi: 10.1128/IAI.73.6.3531-3539.2005
13. Graham AL, Lamb TJ, Read AF, Allen JE. Malaria-filaria coninfection in mice makes malarial disease more severe unless filarial infection achieves patency. *J Infect Dis.* (2005) 191:410–21. doi: 10.1086/426871
14. Moriyasu T, Nakamura R, Deloer S, Senba M, Kubo M, Inoue M, et al. *Schistosoma mansoni* infection suprresses the growth of *Plasmodium yoelli* parasites in the liver and reduces gametocyte infectivity in mosquitoes. *PLoS Neglect Trop Dis.* (2018) 12:e0006197. doi: 10.1371/journal.pntd.0006197
15. Nyakundi RK, Nyamongo O, Maamun J, Akinyi M, Mulei I, Farah IO, et al. Protective effect of chronic schistosomiasis in baboons coinfected with *Schistosoma mansoni* and *Plasmondium knowlesi*. *Infect Immun.* (2016) 84:1320–30. doi: 10.1128/IAI.00490-15
16. Lemaitre M, Watier L, Briand V, Garcia A, Le Hesran JY, Cot M. Coinfection with *Plasmodium falciparum* and *Schistosoma haematobium*: additional evidence of the protective effect of schistosomiasis on malaria in Senegalese children. *Am J Trop Med Hyg.* (2014) 90:329–34. doi: 10.4269/ajtmh.12-0431
17. Lyke KE, Dabo A, Arama C, Daou M, Diarra I, Wang A, et al. Reduced T regulatory cell response during acute *Plasmodium falciparum* infection in Malian children co-infected with *Schistosoma haematobium*. *PLoS ONE* (2012) 7:e31647. doi: 10.1371/journal.pone.0031647
18. Cunnington AJ, Walther M, Riley EM. Piecing together the puzzle of malaria. *Sci Trans Med.* (2013) 5:211–8. doi: 10.1126/scitranslmed.3007432
19. Teo T-H, Howland SW, Claser C, Gun SY, Poh CM, Lee WW, et al. Conversely, co-infection with Chikungunya virus alters the trafficking of pathogenic $CD8^+$ T cells into the brain and prevents *Plasmodium*-induced neuropathology. *EMBO Mol Med.* (2018) 10:121–38. doi: 10.15252/emmm.201707885
20. Waknine-Grinberg JH, Gold D, Ohayon A, Flescher E, Heyfets A, Doenhoff MJ, et al. *Schistosoma mansoni* infection reduces the incidence of murine cerebral malaria. *Malaria J.* (2010) 9:5. doi: 10.1186/1475-2875-9-5
21. Wang ML, Feng YH, Pang W, Qi ZM, Zhang Y, Guo YJ, et al. Parasite densities modulate susceptibility of mice to cerebral malaria during co-infection with *Schistosoma japonicum* and *Plasmodium berghei*. *Malaria J.* (2014) 13:116. doi: 10.1186/1475-2875-13-116
22. Abbate JL, Ezenwa VO, Guégan JF, Choisy M, Nacher M, Roche B. Disentangling complex parasite interactions: protection against cerebral malaria by one helminth species is jeopardized by co-infection with another. *PLoS Neglect Trop Dis.* (2018) 12:e0006483. doi: 10.1371/journal.pntd.0006483
23. O'Neill SM, Brady MT, Callanan JJ, Mulcahy G, Joyce P, Mills KH, et al. *Fasciola hepatica* infection downregulates Th1 responses in mice. *Parasite Immunol.* (2000) 22:147–55. doi: 10.1046/j.1365-3024.2000.00290.x
24. Lucena AN, Cuatero LG, Mulcahy G, Zintl A. The immunomodulatory effects of co-infection with *Fasciola hepatica*: from bovine tuberculosis to Johne's disease. *Vet J.* (2017) 222:9–16. doi: 10.1016/j.tvjl.2017.02.007
25. O'Neill SM, Mills KH, Dalton JP. *Fasciola hepatica* cathepsin L cysteine proteinase suppresses *Bordatella pertussis*-specific interferon-gamma production *in vivo*. *Parasite Immunol.* (2001) 23:541–7. doi: 10.1046/j.1365-3024.2001.00411.x
26. Claridge J, Diggle P, McCann CM, Mulcahy G, Flynn R, McNair J, et al. *Fasciola hepatica* is associated with the failure to detect bovine tuberculosis in dairy cattle. *Nat Commun.* (2012) 3:853. doi: 10.1038/ncomms1840
27. Flynn RJ, Mannion C, Golden O, Hacariz O, Mulcahy G. Experimental *Fasciola hepatica* infection alters responses to tests used for diagnosis of bovine tuberculosis. *Infect Immun.* (2007) 75:1373–81. doi: 10.1128/IAI.01445-06
28. Byrne AW, Graham J, Brown C, Donaghy A, Guelbenzu-Gonzalo M, McNair J, et al. Bovine tuberculosis visible lesions in cattle culled during herd breakdowns: the effects of individual characteristics trade movement and co-infecion. *BMC Vet Res.* (2017) 13:400. doi: 10.1186/s12917-017-1321-z

29. Garza-Cuartero L, O'Sullivan J, Blanco A, McNair J, Welsh M, Flynn RJ, et al. *Fasciola hepatica* infection reduces *Mycobacterium bovis* burden and mycobacterial uptake and suppresses the pro-inflammatory response. *Parasite Immunol.* (2016) 38:387–402. doi: 10.1111/pim.12326
30. Mavrogianni VS, Papadopoulos E, Spanos SA, Mitsoura A, Ptochos S, Gougoulis DA, et al. Trematode infections in pregnant ewes can predispose to mastitis during the subsequent lactation period. *Res Vet Sci.* (2014) 96:171–9. doi: 10.1016/j.rvsc.2013.11.009
31. Boonyanugomol W, Chomvarin C, Sripa B, Bhudhisawasdi V, Khuntikeo N, Hahnvajanawong C, et al. *Helicobacter pylori* in Thai patients with cholangiocarcinoma and its association with biliary inflammation and proliferation. *HPB* (2012) 14:177–84. doi: 10.1111/j.1477-2574.2011.00423.x
32. Dangtakot R, Pinlaor S, Itthitaetrakool U, Chaidee A, Chomvarin C, Sangka A, et al. Coinfection with *Helicobacter pylori* and *Opisthorchis viverrini* enhances the severity of hepatobiliary abnormalities in hamsters. *Infect Immun.* (2017) 85:e00009–19. doi: 10.1128/IAI.00009-17
33. Pearce EJ, MacDonald AS. The immunobiology of schistosomiasis. *Nat Rev Immunol.* (2002) 2:499–511. doi: 10.1038/nri843
34. Bickle QD, Solum J, Helmby H. Chronic intestinal nematode infection exacerbates experimental *Schistosoma mansoni* infection. *Infect Immun.* (2008) 76:5802–9. doi: 10.1128/IAI.00827-08
35. Beechler BR, Jolles AE, Budischak SA, Corstjens PLAM, Ezenwa VO, Smith M, et al. Host immunity, nutrition and coinfection alter longitudinal infection patterns of schistosomes in a free ranging African buffalo population. *PLoS Neglect Trop Dis.* (2017) 11:e0006122. doi: 10.1371/journal.pntd.0006122
36. Kloosterman A, Frankena K, Ploeger HW. Increased establishment of lungworms (*Dictyocaulus viviparus*) in calves after previous infections with gastrointestinal nematodes (*Ostertagia ostertagi* and *Cooperia oncophora*). *Vet Parasitol.* (1989) 33:155–63. doi: 10.1016/0304-4017(89)90063-0
37. Bazzone LE, Smith PM, Rutitzky LI, Shainheit MG, Urban JF, Setiawan T, et al. Coinfection with the intestinal nematode *Heligmosomoides polygyrus* markedly reduces hepatic egg-induced immunopathology and proinflammatory cytokines in mouse models of severe schistosomiasis. *Infect Immun.* (2008) 76:5164–72. doi: 10.1128/IAI.00673-08
38. Tabel H, Wei G, Bull HJ. Immunosuppression: cause for failures of vaccines against African trypanosomiases. *PLoS Neglect Trop Dis.* (2013) 7:e2090. doi: 10.1371/journal.pntd.0002090
39. Caljon G, Van Reet N, De Trez C, Vermeersch M, Pérez-Morga D, Van Den Abbeele J. The dermis as a delivery site of *Trypanosoma brucei* for tsetse flies. *PLoS Pathog.* (2016) 12:e1005744. doi: 10.1371/journal.ppat.1005744
40. Ademola IO, Odeniran PO. Co-infection with *Plasmodium berghei* and *Trypanosoma brucei* increases severity of malaria and trypanosomiasis in mice. *Acta Trop.* (2016) 159:29–35. doi: 10.1016/j.actatropica.2016.03.030
41. Machelart A, Van Vyve M, Potemberg G, Demars A, De Trez C, Tima HG, et al. *Trypanosoma* infection favors *Brucella* elimination via IL-12/IFNγ-dependent pathways. *Front Immunol.* (2017) 8:903. doi: 10.3389/fimmu.2017.00903
42. Teixeira AR, Hecht MM, Guimaro MC, Sousa AO, Nitz N. Pathogenesis of Chagas' disease: parasite persistence and autoimmunity. *Clin Microbiol Rev.* (2011) 24:592–630. doi: 10.1128/CMR.00063-10
43. Rodriguez JPF, Caldas IS, Goncalves V, Almeida LA, Souza RLM, Novaes R. *S. mansoni-T. cruzi* co-infection modulates arginase-1/iNOS expression, liver and heart disease in mice. *Nitric Oxide* (2017) 66:43–52. doi: 10.1016/j.niox.2017.02.013
44. Ahmed N, French T, Rausch S, Kühl A, Hemminger K, Dunay IR, et al. Toxoplasma co-infection prevents Th2 differentiation and leads to a helminth-specific Th1 response. *Front Cell Infect Microbiol.* (2017) 7:341. doi: 10.3389/fcimb.2017.00341
45. Khan IA, Hakak R, Eberle K, Sayles P, Weiss LM, Urban JF. Coninfection with *Heligmosomoides polygyrus* fails to establish $CD8^+$ T-cell immunity against *Toxoplasma gondii*. *Infect Immun.* (2008) 76:1305–13. doi: 10.1128/IAI.01236-07
46. Marple A, Wu W, Shah S, Zhao Y, Du P, Gause WC, et al. Cutting edge: helminth coinfection blocks effector differentiation of CD8 T cells through alternatate host Th2- and IL-10-mediated responses. *J Immunol.* (2016) 198:634–9. doi: 10.4049/jimmunol.1601741
47. Hiob L, Koethe M, Schares G, Goroll T, Daugschies A, Bangoura B. Experimental *Toxoplasma gondii* and *Eimeria tenella* co-infection in chickens. *Parasitol Res.* (2017) 116:3189–203. doi: 10.1007/s00436-017-5636-2
48. Xiao J, Yolken RH. Strain hypothesis of *Toxoplasma gondii* infection on the outcome of human disease. *Acta Physiol.* (2015) 213:828–45. doi: 10.1111/apha.12458
49. Dubey JP, Ruff MD, Camargo ME, Shen SK, Wilkins GL, Kwok OC, et al. Serologic and parasitologic responses of domestic chickens after oral inoculation with *Toxoplasma gondii* oocysts. *Am J Vet Res.* (1993) 54:1668–72.
50. Kaneto CN, Costa AJ, Paulillo AC, Moraes FR, Murakami TO, Meireles MV. Experimental toxoplasmosis in broiler chicks. *Vet Parasitol.* (1997) 69:203–10. doi: 10.1016/S0304-4017(96)01126-0
51. Saeij JP, Boyle JP, Boothroyd JC. Differences among the three major strains of *Toxoplasma gondii* and their specific interactions with the infected host. *Trends Parasitol.* (2005) 21:476–81. doi: 10.1016/j.pt.2005.08.001
52. Mason S, Dubey JP, Smith JE, Boag B. *Toxoplasma gondii* coinfection with diseases and parasites in wild rabbits in Scotland. *Parasitology* (2015) 142:1415–21. doi: 10.1017/S003118201500075X
53. Weatherhead J, Cortes AA, Sandoval C, Vaca M, Chico M, Loor S, et al. Comparison of cytokine responses in Ecuadorian children infected with *Giardia*, *Ascaris*, or both parasites. *Am J Trop Med Hyg.* (2017) 96:1394–9. doi: 10.4269/ajtmh.16-0580
54. Zhou P, Li E, Shea-Donohue T, Singer SM. Tumour necrosis factor α contributes to protection against *Giardia lamblia* infection in mice. *Parasite Immunol.* (2007) 29:367–74. doi: 10.1111/j.1365-3024.2007.00953.x
55. Reynolds LA, Redpath SA, Yurist-Doutsch S, Gill N, Brown EM, van der Heijden J, et al. Enteric helminths promote *Salmonella* coninfection by altering the intestinal microbiome. *J Infect Dis.* (2017) 215:1245–54. doi: 10.1093/infdis/jix141
56. Morpeth SC, Ramadhani HO, Crump JA. Invasive non-Typhi *Salmonella* disease in Africa. *Clin Infect Dis.* (2009) 49:606–11. doi: 10.1086/603553
57. Berkley JA, Bejon P, Mwangi T, Gwer S, Maitland K, Williams TN, et al. HIV infection, malnutrition, and invasive bacterial infection among children with severe malaria. *Clin Infect Dis.* (2009) 49:336–43. doi: 10.1086/600299
58. Mtove G, Amos B, Nadjm B, Hendriksen IC, Dondorp AM, Mwambuli A, et al. Decreasing incidence of severe malaria and community-acquired bacteraemia among hospitalized children in Muhesa, north-eastern Tanzania, 2006–2010. *Malaria J.* (2011) 10:320. doi: 10.1186/1475-2875-10-320
59. Mabey DC, Brown A, Greenwood BM. *Plasmodium falciparum* malaria and *Salmonella* infections in Gambian children. *J Infect Dis.* (1987) 155:1319–21. doi: 10.1093/infdis/155.6.1319
60. Gozzelino R, Jeney V, Soares MP. Mechanisms of cell protection by heme oxygenase-1. *Ann Rev Pharmacol Toxicol.* (2010) 50:323–54. doi: 10.1146/annurev.pharmtox.010909.105600
61. Cunnington AJ, de Souza JB, Walther M, Riley EM. Malaria impairs resistance to *Salmonella* through heme- and heme oxygenase-dependent dysfunctional granulocyte mobilization. *Nat Med.* (2012) 18:120–7. doi: 10.1038/nm.2601
62. Cunnington AJ, Njie M, Correa S, Takem EN, Riley EM, Walther M. Prolonged neutrophil dysfunction after *Plasmodium falciparum* malaria is related to hemolysis and heme oxygenase-1 induction. *J Immunol.* (2012) 189:5336–46. doi: 10.4049/jimmunol.1201028
63. Resende Co T, Hirsch CS, Toossi Z, Dietze R, Ribeiro-Rodrigues R. Intestinal helminth co-infection has a negative impact on both anti-*Mycobacterium tuberculosis* immunity and clinical response to tuberculosis therapy. *Clin Exp Immunol.* (2007) 147:45–52. doi: 10.1111/j.1365-2249.2006.03247.x
64. Verhagen LM, Hermans PW, Warris A, de Groot R, Maes M, Villalba JA, et al. Helminths and skewed cytokine profiles increase tuberculin skin test positivity in Warao Amerindians. *Tuberculosis* (2012) 92:505–12. doi: 10.1016/j.tube.2012.07.004
65. Oktaria S, Effendi EH, Indriatmi W, van Hees CLM, Thio HB, Sjamsoe-Daili ES, et al. Soil-transmitted helminth infections and leprosy: a cross-sectional study of the association between two major neglected tropical diseases in Indonesia. *BMC Infect Dis.* (2016) 16:258. doi: 10.1186/s12879-016-1593-0

66. Flynn JL. Lessons from experimental *Mycobacterium tuberculosis* infections. *Microbes Infect.* (2006) 8:1179–88. doi: 10.1016/j.micinf.2005.10.033
67. Khader SA, Cooper AM. IL-23 and IL-17 in tuberculosis. *Cytokine* (2008) 41:79–83. doi: 10.1016/j.cyto.2007.11.022
68. Toulza F, Tsang L, Ottenhoff TH, Brown M, Dockrell HM. *Mycobacterium tuberculosis*-specific $CD4^+$ T-cell response is increased, and Treg cells decreased, in anthelmintic-treated patients with latent TB. *Eur J Immunol.* (2016) 46:752–61. doi: 10.1002/eji.201545843
69. Babu S, Bhat SQ, Kumar NP, Jayantasri S, Rukmani S, Kumaran P, et al. Human type 1 and 17 responses in latent tuberculosis are modulated by coincident filarial infection through cytotoxic T lymphocyte antigen-4 and programmed death-1. *J Infect Dis.* (2009) 200:288–98. doi: 10.1086/599797
70. George PJ, Anuradha R, Kumaran PP, Chandrasekaran V, Nutman TB, Babu S. Modulation of mycobacterial-specific Th1 and Th17 cells in latent tuberculosis by coincident hookworm infection. *J Immunol.* (2013) 190:5161–8. doi: 10.4049/jimmunol.1203311
71. George PJ, Anuradha R, Kumar NP, Sridhar R, Banurekha VV, Nutman TB, et al. Helminth infections coincident with active pulmonary tuberculosis inhibit mono- and multifunctional $CD4^+$ and $CD8^+$ T cell responses in a process dependent on IL-10. *PLoS Pathog.* (2014) 10:e1004375. doi: 10.1371/journal.ppat.1004375
72. Kahnert A, Seiler P, Stein M, Bandermann S, Hahnke K, Mollenkopf H, et al. Alternative activation deprives macrophages of a coordinated defense program to *Mycobacterium tuberculosis*. *Eur J Immunol.* (2006) 36:631–47. doi: 10.1002/eji.200535496
73. Potian JA, Rafi W, Bhatt K, McBride A, Gause WC, Salgame P. Preexisting helminth infection induces inhibition of innate pulmonary anti-tuberculosis defense by engaging the IL-4 receptor pathway. *J Exp Med.* (2011) 208:1863–74. doi: 10.1084/jem.20091473
74. Aira N, Andersson AM, Singh SK, McKay DM, Blomgran R. Species dependent impact of helminthderived antigens on human macrophages infected with *Mycobacterium tuberculosis*: direct effect on the innate anti-mycobacterial response. *PLoS Neglect Trop Dis.* (2017) 11:e0005390. doi: 10.1371/journal.pntd.0005390
75. du Plessis N, Kleynhans L, Thiart L, van Helden PD, Brombacher F, Horsnell WG, et al. Acute helminth infection enhances early macrophage mediated control of mycobacterial infection. *Mucosal Immunol.* (2013) 6:931–41. doi: 10.1038/mi.2012.131
76. Achkar JM, Chan J, Casadevall A. B cells and antibodies in the defense against *Mycobacterium tuberculosis* infection. *Immunol Rev.* (2015) 264:167–81. doi: 10.1111/imr.12276
77. Anuradha R, Munisankar S, Bhootra Y, Dolla C, Kumaran P, Nutman TB, et al. Modulation of *Mycobacterium tuberculosis*-specific humoral immune responses is associated with *Strongyloides stercoralis* coinfection. *PLoS Neglect Trop Dis.* (2017) 11:e0005569. doi: 10.1371/journal.pntd.0005569
78. Wajja A, Kizito D, Nassanga B, Nalwoga A, Kabagenyi J, Kimuda S, et al. The effect of current *Schistosoma mansoni* infection on the immunogenicity of a candidate TB vaccine, MVA85A, in BCGvaccinated adolescents: an open-label trial. *PLoS Neglect Trop Dis.* (2017) 11:e0005440. doi: 10.1371/journal.pntd.0005440
79. Adeyemi MT, Morenikeji OA, Emikpe BO, Jarikre TA. Interactions between gastrointestinal parasitism and pneumonia in Nigerian goats. *J Parasit Dis.* (2017) 41:726–33. doi: 10.1007/s12639-017-0878-6
80. Howell AK, Tongue SC, Currie C, Evans J, Williams DJL, McNeilly TN. Co-infection with *Fasciola hepatica* may increase the risk of *Escherichia coli* O157 shedding in British cattle destined for the food chain. *Prevent Vet Med.* (2018) 150:70–6. doi: 10.1016/j.prevetmed.2017.12.007
81. Bartelt LA, Bolick DT, Mayneris-Perxachs J, Kolling GL, Medlock GL, Zaenker EI, et al. Cross-modulation of pathogen-specific pathways enhances malnutrition during enteric co-infection with *Giardia lamblia* and enteroaggregative *Escherichia coli*. *PLoS Pathog.* (2017) 13:e1006471. doi: 10.1371/journal.ppat.1006471
82. Beatty JK, Akierman SV, Motta JP, Muise S, Workentine ML, Harrison JJ, et al. *Giardia duodenalis* induces pathogenic dysbiosis of human intestinal microbiota biofilms. *Int J Parasitol.* (2017) 47:311–26. doi: 10.1016/j.ijpara.2016.11.010
83. Manko A, Motta JP, Cotton JA, Feener T, Oyeyemi A, Vallance BA, et al. *Giardia* co-infection promotes the secretion of antimicrobial peptides beta-defensin 2 and trefoil factor 3 and attenuates attaching and effacing bacteria-induced intestinal disease. *PLoS ONE* (2017) 12:e0178647. doi: 10.1371/journal.pone.0178647
84. Osborne LC, Monticelli LA, Nice TJ, Sutherland TE, Siracusa MC, Hepworth MR, et al. Virus-helminth coninfection reveals a microbiota-independent mechanism of immunomodulation. *Science* (2014) 345:579–82. doi: 10.1126/science.1256942
85. Reese TA, Wakeman BS, Choi HS, Hufford MM, Huang SC, Zhang X, et al. Helminth infection reactivates latent γ-herpesvirus via cytokine competition at a viral promoter. *Science* (2014) 345:573–7. doi: 10.1126/science.1254517
86. Attallah AM, Abdallah SO, Albannan MS, Omran MM, Attallah AA, Farid K. Impact of hepatitis C virus/*Schistosoma mansoni* coinfection on the circulating levels of HCV-NS4 protein and extracellular-matrix deposition in patients with different hepatic fibrosis stages. *Am J Trop Med Hyg.* (2016) 95:1044–50. doi: 10.4269/ajtmh.16-0129
87. Morawski BM, Yunus M, Kerukadho E, Turyasingura G, Barbra L, Ojok AM, et al. Hookworm infection is associated with decreased $CD4^+$ T cell counts in HIV-infected adult Ugandans. *PLoS Neglect Trop Dis.* (2017) 11:e0005634. doi: 10.1371/journal.pntd.0005634
88. Dietze KK, Dittmer U, Koudaimi DK, Schimmer S, Reitz M, Breloer M, et al. Filariae-retrovirus co-infection in mice is associated with suppressed virus-specific IgG immune responses and higher viral loads. *PLoS Neglect Trop Dis.* (2016) 10:e0005170. doi: 10.1371/journal.pntd.0005170
89. Modjarrad K, Zulu I, Redden DT, Njobvu L, Lane HC, Bentwich Z, et al. Treatment of intestinal helminths does not reduce plasma concentrations of HIV-1 RNA in coinfected Zambian adults. *J Infect Dis.* (2005) 192:1277–83. doi: 10.1086/444543
90. Elliott AM, Mawa PA, Joseph S, Namujju PB, Kizza M, Nakiyingi JS, et al. Association between helminth infection and $CD4^+$ T cell count, viral load and cytokine responses in HIV-1-infected Ugandan adults. *Trans R Soc Trop Med Hyg.* (2003) 97:103–8. doi: 10.1016/S0035-9203(03)90040-X
91. Carvalho EM, Da Fonseca Porto A. Epidemiological and clinical interaction between HTLV-1 and *Strongyloides stercoralis*. *Parasite Immunol.* (2004) 26:487–97. doi: 10.1111/j.0141-9838.2004.00726.x
92. Vadlamudi RS, Chi DS, Krishnaswamy G. Intestinal strongyloidiasis and hyperinfection syndrome. *Clin Mol Allergy* (2006) 4:8. doi: 10.1186/1476-7961-4-8
93. Montes M, Sanchez C, Verdonck K, Lake JE, Gonzalez E, Lopez G, et al. Regulatory T Cell expansion in HTLV-1 and strongyloidiasis co-infection is associated with reduced IL-5 responses to *Strongyloides stercoralis* antigen. *PLoS Neglect Trop Dis.* (2009) 3:e456. doi: 10.1371/journal.pntd.0000456
94. Herbert DR, Lee JJ, Lee NA, Nolan TJ, Schad GA, Abraham D. Role of IL-5 in Innate and adaptive immunity to larval *Strongyloides stercoralis* in mice. *J Immunol.* (2000) 165:4544–51. doi: 10.4049/jimmunol.165.8.4544
95. Choksi TT, Madison G, Dar T, Asif M, Fleming K, Clarke L, et al. Case report: multiorgan dysfunction syndrome from *Strongyloides stercoralis* hyperinfection in a patient with human T-cell lymphotrophic virus-1 coinfection after initiation of Ivermectin treatment. *Am J Trop Med Hyg.* (2016) 95:864–7. doi: 10.4269/ajtmh.16-0259
96. Gazzinelli-Guimarães PH, de Freitas LF, Gazzinelli-Guimarães AC, Coelho F, Barbosa FS, Nogueira D, et al. Concomitant helminth infection downmodulates the *Vaccinia* virus-specific immune response and potentiates virus-associated pathology. *Int J Parasitol.* (2017) 47:1–19. doi: 10.1016/j.ijpara.2016.08.007
97. Actor JK, Shirai M, Kullberg MC, Buller RM, Sher A, Berzofsky JA. Helminth infection results in decreased virus-specific $CD8^+$ cytotoxic T-cell and Th1 cytokine responses as well as delayed virus clearance. *Proc Nat Acad Sci USA.* (1993) 90:948–52. doi: 10.1073/pnas.90.3.948
98. McFarlane AJ, McSorley HJ, Davidson DJ, Fitch PM, Errington C, Mackenzie KJ, et al. Enteric helminth-induced type I interferon signaling protects against pulmonary virus infection through interaction with the microbiota. *J Allergy Clin Immunol.* (2017) 140:1068–78. doi: 10.1016/j.jaci.2017.01.016
99. Wuerthner VP, Hua J, Hoverman JT. The benefits of coinfection: trematodes alter disease outcomes associated with virus infection. *J Anim Ecol.* (2017) 86:921–31. doi: 10.1111/1365-2656.12665

100. Legname G, Baskakov IV, Nguyen HO, Riesner D, Cohen FE, DeArmond SJ, et al. Synthetic mammalian prions. *Science* (2004) 305:673–6. doi: 10.1126/science.1100195
101. Mabbott NA, Young J, McConnell I, Bruce ME. Follicular dendritic cell dedifferentiation by treatment with an inhibitor of the lymphotoxin pathway dramatically reduces scrapie susceptibility. *J Virol.* (2003) 77:6845–54. doi: 10.1128/JVI.77.12.6845-6854.2003
102. Glaysher BR, Mabbott NA. Role of the GALT in scrapie agent neuroinvasion from the intestine. *J Immunol.* (2007) 178:3757–66. doi: 10.4049/jimmunol.178.6.3757
103. McCulloch L, Brown KL, Bradford BM, Hopkins J, Bailey M, Rajewsky K, et al. Follicular dendritic cell-specific prion protein (PrPC) expression alone is sufficient to sustain prion infection in the spleen. *PLoS Pathog.* (2011) 7:e1002402. doi: 10.1371/journal.ppat.1002402
104. Donaldson DS, Else KJ, Mabbott NA. The gut-associated lymphoid tissues in the small intestine, not the large intestine, play a major role in oral prion disease pathogenesis. *J Virol.* (2015) 15:9532–47. doi: 10.1128/JVI.01544-15
105. Gruner L, Elsen JM, Vu Tien Khang J, Eychenne F, Caritez JC, Jacquiet P, et al. Nematode parasites and scrapie: experiments in sheep and mice. *Parasitol Res.* (2004) 93:493–8. doi: 10.1007/s00436-004-1131-7
106. van Keulen LJ, Schreuder BE, Vromans ME, Langeveld JP, Smits MA. Pathogenesis of natural scrapie in sheep. *Arch Virol Suppl.* (2000) 16:57–71. doi: 10.1007/978-3-7091-6308-5_5
107. van Keulen LJ, Vromans ME, van Zijderveld FG. Ealry and late pathogenesis of natural scrapie infection in sheep. *APMIS* (2002) 110:23–32. doi: 10.1034/j.1600-0463.2002.100104.x
108. Abolins S, King EC, Lazarou L, Weldon L, Hughes L, Drescher P, et al. The comparative immunology of wild and laboratory mice, *Mus musculus domesticus*. *Nat Commun.* (2017) 8:14811. doi: 10.1038/ncomms14811
109. Weldon L, Abolins S, Lenzi L, Bourne C, Riley EM, Viney M. The gut microbiota of wild mice. *PLoS ONE* (2015) 10:e0134643. doi: 10.1371/journal.pone.0134643
110. Johnston C, McSorley H, Smyth D, Anderton S, Wigmore S, Maizels R. A role for helminth parasites in achieving immunological tolerance in transplantation. *Lancet* (2015) 385:S50. doi: 10.1016/S0140-6736(15)60365-8

Conflict of Interest Statement: The author declares that the research was conducted in the absence of any commercial or financial relationships that could be construed as a potential conflict of interest.

frontiers in Immunology

ORIGINAL RESEARCH
published: 19 October 2018
doi: 10.3389/fimmu.2018.02403

Acute *Toxoplasma Gondii* Infection in Cats Induced Tissue-Specific Transcriptional Response Dominated by Immune Signatures

Wei Cong[1,2†], Tania Dottorini[3,4†], Faraz Khan[4], Richard D. Emes[3,4], Fu-Kai Zhang[1], Chun-Xue Zhou[1], Jun-Jun He[1], Xiao-Xuan Zhang[1], Hany M. Elsheikha[3] and Xing-Quan Zhu[1*]*

[1] State Key Laboratory of Veterinary Etiological Biology, Key Laboratory of Veterinary Parasitology of Gansu Province, Lanzhou Veterinary Research Institute, Chinese Academy of Agricultural Sciences, Lanzhou, China, [2] Department of Marine Engineering, Marine College, Shandong University, Weihai, China, [3] Faculty of Medicine and Health Sciences, School of Veterinary Medicine and Science, University of Nottingham, Loughborough, United Kingdom, [4] Advanced Data Analysis Centre, University of Nottingham, Loughborough, United Kingdom

OPEN ACCESS

Edited by:
Xun Suo,
China Agricultural University, China

Reviewed by:
Dolores Correa,
Instituto Nacional de Pediatria, Mexico
Bang Shen,
Huazhong Agricultural University, China

***Correspondence:**
Xing-Quan Zhu
xingquanzhu1@hotmail.com
Hany M. Elsheikha
hany.elsheikha@nottingham.ac.uk

[†] These authors have contributed equally to this work

Specialty section:
This article was submitted to Microbial Immunology, a section of the journal Frontiers in Immunology

Received: 21 June 2018
Accepted: 28 September 2018
Published: 19 October 2018

Citation:
Cong W, Dottorini T, Khan F, Emes RD, Zhang F-K, Zhou C-X, He J-J, Zhang X-X, Elsheikha HM and Zhu X-Q (2018) Acute Toxoplasma Gondii Infection in Cats Induced Tissue-Specific Transcriptional Response Dominated by Immune Signatures. Front. Immunol. 9:2403. doi: 10.3389/fimmu.2018.02403

RNA-sequencing was used to detect transcriptional changes in six tissues of cats, seven days after *T. gondii* infection. A total of 737 genes were differentially expressed (DEGs), of which 410 were up-regulated and 327 were down-regulated. The liver exhibited 151 DEGs, lung (149 DEGs), small intestine (130 DEGs), heart (123 DEGs), brain (104 DEGs), and spleen (80 DEGs)-suggesting tissue-specific transcriptional patterns. Gene ontology and KEGG analyses identified DEGs enriched in immune pathways, such as cytokine-cytokine receptor interaction, Jak-STAT signaling pathway, NOD-like receptor signaling pathway, NF-kappa B signaling pathway, MAPK signaling pathway, T cell receptor signaling pathway, and the cytosolic DNA sensing pathway. C-X-C motif chemokine 10 (CXCL10) was involved in most of the immune-related pathways. PI3K/Akt expression was down-regulated in all tissues, except the spleen. The genes for phosphatase, indoleamine 2,3-dioxygenase, Hes Family BHLH Transcription Factor 1, and guanylate-binding protein 5, playing various roles in immune defense, were co-expressed across various feline tissues. Multivariate K-means clustering analysis produced seven gene clusters featuring similar gene expression patterns specific to individual tissues, with lung tissue cluster having the largest number of DEGs. These findings suggest the presence of a broad immune defense mechanism across various tissues in cats against acute *T. gondii* infection.

Keywords: *Toxoplasma gondii*, host-parasite interaction, transcriptome, differential gene expression, biomarkers

INTRODUCTION

The intracellular protozoan *Toxoplasma gondii* infects almost all warm-blooded animals and approximately one-third of the world's human population, causing toxoplasmosis, a serious illness with fatal consequences in immune-compromised individuals and the unborn fetus (1–3). The emergence of drug-resistant parasite strains (4) together with the adverse effects of the currently-available drug therapies (5), and the inability to clear chronic infection highlight the need for improved treatment strategies to combat toxoplasmosis in humans and animals.

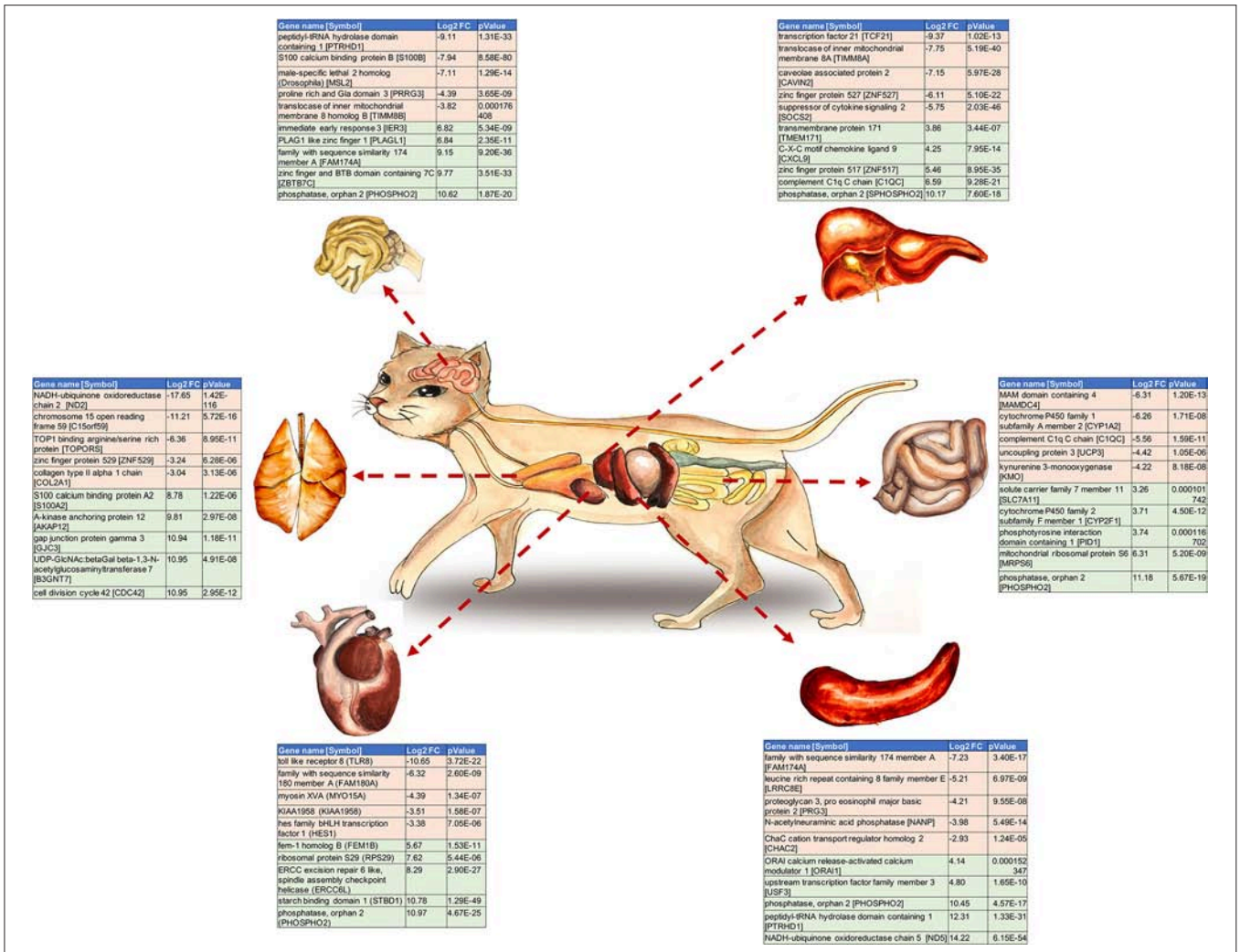

GRAPHICAL ABSTRACT | The top 10 Differentially Expressed Genes (DEGs) per examined cat tissue. The gene name and symbol, the log2 fold change and *P*-value for each gene are shown.

T. gondii has a complex lifecycle, wherein the parasite undergoes asexual reproduction in the intermediate host and sexual reproduction in the definitive host (members of the Felidae family). Cats acquire infection by ingesting prey tissue containing parasite cysts or, more rarely, oocysts. Prenatal infection may also occur in cats and humans (2, 6). Infected cats discharge oocysts (the product of parasite sexual reproduction in the cat's intestine) in their feces. The ability to accommodate both sexual and asexual reproduction of *T. gondii*, makes cats a significant source of infection to humans and animals (1, 7). *T. gondii* is a food-borne pathogen acquired via oral infection; however, it has a dispersive nature and can disseminate throughout the cat's body to infect multiple tissues (8–14).

Recognizing early transcriptional signatures of infection, while knowing the factors that determine tissue susceptibility to *T. gondii* infection in cats, would assist in planning preventative measures against environmental contamination with oocysts. Previous investigations have provided insights into the transcriptome of many intermediate host species during *T. gondii* infection (15–21). However, knowledge of the mechanisms that underpin the feline host transcriptional response to *T. gondii* remains poorly understood; and no genome-wide expression profiling of multiple tissues from cat, has been reported. Single-tissue gene expression can provide information on how a specific tissue responds to infection; however, understanding the patterns of gene expression across various tissues may advance our understanding of *T. gondii* molecular-pathogenesis events occurring during acute infection in cats and reveal the mechanisms by which the definitive host counters a complex infection such as *T. gondii*. RNA sequencing (RNA-Seq) of the whole transcriptome has proved a powerful and versatile tool for global gene expression analysis (22–24), enabling a comparison of transcriptomes between the merozoite and tachyzoite stages of *T. gondii* infecting the cat's intestine (25).

Here, we hypothesized that tissues of *T. gondii*-infected cats exhibit characteristic transcriptional signatures which are dominated by a number of genes, and may be exclusive to

a particular tissue with variance across tissues from the same individual. Differential gene expression and gene clustering analyses were performed on six tissues, individually or combined, in cats infected with *T. gondii*. Our studies provided novel information about the transcriptomic landscape of the major tissue types in cats during acute *T. gondii* infection and revealed tissue responsive signatures during acute *T. gondii* infection.

MATERIALS AND METHODS

Ethics Approval

All efforts were made to minimize suffering and to reduce the number of animals in the experiment. All work with live *T. gondii* was performed at biosafety level 2 and the animal experimental protocols were approved by The Animal Administration and Ethics Committee of Lanzhou Veterinary Research Institute, Chinese Academy of Agricultural Sciences (Protocol Permit Number: LVRIAEC-2014-001).

Animal Husbandry

Twelve domestic cats (*Felis catus;* 2 to 3-months-old; Chinese Li Hua breed) were purchased from a local breeder and housed individually in a controlled environment. Six cats each from two litters– were randomly allocated into four groups (2x infected and 2x control) with three cats per group. All of the cats were tested negative for feline immunodeficiency virus and feline leukemia virus using SNAP FIV/FeLV Combo Test (IDEXX, Westbrook, US), and feline calicivirus and feline parvovirus by ELISA KIT (NuoYuan, Shanghai, China) prior to the experiment. Also, cats tested seronegative for the presence of specific anti-*T. gondii* antibodies using indirect fluorescent antibody test (IFAT). Cats were supplied with a commercial diet (Royal Canine Inc., St. Charles, MO, USA) and water ad libitum during the 3 weeks prior to experimentation. During the experiment cats were fed a maintenance diet, based on their daily energy requirement.

Parasite Strain, Infection and Sample Collection

T. gondii Pru strain (genotype II) was maintained by passage through Kunming mice (26). The number of *T. gondii* cysts (determined using an optical microscope) was adjusted to 100 cysts per 1ml phosphate buffered saline (PBS, pH 7.4). Each experimental animal was infected with 100 cysts in 1 ml PBS by intragrastric inoculation. The enteroepithelial sexual cycle of *T. gondii* is completed within 3-10 days post ingestion of *T. gondii* cysts. This period can be extended to >18 days if cats are infected by oocysts. Control cats were sham-infected with 1 ml PBS only. Six different tissues (brain, heart, liver, lung, small intestine, and spleen) were collected from cats seven days after infection, in order to allow sufficient time for infection to establish. Tissue collection was performed as a terminal procedure from cats under deep isoflurane anesthesia, and unresponsiveness to all stimuli. Collected tissue samples were rinsed in saline, flash frozen in liquid nitrogen and stored at −80°C until processing.

Confirmation of Infection

Total genomic DNA was extracted from all harvested tissues using TIANamp Genomic DNA kit (TianGen™, Beijing, China). A PCR assay targeting *T. gondii* B1 gene was used to detect *T. gondii* infection in all cat tissues (27, 28). The PCR products were subjected to electrophoresis on ethidium bromide-stained 2% agarose–Tris-acetate-EDTA gels, and the banding pattern was visualized by UV transillumination. All of the electrophoresed PCR products were run with positive and negative control. *T. gondii* genotype was confirmed by PCR-restriction fragment length polymorphism (RFLP) analysis of the positive amplicons (29).

RNA Extraction and Qualification

Total RNA was extracted individually from the six tissues of the cats using TRIzol Reagent according to the manufacturer's protocol (Invitrogen, CA, USA). The RNA was checked for degradation and contamination using 1% agarose gels. RNA purity was evaluated with a NanoPhotometer® spectrophotometer (IMPLEN, CA, USA) and RNA concentration was measured using the Qubit® RNA Assay Kit in Qubit® 2.0 Flurometer (Life Technologies, CA, USA). RNA integrity was assessed using the RNA Nano 6000 Assay Kit of the Agilent Bioanalyzer 2100 system (Agilent Technologies, CA, USA).

cDNA Library Preparation and Illumina Deep Sequencing

RNA samples that conformed with Quality Control checks (QC) were used in the transcriptome-sequencing (RNA-seq) analysis. Samples were run in duplicate, and each RNA template consisted of three pooled biological replicates from the same group. 3 μg RNA per sample was used as input material for RNA-seq library preparation using NEBNext® Ultra™ RNA Library Prep Kit for Illumina® (NEB, USA). Index codes were added to correlate sequences to their respective samples. The mRNA was purified from total RNA using poly-T oligo-attached magnetic beads. Fragmentation was carried out using divalent cations under elevated temperature in NEBNext First Strand Synthesis Reaction Buffer (5X). First strand cDNA was synthesized using a random hexamer primer and M-MuLV Reverse Transcriptase (RNase H-). Second strand cDNA was synthesized using DNA Polymerase I and RNase H. Remaining overhangs were converted into blunt ends using exonuclease/polymerase. Following adenylation of the 3′ends of DNA fragments, NEBNext Adaptor with hairpin loop structures were ligated to prepare for hybridization. In order to select cDNA fragments of 150∼200 bp in length, library fragments were purified using the AMPure XP system (Beckman Coulter, Beverly, USA). Then, 3 μl USER Enzyme (NEB, USA) were used with size-selected, adaptor-ligated cDNA at 37°C for 15 min followed by 5 min at 95°C before PCR, which was performed with Phusion High-Fidelity DNA polymerase, Universal PCR primers and Index (X) Primer. PCR products were purified (AMPure XP system) and the library quality was assessed with the Agilent Bioanalyzer 2100 system. The clustering of index-coded samples was performed on a cBot Cluster Generation System

using TruSeq PE Cluster Kit v3-cBot-HS (Illumia) according to the manufacturer's instructions. Following cluster generation, library preparations were sequenced on an Illumina Hiseq 2500 platform and 125 bp paired-end reads were generated.

Quality Trimming of Illumina Paired-End Reads

Before read alignment, all the data files (Fastq) were adaptor trimmed using "scythe" (v0.994 BETA) (https://github.com/vsbuffalo/scythe) and quality trimmed using the library "sickle" (v1.33) (https://github.com/najoshi/sickle).

Read Alignment and Transcript Assembly

Index of the reference genome was built using Hisat2 (v2.1.0) (30). Trimmed paired-end reads were aligned to the reference genome using Hisat2 for expression estimation. StringTie (v1.3.3) was then used to assemble the read alignments into known transcripts for each sample (31). In addition, StringTie also produces a gene abundance table (FPKM and TPM), which was used for clustering analysis.

Tissue-Specific Differential Expression Analysis

A combined read count table at the gene level for all the samples was generated using a python script available from StringTie. The Bioconductor package edgeR (v3.18.1) (32) was used to identify the differentially expressed (DE) genes per-tissue condition (infected vs. uninfected; two biological replicates per condition). Genes with a 5% false discovery rate (FDR < 0.05) and log fold change (logFC) ≥ 1 were considered differentially expressed.

Gene Ontology (GO) and Pathway Analyses

The Bioconductor package GOstats (v2.42.0) (33) was used to test for over-representation of GO terms using a hypergeometric test (hyperGTest). Orthologues for cat gene-sets were found using Ensembl BioMart against human data; then the cat gene orthologues were used for gene ontology analysis. GO terms with a corrected $P < 0.05$ were considered significantly enriched. Pathway analysis was performed using bioconductor package "pathview" (v1.16.5), which implements Kyoto Encyclopedia of Genes and Genomes (KEGG) pathways. The significance level of enrichment of KEGG pathways was identified using FDR < 0.05 and a corrected $P < 0.05$.

K-Means Clustering

The 21,890 genes identified through HiSat2 and StringTie were subjected to clustering analysis. In detail: the FPKM values of the genes from both replicates of each tissue and each treatment (e.g., rep 1 and rep 2 of infected brain tissues) were averaged; the log of the ratio between infected and non-infected conditions for each tissue was calculated; then, two subsequent k-means clustering analyses were performed [MeV_4_8 v10.2 (Multi Experiment viewer)] using Euclidean distance and $k = 10$ number of clusters. A stringent expression cutoff was applied to each sub-group of genes to discard background noise. Specifically, in each of the six generated clusters where genes showed increased expression levels concentrated on a single infected tissue, only those genes with FPKM values >1 in the specific infected condition were considered as expressed and selected for further analysis. To visualize gene expression in each cluster, bean plots (which represent the actual distribution of the individual data sets) were produced using BoxPlotR: a web-tool for generation of box plots.

Quantitative Real Time (RT)-PCR

Total RNA was extracted from various cat tissues using the TRIzol method (Invitrogen) and reverse-transcripted to single strand cDNA using the GoScript^{TM} Reverse Transcription System (Promega, MI, USA). GoTaq® qPCR Master Mix (Promega, MI, USA) was used to perform RT-PCR reactions in a QIAGEN's real-time PCR cycler (Rotor-Gene Q). Amplification reactions were performed under the following conditions: 2 min at 95°C, 40 cycles of 95°C for 15s, 55°C for 30s, and 72°C for 30s. All quantitative measurements were carried out in triplicate and normalized to the housekeeping gene glyceraldehyde-3-phosphatedehydrogenase (*GAPDH*) for every reaction (34). Twelve significant DEGs were selected to validate the sequencing data. Primers used for RT-PCR are listed in **Table 1**. The mRNA fold change was calculated using the following equations (35):

$$^{\Delta}C_T = {}^{\Delta}C_{T(\text{target})} - {}^{\Delta}C_{T(\text{GAPDH})};$$

$$^{\Delta\Delta}C_T = {}^{\Delta}C_{T(\text{infected})} - {}^{\Delta}C_{T(\text{control})};\ \text{mRNA fold change} = 2^{-\Delta\Delta C_T}$$

RESULTS

Presence of *T. Gondii* Infection in Cats

Parasite dissemination from the intestine to other tissues, both close to the inoculation site (small intestine, liver, and spleen) and to distantly placed organs (brain, heart, and lungs) was confirmed seven days post infection. *T. gondii B1* gene-based PCR analysis detected the parasite DNA in the brain, heart, liver, lung, small intestine, and spleen of all infected cats (**Figure S1**). The parasite load did not seem to vary across the cat tissues. However, it is possible that the parasite load may vary over the course of infection. *T. gondii* DNA was not detected in any tissue of the control cats. All positive amplicons that were characterized by RFLP produced a restriction fragment pattern that correlated with *T. gondii* genotype II.

General Features of the Transcriptome Data

Transcriptome-sequencing analysis generated ∼143 million sequence reads (125 bp in length) from 24 libraries. After quality control analysis and the removal of low quality reads, ∼170 Gb clean reads were obtained, with an average of 7 Gb clean reads/tissue. Less than 95% of the clean reads had Phred-like quality scores at the Q20 level and GC content of about 50% (**Table S1**). The clean reads were mapped to the genome of *Felis catus*. The majority of the clean reads were distributed in the exon region, with fewer in the intergenic region and the intron region. Approximately 80% of the clean reads were unique (**Table S2**); and subsequent analyses were based on these uniquely mapped reads.

TABLE 1 | Gene names and primers used in qRT-PCR analysis.

Gene	Primer name*	Primer sequence (5′ to 3′)
ADAM11	ADAM11-F	5′-CTGTGGCTTCCTCCTCTGTGT–3′
	ADAM11-R	5′-TTGCCCTGGTGGTAGAAGGT–3′
APOA2	APOA2-F	5′-CGGTGACTGACTACGGCAAG-3′
	APOA2-R	5′-TAACTGCTCCTGGGTCTTCTCAA–3′
MEP1A	MEP1A-F	5′-CACCATCATCAACATCCTGTCTC–3′
	MEP1A-R	5′-AAGGAAGGTCTGAAGTAGCAAAGGT-3′
ENO4	ENO4-F	5′-TGCATCTCTGTGTTGGTTATGCT–3′
	ENO4-R	5′- CGAAGGGCTACATACCGATTTTAC-3′
IGFI	IGFI-F	5′-GAGAGGAGTGGAAAACGCAGA–3′
	IGFI-R	5′-AGCGGTGAGTCCAAGACAGAG–3′
GKN2	GKN2-F	5′-CATGCTCCTCTACCACGGTTT–3′
	GKN2-R	5′-GCAGGGATGGCTTTATGTTTC–3′
GBP5	GBP5-F	5′-GCTAAAGGAAGGCACCGATAAA–3′
	GBP5-R	5′-AGTGAGCAGGAGAGTCGAAGATAAA–3′
OAS1	OAS1-F	5′-AGCCATCCACATCATCTCCAC–3′
	OAS1-R	5′- AGAGCCACCCTTGACCACTTT-3′
IDO1	IDO1-F	5′-GAACCAAGGCGGTGAAGATG–3′
	IDO1-R	5′-GCATAAACCAGAATAGGAGGCAGA–3′
PI16	PI16-F	5′-CTGCCAGAACTGTCTGCCTCT–3′
	PI16-R	5′-GTCCTTCATCTGCCCCTCAC–3′
ACTG2	ACTG2-F	5′-AACAGGGAGAAGATGACCCAGA–3′
	ACTG2-R	5′-CCAGAAGCATAGAGAGAGAGCACA–3′
ANKFN1	ANKFN1-F	5′-ATACCTCTACACCAGGCAAGGAAC–3′
	ANKFN1-R	5′-GCAGGGAGCAGGAGAAGAAA–3′
GAPDH	GAPDH(CAT)-F	5′-AAGCCCATCACCATCTTCCA–3′
	GAPDH(CAT)-R	5′-TTCACGCCCATCACAAACA–3′

**Forward (F) and reverse (R) primers.*
ADAM11, ADAM metallopeptidase domain 11; APOA2, apolipoprotein A2; MEP1A, Meprin A Subunit Alpha; ENO4, enolase family member 4; IGFI, Insulin-like growth factor 1 level; GKN2, gastrokine 2; GBP5, Guanylate Binding Protein 5; OAS1, 2′-5′-Oligoadenylate Synthetase 1; IDO1, indoleamine 2,3-dioxygenase 1; PI16, Peptidase Inhibitor 16; ACTG2, actin, gamma 2; ANKFN1, ankyrin repeat and fibronectin type III domain containing 1; GAPDH, glyceraldehyde-3-phosphate dehydrogenase.

Infection Induced Significant Alterations in Gene Expression

We investigated the distribution of gene expression values across the six tissues by fragment Per Kilobase of exon per Million mapped reads (FPKM) (**Table S3**). ∼47% of the expressed genes had low expression values ($0 < \text{FPKM} \leq 1$). The number of genes with moderate expression values ($1 < \text{FPKM} \leq 60$) and high expression values ($\text{FPKM} > 60$) accounted for ∼53% of the total annotated genes. Genes with $\text{FPKM} \geq 1$ [ranging from 12,195 (43.80%) to 16,734 (60.10%)] in the six tissues were considered expressed genes. We used the Bioconductor package edgeR (v3.18.1) to identify DEGs in each body tissue of the infected and uninfected cats. A total of 737 genes were differentially expressed in infected vs. uninfected cats, of which 410 were up-regulated and 327 were down-regulated. Large differences in gene expression were observed between cat tissues, indicating heterogenities in the response of cat tissues to *T. gondii* infection. Liver exhibited the highest number of DEGs (151 genes) compared to lung (149 genes), small intestine (130 genes), heart (123 genes), brain (104 genes), and spleen (80 genes) (**Figure 1**). DEGs of each tissue are listed in **Table S4**. We also used quantitative real-time PCR to validate the expression levels of representative genes, across cat tissues, detected by RNA-sequencing analysis (**Figure 2**).

Gene Ontology (GO) Enrichment and Functional Annotation Analyses

GO enrichment analysis was used to identify the significantly enriched GO terms in all DEGs using the GOseq R package. The enriched GO terms of each tissue are shown in **Table S5**. All DEGs were mapped to terms in the KEGG database. DEGs and KEGG pathways related to immune response were highly represented and are summarized in **Table S6**.

Signatures of Gene Co-expression

Differences were detected between the transcriptomes of cat tissues, with significant variations in gene expression between infected and uninfected tissues (**Table S4**). Gene co-expression analysis of DEGs indicated that phosphatase and indoleamine 2,3-dioxygenase (IDO) were co-expressed in five tissues (brain, heart, liver, small intestine, and spleen); while the HES1 (Hes Family BHLH Transcription Factor 1) was co-expressed in brain, heart, liver, and small intestine. Guanylate-binding protein 5 was detected in heart, liver, lung, and spleen (**Figure 3**, **Table S7**). Expression patterns and pathways associated with co-expressed DEGs across the various cat tissues are shown (**Figure S2**).

Global Gene Regulation During *T. Gondii* Infection

We employed cluster analysis, which was based on the partition of genes into clusters according to the log-ratios of gene expression between infected and uninfected tissues using a two-tier K-means algorithm. This analysis identified a set of 10 gene groups each characterized by a unique pattern. The patterns corresponding to individual clusters are visualized as line plots (**Figure 4**). Seven of these 10 clusters showed significant expression levels: spleen (cluster 2); brain (cluster 3); lung (cluster 7); liver (cluster 8), and heart (cluster 9), included up-regulated genes. Small intestine tissue produced two clusters with opposite regulation: cluster 4 (up-regulated genes) and cluster 10 (down-regulated genes). Two clusters (5 and 6) did not exhibit gene expression patterns specific to any tissue. To isolate the most representative genes in each cluster, a second clustering analysis was performed, focusing on genes contained in each of the seven clusters identified by the initial cluster analysis. Ultimately, seven groups of tissue-specific genes were identified, and are shown in heat maps and graphical formats, based on patterns of expression of individual genes across various tissues (**Figures 5A,B**).

Refined Gene Clusters After FPKM Filtering

Here, a stringent expression cutoff was applied to each sub-group of genes to remove background noise. In each of the six clusters where genes showed increased expression concentrated on a single infected tissue, only those genes with FPKM values >1 in the infected condition were selected for further analysis. Five

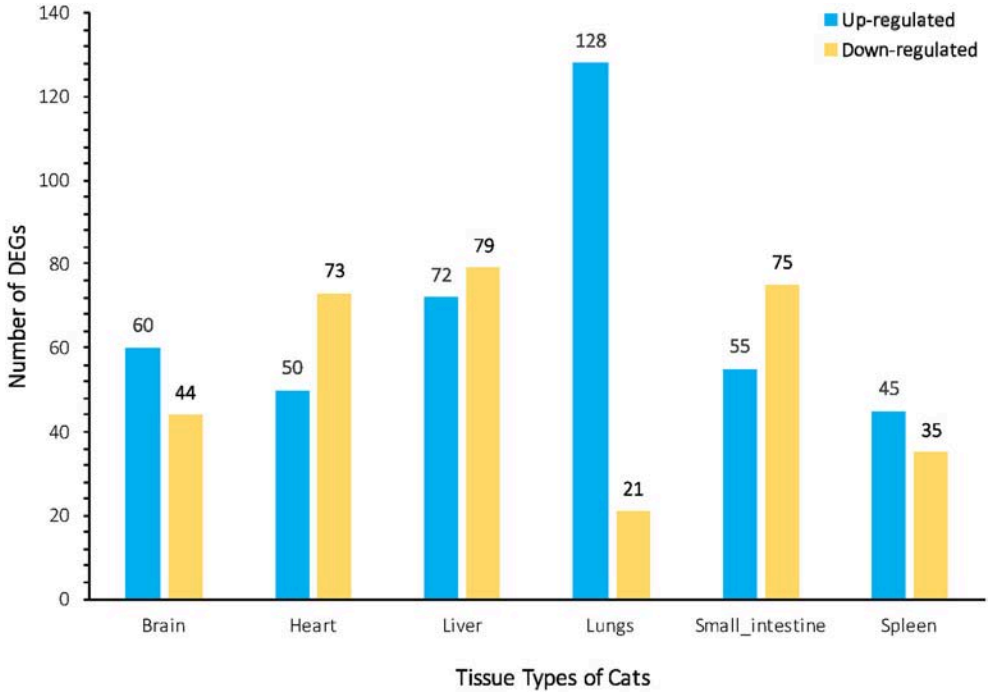

FIGURE 1 | Bar plot representation of the differentially Expressed Genes (DEGs) across the cat tissues after acute *T. gondii* infection. The numbers of up-regulated and down-regulated DEGs assigned to each cat tissue are indicated above the bars. The greatest changes in DEGs between infected and uninfected tissues were observed in the liver and lung.

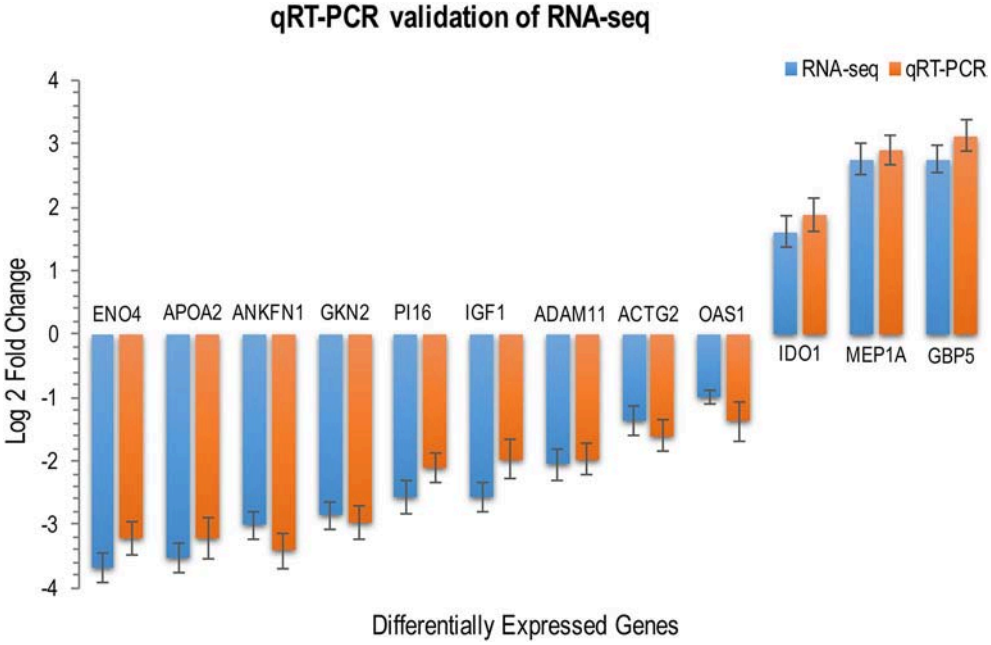

FIGURE 2 | RNA-seq transcriptome analysis and quantitative, real-time RT–PCR produced similar gene expression profiles. The expression levels of 12 DEGs across various cat tissues were determined by qRT-PCR for validation of RNA-seq data. Relative expression levels were calculated using the the $\Delta\Delta CT$ threshold cycle (*CT*) method and *GAPDH* as the reference gene. RNA-seq data are mean of two biological replicates + standard deviation (SD) of normalized read counts. qRT–PCR data are mean of three biological replicates + SD. *P* values are calculated with unpaired, two-tailed *t*-test. The height of the bars represents the log-transformed median fold changes in gene expression between infected and uninfected cats.

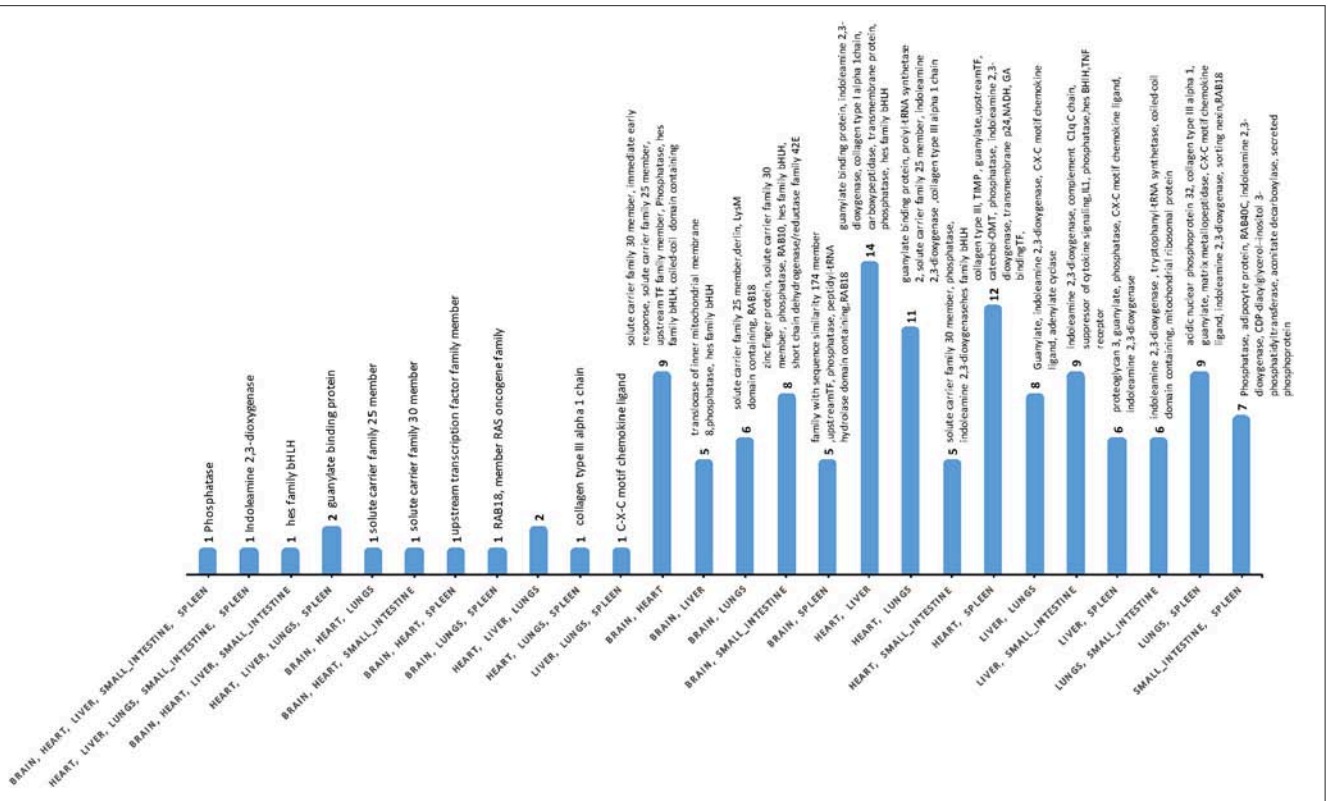

FIGURE 3 | The number of co-expressed DEGs across cat tissues. Phosphatase and indoleamine 2,3-dioxygenase were co-expressed in five tissues, whereas Hes Family BHLH Transcription Factor 1 and Guanylate-binding protein 5 were co-expressed in four tissues. Only fully annotated genes are shown.

of these clusters contained up-regulated genes in the spleen (6 genes), brain (13 genes), lung (75 genes), liver (1 gene), and heart (6 genes). However, the small intestine produced one cluster of 19 up-regulated genes and one cluster of 21 down-regulated genes. GO analysis of genes within these seven clusters provided new insights into biological processes, cellular processes and molecular functions regulated in cats during *T. gondii* infection. The five most highly associated biological process terms with the enrichment *P*-values of each cluster are shown (**Figure 5C**).

KEGG analysis of the DEGs within these seven final clusters was performed to gain more insight into the biological processes influenced during infection. We found no similarity in gene annotation in any cluster in any of the tissues examined. In small intestine cluster, KEGG analysis identified networks associated with hematopoietic cell lineage, metabolism of xenobiotics by cytochrome-P, chemical carcinogenesis and cytokine-cytokine receptor interaction. Lung cluster showed high expression levels of genes involved in nicotine addiction, biosynthesis of unsaturated fatty acids, long-term potentiation, glycosaminoglycan biosynthesis - heparan sulfate/heparin, cell adhesion molecules, insulin secretion, GABAergic synapse, fatty acid metabolism, amyotrophic lateral sclerosis, and adrenergic signaling in cardiomyocytes. The heart cluster showed high expression levels in complement and coagulation cascades and platelet activation. Small intestine cluster showed high expression levels of genes involved in metabolic metabolism, drug metabolism and fatty acid and amino acid metabolism. Genes with different expression patterns across the seven clusters are shown in **Table S8**. All of the analyzed clusters contained genes annotated to GO terms from the three ontologies at roughly equivalent levels. However, we found considerable bias in some tissues in regards to the representation of clustered genes among the three ontologies (**Figure S3**). The high proportion of genes annotated to biological process, reflects a trend toward clustering of metabolic and immune pathways. The most striking example was in the lung cluster, where 253 terms were found in the biological process.

Tissue-Specific Changes in Gene Expression

Even though the number of genes in each cluster was small, large-magnitude gene expression changes between infected and uninfected was observed in most of the tissues (**Figure 6**). The liver gene cluster had the highest magnitude (7.68 fold), followed by lung (5.44 fold), brain (3.58 fold), small intestine cluster 4 (3.55 fold), spleen (3.09 fold), and heart (2.98 fold); whereas small intestine tissue cluster 10 had a magnitude of −3.22 fold. Apart from the liver with only on gene, lung, brain, small intestine, and heart showed large magnitude transcriptional changes occurring in a small number of genes. This suggests that changes induced by *T. gondii* infection seem to rely on a small number of genes, but with large transcriptional changes. The lung was the tissue showing the greatest number of genes with the largest magnitude of transcriptional change. Among all highly expressed genes, the

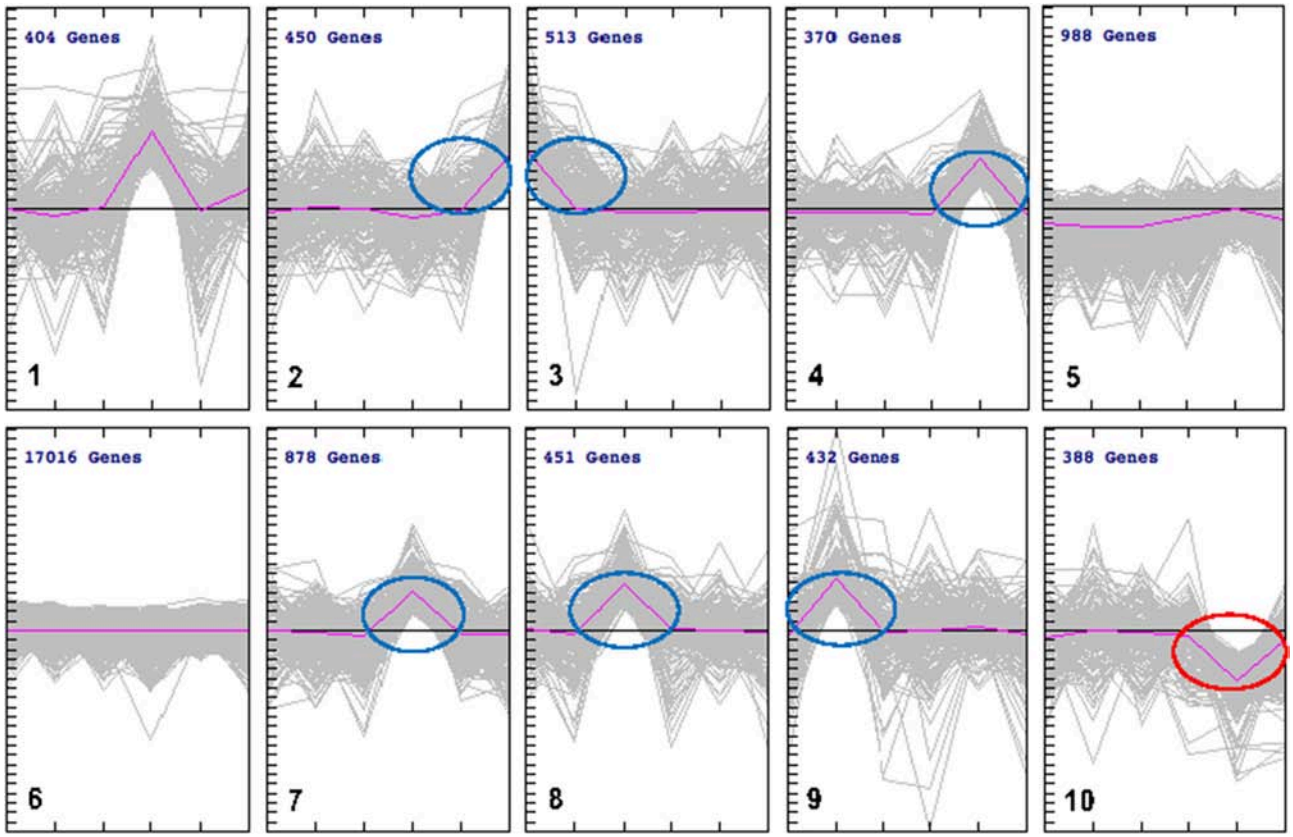

FIGURE 4 | k-Means clustering patterns of the differentially expressed genes across cat tissues. All DEGs were clustered into 10 groups using k-means clustering method and visualized with TM4 software. The pink line shows average expression z-scores to visualize the dominant expression trend of each cluster. Each line in the figure represents an expression value of the corresponding gene. The horizontal axis indicates the type of cat tissues and the vertical axis is the log2 expression ratio. Fold expression changes between various tissues from infected and uninfected cats were calculated using the log2 ratios. The numbers of genes for each cluster are indicated. The clusters included DEGs whose expression was either up regulated (clusters 2, 3, 4, 7, 8, and 9) or down regulated (cluster 10). There were no changes in gene expression observed in clusters 5 and 6. DEGs in cluster 1 was not considered due to lack of specificity to a single tissue.

metallothionein 3 (MT3) gene showed the highest expression in the infected lung, and it was also one of the genes with the highest log ratio between infected and uninfected tissues. Metallothionein-3 protein encoded by MT3 gene binds metals both in natural (such as Zn, Cu, Se) and xenobiotic (such as Ag, Cd) conditions, conferring a protective role against metal toxicity and oxidative stress.

DISCUSSION

The influence of *T. gondii* infection on the transcriptome of different tissue of cats is largely unknown. In this study, we examined the transcriptomes of liver, lung, small intestine, heart, brain, and spleen tissues of cats, seven days post infection. Inter-tissue transcriptome comparison revealed that the levels of DEGs were highest in the liver (151 genes) and lungs (149 genes), indicating a significant gene transcriptional response to infection in the liver and lung compared to other feline tissues. This result supports previous reports, wherein liver and lung seemed to be the most likely tissues to be involved in clinical cases of toxoplasmosis with a rapid fatal outcome (11–13, 34, 36). It is plausible that the timing and duration of infection can influence host tissue transcriptional response to the parasite, as previously indicated by the difference in the transcriptomes of mouse brain between acute and chronic *T. gondii* infection (17), and this could alter cytokine responses of the host to infection.

The transcriptional landscape of infected cat tissues was dominated by an immune gene expression signature, wherein, cytokine-cytokine receptor interaction, Jak-STAT signaling pathway, NOD-like receptor signaling pathway, NF-kappa B signaling pathway, MAPK signaling pathway, T cell receptor signaling pathway and the cytosolic DNA sensing pathway, were amongst the up-regulated immune pathways in almost all tissues. The importance of Toll-like receptor signaling in controlling *T. gondii* infection has been established (37). Many of the upregulated genes (e.g., CXCL10, SOCS3, MAPK13, CXCL9, CD2, CSF2RA, PI4K2B, IGF1, PFKFB1, MMP7, FZD8, TNFSF10, and RelB) identified in the livers are involved in immune-related pathways. Some of these genes are involved in the development of Natural Killer (NK) and adaptive T cell responses, leading to the production of Interferon gamma (IFN-γ) and resistance to infection (38). *T. gondii* is very

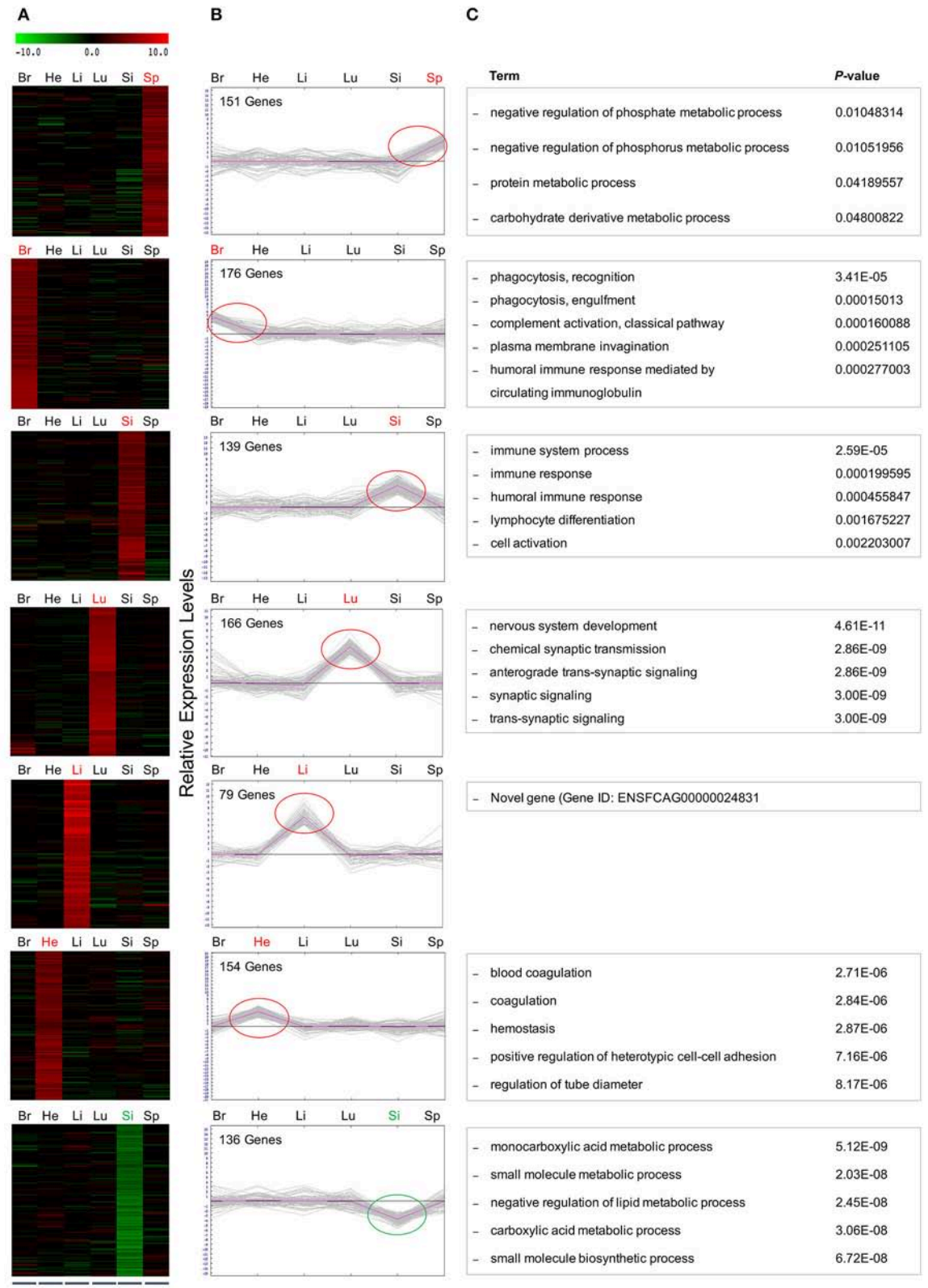

FIGURE 5 | Hierarchical and K-mean clustering analysis of the DEGs within clusters. Differentially expressed, co-regulated genes in each cluster were grouped using k-means clustering. Average cluster size varied considerably among tissues with lung containing the largest cluster with 75 genes. The smallest cluster was found in

(Continued)

FIGURE 5 | the liver, averaging 1 gene per cluster. The DEGs clustered into 7 major groups, demonstrated in **(A)** heat map and **(B)** graphical format, based on patterns of gene expression across the differing cat tissues. Red and green circles indicate the tissue-specific up- and down regulated genes, respectively. Negative values indicate decreased expression, and positive values indicate increased expression. **(C)** GO analysis of DEGs within clusters after FPKM filtering identified the top associated enriched GO terms with corresponding enrichment *P*-values, shown on right.

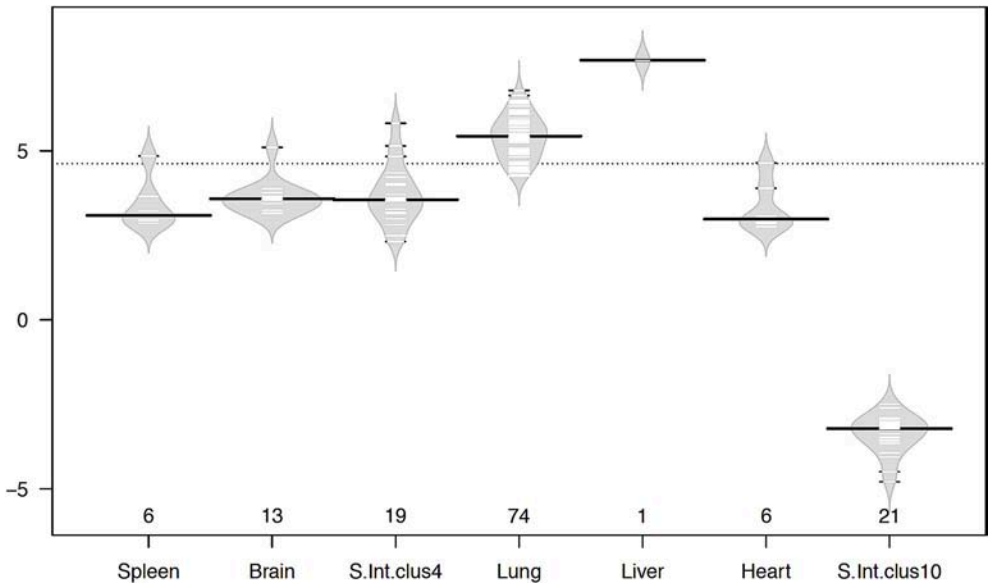

FIGURE 6 | Beanplots showing variation in the magnitude of gene expression within clusters in infected vs. uninfected tissues. The x-axis shows the number of genes of each cluster in the corresponding tissue. The y-axis indicates the average log2 fold change in gene expression. The width of the plot represents the distribution of data, short lines inside the shapes depict individual data points and heavy horizontal lines show the medians within each cluster, while the dotted line indicates the overall average. Plots were drawn using the R beanplot package.

efficient in manipulating the host's immune defense (39, 40); and previous studies have indicated that host immune response is a key determinant of clinical outcome following infection with *T. gondii* (16–20, 41, 42).

Although spleen had the lowest number of DEGs (80 genes) compared to other tissues, KEGG analysis identified multiple immune signaling pathways that were influenced by infection. Most of the immune pathways were up-regulated in spleen of infected cats; such as Toll-like receptor signaling pathway, cytosolic DNA-sensing pathway, RIG-I-like receptor signaling, TNF signaling pathway, FoxO signaling pathway, chemokine signaling pathway, and PI3K/Akt signaling pathway. Of note, C-X-C motif chemokine 10 (CXCL10) was involved in most of the immune-related pathways. Our previous study demonstrated that CXCL10 was up-regulated in pig peripheral blood mononuclear cells during early *T. gondii* infection (20, 21). CXCL10 is a chemokine secreted from cells stimulated with IFN-γ, and plays an important role in chemo-attraction of immune cells (43). This result indicates that *T. gondii* influences chemokine gene expression in spleen during early *T. gondii* infection.

T. gondii is a food-borne pathogen and infection is initially established in the small intestine by consuming prey containing parasite cysts or oocyst-contaminated water (44); leading to enteropathy (45). Therefore, successful infection of the host intestine is essential for subsequent parasite dissemination to different tissues. Others have showed that *in vitro* infection of rat intestinal epithelial cells can trigger an inflammatory response characterized by Tumor Necrosis Factor alpha (TNFα) signaling via NF-κB (46). However, feline host factors that are influenced by intestinal infection remain largely unknown. In our study, the global transcriptomic changes in the intestine of the definitive feline host, have been investigated. A total of 130 DEGs in the small intestine of infected cats were identified; of which 75 were down-regulated and 55 up-regulated. Some of the DEGs were involved in immune processes and signaling pathways, including LOC100302541, TNFSF18, CCL20, TNFRSF6B, IFNG, SOCS3, ICAM1, CD36, and FGF19. Other immune pathways up-regulated in liver and spleen tissues were also up-regulated in the small intestine.

An earlier study investigating the transcriptome of mouse brain during *T. gondii* infection reported an increased expression of genes involved in immune responses and cell activation (16). Also, host immune and inflammatory response was the major feature of genes affected by *T. gondii* infection of mouse peritoneal cells at five days post infection (47). We also showed that the expression of genes and signaling pathways involved in host immune response and cell fate, such as PI3K-Akt signaling pathway, Hippo signaling pathway and MAPK

signaling pathway, was altered in the cat brain. Transcriptional signatures observed in the cat brain tissue showed also that Notch signaling pathway is involved in *T. gondii* neuro-pathogenesis. Previous *T. gondii* host/pathogen KEGG pathway interactome analysis suggested the involvement of six genes of the Notch pathway in psychiatric/neurological disorders (45, 48). Notch signaling interacts with other signaling pathways, including phosphatidylinositol-3-kinase (PI3K)/serine/threonine kinase (Akt) and NF-κB to regulate cell fate. PI3K/Akt signaling pathway regulates diverse cellular activities related to cell growth, metabolism, migration, and apoptosis (49). Notch signaling plays an important role in various facets of *T. gondii* pathogenesis (50). The possibility that PI3K/Akt signaling pathway participates in promoting *T. gondii* survival and proliferation (51) and in mediating cell survival and blockage of apoptotic responses during *T. gondii* infection (50), suggests a link between *T. gondii* and this signal pathway. This finding supports an earlier observation wherein many *T. gondii* strains were found able to regulate genes enriched for processes involved in cell cycle regulation in murine macrophages (15).

T. gondii exploits heterotrimeric Gi-protein-mediated signaling to activate PI3K, leading to phosphorylation of downstream serine/threonine kinase AKT and extracellular signal-regulated protein kinases 1/2 (ERK1/2), and the inhibition of apoptosis (52). In our study, down-regulation of PI3K/AKT signaling in all tissues, except spleen, was detected and this can enhance apoptosis of host tissue and limits parasite growth. Phosphatase (a negative regulator of PI3K/Akt signaling, by converting PIP3 to PIP2, an opposite action to PI3K) can interfere with a number of cellular functions, such as cell proliferation and cell-cycle progression (53), was co-expressed in five cat tissues. These results indicate diverse roles played by PI3K/Akt signaling in *T. gondii*-host interaction. Further investigation into how the PI3K/Akt pathway interacts with other signaling mediators is required. NF-κB and mitogen-activated protein kinase (MAPK) signaling pathways are involved in the innate immune response to *T. gondii* (54). Altered MAPK signaling has been also implicated in toxoplasmosis of mice (55, 56) and humans (57). Considering that NF-κB and MAPK are downstream effectors of Akt, it is of significance to clarify whether this pathway influences the fate of infected cells via the regulation of NF-κB and MAPK.

Gene co-association Across Tissues

Co-expression analysis of DEGs indicated that phosphatase gene expression overlapped in five tissues; including brain, heart, liver, small intestine, and spleen. Transcripts for the inner-membrane complex (IMC) protein phosphatase have been involved in gene expression and cell division (46). Indoleamine 2,3-dioxygenase (IDO) was also co-expressed in five tissues: heart, liver, lung, small intestine, and spleen, but not in the brain tissue. IDO, the rate limiting catabolic enzyme in the degradation pathway of tryptophan, initiates the production of tryptophan degradation products, which exert important immuno-regulatory functions. IDO, through T-cell functions and other mechanisms (58), modulates pathophysiological processes, such as antimicrobial and antioxidant activities, and immune-regulation. IFNγ produced in response to *T. gondii* infection induces IDO enzyme to degrade L-tryptophan, an amino acid for which *T. gondii* is auxotrophic (59, 60). IFNγ-induced L-tryptophan starvation was believed to trigger *T. gondii* clearance via noncanonical, ubiquitin-mediated autophagy (61). Guanylate-binding protein (GBP) was detected in the heart, liver, lung, and spleen. GBP, IFN-γ-inducible effector, is a member of the GTPase family, and plays an essential role in mediating host defense against *T. gondii* (62). Human guanylate-binding protein 1 (hGBP1) functions against *T. gondii* infection in human MSCs (hMSCs). *T. gondii* replication can be significantly inhibited by the recruitment of hGBP1 to the parasitophorous vacuole (PV) membrane in IFN-γ-stimulated hMSCs (63). In mice, the recruitment of mGBP2 to *T. gondii*-containing PV was essential for controlling *T. gondii* replication (64).

Patterns of Gene Clusters

Genes clustered according to their pattern of expressions across the six tissues examined, led to the identification of seven clusters featuring expressions differentiated across tissues and infected/non-infected conditions. We also detected tissue-specific variations in the percentage of clustered genes, and in the properties of gene clusters including functional annotation and magnitude of gene expression. The differences in each tissue's response to infection may imply that some tissue-specific defense mechanisms exist in order to maintain the balance between enhancing the host's response to infection and promoting the parasite's survival. The genes within these clusters after a further processing step imposing a stringent expression cutoff to avoid any background expression noise were analyzed for differential transcriptional changes between infected and uninfected samples (magnitude). Interestingly, the lung besides showing the greater number of genes showed also the largest magnitude of transcriptional changes between infected and non-infected conditions, suggesting that changes induced by infection in lungs seem to rely on genes, which had large transcriptional changes.

CONCLUSION

We used two complementary approaches to characterize alterations in tissue-specific gene expression in cats infected with *T. gondii*. Our results revealed considerable transcriptional differences between cat body tissues, and between infected and healthy cats. We identified significant tissue-specific differences in gene expression, and in gene cluster content and functional annotations. The differences in gene expression and gene clusters may result from tissue-specific differences in the defense processes that shape the host-pathogen interaction. Our data also underlined the importance of immune and inflammatory response to *T. gondii* infection, regardless of tissue types. Genes and pathways discovered in this study, should serve as a basis for further understanding the cellular and molecular basis of cat response to *T. gondii*. These results may assist the selection of biomarkers useful for developing new diagnostic tools or therapeutic interventions to control toxoplasmosis in cats.

ACCESSION NUMBER(S)

The RNA-seq data reported in this study have been deposited in GenBank's Short Read Archive (SRA) database under BioProject number PRJNA296557.

AUTHOR CONTRIBUTIONS

X-QZ, HE, and WC designed the experiment. WC supervised the experimental infection. WC, F-KZ, C-XZ, J-JH, and X-XZ performed the experiments. WC, HE, TD, FK, and RE contributed reagents, materials, and analysis tools. TD, FK, and RE developed computational algorithms and performed the bioinformatics analysis. WC, HE, and X-QZ wrote the paper. All authors commented on the manuscript.

FUNDING

Project support was kindly provided by the International Science and Technology Cooperation Project of Gansu Provincial Key Research and Development Program (Grant No. 17JR7WA031), the National Natural Science Foundation of China (Grant Nos. 31230073 and 31702383), the Elite Program of Chinese Academy of Agricultural Sciences, and the Agricultural Science and Technology Innovation Program (ASTIP) (Grant No. CAAS-ASTIP-2016-LVRI-03).

ACKNOWLEDGMENTS

We thank Hind Mamdowh Saad for excellent drawing of the **Graphical Abstract**.

SUPPLEMENTARY MATERIAL

The Supplementary Material for this article can be found online at: https://www.frontiersin.org/articles/10.3389/fimmu.2018.02403/full#supplementary-material

Figure S1 | Agarose gel electrophoresis of PCR amplicons after nested amplification of *Toxoplasma gondii B1* gene-specific fragment from cat tissue DNA. ∼96-bp products of *B1* gene were amplified from ∼193-bp *B1* PCR products, originally generated from genomic DNA extracted from different cat tissues, using the nested primers 5′-TGCATAGGTTGCAGTCACTG-3′ and 5′-GGCGACCAATCTGCGAATACACC-3′. Samples were analyzed by electrophoresis through 2% (wt/vol) agarose gels. Gels were stained with ethidium bromide and DNA was visualized under UV. Lanes: M, DNA ladder marker (TAKARA, China); 1, positive control; 2, negative control without DNA template; 3–8, positive PCR products from brain, heart, liver, lung, spleen and small intestine of infected cats; 9–14, negative results of samples obtained from the equivalent tissues of uninfected cats. The numbers to the left refer to the size (bp) of marker DNA fragments.

Figure S2 | Differential gene expression patterns across tissues and GO terms of the overlapping DEGs. **(A)** A heatmap of the genes expressed in all six tissues. **(B)** Gene Ontology terms associated with the co-expressed DEGs.

Figure S3 | Gene Ontology terms and KEGG pathways distribution per gene cluster.

Table S1 | Summary of RNA-Sequencing data obtained by Illumina HiSeq 2500 platform.

Table S2 | Summary of read mapping.

Table S3 | The number of gene in different expression level intervals.

Table S4 | Differentially expressed genes in various cat tissues.

Table S5 | Functional enrichment analysis of DEGs in various cat tissues.

Table S6 | DEGs involved in immune-related pathways in cat tissues.

Table S7 | Differentially co-expressed genes across various cat tissues.

Table S8 | Gene Ontology analysis of seven gene clusters.

REFERENCES

1. Montoya JG, Liesenfeld O. Toxoplasmosis. *Lancet* (2004) 363:1965–76. doi: 10.1016/S0140-6736(04)16412-X
2. Elsheikha HM. Congenital toxoplasmosis: priorities for further health promotion action. *Public Health* (2008) 122:335–53. doi: 10.1016/j.puhe.2007.08.009
3. Hill DE, Dubey JP. *Toxoplasma gondii* prevalence in farm animals in the United States. *Int J Parasitol.* (2013) 43:107–13. doi: 10.1016/j.ijpara.2012.09.012
4. Doliwa C, Escotte-Binet S, Aubert D, Sauvage V, Velard F, Schmid A, et al. Sulfadiazine resistance in *Toxoplasma gondii*: no involvement of overexpression or polymorphisms in genes of therapeutic targets and ABC transporters. *Parasite* (2013) 20:19. doi: 10.1051/parasite/2013020
5. Katlama C, De Wit S, O'Doherty E, Van Glabeke M, Clumeck N. Pyrimethamine-clindamycin versus pyrimethamine-sulfadiazine as acute and long-term therapy for toxoplasmic encephalitis in patients with aids. *Clin Infect Dis.* (1996) 22:268–75.
6. Dubey JP, Jones JL. *Toxoplasma gondii* infection in humans and animals in the United States. *Int J Parasitol.* (2008) 38:1257–78. doi: 10.1016/j.ijpara.2008.03.007
7. Hill DE, Dubey JP. *Toxoplasma gondii*: transmission, diagnosis and prevention. *Clin Microbiol Infect.* (2002) 8:634–40. doi: 10.1046/j.1469-0691.2002.00485.x
8. Dubey JP, Zajac SAA, Osofsky TobiasL. Acute primary toxoplasmic hepatitis in an adult cat shedding *Toxoplasma gondii* oocysts. *J Am Vet Med Assoc.* (1990) 197:1616–8.
9. Anfray P, Bonetti C, Fabbrini F, Magnino S, Mancianti F, Abramo F. Feline cutaneous toxoplasmosis: a case report. *Vet Dermatol.* (2005) 16:131–6. doi: 10.1111/j.1365-3164.2005.00434.x
10. Spycher A, Geigy C, Howard J, Posthaus H, Gendron K, Gottstein B, et al. Isolation and genotyping of *Toxoplasma gondii* causing fatal systemic toxoplasmosis in an immunocompetent 10-year-old cat. *J Vet Diagn Invest.* (2011) 23:104–8. doi: 10.1177/104063871102300117
11. Nagel SS, Williams JH, Schoeman JP. Fatal disseminated toxoplasmosis in an immunocompetent cat. *J S Afr Vet Assoc.* (2013) 84: E1–6. doi: 10.4102/jsava.v84i1.299
12. Foster SF, Charles JA, Canfield PJ, Beatty JA, Martin P. Reactivated toxoplasmosis in a FIV-positive cat. *Aus Vet Pract.* (1998) 28:159–63.
13. Atmaca HT, Dincel GC, Macun HC, Terzi OS, Uzunalioglu T, Kalender H, et al. A rare case of feline congenital *Toxoplasma gondii* infection: fatal outcome of systemic toxoplasmosis for the mother and its kitten. *Berl Munch Tierarztl Wochenschr* (2013) 126:216–9.
14. Dubey JP, Prowell M. Ante-mortem diagnosis, diarrhea, oocyst shedding, treatment, isolation, and genetic typing of *Toxoplasma gondii* associated with clinical toxoplasmosis in a naturally infected cat. *J Parasitol.* (2013) 99:158–60. doi: 10.1645/GE-3257.1
15. Melo MB, Nguyen QP, Cordeiro C, Hassan MA, Yang N, McKell R, et al. Transcriptional analysis of murine macrophages infected with different *Toxoplasma* strains identifies novel regulation of host signaling pathways. *PLoS Pathog.* (2013) 9:e1003779. doi: 10.1371/journal.ppat.1003779
16. Tanaka S, Nishimura M, Ihara F, Yamagishi J, Suzuki Y, Nishikawa Y. Transcriptome analysis of mouse brain infected with *Toxoplasma gondii*. *Infect Immun.* (2013) 81:3609–19. doi: 10.1128/IAI.00439-13

17. Pittman KJ, Aliota MT, Knoll LJ. Dual transcriptional profiling of mice and *Toxoplasma gondii* during acute and chronic infection. *BMC Genomics* (2014) 15:806. doi: 10.1186/1471-2164-15-806
18. He JJ, Ma J, Li FC, Song HQ, Xu MJ, Zhu XQ. Transcriptional changes of mouse splenocyte organelle components following acute infection with *Toxoplasma gondii*. *Exp Parasitol.* (2016) 167:7–16. doi: 10.1016/j.exppara.2016.04.019
19. He JJ, Ma J, Song HQ, Zhou DH, Wang JL, Huang SY, et al. Transcriptomic analysis of global changes in cytokine expression in mouse spleens following acute *Toxoplasma gondii* infection. *Parasitol Res.* (2016) 115:703–12. doi: 10.1007/s00436-015-4792-5
20. Zhou CX, Elsheikha HM, Zhou DH, Liu Q, Zhu XQ, Suo X. Dual identification and analysis of differentially expressed transcripts of Porcine PK-15 cells and *Toxoplasma gondii* during *in vitro* infection. *Front Microbiol.* (2016) 7:721. doi: 10.3389/fmicb.2016.00721
21. Zhou CX, Zhou DH, Liu GX, Suo X, Zhu XQ. Transcriptomic analysis of porcine PBMCs infected with *Toxoplasma gondii* RH strain. *Acta Trop.* (2016) 154:82–8. doi: 10.1016/j.actatropica.2015.11.009
22. Emrich SJ, Barbazuk WB, Li L, Schnable PS. Gene discovery and annotation using LCM-454 transcriptome sequencing. *Genome Res.* (2007) 17:69–73. doi: 10.1101/gr.5145806
23. Huang Y, Huang X, Yan Y, Cai J, Ouyang Z, Cui H, et al. Transcriptome analysis of orange-spotted grouper (*Epinephelus coioides*) spleen in response to Singapore grouper iridovirus. *BMC Genomics* (2011) 12:556. doi: 10.1186/1471-2164-12-556
24. Videvall E, Cornwallis CK, Palinauskas V, Valkiunas G, Hellgren O. The avian transcriptome response to *Malaria* infection. *Mol Biol Evol.* (2015) 32:1255–67. doi: 10.1093/molbev/msv016
25. Hehl AB, Basso WU, Lippuner C, Ramakrishnan C, Okoniewski M, Walker RA, et al. Asexual expansion of *Toxoplasma gondii* merozoites is distinct from tachyzoites and entails expression of non-overlapping gene families to attach, invade, and replicate within feline enterocytes. *BMC Genomics* (2015) 16:66. doi: 10.1186/s12864-015-1225-x
26. Yan HK, Yuan ZG, Song HQ, Petersen E, Zhou Y, Ren D, et al. Vaccination with a DNA vaccine coding for perforin-like protein 1 and MIC6 induces significant protective immunity against *Toxoplasma gondii*. *Clin Vaccine Immunol.* (2012) 19:684–9. doi: 10.1128/CVI.05578-11
27. Cong W, Liu GH, Meng QF, Dong W, Qin SY, Zhang FK, et al. *Toxoplasma gondii* infection in cancer patients: prevalence, risk factors, genotypes and association with clinical diagnosis. *Cancer Lett.* (2015) 359:307–13. doi: 10.1016/j.canlet.2015.01.036
28. Jones CD, Okhravi N, Adamson P, Tasker S, Lightman S. Comparison of PCR detection methods for B1, P30, and 18S rDNA genes of *T. gondii* in aqueous humor. *Invest Ophthalmol Vis Sci.* (2000) 41:634–44.
29. Cong W, Meng QF, Song HQ, Zhou DH, Huang SY, Qian AD, et al. Seroprevalence and genetic characterization of *Toxoplasma gondii* in three species of pet birds in China. *Parasit Vectors* (2014) 7:152. doi: 10.1186/1756-3305-7-152
30. Kim D, Langmead B, Salzberg SL. HISAT: a fast spliced aligner with low memory requirements. *Nat Methods* (2015) 12:357-360. doi: 10.1038/nmeth.3317
31. Pertea M, Pertea GM, Antonescu CM, Chang TC, Mendell JT, Salzberg SL. StringTie enables improved reconstruction of a transcriptome from RNA-seq reads. *Nat Biotechnol.* (2015) 33:290–5. doi: 10.1038/nbt.3122
32. Robinson MD, McCarthy DJ, Smyth GK. edgeR: a Bioconductor package for differential expression analysis of digital gene expression data. *Bioinformatics* (2010) 26:139–40. doi: 10.1093/bioinformatics/btp616
33. Falcon S, Gentleman R. Using GOstats to test gene lists for GO term association. *Bioinformatics* (2007) 23:257–8. doi: 10.1093/bioinformatics/btl567
34. Schmittgen TD, Livak KJ. Analyzing real-time PCR data by the comparative CT method. *Nat Protoc.* (2008) 3:1101–8. doi: 10.1038/nprot.2008.73
35. Livak KJ, Schmittgen TD. Analysis of relative gene expression data using realtime quantitative PCR and the $2^{-\Delta\Delta}$ CT method. *Methods* (2001) 25:402–8. doi: 10.1006/meth.2001.1262
36. Tobias S. Acute primary toxoplasmic hepatitis in an adult cat shedding *Toxoplasma gondii* oocysts. *J Am Vet Med Asso.* (1990) 197:1616–8.
37. Yarovinsky F. Innate immunity to *Toxoplasma gondii* infection. *Nat Rev Immunol.* (2014) 14:109–21. doi: 10.1038/nri3598
38. Caamaño J, Alexander J, Craig L, Bravo R, Hunter CA. The NF-kappa B family member RelB is required for innate and adaptive immunity to *Toxoplasma gondii*. *J Immunol.* (1999) 163:4453–61.
39. Butcher BA, Fox BA, Rommereim LM, Kim SG, Maurer KJ, Yarovinsky F, et al. *Toxoplasma gondii* rhoptry kinase ROP16 activates STAT3 and STAT6 resulting in cytokine inhibition and arginase-1-dependent growth control. *PLoS Pathog.* (2011) 7:e1002236. doi: 10.1371/journal.ppat.1002236
40. Hunter CA, Sibley LD. Modulation of innate immunity by *Toxoplasma gondii* virulence effectors. *Nat Rev Microbiol.* (2012) 10:766–78. doi: 10.1038/nrmicro2858
41. Yarovinsky F. Toll-like receptors and their role in host resistance to *Toxoplasma gondii*. *Immunol Lett* (2008) 119:17-21. doi: 10.1016/j.imlet.2008.05.007
42. Pifer R, Yarovinsky F. Innate responses to *Toxoplasma gondii* in mice and humans. *Trends Parasitol.* (2011) 27:388–93. doi: 10.1016/j.pt.2011.03.009
43. Dufour JH, Dziejman M, Liu MT, Leung JH, Lane TE, Luster AD. IFN-γ-inducible protein 10 (IP-10; CXCL10)-deficient mice reveal a role forIP-10 in effector T cell generation and trafficking. *J Immunol.* (2002) 168:3195–204. doi: 10.4049/jimmunol.168.7.3195
44. Dubey JP. Toxoplasmosis - a waterborne zoonosis. *Vet Parasitol.* (2004) 126:57–72. doi: 10.1016/j.vetpar.2004.09.005
45. Schreiner M, Liesenfeld O. Small intestinal inflammation following oral infection with *Toxoplasma gondii* does not occur exclusively in C57BL/6 mice: Review of 70 reports from the literature. *Mem Inst Oswaldo Cruz.* (2009) 104:221–33. doi: 10.1590/S0074-02762009000200015
46. Guiton PS, Sagawa JM, Fritz HM, Boothroyd JC. An *in vitro* model of intestinal infection reveals a developmentally regulated transcriptome of *Toxoplasma* sporozoites and a NF-κB-like signature in infected host cells. *PLoS ONE* (2017) 12:e0173018. doi: 10.1371/journal.pone.0173018
47. Hill RD, Gouffon JS, Saxton AM, Su C. Differential gene expression in mice infected with distinct *Toxoplasma* strains. *Infect Immun.* (2012) 80:968–74. doi: 10.1128/IAI.05421-11
48. Carter CJ. Toxoplasmosis and polygenic disease susceptibility genes: extensive *Toxoplasma gondii* host/pathogen interactome enrichment in nine psychiatric or neurological disorders. *J Pathog.* (2013) 2013:965046. doi: 10.1155/2013/965046
49. Franke TF. Intracellular signaling by Akt: bound to be specific. *Sci Signal.* (2008) 1:pe29. doi: 10.1126/scisignal.124pe29
50. Quan JH, Cha GH, Zhou W, Chu JQ, Nishikawa Y, Lee YH. Involvement of PI 3 kinase/Akt-dependent Bad phosphorylation in *Toxoplasma gondii*-mediated inhibition of host cell apoptosis. *Exp Parasitol.* (2013) 133:462–71. doi: 10.1016/j.exppara.2013.01.005
51. Zhou W, Quan JH, Lee YH, Shin DW, Cha GH. *Toxoplasma gondii* proliferation require down-regulation of host Nox4 expression via activation of PI3 Kinase/Akt signaling pathway. *PLoS ONE* (2013) 8:e66306. doi: 10.1371/journal.pone.0066306
52. Kim L, Denkers EY. *Toxoplasma gondii* triggers Gi-dependent PI 3-kinase signaling required for inhibition of host cell apoptosis. *J Cell Sci.* (2006) 119 (Pt 10):2119–26. doi: 10.1242/jcs.02934
53. Jiang BH, Liu LZ. PI3K/PTEN signaling in angiogenesis and tumorigenesis. *Adv Cancer Res.* (2009) 102:19–65. doi: 10.1016/S0065-230X(09)02002-8
54. Yang CS, Yuk JM, Lee YH, Jo EK. *Toxoplasma gondii* GRA7-induced TRAF6 activation contributes to host protective immunity. *Infect Immun.* (2015) 84:339–50. doi: 10.1128/IAI.00734-15
55. Kim L, Butcher BA, Denkers EY. *Toxoplasma gondii* interferes with lipopolysaccharide-induced mitogen-activated protein kinase activation by mechanisms distinct from endotoxin tolerance. *J Immunol.* (2004) 172:3003–10. doi: 10.4049/jimmunol.172.5.3003
56. Valère A, Garnotel R, Villena I, Guenounou M, Pinon JM, Aubert D. Activation of the cellular mitogen-activated protein kinase pathways ERK, P38 and JNK during *Toxoplasma gondii* invasion. *Parasite* (2003)10:59–64. doi: 10.1051/parasite/2003101p59
57. Braun L, Brenier-Pinchart MP, Yogavel M, Curt-Varesano A, Curt-Bertini RL, Hussain T, et al. A *Toxoplasma* dense granule protein, GRA24, modulates the early immune response to infection by promoting a direct

and sustained host p38 MAPK activation. *J Exp Med.* (2013) 210:2071–86. doi: 10.1084/jem.20130103
58. Mbongue JC, Nicholas DA, Torrez TW, Kim NS, Firek AF, Langridge WH. The Role of Indoleamine 2, 3-Dioxygenase in immune suppression and autoimmunity. Vaccines (Basel) (2015) 3:703-729. doi: 10.3390/vaccines3030703
59. Pfefferkorn ER. Interferon gamma blocks the growth of *Toxoplasma gondii* in human fibroblasts by inducing the host cells to degrade tryptophan. *Proc Natl Acad Sci USA*. (1984) 81:908–12. doi: 10.1073/pnas.81.3.908
60. Hunt NH, Too LK, Khaw LT, Guo J, Hee L, Mitchell AJ, et al. The kynurenine pathway and parasitic infections that affect CNS function. *Neuropharmacology* (2017) 112(Pt B):389–98. doi: 10.1016/j.neuropharm.2016.02.029
61. Krishnamurthy S, Konstantinou EK, Young LH, Gold DA, Saeij JPJ. The human immune response to *Toxoplasma*: Autophagy versus cell death. *PLoS Pathog.* (2017) 13:e1006176. doi: 10.1371/journal.ppat.1006176
62. Kravets E, Degrandi D, Ma Q, Peulen TO, Klümpers V, Felekyan S, et al. Guanylate binding proteins directly attack *Toxoplasma gondii* via supramolecular complexes. *Elife* (2016) 5:e11479. doi: 10.7554/eLife.11479
63. Qin A, Lai DH, Liu Q, Huang W, Wu YP, Chen X, et al. Guanylate-binding protein 1 (GBP1) contributes to the immunity of human mesenchymal stromal cells against *Toxoplasma gondii*. *Proc Natl Acad Sci USA*. (2017) 114:1365–70. doi: 10.1073/pnas.1619665114
64. Degrandi D, Kravets E, Konermann C, Beuter-Gunia C, Klümpers V, Lahme S, et al. Murine guanylate binding protein 2 (mGBP2) controls *Toxoplasma gondii* replication. *Proc Natl Acad Sci USA*. (2013) 110:294–9. doi: 10.1073/pnas.1205635110

Conflict of Interest Statement: The authors declare that the research was conducted in the absence of any commercial or financial relationships that could be construed as a potential conflict of interest.

frontiers in Immunology

ORIGINAL RESEARCH
published: 08 October 2018
doi: 10.3389/fimmu.2018.02282

Parasitic Nematodes Exert Antimicrobial Activity and Benefit From Microbiota-Driven Support for Host Immune Regulation

Sebastian Rausch[1]*, *Ankur Midha*[1], *Matthias Kuhring*[2,3,4,5], *Nicole Affinass*[1], *Aleksandar Radonic*[6,7], *Anja A. Kühl*[8], *André Bleich*[9], *Bernhard Y. Renard*[2] and *Susanne Hartmann*[1]*

[1] Department of Veterinary Medicine, Institute of Immunology, Freie Universität Berlin, Berlin, Germany, [2] Bioinformatics Unit (MF 1), Robert Koch Institute, Berlin, Germany, [3] Core Unit Bioinformatics, Berlin Institute of Health (BIH), Berlin, Germany, [4] Berlin Institute of Health Metabolomics Platform, Berlin Institute of Health (BIH), Berlin, Germany, [5] Max Delbrück Center for Molecular Medicine, Berlin, Germany, [6] Centre for Biological Threats and Special Pathogens (ZBS 1), Robert Koch Institute, Berlin, Germany, [7] Genome Sequencing Unit (MF 2), Robert Koch Institute, Berlin, Germany, [8] iPATH.Berlin, Core Unit for Immunopathology for Experimental Models, Berlin Institute of Health, Charité - Universitätsmedizin Berlin, Corporate Member of Freie Universität Berlin, Humboldt-Universität zu Berlin, Berlin, Germany, [9] Institute for Laboratory Animal Science, Hannover Medical School, Hannover, Germany

OPEN ACCESS

Edited by:
Wenbin Tuo,
Beltsville Agricultural Research Center, Agricultural Research Service (USDA), United States

Reviewed by:
Alan L. Scott,
Johns Hopkins University, United States
William Horsnell,
University of Cape Town, South Africa

***Correspondence:**
Sebastian Rausch
sebastian.rausch@fu-berlin.de
Susanne Hartmann
susanne.hartmann@fu-berlin.de

Specialty section:
This article was submitted to Microbial Immunology, a section of the journal Frontiers in Immunology

Received: *18 June 2018*
Accepted: *14 September 2018*
Published: *08 October 2018*

Citation:
Rausch S, Midha A, Kuhring M, Affinass N, Radonic A, Kühl AA, Bleich A, Renard BY and Hartmann S (2018) Parasitic Nematodes Exert Antimicrobial Activity and Benefit From Microbiota-Driven Support for Host Immune Regulation. Front. Immunol. 9:2282. doi: 10.3389/fimmu.2018.02282

Intestinal parasitic nematodes live in intimate contact with the host microbiota. Changes in the microbiome composition during nematode infection affect immune control of the parasites and shifts in the abundance of bacterial groups have been linked to the immunoregulatory potential of nematodes. Here we asked if the small intestinal parasite *Heligmosomoides polygyrus* produces factors with antimicrobial activity, senses its microbial environment and if the anti-nematode immune and regulatory responses are altered in mice devoid of gut microbes. We found that *H. polygyrus* excretory/secretory products exhibited antimicrobial activity against gram$^{+/-}$ bacteria. Parasites from germ-free mice displayed alterations in gene expression, comprising factors with putative antimicrobial functions such as chitinase and lysozyme. Infected germ-free mice developed increased small intestinal Th2 responses coinciding with a reduction in local Foxp3^{+}RORγt^{+} regulatory T cells and decreased parasite fecundity. Our data suggest that nematodes sense their microbial surrounding and have evolved factors that limit the outgrowth of certain microbes. Moreover, the parasites benefit from microbiota-driven immune regulatory circuits, as an increased ratio of intestinal Th2 effector to regulatory T cells coincides with reduced parasite fitness in germ-free mice.

Keywords: parasite, nematode, immune regulation, germ-free, microbiota, antimicrobial, Treg, Th2

INTRODUCTION

Infections with enteric nematodes are associated with changes in the composition of the host intestinal microbiota in mice, pigs, and primates (1–5). Our previous work showed that nematode-infected mice deficient in IL-4Rα-signaling, hence refractory to IL-4/IL-13-dependent immune sequelae, experience similar microbiota alterations as fully immune-competent mice (2), leaving open the question of the mechanistic basis for structural changes in microbial communities

associated with nematode infections. Our and other groups have shown that products released by parasitic nematodes possess antimicrobial activity (6–8), prompting the question if enteric nematodes sense and actively shape their microbial environment.

To ensure prolonged survival and reproduction, parasitic nematodes have developed strategies suppressing host immune responses, in part driven by the release of immunomodulators interfering with innate and adaptive immune effector mechanisms (9–11), but also by supporting the *de novo* generation, expansion and activation of regulatory T cells (Treg) (12–16). Recent studies provide evidence for a contribution of microbiota alterations to immune regulation during nematode infection. More specifically, the increased abundances of Lactobacilli and Clostridiales family members during nematode-infection have been linked to the expansion and activation of Treg (1, 17), which in turn control the magnitude of anti-parasite and unrelated inflammatory responses (13–16, 18).

Here we focused on the interaction of an enteric parasite infection, microbiota, and host immunity. We surveyed fitness and gene expression of the small intestinal nematode *Heligmosomoides polygyrus* reared in conventional and germ-free mice and investigated products released by the parasite for antimicrobial activity against gram$^-$ and gram$^+$ bacterial species. Furthermore, we compared anti-parasite Th2 immunity and the expansion, cytokine production and phenotypic heterogeneity of Treg in conventional and germfree mice. Our data demonstrate that (I) *H. polygyrus* may actively shape the composition of the host microbiota by releasing antimicrobials and that (II) nematode fitness is compromised in the absence of host microbes. Furthermore, our data suggest that the nematode senses the microbiota, as indicated by differential gene expression of worms from germ-free and conventional hosts, and finally, that microbes support Treg responses regulating anti-parasite Th2 immunity.

MATERIALS AND METHODS

Mice and Parasites

The experiments performed followed the National Animal Protection Guidelines and were approved by the German Animal Ethics Committee for the protection of animals (G0176/16). Female specific pathogen-free (SPF) and germfree C57BL/6 mice were kept in individually ventilated, filter-topped cages with autoclaved bedding, chow and water. Infections with 200 *H. polygyrus* larvae were performed aseptically in a laminar flow. *H. polygyrus* L3 were freshly isolated from fecal cultures of infected mice and treated for 1 week with an antibiotic cocktail (5 mg/ml streptomycin, 1 mg/ml ampicillin, 0.5 mg/ml gentamicin, 1 mg/ml neomycin, 0.5 mg/ml vancomycin; all from AppliChem, Darmstadt, Germany). L3 were shown to be free of aerobic microbes as determined by lack of bacterial growth in antibiotic-free LB medium. Infected and naïve control GF mice received antibiotics (as specified above) via the drinking water. To further reduce the risk of contamination, SPF and GF C57BL/6 mice were kept without bedding change until the dissection 2 weeks post-infection. The axenic status of GF mice was confirmed by qPCR of eubacterial 16s rRNA with colon content collected on the day of infection and dissection. Adult worms were removed from the small intestine, counted and eight females per mouse were kept at 37°C in RPMI-1640 medium containing 200 U/mL penicillin, 200 μg/mL streptomycin (all from PAN Biotech, Aidenbach, Germany) and 1% glucose for 24 h for the determination of individual egg counts. Female worm length was determined after culture.

Parasite Excretory/Secretory Products

Excretory/secretory products of *H. polygyrus* (HES) were collected from adult worms extensively washed before being cultured in phenol-red free RPMI-1640 medium containing 200 U/mL penicillin, 200 μg/mL streptomycin. After 24 h in culture, worms were washed extensively with antibiotic-free worm growth media (RPMI-1640 medium with 1% glucose) and maintained in this medium with daily media changes. Spent media from the first 48 h were discarded. Thereafter, supernatants were harvested every 48 h and sterile filtered through a 0.22 μm syringe-driven filter system, and stored at −20°C until further use.

Bacterial Strains

The strains used to evaluate antibacterial activities of HES in the radial diffusion assay included *Escherichia coli* IMT19224, *Salmonella enterica* serovar Typhimurium ATCC14028, and *Staphylococcus aureus* IMT29828 obtained from the strain collection of the Institute of Microbiology and Epizoonotics, Freie Universität Berlin and *Enterococcus faecium* DSM20477 provided by Dr. Markus Heimesaat (Institute of Microbiology, Charité—Universitätsmedizin Berlin). *E. coli* IMT19224 was used to assess agglutinating activity of HES.

Radial Diffusion Assay

Antibacterial activities of HES were assessed using the radial diffusion assay (19). Overnight bacterial cultures were diluted 1:100 in Mueller-Hinton broth (Carl Roth, Karlsruhe, Germany) and incubated at 37°C with shaking at 250 rpm until reaching an optical density of 0.3–0.4 at 600 nm. Bacteria were washed and resuspended in cold sodium phosphate buffer (100 mM, pH 7.4) by centrifugation (880 × g, 10 min, 4°C). Bacteria were then resuspended in warm (50°C), sterile underlay agar [10 mM sodium phosphate buffer, 1% (v/v) Mueller-Hinton broth, 1.5 (w/v) agar] at 4×10^5 colony forming units per mL. Fifteen milliliter of bacteria-infused underlay agar was poured into 120 mm square petri dishes and allowed to solidify. Evenly spaced wells (5 mm) were formed in the agar using the blunt ends of P10 pipet tips, and treatments and controls added (5 μL/well). Five microliter native HES corresponded to 5 μg protein. The antimicrobial peptide Pexiganan (kindly provided by Jens Rolff, Institute of Biology, Freie Universität Berlin, 0.0125 μg/well) was applied as positive control. PBS and RPMI-1640 medium were included as negative controls. Plates were incubated at 37°C for 3 h and then overlaid with double-strength Mueller-Hinton agar [4.2% (w/v) Mueller-Hinton broth, 1.5% agar]. Petri dishes were incubated for 18 h at 37°C and the growth inhibition zones around each well were measured. Antibacterial activity is

represented as the diameter of the inhibition zone (mm) beyond the 5 mm well.

Agglutination Assay

Agglutinating activity of HES was assessed as described previously (20) using *E. coli* IMT19224. Bacteria were collected at mid-logarithmic phase by centrifugation at 880 × g for 5 min, then washed and resuspended in Tris-buffered saline (50 mM Tris-HCl, 150 mM NaCl, pH 7.5) at approximately 10^9 cells/mL. Thirty microliter of bacteria were mixed with 30 µL of treatments in the presence and absence of 10 mM $CaCl_2$ and incubated for 1 h at room temperature on a glass slide. Concanavalin A from *Canavalia ensiformis* (Con A) and Lectin from *Triticum vulgaris* (Wheat germ agglutinin; WGA, both from Sigma-Aldrich) were included as positive controls. Samples were then visualized and photographed using the 40X objective on a Leica DM750 microscope equipped with an ICC50HD digital camera (Leica Microsystems, Wetzlar, Germany).

Parasite RNA-Isolation and Quality Check

Small intestines and the bulk of removed parasites were kept in ice-cold physiological NaCl solution. Thirty worms (15 males/15 females) were quickly isolated from three individual SPF and GF mice, washed repeatedly in cold physiological NaCl solution, inspected for physical integrity, and absence of host tissue and then snap frozen in liquid nitrogen before storage at −80°C. Samples were homogenized using shredder columns filled with 200 mg sterile sea sand and the FastPrep®-24 instrument (MP Biomedicals, Eschwege, Germany) at 5 m/s for 35 s. Supernatants of homogenized worms were further processed for RNA isolation (InnuPREP RNA isolation, Analytik Jena AG, Germany), DNase treatment (Analytik Jena AG, Germany), and RNA quality control (Agilent 2100 Bioanalyzer, RNA 6000 Nano Kit, Agilent Technologies, Waldbronn, Germany). All RNA samples displayed RIN values of 10.

Sequencing and Data Processing

For transcriptome sequencing on an Illumina platform a TruSeq RNA library generation was utilized. The library was generated by using the TruSeq RNA Sample Prep Kit v2 (Illumina, San Diego, CA, USA) following the manufacturer's instructions. The library was quantified by using the KAPA Library Quantification Kit for Illumina (Kapa Biosystems, Wilmington, MA, USA). The library size was determined by using the High Sensitivity DNA Analysis Kit for the 2100 Bioanalyzer Instrument (Agilent Technologies, Waldbronn, Germany). Libraries were adjusted to a concentration of 12 pM and sequenced on a HiSeq 1500 instrument (Illumina, San Diego, CA, USA) in rapid mode. For cluster generation, the TruSeq Rapid PE Cluster Kit v2 was used. Cluster generation was performed on board. For sequencing the HiSeq Rapid SBS kit v2 was used to sequence 100 + 100 bases.

We sequenced three isolates from SPF and GF mice with a mean library size of 40.15 million paired-end reads and a standard deviation of 10.74. Raw reads were subjected to quality control and trimming via the QCumber pipeline (version 1.0.14, https://gitlab.com/RKIBioinformaticsPipelines/QCumber) utilizing FastQC (v0.11.5, https://www.bioinformatics.babraham.ac.uk/projects/fastqc/), Trimmomatic (0.36) (21) and Kraken (0.10.5-beta) (22). On average, 91.77% of reads remained after trimming.

Preprocessed reads were mapped to a reference genome (as specified below) and corresponding sequence features using the TopHat split-read mapper (v2.1.1) (23) and reference as well as novel features were extracted and merged with the aid of Cufflinks and Cuffmerg (24) (v2.2.1) to obtain one integrated and unified transcriptome for *H. polygyrus* samples. The *H. polygyrus* draft genome nHp_v2.0 was applied as reference genome (database version WBPS10, annotation version 2016-09-WormBase), as available at WormBase ParaSite (25). For each sample, raw expression values were created by counting uniquely mapped reads on gene level using featureCounts (v1.5.0-p3) (26). To identify differentially expressed genes (DEGs) between SPF and GF mice isolates, respectively, DESeq2 (1.12.4) (27) was applied with a classic pairwise design model and a *p*-value threshold of 0.05. In addition, normalized and transformed expression values were extracted from DESeq2 (regularized log transformation) and corrected for batch effects via Limma (3.28.21, removeBatchEffect) (28) to allow for sample comparison with clustered heatmaps and principal component analysis (PCA).

Reference as well as novel transcripts were functionally (re-)annotated using an iterative annotation strategy. First, transcripts were either first-frame translated (reference) or examined for ORFs (novels, Cuffcompare class code "u") using EMBOSS transeq (6.6.0.0) (29) and TransDecoder (v2.1), respectively. Next, resulting protein sequences were passed through a series of database searches until successfully annotated with Gene Ontology (GO) terms (30), either via blastp (2.6.0+) (31), and Blast2GO (4.0.7) (32) or by a final InterProScan (33). Databases used for annotation included (in this order) the UniProt (34) *Heligmosomoides polygyrus bakeri* proteome (UP000050761, downloaded at 07.04.2017), UniProt Swiss-Prot Nematoda proteins, UniProt TrEMBL Nematoda proteins as well as the complete Swiss-Prot database and the complete TrEMBL database (all downloaded at 16.02.2017).

Cell Isolation, Stimulation, and Flow Cytometry

Lymph node single cell suspensions and small intestinal tissue digestion for the isolation of siLP cells were performed as described previously (35). Cultures were kept for 6 h with brefeldin A added after 1 h before surface and intracellular staining. Surface and intracellular markers were stained according to the manufacturer's instructions with the following antibodies obtained from ThermoFisher/eBioscience, if not stated otherwise: CD4-PerCP/-BV510/-A700 (RM4-5), Foxp3-FITC/-PerCP-Cy5.5 (FJK-16s), GATA-3-A660/-PE/-PE-eF610 (TWAJ), T-bet-PE/-PE-Cy7 (eBio4B10), RORγt-BV421 (Q31-378, BD biosciences), IL-10-APC (JES5-16E3), IL-4-PE/-PE-Cy7 (11B11), and IL-17A-PerCP-Cy5.5 (eBio17B7). Live/dead discrimination was performed using fixable viability dye eF780 (ThermoFisher/eBioscience). Unspecific binding was prevented by addition of 20 µg/ml FcgRII/III blocking antibody (2.4G2).

Histology

Formalin-fixed, paraffin-embedded sections (1–2 μm) of duodenum were de-waxed and stained with hematoxylin and eosin for overview, with periodic acid Schiff for goblet cell quantification and by Direct red 80 (Sigma) for the detection of eosinophils. Enteritis was scored using hematoxylin and eosin-stained section as described before (16). PAS^+ goblet cells were counted along five villi per section. Images were acquired using the AxioImager Z1 microscope (Carl Zeiss MicroImaging, Inc., Göttingen, Germany). All evaluations were performed blinded.

Statistical Analyses

Data were assessed for normality using GraphPad Prism software (La Jolla, CA, USA). For comparison between two groups, an unpaired *T*-test was used. Testing of multiple groups was performed using a one-way analysis of variances followed by Tukey's multiple comparison or the Kruskall-Wallis test combined with Dunn's multiple comparison test.

RESULTS

Antimicrobial Activity of Nematode Excretory/Secretory Products

Infection with *H. polygyrus* alters the composition of the intestinal microbiota alongside the intestine, including an increase in $gram^-$ Enterobacteriaceae (2, 17, 36). Similar changes occurred in IL-4Rα$^{-/-}$ mice, hence independently of Th2-mediated changes in gut physiology (2). As both free-living and parasitic nematodes defend themselves against potentially harmful microbes by the production of antimicrobial factors (7), we asked if *H. polygyrus* releases active antimicrobials, possibly interfering with its microbial environment. We used the radial diffusion assay to test the antibacterial activity of *H. polygyrus* excretory/secretory products (HES) in comparison to the antimicrobial peptide Pexiganan. Five micrograms of native HES collected from *H. polygyrus* cultures inhibited the growth of $gram^-$ and $gram^+$ bacteria, including *E. coli*, *S. enterica* var. Typhimurium, *E. faecium*, and *S. aureus* (**Table 1**).

TABLE 1 | Antimicrobial activity* of excretory/secretory products from adult *Heligmosomoides polygyrus* nematodes in the radial diffusion assay.

	E. coli IMT19224	*S. typhimurium* ATCC14028	*E. faecium* DSM20477	*S. aureus* IMT29828
H. polygyrus E/S (5 μg)	5.3 ± 3.1	4.3 ± 0.6	3.7 ± 1.5	5.7 ± 1.5
Pexiganan (0.0125 μg)	9.0 ± 0.0	8.0 ± 0.0	12.0 ± 0.0	13.0 ± 0.0
PBS	–	–	–	–
RPMI-1640	–	–	–	–

**Activity reported as inhibition zone (mm; mean ± standard deviation) produced by 5 μL treatments (n = 3 biological replicates with independent batches of HES). "–"indicates no detectable activity. Data are representative for two independent experiments.*

C-type lectin domain-containing proteins are known to agglutinate bacteria and are important in nematode immune defense against microbial infection (37). As *H. polygyrus* produces a C-type lectin protein (38) we tested the agglutinating activity of nematode products by treating *E. coli* with increasing amounts of native HES in the presence and absence of $CaCl_2$. We observed dose- and calcium-dependent agglutinating activity (**Figure 1**), suggestive of C-type lectin-mediated bacterial agglutination. These data indicate that *H. polygyrus* employs defense mechanisms via released products during its interactions with microbes which may contribute to shaping its microbial environment in the murine gut.

Altered Parasite Gene Expression in Germ-Free Mice

Having demonstrated the ability of nematode products to influence bacterial growth, we sought to investigate if intestinal nematodes sense their microbial environment and hence asked if the complete absence of microbes in the host gut resulted in altered parasite gene expression. To that end, we infected germfree (GF) and conventional (specific pathogen-free; SPF) mice and performed RNA-sequencing with parasites isolated 2 weeks post-infection. Samples clearly clustered according to SPF vs. GF parasite origin (**Figures 2A,B**). We found that a surprisingly small set of 52 genes was differentially expressed in adult worms isolated from GF compared to SPF mice (**Supplementary Table 1**). The majority of genes were upregulated, comprising a venom-like allergen (VAL-1), chitinase-1, lysozyme-3, and orthologs of putative *Caenorhabditis elegans* glutathione S-transferase and *C. elegans*/*C. briggsae* UDP-glucuronosyl- transferases, amongst others (**Supplementary Table 1**). Only four of ten genes downregulated in parasites isolated from GF mice were annotated, including a putative *C. elegans* UDP-glucuronosyl-transferase. Hence, parasitic nematodes reared in a germ-free environment display a distinct gene expression pattern.

Reduced Parasite Fitness in Germ-Free Mice

Previous studies reported on impeded survival and fecundity of intestinal nematodes in the absence of gut microbes (39–41); therefore, we assessed if parasite burden and fitness were altered depending on the host microbial status. While adult worm burdens were similar in SPF and GF mice at 2 weeks post-infection (**Figure 3A**), female worms developing in GF mice were significantly smaller and produced fewer eggs (**Figures 3B,C**). Importantly, *H. polygyrus* resides in the proximal small intestine harboring few microbes and the parasite mainly relies on host tissue as food source (42). Thus, we investigated next if the reduced parasite fitness in GF mice coincided with immune changes.

Altered Treg Responses in Nematode-Infected Germ-Free Mice

The microbiota supports the induction and maintenance of regulatory T cells (Treg) (43–46) and infections with *H. polygyrus*

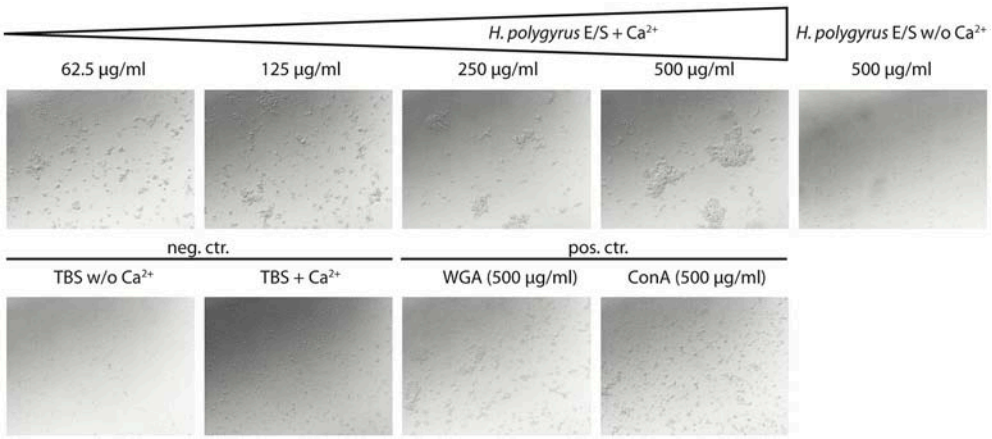

FIGURE 1 | *H. polygyrus* excretory/secretory products cause bacterial agglutination. **(Top)** Bacterial agglutination in the presence and absence of native adult *H. polygyrus* E/S products (HES) and 10 mM $CaCl_2$. Representative images of agglutination of *E. coli* IMT19224 with serial dilutions of *H. polygyrus* E/S products are shown. **(Bottom)** controls of agglutination include tris-buffered saline (TBS) with and without $CaCl_2$ as well as the C-type lectins wheat germ agglutinin (WGA) and concanavalin A (Con A). Magnification x400. Data are representative for two individual experiments performed with two independent HES batches.

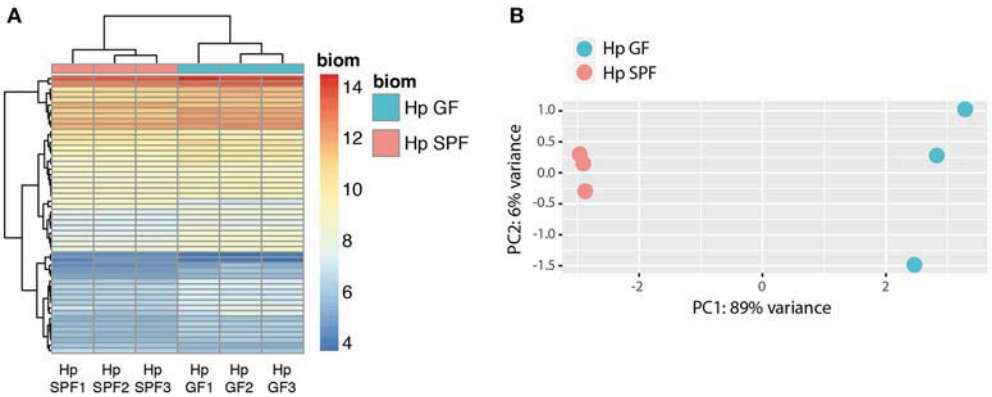

FIGURE 2 | Principle component analysis (PCA) and clustering of differentially expressed genes (DEGs). **(A)** Unsupervised clustering heatmap of differentially expressed genes (DEG, $n = 52$) in *H. polygyrus* samples isolated from SPF and GF mice. Red intensity indicates high gene expression, whereas blue intensity indicates low gene expression. **(B)** Principle component (PC) analysis revealed that 89% of the data variation is explained by the difference between SPF and GF isolates. Data are from one experiment with three biological replicates.

lead to the activation and expansion of regulatory T cells suppressing local immunopathology, but also host protective Th2 immunity (1, 15–17). Therefore, we surveyed if Treg expansion, phenotype and cytokine production in *H. polygyrus* infected mice differed depending on the microbial status.

The overall frequencies of Foxp3$^+$ Treg were similar in mLN of naive SPF and GF mice and did not change significantly upon infection (**Figure 4A**). While Treg frequencies in the small intestinal lamina propria (siLP) were stably maintained in infected SPF mice, Treg frequencies dropped significantly in the small intestines of infected GF mice compared to the respective naive controls (**Figure 4B**).

Intestinal Foxp3$^+$ Treg form a functional heterogeneous population comprising subsets marked by the elevated expression of GATA-3 or RORγt, respectively (47). While GATA-3 expression is necessary for Treg stability under inflammatory conditions (48, 49), RORγt$^+$ Treg exhibit a highly activated phenotype and limit the Th2-driven control of helminth infection and immune pathology in intestinal inflammation (43, 50). Hence, we investigated if the reduced fitness of worms isolated from GF mice was associated with phenotypic alterations in the Treg population. Fewer Treg in mLN and siLP of naïve and infected GF mice expressed RORγt compared to the respective SPF controls (**Figures 4C,D**). Steady state GATA-3 expression by Treg and the expansion of GATA-3$^+$ Treg upon infection was similar in mLN of SPF and GF mice (**Figure 4C**). Upon infection, the increase in GATA-3$^+$Treg reached significance in the small intestine of SPF mice (**Figure 4D**). Thus, naïve and infected GF mice harbored significantly less RORγt$^+$ Treg compared to SPF mice, while GATA-3$^+$Treg expanded similarly.

Next, we asked if Treg activation differed depending on the microbial status and hence assessed their cytokine production.

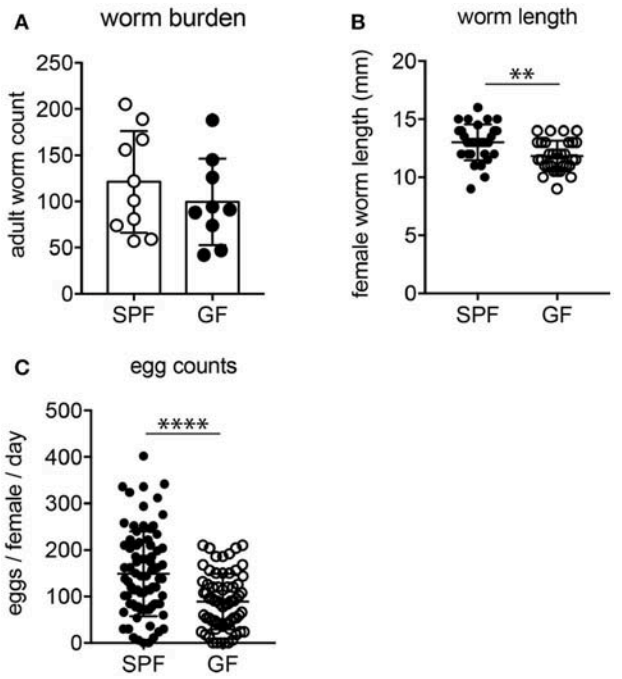

FIGURE 3 | Parasite burden and fitness in SPF and GF mice. **(A)** Number of luminal adults isolated 2 weeks post-*H. polygyrus* infection from SPF and GF mice. **(B)** Length of female parasites. **(C)** Fecundity of female worms determined as egg production within 24 h after isolation. Data are pooled from two independent experiments each performed with four to five infected mice per group. Mean, SD, and individual data points are shown. $^{**}p < 0.01$, $^{****}p < 0.0001$.

IL-10 production by Treg in mLN increased similarly and strongly in SPF and GF mice upon infection (**Figure 4E**). IL-10 production by siLP Treg of SPF mice did not change in response to infection (**Figure 4F**). Small intestinal Treg of GF mice were rather poor IL-10 producers at steady state and upon infection (**Figure 4F**). As intestinal RORγt$^+$ Treg have been reported as superior in IL-10 production compared to other gut Treg (43), we next surveyed IL-10$^+$ Treg of SPF and GF mice for co-expression of RORγt and GATA-3. Expectedly, the reduced frequencies of RORγt$^+$ cells in the Foxp3$^+$Treg pool (**Figures 4C,D**) was reflected by their underrepresentation in the IL-10 producing Treg population of naïve and infected GF mice (**Figures 4G,H**). GATA-3$^+$Treg expanding in mLN of infected SPF and GF mice (**Figure 4C**) clearly dominated the IL-10-expressing Treg pool in both groups upon infection (**Figure 4G**). Reflecting their high frequencies in the total siLP Treg population (**Figure 4D**), GATA-3$^+$Treg dominated in the small intestinal IL-10$^+$ population irrespective of microbial and nematode-infection status (**Figure 4H**). Finally, we investigated if the reduction in RORγt$^+$ Treg in the intestine and the poor IL-10 expression by gut Treg in GF mice was associated with differences in local immunopathology. Duodenal enteritis scores were, however, similar in SPF and GF nematode-infected mice (**Figure 4I**).

Taken together our data show that Treg activation in gut-associated lymphoid tissue seen as increased IL-10 production occurs independently of the presence of gut microbes. Naïve and nematode-infected GF mice display a reduction in RORγt$^+$ Treg in the gut and gut-draining lymph nodes, while GATA-3$^+$ Treg expanded similarly in SPF and GF mice and formed the major IL-10 producing Treg subset upon infection irrespective of the microbial status.

Increased Th2/Treg Ratios in Nematode-Infected Germ-Free Mice

To see if the reduction in RORγt$^+$ Treg and the lower IL-10 expression by small intestinal Treg in GF mice coincided with deregulated Th2 responses we quantified Th2 cells based on GATA-3 expression and IL-4 expression. Significantly more GATA-3$^+$ Th2 cells were present in the small intestines of infected GF mice compared to SPF mice, while IL-4 production was significantly increased in mLN (**Figures 5A,B**). Calculating the ratios of Th2 cells to Treg based on their frequencies in CD4$^+$ T cells, we found significantly elevated Th2 effector to Treg ratios in the small intestine of infected GF compared to SPF mice (**Figure 5C**). We have previously shown that intestinal nematode infections lead to the differentiation of GATA-3$^+$ Th2 and GATA-3$^+$T-bet$^+$ Th2/1 hybrid cells (51, 52). Th2/1 cells developed in infected SPF as well as GF mic, hence microbial signals were dispensable for their induction (**Figures 5D,E**). The increase in intestinal GATA-3$^+$Th2 cells coincided with trends of increased goblet cell and eosinophil counts in the duodenum (**Figures 5F,G**). As the microbiota supports Th17 differentiation (53, 54) we assessed RORγt and IL-17A expression by Foxp3$^-$CD4$^+$ T effector cells. Expectedly, GF mice harbored very few Th17 cells in mLN and small intestine (**Figure S1**). In conclusion, nematode-induced local Th2 responses were significantly increased in the absence of gut microbes and decreased parasite fitness in GF mice was associated with elevated Th2 to Treg ratios at the site of infection.

DISCUSSION

Over the last decade, several studies have shown that intestinal parasite infections lead to changes in the gut microbiota of the host [reviewed in (55, 56)]. Enteric nematodes such as *H. polygyrus*, *Nippostrongylus brasiliensis,* and *Trichuris* species alter the abundance of numerous bacterial genera in the host gut (2–4, 36, 57). Changes in the microbiota composition also result from infections with the protozoan parasites *Toxoplasma gondii* and *Giardia lamblia* (58, 59). Though the mechanistic basis for the microbiome changes provoked by the infections is not well understood, it is speculated that parasites may directly influence the composition of the microbiota. Parasite-driven immune responses resulting from tissue damage (3, 59) and leading to changes in gut physiology and epithelial barrier function (60–63) are likely to be involved. Nutrient competition and changes in host antimicrobial peptide production upon parasite infection may also contribute to structural changes in gut microbial communities (3, 64).

Here, we show that the excretory/secretory (E/S) products of the small intestinal nematode *H. polygyrus* exert antimicrobial

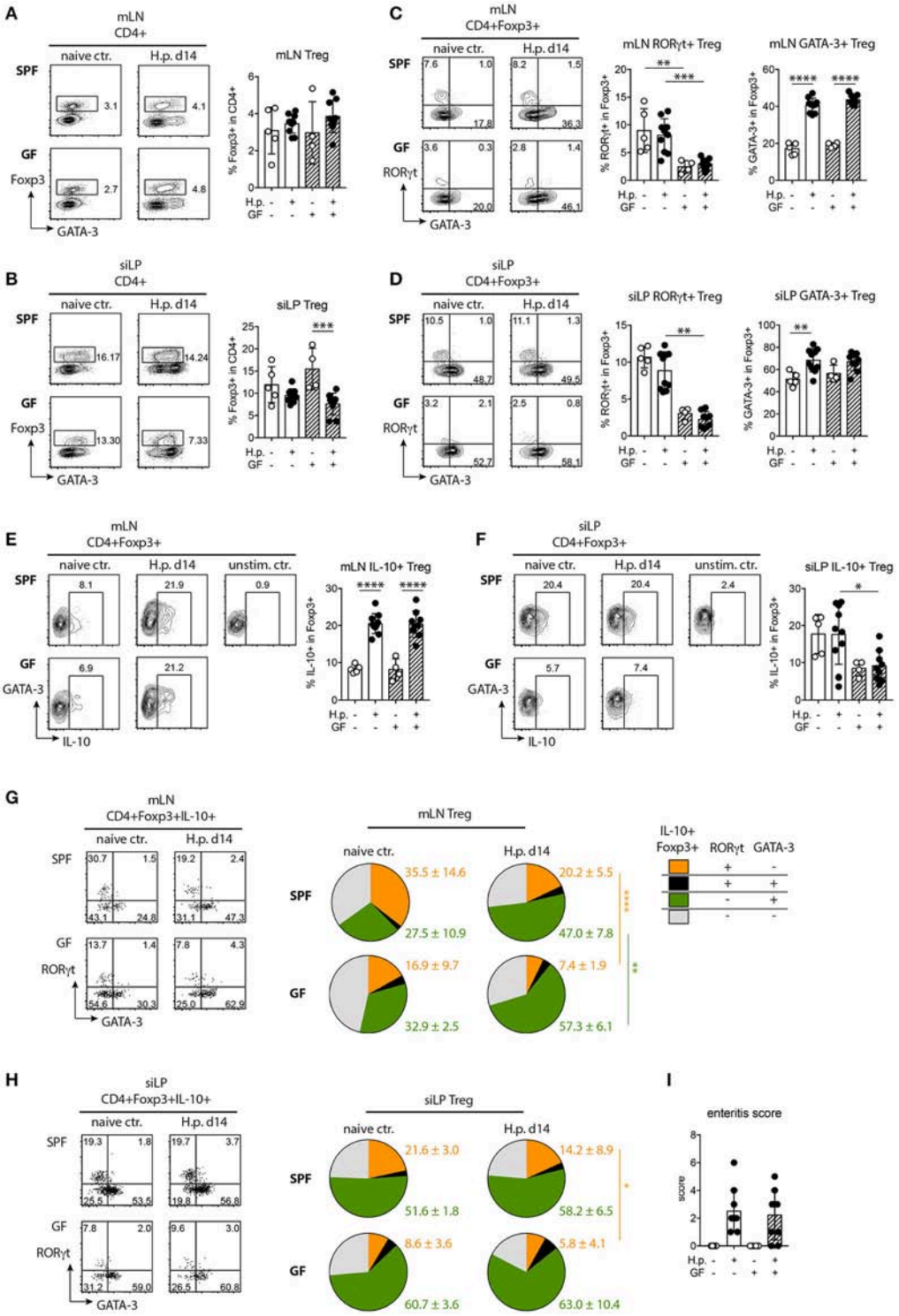

FIGURE 4 | Treg responses in SPF and GF mice infected with *H. polygyrus*. **(A,B)** Representative plots of Foxp3$^+$ Treg detection in CD4$^+$ T cells and Treg frequencies in mesenteric lymph nodes (mLN, **A**) and small intestinal lamina propria (siLP, **B**) of uninfected controls and mice infected with *H. polygyrus* for 2 weeks. **(C,D)** Representative plots of RORγt and GATA-3 expression by Treg and frequencies of RORγt$^+$ and GATA-3$^+$ Treg in mLN **(C)** and siLP **(D)**. **(E,F)** Representative plots of IL-10 expression and frequencies of IL-10$^+$ Treg in mLN **(E)** and siLP **(F)**. **(G,H)** Representation of RORγt$^+$, RORγt$^+$GATA-3$^+$, GATA-3$^+$, and RORγt$^-$GATA-3$^-$ Treg in the IL-10$^+$ Treg population in mLN and siLP of naïve and infected mice. Numbers express group means and SD. **(I)** Duodenal enteritis scores. Data are pooled from two independent experiments each performed with two to three uninfected and four to five infected mice per group. Mean, SD, and individual data points are shown in **(A–H)**. $^*p < 0.05$; $^{**}p < 0.01$, $^{***}p < 0.001$, $^{****}p < 0.0001$.

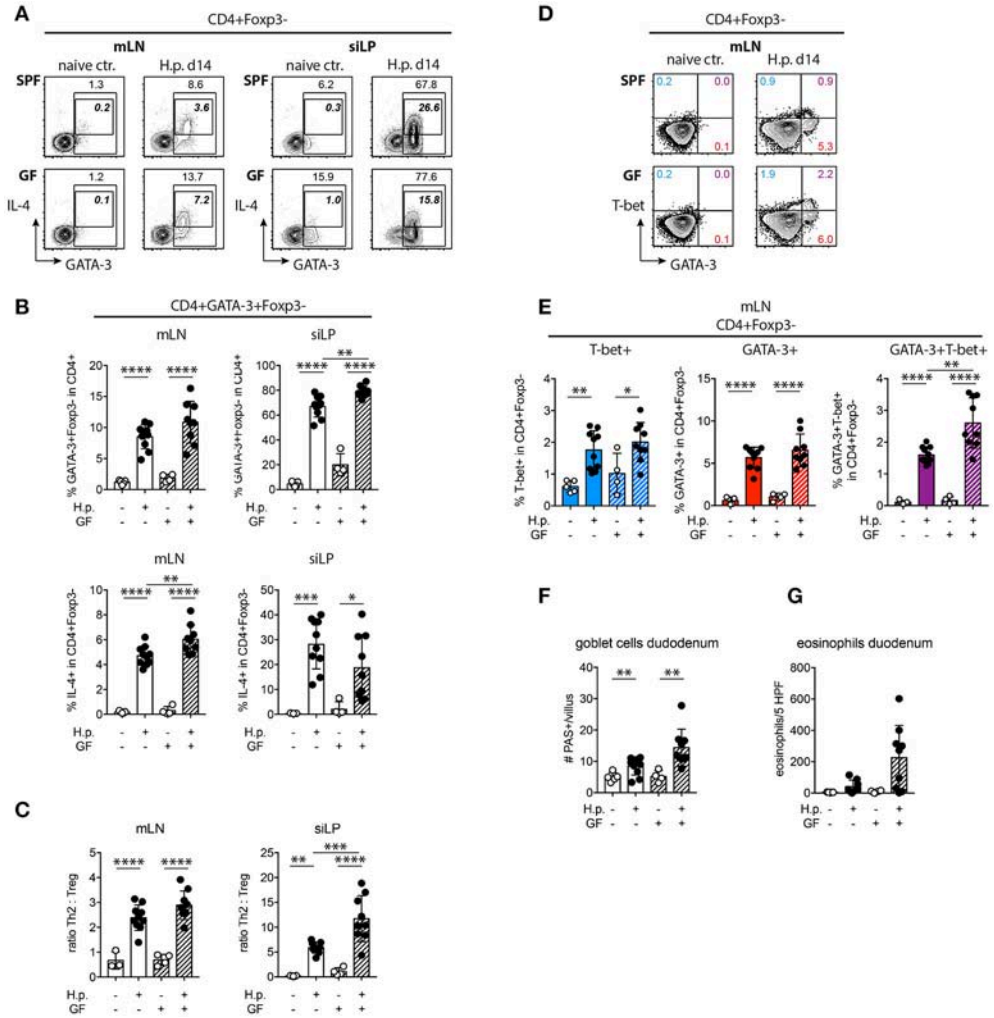

FIGURE 5 | Th2 response and Th2/Treg ratios in SPF and GF mice. **(A,B)** Representative plots of GATA-3 and IL-4 expression by $CD4^+Foxp3^-$ T cells **(A)** and frequencies **(B)** of GATA-3^+ and IL-4^+ Th2 cells in mLN and siLP. Bold italic numbers in FACS plots refer to IL-4^+ cells. **(C)** Ratios of GATA-3^+ Th2 cells to $Foxp3^+$ Treg in mLN and siLP determined based on frequencies in $CD4^+$ T cells. **(D,E)** Representative plots of GATA-3 and T-bet expression by $CD4^+Foxp3^-$ T cells **(D)** and frequencies of T-bet^+ Th1, GATA-3^+ Th2, and GATA-3^+T-bet^+ Th2/1 cells in mLN **(E)**. **(F,G)** Histological goblet cell **(F)** and eosinophil **(G)** quantification in the small intestine of naïve and infected mice. Data are pooled from two independent experiments each performed with two to three uninfected and four to five infected mice per group. Mean, SD, and individual data points are shown. $^*p < 0.05$; $^{**}p < 0.01$, $^{***}p < 0.001$, $^{****}p < 0.0001$.

activities seen as inhibited growth of several bacterial species including commensal intestinal species such as *E. faecium*, and agglutination of *E. coli*. Previous studies have reported on antimicrobial activity of nematode products, such as *Ascaris suum* antibacterial factors (ASABF) and cecropins (65, 66). We have recently shown that E/S products of the porcine roundworm *A. suum* possess antibacterial and agglutinating activity and impair biofilm formation (8). *Ascaris* E/S products comprise proteins and peptides with known and predicted antimicrobial activity, such as cecropins, ASABF, lysozymes, and C-type lectins (8). As our previous studies showed that changes in the gut microbiota of *H. polygyrus*-infected mice occurred independently of the parasite-driven Th2 response and subsequent changes in gut physiology (2), the detection of antimicrobial activities of nematode E/S products offers an attractive explanation of how these parasites may directly shape their microbial environment. On the other hand, strong Th2 responses, and the subsequent changes in host antimicrobial peptide and mucin production have been shown to be related to the decrease of segmented filamentous bacteria during infections with *N. brasiliensis* (3).

Of note, our previous studies showed an increase in Enterobacteriaceae along the small and large intestine upon infection with *H. polygyrus* (2). Whether the antimicrobial activity of *H. polygyrus* E/S products against Enterobacteriaceae family members such as *E. coli* and *S. enterica* prevents a more vigorous increase of such potentially pathogenic bacteria benefitting from intestinal inflammation can only be speculated on. It is conceivable that during coevolution, parasitic worms

have not only developed intricate mechanisms interfering with host immunity, but also adapted to directly support or restrict the growth of commensal families which might be beneficial or detrimental to parasite survival and host health via the release of antimicrobial factors. Furthermore, the parasites may benefit from the support of immune regulatory circuits fostered by microbiome changes upon infection. Indeed, others have shown that *H. polygyrus* infection leads to the outgrowth of *Lactobacillus* species and members of the Clostridiales family, which in turn support the expansion and activation of regulatory T cells (1, 17). Our unpublished data show strong and selective antimicrobial activity of E/S products of *A. suum* on several members of the porcine microbiota, whereas *Clostridia* species displayed a growth advantage in presence of *A. suum* E/S. It hence seems that nematode infections provoke fine-tuned changes in the structure of the gut microbiome in favor of commensals supporting anti-inflammatory circuits, assisting host health and facilitating parasite survival. Future work will address if nematode antimicrobial factors such as cecropins, ASABF, lysozymes, and c-type lectins present in nematode E/S products differentially affect the growth of commensal and potentially pathogenic gut bacteria.

The release of antimicrobial factors by enteric nematodes and potential interference with the growth of certain bacterial species suggest that the parasites sense their microbial environment similar to free living worms such as *C. elegans* or *Pristionchus pacificus* (67, 68). However, whether intestinal parasites react by the differential expression of antimicrobial factors to environmental changes has not been assessed before. Here, we show that nematode gene expression is altered in the absence of host microbes. Our data provide evidence for microbial sensing by *H. polygyrus*, as factors with putative antimicrobial defense functions, such as chitinase (69) and lysozyme (70), were differentially expressed in nematodes isolated from germ-free in comparison to conventional mice, in addition to xenobiotic detoxification genes which are upregulated during bacterial infection of *C. elegans* (71). Interestingly, while lysozymes are thought to play an important role in nematode antimicrobial defenses (72), lysozyme-3 was upregulated in nematodes isolated from germ-free mice. Compared to worms reared in conventional mice, nematodes from germ-free mice develop in the face of a stronger Th2 response and are likely negatively impacted by the lack of a host microbiota, as evidenced by their reduced size and fecundity. Hence, upregulation of defense factors such as lysozyme-3 may be due to a stress response rather than a lack of microbial stimulation. This view is supported by the fact that also putative detoxification genes were upregulated in parasites isolated from germ-free mice. The altered gene expression of nematodes from germ-free mice might further result from the lack of microbial metabolic factors in the germ-free host gut. A direct dependence of *H. polygyrus* on small intestinal microbes as food source appears, however, unlikely, as host tissue, but not ingesta provide the main food source of the adult worms (42).

Several reports linked the host microbial status to differences in susceptibility for infections with intestinal helminths [reviewed in (56)]. We show here that *H. polygrus* adult worms display signs of reduced fitness when developing in GF mice, confirming early studies reporting impeded nematode infectivity and fitness in the absence of gut microbes (39–41). *H. polygyrus* fitness is determined by the magnitude of the anti-parasite Th2 response, evident as disparate worm fecundity and duration of infection in inbred mouse lines differing in Th2 reactivity (73). Anti-nematode immune responses are regulated by Treg, seen as increased Th2 and associated innate responses after Treg depletion, leading to lower worm burdens or shortened retention of adult worms in some experimental systems (12, 15, 74). Microbial signals are important for the activation and instruction of thymus-derived and peripherally induced Foxp3$^+$ Treg in the gut (75). Here we show that the frequencies of Foxp3$^+$ Treg were similar in conventional and GF mice infected with *H. polygyrus*, but the phenotypic composition of Foxp3$^+$ Treg was altered in the small intestine and gut-associated lymphoid tissue of germ-free mice. Confirming a previous report (43), RORγt$^+$Foxp3$^+$ Treg were reduced in GF mice at steady state and after *H. polygyrus* infection, while the expansion of GATA-3$^+$Foxp3$^+$ Treg did not differ between infected SPF and GF mice. Whereas the complete absence of microbiota-induced RORgt$^+$Foxp3$^+$ Treg during *H. polygyrus* infection has been shown to result in the overt production of Th2 cytokines and reduced parasite fitness (43), our study provides evidence that more subtle changes in the intestinal Th2/Treg ratio are resulting from the germ-free status and, presumably, a reduction of microbiota-induced RORγt$^+$Treg is sufficient to significantly stunt parasite fitness.

The production of IL-10 by regulatory T cells has been shown to be of central importance for the prevention of gut inflammation at steady state and in experimental settings of lung and skin inflammation (76). We show here that while IL-10 production by mLN-derived Treg increased significantly upon nematode infection irrespective of the host microbial status, IL-10 production by small intestinal Treg was not altered in response to infection. Furthermore, small intestinal Treg of GF mice displayed reduced IL-10 production at steady state and after nematode infection. The reduced IL-10 expression by small intestinal Treg of GF mice may in part be explained by the reduction in RORγt$^+$ Treg, which have been previously reported as superior in IL-10 production compared to other intestinal Treg (43). Upon infection, however, we detected GATA-3$^+$Treg as the dominant IL-10$^+$ Treg source in the small intestine and mLN of SPF as well as GF mice. While our earlier studies have shown that Treg depletion during *H. polygyrus* infection results in increased small intestinal immunopathology (16), neither the decreased IL-10 production nor the reduction in RORγt$^+$ Treg detected in nematode-infected GF mice reported here were associated with signs of increased gut inflammation.

In conclusion, the antimicrobial activity of nematode products reported here suggests that enteric helminths actively shape their microbial environment, possibly facilitating the outgrowth of microbes supporting immune regulatory circuits, and restricting the expansion of potentially harmful species. Our finding of stunted parasite fitness in germ-free mice associated with locally increased Th2 and blunted Treg responses is in

line with previous reports on gut microbes affecting host susceptibility and Th2 reactivity during nematode infection. Future studies should assess if altering the gut microbiota could be used to shift the Th2/Treg balance in favor of parasite-specific effector cells and if parasite products may be employed to counteract states of pathological dysbiosis resulting from and perpetuating inflammation in intestinal inflammatory disorders.

DATA DEPOSITION

All sequencing data generated in this project are available from the NCBI Sequence Read Archive (SRA) and collectively available via the BioProject: PRJNA486010 and the SRA accession SRP157940, available at https://www.ncbi.nlm.nih.gov/bioproject/486010 and https://www.ncbi.nlm.nih.gov/sra/SRP157940.

AUTHOR CONTRIBUTIONS

SH and SR conceptualized and designed the research. SR, AM, NA, and AR performed all the experiments. SR, AM, MK, NA, AR, AK and BR analyzed the data. SR, AM, MK, and SH wrote the manuscript. AR, AK, AB, and BR provided additional resources and edited the manuscript. All authors approved the final manuscript version.

FUNDING

This work was funded by the Deutsche Forschungsgemeinschaft (GRK 2046, SH, SR). AM received funding by the IMPRS-IDI and is an associated doctoral researcher in the GRK 2046. NA received a stipend of the GRK 2046. The Freie Universität provided start-up funding for RNA-sequencing within the framework of a collaborative research center initiative.

ACKNOWLEDGMENTS

The excellent support by the technicians Y. Weber, B. Sonnenburg, M. Müller, C. Palissa, and S. Spieckermann and by the Robert Koch sequencing lab (ZBS1/MF 2) is acknowledged gratefully. Bacterial strains were generously provided by Prof. Marcus Fulde, Institute of Microbiology and Epizoonotics, Freie Universität Berlin and Dr. Markus Heimesaat, Institute of Microbiology, Charité – Universitätsmedizin Berlin. Pexiganan was generously provided by Prof. Jens Rolff, Institute of Biology, Freie Universität Berlin.

SUPPLEMENTARY MATERIAL

The Supplementary Material for this article can be found online at: https://www.frontiersin.org/articles/10.3389/fimmu.2018.02282/full#supplementary-material

REFERENCES

1. Zaiss MM, Rapin A, Lebon L, Dubey LK, Mosconi I, Sarter K, et al. The intestinal microbiota contributes to the ability of helminths to modulate allergic inflammation. *Immunity* (2015) 43:998–1010. doi: 10.1016/j.immuni.2015.09.012
2. Rausch S, Held J, Fischer A, Heimesaat MM, Kühl AA, Bereswill S, et al. Small intestinal nematode infection of mice is associated with increased enterobacterial loads alongside the intestinal tract. *PLoS ONE* (2013) 8:e74026. doi: 10.1371/journal.pone.0074026
3. Fricke WF, Song Y, Wang A-J, Smith A, Grinchuk V, Pei C, et al. Type 2 immunity-dependent reduction of segmented filamentous bacteria in mice infected with the helminthic parasite *Nippostrongylus brasiliensis*. *Microbiome* (2015) 3:40. doi: 10.1186/s40168-015-0103-8
4. Li RW, Wu S, Li W, Navarro K, Couch RD, Hill D, et al. Alterations in the porcine colon microbiota induced by the gastrointestinal nematode *Trichuris suis*. *Infect Immun.* (2012) 80:2150–7. doi: 10.1128/IAI.00141-12
5. Broadhurst MJ, Ardeshir A, Kanwar B, Mirpuri J, Gundra UM, Leung JM, et al. Therapeutic helminth infection of macaques with idiopathic chronic diarrhea alters the inflammatory signature and mucosal microbiota of the colon. *PLoS Pathog.* (2012) 8:e1003000. doi: 10.1371/journal.ppat.1003000
6. Abner SR, Parthasarathy G, Hill DE, Mansfield LS. *Trichuris suis*: detection of antibacterial activity in excretory-secretory products from adults. *Exp Parasitol.* (2001) 99:26–36. doi: 10.1006/expr.2001.4643
7. Midha A, Schlosser J, Hartmann S. Reciprocal interactions between nematodes and their microbial environments. *Front. Cell. Infect. Microbiol.* (2017) 7:144. doi: 10.3389/fcimb.2017.00144
8. Midha A, Janek K, Niewienda A, Henklein P, Guenther S, Serra DO, et al. The intestinal roundworm ascaris suum releases antimicrobial factors which interfere with bacterial growth and biofilm formation. *Front. Cell. Infect. Microbiol.* (2018) 8:271. doi: 10.3389/fcimb.2018.00271.
9. Maizels RM, Hewitson JP, Murray J, Harcus YM, Dayer B, Filbey KJ, et al. Immune modulation and modulators in *Heligmosomoides polygyrus* infection. *Exp Parasitol.* (2012) 132:76–89. doi: 10.1016/j.exppara.2011.08.011
10. Maizels RM, McSorley HJ. Regulation of the host immune system by helminth parasites. *J Allergy Clin Immunol.* (2016) 138:666–75. doi: 10.1016/j.jaci.2016.07.007
11. Ziegler T, Rausch S, Steinfelder S, Klotz C, Hepworth MR, Kühl AA, et al. A novel regulatory macrophage induced by a helminth molecule instructs IL-10 in CD4+ T cells and protects against mucosal inflammation. *J Immunol.* (2015) 194:1555–64. doi: 10.4049/jimmunol.1401217
12. Blankenhaus B, Reitz M, Brenz Y, Eschbach M-L, Hartmann W, Haben I, et al. Foxp3+ regulatory T cells delay expulsion of intestinal nematodes by suppression of IL-9-driven mast cell activation in BALB/c but not in C57BL/6 mice. *PLoS Pathog.* (2014) 10:e1003913. doi: 10.1371/journal.ppat.1003913
13. Finney CAM, Taylor MD, Wilson MS, Maizels RM. Expansion and activation of CD4+CD25+ regulatory T cells in *Heligmosomoides polygyrus* infection. *Eur J Immunol.* (2007) 37:1874–86. doi: 10.1002/eji.200636751
14. Grainger JR, Smith KA, Hewitson JP, McSorley HJ, Harcus Y, Filbey KJ, et al. Helminth secretions induce de novo T cell Foxp3 expression and regulatory function through the TGF-β pathway. *J Exp Med.* (2010) 207:2331–41. doi: 10.1084/jem.20101074
15. Rausch S, Huehn J, Kirchhoff D, Rzepecka J, Schnoeller C, Pillai S, et al. Functional analysis of effector and regulatory T cells in a parasitic nematode infection. *Infect Immun.* (2008) 76:1908–19. doi: 10.1128/IAI.01233-07
16. Rausch S, Huehn J, Loddenkemper C, Hepworth MR, Klotz C, Sparwasser T, et al. Establishment of nematode infection despite increased Th2 responses and immunopathology after selective depletion of Foxp3+ cells. *Eur. J. Immunol.* (2009) 39:3066–77. doi: 10.1002/eji.200939644
17. Reynolds LA, Smith KA, Filbey KJ, Harcus Y, Hewitson JP, Redpath SA, et al. Commensal-pathogen interactions in the intestinal tract. *Gut Microb.* (2014) 5:522–32. doi: 10.4161/gmic.32155

18. Wilson MS, Taylor MD, Balic A, Finney CAM, Lamb JR, Maizels RM. Suppression of allergic airway inflammation by helminth-induced regulatory T cells. *J Exp Med.* (2005) 202:1199–212. doi: 10.1084/jem.20042572
19. Takemura H, Kaku M, Kohno S, Hirakata Y, Tanaka H, Yoshida R, et al. Evaluation of susceptibility of gram-positive and -negative bacteria to human defensins by using radial diffusion assay. *Antimicrob Agents Chemother.* (1996) 40:2280–4.
20. Gasmi L, Ferré J, Herrero S. High bacterial agglutination activity in a single-CRD C-type lectin from *Spodoptera exigua* (Lepidoptera: Noctuidae). *Biosensors* (2017) 7:12. doi: 10.3390/bios7010012
21. Bolger AM, Lohse M, Usadel B. Trimmomatic: a flexible trimmer for Illumina sequence data. *Bioinformatics* (2014) 30:2114–20. doi: 10.1093/bioinformatics/btu170
22. Wood DE, Salzberg SL. Kraken: ultrafast metagenomic sequence classification using exact alignments. *Genome Biol.* (2014) 15:R46. doi: 10.1186/gb-2014-15-3-r46
23. Kim D, Pertea G, Trapnell C, Pimentel H, Kelley R, Salzberg SL. TopHat2: accurate alignment of transcriptomes in the presence of insertions, deletions and gene fusions. *Genome Biol.* (2013) 14:R36. doi: 10.1186/gb-2013-14-4-r36
24. Trapnell C, Hendrickson DG, Sauvageau M, Goff L, Rinn JL, Pachter L. Differential analysis of gene regulation at transcript resolution with RNA-seq. *Nat Biotechnol.* (2013) 31:46–53. doi: 10.1038/nbt.2450
25. Howe KL, Bolt BJ, Shafie M, Kersey P, Berriman M. WormBase ParaSite – a comprehensive resource for helminth genomics. *Mol Biochem Parasitol.* (2017) 215:2–10. doi: 10.1016/j.molbiopara.2016.11.005
26. Liao Y, Smyth GK, Shi W. featureCounts: an efficient general purpose program for assigning sequence reads to genomic features. *Bioinformatics* (2014) 30:923–30. doi: 10.1093/bioinformatics/btt656
27. Love MI, Huber W, Anders S. Moderated estimation of fold change and dispersion for RNA-seq data with DESeq2. *Genome Biol.* (2014) 15:550. doi: 10.1186/s13059-014-0550-8
28. Ritchie ME, Phipson B, Wu D, Hu Y, Law CW, Shi W, et al. limma powers differential expression analyses for RNA-sequencing and microarray studies. *Nucleic Acids Res.* (2015) 43:e47. doi: 10.1093/nar/gkv007
29. Rice P, Longden I, Bleasby A. EMBOSS: the European molecular biology open software suite. *Trends Genet.* (2000) 16:276–7. doi: 10.1016/S0168-9525(00)02024-2
30. Ashburner M, Ball CA, Blake JA, Botstein D, Butler H, Cherry JM, et al. Gene ontology: tool for the unification of biology. *Nat. Genet.* (2000) 25:25–9. doi: 10.1038/75556
31. Camacho C, Coulouris G, Avagyan V, Ma N, Papadopoulos J, Bealer K, et al. BLAST+: architecture and applications. *BMC Bioinformatics* (2009) 10:421. doi: 10.1186/1471-2105-10-421
32. Conesa A, Götz S, García-Gómez JM, Terol J, Talón M, Robles M. Blast2GO: a universal tool for annotation, visualization and analysis in functional genomics research. *Bioinformatics* (2005) 21:3674–6. doi: 10.1093/bioinformatics/bti610
33. Jones P, Binns D, Chang H-Y, Fraser M, Li W, McAnulla C, et al. InterProScan 5: genome-scale protein function classification. *Bioinformatics* (2014) 30:1236–40. doi: 10.1093/bioinformatics/btu031
34. The UniProt Consortium (2017). UniProt: the universal protein knowledgebase. *Nucleic Acids Res.* 45: D158–69.
35. Strandmark J, Steinfelder S, Berek C, Kühl AA, Rausch S, Hartmann S. Eosinophils are required to suppress Th2 responses in Peyer's patches during intestinal infection by nematodes. *Mucosal Immunol.* (2017) 10:661–72. doi: 10.1093/nar/gkh131
36. Walk ST, Blum AM, Ewing SA-S, Weinstock JV, Young VB. Alteration of the murine gut microbiota during infection with the parasitic helminth *Heligmosomoides polygyrus*. *Inflamm Bowel Dis.* (2010) 16:1841–9. doi: 10.1002/ibd.21299
37. Miltsch SM, Seeberger PH, Lepenies B. The C-type lectin-like domain containing proteins Clec-39 and Clec-49 are crucial for *Caenorhabditis elegans* immunity against *Serratia marcescens* infection. *Dev Comp Immunol.* (2014) 45:67–73. doi: 10.1016/j.dci.2014.02.002
38. Harcus Y, Nicoll G, Murray J, Filbey K, Gomez-Escobar N, Maizels RM. C-type lectins from the nematode parasites *Heligmosomoides polygyrus* and *Nippostrongylus brasiliensis*. *Parasitol Int.* (2009) 58:461–70. doi: 10.1016/j.parint.2009.08.011
39. Chang J, Wescott RB. Infectivity, fecundity, and survival of Nematospiroides dubius in gnotobiotic mice. *Exp Parasitol.* (1972) 32:327–34. doi: 10.1016/0014-4894(72)90060-4
40. Wescott RB. Experimental Nematospiroides dubius infection in germfree and conventional mice. *Exp Parasitol.* (1968) 22:245–9. doi: 10.1016/0014-4894(68)90099-4
41. Wescott RB, Todd AC. A Comparison of the development of *Nippostrongylus brasiliensis* in germ-free and conventional mice. *J Parasitol.* (1964) 50:138–43. doi: 10.2307/3276048
42. Bansemir AD, Sukhdeo MV. The food resource of adult *Heligmosomoides polygyrus* in the small intestine. *J Parasitol.* (1994) 80:24–8. doi: 10.2307/3283340
43. Ohnmacht C, Park J-H, Cording S, Wing JB, Atarashi K, Obata Y, et al. The microbiota regulates type 2 immunity through RORγt$^+$ T cells. *Science* (2015) 349:989–93. doi: 10.1126/science.aac4263
44. Smith PM, Howitt MR, Panikov N, Michaud M, Gallini CA, Bohlooly YM, et al. The microbial metabolites, short-chain fatty acids, regulate colonic treg cell homeostasis. *Science* (2013) 341:569–73. doi: 10.1126/science.1241165
45. Round JL, Mazmanian SK. Inducible Foxp3+ regulatory T-cell development by a commensal bacterium of the intestinal microbiota. *Proc Natl Acad Sci USA.* (2010) 107:12204–9. doi: 10.1073/pnas.0909122107
46. Korn LL, Hubbeling HG, Porrett PM, Yang Q, Barnett LG, Laufer TM. Regulatory T cells occupy an isolated niche in the intestine that is antigen independent. *Cell Rep.* (2014) 9:1567–73. doi: 10.1016/j.celrep.2014.11.006
47. Luu M, Steinhoff U, Visekruna A. Functional heterogeneity of gut-resident regulatory T cells. *Clin Transl Immunol.* (2017) 6:e156. doi: 10.1038/cti.2017.39
48. Wang Y, Su MA, Wan YY. An essential role of the transcription factor GATA-3 for the function of regulatory t cells. *Immunity* (2011) 35:337–48. doi: 10.1016/j.immuni.2011.08.012
49. Wohlfert EA, Grainger JR, Bouladoux N, Konkel JE, Oldenhove G, Ribeiro CH, et al. GATA3 controls Foxp3$^+$ regulatory T cell fate during inflammation in mice. *J Clin Invest.* (2011) 121:4503–15. doi: 10.1172/JCI57456
50. Yang B-H, Hagemann S, Mamareli P, Lauer U, Hoffmann U, Beckstette M, et al. Foxp3$^+$ T cells expressing RORγt represent a stable regulatory T-cell effector lineage with enhanced suppressive capacity during intestinal inflammation. *Mucosal Immunol.* (2016) 9:444–57. doi: 10.1038/mi.2015.74
51. Bock CN, Babu S, Breloer M, Rajamanickam A, Boothra Y, Brunn M-L, et al. Th2/1 hybrid cells occurring in murine and human strongyloidiasis share effector functions of Th1 cells. *Front. Cell. Infect. Microbiol.* (2017) 7:261. doi: 10.3389/fcimb.2017.00261
52. Peine M, Rausch S, Helmstetter C, Fröhlich A, Hegazy AN, Kühl AA, et al. Stable T-bet(+)GATA-3(+) Th1/Th2 hybrid cells arise *in vivo*, can develop directly from naive precursors, and limit immunopathologic inflammation. *PLoS Biol.* (2013) 11:e1001633. doi: 10.1371/journal.pbio.1001633
53. Atarashi K, Tanoue T, Ando M, Kamada N, Nagano Y, Narushima S, et al. Th17 cell induction by adhesion of microbes to intestinal epithelial cells. *Cell* (2015) 163:367–80. doi: 10.1016/j.cell.2015.08.058
54. Ivanov II, Atarashi K, Manel N, Brodie EL, Shima T, Karaoz U, et al. Induction of intestinal Th17 cells by segmented filamentous bacteria. *Cell* (2009) 139:485–98. doi: 10.1016/j.cell.2009.09.033
55. Burgess SL, Gilchrist CA, Lynn TC, Petri WA. Parasitic protozoa and interactions with the host intestinal microbiota. *Infect Immun.* (2017) 85:e00101–17. doi: 10.1128/IAI.00101-17
56. Zaiss MM, Harris NL. Interactions between the intestinal microbiome and helminth parasites. *Parasite Immunol.* (2016) 38:5–11. doi: 10.1111/pim.12274
57. Holm JB, Sorobetea D, Kiilerich P, Ramayo-Caldas Y, Estellé J, Ma T, et al. Chronic trichuris muris infection decreases diversity of the intestinal microbiota and concomitantly increases the abundance of Lactobacilli. *PLOS ONE* (2015) 10:e0125495. doi: 10.1371/journal.pone.0125495
58. Barash NR, Maloney JG, Singer SM, Dawson SC. Giardia alters commensal microbial diversity throughout the murine gut. *Infect Immun.* (2017) 85:e00948–16. doi: 10.1128/IAI.00948-16
59. Heimesaat MM, Bereswill S, Fischer A, Fuchs D, Struck D, Niebergall J, et al. Gram-negative bacteria aggravate murine small intestinal Th1-type immunopathology following oral infection with *Toxoplasma gondii*. *J Immunol.* (2006) 177:8785–95. doi: 10.4049/jimmunol.177.12.8785

60. Zhao A, McDermott J, Urban JF, Gause W, Madden KB, Yeung KA, et al. Dependence of IL-4, IL-13, and nematode-induced alterations in murine small intestinal smooth muscle contractility on Stat6 and enteric nerves. *J Immunol.* (2003) 171:948–54. doi: 10.4049/jimmunol.171.2.948
61. Marillier RG, Michels C, Smith EM, Fick LC, Leeto M, Dewals B, et al. IL-4/IL-13 independent goblet cell hyperplasia in experimental helminth infections. *BMC Immunol.* (2008) 9:11. doi: 10.1186/1471-2172-9-11
62. McKay DM, Shute A, Lopes F. Helminths and intestinal barrier function. *Tissue Barr.* (2017) 5:e1283385. doi: 10.1080/21688370.2017.1283385
63. Finkelman FD, Shea-Donohue T, Morris SC, Gildea L, Strait R, Madden KB, et al. Interleukin-4- and interleukin-13-mediated host protection against intestinal nematode parasites. *Immunol. Rev.* (2004) 201:139–55. doi: 10.1111/j.0105-2896.2004.00192.x
64. Manko A, Motta J-P, Cotton JA, Feener T, Oyeyemi A, Vallance BA, et al. Giardia co-infection promotes the secretion of antimicrobial peptides beta-defensin 2 and trefoil factor 3 and attenuates attaching and effacing bacteria-induced intestinal disease. *PLOS ONE* (2017) 12:e0178647. doi: 10.1371/journal.pone.0178647
65. Pillai A, Ueno S, Zhang H, Kato Y. Induction of ASABF (*Ascaris suum* antibacterial factor)-type antimicrobial peptides by bacterial injection: novel members of ASABF in the nematode *Ascaris suum. Biochem J.* (2003) 371:663–8. doi: 10.1042/bj20021948
66. Pillai A, Ueno S, Zhang H, Lee JM, Kato Y. Cecropin P1 and novel nematode cecropins: a bacteria-inducible antimicrobial peptide family in the nematode *Ascaris suum*. *Biochem J.* (2005) 390:207–14. doi: 10.1042/BJ20050218
67. Samuel BS, Rowedder H, Braendle C, Félix M-A, Ruvkun G. *Caenorhabditis elegans* responses to bacteria from its natural habitats. *Proc Natl Acad Sci USA.* (2016) 113:E3941–9. doi: 10.1073/pnas.1607183113
68. Sinha A, Rae R, Iatsenko I, Sommer RJ. System wide analysis of the evolution of innate immunity in the nematode model species *Caenorhabditis elegans* and *Pristionchus pacificus*. *PLoS ONE* (2012) 7:e44255. doi: 10.1371/journal.pone.0044255
69. Chung MC, Dean S, Marakasova ES, Nwabueze AO, van Hoek ML. Chitinases are negative regulators of *Francisella novicida* biofilms. *PLoS ONE* (2014) 9:e93119. doi: 10.1371/journal.pone.0093119
70. Dierking K, Yang W, Schulenburg H. Antimicrobial effectors in the nematode *Caenorhabditis elegans*: an outgroup to the Arthropoda. *Philos Trans R Soc B Biol Sci.* (2016) 371:20150299. doi: 10.1098/rstb.2015.0299
71. Pukkila-Worley R. Surveillance immunity: an emerging paradigm of innate defense activation in *Caenorhabditis elegans*. *PLOS Pathog.* (2016) 12:e1005795. doi: 10.1371/journal.ppat.1005795
72. Schulenburg H, Boehnisch C. Diversification and adaptive sequence evolution of Caenorhabditislysozymes (Nematoda: Rhabditidae). *BMC Evol Biol.* (2008) 8:114. doi: 10.1186/1471-2148-8-114
73. Filbey KJ, Grainger JR, Smith KA, Boon L, van Rooijen N, Harcus Y, et al. Innate and adaptive type 2 immune cell responses in genetically controlled resistance to intestinal helminth infection. *Immunol Cell Biol.* (2014) 92:436–48. doi: 10.1038/icb.2013.109
74. Smith KA, Filbey KJ, Reynolds LA, Hewitson JP, Harcus Y, Boon L, et al. Low-level regulatory T-cell activity is essential for functional type-2 effector immunity to expel gastrointestinal helminths. *Mucosal Immunol.* (2016) 9:428–43. doi: 10.1038/mi.2015.73
75. Geuking MB, Cahenzli J, Lawson MAE, Ng DCK, Slack E, Hapfelmeier S, et al. Intestinal bacterial colonization induces mutualistic regulatory T cell responses. *Immunity* (2011) 34:794–806. doi: 10.1016/j.immuni.2011.03.021
76. Rubtsov YP, Rasmussen JP, Chi EY, Fontenot J, Castelli L, Ye X, et al. Regulatory T cell-derived interleukin-10 limits inflammation at environmental interfaces. *Immunity* (2008) 28:546–58. doi: 10.1016/j.immuni.2008.02.017

Conflict of Interest Statement: The authors declare that the research was conducted in the absence of any commercial or financial relationships that could be construed as a potential conflict of interest.

frontiers in Immunology

REVIEW
published: 02 October 2018
doi: 10.3389/fimmu.2018.02253

Salivarian Trypanosomosis: A Review of Parasites Involved, Their Global Distribution and Their Interaction With the Innate and Adaptive Mammalian Host Immune System

Magdalena Radwanska[1], *Nick Vereecke*[1,2], *Violette Deleeuw*[2], *Joar Pinto*[2] *and Stefan Magez*[1,2]*

[1] Laboratory for Biomedical Research, Ghent University Global Campus, Incheon, South Korea, [2] Laboratory of Cellular and Molecular Immunology, Vrije Universiteit Brussel, Brussels, Belgium

OPEN ACCESS

Edited by:
Xun Suo,
China Agricultural University, China

Reviewed by:
Debora Decote-Ricardo,
Universidade Federal Rural do Rio de Janeiro, Brazil
Dolores Correa,
Instituto Nacional de Pediatria, Mexico
Xin Zhao,
Institute of Microbiology (CAS), China

***Correspondence:**
Stefan Magez
stefan.magez@vub.be

Specialty section:
This article was submitted to Microbial Immunology, a section of the journal Frontiers in Immunology

Received: 31 May 2018
Accepted: 11 September 2018
Published: 02 October 2018

Citation:
Radwanska M, Vereecke N, Deleeuw V, Pinto J and Magez S (2018) Salivarian Trypanosomosis: A Review of Parasites Involved, Their Global Distribution and Their Interaction With the Innate and Adaptive Mammalian Host Immune System. Front. Immunol. 9:2253. doi: 10.3389/fimmu.2018.02253

Salivarian trypanosomes are single cell extracellular parasites that cause infections in a wide range of hosts. Most pathogenic infections worldwide are caused by one of four major species of trypanosomes including (i) *Trypanosoma brucei* and the human infective subspecies *T. b. gambiense* and *T. b. rhodesiense*, (ii) *Trypanosoma evansi* and *T. equiperdum*, (iii) *Trypanosoma congolense* and (iv) *Trypanosoma vivax*. Infections with these parasites are marked by excessive immune dysfunction and immunopathology, both related to prolonged inflammatory host immune responses. Here we review the classification and global distribution of these parasites, highlight the adaptation of human infective trypanosomes that allow them to survive innate defense molecules unique to man, gorilla, and baboon serum and refer to the discovery of sexual reproduction of trypanosomes in the tsetse vector. With respect to the immunology of mammalian host-parasite interactions, the review highlights recent findings with respect to the B cell destruction capacity of trypanosomes and the role of T cells in the governance of infection control. Understanding infection-associated dysfunction and regulation of both these immune compartments is crucial to explain the continued failures of anti-trypanosome vaccine developments as well as the lack of any field-applicable vaccine based anti-trypanosomosis intervention strategy. Finally, the link between infection-associated inflammation and trypanosomosis induced anemia is covered in the context of both livestock and human infections.

Keywords: trypanosomosis, immunology, pathology, anemia, transmission

INTRODUCTION

Human African Trypanosomosis and Animal African Trypanosomosis are two well-known diseases that affect sub-Saharan Africa and have historically prevented the development of vast lands of the African continent into highly productive agricultural areas. However, the first salivarian pathogenic trypanosome to be discovered was *T. evansi*, a parasite identified by Dr. Griffith Evans in 1880, in horses and camels suffering from a disease called Surra on the Indian subcontinent (1). Almost 140 years after this initial discovery, a wealth of world-wide epidemiological data

on pathogenic trypanosomes shows they are present on four different continents. Molecular parasite mechanisms, that allow the escape from the hosts' immune and non-immune defense systems, have been discovered and various interactions in the context of vector biology have been described. However, in the end the data available today has still not given us a way to intervene in trypanosomosis transmission by means of an effective anti-parasite vaccination strategy. Hence, control still relies on a combination of active case diagnosis and treatment, as well as vector control (2, 3). In this review we cover the classification of trypanosomes, which has recently become under scrutiny (4), as well as new discoveries with respect to genetic exchange between trypanosomes that takes place in the insect vector (5, 6). In addition, the paper provides an update on recent discoveries with respect to the B cell destructive potential of trypanosomes (7, 8), T cell biology (9), and the impact of trypanosomosis on red blood cell (RBC) homeostasis and infection-associated anemia (10). Throughout the data review, both animal trypanosomosis (AT) and human trypanosomosis (HT) have been considered. However, as most recent data shows, this "artificial" distinction might be less useful than previously thought, as atypical human trypanosomosis (a-HT), which can be caused by various animal trypanosomes, is now gaining more and more attention in the field (11).

SETTING THE SCENE FOR SALIVARIAN TRYPANOSOMOSIS

Trypanosomes are unicellular protozoan organisms of the class Kinetoplastida that cause a wide range of infections in a broad range of hosts. The latter includes not just mammals but also fish (12), birds (13), and reptiles (14), while insect vectors actually should be considered not just as transmission "tools" but also as definite hosts. Indeed, it is only here that sexual reproduction stages have been reported, as comprehensively outlined in a recent review by Gibson W. (5). In mammals, both salivarian and stercorarian trypanosomes cause diseases that affect the health status of the infected host in multiple ways. While the stercorarian trypanosomes are an important group of parasites, the main focus of this review is directed toward the pathogenic salivarian trypanosomes that cause infections in human, livestock, and game animals. These infections are marked by the extracellular nature of the infecting agent, causing pathologies and health complications that are very different from the features that characterize intracellular pathogenic infections such as those caused by the stercorarian *T. cruzi* parasite. An additional complication that arises when describing trypanosomosis, is the use of the term *African Trypanosomosis*. This denomination is very often used in an incorrect way. Indeed, as will be described in this review, all major pathogenic salivarian trypanosome infections do occur on the African continent. However several of the pathogens responsible for these diseases have moved "out of Africa" and infections are progressing throughout the world. A last introductory remark for this paper is the fact that Human African Trypanosomosis or HAT has recently been brought under control in a very significant manner by huge consorted international efforts of the last decennium (15). Hence, this might give the impression that trypanosomosis has become a disease of the past. This however could very well be a wrong assumption for three main reasons. First, there are no reports that suggest that AT is near to being controlled on a world-wide scale. Second, the most aggressive form of HAT caused by *T. b. rhodesiense* has a zoonotic origin, so as long as human infective trypanosomes are present in a wildlife reservoir, re-emergence of the disease remains a risk (16, 17). This holds true even if the majority of infections caused by *T. b gambiense* are being brought under control. Third, reports of a-HT in- and outside Africa show that "African" trypanosomosis is only part of the problem (11). Hence, for now trypanosome diseases still remain a threat to human health and to agriculture systems of emerging economies. In the absence of any vaccine strategy preventing the spread of these infections, continued research into host-parasite interactions is needed. This will provide a better understanding of trypanosome diseases itself, the mechanisms of disease resistance, modes of immune evasion, and ultimately the reasons for continued failure of vaccination attempts.

CLASSIFICATION OF THE MAIN PATHOGENIC SALIVARIAN TRYPANOSOMES

Trypanosomes belong to the sub-kingdom Protozoa, the order Kinetoplastida, the family Trypanosomatidae, and genus *Trypanosoma*. The large numbers of different species belonging to this genus have been classified in several subgenera according to their morphology. For the salivarian pathogenic trypanosomes the subgenera include *Trypanozoon*, *Duttonella*, *Nannomonas,* and *Pycnomonas*, of which the first three account for the vast majority of human and animal infections and are the subject of this review. Their combined geographic spread covers most of the developing world (**Figure 1**).

The first trypanosome subgenus, *Trypanozoon,* is composed of several *Trypanosoma* species, which are human and animal infective and includes the first pathogenic trypanosome ever to be discovered i.e. *Trypanosoma evansi*. Today, *T. evansi* is a parasite that is considered to have mainly a veterinary importance (1), causing the disease Surra in a wide range of economically important mammals such as horses, cattle, goats, buffalos, dogs, and camels. In addition, the parasite can be found in game animals such as deer, wild pigs, and capybaras, representing a reservoir that often might escape attention. Today, *T. evansi* is found across Central and South America, North Africa, the Russian territories, the Indian subcontinent, China, and Southeast Asia (23). Transmission mainly occurs mechanically through the bite of bloodsucking insects from the family Tabanidae (genus *Tabanus*) (24), Chrysops (25), Atylotus (26), and Muscidae (genus *Stomoxys* and *Haematobia*) (18). It is this mechanical transmission that has allowed the parasite to move beyond the tsetse fly region and out of Africa. Morphologically, *T. evansi* has long been considered as a monomorphic parasite with the main bloodstream form appearing as so called "long slender" forms. However, the appearance of short intermediate

FIGURE 1 | Geographic distribution of salivarian trypanosomosis. Salivarian trypanosomosis is a worldwide problem caused in large by *Trypanosoma evansi*, *Trypanosoma brucei* (including the human infective subspecies *T. b. gambiense* and *T. b. rhodesiense*), *Trypanosoma vivax* and *Trypanosoma congolense*. *T. brucei,* and *T. congolense* infections are limited to the sub-Saharan tsetse belt. In contrast, as *T. vivax* and *T. evansi* can be mechanically transmitted, these parasites have migrate beyond the tsetse belt, out of Africa and into South America and Asia [adapted from (18–22)].

forms has also been reported, but only in blood smears of infected cat and monkey (27). Important is that the parasite has a peculiar kinetoplast, characterized by either a reduced (lack of maxi-circles and homogenous mini-circles) or a total absence of kinetoplast DNA (kDNA) (28). This deficiency is thought to lock *T. evansi* in the bloodstream form, as they are unable to transcribe the kDNA genes required to perform the oxidative phosphorylation required for the developmental processes in the midgut of the tsetse (29). For long, this altered kDNA characteristic has been used to differentiate *T. evansi* from African *T. brucei* subspecies. Recently however, genetic analysis of a large battery of both *T. evansi* and *T. brucei* parasites has shown that the situation is more complex, and that many *T. evansi* parasites are closely related to *T. brucei*, even more closely than the relation between *T. evansi* parasites from different geographic locations (30–32). In addition, these data suggest that *T. evansi* arose multiple times from a different *T. brucei* ancestor. Hence, this has sparked a debate about the nomenclature of the *Trypanozoon* parasites. While it has been suggested by some to consider *T. evansi* as a *T. brucei* variant, a most recent revision has been proposed based on the proper application of the principles of biological nomenclature. This proposal suggests to rename all *T. brucei* subspecies as *T. evansi* subspecies, and even adopt the use of *T. evansi gambiense* and *T. evansi rhodesiense* for human

infective African Trypanosomes (4). Important in the context of the parasite-host interplay of *T. evansi* is the notion that several human *T. evansi* infections have been reported in- and outside Africa (11). However, despite the wide geographic distribution of *T. evansi*, the reports on human non-African trypanosomosis are overall extremely rare. However, it cannot be excluded that one of the reasons for the scarce amount of data on a-HT is simply due to the lack of proper diagnostic practices that are able to correctly identify human trypanosomosis in *T. evansi* endemic areas.

The second *Trypanozoon* subspecies to be discovered was *T. brucei,* endemic to sub-Saharan Africa and transmitted by biting flies of the genus *Glossina*, commonly known as tsetse, with tsetse meaning "fly" in the Tswana language of Southern Africa. *T. brucei* parasites present a major health problem for humans, as the causative agent of the disease called HAT, or sleeping sickness. Domestic animals such as cattle, pigs, small ruminants, and game animals are also common hosts for *T. brucei*, in which the latter serve as a natural reservoir of the parasite. Three morphological indistinguishable subspecies of *T. brucei* are known (namely *T. b. gambiense, T. b. rhodesiense,* and *T. b. brucei.)* with *T. b. gambiense* and *T. b. rhodesiense* responsible for human trypanosome diseases in West/Central and East Africa, respectively. Uganda is one of the only countries where the two forms of HAT appear in adjacent regions. *T. b. brucei*, on the other hand, is unable to infect humans and is responsible for animal trypanosomosis only. The correct identification of the *T. brucei* subspecies is nearly impossible when solely based on their morphology or geographical origin. Indeed, all three subspecies appear as pleomorphic bloodstream parasites, having both long slender and short stumpy forms. However, molecular approaches have shown that this group is highly heterogeneous (33). The exclusive presence of the serum resistance associated (*SRA*) gene in *T. b. rhodesiense* has been used as a marker for the identification of this subspecies (34, 35). *T. b. gambiense* specific identification can be done through PCR amplification of the *T. b. gambiense*-specific glycoprotein (*TgsGP)* gene that encodes for a receptor-like glycoprotein, which is also involved in normal human serum resistance (36).

The third species within the subgenera of *Trypanozoon*, responsible for livestock infections, is *Trypanosoma equiperdum*. This parasite can be sexually transmitted amongst species from the family Equidae (horses and donkey), causing a venereal disease known as Dourine. Due to this transmission mode, the parasite has also acquired a wide geographic distribution. As for *T. evansi*, to which it is very closely related, also the classification of *T. equiperdum* as a separate species has been under scrutiny for many years (37), and several authors have suggested that there is no scientific argument to make a species level distinction between the two.

The second trypanosome subgenus responsible for salivarian trypanosomosis is *Dutonella*, which is mainly composed of two species, i.e., *T. vivax* and *T. uniforme*. Due to the global socio-economic impact caused by *T. vivax* infections in domestic animals, most of the studies of this subgenus have been carried out on this particular parasite species. This trypanosome is a pathogenic parasite species mainly found in Africa and South America (38). So far, only a single human infection has ever been reported (11). In Africa, transmission occurs in large through the bite of tsetse flies, having the highest infection rate of any tsetse-transmitted trypanosome species (39, 40). This high infectivity could be attributed to the relatively simple cycle of development in the vector's mouthparts. The transmission beyond Africa is mainly carried out mechanically by hematophagous flies from the genus *Stomoxys* and *Tabanus*, which transmit the disease to domestic animals such as cattle and goats, as well as to endemic wild animals such as capybaras, deer, and bubaline antelopes. Despite its large economic impact, especially in South America, *T. vivax* remains one of the less studied animal-infective *Trypanosoma* species. The main issue with *T. vivax* in the context of experimental parasitology and immunology research is the fact that virtually no parasites of this species are capable to be grown in mice. Hence, virtually all laboratory infections in mouse models (incl. Tv700, STIB 719, STIB 731-A, ILRAD 560, IL 1392) are being executed with the derivatives of Y468 *T. vivax* clone that was originally isolated in Nigeria that happened to "grow well" in mice after extensive adaptation (41). Hence, it remains to be seen if the TvY486 *T. vivax* reference strain is a good representative parasite for the general population of parasites found both in Africa and South America regarding host-parasite interaction mechanisms.

The third subgenus of pathogenic salivarian trypanosomes is *Nannomonas*, encompassing three species of animal-infective trypanosomes, i.e., *Trypanosoma simiae*, *Trypanosoma godfreyi*, and *Trypanosoma congolense*. The two first species are mainly infective to mammals belonging to the Suidae family (domestic pigs, warthogs etc.) while *T. congolense* has a broader range of hosts including livestock and game animals, but is generally accepted to be non-infective to humans. It should however be mentioned that a mixed *T. b. gambiense*/*T. congolense* infection has been reported in a human (42) and that *in vitro* testing of human serum-induced trypanolysis has shown a resistance phenotype in several stocks (43). *T. congolense* is the major tsetse transmitted pathogenic salivarian livestock trypanosome present in sub-Saharan Africa and causes large economical losses in the countries where it is endemic. The disease caused by this parasite is referred to as Nagana, meaning *depressed spirit* in the Zulu language of Southern Africa. During transmission, *T. congolense* develops in the midgut and proboscis of the tsetse vector. Mechanical transmission can occur, involving mainly *Tabanus* and *Stomoxys* species (44). In general, *T. congolense* is considered to be a monomorphic parasite. The host-parasite interaction as well as immunopathology associated with *T. congolense* infections has been better studied than in the case of *T. evansi* and *T. vivax*. However, it is important to point out the fact that while the molecular parasite surface structure has been well-described and compared to *T. brucei* (45), the regulation and kinetics of surface coat variation, as well as the infection of the coat with the immune system have never been analyzed in detail. Hence, most statements about these interactions and regulations are based on the assumption that *T. congolense* should behave the same way as *T. brucei*. A second scientific issue that plagues the *T. congolense* research literature is the fact that it is often used as a "chronic" model in comparison to "acute" *T. brucei* infections. This artifact originates from the fact that a specific

chronic *T. congolense* clone, i.e., Tc13, has been used in major immunological investigations for almost three decades (46). In contrast, the vast majority of experimental host-parasite research in *T. brucei brucei* and *T. brucei rhodesiense* models has been done with much more virulent *T. b.* AnTat 1 or LouTat 1 clones (47–49). While these studies by themselves all resulted in valid experimental data, it should be said that there are virulent *T. congolense* strains, resulting in infections in mice which display very similar survival times as the *T. brucei* clones mentioned above (50). Unfortunately, these more virulent *T. congolense* isolates have not been systematically used in comparative studies with *T. brucei*. Hence, reports that compare highly virulent *T. brucei* infections with low virulent *T. congolense* infections, and subsequently provide conclusion in which infection outcome is linked to the species-specific background of the parasite, should be taken with utmost caution. Of note is that the high genetic heterogeneity of *T. congolense* has led to the division of this parasite in three different subgroups i.e., Savannah, Kilifi, and Forest within the same species (51).

GENERAL LIFE CYCLE OF SALIVARIAN TRYPANOSOMES AND INTERACTION WITH BOTH INSECT AND MAMMALIAN HOSTS

The life cycle of cyclically transmitted salivarian trypanosomes inside their vector shows the plasticity of those parasites to adapt to new environments (**Figure 2**). Today, most of the knowledge on parasite transmission comes from the *T. brucei* model in which infection of tsetse flies occurs when the non-dividing short stumpy bloodstream form parasites are taken up during a fly's blood meal, reaching the fly's midgut and transforming into procyclic trypomastigotes (52). Once the parasite infection is established in the fly's midgut, the parasites migrate anteriorly to the proventriculus of the fly. Here, elongated trypomastigotes start to divide asymmetrically into both long and short epimastigotes of which the latter migrate toward the salivary glands and attach to the epithelial cells of the gland. Next, a final division occurs giving rise to the host-infective metacyclic forms. Once in the host's bloodstream, metacyclic parasites transform into long slender shaped bloodstream form parasites, which further divide by binary fission and represent the active dividing parasite form during the mammalian infection stage. It is at this stage that trypanosomes express the Variant Surface Glycoprotein (VSG) (55). This coat protein is encoded by a battery of over 1,000 different genes, mosaics and pseudogenes (56) and serves as an antibody decoy defense system (57). Indeed, VSGs are highly immunogenic and induce VSG-specific antibody responses. Hence, by regularly altering VSG variant expression, the parasite avoids efficient immune recognition and destruction (58). Genetic regulation of antigenic variation has been studied in detail and has been shown to involve various mechanisms of DNA recombination and transcription regulation of VSG genes (59, 60). With respect to mechanisms of genetic variation in trypanosomes, there is now ample evidence supporting the fact that *T. brucei* parasite mating or sexual reproduction does take place in the tsetse (5, 6). Hence, while the tsetse is conventionally referred as the insect vector for trypanosomosis, it should actually be considered as the definite host for the parasite. To put it in other words: mammals are merely the vessel that is used to ensure that trypanosomes are able to migrate from one tsetse to the next, and in addition provide long-term reservoirs that allow trypanosomes to survive seasonal periods in which fly populations are diminished. Sexual reproduction inside the insect vector offers the parasite in theory the chance of generating new hybrids, combining different parental characteristics. Important to note however is the fact that the effectiveness of trypanosome infection in the fly rapidly decreases with the age of the fly, hence also affecting the chance to generate hybrid descendants. Using both green and red fluorescent trypanosomes to study hybrid formation, it was shown that midgut and salivary gland infection rates were highest when flies were exposed to parasites in their first feed (53). Waiting $2^{1/2}$ weeks for a first parasite exposure reduced the infection success by half. Interestingly, exposing tsetse flies to two different trypanosome lines in a consecutive feeding experiment resulted most often in the establishment of the first infection only, as if the primary infection was able to push the vector to mount a protective immune response preventing secondary infection. Under natural circumstances, this would greatly reduce the chance of hybrids being formed, although the experimental conditions used above showed that in all combinations tested, hybrid formation did take place (53). As will be outlined later in this review, even the rarest hybrid formation events can have a significant impact on the transition from AAT to HAT, as it allows generation of a continuous pool of new human infective *T. rhodesiense* parasite strains (54). With respect to the vector immunity mentioned above, several studies published in the recent past have made contributions to the understanding of the mechanism underlying tsetse anti-trypanosome immunity. It is interesting to note that tsetse immunity development *per se* requires the presence of the obligate symbiont *Wigglesworthia* in the larval stage of the fly, transmitted through maternal milk gland secretion (61, 62). This finding complements the notion that the development of a fully functional innate immune system of the mature adult tsetse fly depends on the establishment of a bacterial microbiome population, and that the immaturity of the immune system is responsible for the high susceptibility to trypanosome infections during a first blood feeding (63). The fly immunity itself relies on multiple mechanisms. Indeed, the action of scavenger receptor peptidoglycan-recognition protein LB (PGRP-LP) is crucial for the colonization of the fly by its *Wigglesworthia* symbiont, and in addition has a direct trypanocidal activity on both procyclic and bloodstream form trypanosomes (64, 65). In addition, anti-trypanosome immunity relies on activation of the immune deficiency regulated pathway and antimicrobial peptides (66, 67), as well as reactive oxygen species (ROS) mediated defenses (68), which provides combined protective immunity at the level of the midgut and hemocoel. Interesting here is that for some time the peritrophic matrix, which is a chitinous protective layer lining the insect gut, has been considered as a physical barrier that could provide protection against invading infections. However, RNA interference-based reversed genetic approaches

have shown that the matrix is a true immunological regulator. Its integrity is necessary to build a proper immune context in the defense against different microbes, including trypanosomes, through its role in the expression of the antimicrobial peptide attacin as well as dual oxidase and iNOS, both involved in the production of reactive oxygen intermediates (ROIs) (65). Finally, the tsetse fly's specific TsetseEP protein was shown to provide anti-trypanosome protection at the level of the midgut (69). Interestingly, starvation of flies reduces immune responsiveness and increases susceptibility toward trypanosome infections both in young and older flies (70–72).

Naturally, from a human and economic point of view, it is the mammalian infection stage that has attracted most attention in the past. It is only more recently that the parasite-vector interaction and biology has received more detailed attention and that also non-*T. brucei* infections have been studied in tsetse (73, 74). These reports show that in fact both *T. congolense* and *T. vivax* are much more effective in establishing tsetse infections than *T. brucei*. In particular, for *T. congolense* it has been shown that this parasite is particularly effective in reaching the proboscis of the fly, where the trypomastigote-epimastigote transformation takes place. In this case, migration from the foregut to the mouthparts appeared to occur with high efficiency. In contrast, *T. brucei* is much less efficient in colonizing the tsetse, as most parasites do not survive the migration from the foregut to the salivary glands. Investigating both *T. brucei* and *T. congolense* infections in parallel have suggested that *T. brucei* adopted to final survival in the salivary gland, as this niche would not be preoccupied by the much more efficiently growing *T. congolense* parasites. Hence, despite the fact that both parasites use the same transmission vector, and that also for *T. congolense* meiotic reproduction has been reported in the teste vector (75), there are remarkable differences in the way the two trypanosomes infect and occupy the body of the insect host. In recent years, specific attention has also been given to the immunological events that take place at the bite site of the tsetse, in order to explain how successful mammalian infections are initiated. Here, it has become clear that there is a crucial role for tsetse saliva components in preventing local blood clothing, vasodilation, and neutrophil influx, all leading to the successful establishment of a primary infection and allowing metacyclic saliva parasites to be transformed successfully into long slender bloodstream form parasites (76, 77).

Besides the biological vector transmission described above, mechanical transmission is a second way of ensuring parasites can move from one mammalian host to the next. This mode has been described for *T. congolense*, *T. evansi*, and *T. vivax*, but only the latter two have successfully used this way of transmission to migrate out of Africa, into other continents. The main vectors that have been reported today for both trypanosome species are the horsefly, stable fly, horn fly, and deerfly. In all cases, mechanical transmission occurs when a fly with blood-contaminated mouthparts, containing living bloodstream form parasites, rapidly changes feeding hosts allowing the parasites to be transmitted without any intermediate insect-specific forms. To date, virtually no information is available on possible immune interactions that could make this way of parasite transmission more or less successful. Interestingly, also nothing is known about the immune events that aid in parasite transfer back to the fly. Indeed, it is remarkable that livestock parasitaemia levels are often extremely low, presenting blood parasite load levels that are hardly detectable by microscopy. Yet, even when circulating parasite numbers are extremely low, flies still manages to successfully pick up parasites while taking very small blood meal volumes. Whether this is due to the fact that parasitaemia in the skin microvasculature is uniquely high as compared to the general blood circulation, or whether fly saliva has unique and potent trypanosome chemoattractant, remains to be elucidated.

HUMAN TRYPANOSOMOSIS IN AFRICA IS ONLY PART OF THE PROBLEM

In 2009, the number of reported HAT cases dropped below 10.000 for the first time in 50 years, and the most recent figures available for 2015 indicate that the global incidence of HAT has dropped below 3.000. It is now estimated that by 2020 HAT will no longer be considered as a major human health problem in Africa and hence will also no longer be listed as a neglected disease (78). With HAT being caused by either *Trypanosoma brucei gambiense* (>97%) or *Trypanosoma brucei rhodesiense* (<3%) (79), these numbers and assumptions are mainly based on the current West/Central African situation. Considering however that *T. b. rhodesiense* is a zoonotic parasite with a cattle and wildlife reservoir, re-emergence of HAT is going to remain a crucial concern in Africa. Indeed, whether or not the reservoir of *T. b rhodesiense* has been brought under control is hard to verify due to the insufficient systemic reporting on *T. b. rhodesiense* game and cattle infections. In addition, beyond the borders of the African continent the existence of non-*T. brucei* human trypanosomosis could become a future problem as *T. evansi* infections spread around the globe. Despite the reports of *T. evansi* infections in humans (80–83), this parasite is still not widely considered as a human pathogen. The lack of interest in these infections, combined with the continued spread of these trypanosomes mainly in South America, the Indian subcontinent, and Asia, risks of exposing humans to a new type of "unconventional" disease that will require a whole new approach to trypanosomosis world-wide. In addition, the lack of experimental studies on *T. evansi* infections as compared to *T. brucei* infections makes it harder to link the discussion about the genetic classification of *T. evansi* as a *T. brucei* subspecies to data dealing with the cellular and molecular mechanisms that govern host-pathogen interactions, pathology development, and zoonotic behavior.

Taken the importance of the zoonotic aspect of most remaining human trypanosome infections, it is clear that (African) Animal Trypanosomosis (AAT) *per se* deserves particular attention. In fact, there is a wealth of information available with respect to geographic distribution of AAT, immune pathologies including anemia and vaccine efforts as well as failures. These reports outnumber the scientific data published on host-pathogen aspect of human trypanosomosis. However, this contrasts very much the situation with respect to the actual

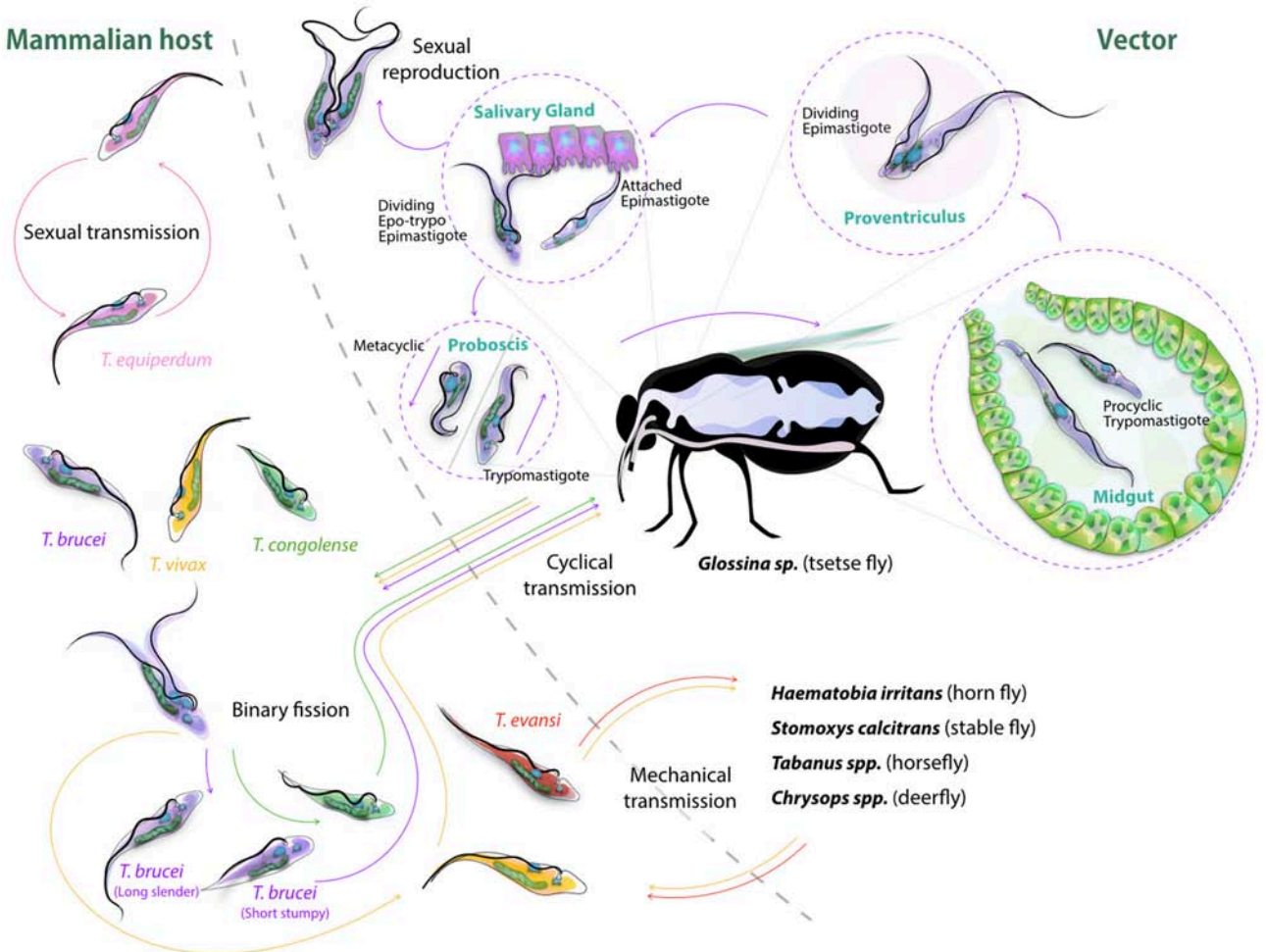

FIGURE 2 | Cyclic transmission of salivarian trypanosomes mediated by tsetse and other biting flies. Most lifecycle data of African Trypanosomes is based on the *T. brucei* cycle involving the tsetse (52). Here, short stumpy form parasite are taken up by the fly, progress through the body of the insect vector passing via the midgut, proventiculus and salivary gland, to be re-injected though the proboscis as infective metacyclic trypomastigotes into a new target. In the bloodstream, differentiation to long slender forms occurs followed by binary fission proliferation. Differentiation back to short stumpy forms will complete the cycle. While *T. congolense* and *T. vivax* can follow a similar cyclic transmission mode, the latter also is known to be spread through mechanical transmission (53, 54), as is the case for *T. evansi* (1). *T. equiperdum* spreads through sexual transmission only (37). Sexual reproduction of trypanosomes itself has been reported to take part in the teste, and has been reported for both *T. brucei* and *T. congolense* (5).

understanding of trypanosome diseases. Indeed, while many have focused on experimental models to understand human trypanosomosis in the past, much less effort has been made to understand the fundamentals of animal trypanosomosis. A fine example to illustrate this is the issue of antigenic variation. For more than four decades, scientists have been studying antigenic variation of the VSG coat used by trypanosomes to deliver a protective response against the host antibody defense system. All work that included genetic approaches as well as molecular biology approaches combined with computer modeling, has been done for *T. brucei*, largely ignoring the fact that the main cattle parasites i.e., *T. congolense* and *T. vivax* are very different trypanosomes that might use other systems of regulation and defense. For example, comparative studies of the VSG repertoire conducted in *T. congolense* and *T. vivax* indicated that the scale of the VSG recombination differs between two species, being more frequent in *T. congolense* than in *T. vivax*. Moreover, *T. vivax* populations were shown to be consistent with clonal reproduction (84), while the *T. congolense* ability to undergo sexual reproduction generates opportunities for allelic recombination among VSG genes (85). Hence, to date we are left with molecular tools that are very suitable to study a wide range of host-parasite interactions in mice which could model human infections, but at the same time we have very little experimental models and tools to study AT. One striking example is *T. equiperdum, which* is hardly studied in comparison to other infections due to the fact that it causes a disease characterized by sexual transmission in horses, a feature so far not reported in mice. In fact, only a single report is available on experimental sexual transmission of trypanosomosis in mice, and this report

is dealing with *T. b. gambiense* (86). However, whether sexual transmission of *T. brucei gambiense* is a real issue in human trypanosomosis, remains a matter of debate (87) and more species-specific research is needed to resolve these issues.

ADAPTATIONS OF ANIMAL INFECTIVE TRYPANOSOMES TO HUMAN HOST

Humans are considered naturally resistant to pathogenic animal trypanosomes such as *T. b. brucei, T. evansi, T. equiperdum, T. congolense*, and *T. vivax.* The mechanism of human resistance to those trypanosomes is based on the presence of cytolytic factors in the high density lipoprotein (HDL) fraction of normal human serum (NHS) (88) and is attributed to two fractions called trypanosome lytic factor 1 and 2 (TLF1 and TLF2), with the latter being the major active compound (89). The human infective *T. brucei* subspecies *T. b. gambiense* and *T. b. rhodesiense* are known to be resistant to TLF lysis through various mechanisms. A number of reports demonstrating *T. evansi* infections in humans has triggered a new wave of interest in molecular mechanisms underlying human infectivity in the context of the transition from an animal infective trypanosome to a zoonotic pathogen causing disease in humans. While TLF1 and TLF2 have slightly different compositions, they both contain the haptoglobin related protein (HPR) and Apolipoprotein L1 (ApoL1), of which the latter is considered the main active lytic compound. Furthermore, TLF2 is complexed with IgM molecules and has a much higher molecular mass than TLF1, but is lipid poor (90). With respect to the mechanisms of lysis and resistance to NHS, initial data was obtained in an experimental model for *T. b. rhodesiense*. Here, it was shown that resistant and susceptible sub-clones can be derived from a common ancestor by passaging trypanosomes in either the presence or absence of human serum. This work gave rise to the discovery of the *SRA* gene, encoding a truncated VSG and located within the VSG expression site (91). Transfer of the gene to *T. b. brucei* showed that the presence of this single gene indeed was enough to confer resistance to NHS (92). Subsequently, the identity of SRA allowed to characterize ApoL1 as the active serum compound (93) that acts through both lysosomal and mitochondrial membrane permeabilization (94). The inhibitory mechanism of SRA was shown to rely on its capacity to block the membrane pore-forming capacity of ApoL1 upon entering the acid compartments of the lysosomal system (95–98). Finally, the haptoglobin-hemoglobin receptor (HpHbR), localized in the flagellar pocket, was identified as the trypanosome receptor involved in TLF1 uptake (99), while the mechanism for TLF2 uptake has still not been elucidated (100). Indeed, HpHbR knock down *T. b. brucei* parasites remain sensitive to both NHS and TLF2 lysis (101). However, as both TLFs contain the same active ApoL1 compound, the SRA is capable of blocking all NHS activity. Interestingly, the *SRA* gene is only present in *T. b. rhodesiense* and hence has been used in a string of different diagnostic approaches for HAT, including PCR and LAMP, targeting not just human samples but also livestock and game reservoirs as well as the tsetse vector, in various regions in Eastern Africa. Of note is a report in which a Ugandan HAT survey indicated that 20% of parasitologicaly confirmed *T. b. rhodesiense* cases resulted from infections that could not be detected by any of the *SRA* PCR methods described so far. Whether this indicates that *SRA*-negative human infective *T. b. rhodesiense* parasites exist, implying these parasites have alternative NHS resistance mechanisms, or whether the negative results were due to *SRA* gene polymorphism that prevented PCR primer annealing, remains a matter of debate (102). The existence of such *SRA* gene polymorphisms has been studied in the context of human disease severity (54). Most recently, using *SRA* as a genetic tracer, it has been shown that genetic recombination between *T. b rhodesiense* and the much larger pool of *T. b. brucei* animal trypanosomes allows for the continuous generation of new *SRA*-positive human infective parasites (103, 104). This once again indicates that in order to really bring HAT under control, AAT and particularly the animal *T. b. rhodesiense* reservoir has to be eliminated as well.

Interestingly, more than 97% of all human trypanosomosis infections are caused by *SRA*-negative *T. b. gambiense* (79), a parasite that is subdivided in Group 1 and Group 2 *T. b. gambiense* (105). While Group 1 parasites have an invariant phenotype toward NHS resistance, Group 2 parasites show a variable degree of resistance, modulated by the actual exposure to NHS. Neither Group 1, nor Group 2 parasites have the *SRA* gene (8), indicating that there are multiple ways to mount resistance to NHS. Literature of the last 5 years has mainly focused on the Group 1 *T. b. gambiense* resistance, showing that these parasites have acquired a combination of defense systems which allows them to resist the lytic action of NHS. This includes a specific point mutation in the HpHbR in combination with reduced receptor expression, reducing TLF1 uptake (106, 107). However, as this receptor is not a main player in TLF2 uptake, *T. b. gambiense* needs additional mechanisms to survive in human blood. These involve the alteration of lipid membrane fluidity by the *T. b. gambiense*-specific glycoprotein (TgsGP) (108, 109), as well as increased cysteine protease activity in the digestive vacuoles of the parasite. The latter is believed to directly affect ApoL1 activity (110). Today, it remains unclear how *T. b. gambiense* Group 2 parasites deal with the toxicity of NHS.

T. evansi parasites express neither SRA, nor TgsGP, but now have been reported in several instances as human pathogens causing a-HT (11, 18, 80, 82, 111). Similarly to *T. b. rhodesiense* and *T. b. gambiense* Group 2 parasites, a remarkable phenotypic plasticity of *T. evansi* has been described upon exposure to NHS, with resistance occurring after prolonged NHS exposure and being absent when NHS selective pressure is removed. Screenings of various *T. evansi* isolates indicated that some even display natural resistance to NHS, while others were found to be fully sensitive (112). In line with these observations in *T. evansi*, even *T. b. brucei* NHS resistance has now been reported. In the latter, a switch to a resistant phenotype was recorded to occur upon repetitive exposure to NHS or TLF1 in the absence of the *SRA* gene (113). However, a fragment homolog to *SRA,* named SRA basic copy (*SRAbc*), was found in the *T. brucei brucei* TREU927/4 strain, which exhibits low resistance to NHS (114). Similarly, one of the

human infective *T. evansi* isolates was shown to contain the *SRAbc* homolog (115). Interestingly, the *T. b. brucei* parasites exhibiting increased NHS resistance had a significant reduction in TLF1 uptake, which coincided with downregulation of *T. b. brucei HpHbR* mRNA levels (100). Hence, it seems that the resistance mechanism in these parasites shows a mixed but attenuated phenotype of those found in either *T. b. gambiense* or *T. b. rhodesiense*, as if the latter could have been selected as "optimized" derivatives of *T. b. brucei* semi-resistant predecessors.

With respect to human *T. evansi,* it is important to highlight that at least one human infective case has been attributed to the lack of functional ApoL1 (81). Indeed, a frameshift mutation, found in both *ApoL1* alleles of the patient, resulted in the ability of trypanosomes to establish infection and to survive in the human bloodstream. This strongly suggests that human trypanosome resistance in large relies on a non-classical immune mechanism, i.e., lipid membrane disruption by TLF. However, a Vietnamese a-HT *T. evansi* victim was shown to have fully functional *ApoL1* alleles and a normal concentration of serum ApoL1 (116). Hence, this shows that there is an additional role for the immune system in the overall defense against trypanosomes, most likely involving a combination of the action of antibodies, cytokines, and complement factors. In at least two confirmed human *T. evansi* infections, the infected individuals were shown to have a compromised immune system. One case relates to a pregnant woman from Mumbai, India suffering from HIV/AIDS, anemia, and upper respiratory tract infection (117). The second case relates to the above mentioned Vietnamese woman who had just given birth (116), with pregnancy itself being known as a unique immune condition that is modulated by fetus development resulting in immune alterations that in some cases in facilitation of parasite growth. Important is that also in experimental *T. evansi* infections in mice, in particular IgM antibodies are crucial for parasitaemia control (118). This indicates that when "natural resistance" such as the resistance conferred by ApoL1 fails, the antibody-mediated immune response does provide a second defense barrier against the progressing of infection.

Finally, it should also be mentioned that several reports in the past have indicated the existence of a-HT caused by the stercorarian *T. lewisi* parasite (119). Here, resistance to NHS lysis was correlated with resistance to human ApoL1 as well. Hence, it seems that while multiple mechanisms have been acquired by various trypanosomes to block the lysosomal pore-forming catalytic activity of NHS, this activity itself is executed in large by a single factor, i.e., ApoL1. This finding itself has attracted scientific attention over the last years with respect to primate evolution (120), and has resulted in the findings that (i) ApoL1 is the common lytic factor in human, gorilla, and baboon primate sera (7, 8, 121), (ii) the chimpanzee, orangutan, and macaque, which are susceptible to all *T. brucei* subspecies, lack functional ApoL1 (121), and (iii) the baboon ApoL1 variant is capable of killing even *T. b. gambiense* and *T. b. rhodesiense*, as opposed to the human ApoL1 (122, 123). The latter finding has prompted an attempt to generate genetically modified TLF transgenic livestock that would be able to resist all known pathogenic trypanosome species (122).

THE ROLE OF B CELLS AND ANTIBODIES IN SALIVARIAN TRYPANOSOMOSIS

As outlined above, VSG switching and antigenic variation, including the generation of VSG mosaic genes, have generally be considered as the major defense systems that parasites have developed against the host's adaptive immune system (56, 124, 125). However, in recent years it has become clear that trypanosomes have developed several precautionary adaptations that provide a rescue in case they do get recognized by antibodies. The reason for this is obvious: even if different VSG variants exhibit different hypervariable loops, and even if mosaic VSG present new epitopes to the immune system, there is no reason to assume that the overall pool of infection-induced antibodies is not at all capable of detecting new parasite variants. In fact, the existence of the cross-reactive nature of anti-VSG antibodies has been used since the beginning of trypanosome immunology research. Here, the VSG of the first arising variant or living cloned parasites, expressing a single VSG, have been used to monitor fluctuating anti-VSG titers throughout infection for weeks or months (57, 126). More interestingly maybe is the fact that reinfection models have shown that weeks into a primary infection, mice can be killed by a secondary infection with virulent trypanosomes expressing exactly the same VSG as the primary infection (127). In order to understand these results, three major host-parasite interactions mechanisms have to be considered. First, trypanosomes have developed a very efficient way of driving endocytosis. This system allows to continuously clear surface bound antibodies from the VSG coat, preventing antibody-mediated lysis (128). Secondly, while antibody/complement-mediated lysis has long been proposed to result in antibody-mediated trypanosome killing, it is important to note that AKR mice, which are natural C5 complement knockout mice, are able to clear peaks of parasitaemia in a similar way as other mice. This shows that the lack of complement-mediated lysis does not prevent the immune system of controlling peak stage parasite levels (129). Third, there is now ample evidence that trypanosomes cause a B cell depletion pathology, which is initiated by the very rapid disappearance of immature B cells in the bone marrow, as well as transitional and IgM^+ marginal zone B cells from the spleen, followed by a gradual depletion of Follicular B cells (FoB) (127, 130). This has now been reported for *T. b. gambiense* and *T. congolense* infections (50, 131). Mechanisms involved in the depletion process have been linked to IFNγ-mediated inflammation (132), NK-mediated B cell destruction (133), and direct cell-cell contact-mediated B cell apoptosis (111, 127). Once FoB cell depletion is accomplished by the parasite, it becomes impossible for the host to generate new efficient antibody responses against newly arising VSG variants (**Figure 3**). In addition, it hampers anti-VSG memory recall responses against previously encountered variants, hence making the host susceptible to

secondary infections with old variants. This might also explain the accumulation of mosaic VSG variants during later stages of infection (56). Indeed, the question whether later variants are immunologically distinct (or not) from their ancestral variants, which has so far not been answered, might not be important at all. Possibly, these variants arise simply from the continuous gene rearrangements that are ongoing at the telemoric ends of the VSG expression sites and are tolerated, due to the lack of antibody-mediated elimination by the host, rather than being produced in order to evade the already existing antibodies.

B cell dysfunction, associated to trypanosomosis, also has a secondary detrimental effect on the mammalian host, i.e., the elimination of vaccine-induced memory recall responses. Indeed, in an experimental model for DTPa vaccination, it was shown that *T. b. brucei* is capable of destroying immunological memory rendering vaccinated mice susceptible to infections with *Bordetella pertussis* (130). This was not a result of an infection-associated immunosuppression, as it persisted after anti-trypanosome drug treatment and the elimination of active trypanosome infections. This detrimental effect of trypanosomes on non-related vaccine efficacy has also been reported in other models and natural infections. Although not thoroughly studied in human infections, one study has shown that antibody titers induced by the anti-measles vaccine are significantly downregulated in HAT patients, and that curative HAT treatment did not result in a restauration of antibody titers (**Figure 4**). For obvious ethical reasons, this study stopped short of assessing whether or not the remaining titers would still confer protection. In addition, the study did not address the question whether vaccine-induced memory recall responses were affected (138). With respect to AT, more data is available in particular with respect to *T. evansi* and *T. congolense* infections. Indeed, such infections in pigs were shown to abrogate protective immune responses generated against the classical swine fever vaccine (139). They were characterized by significantly reduced antibody responses, leukopenia, and high fever. Similarly, *T. evansi* infections in water buffalos, vaccinated against *Pasteurella multocida* (hemorrhagic septicemia), showed impaired capacity to mount a humoral and cell-mediated immune response upon challenge (140). When cattle, harboring *T. congolense* and *T. vivax*, were given a *Brucella abortus* vaccine or were vaccinated against contagious bovine pleuropneumonia, specific antibody responses to the vaccine were shown to be severely depressed (135, 141–143). Similarly, *T. congolense* infected goats vaccinated with *Bacillus anthracis* showed a profoundly diminished anti-anthrax antibody responses (144), while *T. congolense* infected cattle were shown to suffer from immunosuppression and failed recall responses in a foot-and-mouth vaccination setting (145). Taken together, these studies, conducted in natural hosts for animal trypanosomes such as cattle, water buffalos, goats, and pigs, confirmed studies in mice showing that trypanosome infection induces severe impairment of B cell responses and antibody production to a number of non-trypanosome related commercial veterinary vaccines.

THE ROLE OF T CELLS AND T CELL-DERIVED CYTOKINES IN SALIVARIAN TRYPANOSOMOSIS

Taken the extracellular nature of salivarian trypanosome infections, initial thoughts on the control of infection were naturally focused on the role of antibodies and B cells. However, already early in the 1980's it became obvious that while the virulence of experimental trypanosomosis was not linked to the expression of a specific VSG variant, or the use of a specific MHC-II type, $CD4^+$ T cells played an absolutely crucial role in infection control (146). Twenty-five years after this initial discovery, it was shown that major T cell responses against cryptic T cell epitopes play a major role in trypanosomosis control (147, 148). This observation caused a major paradigm shift in the way trypanosomosis control is thought to occur, as it shows that T cell help is not just needed to support effective B cell functioning and antibody production, but that it plays a crucial second B cell-independent role during the progression of infection. This role of T cell biology might initially have been underestimated, as a multitude of studies had shown that trypanosomosis, both in mice and cattle, results in the occurrence of T cell immunosuppression (49, 149). However, these reports mostly referred to suppression of T cell proliferation and not to cytokine secretion. To date, the active disease controlling role of T cells is mainly attributed to the cytokine production in which polarization toward a Th1-type response is crucial for initial parasitaemia control (137). Detailed analysis of both *T. brucei* and *T. congolense* infections has indeed shown that early IFNγ production is crucial for the control of the onset of infection (**Figure 3**). This hypothesis was initially driven by the description of the cytokine production profile of $CD4^+$T cells, and was later corroborated by the use of neutralizing anti-IFNγ antibodies as well as the use of IFNγ knockout mice (150, 151). The latter were shown to have an impaired control of the first peak of parasitaemia, followed by their inability to clear increasing parasite numbers, leading to the early death of the mice using the C57Bl/6 model (152). In experimental *T. congolense* infections, it was demonstrated that while hyper-susceptible BALB/c mice preferentially mount an infection associated Th2-type response against the Tc13 *T. congolense* parasite, Th1-biased C57Bl/6 mice were able to survive for up to 6 months when infected with the same clone (136). Also here it was shown that altering immune balances, by treatment with neutralizing anti-cytokine (or cytokine receptor) monoclonal antibodies, drastically alters the outcome of infection (153). Most recently, it was reported for *T. brucei* that the $CD4^+$ IFNγ response is preceded by the production of this cytokine by NK and NKT cells, followed by a marked upregulation of IFNγ production by $CD8^+$ T cells (154). This was observed in both the spleen and the liver of infected mice. However, by 10 days post infection it was clear that these cell populations were either drastically reduced in numbers or became totally depleted, leaving the $CD4^+$ T cells to execute the major task of cytokine production. A comprehensive report on the overall role of IFNγ in various trypanosome infection models was recently published by Wu *et al.* (155). Interestingly,

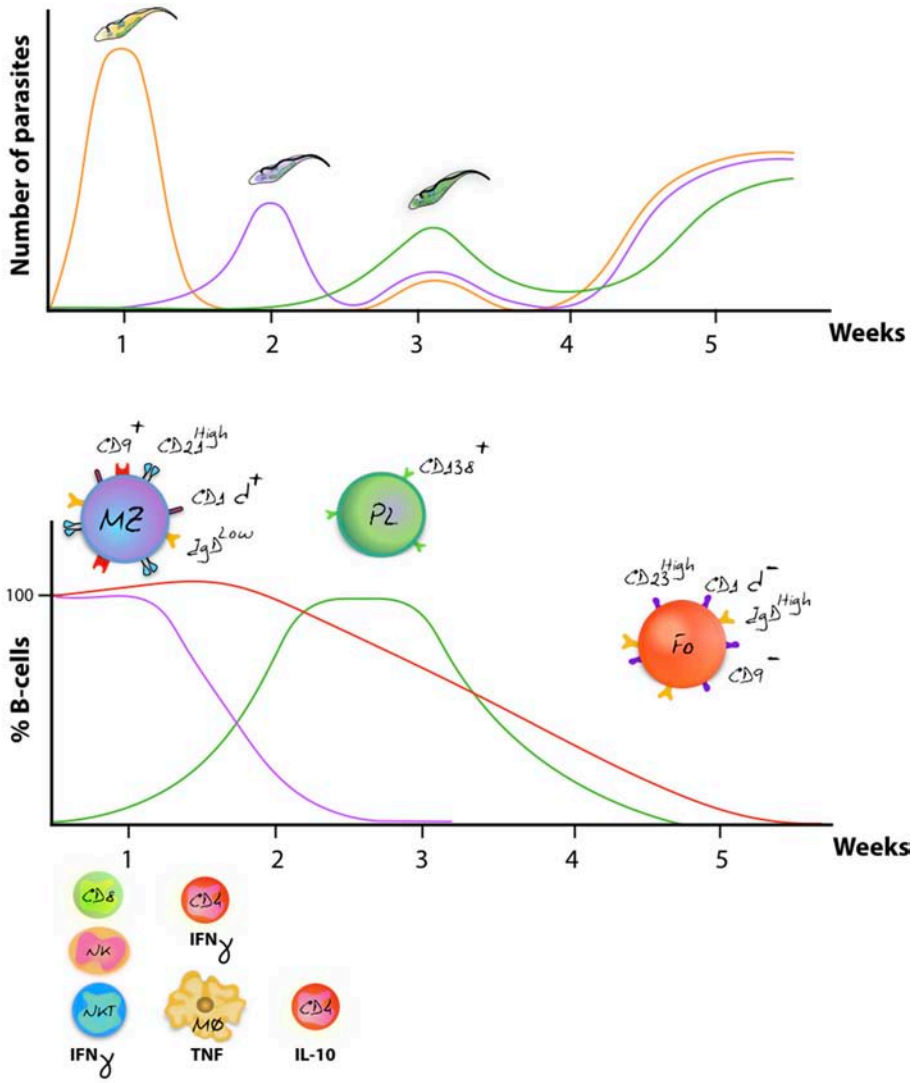

FIGURE 3 | Antigenic variation and host immune destruction are closely linked. Antigenic variation of the trypanosome VSG surface coat enables trypanosomes to escape specific antibody-mediated destruction, resulting in immunologicaly distinct parasites occurring at regular intervals (upper panel). To prevent total eradication, trypanosomes undermine the immune system by ablation of the B cell compartment. In mice, this results in abrogation of an efficient antibody mediated immune defense system, allowing different parasite variants to occur simultaneously (schematically represented as the week 3 situation). Despite to co-occurrence of several variants, later-stage parasitaemia peaks usually have a reduced magnitude in terms of actual parasite numbers as various non-B cell defense systems aid in parasiteamia control [upper panel, adapted from (134)]. The lower panel schematically represent the finding that onset of infection is followed by a rapid depletion of the MZ B cell compartment (purple), followed by a gradual destruction of the FoB cell compartment (red) (116, 119). While the initially host immune response generates effector Plasma B cells, later waves of newly arising parasite variants fail to be efficiently depleted due to the impaired capacity of the host to deliver a renewed Plasma B cell response (green). Overall immunopathology is initiated by excessive production of IFNγ during the first week of infection, involving mainly $CD8^+$ T cells, NK cells, and NKT cells. By 7 days post infection, IFNγ production is taken over by $CD4^+$ T cells, while activated macrophages now produce excessive amounts of TNF that contribute to pathology (135, 136). Later-on in infection, production of IL-10 has been documented to counteract the initial inflammation (137).

to date only one single trypanosome factor has been identified as being able to induce IFNγ production by T cells, $CD8^+$ T cells in particular. This molecule, named TLTF (trypanosome lymphocyte triggering factor) (10) has been characterized in *T. brucei* and *T. evansi* parasites (156), but a homolog has not been described for other trypanosomes. TLTF was shown to be capable of inducing IFNγ production by astrocytes, suggesting a direct role of the molecule in the pathology development of sleeping sickness (157). This hypothesis has been further supported by the finding that IFNγ deficient mice show reduced $CD4^+$ and $CD8^+$ T cell influx into the brain parenchyma of *T. brucei* infected mice (158). Important is that when the role of T cells and IFNγ are considered within a trypanosomosis context, IL-10 was shown to be the main counter regulator of infection-associated inflammation in both *T. brucei* and *T. congolense* models. The source of the latter was proposed to be the regulatory

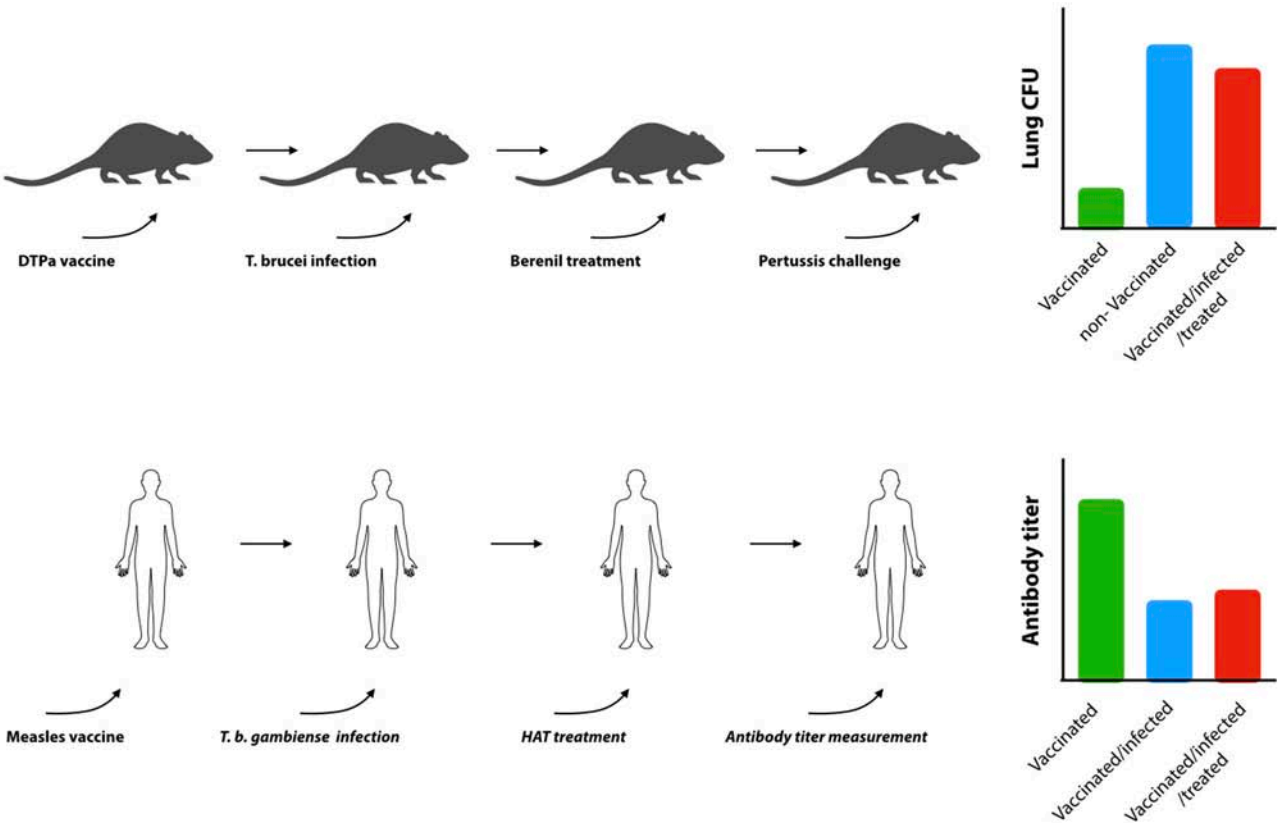

FIGURE 4 | Trypanosomosis-induced B cell destruction results in prolonged B cell dysfunction. Experimental infections in mice have shown that trypanosomes can destroy non-related DTPa induced vaccine responses (upper panel). Vaccinated mice that have been confronted with trypanosomes fail to clear diphtheria bacteria from their lungs, even when the bacterial challenge is performed after the trypanosome infection has been cleared by drug treatment [adapted from (119)]. Indeed is was shown that while the commercial vaccine Boostrix® provides significant protection against a *B. pertussis* challenge (green bar: vaccinated, blue bar: non-vaccinated), exposure to trypanosomes abrogated vaccine-induced protection (red bar). In humans (lower panel), trypanosome infections were shown to suppress vaccine induced anti-measles antibodies. Serum antibody titers in vaccinated *T. gambiense* HAT patients (blue bar) were shown to be significantly lower as compared to vaccinated control individuals (green bar), and specific antibody titers did not recover after curative anti-HAT treatment (red bar) (121).

T cells (9). However, a most recent effort to understand the full kinetics of IL-10 production during trypanosomosis, using the IL-10 reporter mouse system, has indicated that a whole range of cells is capable of producing IL-10 during infection and that most notably $CD4^+$ T cells, that do not have a defined regulatory phenotype, are the main producers of this cytokine (159).

As for the role of IFNγ in parasitaemia control, early reports characterized this cytokine as a trypanosome growth factor (160). In contrast, a number of follow-up reports have indicated that IFNγ is crucial for inhibition of trypanosome growth, as well as for trypanosomosis-associated NO production and TNF production that both limit trypanosome growth (152, 161, 162). Both these factors have subsequently been identified as direct players in the control of peak parasitaemia levels in *T. brucei* as well as *T. congolense* infections. Using TNF knockout mice, it was shown that parasitaemia control in relatively resistant C57Bl/6 mice depends on TNF production during the first peak of parasitaemia (163, 164). This confirmed initial reports in which neutralizing anti-TNF antibodies had a negative effect on *T. brucei* parasitaemia control (165). Subsequently, a comparative infection model using BALB/c, C57Bl/6, C3H/HeN, and CBA/Ca mice showed that while TNF production *per se* was required for proper parasitaemia control, infected mice responded to TNF-associated inflammation with the shedding of TNF-R2 receptors. This, in turn resulted in limiting the TNF-mediated infection-associated immunopathology (166). Based on these results, and placing these observations in the wider context of trypanosome infections using various gene-deficient mouse models, it has been proposed that while soluble TNF could plays a pivotal role in parasitaemia control, it is the membrane-bound form of the cytokine that has a major impact on progressing inflammation and inducing pathology (167). When analyzing the possible direct effect of TNF on trypanosomes, results showed a differential outcome depending upon the model studied. First, it was reported for the *T. brucei brucei* AnTat 1.1 clone that TNF has a direct trypanolytic effect. The latter is mediated by a lectin binding domain of the TNF molecule that is located at the opposite site of the molecule as compared to the mammalian receptor binding site (168). Interestingly, the lectin specificity of TNF exhibits a high affinity for complex branched mannose

sugars, such as those found on the trypanosome VSG molecule (169). Using a model for *T. brucei gambiense*, these findings were independently confirmed in an *in vitro* co-culture system (170). In contrast, experimental mouse studies with the human infective *T. brucei rhodesiense* LouTat 1 clone did not show a direct effect of TNF (171), suggesting that various trypanosome stocks can exhibit different levels of susceptibility to host cytokine-mediated growth regulation, as might be the case for IFNγ. Studies in trypanotolerant vs. trypanosusceptible cattle, using a *T. congolense* model, confirmed the possible role of TNF in parasitaemia control in natural infections (172), but here no link was made to a possible direct trypanolytic effect of the cytokine. Also, for the *T. congolense* infection mouse model, the direct action of TNF has not been reported but here TNF-R1 signaling has been associated to the combined release of soluble TNF and NO by activated macrophages. Those two combined were shown to play a crucial role in parasitaemia control, in conjunction with infection-induced anti-trypanosome antibodies (118). Interesting to note here is that in contrast to the limited knowledge on the molecular mechanisms of trypanosomosis-driven T cell IFNγ production, detailed research into the mechanisms of macrophage-derived TNF induction have been able to provide a more in-depth understanding of the host-parasite interplay. Indeed, first the VSG-GPI anchor was identified as the major trypanosome molecule responsible for TNF induction, with the trypanosome-specific galactose side-branch of the anchor playing a major role in macrophage activation (173, 174). Subsequently, it was shown that IFNγ could prime macrophages to become responsive to GPI-VSG and trypanosome stimulation (175). These results are in line with *in vivo* data showing that a rise in serum IFNγ values precedes the induction of infection-associated TNF (154). However, when macrophages are primed with VSG, prior to IFNγ, the cells are de-sensitize with respect to cytokine secretion (175). This may represent a way to prevent hyper-inflammation during the phase that corresponds to peak parasitaemia clearance, in which massive amounts of VSG are being released into the hosts' circulation. This information has been used to try and design an anti-disease vaccination approach for trypanosomosis (176). Although it was shown that repeated exposure to VSG-GPI prior to infection could indeed reduce the infection-associated pathology related to excessive macrophage activation, the results indicated that the vaccine approach did not result in the buildup of immunological memory involving antibodies or B cells. Instead, the reduction of inflammation, following the repeated GPI exposure related to an alteration of macrophage phenotypes, shifted the balance from infection-induced inflammatory type 1 cells to more anti-inflammatory type 2 cells or macrophages. This response was short-lived. Moreover, as the beneficial effect of the VSG-GPI treatment was observed to the same extent in both B cell deficient mice and in wild-type littermates, it became clear the approach could no longer be considered as a possible vaccine approach (177). In addition to the VSG-GPI, trypanosome DNA that contains high levels of unmethylated CpG sequences has been reported to be responsible for driving NF-κB an MAPK signaling pathways, resulting in the transcription of pro-inflammatory cytokine genes including *tnf*, in case of *T. brucei* infection(178). As for infection with *T. evansi*, the information on the role of IFNγ is limited, but data has shown that in addition to anti-trypanosome antibodies, this cytokine is required for parasitaemia control (179). Most recently, a comparative cytokine analysis using different *T. evansi* infections confirmed the induction of IFNγ in all infections (180). For *T. vivax* infections, there is a general lack of published information on the role of T cells and their cytokines in the control of onset in infection, but it appears reasonable to assume that a similar cytokine environment is needed to obtain the best parasitaemia control possible. As for human (*T. b. rhodesiense*) and cattle (*T. congolense*) infection, the role of IFNγ in inducing inflammatory pathology has been confirmed in both (181, 182), and as already outlined above, IFNγ has been shown to play a major role in the actual cerebral complications that characterize human sleeping sickness (183).

ANEMIA IS A MAJOR PATHOLOGICAL FEATURE OF ANIMAL TRYPANOSOMOSIS

From the data reviewed above, it has become clear that the IFNγ/TNF driven immunopathology is a hallmark of trypanosomosis in both human and livestock. When focusing on the latter it has been amply documented that TNF-linked infection-associated anemia is the major pathological feature that marks both *T. congolense* and *T. vivax* trypanosomosis. In fact, the classification of so-called trypanotolerant and trypanosusceptible animals is based on the relative capacity to control anemia during infection which consequently is directly linked to whether or not animals remain productive while infected with trypanosomes (184). Mechanisms that underlie this tolerance are complex and to date still not clearly understood, but most likely include differences in erythropoeitic potential and hemodilution (185), factors involved in erythrolysis (186), eryhtrophagocytosis (187), the regulation of the erythropoietin homeostasis (188), the host's potential to raise neutralizing antibodies against secreted trypanosome virulence factors (189), and the general mechanism involved in inflammation control such as the regulation of the IFNγ/IL-10 balance as well as other cytokines (167). With respect to cytokine regulation during infection, it is worth mentioning that MIF (Macrophage migration Inhibitory Factor) was recently shown to be one of the key trypanosomosis-associated inflammation inducing cytokines involved in the promotion of so-called anemia of inflammation, in which classically activated macrophages also play a major role (190). Indeed, it was shown that MIF promotes the storage of iron in liver myeloid cells, subsequently depriving iron from the eythropoeitic system and preventing the maturation of RBCs. Important here is that the *T. congolense* C57Bl/6 mouse model has been proven useful over the years to unravel the molecular mechanisms that govern anemia pathology. Gene expression profiling studies in these mice have pinpointed infection-induced deregulation of erythropoiesis as well as the involvement of stress-induced acute phase responses linked to *T. congolense*-associated anemia (191). More recently, the C57Bl/6 model was also shown to be suitable for unraveling the pathology of *T.*

vivax infections (129, 192, 193). In addition, the use of various knockout mouse strains generated on the C56Bl/6 background, such as TNF$^{-/-}$ and Lymphytoxin$^{-/-}$ (194), TNFp75$^{-/-}$ (166), IFNγR$^{-/-}$ (152), IL-10$^{-/-}$ (195), and Gal3$^{-/-}$ (196) have all been used to study specific aspects of the inflammatory cascade that drive trypanosomosis-associated inflammation. One of the most recent finding here has shown that the reduced PCV, associated with experimental mouse trypanosomosis, is not just the result of reduced circulating RBC numbers, but also of increased plasma volume, leading to hemodilution. The reduction of platelet concentrations in *T. congolense*-infected mice has also been reported in *T. congolense*-infected cattle and sheep (197, 198) suggesting that hemodilution could be a major pathogenic characteristic of livestock trypanosomosis, as well.

To date, the characteristics of anemia are probably the most and best described features of AT. Whenever new surveillance efforts result in the discovery of new infection foci, anemia is usually the parameter that is used to describe disease severity. This is the case for *T. evansi*, *T. congolense,* and *T. vivax* independently of the geographic location of infection or host species. As described for *T. congolense*, *T. evansi*-induced anemia was linked to infection-associated deregulation of the iron metabolism as well (199), although the number of detailed mechanistic studies available for this infection are rare. Interestingly, trypanosomosis-associated anemia has even been observed in more rare infection cases of wildlife in the Australian little red flying fox infected with *T. minasense* and *T. rangeli* (200). Together, all these reports indicate that the general occurrence of trypanosomosis-associated anemia is most likely due to the multitude of inflammatory pathways, and linked to various aspects of impaired RBC development and clearance. Taken this into account, it is very intriguing that reports of severe infection-associated anemia are missing in the case of HAT. Indeed, most reports documenting HAT-associated anemia describe the induction of RBC lysis and acute anemia as the result of treatment rather than the infection itself. This is particularly the case for *T. b. gambiense* infections (201–204). For *T. b. rhodesiense* rare reports do exist on the occurrence of infection-associated anemia and hemolysis (205), and models have been developed using vervet monkeys to investigate this aspect of acute HAT pathology in details (206). However, at the same time other reports have shown the lack of any correlation between *T. b. rhodesiense* severity in humans and the presence or absence of anemia (207–209). Hence, it seems that the human immune system might have found unique ways of dealing with trypanosomosis both in terms of dealing with parasite killing through the TLF1/2 ApoL1 mechanisms, as well as the control of infection-associated anemia.

CONCLUSION

Over the past years, international joint efforts to control Human African Trypanosomosis have resulted in a drastic reduction in the number of confirmed disease cases. In addition, it might be feasible that by 2020 the incidence of this neglected tropic disease will be reduced to levels where it is no longer considered as a public health threat. However, at the same time the incidence of animal trypanosomosis is on the rise, affecting animal productivity through the detrimental health effects caused by excessive host-parasite immune interactions. This has now become a world-wide issue that affects agricultural infrastructures in emerging economy countries, not just in Africa but also in Asia and South America. In addition, AT even threatens the livestock industry of developed countries when sudden outbreaks occur due to importation of the disease either through infected vectors or host animals. To date, not a single vaccine strategy is available to control AT. Detrimental infection-associated mechanisms undermine both T cell and B cell compartments, making it virtually impossible to develop methods that allow the generation of long-term sustainable immunological memory. It appears that in the evolutionary battle between the trypanosome and the host immune system, the parasite has not only been able to find ways to evade innate trypanosome killing mechanisms, but has also acquired tools to undermine the crucial immunological defense and memory systems of the host. Only recently, it has become obvious that one of the major strengths of the African Trypanosomes' defense system is the capacity of genetic exchanges between individual parasites, while residing in the insect vector. Through this mechanism, new human-infective parasites can be generated and this by combining resistant genes from existing *T. b. rhodesiense* parasites with the vast repertoire of the *T. b. brucei* animal parasite reservoir. In addition, it has become clear that mechanisms of genetic plasticity also have allowed *T. b. brucei* to transform into *T. equiperdum* and *T. evansi*, parasites that have now successfully conquered large areas of the developing world, as they no longer need the tsetse vector for transmission. In particular, the latter risks to become a future health problem, as human infective cases of *T. evansi* have already been reported in India, Vietnam, Egypt, and Algeria. Together, these results show that while classic *T. gambiense* trypanosomosis is becoming rare, AT and new atypical human trypanosomosis remain a serious risk for the human population. Future research into the host-parasite interactions and trypanosomosis- associated inflammation of these new atypical infections should allow to obtain a better understanding of problems, including vaccine failure, and hopefully lead us to a long-term solution that can deal with both human and livestock infections, as well as the ever surviving wildlife trypanosome reservoir.

AUTHOR CONTRIBUTIONS

All authors contributed to the writing of the paper. In addition all artwork was prepared by JP.

FUNDING

We acknowledge the financial support grants from the FWO (FWO G015016N and G.0.028.10.N.10) and the Bill and Melinda Gates Foundation, grant 641K760.

REFERENCES

1. Desquesnes M, Holzmuller P, Lai D, Dargantes A, Lun Z, Jittaplapong S. *Trypanosoma evansi* and surra: a review and perspectives on origin, history, distribution, taxonomy, morphology, hosts, and pathogenic effects. *Biomed Res Int.* (2013) 2013:194176. doi: 10.1155/2013/194176
2. Büscher P, Cecchi G, Jamonneau V, Priotto G. Human African trypanosomiasis. *Lancet* (2017) 390:2397–409. doi: 10.1016/S0140-6736(17)31510-6
3. Diall O, Cecchi G, Wanda G, Argilés-Herrero R, Vreysen MJB, Cattoli G, et al. Developing a progressive control pathway for African animal trypanosomosis. *Trends Parasitol.* (2017) 33:499–509. doi: 10.1016/j.pt.2017.02.005
4. Molinari J, Moreno SA. *Trypanosoma brucei* Plimmer & Bradford, 1899 is a synonym of T. evansi (Steel, 1885) according to current knowledge and by application of nomenclature rules. *Syst Parasitol.* (2018) 95:249–56. doi: 10.1007/s11230-018-9779-z
5. Gibson W. Liaisons dangereuses: sexual recombination among pathogenic trypanosomes. *Res Microbiol.* (2015) 166:459–66. doi: 10.1016/j.resmic.2015.05.005
6. Peacock L, Ferris V, Sharma R, Sunter J, Bailey M, Carrington M, et al. Identification of the meiotic life cycle stage of *Trypanosoma brucei* in the tsetse fly. *Proc Natl Acad Sci USA*. (2011) 108:3671–6. doi: 10.1073/pnas.1019423108
7. Lugli EB, Pouliot M, Portela MDPM, Loomis MR, Raper J. Characterization of primate trypanosome lytic factors. *Mol Biochem Parasitol.* (2004) 138:9–20. doi: 10.1016/j.molbiopara.2004.07.004
8. Capewell P, Cooper A, Clucas C, Weir W, MacLeod A. A co-evolutionary arms race: trypanosomes shaping the human genome, humans shaping the trypanosome genome. *Parasitology* (2015) 142:S108–19. doi: 10.1017/S0031182014000602
9. Guilliams M, Bosschaerts T, Hérin M, Hünig T, Loi P, Flamand V, et al. Experimental expansion of the regulatory T cell population increases resistance to African trypanosomiasis. *J Infect Dis.* (2008) 198:781–91. doi: 10.1086/590439
10. Bakhiet M, Mix E, Kristensson K, Wigzell H, Olsson T. T cell activation by a*Trypanosoma brucei* brucei-deriyed lymphocyte triggering factor is dependent on tyrosine protein kinases but not on protein kinase C and A. *Eur J Immunol.* (1993) 23:1535–1539. doi: 10.1002/eji.1830230721
11. Truc P, Büscher P, Cuny G, Gonzatti MI, Jannin J, Joshi P, et al. A typical human infections by animal trypanosomes. *PLoS Negl Trop Dis.* (2013) 7:e2256. doi: 10.1371/journal.pntd.0002256
12. Overath P, Haag J, Mameza MG, Lischke A. Freshwater fish trypanosomes: definition of two types, host control by antibodies and lack of antigenic variation. *Parasitology* (1999) 119(Pt 6):591–601. doi: 10.1017/S0031182099005089
13. Zídková L, Cepicka I, Szabová J, Svobodová M. Biodiversity of avian trypanosomes. *Infect Genet Evol.* (2012) 12:102–12. doi: 10.1016/j.meegid.2011.10.022
14. Haag J, O'hUigin C, Overath P. The molecular phylogeny of trypanosomes: evidence for an early divergence of the Salivaria. *Mol Biochem Parasitol.* (1998) 91:37–49. doi: 10.1016/S0166-6851(97)00185-0
15. Pandey A, Galvani A. Strategies for *Trypanosoma brucei* gambiense elimination. *Lancet Glob Health* (2017) 5:e10–1. doi: 10.1016/S2214-109X(16)30284-4
16. Holmes P. On the road to elimination of rhodesiense human African trypanosomiasis: first WHO meeting of stakeholders. *PLoS Negl Trop Dis.* (2015) 9:10–12. doi: 10.1371/journal.pntd.0003571
17. Informal Expert Group on Gambiense HAT Reservoirs, Büscher P, Bart J-M, Boelaert M, Bucheton B, Cecchi G, et al. Do cryptic reservoirs threaten gambiense-sleeping sickness elimination? *Trends Parasitol.* (2018) 34:197–207. doi: 10.1016/j.pt.2017.11.008
18. Desquesnes M, Dargantes A, Lai D-H, Lun Z-R, Holzmuller P, Jittapalapong S. *Trypanosoma evansi* and Surra: a review and perspectives on transmission, epidemiology and control, impact, and zoonotic aspects. *Biomed Res Int.* (2013) 1–20. doi: 10.1155/2013/321237
19. Morrison LJ, Vezza L, Rowan T, Hope JC. Animal African trypanosomiasis: time to increase focus on clinically relevant parasite and host species. *Trends Parasitol.* (2016) 32:599–607. doi: 10.1016/j.pt.2016.04.012
20. Auty H, Torr SJ, Michoel T, Jayaraman S, Morrison LJ. Cattle trypanosomosis: the diversity of trypanosomes and implications for disease epidemiology and control. *Rev Sci Tech.* (2015) 34:587–98.
21. Giordani F, Morrison LJ, Rowan TG, DE Koning HP, Barrett MP. The animal trypanosomiases and their chemotherapy: a review. *Parasitology* (2016) 143:1862–89. doi: 10.1017/S0031182016001268
22. P. Finelle. African animal trypanosomiasis transmission of trypanosomes. *World Anim Rev.* (1973) 7:1–6.
23. Lun ZR, Lai DH, Li FJ, Lukeš J, Ayala FJ. *Trypanosoma brucei*: two steps to spread out from Africa. *Trends Parasitol.* (2010) 26:424–7. doi: 10.1016/j.pt.2010.05.007
24. Baldacchino F, Desquesnes M, Mihok S, Foil LD, Duvallet G, Jittapalapong S. Tabanids: neglected subjects of research, but important vectors of disease agents! *Infect Genet Evol.* (2014) 28:596–615. doi: 10.1016/j.meegid.2014.03.029
25. Banerjee D, Kumar V, Maity A, Ghosh B, Tyagi K, Singha D, et al. Identification through DNA barcoding of Tabanidae (Diptera) vectors of surra disease in India. *Acta Trop.* (2015) 150:52–8. doi: 10.1016/j.actatropica.2015.06.023
26. Taioe MO, Motloang MY, Namangala B, Chota A, Molefe NI, Musinguzi SP, et al. Characterization of tabanid flies (Diptera: Tabanidae) in South Africa and Zambia and detection of protozoan parasites they are harboring. *Parasitology* (2017) 144:1162–78. doi: 10.1017/S0031182017000440
27. Misra KK, Roy S, Choudhury A. Biology of *Trypanosoma* (Trypanozoon) evansi in experimental heterologous mammalian hosts. *J Parasit Dis.* (2016) 40:1047–61. doi: 10.1007/s12639-014-0633-1
28. Borst P, Fase-Fowler F, Gibson WC. Kinetoplast DNA of *Trypanosoma evansi*. *Mol Biochem Parasitol.* (1987) 23:31–8.
29. Paris Z, Hashimi H, Lun S, Alfonzo JD, Lukeš J. Futile import of tRNAs and proteins into the mitochondrion of *Trypanosoma brucei evansi*. *Mol Biochem Parasitol.* (2011) 176:116–20. doi: 10.1016/j.molbiopara.2010.12.010
30. Carnes J, Anupama A, Balmer O, Jackson A, Lewis M, Brown R, et al. Genome and phylogenetic analyzes of *Trypanosoma evansi* reveal extensive similarity to *T. brucei* and multiple independent origins for dyskinetoplasty. *PLoS Negl Trop Dis.* (2015) 9:e3404. doi: 10.1371/journal.pntd.0003404
31. Cuypers B, Van den Broeck F, Van Reet N, Meehan CJ, Cauchard J, Wilkes JM, et al. Genome-Wide SNP analysis reveals distinct origins of *Trypanosoma evansi* and *Trypanosoma equiperdum*. *Genome Biol Evol.* (2017) 9:1990–7. doi: 10.1093/gbe/evx102
32. Richardson JB, Lee K-Y, Mireji P, Enyaru J, Sistrom M, Aksoy S, et al. Genomic analyses of African Trypanozoon strains to assess evolutionary relationships and identify markers for strain identification. *PLoS Negl Trop Dis.* (2017) 11:e0005949. doi: 10.1371/journal.pntd.0005949
33. Gibson W. Molecular characterization of field isolates of human pathogenic trypanosomes. *Trop Med Int Health* (2001) 6:401–6. doi: 10.1046/j.1365-3156.2001.00711.x
34. Radwanska M, Chamekh M, Vanhamme L, Claes F, Magez S, Magnus E, et al. The serum resistance-associated gene as a diagnostic tool for the detection of *Trypanosoma brucei rhodesiense*. *Am J Trop Med Hyg.* (2002) 67:684–90. doi: 10.4269/ajtmh.2002.67.684
35. Welburn SC, Picozzi K, Fèvre EM, Coleman PG, Odiit M, Carrington M, et al. Identification of human-infective trypanosomes in animal reservoir of sleeping sickness in Uganda by means of serum-resistance-associated (SRA) gene. *Lancet* (2001) 358:2017–9. doi: 10.1016/S0140-6736(01)07096-9
36. Radwanska M, Claes F, Magez S, Magnus E, Perez-Morga D, Pays E, et al. Novel primer sequences for polymerase chain reaction-based detection of *Trypanosoma brucei gambiense*. *Am J Trop Med Hyg.* (2002) 67:289–95. doi: 10.4269/ajtmh.2002.67.289
37. Claes F, Büscher P, Touratier L, Goddeeris BM. *Trypanosoma equiperdum*: master of disguise or historical mistake? *Trends Parasitol.* (2005) 21:316–21. doi: 10.1016/j.pt.2005.05.010
38. Jones TW, Dávila AMR. *Trypanosoma vivax*–out of Africa. *Trends Parasitol.* (2001) 17:99–101. doi: 10.1016/S1471-4922(00)01777-3

39. Moloo SK, Sabwa CL, Kabata JM. Vector competence of Glossina pallidipes and G. morsitans centralis for *Trypanosoma vivax*, *T. congolense* and *T. b. brucei*. *Acta Trop.* (1992) 51:271–80. doi: 10.1016/0001-706X(92)90045-Y
40. Croft SL, Kuzoe FA, Ryan L, Molyneux DH. Trypanosome infection rates of *Glossina* spp. (Diptera: Glossinidae) in transitional forest-savanna near Bouaflé, Ivory Coast. *Tropenmed Parasitol.* (1984) 35:247–50.
41. Gibson W. The origins of the trypanosome genome strains *Trypanosoma brucei brucei* TREU 927, *T. b. gambiense* DAL 972, *T. vivax* Y486 and *T. congolense* IL3000. *Parasit Vectors* (2012) 5:71. doi: 10.1186/1756-3305-5-71
42. Truc P, Jamonneau V, N'Guessan P, N'Dri L, Diallo PB, Cuny G. *Trypanosoma brucei* ssp. and *T congolense*: mixed human infection in Côte d'Ivoire. *Trans R Soc Trop Med Hyg.* (1996) 92:537–8.
43. Van Xong H, De Baetselier P, Pays E, Magez S. Selective pressure can influence the resistance of *Trypanosoma congolense* to normal human serum. *Exp Parasitol.* (2002) 102:61–5. doi: 10.1016/S0014-4894(03)00032-8
44. Wiesenhütter E. Research into the relative importance of tabanidae (Diptera) in mechanical disease transmission I. the seasonal occurrence and relative abundance of tabanidae in a dar es salaam dairy farm. *J Nat Hist.* (1975) 9:377–84. doi: 10.1080/00222937500770271
45. Gerold P, Striepen B, Reitter B, Geyer H, Geyer R, Reinwald E, et al. Glycosyl-phosphatidylinositols of *Trypanosoma congolense*: two common precursors but a new protein-anchor. *J Mol Biol.* (1996) 261:181–94. doi: 10.1006/jmbi.1996.0451
46. Okwor I, Onyilagha C, Kuriakose S, Mou Z, Jia P, Uzonna JE. Regulatory T cells enhance susceptibility to experimental *Trypanosoma Congolense* infection independent of mouse genetic background. *PLoS Negl Trop Dis.* (2012) 6:e1761. doi: 10.1371/journal.pntd.0001761
47. Inverso JA, De Gee AL, Mansfield JM. Genetics of resistance to the African trypanosomes. VII. Trypanosome virulence is not linked to variable surface glycoprotein expression. *J Immunol.* (1988) 140:289–93.
48. Magez S, Stijlemans B, Radwanska M, Pays E, Ferguson MA, De Baetselier P. The glycosyl-inositol-phosphate and dimyristoylglycerol moieties of the glycosylphosphatidylinositol anchor of the trypanosome variant-specific surface glycoprotein are distinct macrophage-activating factors. *J Immunol.* (1998) 160:1949–56. doi: 10.4049/jimmunol.164.4.2070
49. Sileghem M, Flynn JN. Suppression of interleukin 2 secretion and interleukin 2 receptor expression during tsetse-transmitted trypanosomiasis in cattle. *Eur J Immunol.* (1992) 22:767–73. doi: 10.1002/eji.1830220321
50. Obishakin E, de Trez C, Magez S. Chronic *Trypanosoma congolense* infections in mice cause a sustained disruption of the B-cell homeostasis in the bone marrow and spleen. *Parasite Immunol.* (2014) 36:187–98. doi: 10.1111/pim.12099
51. Garside LH, Gibson WC. Molecular characterization of trypanosome species and subgroups within subgenus Nannomonas. *Parasitology* (1995) 111(Pt 3):301–12. doi: 10.1017/S0031182000081853
52. Vickerman K. Developmental cycles and biology of pathogenic trypanosomes. *Br Med Bull.* (1985) 41:105–14. doi: 10.1093/oxfordjournals.bmb.a072036
53. Peacock L, Bailey M, Gibson W. Dynamics of gamete production and mating in the parasitic protist *Trypanosoma brucei*. *Parasit Vectors* (2016) 9:404. doi: 10.1186/s13071-016-1689-9
54. Maclean L, Chisi JE, Odiit M, Gibson WC, Ferris V, Picozzi K, et al. Severity of human African trypanosomiasis in East Africa is associated with geographic location, parasite genotype, and host in ammatory cytokine response pro le. *Infect Immun.* (2004) 72:7040–4. doi: 10.1128/IAI.72.12.7040
55. Murphy WJ, Brentano ST, Rice-Ficht AC, Dorfman DM, Donelson JE. DNA rearrangements of the variable surface antigen genes of the trypanosomes1. *J Protozool* (1984) 31:65–73. doi: 10.1111/j.1550-7408.1984.tb04291.x
56. Hall JPJ, Wang H, David Barry J. Mosaic VSGs and the scale of *Trypanosoma brucei* antigenic variation. *PLoS Pathog.* (2013) 9:e1003502. doi: 10.1371/journal.ppat.1003502
57. Levine RF, Mansfield JM. Genetics of resistance to the African trypanosomes. III. Variant-specific antibody responses of H-2-compatible resistant and susceptible mice. *J Immunol.* (1984) 133:1564–9.
58. Mugnier MR, Stebbins CE, Papavasiliou FN. Masters of disguise: antigenic variation and the VSG coat in *Trypanosoma brucei*. *PLoS Pathog.* (2016) 12:e1005784. doi: 10.1371/journal.ppat.1005784
59. Pays E. Regulation of antigen gene expression in *Trypanosoma brucei*. *Trends Parasitol.* (2005) 21:517–20. doi: 10.1016/j.pt.2005.08.016
60. Horn D. Antigenic variation in African trypanosomes. *Mol Biochem Parasito* (2014) 195:123–9. doi: 10.1016/j.molbiopara.2014.05.001
61. Weiss BL, Wang J, Aksoy S. Tsetse immune system maturation requires the presence of obligate symbionts in larvae. *PLoS Biol.* (2011) 9:e1000619. doi: 10.1371/journal.pbio.1000619
62. Weiss BL, Maltz M, Aksoy S. Obligate symbionts activate immune system development in the tsetse fly. *J Immunol.* (2012) 188:3395–403. doi: 10.4049/jimmunol.1103691
63. Weiss BL, Wang J, Maltz MA, Wu Y, Aksoy S. Trypanosome infection establishment in the tsetse fly gut is influenced by microbiome-regulated host immune barriers. *PLoS Pathog.* (2013) 9:e1003318. doi: 10.1371/journal.ppat.1003318
64. Wang J, Wu Y, Yang G, Aksoy S. Interactions between mutualist Wigglesworthia and tsetse peptidoglycan recognition protein (PGRP-LB) influence trypanosome transmission. *Proc Natl Acad Sci USA.* (2009) 106:12133–8. doi: 10.1073/pnas.0901226106
65. Weiss BL, Savage AF, Griffith BC, Wu Y, Aksoy S. The peritrophic matrix mediates differential infection outcomes in the tsetse fly gut following challenge with commensal, pathogenic, and parasitic microbes. *J Immunol.* (2014) 193:773–82. doi: 10.4049/jimmunol.1400163
66. Hao Z, Kasumba I, Lehane MJ, Gibson WC, Kwon J, Aksoy S. Tsetse immune responses and trypanosome transmission: implications for the development of tsetse-based strategies to reduce trypanosomiasis. *Proc Natl Acad Sci USA.* (2001) 98:12648–53. doi: 10.1073/pnas.221363798
67. Hu C, Aksoy S. Innate immune responses regulate trypanosome parasite infection of the tsetse fly glossina morsitans morsitans. *Mol Microbiol.* (2006) 60:1194–204. doi: 10.1111/j.1365-2958.2006.05180.x
68. Hao Z, Kasumba I, Aksoy S. Proventriculus (cardia) plays a crucial role in immunity in tsetse fly (Diptera: Glossinidiae). *Insect Biochem Mol Biol.* (2003) 33:1155–64. doi: 10.1016/j.ibmb.2003.07.001
69. Haines LR, Lehane SM, Pearson TW, Lehane MJ. Tsetse EP protein protects the fly midgut from trypanosome establishment. *PLoS Pathog.* (2010) 6:e1000793. doi: 10.1371/journal.ppat.1000793
70. Akoda K, Van Den Abbeele J, Marcotty T, De Deken R, Sidibe I, Van den Bossche P. Nutritional stress of adult female tsetse flies (Diptera: Glossinidae) affects the susceptibility of their offspring to trypanosomal infections. *Acta Trop.* (2009) 111:263–7. doi: 10.1016/j.actatropica.2009.05.005
71. Akoda K, Van den Bossche P, Marcotty T, Kubi C, Coosemans M, De Deken R, et al. Nutritional stress affects the tsetse fly's immune gene expression. *Med Vet Entomol.* (2009) 23:195–201. doi: 10.1111/j.1365-2915.2009.00799.x
72. Akoda K, Van den Bossche P, Lyaruu E A, De Deken R, Marcotty T, Coosemans M, et al. Maturation of a *Trypanosoma Brucei* infection to the infectious metacyclic stage is enhanced in nutritionally stressed tsetse flies : table 1. *J Med Entomol.* (2009) 46:1446–9. doi: 10.1603/033.046.0629
73. Peacock L, Cook S, Ferris V, Bailey M, Gibson W. The life cycle of Trypanosoma (Nannomonas) congolense in the tsetse fly. *Parasit Vectors* (2012) 5:109. doi: 10.1186/1756-3305-5-109
74. Gibson W, Peacock L, Hutchinson R. Microarchitecture of the tsetse fly proboscis. *Parasit Vectors* (2017) 10:430. doi: 10.1186/s13071-017-2367-2
75. Morrison LJ, Tweedie A, Black A, Pinchbeck GL, Christley RM, Schoenefeld A, et al. Discovery of mating in the major African livestock pathogen trypanosoma congolense. *PLoS ONE* (2009) 4:e5564. doi: 10.1371/journal.pone.0005564
76. Caljon G, Van Den Abbeele J, Stijlemans B, Coosemans M, De Baetselier P, Magez S. Tsetse fly saliva accelerates the onset of *Trypanosoma brucei* infection in a mouse model associated with a reduced host inflammatory response. *Infect Immun.* (2006) 74:6324–30. doi: 10.1128/IAI.01046-06
77. Caljon G, De Ridder K, De Baetselier P, Coosemans M, Van Den Abbeele J. Identification of a tsetse fly salivary protein with dual inhibitory action on human platelet aggregation. *PLoS ONE* (2010) 5:e9671. doi: 10.1371/journal.pone.0009671
78. Sutherland CS, Stone CM, Steinmann P, Tanner M, Tediosi F. Seeing beyond 2020: an economic evaluation of contemporary and emerging strategies for elimination of *Trypanosoma brucei gambiense*. *Lancet Glob Health* (2017) 5:e69–79. doi: 10.1016/S2214-109X(16)30237-6

79. Simarro PP, Diarra A, Postigo JAR, Franco JR, Jannin JG. The human african trypanosomiasis control and surveillance program of the World Health Organization 2000-2009: the way forward. *PLoS Negl Trop Dis.* (2011) 5:e1007. doi: 10.1371/journal.pntd.0001007
80. Joshi PP, Shegokar VR, Powar RM, Herder S, Katti R, Salkar HR, et al. Human trypanosomiasis caused by *Trypanosoma evansi* in India: the first case report. *Am J Trop Med Hyg.* (2005) 73:491–5. doi: 10.4269/ajtmh.2005.73.491
81. Vanhollebeke B, Truc P, Poelvoorde P, Pays A, Joshi PP, Katti R, et al. Human *Trypanosoma evansi* infection linked to a lack of apolipoprotein L-I. *N Engl J Med.* (2006) 355:2752–6. doi: 10.1056/NEJMoa063265
82. Truc P, Gibson W, Herder S. Genetic characterization of *Trypanosoma evansi* isolated from a patient in India. *Infect Genet Evol.* (2007) 7:305–7. doi: 10.1016/j.meegid.2006.07.004
83. Haridy FM, El-Metwally MT, Khalil HHM, Morsy TA. *Trypanosoma evansi* in dromedary camel: with a case report of zoonosis in greater Cairo, Egypt. *J Egypt Soc Parasitol.* (2011) 41:65–76.
84. Duffy CW, Morrison LJ, Black A, Pinchbeck GL, Christley RM, Schoenefeld A, et al. *Trypanosoma vivax* displays a clonal population structure. *Int J Parasitol.* (2009) 39:1475–83. doi: 10.1016/j.ijpara.2009.05.012
85. Jackson AP, Berry A, Aslett M, Allison HC, Burton P, Vavrova-Anderson J, et al. Antigenic diversity is generated by distinct evolutionary mechanisms in African trypanosome species. *Proc Natl Acad Sci USA.* (2012) 109:3416–21. doi: 10.1073/pnas.1117313109
86. Biteau N, Asencio C, Izotte J, Rousseau B, Fèvre M, Pillay D, et al. *Trypanosoma brucei* gambiense infections in mice lead to tropism to the reproductive organs, and horizontal and vertical transmission. *PLoS Negl Trop Dis.* (2016) 10:1–15. doi: 10.1371/journal.pntd.0004350
87. Rocha G, Martins A, Gama G, Brandão F, Atouguia J. Possible cases of sexual and congenital transmission of sleeping sickness [5]. *Lancet* (2004) 363:247. doi: 10.1016/S0140-6736(03)15345-7
88. Seed JR, Sechelski JB, Ortiz JC, Chapman JF. Relationship between human serum trypanocidal activity and host resistance to the African trypanosomes. *J Parasitol.* (1993) 79:226–32. doi: 10.1016/j.molbiopara.2015.03.007
89. Raper J, Fung R, Ghiso J, Nussenzweig V, Tomlinson S. Characterization of a novel trypanosome lytic factor from human serum. *Infect Immun.* (1999) 67:1910–6.
90. Raper J, Portela MP, Lugli E, Frevert U, Tomlinson S. Trypanosome lytic factors: novel mediators of human innate immunity. *Curr Opin Microbiol.* (2001) 4:402–8. doi: 10.1016/S1369-5274(00)00226-5
91. De Greef C, Hamers R. The serum resistance-associated (SRA) gene of *Trypanosoma brucei* rhodesiense encodes a variant surface glycoprotein-like protein. *Mol Biochem Parasitol.* (1994) 68:277–84. doi: 10.1016/0166-6851(94)90172-4
92. Xong H V, Vanhamme L, Chamekh M, Chimfwembe CE, Van Den Abbeele J, Pays A, et al. A VSG expression site-associated gene confers resistance to human serum in *Trypanosoma rhodesiense*. *Cell* (1998) 95:839–46.
93. Vanhamme L, Paturiaux-Hanocq F, Poelvoorde P, Nolan DP, Lins L, Abbeele J Van Den, et al. Apolipoprotein L-1 is the trypanosome lytic factor of human serum. *Nature* (2003) 422:83–7. doi: 10.1038/nature01457.1.
94. Vanwalleghem G, Fontaine F, Lecordier L, Tebabi P, Klewe K, Nolan DP, et al. Coupling of lysosomal and mitochondrial membrane permeabilization in trypanolysis by APOL1. *Nat Commun* .(2015) 6:8078. doi: 10.1038/ncomms9078
95. Pérez-Morga D, Vanhollebeke B, Paturiaux-Hanocq F, Nolan DP, Lins L, Homblé F, et al. Apolipoprotein L-I promotes trypanosome lysis by forming pores in lysosomal membranes. *Science* (2005) 309:469–72. doi: 10.1126/science.1114566
96. Vanhollebeke B, Lecordier L, Perez-Morga D, Amiguet-Vercher A, Pays E. Human serum lyses *Trypanosoma brucei* by triggering uncontrolled swelling of the parasite lysosome. *J Eukaryot Microbiol.* (2007) 54:448–51. doi: 10.1111/j.1550-7408.2007.00285.x
97. Oli MW, Cotlin LF, Shiflett AM, Hajduk SL. Serum resistance-associated protein blocks lysosomal targeting of trypanosome lytic factor in *Trypanosoma brucei*. *Eukaryot Cell* (2006) 5:132–9. doi: 10.1128/EC.5.1.132-139.2006
98. Greene AS, Hajduk SL. Trypanosome lytic factor-1 initiates oxidation-stimulated osmotic lysis of *Trypanosoma brucei brucei*. *J Biol Chem.* (2016) 291:3063–75. doi: 10.1074/jbc.M115.680371
99. DeJesus E, Kieft R, Albright B, Stephens NA, Hajduk SL. A single amino acid substitution in the group 1 *Trypanosoma brucei* gambiense haptoglobin-hemoglobin receptor abolishes TLF-1 binding. *PLoS Pathog.* (2013) 9:1–10. doi: 10.1371/journal.ppat.1003317
100. Bullard W, Kieft R, Capewell P, Veitch NJ, Macleod A, Hajduk SL. Haptoglobin-hemoglobin receptor independent killing of African trypanosomes by human serum and trypanosome lytic factors. *Virulence* (2012) 3:72–6. doi: 10.4161/viru.3.1.18295
101. Vanhollebeke B, De Muylder G, Nielsen MJ, Pays A, Tebabi P, Dieu M, et al. A haptoglobin-hemoglobin receptor conveys innate immunity to *Trypanosoma brucei* in humans. *Science* (2008) 320:677–81. doi: 10.1126/science.1156296
102. Enyaru JCK, Matovu E, Nerima B, Akol M, Sebikali C. Detection of *T.b. rhodesiense* trypanosomes in humans and domestic animals in South East Uganda by amplification of serum resistance-associated gene. *Ann N Y Acad Sci.* (2006) 1081:311–9. doi: 10.1196/annals.1373.041
103. Gibson W, Peacock L, Ferris V, Fischer K, Livingstone J, Thomas J, et al. Genetic recombination between human and animal parasites creates novel strains of human pathogen. *PLoS Negl Trop Dis.* (2015) 9:1–16. doi: 10.1371/journal.pntd.0003665
104. Echodu R, Sistrom M, Bateta R, Murilla G, Okedi L, Aksoy S, et al. Genetic diversity and population structure of <italic>*Trypanosoma brucei*</italic> in uganda: implications for the epidemiology of sleeping sickness and nagana. *PLoS Negl Trop Dis.* (2015) 9:e0003353. doi: 10.5061/dryad.m7q4c
105. Capewell P, Veitch NJ, Turner CMR, Raper J, Berriman M, Hajduk SL, et al. Differences between *Trypanosoma brucei* gambiense groups 1 and 2 in their resistance to killing by trypanolytic factor 1. *PLoS Negl Trop Dis.* (2011) 5:e1287. doi: 10.1371/journal.pntd.0001287
106. Higgins MK, Tkachenko O, Brown A, Reed J, Raper J, Carrington M. Structure of the trypanosome haptoglobin-hemoglobin receptor and implications for nutrient uptake and innate immunity. *Proc Natl Acad Sci USA.* (2013) 110:1905–10. doi: 10.1073/pnas.1214943110
107. Kieft R, Capewell P, Turner CMR, Veitch NJ, MacLeod A, Hajduk S. Mechanism of *Trypanosoma brucei* gambiense (group 1) resistance to human trypanosome lytic factor. *Proc Natl Acad Sci USA.* (2010) 107:16137–41. doi: 10.1073/pnas.1007074107
108. Berberof M, Pérez-Morga D, Pays E. A receptor-like flagellar pocket glycoprotein specific to *Trypanosoma brucei gambiense*. *Mol Biochem Parasitol.* (2001) 113:127–38. doi: 10.1016/S0166-6851(01)00208-0
109. Capewell P, Clucas C, DeJesus E, Kieft R, Hajduk S, Veitch N, et al. The TgsGP gene is essential for resistance to human serum in *Trypanosoma brucei gambiense*. *PLoS Pathog.* (2013) 9:2–7. doi: 10.1371/journal.ppat.1003686
110. Uzureau P, Uzureau S, Lecordier L, Fontaine F, Tebabi P, Homblé F, et al. Mechanism of *Trypanosoma brucei* gambiense resistance to human serum. *Nature* (2013) 501:430–4. doi: 10.1038/nature12516
111. Radwanska M, Bockstal V, Brombacher F, Magez S. Parasite-induced B-cell apoptosis results in loss of specific protective anti-trypanosome antibody responses, and abolishment of vaccine induced protective memory. In: *XII INTERNATIONAL CONGRESS OF PARASITOLOGY (ICOPA)* (Melbourne, VIC). (2010). p. 31–38.
112. Lai D-H, Wang Q-P, Li Z, Luckins AG, Reid SA, Lun Z-R. Investigations into human serum sensitivity expressed by stocks of *Trypanosoma brucei evansi*. *Int J Parasitol.* (2010) 40:705–10. doi: 10.1016/j.ijpara.2009.11.009
113. Faulkner SD, Oli MW, Kieft R, Cotlin L, Widener J, Shiflett A, et al. *In vitro* generation of human high-density-lipoprotein-resistant *Trypanosoma brucei brucei*. *Eukaryot Cell* (2006) 5:1276–86. doi: 10.1128/EC.00116-06
114. Vanhamme L, Renauld H, Lecordier L, Poelvoorde P, Van Den Abbeele J, Pays E. The *Trypanosoma brucei* reference strain TREU927/4 contains T. brucei rhodesiense-specific SRA sequences, but displays a distinct phenotype of relative resistance to human serum. *Mol Biochem Parasitol.* (2004) 135:39–47. doi: 10.1016/j.molbiopara.2004.01.004
115. Lai D, Wang Q, Li Z, Julius L, Lun Z. Evolution of the serum resistance-associated SRA gene in African trypanosomes. *Sci Bull.* (2009) 54:1275–8. doi: 10.1007/s11434-009-0137-z

116. Van Vinh Chau N, Buu Chau L, Desquesnes M, Herder S, Phu Huong Lan N, Campbell JI, et al. A clinical and epidemiological investigation of the first reported human infection with the zoonotic parasite *Trypanosoma evansi* in Southeast Asia. *Clin Infect Dis.* (2016) 62:1002–8. doi: 10.1093/cid/ciw052
117. Wabale V, Nalage P, Joshi A, Bharadwaj R, Deshpande K, Chowdhary A. Human Asian Trypanosomiasis due to *Trypanosoma evansi:* a rare case. *J Adv Parasitol.* (2015) 3:65–8. doi: 10.14737/journal.jap/2015/2.3.65.68
118. Baral TN, De Baetselier P, Brombacher F, Magez S. Control of *Trypanosoma evansi* infection is IgM mediated and does not require a type I inflammatory response. *J Infect Dis.* (2007) 195:1513–20. doi: 10.1086/515577
119. Desquesnes M, Yangtara S, Kunphukhieo P, Chalermwong P, Jittapalapong S, Herder S. Zoonotic trypanosomes in South East Asia: attempts to control *Trypanosoma lewisi* using veterinary drugs. *Exp Parasitol.* (2016) 165:35–42. doi: 10.1016/j.exppara.2016.03.009
120. Thomson R, Genovese G, Canon C, Kovacsics D, Higgins MK, Carrington M, et al. Evolution of the primate trypanolytic factor APOL1. *Proc Natl Acad Sci USA.* (2014) 111:E2130–9. doi: 10.1073/pnas.1400699111
121. Smith EE, Malik HS. The apolipoprotein L family of programmed cell death and immunity genes rapidly evolved in primates at discrete sites of host-pathogen interactions. *Genome Res.* (2009) 19:850–8. doi: 10.1101/gr.085647.108
122. Thomson R, Molina-Portela P, Mott H, Carrington M, Raper J. Hydrodynamic gene delivery of baboon trypanosome lytic factor eliminates both animal and human-infective African trypanosomes. *Proc Natl Acad Sci USA.* (2009) 106:19509–14. doi: 10.1073/pnas.0905669106
123. Cooper A, Capewell P, Clucas C, Veitch N, Weir W, Thomson R, et al. A primate APOL1 variant that kills *Trypanosoma brucei gambiense*. *PLoS Negl Trop Dis.* (2016) 10:e0004903. doi: 10.1371/journal.pntd.0004903
124. Borst P. Antigenic variation and allelic exclusion. *Cell* (2002) 109:5–8. doi: 10.1016/S0092-8674(02)00711-0
125. Pays E, Vanhamme L, Pérez-Morga D. Antigenic variation in *Trypanosoma brucei*: facts, challenges and mysteries. *Curr Opin Microbiol.* (2004) 7:369–74. doi: 10.1016/j.mib.2004.05.001
126. Radwanska M, Magez S, Michel A, Stijlemans B, Geuskens M, Pays E. Comparative analysis of antibody responses against HSP60, invariant surface glycoprotein 70, and variant surface glycoprotein reveals a complex antigen-specific pattern of immunoglobulin isotype switching during infection by *Trypanosoma brucei*. *Infect Immun.* (2000) 68:848–60. doi: 10.1128/IAI.68.2.848-860.2000
127. Bockstal V, Guirnalda P, Caljon G, Goenka R, Telfer JC, Frenkel D, et al. *T. brucei* infection reduces B lymphopoiesis in bone marrow and truncates compensatory splenic lymphopoiesis through transitional B-cell apoptosis. *PLoS Pathog.* (2011) 7:e1002089. doi: 10.1371/journal.ppat.1002089
128. Engstler M, Pfohl T, Herminghaus S, Boshart M, Wiegertjes G, Heddergott N, et al. Hydrodynamic flow-mediated protein sorting on the cell surface of trypanosomes. *Cell* (2007) 131:505–15. doi: 10.1016/j.cell.2007.08.046
129. La Greca F, Haynes C, Stijlemans B, De Trez C, Magez S. Antibody-mediated control of *Trypanosoma vivax* infection fails in the absence of tumor necrosis factor. *Parasite Immunol.* (2014) 36:271–6. doi: 10.1111/pim.12106
130. Radwanska M, Guirnalda P, De Trez C, Ryffel B, Black S, Magez S. Trypanosomiasis-induced B cell apoptosis results in loss of protective anti-parasite antibody responses and abolishment of vaccine-induced memory responses. *PLoS Pathog.* (2008) 4:e1000078. doi: 10.1371/journal.ppat.1000078
131. Cnops J, Kauffmann F, De Trez C, Baltz T, Keirsse J, Radwanska M, et al. Maintenance of B cells during chronic murine *Trypanosoma brucei* gambiense infection. *Parasite Immunol.* (2016) 38:642–7. doi: 10.1111/pim.12344
132. Cnops J, De Trez C, Bulte D, Radwanska M, Ryffel B, Magez S. IFN-γ mediates early B-cell loss in experimental African trypanosomosis. *Parasite Immunol.* (2015) 37:479–84. doi: 10.1111/pim.12208
133. Frenkel D, Zhang F, Guirnalda P, Haynes C, Bockstal V, Radwanska M, et al. *Trypanosoma brucei* Co-opts NK cells to kill splenic B2 B cells. *PLoS Pathog.* (2016) 12:e1005733. doi: 10.1371/journal.ppat.1005733
134. Cnops J, Magez S, De Trez C. Escape mechanisms of African trypanosomes: why trypanosomosis is keeping us awake. *Parasitology* (2015) 142:417–27. doi: 10.1017/S0031182014001838
135. Tizard IR, Mittal KR, Nielsen K. Depressed immunoconglutinin responses in calves experimentally infected with *Trypanosoma congolense*. *Res Vet Sci.* (1980) 28:203–6.
136. Uzonna JE, Kaushik RS, Gordon JR, Tabel H. Cytokines and antibody responses during *Trypanosoma congolense* infections in two inbred mouse strains that differ in resistance. *Parasite Immunol.* (1999) 21:57–71. doi: 10.1046/j.1365-3024.1999.00202.x
137. Schopf LR, Filutowicz H, Bi XJ, Mansfield JM. Interleukin-4-dependent immunoglobulin G1 isotype switch in the presence of a polarized antigen-specific Th1-cell response to the trypanosome variant surface glycoprotein. *Infect Immun.* (1998) 66:451–61.
138. Lejon V, Mumba Ngoyi D, Kestens L, Boel L, Barbé B, Kande Betu V, et al. Gambiense human african trypanosomiasis and immunological memory: effect on phenotypic lymphocyte profiles and humoral immunity. *PLoS Pathog.* (2014) 10:e1003947. doi: 10.1371/journal.ppat.1003947
139. Holland WG, Do TT, Huong NT, Dung NT, Thanh NG, Vercruysse J, et al. The effect of *Trypanosoma evansi* infection on pig performance and vaccination against classical swine fever. *Vet Parasitol.* (2003) 111:115–23. doi: 10.1016/S0304-4017(02)00363-1
140. Holland WG, My LN, Dung TV, Thanh NG, Tam PT, Vercruysse J, et al. The influence of T. evansi infection on the immuno-responsiveness of experimentally infected water buffaloes. *Vet Parasitol.* (2001) 102:225–34. doi: 10.1016/S0304-4017(01)00534-9
141. Rurangirwa FR, Musoke AJ, Nantulya VM, Tabel H. Immune depression in bovine trypanosomiasis: effects of acute and chronic *Trypanosoma congolense* and chronic *Trypanosoma vivax* infections on antibody response to *Brucella abortus* vaccine. *Parasite Immunol.* (1983) 5:267–76. doi: 10.1111/j.1365-3024.1983.tb00743.x
142. Rurangirwa FR, Tabel H, Losos GJ, Tizard IR. Suppression of antibody response to Leptospira biflexa and Brucella abortus and recovery from immunosuppression after Berenil treatment. *Infect Immun.* (1979) 26:822–6.
143. Ilemobade AA, Adegboye DS, Onoviran O, Chima JC. Immunodepressive effects of trypanosomal infection in cattle immunized against contagious bovine pleuropneumonia. *Parasite Immunol.* (1982) 4:273–82. doi: 10.1111/j.1365-3024.1982.tb00438.x
144. Mwangi DM, Munyua WK, Nyaga PN. Immunosuppression in caprine trypanosomiasis: effects of acute *Trypanosoma congolense* infection on antibody response to anthrax spore vaccine. *Trop Anim Health Prod.* (1990) 22:95–100. doi: 10.1007/BF02239832
145. Sharpe RT, Langley AM, Mowat GN, Macaskill JA, Holmes PH. Immunosuppression in bovine trypanosomiasis: response of cattle infected with *Trypanosoma congolense* to foot-and-mouth disease vaccination and subsequent live virus challenge. *Res Vet Sci.* (1982) 32:289–293.
146. De Geea L, Levine RF, Mansfield JM. Genetics of resistance to the African trypanosomes. VI. Heredity of resistance and variable surface glycoprotein-specific immune responses. *J Immunol.* (1988) 140:283–8.
147. Dagenais TR, Demick KP, Bangs JD, Forest KT, Paulnock DM, Mansfield JM. T-cell responses to the trypanosome variant surface glycoprotein are not limited to hypervariable subregions. *Infect Immun.* (2009) 77:141–51. doi: 10.1128/IAI.00729-08
148. Dagenais TR, Freeman BE, Demick KP, Paulnock DM, Mansfield JM. Processing and presentation of variant surface glycoprotein molecules to T cells in African trypanosomiasis. *J Immunol.* (2009) 183:3344–55. doi: 10.4049/jimmunol.0802005
149. Schleifer KW, Mansfield JM. Suppressor macrophages in African trypanosomiasis inhibit T cell proliferative responses by nitric oxide and prostaglandins. *J Immunol.* (1993) 151:5492–503.
150. Hertz CJ, Filutowicz H, Mansfield JM. Resistance to the African trypanosomes is IFN-gamma dependent. *J Immunol.* (1998) 161:6775–83.
151. Hertz CJ, Mansfield JM. IFN-gamma-dependent nitric oxide production is not linked to resistance in experimental African trypanosomiasis. *Cell Immunol.* (1999) 192:24–32. doi: 10.1006/cimm.1998.1429
152. Magez S, Radwanska M, Drennan M, Fick L, Baral TN, Brombacher F, et al. Interferon-gamma and nitric oxide in combination with antibodies are key protective host immune factors during *trypanosoma congolense* Tc13 infections. *J Infect Dis.* (2006) 193:1575–83. doi: 10.1086/503808

153. Uzonna JE, Kaushik RS, Gordon JR, Tabel H. Experimental murine *Trypanosoma congolense* infections. I. Administration of anti-IFN-gamma antibodies alters trypanosome-susceptible mice to a resistant-like phenotype. *J Immunol.* (1998) 161:5507–15.
154. Cnops J, De Trez C, Stijlemans B, Keirsse J, Kauffmann F, Barkhuizen M, et al. NK-, NKT- and CD8-Derived IFNγ drives myeloid cell activation and erythrophagocytosis, resulting in trypanosomosis-associated acute anemia. *PLoS Pathog.* (2015) 11:e1004964. doi: 10.1371/journal.ppat.1004964
155. Wu H, Liu G, Shi M. Interferon gamma in African Trypanosome infections: friends or foes? *Front Immunol.* (2017) 8:1105. doi: 10.3389/fimmu.2017.01105
156. Bakhiet M, Büscher P, Harris RA, Kristensson K, Wigzell H, Olsson T. Different trypanozoan species possess CD8 dependent lymphocyte triggering factor-like activity. *Immunol Lett.* (1996) 50:71–80. doi: 10.1016/0165-2478(96)02521-7
157. Bakhiet M, Hamadien M, Tjernlund A, Mousal A, Seiger A. African trypanosomes activate human fetal brain cells to proliferation and IFN-gamma production. *Neuroreport* (2002) 13:53–6. doi: 10.1097/00001756-200201210-00015
158. Masocha W, Robertson B, Rottenberg ME, Mhlanga J, Sorokin L, Kristensson K. Cerebral vessel laminins and IFN-gamma define *Trypanosoma brucei* brucei penetration of the blood-brain barrier. *J Clin Invest.* (2004) 114:689–94. doi: 10.1172/JCI22104
159. Liu G, Sun D, Wu H, Zhang M, Huan H, Xu J, et al. Distinct contributions of CD4+ and CD8+ T cells to pathogenesis of *Trypanosoma brucei* infection in the context of gamma interferon and interleukin-10. *Infect Immun.* (2015) 83:2785–95. doi: 10.1128/IAI.00357-15
160. Olsson T, Bakhiet M, Edlund C, Höjeberg B, Van der Meide PH, Kristensson K. Bidirectional activating signals between *Trypanosoma brucei* and CD8+ T cells: a trypanosome-released factor triggers interferon-gamma production that stimulates parasite growth. *Eur J Immunol.* (1991) 21:2447–54. doi: 10.1002/eji.1830211022
161. Sternberg JM, Mabbott NA. Nitric oxide-mediated suppression of T cell responses during*Trypanosoma brucei* infection: soluble trypanosome products and interferon-γ are synergistic inducers of nitric oxide synthase. *Eur J Immunol.* (1996) 26:539–43. doi: 10.1002/eji.1830260306
162. Lopez R, Demick KP, Mansfield JM, Paulnock DM. Type I IFNs play a role in early resistance, but subsequent susceptibility, to the African trypanosomes. *J Immunol.* (2008) 181:4908–17. doi: 10.4049/jimmunol.181.7.4908
163. Magez S, Radwanska M, Beschin A, Sekikawa K, De Baetselier P. Tumor necrosis factor alpha is a key mediator in the regulation of experimental *Trypanosoma brucei* infections. *Infect Immun.* (1999) 67:3128–32.
164. Iraqi F, Sekikawa K, Rowlands J, Teale A. Susceptibility of tumor necrosis factor-alpha genetically deficient mice to *Trypanosoma congolense* infection. *Parasite Immunol.* (2001) 23:445–51. doi: 10.1046/j.1365-3024.2001.00401.x
165. Magez S, Lucas R, Darji A, Songa EB, Hamers R, De Baetselier P. Murine tumor necrosis factor plays a protective role during the initial phase of the experimental infection with *Trypanosoma brucei* brucei. *Parasite Immunol.* (1993) 15:635–41. doi: 10.1111/j.1365-3024.1993.tb00577.x
166. Magez S, Truyens C, Merimi M, Radwanska M, Stijlemans B, Brouckaert P, et al. P75 tumor necrosis factor-receptor shedding occurs as a protective host response during African trypanosomiasis. *J Infect Dis.* (2004) 189:527–39. doi: 10.1086/381151
167. Stijlemans B, De Baetselier P, Magez S, Van Ginderachter JA, De Trez C. African trypanosomiasis-associated anemia: the contribution of the interplay between parasites and the mononuclear phagocyte system. *Front Immunol.* (2018) 9:218. doi: 10.3389/fimmu.2018.00218
168. Lucas R, Magez S, De Leys R, Fransen L, Scheerlinck JP, Rampelberg M, et al. Mapping the lectin-like activity of tumor necrosis factor. *Science* (1994) 263:814–7. doi: 10.1126/science.8303299
169. Magez S, Radwanska M, Stijlemans B, Xong H V, Pays E, De Baetselier P. A conserved flagellar pocket exposed high mannose moiety is used by African trypanosomes as a host cytokine binding molecule. *J Biol Chem.* (2001) 276:33458–64. doi: 10.1074/jbc.M103412200
170. Daulouède S, Bouteille B, Moynet D, De Baetselier P, Courtois P, Lemesre JL, et al. Human macrophage tumor necrosis factor (TNF)-alpha production induced by *Trypanosoma brucei* gambiense and the role of TNF-alpha in parasite control. *J Infect Dis.* (2001) 183:988–91. doi: 10.1086/319257
171. Paulnock DM, Freeman BE, Mansfield JM. Modulation of innate immunity by African trypanosomes. *Parasitology* (2010) 137:2051–63. doi: 10.1017/S0031182010001460
172. O'Gorman GM, Park SDE, Hill EW, Meade KG, Mitchell LC, Agaba M, et al. Cytokine mRNA profiling of peripheral blood mononuclear cells from trypanotolerant and trypanosusceptible cattle infected with *Trypanosoma congolense*. *Physiol Genomics* (2006) 28:53–61. doi: 10.1152/physiolgenomics.00100.2006
173. Magez S, Stijlemans B, Baral T, De Baetselier P. VSG-GPI anchors of African trypanosomes: their role in macrophage activation and induction of infection-associated immunopathology. *Microbes Infect.* (2002) 4:999–1006. doi: 10.1016/S1286-4579(02)01617-9
174. Leppert BJ, Mansfield JM, Paulnock DM. The soluble variant surface glycoprotein of African trypanosomes is recognized by a macrophage scavenger receptor and induces I kappa B alpha degradation independently of TRAF6-mediated TLR signaling. *J Immunol.* (2007) 179:548–56. doi: 10.4049/jimmunol.179.1.548
175. Coller SP, Mansfield JM, Paulnock DM. Glycosylinositolphosphate soluble variant surface glycoprotein inhibits IFN- -induced nitric oxide production via reduction in STAT1 phosphorylation in African Trypanosomiasis. *J Immunol.* (2003) 171:1466–72. doi: 10.4049/jimmunol.171.3.1466
176. Stijlemans B, Baral TN, Guilliams M, Brys L, Korf J, Drennan M, et al. A glycosylphosphatidylinositol-based treatment alleviates trypanosomiasis-associated immunopathology. *J Immunol.* (2007) 179:4003–14. doi: 10.4049/jimmunol.179.6.4003
177. Stijlemans B, Vankrunkelsven A, Brys L, Raes G, Magez S, De Baetselier P. Scrutinizing the mechanisms underlying the induction of anemia of inflammation through GPI-mediated modulation of macrophage activation in a model of African trypanosomiasis. *Microbes Infect.* (2010) 12:389–99. doi: 10.1016/j.micinf.2010.02.006
178. Harris TH, Cooney NM, Mansfield JM, Paulnock DM. Signal transduction, gene transcription, and cytokine production triggered in macrophages by exposure to trypanosome DNA. *Infect Immun.* (2006) 74:4530–7. doi: 10.1128/IAI.01938-05
179. Barkhuizen M, Magez S, Ryffel B, Brombacher F. Interleukin-12p70 deficiency increases survival and diminishes pathology in *Trypanosoma congolense* infection. *J Infect Dis.* (2008) 198:1284–91. doi: 10.1086/592048
180. Krishnamoorthy P, Sengupta PP, Das S, Ligi M, Shome BR, Rahman H. Cytokine gene expression and pathology in mice experimentally infected with different isolates of *Trypanosoma evansi*. *Exp Parasitol.* (2016) 170:168–76. doi: 10.1016/j.exppara.2016.09.019
181. Flynn JN, Sileghem M. The role of the macrophage in induction of immunosuppression in *Trypanosoma congolense*-infected cattle. *Immunology* (1991) 74:310–6.
182. Maclean L, Odiit M, Macleod A, Morrison L, Sweeney L, Cooper A, et al. Spatially and genetically distinct African Trypanosome virulence variants defined by host interferon-gamma response. *J Infect Dis.* (2007) 196:1620–8. doi: 10.1086/522011
183. Kennedy PGE. Cytokines in central nervous system trypanosomiasis: cause, effect or both? *Trans R Soc Trop Med Hyg.* (2009) 103:213–4. doi: 10.1016/j.trstmh.2008.08.013
184. Murray M, Morrison WI, Whitelaw DD. Host susceptibility to African trypanosomiasis: trypanotolerance. *Adv Parasitol.* (1982) 21:1–68. doi: 10.1016/S0065-308X(08)60274-2
185. Naessens J. Bovine trypanotolerance: a natural ability to prevent severe anemia and haemophagocytic syndrome? *Int J Parasitol.* (2006) 36:521–8. doi: 10.1016/j.ijpara.2006.02.012
186. Rifkin MR, Landsberger FR. Trypanosome variant surface glycoprotein transfer to target membranes: a model for the pathogenesis of trypanosomiasis. *Proc Natl Acad Sci USA*. (1990) 87:801–5. doi: 10.1073/pnas.87.2.801
187. Guegan F, Plazolles N, Baltz T, Coustou V. Erythrophagocytosis of desialylated red blood cells is responsible for anemia during *Trypanosoma vivax* infection. *Cell Microbiol.* (2013) 15:1285–303. doi: 10.1111/cmi.12123

188. Suzuki T, Ueta YY, Inoue N, Xuan X, Saitoh H, Suzuki H. Beneficial effect of erythropoietin administration on murine infection with *Trypanosoma congolense*. *Am J Trop Med Hyg.* (2006) 74:1020–5. doi: 10.4269/ajtmh.2006.74.1020
189. Authié E, Boulangé A, Muteti D, Lalmanach G, Gauthier F, Musoke AJ. Immunisation of cattle with cysteine proteinases of *Trypanosoma congolense*: targetting the disease rather than the parasite. *Int J Parasitol.* (2001) 31:1429–33. doi: 10.1016/S0020-7519(01)00266-1
190. Stijlemans B, Brys L, Korf H, Bieniasz-Krzywiec P, Sparkes A, Vansintjan L, et al. MIF-mediated hemodilution promotes pathogenic anemia in experimental African trypanosomosis. *PLOS Pathog.* (2016) 12:e1005862. doi: 10.1371/journal.ppat.1005862
191. Thompson PD, Tipney H, Brass A, Noyes H, Kemp S, Naessens J, et al. Claudin 13, a member of the claudin family regulated in mouse stress induced erythropoiesis. *PLoS ONE* (2010) 5:e12667. doi: 10.1371/journal.pone.0012667
192. Blom-Potar MC, Chamond N, Cosson A, Jouvion G, Droin-Bergère S, Huerre M, et al. *Trypanosoma vivax* infections: pushing ahead with mouse models for the study of Nagana. II. Immunobiological dysfunctions. *PLoS Negl Trop Dis.* (2010) 4:e793. doi: 10.1371/journal.pntd.0000793
193. Chamond N, Cosson A, Blom-Potar MC, Jouvion G, D'Archivio S, Medina M, et al. *Trypanosoma vivax* infections: pushing ahead with mouse models for the study of Nagana. I. Parasitological, hematological and pathological parameters. *PLoS Negl Trop Dis.* (2010) 4:e792. doi: 10.1371/journal.pntd.0000792
194. Magez S, Stijlemans B, Caljon G, Eugster H-P, De Baetselier P. Control of experimental *Trypanosoma brucei* infections occurs independently of lymphotoxin-alpha induction. *Infect Immun.* (2002) 70:1342–51. doi: 10.1128/IAI.70.3.1342
195. Bosschaerts T, Guilliams M, Noel W, Hérin M, Burk RF, Hill KE, et al. Alternatively activated myeloid cells limit pathogenicity associated with African trypanosomiasis through the IL-10 inducible gene selenoprotein P. *J Immunol.* (2008) 180:6168–75. doi: 10.1186/1756-3305-4-74
196. Vankrunkelsven A, De Ceulaer K, Hsu D, Liu F-T, De Baetselier P, Stijlemans B. Lack of galectin-3 alleviates trypanosomiasis-associated anemia of inflammation. *Immunobiology* (2016) 215:833–41. doi: 10.1016/j.imbio.2010.05.028
197. Katunguka-Rwakishaya E, Murray M, Holmes PH. Pathophysiology of *Trypanosoma congolense* infection in two breeds of sheep, Scottish blackface and Finn dorset. *Vet Parasitol.* (1997) 68:215–25. doi: 10.1016/S0304-4017(96)01075-8
198. Katunguka-Rwakishaya E, Murray M, Holmes PH. Pathophysiology of ovine trypanosomiasis: ferrokinetics and erythrocyte survival studies. *Res Vet Sci.* (1992) 53:80–6. doi: 10.1016/0034-5288(92)90089-K
199. da Silva CB, Wolkmer P, Paim FC, Da Silva AS, Siqueira LC, de Souza CL, et al. Iron metabolism and its relationship to anemia and immune system in *Trypanosoma evansi* infected rats. *Exp Parasitol.* (2013) 133:357–64. doi: 10.1016/j.exppara.2012.12.010
200. Mackie JT, Stenner R, Gillett AK, Barbosa A, Ryan U, Irwin PJ. Trypanosomiasis in an Australian little red flying fox (*Pteropus scapulatus*). *Aust Vet J.* (2017) 95:259–61. doi: 10.1111/avj.12597
201. Doua F, Yapo FB. Human trypanosomiasis in the Ivory Coast: therapy and problems. *Acta Trop.* (1993) 54:163–8. doi: 10.1016/0001-706X(93)90090-X
202. Doua F, Boa FY, Schechter PJ, Miézan TW, Diai D, Sanon SR, et al. Treatment of human late stage gambiense trypanosomiasis with alpha-difluoromethylornithine (eflornithine): efficacy and tolerance in 14 cases in Côte d'Ivoire. *Am J Trop Med Hyg.* (1987) 37:525–33.
203. Burri C, Brun R. Eflornithine for the treatment of human African trypanosomiasis. *Parasitol Res.* (2003) 90(Supp 1):S49–52. doi: 10.1007/s00436-002-0766-5
204. Milord F, Pépin J, Loko L, Ethier L, Mpia B. Efficacy and toxicity of eflornithine for treatment of *Trypanosoma brucei* gambiense sleeping sickness. *Lancet* (1992) 340:652–5. doi: 10.1016/0140-6736(92)92180-N
205. Paul M, Stefaniak J, Smuszkiewicz P, Van Esbroeck M, Geysen D, Clerinx J. Outcome of acute East African trypanosomiasis in a polish traveler treated with pentamidine. *BMC Infect Dis.* (2014) 14:111. doi: 10.1186/1471-2334-14-111
206. Ngotho M, Kagira JM, Kariuki C, Maina N, Thuita JK, Mwangangi DM, et al. Influence of trypanocidal therapy on the hematology of vervet monkeys experimentally infected with *Trypanosoma brucei* rhodesiense. *Acta Trop.* (2011) 119:14–8. doi: 10.1016/j.actatropica.2011.02.013
207. Chisi JE, Misiri H, Zverev Y, Nkhoma A, Sternberg JM. Anaemia in human African trypanosomiasis caused by *Trypanosoma brucei* rhodesiense. *East Afr Med J.* (2004) 81:505–8. doi: 10.4314/eamj.v81i10.9232
208. MacLean L, Chisi JE, Odiit M, Gibson WC, Ferris V, Picozzi K, et al. Severity of human African trypanosomiasis in east Africa is associated with geographic location, parasite genotype, and host inflammatory cytokine response profile. *Infect Immun.* (2004) 72:7040–4. doi: 10.1128/IAI.72.12.7040-7044.2004
209. Songa EB, Hamers R, Rickman R, Nantulya VM, Mulla AF, Magnus E. Evidence for widespread asymptomatic *Trypanosoma rhodesiense* human infection in the Luangwa Valley (Zambia). *Trop Med Parasitol.* (1991) 42:389–93.

Conflict of Interest Statement: The authors declare that the research was conducted in the absence of any commercial or financial relationships that could be construed as a potential conflict of interest.

frontiers in Immunology

REVIEW
published: 28 February 2019
doi: 10.3389/fimmu.2019.00196

Innate Lymphoid Cells in Protection, Pathology, and Adaptive Immunity During Apicomplexan Infection

*Daria L. Ivanova[1], Stephen L. Denton[1], Kevin D. Fettel[1], Kerry S. Sondgeroth[2], Juan Munoz Gutierrez[3], Berit Bangoura[2], Ildiko R. Dunay[4] and Jason P. Gigley[1]**

[1] Molecular Biology, University of Wyoming, Laramie, WY, United States, [2] Veterinary Sciences, University of Wyoming, Laramie, WY, United States, [3] Microbiology, Immunology and Pathology, College of Veterinary Medicine and Biomedical Sciences, Colorado State University, Fort Collins, CO, United States, [4] Institute of Inflammation and Neurodegeneration, Otto-von-Guericke Universität Magdeburg, Magdeburg, Germany

OPEN ACCESS

Edited by:
Hyun Soon Lillehoj,
United States Department of Agriculture, United States

Reviewed by:
Wongi Min,
Gyeongsang National University, South Korea
Yeong Ho Hong,
Chung-Ang University, South Korea

***Correspondence:**
Jason P. Gigley
jgigley@uwyo.edu

Specialty section:
This article was submitted to Microbial Immunology, a section of the journal Frontiers in Immunology

Received: 30 May 2018
Accepted: 23 January 2019
Published: 28 February 2019

Citation:
Ivanova DL, Denton SL, Fettel KD, Sondgeroth KS, Munoz Gutierrez J, Bangoura B, Dunay IR and Gigley JP (2019) Innate Lymphoid Cells in Protection, Pathology, and Adaptive Immunity During Apicomplexan Infection. Front. Immunol. 10:196. doi: 10.3389/fimmu.2019.00196

Apicomplexans are a diverse and complex group of protozoan pathogens including *Toxoplasma gondii, Plasmodium* spp., *Cryptosporidium* spp., *Eimeria* spp., and *Babesia* spp. They infect a wide variety of hosts and are a major health threat to humans and other animals. Innate immunity provides early control and also regulates the development of adaptive immune responses important for controlling these pathogens. Innate immune responses also contribute to immunopathology associated with these infections. Natural killer (NK) cells have been for a long time known to be potent first line effector cells in helping control protozoan infection. They provide control by producing IL-12 dependent IFNγ and killing infected cells and parasites via their cytotoxic response. Results from more recent studies indicate that NK cells could provide additional effector functions such as IL-10 and IL-17 and might have diverse roles in immunity to these pathogens. These early studies based their conclusions on the identification of NK cells to be CD3–, CD49b+, NK1.1+, and/or NKp46+ and the common accepted paradigm at that time that NK cells were one of the only lymphoid derived innate immune cells present. New discoveries have lead to major advances in understanding that NK cells are only one of several populations of innate immune cells of lymphoid origin. Common lymphoid progenitor derived innate immune cells are now known as innate lymphoid cells (ILC) and comprise three different groups, group 1, group 2, and group 3 ILC. They are a functionally heterogeneous and plastic cell population and are important effector cells in disease and tissue homeostasis. Very little is known about each of these different types of ILCs in parasitic infection. Therefore, we will review what is known about NK cells in innate immune responses during different protozoan infections. We will discuss what immune responses attributed to NK cells might be reconsidered as ILC1, 2, or 3 population responses. We will then discuss how different ILCs may impact immunopathology and adaptive immune responses to these parasites.

Keywords: innate lymphoid cells (ILC), IL-12 family, IFN-gamma, IL-17, apicomplexan parasites

INTRODUCTION

Apicomplexa are a large family of protozoan parasites, which are obligate intracellular parasites of warm-blooded animals. Almost all of them are considered to be major health threats to humans and livestock throughout the world. These include but are not limited to *Toxoplasma gondii* (*T. gondii*), *Plasmodium* spp., *Cryptosporidium* spp., *Eimeria* spp., and *Babesia* spp. Others do exist, but this review will focus on the genera listed above. They can be generally divided into either vector borne or orally transmitted pathogens. Apicomplexans have reduced genome sizes compared to higher eukaryotes, but they encode several different types effector proteins that allow them to develop a very complex relationship with their hosts and contribute to virulence. The vector borne apicomplexans include the mosquito borne *Plasmodium* spp. and the tick borne *Babesia* spp. Orally infectious apicomplexans include *T. gondii*, *Cryptosporidium* spp. and *Eimeria* spp. *Plasmodium* spp. infects ∼200 million people and kills around 400,000 a year (1). *Babesia* spp. is a newly emerging parasitic infection of humans (2, 3). *Toxoplasma gondii* infects ∼30% of people worldwide and is the third leading cause of food borne illness in the U.S (4). There are on average 750,000 new cases of *Cryptosporidium* spp. per year in the U.S. alone and the parasite is distributed worldwide (5). *Eimeria* spp. infections can be devastating to chicken and beef farms, but it does not appear to be infectious to humans (6). Many of these protozoan parasites can be problematic for people with compromised immune systems especially those with HIV/AIDS. Moreover, in immune competent individuals the majority of these infections can cause considerable tissue morbidity and pathology resulting in long term damage to the host. In the case of *T. gondii* infection there is increasing evidence that persistent infection could contribute to psychiatric disorders and neurodegenerative disorders (7). Thus, gaining a better understanding of the immune factors involved in control of these pathogens as well as the factors that contribute to immunopathology is important to reduce negative health outcome caused by these common infections.

Immune control of apicomplexans largely depends upon induction of adaptive immunity via a T helper type 1 (Th1) response and production of IFNγ (8). In addition to Th1 response, IL-17 production and associated inflammation also are induced (9–12). In many cases this Th17 response appears to contribute to immune pathology associated with these infections. In order to develop either a Th1 or Th17 response, innate immune cells have to be triggered to produce the cytokines important in directing which types of T helper responses develop. In comparison to viral infections where much is known about innate immune cell composition and how these cells function in protection and immunopathology, less is known in the context of apicomplexan infection. Active areas of research to expand this knowledge in protozoan infection exist including an understanding of how innate immune responses contribute to control, cause pathology and influence the development of adaptive responses. However, a major gap in knowledge still exists in understanding all of the innate immune cell populations that are recruited and activated during protozoan infections and what role they each have in protection, causing pathology and/or regulating adaptive immune responses.

Innate immune responses are critical in setting the stage for how the adaptive immune system responds to infection. Many types of cells of either myeloid or lymphoid origin within the innate immune cell compartment contribute to this process. Common myeloid progenitor derived cells include, granulocytes, monocytes/macrophages, dendritic cells, and mast cells (13). These myeloid populations initiate a response to infection and activate the lymphoid cell populations by producing chemokines and cytokines, presenting antigen, and providing costimulation. Innate immune cells are derived from the common lymphoid progenitor and were originally only thought to include Natural Killer cells and some innate B cell like populations. However, in 2013 after a continuous flow of new discoveries about innate immune responses by lymphoid derived cells, the newly appreciated complexity of lymphoid progenitor derived innate immune cells was acknowledged and the Innate Lymphoid Cell classification was proposed (14). As a result, NK cells were formally recognized to not be the only cell comprising this population and there exist 3 groups of innate lymphoid cells (ILC) (**Figure 1**). Group 1 ILC include what are now considered to be conventional NK (NK) cells and ILC1 (15). Currently, group 2 ILCs include ILC2s, and group 3 ILC include ILC3 and Lymphoid Tissue inducer like cells (LTi-like ILC3) (16, 17). Conventional NK cells appear to be the only cytotoxic cell while all the other ILCs follow the pattern of helper CD4 T cells and produce cytokines and other soluble factors that help adaptive immune responses develop. Conventional NK cells have been studied for years in apicomplexan infection and their importance in producing IFNγ during acute infection is very well-established (1, 4). However, several studies demonstrate that what were considered to be NK cell responses during parasitic infection might be responses of other ILCs to infection. Given the updated view of the diversity of ILC populations, a major gap in knowledge in the apicomplexan field is how do different ILC populations contribute to innate and adaptive immunity and/or immunopathology associated with these infections. Another important question to address is whether and how ILC populations positively and negatively regulate adaptive immunity to apicomplexans. Where published data is available, we will detail what is known about the development, activation, and effector functions of NK cells and other ILCs in the context of different apicomplexan infections. We will also discuss the possible roles of non-NK cell ILC populations in protection or pathology associated with the different apicomplexan infections and how they may impact adaptive immunity during infection with these parasitic protozoans.

GROUP 1 ILC

Group 1 ILCs include the conventional NK cell and ILC1 (**Figure 1**). NK cells have been extensively studied in the context of Apicomplexan infection (1, 4, 18, 19). ILC1 have only recently been investigated (20). Group 1 ILCs can be identified by

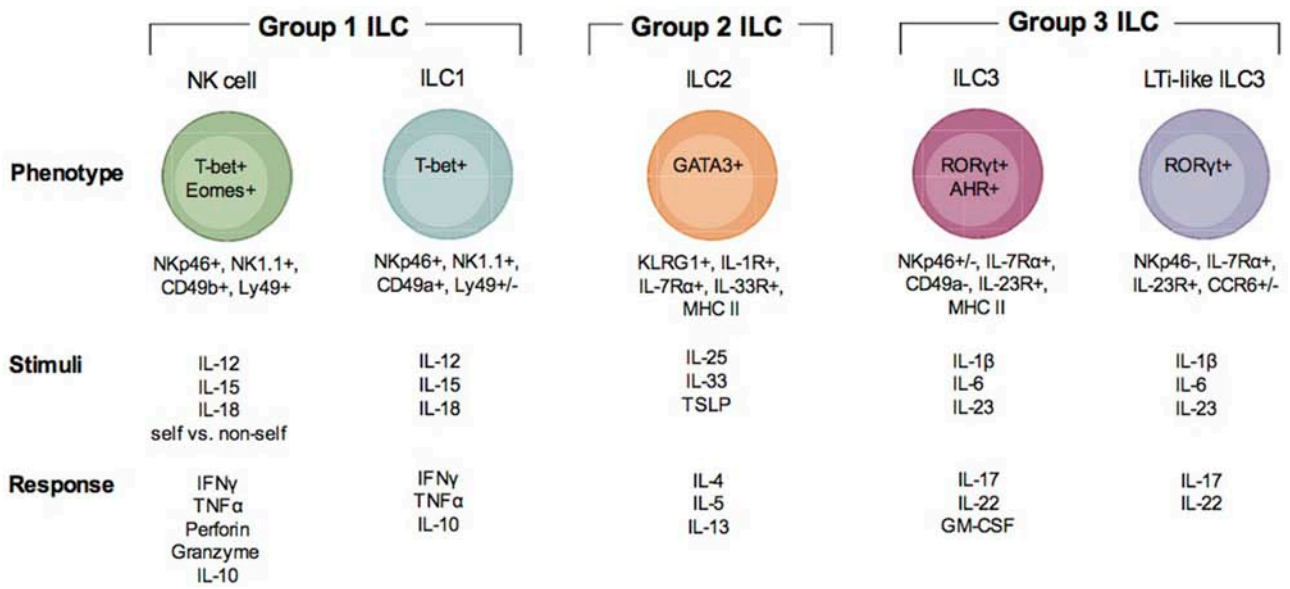

FIGURE 1 | Description of ILC subsets. There are three groups of ILC, group 1 ILC, group 2 ILC, and group 3 ILC. Within each of these groups, subsets of cells are indicated (group 1: NK cells and ILC1; group 2: ILC2; group 3 ILC3 and LTi-like ILC3). Each ILC is illustrated with the transcription factors important for their development and function, their surface phenotype, the stimuli that is known to activate them and the immune factors produced when they are activated and responding to infection.

surface expression of the natural cytotoxicity receptor NKp46 and NK1.1 (only in mice that express *NKrp1*). ILC1 can be distinguished from NK cells by their surface expression of very late antigen 1 (VLA-1) or CD49a and TNF—related apoptosis inducing ligand (TRAIL) (15). In the resting state, NK cells are negative for CD49a and positive for very late antigen 2 (VLA-2) or CD49b. Although TRAIL is considered a marker specific for ILC1s, evidence supports that it is also expressed by immature NK cells (iNK) prior to their maturation in the mature NK cells (mNK) which are TRAIL negative (21). NK cells can be found in many tissues and are continuously circulating through the blood. ILC1s are considered to have tissue residence and have been found in both mucosal and non-mucosal tissues (15). These include the spleen, liver, salivary glands, peritoneal cavity, gut, and uterus. NK cells are dependent on expression of T-bet and Eomes for their development and function (21, 22). ILC1 are only dependent upon T-bet (15). Due to the apparent plasticity in ILC populations, ILC1-like cells can arise from both ILC2 and ILC3 (23). Transdifferentiation of ILC2 and ILC3 into ex-ILC2 and ex-ILC3 ILC1 are marked by their increase in NKp46, NK1.1, CD49a, and T-bet expression. These types of ILC1 are also positive for the high affinity IL-7 receptor subunit alpha (IL-7Rα) or CD127 (23). NK cells are the only group 1 ILC that can be cytotoxic. NK cell cytotoxicity is important for killing virally infected cells and tumor cells. The importance of NK cell cytotoxicity in apicomplexan infection is still unclear. NK cells and ILC1 and ex ILC2 and 3 ILC1s produce high levels of IFNγ and TNFα in response to Th1 inducing cytokines IL-12, IL-15, and IL-18 (15). Via their IFNγ production they help control apicomplexan infection.

GROUP 2 ILC

Group 2 ILC includes ILC2 (**Figure 1**) (16). ILC2 could be involved in apicomplexan infection, however, their importance is still not well defined (24, 25). An important distinction between ILC2 and other ILCs is that to date a distinct surface marker has not been identified. ILC2 are lineage (CD3, CD19), NKp46, and NK1.1 negative and CD127, c-Kit(CD117), KLRG1, and the IL-33 receptor (ST2) positive (16, 26). The ILC2 is tissue resident similar to ILC1 and is found at mucosal tissues including the intestine and lungs. ILC2 development and activation depend on the transcription factor GATA3 and they contribute to Th2 responses by producing IL-4, IL-5, IL-9, and IL-13. ILC2 can also express MHC Class II and may be able to prime CD4 T cells (16). ILC2 are known for their importance in immunity against helminth infections to promote tissue repair. Since they express the IL-33 receptor ST2 they can sense tissue damage and respond to promote tissue repair. They are also damaging as they can contribute to allergic inflammation and asthma. As mentioned above, ILC2 demonstrate a high level of plasticity (27–30). IL-1β and IL-12 can drive them to differentiate into an ILC1-like cells. Thus, in addition to their importance in Th2 responses, when given the proper signals they can produce IFNγ and contribute to Th1 dependent immunity. Therefore, ILC2 could contribute to immune protection and immune system regulation during apicomplexan infections.

GROUP 3 ILC

Group 3 ILCs include ILC3 and LTi and LTi-like ILC3 (**Figure 1**) (17). Recent studies suggest that ILC3 can contribute to

immunity during apicomplexan infections, however, much is not known about how these cells impact immunity against these parasites (31). Based on surface phenotype ILC3 can be either positive or negative for NKp46 (17). They are also positive for CD127, CD117, and receptors for IL-1(IL-1R) and IL-23 (IL-23R). LTi and LTi-like-ILC3 are NKp46 and CD49a negative, but positive or negative for CCR6 depending on the tissue in which they reside (32). Some LTi cells can also be CD4 positive and ILC3 can express MHC Class II. Group 3 ILC have a wide tissue distribution and reside in mucosal tissues and their associated lymphoid organs. ILC3 and LTi-like-ILC3 differentiation and function depend on the transcription factors RORγt and the aryl hydrocarbon receptor (AHR). Given their tissue residency they are poised to respond to different environmental cues to either maintain barrier homeostasis or provide an inflammatory response against infection. In response to IL-1β and IL-23, ILC3 produce IL-17A, IL-22 and GM-CSF and LTi-like-ILC3s produce IL-17F and IL-22. LTi-like ILC3 also can produce lymphotoxin α/β (LTα/β) to promote lymphoid tissue development. Since group 3 ILC can produce IL-17 and IL-22, they could contribute significantly to Th17 responses observed in many apicomplexan infections, yet their importance is unclear.

ILC PLASTICITY

The border between ILC subtypes has become more defined, however as noted above, ILC are highly plastic and can convert into each other depending on the environment they experience (23). For example, under certain inflammatory conditions, ILC2 and ILC3 can express T-bet and produces Th1 cytokines (27, 29, 33). When the conditions permit, these newly generated ILC1 can convert back into ILC2 and ILC3. This cellular plasticity is likely essential for the generation of optimal responses against pathogens and maintenance of tissue integrity. Due to this new appreciation of ILC diversity, how different ILC populations participate in immunity to apicomplexan infection has not been well defined. We will next discuss what is currently known about ILCs during these parasitic infections and highlight situations where different ILCs may be involved. We will also discuss how different ILCs could be implicated in adaptive immunity to these pathogens.

ILC AND *TOXOPLASMA GONDII*

Even though the ILC classification was recently established to define the innate immune cells of lymphoid lineage, the importance of ILC function for control of *T. gondii* infection has been investigated for many years (4, 34) (**Figure 2**). Infection with *T. gondii* begins after ingestion of oocysts from cat feces or bradyzoite containing tissue cysts from undercooked meat (4, 8). Acute infection is followed by chronic infection in the CNS and muscle for the life of the host. Innate immune responses at mucosal sites and in secondary lymphoid organs are critical for early control of the parasite. In early studies NK cells were shown to be activated by *T. gondii* infection to be cytotoxic (35). Later on NK cells were shown to be a non-T cell source of IFNγ and were essential for innate immunity to *T. gondii* infection (36, 37). Whether NK cell cytotoxicity is important for early control of *T. gondii* infection is not known and had not been thoroughly tested (4). Importantly, these early studies were some of the first to demonstrate the importance of the IL-12/IFNγ axis in development of Th1 biased immunity (36–38). Indeed IL-12 is required for activation of NK cells to produce IFNγ during *T. gondii* infection (37). Additional cytokines can help stimulate NK cell activation including IL-1β and IL-18 (39, 40). Whether recognition of self-vs. non-self is an important stimulant for NK cells during *T. gondii* infection is not clear (41). To date there have been no observed dominant NK cell populations based on NK cell receptor expression in mice that arise during acute infection suggesting their response is mostly to inflammatory cytokines. Verification of the importance of NK cells in protection against *T. gondii* infection was tested using lymphocyte deficient animals including RAG knockout and SCID mice. In addition NK cell antibody depletion regimes *in vivo* targeting asialo ganglio-N-tetraosylceramide (anti-ASGM1) or anti-NK1.1 were used. These studies laid the foundation for the importance of NK cells in control of *T. gondii* infection.

More recently, studies have addressed how NK cells are involved in immunity against *T. gondii* infection through their impact on other immune cells. NK cell IFNγ can help prime CD8 T cells in the absence of CD4 T cell help (42). NK cell IFNγ can also help activate CD4 T cells during acute *T. gondii* infection (43). Infection of TAP1$^{-/-}$ mice results in reduced CD4 T cell IFNγ production. Adoptive transfer of IFNγ+ but not IFNγ- NK cells restore this deficient CD4+ T cell response. NK cell activity during early during infection could also impact the myeloid cell compartment (44–46). NK cells may enhance DC maturation via NKG2D on the NK cell resulting in more robust CD8 T cell priming during acute infection (44). NK cell IFNγ may be required for the loss of resident mononuclear phagocytes followed by recruitment of circulating monocytes that locally differentiate into macrophages and monocyte derived DC (MoDC) (45). These MoDC then serve as the main source of IL12p40 at the site of infection, which in this study was the peritoneum. Early NK cell (CD49b+CD49a-CD45+TCRb-NK1.1+) IFNγ production during *T. gondii* infection has also been shown to educate the myeloid compartment in the bone marrow. The IFNγ generated by NK cells in the bone marrow skewed monocyte development at that site into a more regulatory phenotype (46). In summary, NK cells via their IFNγ production are able to both positively and negatively regulate other immune cells during *T. gondii* infection. The impact of NK cells on other immune cells could therefore positively or negatively impact the generation of adaptive immune responses to the parasite.

A small number of studies have investigated whether parasite infection of NK cells affects their behavior (47–49). NK cells can be parasitized, however, this occurs at a very low frequency *in vitro* and *in vivo*. These infected NK cells display a hypermotility phenotype and defective function. A recent study indicates that infected NK cells do not contribute to parasite dissemination in the mouse (47). Thus, how direct parasite infection of NK cells impacts the disease course is not known and needs to be further explored.

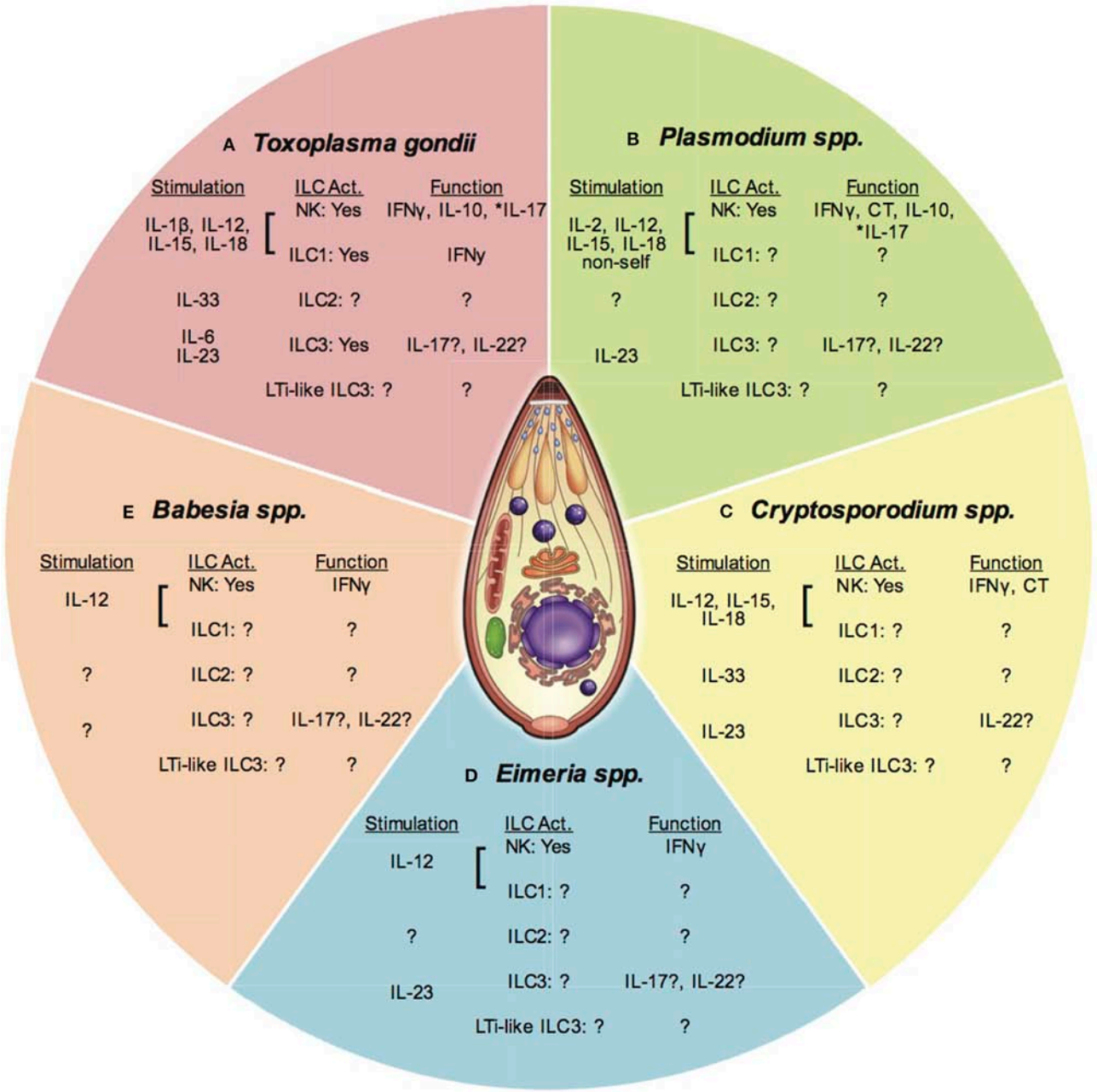

FIGURE 2 | ILC and apicomplexan infection. This figure presents an overview of ILC responses to different apicomplexan infections covered in this article. Each section represents one parasitic protozoan. Under each genus heading there are listed 3 subheadings indicating; (1) Stimuli for each ILC subset (stimulation), (2) The ILC subpopulation activated (ILC Act.), and (3) The function of the activated ILC subset. Question marks indicate where there is no or limited data available. An * denotes where function attributed to NK cells may be from a different ILC population. **(A)** *Toxoplasma gondii* stimulates the production of IL-1β, IL-12, IL-15, and IL-18 that activate NK cells and possibly ILC1 to produce IFNγ and IL-10. IL-17 produced by NK cells may also be produced by other ILC. IL-33 is produced and may activate ILC2. IL-6 and IL-23 are produced and could activate ILC3 for IL-17 and IL-22 production. The importance of LTi-like ILC3 are not known. **(B)** *Plasmodium spp.* stimulates IL-2, IL-12, IL-15, and IL-18, which activate NK cells to produce IFNγ. Recognition of non-self may stimulate NK cell cytotoxicity (CT). These cytokines also stimulate NK cells to produce IL-10. NK cell IL-17 may also be produced by other ILC. The role of ILC2, ILC3, and LTi-like ILC3 are not clear. **(C)** *Cryptosporidium* spp. infection stimulates the production of IL-12, IL-15, and IL-18. These cytokines can activate NK cells to produce IFNγ. NK cell cytotoxicity is also increased after infection, but the stimulus is not known. The importance of ILC1, ILC2, ILC3, and LTi-like ILC3 has not been tested. **(D)** *Eimeria* spp. infection induces IL-12 production that activates NK cells to produce IFNγ. The importance of ILC1, ILC2, ILC3, and LTI-like ILC3 are not known, however evidence suggests IL-17 and IL-22 are produced during infection highlighting the potential activity of non-NK cell ILCs. **(E)** *Babesia* spp. infection stimulates the production of IL-12, which activates NK cells to produce IL-12. The importance of other ILCs has not been investigated at this time.

A major question that now needs to be considered based on the increase in knowledge about additional ILC subsets is can the observations discussed above involve other ILC populations during *T. gondii* infection? This question arises because for many of these studies, the importance of NK cells was further demonstrated by using anti-NK1.1 or anti-ASGM1 to deplete the cells *in vivo* (12, 36). These treatments could easily target other ILC types because of their expression of NK1.1 and or asialo GM1 on their surfaces. One population of ILC that could also be involved in parasite control and in shaping the immune response to the parasite is the ILC1. ILC1 are tissue resident cells that produce large amounts of IFNγ (15). Support for this idea was demonstrated by a study that identified the common helper innate lymphoid progenitor cell or CHILP (20). In these studies, ILC1 as defined by their phenotype Lin-NKp46+NK1.1+Tbet+Eomes- in the small intestine produced the highest amount of IFNγ compared to NK cells and NKp46+NK1.1+ ILC3. Using T-bet deficient ($Tbx21^{-/-}$) mice to eliminate ILC1 development, ILC1 IFNγ was significantly reduced and parasite burdens were significantly increased in the gut. These results suggest that ILC1 resident in specific tissues can also influence the outcome of *T. gondii* infection. A good example that different ILC subsets are involved in different tissues was shown by a separate study using the same T-bet deficient animals (50). In this study the authors found that the NK cells still produced a high level of IFNγ in response to *T. gondii* in the spleen in the absence of this transcription factor. These results demonstrate that in different tissues different transcription factors are important for ILC (NK cell vs. ILC1) responses to *T. gondii.* They also suggest the potential critical role of Eomes and not T-bet in development of NK cell responses in the spleen. Thus, where group 1 ILC IFNγ is impacting immunity to *T. gondii* further investigation is needed to distinguish between NK cells and ILC1 as the source of this cytokine and in what tissues they are working.

Other ILC populations may also be playing an important role in immunity to *T. gondii.* These include the ILC2, ILC3, and LTi-like ILC3 populations. Although ILC2 are helper cells that drive Th2 responses, they could be important during *T. gondii* infection. ILC2 could have a role in dampening the inflammatory response to *T. gondii* infection. ILC2 respond to tissue damage at mucosal sites associated with parasitic helminth infections (16). Their response is controlled by alarmins including IL-33 and IL-1β. Interestingly, a previous report using ST2 (IL-33R) deficient mice demonstrated that these mice were more susceptible to developing inflammatory lesions and Toxoplasmic encephalitis associated with increases in iNOS, IFNγ, and TNFα (25). However, a separate study demonstrated that IL-33 and ST2 correlated with greater immunopathology, inflammation and ocular toxoplasmosis (51). Therefore, whether ILC2 are important or not is unclear. It is still possible that as a result of mucosal tissue damage caused by acute *T. gondii* infection, the release of IL-33 and signaling induced via ST2 could dampen the Th1 biased inflammatory response to the parasite by activating ILC2 to produce Th2 biased cytokines. Whether ILC2s are an important cell type involved as a negative regulator of inflammation and T cell responses during *T. gondii* infection has not been tested and would be important to address in future studies.

Group 3 ILCs could also be an important immune cell involved in *T. gondii* infections, however, very little is known about them. Group 3 ILCs include LTi-like ILC3 and ILC3, both important cell types that are tissue resident and present in several tissues including the gut. They are important for maintaining tissue homeostasis at these sites, but can also promote tissue damage when they are highly activated (17). ILC3 production of IL-22 is thought to help maintain tissue integrity while ILC3 derived IL-17 can be inflammatory and associated with pathology. ILC3 are thought to be resident at mucosal barriers, but are also found in the spleen (32). During *T. gondii* infection a study revealed that IL-17 was produced and signaling through the IL-17 receptor was important for protection by stimulating neutrophil recruitment (52). A separate study demonstrated that IL-17 via IL-17 receptor signaling caused gut immunopathology associated with infection and was important in promoting chronic *T. gondii* infection (53). At this time, the cellular source of IL-17 was not known. One report suggested that NK cells were the source of *T. gondii* induced IL-17 (12). In this study IL-17 levels increased in infected $Rag1^{-/-}$ mice and anti-ASGM1 treatment significantly reduced the levels of this cytokine in these animals. IL-17 production was induced by IL-6, followed by IL-23 and TGFβ, and suppressed by addition of Th1 cytokines (IL-12, 15, and 27). The splenic NK1.1+CD3- cells that produced IL-17 were not secreting IFNγ as no double positive IFNg+IL17+ NK1.1+CD3- cells were detected. These results suggested that this NK cell population might be distinct from the NK cell population involved in early control of the parasite. Taking into consideration the experimental approaches used to define that these cells were NK cells ($Rag1^{-/-}$ and anti-ASGM1) and that these same approaches can target ILC3 may suggest that the ILC3 populations were the IL-17 producers in these studies and not NK cells. Further support for this idea was revealed because the ILC population studied expressed IL-6Ra and the transcription factor RORγt rather than T-bet (12). Group 3 ILC are now known to depend upon expression of RORγt (17). Since ILC3 are also found in the gut, additional studies indicate that an NKp46+ ILC cell develops in the lamina propria and in response to IL-18 recruits inflammatory monocytes into the gut that increase immunopathology associated with *T. gondii* infection (54). A recent study has investigated more specifically the role of ILC3 in the gut during *T. gondii* infection using aryl hydrocarbon receptor deficient mice and demonstrates that these cells appear to negatively regulate T cell activity (31). Thus, again depending on the tissue investigated, ILC3 may have multiple roles including causing disease pathology and potentially as a negative regulator of adaptive immune responses during *T. gondii* infection. Many questions remain unanswered about these cells during this infection including formal dissection of whether ILC3 could positively or negatively impact development and maintenance of T cell responses against *T. gondii*. In addition, ILC3 and LTi-like ILC3 plasticity would be important to investigate during *T. gondii* infection.

As discussed above, ILCs may also play a role as negative regulators of immunity against *T. gondii*. Using systemic *T.*

gondii as a model infection, NK cells were shown to be capable of producing IL-10 (55). These IL-10 producing cells were defined as conventional NK cells because they were lineage negative (CD3-CD19-TCRβ-) and NK1.1 positive. These cells were also CD127 negative suggesting that they were not ILC2 or ILC3. This regulatory NK cell population was induced by systemic inflammation, and IL-12 and NK cell IL-10 limited IL-12 production by DC. These cells were found to produce IL-10 in lung, liver, brain, blood, but not in spleen and MLN during acute *T. gondii* infection. In another study, NK cells (CD3-CD19-DX5+NK1.1+) were shown to be the major source of IL-10 in spleen, PEC, liver during acute infection (56). Both IL-12 and aryl hydrocarbon receptor (AHR) were required for maximal IL-10 production by these cells. These regulatory NK cells also expressed T-bet, KLRG1 and co-produced IFNγ. The presence of the IL-10 producing NK cells reduced the ability of the mice to control *T. gondii* infection. These data suggest that IL-10 producing cells are present during acute *T. gondii* infection, could be members of group 1 ILC and are important for regulating adaptive immune responses to *T. gondii*. A major open question still is where do these cells originate, what are the long term affects of these cells on T cell responses to the parasite and could they have a negative impact on chronic toxoplasmosis.

There are still many open questions about the roles of different populations of ILCs and *T. gondii* infection. The importance of each ILC subtype has not been fully addressed and there are questions about NK cells that will have to be reinvestigated because of the increase in knowledge of the different ILC subsets in the context of infection. Many studies investigating ILCs during *T. gondii* infection have focused on the acute stage of infection. Their importance in long-term control of the parasite is still not clear especially in chronic *T. gondii* infection and the CNS, which is the current focus of our laboratory.

ILC AND PLASMODIUM

As with *T. gondii* infection, investigations of ILCs in *Plasmodium* spp. infection have been ongoing for many years. Of the ILCs researched the majority of data has been generated from NK cell specific studies [reviewed in (1)]. Infection with *Plasmodium* spp. in humans begins with the injection of sporozoites of the parasite from the salivary gland of the mosquito into the blood stream of the host (57). Once the parasite is inside the host, it migrates to the liver where hepatocytes are infected. The parasite transforms as it replicates into the merozoite stage, which is released from the infected hepatocyte after lysis of the cell. The merozoites then infect erythrocytes (RBC) and develop into male and female gametes and the cycle is repeated. The innate immune response is important in early control of the parasite in liver, periphery, and secondary lymphoid structures where many innate immune cells including ILCs reside. Inflammation generated by the innate immune response including ILC may contribute to *Plasmodium* spp. pathogenesis and pathology such as cerebral malaria (58). NK cells are critical immune cell type in early and continuous control of *Plasmodium* spp. infections in both mouse models of infection and humans (1) (**Figure 2**). NK cells and/or other ILC types may also be pathogenic by contributing to the development of cerebral malaria. Additionally, the diverse life stages and tissue locations of the parasite likely require the involvement of distinct ILC subsets. Much is still not known about how each ILC type contributes to these processes during *Plasmodium* spp. infection.

In mice splenic, hepatic and peripheral NK (NK1.1+) cells protect against early stages of malaria infection by producing IFNγ and TNFα (59–62). After anti-ASGM1 treatment and NK cell depletion there was a decrease in IFNγ production and an increase in parasitemia in mice (59, 60). In humans, NK cells are thought to be some of the first cells to produce IFNγ during infection (1, 58). Human NK cells (CD56+) produce IFNγ and TNFα after *Plasmodium falciparum* infection (63–65). Human NK cells (can produce IFNγ after stimulation with *Plasmodium* infected erythrocytes *in vitro* (66). In addition to IFNγ production, peripheral blood NK cells are thought to be stimulated to be cytotoxic in response to parasite infection (67, 68). Human NK cells release cytotoxic molecules when cultured with infected hepatocytes and erythrocytes *in vitro*. NK cells have been observed to directly interact with infected erythrocytes forming conjugates (66, 69, 70). Human NK cells have been shown to kill infected erythrocytes (71). Whether NK cell specific cytotoxicity is important in controlling the parasite *in vivo* is still unclear and still needs to be formally tested in mouse models of infection or in humans.

NK cell activation during *Plasmodium* spp. infection is mediated by several signals including cytokines produced by other immune cells and potentially via self-vs. non-self-recognition. Generally, the classic IL-12/IFNγ axis applies to this infection as well as it does to other Apicomplexan infections. Studies are consistent in showing that IL-12 is essential for IFNγ production by NK cells during *Plasmodium* spp. infection (72). Not only is IL-12 important for activation, but also there is interplay between several cytokines and the activation of NK cells to produce IFNγ in response to IL-12. IL-18 in combination with IL-12 can enhance NK cell IFNγ production in mice in response to *Plasmodium* spp. infection (73). This is via IL-18 dependent up regulation of CD25 (IL-2Rα) expression on NK cells allowing them to be more sensitive to IL-2 and produce IFNγ. This IL-18-IL-12-IL-2-NK cell IFNγ is thought to also be occurring in humans exposed to *Plasmodium* spp. infection (65, 74, 75). IL-2 produced by antigen-specific CD4 T cells augmented NK cell activation in immunized individuals. These human studies also demonstrated that different individuals had variable NK cell activation after exposure to infected erythrocytes (75). One hypothesis is that the variability in human NK cell responses is caused by polymorphisms in KIR and/or HLA genes. IL-15 is another cytokine important in NK cell development and function. The role of IL-15 in NK cell activation during *Plasmodium* spp. infection is less clear. One study showed that IL-15 enhanced NK cell IFNγ production (76). In another study $IL15^{-/-}$ DC were as good as WT DC in activating NK cell IFNγ production *in vitro* (72). This is similar to a study with *T. gondii* infection that demonstrated IL-15 is dispensable for NK cell activation (77). In response to *Plasmodium* spp. infection, NK cells are also activated by interactions with monocytes and monocyte derived DCs (70, 78). One of the interactions

is dependent upon IL-18. Another interaction is dependent upon direct macrophage to NK cell contact. This cell-to-cell interaction is thought to promote NK cell IFNγ production via interaction between LFA-1 on the macrophage and intercellular adhesion molecule-1 (ICAM-1) on the NK cell (79). In regard to cytotoxicity targeted against hepatocytes and erythrocytes, the exact mechanism of NK cell recognition of these cells remains unknown. Several studies addressed whether NK cell expression of ICAM-1, PECAM, VCAM, CD36, CSA, NKp30, NKp44, NKp46, NKG2D, and the expression of PfEMP1 or heat shock protein 70 on infected erythrocytes facilitated this interaction, however, an exact mechanism is still not known and needs further exploration (71, 79–81).

As with *T. gondii* infection, NK cells may also impact the function of other immune cells and development of adaptive immune responses to *Plasmodium* spp. infection. However, very little has been investigated about how NK cells or other ILCs are involved. NK cells may increase DC maturation and cytokine production facilitating T cell priming (72). In one study, after infection with *P. chabaudi* NK cells promoted DC maturation *in vitro*, IL-12 production and ability to prime CD4 T cells to proliferate and produce IFNγ. Another study demonstrated that NK cell activation *in vivo* was not required for DC maturation or DC-mediated priming of $CD4^+$ T cells specific for OVA antigens expressed by *P. berghei* ANKA (82). This study demonstrated that NK cells (NK1.1+) contributed to the DC-mediated priming of $CD8^+$ T cells *via* a mechanism that required IL-12. Although these studies may differ in mechanism, it appears that similar to *T. gondii* infection, activated NK cells are important for DC priming of adaptive immunity against *Plasmodium* spp. This NK cell dependent enhancement of T cell priming appears to depend upon IFNγ. Whether activated NK cells can take the place of helper T cells in helping the priming of CD8 T cells has not been addressed during *Plasmodium* spp. infection. How NK cell IFNγ could impact development of long-term immunity to *Plasmodium* spp. is also not understood. There are still many questions about the importance of NK cells in their role during *Plasmodium* spp. infection.

To date very little is known about other ILCs and *Plasmodium* spp. infection. Many of the observations about NK cells in malaria could also be attributed to other ILC subsets. Again, this is because NK cell targeting experimental strategies (phenotype: NK1.1+, *in vivo* depletion: anti-NK1.1, anti-ASGM1) also can target the other ILC populations. Evidence supporting the involvement of other ILC in immunity to *Plasmodium* spp. is found in studies elucidating the mechanisms involved in development of cerebral malaria (CM) (83). The first ILC to consider is the ILC1 because of its tissue residency in the liver and ability to produce high levels of IFNγ (84). Although NK cell IFNγ production is important for reducing parasite numbers early during infection, the IFNγ producing liver ILCs could be ILC1. T-$bet^{-/-}$ animals have elevated parasitemia after *Plasmodium berghei* ANKA infection (83). T-bet deficiency would implicate ILC1 as a controller of acute infection because development of ILC1 is T-bet dependent (15). Interestingly, although parasite burden was increased, T-bet deficiency reduced the severity of CM suggesting that T-bet dependent ILC1 development and activation could also cause immunopathology. A recent study indicates that NK cells and ILC1 are lost in peripheral blood of humans infected with *Plasmodium falciparum* and spleens and livers of mice infected with *Plasmodium chaubaudi chabaudi* AS (85). Using NKp46-iCre mice crossed onto myeloid cell leukemia sequence-1 floxed mice (Mcl1) to genetically ablate mature NK cells, there was no difference in parasitemia compared to WT controls. Using NKp46 iCre mice crossed onto TGFβR2 floxed mice to genetically ablate ILC1, again there was no difference in parasitemia. The results of these studies may suggest that early liver control by NK cells and ILC1s is important, but once the parasite reaches the blood, group 1 ILC may be less able to control the infection.

ILCs are not only important for protecting against infection, but they can also cause immunopathology associated with infections (17). As noted above, the data from studies of CM support this hypothesis (58). In CM susceptible C57BL6 mice, experimental CM is characterized by overproduction of Th1 cytokines (IFNγ, IL-12, and TNFα) (83, 86). Therefore, NK cells and ILC1 could promote CM through the production of inflammatory cytokines including IFNγ. NK cell IFNγ production has been shown to help recruit CXCR3+ T cells into the brain (86). T-bet deficient mice survived experimental CM longer but had higher parasite burdens, indirectly suggesting the potential involvement of group I ILC in contributing to CM pathogenesis (83). While group 1 ILC may be both protective and a cause of immune pathology during *Plasmodium spp.* infection, group 2 ILC may help negatively regulate inflammation and thus prevent development of CM. A recent study suggests that ILC2 may contribute to protection against development of CM (24). ILC2 are sensitive to IL-33 via the expression of the IL-33 receptor ST2 (17). Administration of IL-33 prevented development of CM (24). The therapeutic effect of IL-33 was associated with the expansion of ILC2 and their production of IL-4, IL-5, and IL-13. Adoptive transfer of ILC2 into *Plasmodium berghei* ANKA infection mice increased the frequency of alternatively activated macrophages and T regulatory cells and reduced the severity of CM.

To date there have been no published studies on group 3 ILC including ILC3 and LTi-like ILC3 and *Plasmodium* spp. infection. ILC3 can produce IL-17, IL-22 and GM-CSF in response to IL-1β and IL-23 (17, 32). Based on the function of ILC3 there could be support that they are responding during *Plasmodium* spp. infection. Whether they are protective or causing pathology has not been established. However, during malaria infection in mouse experimental models and humans IL-17 levels increase (87–89). In several cases the increased IL-17 was independent of CD4+ Th17 cells. Macrophages may be one source, but another source not measured in this study could be ILC3s (87). Whether IL-17 is protective or pathogenic is not clear because the data from multiple studies is contradictory (9, 87–91). In mice, IL-17 may help in protection because IL-17 KO mice have higher parasitemia (87). However, in a human study looking at the association of inflammation including IL-17 in Plasmodium induced multiple organ dysfunction (MOD) and CM, high levels of IL-17 in patients was associated with the highest level of MOD

(89). *Plasmodium* spp. infection of AhR KO mice, which are deficient in ILC3, were more susceptible to CM and generated higher IL-17 and IL-6 in brain (91). Lastly, IL-17 deficient and IL-23 deficient mice developed CM similarly to WT mice and similar levels of parasitemia (87, 90). Another important function of ILC3 is the maintenance of tissue immune homeostasis through IL-22 production. Two independent studies have demonstrated that in the absence of IL-22 (IL-22 KO mice) pathology cause by *Plasmodium* spp. infection is more severe (88, 92). Again, whether this IL-22 is coming from ILC3 is not known. Current information about IL-17 and IL-22 produced during *Plasmodium* spp. infection does not definitively suggest ILC3 are an important cell type for immunity. However, given the lack of ILC3 specific studies performed, their production of these cytokines may make these studies important to explore. LTi-like ILC3 have not been explored in *Plasmodium* spp. infection. Overall, even though a recent study suggests that ILCs are irrelevant (85), there are still substantial gaps in knowledge about ILCs and *Plasmodium* spp. that would be important to investigate.

Another open question that has not been investigated in *Plasmodium* spp. infection is whether and how ILC populations can regulate adaptive immune responses. ILCs can both positively and negatively regulate adaptive immunity. NK cell IFNγ may help prime T cell responses during *Plasmodium* spp. infection (72). During *T. gondii* infection, NK cells and/or other ILC produce IL-10 (55, 56). This NK cell IL-10 may negatively regulate the adaptive immune response against the parasite likely to prevent immunopathology. A recent study has now demonstrated that treatment of mice with an IL-15 complex (IL-15C) stimulates NK cells to produce IL-10 during *Plasmodium berghei* ANKA infection (93). This NK cell IL-10 was required to protect against CM. Whether NK cell or other ILC IL-10 production in response to *Plasmodium* spp. infection has an impact on development of adaptive immunity to *Plasmodium* spp. infection will be important to further explore.

ILC AND *CRYPTOSPORIDIUM*

There is very limited information of the importance of ILCs during *Cryptosporidium* spp. infection (**Figure 2**). Infection with *Cryptosporidium* spp. occurs via ingestion of oocysts in contaminated water (5). The parasite remains in the small intestine living inside of gut epithelial cells and is a major cause of diarrhea in people. Innate immunity against the parasite is important for control of the parasite, however there is still limited knowledge about the factors that are critical for this response. This is especially important to investigate because of the mucosal barrier location of the infection where NK cell, ILC1, ILC2, ILC3, and LTi-like ILC3 can all be present (15–17). The level of inflammation generated by these cells could have a positive and or negative impact on infection pathology with this parasite. Results from an early study suggested that a non T cell source of IFNγ was important for control of *Cryptosporidium* spp. infection in mice (94). Subsequent studies suggested that NK cells were not involved into the control of infection (95, 96). Anti-ASGM1 treatment of SCID mice to deplete NK cells did not result in increased infection pathology. However, more recent studies indicate that innate lymphoid cells are protective against *Cryptosporidium* spp. infection (97). Both adult $Rag2^{-/-}$ and $Rag2^{-/-}\gamma c^{-/-}$ mice developed chronic infection but parasite burdens were higher and intestinal pathology was worse in $Rag2^{-/-}\gamma c^{-/-}$ mice, which eventually succumbed to the infection. Interestingly, in contrast to adult mice, neonatal mice of both genotypes were able to survive the infection, however, $Rag2^{-/-}\gamma c^{-/-}$ had higher parasite burdens for a more extended period of time as compared to $Rag2^{-/-}$ (18). Neonatal C57BL6 mice treated with anti-NK1.1 were slower in controlling the infection and had higher parasite burdens (97). In $Rag2^{-/-}\gamma c^{-/-}$ protection was attributed to IFNγ produced by peritoneal macrophages that were IL-18 and IL-12-dependent (98). Whether NK cell IFNγ is also important for control of *Cryptosporidium* spp. infection is still not clear and needs further investigation. In addition the mechanisms by which NK cells could be activated in *Cryptosporidium* spp. infection have not been thoroughly tested. IL-12, one of the potent activators of NK cell IFNγ production, is produced and is needed for immunity against *Cryptosporidium* spp. in mice (99, 100). In humans, peripheral blood NK cells (CD3-CD16+CD56+) were shown to be cytotoxic against cryptosporidium infected intestinal epithelial cells in the presence of IL15 *in vitro* (101). IL-15 induced increased expression of NKG2D receptor on NK cells and that correlated with increased expression of the NKG2D ligands MHC class I-related molecules MICA and MICB on infected intestinal epithelial cells. This data suggests that there may be direct recognition of the infected epithelium by NK cells during this infection (101). Therefore, it is possible that IL-12 and IL-15 are important NK cell activation signals during *Cryptosporidium* spp. infection. However, this has not been thoroughly tested and whether these signals are critical for parasite control is still unclear.

Beyond this very basic knowledge about NK cells and their involvement in protection against *Cryptosporidium* spp. infection, nothing is known about other ILCs and their role in immunity against infection. In addition it has not been tested whether and how ILCs can (1) impact the function of other immune cells (monocytes, macrophages, DCs and T cells); (2) affect the pathology associated with disease; (3) positively or negatively regulate adaptive immunity to this parasite. A small hint that other ILCs may be involved was discovered in a neonatal lamb infection model of *Cryptosporidium parvum* (102). After infection of neonatal lambs, total NKp46+ cells increased in numbers. The frequency of perforin+ cells increased in NKp46+CD16+ and NKp46+CD16- subsets. In addition, IL-22 mRNA expression was upregulated in small intestines of infected lambs. Whether these NKp46+ cells were ILC3s or other ILC is not known (102). ILC3 could be responding to infection because IL-17 is produced in response to *Cryptosporidium* spp. Infection (10, 103, 104). However, no clear links have been established and more research is needed to dissect the roles of different ILCs in *Cryptosporidium* spp. infection. Elucidating the role of different ILCs in control of *Cryptosporidium* spp. could lead to better therapy and vaccine design to help treat this infection.

ILC AND *EIMERIA*

Similar to *Cryptosporidium* spp., very little is known about NK cells and other ILC and their role in protection vs. pathology during *Eimeria* spp. infection. This is a difficult infection to study ILCs because the host animals are chickens and other livestock and thus have limited reagents available. However, this is another important apicomplexan infection that could provide more insight into how the immune system functions in response to other gut tropic apicomplexans. Infection with *Eimeria* spp. occurs via ingestion of fecal matter containing oocysts of the parasite, which then cause severe inflammation in the mucosa of the gut (105). *Eimeria* spp. is a major cause of disease that can impair productivity in livestock including chickens. Similar to other apicomplexan infections, *Eimeria* spp. stimulates a very strong Th1 response that is initiated by innate immune cells that could include ILC (105). Studies investigating innate immunity to this parasite have focused mainly on NK cells and not other ILCs (**Figure 2**). Early investigations of the importance of NK cells in *Eimeria* spp. infection in mice suggested that NK cells were not involved in providing protection (106). Even though infection of BALBC mice with *E. vermifornis* induced an increase in splenic and mesenteric lymph node (MLN) NK cell cytolytic activity, treatment with anti-ASGM1 to deplete the NK cells did not increase parasite burdens in BALBC mice. A later study demonstrated that in chickens, splenic and intestinal NK cell activity via cytotoxicity as measured by ^{51}Cr-release assay decreased after primary infection followed by recovery of this activity (19). However, during secondary *Eimeria* spp. infection, NK cell activity was increased. Secondary intraepithelial lymphocyte derived NK cell activity was accompanied by increase in number of ASGM1-expressing cells. In beige/beige (bg) mice that are NK cell deficient, replication of *E. vermiformis* was reduced (107). A protective role of NK cells in the immune response against *Eimeria* spp. was demonstrated using SCID, SCID/bg and C57BL6 mice treated with anti-NK1.1 (108). After primary infection with *E. papillata*, WT mice depleted of their NK cells with anti-NK1.1 had higher parasite shedding compared to isotype control treated animals. This NK cell dependent protection may have been due to IFNγ production however this was not test directly. The mechanisms underlying the activation of NK cells during *Eimeria* spp. infection most likely involve IL-12 as it is upregulated after infection, however there are no studies that have tested this directly (109). Whether and how other cytokines and signals impact the development of NK cells responses to *Eimeria* spp. infection have not been addressed.

The role of non-NK cell ILCs has not been addressed in *Eimeria* spp. Given the gut pathology that develops in infected animals ILC1, ILC2, and ILC3 (both ILC3 and LTi-like ILC3) may be involved. Based on research into IL-17 and IL-22 production and its importance in this disease implicates ILC3 may be responding to infection (11, 110). In the absence of IFNγ signaling, mice infected with *Eimeria falciformis* had greater body weight loss and gut pathology, but had a lower parasite burden (110). In these animals IL-17A and IL-22 expression was significantly increased. Importantly antibody blockade of IL-17 and IL-22 reduced the pathology associated with infection. This infection pathology was thought to be CD4 T cell dependent because Th17 CD4 T cells expanded in the absence of IFNγ. Whether ILC3 were also producing IL-17 and IL-22 was not tested in this study. A second also demonstrated that IL-17 was a cause of gut pathology in chickens (11). Since ILC3 can help maintain tissue integrity and also cause pathology at mucosal sites, it is possible they contribute to *Eimeria* spp. associated pathology. Outstanding questions are the importance of ILC in protection and immunopathology, impact of ILC on other immune cells function and impact of ILC on positive and negative regulation of adaptive immune responses to *Eimeria* spp. Understanding their role in infection may help to develop therapies to treat this infection.

ILC AND *BABESIA*

Knowledge about ILCs and *Babesia* spp. infection is very limited. How ILC function in response to this infection is still not thoroughly explored, however, based on other apicomplexan infections, they could be very important for at least early control of *Babesia* spp. infection (**Figure 2**). *Babesia* spp. infection of humans begins after the tick *Ixodes scapularis* harboring sporozoites of the parasite has a blood meal from the host (3). Sporozoites infect RBCs where they replicate as trophozoites eventually transforming into merozoites. Blood stage infection causes hemolysis, fever and fatigue in individuals infected. Increasing rates of infection in people have been observed in endemic regions and *Babesia* spp. has severe health consequences for immunocompromised people. Interestingly, this parasite remains in the blood stream during infection and immunity seems to depend upon the spleen as splenectomyzed people are more susceptible to infection (3). NK cell activity was increased in spleen and peritoneal excudate cells (PEC) of infected with *Babesia microti* mice. However, the course of infection in NK cell deficient bg mice was unaltered (111). NK cell frequencies increased in blood, spleen, and liver of BALBC mice infected with *Babesia* spp. (112). Experiments performed in SCID mice on the C57BL6 background indicated that control of *Babesia* spp. was independent of adaptive immune cells (113). Control of *Babesia* spp. in mice was shown to be dependent upon IL-12 and IFNγ signaling because STAT4 and IFNγR2 deficient animals were more susceptible to infection (114). Loss of NK cells from anti-ASGM1 treatment also resulted in elevated susceptibility to *Babesia* spp. Infection (114). *Babesia* spp. is a dangerous pathogen for cattle (3). NK-like cells proliferated in the spleens of young calves during early response to *B. bovis* (115). Bovine splenic NK cells (NKp46+CD3-CD2+/–CD8+/–) produced IFNγ in the presence of supernatants from *Babesia bovis*-exposed monocytes in an IL-12 dependent manner (116). Bovine NK cell IFNγ production required direct cell-to-cell contact with DCs in co-culture after cytokine stimulation (117). Interestingly, bovine NK cells were more cytotoxic when co-cultured with non-cytokine stimulated DCs. Taken together as with other apicomplexans, group 1 ILCs and specifically NK cells play an important role in early control of *Babesia* spp. infection.

Whether other ILCs are responding and playing a role in *Babesia* spp. infection is not known. However, due to the location of this infection (blood and spleen) other ILC may be less important for this infection. Interestingly, *Babesia* spp. appears to predominantly induce a Th1 response as IL-17 and IL-22 levels did not significantly change in a mouse model of infection (2). More in depth investigation of ILC subsets will be needed to fully assess the role of these cells in immunity against *Babesia* spp. infection. This would include studies exploring how ILC can positively and negatively impact adaptive immune responses.

ILCS AND APICOMPLEXA CONCLUSIONS AND FUTURE DIRECTIONS

ILCs are important cells for the early control of Apicomplexan infections via their production of IFNγ (**Figure 2**). NK cells and possibly ILC1 in many of these infections are the source of this cytokine, which is made in response to IL-12, IL-15, IL-18, and IL-2. Although very few studies have dissected the importance of ILC2 and ILC3 in apicomplexan infection, there are hints that these cells are responding to these infections and could either be protective, helping to dampen inflammation (NK-ILC1-IL-10, ILC2-IL-33, ILC3-IL22) or potentiating inflammatory pathology (NK-ILC1-IFNγ ILC3-IL-17). However, there are still major gaps in knowledge for apicomplexan infections about all of the ways ILC contribute to protection and impact overall immunity to these protozoan pathogens. ILC not only provide early protection, but could also participate in the generation and maintenance of adaptive immune responses against these important parasitic infections. ILCs are important in priming T cell responses either indirectly by maturing APCs or directly via their cytokine production. Immune factors such as cytokines or signaling molecules produced by ILC could have a positive or negative impact on primed T cell long-term fate and memory differentiation. ILC could also contribute to long-term protection by developing memory-like responses to these protozoan pathogens as they do to viral infections (118). Interestingly, during *Plasmodium* spp. vaccination, memory CD4 T cells directed memory-like NK cell responses during secondary infection in vaccinated people (65). How important the ILC contribution to adaptive recall responses during all apicomplexan infections is not well-understood. Lastly, ILC could be cells that are important in honing the adaptive response against these pathogens either making the memory T cell pools better or decreasing their ability to protect against these infections and promoting parasite persistence or susceptibility to reinfection. There are several situations now known during viral infections, in the tumor microenvironment and in autoimmunity where ILC appear to have a negative impact on adaptive immune responses in these different disease situations (4, 119–129). All of these questions will be an important area of research to investigate. Results from future studies of ILC and apicomplexan infections could help improve knowledge of the biology of these complex cells and promote better therapeutic development against these important parasitic pathogens.

AUTHOR CONTRIBUTIONS

JG conceived the review. JG, DI, SD, and KF wrote the review. JG, DI, SD, KF, KS, JM, BB, and ID helped edit the review.

FUNDING

This work is supported by grants from the American Heart Association (AHA 17GRNT33700199) and NIH Wyoming INBRE DRPP P20 GM103432 awarded to JG and NIH Wyoming INBRE graduate student GA awarded to DI. This project is supported in part by a grant from the National Institute of General Medical Sciences (2P20GM103432) from the National Institutes of Health. The content is solely the responsibility of the authors and does not necessarily represent the official views of the National Institutes of Health.

REFERENCES

1. Wolf AS, Sherratt S, Riley EM. NK cells: uncertain allies against malaria. *Front Immunol.* (2017) 8:212. doi: 10.3389/fimmu.2017.00212
2. Djokic V, Akoolo L, Parveen N. *Babesia microti* infection changes host spleen architecture and is cleared by a Th1 immune response. *Front Microbiol.* (2018) 9:85. doi: 10.3389/fmicb.2018.00085
3. Westblade LF, Simon MS, Mathison BA, Kirkman LA. *Babesia microti*: from mice to ticks to an increasing number of highly susceptible humans. *J Clin Microbiol.* (2017) 55:2903–12. doi: 10.1128/JCM.00504-17
4. Gigley JP. The diverse role of nk cells in immunity to *Toxoplasma Gondii* infection. *PLoS Pathog.* (2016) 12:E1005396. doi: 10.1371/journal.ppat.1005396
5. Certad G, Viscogliosi E, Chabe M, Caccio SM. Pathogenic mechanisms of cryptosporidium and giardia. *Trends Parasitol.* (2017) 33:561–76. doi: 10.1016/j.pt.2017.02.006
6. Goff WL, Bastos RG, Brown WC, Johnson WC, Schneider DA. The bovine spleen: interactions among splenic cell populations in the innate immunologic control of hemoparasitic infections. *Vet Immunol Immunopathol.* (2010) 138:1–14. doi: 10.1016/j.vetimm.2010.07.006
7. Donley DW, Olson AR, Raisbeck MF, Fox JH, Gigley JP. Huntingtons disease mice infected with toxoplasma gondii demonstrate early kynurenine pathway activation, altered Cd8+ T-cell responses, and premature mortality. *PLoS ONE.* (2016) 11:E0162404. doi: 10.1371/journal.pone.0162404
8. Hunter CA, Sibley LD. Modulation of innate immunity by *Toxoplasma Gondii* virulence effectors. *Nat Rev Microbiol.* (2012) 10:766–78. doi: 10.1038/nrmicro2858
9. Raballah E, Kempaiah P, Karim Z, Orinda GO, Otieno MF, Perkins DJ, et al. Cd4 T-cell expression of ifn-gamma and Il-17 in pediatric malarial anemia. *PLoS ONE.* (2017) 12:E0175864. doi: 10.1371/journal.pone.0175864
10. Drinkall E, Wass MJ, Coffey TJ, Flynn RJ. A rapid Il-17 response to *Cryptosporidium parvum* in the bovine intestine. *Vet Immunol Immunopathol.* (2017) 191:1–4. doi: 10.1016/j.vetimm.2017.07.009
11. Zhang L, Liu R, Song M, Hu Y, Pan B, Cai J, et al. *Eimeria tenella*: interleukin 17 contributes to host immunopathology in the gut during experimental infection. *Exp Parasitol.* (2013) 133:121–30. doi: 10.1016/j.exppara.2012.11.009
12. Passos ST, Silver J S, O'hara AC, Sehy D, Stumhofer JS, Hunter CA. Il-6 promotes Nk cell production of Il-17 during toxoplasmosis. *J Immunol.* (2010) 184:1776–83. doi: 10.4049/jimmunol.0901843

13. Iwasaki H, Akashi K. Myeloid lineage commitment from the hematopoietic stem cell. *Immunity.* (2007) 26:726–40. doi: 10.1016/j.immuni.2007.06.004
14. Spits H, Artis D, Colonna M, Diefenbach A, Di Santo JP, Eberl G, et al. Innate lymphoid cells–a proposal for uniform nomenclature. *Nat Rev Immunol.* (2013) 13:145–9. doi: 10.1038/nri3365
15. Cortez VS, Colonna M. Diversity and function of group 1 innate lymphoid cells. *Immunol Lett.* (2016) 179:19–24. doi: 10.1016/j.imlet.2016.07.005
16. Schuijs MJ, Halim TYF. Group 2 innate lymphocytes at the interface between innate and adaptive immunity. *Ann N Y Acad Sci.* (2018) 1417:87–103. doi: 10.1111/nyas.13604
17. Withers DR, Hepworth MR. Group 3 innate lymphoid cells: communications hubs of the intestinal immune system. *Front Immunol.* (2017) 8:1298. doi: 10.3389/fimmu.2017.01298
18. Barakat FM, Mcdonald V, Di Santo JP, Korbel DS. Roles for NK cells and an NK cell-independent source of intestinal gamma interferon for innate immunity to *Cryptosporidium parvum* infection. *Infect Immun.* (2009) 77:5044–9. doi: 10.1128/IAI.00377-09
19. Lillehoj HS. Intestinal intraepithelial and splenic natural killer cell responses to eimerian infections in inbred chickens. *Infect Immun.* (1989) 57:1879–84.
20. Klose CSN, Flach M, Mohle L, Rogell L, Hoyler T, Ebert K, et al. Differentiation of type 1 Ilcs from a common progenitor to all helper-like innate lymphoid cell lineages. *Cell.* (2014) 157:340–56. doi: 10.1016/j.cell.2014.03.030
21. Gordon SM, Chaix J, Rupp LJ, Wu J, Madera S, Sun JC, et al. The transcription factors T-bet and eomes control key checkpoints of natural killer cell maturation. *Immunity.* (2012) 36:55–67. doi: 10.1016/j.immuni.2011.11.016
22. Daussy C, Faure F, Mayol K, Viel S, Gasteiger G, Charrier E, et al. T-bet and Eomes instruct the development of two distinct natural killer cell lineages in the liver and in the bone marrow. *J Exp Med.* (2014) 211:563–77. doi: 10.1084/jem.20131560
23. Lim AI, Verrier T, Vosshenrich CA, Di Santo JP. Developmental options and functional plasticity of innate lymphoid cells. *Curr Opin Immunol.* (2017) 44:61–8. doi: 10.1016/j.coi.2017.03.010
24. Besnard AG, Guabiraba R, Niedbala W, Palomo J, Reverchon F, Shaw TN, et al. IL-33-mediated protection against experimental cerebral malaria is linked to induction of type 2 innate lymphoid cells, M2 macrophages and regulatory T cells. *PLoS Pathog.* (2015) 11:e1004607. doi: 10.1371/journal.ppat.1004607
25. Jones LA, Roberts F, Nickdel MB, Brombacher F, Mckenzie AN, Henriquez FL, et al. Il-33 Receptor (T1/St2) signalling is necessary to prevent the development of encephalitis in mice infected with *Toxoplasma Gondii*. *Eur J Immunol.* (2010) 40:426–36. doi: 10.1002/eji.200939705
26. Eberl G, Di Santo JP, Vivier E. The brave new world of innate lymphoid cells. *Nat Immunol.* (2015) 16:1–5. doi: 10.1038/ni.3059
27. Bal SM, Bernink JH, Nagasawa M, Groot J, Shikhagaie MM, Golebski K, et al. IL-1beta, IL-4 and IL-12 control the fate of group 2 innate lymphoid cells in human airway inflammation in the lungs. *Nat Immunol.* (2016) 17:636–45. doi: 10.1038/ni.3444
28. Lim AI, Menegatti S, Bustamante J, Le Bourhis L, Allez M, Rogge L, et al. Il-12 drives functional plasticity of human group 2 innate lymphoid cells. *J Exp Med.* (2016) 213:569–83. doi: 10.1084/jem.20151750
29. Ohne Y, Silver JS, Thompson-Snipes L, Collet MA, Blanck JP, Cantarel BL, et al. Il-1 is a critical regulator of group 2 innate lymphoid cell function and plasticity. *Nat Immunol.* (2016) 17:646–55. doi: 10.1038/ni.3447
30. Silver JS, Kearley J, Copenhaver AM, Sanden C, Mori M, Yu L, et al. Inflammatory triggers associated with exacerbations of copd orchestrate plasticity of group 2 innate lymphoid cells in the lungs. *Nat Immunol.* (2016) 17:626–35. doi: 10.1038/ni.3443
31. Wagage S, Harms Pritchard G, Dawson L, Buza EL, Sonnenberg GF, Hunter CA. The group 3 innate lymphoid cell defect in aryl hydrocarbon receptor deficient mice is associated with t cell hyperactivation during intestinal infection. *PloS ONE.* (2015) 10:E0128335. doi: 10.1371/journal.pone.0128335
32. Melo-Gonzalez F, Hepworth MR. Functional and phenotypic heterogeneity of group 3 innate lymphoid cells. *Immunology.* (2017) 150:265–75. doi: 10.1111/imm.12697
33. Bernink JH, Krabbendam L, Germar K, De Jong E, Gronke K, Kofoed-Nielsen M, et al. Interleukin-12 and−23 control plasticity of CD127(+) group 1 and group 3 innate lymphoid cells in the intestinal lamina propria. *Immunity* (2015) 43:146–60. doi: 10.1016/j.immuni.2015.06.019
34. Dunay IR, Diefenbach A. Group 1 innate lymphoid cells in *Toxoplasma gondii* infection. *Parasite Immunol.* (2018) 40:e12516. doi: 10.1111/pim.12516
35. Hauser WEJr, Sharma SD, Remington JS. Natural killer cells induced by acute and chronic toxoplasma infection. *Cell Immunol.* (1982) 69:330–46. doi: 10.1016/0008-8749(82)90076-4
36. Denkers EY, Gazzinelli RT, Martin D, Sher A. Emergence Of Nk1.1+ cells as effectors of ifn-gamma dependent immunity to *Toxoplasma gondii* in MHC class I-deficient mice. *J Exp Med.* (1993) 178:1465–72. doi: 10.1084/jem.178.5.1465
37. Gazzinelli RT, Hieny S, Wynn TA, Wolf S, Sher A. Interleukin 12 is required for the t-lymphocyte-independent induction of interferon gamma by an intracellular parasite and induces resistance in t-cell-deficient hosts. *Proc Natl Acad Sci USA.* (1993) 90:6115–9. doi: 10.1073/pnas.90.13.6115
38. Hunter CA, Subauste CS, Van Cleave VH, Remington JS. Production of gamma interferon by natural killer cells from toxoplasma gondii-infected scid mice: regulation by interleukin-10, interleukin-12, and tumor necrosis factor alpha. *Infect Immun.* (1994) 62:2818–24.
39. Cai G, Kastelein R, Hunter CA. Interleukin-18 (IL-18) enhances innate IL-12-mediated resistance to *Toxoplasma gondii*. *Infect Immun.* (2000) 68:6932–8. doi: 10.1128/IAI.68.12.6932-6938.2000
40. Hunter CA, Chizzonite R, Remington JS. Il-1 beta is required for Il-12 to induce production of Ifn-gamma by NK cells. A role for Il-1 beta in the T cell-independent mechanism of resistance against intracellular pathogens. *J Immunol.* (1995) 155:4347–54.
41. Ivanova DL, Fatima R, Gigley JP. Comparative analysis of conventional natural killer cell responses to acute infection with *Toxoplasma Gondii* strains of different virulence. *Front Immunol.* (2016) 7:347. doi: 10.3389/fimmu.2016.00347
42. Combe CL, Curiel TJ, Moretto MM, Khan IA. NK cells help to induce CD8(+)-T-cell immunity against *Toxoplasma gondii* in the absence of CD4(+) T cells. *Infect Immun.* (2005) 73:4913–21. doi: 10.1128/IAI.73.8.4913-4921.2005
43. Goldszmid RS, Bafica A, Jankovic D, Feng CG, Caspar P, Winkler-Pickett R, et al. Tap-1 indirectly regulates Cd4+ T cell priming in toxoplasma gondii infection by controlling NK cell ifn-gamma production. *J Exp Med.* (2007) 204:2591–602. doi: 10.1084/jem.20070634
44. Guan H, Moretto M, Bzik DJ, Gigley J, Khan IA. NK cells enhance dendritic cell response against parasite antigens via Nkg2d pathway. *J Immunol.* (2007) 179:590–6. doi: 10.4049/jimmunol.179.1.590
45. Goldszmid RS, Caspar P, Rivollier A, White S, Dzutsev A, Hieny S, et al. NK cell-derived interferon-gamma orchestrates cellular dynamics and the differentiation of monocytes into dendritic cells at the site of infection. *Immunity* (2012) 36:1047–59. doi: 10.1016/j.immuni.2012.03.026
46. Askenase MH, Han SJ, Byrd AL, Morais DA Fonseca D, Bouladoux N, et al. Bone-marrow-resident NK cells prime monocytes for regulatory function during infection. *Immunity* (2015) 42:1130–42. doi: 10.1016/j.immuni.2015.05.011
47. Petit-Jentreau L, Glover C, Coombes JL. Parasitized natural killer cells do not facilitate the spread of *Toxoplasma Gondii* to the brain. *Parasite Immunol.* (2018) 40:E12522. doi: 10.1111/pim.12522
48. Sultana MA, Du A, Carow B, Angbjar CM, Weidner JM, Kanatani S, et al. Downmodulation of effector functions in nk cells upon *Toxoplasma gondii* infection. *Infect Immun.* (2017) 85:e00069–17. doi: 10.1128/IAI.00069-17
49. Ueno N, Lodoen MB, Hickey GL, Robey EA, Coombes JL. *Toxoplasma gondii*-infected natural killer cells display a hypermotility phenotype *in vivo*. *Immunol Cell Biol.* (2015) 93:508–13. doi: 10.1038/icb.2014.106
50. Harms Pritchard G, Hall AO, Christian DA, Wagage S, Fang Q, Muallem G, et al. Diverse Roles For T-Bet in the effector responses required for resistance to infection. *J Immunol.* (2015) 194:1131–40. doi: 10.4049/jimmunol.1401617
51. Tong X, Lu F. Il-33/St2 involves the immunopathology of ocular toxoplasmosis in murine model. *Parasitol Res.* (2015) 114:1897–905. doi: 10.1007/s00436-015-4377-3
52. Kelly MN, Kolls JK, Happel K, Schwartzman JD, Schwarzenberger P, Combe C, et al. Interleukin-17/Interleukin-17 receptor-mediated signaling

is important for generation of an optimal polymorphonuclear response against *Toxoplasma gondii* infection. *Infect Immun.* (2005) 73:617–21. doi: 10.1128/IAI.73.1.617-621.2005
53. Guiton R, Vasseur V, Charron S, Arias MT, Van Langendonck N, Buzoni-Gatel D, et al. Interleukin 17 receptor signaling is deleterious during *Toxoplasma gondii* infection in susceptible Bl6 mice. *J Infect Dis.* (2010) 202:427–35. doi: 10.1086/653738
54. Schulthess J, Meresse B, Ramiro-Puig E, Montcuquet N, Darche S, Begue B, et al. Interleukin-15-dependent Nkp46+ innate lymphoid cells control intestinal inflammation by recruiting inflammatory monocytes. *Immunity* (2012) 37:108–21. doi: 10.1016/j.immuni.2012.05.013
55. Perona-Wright G, Mohrs K, Szaba FM, Kummer LW, Madan R, Karp CL, et al. Systemic but not local infections elicit immunosuppressive Il-10 production by natural killer cells. *Cell Host Microbe* (2009) 6:503–12. doi: 10.1016/j.chom.2009.11.003
56. Wagage S, John B, Krock BL, Hall AO, Randall LM, Karp CL, et al. The aryl hydrocarbon receptor promotes Il-10 production by NK cells. *J Immunol.* (2014) 192:1661–70. doi: 10.4049/jimmunol.1300497
57. Gazzinelli RT, Kalantari P, Fitzgerald KA, Golenbock DT. Innate sensing of malaria parasites. *Nat Rev Immunol.* (2014) 14:744–57. doi: 10.1038/nri3742
58. Palomo J, Quesniaux VFJ, Togbe D, Reverchon F, Ryffel B. Unravelling the roles of innate lymphoid cells in cerebral malaria pathogenesis. *Parasite Immunol.* (2018) 40:e12502. doi: 10.1111/pim.12502
59. Choudhury HR, Sheikh NA, Bancroft GJ, Katz DR, De Souza JB. Early nonspecific immune responses and immunity to blood-stage nonlethal *Plasmodium yoelii* malaria. *Infect Immun.* (2000) 68:6127–32. doi: 10.1128/IAI.68.11.6127-6132.2000
60. Mohan K, Moulin P, Stevenson MM. Natural killer cell cytokine production, not cytotoxicity, contributes to resistance against blood-stage *Plasmodium chabaudi* as infection. *J Immunol.* (1997) 159:4990–8.
61. Roland J, Soulard V, Sellier C, Drapier AM, Di Santo JP, Cazenave PA, et al. NK cell responses to plasmodium infection and control of intrahepatic parasite development. *J Immunol.* (2006) 177:1229–39. doi: 10.4049/jimmunol.177.2.1229
62. Miller JL, Sack BK, Baldwin M, Vaughan AM, Kappe SH. Interferon-mediated innate immune responses against malaria parasite liver stages. *Cell Rep.* (2014) 7:436–47. doi: 10.1016/j.celrep.2014.03.018
63. Agudelo O, Bueno J, Villa A, Maestre A. High IFN-gamma and TNF production by peripheral NK cells of Colombian patients with different clinical presentation of *Plasmodium falciparum*. *Malar J.* (2012) 11:38. doi: 10.1186/1475-2875-11-38
64. Teirlinck AC, Mccall MB, Roestenberg M, Scholzen A, Woestenenk R, De Mast Q, et al. Longevity and composition of cellular immune responses following experimental *Plasmodium falciparum* malaria infection in humans. *Plos Pathog.* (2011) 7:E1002389. doi: 10.1371/journal.ppat.1002389
65. Mccall MB, Roestenberg M, Ploemen I, Teirlinck A, Hopman J, De Mast Q, et al. Memory-like Ifn-gamma response by nk cells following malaria infection reveals the crucial role of t cells in NK cell activation by *P. falciparum*. *Eur J Immunol.* (2010) 40:3472–7. doi: 10.1002/eji.201040587
66. Artavanis-Tsakonas K, Riley EM. Innate immune response to malaria: rapid induction of IFN-gamma from human NK cells by live *Plasmodium falciparum*-infected erythrocytes. *J Immunol.* (2002) 169:2956–63. doi: 10.4049/jimmunol.169.6.2956
67. Hermsen CC, Konijnenberg Y, Mulder L, Loe C, Van Deuren M, Van Der Meer JW, et al. Circulating concentrations of soluble granzyme A and B increase during natural and experimental *Plasmodium falciparum* infections. *Clin Exp Immunol.* (2003) 132:467–72. doi: 10.1046/j.1365-2249.2003.02160.x
68. Orago AS, Facer CA. Cytotoxicity of human natural killer (Nk) cell subsets for *Plasmodium falciparum* erythrocytic schizonts: stimulation by cytokines and inhibition by neomycin. *Clin Exp Immunol.* (1991) 86:22–9. doi: 10.1111/j.1365-2249.1991.tb05768.x
69. Korbel DS, Newman KC, Almeida CR, Davis DM, Riley EM. Heterogeneous human NK cell responses to *Plasmodium falciparum*-infected erythrocytes. *J Immunol.* (2005) 175:7466–73. doi: 10.4049/jimmunol.175.11.7466
70. Baratin M, Roetynck S, Lepolard C, Falk C, Sawadogo S, Uematsu S, et al. Natural killer cell and macrophage cooperation in MyD88-dependent innate responses to *Plasmodium falciparum*. *Proc Natl Acad Sci USA* (2005) 102:14747–52. doi: 10.1073/pnas.0507355102
71. Chen Q, Amaladoss A, Ye W, Liu M, Dummler S, Kong F, et al. Human natural killer cells control *Plasmodium falciparum* infection by eliminating infected red blood cells. *Proc Natl Acad Sci USA*. (2014) 111:1479–84. doi: 10.1073/pnas.1323318111
72. Ing R, Stevenson MM. Dendritic cell and NK cell reciprocal cross talk promotes gamma interferon-dependent immunity to blood-stage *Plasmodium chabaudi* as infection in mice. *Infect Immun.* (2009) 77:770–82. doi: 10.1128/IAI.00994-08
73. Stegmann KA, De Souza JB, Riley EM. Il-18-induced expression of high-affinity Il-2r on murine NK cells is essential for NK-cell Ifn-gamma production during murine *Plasmodium yoelii* infection. *Eur J Immunol.* (2015) 45:3431–40. doi: 10.1002/eji.201546018
74. Horowitz A, Hafalla JC, King E, Lusingu J, Dekker D, Leach A, et al. Antigen-specific Il-2 secretion correlates with NK cell responses after immunization of tanzanian children with the Rts,S/As01 malaria vaccine. *J Immunol.* (2012) 188:5054–62. doi: 10.4049/jimmunol.1102710
75. Artavanis-Tsakonas K, Eleme K, Mcqueen KL, Cheng NW, Parham P, Davis DM, et al. Activation of a subset of human NK cells upon contact with *Plasmodium falciparum*-infected erythrocytes. *J Immunol.* (2003) 171:5396–405. doi: 10.4049/jimmunol.171.10.5396
76. Ing R, Gros P, Stevenson MM. Interleukin-15 enhances innate and adaptive immune responses to blood-stage malaria infection in mice. *Infect Immun.* (2005) 73:3172–7. doi: 10.1128/IAI.73.5.3172-3177.2005
77. Lieberman LA, Villegas EN, Hunter CA. Interleukin-15-deficient mice develop protective immunity to *Toxoplasma gondii*. *Infect Immun.* (2004) 72:6729–32. doi: 10.1128/IAI.72.11.6729-6732.2004
78. Newman KC, Korbel DS, Hafalla JC, Riley EM. Cross-talk with myeloid accessory cells regulates human natural killer cell interferon-gamma responses to malaria. *PLoS Pathog.* (2006) 2:E118. doi: 10.1371/journal.ppat.0020118
79. Baratin M, Roetynck S, Pouvelle B, Lemmers C, Viebig NK, Johansson S, et al. Dissection of the role of PfEMP1 and ICAM-1 in the sensing of *Plasmodium-falciparum*-infected erythrocytes by natural killer cells. *PLoS ONE.* (2007) 2:e228. doi: 10.1371/journal.pone.0000228
80. Mavoungou E, Held J, Mewono L, Kremsner PG. A duffy binding-like domain is involved in the Nkp30-mediated recognition of *Plasmodium falciparum*-parasitized erythrocytes by natural killer cells. *J Infect Dis.* (2007) 195:1521–31. doi: 10.1086/515579
81. Bottger E, Multhoff G, Kun JF, Esen M. *Plasmodium falciparum*-infected erythrocytes induce granzyme B by NK cells through expression of host-Hsp70. *PLoS ONE.* (2012) 7:e33774. doi: 10.1371/journal.pone.0033774
82. Ryg-Cornejo V, Nie CQ, Bernard NJ, Lundie RJ, Evans KJ, Crabb BS, et al. NK cells and conventional dendritic cells engage in reciprocal activation for the induction of inflammatory responses during *Plasmodium berghei* anka infection. *Immunobiology* (2013) 218:263–71. doi: 10.1016/j.imbio.2012.05.018
83. Oakley MS, Sahu BR, Lotspeich-Cole L, Solanki NR, Majam V, Pham PT, et al. The transcription factor T-bet regulates parasitemia and promotes pathogenesis during *Plasmodium berghei* anka murine malaria. *J Immunol.* (2013) 191:4699–708. doi: 10.4049/jimmunol.1300396
84. Spits H, Bernink JH, Lanier L. NK cells and type 1 innate lymphoid cells: partners in host defense. *Nat Immunol.* (2016) 17:758–64. doi: 10.1038/ni.3482
85. Ng SS, Souza-Fonseca-Guimaraes F, Rivera FL, Amante FH, Kumar R, Gao Y, et al. Rapid loss of group 1 innate lymphoid cells during blood stage plasmodium infection. *Clin Transl Immunol.* (2018) 7:E1003. doi: 10.1002/cti2.1003
86. Hansen DS, Bernard NJ, Nie CQ, Schofield L. NK cells stimulate recruitment of Cxcr3+ T cells to the brain during *Plasmodium berghei*-mediated cerebral malaria. *J Immunol.* (2007) 178:5779–88. doi: 10.4049/jimmunol.178.9.5779
87. Ishida H, Matsuzaki-Moriya C, Imai T, Yanagisawa K, Nojima Y, Suzue K, et al. Development of experimental cerebral malaria is independent Of Il-23 AND Il-17. *Biochem Biophys Res Commun.* (2010) 402:790–5. doi: 10.1016/j.bbrc.2010.10.114
88. Mastelic B, Do Rosario AP, Veldhoen M, Renauld JC, Jarra W, Sponaas AM, et al. Il-22 protects against liver pathology and lethality of an

experimental blood-stage malaria infection. *Front Immunol.* (2012) 3:85. doi: 10.3389/fimmu.2012.00085
89. Herbert F, Tchitchek N, Bansal D, Jacques J, Pathak S, Becavin C, et al. Evidence Of Il-17, Ip-10, and Il-10 involvement in multiple-organ dysfunction and Il-17 pathway in acute renal failure associated to *Plasmodium falciparum* malaria. *J Transl Med.* (2015) 13:369. doi: 10.1186/s12967-015-0731-6
90. Ishida H, Imai T, Suzue K, Hirai M, Taniguchi T, Yoshimura A, et al. Il-23 protection against *Plasmodium berghei* infection in mice is partially dependent on Il-17 from macrophages. *Eur J Immunol.* (2013) 43:2696–706. doi: 10.1002/eji.201343493
91. Brant F, Miranda AS, Esper L, Rodrigues DH, Kangussu LM, Bonaventura D, et al. Role of the aryl hydrocarbon receptor in the immune response profile and development of pathology during *Plasmodium berghei* anka infection. *Infect Immun.* (2014) 82:3127–40. doi: 10.1128/IAI.01733-14
92. Sellau J, Alvarado CF, Hoenow S, Mackroth MS, Kleinschmidt D, Huber S, et al. Il-22 dampens the T cell response in experimental malaria. *Sci Rep.* (2016) 6:28058. doi: 10.1038/srep28058
93. Burrack KS, Huggins MA, Taras E, Dougherty P, Henzler CM, Yang R, et al. Interleukin-15 complex treatment protects mice from cerebral malaria by inducing interleukin-10-producing natural killer cells. *Immunity* (2018) 48:e4. doi: 10.1016/j.immuni.2018.03.012
94. Ungar BL, Kao TC, Burris JA, Finkelman FD. Cryptosporidium infection in an adult mouse model. independent roles for Ifn-gamma and Cd4+ T lymphocytes in protective immunity. *J Immunol.* (1991) 147:1014–22.
95. Mcdonald V, Bancroft GJ. Mechanisms of innate and acquired resistance to *Cryptosporidium parvum* infection in scid mice. *Parasite Immunol.* (1994) 16:315–20. doi: 10.1111/j.1365-3024.1994.tb00354.x
96. Rohlman VC, Kuhls TL, Mosier DA, Crawford DL, Greenfield RA. *Cryptosporidium parvum* infection after abrogation of natural killer cell activity in normal and severe combined immunodeficiency mice. *J Parasitol.* (1993) 79:295–7. doi: 10.2307/3283525
97. Korbel DS, Barakat FM, Di Santo JP, Mcdonald V. Cd4+ T cells are not essential for control of early acute *Cryptosporidium parvum* infection in neonatal mice. *Infect Immun.* (2011) 79:1647–53. doi: 10.1128/IAI.00922-10
98. Choudhry N, Petry F, Van Rooijen N, Mcdonald V. A protective role for interleukin 18 in interferon gamma-mediated innate immunity to *Cryptosporidium parvum* that is independent of natural killer cells. *J Infect Dis.* (2012) 206:117–24. doi: 10.1093/infdis/jis300
99. Urban JF Jr, Fayer R, Chen SJ, Gause WC, Gately MK, Finkelman FD. Il-12 Protects immunocompetent and immunodeficient neonatal mice against infection with *Cryptosporidium parvum*. *J Immunol.* (1996) 156:263–8.
100. Takeda K, Omata Y, Koyama T, Ohtani M, Kobayashi Y, Furuoka H, et al. Increase Of Th1 type cytokine mRNA expression in peripheral blood lymphocytes of calves experimentally infected with *Cryptosporidium parvum*. *Vet Parasitol.* (2003) 113:327–31. doi: 10.1016/S0304-4017(03)00080-3
101. Dann SM, Wang HC, Gambarin KJ, Actor JK, Robinson P, Lewis DE, et al. Interleukin-15 activates human natural killer cells to clear the intestinal protozoan cryptosporidium. *J Infect Dis.* (2005) 192:1294–302. doi: 10.1086/444393
102. Olsen L, Akesson CP, Storset AK, Lacroix-Lamande S, Boysen P, Metton C, et al. The early intestinal immune response in experimental neonatal ovine cryptosporidiosis is characterized by an increased frequency of perforin expressing Ncr1(+) NK cells and by Ncr1(-) Cd8(+) cell recruitment. *Vet Res.* (2015) 46:28. doi: 10.1186/s13567-014-0136-1
103. Zhao GH, Cheng WY, Wang W, Jia YQ, Fang YQ, Du SZ, et al. The expression dynamics of Il-17 and Th17 response relative cytokines in the trachea and spleen of chickens after infection with *Cryptosporidium baileyi*. *Parasit Vectors* (2014) 7:212. doi: 10.1186/1756-3305-7-212
104. Zhao GH, Fang YQ, Ryan U, Guo YX, Wu F, Du SZ, et al. Dynamics Of Th17 associating cytokines in *Cryptosporidium parvum*-infected mice. *Parasitol Res.* (2016) 115:879–87. doi: 10.1007/s00436-015-4831-2
105. Lillehoj HS, Trout JM. Avian gut-associated lymphoid tissues and intestinal immune responses to eimeria parasites. *Clin Microbiol Rev.* (1996) 9:349–60. doi: 10.1128/CMR.9.3.349
106. Smith AL, Rose ME, Wakelin D. The role of natural killer cells in resistance to coccidiosis: investigations in a murine model. *Clin Exp Immunol.* (1994) 97:273–9. doi: 10.1111/j.1365-2249.1994.tb06080.x
107. Rose ME, Hesketh P, Wakelin D. Cytotoxic effects of natural killer cells have no significant role in controlling infection with the intracellular protozoon eimeria vermiformis. *Infect Immun.* (1995) 63:3711–4.
108. Schito ML, Barta JR. Nonspecific Immune responses and mechanisms of resistance to eimeria papillata infections in mice. *Infect Immun.* (1997) 65:3165–70.
109. Rosenberg B, Juckett DA, Aylsworth CF, Dimitrov NV, Ho SC, Judge JW, et al. Protein from intestinal eimeria protozoan stimulates Il-12 release from dendritic cells, exhibits antitumor properties *in vivo* and is correlated with low intestinal tumorigenicity. *Int J Cancer* (2005) 114:756–65. doi: 10.1002/ijc.20801
110. Stange J, Hepworth MR, Rausch S, Zajic L, Kuhl AA, Uyttenhove C, et al. Il-22 mediates host defense against an intestinal intracellular parasite in the absence of ifn-gamma at the cost of Th17-driven immunopathology. *J Immunol.* (2012) 188:2410–8. doi: 10.4049/jimmunol.1102062
111. Wood PR, Clark IA. Apparent irrelevance of NK cells to resolution of infections with *Babesia microti* And *Plasmodium vinckei* petteri in mice. *Parasite Immunol.* (1982) 4:319–27. doi: 10.1111/j.1365-3024.1982.tb00443.x
112. Igarashi I, Honda R, Shimada T, Miyahara K, Sakurai H, Saito A, et al. Changes of lymphocyte subpopulations and natural killer cells in mice sensitized with toxoplasma lysate antigen before and after babesia infection. *Nihon Juigaku Zasshi* (1990) 52:969–77. doi: 10.1292/jvms1939.52.969
113. Aguilar-Delfin I, Homer MJ, Wettstein PJ, Persing DH. Innate resistance to Babesia infection is influenced by genetic background and gender. *Infect Immun.* (2001) 69:7955–8. doi: 10.1128/IAI.69.12.7955-7958.2001
114. Aguilar-Delfin I, Wettstein PJ, Persing DH. Resistance to acute babesiosis is associated with interleukin-12- and gamma interferon-mediated responses and requires macrophages and natural killer cells. *Infect Immun.* (2003) 71:2002–8. doi: 10.1128/IAI.71.4.2002-2008.2003
115. Goff WL, Johnson WC, Horn RH, Barrington GM, Knowles DP. The innate immune response in calves to boophilus microplus tick transmitted *Babesia bovis* involves type-1 cytokine induction and NK-like cells in the spleen. *Parasite Immunol.* (2003) 25:185–8. doi: 10.1046/j.1365-3024.2003.00625.x
116. Goff WL, Storset AK, Johnson WC, Brown WC. Bovine splenic NK cells synthesize ifn-gamma in response To Il-12-containing supernatants from *Babesia bovis*-exposed monocyte cultures. *Parasite Immunol.* (2006) 28:221–8. doi: 10.1111/j.1365-3024.2006.00830.x
117. Bastos RG, Johnson WC, Mwangi W, Brown WC, Goff WL. Bovine NK cells acquire cytotoxic activity and produce IFN-gamma after stimulation by *Mycobacterium bovis* BCG- or *Babesia bovis*-exposed splenic dendritic cells. *Vet Immunol Immunopathol.* (2008) 124:302–12. doi: 10.1016/j.vetimm.2008.04.004
118. Sun JC, Ugolini S, Vivier E. Immunological memory within the innate immune system. *Embo J.* (2014) 33:1295–303. doi: 10.1002/embj.201387651
119. Kwong B, Rua R, Gao Y, Flickinger JJr, Wang Y, Kruhlak MJ, et al. T-bet-dependent Nkp46+ innate lymphoid cells regulate the onset of Th17-induced neuroinflammation. *Nat Immunol.* (2017) 18:1117–27. doi: 10.1038/ni.3816
120. Crome SQ, Nguyen LT, Lopez-verges S, Yang SY, Martin B, Yam JY, et al. A distinct innate lymphoid cell population regulates tumor-associated T cells. *Nat Med.* (2017) 23:368–75. doi: 10.1038/nm.4278
121. Rydyznski C, Daniels KA, Karmele EP, Brooks TR, Mahl SE, Moran MT, et al. Generation of cellular immune memory and B-cell immunity is impaired by natural killer cells. *Nat Commun.* (2015) 6:6375. doi: 10.1038/ncomms7375
122. Cook KD, Kline HC, Whitmire JK. NK cells inhibit humoral immunity by reducing the abundance of CD4+ T follicular helper cells during a chronic virus infection. *J Leukoc Biol.* (2015) 98:153–62. doi: 10.1189/jlb.4HI1214-594R
123. Crouse J, Xu HC, Lang PA, Oxenius A. NK cells regulating T cell responses: mechanisms and outcome. *Trends Immunol.* (2015) 36:49–58. doi: 10.1016/j.it.2014.11.001
124. Waggoner SN, Daniels KA, Welsh RM. Therapeutic depletion of natural killer cells controls persistent infection. *J Virol.* (2014) 88:1953–60. doi: 10.1128/JVI.03002-13

125. Xu HC, Grusdat M, Pandyra AA, Polz R, Huang J, Sharma P, et al. Type I interferon protects antiviral Cd8+ T cells from NK cell cytotoxicity. *Immunity* (2014) 40:949–60. doi: 10.1016/j.immuni.2014.05.004
126. Schuster IS, Wikstrom ME, Brizard G, Coudert JD, Estcourt MJ, Manzur M, et al. Trail+ NK cells control Cd4+ T cell responses during chronic viral infection to limit autoimmunity. *Immunity* (2014) 41:646–56. doi: 10.1016/j.immuni.2014.09.013
127. Peppa D, Gill US, Reynolds G, Easom NJ, Pallett LJ, Schurich A, et al. Up-regulation of a death receptor renders antiviral t cells susceptible to NK cell-mediated deletion. *J Exp Med.* (2013) 210:99–114. doi: 10.1084/jem.20121172
128. Cook KD, Whitmire JK. The depletion of NK cells prevents T cell exhaustion to efficiently control disseminating virus infection. *J Immunol.* (2013) 190:641–9. doi: 10.4049/jimmunol.1202448
129. Lang PA, Lang KS, Xu HC, Grusdat M, Parish IA, Recher M, et al. Natural killer cell activation enhances immune pathology and promotes chronic infection by limiting Cd8+ T-cell immunity. *Proc Natl Acad Sci USA*. (2012) 109:1210–5. doi: 10.1073/pnas.1118834109

Conflict of Interest Statement: The authors declare that the research was conducted in the absence of any commercial or financial relationships that could be construed as a potential conflict of interest.

frontiers in Immunology

REVIEW
published: 27 July 2018
doi: 10.3389/fimmu.2018.01734

Oral Versus Intragastric Inoculation: Similar Pathways of *Trypanosoma cruzi* Experimental Infection? From Target Tissues, Parasite Evasion, and Immune Response

*Juliana Barreto de Albuquerque[1], Danielle Silva dos Santos[2], Jens V. Stein[1] and Juliana de Meis[2,3]**

[1] Theodor Kocher Institute, University of Bern, Bern, Switzerland, [2] Laboratory on Thymus Research, Oswaldo Cruz Institute, Oswaldo Cruz Foundation, Rio de Janeiro, Brazil, [3] National Institute of Science and Technology on Neuroimmunomodulation (INCT-NIM), Rio de Janeiro, Brazil

OPEN ACCESS

Edited by:
Xun Suo,
China Agricultural University, China

Reviewed by:
Phileno Pinge-Filho,
Universidade Estadual de Londrina, Brazil
Marisa Mariel Fernandez,
Instituto de Estudios de la Inmunidad Humoral (IDEHU), Argentina

***Correspondence:**
Juliana de Meis
jdemeis@ioc.fiocruz.br

Specialty section:
This article was submitted to Microbial Immunology, a section of the journal Frontiers in Immunology

Received: 30 May 2018
Accepted: 13 July 2018
Published: 27 July 2018

Citation:
Barreto de Albuquerque J, Silva dos Santos D, Stein JV and de Meis J (2018) Oral Versus Intragastric Inoculation: Similar Pathways of Trypanosoma cruzi Experimental Infection? From Target Tissues, Parasite Evasion, and Immune Response. Front. Immunol. 9:1734. doi: 10.3389/fimmu.2018.01734

Currently, oral infection is the most frequent transmission mechanism of Chagas disease in Brazil and others Latin American countries. This transmission pathway presents increased mortality rate in the first 2 weeks, which is higher than the calculated mortality after the biting of infected insect vectors. Thus, the oral route of *Trypanosoma cruzi* infection, and the consequences in the host must be taken into account when thinking on the mechanisms underlying the natural history of the disease. Distinct routes of parasite entry may differentially affect immune circuits, stimulating regional immune responses that impact on the overall profile of the host protective immunity. Experimental studies related to oral infection usually comprise inoculation in the mouth (oral infection, OI) or gavage (gastrointestinal infection, GI), being often considered as similar routes of infection. Hence, establishing a relationship between the inoculation site (OI or GI) with disease progression and the mounting of *T. cruzi*-specific regional immune responses is an important issue to be considered. Here, we provide a discussion on studies performed in OI and GI in experimental models of acute infections, including *T. cruzi* infection.

Keywords: *Trypanosoma cruzi*, oral cavity, intragastric infection, immune response, T cell activation

INTRODUCTION

Chagas disease, or American trypanosomiasis, caused by the hemoflagellate protozoan *Trypanosoma cruzi*, is a tropical neglected illness *Trypanosoma cruzi* (*T. cruzi*). Infection was initially enzooty and maintained among wild animals and insect vectors of the *Reduviidae* family. Deforestation in rural areas allowed vectors to invade human homes (1, 2).

Chagas disease transmission to humans can be classified in primary (vectorial, blood transfusion, congenital, and orally) and secondary (less frequent, such as laboratory accident, handling of infected animals, organ transplantation from infected donors, and hypothetically through sexual) routes of *T. cruzi* infection (3, 4). Different transmission routes present variable incubation period, such as oral, 3–22 days; vector feces near the bite, 4–15 days; blood transfusion, 8–120 days; and organ transplantation, 23–420 days (5–9). Besides the transmission pathway, mortality rates depend

also on the patients' clinical condition and on the time between disease diagnosis and beginning of treatment. Oral transmission results in a higher mortality, estimated between 8 and 35%, than the classical vector-borne infection (<5–10%) (5, 7–10).

From 1990 to 1993, the Brazilian Health Minister started to insert the Notifiable Diseases System of Information-SINAN (DATASUS) to control the number of acute cases in the country. Although underestimated, from 2002 to 2006 Brazil registered 2510 cases of acute Chagas disease according to the DATASUS system. Number of notifications decreased at the time that the pan-American Health Organization registered the interruption of *Triatoma infestans* population in the area in 2006 (11); however, numbers still reached 1,539 new cases in the DATASUS from 2007 to 2014. Nowadays, oral transmission of Chagas disease is the most frequent transmission route in the Brazilian Amazon region (12). Food/beverages contamination with *T. cruzi*-infected insect excreta, macerate, or reservoir meal is responsible for oral transmission in one to more than a hundred cases (outbreaks). It is noteworthy that oral transmission has been associated with high mortality and morbidity, including increased prevalence and severity of the cardiac pathology (myocarditis) (13–16). Argentina, Bolivia, Colombia, Ecuador, French Guiana, and Venezuela have also reported acute Chagas disease outbreaks associated with contaminated food consumption [revised in Ref. (11, 17)]. Fruits pasteurization is the appropriate pathway to kill the parasite, and it has been shown that outbreaks of oral infection in Brazilian Amazonia increase with seasonal months of higher açaí pulp production. Moreover, epidemiological data suggest that in the Pará state most of the cases are caused by consumption of artisanal açaí. Therefore, good practices of quality control could avoid the transmission, such as good agricultural practice and "bleaching" or "whitening" of the fruits (12, 18).

The infection is presently considered as a worldwide health problem with deficiencies in treatment, absence of vaccines, and world spreading (19–22).

PARASITE–HOST INTERACTION AND TARGET TISSUES

T. cruzi presents one of the most complex life cycles among the trypanosomatids, alternating between vertebrate hosts, which comprises a wide range of mammals including humans and invertebrate hematophagous insects from the Reduviidae family (23, 24). Mammalian cell invasion by the *T. cruzi* is critical to its survival in the host. Once inside the vertebrate host, the metacyclic trypomastigotes are able to infect several nucleated mammalian cells at the inoculation site, such as macrophages, fibroblasts, epithelial cells, and others. The intracellular cycle in a mammalian cell presents different steps and begins at the moment that infective forms of *T. cruzi* interact with phagocytic or non-phagocytic surface molecules. These processes lead to cell signaling and internalization of the parasite through multiple endocytic pathways (25–27). *T. cruzi* proteins such as gp82, gp80, gp35/50, gp85, trans-sialidase, and host cell adhesion molecules such as mucins, VLA (very late antigen), and extracellular matrix proteins (ECM) such as laminin and fibronectin have been reported to contribute to parasite infection (23, 25, 28–33). In addition, *T. cruzi* proteases as cruzipain, oligopeptidase B, and Tc80 have been implicated in *T. cruzi* internalization (23, 31). In addition to presenting a large variety of surface molecules that can participate in host–parasite interaction, strain and forms (metacyclic trypomastigotes, tissue culture-derived trypomastigotes, and amastigotes) of the parasite differently express these molecules in the membrane. The capacity of trypomastigotes to interact with a diverse number of molecules on cell surface is determinant to improve invasion processes and allows the parasite to explore survival and multiplicative strategies in the host (23, 31, 34).

It is believed that any mammalian host cell class of molecules in the membrane are potential partners for *T. cruzi* recognition, and the expression of these molecules can vary depending on the cell type involved. Well-characterized groups of receptor are carbohydrates that contain galactosyl, mannosyl, and sialyl residues and lectin-like proteins (23, 26). Interestingly, *T. cruzi* is either able to use and increase expression of ECM in the host cell during the initial process of infection. Regarding *T. cruzi* surface molecules, it has been shown that trypomastigote forms present motifs that bind to cytokeratin 18, fibronectin, laminin, heparan sulfate proteoglycans, and integrins (35, 36).

The components involved in *T. cruzi* oral infection were suggested in experimental models. Hoft and colleagues demonstrated by histological analysis that after oral infection, *T. cruzi* invades and replicates inside epithelial cells within the gastric mucosa. This initial invasion is followed by the establishment of a progressive gastritis and further systemic dissemination of the parasite. Furthermore, hypertrophy and the presence of parasites in adjacent lymph nodes of stomach and inflammatory infiltrates in various organs (pancreas, liver, spleen, bone marrow, heart, duodenum, adrenal, brain, and/or skeletal muscle) were also described. Amastigote nests were detected in the gastric mucosal epithelium, but not in the upper gastrointestinal tract, like esophagus and oropharynx after oral infection. These data suggested that oral infection initiates in gastric mucosal followed by systemic dissemination (37).

Analysis of molecular mechanisms involved in *T. cruzi* interaction with host cells during oral infection is under investigation. It has been suggested that gastric epithelium express mucins that interacts with *T. cruzi* glycoproteins, such as gp82 and gp30, triggering a cascade of intracellular signaling in the parasite and at the host cell, leading to the mobilization of intracellular Ca^{2+} that is essential for parasite internalization (32, 34, 38, 39).

In line with this, previous studies of intrapharyngeal infection in mice, and *in vitro* studies of human epithelial cells have demonstrated the key role of glycoprotein gp82 during *T. cruzi* invasion in gastric of mucosal (40). Gp82 is present in metacyclic trypomastigotes forms, but not in amastigotes, epimastigotes, or tissue culture-derived trypomastigotes forms (41, 42). Interestingly, gp82 expressed in different *T. cruzi* strains is resistant to degradation by pepsin or proteinase K (43, 44). Metacyclic forms of *T. cruzi* recovered from the stomach 1 h after an intrapharyngeal inoculation in mice preserve the gp82 intact, and the parasite infectivity was not altered. Furthermore, *T. cruzi* gp82$^{-/-}$ metacyclic forms have reduced gastric mucin-binding capacity, less efficient migration through the gastric mucin-coated and low

infectivity in mice by the intrapharyngeal route when compared with metacyclic forms that express gp82 (44, 45).

GP30 is another glycoprotein involved in *T. cruzi* interaction with the gastric epithelium, binding the target cells in a receptor-dependent manner, inducing Ca^{2+} response and lysosome exocytosis, both required for the parasite internalization in the cell (44, 45). Interestingly, gp30 shows a lower affinity to gastric mucin-binding proteins as compared to gp82, and this seems to be associated with low infective capacity of gp82-deficient strains *in vivo* (45, 46). Different isolates of Y strain differ in the expression of gp82 and gp30 surface molecules and the ability to infect mice by the intragastric/intrapharyngeal inoculation (46).

The infection process is also influenced by gp90, a metacyclic stage-specific molecule, that binds to mammalian cells in receptor-dependent manner but, differently from gp82, this protein is unable to trigger Ca^{2+} signal and downmodulates the parasite cell invasion capacity (47). It has been shown that *T. cruzi* strains that express high levels of gp90 on the surface, in addition to gp82 and gp30, have low cellular infection capacity *in vitro*. However, recent *in vivo* studies indicated that infectivity of *T. cruzi* is also influenced by the susceptibility of g90 molecules to peptic digestion. *T. cruzi* strains expressing pepsin-resistant gp90 isoform show a low capacity to invade gastric mucosal epithelium after intrapharyngeal inoculation in mice, resulting in subpatent or low parasitemia. By contrast, *T. cruzi* strains expressing pepsin-susceptible gp90 produced high parasitemia and high mortality when given to mice by the intrapharyngeal route (43). In addition, analysis of extracellular vesicles and soluble proteins released by metacyclic trypomastigotes forms of *T. cruzi* has revealed presence of gp82 and gp90 surface molecules in these compartments (48, 49).

A variety number of molecules involved in parasite–host cell interactions are potential candidates in oral infection. During the oral infection, parasites come across different cells throughout the gastrointestinal tract, from tissues as the mouth to intestines. In previous data, Diaz-Ungría and Bracho showed signs of a possible *T. cruzi* penetration in the oral, esophageal, gastric, and intestinal mucosa with local eosinophilia, infiltrated lymphocytes and monocytes in histological sections from dogs after oral infection (50). We have recently demonstrated that the site of parasite entrance, through the mouth (oral infection—OI), which is more similar to natural infection, versus gastrointestinal infection (GI) promotes different host immune response and mortality. Thus, compared with GI mice, OI mice presented elevated infection rate, parasitemia, and higher Th1 cytokines (51) (**Figures 1A,B**). This distinct immunological response and infection severity according to the different mucosal pathways highlighted important considerations concerning the primary site of *T. cruzi* infection in the oral route and indicated that the pathophysiology in this model may not be the same when parasites are administrated into the oral cavity or by gavage into the stomach (intrapharyngeal/intragastric).

In a recent study, the site of parasite entry in OI mice, inoculating *T. cruzi* directly in the mouth and analyzing by bioluminescence imaging corroborates the hypothesis that oral cavity is a potential critical site of initial *T. cruzi* infection before spreading to other organs in the acute phase. Moreover, OI leads to *T. cruzi* entrance in the palate, multiplication at the nasal cavity and dissemination to central nervous system and peripheral tissues. These evidences suggest that oral cavity is the primary site of infection and the nasal cavity comprises most of the parasite replication (52) (**Figures 1C,D**). Interestingly, facial edema and paresthesia of the tongue were already described in patients infected with *T. cruzi* by the oral route (53).

The mouth/oral cavity is also a target tissue for different viral, bacterial, and fungal infections disease, such as Herpes virus type 1 and 2, *Helicobacter pylori*, *Candida albicans*, and others disease (54–56). The oral cavity contains distinct mucosal surfaces and molecules expression, such as mucins, in which microorganisms can bind and, consequently colonize this anatomical region (57). The oral mucosa is coated by a film of mucus consisting of lipids, glycosylated proteins, such as mucin immunoglobulins, as well as growth factors and others. The mucins are considered as the first line of defense in the oral cavity, preventing the attachment of certain pathogens to the epithelium or forming aggregates facilitating the elimination of pathogens by the organism. However, some pathogens can bind in the carbohydrate structures present in the mucins, such as sialic acids, which favors access to epithelial cells and cell invasion (57–59).

Previous data demonstrated that *Streptococcus* sp. binds to salivary mucins on the surface of the tooth, being one of the first steps in the formation of dental plaque (60). Studies using *Tannerella forsythia*, one of the major bacterial pathogens associated with periodontitis, uncovered that glycoprotein-associated sialic acid in terminal sugars on the surface of oral cavity epithelium is important for the adhesion and invasion of these bacteria. In this study, parasite inactivation by mutation or inhibition of NanH sialidase decreased the adhesion and invasion of *T. forsythia* in human gingival epithelial cell culture lines (OBA-9). The NanH sialidase activity is specific for α-2,3 sialic acid present on the surface of gingival epithelial cells, suggesting its role in parasite adhesion and invasion (61, 62).

In line with these findings, Lakdawala and colleagues demonstrated that the soft palate is a relevant focus of influenza viruses' infection. The soft palate is a mucin-rich environment, which favors the infection and may contribute to airborne transmission. Furthermore, the expression of α-2,3 sialic acids, the viral hemagglutinin ligands, is detected on the soft palate, in the regions of the oral surface and the nasopharyngeal tissues from humans and ferret (63).

Interestingly, α-2,3 sialic acids are the main molecule involved in *T. cruzi* trans-sialidase-mediated binding. Trans-sialidase are considered as an important virulence factor, since this enzyme is able to reduce host cell immune response and mediates *T. cruzi* and host cells adhesion (33). It has been shown that trans-sialidase binds to host sialoglycans, generating "eat me" signals in epithelial cells, which facilitates parasite entry into non-phagocytic cells (64). Notably, the mouth seems to be a potential source of infection and this knowledge contributes to the elucidation of the target tissue/organs and the molecular components regulating the establishment of *T. cruzi* oral infection and its pathogenesis.

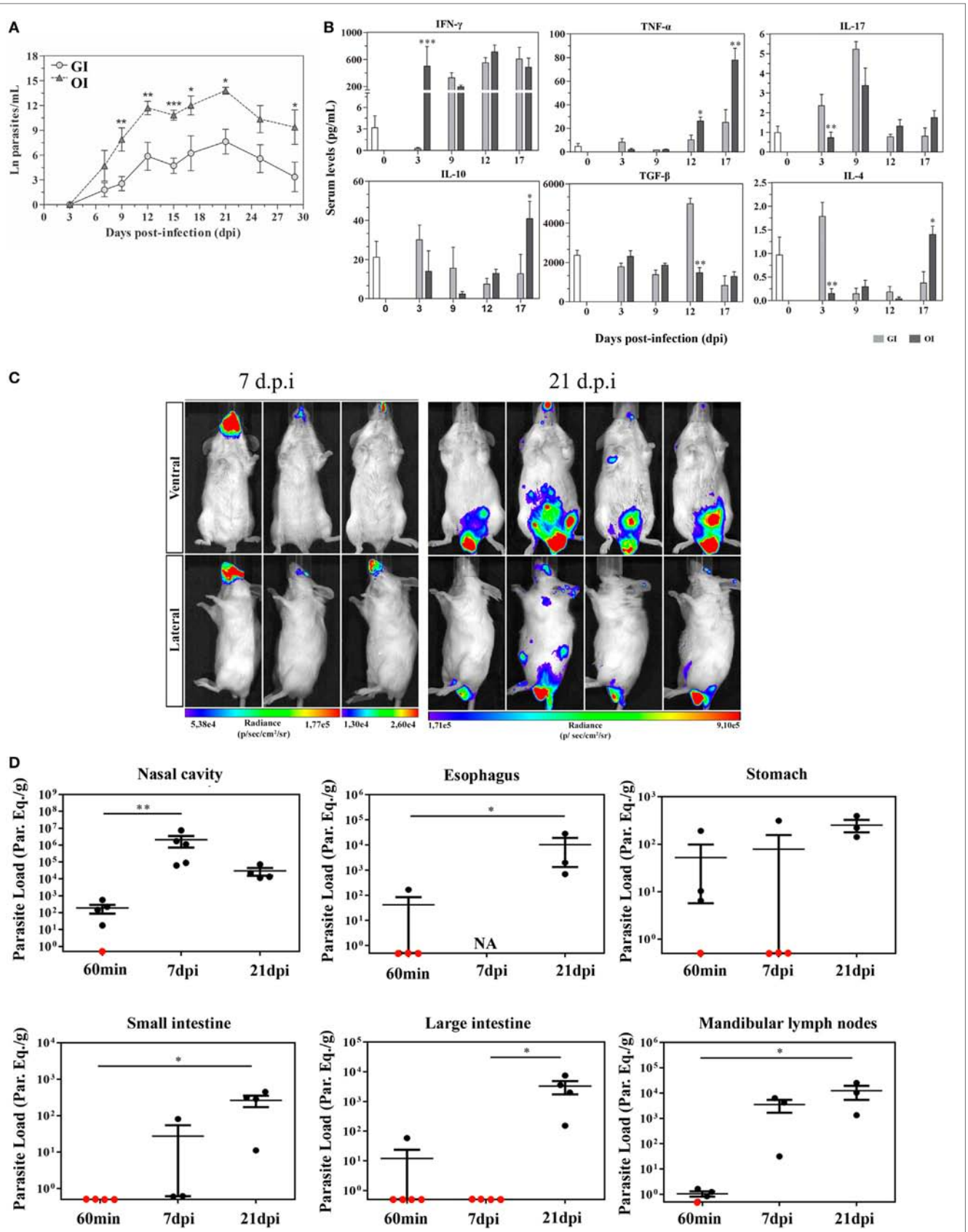

FIGURE 1 | Continued

FIGURE 1 | Severity and target tissues during acute phase of *Trypanosoma cruzi* orally infected mice. **(A)** Male BALB/c mice were infected with 5×10^4 tissue culture-derived trypomastigotes forms of *T. cruzi* (Tulahuén strain) through gavage [gastrointestinal infection (GI)] or oral cavity (OI). Parasitemia (mean and SEM) was assessed during the acute phase and expressed as ln parasites per milliliter for statistical analysis. Parasites were counted by light microscopy, and parasitemia calculated by the Brenner method. Parasitemia comparisons were performed at different days post-infection (dpi), Kruskal–Wallis, Dunn's post-test (until 15 dpi), and one-tailed Mann–Whitney (after 15 dpi) tests were used. **(A)** *n*: GI, 3 dpi = 7; 7 dpi = 22; 9 dpi = 29; 12 dpi = 17; 15 dpi = 45; 17 dpi = 10; 21 dpi = 24; 25 dpi = 16; 29 dpi = 11 and OI, 3 dpi = 4; 7 dpi = 9; 9 dpi = 14; 12 dpi = 22; 15 dpi = 40; 17 dpi = 12; 21 dpi = 14; 25 dpi = 8; 29 dpi = 6. Lower numbers represent early stages, when parasitemia was still undetectable and final stages, when mortality rates were too high. **(B)** Cytokine analysis in GI and OI mice. Male BALB/c mice were infected with 5×10^4 tissue culture-derived trypomastigotes forms of *T. cruzi* (Tulahuén strain) through gavage (GI) or within oral cavity (OI). In the course of acute infection, serum was isolated and levels of cytokines (IFN-γ, TNF, IL-17, IL-10, and TGF-β) were quantified in uninfected control and infected mice by a multiplex analysis. The results are expressed as the mean values (±SEM) for each group/day post-infection. *n*: IFN-γ, uninfected (0) = 12; 3 dpi GI = 11, OI = 5; 9 dpi GI = 8, OI = 5; 12 dpi GI = 9, OI = 4; 17 dpi GI = 4, OI = 6. TNF, uninfected (0) = 11; 3 dpi GI = 10, OI = 10; 9, 12 dpi, GI = 3, OI = 3; 17 dpi, GI = 6, OI = 11. IL-17, uninfected (0) = 12; 3 dpi, GI = 10, OI = 10; 9 dpi, GI = 3, OI = 3; 12 dpi, GI = 5, OI = 5; 17 dpi, GI = 6, OI = 14. TGF-β, uninfected (0) = 6; 3 dpi, GI = 4, OI = 4; 9 dpi, GI = 5, OI = 5; 12 dpi, GI = 5, OI = 4; 17 dpi, GI = 2, OI = 5. IL-10 and IL-4, uninfected (0) = 6; 3, 9, 12 dpi, GI = 6, OI = 6; 17 dpi, GI = 3, OI = 8. Statistical analysis was performed using GraphPad Prism 5. $^*p = 0.05$; $^{**}p = 0.01$; $^{***}p = 0.001$. **(C)** Course of parasite distribution in oral infection. Male BALB/c mice were infected in the oral cavity (OI) with 1×10^6 trypomastigotes forms of *T. cruzi* expressing luciferase (Dm28c-luc). Representative *in vivo* bioluminescence images were acquired in the same mice (*n* = 6), at 7 and 21 dpi, after 15 min of D-luciferin intraperitoneal administration (150 mg/kg), using IVIS® Lumina image system (Xenogen). **(D)** *T. cruzi* loads in orally infected mice. Male BALB/c mice were infected in the oral cavity (OI) with 1×10^6 trypomastigotes forms of *T. cruzi* expressing luciferase (Dm28c-luc). Organs and tissues were harvested for qPCR analysis to determine the parasite load (parasite equivalent/g) at 60 min, 7, and 21 dpi. The qPCR was performed in multiplex, targeting *T. cruzi* nuclear satellite DNA (Sat DNA) and IAC (internal amplification control), as a quality control. Parasite load in the nasal cavity (*n*: 60 min and 7 dpi = 5; 21 dpi = 4), esophagus (*n*: 60 min = 4; 21 dpi = 3), stomach (*n*: 60 min and 7 dpi = 4; 21 dpi = 3), small intestine (*n*: 60 min = 5; 7 dpi = 3; 21 dpi = 4), large intestine (*n*: 60 min = 5; 7 and 21 dpi = 4), and mandibular lymph nodes (*n*: 60 min = 4; 7 and 21 dpi = 3). Red dots: no parasite detection. Values present mean ± SEM. Kruskal–Wallis (Dunn's post-test) for group kinetics. Statistical analysis was performed using Graph Pad Prism 5. $^*p < 0.05$, $^{**}p < 0.01$. Adapted from Barreto-de-Albuquerque et al. (51) and Silva-dos Santos et al. (52).

IMMUNE RESPONSE AND DISEASE OUTCOME IN EXPERIMENTAL MODELS

The most widely used experimental model to study *T. cruzi* infection has been for years the intraperitoneal (IP) inoculation of the parasite in mice, in which 10^2 trypomastigotes are able to promote functional alterations in the immune system from 14 days post-infection (dpi) (65). However, this pathway does not mimic the natural infection through contaminated excreta left by the vector after biting. More importantly, especially in Brazil and other endemic countries, the most frequent transmission route has been reported to be by ingestion of contaminated food and beverages (7, 17, 66, 67). Several approaches to address oral infection in mice have been described in the literature, such as intrapharyngeal, intragastric, and in the oral cavity inoculation (37, 44, 45, 51, 68–70).

Comparing mucosal routes through the digestive tube with systemic inoculation, differences in disease outcome and immune response can be observed. Intraperitoneally infected mice present higher parasitemia and mortality than intragastric or oral cavity-inoculated mice with the same inoculum (51, 69, 71). Besides, IP-infected mice also start to die earlier than GI/OI-infected and present 80–100% mortality, while GI/OI results in higher survival rates. Still, OI leads to parasitemia and mortality levels higher than in GI models. Infection through gavage (intragastrically) presents less percentage of mice with patent parasitemia, parasitemia, and mortality than IP injection (51, 70). Despite intermediate parasitemia and mortality levels between GI and IP, OI infection leads to a percentage of mice with patent parasitemia similar to IP (49.3% for GI and 97.5% for OI) (51). These temporal and quantitative differences in parasitemia might be related to the distinct barriers the parasite needs to cross after these inoculation routes. As it has been discussed in the literature, the route of parasite inoculation affects the pathogenesis and disease outcome of experimental *T. cruzi* infection (72).

After oral infection, parasites have been detected in several tissues, and even where they are not detected, inflammatory infiltrates are found (37, 52). Systemic *versus* mucosal *T. cruzi* infection leads to distinct disease patterns. Systemic infections with Peruvian strain, such as IP, IV (intravenous), or SC (subcutaneous) promote higher infection rates (67–100%) and mortality than mucosal, such as OI, GI, intrarectal, genitalia, or conjunctival infection (17–67%) (73). By contrast, the study by Caradonna and Pereiraperrin (74), mice infected with Tulahuén strain through intranasal (IN) route present higher mortality than SC. In addition, after an oral inoculation (oropharynx), insect-derived metacyclic trypomastigotes are more infective when compared to cutaneous challenge (over puncture wound that is not the same as the SC) (75).

Inoculation route can also lead to preferential tropism, as well as distinct local and systemic immune responses (51, 52, 72, 74) (**Table 1**). Inflammatory infiltrates can be found in the heart and the severity is not necessarily the main cause of death (37, 51, 69). Infiltration of immune cells is observed in several organs regardless the presence of parasite (37). The literature shows that Tulahuén strain of *T. cruzi* induces TNF production and apoptosis of hepatocytes (76). In this regard, OI and GI infection leads to apoptosis in the liver and in the heart of acute infected mice and the macrophages are the main source of TNF. These different pathways can also lead to elevated serum IFN-γ levels and TNF, especially in OI (51). Also in the heart higher levels of TNF mRNA is detected in OI when compared with GI. This elevated TNF levels in OI may be associated with cardiac, spleen, and hepatic damage, as well as toxic shock in mice, as reported in studies with other models (51, 77, 78). Besides, it can be considered one of the factors for death in mice, since blockage of this cytokine improves the survival (51).

After OI or GI, different cell types can be found within the heart and liver, such as $CD4^+$ and $CD8^+$ cells, neutrophils, and macrophages. Among them, macrophages constitute the main source

TABLE 1 | Cytokines are differentially expressed according to the infection route.

	GI	Reference	OI	Reference
CCL3	↑ stomach (a; c)/spleen (c)	(79)	N.A.	–
CCL5	↑ stomach (c)/heart (c)	(79)	N.A.	–
CXCL1	↑ stomach (c)/heart (c)	(79)	N.A.	–
CXCL10	↑ stomach (c)/heart (c)/ spleen (c)	(79)	N.A.	–
CXCL9	↑ stomach (c)/heart (c)/ spleen (c)	(79)	N.A.	–
G-CSF	↑ stomach (c)	(79)	N.A.	–
IFN-γ	↑ stomach (a; c)/spleen (c)/ serum (a)	(51, 79)	↑ IEL (a)/ LP (a)/↑↑ serum (a)	(37, 51)
IL-10	↑ stomach (a; c)/heart (c)/ spleen (a)	(79)	↑ serum (a)	(51)
IL-12	↑ stomach (a; c)/heart (c)/ spleen (a)	(79)	N.A.	
IL-17	↑ serum (a)	(51, 79)	↑↑ serum (a)	(51)
IL-2	↑ stomach (c)/spleen (c)	(79)	N.A.	–
IL-3	↑ stomach (a; c)	(79)	N.A.	–
IL-4	↑ stomach (a; c)/spleen (c)	(79)	↑ serum (a)	(51)
IL-6	↑ spleen (c)	(79)	N.A.	–
IL-7	↑ stomach (c)/spleen (c)	(79)	N.A.	–
IL-9	↑ spleen (c)	(79)	N.A.	–
M-CSF	↑ stomach (c)	(79)	N.A.	–
TGF-β	↑↑ serum (a)	(51)	↑ serum (a)	(51)
TNF	↑ stomach (c)/spleen (c)/liver (a)/heart (a)/↑ serum (a)	(51, 79)	↑ liver/ heart/↑↑ serum (a)	(51)
GM-CSF	↑ spleen (a; c)	(79)	N.A.	–

GI, gastrointestinal infection; OI, oral infection; a, acute phase; c, chronic phase; N.A., not analyzed; IEL, intraephitelial lymphocytes; LP, lamina propria.

of tissue TNF (51). In acute and chronic phase, inflammation can be detected in the stomach and heart after GI infection, followed by alterations in cytokine production. An increase of IL-12, IFN-γ, IL-4, IL-10, CCL3/4, and IL-3 is observed in the stomach during the acute phase of the disease and IL-12, TNF-α, CCL3/4, CXCL1, CCL5, CXCL9, CXCL10, G-CSF, M-CSF, IL-2, and IL-7 in the chronic phase. Hoft and collaborators demonstrated that after oral inoculation, *T. cruzi* infection within the gastric epithelium is able to stimulate B cell responses with parasite-specific IgA and IgG, suggesting activation of these cells in mucosal inductive sites, such as Peyer's patches, although the presence of parasite was not proven there. Furthermore, gastric intraepithelial lymphocytes and from lamina propria produce IFN-γ (37). In the heart, IL-10 and CXCL1 increase in animals GI-infected with the CL strain, in addition to IL-12, IL-10, CXCL9, and CXCL10 during the chronic phase. Of note, this profile can vary according to strain (79). Yet, little is known after oral inoculation of the parasite.

It was already described after IP infection, alterations in secondary lymphoid organs are observed in acute infection with an increase in total cell numbers and individual subsets as well as cytokine production in the subcutaneous lymph nodes and spleen, and a decrease in mesenteric lymph nodes and thymus (65, 80). After GI, there is an increase of neutrophils, lymphocytes, and monocytes and a reduction of the number of eosinophils in GI- and IP-infected mice. As demonstrated in Domingues and colleagues study, the peak of parasitemia in GI at 18 dpi is correlated with an increase in monocytes in the blood. The spleen also increases in GI, mainly $CD8^+$ cells and double-positive $CD8^+CD4^+$, but at a later time and the thymus is slightly increased instead of the atrophy observed after IP (70). High levels of IL-12, IL-10, and GM-CSF are expressed in the spleen during the acute phase of CL strain-infected mice, while IFN-γ, TNF-α, IL-6, IL-4, IL-9, CCL3/4, CXCL9, CXCL10, GM-CSF, IL-2, and IL-7 are elevated during chronic infection (79). The mesenteric lymph nodes decrease in GI with reduction of $CD4^+$ cells (70). Of note, the only study addressing lymphoid organ alteration after oral infection (oral cavity inoculation) reports an increase of gastric lymph nodes (37).

Regarding systemic cytokines GI and OI mice have a high concentration of serum IL-4, while OI leads to lower amounts of the regulatory cytokine IL-10 and TGF-β. These cytokines are known to inhibit macrophage microbicidal function, protecting the host from tissue damage (77, 81). Furthermore, inoculation of parasite through digestive mucosa (oral and more in GI) triggers IL-17 production, which is reflected in the serum. IL-17-producing cells have also been described to contribute to the formation of the gastrointestinal barrier (82). Moreover, mucosal infections (IN or OI/GI) with bacteria, such as *Listeria monocytogenes* (Lm), *Streptococcus pyogenes*, and *Francisella tularensis* leads to Th17 responses, while the systemic routes (IV or SC) trigger a Th1 response (83).

For different infection models systemic inoculations, IP, IV, and SC have been widely used. Although these approaches do not always necessarily mimic the natural transmission pathway. Our group and others have already demonstrated that the route of parasite administration is relevant for the disease outcome in infections by different pathogens (72, 84). Besides as ideal experimental model should mimic all phases of infection, including the transmission pathway (84). In this regard, for food-borne diseases, oral inoculation is an essential issue to consider.

Considering the human counterpart in Chagas disease, oral transmission has become more epidemiologically relevant and the outbreaks are related to contaminated food ingestion (85). Interestingly, facial edema is frequently observed in these patients (53). In experimental models, we described that host response is distinct when parasites are delivered into the oral cavity or by gavage (51). As it has been discussed also in non-infectious models, the oral cavity represents the first contact with the organism after ingestion and presents an underexplored environment. Thus, it should really be considered as more than just the entrance for the gastrointestinal tract (86). Tolerogenic dendritic cells producing IL-10 and IL-12 (regulatory and inflammatory profiles) can capture parasite/antigens within the mucosa in the oral cavity and in the gastrointestinal tract from where they can also be drained to the liver by the portal system (87, 88). Thus, regarding oral infections, parasite delivery into the oral cavity or by gavage (intrapharyngeal/gastrointestinal) should not be assumed as equivalent processes.

The importance to standardize the nomenclature and the choice among different approaches to address "oral" infection, such as *ad libitum*, oral gavage and in the oral cavity has been discussed also in the context of other food-borne diseases, such

as Listeriosis, caused by the bacteria Lm (84). After GI Lm inoculation, high amounts of Lm and specific T cells are found in the intestinal mucosa, mesenteric lymph nodes, spleen, and liver, whereas ingestion of Lm-contaminated bread promotes increased and phenotypically distinct intestinal resident memory cells (T_{RM}) compared with other routes of infection (89–91). Moreover, IV and IN routes are able to induce T_H1 and T_H17 $CD4^+$ cells, respectively, but T_H1 cells from IV were are more likely to originate a memory cell pool than T_H17 from IN (92).

CONCLUSION AND PERSPECTIVES

Nowadays, *T. cruzi* oral transmission is an important route of infection in Latin American countries. Despite its relevance, significant studies about this form of parasite infection are largely lacking. Experimental studies related to oral *T. cruzi* and other infective agents usually comprise inoculation in the mouth (OI) or intragastrically/intrapharyngeal (GI), being roughly considered as similar routes of infection. In this review, we unraveled the intrinsic importance of specific (and distinct) tissues involved in the primary site of an infective agent entrance, resulting in regional immune response and differential disease outcome. New studies investigating the influence of target tissues and host–parasite interactions in OI and GI must be performed.

AUTHOR CONTRIBUTIONS

JM, JBA, DSS, and JS contributed with text writing and review construction.

FUNDING

This work was funded with grants from FOCEM, Fiocruz, Oswaldo Cruz Institute, CNPq, and Faperj (Brazil).

REFERENCES

1. Schofield CJ, Diotaiuti L, Dujardin JP. The process of domestication in Triatominae. *Mem Inst Oswaldo Cruz* (1999) 94(Suppl 1):375–8. doi:10.1590/S0074-02761999000700073
2. Coura JR, Vinas PA, Junqueira AC. Ecoepidemiology, short history and control of Chagas disease in the endemic countries and the new challenge for non-endemic countries. *Mem Inst Oswaldo Cruz* (2014) 109(7):856–62. doi:10.1590/0074-0276140236
3. Dorn P, Buekens P, Hanford E. Whac-a-mole: future trends in Chagas transmission and the importance of a global perspective on disease control. *Future Microbiol* (2007) 2:365–7. doi:10.2217/17460913.2.4.365
4. Tarleton RL, Reithinger R, Urbina JA, Kitron U, Gurtler RE. The challenges of Chagas disease – grim outlook or glimmer of hope. *PLoS Med* (2007) 4:e332. doi:10.1371/journal.pmed.0040332
5. Wendel S. Transfusion transmitted Chagas disease: is it really under control? *Acta Trop* (2010) 115:28–34. doi:10.1016/j.actatropica.2009.12.006
6. Bern C, Kjos S, Yabsley MJ, Montgomery SP. *Trypanosoma cruzi* and Chagas' disease in the United States. *Clin Microbiol Rev* (2011) 24:655–81. doi:10.1128/CMR.00005-11
7. Shikanai-Yasuda MA, Carvalho NB. Oral transmission of Chagas disease. *Clin Infect Dis* (2012) 54:845–52. doi:10.1093/cid/cir956
8. Noya BA, Diaz-Bello Z, Colmenares C, Ruiz-Guevara R, Mauriello L, Munoz-Calderon A, et al. Update on oral Chagas disease outbreaks in Venezuela: epidemiological, clinical and diagnostic approaches. *Mem Inst Oswaldo Cruz* (2015) 110:377–86. doi:10.1590/0074-02760140285
9. Alarcón de Noya B, Noya González O, Robertson LJ. *Trypanosoma cruzi* as a foodborne pathogen. *SpringerBriefs in Food, Health, and Nutrition*. New York, Heidelberg, Dordrecht, London: Springer (2016). 92 p.
10. Rassi A Jr, Rassi A, Marin-Neto JA. Chagas disease. *Lancet* (2010) 375:1388–402. doi:10.1016/S0140-6736(10)60061-X
11. Sanchez LV, Ramirez JD. Congenital and oral transmission of American trypanosomiasis: an overview of physiopathogenic aspects. *Parasitology* (2013) 140:147–59. doi:10.1017/S0031182012001394
12. Santos V, Meis J, Savino W, Andrade JAA, Vieira J, Coura JR, et al. Acute Chagas disease in the state of para, Amazon region: is it increasing? *Mem Inst Oswaldo Cruz* (2018) 113:e170298. doi:10.1590/0074-02760170298
13. Barbosa-Ferreira JM, Nobre AF, Maldonado JG, Borges-Pereira J, Zauza PL, Coura JR. [Stroke in a chronic autochthonous chagasic patient from the Brazilian Amazon]. *Rev Soc Bras Med Trop* (2010) 43:751–3. doi:10.1590/S0037-86822010000600034
14. Pinto AY, Harada GS, Valente V, Abud JE, Gomes F, Souza GC, et al. [Cardiac attacks in patients with acute Chagas disease in a family micro-outbreak, in Abaetetuba, Brazilian Amazon]. *Rev Soc Bras Med Trop* (2001) 34:413–9. doi:10.1590/S0037-86822001000500003
15. Vinas Albajar P, Laredo SV, Terrazas MB, Coura JR. [Dilated cardiomyopathy in patients with chronic chagasic infection: report of two fatal autochthonous cases from Rio Negro, state of Amazonas, Brazil]. *Rev Soc Bras Med Trop* (2003) 36:401–7. doi:10.1590/S0037-86822003000300013
16. Ianni BM, Mady C. [The sugarcane juice was delicious, but…]. *Arq Bras Cardiol* (2005) 85:379–81. doi:10.1590/S0066-782X2005001900001
17. de Noya BA, Gonzalez ON. An ecological overview on the factors that drives to *Trypanosoma cruzi* oral transmission. *Acta Trop* (2015) 151:94–102. doi:10.1016/j.actatropica.2015.06.004
18. Barbosa RL, Pereira KS, Dias VL, Schmidt FL, Alves DP, Guaraldo AM, et al. Virulence of *Trypanosoma cruzi* in Acai (*Euterpe oleraceae* Martius) pulp following mild heat treatment. *J Food Prot* (2016) 79:1807–12. doi:10.4315/0362-028X.JFP-15-595
19. Hotez PJ, Molyneux DH, Stillwaggon E, Bentwich Z, Kumaresan J. Neglected tropical diseases and HIV/AIDS. *Lancet* (2006) 368:1865–6. doi:10.1016/S0140-6736(06)69764-X
20. Savino W, Villa-Verde DM, Mendes-Da-Cruz DA, Silva-Monteiro E, Perez AR, Aoki Mdel P, et al. Cytokines and cell adhesion receptors in the regulation of immunity to *Trypanosoma cruzi*. *Cytokine Growth Factor Rev* (2007) 18:107–24. doi:10.1016/j.cytogfr.2007.01.010
21. Malik LH, Singh GD, Amsterdam EA. Chagas heart disease: an update. *Am J Med* (2015) 128(1251):e1257–9. doi:10.1016/j.amjmed.2015.04.036
22. Thakare R, Dasgupta A, Chopra S. An update on benznidazole for the treatment of patients with Chagas disease. *Drugs Today (Barc)* (2018) 54:15–23. doi:10.1358/dot.2018.54.1.2753402
23. de Souza W, de Carvalho TM, Barrias ES. Review on *Trypanosoma cruzi*: host cell interaction. *Int J Cell Biol* (2010) 2010:295394. doi:10.1155/2010/295394
24. Coura JR, Junqueira AC. Ecological diversity of *Trypanosoma cruzi* transmission in the Amazon basin. The main scenaries in the Brazilian Amazon. *Acta Trop* (2015) 151:51–7. doi:10.1016/j.actatropica.2015.04.029
25. Maeda FY, Cortez C, Yoshida N. Cell signaling during *Trypanosoma cruzi* invasion. *Front Immunol* (2012) 3:361. doi:10.3389/fimmu.2012.00361
26. Barrias ES, de Carvalho TM, De Souza W. *Trypanosoma cruzi*: entry into mammalian host cells and parasitophorous vacuole formation. *Front Immunol* (2013) 4:186. doi:10.3389/fimmu.2013.00186
27. Cardoso MS, Reis-Cunha JL, Bartholomeu DC. Evasion of the immune response by *Trypanosoma cruzi* during acute infection. *Front Immunol* (2015) 6:659. doi:10.3389/fimmu.2015.00659
28. Schenkman S, Jiang MS, Hart GW, Nussenzweig V. A novel cell surface trans-sialidase of *Trypanosoma cruzi* generates a stage-specific epitope required for invasion of mammalian cells. *Cell* (1991) 65:1117–25. doi:10.1016/0092-8674(91)90008-M
29. Buscaglia CA, Campo VA, Frasch AC, Di Noia JM. *Trypanosoma cruzi* surface mucins: host-dependent coat diversity. *Nat Rev Microbiol* (2006) 4:229–36. doi:10.1038/nrmicro1351

30. Yoshida N, Cortez M. *Trypanosoma cruzi*: parasite and host cell signaling during the invasion process. *Subcell Biochem* (2008) 47:82–91. doi:10.1007/978-0-387-78267-6_6
31. Villalta F, Scharfstein J, Ashton AW, Tyler KM, Guan F, Mukherjee S, et al. Perspectives on the *Trypanosoma cruzi*-host cell receptor interactions. *Parasitol Res* (2009) 104:1251–60. doi:10.1007/s00436-009-1383-3
32. Yoshida N. Molecular mechanisms of *Trypanosoma cruzi* infection by oral route. *Mem Inst Oswaldo Cruz* (2009) 104(Suppl 1):101–7. doi:10.1590/S0074-02762009000900015
33. Freire-de-Lima L, Fonseca LM, Oeltmann T, Mendonca-Previato L, Previato JO. The trans-sialidase, the major *Trypanosoma cruzi* virulence factor: three decades of studies. *Glycobiology* (2015) 25:1142–9. doi:10.1093/glycob/cwv057
34. Yoshida N. *Trypanosoma cruzi* infection by oral route: how the interplay between parasite and host components modulates infectivity. *Parasitol Int* (2008) 57:105–9. doi:10.1016/j.parint.2007.12.008
35. Ortega-Barria E, Pereira ME. A novel *T. cruzi* heparin-binding protein promotes fibroblast adhesion and penetration of engineered bacteria and trypanosomes into mammalian cells. *Cell* (1991) 67:411–21. doi:10.1016/0092-8674(91)90192-2
36. Calvet CM, Melo TG, Garzoni LR, Oliveira FO Jr, Neto DT, Meirelles MNSL, et al. Current understanding of the *Trypanosoma cruzi*-cardiomyocyte interaction. *Front Immunol* (2012) 3:327. doi:10.3389/fimmu.2012.00327
37. Hoft DF, Farrar PL, Kratz-Owens K, Shaffer D. Gastric invasion by *Trypanosoma cruzi* and induction of protective mucosal immune responses. *Infect Immun* (1996) 64:3800–10.
38. Staquicini DI, Martins RM, Macedo S, Sasso GR, Atayde VD, Juliano MA, et al. Role of GP82 in the selective binding to gastric mucin during oral infection with *Trypanosoma cruzi*. *PLoS Negl Trop Dis* (2010) 4:e613. doi:10.1371/journal.pntd.0000613
39. Yoshida N, Tyler KM, Llewellyn MS. Invasion mechanisms among emerging food-borne protozoan parasites. *Trends Parasitol* (2011) 27:459–66. doi:10.1016/j.pt.2011.06.006
40. Neira I, Silva FA, Cortez M, Yoshida N. Involvement of *Trypanosoma cruzi* metacyclic trypomastigote surface molecule gp82 in adhesion to gastric mucin and invasion of epithelial cells. *Infect Immun* (2003) 71:557–61. doi:10.1128/IAI.71.1.557-561.2003
41. Teixeira MM, Yoshida N. Stage-specific surface antigens of metacyclic trypomastigotes of *Trypanosoma cruzi* identified by monoclonal antibodies. *Mol Biochem Parasitol* (1986) 18:271–82. doi:10.1016/0166-6851(86)90085-X
42. Araya JE, Cano MI, Yoshida N, Da Silveira JF. Cloning and characterization of a gene for the stage-specific 82-kDa surface antigen of metacyclic trypomastigotes of *Trypanosoma cruzi*. *Mol Biochem Parasitol* (1994) 65:161–9. doi:10.1016/0166-6851(94)90124-4
43. Cortez M, Silva MR, Neira I, Ferreira D, Sasso GR, Luquetti AO, et al. *Trypanosoma cruzi* surface molecule gp90 downregulates invasion of gastric mucosal epithelium in orally infected mice. *Microbes Infect* (2006) 8:36–44. doi:10.1016/j.micinf.2005.05.016
44. Cortez C, Yoshida N, Bahia D, Sobreira TJ. Structural basis of the interaction of a *Trypanosoma cruzi* surface molecule implicated in oral infection with host cells and gastric mucin. *PLoS One* (2012) 7:e42153. doi:10.1371/journal.pone.0042153
45. Cortez M, Neira I, Ferreira D, Luquetti AO, Rassi A, Atayde VD, et al. Infection by *Trypanosoma cruzi* metacyclic forms deficient in gp82 but expressing a related surface molecule, gp30. *Infect Immun* (2003) 71:6184–91. doi:10.1128/IAI.71.11.6184-6191.2003
46. Cortez C, Martins RM, Alves RM, Silva RC, Bilches LC, Macedo S, et al. Differential infectivity by the oral route of *Trypanosoma cruzi* lineages derived from Y strain. *PLoS Negl Trop Dis* (2012) 6:e1804. doi:10.1371/journal.pntd.0001804
47. Malaga S, Yoshida N. Targeted reduction in expression of *Trypanosoma cruzi* surface glycoprotein gp90 increases parasite infectivity. *Infect Immun* (2001) 69:353–9. doi:10.1128/IAI.69.1.353-359.2001
48. Bayer-Santos E, Cunha-E-Silva NL, Yoshida N, Franco Da Silveira J. Expression and cellular trafficking of GP82 and GP90 glycoproteins during *Trypanosoma cruzi* metacyclogenesis. *Parasit Vectors* (2013) 6:127. doi:10.1186/1756-3305-6-127
49. Clemente TM, Cortez C, Novaes Ada S, Yoshida N. Surface molecules released by *Trypanosoma cruzi* metacyclic forms downregulate host cell invasion. *PLoS Negl Trop Dis* (2016) 10:e0004883. doi:10.1371/journal.pntd.0004883
50. Diaz-Ungría C, Bracho JS. Camino que sigue el *Trypanosoma cruzi* en perros infectados por vía bucal: nuevos estudios. *Rev Vet Venezuelana* (1970) 44:114–9.
51. Barreto-de-Albuquerque J, Silva-dos-Santos D, Perez AR, Berbert LR, de Santana-Van-Vliet E, Farias-de-Oliveira DA, et al. *Trypanosoma cruzi* infection through the oral route promotes a severe infection in mice: new disease form from an old infection? *PLoS Negl Trop Dis* (2015) 9:e0003849. doi:10.1371/journal.pntd.0003849
52. Silva-dos-Santos D, Barreto-de-Albuquerque J, Guerra B, Moreira OC, Berbert LR, Ramos MT, et al. Unraveling Chagas disease transmission through the oral route: gateways to *Trypanosoma cruzi* infection and target tissues. *PLoS Negl Trop Dis* (2017) 11:e0005507. doi:10.1371/journal.pntd.0005507
53. Pinto AY, Ferreira AG Jr, Valente Vda C, Harada GS, Valente SA. Urban outbreak of acute Chagas disease in Amazon region of Brazil: four-year follow-up after treatment with benznidazole. *Rev Panam Salud Publica* (2009) 25:77–83. doi:10.1590/S1020-49892009000100012
54. Stoopler ET, Sollecito TP. Oral mucosal diseases: evaluation and management. *Med Clin North Am* (2014) 98:1323–52. doi:10.1016/j.mcna.2014.08.006
55. Salvatori O, Puri S, Tati S, Edgerton M. Innate immunity and saliva in *Candida albicans*-mediated oral diseases. *J Dent Res* (2016) 95:365–71. doi:10.1177/0022034515625222
56. Yee JK. Helicobacter pylori colonization of the oral cavity: a milestone discovery. *World J Gastroenterol* (2016) 22:641–8. doi:10.3748/wjg.v22.i2.641
57. Wu RQ, Zhang DF, Tu E, Chen QM, Chen W. The mucosal immune system in the oral cavity—an orchestra of T cell diversity. *Int J Oral Sci* (2014) 6:125–32. doi:10.1038/ijos.2014.48
58. Tabak LA. In defense of the oral cavity: structure, biosynthesis, and function of salivary mucins. *Annu Rev Physiol* (1995) 57:547–64. doi:10.1146/annurev.ph.57.030195.002555
59. Derrien M, van Passel MW, van de Bovenkamp JH, Schipper RG, de Vos WM, Dekker J. Mucin-bacterial interactions in the human oral cavity and digestive tract. *Gut Microbes* (2010) 1:254–68. doi:10.4161/gmic.1.4.12778
60. Murray PA, Prakobphol A, Lee T, Hoover CI, Fisher SJ. Adherence of oral streptococci to salivary glycoproteins. *Infect Immun* (1992) 60:31–8.
61. Honma K, Mishima E, Sharma A. Role of *Tannerella forsythia* NanH sialidase in epithelial cell attachment. *Infect Immun* (2011) 79:393–401. doi:10.1128/IAI.00629-10
62. Roy S, Honma K, Douglas CW, Sharma A, Stafford GP. Role of sialidase in glycoprotein utilization by *Tannerella forsythia*. *Microbiology* (2011) 157:3195–202. doi:10.1099/mic.0.052498-0
63. Lakdawala SS, Jayaraman A, Halpin RA, Lamirande EW, Shih AR, Stockwell TB, et al. The soft palate is an important site of adaptation for transmissible influenza viruses. *Nature* (2015) 526:122–5. doi:10.1038/nature15379
64. Butler CE, de Carvalho TM, Grisard EC, Field RA, Tyler KM. Trans-sialidase stimulates eat me response from epithelial cells. *Traffic* (2013) 14:853–69. doi:10.1111/tra.12078
65. de Meis J, Morrot A, Farias-de-Oliveira DA, Villa-Verde DM, Savino W. Differential regional immune response in Chagas disease. *PLoS Negl Trop Dis* (2009) 3:e417. doi:10.1371/journal.pntd.0000417
66. Benchimol Barbosa PR. The oral transmission of Chagas' disease: an acute form of infection responsible for regional outbreaks. *Int J Cardiol* (2006) 112:132–3. doi:10.1016/j.ijcard.2005.11.087
67. Dias JC. [Notes about of *Trypanosoma cruzi* and yours bio-ecology characteristics with agents of the transmission by meals]. *Rev Soc Bras Med Trop* (2006) 39:370–5. doi:10.1590/S0037-86822006000400010
68. Kirchhoff LV, Hoft DF. Immunization and challenge of mice with insect-derived metacyclic trypomastigotes of *Trypanosoma cruzi*. *Parasite Immunol* (1990) 12:65–74. doi:10.1111/j.1365-3024.1990.tb00936.x
69. Camandaroba EL, Pinheiro Lima CM, Andrade SG. Oral transmission of Chagas disease: importance of *Trypanosoma cruzi* biodeme in the intragastric experimental infection. *Rev Inst Med Trop Sao Paulo* (2002) 44:97–103. doi:10.1590/S0036-46652002000200008
70. Domingues CS, Hardoim DJ, Souza CS, Cardoso FO, Mendes VG, Previtalli-Silva H, et al. Oral Outbreak of Chagas disease in Santa Catarina, Brazil: experimental evaluation of a patient's strain. *PLoS One* (2015) 10:e0122566. doi:10.1371/journal.pone.0122566

71. Dias GB, Gruendling AP, Araujo SM, Gomes ML, Toledo MJ. Evolution of infection in mice inoculated by the oral route with different developmental forms of *Trypanosoma cruzi* I and II. *Exp Parasitol* (2013) 135:511–7. doi:10.1016/j.exppara.2013.08.013
72. de Meis J, Barreto de Albuquerque J, Silva dos Santos D, Farias-de-Oliveira DA, Berbert LR, Cotta-de-Almeida V, et al. *Trypanosoma cruzi* entrance through systemic or mucosal infection sites differentially modulates regional immune response following acute infection in mice. *Front Immunol* (2013) 4:216. doi:10.3389/fimmu.2013.00216
73. Marsden PD. *Trypanosoma cruzi* infections in CFI mice. II. Infections induced by different routes. *Ann Trop Med Parasitol* (1967) 61:62–7. doi:10.1080/00034983.1967.11686458
74. Caradonna K, Pereiraperrin M. Preferential brain homing following intranasal administration of *Trypanosoma cruzi*. *Infect Immun* (2009) 77:1349–56. doi:10.1128/IAI.01434-08
75. Eickhoff CS, Dunn BA, Sullivan NL, Hoft DF. Comparison of the infectivity of *Trypanosoma cruzi* insect-derived metacyclic trypomastigotes after mucosal and cutaneous contaminative challenges. *Mem Inst Oswaldo Cruz* (2013) 108:508–11. doi:10.1590/S0074-02762013000400018
76. Ronco MT, Frances DE, Ingaramo PI, Quiroga AD, Alvarez ML, Pisani GB, et al. Tumor necrosis factor alpha induced by *Trypanosoma cruzi* infection mediates inflammation and cell death in the liver of infected mice. *Cytokine* (2010) 49:64–72. doi:10.1016/j.cyto.2009.09.012
77. Holscher C, Mohrs M, Dai WJ, Kohler G, Ryffel B, Schaub GA, et al. Tumor necrosis factor alpha-mediated toxic shock in *Trypanosoma cruzi*-infected interleukin 10-deficient mice. *Infect Immun* (2000) 68:4075–83. doi:10.1128/IAI.68.7.4075-4083.2000
78. Andrade SG, Magalhaes Ldos A, Pessina DH. Importance of TNF-alpha in the course of acute infection with *Trypanosoma cruzi*: influence of its inhibition by pentoxifylline treatment. *Mem Inst Oswaldo Cruz* (2008) 103:21–6. doi:10.1590/S0074-02762008005000006
79. Rodrigues AA, Notario AF, Teixeira TL, Silva E, Quintal RT, Alves AP. A high throughput analysis of cytokines and chemokines expression during the course of *Trypanosoma cruzi* experimental oral infection. *Acta Trop* (2016) 157:42–53. doi:10.1016/j.actatropica.2016.01.025
80. de Meis J, Ferreira LM, Guillermo LV, Silva EM, Dosreis GA, Lopes MF. Apoptosis differentially regulates mesenteric and subcutaneous lymph node immune responses to *Trypanosoma cruzi*. *Eur J Immunol* (2008) 38:139–46. doi:10.1002/eji.200737582
81. Reed SG, Brownell CE, Russo DM, Silva JS, Grabstein KH, Morrissey PJ. IL-10 mediates susceptibility to *Trypanosoma cruzi* infection. *J Immunol* (1994) 153:3135–40.
82. Blaschitz C, Raffatellu M. Th17 cytokines and the gut mucosal barrier. *J Clin Immunol* (2010) 30:196–203. doi:10.1007/s10875-010-9368-7
83. Hu W, Pasare C. Location, location, location: tissue-specific regulation of immune responses. *J Leukoc Biol* (2013) 94:409–21. doi:10.1189/jlb.0413207
84. D'Orazio SE. Animal models for oral transmission of *Listeria monocytogenes*. *Front Cell Infect Microbiol* (2014) 4:15. doi:10.3389/fcimb.2014.00015
85. Toso MA, Vial UF, Galanti N. [Oral transmission of Chagas' disease]. *Rev Med Chil* (2011) 139:258–66. doi:10.4067/S0034-98872011000200017
86. Novak N, Haberstok J, Bieber T, Allam JP. The immune privilege of the oral mucosa. *Trends Mol Med* (2008) 14:191–8. doi:10.1016/j.molmed.2008.03.001
87. Weiner HL, Da Cunha AP, Quintana F, Wu H. Oral tolerance. *Immunol Rev* (2011) 241:241–59. doi:10.1111/j.1600-065X.2011.01017.x
88. Moingeon P, Mascarell L. Induction of tolerance via the sublingual route: mechanisms and applications. *Clin Dev Immunol* (2012) 2012:623474. doi:10.1155/2012/623474
89. Kursar M, Bonhagen K, Kohler A, Kamradt T, Kaufmann SH, Mittrucker HW. Organ-specific CD4+ T cell response during *Listeria monocytogenes* infection. *J Immunol* (2002) 168:6382–7. doi:10.4049/jimmunol.168.12.6382
90. Kursar M, Kohler A, Kaufmann SH, Mittrucker HW. Depletion of CD4+ T cells during immunization with nonviable *Listeria monocytogenes* causes enhanced CD8+ T cell-mediated protection against listeriosis. *J Immunol* (2004) 172:3167–72. doi:10.4049/jimmunol.172.5.3167
91. Sheridan BS, Pham QM, Lee YT, Cauley LS, Puddington L, Lefrancois L. Oral infection drives a distinct population of intestinal resident memory CD8(+) T cells with enhanced protective function. *Immunity* (2014) 40:747–57. doi:10.1016/j.immuni.2014.03.007
92. Pepper M, Linehan JL, Pagan AJ, Zell T, Dileepan T, Cleary PP, et al. Different routes of bacterial infection induce long-lived TH1 memory cells and short-lived TH17 cells. *Nat Immunol* (2010) 11:83–9. doi:10.1038/ni.1826

Conflict of Interest Statement: The authors declare that the research was conducted in the absence of any commercial or financial relationships that could be construed as a potential conflict of interest.

frontiers in Immunology

ORIGINAL RESEARCH
published: 12 November 2018
doi: 10.3389/fimmu.2018.02487

Immunoproteomics and Surfaceomics of the Adult Tapeworm *Hymenolepis diminuta*

Daniel Młocicki[1,2], Anna Sulima[1], Justyna Bień[2], Anu Näreaho[3], Anna Zawistowska-Deniziak[2], Katarzyna Basałaj[2], Rusłan Sałamatin[1,4], David Bruce Conn[5,6] and Kirsi Savijoki[7]*

[1] Department of General Biology and Parasitology, Medical University of Warsaw, Warsaw, Poland, [2] Witold Stefański Institute of Parasitology, Polish Academy of Sciences, Warsaw, Poland, [3] Department of Veterinary Biosciences, University of Helsinki, Helsinki, Finland, [4] Department of Parasitology and Vector-Borne Diseases, National Institute of Public Health–National Institute of Hygiene, Warsaw, Poland, [5] Department of Invertebrate Zoology, Museum of Comparative Zoology, Harvard University, Cambridge, MA, United States, [6] One Health Center, Berry College, Mount Berry, GA, United States, [7] Division of Pharmaceutical Biosciences, University of Helsinki, Helsinki, Finland

OPEN ACCESS

Edited by:
Xun Suo,
China Agricultural University, China

Reviewed by:
Maria Doligalska,
University of Warsaw, Poland
Abu Hena Mostafa Kamal,
University of Texas at Arlington, United States

***Correspondence:**
Daniel Młocicki
danmlo@twarda.pan.pl

Specialty section:
This article was submitted to Microbial Immunology, a section of the journal Frontiers in Immunology

Received: *29 May 2018*
Accepted: *08 October 2018*
Published: *12 November 2018*

Citation:
Młocicki D, Sulima A, Bień J, Näreaho A, Zawistowska-Deniziak A, Basałaj K, Sałamatin R, Conn DB and Savijoki K (2018) Immunoproteomics and Surfaceomics of the Adult Tapeworm Hymenolepis diminuta. Front. Immunol. 9:2487. doi: 10.3389/fimmu.2018.02487

In cestodiasis, mechanical and molecular contact between the parasite and the host activates the immune response of the host and may result in inflammatory processes, leading to ulceration and intestinal dysfunctions. The aim of the present study was to identify antigenic proteins of the adult cestode *Hymenolepis diminuta* by subjecting the total protein extracts from adult tapeworms to 2DE immunoblotting (two-dimensional electrophoresis combined with immunoblotting) using sera collected from experimentally infected rats. A total of 36 protein spots cross-reacting with the rat sera were identified using LC-MS/MS. As a result, 68 proteins, including certain structural muscle proteins (actin, myosin, and paramyosin) and moonlighters (heat shock proteins, kinases, phosphatases, and glycolytic enzymes) were identified; most of these were predicted to possess binding and/or catalytic activity required in various metabolic and cellular processes, and reported here as potential antigens of the adult cestode for the first time. As several of these antigens can also be found at the cell surface, the surface-associated proteins were extracted and subjected to in-solution digestion for LC-MS/MS identification (surfaceomics). As a result, a total of 76 proteins were identified, from which 31 proteins, based on 2DE immunoblotting, were predicted to be immunogenic. These included structural proteins actin, myosin and tubulin as well as certain moonlighting proteins (heat-shock chaperones) while enzymes with diverse catalytic activities were found as the most dominating group of proteins. In conclusion, the present study shed new light into the complexity of the enteric cestodiasis by showing that the *H. diminuta* somatic proteins exposed to the host possess immunomodulatory functions, and that the immune response of the host could be stimulated by diverse mechanisms, involving also those triggering protein export via yet unknown pathways.

Keywords: *Hymenolepis diminuta*, tapeworm, cestoda, host–parasite interactions, proteomics, mass spectrometry, immunoblotting, surface proteins

INTRODUCTION

Cestodes have been recognized for many years as being among the most important human parasites, causing diseases that remain within the top health priorities in many parts of the world (1). Indeed, cestode diseases are explicit targets for control efforts, especially in developing countries (2, 3). Such diseases are emerging threats even in more developed countries, where hymenolepiasis remains among the cestode diseases that have the highest morbidity globally (4, 5).

Similarly to other cestode species the life-cycle of *Hymenolepis diminuta* is complex and involve three morphologically distinct developmental stages: the hexacanth larva, the metacestode juvenile, and the sexual adult stage (6). The hexacanth is enclosed within its oncospheral envelopes, forming the cestode egg (7) that undergoes progressive metamorphosis into the metacestode stage in the intermediate host's body tissues and/or cavities. In most of the cases, the metacestode needs to be ingested to reach the vertebrate definitive host's small intestine and grow into the adult parasite. In the intestinal lumen, developing immature and adult cestodes are exposed to the hostile intestinal environment, including digestive enzymes, immune responses, bacteria, and active peristaltic movements of the small intestine. Adult tapeworms utilize their scolex that is armed with adhesive structures (suckers), for anchoring themselves to the intestinal epithelium. In addition, juvenile, premature and adult cestodes use tegumental surface structures—microtiches—to mediate broad adherence to the intestinal epithelium. In a number of cases, this mechanical contact between the parasite and host intestinal tissue can irritate the intestinal mucosa, which may finally result in inflammatory processes leading to ulceration and intestinal dysfunctions (8). In this way parasite-derived molecules interact with the host immune system as antigens associated with three sources: excretory-secretory, surface, and tegumental proteins (9–11). Many of these molecules are proteins involved in the parasite's metabolism and survival strategies. In our previous study we identified numerous excretory-secretory proteins (ESPs), among which several were found as antigens with potential impact on the parasite–host interaction (10).

However, despite the current progress in understanding the parasite–host cross-talk mechanisms, the immunoparasitology and related proteomes of the adult cestodes have remained largely unknown. The only available data related to immunoproteomics of these organisms is based on the adult tapeworms *Echinococcus granulosus* infecting dogs (9). Comparing the number of reports regarding the immunoparasitology of cestode metacestode stages (predominantly hydatidosis), adult trematodes and nematodes, there is still a gap in our knowledge related to the adult cestode.

Human or other mammalian cestodiases are mostly caused by the metacestode juvenile stages of *Echinococcus* spp. (hydatid cysts) and *Taenia* spp. (cysticerci). Selected *Hymenolepis* species may infect humans in the adult stage, and *H. diminuta* has been extensively studied as it can be maintained in laboratory animal hosts (12). From these species, *H. diminuta* can establish successful invasion in both rodent and human hosts, and has become an important model for studying cestode-host interrelationships. However, from immunological perspectives, the adult stage of this organism has remained largely unexplored (13–23). The presence of adult tapeworms in the host intestine may also influence the function of this organ, thereby affecting the immunity and host condition. In support of this, Kosik-Bogacka et al. (24–31) have reported that *H. diminuta* had impact on ion transport, oxidative stress, the expression and/or activity of toll-like receptors and cyclooxygenases in rat intestines. Due to its low pathogenicity and immunomodulatory activity, *H. diminuta* is also considered a source of potential therapeutic molecules for treating autoimmune and inflammatory diseases activity (32–34).

In the present study, we applied 2DE immunoblotting (two-dimensional gel electrophoresis followed by immunoblotting) of *H. diminuta* proteins using antisera raised against this organism in rats to indicate antigenic proteins with potential role in adaptation and host–parasite interaction. In addition, the surface-associated proteins were identified to complement the 2DE results and to pinpoint the subcellular location of the identified antigens. Our study, besides uncovering plausible antigens in the adult cestodes, demonstrates that gel-based proteomic approach investigating individual proteins still offers an effective way for finding new candidates for immunodiagnostics and therapeutic strategies.

ANIMALS AND METHODS

Experimental Animals

Healthy and pathogen-free male Lewis rats, aged 3 months, were used as definitive hosts for adult *H. diminuta*. They were kept in plastic cages in the laboratory animal facilities of the Institute of Parasitology, PAS. They were provided feed and water *ad libitum*.

Ethics Statement

This study was approved by the 3rd Local Ethical Committee for Scientific Experiments on Animals in Warsaw, Poland (Permit number 51/2012, 30th of May 2012).

Cultivation of *H. diminuta* Adult Cestodes

Six-week-old *H. diminuta* cysticercoids were extracted from dissected *Tenebrio molitor* beetles under a microscope (magnification 100×). Three-month-old rats (10) were infected by voluntary oral uptake of six cysticercoids of *H. diminuta* per rat and the fecal sample direct smears were examined under a microscope (magnification 400×) after 5–6 weeks from the initial infection to verify the presence of adult parasites by finding eggs. Rats were euthanized with 100 mg/kg intraperitoneal tiopenthal anesthesia (Biochemie GmbH, Austria). The rat small intestines were removed immediately, adult parasites were isolated and washed up to five times with 100 mM PBS with antibiotics added (1% penicillin) to remove debris. Before protein extraction and proteomic analysis the parasitic material was stored at −80°C.

Collection of Serum From Infected Rats

Blood samples were collected 4–5 weeks after infection from rats, infected with *H. diminuta* and serum was separated. Sera before the infection at day 0 and from uninfected rats were used as negative controls (**Supplementary Figure 1**). Blood

samples were collected to tubes by cardiac puncture at the time of euthanasia from heavily sedated animals. After collection, samples were allow to clot by leaving them undisturbed at room temperature for 20–25 min. The clot was removed by centrifugation (1,500 × *g* for 15 min, +4°C), serum samples were collected immediately and transferred into a clean polypropylene tube using a pipette. If not used immediately samples were stored at −80°C.

Protein Extraction

Hymenolepis diminuta adult worms in whole (size between 40 and 60 cm in length) were suspended in lysis buffer, containing 8 M Urea, 4% CHAPS and 40 mM Tris-base supplemented with protease inhibitor cocktail (Roche, Germany) and homogenized by sonication on ice until the suspension became clear. The homogenate was centrifuged at 15,000 × *g* at 4°C for 25 min to collect the supernatant containing soluble proteins, which were either used directly or stored at −80°C until use. The protein concentration was measured using a Spectrometer ND-1000 UV/Vis (NanoDrop Technologies, United States). Three biological replicates (three adult worms at the same age collected from different animals) taken from independent experiments were used in the present study.

Two-Dimensional Gel Electrophoresis (2DE)

The protein samples (150 ±10 μg from each replicate) were rehydrated overnight in 250 μl of the rehydration solution (ReadyPrep™ 2-D Rehydration Buffer, Bio-Rad, USA) with immobilized pH gradient (IPG) gel 7 cm strips having pH ranging from 4 to 7. Isoelectric focusing (IEF) was performed using a Protean IEF Cell (BioRad, United States) at 20°C as follows: 15 min at 250 V, then rapid ramping to 4,000 V for 2 h, and 4,000 V for 16,000 Vh (using a limit of 50 μA/strip). After IEF, the strips were first equilibrated for 25 min in equilibration buffer (ReadyPrep™ 2-D Starter Kit Equilibration Buffer I, Bio-Rad, USA), followed by a 25-min equilibration in the same buffer supplemented with 2.5% iodoacetamide (ReadyPrep™ 2-D Starter Kit Equilibration Buffer II). The second dimension, SDS-PAGE, was run on 12% polyacrylamide gel in the Midi-Protean Tera Cell (Bio-Rad, United States) with 200 V, for approximately 45 min. All the replica gels were run in the same conditions.

After 2DE, the proteomes were visualized using the Silver Staining Kit according to the manufacturer's protocol (Krzysztof Kucharczyk Techniki Elektroforetyczne, Poland), or the 2DE gels were used without staining for immunoblotting. The silver-stained gels were scanned with a GS-800 densitometer (Bio-Rad, United States) and quantitatively analyzed using Quantity One and PDQuest Analysis Software (Bio-Rad, United States). To minimize the risk of protein overstaining, the time used in the developing step was reduced to a minimum.

2DE-Immunoblotting

Proteins from 2DE-gels were transferred by a wet transfer system (Bio-Rad, United States) to a nitrocellulose membrane (Bio-Rad, United States) that was then treated with sera collected from rats experimentally infected with *H. diminuta* diluted 1:500 in Protein-Free T20 (TBS) Blocking Buffer (Thermo Scientific, Rockford, United States) and then with anti-rat IgG-conjugated to horseradish peroxidase (1:8,000, Sigma Aldrich, United States). The blots were developed using the SuperSignal West Pico Chemiluminescent Substrate (ThermoFisher Scientific, United States) according to the provided instructions, and visualized using the GS-800 Densitometer (Bio-Rad, United States) and analyzed by the 1-D Analysis Software Quantity 1 (Bio-Rad, United States). The experiment was performed with three biological replicate samples.

LC-MS/MS Identification

Spots of interest were manually excised from the silver-stained gels and subjected to standard "in-gel digestion" procedure, in which they were first dehydrated with acetonitrile (ACN) and then reduced, alkylated, and digested with trypsin as previously described by Kordan et al. (35). Briefly, the gel pieces were first treated with 10 mM DTT in 100 mM NH_4HCO_3 for 30 min at 57°C, and then with 0.5 M iodoacetamide in 100 mM NH_4HCO_3 (45 min in the dark at room temperature). Proteins were digested overnight with 10 ng/μl trypsin in 25 mM NH_4HCO_3, at pH 8.5 (Promega, Madison, WI, United States) at 37°C. The resulting tryptic peptides were extracted in a solution containing 0.1% formic acid and 2% ACN.

The tryptic peptides were subjected to liquid chromatography and tandem mass spectrometry (LC-MS/MS) in the Laboratory of Mass Spectrometry, Institute of Biochemistry and Biophysics, Polish Academy of Sciences (Warsaw, Poland). Samples were concentrated and desalted on a RP-C18 pre-column (Waters, United States), and further peptide separation was achieved on a nano-Ultra Performance Liquid Chromatography (UPLC) RP-C18 column (Waters, BEH130 C18 column, 75 μm i.d., 250 mm long) of a nanoACQUITY UPLC system, using a 45-min linear acetonitrile gradient. The column outlet was directly coupled to the Electrospray ionization (ESI) ion source of the Orbitrap Velos type mass spectrometer (Thermo, United States), working in the regime of data dependent MS to MS/MS switch with HCD type peptide fragmentation. An electrospray voltage of 1.5 kV was used. Raw data files were pre-processed with Mascot Distiller software (version 2.5, MatrixScience).

The obtained peptide masses and fragmentation spectra were matched to the National Center Biotechnology Information (NCBI) non-redundant database NCBInr 20150115 (57,412,064 sequences; 20,591,031,683 residues), with a Cestoda filter (44,695 sequences) using the Mascot search engine (Mascot Server v. 2.4.1, MatrixScience). The following search parameters were applied: enzyme specificity was set to trypsin, peptide mass tolerance to ± 30 ppm and fragment mass tolerance to ± 0.1 Da. The protein mass was left as unrestricted, and mass values as monoisotopic with one missed cleavage being allowed. Alkylation of cysteine by carbamidomethylation as fixed and oxidation of methionine was set as a variable modification.

Multidimensional protein Identification Technology–type (MudPIT-type) and/or the highest number of peptide sequences, were selected. The expected value threshold of 0.05 was used

for analysis, which means that all peptide identifications had a <1 in 20 chance of being a random match. Spectra derived from silver-stained gel pieces usually do not contain enough MS/MS fragmentations to calculate a meaningful FDR, therefore a Mascot score threshold of 30 or above ($p < 0.05$) was used.

Extraction and Identification of Surface-Associated Proteins

Adult *H. diminuta* worms were first washed 3 times in sterile phosphate-buffered saline (PBS), followed by quick wash in sterile PBS with antibiotics (1% penicillin) to remove debris. Then they were washed again in sterile PBS without antibiotics and incubated in 3 ml of 1% Nonidet P-40 (NP-40 [Sigma Aldrich]) in 50 mM Ambic/AMBIC buffer for 30 min on a roller mixer at room temperature. After incubation samples were centrifuged at 15,000 × *g* and the supernatant was collected to a new tube. In order to perform mass spectrometry analysis Nonidet P-40 was removed using detergent Removal Spin Columns (Pierce) according to manufacturer's instructions. Columns were first equilibrated with 50 mM AMBIC without the detergent and then the sample was carefully applied on the column and incubated for 2 min in room temperature and eluted by centrifugation (1,000 × *g*, 2 min) to a new tube. The protein concentration was measured using a Spectrometer ND-1000 UV/Vis (NanoDrop Technologies, United States). Three replicates from the collected surface proteins were subjected to LC-MS/MS identification.

Proteins were identified by LC-MS/MS (Laboratory of Mass Spectrometry, Institute of Biochemistry and Biophysics, Polish Academy of Sciences (Warsaw, Poland) as described above. Protein solutions were subjected to standard procedure of trypsin digestion, during which proteins were reduced with 0.5 M (5 mM f.c.) TCEP for 1 h at 60°C, blocked with 200 mM MMTS (10 mM f.c.) for 10 min at RT and digested overnight with 10 μl of 0.1 ug/ul trypsin. The resulting peptide mixtures were applied in equal volumes of 20 μl to RP-18 pre-column (Waters, Milford, MA) using water containing 0.1% FA as a mobile phase and then transferred to a nano-HPLC RP-18 column (internal diameter 75 μM, Waters, Milford MA) using ACN gradient (0–35% ACN in 160 min) in the presence of 0.1% FA at a flow rate of 250 nl/min. The column outlet was coupled directly to the ion source of the Orbitrap Elite mass spectrometer (Thermo Electron Corp., San Jose, CA, United States) working in the regime of data-dependent MS to MS/MS switch with HCD type peptide fragmentation. A blank run ensuring absence of cross-contamination from previous samples preceded each analysis.

Raw data files were pre-processed with Mascot Distiller software (v. 2.6, MatrixScience, London, UK). The obtained peptide masses and fragmentation spectra were matched to the NCBInr database (167,148,673 sequences; 60,963,227,986 residues), with a *Cestoda* filter (49,619 sequences) using the Mascot Search Engine (MatrixScience, London, UK, Mascot Server 2.5). To reduce mass errors, the peptide and fragment mass tolerance settings were established separately for individual LC-MS/MS runs after a measured mass recalibration, resulting in values 5 ppm for parent and 0.01 Da for fragment ions. The rest of search parameters were as follows: enzyme, Trypsin; missed cleavages, 1; fixed modifications, Alkylation of cysteine by carbamidomethylation; oxidation of methionine was set as a variable modification. In each Mascot search, the score cutoff was determined automatically to obtain an FDR below 1%? The Decoy Mascot functionality was used for keeping FDR for peptide identifications below 1%.

Proteome Bioinformatics

The presence of potential N-terminal signal peptide cleavage site for the identified proteins was analyzed using the SignalP 4.1 tool (36). The identified proteins were classified according to their predicted molecular function, biological process, and cellular component using the UniProtKB database (http://www.uniprot.org/) and QuickGO (http://www.ebi.ac.uk/QuickGO/). Proteins with enzymatic properties were further classified according to Kyoto Encyclopedia of Genes and Genomes (KEGG) database (http://www.genome.jp/kegg/).

RESULTS

2DE of the *H. diminuta* Adult-Stage Proteins

The stained 2DE-protein patterns in each three biological replica gels were comparable. As our preliminary 2DE analyses indicated that most of the adult-stage proteins migrated with pI values ranging from 4 to 7 (data not shown), the present study focused on proteins covering this proteome region. The PDQuest software analyses of the silver-stained proteomes enabled us to distinguish more than 580 adult-stage protein spots from *H. diminuta*. **Figure 1** showing the representative silver-stained master gel indicates that majority of the protein spots migrated with molecular weights (MWs) between 15 and 130 kDa.

With the use of the 2DE-immunoblotting we detected 36 spots as positively recognized by the *H. diminuta*-infected rat sera, whereas sera collected form uninfected rats were signal free (**Figure 2** and **Supplementary Figure 1**). Potentially immunogenic proteins migrated predominantly with MWs between 35 and 250 kDa and pHs ranging from 4 to 5 and 6 to 7 (**Figure 2**). Several immunoreactive spots were also detected in the area between 10 and 35 kDa. The proteins were organized in eight groups of horizontally adjacent immunoreactive spots as shown in **Figures 1**, **2**.

LC-MS/MS Identification of Antigenic and Surface Proteins of *H. diminuta* Adult Stage

Thirty-six protein spots cross-reacting with the rat antisera were excised from the silver-stained replica 2DE-gel and subjected to in-gel tryptic digestion and LC-MS/MS analyses. As a result, 68 potentially antigenic proteins were identified and are listed in **Table 1** and **Supplementary File 1**. As shown in **Table 1** numerous proteins were identified from multiple spots; 38 of the identified proteins were present in more than one spot (**Table 1** and **Supplementary File 1**). Similarly, the number

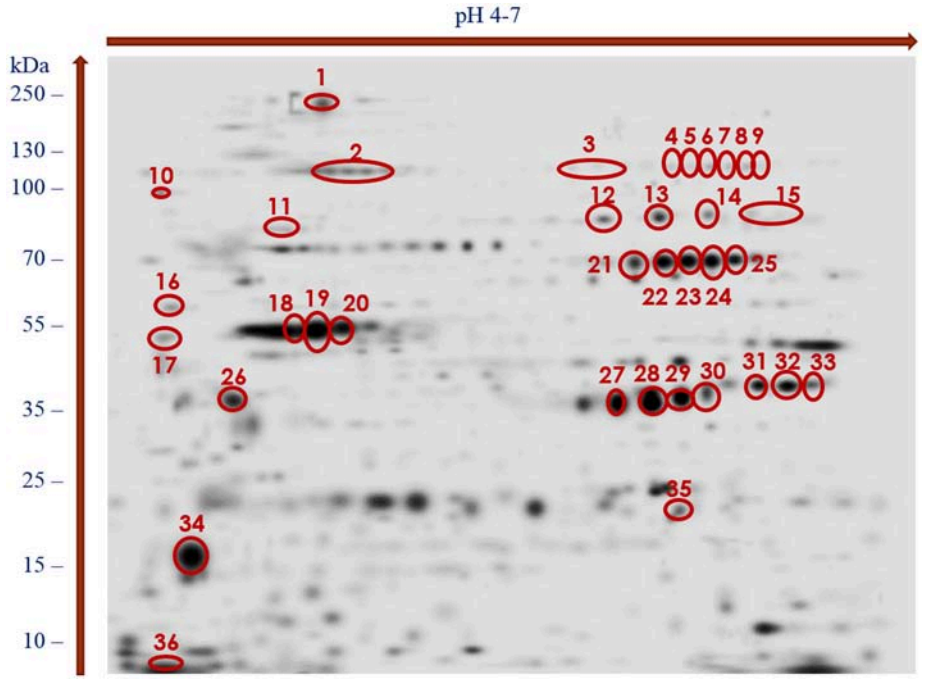

FIGURE 1 | Master gel of silver-stained 2-DE protein maps of *H. diminuta* adult-stage somatic proteome showing spots recognized as immunogenic and excised from the gel for LC-MS/MS analysis (indicated by red color).

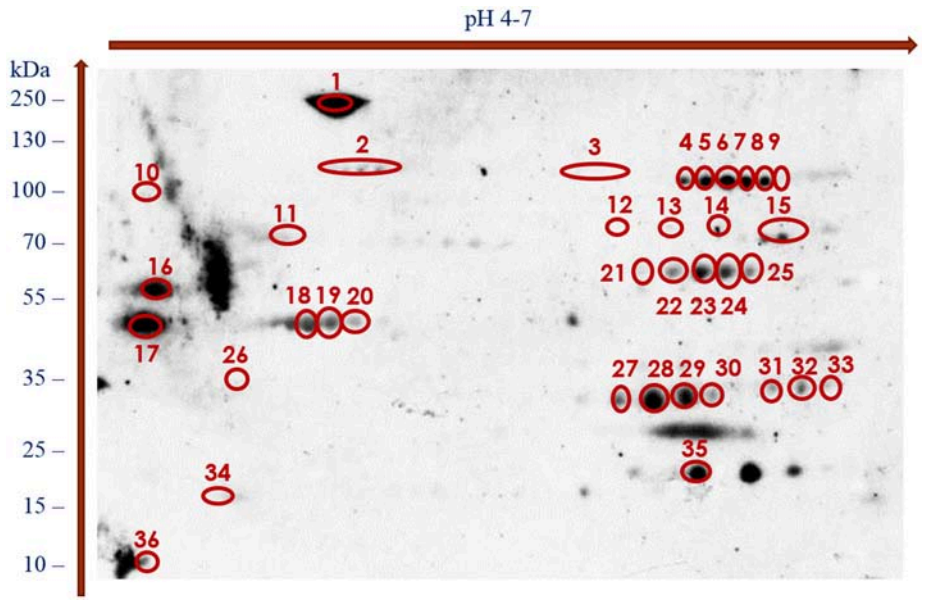

FIGURE 2 | Recognition pattern of *H. diminuta* adult-stage immunoreactive protein spots by antibodies of *H. diminuta*-infected rats visualized using chemiluminescence.

of proteins identified per spot varied from spot to spot; the highest number of proteins were identified from the spot number 12 (with 11 proteins) (**Supplementary File 2**). Only one protein was present in spots 10 (spectrin beta chain) and 36 (myosin essential light chain). Proteins that were most frequently identified from multiple spots included the aldo-keto reductase family 1 (present in 8 spots) proteins, glutamate dehydrogenase (in 9 spots), glyceraldehyde-3-phosphate dehydrogenase—GAPDH (in 8 spots), enolase, phosphoenolpyruvate carboxykinase and pyruvate kinase—PYK (in 7 spots).

TABLE 1 | Alphabetical list of identified adult *Hymenolepis diminuta* antigenic proteins with spot numbers and recognition of potentially signaling/secretory proteins (antigenic proteins identified for the first time in the adult cestode are indicated in bold).

Protein [Organism]	Spot number (Number of spots)	SP*
3-oxoacyl-acyl-carrier-protein reductase# [*Hm*]	35 (1)	N
Actin, cytoplasmic 2 [*Eg*]	1, 2, 11, 18, 19, 20 (6)	N
Actin, partial [*Dd*]	18, 19, 20, 26 (4)	N
Actin-1 [*Eg*]	19 (1)	N
Actin-5#, partial [*Dd*]	19 (1)	N
Alanine aminotransferase 2# [*Hm*]	12, 21, 22 (3)	N
Aldo-keto reductase family 1, member B4# [*Hm*]	22, 27, 28, 29, 30, 32, 33, 35 (8)	N
Alpha-tubulin [*Hd*]	11 (1)	N
Annexin A8 [*Eg*]	18, 25 (2)	N
Aspartyl tRNA synthetase, cytoplasmic [*Hm*]	12, 13 (2)	N
Calpain A# [*Hm*]	11 (1)	N
Calumenin-B [*Eg*]	26 (1)	**Y**
Capping protein (actin filament) muscle Z line [*Hm*]	31 (1)	N
Cytosolic malate dehydrogenase# [*Hm*]	27, 28, 29, 30, 31 (5)	N
Deoxyhypusine hydroxylase:monooxygenase# [*Hm*]	18, 19 (2)	N
Dnaj subfamily A [*Hm*]	21 (1)	N
Ef hand family protein [*Hm*]	27 (1)	**Y**
Elongation factor 2# [*Hm*]	15 (1)	N
Enolase# [*Hm*]	4, 12, 21, 22, 23, 24, 25 (7)	N
Estradiol 17 beta-dehydrogenase [*Eg*]	27 (1)	N
Eukaryotic initiation factor 4A [*Hm*]	19, 33 (2)	N
Filamin# [*Hm*]	1, 2, 11 (3)	N
Fructose-1,6-bisphosphate aldolase# [*Hm*]	32, 33 (2)	N
Fumarate hydratase class I# [*Hm*]	14, 15 (2)	N
Glucose-6-phosphate isomerase [*Eg*]	15, 31 (2)	N
Glutamate dehydrogenase# [*Hm*]	6, 7, 12, 14, 21, 22, 23, 24, 25 (9)	N
Glutamate dehydrogenase, mitochondrial# [*Hm*]	12, 23 (2)	N
Glyceraldehyde-3-phosphate dehydrogenase# [*Hm*]	9, 15, 28, 29, 30, 31, 32, 33 (8)	N
Glycogen phosphorylase# [*Hm*]	1 (1)	N
GTP-binding nuclear protein Ran [*Hm*]	35 (1)	N
Heat shock cognate protein [*Eg*]	2 (1)	N
Heat shock protein [*Eg*]	2, 11 (2)	N
Heat shock protein 60 [*Em*]	11 (1)	N
Heat shock protein 70# [*Hm*]	2, 3 (2)	N
Heterogeneous nuclear ribonucleoprotein 87F [*Eg*]	31, 32, 33 (3)	N
Hypothetical transcript [*Hm*]	2, 12, 13 (3)	N
Inosine-5- monophosphate dehydrogenase 2 [*Hm*]	25 (1)	N
Lactate dehydrogenase# [*Hm*]	28, 30 (2)	N
Lamin [*Hm*]	2, 3 (2)	N
Leucyl aminopeptydase [*Eg*]	13 (1)	N
Major egg antigen [*Hm*]	11 (1)	N
Major vault protein# [*Hm*]	1 (1)	N
Myosin essential light chain [*Hm*]	36 (1)	N
Myosin heavy chain# [*Hm*]	1, 2 (2)	N
Myosin regulatory light chain [*Eg*]	34 (1)	N
NADP-dependent malic enzyme# [*Hm*]	12, 13, 14, 15 (4)	N
Neuronal calcium sensor [*Hm*]	12, 13 (2)	N
Paramyosin [*Hm*]	1, 2, 3, 4, 11 (4)	N
Phosphoenolpyruvate carboxykinase# [*Hm*]	4, 5, 6, 7, 8, 9, 15 (7)	N
Phosphoglucomutase# [*Hm*]	12, 14 (2)	N
Pseudouridine metabolizing bifunctional protein [*Hm*]	9 (1)	N
Pyruvate kinase# [*Hm*]	6, 9, 12, 13, 14, 15 (7)	N
Spectrin alpha actinin# [*Hm*]	18, 26 (2)	N
Spectrin beta chain [*Hm*]	10, 16, 20 (3)	N
Stress-70 protein [*Eg*]	2 (1)	N
Subfamily T1A non peptidase [*Hm*]	34 (1)	N
Succinate dehydrogenase flavoprotein# [*Eg*]	3 (1)	N
Succinyl coenzyme A ligase# [*Hm*]	19, 20 (2)	N
T-complex protein 1 subunit delta [*Hm*]	14, 15 (2)	N
T-complex protein 1 subunit zeta [*Hm*]	12, 13 (2)	N
Transketolase# [*Hm*]	4, 5 (2)	N
Triosephosphate isomerase# [*Hm*]	35 (1)	N
Tropomyosin [*Hm*]	16, 17 (2)	N
Tropomyosin 2 high molecular weight [*Mc*]	17 (1)	N
Tubulin# [*Se*]	11 (1)	N
Tubulin beta chain# [*Eg*]	11, 26 (2)	N
Vacuolar H+ atpase v1 sector subunit A [*Hm*]	2 (1)	N
V-type proton atpase catalytic subunit A [*Eg*]	2 (1)	N

*SP - signal peptide; * - the presence of secretory/signal proteins predicted with the use of SignalP 4.1 Server software; Y - potentially secretory protein; N - negative search results; # - protein recognized among surface proteins; Dd - Diphyllobothrium dendriticum; Eg - Echinococcus granulosus; Em - Echinococcus multilocularis; Hd - Hymenolepis diminuta; Hm - Hymenolepis microstoma; Mc - Mesocestoides corti; Se - Spirometra erinaceieuropaei.*

Altogether, 30 proteins were identified from individual spots (**Table 1**).

Figure 1 shows the cross-reactive protein spots numbered with 1, 5–8, 18–20, 22–23, 28–29, and 35. They were found to match with the following proteins: actin, aldo keto reductase family 1 proteins, enolase, filamin, glutamate dehydrogenase, paramyosin, myosin, malate dehydrogenase, phosphoenolpyruvate carboxykinase, succinyl coenzyme-A ligase, spectrin, triosephosphate isomerase (TPI), and 3 oxoacyl

TABLE 2 | Enzymatic proteins identified by LCMS/MS in immunoreactive spots of the adult tapeworm *Hymenolepis diminuta*.

Enzyme classes	Protein names
Fructose-bisphosphate aldolase	Fructose-1,6-bisphosphate aldolase
Hydrolases	Calpain A
	Leucyl aminopeptidase
	Vacuolar H+ ATPase v1 sector subunit A
	V-type proton ATPase catalytic subunit A
Interconverting aldoses and ketoses	Glucose-6-phosphate isomerase
	Triosephosphate isomerase
Isomerases	Phosphoglucomutase
	Triosephosphate isomerase
Ligase	Aspartyl tRNA synthetase cytoplasmic
	Succinyl coenzyme A ligase
Lyases	Enolase
	Fumarate hydratase
	Phosphoenolpyruvate carboxykinase
Oxidoreductases	3-oxoacyl-[acyl-carrier-protein] reductase
	Aldo keto reductase family 1 member B4
	Cytosolic malate dehydrogenase
	Deoxyhypusine hydroxylase
	Estradiol 17 beta-dehydrogenase
	Glutamate dehydrogenase
	Glutamate dehydrogenase, mitochondrial
	Glyceraldehyde-3-phosphate dehydrogenase
	Inosine-5′-monophosphate dehydrogenase
	Lactate dehydrogenase
	NADP-dependent malic enzyme
	Succinate dehydrogenase flavoprotein
Proteasome endopeptidase complex	Proteasome subunit alpha type
Transferases	Alanine aminotransferase 2
	Pyruvate kinase
	Transketolase

acyl carrier protein reductase. The MW and pH values of these potential antigens ranged between 55 and 250 kDa and 4 and 7, respectively.

Several of the potentially antigenic *H. diminuta* adult-stage proteins could be classified as enzymes with 9 different subclasses, structural proteins and heat shock proteins (HSPs) (**Tables 1**, **2**). The oxidoreductases were found to be the most dominating enzyme group for the identified proteins (13 proteins) (**Table 2**).

Using non-gel based proteomic approach (in-solution tryptic digestion of proteins coupled with LC-MS/MS identification) we were able to identify 76 proteins from the surface of *H. diminuta* adult stage worms. All these proteins were identified in each replicate with at least three matching peptides (**Supplementary File 3**). Among these surface-associated proteins, enzymes involved in various catalytic activities were suggested to be the most abundant protein group. In addition, heat shock proteins with potential moonlighting functions and classical structural proteins including actins, myosins, and tubulins were also identified. Notably, 31 from these surface proteins were detected as potential antigens in 2DE immunoblotting (**Table 1**, proteins marked with hashtag), which indicates that several of these antigens are excreted out of the worm.

Gene Ontology (GO) of the Potentially Antigenic Proteins of *H. diminuta* Adult Stage

According to bioinformatics predictions only 2 of the proteins were predicted to be secreted via the classical secretion pathway (calumenin-B, ef-hand family protein) (**Table 1**). Based on the GO annotation the identified proteins were classified into 3 different categories; molecular function (62 proteins), biological process (35 proteins), and as cellular components (30 proteins) (**Figures 3**–**5**). Twenty subcategories were assigned to molecular functions (**Figure 3**), with predominant groups related to binding, e.g., ion binding (42 proteins), organic cyclic compound binding (29), heterocyclic compound binding (29), and small molecule binding (27). Biological processes could be assigned to 35 proteins, most of them engaged with carboxylic acid metabolism (12), cellular nitrogen compound metabolism (9), aromatic compound metabolism (9), heterocycle (9) and phosphorus (8) metabolic processes (**Figure 4**). **Figure 5** shows the distribution of the identified proteins according to their subcellular location; 30 proteins were associated with cellular structures (**Figure 5**), majority of them predicted to be localized in different cell (25) and organelle parts (9) or macromolecular complexes (9).

According to GO annotation 75 of the identified surface proteins were classified to molecular function, 48 to biological processes and 32 to associated cellular components (**Figures 6**–**8**). Among molecular functions the recognized proteins could be divided into 21 subcategories related mainly to molecule binding ion binding (43 proteins), organic (35) and heterocyclic compound binding (35), and small molecule binding (33) (**Figure 6**). The identified surface proteins associated with biological processes (**Figure 7**) are involved in cellular processes (40 proteins), organic substance (29) and primary metabolic (26) processes as well as in electron transport chain (25). **Figure 8** illustrates the division of the identified surface proteins into different cellular compartments.

DISCUSSION

The present study shows that somatic proteins of the adult *H. diminuta* tapeworms exhibit immunogenicity in the rat host, and that the revealed immunoproteome could be used to propose new candidate proteins taking part in parasite–host interactions. Our previously published proteomic results of the *H. diminuta* (ESPs) show that the adult cestode immunogenic proteins were involved in stress response, various metabolic processes and structurally related functions (10). Some of these proteins have been considered as potential vaccine candidates and drug targets for treating e.g., schistosomiasis (37–39) and hydatidosis (40–42). Present study indicates slight differences between the protein profiles

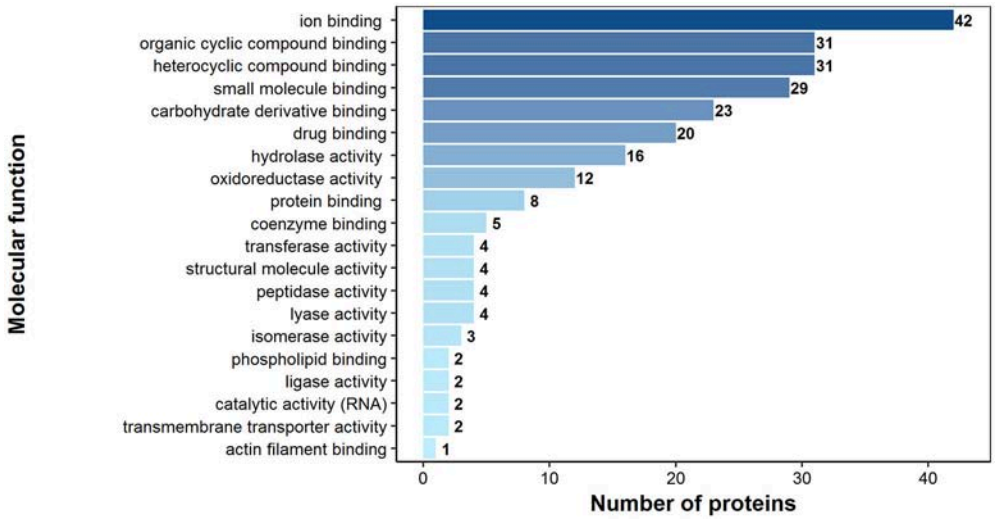

FIGURE 3 | Identified *H. diminuta* adult stage antigenic proteins categorized by their molecular functions according to gene ontology (GO) information obtained from UniProtKB and QuickGO databases.

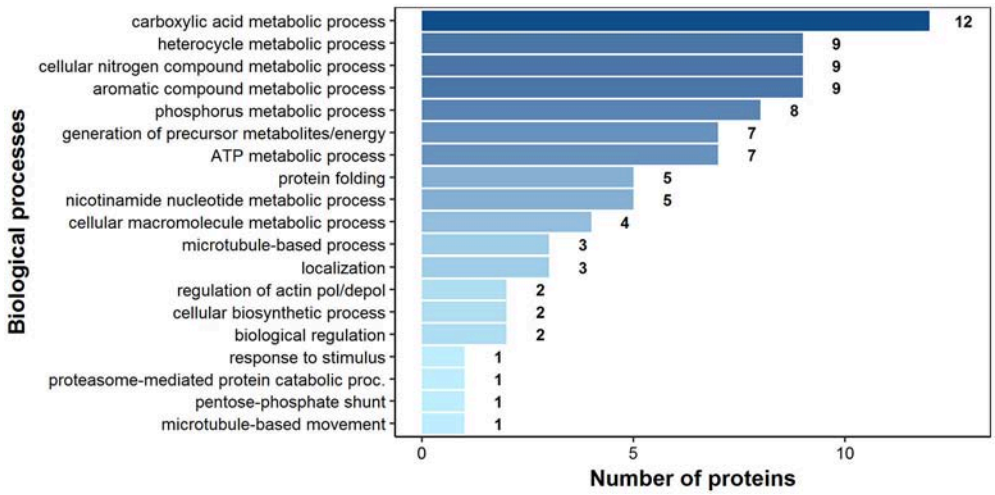

FIGURE 4 | Identified *H. diminuta* adult-stage antigenic proteins categorized by their biological processes according to gene ontology (GO) information obtained from UniProtKB and QuickGO databases.

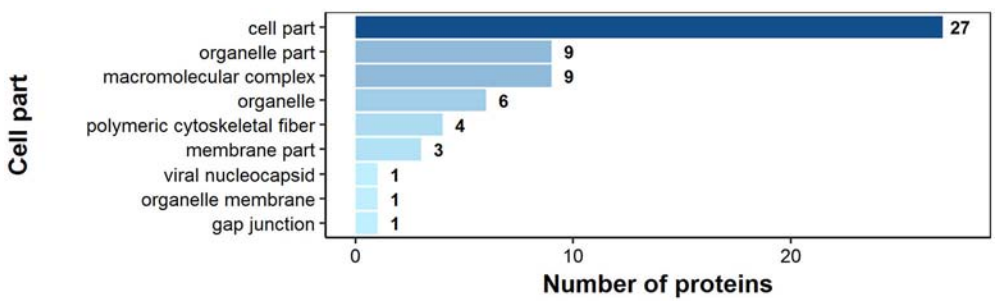

FIGURE 5 | Identified *H. diminuta* adult-stage antigenic proteins categorized by their cellular component category according to gene ontology (GO) information obtained from UniProtKB and QuickGO databases.

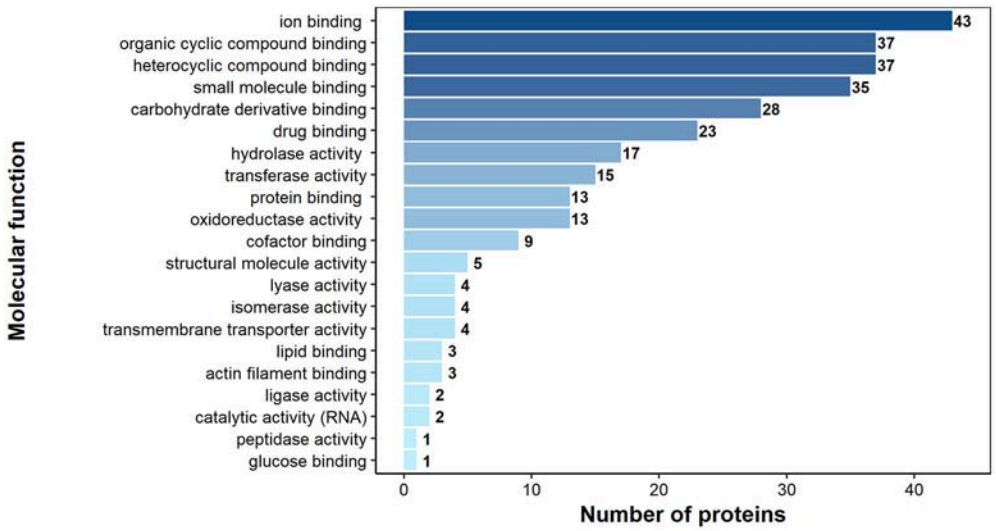

FIGURE 6 | Identified *H. diminuta* adult stage surface proteins categorized by their molecular functions according to gene ontology (GO) information obtained from UniProtKB and QuickGO databases.

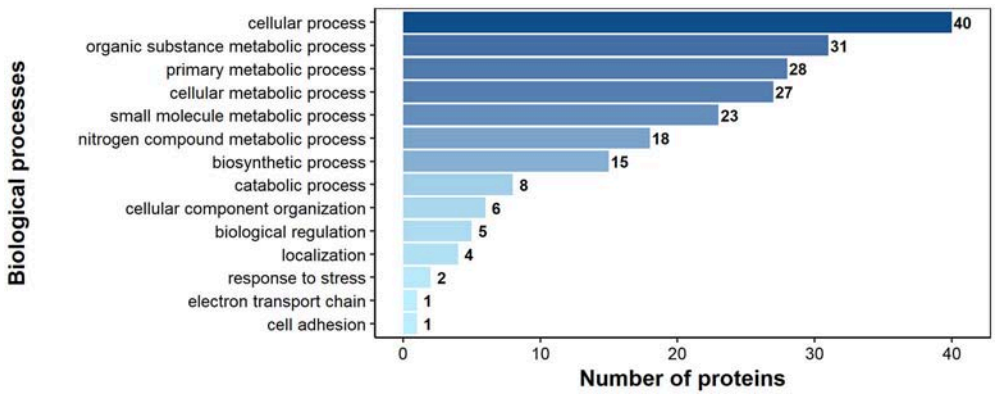

FIGURE 7 | Identified *H. diminuta* adult stage surface proteins categorized by their biological processes according to gene ontology (GO) information obtained from UniProtKB and QuickGO databases.

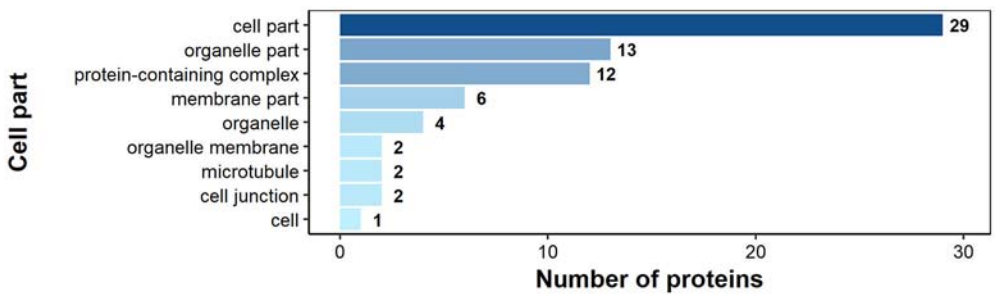

FIGURE 8 | Identified *H. diminuta* adult stage surface proteins categorized by their cellular component category according to gene ontology (GO) information obtained from UniProtKB and QuickGO databases.

obtained from ESPs and somatic proteome. The ESPs, cross-reacting with the specific antibodies and not recognized in the somatic proteome, were predominantly identified as structural proteins (titin, myoferlin, gelsolin, and neurogenic locus notch protein), proteins associated with transport (basement membrane-specific heparan sulfate, phospholipid transporting ATPase, armadillo type fold) and ion-binding and/or ion channels (anoctamin, sarcoplasmic calcium-binding protein).

The identified immunoproteome of the adult *H. diminuta* tapeworm could be divided into two main groups: (i) structural proteins engaged in diverse parasite–host interactions and (ii) enzymes involved in key metabolic processes (NADP dependent malic enzyme, pyruvate kinase–PYK) or conferring moonlighting activity (43, 44) (e.g., triosephosphate isomerase—TPI, glycogen phosphorylase, L- lactate dehydrogenase–L-LDH, glyceraldehyde 3-phosphate dehydrogenase—GAPDH, glucose-6-phosphate isomerase-GPI, fructose 1,6-bisphosphate aldolase-FBA, inosine-5′-monophosphate dehydrogenase-IMP, succinate dehydrogenase, and deoxyhypusine hydroxylase) to the cells. Majority of these proteins are catalytic enzymes with a role in glycolysis, glyconeogenesis, tricarboxylic acid cycle, pyruvate fermentation or purine metabolism, which are cytosolic proteins predicted to be exported via non-classical secretion pathways and having adhesive moonlighting functions after entering the cell surface of an organism (43, 44). Since cestodes take the nutrients through the tegument and directly from the host, the direct contact of the host with the parasite-derived enzymes is highly probable. We may then hypothesize that the constant release of enzymes by the parasite not only influence host immunity but may also change the environment, and could explain the ability of the cestode to modify and alter the microbiome communities of the host intestine (14, 45–47). This is in consistent with the results of Kosik-Bogacka et al. who studied the impact of *H. diminuta* on transepithelial ion transport in intestines, and blood parameters of infected rats at different stages of the infection (24, 26). According to these observations cestodiasis reduced the transepithelial electrical potential and caused a leakage of tight junctions. Another effect of active hymenolepidosis was related to increased lipid peroxidation, changes in anti-oxidant enzyme activity and altered glutathion level in the infected rat gastrointestinal tract (25). This suggests decreased efficiency of intestinal protection against oxidative stress induced by the presence of the parasite. All of the aforementioned processes and the presence of parasite derived molecules may change the intestinal environment and provoke changes in microbiome composition.

On the other hand, as suggested by Kosik-Bogacka (24–26) imbalance between oxidant and anti-oxidant processes can play a major role in pathology associated with hymenolepidosis, including its proinflamatory role associated with the expression and activation of cyclooxygenases in the rat gastrointestinal tract (31). Pathomechanisms observed during infection with *H. diminuta* may be connected with the changes in the expression of toll-like receptors (TLR) important for pathogen recognition. Kosik-Bogacka et al. (28, 29), studying the expression of TLR in *H. diminuta* infected rats, observed increased TLR2 and TLR4 expression compared to the control group, especially in the small intestine. Similarly, the TLR3 snf TLT9 expression was higher in infected rats (30). These analyses confirmed the role of TLR in hymenolepidosis and suggest that *H. diminuta* releases antigens stimulating immune response, which results in adaptation of the host organism to parasite derived molecules (32). Our previous research demonstrated the presence of PYK and GAPDH among the ESP of adult *H. diminuta* (10) and here we confirmed their immunogenic potential. In addition to glycolytic enzymes (PYK and GAPDH), also these taking part in fatty enzyme metabolism are considered important drug targets. Similarly to 3-oxoacyl-ACP reductase, an important candidate in antischistosomal combat (48). As the above mentioned enzymatic proteins have not been identified as immunogenic in the adult *E. granulosus* (9), our study reports their possible antigenicity in an adult tapeworms for the first time. This suggests that similarly to metacestodes, adult tapeworm enzymes (moonlighters) take part in parasite-host interplay. Some of these metabolic enzymes may be derived from the tegument by shedding of glycocalyx (present paper) or are released with secretory vesicles as described by Ancarola et al. (49) for metacestodes.

Our findings suggest that the non-classical protein export, possibly involving protein moonlighters, could contribute to increased viability and interaction with the host. Intriguingly, a recent study reported that this interplay may be mediated by the involvement of extracellular vesicles (EVs) to export cytosolic proteins in a protected and concentrated manner, as proved for metacestodes (49). Similarly, EVs released by hexacanth larvae were proved to be a source of *Taenia ovis* vaccine antigens (50). Since our immunoproteomic approach shows the presence of certain cytosolic and structural proteins as possible antigens, we suppose that the mechanism of their trafficking may have involved EVs. These include for instance antigens considered as vaccine candidates such as calpain (51, 52) and the major egg antigen p40 (mp40) (53–55).

Structural and enzymatic proteins are the most typical immunodominant antigens represented by the somatic proteome of the adult stage of *H. diminuta*. Among cestodes, antigenicity of certain structural proteins was first described in studies focusing on the metacestode stages (40–42, 56–61). Our recent study on antigenic proteins of *H. diminuta* cysticercoid metacestodes (57) supported these findings and confirmed the immunogenic importance of structural proteins, in host's immune response to infection. This indicated that structural proteins, for example beta-tubulin, should be considered as vaccine candidates and/or drug targets against cestode metacestode and adult stages. Another interesting example of structural protein is paramyosin identified at the helminths' surface or among the secreted proteins. This structural protein is believed to function as a multifunctional modulator of the host immune response (62, 63), and together with actin is involved in tegumental repair and considered to represent an important vaccine target molecule. The localization of this protein in the tegument of the parasite is the likely basis for resistance observed in mice immunized with paramyosin (64). Interestingly, it has been speculated that

paramyosin protects invading helminths from the immune attack by "decoy" binding proteins of the complement pathway (62). The presence of paramyosin has also been identified as a potential antigen in adult tapeworms (51). Antigenicity of paramyosin was further confirmed by Wang et al. (9), as this protein was one of the major antigens recognized by the antisera from dogs infected with adult *Echinococcus granulosus*.

Immunoproteomic analysis of adult *E. granulosus* has revealed the presence of 12 and 8 potentially antigenic proteins associated, respectively with the somatic proteome and the secretome of this organism (9). Only 7 potentially immunogenic proteins were commonly identified from *E. granulosus* and by us in *H. diminuta* adult worms. These included actin, paramyosin and several moonlighters such as enolase (ENO), malate dehydrogenase (MDH), TPI as well as the stress-related HSP60 and HSP70 proteins. Two other proteins, namely, calreticulin and superoxide dismutase (SOD) were previously identified in *H. diminuta* cysticercoids (11), but they have not been recognized as immunogenic (57). The revealed immunoproteome of the *H. diminuta* indicated potential vaccine candidates against echinococcosis, such as ENO, calpain, and GAPDH and the stress proteins HSP60 and HSP70 (51). Heat shock proteins (HSPs) are known key players in processes associated with development, differentiation, survival, aging, and death. While the antigenic potential of HSPs was shown in previous studies on cestode metacestode stages (56, 57, 65), their immunogenicity in the adult tapeworms has been confirmed only in *E. granulosus* (9), in the present and in our previous studies on *H. diminuta* ESP (10). For as much as HSPs are considered as potential vaccine target proteins (66), their presence throughout the cestode life cycle suggests their importance in cestode biology and survival in the host. The balanced interplay between structural and stress molecules is probably one of the survival factors adopted by parasites during coevolution with their hosts (11). Comparative proteomic analyses of adult and metacestode stages suggest stage-specific mechanisms engaged in the parasite's survival at different life-cycle stages (11, 67). In *H. diminuta*, proteins with antigenic potential, common for these two stages are structural proteins (actins, annexin, lamin, myosin, paramyosin, tubulin), enzymes (calpain, NADP dependent malic enzyme, phosphoenolpyruvate carboxykinase, succinyl co-A), HSPs, and major egg antigen (57). Differences in the expression of immunogenic proteins observed in these two distinct stages are associated predominantly with enzymes and may reflect variability in metabolic activity and stage-specific survival strategies.

There has been interest in targeting metabolic enzymes in the treatment of infectious diseases (68). Fumarate hydratase, involved in canalization of the stereospecific reversible hydration of fumarate to l-malate during the citric acid cycle, was one of the enzymes we have previously identified as one of the immunogens characteristic for the adult *H. diminuta* (11). It has been shown that this enzyme takes part in dismutation of malate in the nematode mitochondria (69), thereby making this enzyme one of the promising targets for designing efficient anthelminthic drugs. The present study also suggests that non-classically exported cytoplasmic proteins, i.e., moonlighters (e.g., enzymes, structural proteins, and HSPs), form another group of proteins playing important roles in host–parasite interactions. One of these moonlighters may be TPI that has also been identified as one of the somatic and surface proteins in *H. diminuta* (9) and in the present study. This enzyme is involved in glycolysis and has been proposed to represent a potential drug target and vaccine candidate to treat schistosomiasis (70).

The potential role of parasite antigens in contributing to increased viability via their immunomodulatory and anti-inflammatory activity has resulted in the concept of helminth-derived molecules as a source of immunomodulatory agents (32, 71, 72). The immunogenic proteins in the crude extract and among the identified surface proteins of *H. diminuta* adult worms may show potential in search of new drug targets and diagnostic methods, since the helminth-derived molecules are considered as potential therapeutics of autoimmune and inflammatory diseases (32–34, 72–74). Recent reports indicated that adult *H. diminuta* tapeworms can effectively modulate the host immune system (15, 16, 20, 47, 75, 76), and that *H. diminuta*-derived molecules can be used to control inflammation (20, 75, 77–79). The results here indicate that *H. diminuta* somatic proteins have been exposed to the host immune system as antigens. However, to uncover full immunomodulatory potential of the identified *H. diminuta* proteins, further studies and finally *in vivo* experiments are needed.

CONCLUSIONS

The somatic proteome and surfaceome of the adult *H. diminuta* with the use of 2DE immunoblotting and LC-MS/MS identification is reported here. The present study proposed a number of new immunogenic proteins involved in key metabolic processes and with likely roles in mediating parasite–host interactions. The identified immunodominant antigens, classified as proteins having structural and enzymatic functions, suggest contributory role of these molecules in mediating host–parasite interaction and during the adult cestode infection. Here we point to enzymes, structural and heat-shock proteins as potential mediators in the interactions between the parasite and the host. Most of these molecules are predicted to trafficate by non-classical ways by motifs or signals that remain to be uncovered. Thus, the present study shed new light on the complexity of the parasite-host interplay during cestodiasis, and highlights the importance of non-classical protein export (e.g., EVs and protein moonlighters) in modulating the parasite–host interaction. This study also provides valuable data not only for understanding the adult cestode biology but also for searching new targets for diagnostic and drug innovations.

AUTHOR CONTRIBUTIONS

DM supervised the work and all its proteomic features and drafted the manuscript. KS and AN participated in the planning of the study. AN, DM, JB, and KS conceived and designed the experiments. AS, JB, and DM conceived and performed the immunological study with rats. KS supported AS and DM in mass

spectrometry data analyses. AN, AZ-D, DBC, JB, KB, KS, and RS participated in data analyses and final editing of the manuscript. All authors were actively involved in preparing the manuscript with the responsible author. All authors read and approved the final version of the manuscript.

FUNDING

Financial support for this study was provided by the National-Science-Center-Poland (grants 2012/05/B/NZ6/00769 and 2017/01/X/NZ6/00260).

ACKNOWLEDGMENTS

The equipment used for protein identification by LC-MS/MS analysis was sponsored in part by the Center for Preclinical Research and Technology (CePT), a project co-sponsored by the European Regional Development Fund and Innovative Economy, The National Cohesion Strategy of Poland.

SUPPLEMENTARY MATERIAL

The Supplementary Material for this article can be found online at: https://www.frontiersin.org/articles/10.3389/fimmu.2018.02487/full#supplementary-material

Supplementary Figure 1 | Negative control showing Western blot recognition pattern of *H. diminuta* adult-stage proteins with sera collected from *H. diminuta*-uninfected rats and visualized using chemiluminescence.

Supplementary File 1 | Results of the LC-MS/MS analysis of immunoreactive protein spots of the adult tapeworm somatic proteome recognized by sera from *Hymenolepis diminuta* infected rats.

Supplementary File 2 | *Hymenolepis diminuta* adult stage proteins identified from immunoreactive spots selected for LC-MS/MS analysis.

Supplementary File 3 | Results of the LC-MS/MS analysis of collected surface proteins of the adult tapeworm *Hymenolepis diminuta*.

REFERENCES

1. Ito A, Budke CM. Culinary delights and travel? a review of zoonotic cestodiases and metacestodiases. *Travel Med Infect Dis.* (2014) 12:582–91. doi: 10.1016/j.tmaid.2014.06.009
2. Torgerson PR, Devleesschauwer B, Praet N, Speybroeck N, Willingham AL, Kasuga F, et al. World Health Organization estimates of the global and regional disease burden of 11 foodborne parasitic diseases, 2010: a data synthesis. *PLoS Med.* (2015) 12:e1001920. doi: 10.1371/journal.pmed.1001920
3. Thompson RCA. Neglected zoonotic helminths: *Hymenolepis nana*, *Echinococcus Canadensis,* and *Ancylostoma ceylanicum*. *Clin Microbiol Infect.* (2015) 21:426–32. doi: 10.1016/j.cmi.2015.01.004
4. Crompton DWT. How much human helminthiasis is there in the world? *J Parasitol.* (1999) 85:397–403. doi: 10.2307/3285768
5. Rabiee MH, Mahmoudi A, Siahsarvie R, Kryštufek B, Mostafavi E. Rodent-borne diseases and their public health importance in Iran. *PLoS Negl Trop Dis.* (2018) 12:e0006256. doi: 10.1371/journal.pntd.0006256
6. Conn DB. *Atlas of Invertebrate Reproduction and Development*. 2nd ed. New York, NY: John Wiley & Sons (2000).
7. Conn DB, Swiderski Z. A standardised terminology of the embryonic envelopes and associated developmental stages of tapeworms (Platyhelminthes: *Cestoda*). *Folia Parasitol.* (2008) 55:42–52. doi: 10.14411/fp.2008.006
8. Webb C, Cabada MM. Intestinal cestodes. *Curr Opin Infect Dis.* (2017) 30:504–10. doi: 10.1097/QCO.0000000000000400
9. Wang Y, Xiao D, Shen Y, Han X, Zhao F, Li X, et al. Proteomic analysis of the excretory/secretory products and antigenic proteins of *Echinococcus granulosus* adult worms from infected dogs. *BMC Vet Res.* (2015) 11:1–7. doi: 10.1186/s12917-014-0312-6
10. Bien J, Sałamatin R, Sulima A, Savijoki K, Conn DB, Näreaho A, et al. Mass spectrometry analysis of the excretory-secretory (E-S) products of the model cestode *Hymenolepis diminuta* reveals their immunogenic properties and the presence of new E-S proteins in *cestodes*. *Acta Parasitol.* (2016) 61:429–42. doi: 10.1515/ap-2016-0058
11. Sulima A, Savijoki K, Bien J, Näreaho A, Salamatin R, Conn DB, et al. Comparative proteomic analysis of *Hymenolepis diminuta* cysticercoid and adult stages. *Front Microbiol.* (2018) 8:2672. doi: 10.3389/fmicb.2017.02672
12. Siles-Lucas M, Hemphill A. *Cestode* parasites: application of *in vivo* and *in vitro* models for studies on the host-parasite relationship. *Adv Parasitol.* (2002) 51:133–230. doi: 10.1016/S0065-308X(02)51005-8
13. Graepel R, Leung G, Wang A, Villemaire M, Jirik FR, Sharkey KA, et al. Murine autoimmune arthritis is exaggerated by infection with the rat tapeworm, *Hymenolepis diminuta*. *Int J Parasitol.* (2013) 43:593–601. doi: 10.1016/j.ijpara.2013.02.006
14. McKenney EA, Williamson L, Yoder AD, Rawls JF, Bilbo SD, Parker W. Alteration of the rat cecal microbiome during colonization with the helminth *Hymenolepis diminuta*. *Gut Microbes* (2015) 6:182–93. doi: 10.1080/19490976.2015.1047128
15. Hunter MM, Wang A, Parhar KS, Johnston MJG, Van Rooijen N, Beck PL, et al. *In vitro*-derived alternatively activated macrophages reduce colonic inflammation in mice. *Gastroenterology* (2010) 138:1395–405. doi: 10.1053/j.gastro.2009.12.041
16. Zawistowska-Deniziak A, Basałaj K, Strojny B, Młocicki D. New data on human macrophages polarization by *Hymenolepis diminuta* tapeworm-An *in vitro* study. *Front Immunol.* (2017) 8:148. doi: 10.3389/fimmu.2017.00148
17. Melon A, Wang A, Phan V, McKay DM. Infection with *Hymenolepis diminuta* is more effective than daily corticosteroids in blocking chemically induced colitis in mice. *J Biomed Biotechnol.* (2010) 2010:384523. doi: 10.1155/2010/384523
18. Jones P, Binns D, Chang H-Y, Fraser M, Li W, McAnulla C, et al. InterProScan 5: genome-scale protein function classification. *Bioinformatics* (2014) 30:1236–40. doi: 10.1093/bioinformatics/btu031
19. Aira N, Andersson AM, Singh SK, McKay DM, Blomgran R. Species dependent impact of helminth-derived antigens on human macrophages infected with *Mycobacterium tuberculosis*: direct effect on the innate anti-mycobacterial response. *PLoS Negl Trop Dis.* (2017) 11: e0005390. doi: 10.1371/journal.pntd.0005390
20. Reyes JL, Fernando MR, Lopes F, Leung G, Mancini NL, Matisz CE, et al. IL-22 restrains tapeworm-mediated protection against experimental colitis via regulation of IL-25 expression. *PLoS Pathog.* (2016) 12:e1005481. doi: 10.1371/journal.ppat.1005481
21. Wang A, McKay DM. Immune modulation by a high molecular weight fraction from the rat tapeworm *Hymenolepis diminuta*. *Parasitology* (2005) 130:575–85. doi: 10.1017/S0031182004006985
22. Persaud R, Wang A, Reardon C, McKay DM. Characterization of the immuno-regulatory response to the tapeworm *Hymenolepis diminuta* in the non-permissive mouse host. *Int J Parasitol.* (2007) 37:393–403. doi: 10.1016/j.ijpara.2006.09.012
23. Matisz CE, McDougall JJ, Sharkey KA, McKay DM. Helminth parasites and the modulation of joint inflammation. *J Parasitol Res.* (2011) 2011:942616. doi: 10.1155/2011/942616
24. Kosik-Bogacka DI, Baranowska-Bosiacka I, Salamatin R. *Hymenolepis diminuta:* effect of infection on ion transport in colon and blood picture of rats. *Exp Parasitol.* (2010) 124:285–94. doi: 10.1016/j.exppara.2009.10.014
25. Kosik-Bogacka DI, Baranowska-Bosiacka I, Nocen I, Jakubowska K, Chlubek D. *Hymenolepis diminuta*: activity of anti-oxidant enzymes in different parts of rat gastrointestinal tract. *Exp Parasitol.* (2011) 128:265–71. doi: 10.1016/j.exppara.2011.02.026

26. Kosik-Bogacka DI, Kolasa A, Baranowska-Bosiacka I, Marchlewicz M. *Hymenolepis diminuta*: the effects of infection on transepithelial ion transport and tight junctions in rat intestines. *Exp Parasitol.* (2011) 127:398–404. doi: 10.1016/j.exppara.2010.09.001
27. Kosik-Bogacka DI, Kolasa A. Histopathological changes in small and large intestines during hymenolepidosis in rats. *Folia Biol.* (2012) 60:195–8. doi: 10.3409/fb60_3-4.195-198
28. Kosik-Bogacka DI, Wojtkowiak-Giera A, Kolasa A, Czernomysy-Furowicz D, Lanocha N, Wandurska-Nowak E, et al. *Hymenolepis diminuta*: analysis of the expression of Toll-like receptor genes (TLR2 and TLR4) in the small and large intestines of rats. Part II. *Exp Parasitol.* (2013) 130:261–6. doi: 10.1016/j.exppara.2013.08.002
29. Kosik-Bogacka DI, Wojtkowiak-Giera A, Kolasa A, Salamatin R, Jagodzinski PP, Wandurska-Nowak E. *Hymenolepis diminuta*: analysis of the expression of Toll-like receptor genes (TLR2 and TLR4) in the small and large intestines of rats. *Exp Parasitol.* (2012) 130:261–6. doi: 10.1016/j.exppara.2011.12.002
30. Kosik-Bogacka DI, Wojtkowiak-Giera A, Kolasa A, Baranowska-Bosiacka I, Lanocha N, Wandurska-Nowak E, et al. *Hymenolepis diminuta*: analysis of the expression of Toll-like receptor genes and protein (TLR3 and TLR9) in the small and large intestines of rats. *Exp Parasitol.* (2014) 145:61–7. doi: 10.1016/j.exppara.2014.07.009
31. Kosik-Bogacka DI, Baranowska-Bosiacka I, Kolasa-Wołosiuk A, Lanocha-Arendarczyk N, Gutowska I, Korbecki J, et al. The inflammatory effect of infection with *Hymenolepis diminuta* via the increased expression and activity of COX-1 and COX-2 in the rat jejunum and colon. *Exp Parasitol.* (2016) 169:69–76. doi: 10.1016/j.exppara.2016.07.009
32. Maizels RM, McSorley HJ. Regulation of the host immune system by helminth parasites. *J Allergy Clin Immunol.* (2016) 138:666–75. doi: 10.1016/j.jaci.2016.07.007
33. Smallwood TB, Giacomin PR, Loukas A, Mulvenna JP, Clark RJ, Miles JJ. Helminth immunomodulation in autoimmune disease. *Front Immunol.* (2017) 8:453. doi: 10.3389/fimmu.2017.00453
34. Wang M, Wu L, Weng R, Zheng W, Wu Z, Lv Z. Therapeutic potential of helminths in autoimmune diseases: helminth-derived immune-regulators and immune balance. *Parasitol Res.* (2017) 116:2065–74. doi: 10.1007/s00436-017-5544-5
35. Kordan W, Malinowska A, Lecewicz M, Wysocki P, Fraser L, Strzezek J. The structure of platelet-activating factor acetylhydrolase (PAF-AH) isolated from boar seminal plasma and examined using mass spectrometry. *Anim Sci Pap Rep.* (2007) 25:289–95.
36. Nielsen H. Predicting secretory proteins with signalP. *Methods Mol Biol.* (2017) 1611:59–73. doi: 10.1007/978-1-4939-7015-5_6
37. Sotillo J, Pearson M, Becker L, Mulvenna J, Loukas A. A quantitative proteomic analysis of the tegumental proteins from *Schistosoma mansoni* schistosomula reveals novel potential therapeutic targets. *Int J Parasitol.* (2015) 45:505–16. doi: 10.1016/j.ijpara.2015.03.004
38. DeMarco R, Verjovski-Almeida S. Schistosomes-proteomics studies for potential novel vaccines and drug targets. *Drug Discov Today* (2009) 14:472–78. doi: 10.1016/j.drudis.2009.01.011
39. Verjovski-Almeida S, DeMarco R. Current developments on *Schistosoma* proteomics. *Acta Trop.* (2008) 108:183–5. doi: 10.1016/j.actatropica.2008.04.017
40. Chemale G, Van Rossum AJ, Jefferies JR, Barrett J, Brophy PM, Ferreira HB, et al. Proteomic analysis of the larval stage of the parasite *Echinococcus granulosus*: causative agent of cystic hydatid disease. *Proteomics* (2003) 3:1633–6. doi: 10.1002/pmic.200300487
41. Virginio VG, Monteiro KM, Drumond F, De Carvalho MO, Vargas DM, Zaha A, et al. Excretory/secretory products from *in vitro*-cultured *Echinococcus granulosus* protoscoleces. *Mol Biochem Parasitol.* (2012) 183:15–22. doi: 10.1016/j.molbiopara.2012.01.001
42. Monteiro KM, De Carvalho MO, Zaha A, Ferreira HB. Proteomic analysis of the *Echinococcus granulosus* metacestode during infection of its intermediate host. *Proteomics* (2010) 10:1985–99. doi: 10.1002/pmic.200900506
43. Jeffery CJ. Moonlighting proteins – nature's Swiss army knives. *Sci Prog.* (2017) 100:363–73. doi: 10.3184/003685017X15063357842574
44. Chen C, Zabad S, Liu H, Wang W, Jeffery C. MoonProt 2.0: an expansion and update of the moonlighting proteins database. *Nucleic Acids Res.* (2018) 46:D640–4. doi: 10.1093/nar/gkx1043
45. Aivelo T, Norberg A. Parasite-microbiota interactions potentially affect intestinal communities in wild mammals. *J Anim Ecol.* (2018) 87:438–47. doi: 10.1111/1365-2656.12708
46. Wegener Parfrey L, Jirku M, Šíma R, Jalovecká M, Sak B, Grigore K, et al. A benign helminth alters the host immune system and the gut microbiota in a rat model system. *PLoS ONE* (2017) 12:e0182205. doi: 10.1371/journal.pone.0182205
47. Kapczuk P, Kosik-Bogacka D, Łanocha-Arendarczyk N, Gutowska I, Kupnicka P, Chlubek D, et al. Selected molecular mechanisms involved in the parasite—host system *Hymenolepis diminuta—Rattus norvegicus*. *Int J Mol Sci.* (2018) 19:2435. doi: 10.3390/ijms19082435
48. Liu J, Dyer D, Wang J, Wang S, Du X, Xu B, et al. 3-Oxoacyl-ACP reductase from *Schistosoma japonicum*: integrated *in silico-in vitro* strategy for discovering antischistosomal lead compounds. *PLoS ONE* (2013) 8:e64984. doi: 10.1371/journal.pone.0064984
49. Ancarola ME, Marcilla A, Herz M, Macchiaroli N, Pérez M, Asurmendi S, et al. Cestode parasites release extracellular vesicles with microRNAs and immunodiagnostic protein cargo. *Int J Parasitol.* (2017) 47:675–86. doi: 10.1016/j.ijpara.2017.05.003
50. Jabbar A, Swiderski Z, Mlocicki D, BeveridgeEI, Lightowlers MW. The ultrastructure of taeniid cestode oncospheres and localization of host-protective antigens. *Parasitology* (2010) 137:521–35. doi: 10.1017/S0031182009991260
51. Cui SJ, Xu LL, Zhang T, Xu M, Yao J, Fang CY, et al. Proteomic characterization of larval and adult developmental stages in *Echinococcus granulosus* reveals novel insight into host-parasite interactions. *J Proteomics* (2013) 84:158–75. doi: 10.1016/j.jprot.2013.04.013
52. Zhang Y, Taylor MG, Johansen MV, Bickle QD. Vaccination of mice with a cocktail DNA vaccine induces a Th1-type immune response and partial protection against Schistosoma japonicum infection. *Vaccine* (2001) 20:724–30. doi: 10.1016/S0264-410X(01)00420-0
53. Anthony RM, Rutitzky LI, Urban JF, Stadecker MJ, Gause WC, Urban JF Jr, et al. Protective immune mechanisms in helminth infection. *Nat Rev Immunol.* (2007) 7:975–87. doi: 10.1038/nri2199
54. Cass CL, Johnson JR, Califf LL, Xu T, Hernandez HJ, Stadecker MJ, et al. Proteomic analysis of *Schistosoma mansoni* egg secretions. *Mol Biochem Parasitol.* (2007) 155:84–93. doi: 10.1016/j.molbiopara.2007.06.002
55. Abouel-Nour MF, Lotfy M, Attallah AM, Doughty BL. *Schistosoma mansoni* major egg antigen Smp40: molecular modeling and potential immunoreactivity for anti-pathology vaccine development. *Mem Inst Oswaldo Cruz.* (2006) 101:365–72. doi: 10.1590/S0074-02762006000400004
56. Aziz A, Zhang W, Li J, Loukas A, McManus DP, Mulvenna J. Proteomic characterisation of *Echinococcus granulosus* hydatid cyst fluid from sheep, cattle and humans. *J Proteomics* (2011) 74:1560–72. doi: 10.1016/j.jprot.2011.02.021
57. Sulima A, Bien J, Savijoki K, Näreaho A, Sałamatin R, Conn DB, et al. Identification of immunogenic proteins of the cysticercoid of *Hymenolepis diminuta*. *Parasit. Vectors* (2017) 10:577. doi: 10.1186/s13071-017-2519-4
58. Vendelova E, Camargo de Lima J, Lorenzatto KR, Monteiro KM, Mueller T, Veepaschit J, et al. Proteomic analysis of excretory-secretory products of *mesocestoides corti* metacestodes reveals potential suppressors of dendritic cell functions. *PLoS Negl Trop Dis.* (2016) 10:e0005061. doi: 10.1371/journal.pntd.0005061
59. Cantacessi C, Mulvenna J, Young ND, Kasny M, Horak P, Aziz A, et al. A deep exploration of the transcriptome and "Excretory/Secretory" proteome of adult *Fascioloides magna*. *Mol Cell Proteomics* (2012) 11:1340–53. doi: 10.1074/mcp.M112.019844
60. Liu F, Hu W, Cui SJ, Chi M, Fang CY, Wang ZQ, et al. Insight into the host-parasite interplay by proteomic study of host proteins copurified with the human parasite, *Schistosoma japonicum*. *Proteomics* (2007) 7:450–62. doi: 10.1002/pmic.200600465
61. Wang Y, Cheng Z, Lu X, Tang C. *Echinococcus multilocularis*: proteomic analysis of the protoscoleces by two-dimensional electrophoresis and mass spectrometry. *Exp Parasitol.* (2009) 123:162–7. doi: 10.1016/j.exppara.2009.06.014
62. Santivañez SJ, Hernández-González A, Chile N, Oleaga A, Arana Y, Palma S, et al. Proteomic study of activated *Taenia solium* oncospheres. *Mol Biochem Parasitol.* (2010) 171:32–9. doi: 10.1016/j.molbiopara.2010.01.004

63. Laschuk A, Monteiro KM, Vidal NM, Pinto PM, Duran R, Cerveñanski C, et al. Proteomic survey of the cestode *Mesocestoides corti* during the first 24 hours of strobilar development. *Parasitol Res.* (2011) 108:645–56. doi: 10.1007/s00436-010-2109-2
64. Matsumoto Y, Perry G, Levine RJ, Blanton R, Mahmoud AA, Aikawa M. Paramyosin and actin in schistosomal teguments. *Nature* (1988) 333:76–8. doi: 10.1038/333076a0
65. Kouguchi H, Matsumoto J, Katoh Y, Suzuki T, Oku Y, Yagi K. *Echinococcus multilocularis*: two-dimensional Western blotting method for the identification and expression analysis of immunogenic proteins in infected dogs. *Exp Parasitol.* (2010) 124:238–43. doi: 10.1016/j.exppara.2009.09.016
66. Colaco CA, Bailey CR, Walker KB, Keeble J. Heat shock proteins: stimulators of innate and acquired immunity. *Biomed Res Int.* (2013) 2013:461230. doi: 10.1155/2013/461230
67. Camargo de Lima J, Monteiro KM, Basika Cabrera TN, Paludo GP, Moura H, Barr JR, et al. Comparative proteomics of the larval and adult stages of the model cestode parasite *Mesocestoides corti*. *J Proteomics* (2018) 175:127–35. doi: 10.1016/j.jprot.2017.12.022
68. Srinivasan V, Morowitz HJ. Ancient genes in contemporary persistent microbial pathogens. *Biol Bull.* (2006) 210:1–9. doi: 10.2307/4134531
69. Kulkarni G, Sabnis NA, Harris BG. Cloning, expression, and purification of fumarase from the parasitic nematode *Ascaris suum*. *Protein Expr Purif.* (2004) 33:209–13. doi: 10.1016/j.pep.2003.09.005
70. Zinsser VL, Farnell E, Dunne DW, Timson DJ. Triose phosphate isomerase from the blood fluke *Schistosoma mansoni* : biochemical characterisation of a potential drug and vaccine target. *FEBS Lett.* (2013) 587:3422–7. doi: 10.1016/j.febslet.2013.09.022
71. Harnett W. Secretory products of helminth parasites as immunomodulators. *Mol Biochem Parasitol.* (2014) 195:130–6. doi: 10.1016/j.molbiopara.2014.03.007
72. McSorley HJ, Maizels RM. Helminth infections and host immune regulation. *Clin Microbiol Rev.* (2012) 25:585–608. doi: 10.1128/CMR.05040-11
73. Vendelova E, Lutz MB, Hrčková G. Immunity and immune modulation elicited by the larval cestode *Mesocestoides vogae* and its products. *Parasite Immunol.* (2015) 37:493–504. doi: 10.1111/pim.12216
74. Steinfelder S, O'Regan NL, Hartmann S. Diplomatic assistance: can helminth-modulated macrophages act as treatment for inflammatory disease? *PLOS Pathog.* (2016) 12:e1005480. doi: 10.1371/journal.ppat.1005480
75. Matisz CE, Leung G, Reyes JL, Wang A, Sharkey KA, McKay DM. Adoptive transfer of helminth antigen-pulsed dendritic cells protects against the development of experimental colitis in mice. *Eur J Immunol.* (2015) 45:3126–39. doi: 10.1002/eji.201545579
76. Hernandez JLR, Leung G, McKay DM. Cestode regulation of inflammation and inflammatory diseases. *Int J Parasitol.* (2013) 43:233–43. doi: 10.1016/j.ijpara.2012.09.005
77. Johnston MJG, MacDonald JA, McKay DM. Parasitic helminths: a pharmacopeia of anti-inflammatory molecules. *Parasitology* (2009) 136:125–47. doi: 10.1017/S0031182008005210
78. Johnston MJG, Wang A, Catarino MED, Ball L, Phan VC, MacDonald JA, et al. Extracts of the rat tapeworm, *Hymenolepis diminuta*, suppress macrophage activation *in vitro* and alleviate chemically induced colitis in mice. *Infect Immun.* (2010) 78:1364–75. doi: 10.1128/IAI.01349-08
79. Reyes JL, Wang A, Fernando MR, Graepel R, Leung G, van Rooijen N, et al. Splenic B cells from *Hymenolepis diminuta*– infected mice ameliorate colitis independent of T cells and via cooperation with macrophages. *J Immunol.* (2015) 194:364–78. doi: 10.4049/jimmunol.1400738

Conflict of Interest Statement: The authors declare that the research was conducted in the absence of any commercial or financial relationships that could be construed as a potential conflict of interest.

frontiers in Immunology

ORIGINAL RESEARCH
published: 19 September 2018
doi: 10.3389/fimmu.2018.02073

Toxoplasma Effector TgIST Targets Host IDO1 to Antagonize the IFN-γ-Induced Anti-parasitic Response in Human Cells

Hironori Bando[1,2†], *Naoya Sakaguchi*[1†], *Youngae Lee*[1,2], *Ariel Pradipta*[1], *Ji Su Ma*[1,2], *Shun Tanaka*[1,2], *De-Hua Lai*[3], *Jianfa Liu*[4], *Zhao-Rong Lun*[3], *Yoshifumi Nishikawa*[5], *Miwa Sasai*[1,2] *and Masahiro Yamamoto*[1,2*]

[1] *Department of Immunoparasitology, Research Institute for Microbial Diseases, Osaka University, Osaka, Japan,* [2] *Laboratory of Immunoparasitology, WPI Immunology Frontier Research Center, Osaka University, Osaka, Japan,* [3] *State Key Laboratory of Biocontrol, Center for Parasitic Organisms, School of Life Sciences, Guangzhou, China,* [4] *Department of Pathology and Pathogenic Biology, Medical College of Ningbo University, Ningbo, China,* [5] *National Research Center for Protozoan Diseases, Obihiro University of Agriculture and Veterinary Medicine, Obihiro, Japan*

OPEN ACCESS

Edited by:
Xun Suo,
China Agricultural University, China

Reviewed by:
Tiago W. P. Mineo,
Federal University of Uberlandia, Brazil
Eva Frickel,
Francis Crick Institute,
United Kingdom

***Correspondence:**
Masahiro Yamamoto
myamamoto@biken.osaka-u.ac.jp

[†]These authors have contributed equally to this work

Specialty section:
This article was submitted to Microbial Immunology, a section of the journal Frontiers in Immunology

Received: *07 May 2018*
Accepted: *21 August 2018*
Published: *19 September 2018*

Citation:
Bando H, Sakaguchi N, Lee Y, Pradipta A, Ma JS, Tanaka S, Lai D-H, Liu J, Lun Z-R, Nishikawa Y, Sasai M and Yamamoto M (2018) Toxoplasma Effector TgIST Targets Host IDO1 to Antagonize the IFN-γ-Induced Anti-parasitic Response in Human Cells. Front. Immunol. 9:2073. doi: 10.3389/fimmu.2018.02073

Toxoplasma gondii is an important human and animal pathogen that causes life-threatening toxoplasmosis. Interferon-γ (IFN-γ) is critical for anti-*T. gondii* cell-autonomous immunity in both humans and mice. To proliferate efficiently within the hosts, virulent strains of *T. gondii* can suppress IFN-γ-dependent immunity. During parasite infection, it is well-characterized that various virulence effectors are secreted to transcriptionally or post-translationally target IFN-γ-inducible GTPases, which are essential for anti-parasite responses in mice. However, the role of IFN-γ-inducible GTPases in anti-*T. gondii* responses in human cells is controversial since they are non-functional or absent in humans. Instead, IFN-γ-induced tryptophan degradation by indole-2,3-dioxygenase (IDO) is important for the anti-*T. gondii* human response. To date, the *T. gondii* virulent mechanism targeting IDO in human cells remains elusive. Here we show that although humans possess two IDO isozymes, IDO1 and IDO2, human cells of various origins require IDO1 but not IDO2 for IFN-γ-induced cell-autonomous immunity to *T. gondii*. *T. gondii* secretes an effector TgIST to inhibit IDO1 mRNA expression. Taken together, the data suggests that *T. gondii* possesses virulence programs operated by TgIST to antagonize IFN-γ-induced IDO1-mediated anti-parasite cell-autonomous immunity in human cells.

Keywords: IFN-γ, IDO1, IDO2, virulence, human, TgIST

INTRODUCTION

Toxoplasma gondii is an intracellular apicomplexan protozoan that has a broad range of intermediate hosts, including humans (1, 2). Although it is estimated that at least one-third of the world's population is infected with *T. gondii*, most of these infections are asymptomatic. However, the parasite remains in a latent state and may reactivate and lead to severe diseases including hepatitis, encephalitis, and myocarditis if that individual becomes immunocompromised (3, 4). Moreover, toxoplasmosis caused by *T. gondii* infection may lead to congenital diseases in fetuses

and newborn infants from primarily-infected pregnant women (5). Thus, *T. gondii* is one of the most important human and animal pathogens.

The host immune system plays a critical role in the course of *T. gondii* infection and in the progression of toxoplasmosis. In particular, the type I cytokine interferon-γ (IFN-γ), which is produced by $CD4^+$ T cells and natural killer cells (NK), is an essential host factor for anti-*T. gondii* responses in host cells (6). This is because IFN-γ activates the transcription factor STAT1 and induces the expression of hundreds of genes (7). In the mouse model, IFN-γ-induced anti-*T. gondii* responses have been extensively analyzed. Parasitocidal and parasitostatic effects mediated by IFN-γ-inducible gene products have been observed in mice. The parasitocidal effects are coordinated by IFN-γ-inducible GTPases such as p47 immunity-related GTPases (IRGs) and p65 guanylate-binding proteins (GBPs) (8, 9). These GTPases accumulate on parastitophorous vacuoles (PVs), leading to their destruction (10). In mice, the accumulation of IRGs and GBPs on *T. gondii* requires some essential autophagy-related (Atg) proteins such as Atg3, Atg5, Atg7, Atg16L1, and GABARAPs but not other Atg proteins such as Atg9, Atg14, FIP200, and LC3s (11), suggesting the non-autophagic role of these Atg proteins in IFN-γ-mediated anti-*T. gondii* responses in mice. Atg16L1-deficient murine cells are severely defective in the IFN-γ-induced clearance of *T. gondii* due to impaired recruitment of GBPs and IRGs to *T. gondii* (12, 13), suggesting the essential role of Atg16L1 in anti-*T. gondii* responses in mice. In addition, this parasitostatic mechanism involves nitric oxide (NO), which is produced by IFN-γ-inducible NO synthase (iNOS) (14). Mice lacking IRGs, GBPs, and iNOS are susceptible to *T. gondii* infection (8, 15–20). Thus, the significance of these IFN-γ-inducible factors for anti-*T. gondii* immune responses in mice has previously been established.

However, the importance of IFN-γ-inducible GTPase- and NO-mediated mechanisms in humans is less certain. For example, compared with more than 20 IRG members in mice, humans only possess one IRG, which is not inducible by IFN-γ (21). Furthermore, inhibition of NO production does not affect *T. gondii* growth in IFN-γ-stimulated human macrophages (22). Regarding GBPs, a human reprogrammed fibroblast-like cell line (HAP1) lacking all GBPs shows a normal IFN-γ-dependent reduction in *T. gondii* growth (12, 23). However, knockout of GBP1 in a human lung epithelial cell line (A549) and knockdown of GBP1 in human mesenchymal stem cells (MSCs) results in impaired restriction of *T. gondii* growth in response to IFN-γ (24, 25). Thus, the involvement of IFN-γ-inducible GTPases and NO in the human anti-*T. gondii* response is controversial (12, 23–26). Regarding the role of autophagy proteins in human cells, ATG16L1 is dispensable for IFN-γ-induced inhibition of *T. gondii* growth in HAP1 cells and HUVECs (12, 27), whereas ATG16L1 is required for anti-parasite responses in HeLa cells via IFN-γ-inducible ubiquitination of *T. gondii* PVs (23). Thus, the anti-*T. gondii* role of ATG16L1 in humans may be cell-type specific. By contrast, IFN-γ-dependent nutrient deprivation or cell death has been established as an anti-*T. gondii* response in human cells (28, 29). Regarding nutrient deprivation, IFN-γ stimulates the expression of indoleamine 2,3-dioxygenases (IDO) to degrade tryptophan, which is an essential amino acid for *T. gondii* intracellular growth (30, 31). The treatment of IFN-γ-activated human cells with a pharmacological inhibitor of IDO called 1-methyl-DL- tryptophan (1-DL-MT) leads to defects in the IFN-γ-induced reduction of *T. gondii* numbers (32), establishing the significance of IDO in the IFN-γ-induced anti-*T. gondii* response in human cells. IDO consists of two closely related family members, IDO1 and IDO2 (33). Previous studies using 1-DL-MT concluded that IDO is responsible for the IFN-γ-inducible anti-*T. gondii* response (32, 34). However, given that both IDO1 and IDO2 are sensitive to 1-DL-MT (35, 36), it remains unclear whether either IDO1 or IDO2 (or both) is more important.

To antagonize the IFN-γ-induced anti-parasitic host response, *T. gondii* secretes various effector molecules into host cells upon infection (37, 38). The effector mechanisms are also extensively analyzed in the mouse model. ROP5, ROP17, and ROP18 are secreted from the rhoptry organelles to suppress IRG/GBP-dependent immune responses at PV membranes, resulting in increased virulence in mice (39–43). In addition, a dense granule-derived effector GRA7 is also injected into host cells to enhance ROP18-mediated inhibition of IRGs in mice (44). Furthermore, *T. gondii* infection is shown to impede STAT1-mediated gene expression (45, 46). TgIST was recently shown to be secreted from dense granules and finally localized at the host nucleus, where TgIST associates with the remodeled host nucleosome and the deacetylase complex to inhibit the expression of STAT1-dependent genes including iNOS, chemokines, IRGs, and GBPs, leading to enhanced virulence in mice (47, 48). Although ROP5 and ROP18 are virulence factors in mice, these effectors do not affect the ability of *T. gondii* to survive in IFN-γ-stimulated human fibroblasts (49). Regarding TgIST, although TgIST-deficient parasites are defective in STAT1-depdendent gene expression in human cells (47, 48), whether TgIST affects parasite survival in IFN-γ-stimulated host cells and which, if any, of the STAT1-regulated human gene products is targeted by TgIST remains elusive, given the differences between humans and mice in terms of IFN-γ-induced anti-*T. gondii* cell-autonomous immunity.

In the present study, we first demonstrated that IDO1, but not IDO2, is required for IFN-γ-induced inhibition of *T. gondii* growth of human cell lines of various origins. In terms of *T. gondii* virulence mechanisms, we have shown that TgIST directly suppresses IDO1 gene expression to promote parasite growth in IFN-γ-activated human cells. Taken together, these data have revealed that *T. gondii* uses TgIST as a virulence mechanism to impede the IDO1-dependent cell-autonomous response in IFN-γ-activated human cells.

RESULTS

ATG16L1-Independent IFN-γ-Induced Reduction of *T. gondii* Numbers in the Human HAP1 Cell Line

We have previously shown that ATG16L1 plays an important role in the IFN-γ-induced reduction of type II *T. gondii* (ME49)

in mouse cells (mouse embryonic fibroblasts; MEFs) but not in human HAP1 cells (**Figure 1A**), suggesting an ATG16L1-independent IFN-γ-induced anti-*T. gondii* response in human cells (12). To elucidate the molecular mechanism, we next challenged MEFs and HAP1 cells with type I (RH) or type II (ME49) parasites. As shown previously (12), MEFs showed more efficient IFN-γ-induced reduction of type II parasites than of type I parasites. By contrast, IFN-γ stimulation could similarly and efficiently reduce the numbers of both type I and II parasites in HAP1 cells (**Figure 1B**). IFN-γ-induced degradation of arginine by iNOS, or of tryptophan by IDO, which consists of two members, IDO1 and IDO2, have been shown to be important for the anti-*T. gondii* response in mouse or human cells (18, 30, 31). To test whether iNOS or IDO (or both) are involved in the process in HAP1 cells, we examined iNOS, IDO1, or IDO2 mRNA expression in HAP1 cells (**Figure 1C**). Stimulation of IFN-γ led to strong induction of IDO1 and IDO2 mRNAs and weak induction of iNOS mRNA. Second, we tested the expression levels of these mRNAs in IFN-γ-stimulated cells followed by *T. gondii* infection (**Figure 1C**). *T. gondii* infection at 24 hours after IFN-γ stimulation did not interfere with the expression of iNOS, IDO1, and IDO2 mRNAs in HAP1 cells (**Figure 1C**). Furthermore, we treated HAP1 cells with a pharmacological inhibitor of iNOS known as aminoguanidine or an inhibitor of IDO known as 1-methyl-DL-tryptophan (1-DL-MT), and compared the parasite numbers. 1-DL-MT but not aminoguanidine treatment abolished the IFN-γ-induced reduction of *T. gondii* numbers in HAP1 cells (**Figure 1D**), strongly suggesting the anti-*T. gondii* function of IDO in the human HAP1 cell line.

IDO1 but Not IDO2 Plays a Critical Role in the Anti-*T. gondii* Response in HAP1 Cells

Both IDO1 and IDO2 could be inhibited by 1-DL-MT (35, 36). Although both IDO1 and IDO2 mRNAs were highly induced by IFN-γ stimulation in HAP1 cells (**Figure 1C**), it remained to be seen which was more important for the IFN-γ-induced response in HAP1 cells. To clarify the contribution of IDOs in HAP1 cells, we generated IDO1 singly deficient (IDO1-KO), IDO2 singly deficient (IDO2-KO), and doubly deficient (IDO1/IDO2-DKO) HAP1 cells by CRISPR/Cas9 genome editing (**Figures 2A,B, Figure S1A**) and tested the IFN-γ-induced reduction of type II parasite numbers. Although IDO2-KO HAP1 cells functioned normally, IDO1-KO cells as well as IDO1/IDO2-DKO cells were completely defective in IFN-γ-induced parasite reduction (**Figure 2C**), suggesting that IDO1 but not IDO2 is essential for the IFN-γ-induced anti-*T. gondii* response in the human cell line. Kynurenine is a tryptophan metabolite of IDOs (50). Therefore, we measured kynurenine concentrations in HAP1 cells lacking IDOs (**Figure S1B**). Whereas, the kynurenine concentrations were increased upon IFN-γ treatment in wild-type HAP1 cells, such an increment was not observed in IDO1-KO or IDO1/IDO2-DKO HAP1 cells (**Figure S1B**). By contrast, IDO2-KO cells showed normal induction of kynurenine after IFN-γ stimulation (**Figure S1B**), correlating with the importance of IDO1 in the IFN-γ-induced reduction of parasite numbers and the degree of tryptophan degradation. In mouse cells, a *T. gondii* strain-dependent difference was observed in the IFN-γ-induced anti-*T. gondii* response (**Figure 1B**) (12, 13). By contrast, although wild-type cells exhibited greatly reduced numbers of type I parasites after IFN-γ stimulation, this IFN-γ-mediated reduction was not observed in IDO1-KO HAP1 cells (**Figure S1C**), suggesting the lack of strain dependence in this human cell line. Next, we analyzed whether IDO1 expression could rescue the defective anti-*T. gondii* response of IDO1-KO cells. To achieve this, IDO1-KO cells were transfected with a doxycycline-inducible IDO1 or the empty control vectors and the IFN-γ-induced anti-*T. gondii* response was tested (**Figure 2D**, **Figure S1D**). The doxycycline-inducible IDO1 expression led to a reduction of parasite numbers in the IFN-γ-stimulated IDO1-KO cells (**Figure 2D**). Next we tested whether IDO1 plays a role in the inhibition of *T. gondii* replication or in parasite elimination. The parasite numbers per vacuole in IFN-γ-stimulated IDO1-KO HAP1 cells were significantly higher than those of wild-type cells (**Figures 2E,F**). Whereas, the rates of *T. gondii*-infected wild-type or IDO1-KO cells were comparable 3 and 24 h post infection (**Figures 2E,G**), indicating that IDO1 inhibits *T. gondii* replication in IFN-γ-stimulated HAP1 cells. Taken together, these data suggest that IDO1 plays a critical role in the IFN-γ-induced anti-*T. gondii* response in HAP1 cells.

IDO1 Is Required for the Anti-*T. gondii* Response in Various Human Cell Lines

Next we assessed whether IDO1 is important for the IFN-γ-induced anti-*T. gondii* response in other human cells. IDO1 mRNAs were highly induced in foreskin fibroblasts (HFFs), a hepatocyte cell line (Huh7), and an epithelial cell line (HeLa) upon IFN-γ stimulation regardless of the subsequent *T. gondii* infection (**Figure 3A**). Then we generated IDO1-KO HFFs, Huh7, or HeLa cells by CRISPR/Cas9-genome editing (**Figure 3B**, **Figure S2A**) and analyzed the IFN-γ-induced reduction in *T. gondii* numbers. Among all of the cell types tested, IDO1-KO cells were defective in the IFN-γ-mediated anti-*T. gondii* response (**Figure 3C**). However, compared with IDO1-KO HAP1 cells or HFFs, both of which displayed complete loss of an anti-parasite response (**Figures 2C**, **3C**), IDO1 deficiency in Huh7 or HeLa cells resulted in severely impaired or modest defects (**Figure 3C**), suggesting an IDO1-independent anti-*T. gondii* response in Huh7 and HeLa cells. In addition, Tryptophan 2,3-dioxygenase (TDO) was not involved to IFN-γ induced anti-*T. gondii* responses in Huh7 cells (**Figure S2B**).

ATG16L1 Is Required for the Anti-*T. gondii* Response in a Cell Type-Specific Manner

A previous study demonstrated that ATG16L1 is involved in the IFN-γ-induced anti-*T. gondii* response in HeLa cells (23). Therefore, we hypothesized that ATG16L1 plays a role in the IDO1-independent response in Huh7 and HeLa cells. To examine this possibility, we generated ATG16L1-deficient (ATG16L1-KO) HFFs, Huh7, and HeLa cells by CRISPR/Cas9 genome editing (**Figure 4A**). Although ATG16L1-KO HFFs and Huh7 cells showed no increment of parasite

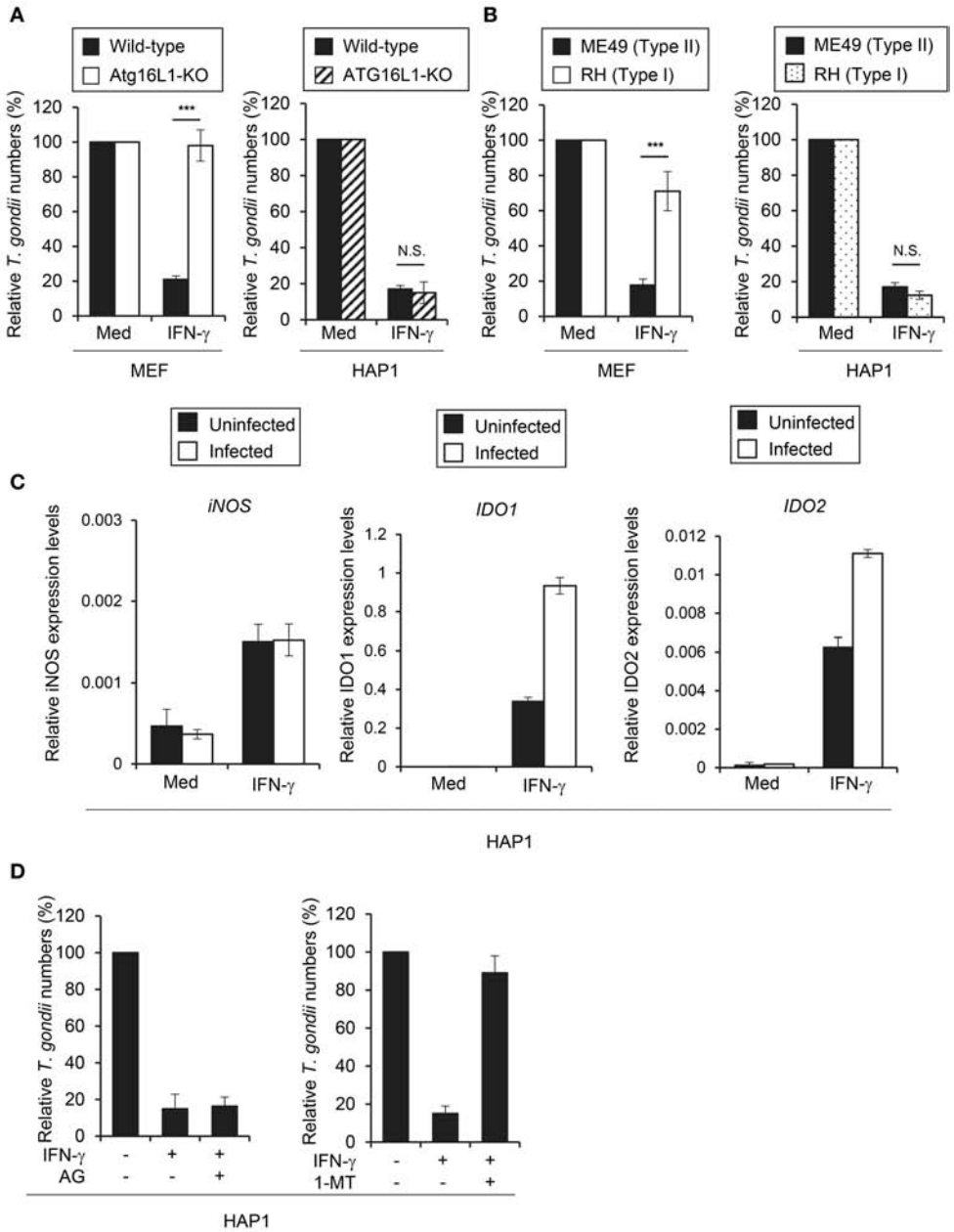

FIGURE 1 | IDO plays a critical role in anti *T. gondii* response in HAP1 cells. **(A)** WT or Atg16L1-KO MEFs or HAP1 cells were untreated or pre-treated with IFN-γ for 24 h, and then infected with *T. gondii*. The parasite survival rate after 24 h post infection was measured by luciferase assay. **(B)** MEFs or HAP1 cells were untreated or pre-treated with IFN-γ for 24 h, and then infected with Type I or Type II *T. gondii*. The parasite survival rate after 24 h post infection was measured by luciferase assay. **(C)** Quantitative RT-PCR analysis of iNOS, IDO1 or IDO2 mRNA level in HAP1 cells that were untreated or treated with IFN-γ for 24 h, and then infected with or without *T. gondii* was performed. (**D**) HAP1 cells were untreated or treated with IFN-γ and/or Aminoguanidine and/or 1-DL-MT for 24 h, and then infected with *T. gondii*. The parasite survival rate after 24 h post infection was measured by luciferase assay. Indicated values are means of ± s.d. (three biological replicates per group from three independent experiments) **(A–D)**. ***$p < 0.001$; N.S., not significant; (Student's *t*-test).

numbers (**Figure 4B**) or parasite numbers per vacuole upon IFN-γ stimulation (**Figures 4C,D**), ATG16L1-KO HeLa cells exhibited modest defects (**Figures 4C,D**). Furthermore, 1-DL-MT treatment in ATG16L1-KO HeLa cells resulted in a less efficient IFN-γ-mediated response than in non-treated control cells (**Figure S2C**), suggesting that ATG16L1 is involved in the IFN-γ-induced anti-parasite response in a cell type-specific manner. Thus, IDO1 is involved in the IFN-γ-induced anti-*T. gondii* response in human cells of various origins (**Figure 6A**). However, given the dispensable role of IDO in HUVECs (51), the degree of importance of IDO1 in the anti-*T. gondii* response depends on cell type.

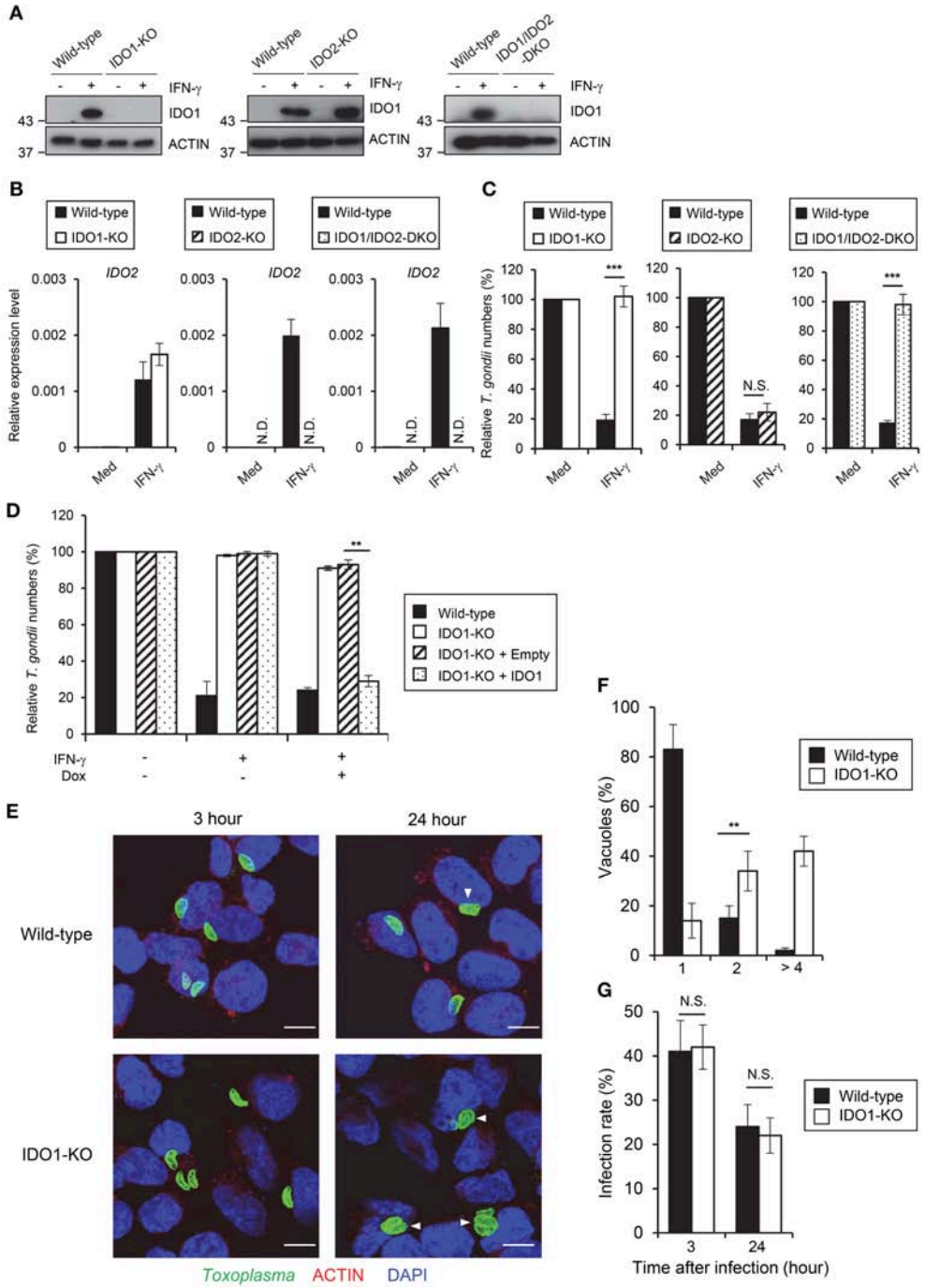

FIGURE 2 | IDO1 but not IDO2 has a critical role in anti-*T. gondii* response in HAP1 cells. **(A)** WT, IDO1-KO, IDO2-KO, or IDO1/IDO2-DKO HAP1 cells were stimulated with IFN-γ for 24 h, and then lysates were detected by Western blot. **(B)** Quantitative RT-PCR analysis of IDO2 mRNA level in IDO1-KO, IDO2-KO, or IDO1/IDO2-DKO HAP1 cells that were untreated or treated with IFN-γ for 24 h was performed. **(C)** WT, IDO1-KO, IDO2-KO, or IDO1/IDO2-DKO HAP1 cells were untreated or treated with IFN-γ for 24 h, and then infected with *T. gondii*. The parasite survival rate after 24 h post infection was measured by luciferase assay. **(D)** WT, IDO1-KO, IDO1-KO+empty, or IDO1-KO+IDO1 HAP1 cells were untreated or treated with IFN-γ for 24 h, and then infected with *T. gondii*. The parasite survival rate after 24 h post infection was measured by luciferase assay. **(E)** Fluorescence confocal microscopy of WT and IDO1-KO HAP1 cells stimulated by IFN-γ for 24 h, subsequently infected with *T. gondii* for 3 or 24 h, and immunostained for ACTIN (red) and *T. gondii* GAP45 (green). The nucleus was stained with DAPI (blue). Arrow heads show vacuoles containing 2 or more parasites. Scale bars correspond to 5 μm. **(F,G)** WT or IDO1-KO HAP1 cells were stimulated with IFN-γ for 24 h, and then infected with *T. gondii*. The parasite number per vacuole after 24 h post infection **(F)** or the parasite infection rate after 3 or 24 h post infection **(G)** was measured by IFA. Western blot and immunofluorescence images are representative of three independent experiments **(A,E)**. Indicated values are means of ± s.d. (three biological replicates per group from three independent experiments) **(B,C,D,F,G)**. ***$p < 0.001$, **$p < 0.01$; N.S., not significant; (Student's *t*-test). N.D., not detected.

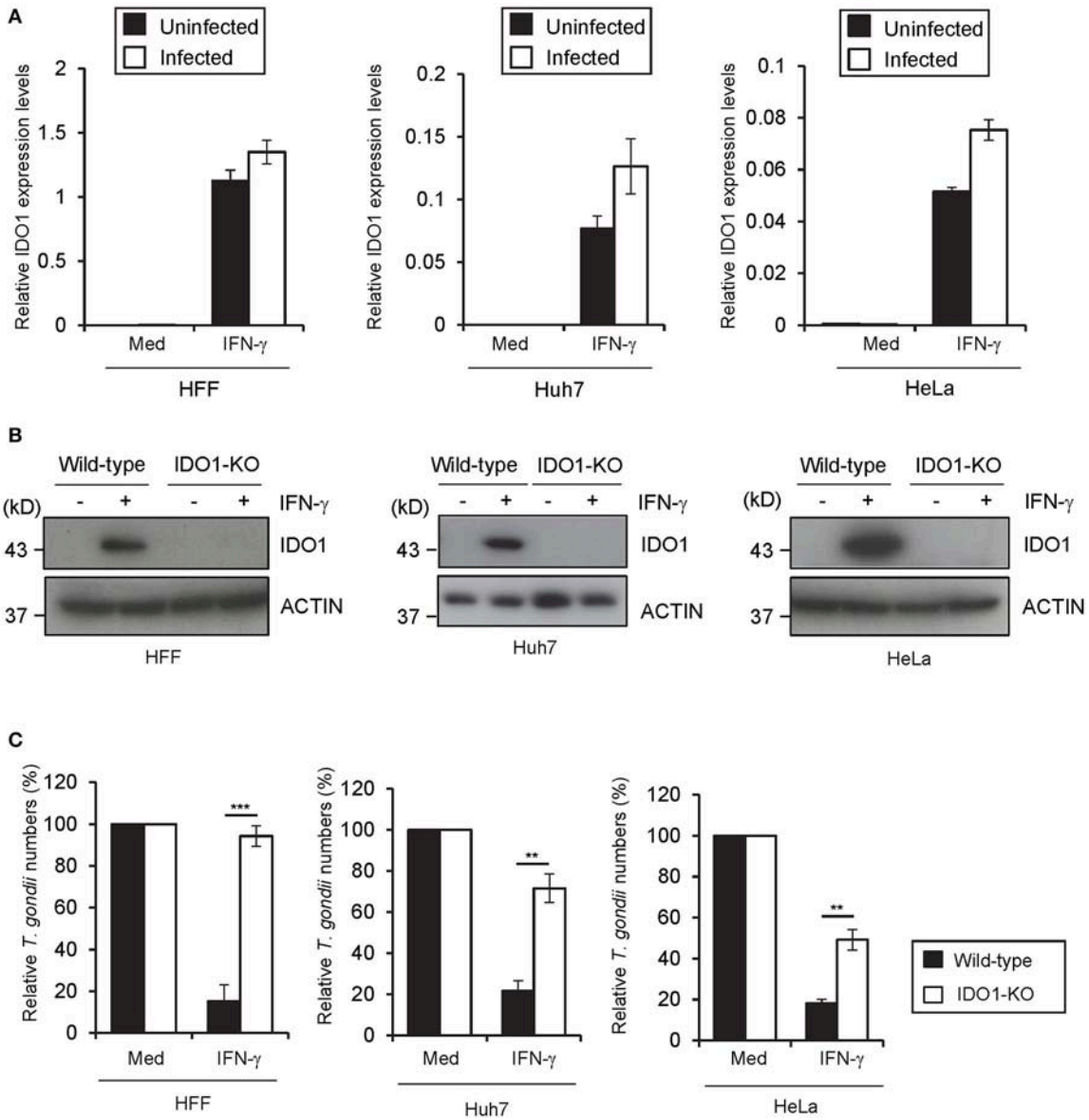

FIGURE 3 | IDO1 has a critical role in anti-*T. gondii* response in various human cells. **(A)** Quantitative RT-PCR analysis of IDO1 mRNA level in HFFs, Huh7 or HeLa cells that were untreated or treated with IFN-γ for 24 h, and then infected with or without *T. gondii* was performed. **(B)** WT or IDO1-KO HFFs, Huh7 or Hela cells were untreated or treated with IFN-γ for 24 h, and then lysates were detected by Western blot. **(C)** WT or IDO1-KO HFFs, Huh7 or Hela cells were untreated or treated with IFN-γ for 24 h, and then infected with *T. gondii*. The parasite survival rate after 24 h post infection was measured by luciferase assay. Western blot image is representative of three independent experiments **(B)**. Indicated values are means of ± s.d. (three biological replicates per group from three independent experiments) **(A,C)**. ***$p < 0.001$, **$p < 0.01$; N.S., not significant; (Student's *t*-test). N.D., not detected.

TgIST Directly Suppresses IDO1 Expression to Inhibit the IFN-γ-Induced Anti-*T. gondii* Response in Human Cell Lines

Since IDO1 plays a critical role in the IFN-γ-induced anti-*T. gondii* response in various human cells, we next explored the possible *T. gondii* virulence mechanisms targeting IDO1 in human cells. We selected TgIST, a *T. gondii* secreting effector molecule, as the candidate (47, 48), since the regulation of IDO1 expression by IFN-γ was shown to be regulated by STAT1 (52). To assess this possibility, we generated TgIST-KO type II parasites by CRISPR/Cas9 genome editing (**Figures S3A,B**) and asked whether TgIST deficiency affects *T. gondii* virulence in human cells (**Figure 5A**). As previously reported (47, 48), we also confirmed that TgIST-dependent suppression of the anti-*T. gondii* effect could be detected only when *T. gondii*-infected cells were subsequently stimulated with IFN-γ but not when IFN-γ-pre-treated cells were followed by *T. gondii* infection (**Figure 5A**, **Figure S4A**). By contrast, we observed

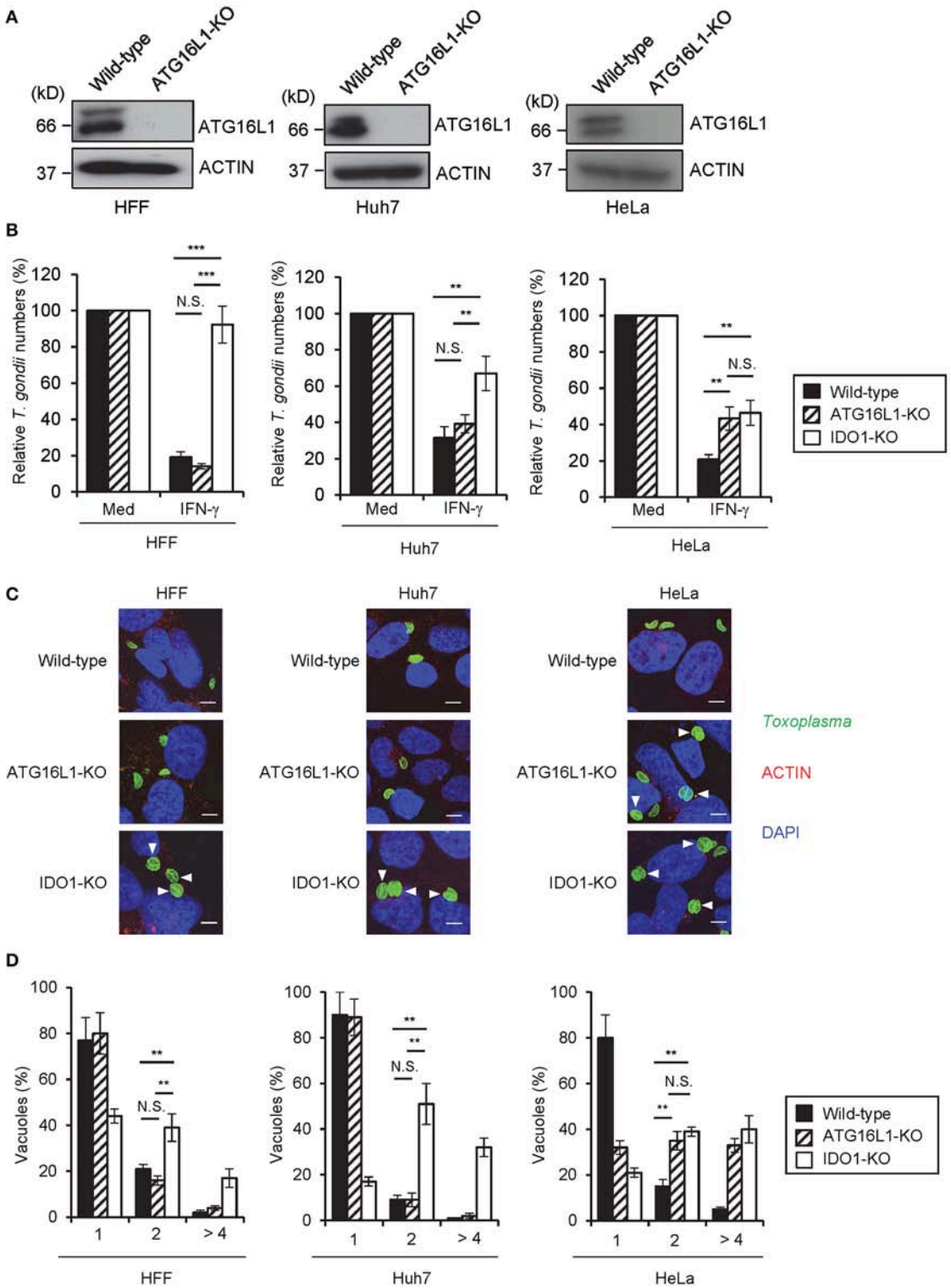

FIGURE 4 | IDO1 but not ATG16L1 extensively participate in anti-*T. gondii* response in human cell lines. **(A)** WT or ATG16L1-KO HFFs, Huh7 or Hela cells were untreated or treated with IFN-γ for 24 h, and then lysates were detected by Western blot. **(B)** WT, IDO1-KO, or ATG16L1-KO HFFs, Huh7 or Hela cells were untreated or treated with IFN-γ for 24 h, and then infected with *T. gondii*. The parasite survival rate after 24 h post infection was measured by luciferase assay. **(C)** Fluorescence confocal microscopy of WT, ATG16L1-KO and IDO1-KO HFF, Huh7 or HeLa cells stimulated by IFN-γ for 24 h, subsequently infected with *T. gondii* for 24 h, and immunostained for ACTIN (red) and *T. gondii* GAP45 (green). The nucleus was stained with DAPI (blue). Arrow heads show vacuoles containing 2 or more parasites.

(Continued)

FIGURE 4 | Scale bars correspond to 5 μm. **(D)** WT, IDO1-KO or ATG16L1-KO HFFs, Huh7 or Hela cells were untreated or treated with IFN-γ for 24 h, and then infected with *T. gondii*. The number of parasites per vacuole after 24 h post infection was measured by IFA. Western blot and immunofluorescence images representative of three independent experiments **(A,C)**. Indicated values are means of ± s.d. (three biological replicates per group from three independent experiments) **(B,D)**. ***$p < 0.001$, **$p < 0.01$; N.S., not significant; (Student's *t*-test). N.D., not detected.

an IFN-γ-dependent reduction in TgIST-KO parasite numbers (**Figure 5A**), suggesting that TgIST promotes parasite growth in the IFN-γ-post-stimulated cells. Phosphorylation of the Y701 residue of STAT1 (STAT1 Y701-p) was previously shown to be induced by *T. gondii* infection without IFN-γ stimulation and STAT1 Y701-p proteins were translocated to the nucleus (48). TgIST directly binds to STAT1 and recruits the chromatin-modifying Mi-2/NuRD complex to STAT1 transcriptional complexes. As a result, chromatin is remodeled and interferon-stimulated gene expression, including that of IRF-1, is decreased (47, 48). We tested whether *T. gondii* infection inhibits STAT1-dependent transcription in IFN-γ-post-treated HFF, Huh7, or HAP1 cells in a TgIST-dependent manner. Although phospho-STAT1 (STAT1 Y701-p) proteins were not detected in the nucleus in unstimulated cells, STAT1 Y701-p proteins were translocated to the nucleus upon IFN-γ-treatment. As previously reported (47, 48), wild-type *T. gondii* infection caused STAT1 Y701-p nuclear translocation even in unstimulated cells (**Figure 5B**). The subsequent IFN-γ-stimulation further induced translocation of STAT1 Y701-p to the nucleus (**Figure 5B**); however, STAT1 Y701-p was not active since STAT1-regulated gene products such as IRF1 and IDO1 mRNAs and proteins were not induced (**Figure 5C**, **Figures S4B,C**). By contrast, infection of TgIST-KO *T. gondii* did not result in STAT1 Y701-p nuclear translocation in unstimulated cells. Furthermore, the subsequent IFN-γ stimulation in TgIST-KO parasite-infected cells normally induced STAT1 Y701-p nuclear translocation in comparison with uninfected cells. Moreover, normal levels of IFN-γ-induced IRF1 and IDO1 expression suggested that the STAT1 activity in TgIST-KO *T. gondii*-infected cells was normal (**Figure 5C**, **Figures S4B,C**). Furthermore, IDO1-KO cells did not exhibit an IFN-γ-induced reduction in TgIST-KO parasites (**Figure 5D**). Conversely, growth of TgIST-intact wild-type *T. gondii* as well as TgIST-KO parasite growth was strongly inhibited by doxycycline-induced (thereby, STAT1-independent) IDO1 overexpression (**Figure 5E**), indicating that the pro-parasitic role of TgIST for *T. gondii* growth in IFN-γ-post-stimulated human cells is mainly due to inhibition of IDO1 but not other IFN-γ-inducible proteins (**Figure 6B**).

DISCUSSION

In the present study, we have demonstrated that IDO1 but not IDO2 plays an essential role in the IFN-γ-induced anti-*T. gondii* response in several human cell lines and primary fibroblasts. This finding is further strengthened by subsequent findings that treatment of an IDO inhibitor 1-DL-MT, consisting of 1-D-MT and 1-L-MT, reverses IFN-γ-dependent growth inhibition (32). However, IDO2 as well as IDO1 are possibly inhibited by both 1-D-MT and 1-L-MT (35, 36). Thus, whether the inhibitory effect of 1-DL-MT is on IDO1 or/and IDO2 remained unclear. Here we found that, by complete genetic deletion of IDO1 or/and IDO2 in HAP1 cells, IDO2-KO cells were able to reduce parasite numbers similarly to wild-type cells. By contrast, IDO1-KO cells as well as IDO1/IDO2-DKO cells could not control the parasite in response to IFN-γ. In addition, *T. gondii* numbers per vacuole at 24 h post infection in IDO1-KO cells were higher than in wild-type cells, whereas the infection rates were comparable. Thus, we have formally clarified that IDO1 is more important for the IFN-γ-induced inhibition of *T. gondii* growth in human cells than IDO2. Moreover, given that assessment in *T. gondii* numbers in PVs and the infection rate have been established as being indicative of the restriction of parasite replication and of parasite elimination/killing (20), IDO1 is required for *T. gondii* replication control rather than parasite elimination.

The ATG16L1-dependent cell-autonomous response mediated by IFN-γ-inducible GTPases such as IRGs and GBPs is important for the IFN-γ-mediated anti-*T. gondii* response in mice (12, 13). However, humans lack most of the IRGs (21). Moreover, human GBPs have been shown to be dispensable for the IFN-γ-inducible response (12, 24, 29). Recently, the IFN-γ-induced ubiquitination of *T. gondii* PVs has been shown to be required for the anti-*T. gondii* response in human cells such as HeLa cells and HUVECs (23, 27). Furthermore, ATG16L1 together with ATG7 are also important for the ubiquitin-mediated reduction of parasite numbers in HeLa cells (23). We have confirmed the anti-parasitic role of ATG16L1 in HeLa cells in this study. Moreover, although ATG16L1 is dispensable for the IFN-γ-induced reduction of *T. gondii* numbers in HAP1 cells, HFFs, and Huh7 cells, this autophagy protein is required in HeLa cells. The specific participation of ATG16L1 in the anti-*T. gondii* response in HeLa cells might be partly due to constitutively high levels of basal autophagy in HeLa cells (53, 54). Although the involvement of ATG16L1 in the human IFN-γ-induced anti-*T. gondii* response may be cell type-specific, complete genetic deletion of IDO1 in all human cells tested led to the impaired control of *T. gondii* growth by IFN-γ, suggesting that IDO1 is mainly used for the IFN-γ-mediated anti-*T. gondii* response in normal cells and various human cell lines. Given that ATG16L1-KO HeLa cells treated with 1-DL-MT still exhibit a modest IFN-γ-dependent reduction of *T. gondii* numbers, an ATG16L1 and IDO-independent anti-*T. gondii* response may exist in HeLa cells. It has been shown that IFN-γ stimulates cell death before parasite replication, reducing the parasite number in HFFs. In addition, IFN-γ-inducible cell death is independent of ATG5 and IDOs (29). Although we have not tested cell death in 1-DL-MT-treated ATG16L1-KO HeLa cells, it is possible that IFN-γ-dependent cell death might be responsible for the ATG16L1 and IDO-independent response.

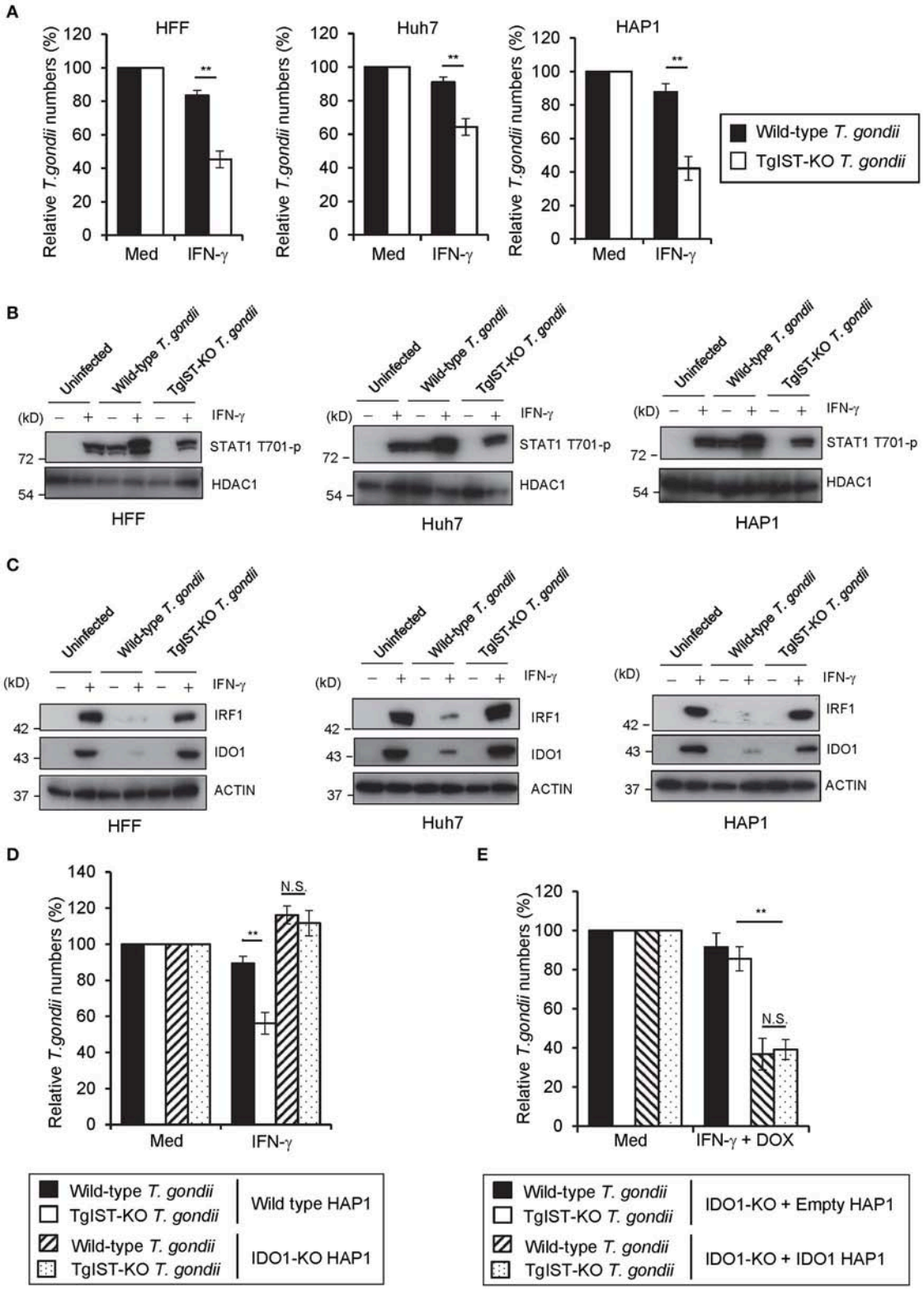

FIGURE 5 | TgIST directly inhibits IDO1 mRNA induction in IFN-γ-post-treated human cells **(A)** HFFs, Huh7, or HAP1 cells were infected with WT or TgIST-KO *T. gondii* for 8 h, and subsequently treated with IFN-γ for 24 h or untreated. The parasite survival rate after 24 h post IFN-γ treatment was measured by luciferase assay. **(B,C)** HFFs, Huh7 or HAP1 cells infected with WT or TgIST-KO *T. gondii* for 8 h or uninfected, and subsequently treated with IFN-γ for 24 h or untreated. Cell lysates

(Continued)

FIGURE 5 | were detected by Western blot to detect phospho-STAT1 and HDAC1 **(B)** or IRF1, IDO1, and Actin **(C)**. **(D)** WT or IDO1-KO HAP1 cells were infected with WT or TgIST-KO *T. gondii* for 8 h, and subsequently treated with IFN-γ for 24 h or untreated. The parasite survival rate after 24 h post IFN-γ treatment was measured by luciferase assay. **(E)** IDO1-KO + Empty or IDO1-KO + IDO1 HAP1 cells were infected with WT or TgIST-KO *T. gondii* for 8 h, and subsequently treated with IFN-γ and doxycycline for 24 h or untreated. The parasite survival rate 24 h post treatment was measured by luciferase assay. Western blot image is representative of three independent experiments **(B,C)**. Indicated values are means of ± s.d. (three biological replicates per group from three independent experiments) **(A,D,E)**. $^{**}p < 0.01$; N.S., not significant; (Student's *t*-test).

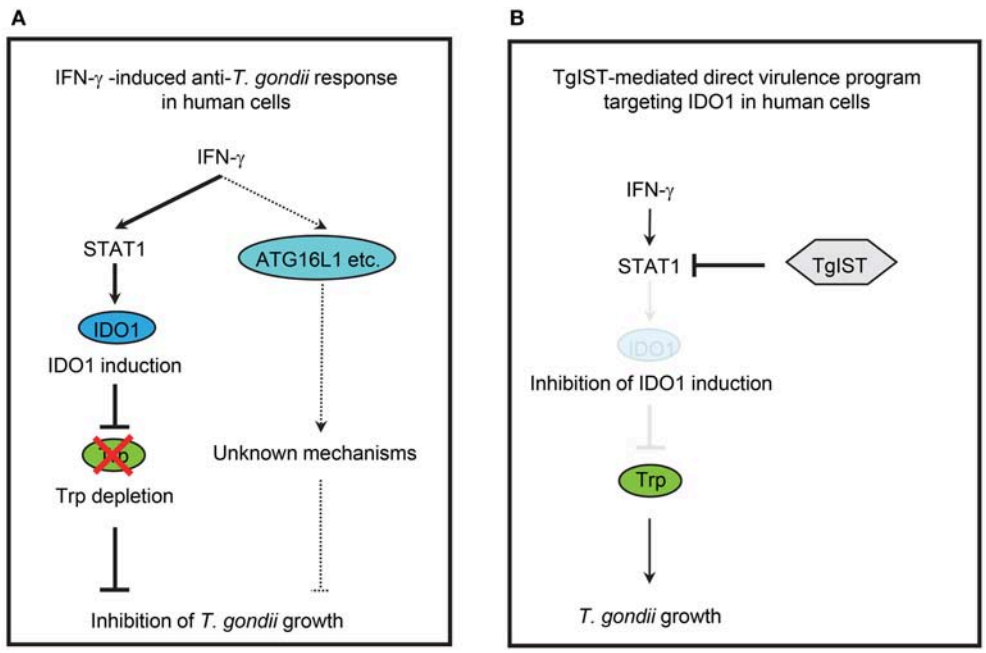

FIGURE 6 | Simplified scheme of IFN-γ-induced anti-*T. gondii* host immune response and *T. gondii* virulence programs in human cells. **(A)** IFN-γ-induced anti-*T. gondii* response in human cells. IFN-γ induce the expression of IDO1, which results in depletion of L-tryptophan (Trp), leading to inhibition of *T. gondii* growth in various human cells. IFN-γ also induce ATG16L1-dependent cell—autonomous response, but the involvement of ATG16L1 in the human IFN-γ-induced anti-*T. gondii* response is cell type-specific manner. **(B)** TgIST-mediated direct virulence program targeting IDO1 in human cells. *T. gondii* secrete effector TgIST in the infected human cells, which results in the inhibition of host STAT1-dependent gene expression, leading to directly inhibition of IDO1 mRNA induction and allowing the *T. gondii* growth.

We report a novel *T. gondii* virulence strategy in human cells, where IDO1 mRNA transcription is targeted by TgIST that directly binds to STAT1 and recruits the Mi-2/NuRD chromatin remodeling repressor complex to inhibit STAT1-dependent gene expression (47, 48). Expression of STAT1-regulated genes such as IRF1, CXCL9, CIITA, MX, GBP2, SOCS1, and ICAM1 is shown to be inhibited by TgIST in human cells (47, 48). Here we added IDO1 to the list of genes down-regulated by TgIST. Moreover, TgIST-independent (STAT1-independent) expression of IDO1 fully recovered the IFN-γ-induced growth inhibition by TgIST-sufficient parasite infection. In addition, TgIST-KO parasites can proliferate in IDO1-KO cells. Given that mRNA and protein levels of IRF1 as well as IDO1 were also inhibited in a TgIST-dependent manner, *T. gondii* may secrete TgIST to directly target STAT1 and non-specifically suppress expression of STAT1-regulated genes including IDO1 and IRF1 in the infected human cells.

In summary, we have demonstrated that IDO1 plays an important role in IFN-γ-inducible anti-*T. gondii* responses in various human cell types. Furthermore, TgIST suppresses the IFN-γ-induced anti-*T. gondii* response by directly targeting IDO1, which plays an important role in various human cells. By focusing on the difference between human and mouse immune responses, unidentified virulence mechanisms by known or unknown *T. gondii* effectors might be discovered in the future. In addition, STAT1-independent artificial induction of IDO1 could evade the TgIST-dependent virulence mechanism and offer a novel therapeutic strategy for treating human toxoplasmosis.

MATERIALS AND METHODS

Cells and Parasites

All *T. gondii* strains were maintained in Vero cells in RPMI (Nacalai Tesque) supplemented with 2% heat-inactivated FBS (JRH Bioscience), 100 U/ml penicillin, and 0.1 mg/ml streptomycin (Nacalai Tesque), as previously described (55). HAP1 cells were maintained in IMDM (Nacalai Tesque) containing 10% heat-inactivated FBS, and 100 U/ml penicillin, and 0.1 mg/ml streptomycin. HFFs, Huh7 cells were maintained

in RPMI (Nacalai Tesque) containing 10% heat-inactivated FBS, and 100 U/ml penicillin, and 0.1 mg/ml streptomycin. HeLa cells and MEF cells were maintained in DMEM (Nacalai Tesque) containing 10% heat-inactivated FBS, 100 U/ml penicillin, and 0.1 mg/ml streptomycin.

Reagents

Antibodies against IDO1 (13268-1-AP), HDAC1 (10197-1-AP), and IRF1 (11335-1-AP) was obtained from Proteintech. Antibodies against Phospho-Stat1 (Tyr701) (#9167) was obtained from Cell Signaling. Antibodies against ATG16L1 (PM040) was obtained from MBL. Anti-β-actin antibody (A1978) was obtained from Sigma. Antibodies against GAP45 was described previously (56). Recombinant human and mouse IFN-γ were obtained from Peprotech. 1-Methyl-DL-tryptophan (sc-224746) was obtained from Santa Cruz Biotechnology, Inc. Aminoguanidine hydrochloride (396494) was obtained from Sigma.

Plasmid Construction for Generation of Human Cell Lines

All genomic deficient cell lines were generated with the px330 plasmid CRISPR/Cas9 system. The insert fragment of IDO1, IDO2 ATG16L1 gRNA were generated by annealing primers. All the primers used in this study are listed in **Table S1**. These insert fragments were inserted into the BbsI site of the cloning vector containing U6 promoter to generate gRNA expressing plasmids pIDO1_gRNA1, pIDO1_gRNA2, pIDO2_gRNA1, pIDO2_gRNA2, pATG16L1_gRNA1, and pATG16L1_gRNA2, respectively. The insert fragment was cut out by XhoI and SalI from the pIDO1_gRNA2, pIDO2_gRNA2, and pATG16L1_gRNA2 vector, and ligated into the XhoI site of the pIDO1_gRNA1, pIDO2_gRNA1, and pATG16L1_gRNA1 vector to generate plasmids pIDO1_gRNA1/2, pIDO2_gRNA1/2, and pATG16L1_gRNA1/2. The insert fragment was cut out by KpnI and MluI from pIDO1_gRNA1/2, pIDO2_gRNA1/2, and pATG16L1_gRNA1/2 vector, respectively, and ligated into the KpnI and MluI site of the pEF6-hCas9-Puro vector.

Generation of Gene-Targeted Human Cell Lines by CRISPR/Cas9 Genome Editing

Human cells were electroporated with the pEF6-hCas9-Puro vector containing target gRNA1/2 using NEPA21 (nepa gene). And then 24 h post-electroporation, 0.5–5 μg/ml puromycin was added for 5–10 days to select for cells with a stably integrated. Cells were plated in limiting dilution in 96-well plates to isolate single cell clones. To confirm complete target gene deficient, the IDO1, IDO2 and ATG16L1 protein expression were analyzed by Western blot. Atg16L1 KO MEF cells were described previously (12).

Plasmid Construction for Generation of Knockout *T. gondii* Strain

Plasmid pSAG1::Cas9-U6::sgUPRT that encoding Cas9 nuclease (GFP fusion) under control of the *T. gondii* SAG1 promotor was obtained from addgene (plasmid 54467). The primer sequences are listed in **Table S1**. The TgIST-targeting CRISPR/Cas9 plasmid (pSAG1::Cas9-U6::sgTgIST-1 or pSAG1::Cas9-U6::sgTgIST-2) was constructed in two steps. First, the overlap PCR method was used to generate gRNA expressing plasmids. The U6 promoter from ME49 driving expression of the TgIST specific sgRNA (pgTgIST-1 or pgTgIST-2) was amplified from pSAG1::Cas9-U6::sgUPRT. For first-step PCR, primer pairs TgU6_F and TgISTgRNA1-R, TgISTgRNA1-F and TgU6_R, TgU6_F and TgISTgRNA2-R, TgISTgRNA2-F and TgU6_R were used. For second-step PCR primer pairs TgU6_F and TgU6_R were used, and cloning it into the NotI and SacI sites of the pBluescript II SK(+) (plasmid 54467). Second, the Cas9-Ds-Red monomer cassette under the SAG1 promoter was cut out from pSAG1::Cas9-U6::sgUPRT (Ds-Red monomer fusion), and ligated into the KpnI and NotI site of the pgTgIST-1 or pgTgIST-2. To generate a construct for deleting the entire coding sequence of TgIST, flanking regions of 5′ outside the sgTgIST-1 and 3′ outside the sgTgIST-2 regions were used to surround the TgIST cassette. To generate a plasmid for inserting HXGPRT into the TgIST gene, upstream regions of sgTgIST-1 (894-bp) and downstream regions of sgTgIST-2 (670-bp) were amplified from ME49 genomic DNA by using primers TgIST targeting 5′_F and TgIST targeting 5′_R or TgIST targeting 3′_F and TgIST targeting 3′_R. These two fragments were ligated into the KpnI and XhoI or BamHI and NotI sites of pHXGPRT vector.

Generation of TgIST-KO *T. gondii* by CRISPR/Cas9 Genome Editing

Prugniaud (Pru) *T. gondii*-expressing luciferase were filtered, washed and resuspended in Cytomix (10 mM KPO_4, 120 mM KCl, 0.15 mM $CaCl_2$, 5 mM $MgCl_2$, 25 mM HEPES, 2 mM EDTA). Parasites were mixed with 50 μg of sgTgIST-1 and sgTgIST-2 CRISPR plasmid along with 40 μg of the targeting vector linearized by KpnI and SacI, and supplemented with 2 mM ATP, 5 mM GSH. Parasites were electroporated by GENE PULSER II (Bio-Rad Laboratories). Selection by growth for 14 days in 25 μg/ml mycophenolic acid (Sigma) and 25 μg/ml xanthine (Wako) were used to obtain stably resistant clone. And then parasites were plated in limiting dilution in 96-well plates to isolate single clones. To confirm the disruption of the gene encoding TgIST, we analyzed messenger RNA of TgIST from WT and TgIST-KO parasites by quantitative RT-PCR. In addition, we observed comparable *in vitro* growth and *in vivo* virulence to each other and to the parental line.

Quantitative RT-PCR

Total RNA was extracted, and cDNA was synthesized using Verso Reverse transcription (Thermo Fisher Scientic). Quantitative RT-PCR was performed with a CFX connect real-time PCR system (Bio-Rad Laboratories) using the Go-Taq Real-Time PCR system (Promega). The values were normalized to the amount of beta actin (β-actin) for human cells or tubulin for *T. gondii* in each sample. The primer sequences are listed in **Table S1**.

Western Blot Analysis

Cells were lysed in a lysis buffer (0.5% Nonidet P-40, 150 mM NaCl, and 20 mM Tris-HCl, pH 7.5) containing a protease inhibitor cocktail (Roche) and phosphatase inhibitor cocktail

(Nacalai Tesque). The cell lysates were separated by SDS-PAGE and transferred to polyvinylidene uoride membranes and subjected to Western blot analysis using the indicated antibodies as described previously (57).

Luciferase Assay

For the experiment using IFN-γ pre-stimulated cells, HFFs (6×10^5), HAP1 (2×10^6), HeLa (8×10^5), or Huh7 (6×10^5) cells were untreated or treated with 10 ng/ml IFN-γ for 24 h, and subsequently infected with the luciferase-expressing *T. gondii* (MOI = 0.5) for 24 h. For the experiment using IFN-γ post-stimulation cells, HFFs (6×10^5), HAP1 (2×10^6), HeLa (8×10^5), or Huh7 (6×10^5) cells were infected with the luciferase-expressing *T. gondii* (MOI = 0.5) for 8 h, and subsequently untreated or treated with 10 ng/ml IFN-γ for 24 h. To measure the number of *T. gondii*, all infected cells were collected and lysed by 100 μl of lysis buffer (Promega) and sonicated. After centrifugation at 20,000 × g at 4°C, the luciferase activity of the supernatant was measured using the Dual Luciferase Reporter Assay System (Promega) and GLOMAX 20/20 luminometer (Promega). The percentages of the activities in cytokines stimulated cells over those in unstimulated cells were shown as "Relative *T. gondii* numbers" in figures.

Immunofluorescence Assays

HFFs, Huh7, or HeLa cells were cultured on glass coverslips, and infected with *T. gondii* (MOI = 2) for the indicated time, and fixed in PBS containing 3.7% paraformaldehyde for 10 min at room temperature. Cells were permeabilized with PBS containing 0.002% Digitonin for 5 min and then blocked with 8% FBS in PBS for 1 h at room temperature. And then, cells were incubated with the indicated primary antibodies for 1 h at 37°C, followed by incubation with Alexa 488-, Alexa 594-, or Alexa 647-conjugated secondary antibodies (Molecular Probes) and DAPI for 1 h at 37°C in the dark. Finally, coverslips were mounted onto glass slides with PermaFluor (Thermo Scientific) and analyzed using confocal laser microscopy (FV1200 IX-83, Olympus).

IDO Activity Assay

The enzymatic IDO activity was evaluated by the calculation of the kynurenine concentration in the cell culture supernatant as previously described (58). Cells were cultured in 12-well plates and untreated or treated with 10 ng/ml IFN-γ for 24 h. The concentration of kynurenine in culture supernatant was measured using Ehrlich reagent method (59). Seventy microliters of culture supernatant was mixed with 35 μl of 30% trichloroacetic acid, and centrifuged at 8,000 x g for 5 min. Then 75 μl of the supernatant was added to an equal volume of Ehrlich reagent (0.8% p-dimethylaminobenzaldehyde in acetic acid) in a 96-well plate, and the absorbance was read at 490 nm. The values were compared with a standard curve with defined concentrations of kynurenine (Sigma Aldrich).

Statistical Analysis

All statistical analyses were performed using Excel (Microsoft). All the experimental points and n values represent an average of each three biological replicates (three independent experiments). The statistical significance of differences in mean values was analyzed by using an unpaired two-tailed Student's *t*-test. *P*-values less than 0.05 were considered to be statistically significant.

AUTHOR CONTRIBUTIONS

HB, NS, ST, YN, and MY designed the experiments. AP, JM, ST, and MS prepared the materials. HB, NS, JL, Z-RL, and MY analyzed the data. HB, NS, DL, Z-RL, and MY wrote the paper. All authors listed contributed to revised work and approved the final manuscript.

FUNDING

This work was Supported by the Research Program on Emerging and Re-emerging Infectious Diseases (18fk0108047h0002) and Japanese Initiative for Progress of Research on Infectious Diseases for global Epidemic (18fm0208018h0002) from Agency for Medical Research and Development (AMED), Grant-in-Aid for Scientific Research on Innovative Areas (17K15677) from Ministry of Education, Culture, Sports, Science and Technology, Cooperative Research Grant of the Institute for Enzyme Research, Joint Usage/Research Center, Tokushima University, Takeda Science Foundation, Mochida Memorial Foundation on Medical and Pharmaceutical Research, Uehara Memorial Foundation and Research Foundation for Microbial Diseases of Osaka University for MY and National Science Foundation of China (#31772445) for DL and Z-RL.

ACKNOWLEDGMENTS

We thank Mari Enomoto (Osaka University) for secretarial and technical assistance.

SUPPLEMENTARY MATERIAL

The Supplementary Material for this article can be found online at: https://www.frontiersin.org/articles/10.3389/fimmu.2018.02073/full#supplementary-material

REFERENCES

1. Dubey JP. *Toxoplasmosis of Animals and Humans*. Boca; Raton, FL: CRC Press (2010).
2. Boothroyd JC. *Toxoplasma gondii*: 25 years and 25 major advances for the field. *Int J Parasitol.* (2009) 39:935–46. doi: 10.1016/j.ijpara.2009.02.003
3. Weitberg AB, Alper JC, Diamond I, Fligiel Z. Acute granulomatous hepatitis in the course of acquired toxoplasmosis. *N Engl J Med.* (1979) 300:1093–96. doi: 10.1056/NEJM197905103001907
4. Frenkel JK, Remington JS. Hepatitis in toxoplasmosis. *N Engl J Med.* (1980) 302:178–9.

5. Montoya JG, Remington JS. Management of *Toxoplasma gondii* infection during pregnancy. *Clin Infect Dis.* (2008) 47:554–66. doi: 10.1086/590149
6. Suzuki Y, Orellana MA, Schreiber RD, Remington JS. Interferon-gamma: the major mediator of resistance against *Toxoplasma gondii*. *Science* (1988) 240:516–8. doi: 10.1126/science.3128869
7. Platanias LC. Mechanisms of type-I- and type-II-interferon-mediated signalling. *Nat Rev Immunol.* (2005) 5:375–86. doi: 10.1038/nri1604
8. Yamamoto M, Okuyama M, Ma JS, Kimura T, Kamiyama N, Saiga H, et al. A cluster of interferon-gamma-inducible p65 GTPases plays a critical role in host defense against *Toxoplasma gondii*. *Immunity* (2012) 37:302–13. doi: 10.1016/j.immuni.2012.06.009
9. Gazzinelli RT, Mendonca-Neto R, Lilue J, Howard J, Sher A. Innate resistance against Toxoplasma gondii: an evolutionary tale of mice, cats, and men. *Cell Host Microbe* (2014) 15:132–8. doi: 10.1016/j.chom.2014.01.004
10. MacMicking JD. Interferon-inducible effector mechanisms in cell-autonomous immunity. *Nat Rev Immunol.* (2012) 12:367–82. doi: 10.1038/nri3210
11. Sasai M, Sakaguchi N, Ma JS, Nakamura S, Kawabata T, Bando H, et al. Essential role for GABARAP autophagy proteins in interferon-inducible GTPase-mediated host defense. *Nat Immunol.* (2017) 18:899–910. doi: 10.1038/ni.3767
12. Ohshima J, Lee Y, Sasai M, Saitoh T, Su Ma J, Kamiyama N, et al. Role of mouse and human autophagy proteins in IFN-gamma-induced cell-autonomous responses against *Toxoplasma gondii*. *J Immunol.* (2014) 192:3328–35. doi: 10.4049/jimmunol.1302822
13. Choi J, Park S, Biering SB, Selleck E, Liu CY, Zhang X, et al. The parasitophorous vacuole membrane of *Toxoplasma gondii* is targeted for disruption by ubiquitin-like conjugation systems of autophagy. *Immunity* (2014) 40:924–35. doi: 10.1016/j.immuni.2014.05.006
14. Sibley LD, Adams LB, Fukutomi Y, Krahenbuhl JL. Tumor necrosis factor-alpha triggers antitoxoplasmal activity of IFN-gamma primed macrophages. *J Immunol.* (1991) 147:2340–5.
15. Ling YM, Shaw MH, Ayala C, Coppens I, Taylor GA, Ferguson DJ, et al. Vacuolar and plasma membrane stripping and autophagic elimination of *Toxoplasma gondii* in primed effector macrophages. *J Exp Med.* (2006) 203:2063–71. doi: 10.1084/jem.20061318
16. Selleck EM, Fentress SJ, Beatty WL, Degrandi D, Pfeffer K, Virgin HWT, et al. Guanylate-binding protein 1 (Gbp1) contributes to cell-autonomous immunity against *Toxoplasma gondii*. *PLoS Pathog.* (2013) 9:e1003320. doi: 10.1371/journal.ppat.1003320
17. Degrandi D, Kravets E, Konermann C, Beuter-Gunia C, Klumpers V, Lahme S, et al. Murine guanylate binding protein 2 (mGBP2) controls Toxoplasma gondii replication. *Proc Natl Acad Sci USA*. (2013) 110:294–9. doi: 10.1073/pnas.1205635110
18. Scharton-Kersten TM, Yap G, Magram J, Sher A. Inducible nitric oxide is essential for host control of persistent but not acute infection with the intracellular pathogen *Toxoplasma gondii*. *J Exp Med.* (1997) 185:1261–73. doi: 10.1084/jem.185.7.1261
19. Collazo CM, Yap GS, Sempowski GD, Lusby KC, Tessarollo L, Woude GF, et al. Inactivation of LRG-47 and IRG-47 reveals a family of interferon gamma-inducible genes with essential, pathogen-specific roles in resistance to infection. *J Exp Med.* (2001) 194:181–8. doi: 10.1084/jem.194.2.181
20. Zhao Y, Ferguson DJ, Wilson DC, Howard JC, Sibley LD, Yap GS. Virulent Toxoplasma gondii evade immunity-related GTPase-mediated parasite vacuole disruption within primed macrophages. *J Immunol.* (2009) 182:3775–81. doi: 10.4049/jimmunol.0804190
21. Bekpen C, Hunn JP, Rohde C, Parvanova I, Guethlein L, Dunn DM, et al. The interferon-inducible p47 (IRG) GTPases in vertebrates: loss of the cell autonomous resistance mechanism in the human lineage. *Genome Biol.* (2005) 6:R92. doi: 10.1186/gb-2005-6-11-r92
22. Murray HW, Teitelbaum RF. L-arginine-dependent reactive nitrogen intermediates and the antimicrobial effect of activated human mononuclear phagocytes. *J Infect Dis.* (1992) 165:513–7. doi: 10.1093/infdis/165.3.513
23. Selleck EM, Orchard RC, Lassen KG, Beatty WL, Xavier RJ, Levine B, et al. A Noncanonical autophagy pathway restricts *Toxoplasma gondii* growth in a strain-specific manner in IFN-gamma-activated human cells. *MBio* (2015) 6:e01157-01115. doi: 10.1128/mBio.01157-15
24. Johnston AC, Piro A, Clough B, Siew M, Virreira Winter S, Coers J, et al. Human GBP1 does not localize to pathogen vacuoles but restricts *Toxoplasma gondii*. *Cell Microbiol.* (2016) 18:1056–64. doi: 10.1111/cmi.12579
25. Qin A, Lai DH, Liu Q, Huang W, Wu YP, Chen X, et al. Guanylate-binding protein 1 (GBP1) contributes to the immunity of human mesenchymal stromal cells against *Toxoplasma gondii*. *Proc Natl Acad Sci USA*. (2017) 114:1365–70. doi: 10.1073/pnas.1619665114
26. Gomez-Marin JE. No NO production during human Toxoplasma infection. *Parasitol Today* (2000) 16:131. doi: 10.1016/S0169-4758(99)01614-2
27. Clough B, Wright JD, Pereira PM, Hirst EM, Johnston AC, Henriques R, et al. K63-linked ubiquitination targets *Toxoplasma gondii* for endo-lysosomal destruction in IFNgamma-stimulated human cells. *PLoS Pathog.* (2016) 12:e1006027. doi: 10.1371/journal.ppat.1006027
28. Pfefferkorn ER. Interferon gamma blocks the growth of *Toxoplasma gondii* in human fibroblasts by inducing the host cells to degrade tryptophan. *Proc Natl Acad Sci USA*. (1984) 81:908–12. doi: 10.1073/pnas.81.3.908
29. Niedelman W, Sprokholt JK, Clough B, Frickel EM, Saeij JP. Cell death of gamma interferon-stimulated human fibroblasts upon *Toxoplasma gondii* infection induces early parasite egress and limits parasite replication. *Infect Immun.* (2013) 81:4341–9. doi: 10.1128/IAI.00416-13
30. Pfefferkorn ER, Eckel M, Rebhun S. Interferon-gamma suppresses the growth of *Toxoplasma gondii* in human fibroblasts through starvation for tryptophan. *Mol. Biochem. Parasitol.* (1986) 20:215–24.
31. Pfefferkorn ER, Rebhun S, Eckel M. Characterization of an indoleamine 2,3-dioxygenase induced by gamma-interferon in cultured human fibroblasts. *J Interferon Res.* (1986) 6:267–79. doi: 10.1089/jir.1986.6.267
32. Heseler K, Spekker K, Schmidt SK, MacKenzie CR, Daubener W. Antimicrobial and immunoregulatory effects mediated by human lung cells: role of IFN-gamma-induced tryptophan degradation. *FEMS Immunol Med Microbiol.* (2008) 52:273–81. doi: 10.1111/j.1574-695X.2007.00374.x
33. Ball HJ, Sanchez-Perez A, Weiser S, Austin CJ, Astelbauer F, Miu J, et al. Characterization of an indoleamine 2,3-dioxygenase-like protein found in humans and mice. *Gene* (2007) 396:203–13. doi: 10.1016/j.gene.2007.04.010
34. Murakami Y, Hoshi M, Hara A, Takemura M, Arioka Y, Yamamoto Y, et al. Inhibition of increased indoleamine 2,3-dioxygenase activity attenuates *Toxoplasma gondii* replication in the lung during acute infection. *Cytokine* (2012) 59:245–51. doi: 10.1016/j.cyto.2012.04.022
35. Qian F, Liao J, Villella J, Edwards R, Kalinski P, Lele S, et al. Effects of 1-methyltryptophan stereoisomers on IDO2 enzyme activity and IDO2-mediated arrest of human T cell proliferation. *Cancer Immunol Immunother.* (2012) 61:2013–20. doi: 10.1007/s00262-012-1265-x
36. Yuasa HJ, Ball HJ, Austin CJ, Hunt NH. 1-L-methyltryptophan is a more effective inhibitor of vertebrate IDO2 enzymes than 1-D-methyltryptophan. *Comp Biochem Physiol. B Biochem Mol Biol.* (2010) 157:10–5. doi: 10.1016/j.cbpb.2010.04.006
37. Hunter CA Sibley LD. Modulation of innate immunity by *Toxoplasma gondii* virulence effectors. *Nat Rev Microbiol.* (2012) 10:766–78. doi: 10.1038/nrmicro2858
38. Hakimi MA, Olias P, Sibley LD. Toxoplasma effectors targeting host signaling and transcription. *Clin Microbiol Rev.* (2017) 30:615–45. doi: 10.1128/CMR.00005-17
39. Steinfeldt T, Konen-Waisman S, Tong L, Pawlowski N, Lamkemeyer T, Sibley LD, et al. Phosphorylation of mouse immunity-related GTPase (IRG) resistance proteins is an evasion strategy for virulent *Toxoplasma gondii*. *PLoS Biol.* (2010) 8:e1000576. doi: 10.1371/journal.pbio.1000576
40. Reese ML, Zeiner GM, Saeij JP, Boothroyd JC, Boyle JP. Polymorphic family of injected pseudokinases is paramount in Toxoplasma virulence. *Proc Natl Acad Sci USA*. (2011) 108:9625–30. doi: 10.1073/pnas.1015980108
41. Fentress SJ, Behnke MS, Dunay IR, Mashayekhi M, Rommereim LM, Fox BA, et al. Phosphorylation of immunity-related GTPases by a *Toxoplasma gondii*-secreted kinase promotes macrophage survival and virulence. *Cell Host Microbe* (2010) 8:484–95. doi: 10.1016/j.chom.2010.11.005
42. Behnke MS, Khan A, Wootton JC, Dubey JP, Tang K, Sibley LD. Virulence differences in Toxoplasma mediated by amplification of a family of polymorphic pseudokinases. *Proc Natl Acad Sci USA*. (2011) 108:9631–6. doi: 10.1073/pnas.1015338108

43. Etheridge RD, Alaganan A, Tang K, Lou HJ, Turk BE, Sibley LD. The Toxoplasma pseudokinase ROP5 forms complexes with ROP18 and ROP17 kinases that synergize to control acute virulence in mice. *Cell Host Microbe* (2014) 15:537–50. doi: 10.1016/j.chom.2014.04.002
44. Alaganan A, Fentress SJ, Tang K, Wang Q, Sibley LD. Toxoplasma GRA7 effector increases turnover of immunity-related GTPases and contributes to acute virulence in the mouse. *Proc Natl Acad Sci USA.* (2014) 111:1126–31. doi: 10.1073/pnas.1313501111
45. Rosowski EE, Saeij JP. *Toxoplasma gondii* clonal strains all inhibit STAT1 transcriptional activity but polymorphic effectors differentially modulate IFNgamma induced gene expression and STAT1 phosphorylation. *PLoS ONE* (2012) 7:e51448. doi: 10.1371/journal.pone.0051448
46. Rosowski EE, Nguyen QP, Camejo A, Spooner E, Saeij JP. *Toxoplasma gondii* Inhibits gamma interferon (IFN-gamma)- and IFN-beta-induced host cell STAT1 transcriptional activity by increasing the association of STAT1 with DNA. *Infect Immun.* (2014) 82:706–19. doi: 10.1128/IAI.01291-13
47. Olias P, Etheridge RD, Zhang Y, Holtzman MJ, Sibley LD. Toxoplasma effector recruits the Mi-2/NuRD complex to repress STAT1 transcription and block IFN-gamma-dependent gene expression. *Cell Host Microbe* (2016) 20:72–82. doi: 10.1016/j.chom.2016.06.006
48. Gay G, Braun L, Brenier-Pinchart MP, Vollaire J, Josserand V, Bertini RL, et al. *Toxoplasma gondii* TgIST co-opts host chromatin repressors dampening STAT1-dependent gene regulation and IFN-gamma-mediated host defenses. *J Exp Med.* (2016) 213:1779–98. doi: 10.1084/jem.20160340
49. Niedelman W, Gold DA, Rosowski EE, Sprokholt JK, Lim D, Farid Arenas A, et al. The rhoptry proteins ROP18 and ROP5 mediate *Toxoplasma gondii* evasion of the murine, but not the human, interferon-gamma response. *PLoS Pathog.* (2012) 8:e1002784. doi: 10.1371/journal.ppat.1002784
50. Yamamoto S, Hayaishi O. Tryptophan pyrrolase of rabbit intestine. D- and L-tryptophan-cleaving enzyme or enzymes. *J Biol Chem.* (1967) 242:5260–6.
51. Woodman JP, Dimier IH, Bout DT. Human endothelial cells are activated by IFN-gamma to inhibit *Toxoplasma gondii* replication. Inhibition is due to a different mechanism from that existing in mouse macrophages and human fibroblasts. *J Immunol.* (1991) 147:2019–23.
52. Sotero-Esteva WD, Wolfe D, Ferris M, Taylor MW. An indoleamine 2,3-dioxygenase-negative mutant is defective in stat1 DNA binding: differential response to IFN-gamma and IFN-alpha. *J Interferon Cytokine Res.* (2000) 20:623–32. doi: 10.1089/107999000414790
53. Mizushima N, Yoshimori T, Levine B. Methods in mammalian autophagy research. *Cell* (2010) 140:313–26. doi: 10.1016/j.cell.2010.01.028
54. Klionsky DJ, Abdelmohsen K, Abe A, Abedin MJ, Abeliovich H, Acevedo Arozena A, et al. Guidelines for the use and interpretation of assays for monitoring autophagy (3rd edition). *Autophagy* (2016) 12:1–222. doi: 10.1080/15548627.2015.1100356
55. Ma JS, Sasai M, Ohshima J, Lee Y, Bando H, Takeda K, et al. Selective and strain-specific NFAT4 activation by the *Toxoplasma gondii* polymorphic dense granule protein GRA6. *J Exp Med.* (2014) 211:2013–32. doi: 10.1084/jem.20131272
56. Terkawi MA, Kameyama K, Rasul NH, Xuan X, Nishikawa Y. Development of an immunochromatographic assay based on dense granule protein 7 for serological detection of *Toxoplasma gondii* infection. *Clin Vaccine Immunol.* (2013) 20:596–601. doi: 10.1128/CVI.00747-12
57. Yamamoto M, Standley DM, Takashima S, Saiga H, Okuyama M, Kayama H, et al. A single polymorphic amino acid on *Toxoplasma gondii* kinase ROP16 determines the direct and strain-specific activation of Stat3. *J Exp Med.* (2009) 206:2747–60. doi: 10.1084/jem.20091703
58. Daubener W, Wanagat N, Pilz K, Seghrouchni S, Fischer HG, Hadding U. A new, simple, bioassay for human IFN-gamma. *J Immunol Methods* (1994) 168:39–47. doi: 10.1016/0022-1759(94)90207-0
59. Braun D, Longman RS, Albert ML. A two-step induction of indoleamine 2,3 dioxygenase (IDO) activity during dendritic-cell maturation. *Blood* (2005) 106:2375–81. doi: 10.1182/blood-2005-03-0979

Conflict of Interest Statement: The authors declare that the research was conducted in the absence of any commercial or financial relationships that could be construed as a potential conflict of interest.

frontiers in Immunology

ORIGINAL RESEARCH
published: 15 August 2018
doi: 10.3389/fimmu.2018.01868

Silent Witness: Dual-Species Transcriptomics Reveals Epithelial Immunological Quiescence to Helminth Larval Encounter and Fostered Larval Development

Friederike Ebner[1], Mathias Kuhring[2,3,4,5], Aleksandar Radonić[6], Ankur Midha[1], Bernhard Y. Renard[2] and Susanne Hartmann[1]*

[1] Department of Veterinary Medicine, Institute of Immunology, Freie Universität Berlin, Berlin, Germany, [2] Bioinformatics Unit (MF1), Department for Methods Development and Research Infrastructure, Robert Koch Institute, Berlin, Germany, [3] Core Unit Bioinformatics, Berlin Institute of Health (BIH), Berlin, Germany, [4] Berlin Institute of Health Metabolomics Platform, Berlin Institute of Health (BIH), Berlin, Germany, [5] Max Delbrück Center (MDC) for Molecular Medicine, Berlin, Germany, [6] Center for Biological Threats and Special Pathogens: Highly Pathogenic Viruses (ZBS 1), Robert Koch Institute, Berlin, Germany

OPEN ACCESS

Edited by:
Wenbin Tuo, Beltsville Agricultural Research Center, Agricultural Research Service (USDA), United States

Reviewed by:
Alan L. Scott, Johns Hopkins University, United States
William Horsnell, University of Cape Town, South Africa

***Correspondence:**
Friederike Ebner
friederike.ebner@fu-berlin.de

Specialty section:
This article was submitted to Microbial Immunology, a section of the journal Frontiers in Immunology

Received: *01 May 2018*
Accepted: *30 July 2018*
Published: *15 August 2018*

Citation:
Ebner F, Kuhring M, Radonić A, Midha A, Renard BY and Hartmann S (2018) Silent Witness: Dual-Species Transcriptomics Reveals Epithelial Immunological Quiescence to Helminth Larval Encounter and Fostered Larval Development. Front. Immunol. 9:1868. doi: 10.3389/fimmu.2018.01868

Gastrointestinal nematodes are among the most prevalent parasites infecting humans and livestock worldwide. Infective larvae of the soil-transmitted nematode *Ascaris* spp. enter the host and start tissue migration by crossing the intestinal epithelial barrier. The initial interaction of the intestinal epithelium with the parasite, however, has received little attention. In a time-resolved interaction model of porcine intestinal epithelial cells (IPEC-J2) and infective *Ascaris suum* larvae, we addressed the early transcriptional changes occurring simultaneously in both organisms using dual-species RNA-Seq. Functional analysis of the host response revealed an overall induction of metabolic activity, without induction of immune responsive genes or immune signaling pathways and showing suppression of chemotactic genes like CXCL8/IL-8 or CHI3L1. *Ascaris* larvae, when getting in contact with the epithelium, showed induction of genes that orchestrate motor activity and larval development, such as myosin, troponin, myoglobin, and protein disulfide isomerase 2 (PDI-2). In addition, excretory-secretory products that likely facilitate parasite invasion were increased, among them, aspartic protease 6 or hyaluronidase. Integration of host and pathogen data in an interspecies gene co-expression network indicated links between nematode fatty acid biosynthesis and host ribosome assembly/protein synthesis. In summary, our study provides new molecular insights into the early factors of parasite invasion, while at the same time revealing host immunological unresponsiveness. Reproducible software for dual RNA-Seq analysis of non-model organisms is available at https://gitlab.com/mkuhring/project_asuum and can be applied to similar studies.

Keywords: host–pathogen, parasitic nematode, IPEC-J2, *Ascaris suum*, dual-species, RNA sequencing, transcriptomics, epithelial communication

INTRODUCTION

The large roundworms *Ascaris (A.) lumbricoides* and *Ascaris suum* are the most prevalent soil-transmitted helminths worldwide and parasitize the gastrointestinal tract of humans and pigs, respectively. With an estimated 800 million people currently infected, typically in the most impoverished populations, Ascariasis belongs to the group of neglected tropical diseases (1–3). Among pigs, the prevalence of *A. suum* in high intensity production farms remains high all over the world and *A. suum* infections are known to cause major economic losses in the pig industry due to reduced growth performance, liver condemnation, and reduced vaccination responses (4, 5). Due to the genetic closeness of *A. lumbricoides* and *A. suum* (6, 7), studying host–parasite interactions in pigs is not only of veterinary importance but also represents an ideal research model for the human condition (8).

Ascariasis is caused by ingesting infective eggs containing L3 larvae from contaminated food and water, or with regard to pigs, coprophagy (9). The eggs hatch in the intestine and parasites undergo larval migration through the body before developing into adult worms that inhabit the small intestine. The early, intestinal migratory path involves newly hatched L3 larvae penetrating the walls of the distal small intestine, cecum, and proximal colon (10, 11) and migrating toward the liver.

Given the initial invasion and chronic infestation at gastrointestinal barriers, the mucosal immune response is of fundamental importance for defending against the parasite. The first cells to encounter invading *Ascaris* larvae are epithelial cells. The intestinal epithelium represents a tight barrier that prevents pathogen invasion. However, rather than being just a physical barrier, epithelial cells are equipped with microbial-detection mechanisms, signaling circuits, and both homeostatic and inflammatory mediators (12, 13). At the interface between host and environment, the epithelium defends the host against infection to the one side while fostering innate immune recognition and transmission of danger signals to the other side (12). While many types of pattern recognition receptors (PRRs) facilitate sensing of microbes, it is less clear how enteric parasites like *Ascaris* spp., which do not express known PAMPs, are sensed and detected by the epithelium. Conversely, whether a targeted host–pathogen interaction at the epithelial barrier drives larval tissue migration is not yet known.

The site-specific mucosal penetration of invading *Ascaris* L3 occurs within 3–6 h after oral infection (11) and restricts the window for an early intervention. Infection and challenge studies have greatly contributed to our understanding of hepatic- and pulmonary immune responses against *A. suum* (11, 14, 15); however, not much is known concerning the initial steps of immune recognition and modulation during early larval migration. Understanding to what extend host and parasite might sense, interact, regulate, or harm each other at the epithelial interface might clarify how mucosal immunity is initiated and reveal possible intervention strategies.

Therefore, we performed a time-resolved transcriptional analysis of infective *A. suum* third-stage larvae (AscL3) co-incubated with porcine intestinal-epithelial cells (IPEC-J2), an *in vitro* model widely used to study microbial pathogen–host interaction (16, 17). In that context, RNA-Seq is extremely useful for addressing non-model organisms such as a parasitic nematode (*A. suum*) and the pig. Addressing the limitations of most current dual RNA-Seq pathogen–host studies, pointed out by Westerman and colleagues (18) in a recent review, we do not restrict our analysis to pairwise differential comparisons of sets of time points, but account for the complete temporal behavior. By contrasting splines fitted across the time lines to baseline models rather than individual time point comparisons, statistical power can be increased (19) and the statistical model can capture trends that otherwise may be missed due to the restricted temporal granularity of individual time points (18).

In contrast to intracellular microbial pathogens, the possibility of separating larvae and host tissue after incubation enables purer sequencing and thus transcriptome analysis is unaffected by asymmetric read coverage as well as cross read mappings. In addition, we complement annotation of the non-model *A. suum* transcriptome for functional analysis by implementing a unique iterative annotation strategy favoring transfer from closely related species. This workflow builds upon continuously increasing the search space of species, thereby favoring results from closely related species were available, but still annotating sequences were no hits on closely related species can be found.

While many software solutions for individual steps are available, we are not aware of any interconnected analysis pipeline for dual RNA-Seq studies of non-model organisms. Here, we rely on Snakemake (20) as a current bioinformatics community standard to provide workflows at https://gitlab.com/mkuhring/project_asuum/. These workflows not only allow full reproduction of our analyses but are provided for reusage in related experiments and capture all relevant steps. Particularly, we integrated and primarily automated the annotation steps for both non-model organisms with the differential expression and functional analysis.

Our time-resolved, dual-species whole-transcriptome approach provides molecular insights into host–parasite interactions during direct physical interaction and in the absence of surrounding microbes, their metabolites and second line immune cells, enabling us to focus exclusively on parasite-epithelial cross-talk. Our results demonstrate that *Ascaris* larvae invade the host soft-footed without initiating immune alarming responses while expressing genes ensuring invasion and their further development.

MATERIALS AND METHODS

Generation of Infective *A. suum* L3 Stage Larvae and Hatching

Infective third-stage larvae of *A. suum* were generated as previously described (21). In brief, secreted *A. suum* eggs were collected from the culture fluid of female worms obtained from a local slaughter house. Eggs were decoated in 0.5 M sodium hydroxide, washed, and embryonated in 0.1 N H_2SO_4 for 6–8 weeks under weekly aeration. For hatching, embryonated eggs were treated with 5.25% sodium hypochlorite to remove the chitinous layer from the eggs. Hypochlorite-treated eggs were further layered below slowly moving sterile glass beads (4 mm) to facilitate hatching. Subsequently, intact and motile *A. suum* larvae were collected,

washed, counted, and adapted to mammalian cell culture media (IMDM, 5% FCS, 1% P/S) over night.

Parasite and Epithelial Cell Co-Incubation

Porcine intestinal epithelial cells (IPEC-J2 cell line) were cultured as monolayers for complete confluence in 35 mm Petri dishes [IMDM, 5% FCS, 1% P/S (all from PAN-Biotech, Aidenbach, Germany)]. L3 stage *A. suum* worms (50,000/dish, resulting in a larva to cell ratio of 1:10) were layered on top of epithelial cells and co-incubated for the indicated time points at 37°C, 5% CO_2. Three biological replicates of a time-resolved co-incubation series of pathogen and epithelial cells were performed, with five time points (0, 1, 2, 3, and 9 h) being interrogated with regard to the early migratory pathway of *A. suum* (10, 11). Monocultures of either worms or epithelial cells served as controls (referred to as time point 0 h). Following co-incubation, *A. suum* larvae were removed from the epithelial layer and worms and epithelial cells were processed separately for RNA isolation. Viability of IPEC-J2 cells following larval coculture was verified in separate experiments by vital cell counting, measuring ATP as indicator for metabolically active cells and by documenting the monolayer appearance using Giemsa staining (Figures S6A–C in Supplementary Material). Asc L3 were visually inspected for larval motility throughout the entire coculture period and assayed for migration capacity and viability [excretory-secretory (ES) production] after 9 h of coculture (Figures S6E,F in Supplementary Material).

RNA Isolation and Quality Check

Worm samples were homogenized using shredder columns filled with 200 mg sterile sea sand and the FastPrep®-24 instrument (MP Biomedicals) at 5 m/s for 35 s. Supernatants of homogenized worms and epithelial cell lysates were further processed for RNA isolation (InnuPREP RNA isolation, Analytik Jena AG, Germany), DNase treatment (Analytik Jena AG, Germany), and RNA quality control (Agilent 2100 Bioanalyzer, RNA 6000 Nano Kit, Agilent Technologies, Waldbronn, Germany). RNA sample RIN values ranged between 7.9 and 10 for porcine epithelial cells and 7.3 and 9.5 for AscL3, respectively.

Sequencing and Mapping

For transcriptome sequencing on an Illumina platform a TruSeq RNA library generation was utilized. The library was generated by using the TruSeq RNA Sample Prep Kit v2 (Illumina, San Diego, CA, USA) following the manufacturer's instructions. The library was quantified by using the KAPA Library Quantification Kit for Illumina (Kapa Biosystems, Wilmington, MA, USA). The library size was determined by using the High Sensitivity DNA Analysis Kit for the 2100 Bioanalyzer Instrument (Agilent Technologies, Waldbronn, Germany). Libraries were adjusted to a concentration of 12 pM and sequenced on a HiSeq 1500 instrument (Illumina, San Diego, CA, USA) in high-output mode. For cluster generation, the TruSeq PE Cluster Kit v3 was used. Cluster generation was performed on a cBot instrument. For sequencing, the TruSeq SBS Kit v3 was used to sequence 100 + 100 bases.

Sequence data processing and analysis were conducted as illustrated in **Figure 1B**. We sequenced 15 (resulting in three replicates for each of the five time points) AscL3 and IPEC-J2 samples each, with a mean library size of 45.5 million paired-end reads and a SD of 25.4. Raw reads were subjected to quality control and trimming *via* the QCumber pipeline (version 1.0.0)[1] utilizing FastQC (v0.11.5)[2], Trimmomatic (0.33) (22), and Kraken (0.10.5-beta) (23). On average, 88.21% of reads remained after trimming.

Preprocessed reads were mapped to reference genomes as specified below and corresponding sequence features using the TopHat split-read mapper (v2.1.1) (24) and reference as well as novel features were extracted and merged with the aid of Cufflinks (25) and Cuffmerge (25) (v2.2.1) to obtain one integrated and unified transcriptome for AscL3 and IPEC-J2 samples,

[1]https://gitlab.com/RKIBioinformaticsPipelines/QCumber (Accessed: March 17, 2018).

[2]https://www.bioinformatics.babraham.ac.uk/projects/fastqc/ (Accessed: March 17, 2018).

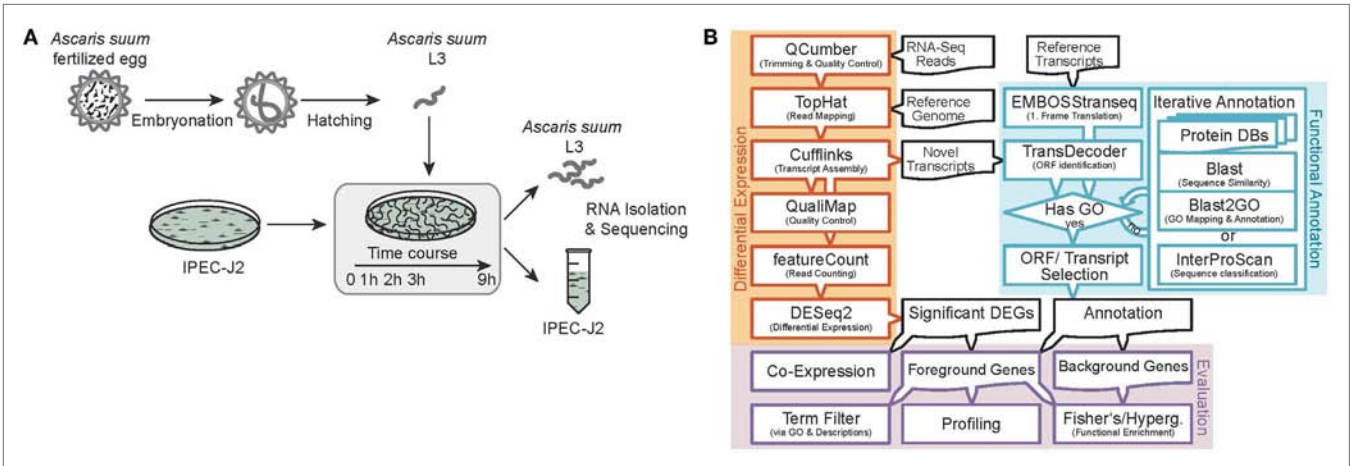

FIGURE 1 | Experimental design and RNA-Seq data processing. **(A)** Analysis of the early host–parasite interaction of *Ascaris suum* L3 and porcine epithelial cells (IPEC-J2) by studying dual-species gene expression dynamics over a time course (0–9 h). **(B)** Paired RNA samples were Illumina sequenced, preprocessed, mapped to reference genomes, annotated, and differential gene expression and functional analysis was performed using the illustrated bioinformatics pipeline.

respectively. Reference genomes used included the original *A. suum* draft genome from Jex et al. (26) as available from the WormBase ParaSite (27) FTP server (ftp.wormbase.org/pub/wormbase/species/a_suum/assemblies/v1/) and the *Sus scrofa* genome assembly from Ensembl (28) (Sscrofa10.2, release 85).

Differential Expression

For each sample, raw expression values were created by counting uniquely mapped reads on gene level using featureCounts (v1.5.0-p3) (29). To identify differentially expressed genes (DEGs) within AscL3 and IPEC-J2 samples, respectively, DESeq2 (1.12.4) (19) was adjusted for a time series design model based on natural splines to account for the time points in the experiment. A likelihood-ratio test against fits of a reduced null model including only intercept and the batch variable was applied to infer significant DEGs. However, pairwise fold-changes for each time point greater than 0 h were extracted *via* a classic DESeq2 model and pairwise contrasts with the base time point 0 h (indicating expression changes in comparison to 0 h). In addition, normalized and transformed expression values were extracted from DESeq2 (regularized log transformation) and corrected for batch effects *via* Limma (3.28.21, removeBatchEffect) (30) to allow for sample quality control with clustered heatmaps and principal component analysis (PCA).

Functional Annotation

Reference as well as novel transcripts were functionally annotated with focus on Gene Ontology (GO) terms (31, 32) using a novel iterative annotation strategy. First, transcripts were either first-frame translated (reference) or examined for ORFs (novels, Cuffcompare class code "u") using EMBOSS transeq (6.6.0.0) (33) and TransDecoder (v2.1)[3], respectively. Next, resulting protein sequences were passed through a series of database searches until successfully annotated with GO, either *via* blastp (2.6.0+) (34) and Blast2GO (4.0.7) (35) or by a final InterProScan classification (5.23–62.0 for *A. suum*, 5.22–61.0 for *S. scrofa*) (36). Databases used for *A. suum* sequences annotation included (in this order) the UniProt (37) *A. suum* proteome (UP000017900), UniProt Swiss-Prot Nematoda proteins, UniProt TrEMBL Nematoda proteins as well as the complete Swiss-Prot database and the complete TrEMBL database (all downloaded at 16.02.2017). For *S. scrofa* sequences, Ensembl reference annotations were obtained *via* the Ensembl BioMart server (38, 39) (with date of 30.10.2016). In addition, remaining non-annotated transcripts were searched against the UniProt *S. scrofa* proteome (UP000008227), Swiss-Prot Mammalia proteins, TrEMBL Mammalia proteins (all downloaded at 27.02.2017) as well as the complete Swiss-Prot database and the complete TrEMBL database (both downloaded at 16.02.2017).

In addition to GO terms, protein sequences were annotated with KEGG Orthology terms (KO) (40) *via* the BlastKOALA web interface (2.1) (41) using the "family_eukaryotes" and "genus_prokaryotes" databases for *A. suum* sequences and the "genus_eukaryotes" database for *S. scrofa* sequences, respectively (database builds 02.05.2017). However, for *S. scrofa,* reference annotations obtained *via* biomaRt (2.28.0) (42) and KEGGREST (1.12.3)[4] were preferred if available. KO terms were then mapped to KEGG pathways *via* KEGGREST. Furthermore, *A. suum* sequences were examined for potential excretory and secretory proteins as previously described by others (43). In brief, ES proteins were annotated as classical or non-classical secretory proteins by combining SignalP (4.1 Server, organism group "Eukaryotes") (44) and SecretomeP (2.0 Server, organism groups "Gram-negative bacteria," "Gram-positive bacteria," and "Mammalian") (45, 46). Mitochondrial proteins were excluded from that list using TargetP (1.1 Server, organism group "Non-plant") (47) as well as proteins predicted for transmembrane regions by TMHMM (Server v. 2.0) (48). The remaining predicted ES proteins were further categorized by KEGG ENZYME enzyme codes derived from KO-terms with the use of KEGGREST.

Functional Analysis

Functional profiles and enrichment analysis of significant DEGs were calculated based on GO term annotations (projected onto level 2) of the three classes of molecular function (MF), cellular component (CC), and biological process (BP) as well as on KEGG Pathways. For enrichment analysis, significant DEGs were tested against background gene sets representing the expression potential in the experiment, i.e., all expressed and sufficiently annotated genes in the AscL3 and IPEC-J2 samples, respectively. Significantly over- and underrepresented GO terms were determined by the two-sided Fisher's Exact test in Blast2GO (adjusted $p < 0.05$) while enriched KEGG pathways were determined with a hypergeometric test in clusterProfiler (3.0.5) (49) (adjusted $p < 0.05$). In addition to global analysis, significant DEGs were mined for specific functions of particular interest *via* filters based on specifically selected GO terms, free-text searched GO term collections, as well as gene description analysis. Thereby, GO term filters were recursively extended with corresponding child terms to account for descending functionality using GO.db (3.3.0)[5]. Target functions as well as corresponding GO-terms and description filter are found in Table S3 in Supplementary Material.

Co-Expression Analysis

The normalized, transformed, and batch-corrected expression values were used to infer an interspecies gene co-expression network (GEN) between *A. suum* and *S. scrofa*. The AscL3 and IPEC-J2 expression matrices were combined (excluding replicate C of time point 2 h due to quality issues) and subjected to pairwise Spearman rank correlation tests using the psych R package (1.7.5) (50) with FDR *p*-value adjustment for multiple testing. Resulting gene pairs (edges in the GEN) were filtered by significance (adjusted $p < 0.05$) and correlation strength (rho > 0.95) before further analysis and visualization within Cytoscape (3.2.1) (51). In Cytoscape, duplicated edges and self-loops were removed and the network was reduced to nodes participating in interspecies interactions (GEN1). Node degrees were calculated based once on all edges and once on interspecies edges alone (GEN2) to identify highly interacting genes between species. In addition, node (resp. gene) clusters were calculated on GEN1 with the MCODE plugin (v1.4.1) (52).

[3]https://github.com/TransDecoder/TransDecoder (Accessed: March 17, 2018).

[4]http://bioconductor.org/packages/KEGGREST/ (Accessed: March 17, 2018).

[5]http://bioconductor.org/packages/GO.db/ (Accessed: March 17, 2018).

RESULTS AND DISCUSSION

Transcriptional Response Reveals Temporal Dynamics of Early Host–Pathogen Interaction

A critical event during initial invasion of *Ascaris* parasites is crossing the intestinal epithelial barrier of their mammalian hosts. The initial dialog of host epithelium and parasite before the parasite starts tissue migration has, however, received little attention. We thus performed a time-resolved RNA-Seq transcriptional profiling of both, *A. suum* L3 larvae and porcine epithelial cells (IPEC-J2) to examine the early and comprehensive transcription of genes potentially involved in sensing, attachment, barrier disruption, and immune response early after initial parasite–host contact.

We sequenced *A. suum* larvae (AscL3) and IPEC-J2 at five different time points during co-incubation (0, 1, 2, 3, and 9 h) with $n = 3$ biological replicates each (**Figure 1A**). Mapping quality control of raw reads using QualiMap (v.2.2.1, **Figure 1B**) (53) indicated one sample (IPEC-J2, 2 h, replicate C) being inconsistent

TABLE 1 | Numbers of differentially expressed and annotated genes.

	Total DEG	FC ≥ 1.5[a]	FC ≥ 1.8[a]	FC ≥ 2[a]
Complete				
Ascaris suum (α = 0.05)	146	74	17	9
Sus scrofa (α = 0.01)	1,423	763	181	56
GO-annotated				
A. suum	87	34	11	5
S. scrofa	1,214	621	121	33

[a]*abs(log(fold-change)) ≥ log(n).*

Total and gene ontology (GO) annotated numbers of differentially expressed genes (DEG) and DEG numbers for distinct fold-change cut-offs (with respect to the maximal pairwise fold-change) are depicted for A. suum L3 and S. scrofa epithelial cell (IPEC-J2) expression data.

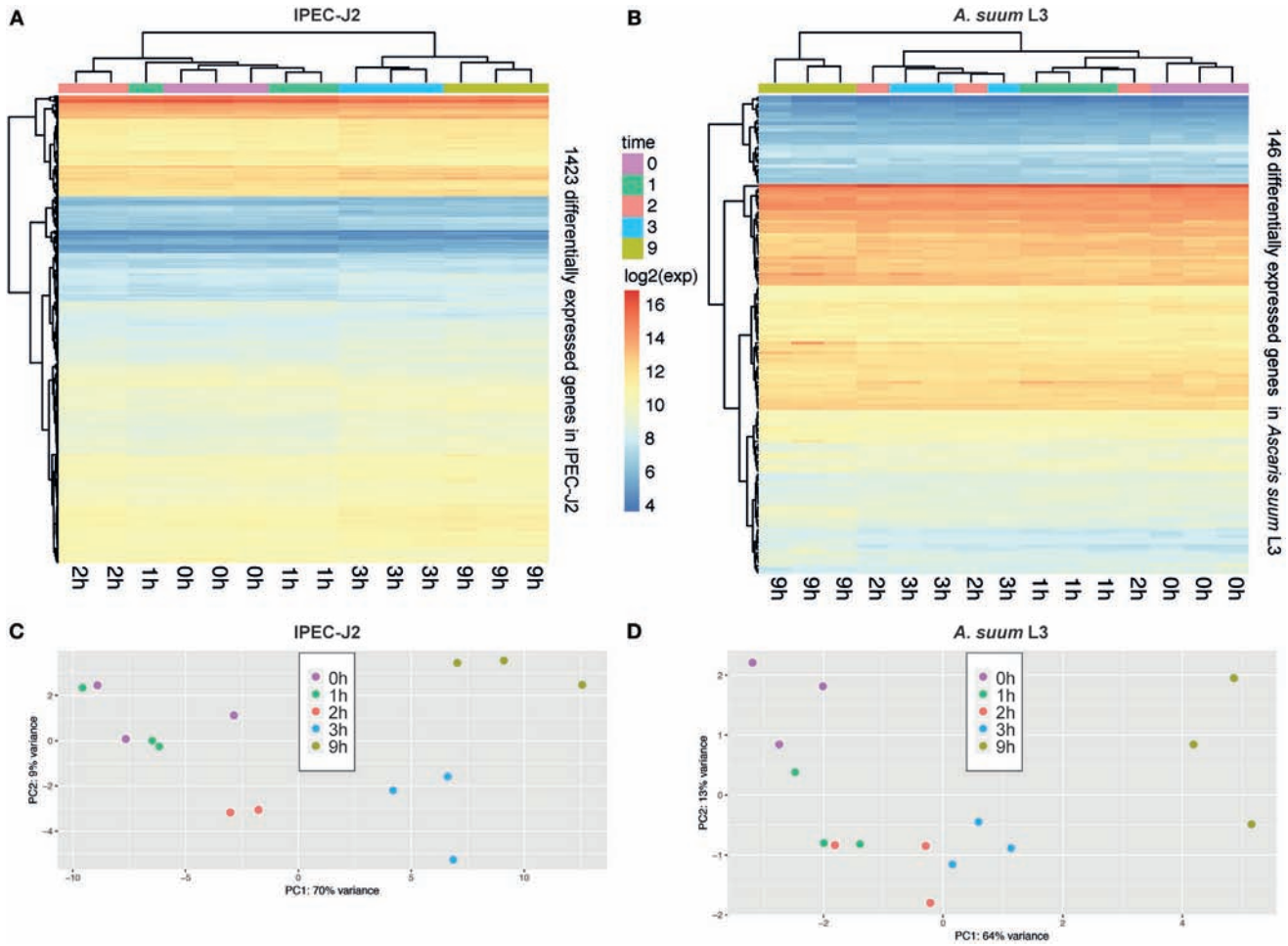

FIGURE 2 | Principal component analysis (PCA) of porcine epithelial cells (IPEC-J2) and *Ascaris suum* L3 expression data and clustering of differentially expressed genes (DEGs). **(A)** Unsupervised clustering heatmap of DEG in porcine epithelial cells (n = 1,423, IPEC-J2) and **(B)** *A. suum* L3 (n = 146). Red intensity indicates high gene expression during the time-course of host–parasite co-incubation, whereas blue intensity indicates low gene expression. PCA of RNA-Seq samples of **(C)** porcine epithelial cells and **(D)** *A. suum* L3 reveals that 79% (IPEC-J2) and 77% (*A. suum*) of the data variation is explained by the first two PCs, respectively. The five time points are color-coded (0, 1, 2, 3, and 9 h) and comprise $n = 3$ biological replicates (exception: $n = 2$ for IPEC-J2; 2 h, due to RNA-Seq quality control exclusion).

in comparison to all the other samples in the experiment, which consequently was excluded from further analysis.

In total, our exploratory study identified 146 *A. suum* genes and 1,423 *S. scrofa* genes with significant differential expression over time (**Table 1**, with adjusted *p*-value < 0.05 for *A. suum* and 0.01 for *S. scrofa*, respectively). Normalized expression values of both IPEC-J2 and *A. suum* L3 genes demonstrated successful clustering of replicates by time with minor exceptions of earlier time points for IPEC-J2 (**Figure 2A**) and median time points for AscL3 (**Figure 2B**). Clustering analysis indicates that most distinct changes in expression occur in later time points, additionally confirmed by the pairwise fold-changes (Table S1 in Supplementary Material). PCA of IPEC-J2 (**Figure 2C**) and *A. suum* L3 (**Figure 2D**) expression data indicate a relation of the first principal component with time direction and thus confirms that most of the variance and, therefore, change in expression is occurring over time.

Particularly for genes of the non-model nematode *A. suum*, available GO annotation was limited. We, therefore, implemented an iterative annotation strategy, depicted in **Figure 1B** and Figure S1 in Supplementary Material, which enabled us to assign GO terms to 13,683 reference and 410 novel *A. suum* genes as well as to 21,265 reference and 890 novel *S. scrofa* genes (including Ensembl reference GO-annotations). Regarding our co-incubation experiment, 59.6% of the *A. suum* DEGs (87 of the 146) and 85.3% of the *S. scrofa* DEGs (1,214 of the 1,423) were adequately annotated and thereby eligible for further functional analysis (**Table 1**). In parallel, a total of 8,034 *A. suum* genes could be annotated with KEGG Orthology (KO) identifiers including 7,306 reference and 728 novel genes. Furthermore, 9,711 *S. scrofa* genes could be annotated with KOs comprising 8,954 reference and 757 novel genes. KEGG pathways were assigned to 59 *A. suum* and 471 *S. scrofa* DEGs, respectively. These data highlight the GO annotation gap for *A. suum* genes and point out a need for improving methods to functional annotate nematode genes in general. A complete list of all *A. suum* L3 and IPEC-J2 genes (annotated and not annotated) is provided as Table S4 in Supplementary Material.

The Epithelial Cell Response to Worm Invasion

Epithelial Cells Are Not Intensely "Alarmed"

The IPEC-J2 cell line is a non-transformed, porcine epithelial cell line derived from the small intestine and currently the most convincing model for porcine infection studies (16, 54). The initial contact of *A. suum* larvae with the intestinal epithelial cells over 9 h results in a transcriptomic response of 1,423 *S. scrofa* genes (982 upregulated/441 downregulated, with respect to the maximal pairwise fold-change). To functionally describe the regulated *S. scrofa* genes, level 2 GO term profiles are illustrated (**Figure 3A**), categorizing MF, CC, and BP. To gain insight into the biological significance of alterations in gene expression levels, GO enrichment analysis was used to determine whether certain GO terms are over- or underrepresented within the gene set of interest. GO terms significantly overrepresented (adjusted $p < 0.05$) among *S. scrofa* DEGs were *binding* (as part of MF), *CC organization* or *biogenesis and cellular process* (BP) as well as several CC including *cell*, *cell part*, *macromolecular complex*, *membrane-enclosed lumen*, *organelle*, *organelle part*, and *supramolecular fiber* (**Figure 3A**). Surprisingly, the few underrepresented terms are almost exclusively attributed to extracellular matrix (ECM), membrane, and membrane part (CC), a group of terms that we expected to be specifically addressed while being co-incubated with a comparably large and motile extracellular parasite. Further global analysis as subcellular location of *S. scrofa* DEGs and KEGG pathway annotation are depicted in **Figures 3B,C**. *S. scrofa* KEGG profiling features several significantly enriched pathways (hypergeometric test, adjusted $p < 0.05$) including induced cell cycle activity, FoxO signaling, homologous recombination and RNA degradation as well as a suppressed ribosome pathway. In addition, though not significant, oxidative phosphorylation and purine metabolism show distinct repression (**Figure 3C**). Genes of the FoxO family that are central for the here enriched *FoxO signaling* pathway regulate transcriptional responses including apoptosis, cell-cycle control, glucose metabolism, oxidative stress resistance, and longevity. A recent study revealed that intestinal FoxO-mediated signaling is required for epithelial antimicrobial response and AMP synthesis by enterocytes (55). Factors inducing FoxO signaling include oxidative and nutrient stress stimuli, such as insulin or several growth factors. The induced oxidative stress response is in line with the repression of the oxidative phosphorylation pathway, and together imply increased nutrient consumption or even nutritional competition between IPEC-J2 and *A. suum* larvae.

KEGG pathway analysis further highlights that pathways linked to extracellular recognition such as TLR signaling are not regulated (**Figure 3C**). This is supported by several other studies showing that host PRRs such as TLR are modulated by nematode species to limit inflammation (56–58) but TLR signaling in generating an anti-helminth immune response remains controversial (59). Since epithelial cells are known to express all kinds of PRRs, we more specifically considered the role of C-type lectin receptors such as mannose receptor, DC-sign, ICAM-3, collectins, or selectins (59, 60) to be addressed, but found no transcriptional evidence that these receptors or corresponding receptor signaling pathways are affected by the presence of *A. suum* larvae. Interestingly, we observe a generally low presence of *S. scrofa* DEGs in several other signal transduction pathways, such as HIF-1, MAPK, mTOR, NF-kappa B, Rap1, TGF-ß, or RAS indicating that IPEC-J2 cells overall were not in an "alarmed state" as expected.

Although we hypothesized that epithelial cells somehow sense incoming *Ascaris* larvae and might orchestrate an appropriate response, we were surprised to find such a low magnitude of response (indicated by fold-change values) and the lack of conclusive activation signatures. We then specifically looked for genes involved in inflammatory responses (**Figure 4A**, GO declination in Table S3 in Supplementary Material) and chemotactic responses (**Figure 4B**, GO declination in Table S3 in Supplementary Material) and found chemokine transcripts (CCL5, IL8, and CXCL18), the chitinase 3 like 1 protein, and the cytokines genes for IL17D to be suppressed. Interleukin-8, one

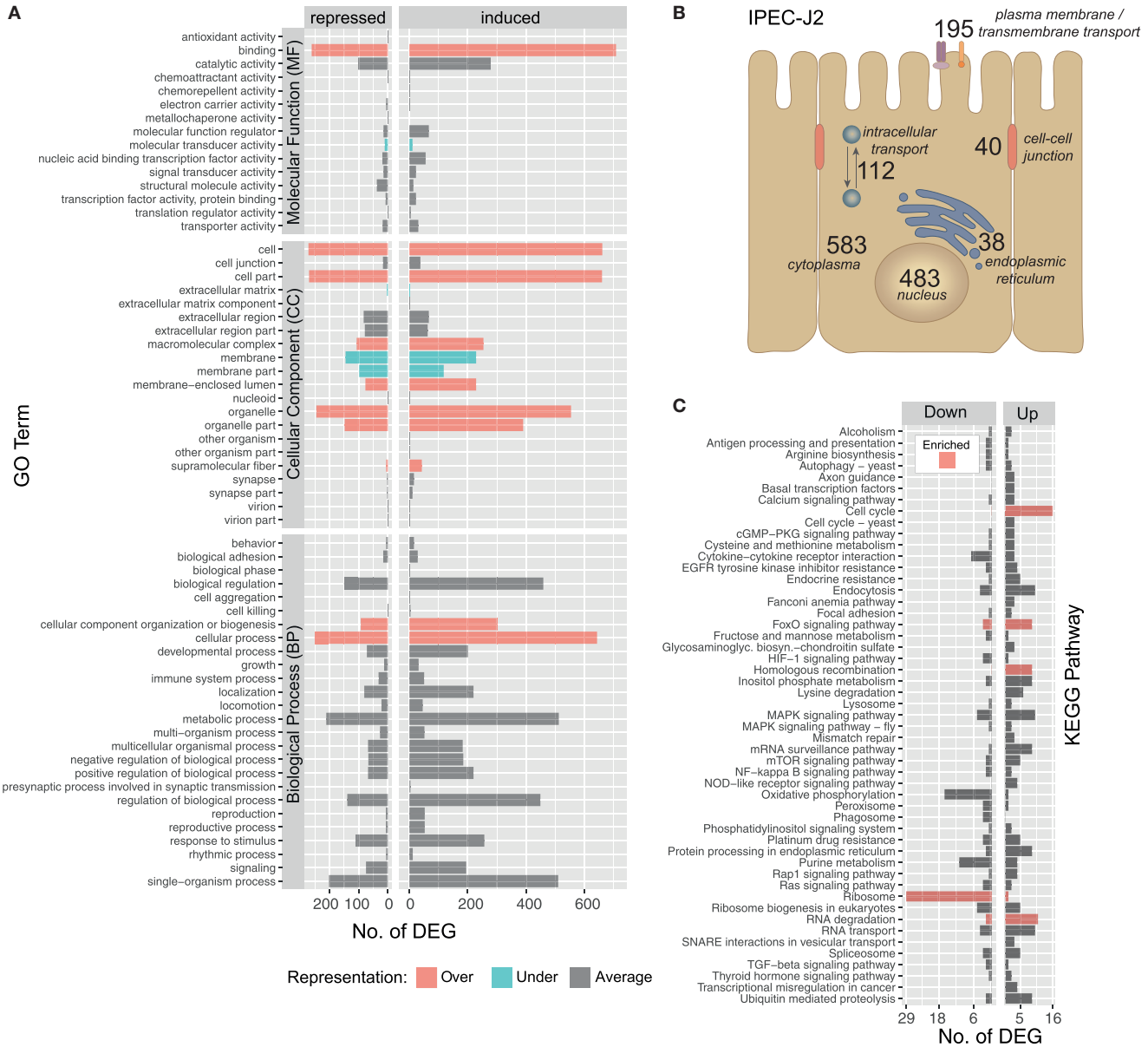

FIGURE 3 | Gene ontology (GO) and pathway profiling of porcine intestinal epithelial cell differentially expressed genes (DEGs). An iterative annotation strategy was used to assign GO terms to reference and novel porcine transcripts. **(A)** For 1,214 GO-annotated porcine DEGs, the level 2 of GO hierarchy is illustrated and classified into Molecular Function (MF), Cellular Component (CC) and Biological Process (BP). GO terms significantly enriched among differentially expressed *S. scrofa* genes (Fischer's Exact Test, two-sided, $p < 0.05$) are highlighted as over-( ) and under-( ) represented terms alongside with averagely represented terms ( ) with regard to the reference genome. **(B)** Subcellular localization of DEG encoding proteins deduced from binning relevant GO terms (Table S3 in Supplementary Material) and offsprings [*nucleus* (CC, 483), *endoplasmic reticulum* (CC, 38), *cytoplasm* (CC, 583), *intracellular transport* (BP, 112), *plasma membrane* (CC, 128), *transmembrane transport* (BP, 34), *transmembrane transporter activity* (MF, 33), *cell–cell-junction* (CC, 31), and *cell–cell junction organization* (BP, 9)]. **(C)** Sequences were annotated with KEGG pathways and pathways with three or more assigned DEGs are visualized including color-coded ( ) enrichment analysis (hypergeometric test, $p < 0.05$).

of the repressed immunity genes, is a potent chemoattractant for primary neutrophils but also other granulocytes, and is secreted by epithelial cells in response to bacterial stimuli (61). Upon LPS stimulation, also porcine IPEC-J2 cells rapidly upregulate IL-8 transcripts (Figure S6D in Supplementary Material). Intriguingly, Aprianto and colleagues (62) showed that a highly adherent, unencapsulated form of *S. pneumoniae* suppressed IL-8 production from epithelial cells compared to a free-floating, non-adherent form of the same strain early during infection. Their RNA-Seq study thereby links repression of epithelial innate immune response with the adherence mechanisms of the invading pathogen and provides evidence for targeted immune evasion. Hence, active suppression of the innate chemokine response combined with restricted epithelial recognition of AscL3 larvae,

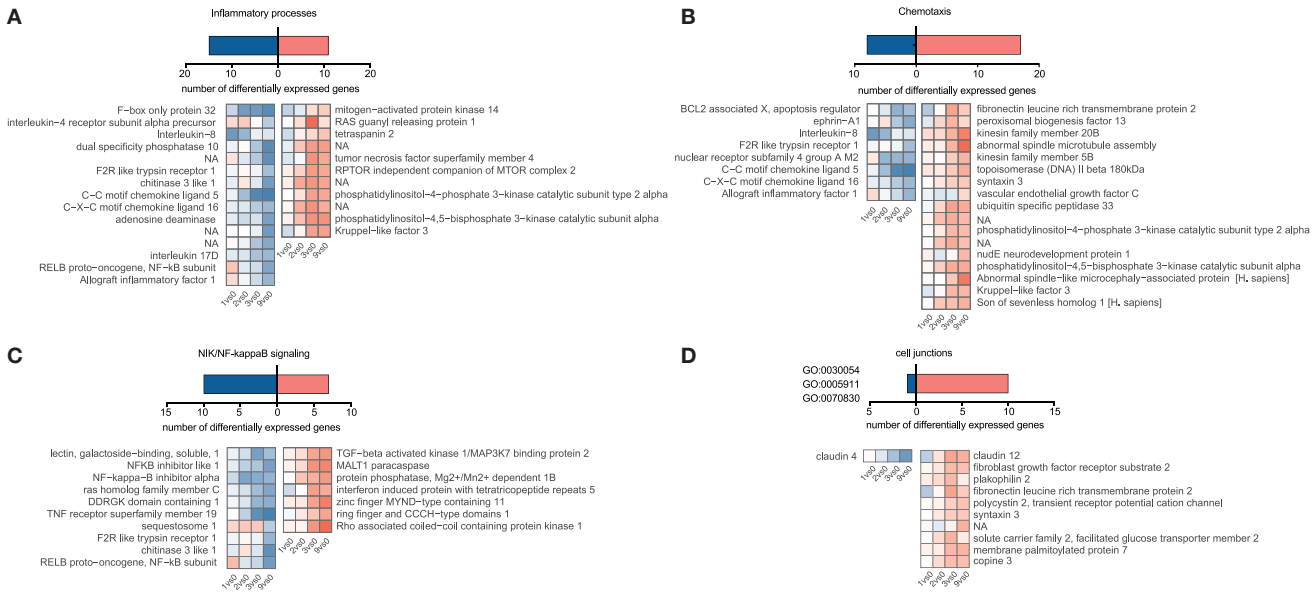

FIGURE 4 | Temporal gene expression changes in porcine intestinal epithelial cells in response to *A. suum* larvae. Blastp, Blast2GO, and InterProScan were used to identify *S. scrofa* differentially expressed genes associated with distinct immune responses or cell junction for **(A)** "Inflammatory processes," **(B)** "Chemotaxis," and **(C)** "NIK/NF-kappaB signaling." For **(D)** "Cell junctions," the cell–cell junction localization filter was manually selected for GO:0030054, GO:0005911, and GO:0070830.

weak induction and even suppression of NIK/NF kappaB signaling (**Figure 4C**), could explain the poor response of immune-related genes that we observed. Following this line, mice lacking NF kappaB signaling specifically in epithelial cells are incapable of mounting protective type 2 cell-mediated immunity to the nematode *Trichuris muris* in its rodent host (63). The initiation of protective type 2 responses against helminth typically begins with production of epithelial cell-derived cytokines (IL-25, IL-33, and thymic stromal lymphopoietin), but none of them was found to be regulated in porcine IPEC-J2 cells early after *A. suum* co-incubation. However, it has to be taken into account that it was recently found that rather than every epithelial cell, a very rare epithelial cell type, intestinal tuft cells, initiated mucosal type 2 responses to helminth parasites through IL-25 secretion after TRMP5 taste chemoreception (64, 65).

Studies in the mouse model parasitic nematode *Heligmosomoides polygyrus* showed that factors secreted by the nematodes directly suppressed IL-33 release (66), but the upstream mechanisms of IL-33 release are somewhat controversial and suggest that IL-33 might also be released from intracellular stores when cells undergo necrosis or even after mechanical stress (67). However, from our data, we cannot conclude that IL-33 is not released. We, therefore, speculated that during co-incubation, worms cause epithelial barrier damage and induce mechanical stress responses or cell death, but the latter was only poorly reflected in the epithelial transcriptome response [no wound healing, apoptosis, or necroptosis pathways (**Figure 3C**)]. From 247 DEGs associated with stress response in general (GO declination Table S3 and Figure S4 in Supplementary Material), only 10 are connected to mechanically induced stress responses/mechanical stimulus (Figure S5 in Supplementary Material). However, when genes associated to cell junction or bicellular junction formation (GO:0030054, GO:0070830, and GO:0005911) were considered, we noticed a clear trend toward an induced gene response, including claudin-12, plakophilin 2, and FLRT3 (**Figure 4D**). This highlights an active response to promote barrier integrity of IPEC-J2 and raises the question whether *A. suum* larvae and/or their secreted products specifically target tight junction formation. Moreover, the only downregulated gene in this functional group was claudin-4 (**Figure 4D**). This is particularly interesting, because researchers suggest that claudin-4 acts to tighten the paracellular pathway (68) and downregulation of claudin-4 is observed under conditions leading to increased permeability (69). The differential regulation of claudin-12 and claudin-4 and the downregulation of IL-8 was additionally validated by quantitative PCR (Figure S7A in Supplementary Material).

Together, our results indicate that small intestinal epithelial cells show poor innate immune responses to co-incubated *A. suum* L3, reduced ribosome function and oxidative phosphorylation pathways, but specifically induce tight junction formation. Whether IPEC-J2 cells do not possess an adequate detection system or whether the parasite is inactivating the host detection systems that would otherwise raise the alarm remains unknown.

The Worm Response to the Epithelial Barrier

Ascaris suum Larvae Drive Invasion and Migration

The initial contact of *Ascaris suum* L3 with intestinal epithelial cells resulted in a transcriptomic response of 146 *A. suum* genes

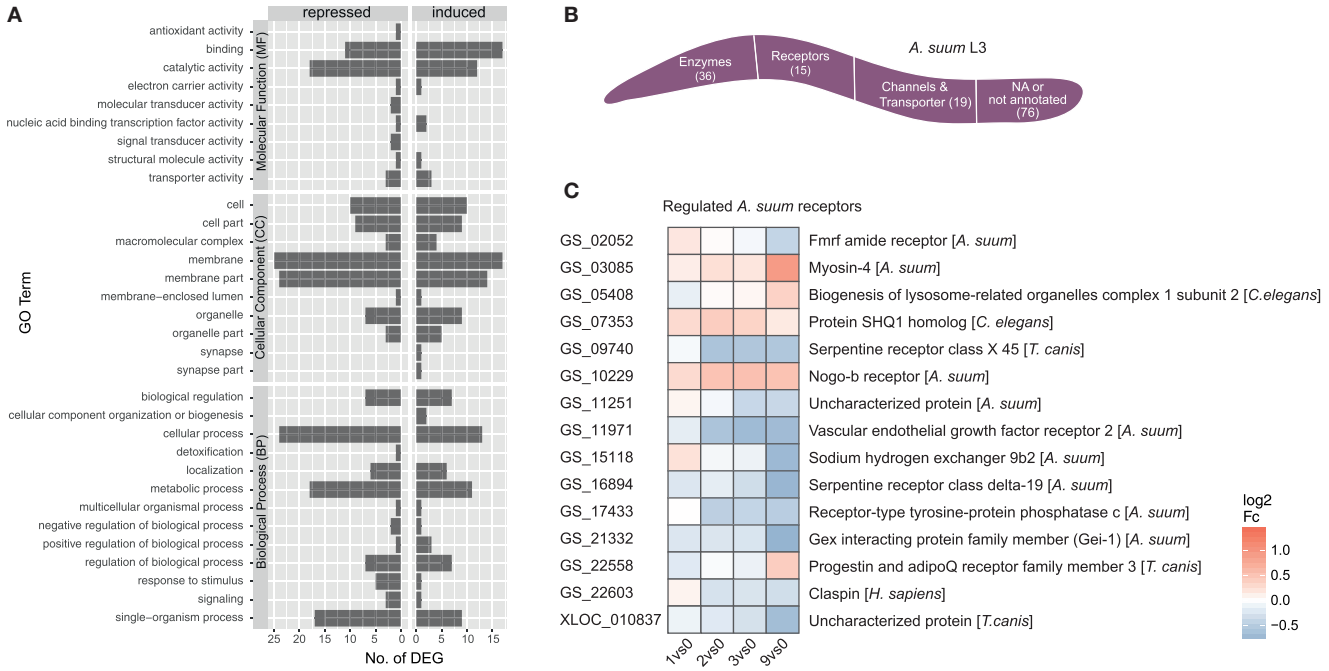

FIGURE 5 | Gene ontology (GO) profiling of *Ascaris suum* differentially expressed genes (DEGs). **(A)** Distribution of level 2 GO terms for *A. suum* L3 DEGs, categorized into molecular function, cellular component (CC), and biological process (BP). **(B)** Global classification of *A. suum* L3 DEGs into enzymes, receptors, and channels/transporter based on GO-term filter and gene description analysis (Table S3 in Supplementary Material). **(C)** Time-resolved expression of *A. suum* DEGs with GO assigned receptor function.

(68 upregulated/78 downregulated, with respect to the maximal pairwise fold-change). A total of 87 genes mapped to GO terms showed regulated functions such as *binding* and *catalytic activity* (MF), *membrane and membrane part* (CC) as well as *cellular*, *metabolic,* and *single-organism processes* (BP) (**Figure 5A** GO level 2). However, no significant enrichments (two-sided Fisher's Exact test in Blast2GO; adjusted $p < 0.05$) could be observed with respect to the background genome. Due to the small number of *A. suum* DEGs in general, only a few KEGG pathways could be assigned more than once, namely ABC transporters (2), cAMP signaling pathway (2, repressed), cysteine and methionine metabolism (2, repressed), glycosaminoglycan degradation (2, activated), protein digestion and absorption (3), pyrimidine metabolism (2), RNA degradation (2), and spliceosome (2) (Figure S2 in Supplementary Material). GO term filtering and gene description analysis were used to classify *A. suum* L3 DEGs into enzymes (36), receptors (15), and channels/transporters (19) (**Figure 5B**). Surprisingly, most receptor associated genes were indeed downregulated (10 out of 15, **Figure 5C**). We specifically looked for *Ascaris* C-type lectins (C-TL), a superfamily potentially involved in either site-specific tissue recognition or interference with mammalian C-TL-mediated inflammation (70), but found no C-TL within the *A. suum* DEGs of our early response experiment.

In contrast, the 20 most upregulated *A suum* L3 genes (Table S1 in Supplementary Material) included genes associated with motor activity (GS_03085 Myosin-4, GS_04138 Troponin T, GS_00138 Myoglobin) and structure (GS_04352 Cuticle collagen domain-containing protein, GS_11610 Cuticle collagen 6, GS_09547 Cuticle collagen 34, GS_00653 Protein disulfide-isomerase 2). The upregulation of genes associated with motor activity/motility driven by epithelial-contact is particularly interesting in the absence of host peristalsis, the luminal content/microbes, or mucus production and could be indicative of increased locomotion either in order to penetrate host tissue or to counteract passive movement after site-specific recognition. Increased muscular locomotor activity together with proteolytic enzymes secreted by glandular structures are thought to be essential for host tissue penetration.

The subset of upregulated genes involved in cuticle formation such as protein disulfide-isomerase 2 (PDI-2) (Table S1 in Supplementary Material and qPCR-validated in Figure S7B in Supplementary Material) suggests an epithelial trigger for driving further larval development. Nematode cuticles are formed by multiple collagenous layers that contain extensive disulfide linkages (71) and new cuticles are synthesized sequentially for each developmental stage. Cuticle biogenesis in the endoplasmic reticulum involves proline hydoxylation and disulfide bond formation by PDI (72). Mutations in the Protein disulfide-isomerase 2 (PDI-2) gene of *Caenorhabditis elegans* resulted in severe body morphology defects, uncoordinated movement, adult sterility, abnormal molting, and aberrant collagen deposition (73). The importance of PDI-2 activity for ECM formation demonstrated for *C. elegans* and more recently also for *Brugia malayi* (74) highlights its relevance as a potential anthelmintic drug target (72), including for *Ascaris* species.

At the host–parasite interface, ES proteins released by helminths play an important role in mediating host–parasite interaction, regulation, and control (75–78). To assess the transcriptional regulation of proteins potentially secreted by larval *Ascaris* parasites, we merged predicted DEGs for classical (SignalP) and non-classical (SecretomeP) secretory proteins and removed mitochondrial (TargetP) and transmembrane (TMHMM) proteins (**Figure 6A**). From the 55 ES proteins, 20 can be assigned to enzymatic activity with diverse functions including hydrolases ($n = 9$), transferases ($n = 6$), isomerases ($n = 2$), oxidoreductases ($n = 2$), and lyases ($n = 1$) as depicted in **Figure 6A**.

We hypothesized that proteolytic enzymes would be essential for parasite invasion and, therefore, upregulated by *A. suum* larvae once the epithelial barrier was detected. Within the class of proteases, nematode serine proteases have received considerable interest as they are widely distributed in parasitic nematodes with a wide variety of functions (79). Indeed, the parasite transcript with the highest maximal fold-change (comparing 0 versus 9 h time point, Table S1 in Supplementary Material) was identified as being *A. suum* aspartic protease 6 (**Figure 6B**). Aspartic proteases are a group of endopeptidases characterized by their catalytic aspartic residues that are known to drive host hemoglobin digestion by the blood-feeding nematodes *Haemonchus contortus*, *Ancylostoma caninum*, and *Necator americanus* (80, 81). Moreover, aspartic protease 1 from *N. americanus* is targeted by the bivalent human hookworm vaccine [Na-APR-1(M74), carrying a site-directed mutation abolishing its catalytic activity, and glutathione *S*-transferase (Na-GST-1)] currently being tested in clinical phase 1 studies in the US and Brazil (82–84). The Na-APR-1(M74) vaccine strategy is based on the induction of neutralizing antibodies against aspartic protease 1, thereby preventing hemoglobin degradation in the brush border membrane of the parasite's digestive tract and finally leading to diminished parasite-related blood loss and reduced numbers of hookworms [reviewed in Ref. (83, 85)]. For nematode parasites that do not feed on blood but express aspartic proteases, different functions such as skin macromolecule and epithelial degradation, aiding in tissue penetration, or host-derived nutrient digestion are suggested (86–88). Interestingly, a proteomic study on ES products of different larval stages of *A. suum* shows the presence of aspartic

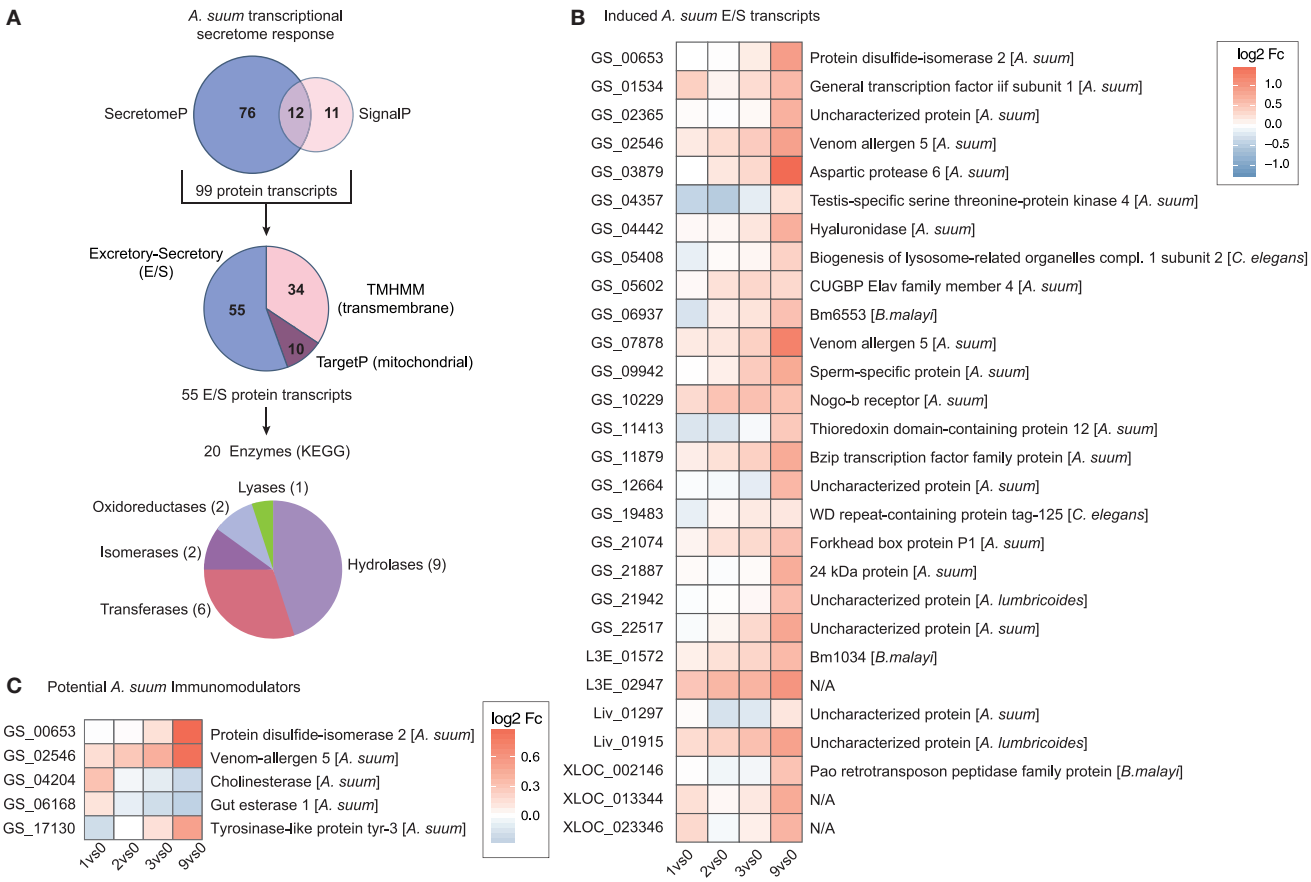

FIGURE 6 | The secretome response of *Ascaris suum*. **(A)** The pipeline to identify *A. suum* excretory-secretory (ES) transcripts used SignalP and SecretomeP to annotate classical ($n = 23$) and non-classical ($n = 88$) ES genes and excluded mitochondrial ($n = 10$; TargetP) and transmembrane ($n = 34$; TMHMM) protein transcripts. KEGG ENZYME identified enzyme classes of ES transcripts are depicted in the bottom pie chart. **(B)** Time-resolved expression of $n = 28$ induced *A. suum* ES transcripts. **(C)** Differentially expressed *A. suum* transcripts that matched to genome prediction of *A. suum* immunomodulatory ES products based on homology to other nematodes (26).

protease 6 protein in ES collected from L3-lung stage worms, but its absence in the ES of hatched L3 larvae (89), thereby directly supporting our findings on the protein level and highlighting an epithelial trigger and early role for this specific enzyme.

The same study revealed the high abundance of glycosyl hydrolases (family 31, GH31) in *A. suum* L4 ES (89) suggesting degradation of complex carbohydrates to be essential for its energy metabolism. Among the ES enzymes upregulated directly in response to epithelial cell contact, we indeed identified a hyaluronidase (**Figure 6**, GS_04442). There is evidence that some bacterial species use hyaluronidases to utilize host hyaluronic acid (HA), an essential part of the ECM of epithelial tissue, as a carbon source for their energy metabolism (90). This might indicate that *A. suum* L3 not only produce proteolytic enzymes that help in epithelial tissue invasion but that epithelial ECM components can be directly hydrolyzed to feed on. Moreover, the release of hyaluronidase by *A. suum* has been described earlier for larvae isolated from the lungs of infected pigs (91). Besides its role in facilitating larval migration, the authors added another functional point: the modulation of developmental processes by hydrolyzing HA present in extracellular cuticle during molting. The role of *A. suum* hyaluronidase in either breaking up the internal cuticle-epidermal connection critical for molting (91), larval migration (92), or larval energy metabolism, therefore, remains speculative.

A comparison of the herein identified *A. suum* DEGs with a draft genome-based list of potential *A. suum* immunomodulators (26) revealed three upregulated transcripts (**Figure 6C**, GS_00653 PDI-2, GS_02546 venom allergen-5 and GS_17130 tyrosinase like protein tyr-3). Genomic and proteomic evidence suggest the abundance of venom allergen-like (VAL) proteins (SCP/TAPs superfamily) also in the ES compartment of *A. suum*. The early upregulation of VAL genes (venom allergen-5: qPCR validated in Figure S7B in Supplementary Material) is perhaps not surprising and has been associated in previous studies with larval invasion (78, 93, 94), although there is only limited understanding on the detailed function of those proteins in the host–parasite relationship.

In summary, we provide transcriptomic evidence for an early response pattern of genes that *A. suum* L3 specifically regulate during contact with host epithelial cells. Among those genes are factors that might facilitate parasite invasion through the epithelial barrier (aspartic protease 6), migration (myosin, troponin, and myoglobin), feeding (hyaluronidase), and development (PDI2) of the parasite. However, the parasite–host interaction not only depends on proteins but might also include glycans, lipids, miRNAs, or other small molecules and metabolites that have not been studied here, but can also contribute to parasite-epithelial communication (75). Furthermore, intestinal parasites and microbes have co-evolved together in their respective hosts. For that reason, the complex interaction of parasites with the bacterial community and the microbiota–host interaction likely also contributes to the parasite–host communication.

Interspecies Interaction Is Dominated by Four *A. suum* Genes

Inference of interspecies gene co-expression networks (GENs) is an important systems biology approach to predict pathogen–host interactions. We applied established and efficient procedures to infer and analyze GENs including pairwise correlation, cluster (module) analysis, and functional enrichment (95, 96). Thereby, genes featuring a similar expression profile over time are associated by direct network links as well as gene clusters and are considered to participate in common functionality or in concurrent and thus interlinked processes. It must be noted that the recommended sample number of 20 is not met; however, our analysis compensates with distinctly higher read coverage than recommended (>10 million), an encompassing context of all samples due to the time series as well as strict GEN creation parameters ($p < 0.05$, rho > 0.95), resulting in a few but prominent and explicit signals.

Based on node degrees of the co-expression network that was reduced to interspecies nodes and interspecies edges (**Figure 7A**, GEN2), we identified four highly interacting *A. suum* genes (**Figures 7B,C**). Three of the four highly interacting *A. suum* genes could be annotated by the iterative strategy (**Figure 1B**); GS_12056 with the "elongation of very long-chain fatty acids" (UniProt:ASU_11627, GO:0016021 integral components of the membrane), GS_09942 as "sperm-specific protein" (UniProt:ASU_04668, PROSITE:PS50202) and GS_11251 as "Uncharacterized protein," or with the InterProScan classification, "rhodopsin-like G protein-coupled receptors (GPCRs)" (UniProt:ASU_01462, GO:0016021 integral components of membrane) (**Figure 7E**). The one gene lacking thorough characterization, L3E_01572, is annotated only with the associated GO-term (UniProt:Bm1034, GO:0016021 integral component of membrane). The overall gene regulation, based on maximal fold change values, of *S. scrofa* genes connected to the four *A. suum* genes was diverse as illustrated in **Figure 7D**. In addition to node degrees, the four *A. suum* genes are further emphasized by the fact that they participate in the four largest clusters of GEN1 identified by MCODE (Cluster 1, 2, 4, and 5, **Figure 7B**; Table S2 in Supplementary Material). Those four clusters are dominated by *S. scrofa* genes except for one *A. suum* gene each. The network data links the parasite's fatty acid biosynthesis with host cluster 1, which is comprised of mostly repressed genes like Cystatin E/M and macrophage inhibitory factor 1 (MIF), known to be induced by bacterial invaders (97), and ribosomal proteins (RPS21, RPS16, RPL13, RPL18, RPL8) involved in peptide and protein synthesis (Table S2 in Supplementary Material). GO profiling of *S. scrofa* DEGs per cluster revealed significantly over-represented terms (two-sided Fisher's Exact test, $p < 0.05$) in cluster 1 (**Figures 7B,C**; Figure S3 in Supplementary Material) associated with structural molecule activity (MF), cell, cell part and macromolecular complex (CC). In parallel, the sperm-specific protein of *A. suum* interacted with cluster 2 that contained mostly repressed genes for cellular and metabolic processes (BP). A dominant activation of genes was found in cluster 5 with the interspecies link to GS_11251 (*A. suum*) that shares structural similarity to known rhodopsin-like G protein-coupled receptors according to InterPro. GPCRs transduce extracellular signals through interaction with guanine nucleotide-binding (G) proteins, highlighting its potential for interspecies linkage.

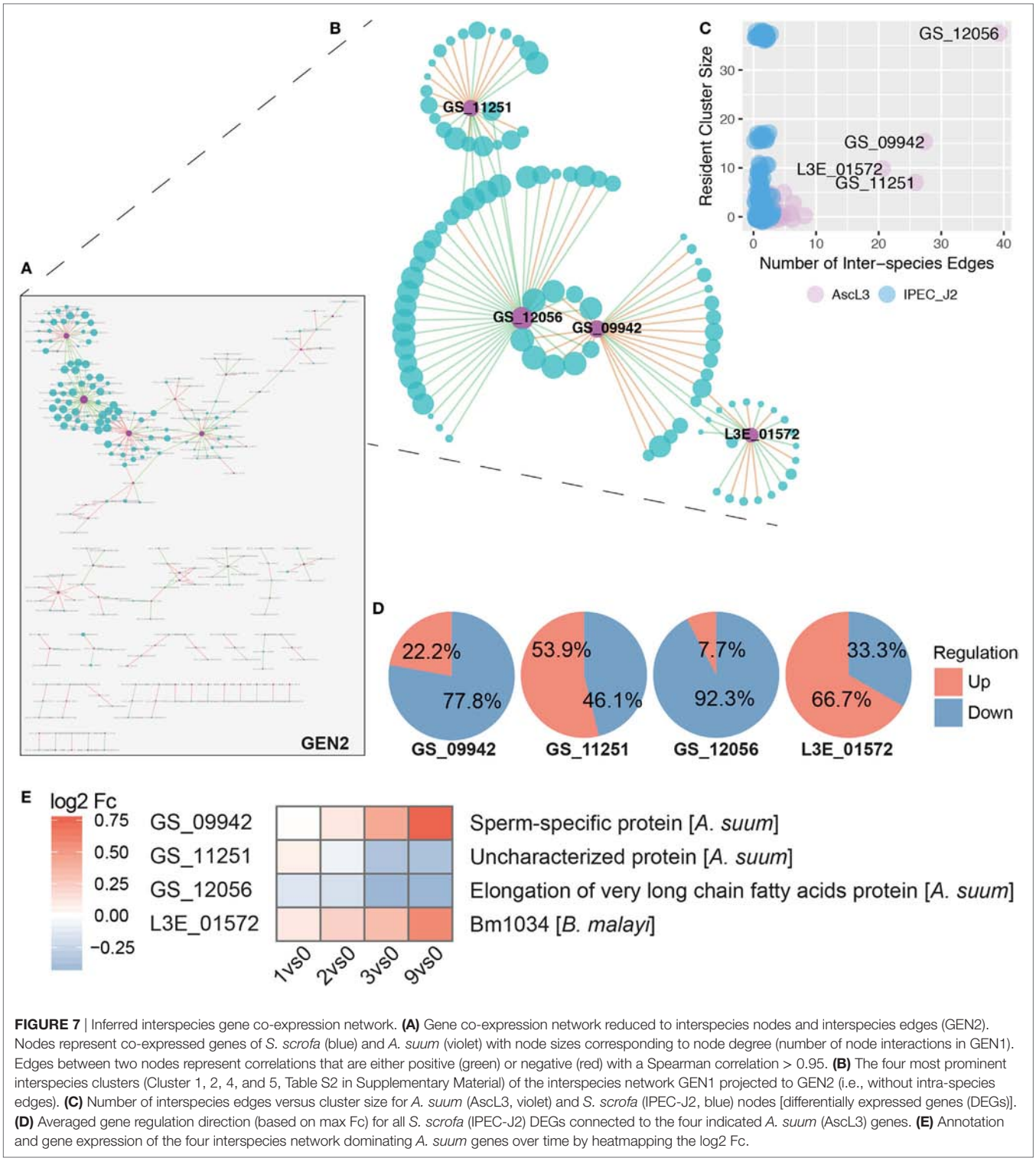

FIGURE 7 | Inferred interspecies gene co-expression network. **(A)** Gene co-expression network reduced to interspecies nodes and interspecies edges (GEN2). Nodes represent co-expressed genes of *S. scrofa* (blue) and *A. suum* (violet) with node sizes corresponding to node degree (number of node interactions in GEN1). Edges between two nodes represent correlations that are either positive (green) or negative (red) with a Spearman correlation > 0.95. **(B)** The four most prominent interspecies clusters (Cluster 1, 2, 4, and 5, Table S2 in Supplementary Material) of the interspecies network GEN1 projected to GEN2 (i.e., without intra-species edges). **(C)** Number of interspecies edges versus cluster size for *A. suum* (AscL3, violet) and *S. scrofa* (IPEC-J2, blue) nodes [differentially expressed genes (DEGs)]. **(D)** Averaged gene regulation direction (based on max Fc) for all *S. scrofa* (IPEC-J2) DEGs connected to the four indicated *A. suum* (AscL3) genes. **(E)** Annotation and gene expression of the four interspecies network dominating *A. suum* genes over time by heatmapping the log2 Fc.

Even though more extensive interpretations are limited for the DEGs that have no functional information assigned, the prominent appearance of the four *A. suum* genes in the GENs and clusters render them into attractive and suitable candidates for targeted approaches.

DATA DEPOSITION

All sequencing data generated in this project are available from the NCBI Sequence Read Archive (SRA) and collectively available *via* the BioProject: PRJNA450204.

All analysis code is provided at https://gitlab.com/mkuhring/project_asuum.

AUTHOR CONTRIBUTIONS

Conceptualization: FE, BR, and SH. Investigation: FE, MK, AR, and AM. Formal analysis: MK and BR. Visualization: FE and MK. Writing—original draft: FE and MK. Writing—review and editing: FE, AM, MK, AR, BR, and SH. Funding acquisition: SH and BR. Resources: AM and AR. Supervision: SH and BR.

ACKNOWLEDGMENTS

The authors thank Christiane Palissa, Bettina Sonnenburg, Marion Müller, Yvonne Weber, Beate Anders, and Julia Hinzmann for excellent technical support and Ulrike Lodemann and Henriette Loß for their help in RNA quality assessment. The study was supported by the Federal Ministry of Education and Research (BMBF) within the consortium "InfectControl 2020," project Art4Fun to SH and by the German Research Foundation (DFG), national research training group (GRK) 2046 to SH, and a starting grant of Freie Universität Berlin to SH and BR.

SUPPLEMENTARY MATERIAL

The Supplementary Material for this article can be found online at https://www.frontiersin.org/articles/10.3389/fimmu.2018.01868/full#supplementary-material.

TABLE S1 | Differentially expressed genes pig and worm total.

TABLE S2 | Co-expression analysis: GEN nodes, GEN edges, GEN cluster.

TABLE S3 | Gene ontology (GO) term declination for GO filters.

TABLE S4 | Genome of Ascaris suum L3 and IPEC-J2.

REFERENCES

1. Bethony J, Brooker S, Albonico M, Geiger SM, Loukas A, Diemert D, et al. Soil-transmitted helminth infections: ascariasis, trichuriasis, and hookworm. *Lancet* (2006) 367:1521–32. doi:10.1016/S0140-6736(06)68653-4
2. Hotez PJ, Alvarado M, Basáñez M-G, Bolliger I, Bourne R, Boussinesq M, et al. The global burden of disease study 2010: interpretation and implications for the neglected tropical diseases. *PLoS Negl Trop Dis* (2014) 8(7):e2865. doi:10.1371/journal.pntd.0002865
3. Utzinger J, Becker SL, Knopp S, Blum J, Neumayr AL, Keiser J, et al. Neglected tropical diseases: diagnosis, clinical management, treatment and control. *Swiss Med Wkly* (2012) 142:w13727. doi:10.4414/smw.2012.13727
4. Thamsborg SM, Nejsum P, Mejer H. Chapter 14 – Impact of *Ascaris suum* in livestock. In: Holland C, editor. *Ascaris: The Neglected Parasite*. Amsterdam: Elsevier (2013). p. 363–81.
5. Vlaminck J, Geldhof P. Chapter 16 – Diagnosis and control of *Ascariasis* in pigs. In: Holland C, editor. *Ascaris: The Neglected Parasite*. Amsterdam: Elsevier (2013). p. 395–425.
6. Leles D, Gardner SL, Reinhard K, Iñiguez A, Araujo A. Are *Ascaris lumbricoides* and *Ascaris suum* a single species? *Parasit Vectors* (2012) 5:42. doi:10.1186/1756-3305-5-42
7. Shao C-C, Xu M-J, Alasaad S, Song H-Q, Peng L, Tao J-P, et al. Comparative analysis of microRNA profiles between adult *Ascaris lumbricoides* and *Ascaris suum*. *BMC Vet Res* (2014) 10:99. doi:10.1186/1746-6148-10-99
8. Rosa BA, Jasmer DP, Mitreva M. Genome-wide tissue-specific gene expression, co-expression and regulation of co-expressed genes in adult nematode *Ascaris suum*. *PLoS Negl Trop Dis* (2014) 8:e2678. doi:10.1371/journal.pntd.0002678
9. Katakam KK, Thamsborg SM, Dalsgaard A, Kyvsgaard NC, Mejer H. Environmental contamination and transmission of *Ascaris suum* in Danish organic pig farms. *Parasit Vectors* (2016) 9:80. doi:10.1186/s13071-016-1349-0
10. Douvres FW, Tromba FG, Malakatis GM. Morphogenesis and migration of *Ascaris suum* larvae developing to fourth stage in swine. *J Parasitol* (1969) 55:689–712. doi:10.2307/3277198
11. Murrell KD, Eriksen L, Nansen P, Slotved HC, Rasmussen T. *Ascaris suum*: a revision of its early migratory path and implications for human ascariasis. *J Parasitol* (1997) 83:255–60. doi:10.2307/3284450
12. Fritz JH, Le Bourhis L, Magalhaes JG, Philpott DJ. Innate immune recognition at the epithelial barrier drives adaptive immunity: APCs take the back seat. *Trends Immunol* (2008) 29:41–9. doi:10.1016/j.it.2007.10.002
13. Ganz T. Epithelia: not just physical barriers. *Proc Natl Acad Sci U S A* (2002) 99:3357–8. doi:10.1073/pnas.072073199
14. Dawson H, Solano-Aguilar G, Beal M, Beshah E, Vangimalla V, Jones E, et al. Localized Th1-, Th2-, T regulatory cell-, and inflammation-associated hepatic and pulmonary immune responses in *Ascaris suum*-infected swine are increased by retinoic acid. *Infect Immun* (2009) 77:2576–87. doi:10.1128/IAI.00827-07
15. Masure D, Wang T, Vlaminck J, Claerhoudt S, Chiers K, Van den Broeck W, et al. The intestinal expulsion of the roundworm *Ascaris suum* is associated with eosinophils, intra-epithelial T cells and decreased intestinal transit time. *PLoS Negl Trop Dis* (2013) 7:e2588. doi:10.1371/journal.pntd.0002588
16. Nossol C, Barta-Böszörményi A, Kahlert S, Zuschratter W, Faber-Zuschratter H, Reinhardt N, et al. Comparing two intestinal porcine epithelial cell lines (IPECs): morphological differentiation, function and metabolism. *PLoS One* (2015) 10:e0132323. doi:10.1371/journal.pone.0132323
17. Schierack P, Nordhoff M, Pollmann M, Weyrauch KD, Amasheh S, Lodemann U, et al. Characterization of a porcine intestinal epithelial cell line for in vitro studies of microbial pathogenesis in swine. *Histochem Cell Biol* (2006) 125:293–305. doi:10.1007/s00418-005-0067-z
18. Westermann AJ, Barquist L, Vogel J. Resolving host–pathogen interactions by dual RNA-seq. *PLoS Pathog* (2017) 13(2):e1006033. doi:10.1371/journal.ppat.1006033
19. Love MI, Huber W, Anders S. Moderated estimation of fold change and dispersion for RNA-seq data with DESeq2. *Genome Biol* (2014) 15:550. doi:10.1186/s13059-014-0550-8
20. Köster J, Rahmann S. Snakemake—a scalable bioinformatics workflow engine. *Bioinformatics* (2012) 28:2520–2. doi:10.1093/bioinformatics/bts480
21. Urban JF Jr, Douvres FW, Tromba FG. A rapid method for hatching *Ascaris suum* eggs in vitro. *Proc Helminthol Soc Wash* (1981) 48(2):241–3.
22. Bolger AM, Lohse M, Usadel B. Trimmomatic: a flexible trimmer for Illumina sequence data. *Bioinformatics* (2014) 30:2114–20. doi:10.1093/bioinformatics/btu170
23. Wood DE, Salzberg SL. Kraken: ultrafast metagenomic sequence classification using exact alignments. *Genome Biol* (2014) 15:R46. doi:10.1186/gb-2014-15-3-r46
24. Kim D, Pertea G, Trapnell C, Pimentel H, Kelley R, Salzberg SL. TopHat2: accurate alignment of transcriptomes in the presence of insertions, deletions and gene fusions. *Genome Biol* (2013) 14:R36. doi:10.1186/gb-2013-14-4-r36
25. Trapnell C, Hendrickson DG, Sauvageau M, Goff L, Rinn JL, Pachter L. Differential analysis of gene regulation at transcript resolution with RNA-seq. *Nat Biotechnol* (2013) 31:46–53. doi:10.1038/nbt.2450
26. Jex AR, Liu S, Li B, Young ND, Hall RS, Li Y, et al. *Ascaris suum* draft genome. *Nature* (2011) 479:529–33. doi:10.1038/nature10553
27. Howe KL, Bolt BJ, Shafie M, Kersey P, Berriman M. WormBase ParaSite – a comprehensive resource for helminth genomics. *Mol Biochem Parasitol* (2017) 215:2–10. doi:10.1016/j.molbiopara.2016.11.005
28. Zerbino DR, Achuthan P, Akanni W, Amode MR, Barrell D, Bhai J, et al. Ensembl 2018. *Nucleic Acids Res* (2018) 46:D754–61. doi:10.1093/nar/gkx1098

29. Liao Y, Smyth GK, Shi W. featureCounts: an efficient general purpose program for assigning sequence reads to genomic features. *Bioinformatics* (2014) 30:923–30. doi:10.1093/bioinformatics/btt656
30. Ritchie ME, Phipson B, Wu D, Hu Y, Law CW, Shi W, et al. limma powers differential expression analyses for RNA-sequencing and microarray studies. *Nucleic Acids Res* (2015) 43:e47. doi:10.1093/nar/gkv007
31. Ashburner M, Ball CA, Blake JA, Botstein D, Butler H, Cherry JM, et al. Gene ontology: tool for the unification of biology. The Gene Ontology Consortium. *Nat Genet* (2000) 25:25–9. doi:10.1038/75556
32. The Gene Ontology Consortium. Expansion of the gene ontology knowledgebase and resources. *Nucleic Acids Res* (2017) 45:D331–8. doi:10.1093/nar/gkw1108
33. Rice P, Longden I, Bleasby A. EMBOSS: the European molecular biology open software suite. *Trends Genet* (2000) 16:276–7. doi:10.1016/S0168-9525(00)02024-2
34. Camacho C, Coulouris G, Avagyan V, Ma N, Papadopoulos J, Bealer K, et al. BLAST+: architecture and applications. *BMC Bioinformatics* (2009) 10:421. doi:10.1186/1471-2105-10-421
35. Conesa A, Götz S, García-Gómez JM, Terol J, Talón M, Robles M. Blast2GO: a universal tool for annotation, visualization and analysis in functional genomics research. *Bioinformatics* (2005) 21:3674–6. doi:10.1093/bioinformatics/bti610
36. Jones P, Binns D, Chang H-Y, Fraser M, Li W, McAnulla C, et al. InterProScan 5: genome-scale protein function classification. *Bioinformatics* (2014) 30:1236–40. doi:10.1093/bioinformatics/btu031
37. The UniProt Consortium. UniProt: the universal protein knowledgebase. *Nucleic Acids Res* (2017) 45:D158–69. doi:10.1093/nar/gkw1099
38. Kinsella RJ, Kähäri A, Haider S, Zamora J, Proctor G, Spudich G, et al. Ensembl BioMarts: a hub for data retrieval across taxonomic space. *Database (Oxford)* (2011) 2011:bar030. doi:10.1093/database/bar030
39. Smedley D, Haider S, Durinck S, Pandini L, Provero P, Allen J, et al. The BioMart community portal: an innovative alternative to large, centralized data repositories. *Nucleic Acids Res* (2015) 43:W589–98. doi:10.1093/nar/gkv350
40. Kanehisa M, Sato Y, Kawashima M, Furumichi M, Tanabe M. KEGG as a reference resource for gene and protein annotation. *Nucleic Acids Res* (2016) 44:D457–62. doi:10.1093/nar/gkv1070
41. Kanehisa M, Sato Y, Morishima K. BlastKOALA and GhostKOALA: KEGG tools for functional characterization of genome and metagenome sequences. *J Mol Biol* (2016) 428:726–31. doi:10.1016/j.jmb.2015.11.006
42. Durinck S, Spellman PT, Birney E, Huber W. Mapping identifiers for the integration of genomic datasets with the R/Bioconductor package biomaRt. *Nat Protoc* (2009) 4:1184–91. doi:10.1038/nprot.2009.97
43. Gomez S, Adalid-Peralta L, Palafox-Fonseca H, Cantu-Robles VA, Soberón X, Sciutto E, et al. Genome analysis of excretory/secretory proteins in *Taenia solium* reveals their abundance of antigenic regions (AAR). *Sci Rep* (2015) 5:9683. doi:10.1038/srep09683
44. Petersen TN, Brunak S, von Heijne G, Nielsen H. SignalP 4.0: discriminating signal peptides from transmembrane regions. *Nat Methods* (2011) 8:785–6. doi:10.1038/nmeth.1701
45. Bendtsen JD, Jensen LJ, Blom N, Von Heijne G, Brunak S. Feature-based prediction of non-classical and leaderless protein secretion. *Protein Eng Des Sel* (2004) 17:349–56. doi:10.1093/protein/gzh037
46. Bendtsen JD, Kiemer L, Fausbøll A, Brunak S. Non-classical protein secretion in bacteria. *BMC Microbiol* (2005) 5:58. doi:10.1186/1471-2180-5-58
47. Emanuelsson O, Nielsen H, Brunak S, von Heijne G. Predicting subcellular localization of proteins based on their N-terminal amino acid sequence. *J Mol Biol* (2000) 300:1005–16. doi:10.1006/jmbi.2000.3903
48. Krogh A, Larsson B, von Heijne G, Sonnhammer EL. Predicting transmembrane protein topology with a hidden Markov model: application to complete genomes. *J Mol Biol* (2001) 305:567–80. doi:10.1006/jmbi.2000.4315
49. Yu G, Wang L-G, Han Y, He Q-Y. clusterProfiler: an R package for comparing biological themes among gene clusters. *OMICS* (2012) 16:284–7. doi:10.1089/omi.2011.0118
50. Revelle W. *psych: Procedures for Personality and Psychological Research*. Evanston: Northwestern University (2018). Available from: https://CRAN.R-project.org/package=psych Version = 1.8.4
51. Shannon P, Markiel A, Ozier O, Baliga NS, Wang JT, Ramage D, et al. Cytoscape: a software environment for integrated models of biomolecular interaction networks. *Genome Res* (2003) 13:2498–504. doi:10.1101/gr.1239303
52. Bader GD, Hogue CWV. An automated method for finding molecular complexes in large protein interaction networks. *BMC Bioinformatics* (2003) 4:2. doi:10.1186/1471-2105-4-2
53. Okonechnikov K, Conesa A, García-Alcalde F. Qualimap 2: advanced multi-sample quality control for high-throughput sequencing data. *Bioinformatics* (2016) 32:292–4. doi:10.1093/bioinformatics/btv566
54. Zakrzewski SS, Richter JF, Krug SM, Jebautzke B, Lee I-FM, Rieger J, et al. Improved cell line IPEC-J2, characterized as a model for porcine jejunal epithelium. *PLoS One* (2013) 8:e79643. doi:10.1371/journal.pone.0079643
55. Fink C, Hoffmann J, Knop M, Li Y, Isermann K, Roeder T. Intestinal FoxO signaling is required to survive oral infection in *Drosophila*. *Mucosal Immunol* (2016) 9:927–36. doi:10.1038/mi.2015.112
56. Goodridge HS, Marshall FA, Else KJ, Houston KM, Egan C, Al-Riyami L, et al. Immunomodulation via novel use of TLR4 by the filarial nematode phosphorylcholine-containing secreted product, ES-62. *J Immunol* (2005) 174:284–93. doi:10.4049/jimmunol.174.1.284
57. Kane CM, Cervi L, Sun J, McKee AS, Masek KS, Shapira S, et al. Helminth antigens modulate TLR-initiated dendritic cell activation. *J Immunol* (2004) 173:7454–61. doi:10.4049/jimmunol.173.12.7454
58. MacDonald AS, Maizels RM. Alarming dendritic cells for Th2 induction. *J Exp Med* (2008) 205:13–7. doi:10.1084/jem.20072665
59. Perrigoue JG, Marshall F, Artis D. On the hunt for helminths: innate immune cells in the recognition and response to helminth parasites. *Cell Microbiol* (2008) 10:1757–64. doi:10.1111/j.1462-5822.2008.01174.x
60. Cohen-Kedar S, Baram L, Elad H, Brazowski E, Guzner-Gur H, Dotan I. Human intestinal epithelial cells respond to β-glucans via Dectin-1 and Syk. *Eur J Immunol* (2014) 44:3729–40. doi:10.1002/eji.201444876
61. Patel S, McCormick BA. Mucosal inflammatory response to *Salmonella typhimurium* infection. *Front Immunol* (2014) 5:311. doi:10.3389/fimmu.2014.00311
62. Aprianto R, Slager J, Holsappel S, Veening J-W. Time-resolved dual RNA-seq reveals extensive rewiring of lung epithelial and pneumococcal transcriptomes during early infection. *Genome Biol* (2016) 17:198. doi:10.1186/s13059-016-1054-5
63. Zaph C, Troy AE, Taylor BC, Berman-Booty LD, Guild KJ, Du Y, et al. Epithelial-cell-intrinsic IKK-β expression regulates intestinal immune homeostasis. *Nature* (2007) 446:552–6. doi:10.1038/nature05590
64. Gerbe F, Sidot E, Smyth DJ, Ohmoto M, Matsumoto I, Dardalhon V, et al. Intestinal epithelial tuft cells initiate type 2 mucosal immunity to helminth parasites. *Nature* (2016) 529:226–30. doi:10.1038/nature16527
65. Howitt MR, Lavoie S, Michaud M, Blum AM, Tran SV, Weinstock JV, et al. Tuft cells, taste-chemosensory cells, orchestrate parasite type 2 immunity in the gut. *Science* (2016) 351:1329–33. doi:10.1126/science.aaf1648
66. McSorley HJ, Blair NF, Smith KA, McKenzie ANJ, Maizels RM. Blockade of IL-33 release and suppression of type 2 innate lymphoid cell responses by helminth secreted products in airway allergy. *Mucosal Immunol* (2014) 7(5):1068–78. doi:10.1038/mi.2013.123
67. Kakkar R, Hei H, Dobner S, Lee RT. Interleukin 33 as a mechanically responsive cytokine secreted by living cells. *J Biol Chem* (2012) 287:6941–8. doi:10.1074/jbc.M111.298703
68. Günzel D, Yu ASL. Claudins and the modulation of tight junction permeability. *Physiol Rev* (2013) 93:525–69. doi:10.1152/physrev.00019.2012
69. Günzel D, Fromm M. Claudins and other tight junction proteins. *Compr Physiol* (2012) 2:1819–52. doi:10.1002/cphy.c110045
70. Loukas A, Maizels RM. Helminth C-type lectins and host–parasite interactions. *Parasitol Today* (2000) 16:333–9. doi:10.1016/S0169-4758(00)01704-X
71. Cox GN, Staprans S, Edgar RS. The cuticle of *Caenorhabditis elegans*: II. Stage-specific changes in ultrastructure and protein composition during postembryonic development. *Dev Biol* (1981) 86:456–70. doi:10.1016/0012-1606(81)90204-9
72. Page AP, Stepek G, Winter AD, Pertab D. Enzymology of the nematode cuticle: a potential drug target? *Int J Parasitol Drugs Drug Resist* (2014) 4:133–41. doi:10.1016/j.ijpddr.2014.05.003

73. Winter AD, McCormack G, Page AP. Protein disulfide isomerase activity is essential for viability and extracellular matrix formation in the nematode *Caenorhabditis elegans*. *Dev Biol* (2007) 308:449–61. doi:10.1016/j.ydbio.2007.05.041
74. Winter AD, McCormack G, Myllyharju J, Page AP. Prolyl 4-hydroxlase activity is essential for development and cuticle formation in the human infective parasitic nematode *Brugia malayi*. *J Biol Chem* (2013) 288:1750–61. doi:10.1074/jbc.M112.397604
75. Coakley G, Buck AH, Maizels RM. Host parasite communications – messages from helminths for the immune system. *Mol Biochem Parasitol* (2016) 208:33–40. doi:10.1016/j.molbiopara.2016.06.003
76. Cooper D, Eleftherianos I. Parasitic nematode immunomodulatory strategies: recent advances and perspectives. *Pathogens* (2016) 5(3):58. doi:10.3390/pathogens5030058
77. Ebner F, Schwiertz P, Steinfelder S, Pieper R, Zentek J, Schütze N, et al. Pathogen-reactive T helper cell analysis in the pig. *Front Immunol* (2017) 8:565. doi:10.3389/fimmu.2017.00565
78. Hewitson JP, Grainger JR, Maizels RM. Helminth immunoregulation: the role of parasite secreted proteins in modulating host immunity. *Mol Biochem Parasitol* (2009) 167:1–11. doi:10.1016/j.molbiopara.2009.04.008
79. Yang Y, Wen YJ, Cai YN, Vallée I, Boireau P, Liu MY, et al. Serine proteases of parasitic helminths. *Korean J Parasitol* (2015) 53:1–11. doi:10.3347/kjp.2015.53.1.1
80. Williamson AL, Brindley PJ, Abbenante G, Prociv P, Berry C, Girdwood K, et al. Cleavage of hemoglobin by hookworm cathepsin D aspartic proteases and its potential contribution to host specificity. *FASEB J* (2002) 16:1458–60. doi:10.1096/fj.02-0181fje
81. Yatsuda AP, Bakker N, Krijgsveld J, Knox DP, Heck AJR, de Vries E. Identification of secreted cysteine proteases from the parasitic nematode *Haemonchus contortus* detected by biotinylated inhibitors. *Infect Immun* (2006) 74:1989–93. doi:10.1128/IAI.74.3.1989-1993.2006
82. Bottazzi ME. The human hookworm vaccine: recent updates and prospects for success. *J Helminthol* (2015) 89:540–4. doi:10.1017/S0022149X15000206
83. Hotez PJ, Diemert D, Bacon KM, Beaumier C, Bethony JM, Bottazzi ME, et al. The human hookworm vaccine. *Vaccine* (2013) 31:B227–32. doi:10.1016/j.vaccine.2012.11.034
84. Seid CA, Curti E, Jones RM, Hudspeth E, Rezende W, Pollet J, et al. Expression, purification, and characterization of the *Necator americanus* aspartic protease-1 (Na-APR-1 (M74)) antigen, a component of the bivalent human hookworm vaccine. *Hum Vaccin Immunother* (2015) 11:1474–88. doi:10.1080/21645515.2015.1036207
85. Hotez PJ, Bethony JM, Diemert DJ, Pearson M, Loukas A. Developing vaccines to combat hookworm infection and intestinal schistosomiasis. *Nat Rev Microbiol* (2010) 8:814. doi:10.1038/nrmicro2438
86. Brown A, Girod N, Billett EE, Pritchard DI. *Necator americanus* (human hookworm) aspartyl proteinases and digestion of skin macromolecules during skin penetration. *Am J Trop Med Hyg* (1999) 60:840–7. doi:10.4269/ajtmh.1999.60.840
87. Jolodar A, Fischer P, Büttner DW, Miller DJ, Schmetz C, Brattig NW. Onchocerca volvulus: expression and immunolocalization of a nematode cathepsin D-like lysosomal aspartic protease. *Exp Parasitol* (2004) 107:145–56. doi:10.1016/j.exppara.2004.06.006
88. Mello LV, O'Meara H, Rigden DJ, Paterson S. Identification of novel aspartic proteases from *Strongyloides ratti* and characterisation of their evolutionary relationships, stage-specific expression and molecular structure. *BMC Genomics* (2009) 10:611. doi:10.1186/1471-2164-10-611
89. Wang T, Van Steendam K, Dhaenens M, Vlaminck J, Deforce D, Jex AR, et al. Proteomic analysis of the excretory-secretory products from larval stages of *Ascaris suum* reveals high abundance of glycosyl hydrolases. *PLoS Negl Trop Dis* (2013) 7:e2467. doi:10.1371/journal.pntd.0002467
90. Starr CR, Engleberg NC. Role of hyaluronidase in subcutaneous spread and growth of group A *Streptococcus*. *Infect Immun* (2006) 74:40–8. doi:10.1128/IAI.74.1.40-48.2006
91. Rhoads ML, Fetterer RH, Urban JF. Release of hyaluronidase during in vitro development of *Ascaris suum* from the third to fourth larval stage. *Parasitol Res* (2001) 87:693–7. doi:10.1007/s004360100410
92. Hotez PJ, Narasimhan S, Haggerty J, Milstone L, Bhopale V, Schad GA, et al. Hyaluronidase from infective *Ancylostoma* hookworm larvae and its possible function as a virulence factor in tissue invasion and in cutaneous larva migrans. *Infect Immun* (1992) 60:1018–23.
93. Bower MA, Constant SL, Mendez S. *Necator americanus*: the Na-ASP-2 protein secreted by the infective larvae induces neutrophil recruitment in vivo and in vitro. *Exp Parasitol* (2008) 118:569–75. doi:10.1016/j.exppara.2007.11.014
94. Murray J, Gregory WF, Gomez-Escobar N, Atmadja AK, Maizels RM. Expression and immune recognition of *Brugia malayi* VAL-1, a homologue of vespid venom allergens and *Ancylostoma* secreted proteins. *Mol Biochem Parasitol* (2001) 118:89–96. doi:10.1016/S0166-6851(01)00374-7
95. Ballouz S, Verleyen W, Gillis J. Guidance for RNA-seq co-expression network construction and analysis: safety in numbers. *Bioinformatics* (2015) 31:2123–30. doi:10.1093/bioinformatics/btv118
96. van Dam S, Võsa U, van der Graaf A, Franke L, de Magalhães JP. Gene co-expression analysis for functional classification and gene-disease predictions. *Brief Bioinform* (2017) 19(4):575–92. doi:10.1093/bib/bbw139
97. Beswick EJ, Reyes VE. Macrophage migration inhibitory factor and interleukin-8 produced by gastric epithelial cells during *Helicobacter pylori* exposure induce expression and activation of the epidermal growth factor receptor. *Infect Immun* (2008) 76:3233–40. doi:10.1128/IAI.01534-07

Conflict of Interest Statement: The authors declare that the research was conducted in the absence of any commercial or financial relationships that could be construed as a potential conflict of interest.

frontiers in Microbiology

ORIGINAL RESEARCH
published: 04 December 2018
doi: 10.3389/fmicb.2018.02965

Protective Efficacy Against Acute and Chronic *Toxoplasma gondii* Infection Induced by Immunization With the DNA Vaccine TgDOC2C

Nian-Zhang Zhang[1], Qi Gao[1,2], Meng Wang[1], Jun-Ling Hou[1], Fu-Kai Zhang[1], Ling-Ying Hu[3] and Xing-Quan Zhu[1,4]**

[1] State Key Laboratory of Veterinary Etiological Biology, Key Laboratory of Veterinary Parasitology of Gansu Province, Lanzhou Veterinary Research Institute, Chinese Academy of Agricultural Sciences, Lanzhou, China, [2] Hunan Entry-Exit Inspection and Quarantine Bureau, Changsha, China, [3] Fujian Yongcheng Agricultural and Animal Husbandry Sci-Tech Group, Fuzhou, China, [4] Jiangsu Co-innovation Center for the Prevention and Control of Important Animal Infectious Diseases and Zoonoses, College of Veterinary Medicine, Yangzhou University, Yangzhou, China

OPEN ACCESS

Edited by:
Wenbin Tuo, Beltsville Agricultural Research Center, Agricultural Research Service (USDA), United States

Reviewed by:
Sunil Joshi, University of Miami, United States
Rui Fang, Huazhong Agricultural University, China

***Correspondence:**
Nian-Zhang Zhang
nianzhang919@163.com
Xing-Quan Zhu
xingquanzhu1@hotmail.com

Specialty section:
This article was submitted to Microbial Immunology, a section of the journal Frontiers in Microbiology

Received: *20 April 2018*
Accepted: *18 November 2018*
Published: *04 December 2018*

Citation:
Zhang N-Z, Gao Q, Wang M, Hou J-L, Zhang F-K, Hu L-Y and Zhu X-Q (2018) Protective Efficacy Against Acute and Chronic Toxoplasma gondii Infection Induced by Immunization With the DNA Vaccine TgDOC2C. Front. Microbiol. 9:2965. doi: 10.3389/fmicb.2018.02965

Toxoplasma gondii is a ubiquitous intracellular apicomplexan parasite that can cause zoonotic toxoplasmosis. Effective vaccines against *T. gondii* infection are necessary to prevent and control the spread of toxoplasmosis. The present study analyzed the B-linear epitopes of *T. gondii* DOC2 (TgDOC2) protein and then cloned the C-terminus of the TgDOC2 gene (TgDOC2C) to construct the pVAX-TgDOC2C eukaryotic vector. After intramuscular injection of pVAX-TgDOC2C, immune responses were monitored. Two weeks after the last immunization, the protective effects of pVAX-TgDOC2C against acute and chronic toxoplasmosis were evaluated by challenges with *T. gondii* RH tachyzoites (genotype I) and PRU cysts (genotype II). The DNA vaccine elicited strong humoral and cellular immune responses with high levels of IgG antibody, IL-2 and IFN-γ production compared to those of the controls. The percentage of CD4+ and CD8+ T cells in mice immunized with pVAX-TgDOC2C was significantly increased compared to that of mice injected with empty pVAX I or PBS. After acute infection with 10^3 lethal tachyzoites, mice immunized with pVAX-TgDOC2C survived longer (12.5 days) than mice treated with pVAX I (8 days) and PBS (7.5 days). Mice immunized with pVAX-TgDOC2C had significantly less brain cysts (1600.83 ± 284.61) compared to mice immunized with pVAX I (3016.67 ± 153.84) or PBS (3100 ± 246.98). Together, these results demonstrated that TgDOC2C confers protective immunity against *T. gondii* infection and may be a promising candidate antigen for further development of an effective multicomponent vaccine for veterinary use against toxoplasmosis in livestock animals.

Keywords: *Toxoplasma gondii*, toxoplasmosis, TgDOC2C, DNA vaccine, protective efficacy

INTRODUCTION

Infections by the intracellular parasite *Toxoplasma gondii* are common in all warm-blooded animals, including birds and humans (Dubey, 2008; Innes, 2010; Zhou et al., 2011). If women acquire primary infection with the parasite during gestation, the fetus is at high risk of developing congenital toxoplasmosis that would manifest clinical signs of chorioretinitis, cerebral

calcifications, mental retardation and hydrocephalus (Gao et al., 2012; Robert-Gangneux and Dardé, 2012; Aleixo et al., 2016). For immunocompromised individuals, reactivation of latent *Toxoplasma* infection may lead to encephalitis, ophthalmopathy and focal neurological lesions or even fatal damage (Holland, 1989; Pereira-Chioccola et al., 2009; Robert-Gangneux and Dardé, 2012; Wang et al., 2017). Toxoplasmosis in animals can cause heavy economic losses, especially in sheep and goats, arising from miscarriage, stillbirth, and neonatal death (Innes et al., 2009; Gebremedhin et al., 2014). Of more serious concern is the fact that the infected meat-producing animal is considered an important source of infection for humans (Dubey, 2009; Belluco et al., 2017; Pan et al., 2017).

Development of a safe and effective vaccine against *T. gondii* is an attractive option to prevent tissue cyst formation that can improve food safety in meat production (Zhang et al., 2013; Hiszczyńska-Sawicka et al., 2014). A DNA vaccine has elicited strong Th1-bias humoral and cellular immune responses in a mouse model to prolong the survival time after *Toxoplasma* acute infection and reduce brain cyst formation after chronic infection, which is considered a promising strategy to prevent toxoplasmosis (Gurunathan et al., 2000; Zhang et al., 2015a; Li and Zhou, 2018). Because no evaluated antigen can completely protect hosts against *T. gondii* infection, the identification of new potential vaccine candidates is a crucial step toward the development of an effective vaccine against *T. gondii* infection (Zhang et al., 2013; Li and Zhou, 2018).

Ca^{2+} is a crucial secondary messenger in the regulation of intracellular parasite attachment, invasion and egress of eukaryotic cells (Nagamune et al., 2008; Billker et al., 2009; Stewart et al., 2017). Calcium-dependent protein kinases (CDPKs) have been shown to participate in the downstream calcium-related signaling cascades as signaling mediators involved in distinct developmental processes of *T. gondii* (Billker et al., 2009; McCoy et al., 2012). TgDOC2 is another identified calcium signaling mediator that constitutes a second level of the pathway, operating downstream of CDPKs (Farrell et al., 2012; Jean et al., 2014). The DOC2 protein facilitates the membrane fusion of *T. gondii* secretory vesicles with the plasma membrane during the process of egress through regulating the Ca^{2+} signal pathway (Farrell et al., 2012). A previous study has shown that a TgDOC2-deficient strain has a disability in microneme secretion (Farrell et al., 2012). Together, these findings suggested that TgDOC2 may be a novel drug target or a vaccine candidate (Lourido and Moreno, 2015). However, there are no reports about the immunogenicity of TgDOC2 and its potential application as a vaccine candidate.

Thus, the aims of this study were to predict the potential epitopes of TgDOC2 and to evaluate its immunogenicity in the Kunming mouse model through a DNA strategy. Furthermore, the present study aimed to analyze the ability of the DNA vaccine against the infection with the highly virulent RH strain and the less virulent PRU strain.

MATERIALS AND METHODS

Animals

Specific pathogen-free (SPF) female Kunming mice aged 6–8 weeks were obtained from the Center of Laboratory Animals, Lanzhou Institute of Biological Products (Lanzhou, China). The present study was approved by the Animal Administration and Ethics Committee of Lanzhou Veterinary Research Institute, Chinese Academy of Agricultural Sciences (Approval No. LVRIAEC2012-011). All mice used for the experiments were raised and handled in strict accordance with the Good Animal Practice requirements of the Animal Ethics Procedures and Guidelines of the People's Republic of China.

Parasites

Tachyzoites of the *T. gondii* RH strain (genotype I) were maintained in the State Key Laboratory of Veterinary Etiological Biology through serial passage in Kunming mice *via* intraperitoneal injection. Tachyzoites were harvested from the peritoneal exudates. The obtained tachyzoites were also used for the preparation of *Toxoplasma* lysate antigen (TLA). The PRU cysts (genotype II) were maintained monthly through oral passage in Kunming mice, and they were purified from infected brains.

Amplification and Bioinformatics Analysis of the TgDOC2 Gene

Total RNA of *T. gondii* was extracted from the tachyzoites of the RH strain using the Trizol reagent (Invitrogen) according to the manufacturer's protocol. The TgDOC2 gene was amplified by reverse transcription-polymerase chain reaction (RT-PCR) using the following pair of primers: C2F (5′-ATGATGAAACTAAAGGAAATGG-3′) and C2R (5′-TCAGGTGCGCCCAGCCAGATCCAGTTG-3′). The PCR product was sequenced by Sangon Biotech Co., Ltd. (China). The potential epitopes of TgDOC2 were predicted using DNAStar 8.0 (DNAStar, United States) software with the Jameson-Wolf index.

Construction of Recombinant Plasmids

The C-terminus of the TgDOC2 gene (TgDOC2C) was amplified by PCR from the TgDOC2 gene using a pair of primers, namely, C2CF (5′-CGGGGTACCACGGAGAGAGAACGGAGAC-3′) and C2CR (5′-CCGGAATTCTCAGGTGCGCCCAGCCAGATCCAGT-3′), in which *Kpn* I and *Eco*R I restriction sites were introduced and underlined. PCR products were ligated into the pVAX I eukaryotic vector (Invitrogen, United States) through *Kpn* I/*Eco*R I sites to construct the recombinant pVAX-TgDOC2C plasmid. The concentration of extracted recombinant plasmids was determined by spectrophotometry at OD260 and OD280. The pVAX-TgDOC2C vector was diluted in sterile phosphate buffered saline (PBS) at a concentration of 1 μg/μl.

Expression of pVAX-TgDOC2C *in vitro*

The pVAX-TgDOC2C recombinant plasmid was transfected into HEK293 cells using Lipofectamine™ 2000 reagent

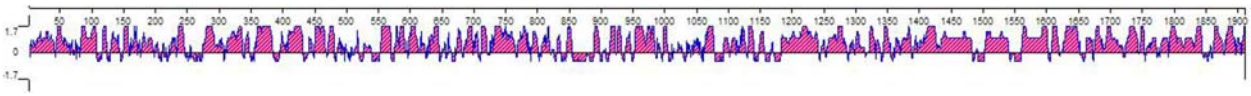

FIGURE 1 | Analysis of the antigenic index of TgDOC2 protein by DNAStar 8.0 software with the Jameson-Wolf index. Linear B-cell epitopes were predicted to widely distribute in the whole TgDOC2 protein but were mainly clustered in the C-terminal.

(Invitrogen, United States) following the manufacturer's instructions. Forty-eight hours posttransfection, the expression of pVAX-TgDOC2C *in vitro* was assayed by indirect immunofluorescence assay (IFA). In brief, pVAX-TgDOC2C-transfected cells were fixed with absolute acetone and washed with PBSTr (0.1% Triton-X-100 in PBS). Cells were then incubated with goat anti-*T. gondii* tachyzoites polyclonal antibody (in PBSTr at 1:50) for 1 h. After washing with PBSTr, cells were stained by fluorescein isothiocyanate (FITC)-labeled rabbit anti-goat IgG antibody (1:2000, Sigma, United States) for 1 h. HEK293 cells transfected with the empty pVAX I vector were treated as the negative control.

The expression of pVAX-TgDOC2C in HEK293 cells was detected by Western blot analysis. Briefly, transfected HEK293 cells (approximately 10^6) were lysed by freezing and thawing five times, and the lysates were then subjected to SDS-PAGE. After electrotransfer, the nitrocellulose (NC) membrane (Pall, United States) was incubated with 5% bovine serum albumin (BSA) in PBST (PBS with 0.05% Tween-20) at room temperature (RT) for 1 h to block the non-specific binding sites. The membrane was washed 3 times with PBST and then was cultured with pVAX-TgDOC2C-vaccinated mouse sera (diluted in 1:500; collected at 2 weeks after the third immunization) at RT for 1 h. After washing 3 times with PBST, the membrane was incubated with goat anti-mouse IgG-HRP antibody (diluted at 1:3000, Sigma, United States) for 1 h at RT. The specific band was visualized with Clarity™ Western ECL Blotting Substrates (Bio-Rad, United States) according to the manufacturer's protocol. Mouse sera from PBS-treated mice were used as the negative control.

Immunization and Challenge

Sixty-six female Kunming mice were randomly divided equally into three groups. Mice were intramuscularly immunized with 100 μl of pVAX-TgDOC2C and boosted with a 2-week interval. Mice treated with pVAX I vector alone or PBS served as controls. Blood samples were collected prior to each vaccination from the mouse tail vein and were centrifuged at 3,000 × *g* for 10 min to separate blood samples. Preimmune serum samples were used as negative controls.

For evaluation of the protective effect against acute *T. gondii* infection, 10 mice from each group were intraperitoneally infected with 10^3 tachyzoites of the virulent RH strain 2 weeks after the final immunization. The challenged mice were monitored daily until total death. In addition, another six mice from each group were orally infected with 10 brain cysts of the PRU strain as the chronic infection model. Five weeks after the challenge, the numbers of brain cysts were determined under microscopic examination.

IgG Antibody Assay

The levels of IgG antibodies in sera from mice in each group were determined by ELISA using the SBA Clonotyping System-HRP Kit (Southern Biotech Co., Ltd., Birmingham, AL, United States) following the manufacturer's protocol. In brief, 96-well microtiter plates were coated with 5 μg/ml TLA at 4°C overnight. After washing with PBST, plates were then treated with 1% skim milk in PBST for 1 h while shaking at RT to block non-specific binding sites. Serum (100 μl; 1:10 diluted with PBS) from each mouse was pipetted into a well and incubated for 1 h at 37°C. Each well was then incubated with 100 μl of anti-mouse IgG (HRP, 1:250 dilution, Sigma, United States) for 1 h at 37°C. Peroxidase activity was revealed by incubating with 100 μl of substrate solution (pH 4.0; 1.5% ABST, 0.03% H_2O_2 and 1.05% citrate substrate buffer). The reaction was stopped after the addition of 1 M H_2SO_4, and the absorbance was measured at 450 nm. All samples were performed in triplicate.

Purified Splenocyte Collection

Two weeks after the last immunization, six mice per group were sacrificed to aseptically harvest the spleen. Splenocytes were obtained by filtering spleens through a nylon membrane and were purified using erythrocyte lysis buffer (Solarbio, Shanghai, China). Harvested splenocytes were resuspended in DMEM medium supplemented with penicillin/streptomycin (p/s) and 10% fetal bovine serum (FBS).

Lymphocyte Proliferation Assay by MTS Assay

The density of purified splenocytes was adjusted into 2×10^5/well in 96-well microtiter plates. Cells were cultured in DMEM medium supplemented with 10% FBS and 100 U/ml p/s. Splenocytes were then incubated with 10 μg/ml TLA or 5 μg/ml concanavalin A (ConA; Sigma, St. Louis, MO, United States) at 37°C in 5% CO_2. Splenocytes cultured with medium alone (M) served as the blank control. The levels of proliferative responses *in vitro* were estimated using the MTS assay (Promega, Madison, WI, United States) after 92 h. The stimulation index (SI) was calculated using the following equation: OD_{570TLA}/OD_{570M} or $OD_{570ConA}/OD_{570M}$.

Flow Cytometry

CD4+ and CD8+ T lymphocytes were examined according to previous methods (Li et al., 2014). Splenocytes were first adjusted into a concentration of 10^6 cells/ml in PBS containing 2% FBS. Staining with phycoerythrin (PE)-labeled anti-CD3 (eBioscience, San Diego, CA, United States), allophycocyanin (APC)-labeled anti-CD4 (eBioscience) and fluorescein isothiocyanate (FITC)-labeled anti-CD8 (eBioscience) was performed at 4°C for 30 min in the dark. After rinsing twice with PBS, cells were fixed in FACScan solution (1% BSA and 0.1% sodium azide diluted in PBS) and 2% paraformaldehyde. The fluorescence profiles of stained samples were analyzed using a FACScan flow cytometer (BD Biosciences) using SYSTEM II software (Coulter).

Cytokine Assays

Purified splenocytes from mice in each group were stimulated with TLA (10 μg/ml) in 96-well flat-bottom microtiter plates. Supernatants in each well were harvested to determinate IL-4 and IL-2 levels at 24 h and IFN-γ levels at 96 h using ELISA kits according to the manufacturer's instructions (BioLegend, United States). Briefly, the supernatants and assay buffer A were pipetted into the same well, and plates were then incubated while shaking at 200 rpm for 2 h at RT. After washing the plates four times with 1× wash buffer, 100 μl of IL-4, IL-2 or IFN-γ detection solution was added into each well and incubated at RT. After 1 h, the contents of the plates were discarded, and the avidin-HRP solution was added after washing four times and incubated while shaking for 30 min at RT. The substrate solution E was then added and incubated for 20 min in the dark. To stop the reaction, 100 μl of stop solution was added. Absorbance was read by a Model 680 microplate reader (Bio-Rad, Hercules, CA, United States) at 450 nm. Sensitivity limits for the assays were 50 pg/ml for IL-2, 20 pg/ml for IFN-γ and 10 pg/ml for IL-4. Three independent experiments were performed for analysis of the data.

Statistical Analysis

The differences in IgG levels, CD4+ T cells and CD8+ T cells as well as the reduction in brain cysts were calculated by one-way ANOVA among at least three groups and by the *t*-test between two groups. The difference in survival time was calculated by the *Chi*-square test. All figures regarding the statistical analysis were prepared by GraphPad Prism version 5.0 (San Diego, CA, United States). A value of $P < 0.05$ was considered significant.

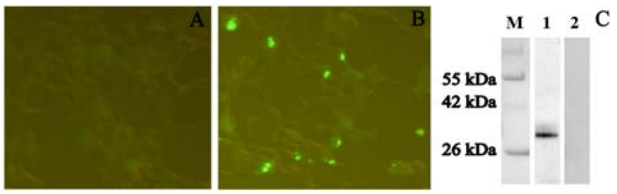

FIGURE 2 | Analysis of pVAX-TgDOC2C expression *in vitro*. Expression of the pVAX I empty vector **(A)** and pVAX-TgDOC2C **(B)** in HEK293 cells was detected by indirect immunofluorescence (IFA). **(C)** The pVAX-TgDOC2C product in HEK293 cell lysate was detected by Western blot analysis. M: protein molecular weight; lane 1: membrane incubated with mouse sera from the pVAX-TgDOC2C-vaccinated group at 2 weeks after the last immunization; lane 2: membrane incubated with mouse sera from the PBS group.

RESULTS

Analysis of the Amplified TgDOC2 Gene

The amplified TgDOC2 gene was identified through alignment with the corresponding sequence from the http://toxodb.org/ website. The cloned TgDOC2 gene showed 100% identity to the reference sequence (Gene ID: TGGT1_240910).

The potential B-linear epitopes of the TgDOC2 protein was predicted using DNAStar 8.0 software. The results showed that potential B-linear epitopes of the TgDOC2 protein were mainly gathered in the C-terminal end (**Figure 1**). Thus, the nucleotide positions distributed between 3550 (position at 1183 aa) and the end were selected for further amplification to construct the DNA vaccine.

Detection of pVAX-TgDOC2C Plasmid Expression in HEK293 Cells

The expression of pVAX-TgDOC2C *in vitro* was first examined by IFA. Green fluorescence was identified in HEK293 cells transfected with pVAX-TgDOC2C plasmids, but no fluorescence was observed in cells transfected with pVAX I alone (**Figures 2A,B**). These results indicated that pVAX-TgDOC2C was successfully expressed in HEK293 cells. As shown in **Figure 2C**, the specific band was detected in the membrane incubated with pVAX-TgDOC2C-vaccinated mouse sera but not in the membrane incubated with sera from the PBS-treated group. The size of the band was approximately 30 kDa, which was the expected size.

TABLE 1 | Splenocyte proliferative responses and the percentages of T cell subsets in immunized mice 2 weeks after the last immunization.

Groups	SI (Mean ± SD)		CD3 + CD4 + CD8 - (%)	CD3 + CD8 + CD4 - (%)
	TLA	ConA		
pVAX-TgDOC2C	1.51 ± 0.08***	1.80 ± 0.04*	13.33 ± 2.86***	8.45 ± 1.27*
pVAX I	1.32 ± 0.04	1.44 ± 0.09	3.28 ± 1.18	5.13 ± 1.84
PBS	1.30 ± 0.05	1.56 ± 0.1	3.27 ± 0.94	5.61 ± 1.11

*SI, stimulation index; TLA, Toxoplasma lysate antigen; ConA, concanavalin A. n = 6, *P < 0.05, **P < 0.001, ***P < 0.0001.*

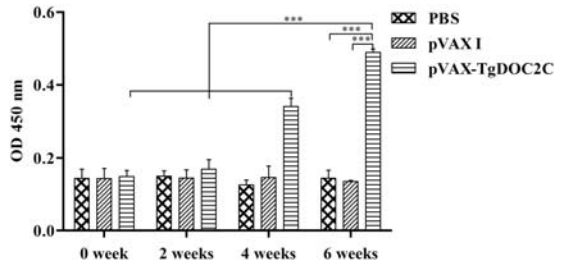

FIGURE 3 | Determination of IgG antibodies in the sera of Kunming mice at 0, 2, 4, and 6 weeks. Each bar represents the mean OD (±SE, $n = 3$). ***$P < 0.0001$.

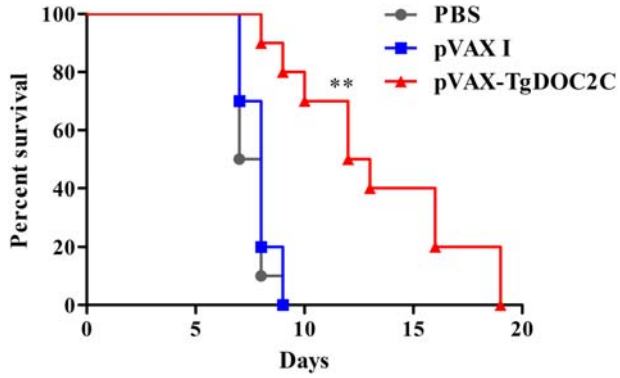

FIGURE 4 | Survival rate of mice immunized with pVAX-TgDOC2C, pVAX I and PBS followed by challenge with 10^3 tachyzoites 2 weeks after the last immunization. The mice immunized with pVAX-TgDOC2C died from day 9 to 19, which resulted in an increased survival time (12.5 days) compared to mice in the pVAX I (8 days) and PBS (7.5 days) groups ($n = 10$). **$P < 0.001$.

Humoral Responses Induced by DNA Immunization of pVAX-TgDOC2C

The antibody levels in the sera of mice injected with pVAX-TgDOC2C increased with successive immunization and were reached the highest levels at 2 weeks after the last vaccination [$F(3,8) = 66.21$, $P < 0.0001$]. However, no differences were detected in serum samples of mice from pVAX I [$F(3,8) = 0.04$, $P = 0.99$] and PBS [$F(3,8) = 0.27$, $P = 0.84$] groups following immunization. After the third immunization, a significantly higher level of IgG antibody was examined in the sera of mice inoculated with pVAX-TgDOC2C compared to those receiving pVAX I [$t(4) = 29.20$, $P < 0.0001$] and PBS [$t(4) = 10.78$, $P < 0.0001$] (**Figure 3**).

Analysis of Cellular Immune Response

As shown in **Table 1**, an enhanced proliferative response was detected in the splenocytes of mice immunized with pVAX-TgDOC2C after incubation with TLA [$F(2,15) = 23.95$, $P < 0.0001$] and ConA [$F(2,15) = 4.131$, $P = 0.04$] compared to those from the pVAX I and PBS groups.

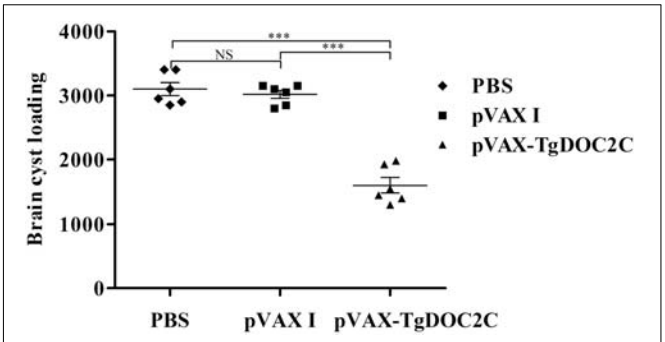

FIGURE 5 | Protection against chronic toxoplasmosis in mice injected with pVAX-TgDOC2C, pVAX I and PBS 2 weeks after the last immunization. Each bar represents the mean number of brain cysts (±SE, $n = 6$). ***$P < 0.0001$. NS, not significant.

Percentages of CD4+ and CD8+ T cells were determined in spleens of mice from each group by flow cytometry analysis. The CD3+ CD4+ T lymphocytes in mice injected with pVAX-TgDOC2C were significantly higher than those in mice from the pVAX I and PBS groups [$F(2,15) = 57.53$, $P < 0.0001$] (**Table 1**). The ratio of CD3+ CD8+ T cells in mice of the pVAX-TgDOC2C group was higher than that in controls [$F(2,15) = 9.3$, $P = 0.002$] (**Table 1**).

Cytokine Assays

Splenocytes from mice injected with pVAX-TgDOC2C had significantly higher levels of IFN-γ [$F(2,15) = 52.66$, $P < 0.0001$] and IL-2 [$F(2,15) = 15.87$, $P = 0.0002$] than those in mice in the pVAX I and PBS groups (**Table 2**). However, the level of IL-4 production was not significantly difference among the three groups ($P > 0.05$).

Protective Efficacy Elicited by pVAX-TgDOC2C Vaccination

To evaluate the protective activity of the pVAX-TgDOC2C recombinant plasmid against acute *T. gondii* infection, 10 mice in each group were intraperitoneally administered with 10^3 lethal tachyzoites 2 weeks after the last vaccination. The average survival time of mice inoculated with pVAX-TgDOC2C (12.5 days) was significantly longer than those injected with pVAX I (8 days) and PBS (7.5 days) ($P = 0.0004$) (**Figure 4**). Moreover, the

TABLE 2 | Cytokine production by splenocytes of immunized Kunming mice after stimulation by toxoplasma lysate antigen[a].

Groups	Cytokine production (pg/ml)		
	IFN-γ	IL-2	IL-4
pVAX-TgDOC2C	1584.8 ± 474.4***	178.03 ± 58.55**	< 10
pVAX I	172.21 ± 11.5	< 50	< 10
PBS	182.12 ± 24.03	< 50	< 10

[a]*Splenocytes from mice were harvested 2 weeks after the last immunization. n = 6, **P < 0.001, ***P < 0.0001.*

survival times of mice in the control groups were not significantly different ($P > 0.05$).

The protective effect of the pVAX-TgDOC2C vaccine against *T. gondii* chronic infection was assessed through examination of brain cyst number per mouse from each group 35 days after infection of 10 cysts of the PRU strain. As depicted in **Figure 5**, mice immunized with pVAX-TgDOC2C (1600.83 ± 284.61) had significantly decreased brain cyst loadings compared to those injected with pVAX I (3016.67 ± 153.84) [$t(10) = 10.72$, $P < 0.0001$] and PBS (3100 ± 246.98) [$t(10) = 9.75$, $P < 0.0001$]. Immunization of mice with pVAX-TgDOC2C resulted in a cyst reduction rate of 48.36% compared to that of PBS-injected mice.

DISCUSSION

The present study showed that a DNA vaccination encoding the TgDOC2C gene in a mouse model promoted humoral and cellular immune responses, which contributed to a prolonged survival time (12.5 days, $P = 0.0004$) during acute infection and a decrease in brain cysts (1600.83 ± 284.61, $P < 0.0001$) during chronic infection. Significant progress has been made in recent years in the investigation of immune effects of various *T. gondii* antigens, such as ASP3 (Zhao et al., 2017), GRA2 (Ching et al., 2016), ROM5 (Zhang et al., 2015b), ROP18 (Yuan et al., 2011), ROP1 (Hiszczyńska-Sawicka et al., 2011), MIC6 (Peng et al., 2009), and SAG1 (Couper et al., 2003), and most of these antigens provide partial protection against *T. gondii* infection. The present results first demonstrated the potentiality of TgDOC2C as a vaccine candidate against acute and chronic toxoplasmosis.

DOC2, a calcium-binding protein, acts on membrane fusion and spontaneous neurotransmission in a murine model (Pinheiro et al., 2016; Ramirez et al., 2017). In intracellular parasites, the DOC2 protein impairs microneme secretion and is an essential component for exocytosis (Farrell et al., 2012; Jean et al., 2014). In the present study, the TgDOC2 protein was used to predict potential B-linear epitopes using DNASTAR software. The C-terminal end of the protein had more epitopes, suggesting that this sequence had potential to become an effective DNA vaccine against *T. gondii*. Analyses of epitopes, functions, or gene structures by emerging bioinformatics programs are widely used to design new vaccine candidates using an experimental methodology that discards non-functional sequences (Bai et al., 2012; Bastos et al., 2016; Zhou et al., 2016; Zhou and Wang, 2017). As expected, TgDOC2C is an effective vaccine candidate to improve the protective immunity against *T. gondii* challenges. Further study should design an epitope-based vaccine using calcium-dependent antigens in view of the ability of several TgCDPKs to protect mice from toxoplasmosis (Zhang et al., 2015a).

T cell-mediated immune defense is relevant to the control of toxoplasmosis (El Bissati et al., 2017), and CD8+ and CD4+ lymphocytes play a critical role during the adaptive immune response against *T. gondii* infection and reactivation (Gazzinelli et al., 1992). CD4+ T cells perform important roles in adaptive immune responses and limit intracellular pathogens in the early stage of infection (Kemball et al., 2007), while CD8+ T cells participate in the resistance in the later stage of intracellular infection through cytolytic activity (Ely et al., 1999). Enhanced CD8+ and CD4+ T cells contribute to the increasing protective immunity against *T. gondii* acute and chronic infection after DNA immunization with TgSOD (Liu et al., 2017), TgROM5 (Zhang et al., 2015b), TgeIF4A (Chen et al., 2013a) and other cocktail vaccines (Cao et al., 2015; Zhang et al., 2018). In the present study, the increased CD8+ and CD4+ T cells in mice immunized with TgDOC2C prolonged the survival time against acute infection and decreased brain cysts against chronic infection.

During the course of CD8+ and CD4+ T cell proliferation, polarization and activation, IFN-γ and IL-2 participate in certain stages and drive the immune response into Th1 type (Suzuki et al., 2011). IFN-γ is not only crucial to restrict tachyzoite growth in the early stage of infection but also important to inhibit the reactivation of dormant *T. gondii* cysts (MacMicking, 2012). Several previous studies have shown the correlation between the Th1 type immune response, characterized by the increase in IFN-γ and IL-2 production, and the enhanced resistance against toxoplasmosis in mice (Li et al., 2014; Zhao et al., 2017; Zheng et al., 2017). In the present study, significantly higher levels of IFN-γ and IL-2 production were detected in mice immunized with pVAX-TgDOC2C compared to those that received empty pVAX I and PBS, which conferred the extent of survival time after acute infection and the decrease in brain cysts after chronic infection. However, IL-4, which is associated with the Th2 immune response, was not significantly changed among the three groups. A promoted protective immunity against *T. gondii* infection along with a low secretion of IL-4 production has also been indicated in mice immunized with TgROP8 (Parthasarathy et al., 2013) and TgIF2α (Chen et al., 2013b).

The IgG antibodies against toxoplasmosis control *T. gondii* infection through inhibiting *T. gondii* duplication, facilitating the parasite attachment to immune cells and promoting macrophages to kill intracellular parasites *via* the process of antibody-dependent cell-mediated cytotoxicity (ADCC). In the present study, the increasing humoral immune response was associated with the enhanced protection against *T. gondii* infection, which was similar to the results from DNA immunization with TgROM5, TgeIF4A, TgROP18, and other antigens (Peng et al., 2009; Yuan et al., 2011; Cui et al., 2012; Chen et al., 2013a; Zhang et al., 2015b).

CONCLUSION

The present study demonstrated that immunization of mice with pVAX-TgDOC2C induces a strong humoral and cellular Th1-type immune response, resulting in reduced brain cyst numbers and the extent of survival time. The vaccine potential of pVAX-TgDOC2C indicates the possibility of

inclusion in further development of a multicomponent or an epitope-based vaccine against toxoplasmosis in food-producing animals.

AVAILABILITY OF DATA AND MATERIAL

The datasets supporting the conclusions of this article are included within the article.

AUTHOR CONTRIBUTIONS

X-QZ and N-ZZ conceived and designed the experiments. QG, MW, F-KZ, and L-YH performed the experiments. N-ZZ and J-LH analyzed the data and wrote the paper. N-ZZ, QG, and X-QZ critically revised the manuscript. All authors read and approved the final version of the manuscript.

FUNDING

Project support was provided by the National Key Research and Development Program of China (Grant No. 2017YFD0501304), the National Natural Science Foundation of China (Grant No. 31602045), the Elite Program of Chinese Academy of Agricultural Sciences, and the Agricultural Science and Technology Innovation Program (ASTIP) (Grant No. CAAS-ASTIP-2016-LVRI-03).

REFERENCES

Aleixo, A. L., Curi, A. L., Benchimol, E. I., and Amendoeira, M. R. (2016). *Toxoplasmic retinochoroiditis*: clinical characteristics and visual outcome in a prospective study. *PLoS Negl. Trop. Dis.* 10:e0004685. doi: 10.1371/journal.pntd.0004685

Bai, Y., He, S. Y., Zhao, G. H., Chen, L., Shi, N., Zhou, H., et al. (2012). *Toxoplasma gondii*: bioinformatics analysis, cloning and expression of a novel protein TgIMP1. *Exp. Parasitol.* 132, 458–464. doi: 10.1016/j.exppara.2012.09.015

Bastos, L. M., Macêdo, A. G. Jr., Silva, M. V., Santiago, F. M., Ramos, E. L., Santos, F. A., et al. (2016). *Toxoplasma gondii*-derived synthetic peptides containing B- and T-cell epitopes from GRA2 protein are able to enhance mice survival in a model of experimental toxoplasmosis. *Front. Cell Infect. Microbiol.* 6:59. doi: 10.3389/fcimb.2016.00059

Belluco, S., Simonato, G., Mancin, M., Pietrobelli, M., and Ricci, A. (2017). *Toxoplasma gondii* infection and food consumption: a systematic review and meta-analysis of case-controlled studies. *Crit. Rev. Food Sci. Nutr.* 11, 1–12. doi: 10.1080/10408398.2017.1352563

Billker, O., Lourido, S., and Sibley, L. D. (2009). Calcium-dependent signaling and kinases in apicomplexan parasites. *Cell Host Microbe* 5, 612–622. doi: 10.1016/j.chom.2009.05.017

Cao, A., Liu, Y., Wang, J., Li, X., Wang, S., Zhao, Q., et al. (2015). *Toxoplasma gondii*: vaccination with a DNA vaccine encoding T- and B-cell epitopes of SAG1, GRA2, GRA7 and ROP16 elicits protection against acute toxoplasmosis in mice. *Vaccine* 33, 6757–6762. doi: 10.1016/j.vaccine.2015.10.077

Chen, J., Huang, S. Y., Li, Z. Y., Yuan, Z. G., Zhou, D. H., Petersen, E., et al. (2013a). Protective immunity induced by a DNA vaccine expressing eIF4A of *Toxoplasma gondii* against acute toxoplasmosis in mice. *Vaccine* 31, 1734–1739. doi: 10.1016/j.vaccine.2013.01.027

Chen, J., Huang, S. Y., Zhou, D. H., Li, Z. Y., Petersen, E., Song, H. Q., et al. (2013b). DNA immunization with eukaryotic initiation factor-2α of *Toxoplasma gondii* induces protective immunity against acute and chronic toxoplasmosis in mice. *Vaccine* 31, 6225–6231. doi: 10.1016/j.vaccine.2013.10.034

Ching, X. T., Fong, M. Y., and Lau, Y. L. (2016). Evaluation of immunoprotection conferred by the subunit vaccines of GRA2 and GRA5 against acute toxoplasmosis in BALB/c mice. *Front. Microbiol.* 7:609. doi: 10.3389/fmicb.2016.00609

Couper, K. N., Nielsen, H. V., Petersen, E., Roberts, F., Roberts, C. W., and Alexander, J. (2003). DNA vaccination with the immunodominant tachyzoite surface antigen (SAG-1) protects against adult acquired *Toxoplasma gondii* infection but does not prevent maternofoetal transmission. *Vaccine* 21, 2813–2820. doi: 10.1016/S0264-410X(03)00163-4

Cui, X., Lei, T., Yang, D., Hao, P., Li, B., and Liu, Q. (2012). *Toxoplasma gondii* immune mapped protein-1 (TgIMP1) is a novel vaccine candidate against toxoplasmosis. *Vaccine* 30, 2282–2287. doi: 10.1016/j.vaccine.2012.01.073

Dubey, J. P. (2008). The history of *Toxoplasma gondii*-the first 100 years. *J. Eukaryot. Microbiol.* 55, 467–475. doi: 10.1111/j.1550-7408.2008.00345.x

Dubey, J. P. (2009). Toxoplasmosis in pigs–the last 20 years. *Vet. Parasitol.* 164, 89–103. doi: 10.1016/j.vetpar.2009.05.018

El Bissati, K., Zhou, Y., Paulillo, S. M., Raman, S. K., Karch, C. P., Roberts, C. W., et al. (2017). Protein nanovaccine confers robust immunity against *Toxoplasma*. *NPJ Vaccines* 2:24. doi: 10.1038/s41541-017-0024-6

Ely, K. H., Kasper, L. H., and Khan, I. A. (1999). Augmentation of the CD8+ T cell response by IFN-gamma in IL-12-deficient mice during *Toxoplasma gondii* infection. *J. Immunol.* 162, 5449–5454.

Farrell, A., Thirugnanam, S., Lorestani, A., Dvorin, J. D., Eidell, K. P., Ferguson, D. J., et al. (2012). A DOC2 protein identified by mutational profiling is essential for apicomplexan parasite exocytosis. *Science* 335, 218–221. doi: 10.1126/science.1210829

Gao, X. J., Zhao, Z. J., He, Z. H., Wang, T., Yang, T. B., Chen, X. G., et al. (2012). *Toxoplasma gondii* infection in pregnant women in China. *Parasitology* 139, 139–147. doi: 10.1017/S0031182011001880

Gazzinelli, R., Xu, Y., Hieny, S., Cheever, A., and Sher, A. (1992). Simultaneous depletion of CD4+ and CD8+ T lymphocytes is required to reactivate chronic infection with *Toxoplasma gondii*. *J. Immunol.* 149, 175–180.

Gebremedhin, E. Z., Abdurahaman, M., Hadush, T., and Tessema, T. S. (2014). Seroprevalence and risk factors of *Toxoplasma gondii* infection in sheep and goats slaughtered for human consumption in Central Ethiopia. *BMC Res. Notes* 7:696. doi: 10.1186/1756-0500-7-696

Gurunathan, S., Wu, C. Y., Freidag, B. L., and Seder, R. A. (2000). DNA vaccines: a key for inducing long-term cellular immunity. *Curr. Opin. Immunol.* 12, 442–447. doi: 10.1016/S0952-7915(00)00118-7

Hiszczyńska-Sawicka, E., Gatkowska, J. M., Grzybowski, M. M., and Długońska, H. (2014). Veterinary vaccines against toxoplasmosis. *Parasitology* 141, 1365–1378. doi: 10.1017/S0031182014000481

Hiszczyńska-Sawicka, E., Li, H., Xu, J. B., Holec-Gąsior, L., Kur, J., Sedcole, R., et al. (2011). Modulation of immune response to *Toxoplasma gondii* in sheep by immunization with a DNA vaccine encoding ROP1 antigen as a fusion protein with ovine CD154. *Vet. Parasitol.* 183, 72–78. doi: 10.1016/j.vetpar.2011.06.010

Holland, G. N. (1989). Ocular toxoplasmosis in the immunocompromised host. *Int. Ophthalmol.* 13, 399–402. doi: 10.1007/BF02306488

Innes, E. A. (2010). A brief history and overview of *Toxoplasma gondii*. *Zoonoses Public Health* 57, 1–7. doi: 10.1111/j.1863-2378.2009.01276.x

Innes, E. A., Bartley, P. M., Buxton, D., and Katzer, F. (2009). Ovine toxoplasmosis. *Parasitology* 136, 1887–1894. doi: 10.1017/S0031182009991636

Jean, S., Zapata-Jenks, M. A., Farley, J. M., Tracy, E., and Mayer, D. C. (2014). *Plasmodium falciparum* double C2 domain protein, PfDOC2, binds to calcium when associated with membranes. *Exp. Parasitol.* 144, 91–95. doi: 10.1016/j.exppara.2014.06.015

Kemball, C. C., Pack, C. D., Guay, H. M., Li, Z. N., Steinhauer, D. A., Szomolanyi-Tsuda, E., et al. (2007). The antiviral CD8+ T cell response is differentially dependent on CD4+ T cell help over the course of persistent infection. *J. Immunol.* 179, 1113–1121. doi: 10.4049/jimmunol.179.2.1113

Li, Y., and Zhou, H. (2018). Moving towards improved vaccines for *Toxoplasma gondii*. *Expert Opin. Biol. Ther.* 18, 273–280. doi: 10.1080/14712598.2018.1413086

Li, Z. Y., Chen, J., Petersen, E., Zhou, D. H., Huang, S. Y., Song, H. Q., et al. (2014). Synergy of mIL-21 and mIL-15 in enhancing DNA vaccine efficacy against acute and chronic *Toxoplasma gondii* infection in mice. *Vaccine* 32, 3058–3065. doi: 10.1016/j.vaccine.2014.03.042

Liu, Y., Cao, A., Li, Y., Li, X., Cong, H., He, S., et al. (2017). Immunization with a DNA vaccine encoding *Toxoplasma gondii* Superoxide dismutase (TgSOD) induces partial immune protection against acute toxoplasmosis in BALB/c mice. *BMC Infect. Dis.* 17:403. doi: 10.1186/s12879-017-2507-5

Lourido, S., and Moreno, S. N. (2015). The calcium signaling toolkit of the *Apicomplexan parasites Toxoplasma gondii* and Plasmodium spp. *Cell Calcium* 57, 186–193. doi: 10.1016/j.ceca.2014.12.010

MacMicking, J. D. (2012). Interferon-inducible effector mechanisms in cell-autonomous immunity. *Nat. Rev. Immunol.* 12, 367–382. doi: 10.1038/nri3210

McCoy, J. M., Whitehead, L., van Dooren, G. G., and Tonkin, C. J. (2012). TgCDPK3 regulates calcium-dependent egress of *Toxoplasma gondii* from host cells. *PLoS Pathog.* 8:e1003066. doi: 10.1371/journal.ppat.1003066

Nagamune, K., Moreno, S. N., Chini, E. N., and Sibley, L. D. (2008). Calcium regulation and signaling in apicomplexan parasites. *Subcell Biochem.* 47, 70–81. doi: 10.1007/978-0-387-78267-6_5

Pan, M., Lyu, C., Zhao, J., and Shen, B. (2017). Sixty Years (1957-2017) of research on toxoplasmosis in China-an overview. *Front. Microbiol.* 8:1825. doi: 10.3389/fmicb.2017.01825

Parthasarathy, S., Fong, M. Y., Ramaswamy, K., and Lau, Y. L. (2013). Protective immune response in BALB/c mice induced by DNA vaccine of the ROP8 gene of *Toxoplasma gondii*. *Am. J. Trop. Med. Hyg.* 88, 883–887. doi: 10.4269/ajtmh.12-0727

Peng, G. H., Yuan, Z. G., Zhou, D. H., He, X. H., Liu, M. M., Yan, C., et al. (2009). *Toxoplasma gondii* microneme protein 6 (MIC6) is a potential vaccine candidate against toxoplasmosis in mice. *Vaccine* 27, 6570–6574. doi: 10.1016/j.vaccine.2009.08.043

Pereira-Chioccola, V. L., Vidal, J. E., and Su, C. (2009). *Toxoplasma gondii* infection and cerebral toxoplasmosis in HIV-infected patients. *Future Microbiol.* 4, 1363–1379. doi: 10.2217/fmb.09.89

Pinheiro, P. S., Houy, S., and Sørensen, J. B. (2016). C2-domain containing calcium sensors in neuroendocrine secretion. *J. Neurochem.* 139, 943–958. doi: 10.1111/jnc.13865

Ramirez, D. M. O., Crawford, D. C., Chanaday, N. L., Trauterman, B., Monteggia, L. M., and Kavalali, E. T. (2017). Loss of Doc2-dependent spontaneous neurotransmission augments glutamatergic synaptic strength. *J. Neurosci.* 37, 6224–6230. doi: 10.1523/JNEUROSCI.0418-17.2017

Robert-Gangneux, F., and Dardé, M. L. (2012). Epidemiology of and diagnostic strategies for toxoplasmosis. *Clin. Microbiol. Rev.* 25, 264–296. doi: 10.1128/CMR.05013-11

Stewart, R. J., Whitehead, L., Nijagal, B., Sleebs, B. E., Lessene, G., McConville, M. J., et al. (2017). Analysis of Ca2+ mediated signaling regulating *Toxoplasma* infectivity reveals complex relationships between key molecules. *Cell Microbiol.* 19:e12685. doi: 10.1111/cmi.12685

Suzuki, Y., Sa, Q., Gehman, M., and Ochiai, E. (2011). Interferon-gamma- and perforin-mediated immune responses for resistance against *Toxoplasma gondii* in the brain. *Expert Rev. Mol. Med.* 13:e31. doi: 10.1017/S1462399411002018

Wang, Z. D., Liu, H. H., Ma, Z. X., Ma, H. Y., Li, Z. Y., Yang, Z. B., et al. (2017). *Toxoplasma gondii* infection in immunocompromised patients: a systematic review and meta-analysis. *Front. Microbiol.* 8:389. doi: 10.3389/fmicb.2017.00389

Yuan, Z. G., Zhang, X. X., Lin, R. Q., Petersen, E., He, S., Yu, M., et al. (2011). Protective effect against toxoplasmosis in mice induced by DNA immunization with gene encoding *Toxoplasma gondii* ROP18. *Vaccine* 29, 6614–6619. doi: 10.1016/j.vaccine.2011.06.110

Zhang, N. Z., Chen, J., Wang, M., Petersen, E., and Zhu, X. Q. (2013). Vaccines against *Toxoplasma gondii*: new developments and perspectives. *Expert Rev. Vaccines* 12, 1287–1299. doi: 10.1586/14760584.2013.844652

Zhang, N. Z., Gao, Q., Wang, M., Elsheikha, H. M., Wang, B., Wang, J. L., et al. (2018). Immunization with a DNA vaccine cocktail encoding TgPF, TgROP16, TgROP18, TgMIC6, and TgCDPK3 genes protects mice against chronic toxoplasmosis. *Front. Immunol.* 9:1505. doi: 10.3389/fimmu.2018.01505

Zhang, N. Z., Wang, M., Xu, Y., Petersen, E., and Zhu, X. Q. (2015a). Recent advances in developing vaccines against *Toxoplasma gondii*: an update. *Expert Rev. Vaccines* 14, 1609–1621. doi: 10.1586/14760584.2015.1098539

Zhang, N. Z., Xu, Y., Wang, M., Petersen, E., Chen, J., Huang, S. Y., et al. (2015b). Protective efficacy of two novel DNA vaccines expressing *Toxoplasma gondii* rhomboid 4 and rhomboid 5 proteins against acute and chronic toxoplasmosis in mice. *Expert Rev. Vaccines* 14, 1289–1297. doi: 10.1586/14760584.2015.1061938

Zhao, G., Song, X., Kong, X., Zhang, N., Qu, S., Zhu, W., et al. (2017). Immunization with *Toxoplasma gondii* aspartic protease 3 increases survival time of infected mice. *Acta Trop.* 171, 17–23. doi: 10.1016/j.actatropica

Zheng, B., Ding, J., Chen, X., Yu, H., Lou, D., Tong, Q., et al. (2017). Immunoefficacy of a *T. gondii* secreted protein with an altered thrombospondin repeat (TgSPATR) as a novel DNA vaccine candidate against acute toxoplasmosis in BALB/c mice. *Front Microbiol.* 8:216. doi: 10.3389/fmicb.2017.00216

Zhou, J., and Wang, L. (2017). SAG4 DNA and peptide vaccination provides partial protection against *T. gondii* infection in BALB/c mice. *Front. Microbiol.* 8:1733. doi: 10.3389/fmicb.2017.01733

Zhou, J., Wang, L., Lu, G., Zhou, A., Zhu, M., Li, Q., et al. (2016). Epitope analysis and protection by a ROP19 DNA vaccine against *Toxoplasma gondii*. *Parasite* 23:17. doi: 10.1051/parasite/2016017

Zhou, P., Chen, Z., Li, H. L., Zheng, H., He, S., Lin, R. Q., et al. (2011). *Toxoplasma gondii* infection in humans in China. *Parasit. Vectors* 4:165. doi: 10.1186/1756-3305-4-165

Conflict of Interest Statement: The authors declare that the research was conducted in the absence of any commercial or financial relationships that could be construed as a potential conflict of interest.

frontiers in Immunology

ORIGINAL RESEARCH
published: 31 July 2018
doi: 10.3389/fimmu.2018.01763

A Role for Epitope Networking in Immunomodulation by Helminths

E. Jane Homan and Robert D. Bremel*

EigenBio LLC, Madison, WI, United States

Helminth infections, by nematodes, trematodes, or cestodes, can lead to the modulation of host immune responses. This allows long-duration parasite infections and also impacts responses to co-infections. Surface, secreted, excreted, and shed proteins are thought to play a major role in modulation. A commonly reported feature of such immune modulation is the role of T regulatory (Treg) cells and IL-10. Efforts to identify helminth proteins, which cause immunomodulation, have identified candidates but not provided clarity as to a uniform mechanism driving modulation. In this study, we applied a bioinformatics systems approach, allowing us to analyze predicted T-cell epitopes of 17 helminth species and the responses to their surface proteins. In addition to major histocompatibility complex (MHC) binding, we analyzed amino acid motifs that would be recognized by T-cell receptors [T-cell-exposed motifs (TCEMs)]. All the helminth species examined have, within their surface proteins, peptides, which combine very common TCEMs with predicted high affinity binding to many human MHC alleles. This combination of features would result in large cognate T cell and a high probability of eliciting Treg responses. The TCEMs, which determine recognition by responding T-cell clones, are shared to a high degree between helminth species and with *Plasmodium falciparum* and *Mycobacterium tuberculosis*, both common co-infecting organisms. The implication of our observations is not only that Treg cells play a significant role in helminth-induced immune modulation but also that the epitope specificities of Treg responses are shared across species and genera of helminth. Hence, the immune response to a given helminth cannot be considered in isolation but rather forms part of an epitope ecosystem, or microenvironment, in which potentially immunosuppressive peptides in the helminth network via their common T-cell receptor recognition signals with T-cell epitopes in self proteins, microbiome, other helminths, and taxonomically unrelated pathogens. Such a systems approach provides a high-level view of the antigen-immune system signaling dynamics that may bias a host's immune response to helminth infections toward immune modulation. It may indicate how helminths have evolved to select for peptides that favor long-term parasite host coexistence.

Keywords: helminth, immunomodulation, bioinformatics, T regulatory, networking, T-cell-exposed motifs

OPEN ACCESS

Edited by:
Wenbin Tuo, Agricultural Research Service (USDA), United States

Reviewed by:
Susanne Hartmann, Freie Universität Berlin, Germany
Peter C. Thompson, Agricultural Research Service (USDA), United States

****Correspondence:***
E. Jane Homan
jane_homan@eigenbio.com

Specialty section:
This article was submitted to Microbial Immunology, a section of the journal Frontiers in Immunology

Received: *15 April 2018*
Accepted: *17 July 2018*
Published: *31 July 2018*

Citation:
Homan EJ and Bremel RD (2018) A Role for Epitope Networking in Immunomodulation by Helminths. Front. Immunol. 9:1763. doi: 10.3389/fimmu.2018.01763

INTRODUCTION

Parasitic helminth infections affect over 2 billion people, mostly in tropical and subtropical countries, causing a vast burden of clinical and subclinical disease (1–3). To allow them to infect their hosts for extended periods, sometimes over decades, helminths have evolved to modulate their host's immune responses (4–6). Down-regulation of the immune response results in many

Abbreviations: APC, antigen-presenting cell; FC, frequency category; GEM, groove-exposed motif; HLA, human leucocyte allele; MHC, major histocompatibility complex; pMHC, peptide MHC; sORF, small open reading frame; TCEM, T-cell-exposed motif; TMH, transmembrane helix.

infected individuals being asymptomatic carriers and thus ensures perpetuation of the parasite life cycle.

Immune modulation by helminths extends to other immune stimulants; in infected individuals the immune response to secondary parasite infections, to other pathogens, and to vaccines is also down-regulated (7–11). While epidemiologic and socioeconomic factors also contribute to the prevalence of co-infections, helminth-induced immune modulation may predispose to infection by *Mycobacterium tuberculosis* or malaria (7, 12–14). A number of helminth infections have been associated with increased risks of cancer. The oriental liver flukes, *Clonorchis sinensis* and *Opisthorchis viverrini*, are risk factors for development of cholangiocarcinoma, typically many decades after initial infection (15). Infection with *Schistosoma haematobium* is associated with an increased risk of bladder carcinoma (16). Intestinal helminths have been thought to reduce risk of *Helicobacter pylori* associated adenocarcinoma (17), but *Opisthorchis* flukes may serve as risk factor by vectoring *H. pylori* and thus increasing associated cancers (18).

Helminth immune modulation has some beneficial effects as allergies, and inflammatory and autoimmune diseases are less common in populations infected with helminths (11, 19–21). Treatment with anthelminthics removes this effect and is reported to increase the incidence of inflammatory, autoimmune and allergic diseases (22, 23). The observation that helminth infection modulates inflammation and allergic responses has raised interest in the use of helminth infections, helminth extracts, or recombinant helminth-derived proteins as therapeutic interventions (24–27).

The mechanisms of immunomodulation arising from helminth infections have been extensively researched and are the subject of a large body of literature and many authoritative reviews (4, 11, 27–29). Among the many reports of possible modes of action (30, 31), two common themes emerge. First, certain groups of proteins appear to play a key role in bringing about changes in the host immune response. This includes proteins, which are secreted or excreted (32–34), proteins that are present in outer surface tegument or gastrointestinal surfaces, or proteins that are continually shed into the environs of the worm, either in isolation or as components of extracellular vesicles (35, 36). Extracts of secreted and surface proteins have been shown experimentally to elicit some of the immunomodulatory effects (32, 34). This has been extended to testing a number of individual proteins and identifying several proteins that can affect immune function (24, 28, 31, 37). The second unifying theme is that T regulatory (Treg) cells, and induction of IL-10, play a central role in helminth-induced host immune modulation (38–44), whether by classical Foxp3+ CD4 cells or other IL-10 secreting populations of CD4+ or CD8+ cells (45–50).

Helminth infections are not uniformly immunosuppressive. Protective immunity does emerge over time and provides the impetus for research toward vaccines (1, 51, 52), although reinfection may follow anthelmintic treatment (53, 54). Allergic responses to some helminths also occur and may also predispose to asthma (55, 56).

Studies of helminth immune modulation have largely focused on how cytokine-mediated effector mechanisms may impact the immune response. However, they have not addressed the question of whether the initial signaling in immune recognition of the parasite causes components of the immune response to be biased toward a suppressive or regulatory pathway.

In this study, we use a computational systems approach to evaluate the initial signal recognition patterns between helminth and host T cells. We evaluate the complete proteomes of 17 representative helminths and three reported co-infections based on the pattern of amino acids that would be exposed to T cells, which determine the interaction of parasite antigen and T cells. Essentially, we are attempting to see the helminth antigens as a T-cell receptor would see them, based on the minimal differentiating signal patterns from major histocompatibility complex (MHC)-bound helminth peptides that would be exposed from the MHC histotope. We have previously examined such interactions between T-cell receptor and amino acid motifs in a variety of bacterial pathogens and commensals and found distinct patterns that appear to relate to the pathogenesis of the organisms (57).

A single T-cell does not recognize, or respond to, a whole helminth; it instead engages with the few amino acids in a bound peptide MHC (pMHC) protruding from a MHC histotope, which is determined by the host human leucocyte allele (HLA) genotype. Protein antigens are processed by antigen-presenting cells (APCs) and presented to T cells as peptides bound in the groove of MHC molecules. The bound peptides (8–11 amino acids for MHC I and 13–22 amino acids for MHC II) comprise inward facing amino acids which determine peptide binding in the groove pockets [the groove-exposed motif (GEM) or pocket positions]. The intervening amino acids protrude outwards from the MHC surface or histotope and are thus exposed to the T-cell receptor, determining binding to that cognate receptor (58, 59). We refer to these amino acid motifs as the T-cell-exposed motif (TCEM). In MHC I-bound peptides, the TCEM comprises a continuous pentamer comprising positions 4, 5, 6, 7, and 8 of a nonamer, whereas in MHC II-bound peptides, the TCEM is a discontinuous pentamer in two possible recognition patterns, denoted here as TCEM IIA and IIB and comprised amino acid positions ~2,3~5~7,8~ or −1~~3~5~7,8~, respectively (where ~ is the intervening positions), relative to the central nonamer core of a longer bound peptide (60, 61). Hence, the signal that determines the outcome of the interaction with the cognate T cell is determined by the pentameric TCEM motif. This enables T cells to be polyspecific, responding to the same TCEM recognition signal, even though the MHC-bound peptide may be derived from antigens of different sources (62). The duration of TCEM signaling is determined by the stability of the pMHC complex and thus the dwell time of the peptide in the MHC groove, a function of the amino acids making up the MHC GEM. The frequency of signaling is determined by the size of the cognate T-cell population encountering the signal, which in turn is influenced by the frequency of occurrence of that TCEM in self proteins, commensal microbiome, and other pathogens.

The proteins of the human microbiome, especially the gastrointestinal microbiome, the human proteome, and the immunoglobulin repertoire are also continually processed by APCs and presented to T cells (63, 64). In examining the immunoglobulinome, it emerged that there is a frequency hierarchy of

TCEM. This includes, at one extreme, common motifs found in most immunoglobulin variable regions. These are not limited to motifs encoded by the germline but also include motifs produced by somatic mutation. At the other extreme, very rare motifs are encountered only once in several million B-cell clones (65, 66). This frequency distribution is representative of that in the rest of the human proteome and gastrointestinal microbiome (57). The frequency of appearance of a TCEM determines the frequency of stimulation of a clone or clones of cognate T cells. Hence, more common motifs would be expected to beget larger cognate T-cell populations than rare motifs. A highly bound peptide that recruits a large T-cell population and a high frequency of signal is more likely to generate a suppressive or Treg response (67–72). The human immunoglobulinome comprises the greatest diversity of motifs relative to the rest of the human proteome and microbiome and undergoes considerably more turnover. We use the immunoglobulinome variable regions as a reference scale of TCEM motif frequency (65). Here, we show that a feature of helminths is their content of common TCEM that, when in the context of a binding GEM, is potentially immunosuppressive and to which the infected host is chronically exposed.

Helminth parasites have large genomes and complex life cycles (73, 74). Considerable progress has been made in helminth genome sequencing, but many proteins remain unannotated, and transcriptomic studies that relate proteins to life stage, while more advanced for a few helminths (75–79) are mostly incomplete. With these limitations, we cannot define an exact combination of T-cell epitope modulation signals functioning within the human host, but the results we present are indicative of the complexity of potential T-cell epitope interactions within and among helminth species and with potential co-infections. Such a systems approach provides a high-level view of the antigen-immune system signaling dynamics that may bias a host immune response to helminth infections toward immune modulation and may suggest approaches to develop a further understanding of the host:parasite interrelationship.

MATERIALS AND METHODS

Helminth Proteomes

Protein FASTA files for 17 complete helminth proteomes were downloaded from Wormbase (www.wormbase.org) (80) as shown in **Table 1**. All infect humans; most have human as their primary definitive host; some (e.g., *Echinococcus granulosus*, *Trichinella spiralis*, *Fasciola hepatica*, and *Loa loa* infect humans as an accidental zoonotic host). Proteomes identified and curated by different originating laboratories varied in the size criteria applied for inclusion as did criteria for inclusion of multiple splice variants. Proteins under 50 amino acids were excluded from our analysis as end effects of the sliding analysis windows preclude making meaningful comparisons to larger proteins.

Comparative Proteomes

The proteins of the human immunoglobulinome, comprising the variable region sequences of 40 million distinct immunoglobulins, were assembled as previously described, supplemented with sequences from clinical samples and other published immunoglobulin sequences, and the TCEM frequency distributions were precomputed as previously described (61, 66, 93). Examination of the frequency of occurrence of TCEM in the large immunoglobulin dataset allows us to assign a frequency category (FC) to each TCEM motif as it occurs in the immunoglobulinome clonotypes. Each motif in each recognition pattern (TCEM I for MHC I and TCEM IIA and IIB for MHC II) is assigned a log base 2 FC based on whether it occurs in half (FC1), 1 in 4 (FC2), and 1 in 8 (FC3)

TABLE 1 | Helminth proteomes analyzed.

Class	Parasite evaluated	Proteome size[a]	15-mer peptides	Secreted and surface proteins selected for complete analysis[b]	Secreted and surface proteins selected as percentage of proteome	Project number on http://parasite.wormbase.org	Reference
Nematodes	*Ancylostoma ceylanicum*	36,687	9,508,454	3,266	8.9	prjna231479	(75)
	Ancylostoma duodenale	27,485	5,447,645	713	2.6	prjna72581	
	Necator americanus	19,153	4,868,515	737	3.8	prjna72135	(81)
	Ascaris lumbricoides	23,604	6,833,958	1,064	4.5	prjeb4950	
	Brugia malayi	11,021	6,125,076	853	7.7	prjna10729	(82)
	Loa loa	12,473	4,931,854	606	4.9	prjna246086	(83)
	Onchocerca volvulus	12,117	4,873,818	736	6.1	prjeb513	(84)
	Wucheria bancrofti	13,058	4,140,788	589	4.5	prjeb536	
	Trichinella spiralis	14,737	8,879,076	1,567	10.6	prjna257433	(85)
	Trichuris trichuria	9,650	4,050,951	522	5.4	prjeb535	(86)
Trematodes	*Clonorchis sinensis*	13,634	7,029,209	933	6.8	prjda72781	(87)
	Opisthorchis viverrini	16,356	6,848,490	874	5.3	prjna222628	(88)
	Fasciola hepatica	22,676	5,851,887	670	3.0	prjeb6687	(89)
	Schistosoma mansoni	10,772	5,443,618	629	5.8	prjea36577	(90, 91)
Cestodes	*Diphylobothrium latum*	19,966	3,872,702	529	2.6	prjeb1206	
	Echinococcus granulosus	10,245	4,932,446	804	7.8	prjeb121	(92)
	Taenia solium	12,481	4,992,618	724	5.8	prjna170813	(92)

[a]*T-cell-exposed motif (TCEM) extraction and ranking were completed on the whole proteome.*

[b]*Proteins for detailed analysis were selected from the proteome based on the presence of a transmembrane domain and/or signal peptide, which are in the top 5% of content of high frequency TCEM (those motifs more common than 1 in 1,024 clones), or which contain TCEM in any pattern (TCEM I, IIA, or IIB).*

immunoglobulin variable regions, up to FC23, which represents 1 in 8.39 million (2^{23}) clonotypes, or approximately one T-cell clone in the entire repertoire that a single human carries. A further category of FC24 designates those motifs not yet encountered in immunoglobulin variable regions analyzed to date. The mean frequency in the human immunoglobulinome is FC10, a motif which is found in 1 in 1,024 (2^{10}) variable regions. Motifs of FC1-3 are referred to as very high frequency and those of FC10 or less as high frequency.

The human proteome, including all known isoforms of each protein (totaling 88,000 proteins), but excluding immunoglobulin sequences, was assembled from Uniprot (www.uniprot.org) and its TCEMs precomputed. The proteomes of constituents of the GI microbiome were assembled and precomputed as previously described (57). This database comprised 67 bacterial species.

Proteomes of reference sequences of *Plasmodium falciparum* (3D7), *M. tuberculosis* (H37Rv), and *H. pylor*i (26695) were downloaded from EupathDb (http://eupathdb.org) and Patric (https://www.patricbrc.org/) (94, 95). These proteomes were screened in their entirety for high frequency TCEM and not filtered by SP and transmembrane helix (TMH) proteins.

Determination of TCEMs and Predicted MHC Binding

T-cell-exposed motif patterns were extracted from the complete proteomes and ranked as previously described for each of three recognition patterns (61, 65). Frequencies of motif occurrence were determined with respect to the immunoglobulinome, the human proteome, and the gastrointestinal microbiome (57). MHC binding was predicted using neural network ensembles trained to the LN ic50 (96) for approximately 230,000 binding reactions using the neural platform of JMP® (SAS Institute). This is an updated version of a system described previously (61). Predicted MHC binding was computed for each sequential 9-mer and 15-mer peptides in selected protein sets, wherein the predicted binding affinity to 37 MHC I and 28 MHC II alleles was determined. To estimate population behavior comprising multiple alleles with varying affinities for any peptide, the LN ic50 binding data estimates were transformed and standardized to a zero mean unit variance within each protein using a Johnson Sb distribution (97). This transformation enables the combination of binding results from different alleles, which is akin to using the principle of the additivity of variance commonly used in quantitative genetics (98, 99). The probability of cleavage of each protein by human cathepsin B, L, or S was determined. Both binding affinity and cleavage predictions were accomplished using previously described methods by neural network predictors based on principal component analysis of amino acid physical properties (100).

Suppressive Indices

To derive an indicator of the probability of a particular peptide generating a Treg response, we combined the prediction of standardized MHC binding and the frequency of occurrence of the TCEM. The combination of these two parameters provides a metric that is directly related to the probability that a collision between a cognate T cell and a pMHC on the surface of an APC will occur. For each peptide, where the standardized predicted binding affinity is greater than the mean for the protein and allele combination, the predicted standardized affinity of each allele (A) is weighted by its cognate encounter number ($nA \times FC^{16\text{-}FC}$) and the sum that product provides the suppressive index. Thus, the final suppressive index is a composite metric of affinity and how often cognate T-cell encounters will occur in the human population (Figure S1 in Supplementary Material).

The suppressive index is therefore an indicator of the predicted response of the human population of diverse immunogenetics; the response of any particular HLA allele will vary around this mean index. Hence the suppressive index, as computed here, does not distinguish the differences in modulation, which may arise between different ethnic or immunogenetic population subsets or between individual immunogenetically distinct hosts.

Bacteria and viruses, with small proteomes, typically comprise peptides with suppressive indices of up to a few hundred and usually under about 8,000, rare motifs have indices of 20,000–50,000 (data not shown). Only exceptional proteins in bacteria and viruses have motifs with indices >200,000. A peptide scoring a suppressive index over 1 million is thus extremely rare and would only be possible with an extremely common motif (FC1-3) that binds to almost all human alleles (in either frames IIA and IIB or MHC I A and B).

Selection of Proteins Comprising Potential Suppressor Motifs

Given the large size of each helminth proteome, we focused attention particularly on proteins of the secreted and surface proteins and on those most likely to elicit a suppressive response. To this end, all proteins with signal peptides and/or transmembrane helices in an organism proteome were selected. To identify transmembrane regions and signal peptides in the primary amino acid sequence of proteins, the online resource Phobius http://phobius.sbc.su.se/was used. This combines the two types of domain identification tools generally used in genome annotation in one resource (101). Signal peptides were predicted for eukaryotic organisms.

From these, in order to focus on the likely immunomodulatory protein candidates, two subsets of proteins were then compiled from each species based on the following criteria: the proteins having the highest content of common TCEM (less than or equal to FC 10) per 100 amino acid length were selected; and those proteins having any TCEM (TCEM I, IIA, or IIB) of FC1-3 (motifs occurring at least as frequently as in one in eight immunoglobulin variable regions). These subsets were combined, duplicates were eliminated, and a full computation of predicted MHC binding and cathepsin excision sites was completed. This comprised from 2.5 to 10% of each proteome. All peptides for each protein in each species set (15-mer for MHC II and 9-mer for MHC I) were ranked by suppressive index. Any peptide having a suppressive index over 300,000 and its source protein were identified.

Proteins Reported to Be Associated With Immunomodulation

A set of sequences for proteins previously reported to be associated with immunomodulation (24, 28, 37) was assembled, using Reference sequences from GenBank. These proteins are listed in Table S1 in Supplementary Material.

Statistical Analysis

All data processing, pattern analysis, and statistical analysis were done with JMP® v13 from SAS Institute (Cary, NC, USA).

RESULTS

Analyses were conducted for all three TCEM recognition patterns in the complete proteomes. To conserve space, in some cases, we show data for TCEM IIA in the body of the paper and provide corresponding TCEM I and TCEM IIB data in Supplementary Tables. Very similar results are seen for each of the TCEM patterns.

TCEM Characteristics of the Entire Organism Proteome

Sharing of TCEMs Is Common

For each TCEM pentameric motif pattern, the maximum possible configurations of the 20 amino acid is 3.2 million (20^5). All possible motifs are found in the immunoglobulinome. The human proteome and GI microbiome comprise approximately 75 and 91%, respectively, of the possible motifs in each recognition pattern.

Table 2 shows the content the TCEM IIA motifs in the helminth species studied and the degree of sharing of motifs (Table S2 in Supplementary Material shows additional motif patterns TCEM I and IIB). The repertoire of each helminth comprises from approximately 53 to 71% of the total possible motifs in each TCEM pattern, indicating the overlap of repertoire with the immunoglobulinome. Among all 17 species of helminth, >96% of all possible TCEMs are collectively represented.

Sharing Between Helminth Species

Given the breadth of the TCEM repertoires of each species of helminth there is inevitably overlap in repertoires between the species. Overall ~415,000 TCEM motifs of each pattern are present in all of the 17 species analyzed. The remaining ~2.6 million motifs are shared in varying combinations among the species. **Figure 1** shows the motif sharing patterns. Each tile represents a unique combination of sharing of the 3.2 million TCEM IIA motifs among the 17 species, in all comprising 112,225 different motif sharing combinations. This indicates the complexity of the potential T-cell epitope sharing and cross-reactivities between species.

Each helminth species has a small set of motifs, less than 0.6%, that are unique to that species relative to the other 16 species (last column **Table 2**). The exact number of these motifs is unlikely to be significant given the different approaches to sequencing and curation adopted for each species, but it is notable that each species does have a unique signature. However, it must be recognized that such unique motifs are overlapped with amino acids comprising non-unique motifs, so their utility in directing a unique immune response is limited.

TABLE 2 | Sharing of total T-cell-exposed motif (TCEM) IIA between helminths, gastrointestinal microbiome, and human proteome.

	Total TCEM IIA	TCEM IIA as percentage of 3.2 million	TCEM IIA shared with GI microbiome	Percentage of TCEM IIA shared with GI microbiome	TCEM IIA shared with human proteome	Percentage of TCEM IIA shared with human proteome	TCEM IIA unique to helminth species	Unique TCEM IIA as percentage of species total
Immunoglobulinome	3,200,000	100.00						
GI microbiome	2,921,445	91.30						
Human proteome #1	2,412,699	75.40						
Total motifs in 17 helminths	3,101,990	96.94						
TCEM IIA common to all 17 species	418,120							
Ancylostoma ceylanicum	2,281,190	71.29	2,193,019	96.13	1,931,093	84.65	13,051	0.57
Ancylostoma duodenale	1,844,757	57.65	1,790,685	97.07	1,609,132	87.23	4,032	0.22
Necator americanus	1,845,715	57.68	1,792,570	97.12	1,611,216	87.29	5,294	0.29
Ascaris lumbricoides	2,075,222	64.85	2,005,287	96.63	1,783,734	85.95	13,400	0.65
Brugia malayi	1,835,074	57.35	1,780,913	97.05	1,595,941	86.97	2,370	0.13
Loa loa	1,796,988	56.16	1,746,152	97.17	1,569,747	87.35	3,397	0.19
Onchocerca volvulus	1,855,127	57.97	1,800,210	97.04	1,610,305	86.80	5,015	0.27
Wucheria bancrofti	1,737,656	54.30	1,689,344	97.22	1,519,185	87.43	1,925	0.11
Trichinella spiralis	1,873,959	58.56	1,811,550	96.67	1,622,466	86.58	12,512	0.67
Trichuris trichura	1,716,725	53.65	1,669,456	97.25	1,507,130	87.79	9,275	0.54
Clonorchis sinensis	2,079,755	64.99	2,006,177	96.46	1,792,125	86.17	7,740	0.37
Opisthorchis viverrini	2,032,485	63.52	1,962,333	96.55	1,758,940	86.54	6,589	0.32
Fasciola hepatica	1,918,592	59.96	1,855,938	96.73	1,670,778	87.08	10,851	0.57
Schistosoma mansoni	1,822,979	56.97	1,767,657	96.97	1,586,723	87.04	9,105	0.50
Diphyllobothrium latum	1,592,066	49.75	1,551,677	97.46	1,417,136	89.01	6,647	0.42
Echinococcus granulosus	1,788,474	55.89	1,735,938	97.06	1,575,786	88.11	4,636	0.26
Taenia solium	1,801,611	56.30	1,748,550	97.05	1,585,759	88.02	5,002	0.28

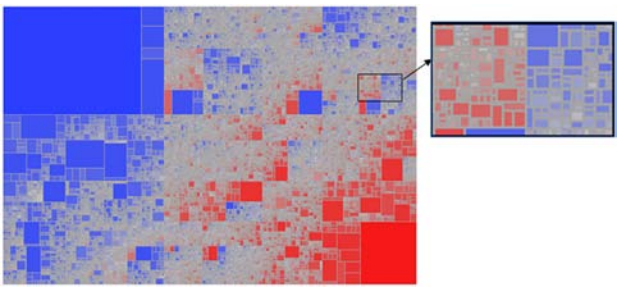

FIGURE 1 | Treemap showing the complexity of sharing patterns of T-cell-exposed motifs (TCEMs) (shown for TCEM IIA) among the 17 helminth species analyzed. A total of 112,225 unique sharing patterns were identified. The sharing pattern refers to the combination of the 17 species of helminths that carries that motif. Some sharing patterns comprised a single TCEM motif represented by a very small tile; other sharing patterns comprise large groups of shared motifs and are shown by large tiles. The tiles are colored from highly shared motif groups (blue) to minimally shared motif groups (red). The large blue box at top left represents the TCEM IIA common to all 17 species; the red box at bottom right represents the TCEM IIA absent from all species. The intervening tiles each have a unique combination of motifs and species sharing pattern. The expanded high resolution cutout provides an appreciation of the number and complexity of different patterns embedded in the lower resolution picture.

Sharing of TCEM Between Helminths and Co-Infecting Pathogens

Three unrelated pathogens cited as common co-infections with heminthiases were selected for comparison. The extent of TCEM IIA sharing with *P. falciparum*, *M. tuberculosis*, and *H. pylori* is shown in Table S3 in Supplementary Material. Across all species of helminth, approximately 50% of TCEM have matches in *P. falciparum*, 28% have matches in *M. tuberculosis*, and 16% have matches in *H. pylori*.

Distribution of High-Frequency TCEMs Within the Helminth Proteome

The frequency of occurrence of TCEMs in each helminth proteome was compared to their frequency in the immunoglobulinome. There is no significant difference in the distribution of motifs found in helminths among the frequency categories observed in the immunoglobulinome (correlation coefficients all >0.9); those motifs that are common in immunoglobulins are commonly found in helminths and rare immunoglobulin motifs are also rare in helminths.

We then examined the distribution of high frequency TCEM in the proteins of each helminth proteome to evaluate whether particular proteins might be contributing more to an immunosuppressive response. **Figure 2** shows examples of the distribution of proteins based on their content of TCEM of FC10 or lower, i.e., those motifs more common than the mean frequency in the immunoglobulin reference database. Each protein is plotted according to its size and the number of the frequent motifs. Comparable plots for the other helminths, and the three comparative co-infections, are provided in Figure S2 in Supplementary Material. While the distribution is not dissimilar from that seen in many other pathogens (57), the scatter

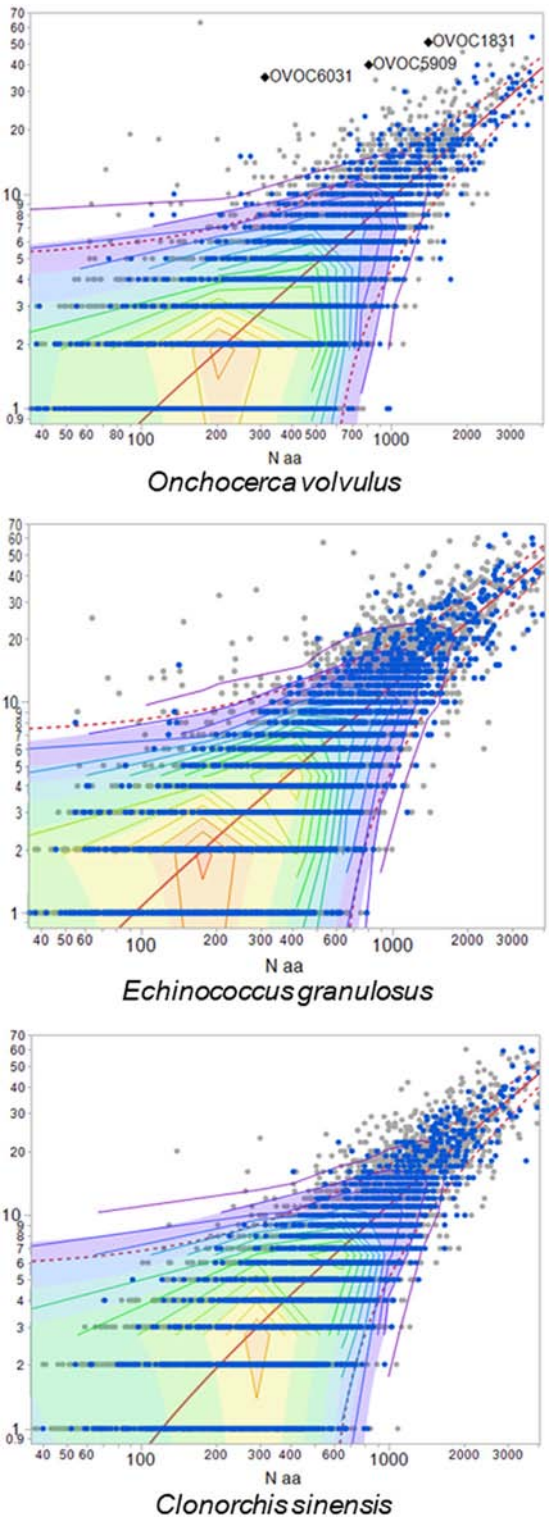

FIGURE 2 | Proteins with high content of common T-cell-exposed motif (TCEM). Each dot represents one protein of the species indicated. *X*-axis shows size of the protein (log_{10} amino acid number). *Y*-axis shows number of TCEM IIA motifs of higher than FC10, i.e., occurring more often than the mean in an immunoglobulinome reference database. Proteins shown in blue are secreted and surface proteins. Three example *Onchocerca volvulus* proteins are labeled, and sequences for these provided in Figure S3 in Supplementary Material.

of outlier proteins with a high content of frequent or rare TCEM is distinctive. As shown in **Figure 2**, the outliers are not proteins with signal peptides or transmembrane domains. Having a high content of high frequency TCEM motifs would be an indicator that a protein may have more immunosuppressive peptides, if such peptides are appropriately processed in APC and bind to MHC. On closer examination, the outliers were found to be proteins which have a high content of repetitive residues, either homorepeats of amino acids or repeats of simple amino acid motifs. Homorepeats of L, S, G, T, and Y emerge as frequent FC categories while those homorepeats of M, C, H, Q, and W are rare motifs in immunoglobulins. Figure S3 in Supplementary Material shows the sequences of those *Onchocerca volvulus* examples labeled in **Figure 2**, which are examples of proteins comprising amino acid repeats. *L. loa* is particularly striking with respect to the number of proteins with extended homorepeats that show as having a high content of common TCEM (Figure S1 in Supplementary Material).

TCEM Characteristics of Surface and TMH Proteins

Sharing of TCEM Associated With High Suppressive Index Between Helminth Species

Given the focus in the literature on the secreted, surface, and shed proteins as potential contributors to immunomodulation (32–35), we elected to focus further analysis on the subset of proteins which have a signal peptide, one or more transmembrane helices or both, along with the highest frequency TCEM. For each helminth species, the top 2.5–10% of protein with respect to their likelihood of comprising suppressive motifs were analyzed, comprising 15,816 proteins overall (**Table 1**). The number of peptides with extremely high suppressive indices over 300,000 was determined and included 903 peptides with high MHC I suppressive indices, of which 627 were unique, and 1,377 peptides with high MHC II suppressive indices, of which 977 were unique. Such highly suppressive index peptides were found in all the helminth species examined. **Table 3** shows the counts by species and suppressive index groupings. Among these, 70 proteins were identified containing more than one high suppressive index peptide at separate positions. Given the differing criteria in helminth proteome assembly, and the criteria imposed for the selection of analysis of a secreted or surface subset of proteins, the absolute numbers shown are not of particular significance except to indicate that such high indices are quite common findings in helminths.

Several helminths have peptides of high suppressive index, which comprise shared TCEM motifs, but in association with the same or different flanking peptides. Not surprisingly, the same flanking sequences are found in closely related helminths, such as *Clonorchis* and *Opisthorchis* as well as in proteins with multiple different transcripts, as shown for *Ancylostoma ceylanicum*. It should also be noted however that the same TCEM motifs may occur in the same parasites in the context of flanking peptides which are not high affinity binders. Depending on their binding affinity, these would have a shorter or even a transitory dwell time within the MHC groove. However, to the degree they may attract cognate Treg cells whose phenotype has already been determined, they may reinforce Treg signaling. **Figure 3** shows an example of peptides from *O. viverrini* and *A. lumbricoides* each comprising the same FC3 TCEM IIA motif SL~L~LV but within an array of peptides, which show different predicted MHC II binding affinities. It also indicates how binding may vary between alleles to generate different outcomes in different hosts.

TABLE 3 | Content of extremely high suppressive index peptides in secreted and surface proteins, showing peptides with suppressive index over 300,000.

	Major histocompatibility complex (MHC) I	MHC II
Ancylostoma ceylanicum	196	322
Ancylostoma duodenale	36	72
Necator americanus	32	63
Ascaris lumbricoides	81	83
Brugia malayi	56	72
Loa loa	32	56
Onchocerca volvulus	46	65
Wucheria bancrofti	34	48
Trichinella spiralis	71	150
Trichuris trichuria	20	64
Clonorchis sinensis	70	85
Opisthorchis viverrini	61	101
Fasciola hepatica	8	17
Schistosoma mansoni	30	58
Diphylobothrium latum	1	6
Echinococcus granulosus	68	62
Taenia solium	61	53
Total	903	1,377

Sharing of TCEM Associated With High Suppressive Index Between Helminths and Co-Infections

High-frequency TCEM associated with high suppressive indices was also shared between helminths and the three co-infecting pathogens examined. **Table 4** shows the count of shared motifs and the TCEM associated with highest suppressive indices in helminths and their matches in the three co-infecting agents. Shared highly suppressive motifs were found particularly for *M. tuberculosis* and *P. falciparum*. We have focused on those with suppressive indices over 300,000. **Figure 4** shows a conceptual model for how such T-cell networking among multiple helminths and co-infections may occur, based on a small illustrative group of five TCEM IIA motifs, which would each engage a finite number of T-cell clonotypes.

Proteins Previously Reported to Be Associated With Immunomodulation

Analysis of suppressive indices in 21 proteins reported to be associated with immunomodulation (Table S1 in Supplementary Material) identified only one, *T. spiralis* p53 with a peptide having a suppressive index over 300,000; the 15-mer at index position 456 has a suppressive index of 305,422, driven by the motif AV~Y~AR, which is found in 25% of all immunoglobulin variable regions. Suppressive indices of the other proteins are noted in Table S1 in Supplementary Material. Several proteins have suppressive indices in the range of 20,000–80,000.

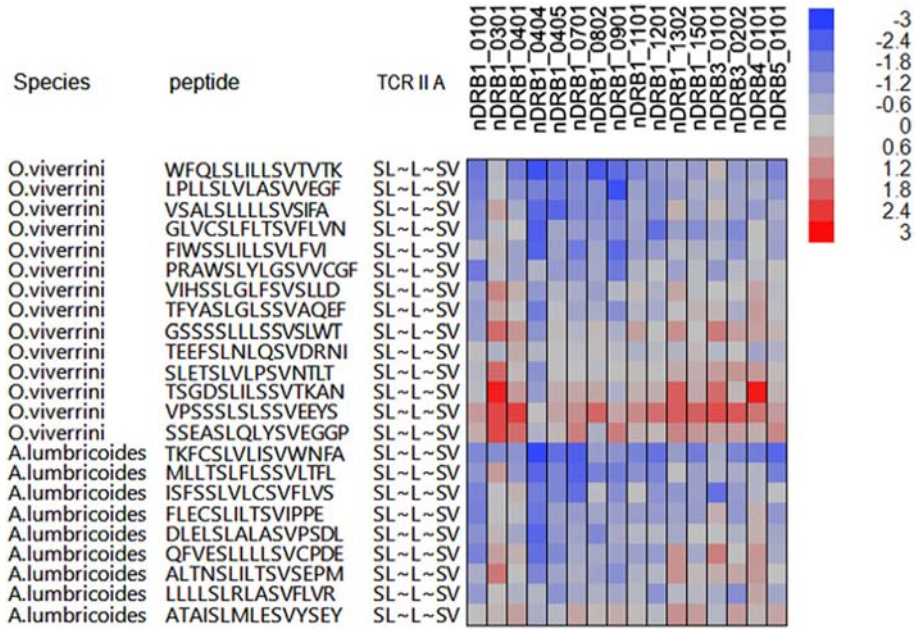

FIGURE 3 | Example of peptides of *Opisthorchis viverrini* and *Ascaris lumbricoides*, which have shared T-cell-exposed motifs (TCEMs) but in the context of differing groove-exposed motifs. *X*-axis of cell plot indicates multiple different major histocompatibility complex (MHC) II DRB alleles. Coloration of the cell plot indicates predicted binding affinity in standard deviation units below the mean for that protein. Blue indicates high binding affinity; red indicates low affinity. The peptides represent a range of suppressive indices: *O. viverrini* ranges from 621,829 to 20,788 and *A. lumbricoides* from 371,273 to 36,698 based on binding to all MHC II alleles evaluated. As the TCEM motif SL~L~LV is a common motif (FC3), these are all relatively high indices.

TABLE 4 | Sharing of helminth T-cell-exposed motifs (TCEMs) associated with extremely high suppressive index motifs with selected co-infections.

	Suppressive indices >300,000								
	***Mycobacterium tuberculosis* motifs shared**			***Plasmodium falciparum* motifs shared**			***Helicobacter pylori* motifs shared**		
	TCEM I	**TCEM IIA**	**TCEM IIB**	**TCEM I**	**TCEM IIA**	**TCEM IIB**	**TCEM I**	**TCEM IIA**	**TCEM IIB**
Ancylostoma ceylanicum	69	51	49	90	47	57	0	0	2
Ancylostoma duodenale	15	10	13	21	12	15	0	1	0
Necator americanus	9	14	8	20	14	14	0	0	1
Ascaris lumbricoides	21	24	6	41	26	14	0	2	1
Brugia malayi	16	13	5	29	16	14	0	1	1
Loa loa	8	7	9	18	9	8	0	1	1
Onchocerca volvulus	14	10	4	24	9	12	0	1	0
Wucheria bancrofti	9	6	7	17	7	11	0	1	0
Trichinella spiralis	15	17	12	32	40	34	0	10	0
Trichuris trichuria	6	11	10	5	11	18	0	1	0
Clonorchis sinensis	24	14	8	37	12	22	0	0	1
Opisthorchis viverrini	20	22	10	35	21	28	0	1	3
Fasciola hepatica	4	8	4	7	5	3	0	0	0
Schistosoma mansoni	7	8	6	17	13	8	0	2	1
Diphyllobothrium latum	0	0	2	0	0	4	0	0	0
Echinococcus granulosus	25	10	13	34	5	18	0	0	3
Taenia solium	26	9	7	33	9	13	0	0	1

DISCUSSION

Reports of immunomodulation by helminths have led to a search for individual proteins, which may cause this effect. A comprehensive explanation of helminth associated immunomodulation has been elusive, but a recurring theme is that Treg cells play a central role (38, 40). In the present analysis, we apply a systems approach examining the potential magnitude of networking of T-cell responses between parasites, host, and co-infecting microrganisms and offering

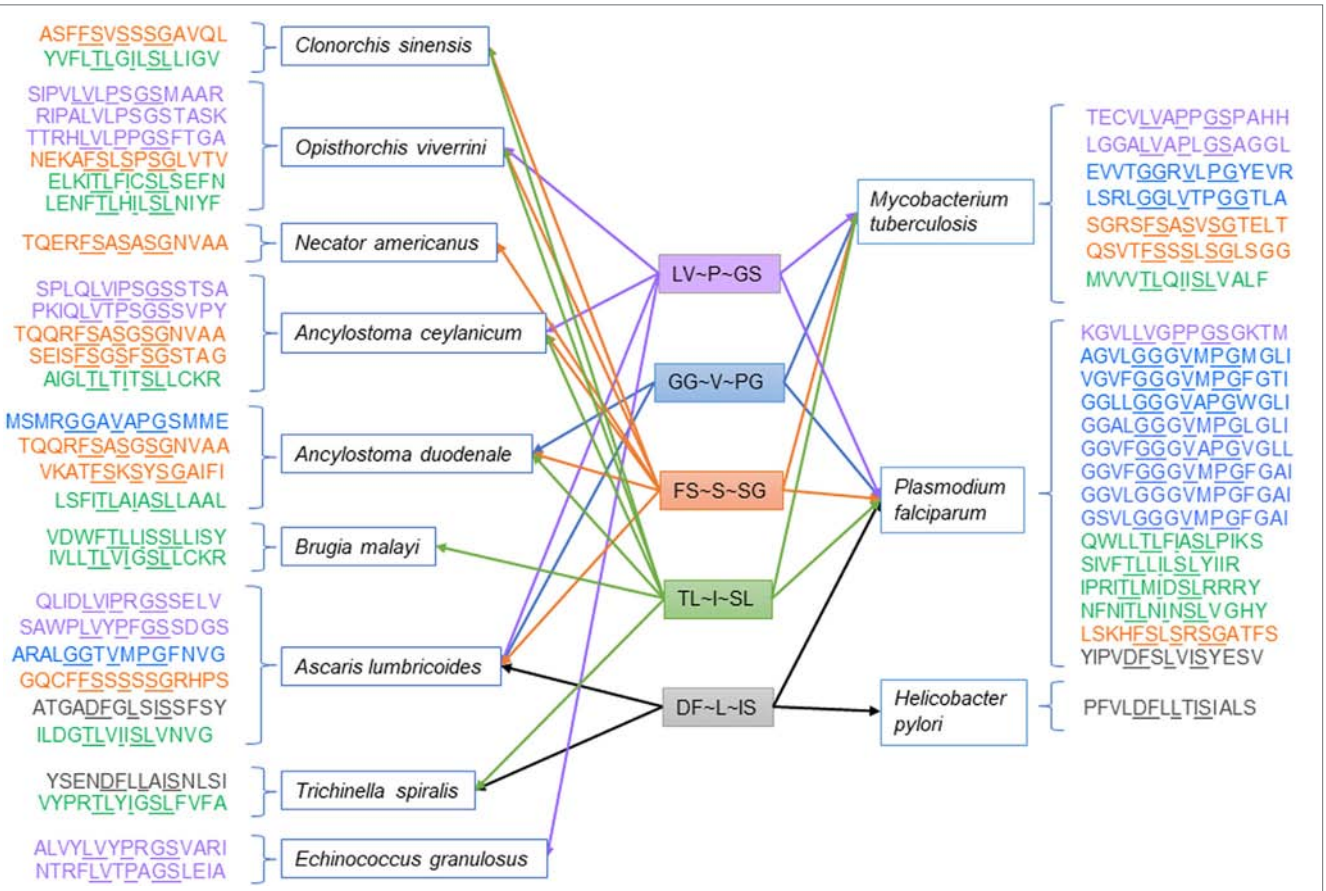

FIGURE 4 | Illustration of networking among high suppressive index T-cell-exposed motifs in helminths and selected co-infections.

a conceptual model, which may shed new light on the immunomodulation phenomenon. The goal of this study was not to identify a definitive set of peptides that are solely responsible for immunomodulation, but rather to highlight potential interplay of T-cell epitopes in an ecosystem in which helminths are present, and also to know how such networking may contribute to immunomodulation of the host.

Our study has several important limitations. Both annotation of helminth proteomes and transcriptomic studies of helminths infecting their hosts are incomplete and challenging (102, 103). Indeed, we do not know in which life stage of the parasite, many proteins are expressed or in which host microenvironment they may have an effect. Thus, we cannot anticipate the quantitative or temporal impact of each protein. In a highly expressed protein, a suppressive motif may be multiplied many times or a moderately suppressive peptide motif may carry more weight if that protein is highly upregulated. Each parasite proteome is large, and to facilitate analysis, we selected certain subsets (surface and secreted proteins) for more detailed evaluation. For most of the helminths studied, only a single proteome is available. We only studied one isolate or reference proteome for each organism, both helminth and the three selected co-infecting pathogens. Polymorphisms of proteins between isolates based on single amino acid changes are sufficient to change MHC binding of peptides and the TCEM presented (104). Furthermore, single amino acid changes impact T-cell interactions across up to 46 potential binding peptides, by changing any of cathepsin processing, MHC binding, or the TCEMs presented (65). Hence, different isolates will have somewhat different networking patterns, but the overall conceptual model will apply.

The starting point for such a networking model is the premise that a T-cell receptor is agnostic as to the source of the amino acid motif of a bound peptide, which the TCR engages in the context of the MHC histotope. A cognate TCR engages a particular pentameric motif whether that occurs in a host protein, a microbiome protein, a helminth, or a co-infecting pathogen. While the flanking and intercalated amino acids in the groove or pocket positions determine MHC binding affinity (and thus the peptide dwell time), they are hidden from the TCR. Only three variables determine the signaling directed to the TCR: whether the TCR engages the pentameric motif or not; how frequently that motif is encountered and hence the population of cognate T cells stimulated to engage it; and the dwell time of the peptide bound in the MHC groove. A precondition is that the peptide is efficiently processed by peptidases in the APC to allow excision of a peptide of appropriate length to bind in the MHC.

The second, and rather obvious, key point is that the repertoire of pentameric amino acid motifs in each recognition pattern is limited to 20^5 or 3.2 million permutations. These may be distributed in at least three different patterns: two recognition patterns based on binding in MHC II and one pattern based on binding in MHC I (58, 60). This limits the maximal repertoire of T-cell differentiation to 9.6 million. This is entirely consistent with estimates of a human's total T-cell count and the essential role of polyspecificity (62, 105). Given this relatively small number, it is not surprising that the large helminth proteomes we examined embodied a large percentage of the total pentameric possibilities, including the common motifs, and showed a high degree of overlap with the other proteomes and organisms examined. This mirrors findings of motif sharing among bacteria, both pathogens and commensal microbiome (57).

A further layer of variables, not addressed in this analysis, lies in the fact that multiple different clones of T cells may have TCR that bind the same TCEM peptide motif but with different affinities, and hence different dwell times, and that may trigger different cytokine outcomes (106). Higher binding affinity, consistent with higher suppressive indices, is reportedly more prone to generate IL-10 upregulation (106, 107). Binding based on less than five amino acid residues, or so-called "near neighbor" binding, further expands the possibilities for lesser binding affinities (108). The multiplicity of T-cell clones, which respond to any specific TCEM with differing binding affinities, do not change the importance of the TCEM cross-reactivity patterns but do expand the degrees of modulation possible.

The examples in **Figures 3** and **4** show, for a small number of TCEM IIA motifs, that shared motifs may be embedded within many different peptides. The differing MHC GEMs, those amino acids that are directed into the MHC pockets (i.e. the non-TCEM amino acids), each determine the affinity of binding to a different set of HLA. We have focused here only on those peptides, which generate the most extreme high suppressive indices. To achieve such a score, a peptide has to be able to bind to almost all HLA alleles with high affinity. Peptides that bind with high affinity to only two or three alleles would not achieve such a high score but would have a potentially suppressive effect in individuals carrying those alleles. This reinforces two points. First, the data shown are illustrations based on the most extreme cases of epitope sharing leading to potential shared immunosuppression, when in fact a much greater span of complexity of epitope networking patterns exists across lesser degrees of binding affinity. Second, regional/ethnic population adaptation to parasites – and by the parasites to their local hosts – may be a selection function of those alleles carried by the native subpopulation binding potentially suppressive peptides with greater affinity, while those of foreign hosts do not. In addition, peptide binding to mouse, or other animal, alleles may differ from human alleles, in some cases limiting the relevance of animal models.

The analyses, even with the limitations noted, suggest that a systems approach in which the immune response is seen as a network of shared T-cell engagement may be needed to fully understand the immunomodulatory functions of helminthiasis. What is extraordinary among the helminths, which initially drew our attention, is the presence of many extremely high suppressive indices, indicative of common TCEM combined with high binding by most or many HLA alleles. In this regard, the helminths, on an individual peptide basis, far outstrip viruses and bacteria we have previously examined, where any suppressive index over 100,000 would be considered very high and where we have only in extremely rare instances observed an index of >1,000,000. Overall, this is likely due to the large helminth proteomes that increase the probability of common TCEM motifs and, when these also bind to MHC, and potentially beneficial modulatory peptides will be selected over evolutionary time.

Where shared TCEM motifs occur between helminth species, it implies that the cognate T-cell population responsive to the first helminth TCEM would also be responsive, or cross-reactive, to the same TCEM where it occurs in a second helminth. If the MHC binding of the first motif is such that it has a long dwell time and is likely to elicit a Treg response (67–70); when that same motif occurs in a second helminth and is bound by the same T-cell clones, the effect of the Treg phenotype would carry over to the response to the second helminth. Induction of relatively few Treg cells may impact the effector cells within the local microenvironment through bystander suppression (109, 110). The lengthy association of the parasite with the host, and the motif sharing among multiple parasites, would ensure a chronic presence of motifs, which have high suppressive indices, thereby fulfilling another requirement for Treg induction, repeated stimulation (111). Whereas protozoal parasites employ antigenic variation as a defensive mechanism to maintain infection (73), helminths employ the continuity of antigenic signaling to modulate the host T cell as a defense, while the surface proteins retain their invasive and other functions. It appears that relatively few Treg responders are needed to overcome a stimulatory response (67).

Mycobacterium tuberculosis, *P. falciparum*, and *H. pylori* were selected as examples of co-infections for analysis based on literature reports of interaction with helminths (7, 13, 14, 18). The widespread sharing of TCEMs among helminths, host, and the three co-infections indicates that there is potential for T-cell repertoires conditioned by exposure to a co-infecting pathogen proteome to be cross-reactive with helminths and vice versa. TCEMs provide the minimal prerequisite for T-cell polyspecificity or cross-reactivity. The shared motif counts in **Table 2** are the maximum possible count of cross-reactions. This count must be further conditioned by MHC binding and peptidase processing and contemporaneous transcription. The degree of sharing is in part a function of the size of the proteome of each organism; the larger the proteome the more chance that rare motifs will be present and also that there will be more shared common motifs. However, such shared motifs can lead to mutual immunomodulatory consequences. Among the motifs that helminths share with the selected co-infections are potentially highly suppressive peptides, indicating, for example, that a Treg response elicited by *M. tuberculosis* may be shared with helminths, or vice versa. Notably, in *M. tuberculosis*, TCEM IIA matches resulting in high suppressive indices were found in 27 proteins of the PE and PE PGRS families, which have been reported to be associated

with Treg induction (112, 113). In *P. falciparum*, shared high suppressive index motifs were most frequently found in rifins and in proteins annotated as conserved plasmodium proteins. Rifins are a family of proteins expressed on *P. falciparum*-infected erythrocytes, which have been implicated in immune evasion through binding to immune inhibitory receptors and the development of severe malaria (114, 115). Less sharing was seen in *H. pylori*, which has a smaller proteome and where the interaction with helminths may not be dependent on immune mechanisms (18).

A networking model in which a helminth infection creates a Treg cell-rich microenvironment and simultaneously causes chronic tissue damage, and thus a high rate of host cell division prone to mutations, may also create an environment tolerant to the progression of neoplasia. Treg cells have been demonstrated to be increased in *Opisthorchis* infections (40) and may lead to impaired response to neoepitopes. While multiple mechanisms may trigger carcinogenesis, such a model could explain the emergence of cholangiocarcinoma following prolonged infection with *Clonorchis* or *Opisthorchis* (15, 18). Conversely, the increase in autoimmune, inflammatory, and allergic disease observed in the absence of helminths, or following anthelminthic application, would be consistent with removal of the peptides driving an immunosuppressive Treg-dominated network.

Helminth proteins contain a large number of homopolymers of amino acids along with repetitious simple amino acid motifs. Only a few homopolymers (glycines, leucines, serines, threonines, and tyrosines) contribute to the counts of higher frequency TCEMs; of these, only leucines and tyrosines result in fairly high binding affinity for multiple alleles. While such repeats are a more common feature of eukaryotes than prokaryotes (116) and may offer some selective advantages (117), they do not emerge as a driver of very high suppressive indices in the helminths examined. However, their presence does raise the question of whether multiple occurrences, especially of leucine or tyrosine observed in *L. loa*, might have an additive suppressive effect.

We omitted from consideration proteins under 50 amino acids in length. Some helminth proteomes included a large number of small open reading frames (sORFs). Whether sORFs which generate peptides large enough to bind MHCs may also contribute to the overall epitope landscape is unknown (118, 119). Given species differences in the curation of proteins for inclusion, a comparative analysis is not possible.

In addressing networking as a factor in immunomodulation, we have focused here on the most common TCEM and those that are shared by many helminths. We also noted that a very small percentage of TCEM motifs are unique to any single helminth among those evaluated; these may or may not be motifs rarely found in the immunoglobulinome but are unlikely to be among the most common motifs. **Figure 1** reflects the sharing patterns of motifs among helminth species. There is a range of less common motifs, which also have sharing patterns among the species (as reflected by the grey and red tiles in **Figure 1**). These are motifs that may elicit immune stimulation and potentially have utility in a vaccine. The challenge in designing a vaccine comprising T-cell epitopes is to identify proteins comprising conserved stimulatory epitopes, appropriately processed by cathepsins for MHC presentation, which are not negated by an immunosuppressive motif (120).

It is likely that many mechanisms are contributing simultaneously to immunomodulation. The proteins previously reported (24, 27, 28, 37) may have a primary or secondary role in immune regulation. The cystatins, which have been reported to play an immunomodulatory role in several parasites (121–123), would likely inhibit cathepsin function and, hence, peptide excision for presentation on the MHC. Others may act through the induction of Treg cells or as a downstream consequence of such regulation. Among the previously reported immunomodulators that we analyzed, only *T. spiralis* p53 was found to have a suppressive index over 300,000. Several others had suppressive indices below this level, indicating that they might have a suppressive effect in individuals of certain alleles, or when present in large amounts; the major egg antigen of *S. mansoni* is one example. However, it is important to keep in mind that several of the proteins previously examined for their immunomodulatory role are from helminths that are not human pathogens and they have been examined in animal models, so our analysis of suppressive index based on human alleles examines those out of the host context in which they were tested.

There has been increasing interest in exploiting the immunomodulatory effects of helminths (23, 26), by administering low level live parasite infections, extracts, or recombinant proteins (24, 25, 31). The TCEM networking model put forth here offers an approach to defining predicted immunomodulatory peptides, which have benefited from selection through an evolutionary filter and which may then be tested in a therapeutic model at less risk than a live parasite.

Given the lack of annotation of many individual proteins in the helminth proteomes, and the recognition that we have only worked with one isolate of each species, we have not focused here on highlighting the particular potential highly suppressive peptides for each parasite. Rather we have addressed this as a conceptual model. For every motif example for which we show an unambiguous predicted outcome for most HLA, there are many more subtle effects based on lower suppressive indices or particular host HLAs. The systems approach we have taken suggests that the immune response to a given parasite cannot be considered in isolation but should be seen as a part of an epitope ecosystem, or microenvironment, in which the potentially highly suppressive peptides in the helminths network through their common T-cell receptor recognition signals with T-cell epitopes in self proteins, microbiome, in other helminths and in taxonomically unrelated pathogens. It indicates the complexity of T-cell interactions, which may have allowed helminths to evolve to select for the peptides that drive an immunosuppressive repertoire of T cells. Such a repertoire would favor long-term coexistence with the host, or an immunogenetic subpopulation thereof, and facilitate polyparasitism and co-infections. This approach suggests that a different paradigm, in which epitope networking is considered, can contribute to understanding helminth associated immunomodulation. It is a paradigm, which is both very simple in conception and profoundly complex to test through a reductionist approach.

AUTHOR CONTRIBUTIONS

RB designed the algorithms, EH planned the study and performed the analyses, and EH and RB wrote the article.

ACKNOWLEDGMENTS

Systems analysis of this type is not possible without the assembly of genomes and proteomes into accessible databases such as EuPathDB, Patric, Wormbase, Uniprot, and the Human Microbiome Project. We are indebted to the consortia, which maintain such databases. The authors thank Erich Marquard Schwarz for insightful discussion and Alleen Hager for computational and editorial assistance.

SUPPLEMENTARY MATERIAL

The Supplementary Material for this article can be found online at https://www.frontiersin.org/articles/10.3389/fimmu.2018.01763/full#supplementary-material.

REFERENCES

1. Hotez PJ, Brindley PJ, Bethony JM, King CH, Pearce EJ, Jacobson J. Helminth infections: the great neglected tropical diseases. *J Clin Invest* (2008) 118(4): 1311–21. doi:10.1172/JCI34261
2. Brooker S, Bethony J, Hotez PJ. Human hookworm infection in the 21st century. *Adv Parasitol* (2004) 58:197–288. doi:10.1016/S0065-308X(04)58004-1
3. Herricks JR, Hotez PJ, Wanga V, Coffeng LE, Haagsma JA, Basanez MG, et al. The global burden of disease study 2013: what does it mean for the NTDs? *PLoS Negl Trop Dis* (2017) 11(8):e0005424. doi:10.1371/journal.pntd.0005424
4. McSorley HJ, Maizels RM. Helminth infections and host immune regulation. *Clin Microbiol Rev* (2012) 25(4):585–608. doi:10.1128/CMR.05040-11
5. Harris AR, Russell RJ, Charters AD. A review of schistosomiasis in immigrants in Western Australia, demonstrating the unusual longevity of *Schistosoma mansoni*. *Trans R Soc Trop Med Hyg* (1984) 78(3):385–8. doi:10.1016/0035-9203(84)90129-9
6. Wright EP, Jain S. Human infestation by *Taenia saginata* lasting over 20 years. *Postgrad Med J* (1984) 60(705):495–6. doi:10.1136/pgmj.60.705.495
7. Wammes LJ, Hamid F, Wiria AE, de Gier B, Sartono E, Maizels RM, et al. Regulatory T cells in human geohelminth infection suppress immune responses to BCG and *Plasmodium falciparum*. *Eur J Immunol* (2010) 40(2):437–42. doi:10.1002/eji.200939699
8. Cooper PJ, Chico M, Sandoval C, Espinel I, Guevara A, Levine MM, et al. Human infection with *Ascaris lumbricoides* is associated with suppression of the interleukin-2 response to recombinant cholera toxin B subunit following vaccination with the live oral cholera vaccine CVD 103-HgR. *Infect Immun* (2001) 69(3):1574–80. doi:10.1128/IAI.69.3.1574-1580.2001
9. Stelekati E, Wherry EJ. Chronic bystander infections and immunity to unrelated antigens. *Cell Host Microbe* (2012) 12(4):458–69. doi:10.1016/j.chom.2012.10.001
10. Supali T, Verweij JJ, Wiria AE, Djuardi Y, Hamid F, Kaisar MM, et al. Polyparasitism and its impact on the immune system. *Int J Parasitol* (2010) 40(10):1171–6. doi:10.1016/j.ijpara.2010.05.003
11. Maizels RM, Yazdanbakhsh M. T-cell regulation in helminth parasite infections: implications for inflammatory diseases. *Chem Immunol Allergy* (2008) 94:112–23. doi:10.1159/000154944
12. Babu S, Bhat SQ, Kumar NP, Jayantasri S, Rukmani S, Kumaran P, et al. Human type 1 and 17 responses in latent tuberculosis are modulated by coincident filarial infection through cytotoxic T lymphocyte antigen-4 and programmed death-1. *J Infect Dis* (2009) 200(2):288–98. doi:10.1086/599797
13. George PJ, Anuradha R, Kumaran PP, Chandrasekaran V, Nutman TB, Babu S. Modulation of mycobacterial-specific Th1 and Th17 cells in latent tuberculosis by coincident hookworm infection. *J Immunol* (2013) 190(10):5161–8. doi:10.4049/jimmunol.1203311
14. Chatterjee S, Nutman TB. Helminth-induced immune regulation: implications for immune responses to tuberculosis. *PLoS Pathog* (2015) 11(1): e1004582. doi:10.1371/journal.ppat.1004582
15. Sripa B, Kaewkes S, Sithithaworn P, Mairiang E, Laha T, Smout M, et al. Liver fluke induces cholangiocarcinoma. *PLoS Med* (2007) 4(7):e201. doi:10.1371/journal.pmed.0040201
16. Mostafa MH, Sheweita SA, O'Connor PJ. Relationship between schistosomiasis and bladder cancer. *Clin Microbiol Rev* (1999) 12(1):97–111.
17. Whary MT, Sundina N, Bravo LE, Correa P, Quinones F, Caro F, et al. Intestinal helminthiasis in Colombian children promotes a Th2 response to *Helicobacter pylori*: possible implications for gastric carcinogenesis. *Cancer Epidemiol Biomarkers Prev* (2005) 14(6):1464–9. doi:10.1158/1055-9965.EPI-05-0095
18. Brindley PJ, da Costa JM, Sripa B. Why does infection with some helminths cause cancer? *Trends Cancer* (2015) 1(3):174–82. doi:10.1016/j.trecan.2015.08.011
19. Cooper PJ. Intestinal worms and human allergy. *Parasite Immunol* (2004) 26(11–12):455–67. doi:10.1111/j.0141-9838.2004.00728.x
20. Correale J, Farez M. Association between parasite infection and immune responses in multiple sclerosis. *Ann Neurol* (2007) 61(2):97–108. doi:10.1002/ana.21067
21. Libbey JE, Cusick MF, Fujinami RS. Role of pathogens in multiple sclerosis. *Int Rev Immunol* (2014) 33(4):266–83. doi:10.3109/08830185.2013.823422
22. Sanya RE, Nkurunungi G, Andia Biraro I, Mpairwe H, Elliott AM. A life without worms. *Trans R Soc Trop Med Hyg* (2017) 111(1):3–11. doi:10.1093/trstmh/trx010
23. Wammes LJ, Mpairwe H, Elliott AM, Yazdanbakhsh M. Helminth therapy or elimination: epidemiological, immunological, and clinical considerations. *Lancet Infect Dis* (2014) 14(11):1150–62. doi:10.1016/S1473-3099(14)70771-6
24. Nascimento Santos L, Carvalho Pacheco LG, Silva Pinheiro C, Alcantara-Neves NM. Recombinant proteins of helminths with immunoregulatory properties and their possible therapeutic use. *Acta Trop* (2017) 166:202–11. doi:10.1016/j.actatropica.2016.11.016
25. Smallwood TB, Giacomin PR, Loukas A, Mulvenna JP, Clark RJ, Miles JJ. Helminth immunomodulation in autoimmune disease. *Front Immunol* (2017) 8: 453. doi:10.3389/fimmu.2017.00453
26. Harnett MM, Harnett W. Can parasitic worms cure the modern world's ills? *Trends Parasitol* (2017) 33(9):694–705. doi:10.1016/j.pt.2017.05.007
27. Finlay CM, Walsh KP, Mills KH. Induction of regulatory cells by helminth parasites: exploitation for the treatment of inflammatory diseases. *Immunol Rev* (2014) 259(1):206–30. doi:10.1111/imr.12164
28. Maizels RM, McSorley HJ. Regulation of the host immune system by helminth parasites. *J Allergy Clin Immunol* (2016) 138(3):666–75. doi:10.1016/j.jaci.2016.07.007
29. McSorley HJ, Loukas A. The immunology of human hookworm infections. *Parasite Immunol* (2010) 32(8):549–59. doi:10.1111/j.1365-3024.2010.01224.x
30. McSorley HJ, Hewitson JP, Maizels RM. Immunomodulation by helminth parasites: defining mechanisms and mediators. *Int J Parasitol* (2013) 43(3–4): 301–10. doi:10.1016/j.ijpara.2012.11.011
31. Navarro S, Pickering DA, Ferreira IB, Jones L, Ryan S, Troy S, et al. Hookworm recombinant protein promotes regulatory T cell responses that suppress experimental asthma. *Sci Transl Med* (2016) 8(362):362ra143. doi:10.1126/scitranslmed.aaf8807
32. Geiger SM, Fujiwara RT, Freitas PA, Massara CL, Dos Santos Carvalho O, Correa-Oliveira R, et al. Excretory-secretory products from hookworm l(3) and adult worms suppress proinflammatory cytokines in infected individuals. *J Parasitol Res* (2011) 2011:512154. doi:10.1155/2011/512154
33. Maizels RM, Philipp M, Ogilvie BM. Molecules on the surface of parasitic nematodes as probes of the immune response in infection. *Immunol Rev* (1982) 61:109–36. doi:10.1111/j.1600-065X.1982.tb00375.x
34. Ferreira I, Smyth D, Gaze S, Aziz A, Giacomin P, Ruyssers N, et al. Hookworm excretory/secretory products induce interleukin-4 (IL-4)+ IL-10+ CD4+

T cell responses and suppress pathology in a mouse model of colitis. *Infect Immun* (2013) 81(6):2104–11. doi:10.1128/IAI.00563-12
35. Lightowlers MW, Rickard MD. Excretory-secretory products of helminth parasites: effects on host immune responses. *Parasitology* (1988) 96(Suppl):S123–66. doi:10.1017/S0031182000086017
36. Coakley G, Maizels RM, Buck AH. Exosomes and other extracellular vesicles: the new communicators in parasite infections. *Trends Parasitol* (2015) 31(10):477–89. doi:10.1016/j.pt.2015.06.009
37. Morais SB, Figueiredo BC, Assis NRG, Alvarenga DM, de Magalhaes MTQ, Ferreira RS, et al. *Schistosoma mansoni* SmKI-1 serine protease inhibitor binds to elastase and impairs neutrophil function and inflammation. *PLoS Pathog* (2018) 14(2):e1006870. doi:10.1371/journal.ppat.1006870
38. Maizels RM, Smith KA. Regulatory T cells in infection. *Adv Immunol* (2011) 112:73–136. doi:10.1016/B978-0-12-387827-4.00003-6
39. Ricci ND, Fiuza JA, Bueno LL, Cancado GG, Gazzinelli-Guimaraes PH, Martins VG, et al. Induction of CD4(+)CD25(+)FOXP3(+) regulatory T cells during human hookworm infection modulates antigen-mediated lymphocyte proliferation. *PLoS Negl Trop Dis* (2011) 5(11):e1383. doi:10.1371/journal.pntd.0001383
40. Kaewraemruaen C, Sermswan RW, Wongratanacheewin S. Induction of regulatory T cells by *Opisthorchis viverrini*. *Parasite Immunol* (2016) 38(11): 688–97. doi:10.1111/pim.12358
41. Taylor MD, Harris A, Babayan SA, Bain O, Culshaw A, Allen JE, et al. CTLA-4 and CD4+ CD25+ regulatory T cells inhibit protective immunity to filarial parasites in vivo. *J Immunol* (2007) 179(7):4626–34. doi:10.4049/jimmunol.179.7.4626
42. Sawant DV, Gravano DM, Vogel P, Giacomin P, Artis D, Vignali DA. Regulatory T cells limit induction of protective immunity and promote immune pathology following intestinal helminth infection. *J Immunol* (2014) 192(6):2904–12. doi:10.4049/jimmunol.1202502
43. Doetze A, Satoguina J, Burchard G, Rau T, Loliger C, Fleischer B, et al. Antigen-specific cellular hyporesponsiveness in a chronic human helminth infection is mediated by T(h)3/T(r)1-type cytokines IL-10 and transforming growth factor-beta but not by a T(h)1 to T(h)2 shift. *Int Immunol* (2000) 12(5):623–30. doi:10.1093/intimm/12.5.623
44. Metenou S, Dembele B, Konate S, Dolo H, Coulibaly SY, Coulibaly YI, et al. At homeostasis filarial infections have expanded adaptive T regulatory but not classical Th2 cells. *J Immunol* (2010) 184(9):5375–82. doi:10.4049/jimmunol.0904067
45. Khan IA, Hakak R, Eberle K, Sayles P, Weiss LM, Urban JF Jr. Coinfection with *Heligmosomoides polygyrus* fails to establish CD8+ T-cell immunity against *Toxoplasma gondii*. *Infect Immun* (2008) 76(3):1305–13. doi:10.1128/IAI.01236-07
46. Marple A, Wu W, Shah S, Zhao Y, Du P, Gause WC, et al. Cutting Edge: helminth coinfection blocks effector differentiation of CD8 T cells through alternate host Th2- and IL-10-mediated responses. *J Immunol* (2017) 198(2): 634–9. doi:10.4049/jimmunol.1601741
47. Walsh CM, Smith P, Fallon PG. Role for CTLA-4 but not CD25+ T cells during *Schistosoma mansoni* infection of mice. *Parasite Immunol* (2007) 29(6):293–308. doi:10.1111/j.1365-3024.2007.00947.x
48. Sachdev D, Gough KC, Flynn RJ. The chronic stages of bovine *Fasciola hepatica* are dominated by CD4 T-cell exhaustion. *Front Immunol* (2017) 8:1002. doi:10.3389/fimmu.2017.01002
49. Huang Y, Mao K, Chen X, Sun MA, Kawabe T, Li W, et al. S1P-dependent interorgan trafficking of group 2 innate lymphoid cells supports host defense. *Science* (2018) 359(6371):114–9. doi:10.1126/science.aam5809
50. Logan J, Navarro S, Loukas A, Giacomin P. Helminth-induced regulatory T cells and suppression of allergic responses. *Curr Opin Immunol* (2018) 54:1–6. doi:10.1016/j.coi.2018.05.007
51. Loukas A, Bethony J, Brooker S, Hotez P. Hookworm vaccines: past, present, and future. *Lancet Infect Dis* (2006) 6(11):733–41. doi:10.1016/S1473-3099(06)70630-2
52. Noon JB, Aroian RV. Recombinant subunit vaccines for soil-transmitted helminths. *Parasitology* (2017) 144(14):1845–70. doi:10.1017/S003118201700138X
53. Jia TW, Melville S, Utzinger J, King CH, Zhou XN. Soil-transmitted helminth reinfection after drug treatment: a systematic review and meta-analysis. *PLoS Negl Trop Dis* (2012) 6(5):e1621. doi:10.1371/journal.pntd.0001621
54. Albonico M, Smith PG, Ercole E, Hall A, Chwaya HM, Alawi KS, et al. Rate of reinfection with intestinal nematodes after treatment of children with mebendazole or albendazole in a highly endemic area. *Trans R Soc Trop Med Hyg* (1995) 89(5):538–41. doi:10.1016/0035-9203(95)90101-9
55. Ahumada V, Garcia E, Dennis R, Rojas MX, Rondon MA, Perez A, et al. IgE responses to *Ascaris* and mite tropomyosins are risk factors for asthma. *Clin Exp Allergy* (2015) 45(7):1189–200. doi:10.1111/cea.12513
56. Loukas A, Prociv P. Immune responses in hookworm infections. *Clin Microbiol Rev* (2001) 14(4):689–703. doi:10.1128/CMR.14.4.689-703.2001
57. Bremel RD, Homan J. Extensive T-cell epitope repertoire sharing among human proteome, gastrointestinal microbiome, and pathogenic bacteria: implications for the definition of self. *Front Immunol* (2015) 6:538. doi:10.3389/fimmu.2015.00538
58. Birnbaum ME, Mendoza JL, Sethi DK, Dong S, Glanville J, Dobbins J, et al. Deconstructing the peptide-MHC Specificity of T cell recognition. *Cell* (2014) 157(5):1073–87. doi:10.1016/j.cell.2014.03.047
59. Wucherpfennig KW. The structural interactions between T cell receptors and MHC-peptide complexes place physical limits on self-nonself discrimination. *Curr Top Microbiol Immunol* (2005) 296:19–37.
60. Rudolph MG, Stanfield RL, Wilson IA. How TCRs bind MHCs, peptides, and coreceptors. *Annu Rev Immunol* (2006) 24:419–66. doi:10.1146/annurev.immunol.23.021704.115658
61. Bremel RD, Homan EJ. An integrated approach to epitope analysis II: a system for proteomic-scale prediction of immunological characteristics. *Immunome Res* (2010) 6(1):8. doi:10.1186/1745-7580-6-8
62. Wucherpfennig KW, Allen PM, Celada F, Cohen IR, De Boer R, Garcia KC, et al. Polyspecificity of T cell and B cell receptor recognition. *Semin Immunol* (2007) 19(4):216–24. doi:10.1016/j.smim.2007.02.012
63. Bogen B, Weiss S. Processing and presentation of idiotypes to MHC-restricted T cells. *Int Rev Immunol* (1993) 10:337–55. doi:10.3109/08830189309061709
64. Weiss S, Bogen B. B-lymphoma cells process and present their endogenous immunoglobulin to major histocompatibility complex-restricted T cells. *Proc Natl Acad Sci U S A* (1989) 86(1):282–6. doi:10.1073/pnas.86.1.282
65. Bremel RD, Homan EJ. Frequency patterns of T-cell exposed amino acid motifs in immunoglobulin heavy chain peptides presented by MHCs. *Front Immunol* (2014) 5:541. doi:10.3389/fimmu.2014.00541
66. Hoglund RA, Lossius A, Johansen JN, Homan J, Benth JS, Robins H, et al. In silico prediction analysis of idiotope-driven T-B cell collaboration in multiple sclerosis. *Front Immunol* (2017) 8:1255. doi:10.3389/fimmu.2017.01255
67. Li MO, Rudensky AY. T cell receptor signalling in the control of regulatory T cell differentiation and function. *Nat Rev Immunol* (2016) 16(4):220–33. doi:10.1038/nri.2016.26
68. Valitutti S. The serial engagement model 17 years after: from TCR triggering to immunotherapy. *Front Immunol* (2012) 3:272. doi:10.3389/fimmu.2012.00272
69. Faroudi M, Zaru R, Paulet P, Muller S, Valitutti S. Cutting edge: T lymphocyte activation by repeated immunological synapse formation and intermittent signaling. *J Immunol* (2003) 171(3):1128–32. doi:10.4049/jimmunol.171.3.1128
70. Gabrysova L, Wraith DC. Antigenic strength controls the generation of antigen-specific IL-10-secreting T regulatory cells. *Eur J Immunol* (2010) 40(5):1386–95. doi:10.1002/eji.200940151
71. Gett AV, Sallusto F, Lanzavecchia A, Geginat J. T cell fitness determined by signal strength. *Nat Immunol* (2003) 4(4):355–60. doi:10.1038/ni908
72. Feng Y, Brazin KN, Kobayashi E, Mallis RJ, Reinherz EL, Lang MJ. Mechanosensing drives acuity of alphabeta T-cell recognition. *Proc Natl Acad Sci U S A* (2017) 114(39):E8204–13. doi:10.1073/pnas.1703559114
73. Zarowiecki M, Berriman M. What helminth genomes have taught us about parasite evolution. *Parasitology* (2015) 142(Suppl 1):S85–97. doi:10.1017/S0031182014001449
74. Blaxter M, Koutsovoulos G. The evolution of parasitism in Nematoda. *Parasitology* (2015) 142(Suppl 1):S26–39. doi:10.1017/S0031182014000791
75. Schwarz EM, Hu Y, Antoshechkin I, Miller MM, Sternberg PW, Aroian RV. The genome and transcriptome of the zoonotic hookworm *Ancylostoma ceylanicum* identify infection-specific gene families. *Nat Genet* (2015) 47(4): 416–22. doi:10.1038/ng.3237
76. Mulvenna J, Sripa B, Brindley PJ, Gorman J, Jones MK, Colgrave ML, et al. The secreted and surface proteomes of the adult stage of the carcinogenic human liver fluke *Opisthorchis viverrini*. *Proteomics* (2010) 10(5):1063–78. doi:10.1002/pmic.200900393

77. Young ND, Campbell BE, Hall RS, Jex AR, Cantacessi C, Laha T, et al. Unlocking the transcriptomes of two carcinogenic parasites, *Clonorchis sinensis* and *Opisthorchis viverrini*. *PLoS Negl Trop Dis* (2010) 4(6):e719. doi:10.1371/journal.pntd.0000719
78. Almeida CR, Stoco PH, Wagner G, Sincero TC, Rotava G, Bayer-Santos E, et al. Transcriptome analysis of *Taenia solium* cysticerci using open reading frame ESTs (ORESTES). *Parasit Vectors* (2009) 2(1):35. doi:10.1186/1756-3305-2-35
79. Bennuru S, Cotton JA, Ribeiro JM, Grote A, Harsha B, Holroyd N, et al. Stage-specific transcriptome and proteome analyses of the filarial parasite *Onchocerca volvulus* and Its *Wolbachia* endosymbiont. *mBio* (2016) 7(6):e2028–2016. doi:10.1128/mBio.02028-16
80. Harris TW, Lee R, Schwarz E, Bradnam K, Lawson D, Chen W, et al. WormBase: a cross-species database for comparative genomics. *Nucleic Acids Res* (2003) 31(1):133–7. doi:10.1093/nar/gkg053
81. Tang YT, Gao X, Rosa BA, Abubucker S, Hallsworth-Pepin K, Martin J, et al. Genome of the human hookworm *Necator americanus*. *Nat Genet* (2014) 46(3):261–9. doi:10.1038/ng.2875
82. Ghedin E, Wang S, Spiro D, Caler E, Zhao Q, Crabtree J, et al. Draft genome of the filarial nematode parasite *Brugia malayi*. *Science* (2007) 317(5845): 1756–60. doi:10.1126/science.1145406
83. Tallon LJ, Liu X, Bennuru S, Chibucos MC, Godinez A, Ott S, et al. Single molecule sequencing and genome assembly of a clinical specimen of *Loa loa*, the causative agent of loiasis. *BMC Genomics* (2014) 15:788. doi:10.1186/1471-2164-15-788
84. Cotton JA, Bennuru S, Grote A, Harsha B, Tracey A, Beech R, et al. The genome of *Onchocerca volvulus*, agent of river blindness. *Nat Microbiol* (2016) 2:16216. doi:10.1038/nmicrobiol.2016.216
85. Korhonen PK, Pozio E, La Rosa G, Chang BC, Koehler AV, Hoberg EP, et al. Phylogenomic and biogeographic reconstruction of the *Trichinella* complex. *Nat Commun* (2016) 7:10513. doi:10.1038/ncomms10513
86. Foth BJ, Tsai IJ, Reid AJ, Bancroft AJ, Nichol S, Tracey A, et al. Whipworm genome and dual-species transcriptome analyses provide molecular insights into an intimate host-parasite interaction. *Nat Genet* (2014) 46(7):693–700. doi:10.1038/ng.3010
87. Huang Y, Chen W, Wang X, Liu H, Chen Y, Guo L, et al. The carcinogenic liver fluke, *Clonorchis sinensis*: new assembly, reannotation and analysis of the genome and characterization of tissue transcriptomes. *PLoS One* (2013) 8(1):e54732. doi:10.1371/journal.pone.0054732
88. Young ND, Nagarajan N, Lin SJ, Korhonen PK, Jex AR, Hall RS, et al. The *Opisthorchis viverrini* genome provides insights into life in the bile duct. *Nat Commun* (2014) 5:4378. doi:10.1038/ncomms5378
89. Cwiklinski K, Dalton JP, Dufresne PJ, La Course J, Williams DJ, Hodgkinson J, et al. The *Fasciola hepatica* genome: gene duplication and polymorphism reveals adaptation to the host environment and the capacity for rapid evolution. *Genome Biol* (2015) 16:71. doi:10.1186/s13059-015-0632-2
90. Berriman M, Haas BJ, LoVerde PT, Wilson RA, Dillon GP, Cerqueira GC, et al. The genome of the blood fluke *Schistosoma mansoni*. *Nature* (2009) 460(7253):352–8. doi:10.1038/nature08160
91. Protasio AV, Tsai IJ, Babbage A, Nichol S, Hunt M, Aslett MA, et al. A systematically improved high quality genome and transcriptome of the human blood fluke *Schistosoma mansoni*. *PLoS Negl Trop Dis* (2012) 6(1):e1455. doi:10.1371/journal.pntd.0001455
92. Tsai IJ, Zarowiecki M, Holroyd N, Garciarrubio A, Sanchez-Flores A, Brooks KL, et al. The genomes of four tapeworm species reveal adaptations to parasitism. *Nature* (2013) 496(7443):57–63. doi:10.1038/nature12031
93. Bremel RD, Homan EJ. An integrated approach to epitope analysis I: dimensional reduction, visualization and prediction of MHC binding using amino acid principal components and regression approaches. *Immunome Res* (2010) 6:7. doi:10.1186/1745-7580-6-7
94. Wattam AR, Abraham D, Dalay O, Disz TL, Driscoll T, Gabbard JL, et al. PATRIC, the bacterial bioinformatics database and analysis resource. *Nucleic Acids Res* (2014) 42(Database issue):D581–91. doi:10.1093/nar/gkt1099
95. Aurrecoechea C, Barreto A, Basenko EY, Brestelli J, Brunk BP, Cade S, et al. EuPathDB: the eukaryotic pathogen genomics database resource. *Nucleic Acids Res* (2017) 45:D581–91. doi:10.1093/nar/gkw1105
96. Vita R, Overton JA, Greenbaum JA, Ponomarenko J, Clark JD, Cantrell JR, et al. The immune epitope database (IEDB) 3.0. *Nucleic Acids Res* (2015) 43(Database issue):D405–12. doi:10.1093/nar/gku938
97. Johnson NL. Systems of frequency curves generated by methods of translation. *Biometrika* (1949) 36(Pt 1–2):149–76. doi:10.2307/2332539
98. Crow JF. Perspective: here's to fisher, additive genetic variance, and the fundamental theorem of natural selection. *Evolution* (2002) 56(7):1313–6. doi:10.1111/j.0014-3820.2002.tb01445.x
99. Lessard S. Fisher's fundamental theorem of natural selection revisited. *Theor Popul Biol* (1997) 52(2):119–36. doi:10.1006/tpbi.1997.1324
100. Bremel RD, Homan EJ. Recognition of higher order patterns in proteins: immunologic kernels. *PLoS One* (2013) 8(7):e70115. doi:10.1371/journal.pone.0070115
101. Kall L, Krogh A, Sonnhammer EL. A combined transmembrane topology and signal peptide prediction method. *J Mol Biol* (2004) 338(5):1027–36. doi:10.1016/j.jmb.2004.03.016
102. Gilabert A, Curran DM, Harvey SC, Wasmuth JD. Expanding the view on the evolution of the nematode dauer signalling pathways: refinement through gene gain and pathway co-option. *BMC Genomics* (2016) 17:476. doi:10.1186/s12864-016-2770-7
103. Viney M. The genomic basis of nematode parasitism. *Brief Funct Genomics* (2018) 17(1):8–14. doi:10.1093/bfgp/elx010
104. Flanagan KL, Wilson KL, Plebanski M. Polymorphism in liver-stage malaria vaccine candidate proteins: immune evasion and implications for vaccine design. *Expert Rev Vaccines* (2016) 15(3):389–99. doi:10.1586/14760584.2016.1125785
105. Mason D. A very high level of crossreactivity is an essential feature of the T-cell receptor. *Immunol Today* (1998) 19(9):395–404.
106. Sprouse ML, Shevchenko I, Scavuzzo MA, Joseph F, Lee T, Blum S, et al. Cutting edge: low-affinity TCRs support regulatory T cell function in autoimmunity. *J Immunol* (2018) 200(3):909–14. doi:10.4049/jimmunol.1700156
107. Sprouse ML, Scavuzzo MA, Blum S, Shevchenko I, Lee T, Makedonas G, et al. High self-reactivity drives T-bet and potentiates Treg function in tissue-specific autoimmunity. *JCI Insight* (2018) 3(2):97322. doi:10.1172/jci.insight.97322
108. Petrova GV, Gorski J. Cross-reactive responses to modified M1(5)(8)-(6)(6) peptides by CD8(+) T cells that use noncanonical BV genes can describe unknown repertoires. *Eur J Immunol* (2012) 42(11):3001–8. doi:10.1002/eji.201242596
109. Belkaid Y, Tarbell K. Regulatory T cells in the control of host-microorganism interactions. *Annu Rev Immunol* (2009) 27:551–89. doi:10.1146/annurev.immunol.021908.132723
110. Tang Q, Bluestone JA. The Foxp3+ regulatory T cell: a jack of all trades, master of regulation. *Nat Immunol* (2008) 9(3):239–44. doi:10.1038/ni1572
111. Levine AG, Arvey A, Jin W, Rudensky AY. Continuous requirement for the TCR in regulatory T cell function. *Nat Immunol* (2014) 15(11):1070–8. doi:10.1038/ni.3004
112. Delogu G, Brennan MJ. Comparative immune response to PE and PE_PGRS antigens of *Mycobacterium tuberculosis*. *Infect Immun* (2001) 69(9):5606–11. doi:10.1128/IAI.69.9.5606-5611.2001
113. Chatrath S, Gupta VK, Dixit A, Garg LC. PE_PGRS30 of *Mycobacterium tuberculosis* mediates suppression of proinflammatory immune response in macrophages through its PGRS and PE domains. *Microbes Infect* (2016) 18(9):536–42. doi:10.1016/j.micinf.2016.04.004
114. Saito F, Hirayasu K, Satoh T, Wang CW, Lusingu J, Arimori T, et al. Immune evasion of *Plasmodium falciparum* by RIFIN via inhibitory receptors. *Nature* (2017) 552(7683):101–5. doi:10.1038/nature24994
115. Goel S, Palmkvist M, Moll K, Joannin N, Lara P, Akhouri RR, et al. RIFINs are adhesins implicated in severe *Plasmodium falciparum* malaria. *Nat Med* (2015) 21(4):314–7. doi:10.1038/nm.3812
116. Sim KL, Creamer TP. Abundance and distributions of eukaryote protein simple sequences. *Mol Cell Proteomics* (2002) 1(12):983–95. doi:10.1074/mcp.M200032-MCP200
117. Haerty W, Golding GB. Low-complexity sequences and single amino acid repeats: not just "junk" peptide sequences. *Genome* (2010) 53(10):753–62. doi:10.1139/G10-063
118. Plaza S, Menschaert G, Payre F. In search of lost small peptides. *Annu Rev Cell Dev Biol* (2017) 33:391–416. doi:10.1146/annurev-cellbio-100616-060516
119. Couso JP, Patraquim P. Classification and function of small open reading frames. *Nat Rev Mol Cell Biol* (2017) 18(9):575–89. doi:10.1038/nrm.2017.58

120. Morais SB, Figueiredo BC, Assis NRG, Homan J, Mambelli FS, Bicalho RM, et al. Schistosoma mansoni SmKI-1 orIts C-terminal fragment induces partial protection against S. mansoni infection in mice. *Front Immunol* (2018) 9:1762. doi:10.3389/fimmu.2018.01762
121. Jang SW, Cho MK, Park MK, Kang SA, Na BK, Ahn SC, et al. Parasitic helminth cystatin inhibits DSS-induced intestinal inflammation via IL-10(+) F4/80(+) macrophage recruitment. *Korean J Parasitol* (2011) 49(3):245–54. doi:10.3347/kjp.2011.49.3.245
122. Sun Y, Liu G, Li Z, Chen Y, Liu Y, Liu B, et al. Modulation of dendritic cell function and immune response by cysteine protease inhibitor from murine nematode parasite *Heligmosomoides polygyrus*. *Immunology* (2013) 138(4):370–81. doi:10.1111/imm.12049
123. Hartmann S, Kyewski B, Sonnenburg B, Lucius R. A filarial cysteine protease inhibitor down-regulates T cell proliferation and enhances interleukin-10 production. *Eur J Immunol* (1997) 27(9):2253–60. doi:10.1002/eji.1830270920

Conflict of Interest Statement: Both authors are employees and equity holders in ioGenetics LLC, the parent company of EigenBio LLC.

The reviewer PT and handling Editor declared their shared affiliation.

frontiers in Immunology

REVIEW
published: 26 November 2018
doi: 10.3389/fimmu.2018.02741

Leptin Functions in Infectious Diseases

Radheshyam Maurya[1]*, *Parna Bhattacharya*[2], *Ranadhir Dey*[2] and *Hira L. Nakhasi*[2]

[1] Department of Animal Biology, School of Life Science, University of Hyderabad, Hyderabad, India, [2] Division of Emerging and Transfusion Transmitted Diseases, Center for Biologics Evaluation and Research, Food and Drug Administration, Silver Spring, MD, United States

Leptin, a pleiotropic protein has long been recognized to play an important role in the regulation of energy homeostasis, metabolism, neuroendocrine function, and other physiological functions through its effects on the central nervous system (CNS) and peripheral tissues. Leptin is secreted by adipose tissue and encoded by the obese (*ob*) gene. Leptin acts as a central mediator which regulates immunity as well as nutrition. Importantly, leptin can modulate both innate and adaptive immune responses. Leptin deficiency/resistance is associated with dysregulation of cytokine production, increased susceptibility toward infectious diseases, autoimmune disorders, malnutrition and inflammatory responses. Malnutrition induces a state of immunodeficiency and an inclination to death from communicable diseases. Infectious diseases are the disease of poor who invariably suffer from malnutrition that could result from reduced serum leptin levels. Thus, leptin has been placed at the center of many interrelated functions in various pathogenic conditions, such as bacterial, viruses and parasitic infections. We review herein, the recent advances on the role of leptin in malnutrition in pathogenesis of infectious diseases with a particular emphasis on parasitic diseases such as Leishmaniasis, Trypanosomiasis, Amoebiasis, and Malaria.

Keywords: leptin, leishmaniasis, trypanosomiasis, amoebiasis, malaria, bacteria, virus, malnutrition

OPEN ACCESS

Edited by:
Xun Suo,
China Agricultural University, China

Reviewed by:
Theo Araújo-Santos,
Universidade Federal do Oeste da Bahia, Brazil
Abhigyan Satyam,
Harvard Medical School, United States

***Correspondence:**
Radheshyam Maurya
rmusl@uohyd.ernet.in;
radhemaurya@rediifmail.com

Specialty section:
This article was submitted to Microbial Immunology, a section of the journal Frontiers in Immunology

Received: *20 March 2018*
Accepted: *07 November 2018*
Published: *26 November 2018*

Citation:
Maurya R, Bhattacharya P, Dey R and Nakhasi HL (2018) Leptin Functions in Infectious Diseases. Front. Immunol. 9:2741. doi: 10.3389/fimmu.2018.02741

INTRODUCTION

Leptin is a hormone derived from adipocytes in response to the nutritional status, and it signals to the central nervous system (CNS) and peripheral organs (1). The circulating plasma leptin concentrations are mostly influenced by the total body fat mass index, metabolic hormones, and gender. Women have higher concentrations of circulating leptin compared to men (2). The central function of leptin is metabolic homeostasis that can be attained by the delivery of information about the total body fat mass to the hypothalamus that in turn alters the CNS function and regulates glucocorticoids, insulin hormone and food intake & energy balance (3, 4). Concurrently, leptin is also a critical regulator of immunity and functions as a pro-inflammatory cytokine-like interleukin (IL)-1, IL-6, IL-8, IL-18, and tumor necrosis factor-α (TNF-α), and its deficiency increases susceptibility to infectious (5–8).

Leptin was identified as the gene defect responsible for the obesity syndrome in Leptin-deficient (*ob*/*ob*) mice and reported as the product of *Ob* gene (9, 10). Leptin is a 16 kDa α-helix type protein like the long-chain helical cytokine family such as IL-6, IL-2, IL-12, leukocyte inhibitory factor (LIF), Granulocyte-colony stimulating factor (G-CSF), Ciliary neurotrophic factor (CNTF),

and Oncostatin M (11, 12). Most of the biological functions of leptin are exerted through leptin receptor (Ob-R) signaling via the Janus kinase/signal transducer and activator of transcription (JAK/STAT) pathway (13, 14). In general, leptin enhances the immune response via activating antigen presenting cells (APCs), Th1 cells function and proliferation, and mediating the secretion of the pro-inflammatory cytokines, such as TNF-α, IL-2, or IL-6 (7, 15, 16). Leptin-deficient (*ob/ob*; double knockout obese gene) and leptin receptor-deficient (*db/db*; double knockout obese receptor gene) mice display marked reduction in the size & thymic atrophy and exhibit defective immune responses (17, 18). Similarly, reduced leptin levels in starved and malnourished individuals is further associated with alterations of the immune response and thymic atrophy. However, these conditions can be reversed by leptin administration (19–22).

Over the past decade, the role leptin in infectious diseases was extensively explored. It has been reported that leptin deficiency is correlated with starvation or nutritional deprivation/malnutrition (23). Malnutrition affects both innate & acquired immunity of the host (24) thereby increasing the incidences of infections and mortality (25). The immune dysfunction in malnutrition or restricted calorie intake reduced the memory T cells, total CD4+ and CD8+ T cell numbers compared to well-nourished infected controls (26–29). Interestingly, leptin has a crucial role in mediating phagocytosis, T cell number, function, and metabolism in both obesity and malnutrition. The systemic circulating leptin deficiency in malnutrition is also correlated with several other bacterial, viral and parasitic infections such as tuberculosis (30), pneumonia (31), sepsis (32), colitis (33), viral infection (34, 35) leishmaniasis (36), trypanosomiasis (37), amoebiasis (38), and malaria (39) due to defective cytokine production (40–45). Hence, nutritional status is critically essential for immune cell function in both malnutrition and infection. Understanding how leptin is altered in malnutrition and infection will lead to better insight of and treatment for diseases where nutritional status determines clinical outcome. Furthermore, there has been increasing evidence that leptin is involved in the pathogenesis of various infectious diseases. In the present review, we will discuss the emerging role of leptin in different infectious diseases and will further highlight how malnutrition or starvation could play a role.

LEPTIN AND IMMUNITY

Leptin is a pleiotropic molecule, which can function as a hormone as well as cytokine (adipokine). Almost all immune cells such as neutrophils, monocytes, lymphocytes express leptin receptor and it belongs to the family of class-I cytokine receptors (46–48). Leptin regulates angiogenesis, hematopoiesis, innate & adaptive immunity and induces the Th1 response by increasing IFN-γ, IL-2, and TNF-α production, subsequently leading to the activation of monocyte/macrophages and prevents the apoptosis of various immune cells by delaying the cleavage of Bid and Bax (49–55).

In innate immunity, leptin enhances the activity and function of neutrophils by the release of oxygen free radicals, increased CD11b expression and intercellular adhesion molecule-1 (ICAM-1), which leads to migration of immune cells at the sites of inflammation (56–58). Leptin activates the monocytes and dendrite cells (DCs) that in turn leads to the production of pro-inflammatory cytokines such as TNF-α, IL-6 along with IL-12, a key cytokine that facilitates the shifting of T-cells toward the Th1 phenotype (59–62). Leptin also promotes DCs survival by triggering the activation of nuclear factor-kappa B (NF-kappa B) and up-regulates B-cell lymphoma 2 (Bcl-2) and B-cell lymphoma-extra-large (Bcl-xL) gene expression via the PI3K-Akt signaling pathway (62). Moreover, upon leptin stimulation, DCs also exhibit increased production of multiple cytokines including IL-1, IL-6, IL-12, TNF-α, MIP-1α and induces the expression of surface molecules, such as CD1a, CD80, CD83, or CD86 (63, 64). Indirectly, leptin leads to the activation of natural killer (NK) cells upon modulation of IL-1, IL-6, and TNF-α via monocytes and macrophages (61) resulting an increased IL-12 and reduced IL-15 expression in NK cells (65, 66).

In adaptive immunity, leptin induces the maturation and survival of thymic T-cells by reducing their rate of apoptosis through inhibition of FAS-directed apoptosis pathway (16, 67). Eventually, leptin has anti-apoptotic effects on mature T-cells, by up-regulating the expression of Bcl-xL (68), T-box transcription factor (T-bet) (69), and synergizes with other cytokines in lymphocyte proliferation and activation possibly via signal transducer and activator of transcription 3 (STAT3) signaling (70, 71). Leptin deficiency in both mouse and human results in severe immune defects characterized by decrease in total lymphocytes, CD4+ helper T cell number, increased thymocyte apoptosis, and a skewing away from the Th1 toward Th2 phenotype thereby resulting in increased susceptibility to intracellular infections (16, 17, 72–74). Leptin mediates T-cells polarization by inducing the cell-mediated immune response through the secretion of IL-2, IL-12, TNF-α, and IFN-γ from Th1 cells and suppresses the production of IL-10 and IL-4 from Th2 cells (13, 75–78). In facts, thymocytes treated with leptin induces CD4+CD8+ cell differentiation mainly to CD4+ mature thymocytes (79). Additionally, leptin also activates human B cells to secrete cytokines, such as IL-6, IL-10, and TNF-α, through the activation of JAK2/STAT3 and p38MAPK/ERK1/2 signaling pathways (80, 81). Leptin-STAT3 signaling also influences the production of C-X-C chemokine receptor type 3 (CXCR3) and C-C chemokine receptor type 5 (CCR5) ligands, which are preferentially expressed on Th1 cells and enhances pro-inflammatory cytokines such as IL-1β, TNF-α, and IL-6 in serum (39, 82, 83). In conclusion, leptin acts as a Th1 cytokine and regulates all immune cells through leptin receptor and affects innate & adaptive immune responses together facilitating a shift toward Th1 response. The brief role of leptin in innate & adaptive immune response was summarized in **Figure 1**.

LEPTIN IN MALNUTRITION

Nutritional deficiency impaired phagocyte function, cell-mediated immunity, cytokine production, antibody response and the complement system (24, 25, 84) and predisposed to

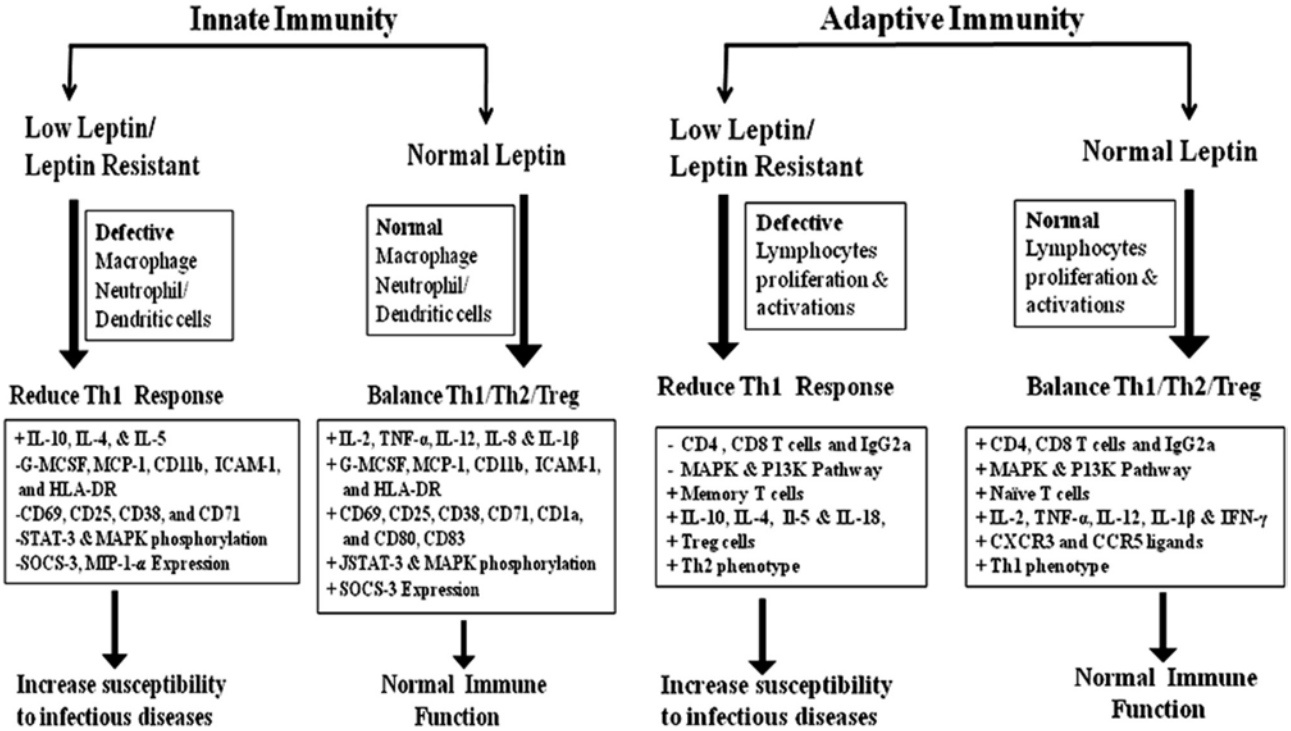

FIGURE 1 | The role of leptin in Innate and adaptive immunity: innate immunity; Leptin plays a crucial role in the activation and proliferation of macrophage, neutrophil, and dendritic cells through the up and down regulation of various cytokine/chemokines. Adaptive immunity; Leptin-induced the activation and proliferation of total lymphocytes (T and B cells), regulatory T cells and Naive T cells through the up and down regulation of pro-inflammatory and anti-inflammatory cytokines. The Innate and adaptive immune response induced by leptin signaling through the phosphorylation of MAKP/STAT-3/P13K pathways (15–18, 49–55).

death from infectious diseases (85). Concurrently, malnutrition is the most common cause of secondary immunodeficiency worldwide associated with protein-energy malnutrition (PEM) (86, 87), a nutritional deficiency in which individuals suffer from protein but not calorific malnutrition (88). Strikingly, PEM causes a drastic reduction in body fat mass and decreases the circulating concentration of leptin, which, in turn, impairs the generation of proinflammatory mediators [IFN-γ, TNF-α and (NO) nitric oxide] (89, 90), and increases the incidence of infectious diseases (72, 83). Malnutrition is a primary risk factor for many infectious diseases. From recent research, it seems that malnutrition is a predictor of tuberculosis disease and is associated with worse outcomes. Active tuberculosis is correlated with weight loss, cachexia, and low serum concentrations of leptin which in turn suppresses the lymphocyte stimulation and Th1 cytokines such as IL-2, IFN-γ, and TNF-α secretion (91–96). PEM significantly reduced the lymphocyte stimulation as well as secretion of the Th1 cytokines such as IL-2, IFN-γ, and TNF-α, in M. tuberculosis-infected guinea pig (92, 97). Furthermore, PEM also diminishes leptin concentrations and increases serum levels of stress hormones, i.e., glucocorticoids which impairs macrophage functions by limiting NF-kB translocation into the nucleus (96). Macrophages from experimental PEM mice are less sensitive to lipopolysaccharides (LPS) due to decreased NF-kB translocation resulting in impairment of active phagocytosis, cytokines response and reactive oxygen intermediates (ROIs) productions (98–101).

Serum leptin concentration decreases as malnutrition becomes more pronounced and thus serves as a biomarker of poor nutritional status in chronic cirrhosis due to viral hepatitis and candidiasis due to *Candida albicans* (102–105). Moreover, during fasting or starvation, leptin levels also fall disproportionately due to the decrease in adipose tissue fat mass (106, 107). The decrease in leptin level during starvation rendered wild-type mice susceptible to LPS and TNF-α induced lethality whereas leptin treatment restores those changes despite ongoing starvation, suggesting that the lack of leptin plays a role in the immune dysfunction during starvation (18, 108). Exogenous leptin administration modulates T cell responses in mice and prevents starvation-induced immune suppression on the development of a delay type of hypersensitivity (DTH) response and protects from starvation-induced lymphoid atrophy in mice (12, 15, 68, 109).

Taken together, Leptin is a protein hormone secreted by adipocytes, regulating body fat and food intake through neuroendocrine-signaling system. Hence, it is possible to speculate that leptin might act in the brain to directly regulate metabolic response along with peripheral immune function thereby contributing to better outcomes in various infectious diseases compared with states of relative or total leptin deficiency. Importantly, recent studies reported that

serum leptin level may be used as a promising diagnostic or prognostic marker for critical illness sepsis that is triggered by an infective agent such as bacteria, viruses, fungi, or parasites (110). Therefore, from here onwards, the review focuses on the role of leptin in various infectious diseases.

LEPTIN AND BACTERIAL INFECTIONS

Leptin-deficient mice and mice rendered leptin-deficient by fasting exhibit impaired pulmonary bacterial clearance (**Table 1**) and enhanced lethality during pulmonary tuberculosis, bacterial pneumonia, and sepsis (30–32). The patients with pulmonary tuberculosis (PTB) have decreased serum leptin levels, and an increase in adiponectin may serve as a reliable biomarker for predicting the development and progression of PTB pathogenesis (111, 145, 146). Mycobacterium infection in *ob/ob* mice was hampered to produce organized granulomatous response and defective in CD4+ and CD8+ T cells functions, IFN-γ and DTH responses (30). The mechanisms underlying the defective leukocyte effector function in cells from leptin-deficient mice were associated with a reduction in leukotriene (LT) synthesis in alveolar macrophage (AMs), reduced complement receptor (CR3) expression and decreased H_2O_2 synthesis in neutrophils (PMNs) infected with *Klebsiella pneumoniae* (112–114). Restoring the level of circulating leptin to physiological levels in fasted and *ob/ob* mice significantly improved the survival and pulmonary bacterial clearance, reduced bacteraemia, reconstituted alveolar macrophage phagocytosis and increased H_2O_2 production in the PMNs resulting in increased killing of *S. pneumonia in vitro* (31, 115). Leptin binding to leptin receptor activates multiple intracellular signaling pathways, including STAT3, STAT5, and ERK1/2. STAT3 activates transcription of suppressor of cytokine signaling (SOCS)-3, a protein that inhibits JAK2 and STAT3 signaling during prolonged stimulation of the Leptin receptor long isoform (*Lep-Rb*) (147, 148). *Lep-Rb* mediated phosphorylation of Tyr^{1077} activates STAT5 signaling pathway (149). Phosphorylation of Tyr^{985} in leptin receptor recruits binding partners SH2-containing tyrosine phosphatase (SHP-2) and growth factor binding 2 (GRB2) which activate extracellular signal-regulated kinase 1 and 2 (ERK 1/2) signaling (147, 150). A mutation of the Try^{985} with L^{985} residue in the leptin receptor exhibited increased mortality and impaired pulmonary bacterial clearance following an intratracheal challenge with *K. pneumoniae* due to the disruption of ERK-dependent activation (151).

Moreover, Leptin-dependent neutrophilic phagocytosis of *L. monocytogenes* was more potent than *Escherichia coli* due to the presence of apoptotic factor Listeriolysin O, which is absent in *E. coli* (116). Exogenous leptin restored the anti-listeria resistance and monocyte chemoattractant protein-1 (MCP-1) and MIP-2 production in leptin-deficient mice (117, 152). *Clostridium difficile colitis* is a primary causative agent of nosocomial infection in humans and murine. The defective STAT3 signaling pathway leads to susceptibility to infectious colitis and bacterial peritonitis (33, 153) and leptin treatment restored the protective mucosal immune response in *C. difficile colitis* by the STAT3 inflammatory pathway (33).

In contrast to above finding, disruption of leptin receptor-mediated STAT3 signaling pathway improved AMs phagocytosis and host defense against *P. pneumonia* in ($Lepr^{s1138/s1138}$) s/s mice following an intratracheal challenge with *S. pneumonia* (154). These effects are mediated by an intracellular signaling pathway that is dependent on ERK1/2 activation in AMs resulting an increased in LT synthesis, which enhanced the phagocytosis in cells from *s/s* mice (154). Mice infected with *Helicobacter pylori*-induced pro-inflammatory cytokine response and enhanced the leptin secretion from gastric mucosa which may be playing a role in weight gain after eradication of *H pylori* infection (118–120) suggesting that leptin has a local effect rather than systemic action in patients with gastritis (121, 155). These findings reveal the existence of a relevant neuroendocrine control of leptin in systemic immune defense in various bacterial diseases thereby highlighting the possible therapeutic potential of leptin analogous to control infectious diseases.

LEPTIN AND VIRAL INFECTIONS

Mice deficient in the leptin receptor or malnourished leads to impaired viral clearance (**Table 1**), diminished lung IFNγ level and reduced survival during influenza-A pneumonia infections (156). The mice lacking functional leptin receptor in T cells ($LepR^{T-/-}$) limits pH1N1 influenza mortality and infection severity in obese mice suggesting that leptin signaling in T cells may be a critical mediator of pH1N1 severity in obese mice (122, 123). Moreover, Leptin resistant obese mice or decreased leptin level in obese individuals may increase the susceptibility to influenza virus infection by suppressing the memory T-cell function and IFN-α, IFN-β, and IFN-γ mRNA expression which leads to an increase in viral titer and infiltration (124). Furthermore, mice lacking functional leptin receptor in tissue-specific lung epithelial and macrophage cells have improved viral clearance and reduced lung injury following influenza-A infection suggesting that leptin signaling is also associated with non-myeloid cells such as natural killer cells and T cells (125). Leptin significantly upregulated the Th17 subset but suppressed Th2 subset differentiation possibly via regulating ERK1/2 phosphorylation in human bronchial epithelial cells (hBECs) infected with the respiratory syncytial virus (RSV) (126). Human immunodeficiency virus (HIV)-infected patients have an exaggerated expression of leptin receptor on their blood mononuclear cells while low leptin levels in their serum leads to an immune deficiency in these patients (127, 128). Importantly, leptin therapy, a novel strategy now in clinical trials, and its beneficial positive role in HIV patients in correction of metabolic complications related to HIV-associated lipodystrophy syndrome (HALS) has been reported recently (129). Leptin also diminishes the oxidative status of monocytes suggesting that leptin can alter the redox status of monocytes, which leads to immunological alterations in HIV infection (35). Therefore, taken together these findings reveal that leptin could control the systemic immune defense failure in viral specific immune cells dysfunction and

TABLE 1 | The distinctive immune responses in various infectious diseases upon leptin treatment were summarized.

Infectious group	Infectious species	Effect of leptin on the Immune response	Model used (*in-vitro & in-vivo*)	References
Bacterial disease	*Mycobacterium tuberculosis*	Increase IFNγ & TNF-α levels and PMN cells & functions. Increase T helper CD4 T cells & CD8 T cells activity. Improve Ag- specific antibody response. Restored DTH response and Granuloma formation. Reduced IL-6 cytokine and bacterial load.	Mice and human	(30, 95, 111)
	Klebsiella pneumonia	Increase phagocytosis index and Leukotriene synthesis. Improve defective alveolar macrophage phagocytosis. Restored CD11b expression level. Decrease bacterial load and reduce mortality.	Mice	(112, 113)
	Pneumococcal pneumonia	Restored defective alveolar macrophage phagocytosis activity. Increase PMN H_2O_2 production. Reduced TNF-α, MIP-2, PGE2 in the lung. Improves pulmonary bacterial clearance and survival.	Mice	(31, 114)
	Clostridium difficile	Leptin receptor Q223R mutation leads to defective STAT3 signaling pathway and associated with an increased risk of colitis. Mutation of tyrosine 1,138 in the intracellular domain of LepRb decreased mucosal chemokine and cell recruitment. Increases inflammation, colonic chemokine expression, and cellular recruitment. Improve the bacterial clearance.	Mice	(33)
	Sepsis	Improve the Neutrophil function. Increase the phosphorylation of p38 MAP kinase. Control sepsis-induced organ damage Supresses IL-6 and MCP-1 level. Control the bacteraemia.	Mice and rat	(32, 110, 115)
	Listeria monocytogenes	Induce CD11b expression on neutrophils and lower the apoptosis. Induce effective bacterial phagocytosis and lymphocytic apoptosis in sever immune-deficiency. Improvement of anti-listerial resistance and the MCP-1 mRNA expression. Decrease defective MCP-1 expression in the liver. Control the bacteraemia.	Mice	(116, 117)
	Helicobactor pylori	Increase mucosal leptin in the infected patients compare to uninfected patients. Amount of gastric leptin correlated positively with the mucosal levels of IL-1β and IL-6, but not IL-8 cytokine. Increase of gastric leptin expression during infection may have a local rather than systemic action. Increase in serum leptin concentration. Circulating leptin correlated with body mass index, but not with bacterial load. There was no change in plasma leptin levels following cure of the infection.	Mice and human	(118–121)
Viral disease	Influenza A/H1N1 pneumonia	Global deficiency of leptin receptor (db/db) have worsened survival following influenza A infection. Leptin receptor deficiency impaired viral clearance & diminished the IFN-γ levels. Loss of leptin receptor within lung epithelium or within macrophages is not associated with worsened lung injury or mortality following infection. Decrease proinflammatory cytokines IL-6 and IL-1β level and increase survival. Disruption of leptin signaling in T cells limits worsened the pH1N1 dependent mortality and infection severity.	Human and mice	(34, 122–125)
	Respiratory Syncytial Virus	Promoted Th17 subset differentiation. Suppressed Th2 subset differentiation. Increased phosphorylation of ERK1/2 in peripheral Lymphocytes.	Human	(126)
	HIV	Leptin inhibits ROS and control oxidative burst mechanism in HIV+ monocyte patients. Leptin receptor (ob-R) expression increased in HIV+ PBMCs than control. Serum leptin level positively correlated with CD4+ T lymphocyte during antiviral therapy in HIV patients. Supresses SOCS3 & mTOR expression and Th2 subset differentiation. Reduced viral load.	Human and mice (*in-vitro* & *in-vivo*)	(35, 127–129)

(Continued)

TABLE 1 | Continued

Infectious group	Infectious species	Effect of leptin on the Immune response	Model used (*in-vitro & in-vivo*)	References
Parasitic disease	*Leishmania major/Leishmania donovani*	Activates macrophage phagocytosis and ROS induction. Enhances the phosphorylation of Erk1/2 & Akt in macrophages. Increases IFN-γ, IL12, IL-1β secretion in macrophage. Improve IFN-γ/IL-10 ratio, GrzA and Th1 cytokine response. Activate CD8+ T-cell compartment and reduces PD-1 & CTLA-4 expression. Increase IgG2a levels and improve IgG2a/IgG1 ratio. Improve granuloma formation and repaired tissue degeneration. Reduced parasite load in visceral organs.	Human (THP-1 and PBMCs) Mice (*in-vitro* & *in-vivo*)	(36, 49, 130–132)
	Trypanosoma cruzi	Defective leptin receptors or reduction in leptin level increase parasitemia and mortality rate. Reconstitution of central leptin signaling in brain reduces tissue parasitism and mortality rates. Improve plasma cytokines and chemokine's.	Mice	(37, 133–136)
	Entamoeba histolytica	Mutation in leptin receptor (LEPR Q223R). Substitution of arginine (223R) in the cytokine receptor homology domain 1 of LEPR are more susceptible than those have glutamine (223Q) amino acid. Q223R polymorphism also decreased leptin-dependent STAT3 activation and defective STAT3 signaling and increase susceptibility to liver & intestinal abscess. Q223R leptin receptor mutation results in defective neutrophil infiltration to the site of infection. Mutation of tyrosine 985 or 1138 in leptin receptor results in defective SHP2/ERK and STAT3 signaling. Leptin-mediated resistance to amebiasis requires leptin receptor signaling through both the STAT3 and SHP2/ERK pathways. Leptin promotes regeneration & mucin secretion by epithelial cell and control apoptosis & integrity in intestinal epithelium lining. Low serum leptin increase liver and intestinal abscess. Intestinal parasites deregulate the secretion of leptin and adiponectin and play a role in enteric parasitosis by modulating body immunity, food intake and blood chemistry.	Human and mice	(38, 137–142)
	Plasmodium berghei ANKA parasite	Higher serum leptin levels. Increase mTORC1 (Mechanistic target of rapamycin complex 1) activity in CD4+ and CD8+ T cells in a dose dependent manner. Leptin act as downstream target for mTORC1 activity in T cells during ECM. The *leptin* gene mutation in *ob/ob* is associated with observed CM resistance phenotype. CM resistance phenotype is due to involvement of Th1 cytokines TNF-α and INF-γ in the regulatory cascade controlling inflammatory responses after malarial infections.	Mice	(39, 143, 144)

further suggests the possible healing potential for leptin analogs in infectious disease.

LEPTIN AND PARASITIC INFECTIONS

Parasitic infections contribute significantly to the burden of communicable diseases worldwide. Reportedly, much of infections and mortality from parasitic illnesses are restricted mainly in developing countries (157). Malnutrition or loss of appetite is a common characteristic of many infectious diseases including parasitic infections which result in reduced serum leptin levels (158). Since, leptin has been reported to induce pro-inflammatory cytokines & chemokines, neutrophil chemotaxis, NK cell cytotoxicity, and T cell functions, therefore its deficiency leads to an increase in susceptibility to infectious diseases (64, 65, 159, 160). Furthermore, leptin exerts central effects on hypothalamic-pituitary function and disruption of these effects have been implicated into severe parasitic diseases due to immune dysfunction in host (35–38).

Moreover, very little is known about the role of leptin in pathogenesis of parasitic infections. There is a need for studying the role of leptin in controlling parasitic infections since preponderance of such infections is associated with malnutrition which goes hand in hand in developing countries. As a first step, we have highlighted some of these studies to generate interest in initiating such studies (**Table 1**).

Leishmaniasis

Leishmaniasis is a vector-borne protozoan disease caused by Leishmania parasites. Leishmaniasis is commonly prevalent in tropical and subtropical regions of the world with different immunopathology and varying degrees of morbidity and mortality. Among which, Visceral Leushmaniasis (VL) is

the deadliest form of the diseases, marked by uncontrolled parasitemia in the spleen, liver, and bone marrow (161, 162).

VL is an endemic disease found mostly in economically poor societies, who invariably suffer from malnutrition. Malnutrition is characterized by the lower serum leptin level which in turn adversely alters the development of innate and adaptive immune responses during VL in both mice and children living in endemic areas (163–165). Hence, malnutrition and low serum leptin level are playing a critical role in *Leishmania* infection and its pathogenesis. Leptin improved cytokine production and phagocytosis of *Leishmania donovani* by murine and human macrophages by increasing the phagolysosome formation and oxidative killing of the parasite via intracellular reactive oxygen species (ROS) generation (36). Leptin in combination with miltefosine, the conventional antileishmanial drug, augments the protective immunity in mouse macrophage during *L. donovani* infection *in vitro* (130). Similarly, it enhances the host protective Th1 cytokine responses in THP-1, and human PMBCs derived macrophages by inducing Erk1/2 and Akt phosphorylation, which is usually dephosphorylated in *L. donovani* infection (36). It can also maintain the protective environment against *L. donovani* infection through the classical macrophage activation (36). Recently we demonstrated that leptin induces the innate immune response in bone marrow-derived antigen presenting dendritic cells, and causes heightened nitric oxide, proinflammatory cytokines (IFN-γ, IL-12, and IL1β) in the splenocytes stimulated with soluble Leishmania antigen. Besides this, leptin-induced IFN-γ production from both CD4+ and CD8+ T cells compared with untreated infected normal mice, indicates that leptin-induced heightened Th1 response (131). Alternatively, leptin deficient *ob/ob* mice had higher splenic and liver parasite burden compared with the normal infected mice. Nevertheless, leptin treatment of *ob/ob* mice failed to reduce the splenic parasite burden and host-protective cytokine response. Moreover, in contrast to DCs from a normal mouse, *ob/ob* mouse-derived DCs showed limitation in the initiation of innate immune response during *Leishmania* infection that could not be restored by leptin treatment suggesting that leptin signaling was differentially regulated in *ob/ob* mice compared with normal mice fed with healthy diet (131, 166). Interestingly, very recently we demonstrated that leptin also induces a protective CD8+ T-cell dependent immune response in malnutrition coupled with *L. donovani* infection through up-regulation of Granzyme A (GrzA) and down-regulation of cytotoxic T-lymphocyte-associated protein 4 (CTLA-4) and Programmed death-1 (PD-1) markers (132). The PD-1 ligand plays a significant role in CD8+ T cell exhaustion during the chronic infections of various infectious diseases including VL (167). It is worth mentioning here that in contrast to the above reports an increased expression or activity of leptin, has been reported in blood samples of dogs with canine leishmaniasis (CanL) and suggested possible use of leptin as a biomarker for CanL (168). In conclusion, leptin treatment may improve parasite clearance in malnourished VL condition through restoration of normal immune cell function via leptin signaling.

Trypanosomiasis

Chagas disease is caused by a protozoan parasite *Trypanosoma cruzi*. The parasite is transmitted to humans and other hosts mainly by feces of infected blood-feeding triatomines, blood transfusion, or by ingestion of contaminated food (169). Chagas disease remains a serious health problem in Central and South America and a major cause of morbidity and mortality (135, 170). *T. cruzi* uses adipocytes as a reservoir for chronic infection and displays a pro-inflammatory phenotype by upregulating cytokines such as IL-1β, IFN-γ, TNF-α, and chemokines such as CCL2, CXCL10, and CCL5 along with innate immune receptors such as Toll-like receptor (TLR)-2 and 9 (171–173). Other pathways, such as ERK and PI3K pathways were also activated upon *T. cruzi* infection (174, 175). Additionally, Adipose tissue profoundly expressed Peroxisome proliferator-activated receptor (PPAR-γ) along with adiponectin, which exerts an anti-inflammatory effect. The levels of PPAR-γ were also decreased in *T. cruzi* infected cells, which leads to the reduced secretion of adiponectin and increased inflammatory reactions (176).

Since parasite infects many organs including adipose tissue which is a source to a variety of adipokines, including leptin and could have significant role in pathogenesis of Trypanosomiasis (133, 134). Mice infected with *T. cruzi* showed significant reduction in leptin levels, possibly due to adipocyte involvement in disease progression (133, 135). It was also reported that chemically induced diabetic mice and genetically susceptible *db/db* diabetic mice with defective leptin receptors had higher parasitemia and mortality after *T. cruzi* infection, which suggests that the dysregulation of host metabolism may be beneficial to parasitic survival in the host (136). Moreover, mice with defective leptin receptor are metabolically challenged and upon infection with *T. cruzi* suffer high mortality (37). In NSE-Rb *db/db* mice, a genetically modified *db/db* mouse, central leptin signaling is reconstituted only in the brain which is sufficient to correct the metabolic defects and when infected with *T. cruzi* showed reduced parasitemia, mortality rates, and tissue parasitism as compared to normal *db/db* mice. The plasma levels of several cytokines and chemokines were also significantly increased in infected *db/db* mice compared with NSE-Rb *db/db* mice (37). In summary, the normalization of the metabolic dysfunction in NSE-Rb *db/db* mice through the restoration of leptin receptor signaling in brain reconstitute the normal immune response against *T. cruzi* infection, but not peripheral restoration, highlighting that leptin may play a role as a central regulator for both metabolic function and immune response.

Amoebiasis

Amoebiasis is the disease caused by an enteric protozoan parasite *Entamoeba histolytica*. Infection results from ingestion of the parasite cyst from feces-contaminated food or water (177). *E. histolytica* primarily lives in the intestinal mucosa and mainly restricted in colon infection causing devastating dysentery, colitis, and liver abscess by producing tissue damages (178, 179) while many deaths are associated with extraintestinal invasive disease (180, 181). Amoebiasis occurs when trophozoites disrupt the mucosal barrier and penetrate the underlying tissue and break down extracellular matrix, destroy cells, and phagocytose cellular

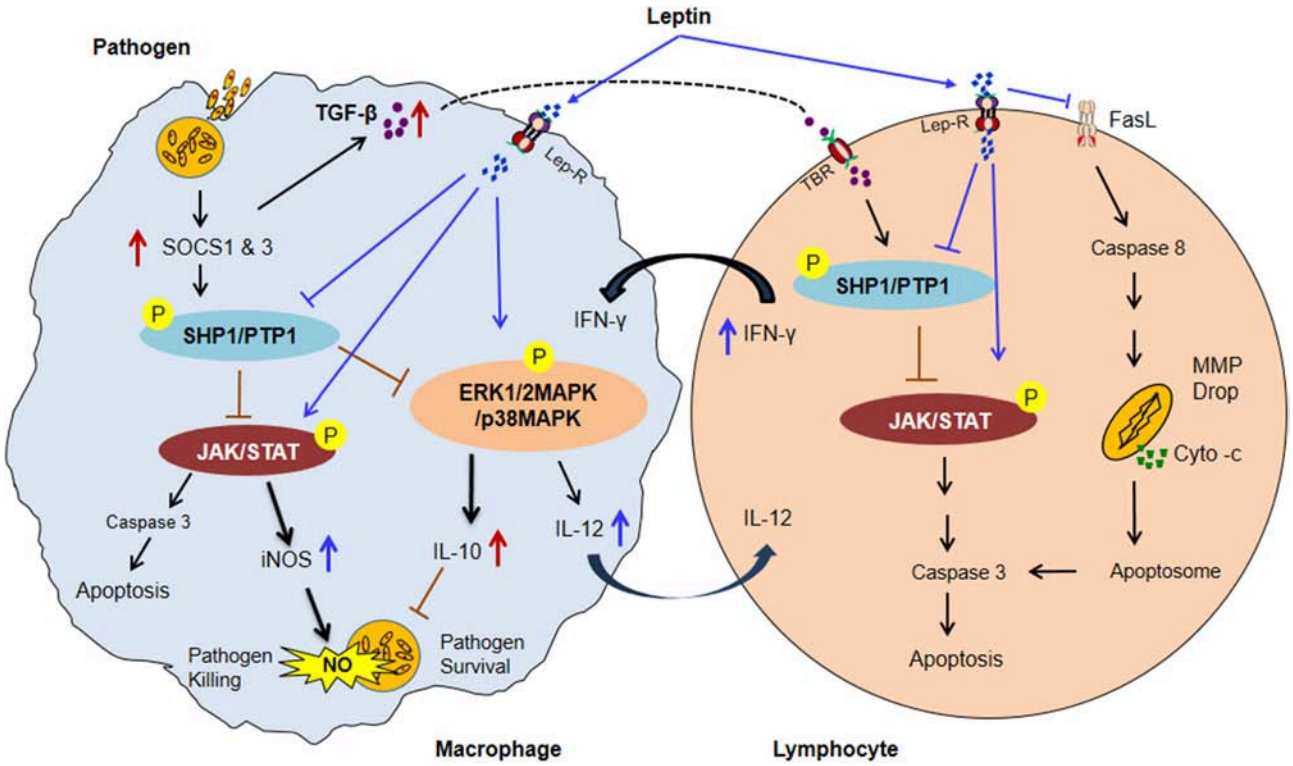

FIGURE 2 | The possible model of Leptin and Immune response in malnutrition coupled infectious diseases. In malnutrition, low adipocyte mass causes a reduction of serum leptin level resultant impairment of normal macrophages and lymphocytes activities. Infected macrophages induce the SOCS1 & 3 proteins expression subsequently upregulates ROS scavenging enzyme Thioredoxin which leads to activates SHP1/PTPase molecules. SHP1/PTP1 negatively regulates the JAK/STAT, and MAP-Kinase pathways thus inhibiting IFN–inducible macrophage functions (increased IL-10 and TGF-β level and decreased the IL-12 cytokines in infected macrophage). IL-10 suppresses the NO activity and improves the parasite survival. TGF-β activates SHP1/PTPase activity in lymphocytes through TGF-β receptor (TBR) which leads to lymphocytes apoptosis. In contrast, Leptin treatment inactivated SHP1/PTPase directed pathways and reversed the macrophage activities by up-regulating the pro-inflammatory cytokines (IFNγ, TNF-α, and IL-12) secretion and NO expression. IL-12 cytokine released from activated macrophage upon leptin treatment inhibits the SHP1/PTPase dependent T lymphocytes apoptosis by activation of JAK/STAT pathway. Moreover, Leptin directly inhibits the FasL-dependent T lymphocytes apoptosis by the inhibition of the caspase 8 activity. Caspase-8 then promotes mitochondrial outer membrane permeabilization (MOMP) by diminishing the inhibitory effect of various antiapoptotic and proapoptotic molecules. MOMP results in cytochrome-c release from the mitochondria, enabling activation of a supramolecular complex, the apoptosome that activates caspase-3 to undertake apoptotic cell death (Suppressors of cytokine signaling: SOCS1 & 3; Protein tyrosine phosphatases: SHP1/PTP1, Mitochondrial membrane potential drop: MMP drop, and P: phosphorylation) (192–206).

debris (182). Studies on amoebic liver abscess (ALA) carried out in Indian subcontinent suggest that malnutrition is associated with ALA outcome (183, 184).

Moreover, malnutrition and serum leptin levels are directly proportional to the pathogenesis of amoebiasis, and low serum leptin plays a critical role in *E. histolytica*- associated diarrheal illness and extent of liver injury (137, 185). The mucosal immune response can be suppressed by a mutation in leptin receptor and defective STAT3 signaling pathways, resulting in susceptibility to intestinal abscess due to *E. histolytica* infections (38, 138). The mechanism of mucosal immune suppression depends on homozygous allelic mutation in leptin receptor Q223R (rs1137101) that ablates STAT3 signaling, results in decreased mucosal chemokine's LIF, CXCL9, CXCL10, CCL3, and CCL4 secretion (68, 69). A mutation or polymorphism in leptin receptor at 233 (from glutamine to arginine) is liable to enhance 4 times more susceptibility to *E. histolytica* infection in children irrespective of nutritional status (139). The leptin-deficient (*ob/ob*) and LepRb-deficient (*db/db*) mice were highly susceptible to infection with *E. histolytica*, whereas wild-type C57BL/6 mice were resistant. Moreover, mice either homozygous or heterozygous for the 223R allele of leptin receptor were significantly more prone to amoebic infection. Both types of mice ceca were shown to have profound epithelial denudation because of trophozoites invasion. Leptin signaling in the intestinal epithelium and downstream STAT3 and SHP2 (Src homology phosphatase 2) signaling was required for protection in the murine model of amoebic colitis (140). Leptin-mediated specific activation of STAT3 and ERK or Akt signaling pathways in gut mucosal epithelial cells offers more resistance against amoebiasis caused by *E. histolytica* infection (141, 142). In conclusion, leptin may control the amoebic infections by the activation of leptin signaling pathway in gut mucosal epithelial cells via up-regulation of various signaling pathway.

Malaria

Malaria is caused by *Plasmodium* species, an intracellular parasite transmitted by the bite of an infected female Anopheles mosquito. It is endemic in most of the tropical countries such as sub-tropical regions of Asia, Africa, South and Central America (186). *Plasmodium falciparum* is the most virulent form of the human malaria parasites and responsible for 90% of malaria-related morbidity and mortality (187). During a mosquito bite, sporozoites are injected into host's skin, enter the bloodstream and reach to the liver. Parasites differentiate and replicate inside hepatocytes, and then released as merozoites into the bloodstream, which subsequently invades red blood cells (RBCs) (186).

Inflection of diet can affect the outcome of parasitic diseases either through the effects on parasite growth and development, or via the host immune response, or both. Leptin is a cytokine predominantly secreted by adipocytes that increases in proportion to total body fat mass, and upon exposure to pro-inflammatory cytokines, it inhibits both appetite and adiposity in malaria infection (39). Moreover, serum leptin levels were approximately five-fold higher in *Plasmodium berghei*-infected mice than in non-infected controls (188). Leptin-deficient mice infected with *P. berghei* ANKA were shown to be resistant to the development of cerebral malaria whereas the normal mice developed signs of cerebral malaria. Dietary restriction prevented severe experimental cerebral malaria (ECM) symptoms and death in mice through modulation of leptin levels and mechanistic target of rapamycin complex 1 (mTORC1) activity in T cells (143). Pharmacological inhibition of either leptin signaling with a mutant peptide, or downstream mTORC1 signaling with rapamycin, blocked ECM symptoms and reduced mortality (39). Furthermore, leptin exerts central effects on hypothalamic-pituitary function and these outcomes might affect the severity of malaria disease. Disturbance in hypothalamic-pituitary-adrenal axis during *P. falciparum* infection have been involved in the pathogenic mechanism of severe malaria (144). Importantly, the level of leptin in serum of malaria patients has been recently reported to be used as prognostic markers of treatment outcomes and pathogenesis of malaria patients (144). In conclusion, leptin could play an important role to control the immuno-compromised malarial infections by the activation of immune cells through leptin signaling pathway.

CONCLUSION AND SUMMARY

Many studies have been conducted in recent past to understand the role of leptin in immune modulation such as activation of phagocytosis, cytokine polarization and cell-mediated immunity in infectious diseases. Both obesity and malnutrition are pandemics associated with immune-deficiencies that lead to increased vulnerability to infectious disease. Interestingly, both obesity and malnutrition are related to aberrant leptin levels, obesity due to chronically elevated leptin levels, whereas malnutrition results in significantly diminished leptin levels. Emerging data from animal models and human indicates that immune dysfunction underlies the etiology of malnutrition and reduced immune-mediated protection from infections, which interplay between nutrition, leptin levels and immune responses (86, 189, 190). Malnutrition is characterized by immune suppression and increased risk of mortality from infectious diseases (191). The immune dysfunction is not only a consequence of inadequate diet but also contributes in various mechanisms, including the energy homeostasis, metabolism, the role of leptin and it signals to the hypothalamic-pituitary-adrenal axis and peripheral organs. Thus, it is likely that the CNS plays a critical role in malnutrition associated immune deficiency. Protein-energy malnutrition reduces leptin concentrations which impairs macrophage functions, ability to engulf pathogens and to produce proinflammatory cytokines (25, 27). Importantly, leptin has a crucial role in mediating innate and adaptive immune response which are significantly affected by nutritional status and play a vital role in the immune adaptation in both malnutrition and infection. Moreover, many infectious diseases directly or indirectly are linked to malnutrition which compromises the innate and adaptive immunity of host and increased susceptibility to infectious disease.

More importantly the mechanism of leptin signaling in various infectious diseases is depends on SOCS3 expression as describes in NF-κB dependent pathway. The SOCS3 expression attenuates the macrophage's response to IFN-γ at both proximal level activation and downstream expression. Hence, taken together above-mentioned observations indicate that the potential role of leptin signaling in various pathogens has been summarized in a schematic diagram (**Figure 2**) (192–205). Therefore, understanding the link between nutrition, leptin, and immune dysfunction in murine and human infectious diseases will inform targeted interventions for a vulnerable population with undernutrition, which is a crucial need for new approaches to reduce global mortality from infectious diseases. Present review provides a rationale for future studies to explore role of leptin as therapeutics to host immune dysfunction in infectious diseases during malnutrition.

AUTHOR CONTRIBUTIONS

RM conceived and conducted literature reviews, figure, and table construction and contributed to the writing of the manuscript. PB, RD, and HN critically edited and reviewed the complete manuscript, tables and figures. All authors approved the final manuscript for submission.

ACKNOWLEDGMENTS

We sincerely thank University Grant Commission (UGC), DST-SERB, DST-FIST, DST-Purse and University of Hyderabad for providing the lab infrastructure and subscription of many scientific journal and books to compile the review. FDA authors' contributions represent their best judgment and do not bind or obligate the FDA.

REFERENCES

1. La Cava A, Matarese G. The weight of leptin in autoimmunity. *Nat Rev Immunol.* (2004) 4:371–9. doi: 10.1038/nri1350
2. Grinspoon S, Gulick T, Askari H, Landt M, Lee K, Anderson E, et al. Serum leptin levels in women with anorexia nervosa. *J Clin Endocrinol Metab.* (1996) 81:3861–3.
3. Mantzoros CS, Magkos F, Brinkoetter M, Sienkiewicz E, Dardeno TA, Kim SY, et al. Leptin in human physiology and pathophysiology. *Am J Physiol Endocrinol Metab.* (2011) 301:E567–84. doi: 10.1152/ajpendo.00315.2011
4. Dardeno TA, Chou SH, Moon HS, Chamberland JP, Fiorenza CG, Mantzoros CS. Leptin in human physiology and therapeutics. *Front Neuroendocrinol.* (2010) 31:377–93. doi: 10.1016/j.yfrne.2010.06.002
5. Faggioni R, Jones-Carson J, Reed DA, Dinarello CA, Feingold KR, Grunfeld C, et al. Leptin-deficient (*ob*/*ob*) mice are protected from T cell-mediated hepatotoxicity: role of tumor necrosis factor α and IL-18. *Proc Natl Acad Sci USA.* (2000) 97:2367–72. doi: 10.1073/pnas.040561297
6. Procaccini C, Jirillo E, Matarese G. Leptin as an immunomodulator. *Mol Aspects Med.* (2012) 33:35–45. doi: 10.1016/j.mam.2011.10.012
7. Fernandez-Riejos P, Najib S, Santos-Alvarez J, Martín-Romero C, Pérez-Pérez A, González-Yanes C, et al. Role of leptin in the activation of immune cells. *Media Inflamm.* (2010) 2010:568343. doi: 10.1155/2010/568343
8. Sharma A, Satyam A, Sharma JB. Leptin, IL-10 and inflammatory markers (TNF-alpha, IL-6 and IL-8) in pre-eclamptic, normotensive pregnant and healthy non-pregnant women. *Am J Reprod Immunol.* (2007) 58:21–30. doi: 10.1111/j.1600-0897.2007.00486.x
9. Zhang Y, Proenca R, Maffei M, Barone M, Leopold L, Friedman JM. Positional cloning of the mouse obese gene and its human homologue. *Nature* (1994) 372:425–32. doi: 10.1038/372425a0
10. Coleman DL. Obese and diabetes: two mutant genes causing diabetes-obesity syndromes in mice. *Diabetologia* (1978) 14:141–8. doi: 10.1007/BF00429772
11. Madej T, Boguski MS, Bryant SH, Threading analysis suggests that the obese gene product may be a helical cytokine. *FEBS Lett.* (1995) 373:13–8. doi: 10.1016/0014-5793(95)00977-H
12. Tartaglia LA, Dembski M, Weng X, Deng N, Culpepper J, Devos R, et al. Identification and expression cloning of a leptin receptor, OB-R. *Cell* (1995) 83:1263–71. doi: 10.1016/0092-8674(95)90151-5
13. Licinio J, Mantzoros C, Negrão AB, Cizza G, Wong ML, Bongiorno PB, et al. Human leptin levels are pulsatile and inversely related to pituitary-adrenal function. *Nat Med.* (1997) 3:575–9. doi: 10.1038/nm0597-575
14. Mansour E, Pereira FG, Araujo EP, Amaral MEC, Morari J, Ferraroni NR, et al. Leptin inhibits apoptosis in thymus through a janus kinase-2-independent, insulin receptor substrate-1/phosphatidylinositol-3 kinase-dependent pathway. *Endocrinology* (2006) 147:5470–9. doi: 10.1210/en.2006-0223
15. Martin-Romero C, Santos-Alvarez J, Governa R, Sanchez-Margalet V. Human leptin enhances activation and proliferation of human circulating T lymphocytes. *Cell Immunol.* (2000) 199:15–24. doi: 10.1006/cimm.1999.1594
16. Matarese G, Moschos S, Mantzoros CS. Leptin in immunology. *J Immunol.* (2005) 174:3137–42. doi: 10.4049/jimmunol.174.6.3137
17. Lord GM, Matarese G, Howard JK, Baker RJ, Bloom SR, Lechler RI. Leptin modulates the T-cell immune response and reverses starvation-induced immunosuppression. *Nature* (1998) 394:897–901. doi: 10.1038/29795
18. Howard JK, Lord GM, Matarese G, Vendetti S, Ghatei MA, Ritter MA, et al. Leptin protects mice from starvation-induced lymphoid atrophy and increases thymic cellularity in *ob/ob* mice. *J Clin Invest.* (1999) 104:1051–9. doi: 10.1172/JCI6762
19. Saucillo DC, Gerriets VA, Sheng J, Rathmell JC, Maciver NJ. Leptin metabolically licenses T cells for activation to link nutrition and immunity. *J Immunol.* (2014) 192:136–44. doi: 10.4049/jimmunol.1301158
20. Faggioni R, Feingold KR, Grunfeld C. Leptin regulation of the immune response and the immunodeficiency of malnutrition. *FASEB J.* (2001) 15:2565–71. doi: 10.1096/fj.01-0431rev
21. Paz-Filho GJ, Delibasi T, Erol HK, Wong ML, Licinio J. Cellular immunity before and after leptin replacement therapy. *J Pediatr Endocrinol Metab.* (2009) 22:1069–74. doi: 10.1515/JPEM.2009.22.11.1069
22. Farooqi IS, Matarese G, Lord GM. Beneficial effects of leptin on obesity, T cell hyporesponsiveness, and neuroendocrine/metabolic dysfunction of human congenital leptin deficiency. *J Clin Invest.* (2002) 110:1093–103. doi: 10.1172/JCI0215693
23. Moore S, Morgan G, Collinson A, Swain J, O'Connell M, Prentice A. Leptin, malnutrition, and immune response in rural Gambian children. *Arch Dis Child.* (2002) 87:192–7. doi: 10.1136/adc.87.3.192
24. Woodward B. Protein, calories, and immune defenses. *Nutr Rev.* (1998) 56:S84–92. doi: 10.1111/j.1753-4887.1998.tb01649.x
25. Schaible UE, Kaufmann SH. Malnutrition and infection: complex mechanisms and global impacts. *PLoS Med.* (2007) 4:e115. doi: 10.1371/journal.pmed.0040115
26. Najera O, Gonzalez C, Toledo G, López L, Cortés E, Betancourt M, et al. CD45RA and CD45RO isoforms in infected malnourished and infected well-nourished children. *Clin Exp Immunol.* (2001) 126:461–5. doi: 10.1046/j.1365-2249.2001.01694.x
27. Iyer SS, Chatraw JH, Tan WG, Wherry EJ, Becker TC, Ahmed R, et al. Protein-energy malnutrition impairs homeostatic proliferation of memory CD8 T cells. *J Immunol.* (2012) 188:77–84. doi: 10.4049/jimmunol.1004027
28. Chatraw JH, Wherry EJ, Ahmed R, Kapasi ZF. Diminished primary CD8 T cell response to viral infection during protein-energy malnutrition in mice is due to changes in microenvironment and low numbers of viral-specific CD8 T cell precursors. *J Nutr.* (2008) 138:806–12. doi: 10.1093/jn/138.4.806
29. Nájera O, González C, Toledo G, López L, Ortiz R. Flow cytometry study of lymphocyte subsets in malnourished and well-nourished children with bacterial infections. *Clin Diagn Lab Immunol.* (2004) 11:577–80. doi: 10.1128/CDLI.11.3.577-580.2004
30. Wieland CW, Florquin S, Chan ED, Leemans JC, Weijer S, Verbon A, et al. Pulmonary *Mycobacterium tuberculosis* infection in leptin-deficient *ob/ob* mice. *Int Immunol.* (2005) 17:1399–408. doi: 10.1093/intimm/dxh317
31. Hsu A, Aronoff DM, Phipps J, Goel D, Mancuso P. Leptin improves pulmonary bacterial clearance and survival in *ob/ob* mice during *Pneumococcal pneumonia*. *Clin Exp Immunol.* (2007) 150:332–9. doi: 10.1111/j.1365-2249.2007.03491.x
32. Tschöp J, Nogueiras R, Haas-Lockie S, Kasten KR, Castañeda TR, Huber N, et al. CNS leptin action modulates immune response and survival in sepsis. *J Neurosci.* (2010) 30:6036–47. doi: 10.1523/JNEUROSCI.4875-09.2010
33. Madan R, Guo X, Naylor C, Buonomo EL, Mackay D, Noor Z, et al. Role of leptin-mediated colonic inflammation in defense against Clostridium difficile Colitis. *Infect Immun.* (2014) 82:341–9. doi: 10.1128/IAI.00972-13
34. Zhang AJ, To KK, Li C, Lau CC, Poon VK, Chan CC, et al. Leptin mediates the pathogenesis of severe 2009 pandemic influenza a (h1n1) infection associated with cytokine dysregulation in mice with diet-induced obesity. *J Infect Dis.* (2013) 207:1270–80. doi: 10.1093/infdis/jit031
35. Sánchez-Pozo C, Rodriguez-baño J, Domínguez-Castellano A, Muniain MA, Goberna R, Sánchez-Margalet V. Leptin stimulates the oxidative burst in control monocytes but attenuates the oxidative burst in monocytes from HIV-infected patients. *Clin Exp Immunol.* (2003) 134:464–9. doi: 10.1111/j.1365-2249.2003.02321.x
36. Dayakar A, Chandrasekaran S, Veronica J, Maurya R. Leptin induces the phagocytosis and protective immune response in *Leishmania donovani* infected THP-1 cell line and human PBMCs. *Exp Parasitol.* (2016) 160:54–9. doi: 10.1016/j.exppara.2015.12.002
37. Nagajyothi F, Zhao D, Machado FS, Weiss, LM Schwartz GJ, Desruisseaux MS, et al. Crucial role of the central leptin receptor in murine *Trypanosoma cruzi* infection. *J Infect Dis.* (2010) 202:1104–13. doi: 10.1086/656189
38. Vedantama G, Viswanathan VK. Leptin signaling protects the gut from *Entamoeba histolytica* infection. *Gut Microb.* (2012) 3:2–3. doi: 10.4161/gmic.19424
39. Pulido-Mendez M, De Sanctis J, Rodriguez-Acosta A. Leptin and leptin receptors during malaria infection in mice. *Folia Parasitol.* (2002) 49:249–51. doi: 10.14411/fp.2002.046
40. Chan J, Tian Y, Tanaka KE, Tsang MS, Yu K, Salgame P, et al. Effects of protein-calorie malnutrition on tuberculosis in mice. *Proc Natl Acad Sci USA.* (1996) 93:14857–61. doi: 10.1073/pnas.93.25.14857
41. Pena-Cruz V, Reiss CS, McIntosh K. Sendai virus infection of mice with protein malnutrition. *J Virol.* (1989) 63:3541–4.
42. Ritz BW, Aktan I, Nogusa S, Gardner EM. Energy restriction impairs natural killer cell function and increases the severity of influenza

infection in young adult male C57BL/6 mice. *J Nutr.* (2008) 138:2269–75. doi: 10.3945/jn.108.093633
43. Goldberg EL, Romero-Aleshire MJ, Renkema KR, Ventevogel MS, Chew WM, Uhrlaub JL, et al. Lifespan-extending caloric restriction or mTOR inhibition impair adaptive immunity of old mice by distinct mechanisms. *Aging Cell* (2015) 14:130–8. doi: 10.1111/acel.12280
44. Kristan DM. Chronic calorie restriction increases susceptibility of laboratory mice (Mus musculus) to a primary intestinal parasite infection. *Aging Cell* (2007) 6:817–25. doi: 10.1111/j.1474-9726.2007.00345.x
45. Rodríguez L, Graniel J, Ortiz R. Effect of leptin on activation and cytokine synthesis in peripheral blood lymphocytes of malnourished infected children. *Clin Exp Immunol.* (2007) 148:478–85. doi: 10.1111/j.1365-2249.2007.03361.x
46. Procaccini C, Lourenco EV, Matarese G, La Cava A. Leptin signaling: a key pathway in immune responses. *Curr Signal Transduct Ther.* (2009) 4:22–30. doi: 10.2174/157436209787048711
47. Fantuzzi G. Three questions about leptin and immunity. *Brain Behav Immun.* (2009) 23:405–10. doi: 10.1016/j.bbi.2008.10.007
48. Sánchez-Margalet V, Martín-Romero C, Santos-Alvarez J, Goberna R, Najib S, Gonzalez-Yanes C. Role of leptin as an immunomodulator of blood mononuclear cells: mechanisms of action. *Clin Exp Immunol.* (2003) 133:11–9. doi: 10.1046/j.1365-2249.2003.02190.x
49. Gainsford T, Willson TA, Metcalf D. Leptin can induce proliferation, differentiation, and functional activation of hemopoietic cells. *Proc Natl Acad Sci USA.* (1996) 93:14564–8. doi: 10.1073/pnas.93.25.14564
50. Raso GM, Pacilio M, Esposito E, Coppola A, Di Carlo R, Meli R. Leptin potentiates IFN-gamma induced expression of nitric oxide synthase and cyclo-oxygenase-2 in murine macrophage J774A. 1. *Br J Pharmacol.* (2002) 137:799–804. doi: 10.1038/sj.bjp.0704903
51. Santos-Alvarez J, Goberna R, Sanchez-Margalet V. Human leptin stimulates proliferation and activation of human circulating monocytes. *Cell Immunol.* (1999) 194:6–11. doi: 10.1006/cimm.1999.1490
52. Bennett BD, Solar GP, Yuan JQ, Mathias J, Thomas GR, Matthews W. A role for leptin and its cognate receptor in hematopoiesis. *Curr Biol.* (1996) 6:1170–80. doi: 10.1016/S0960-9822(02)70684-2
53. Najib S, Sanchez-Margalet V. Human leptin promotes survival of human circulating blood monocytes prone to apoptosis by activation of p42/44 MAPK pathway. *Cell Immunol.* (2002) 220:43–149. doi: 10.1016/S0008-8749(03)00027-3
54. Loffreda S, Yang SQ, Lin HZ, Karp CL, Brengman ML, Wang DJ, et al. Leptin regulates proinflammatory immune responses. *FASEB J.* (1998) 12:57–65. doi: 10.1096/fasebj.12.1.57
55. Oral EA, Javor ED, Ding L, Uzel G, Cochran EK, Young JR, et al. Leptin replacement therapy modulates circulating lymphocyte subsets and cytokine responsiveness in severe lipodystrophy. *J Clin Endocrinol Metab.* (2006) 91:621–8. doi: 10.1210/jc.2005-1220
56. Bruno A, Conus S, Schmid I, Simon H-U. Apoptotic pathways are inhibited by leptin receptor activation in neutrophils. *J Immunol.* (2005) 174:8090–6. doi: 10.4049/jimmunol.174.12.8090
57. Zarkesh-Esfahani H, Pockley AG, Wu Z, Hellewell PG, Weetman AP, Ross RJ, et al. Leptin indirectly activates human Neutrophils via induction of TNF-α. *J Immunol.* (2004) 172:1809–14. doi: 10.4049/jimmunol.172.3.1809
58. Brake DK, Smith EB, Mersmann H, Smith CW, Robker RL. ICAM-1 expression in adipose tissue: effects of diet-induced obesity in mice. *Am J Physiol Cell Physiol.* (2006) 291:C1232–9. doi: 10.1152/ajpcell.00008.2006
59. Kiguchi N, Maeda T, Kobayashi Y, Fukazawa Y, Kishioka S. Leptin enhances CC-chemokine ligand expression in cultured murine macrophage. *Biochem Biophys Res Commun.* (2009) 384:311–5. doi: 10.1016/j.bbrc.2009.04.121
60. Gruen ML, Hao M, Piston DW, Hasty AH. Leptin requires canonical migratory signaling pathways for induction of monocyte and macrophage chemotaxis. *Am J Physiol Cell Physiol.* (2007) 293:C1481–8. doi: 10.1152/ajpcell.00062.2007
61. Rafail S, Ritis K, Schaefer K, Kourtzelis I, Speletas M, Doumas M, et al. Leptin induces the expression of functional tissue factor in human neutrophils and peripheral blood mononuclear cells through JAK2-dependent mechanisms and TNF-α involvement. *Thromb Res.* (2008) 122:366–75. doi: 10.1016/j.thromres.2007.12.018
62. Mattioli B, Straface E, Quaranta MG, Giordani L, Viora M. Leptin promotes differentiation and survival of human dendritic cells and licenses them for Th1 priming. *J Immunol.* (2005) 174:6820–8. doi: 10.4049/jimmunol.174.11.6820
63. Mattioli B, Giordani L, Quaranta MG, Viora M. Leptin exerts an anti-apoptotic effect on human dendritic cells via the PI3K-Akt signalling pathway. *FEBS Lett.* (2009) 583:1102–6. doi: 10.1016/j.febslet.2009.02.029
64. Lam QL, Liu S, Cao X, Lu L. Involvement of leptin signalling in the survival and maturation of bone marrow-derived dendritic cells. *Eur J Immunol.* (2006) 36:3118–30. doi: 10.1002/eji.200636602
65. Tian Z, Sun R, Wei H, Gao B. Impaired natural killer (NK) cell activity in leptin receptor deficient mice: leptin as a critical regulator in NK cell development and activation. *Biochem Biophys Res Commun.* (2002) 298:297–302. doi: 10.1016/S0006-291X(02)02462-2
66. Zhao Y, Sun R, You L, Gao C, Tian Z. Expression of leptin receptors and response to leptin stimulation of human natural killer cell lines. *Biochem Biophys Res Commun.* (2003) 300:247–52. doi: 10.1016/S0006-291X(02)02838-3
67. Velloso LA, Savino W, Mansour E. Leptin action in the thymus. *Ann N Y Acad Sci.* (2009) 1153:29–34. doi: 10.1111/j.1749-6632.2008.03973.x
68. Da Silva SV, Salama C, Renovato-Martins M, Helal-Neto, E, Citelli, M, Savino, W, et al. Increased leptin response and inhibition of apoptosis in thymocytes of young rats offspring from protein deprived dams during lactation. *PLoS ONE* (2013) 8:e64220. doi: 10.1371/journal.pone.0064220
69. Merrick JC, Edelson BT, Bhardwaj V, Swanson PE, Unanue ER. Lymphocyte apoptosis during early phase of Listeria infection in mice. *Am J Pathol.* (1997) 151:785–92.
70. Papathanassoglou E, El-Haschimi K, Li XC, Matarese G, Strom T, Mantzoros C. Leptin receptor expression and signaling in lymphocytes: kinetics during lymphocyte activation, role in lymphocyte survival, and response to high-fat diet in mice. *J Immunol.* (2006) 176:7745–52. doi: 10.4049/jimmunol.176.12.7745
71. Fujita Y, Murakami M, Ogawa Y, Masuzaki H, Tanaka M, Ozaki S, et al. Leptin inhibits stress-induced apoptosis of T lymphocytes. *Clin Ex Immunol.* (2002) 128:21–6. doi: 10.1046/j.1365-2249.2002.01797.x
72. Lord GM, Matarese G, Howard JK, Bloom SR, Lechler RI. Leptin inhibits the anti-CD3-driven proliferation of peripheral blood T cells but enhances the production of proinflammatory cytokines. *J Leukoc Biol.* (2002) 72:330–8. doi: 10.1189/jlb.72.2.330
73. Farooqi IS, Wangensteen T, Collins S, Kimber W, Matarese G, Keogh JM, et al. Clinical and molecular genetic spectrum of congenital deficiency of the leptin receptor. *N Engl J Med.* (2007) 356:237–47. doi: 10.1056/NEJMoa063988
74. Ozata M, Ozdemir IC, Licinio J. Human leptin deficiency caused by a missense mutation: multiple endocrine defects, decreased sympathetic tone, and immune system dysfunction indicates new targets for leptin action, greater central than peripheral resistance to the effects of leptin, and spontaneous correction of leptin-mediated defects. *J Clin Endocrinol Metab.* (1999) 84:3686–95. doi: 10.1210/jcem.84.10.5999
75. Chandra RK. Cell-mediated immunity in genetically obese C57BL/6J (ob/ob) mice. *Am J Clin Nutr.* (1980) 33:13–6. doi: 10.1093/ajcn/33.1.13
76. Banks AS, Davis SM, Bates SH, Myers MG Jr. Activation of downstream signals by the long form of the leptin receptor. *J Biol Chem.* (2000) 275:14563–72. doi: 10.1074/jbc.275.19.14563
77. Dunn SL, Bjornholm M, Bates SH, Chen Z, Seifert M, Myers MG Jr, et al. Feedback inhibition of leptin receptor/Jak2 signaling via Tyr1138 of the leptin receptor and suppressor of cytokine signaling 3. *Mol Endocrinol.* (2005) 19:925–38. doi: 10.1210/me.2004-0353
78. Kim SY, Lim JH, Choi SW, Kim M, Kim ST, Kim MS, et al. Preferential effects of leptin on CD4 T cells in central and peripheral immune system are critically linked to the expression of leptin receptor. *Biochem Biophys Res Commun.* (2010) 394:562–8. doi: 10.1016/j.bbrc.2010.03.019
79. De Rosa V, Procaccini C, Calì G, Pirozzi G, Fontana S, Zappacosta S, et al. A key role of leptin in the control of regulatory T cell proliferation. *Immunity* (2007) 26:241–55. doi: 10.1016/j.immuni.2007.01.011
80. Sanchez-Margalet V, Martin-Romero C. Human leptin signaling in human peripheral blood mononuclear cells: activation of the JAK-STAT pathway. *Cell Immunol.* (2001) 211:30–6. doi: 10.1006/cimm.2001.1815

81. Agrawal S, Gollapudi S, Su H, Gupta S. Leptin activates human B cells to secrete TNF-alpha, IL-6, and IL-10 via JAK2/STAT3 and p38MAPK/ERK1/2 signaling pathway. *J Clin Immunol.* (2011) 31:472–8. doi: 10.1007/s10875-010-9507-1
82. Groom JR, Luster AD. CXCR3 in T cell function. *Exp Cell Res.* (2011) 315:620–31. doi: 10.1016/j.yexcr.2010.12.017
83. Biesiada G, Czepiel J, Ptak-Belowska A, Targosz A, Krzysiek-Maczka G, Strzalka M, et al. Expression and release of leptin and proinflammatory cytokines in patients with ulcerative colitis and infectious diarrhea. *J Physiol Pharmacol.* (2012) 63:471–81.
84. Chandra RK. Nutrition, immunity and infection: from basic knowledge of dietary manipulation of immune responses to practical application of ameliorating suffering and improving survival. *Proc Natl Acad Sci USA.* (1996) 93:14304–7. doi: 10.1073/pnas.93.25.14304
85. Matarese G. Leptin and the immune system: how nutritional status influences the immune response. *Eur Cytokine Netw.* (2000) 11:7–14.
86. Gerriets VA, MacIver NJ. Role of T cells in malnutrition and obesity. *Front Immunol.* (2014) 5:379. doi: 10.3389/fimmu.2014.00379
87. Chandra R. Nutrition, and immunology: from the clinic to cellular biology and back again. *Proc Nutr Soc.* (1999) 58:681–3. doi: 10.1017/S0029665199000890
88. Cederholm T, Arner P, Palmblad J. Low circulating leptin levels in protein-energy malnourished chronically ill elderly patients. *J Intern Med.* (1997) 242:377–82. doi: 10.1046/j.1365-2796.1997.00216.x
89. Soliman AT, Zalabany El, Salama MM, Ansari BM. Serum leptin concentrations during protein-energy malnutrition: correlation with growth parameters and endocrine function. *Metabolism* (2000) 49:819–25. doi: 10.1053/meta.2000.6745
90. Blackburn GL. Pasteur's quadrant and malnutrition. *Nature* (2001) 409:397–401. doi: 10.1038/35053187
91. Dai G, McMurray DN. Altered cytokine production and impaired antimycobacterial immunity in protein-malnourished guinea pigs. *Infect Immun.* (1998) 66:3562–8.
92. Cegielski JP, McMurray DN. The relationship between malnutrition and tuberculosis: evidence from studies in humans and experimental animals. *Int J Tuberc Lung Dis.* (2004) 8:286–98.
93. Cakir B, Yonem A, Guler S, Odabasi E, Demirbas B, Gürsoy G, et al. Relation of leptin and tumor necrosis factor alpha to body weight changes in patients with pulmonary tuberculosis. *Horm Res.* (1999) 52:279–83.
94. Schwenk A, Hodgson L, Rayner CF, Griffin GE, Macallan DC. Leptin and energy metabolism in pulmonary tuberculosis. *Am J Clin Nutr.* (2003) 77:392–8. doi: 10.1093/ajcn/77.2.392
95. van Crevel R, Karyadi E, Netea MG, Verhoef H, Nelwan RH, West CE, et al. Decreased plasma leptin concentrations in tuberculosis patients are associated with wasting and inflammation. *J Clin Endocrinol Metab.* (2002) 87:758–63. doi: 10.1210/jcem.87.2.8228
96. van Lettow M, van der Meer JW, West CE, van Crevel R, Semba RD. Interleukin- 6 and human immunodeficiency virus load, but not plasma leptin concentration, predict anorexia and wasting in adults with pulmonary tuberculosis in Malawi. *J Clin Endocrinol Metab.* (2005) 90:4771–6. doi: 10.1210/jc.2004-2539
97. Hoang T, Agger EM, Cassidy JP, Christensen JP, Andersen P. Protein energy malnutrition during vaccination has limited influence on vaccine efficacy but abolishes immunity if administered during *Mycobacterium tuberculosis* infection. *Infect Immun.* (2015) 83:2118–26. doi: 10.1128/IAI.03030-14
98. Auphan N, Didonato JA, Helmberg A, Rosette C, Karin M. Immunoregulatory genes and immunosuppression by glucocorticoids. *Arch Toxicol Suppl.* (1997) 19:87–95. doi: 10.1007/978-3-642-60682-3_8
99. McCarter MD, Naama HA, Shou J, Kwi LX, Evoy DA, Calvano SE, et al. Altered macrophage intracellular signaling induced by protein-calorie malnutrition. *Cell Immunol.* (1998) 183:131–6. doi: 10.1006/cimm.1998.1241
100. Redmond HP, Gallagher HJ, Shou J, Daly JM. Antigen presentation in protein-energy malnutrition. *Cell Immunol.* (1995) 163:80–7. doi: 10.1006/cimm.1995.1101
101. Redmond HP, Leon P, Lieberman MD, Hofmann K, Shou J, Reynolds JV, et al. Impaired macrophage function in severe protein-energy malnutrition. *Arch Surg.* (1991) 126:192–6. doi: 10.1001/archsurg.1991.01410260080011
102. Palacio A, Lopez M, Perez-Bravo F, Monkeberg F, Schlesinger L. Leptin levels are associated with immune response in malnourished infants. *J Clin Endocrinol Metab.* (2002) 87:3040–6. doi: 10.1210/jcem.87.7.8636
103. Bartz S, Mody A, Hornik C, Bain J, Muehlbauer M, Kiyimba T, et al. Severe acute malnutrition in childhood: hormonal and metabolic status at presentation, response to treatment, and predictors of mortality. *J Clin Endocrinol Metab.* (2014) 99:2128–37. doi: 10.1210/jc.2013-4018
104. Testa R, Franceschini R, Giannini E, Cataldi A, Botta F, Fasoli A, et al. Serum leptin levels in patients with viral chronic hepatitis or liver cirrhosis. *J Hepatol.* (2000) 33:33–7. doi: 10.1016/S0168-8278(00)80156-7
105. Redmond HP, Shou J, Kelly CJ, Leon P, Daly JM. Protein-calorie malnutrition impairs host defense against *Candida albicans*. *J Surg Res.* (1991) 50:552–9. doi: 10.1016/0022-4804(91)90040-S
106. Cason J, Ainley CC, Wolstencroft RA, Norton KR, Thompson RP. Cell-mediated immunity in anorexia nervosa. *Clin Exp Immunol.* (1986) 64:370–5.
107. Ahima RS, Prabakaran D, Mantzoros C, Qu D, Lowell B, Maratos-Flier E, et al. Role of leptin in the neuroendocrine response to fasting. *Nature* (1996) 382:250–2. doi: 10.1038/382250a0
108. Faggioni R, Moser A, Feingold KR, Grunfeld C. Reduced leptin levels in starvation increase susceptibility to endotoxic shock. *Am J Pathol.* (2000) 156:1781–7. doi: 10.1016/S0002-9440(10)65049-3
109. Faggioni R, Fantuzzi G, Gabay C, Moser A, Dinarello CA, Feingold KR, et al. Leptin deficiency enhances sensitivity to endotoxin-induced lethality. *Am J Physiol.* (1999) 276:R136–42.
110. Chen M, Wang B, Xu Y, Deng Z, Xue H, Wang L, et al. Diagnostic value of serum leptin and a promising novel diagnostic model for sepsis. *Exp Therapeutic Med.* (2014) 7:881–6. doi: 10.3892/etm.2014.1506
111. Ye M, Bian L-F. Association of serum leptin levels and pulmonary tuberculosis: a meta-analysis. *J Thorac Dis.* (2018)10:1027–36. doi: 10.21037/jtd.2018.01.70
112. Mancuso P, Gottschalk A, Phare SM, Peters-Golden M, Lukacs NW, Huffnagle GB. Leptin-deficient mice exhibit impaired host defense in Gram-negative pneumonia. *J Immunol.* (2002) 168:4018–24. doi: 10.4049/jimmunol.168.8.4018
113. Moore SI, Huffnagle GB, Chen GH, White ES, Mancuso P. Leptin modulates neutrophil phagocytosis of *Klebsiella pneumoniae*. *Infect Immun.* (2003) 71:4182–5. doi: 10.1128/IAI.71.7.4182-4185.2003
114. Mancuso P, Huffnagle GB, Olszewski MA, Phipps J, Peters-Golden M. Leptin corrects host defense defects after acute starvation in murine *Pneumococcal pneumonia*. *Am J Respir Crit Care Med.* (2006) 173:212–8. doi: 10.1164/rccm.200506-909OC
115. Koca C, Kavakli HS, Alici O. Immunomodulatory role of leptin treatment in experimental sepsis caused by gram negative bacteria. *Turk J Med Sci.* (2011) 41:251–8. doi: 10.3906/sag-1009-1109
116. Morshedi A, Zarkesh-Esfahani HS, Behjati M. Effect of leptin on neutrophils phagocytosis and lymphocytes apoptosis challenge by *Listeria monocytogenes* and *Escherichia coli*. *Jundishapur J Microbiol.* (2013) 6:e6389. doi: 10.5812/jjm.6389
117. Ikejima S, Sasaki S, Sashinami H, Mori F, Ogawa Y, Nakamura T, et al. Impairment of host resistance to *Listeria monocytogenes* infection in the liver of *db/db* and *ob/ob* mice. *Diabetes* (2005) 54:182–9. doi: 10.2337/diabetes.54.1.182
118. Nishi Y, Isomoto H, Uotani S, Wen CY, Shikuwa S, Ohnita K, et al. Enhanced production of leptin in gastric fundic mucosa with *Helicobacter pylori* infection. *World J Gastroenterol.* (2005) 11:695–9. doi: 10.3748/wjg.v11.i5.695
119. Khosravi Y, Seow SW, Amoyo AA, Chiow KH, Tan TL, Wong WY, et al. *Helicobacter pylori* infection can affect energy modulating hormones and body weight in germ free mice. *Sci Rep.* (2015) 5:8731. doi: 10.1038/srep08731
120. Azuma T, Suto H, Ito Y, Ohtani M, Dojo M, Kuriyama M, et al. Gastric leptin and *Helicobacter pylori* infection. *Gut* (2001) 49:324–9. doi: 10.1136/gut.49.3.324
121. Khudhur S, Jameel D, Karhoot J, AL-Khafaji J, Mohsin J. Increase serum leptin level in *Helicobacter pylori* infection in Iraqi gastritis patients. *Al-Kindy Col Med J.* (2011) 7:74–7.

122. Milner J, Meyers M, Sheridan P, Mancuso P, Beck M. The role of T cell leptin signaling in 2009 pandemic *H1N1* influenza infection mortality in obese mice (VIR2P.1013). *J Immunol.* (2014) 192(Suppl. 1):75.2.
123. Milner JJ, Rebeles J, Dhungana S, Stewart DA, Sumner SC, Meyers MH, et al. Obesity increases mortality and modulates the lung metabolome during pandemic *H1N1* influenza virus infection in mice. *J Immunol.* (2015) 194:4846–59. doi: 10.4049/jimmunol.1402295
124. Hur SJ, Kim DH, Chun SC, Lee SK. Effect of adenovirus and influenza virus infection on obesity. *Life Sci.* (2013) 93:531–5. doi: 10.1016/j.lfs.2013.08.016
125. Radigan KA, Morales-Nebreda L, Soberanes S, Nicholson T, Nigdelioglu R, Cho T, et al. Impaired clearance of influenza a virus in obese, leptin receptor-deficient mice is independent of leptin signaling in the lung epithelium and macrophages. *PLoS ONE* (2014) 9:e108138. doi: 10.1371/journal.pone.0108138
126. Qin L, Tan YR, Hu CP, Liu XA, He RX. Leptin is over-secreted by respiratory syncytial virus-infected bronchial epithelial cells and regulates th2 and th17 cell differentiation. *Int Arch Allergy Immunol.* (2015) 167:65–71. doi: 10.1159/000436966
127. Sánchez-Margalet V, Martín-Romero C, González-Yanes C, Goberna R, Rodríguez-Baños J, Muniain MA. Leptin receptor expression is induced in activated mononuclear cells *in vitro* and *in vivo* in HIV-infected patients. *Clin Exp Immunol.* (2002)129:119–24. doi: 10.1046/j.1365-2249.2002.01900.x
128. Azzoni L, Crowther NJ, Firnhaber C, Foulkes AS, Yin X, Glencross D, et al. Association between HIV replication and serum leptin levels: an observational study of a cohort of HIV-1-infected South African women. *J Int AIDS Soc.* (2010) 13:33. doi: 10.1186/1758-2652-13-33
129. Sinha U, Sinharay K, Sengupta N, Mukhopadhyay P. Benefits of leptin therapy in HIV patients. *Ind J Endocrinol Metab.* (2012) 16(Suppl. 3):S637–43. doi: 10.4103/2230-8210.105583
130. Shivahare R, Ali W, Vishwakarma P, Natu SM, Puri SK, Gupta S. Leptin augments protective immune responses in murine macrophages and enhances the potential of miltefosine against experimental visceral leishmaniasis. *Acta Trop.* (2015) 150:35–41. doi: 10.1016/j.actatropica.2015.06.024
131. Maurya R, Bhattacharya P, Ismail N, Dagur PK, Joshi AB, Razdan K, et al. Differential role of leptin as an immunomodulator in controlling visceral leishmaniasis in normal and leptin-deficient mice. *Am J Trop Med Hyg.* (2016) 95:109–19. doi: 10.4269/ajtmh.15-0804
132. Dayakar A, Chandrasekaran S, Veronica J, Bharadwaja V, Maurya R. Leptin regulates Granzyme-A, PD-1 and CTLA-4 expression in T cell to control visceral leishmaniasis in BALB/c Mice. *Sci Rep.* (2017) 7:14664. doi: 10.1038/s41598-017-15288-7
133. Combs TP, Nagajyothi, Mukherjee S, de Almeida CJ, Jelicks LA, Schubert W, et al. The adipocyte as an important target cell for *Trypanosoma cruzi* infection. *J Biol Chem.* (2005) 280:24085–94. doi: 10.1074/jbc.M412802200
134. Gutierrez FR, Guedes PM, Gazzinelli RT, Silva JS. The role of parasite persistence in the pathogenesis of Chagas heart disease. *Parasite Immunol.* (2009) 31:673–85. doi: 10.1111/j.1365-3024.2009.01108.x
135. Matos Ferreira AV, Segatto M, Menezes Z, Macedo AM, Gelape C, de Oliveira Andrade L, et al. Evidence for *Trypanosoma cruzi* in adipose tissue in human chronic Chagas disease. *Microb Infect.* (2011) 13:1002–5. doi: 10.1016/j.micinf.2011.06.002
136. Tanowitz HB, Amole B, Hewlett D, Wittner M. *Trypanosoma cruzi* infection in diabetic mice. *Trans R Soc Tropic Med Hyg.* (1988) 82:90–3. doi: 10.1016/0035-9203(88)90272-6
137. Alam F, Salam A, Mahmood I, Kabir M, Chowdhury S, Haque R**.** Amebic liver abscess is associated with malnutrition and low serum leptin level. *J Infect Dis Ther.* (2016) 4:298. doi: 10.4172/2332-0877.1000298
138. Duggal P, Guo X, Haque R, Peterson KM, Ricklefs S, Mondal D, et al. A mutation in the leptin receptor is associated with *Entamoeba histolytica* infection in children. *J Clin Invest.* (2011) 121:1191–8. doi: 10.1172/JCI45294
139. Naylor C, Burgess S, Madan R, Buonomo E, Razzaq K, Ralston K et al. Leptin receptor mutation results in defective neutrophil recruitment to the colon during *Entamoeba histolytica* infection. *MBio* (2014) 5:e02046–14. doi: 10.1128/mBio.02046-14
140. Guo X, Roberts MR, Becker SM, Podd B, Zhang Y, Chua SC Jr, et al. Leptin signaling in intestinal epithelium mediates resistance to enteric infection by *Entamoeba histolytica*. *Mucosal Immunol.* (2011) 4:294–303. doi: 10.1038/mi.2010.76
141. Marie CS, Verkerke HP, Paul SN, Mackey AJ, Petri WA Jr. Leptin protects host cells from *Entamoeba histolytica* cytotoxicity by a STAT-3 dependent mechanism. *Infect Immun.* (2012) 226:2123–30.
142. Mackey-Lawrence NM, Petri WA Jr. Leptin and mucosal immunity. *Mucosal Immunol.* (2012) 5:472–9. doi: 10.1038/mi.2012.40
143. Mejia P, Treviño-Villarreal JH, Hine C, Harputlugil E, Lang S, Calay E, et al. Dietary restriction protects against experimental cerebral malaria via leptin modulation and T cell mTORC1 suppression. *Nat Commun.* (2015) 6:6050. doi: 10.1038/ncomms7050
144. Al-Fadhli MA, Saraya MA, Qasem JA. Evaluation of leptin, interleukin-1 beta and tumor necrosis factor alpha in the serum of malaria patients as prognostic markers of treatment outcome. *Asian Pac J Trop Biomed.* (2014) 4:441–5. doi: 10.12980/APJTB.4.201414B11
145. Elnemr GM, Elnashar MA, Elmargoushy NM, Elnashar NA, Elnashar MA. Adiponectin levels as a marker of inflammation in pulmonary tuberculosis. *Egypt J Hosp Med.* (2015) 59:208–14. doi: 10.12816/0012177
146. Neeraj Indora N, Sharma K, Karunanand B, Sudan DPS, Shah AK. Assessment of metabolic (Adiponectin, Leptin) and inflammatory markers (TNF-α, hs-CRP & IFN-γ) in pulmonary tuberculosis: prospective Study. *Int J Clin Biochem Res.* (2017) 4:216–9. doi: 10.18231/2394-6377.2017.0051
147. Shirshev SV, Orlova EG. Molecular mechanisms of regulation of the functional activity of mononuclear phagocytes by leptin. *Biochemistry* (2005) 70:841–7. doi: 10.1007/s10541-005-0193-1
148. Bates SH, Stearns WH, Dundon TA, Schubert M, Tso AW, Wang Y, et al. STAT3 signalling is required for leptin regulation of energy balance but not reproduction. *Nature* (2003) 421:856–9. doi: 10.1038/nature01388
149. Gong Y, Ishida-Takahashi R, Villanueva EC, Fingar DC, Münzberg H, Myers MG Jr. The long form of the leptin receptor regulates STAT5 and ribosomal protein S6 via alternate mechanisms. *J Biol Chem.* (2007) 282:31019–27. doi: 10.1074/jbc.M702838200
150. Bjørbaek C, Buchholz RM, Davis SM, Bates SH, Pierroz DD, Gu H, et al. Divergent roles of SHP-2 in ERK activation by leptin receptors. *J Biol Chem.* (2001) 276:4747–55. doi: 10.1074/jbc.M007439200
151. Mancuso P, Myers MG, Goel D, Serezani CH, O'Brien E, Goldberg J, et al. Ablation of leptin receptor-mediated ERK activation impairs host defense against gram-negative pneumonia. *J Immunol.* (2012) 189:867–75. doi: 10.4049/jimmunol.1200465
152. Caldefie-Chezet F, Poulin A, Tridon A, Sion B, Vasson MP. Leptin: a potential regulator of polymorphonuclear neutrophil bactericidal action? *J Leukoc Biol.* (2001) 69:414–8.
153. Moshyedi AK, Josephs MD, Abdalla EK, Mackay SLD, Edwards CK, Copeland EM, et al. Increased leptin expression in mice with bacterial peritonitis is partially regulated by tumor necrosis factor alpha. *Infect Immun.* (1998) 66:1800–2.
154. Mancuso P, Peters-Golden M, Goel D. Disruption of leptin receptor-stat3 signaling enhances leukotriene production and pulmonary host defense against *Pneumococcal pneumonia*. *J Immunol.* (2011) 186:1081–90. doi: 10.4049/jimmunol.1001470
155. Breideri M, Miehlike S, Glasou A, Orban Z, Stolte M, Ehninger G, et al. Leptin and its receptor in normal human gastric mucosa and in *H pylori*-associated gastritis. *Scand J Gastroenterol.* (1999) 34:954–61. doi: 10.1080/003655299750025039
156. Taylor AK, Cao W, Vora KP, De La Cruz J, Shieh WJ, Zaki SR, et al. Protein-energy malnutrition decreases immunity and increases susceptibility to influenza infection in mice. *J Infect Dis.* (2013) 207:501–10. doi: 10.1093/infdis/jis527
157. Ortega YR, Eberhard ML, Kris H. Protozoan diseases: cryptosporidiosis, giardiasis and other intestinal protozoan diseases. *International Encyclopedia of Public Health.* Oxford: Academic Press (2008) p. 354–66.
158. Lõhmus M, Moalem S, Björklund M. Leptin, a tool of parasites? *Biol Lett.* (2012) 8:849–52. doi: 10.1098/rsbl.2012.0385
159. Caldefie-Chezet F, Poulin A, Vasson MP. Leptin regulates functional capacities of polymorphonuclear neutrophils. *Free Radic Res.* (2003) 37:809–14. doi: 10.1080/1071576031000097526

160. Naylor C, Petri WA Jr. Leptin regulation of immune responses. *Trends Mol Med.* (2016) 22:88–98. doi: 10.1016/j.molmed.2015.12.001
161. WHO. Control of the leishmaniasis: report of a meeting of the WHO Expert Committee on the Control of Leishmaniases, Geneva, March 22–26, 2010. *World Health Organ Tech Rep Ser.* (2010) 949:1–186.
162. Desjeux P. Leishmaniasis: current situation and new perspectives. Comp Immunol *Microbiol Infect Dis.* (2004). 27:305–18. doi: 10.1016/j.cimid.2004.03.004
163. Pearson RD, Cox G, Jeronimo SM, Castracane J, Drew JS, Evans T, et al. Visceral leishmaniasis: a model for infection-induced cachexia. *Am J Trop Med Hyg.* (1992) 47(1 Pt 2):8–15. doi: 10.4269/ajtmh.1992.47.8
164. Anstead GM, Chandrasekar B, Zhao W, Yang J, Perez LE, Melby PC. Lalnutrition alters the innate immune response and increases early visceralization following *Leishmania donovani* infection. *Infect Immun.* (2001) 69:4709–18. doi: 10.1128/IAI.69.8.4709-4718.2001
165. Ibrahim MK, Barnes JL, Anstead GM, Jimenez F, Travi BL, Peniche AG, et al. The malnutrition-related increase in early visceralization of *Leishmania donovani* is associated with a reduced number of lymph node phagocytes and altered conduit system flow. *PLoS Negl Tropic Dis.* (2013) 7:e2329. doi: 10.1371/journal.pntd.0002329
166. Macia L, Delacre M, Abboud G, Ouk TS, Delanoye A, Verwaerde C, et al. Impairment of dendritic cell functionality and steady-state number in obese mice. *J Immunol.* (2006) 177:5997. doi: 10.4049/jimmunol.177.9.5997
167. Jin HT, Anderson AC, Tan WG, West EE, Ha SJ, Araki K, et al. Cooperation of Tim-3 and PD-1 in CD8 T-cell exhaustion during chronic viral infection. *Proc Natl Acad Sci USA.* (2010) 107:14733–8. doi: 10.1073/pnas.1009731107
168. Di Loria A, Squillacioti C, De Luca A, Veneziano V, Mirabella N, Guccione J, et al. Increased leptin mRNA expression in the blood of dogs naturally infected by *Leishmania infantum*. *Vet J.* (2014) 202:634–6. doi: 10.1016/j.tvjl.2014.10.010
169. WHO. *Global Plan to Combat Neglected Diseases 2008–2015*. WHO/CDS/NTD/2007. Geneva: WHO (2007).
170. Machado FS, Mukherjee S, Weiss LM, Tanowitz HB, Ashton AW. Bioactive lipids in *Trypanosoma cruzi* infection. *Adv Parasitol.* (2011) 76:1–31. doi: 10.1016/B978-0-12-385895-5.00001-3
171. Miao Q, Ndao M. *Trypanosoma cruzi* infection and host lipid metabolism. *Mediators Inflamm.* (2014) 2014:902038. doi: 10.1155/2014/902038
172. Nagajyothi F, Desruisseaux MS, Thiruvur N, Weiss LM, Braunstein VL, Albanese C, et al. *Trypanosoma cruzi* infection of cultured adipocytes results in an inflammatory phenotype. *Obesity* (2008) 16:1992–7. doi: 10.1038/oby.2008.331
173. Rodrigues CM, Valadares HM, Francisco AF, Arantes JM, Campos CF, Teixeira-Carvalho A, et al. Coinfection with different *Trypanosoma cruzi* strains interferes with the host immune response to infection. *PLoS Negl Trop Dis.* (2010) 4:e846. doi: 10.1371/journal.pntd.0000846
174. Mukherjee S, Huang H, Petkova SB, Albanese C, Pestell RG, Braunstein VL, et al. *Trypanosoma cruizi* infection activates extracellular signal-regulated kinase in cultured endothelial and smooth muscle cells. *Infect Immun.* (2004) 72:5274–82. doi: 10.1128/IAI.72.9.5274-5282.2004
175. Wilkowsky SE, Barbieri MA, Stahl P, Isola ELD. *Trypanosoma cruzi*: phosphatidylinositol 3-kinase and protein kinase B activation is associated with parasite invasion. *Exp Cell Res.* (2001) 264:211–8. doi: 10.1006/excr.2000.5123
176. Hovsepian E, Penas F, Mirkin GA, Goren NB. Role of PPARs in *Trypanosoma cruzi i*nfection: implications for chagas disease therapy. *PPAR Res.* (2011) 2012:528435. doi: 10.1155/2012/528435
177. Stanley SL Jr. Amoebiasis. *Lancet* (2003) 361:1025–34. doi: 10.1016/S0140-6736(03)12830-9
178. Baxt LA, Singh U. New insights into *Entamoeba histolytica* pathogenesis. *Curr Opin Infect Dis.* (2008) 21:489–94. doi: 10.1097/QCO.0b013e32830ce75f
179. Mortimer L, Chadee K. The immunopathogenesis of *Entamoeba histolytica*. *Exp Parasitol.* (2010) 126:366–80. doi: 10.1016/j.exppara.2010.03.005
180. Petri WA Jr, Mondal D, Peterson KM, Duggal P, Haque R. Association of malnutrition with amebiasis. *Nutr Rev.* (2009) 67 (Suppl. 2):S207–15. doi: 10.1111/j.1753-4887.2009.00242.x
181. Ali IK, Clark CG, Petri WA Jr. Molecular epidemiology of amebiasis. *Infect Genet Evol.* (2008) 8:698–707. doi: 10.1016/j.meegid.2008.05.004
182. Haque R, Mondal D, Duggal P, Kabir M, Roy S, Farr BM, et al. *Entamoeba histolytica* infection in children and protection from subsequent amebiasis. *Infect Immun.* (2006) 74:904–9. doi: 10.1128/IAI.74.2.904-909.2006
183. Blessman J, Van LP, Tanich E. Epidemiology of amebiasis in a region of high incidence of amebic liver abscess in central Vietnam. *Am J Trop Med Hyg.* (2002) 66:578–83. doi: 10.4269/ajtmh.2002.66.578
184. Siddiqui MA, Ekram ARSM, Islam QT, Hoque MA, Masum QAAI. Clinico-pathological profile of liver abscess in a teaching hospital. *Teachers Assoc J Rajshahi* (2008) 21:46–8.
185. Mondal D, Haque R, Sack RB, Kirkpatrick BD, Petri WA. Attribution of malnutrition to cause-specific diarrheal illness: evidence from a prospective study of preschool children in Mirpur, Dhaka, Bangladesh. *Am J Trop Med Hyg.* (2009) 80:824–6. doi: 10.4269/ajtmh.2009.80.824
186. World Health Organization. *World Malaria Report*. Geneva: WHO (2015).
187. Bousema T, Drakeley C. Epidemiology and infectivity of *Plasmodium falciparum* and *Plasmodium vivax* gametocytes in relation to malaria control and elimination. *Clin Microbiol Rev.* (2011) 24:377–410. doi: 10.1128/CMR.00051-10
188. Robert V, Bourgouin C, Depoix D, Thouvenot C, Lombard MN, Grellier P. Malaria and obesity: obese mice are resistant to cerebral malaria. *Malaria J.* (2008) 7:81. doi: 10.1186/1475-2875-7-81
189. Finlay D, Cantrell DA. Metabolism, migration and memory in cytotoxic T cells. *Nat Rev Immunol.* (2011) 11:109–17. doi: 10.1038/nri2888
190. Hughes SM, Amadi B, Mwiya M, Nkamba H, Tomkins A, Goldblatt D. Dendritic cell anergy results from endotoxemia in severe malnutrition. *J Immunol.* (2009) 183:2818–26. doi: 10.4049/jimmunol.0803518
191. Bourke CD, Berkley JA, Prendergast AJ. Immune dysfunction as a cause and consequence of malnutrition. *Trends Immunol.* (2016) 37:386–98. doi: 10.1016/j.it.2016.04.003
192. Lam QL, Lu L. Role of leptin in immunity. *Cel Mol Immunol.* (2007) 4:1–13.
193. Vernooy JHJ, Ubags NDJ, Brusselle GG, Tavernier J, Suratt BT, Joos GF, et al. Leptin as regulator of pulmonary immune responses: involvement in respiratory diseases. *Pulmon Pharmacol Therapeut.* (2013) 26:464–72. doi: 10.1016/j.pupt.2013.03.016
194. Duncan SA, Baganizi DR, Sahu R, Singh SR, Dennis VA. SOCS proteins as regulators of inflammatory responses induced by bacterial infections: a review. *Front Microbiol.* (2017) 8:2431. doi: 10.3389/fmicb.2017.02431
195. Paracha RZ, Ahmad J, Ali A, Hussain R, Niazi U, Tareen SHK, et al. Formal modelling of toll like receptor 4 and JAK/STAT signalling pathways: insight into the roles of SOCS-1, interferon-β and proinflammatory cytokines in sepsis. *PLoS ONE* (2014) 9:e108466. doi: 10.1371/journal.pone.0108466
196. Akhtar LN, Qin H, Muldowney MT, Yanagisawa LL, Kutsch O, Clements J E, et al. Suppressor of cytokine signaling 3 inhibits antiviral IFN- β signaling to enhance HIV-1 replication in macrophages. *J Immunol.* (2010) 185:2393–404. doi: 10.4049/jimmunol.0903563
197. Wei H, Wang S, Chen Q, Chen Y, Chi X, Zhang L, et al. Suppression of interferon lambda signaling by SOCS-1 results in their excessive production during influenza virus infection. *PLoS Pathog.* (2014) 10:e1003845. doi: 10.1371/journal.ppat.1003845
198. Michaud F, Coulombe F, Gaudreault E, Paquet-Bouchard C, Rola-Pleszczynski M, Gosselin J. Epstein-Barr virus interferes with the amplification of IFN-α secretion by activating suppressor of cytokine signaling 3 in primary human monocytes. *PLoS ONE* (2010) 5:e11908. doi: 10.1371/journal.pone.0011908
199. Srivastav S, Basu Ball W, Gupta P, Giri J, Ukil A, Das PK. *Leishmania donovani* prevents oxidative burst-mediated apoptosis of host macrophages through selective induction of suppressors of cytokine signaling (SOCS) proteins. *J Biol Chem.* (2014) 289:1092–105. doi: 10.1074/jbc.M113.496323
200. Banerjee R, Kumar S, Sen A, Mookerjee A, Roy S, Pal S, et al. TGF-β-regulated tyrosine phosphatases induce lymphocyte apoptosis in *Leishmania donovani*-infected hamsters. *Immunol Cell Biol.* (2011) 89:466–74. doi: 10.1038/icb.2010.108
201. Bertholet S, Dickensheets H L, Sheikh F, Gam AA, Donnelly R P, Kenney RT. *Leishmania donovani*-induced expression of suppressor of cytokine signaling 3 in human macrophages: a novel mechanism for intracellular

parasite suppression of activation. *Infect Immun.* (2003) 71:2095–101. doi: 10.1128/IAI.71.4.2095-2101.2003

202. Blanchette J, Racette N, Faure R, Siminovitch KA, Olivier M. *Leishmania*-induced increases in activation of macrophage SHP-1 tyrosine phosphatase are associated with impaired IFN-gamma-triggered JAK2 activation. *Eur J Immunol.* (1999) 29:3737–44. doi: 10.1002/(SICI)1521-4141(199911)29:11<3737::AID-IMMU3737>3.0.CO;2-S
203. Forget G, Gregory DJ, Whitcombe LA, Olivier M. Role of host protein tyrosine phosphatase SHP-1 in *Leishmania donovani*-induced inhibition of nitric oxide production. *Infect Immun.* (2006) 74:6272–79. doi: 10.1128/IAI.00853-05
204. Alti D, Sambamurthy C, Kalangi SK. Emergence of leptin in infection and immunity: scope and challenges in vaccines formulation. *Front Cell Infect Microbiol.* (2018) 8:147. doi: 10.3389/fcimb.2018.00147
205. Stahl P, Schwarz RT, Debierre-Grockiego F, Meyer T. *Trypanosoma cruzi* parasites fight for control of the JAK-STAT pathway by disarming their host. *JAKSTAT* (2015) 3:e1012964. doi: 10.1080/21623996.2015.1012964
206. Hovsepian E, Penas F, Siffo S, Mirkin GA, Goren NB. IL-10 inhibits the NF-κB and ERK/MAPK-mediated production of pro-inflammatory mediators by up-regulation of SOCS-3 in *Trypanosoma cruzi*-infected Cardiomyocytes. *PLoS ONE* (2013) 8:e79445. doi: 10.1371/journal.pone.0079445

Conflict of Interest Statement: The authors declare that the research was conducted in the absence of any commercial or financial relationships that could be construed as a potential conflict of interest.

frontiers in Immunology

ORIGINAL RESEARCH
published: 10 August 2018
doi: 10.3389/fimmu.2018.01814

A Lactate Fermentation Mutant of *Toxoplasma* Stimulates Protective Immunity Against Acute and Chronic Toxoplasmosis

*Ningbo Xia[1], Taifang Zhou[1], Xiaohan Liang[1], Shu Ye[1], Pengfei Zhao[1], Jichao Yang[1], Yanqin Zhou[1], Junlong Zhao[1,2,3] and Bang Shen[1,3]**

[1] State Key Laboratory of Agricultural Microbiology, Huazhong Agricultural University, Wuhan, China, [2] Hubei Cooperative Innovation Center for Sustainable Pig Production, Wuhan, China, [3] Key Laboratory of Preventive Medicine in Hubei Province, Wuhan, China

Toxoplasma gondii is an important zoonotic pathogen infecting one-third of the world's population and numerous animals, causing significant healthcare burden and socioeconomic problems. Vaccination is an efficient way to reduce global sero-prevalence, however, ideal vaccines are not yet available. We recently discovered that the *Toxoplasma* mutant lacking both lactate dehydrogenases *LDH1* and *LDH2* (*Δldh*) grew well *in vitro* but was unable to propagate in mice, making it a good live vaccine candidate. Here, we tested the protection efficacy of ME49 *Δldh* using a mouse model. Vaccinated mice were efficiently protected from the lethal challenge of a variety of wild-type strains, including type 1 strain RH, type 2 strain ME49, type 3 strain VEG, and a field isolate of Chinese 1. The protection efficacies of a single vaccination were nearly 100% for most cases and it worked well against the challenges of both tachyzoites and tissue cysts. Re-challenging parasites were unable to propagate in vaccinated mice, nor did they make tissue cysts. High levels of *Toxoplasma*-specific IgG were produced 30 days after immunization and stayed high during the whole tests (at least 125 days). However, passive immunization of naïve mice with sera from vaccinated mice did reduce parasite propagation, but the overall protection against parasite infections was rather limited. On the other hand, *Δldh* immunization evoked elevated levels of Th1 cytokines like INF-γ and IL-12, at early time points. In addition, splenocytes extracted from immunized mice were able to induce quick and robust INF-γ and other pro-inflammatory cytokine production upon *T. gondii* antigen stimulation. Together these results suggest that cellular immune responses are the main contributors to the protective immunity elicited by *Δldh* vaccination, and humoral immunity also contributes partially. We also generated uracil auxotrophic mutants in ME49 and compared their immune protection efficiencies to the *Δldh* mutants. The results showed that these two types of mutants have similar properties as live vaccine candidates. Taken together, these results suggest that mutants lacking LDH were severely attenuated in virulence but were able to induce strong anti-toxoplasma immune responses, therefore are good candidates for live vaccines.

Keywords: *Toxoplasma*, lactate dehydrogenase, live vaccine, toxoplasmosis, cellular immunity

OPEN ACCESS

Edited by:
Xun Suo, China Agricultural University, China

Reviewed by:
Pallab Ghosh, Harvard Medical School, United States
Manuel Vilanova, Universidade do Porto, Portugal

***Correspondence:**
Bang Shen
shenbang@mail.hzau.edu.cn

Specialty section:
This article was submitted to Microbial Immunology, a section of the journal Frontiers in Immunology

Received: *19 March 2018*
Accepted: *23 July 2018*
Published: *10 August 2018*

Citation:
Xia N, Zhou T, Liang X, Ye S, Zhao P, Yang J, Zhou Y, Zhao J and Shen B (2018) A Lactate Fermentation Mutant of Toxoplasma Stimulates Protective Immunity Against Acute and Chronic Toxoplasmosis. Front. Immunol. 9:1814. doi: 10.3389/fimmu.2018.01814

INTRODUCTION

Toxoplasma gondii is an obligate intracellular parasite that infects all warm-blooded animals and humans (1). Generally, its infection in healthy people causes no or mild flu-like symptoms, thus most of the infections are not noticed. However, in susceptible pregnant women, *T. gondii* infection may have severe consequences such as abortion, neonatal death, congenital defects, and mental retardation of delivered babies (2, 3). In addition, it is also a high risk for individuals with compromised immune functions, such as AIDS and organ transplant patients (2). Due to the broad host range, a variety of agricultural important animals such as pigs and sheep are constantly challenged by *T. gondii*, causing substantial economic losses and public health problems (2, 4, 5). Folic acid metabolism inhibitors such as pyrimethamine and sulfadiazine are commonly used to treat toxoplasmosis but they do not work on chronic infections (6).

The control of *Toxoplasma* infection is rather difficult, one reason is that it has complex life cycle and multiple routes of transmission (7, 8). Cats are the definitive hosts of *T. gondii* and the oocysts shed by cats are thought to be a key source of human and animal infections (9). In addition, *T. gondii* can be transmitted between intermediate hosts through predation. Most of the *Toxoplasma* infection cases belong to chronic infection, where the parasites are encysted in muscles and central nerve system (called tissue cysts) of infected animals lifelong (7). Ingestion of raw or undercooked meat from such animals represents another important route of transmitting the parasites to humans and animals (2, 5). As mentioned above, encysted parasites at the chronic infection stage are resistant to most of the current therapeutics. Another challenge to the control of toxoplasmosis is the complex population structure of *T. gondii* strains. North America and Europe are dominated by three clonal strains (type I, II, and III), which display different acute virulence in mice (10, 11). However, in other parts of the world, the strains are much more diverse, particularly in South America (12, 13). A recent study demonstrated that genetically distinct strains may be able to superinfect the same host, indicating the lack of sufficient cross protection from immunization with one single strain (14). This study had important highlights for the design of *Toxoplasma* vaccines, particularly whole parasite-based vaccines.

Scientists have done tremendous amount of work to pursue an ideal vaccine against *T. gondii*. The first generation of vaccines contained killed parasites, or native antigens derived from soluble or secretory proteins of cultured tachyzoites. These vaccines only provided limited protection against further infections (15, 16). Then when the recombinant DNA technology became available, a variety of subunit vaccines were tried, mainly using surface or secretory proteins such as SAG1 and MIC2 (17–20). These recombinant protein or vector-based subunit vaccines were safer and easier to make than native antigen-based vaccines, however, they did not provide sufficient protection either [reviewed in Ref. (21, 22)]. The strategy that holds the most promise for a good *Toxoplasma* vaccine seems to be live attenuated vaccines. Currently there is one commercial vaccine (Toxovax®) available, which is derived from the S48 strain originally isolated from an aborted lamb and licensed for use to avoid congenital toxoplasmosis in ewes (23). The exact mechanisms of Toxovax® as a vaccine are not well understood, but thought to be linked to its inability to form cysts or oocysts to complete the life cycle (24). Tachyzoites can be cleared efficiently by hosts' immunity, therefore mutants defective in cyst formation have the potential to be vaccines. Encouraged by the success of Toxovax® and to design safer live vaccines, scientists turned to genetically modified parasites. Among these, uracil auxotroph mutants defective in *de novo* UMP (uridine 5′-monophosphate) synthesis are promising (25–27). Mutants with inactivated *CPSII* or *OMPDC* grew well *in vitro* in the presence of extra uracil (25–27), but were unable to establish acute infection in animals, therefore were severely attenuated. These mutants were extensively studied in mice and displayed great potential to be good vaccines, but still need to be tested in other animals like pigs, sheep, and cats.

We recently discovered that *T. gondii* mutants with both lactate dehydrogenase genes deleted (*Δldh*) grew robustly *in vitro* but failed to propagate *in vivo* (28), very similar to the uracil auxotroph mutants. The reason for this growth difference is that, under *in vivo* conditions when oxygen is limited, lactate fermentation becomes a key energy supply pathway to support parasite replication. By contrast, oxidative phosphorylation alone provides enough energy for parasite reproduction *in vitro* when oxygen is rich. As such, *Δldh* mutant was greatly attenuated *in vivo*, even in immune-deficient animals (28). In this study, we set to analyze the protective immunity of the *Δldh* mutant as a vaccine using the mouse model. The results showed that vaccination of mice with tachyzoites of this mutant induced efficient protection against the challenge of a variety of strains.

RESULTS

Tissue Cysts Derived From ME49 *Δldh* Were Severely Attenuated in Mice

Our previous study reported that the virulence of ME49 *Δldh* tachyzoites was significantly (>640-fold) reduced compared to that of the wild-type (WT) strain ME49, no mortality was detected even at the infection dose of 3.2×10^4 tachyzoites/mouse (28). However, we did observe that many of the *Δldh* tachyzoites infected mice formed brain cysts, although the amount was much less than that of WT parasites infected mice. To see whether the residual amount of cysts in *Δldh* infected mice have normal virulence, 50 cysts derived from WT or *Δldh* parasites were used to infect ICR mice by oral administration, and the survival of infected mice was monitored for 40 days. The results showed that 50 cysts of ME49 killed 80% of the mice. However, none of the *Δldh* cyst infected mice died (**Figure 1**), nor did they show any obvious clinical symptoms, suggesting that the virulence of the *Δldh* cysts was also significantly attenuated, just like the tachyzoites of this strain.

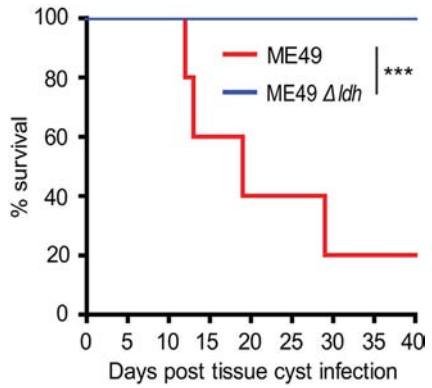

FIGURE 1 | Virulence tests of *Toxoplasma* cysts in mice. ICR mice were infected with brain cysts of ME49 or ME49 *Δldh* (50 cysts/mouse, $n = 5$ mice for ME49 strain and $n = 7$ mice for ME49 *Δldh* strain) by oral administration and their survival was monitored for 40 days. ***$p < 0.001$, Gehan–Breslow–Wilcoxon test.

Δldh Vaccination Elicited Strong Protective Immunity Against Tachyzoites Infection

The *Δldh* mutant grew robustly *in vitro* but was unable to propagate *in vivo*, this unique property makes it a good vaccine candidate (28). To check this possibility and assess the immune protection offered by *Δldh* vaccination, ICR mice were first immunized with ME49 *Δldh* by intraperitoneal injection (10^4 tachyzoites/mouse). Thirty days later, they were challenged with 10^4 tachyzoites of the type 2 strain ME49, type 3 strain VEG, or Chinese 1 strain C7719. Subsequently survival of the mice was monitored for another 30 days. The mortality rates for non-immunized mice were 100% upon the infection of ME49 and C7719, whereas VEG caused 90% mortality. However, for *Δldh*-vaccinated mice, the survival rates were 100% upon the challenge of all three strains and no obvious symptoms were observed during the 30-day infection period (**Figures 2A–C**). These results indicate that *Δldh* vaccination is able to offer efficient protection against lethal parasite infections.

The above results showed that 30 days post *Δldh* vaccination, mice were well protected. To see whether *Δldh* vaccination provides longer time protective immunity, mice were vaccinated with ME49 *Δldh* and 75 days later, they were challenged with type 1 strain RH *Δhxgprt*, type 2 strain ME49, or Chinese 1 strain C7719. The survival rates of immunized mice that were re-infected with ME49 or C7719 were 100% (**Figures 2E,F**), similar to the above infections 30 days post-vaccination. However, if challenged with the most virulent type 1 strain RH *Δhxgprt*, only 60% of the immunized mice survived (**Figure 2D**). As will be discussed below, the protection against RH infection was also 100% if the challenge occurred 20 days after immunization. To examine the efficiency of even longer time protection, ME49 *Δldh* vaccinated mice were challenged with WT parasites 125 days post-vaccination. The results showed that the immune protection against ME49 and VEG challenge was still 100% (**Figures 2G,H**). Together, these results suggest that ME49 *Δldh* immunization can provide both short- and long-term protection against strains with intermediate virulence, but the protection against strongly virulent strains is limited to a short time after vaccination and then decreased gradually.

Δldh Immunization Stimulated Protective Immunity Against Bradyzoites Infection

A significant portion of *T. gondii* infections were acquired through ingestion of tissue cysts that contain bradyzoites. In order to check whether *Δldh* vaccination provided protection against bradyzoites infection, ICR mice were first immunized with 10^4 tachyzoites of ME49 *Δldh*. Thirty days after immunization, they were orally challenged with 50 cysts of the ME49 strain. The results show that 100% of *Δldh*-immunized mice survived the cyst challenging, whereas all naïve mice died of this infection (**Figure 3**). These results suggest that *Δldh* strain also elicited protective immunity against bradyzoite infection.

Δldh Immunization Blocked Cyst Formation From New Infections

One caveat of chemotherapies against acute toxoplasmosis is that the drugs may drive the parasites to slowly replicating bradyzoites to form tissue cysts, which lead to lifelong chronic infection. To examine whether the *Δldh* mutant vaccination could provide protective immunity against chronic *T. gondii* infection, the cyst forming competent but less virulent (compared with ME49) strain TgPIG-WH1 (genotyped as ToxoDB #3) was used to challenge the vaccinated ICR mice. As shown in **Figure 4A**, at the infection dose of 10^4 tachyzoites/mouse through intraperitoneal injection, TgPIG-WH1 killed only 10% of the non-immunized mice, consistent with its reduced virulence. Thirty days post TgPIG-WH1 challenge, survived mice were sacrificed and the numbers of tissue cysts in the brains were determined by DBA-FITC staining, and compared to that of vaccinated but not re-challenged, as well as non-immunized but TgPIG-WH1 infected mice. The results in **Figure 4B** showed that infection of naïve mice by TgPIG-WH1 resulted in about 500 cysts per brain on average. However, cyst number in *Δldh* immunized and subsequently TgPIG-WH1 infected mice was reduced to around 100, which was very similar to that of vaccinated but not re-challenged mice, suggesting that they were probably derived from vaccination but not TgPIG-WH1 infection. Together, these results indicate that *Δldh* immunization also provides protective immunity against chronic toxoplasmosis.

Δldh Vaccinated Mice Were Able to Clear Challenging Parasites Rapidly

The above results demonstrated that vaccinating mice with ME49 *Δldh* provided efficient protection against both acute and chronic toxoplasmosis. To further examine the fate of challenging parasites, the propagation dynamics of a luciferase expressing strain RH-Luc in vaccinated mice were determined by bioluminescent imaging. In naïve mice, RH-Luc infection resulted in rapid replication of the parasites. At the infection dose of 10^4 tachyzoites/mouse, luminescent signals were detectable just 1 day after infection and increased over 1,000-fold 5 days post-infection

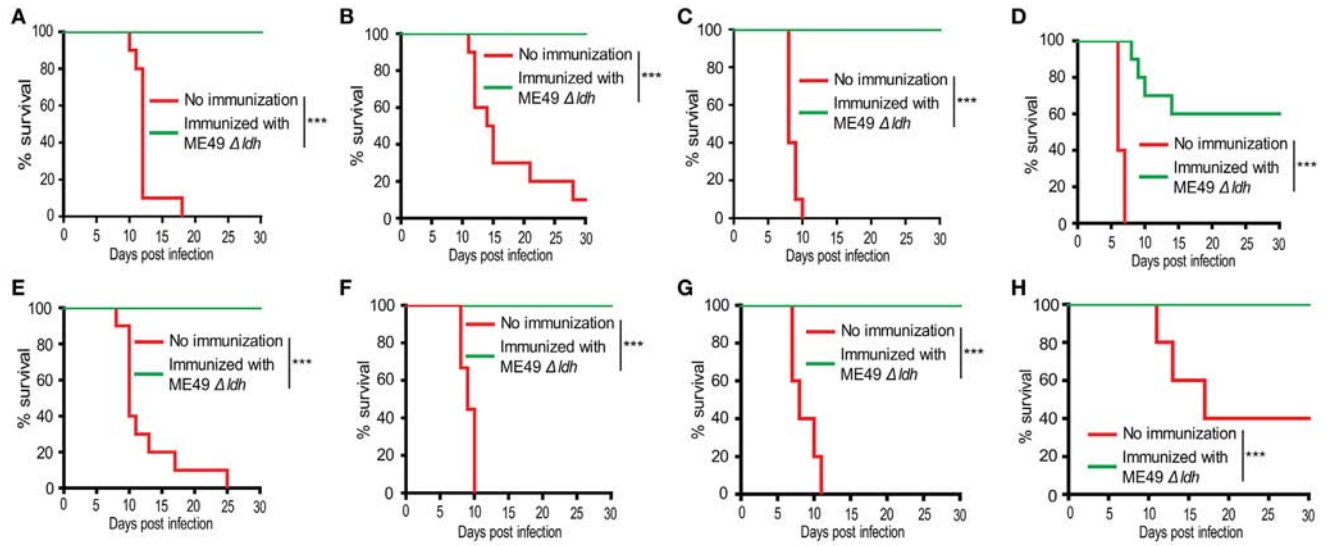

FIGURE 2 | *Δldh* parasite immunization protected mice from *Toxoplasma gondii* tachyzoites infection. ICR mice were pre-immunized with 10^4 tachyzoites of the ME49 *Δldh* mutant. **(A–C)** 30 days post-immunization, they were challenged with 10^4 tachyzoites of the ME49 **(A)**, VEG **(B)**, or C7719 **(C)** strains (10 mice for each strain) by intraperitoneal injection and their survival was monitored for another 30 days. **(D–F)** 75 days post-immunization, 10^4 tachyzoites of the RH *Δhxgprt* **(D)**, ME49 **(E)**, C7719 **(F)** strains were used to challenge the mice and their survival was monitored for another 30 days. **(G,H)** 125 days post-immunization, 10^4 tachyzoites of the ME49 **(G)**, VEG **(H)** strains were used to challenge the mice and their survival was monitored for another 30 days. Non-immunized mice were included as control. ***$p < 0.001$, Gehan–Breslow–Wilcoxon tests.

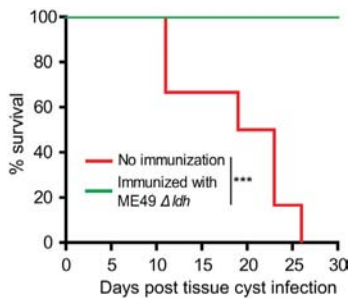

FIGURE 3 | *Δldh* mutant vaccination protected mice from *Toxoplasma gondii* cysts infection. ICR mice were pre-immunized with ME49 *Δldh* as in **Figure 2**, 30 days post-immunization they were challenged with 50 fresh brain cysts of the ME49 strain and their survival was monitored for another 30 days ($n = 10$ mice for each strain). Non-immunized mice were included as control. ***$p < 0.001$, Gehan–Breslow–Wilcoxon test.

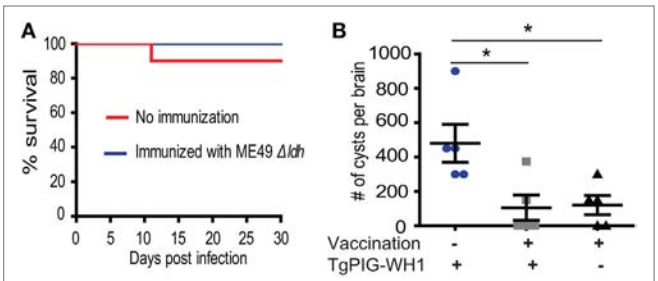

FIGURE 4 | *Δldh* mutant immunization prevented cyst formation from further infections. **(A)** ICR mice were pre-immunized with ME49 *Δldh* as in **Figure 2** and 30 days later challenged with 10^4 tachyzoites of TgPIG-WH1. Non-immunized mice were included as control and survival of mice were monitored for another 30 days ($n = 10$ mice for each strain). **(B)** Cyst loads in the brains of non-immunized but TgPIG-WH1 challenged mice, immunized and TgPIG-WH1 challenged mice, and *Δldh* immunized but not TgPIG-WH1 challenged mice [not shown in **(A)**]. The mice survived at day 30 in **(A)** were sacrificed, and the number of *Toxoplasma* cysts in the brain homogenate was determined by DBA-FITC staining and fluorescent microscopy. Data from the analysis of five mice in each group were graphed, *$p < 0.05$, Student's *t*-test.

(**Figures 5A,B**). However, in the vaccinated mice, luminescent signals were not detectable at both time points, indicating little propagation and probably rapid clearance of the challenging RH-Luc (**Figures 5A,B**). It should be noted that in this experiment, RH-Luc infection was performed 30 days after *Δldh* immunization. We also followed the survival of these RH-Luc infected mice for 20 days, all naïve mice died within 8 days but all vaccinated mice survived with no symptoms (**Figure 5C**). These results suggest that, at least within a limited time period, *Δldh* immunization enables rapid clearance of the challenging parasites, which explains its efficient immune protection.

Δldh Vaccination Significantly Increased the Levels of Pro-Inflammatory Cytokines and *T. gondii* Specific IgG Antibodies

To estimate the potential mechanisms of immune protection offered by *Δldh* vaccination, we first examined the cytokine level changes upon vaccination. Sera samples obtained from vaccinated mice 30, 75, or 125 days post-vaccination were subject to ELISA analysis to check the levels of IFN-γ, IL-12,

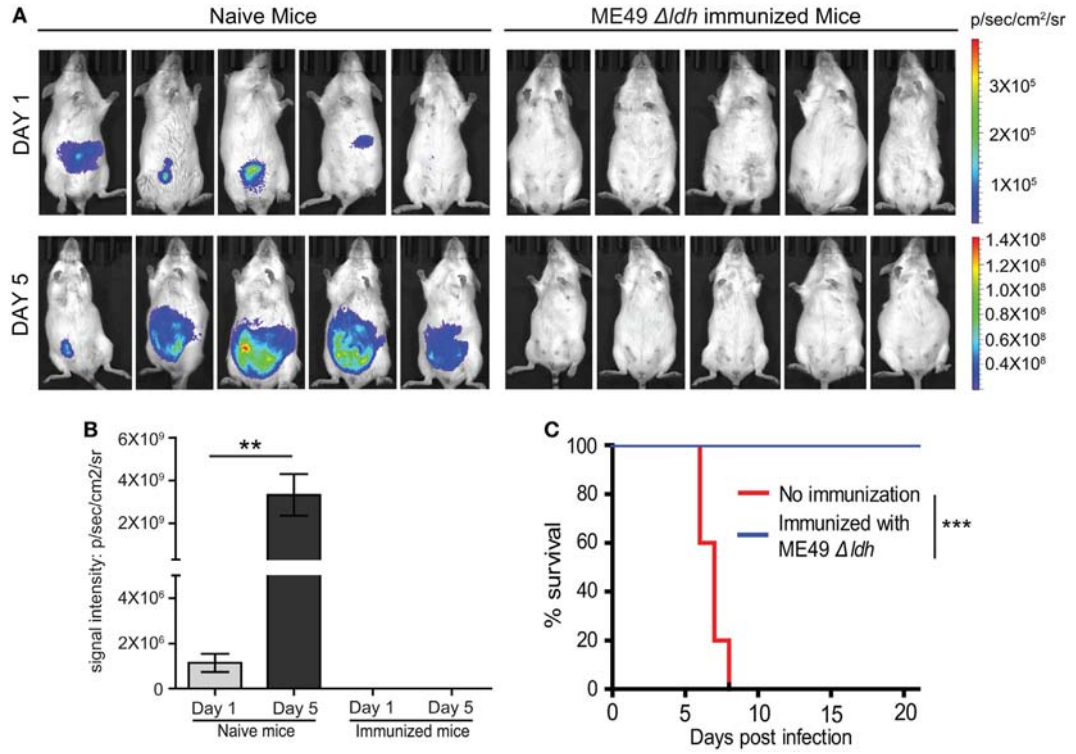

FIGURE 5 | *Δldh* parasite vaccination elicited rapid clearance of challenging parasites. **(A)** Naïve or pre-immunized mice were challenged with 10^4 tachyzoites of RH-Luc (five mice for each group). Parasite loads in mice 1 and 5 days post RH-Luc infection were analyzed by live animal imaging on the IVIS Spectra system. p/sec/cm^2/sr: photons per second per cm^2 per steradian. **(B)** Total bioluminescent signals of mice from **(A)** were calculated and graphed, $^{**}p < 0.01$, Student's *t*-test. **(C)** Survival curves of naïve or *Δldh* immunized mice infected with RH-Luc, $^{***}p < 0.001$, Gehan–Breslow–Wilcoxon test.

IL-10, and TNF-α. The IL-12–IFN-γ axis is key to activate cellular immune clearance of *T. gondii*. Their levels, as well as the levels of another pro-inflammatory cytokine TNF-α, increased significantly both 30 and 75 days post-vaccination, compared to control mice (**Figures 6A–C**). However, the levels at day 75 were lower than that at day 30, which was likely caused by the activation of anti-inflammatory response, as evidenced by high levels of IL-10 in vaccinated mice 30 days post-infection (**Figure 6D**). At 125 days post-infection, the levels of all cytokines were back to normal as in naïve mice (**Figures 6A–D**). We also measured the *T. gondii* specific IgG levels and found that ME49 *Δldh* vaccination induced high levels of IgG 30, 75, and 125 days post-immunization (**Figure 6E**). Although it looked like there was an increase in *T. gondii* specific IgG levels over time, the differences were not statistically significant (**Figure 6E**). The relatively stable levels of parasite-specific IgG were in contrast to the changes of cytokine levels. These results, along with the above-described short- and long-term protective immunity (**Figure 2**), suggest that *Δldh* immunization probably stimulated both humoral and cell-mediated immune responses to control secondary infections.

Passive Immunization With the Sera of *Δldh*-Vaccinated Mice Provided Partial Protection Against *T. gondii* Infection

Above results demonstrated that high levels of *T. gondii* specific IgG were produced in *Δldh*-vaccinated mice. To estimate the contribution of such antisera in restricting further parasite infection, naïve mice were infected with the WT strain ME49 through intraperitoneal injection. At day 0 and day 3 after infection, sera from the ME49 *Δldh*-vaccinated mice were collected 160 days post-immunization and administered into infected mice by tail vein injection. The protection of passive immunization was estimated in two ways, parasite burden and mice survival. One week post-infection, parasite burden in peritoneal fluid was determined by quantitative PCR. The results showed that passive immunization with the sera of *Δldh*-vaccinated mice did result in significantly lower level of parasite burden compared to immunization with sera of naïve mice (**Figure 7A**). However, when the survival of mice were followed, passively immunized mice only survived for two more days, compared with the negative immunization control (**Figure 7B**). Together these results suggested that the sera of *Δldh*-vaccinated mice are able to reduce parasite propagation to some degree but do not offer full protection against lethal infections.

Robust Pro-Inflammatory Cytokine Production by Splenocytes of *Δldh*-Vaccinated Mice Upon *T. gondii* Antigen Stimulation

The above passive immunization results suggested that the contribution of humoral immunity to the protection of *Δldh*

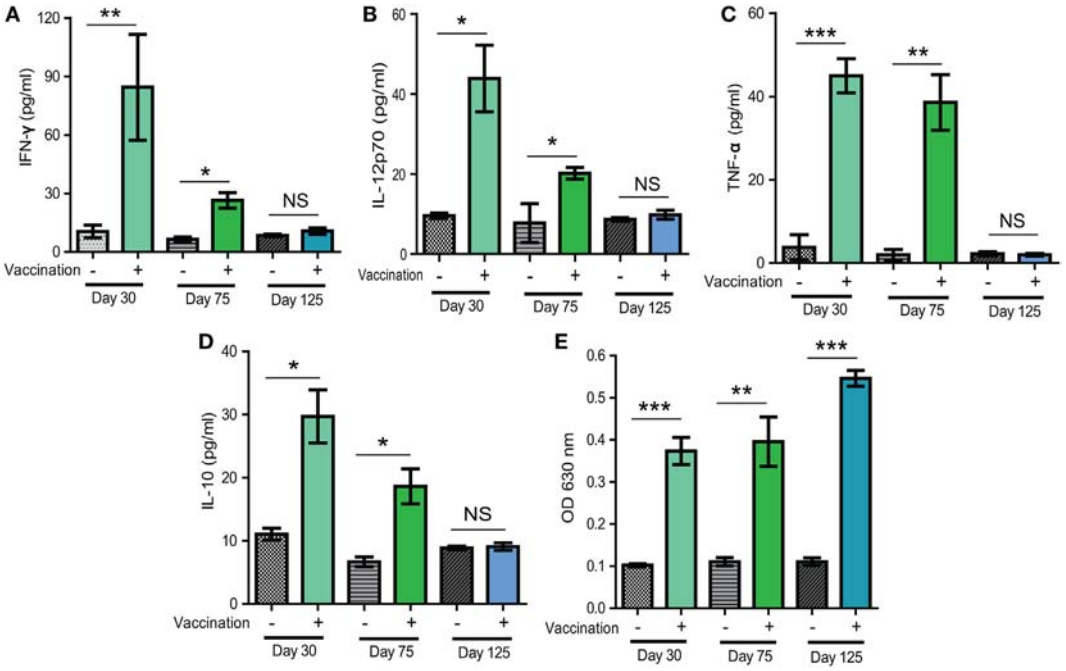

FIGURE 6 | Levels of selected cytokines and *Toxoplasma* specific IgG in sera of mice 30, 75, and 125 days after *Δldh* immunization. **(A–D)** Levels of indicated cytokines measured by ELISA. **(E)** Relative levels of *Toxoplasma* specific IgG, as determined by indirect ELISA. Sera from naïve mice were used as controls and three mice from each group were analyzed. $^{*}p < 0.05$, $^{**}p < 0.01$, $^{***}p < 0.001$, NS: not significant, Student's *t*-test.

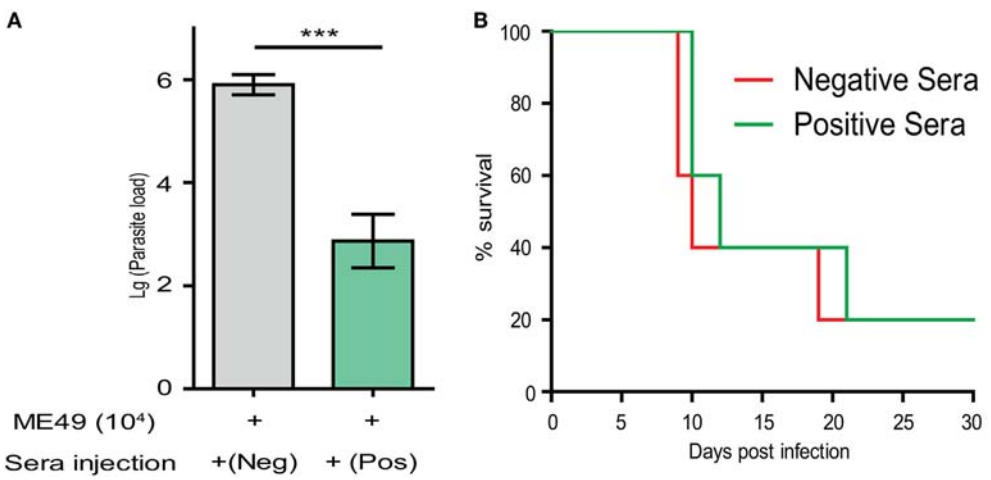

FIGURE 7 | Passive immunization using the sera from *Δldh*-vaccinated mice provided partial protection against parasite infection. **(A)** ICR mice ($n = 3$ for each group) were injected with 10^4 tachyzoites of ME49 by intraperitoneal injection. At day 0 and day 3 post-infection, mice were treated with positive sera collected from the ME49 *Δldh*-vaccinated mice (160 days post-vaccination), or negative serum from naïve mice by tail intravenous injection. Parasite loads in peritoneal fluids 7 days post-infection were estimated by quantitative PCR. $^{***}p < 0.0001$, Student's *t*-test. **(B)** Survival of passively immunized mice.

vaccination is limited. Next, we estimated cell-mediated immunity, as well as the antigen-specific memory responses by checking the antigen recall response in vaccinated mice. To do that, splenocytes from ME49 *Δldh* immunized mice were harvested 160 days post-vaccination, a time point when the cytokine levels in immunized mice was indistinguishable from that of naïve mice. These splenocytes were cultured *in vitro* and stimulated with total soluble Toxoplasma antigen (TSA) prepared from ME49 tachyzoites. Subsequently the supernatants from the cultures were collected to estimate the cytokine levels by ELISA. Compared with the no-stimulation or non-vaccinated splenocyte controls, TSA stimulated high levels of pro-inflammatory cytokines INF-γ and TNF-α (**Figures 8A,B**). Induction of IL-12 production was not as obvious (**Figure 8C**). Given that INF-γ is the key activator of

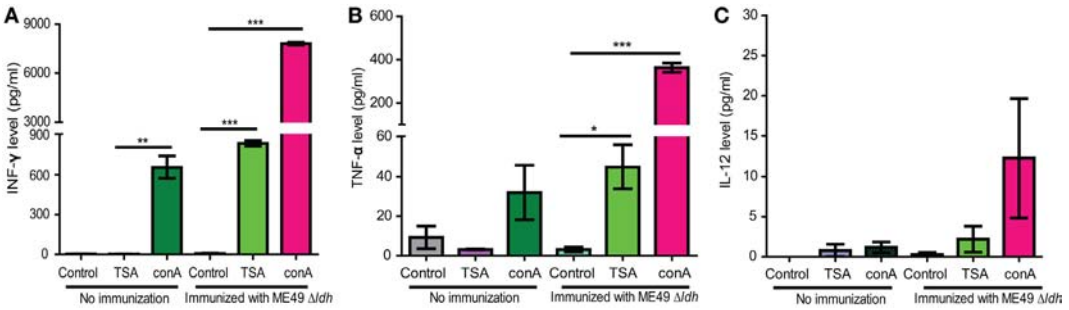

FIGURE 8 | Cytokine production by splenocytes of ME49 *Δldh*-vaccinated mice after *Toxoplasma* antigen stimulation. ICR mice were vaccinated with 10^3 tachyzoites of ME49 *Δldh* and splenocytes were harvested 160 days post-vaccination. The *in vitro* cultured splenocytes were then treated with fetal bovine serum (control), total soluble Toxoplasma antigen (TSA) or Concanavalin A (conA, positive control) for 72 h. Subsequently the levels of IFN-γ **(A)**, TNF-α **(B)** and IL-12 **(C)** in the culture supernatants were measured by ELISA. Splenocytes isolated from non-immunized naïve mice were included as controls. Three mice from each group were analyzed and each treatment condition was repeated three times, $^*p < 0.05$, $^{**}p < 0.01$, $^{***}p < 0.0001$, Student's *t*-test.

cell-mediated immunity for *T. gondii* clearance, quick and robust INF-γ production from vaccinated splenocytes upon TSA stimulation suggests that efficient cellular immune responses would be activated during secondary infections.

Compare the Protection Efficiency of *Δldh*-Based Vaccines to That of Uracil Auxotrophic Mutants

Mutants defective in *de novo* pyrimidine biosynthesis are auxotrophic to uracil, therefore they are not replicating and avirulent *in vivo* (25–27). As such, those types of mutants (such as *CPSII* and *OMPDC* deficient strains) were considered great vaccine candidates. We sought to compare the protection efficiency of our *Δldh*-based vaccines to that based on uracil auxotrophic mutants. For this purpose, we first made an *OMPDC* deletion mutant in ME49, by CRISPR/Cas9-mediated gene replacement to replace *OMPDC* by loxP sites flanked *DHFR** (**Figure 9A**). The resulted ME49 *ompdc:DHFR** (**Figure 9B**) was then transiently transfected with a Cre recombinase expressing plasmid to remove the selection marker *DHFR**, to obtain ME49 *Δompdc* (**Figure 9C**). We also generated a double knockout line (ME49 *Δompdc Δldh1*) by disrupting *LDH1* in ME49 *Δompdc* (**Figures 9D,E**).

First, the virulence of these mutants were compared in mice. With the infection dose of 10^4 tachyzoites per mouse, ME49 killed all mice within 12 days. All mice infected with *Δompdc, Δompdc Δldh1*, or *Δldh* mutants were survived (**Figure 10A**), indicating significant virulence attenuation of these mutants. To further check the ability of these mutants to propagate *in vivo*, mice were infected with each mutant line (10^4 tachyzoites/mouse) and a week later, the parasite burden in peritoneal fluid was examined by qPCR. ME49 displayed robust replication and high parasite burden was detected in mice with this strain (**Figure 10B**). All three mutants showed minimal replication in mice, as the parasite burden in the corresponding mutants were very low, close to (*Δldh*) or below (*Δompdc*, *Δompdc Δldh1*) the reliable detection limit of qPCR (**Figure 10B**). It seemed like there were more parasites in *Δldh*-infected mice than *Δompdc*- and *Δompdc Δldh1*-infected ones, however, because of the sensitivity of the qPCR tests, it is hard to measure the exact parasite burden differences. Next, we compared the immune protection efficiencies of these mutants. Mice were first infected with each of these mutant lines, 30 days post-infection they were challenged with the WT strain ME49 and survival of the mice was monitored. All immunized mice survived the secondary infection (**Figure 10C**), which is consistent with previous results and indicates that these mutants offered similar protection efficiencies against further infections. Together, these results suggest that the *Δldh* mutant worked comparably well as the uracil auxotrophic mutants as a vaccine candidate.

DISCUSSION

Decades of epidemiological and experimental studies have suggested that vaccination is probably the most effective way to control the ubiquitous pathogen *T. gondii*, and live attenuated vaccines hold the most promise among all vaccination strategies tried so far. Toxovax® derived from the incomplete strain S48 has been commercialized to reduce *Toxoplasma* caused abortion in sheep (23), and the uracil auxotroph mutants also look promising under experimental settings (25–27). However, these do not mean that current vaccines are ideal. In this study, we tested the possibility of using a lactate dehydrogenase null mutant (*Δldh*) as a live vaccine candidate to prevent animal toxoplasmosis, since our previous work has shown that this mutant was able to grow efficiently *in vitro* but unable to propagate *in vivo* (28). The results showed that, indeed ME49 *Δldh* immunization stimulated efficient protective immunity against the challenge of a variety of strains.

There is a long history for the search of good anti-toxoplasmic vaccines. Killed parasites, total antigens or secreted antigens extracted from cultured parasites, recombinant antigens in a variety of forms, and live attenuated parasites have all been tried over the last 60 years (16, 29–31). One important lesson from these studies is that live attenuated vaccines are the most efficient in stimulating protective immunity. The only commercially available *Toxoplasma* vaccine Toxovax® is a live vaccine derived from the S48 strain, which is used in breeding ewes to reduce

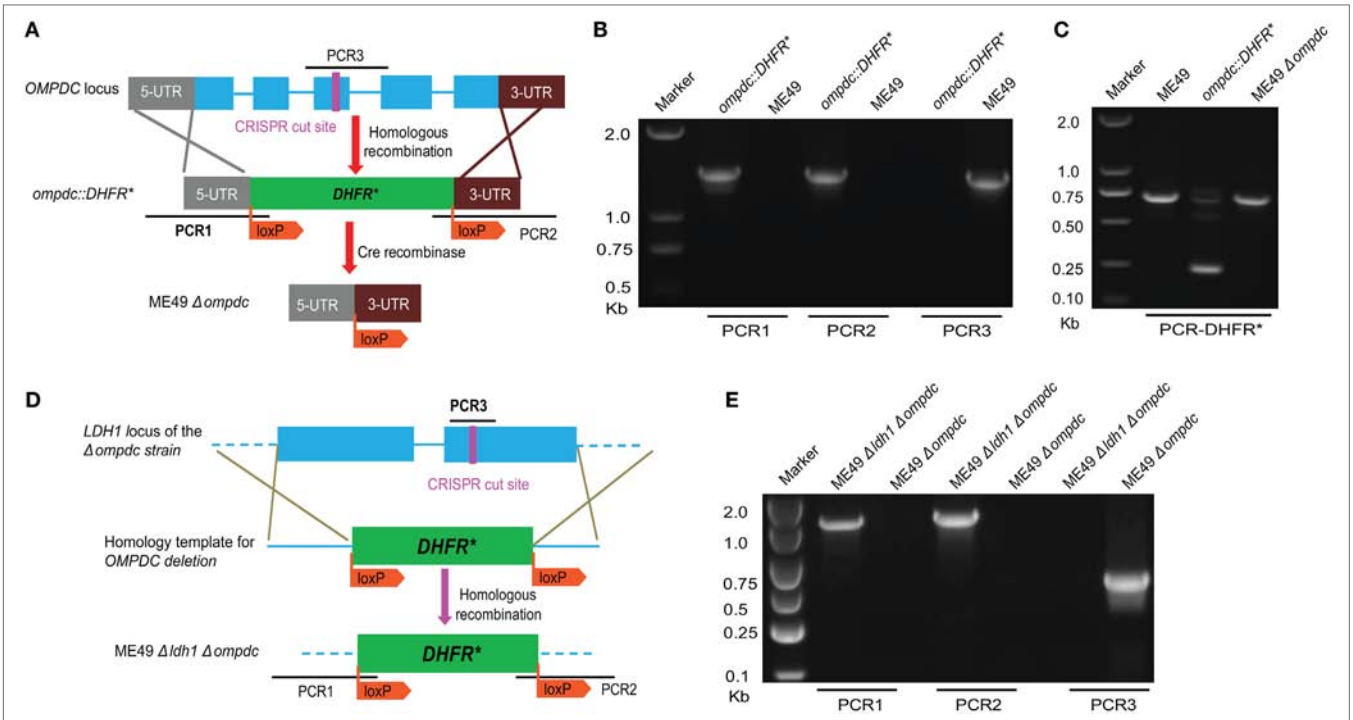

FIGURE 9 | Generation of *OMPDC* deletion mutants. **(A)** Schematic illustration of *OMPDC* replacement by the selection marker *DHFR** and subsequent removal of *DHFR** by Cre recombinase. **(B)** Diagnostic PCR on an *ompdc:DHFR** clone. PCR1 and PCR2 check the integration of *DHFR** at the 5′ and 3′ end of *OMPDC*, respectively, whereas PCR3 examines the presence of *OMPDC* sequence. **(C)** Diagnostic PCR confirming the removal of *DHFR** by Cre recombinase. This PCR generated a 700 bp product from the endogenous *DHFR* locus, and a 250 bp product from *DHFR** due to the absence of introns. Absence of the 250 bp product in *ompdc:DHFR** treated with Cre indicates removal of *DHFR**. **(D)** Diagram illustrating the deletion of *LDH1* in *Δompdc* to make the double mutant *Δompdc ldh1:DHFR**, by CRISPR/Cas9-mediated homologous gene replacement. **(E)** Diagnostic PCR on a *Δompdc ldh1:DHFR** clone.

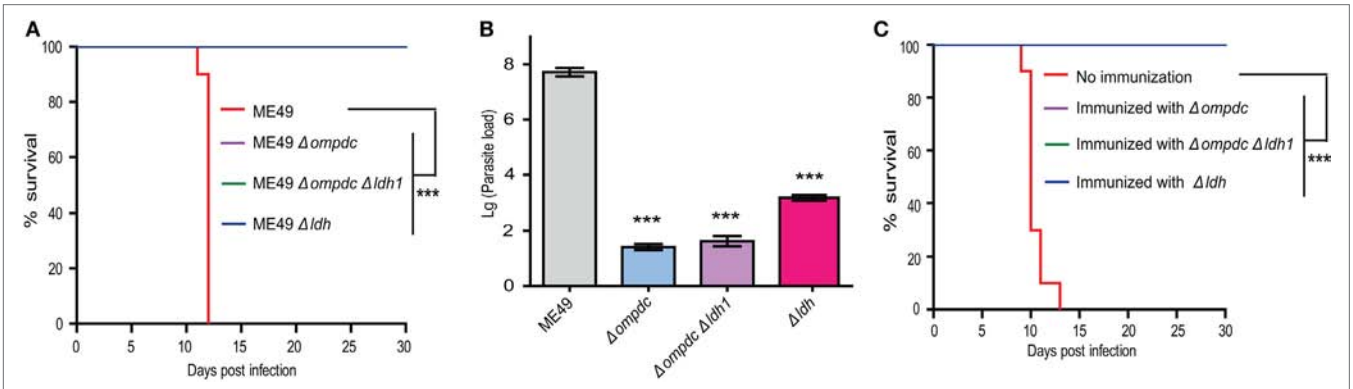

FIGURE 10 | Comparison of *Δldh* mutants-based vaccines to that based on *Δompdc* auxotrophs. **(A)** Survival curves of mice infected with indicated strains. Tachyzoites of indicated strains were used to infect ICR mice (10^4 parasites/mouse, 10 mice for each strain) by intraperitoneal injection and the survival of mice were monitored for 30 days. ***$p < 0.001$, Gehan–Breslow–Wilcoxon test. **(B)** Replication of parasites *in vivo*. ICR mice were infected with 10^4 tachyzoites of indicated strains by intraperitoneal injection and parasite loads in peritoneal fluids 7 days post-infection were determined by quantitative PCR. ***$p < 0.001$, Student's *t*-test. **(C)** Protection efficiency offered by vaccination of indicated *Toxoplasma gondii* mutants. ICR mice were immunized with indicated strains by intraperitoneal injection of 10^4 tachyzoites each. Thirty days post-immunization, they were challenged with 10^4 tachyzoites of the ME49 strain and survival of mice were monitored for another 30 days. Non-immunized mice were included as negative control. ***$p < 0.001$, Gehan–Breslow–Wilcoxon test.

incidences of dry ewes and abortion (23). Inability to complete its life cycle was thought to be why it can be used as a vaccine, since it can only grow as tachyzoites and survive in sheep for about 14 days before being cleared by sheep's immune functions (32). However, this strain is still highly virulent in mice during acute infection. It may also revert to gain cysts or oocysts formation abilities. Because of these limitations, this vaccine is not widely used. Recently the *de novo* pyrimidine synthesis pathway was found to be a good target for vaccine design, as mutants (such as *ΔcpsII* and *Δompdc*) with defective *de novo* UMP biosynthesis

activity were able to grow *in vitro* in the presence of uracil but unable to propagate *in vivo* (25–27). Both *ΔcpsII* and *Δompdc* mutants were reported to induce long-term protection against both acute and chronic toxoplasmosis. Although the uracil auxotroph mutants are promising, their protection is not always 100% (25–27). The *Δldh* mutant tested in this study is similar to the uracil auxotroph mutants as a vaccine candidate, due to its drastic growth differences between *in vitro* and *in vivo* conditions.

An ideal live vaccine not only stimulates efficient protection against further infections but also leaves no parasites behind in order to prevent the risk of parasite dissemination through vaccination, particularly for meat producing animals. In the mouse model, *Δldh* vaccination induced strong protective immune responses against the challenge of a variety of strains, including type 1, 2, 3 strains and natural isolates belonging to ToxoDB #9 and ToxoDB #3. However, it should be noted that the protection to virulent type 1 strain RH-Luc is limited to short term, likely because our *Δldh* was made in the type 2 strain ME49. It was reported previously that vaccinated hosts can also be superinfected by wild strains if they contain virulent ROP5 and ROP18 alleles (14). This explains why ME49 *Δldh* vaccination only provided short-term protection against RH infection. It also suggests that using the endemic strains as starting material to design live vaccines is more likely to be successful. Nonetheless, inactivating *LDH* genes is still a feasible way of producing live attenuated vaccines. The other seemingly caveat of ME49 *Δldh* vaccination is that it still produced very small amount of tissue cysts, although we have shown that these cysts were severely attenuated and likely would not cause diseases in vaccinated animals or new hosts if transmitted to. Nevertheless, we have to admit that, ME49 *Δldh* still needs improvement in this regard, especially for meat producing animals due to the risk of transmitting the infection to humans. One strategy to improve, like we showed, is to combine *Δldh* with mutations that lead to defective *de novo* pyrimidine synthesis. The *Δompdc Δldh1* mutant is as efficient as the *Δldh* mutant in terms of stimulating protective immunity against further infections. Yet, there was little parasite replication and no cyst formation *in vivo* after vaccinating animals with this strain (**Figure 10B** and data not shown), making it safer than the *Δldh* mutant. There is another advantage to combine multiple deletions in one strain for live vaccine design. If the vaccine were to be used in cats, combination of multiple mutations reduces the chance of reversing the vaccine strain back to the virulent parental strain through sexual reproduction, which can happen when the cats are infected with other strains during the vaccination period.

In efforts to assess the potential mechanism of protective immunity from *Δldh* vaccination, we found that it was a combination of humoral and cellular immune responses, with cellular immunity being the major contributor. *Δldh* administration stimulated high levels of IL-12 and IFN-γ, two pro-inflammatory cytokines known to be crucial for activation of cell-mediated clearance of *T. gondii*. The elevated levels of IL-12 and IFN-γ did stay for a while after vaccination and then gradually decreased. They were completely back to normal levels 125 days post-vaccination. At day 160 post *Δldh* immunization, splenocytes extracted from vaccinated mice were able to respond to *T. gondii* antigen quickly and produce high levels of IFN-γ and other pro-inflammatory cytokines, which could activate cellular immune responses and clear secondary infections efficiently. On the other hand, when testing the contribution of humoral immunity by passive immunization, it was found that sera from *Δldh*-vaccinated mice was able to reduce parasite propagation but the overall protection was rather limited, since the passively immunized mice only survived 2 days longer compared to controls (**Figure 7B**). Together these results suggested that cellular immunity, instead of humoral immunity is the main source of protection from *Δldh* vaccination, similar to the uracil auxotroph mutants-based vaccines (25, 27). In our cytokine measurement studies, we noticed that *Δldh* immunization induced relatively long duration of increased IL-12 and IFN-γ levels (**Figures 6A–D**). This was somewhat unexpected, but it may be caused by the unique propagation dynamics of the *Δldh* mutants *in vivo*. As was shown, after immunization *Δldh* parasites could form very low levels of cysts in mice, which suggested that some degree of parasite replication and differentiation must have occurred. The prolonged IL-12 and IFN-γ induction might be a consequence of these parasite activities, but further work is required to completely understand this observation. In addition, it is interesting to note that *Δldh* immunization provided full protection against the challenge of type 1 virulent strain in a relatively short term (30 days). If the challenge occurred too long (>75 days) after vaccination, the protection efficiency decreased significantly. This pattern correlated well with the IL-12 and IFN-γ level changes, which may indicate that the existing of an activated cell-mediated immunity is required for full control of virulent type 1 strains. Nonetheless, even after 75 days, vaccinated mice were still partially protected against RH *Δhxgprt* infection, and fully protected from the challenge of other strain types with intermediate virulence.

In conclusion, our study demonstrated that *Δldh* mutant can potentially be used as a live attenuated vaccine. Its administration stimulated a combination of humoral and cellular immune responses that protected animals from further infections of a variety of *T. gondii* strains. We also combined a uracil auxotroph conferring mutation with *Δldh* deletion to make the double knockout *Δompdc Δldh1*, which exhibited similar protection efficiency as the *Δldh* mutant but with further reduced *in vivo* replication and cyst formation, making it safer to use as vaccines. Although the work from mice models demonstrated the great potential of these mutants as vaccine candidates, further investigations are needed to check the safety of vaccination and efficiency of protection in large animals like pigs and sheep, as well as in cats to see the protection against oocyst shedding.

MATERIALS AND METHODS

Mice and Parasite Strains

All 7-week-old ICR mice were purchased from the Hubei provincial center for disease control and prevention. All animals were maintained under standard conditions according to the regulations specified by Administration of Affairs Concerning Experimental Animals. Animal experiments were approved by the ethical committee of Huazhong Agricultural University (permit #: HZAUMO2016049).

Toxoplasma gondii type 1 strain RH *Δhxgprt* and its derivative RH-Luc that expresses a firefly luciferase, type 2 strain ME49, type 3 strain VEG, RFLP genotype ToxoDB #3 strain TgPIG-WH1, and ToxoDB #9 strain C7719 were used in this study, which were propagated with human foreskin fibroblast cells (purchased from ATCC, USA) and cultured in DMEM medium supplemented with 10% fetal bovine serum (FBS) (LifeTechnologies, Inc., Rockville, MD, USA). In addition, the *Δompdc* and *Δompdc Δldh1* mutant strains were maintained in the presence of extra 250 μM uracil (25, 27) (LifeTechnologies, Inc., Rockville, MD, USA).

Virulence Test of *Δldh* Cysts

Fresh brain cysts derived from ME49 *Δldh* or ME49 were used to infect 7-week-old female ICR mice through oral administration (50 cysts/mouse). Mice survival was monitored for 40 days and blood sample were collected afterward. MIC3-based indirect ELISA was used to check the sera to confirm infection. Sero-negative mice were not included in analysis. Cumulative mortality was graphed as Kaplan–Meier survival plots and analyzed in Prism 5 (GraphPad Software, Inc., La Jolla, CA, USA).

Immune Protection Against Acute Infection Stimulated by *T. gondii* Mutants Vaccination

ICR mice were immunized with 10^4 tachyzoites of ME49 *Δldh*, ME49 *Δompdc*, or ME49 *Δompdc Δldh1* through intraperitoneal injection. 30, 75, or 125 days post-immunization, mice were challenged with 10^4 tachyzoites of RH *Δhxgprt*, ME49, VEG, C7719, or TgPIG-WH1 by intraperitoneal injection (10 mice for each group), or 50 fresh cysts of ME49 by oral administration. Non-immunized naïve mice with the same challenging doses and routes were included as controls and subsequently these animals were monitored for another 30 days to check their clinical symptoms and survival. In addition, naïve or *Δldh* immunized mice were infected with 10^4 tachyzoites of the luciferase expressing RH-Luc strain by intraperitoneal injection (five mice/group). Propagation of RH-Luc in these mice was monitored 1 and 5 days post-infection, by bioluminescent imaging on the IVIS Spectrum imaging system (PerkinElmer, Inc., Boston, MA, USA). To do this, each mouse was injected with 200 μl of 15.4 mg/ml D-luciferin, anesthetized in a chamber containing 2% isoflurane and then imaged by IVIS Spectrum according to the manufacturer's instructions, as well as previous descriptions (33). Data acquisition and analysis were performed using the Living Image 4 software (PerkinElmer, Inc., Boston, MA, USA).

Prevention of Cyst Formation by *Δldh* Immunization

ICR mice were first immunized with ME49 *Δldh* as above and then challenged with 10^4 tachyzoites of TgPIG-WH1. Subsequently the mice were monitored for another 30 days and seropositive mice were sacrificed to harvest the brains. Immunized but not TgPIG-WH1 challenged, and non-immunized but TgPIG-WH1 challenged mice were included as controls (10 mice per group). The number of *Toxoplasma* cysts in each mouse brain was determined by DBA-FITC staining, as previously described (34).

Cytokines and *Toxoplasma*-Specific IgG Level Measurements

Sera samples were collected from mice and stored at −20°C until analysis. The levels of IL12p70, INF-γ, IL-10, and TNF-α were measured using commercial ELISA kits following the manufacturer's instructions (4A Biotech, Inc., Beijing, China). To analyze the levels of *T. gondii* specific IgG by ELISA, 96-well microtiter plates were coated with 100 μl/well 0.5 μg/ml soluble tachyzoite antigens diluted in PBS and incubated at 4°C overnight. The plates were then washed and blocked with 1% BSA. Sera samples were diluted 50-fold and added to each well to incubate for 60 min at 37°C. After extensive washing, the bound IgG antibodies were detected by HRP conjugated goat anti-mouse IgG secondary antibodies and tetramethylbenzidine as substrate. A minimum of three mice was included for each experiment and all sera samples were analyzed three times.

Cytokine Production by Splenocytes After *T. gondii* Antigen Stimulation

ICR mice were immunized with ME49 *Δldh* tachyzoites and seropositive animals were sacrificed 160 days after immunization. Subsequently the spleens were collected from the mice and homogenized in red cell lysis solution (Biosharp, Inc., Beijing, China) to obtain splenocyte suspensions. The recovered splenocytes were washed once in RPMI 1640 (LifeTechnologies, Inc., Rockville, MD, USA), resuspended and counted (35). Viability of the cells was determined by trypan blue staining. Then 3×10^5 viable splenocytes were plated in each well of 96-well plates and cultured in RPMI 1640 supplemented with 20% FBS (LifeTechnologies, Inc., Rockville, MD, USA) and 100 U/ml penicillin–streptomycin. Meanwhile the splenocytes were stimulated with total *T. gondii* soluble antigens (final concentration 50 μg/ml) isolated from tachyzoites of ME49 for 3 days. The supernatants from these cultures were harvested for cytokines level measurements, which was performed as above. *T. gondii* soluble antigens were prepared as the following: freshly egressed tachyzoites of ME49 were collected, purified by filtration, and lysed by sonication in a waterbath sonicator for 30 min. Subsequently the samples were spinned at 12,000 rcf for 10 min at 4°C and the supernatant was collected as TSA, which was subject to protein concentration determination by BCA Protein Assay Kit (Beyotime Biotechnology, Beijing, China) before use. The splenocytes were also stimulated with 5 μg/ml concanavalin A (LifeTechnologies, Inc., Rockville, MD, USA) or 20% FBS as positive and negative controls, respectively. The same experiments were also done with non-immunized naïve mice for further comparisons. Three naïve mice and three immunized mice were analyzed, and each supernatant sample was examined three times by ELISA for technical replication.

Passive Immunization With the Sera of *Δldh*-Vaccinated Mice

ICR mice (16 mice in total, two groups with 8 mice in each group) were infected with the WT strain ME49 through intraperitoneal

injection (10^4 tachyzoites/mouse). At day 0 and day 3 after infection, sera from naïve mice or the ME49 *Δldh*-vaccinated mice 160 days post-immunization were collected and administered into infected mice by tail vein injection (100 µl/mouse). The protection of passive immunization was estimated in two ways. First, three mice from each group were sacrificed 7 days post-infection to measure the parasite burden in peritoneal fluids by quantitative PCR, as previously described (28). Second, the survival of the other five mice in each group was monitored daily for 30 days.

Generation of *Δompdc* and *Δompdc Δldh1* Mutants

Both *OMPDC* and *LDH1* deletions were made by CRISPR/Cas9-mediated homologous gene replacements, using the methods described previously (36, 37). All primers and plasmids used in the mutant constructions are listed in **Tables 1** and **2**, respectively. *LDH1* and *OMPDC* specific CRISPR plasmids were generated by replacing the *UPRT* targeting guide RNA (gRNA) in *pSAG1-Cas9-sgUPRT* with corresponding gRNAs, using Q5 site-directed mutagenesis (36, 37). The plasmid p*OMPDC*:loxp-*DHFR**-loxp was constructed by cloning the 5′- and 3′-homology arms (1,044 and 981 bps, respectively) of *OMPDC*, as well as the loxp-*DHFR**-loxp (3,672 bps) amplified from pDONR-G265-loxP-*DHFR**-loxp into pUC19 through Gibson assembly (New England Biolabs, Ipswich, MA, USA). It was used as the homologous template to replace *OMPDC* with the loxp-*DHFR**-loxp. The plasmid pLDH1:loxp-*DHFR**-loxp used to replace *LDH1* with loxp-*DHFR**-loxp was constructed in a similar way. All the plasmids were verified by DNA sequencing before use. To constructed the *OMPDC* knockout strain, ME49 was co-transfected with the *OMPDC* specific CRISPR plasmid and homologous template (*OMPDC*:loxp-*DHFR**-loxp), selected with 1 µM pyrimethamine and 250 µM uracil (LifeTechnologies, Inc., Rockville, MD, USA), and single cloned by limiting dilution. The resulted ME49 *ompdc:DHFR** was then transiently transfected with a Cre recombinase expressing plasmid (pmin-Cre-eGFP) (38) to remove the selection marker *DHFR**, to obtain ME49 *Δompdc*. All clones were identified by diagnostic PCRs, as demonstrated in **Figures 9A,D**. The *Δompdc Δldh1* double mutant were made by replacing *LDH1* in ME49 *Δompdc* with loxp-*DHFR**-loxp, using the same strategy as the *OMPDC* deletion.

Statistical Analysis

Statistical comparisons were performed in Prism 5 (GraphPad Software, Inc., La Jolla, CA, USA) using Student's *t*-tests,

TABLE 1 | Primers used in this study.

Primer	Sequence	Use
gRNA-LDH1-Fw	5′-GCCGGTCTGACCAAGGTGCCGTTTTAGAGCTAGAAATAGC-3′	To construct the *LDH1* specific CRISPR plasmid
gRNA-OMPDC-Fw	5′-GAGCTTGACTCCACCCTCACGTTTTAGAGCTAGAAATAGC-3′	To construct the *OMPDC* specific CRISPR plasmid
gRNA-R	5′-AACTTGACATCCCCATTTAC-3′	To construct gene specific CRISPR plasmids
pUC19-Fw	5′-GGCGTAATCATGGTCATAGC-3′	Amplification of pUC19 for Gibson assembly
pUC19-Rv	5′-CTCGAATTCACTGGCCGTCG-3′	Amplification of pUC19 for Gibson assembly
loxp-*DHFR**-loxp-Fw	5′-CAACCCGCGCAGAAGACATC-3′	Amplification of loxp-*DHFR**-loxp for Gibson assembly
loxp-*DHFR**-loxp-Rv	5′-GGACACGCTGAACTTGTGGC-3′	Amplification of loxp-*DHFR**-loxp for Gibson assembly
U5ompdc-Fw	5′-CGACGGCCAGTGAATTCGAGGTACGTTTGCGATTGTGAGC-3′	Amplification of 5′-homology of *OMPDC* for pOMPDC:loxp-*DHFR**-loxp construction
U5ompdc-Rv	5′-GATGTCTTCTGCGCGGGTTGCAGTTCTTTGGAATTGTCACGG-3′	Amplification of 5′-homology of *OMPDC* for pOMPDC:loxp-DHFR*-loxp construction
U3ompdc-Fw	5′-GCCACAAGTTCAGCGTGTCCCGTGCTGAAAGCGAAACACTATC-3′	Amplification of 3′-homology of *OMPDC* for pOMPDC:loxp-DHFR*-loxp construction
U3ompdc-Rv	5′-GCTATGACCATGATTACGCCGTCAGTTTCTCTGTGCGAGTTG-3′	Amplification of 3′-homology of *OMPDC* for pOMPDC:loxp-DHFR*-loxp construction
U5ldh1-Rv	5′-GATGTCTTCTGCGCGGGTTGTTCTCCTCTGCACAAGTGCG-3′	Amplification of *PUC19:LDH1-5UTR-3UTR* for pLDH1:loxp-*DHFR**-loxp construction
U3ldh1-Fw	5′-GCCACAAGTTCAGCGTGTCCTGGCAAAACAGGAGCGGAAT-3′	Amplification of *PUC19:LDH1-5UTR-3UTR* for pLDH1:loxp-*DHFR**-loxp construction
5′-UpU5OMPDC	5′-GACAGTTATGGCCCGTCTTC-3′	PCR1 of *Δompdc:DHFR**
3′-In*DHFR**-Fw	5′-CGTGACCACGCCAAAGTAG-3′	PCR1 of *Δompdc:DHFR**
5′-In*DHFR**-Rv	5′-GCACTTGCAGGATGAATTCC-3′	PCR2 of *Δompdc:DHFR**
3′-DnU3OMPDC	5′-GAGCATTGTGCATTTGCGTC-3′	PCR2 of *Δompdc:DHFR**
5′-UpgRNA OMPDC	5′-CGTCAGCTTCGTTAGACCAG-3′	PCR3 of *Δompdc:DHFR**
3′-DngRNA OMPDC	5′-CAGCTGTACTATGAACGGGTG-3′	PCR3 of *Δompdc:DHFR**
5′-In*DHFR*	5′-GTCCGAGTCTGTGCTTCAC-3′	To identify the deletion of loxP-*DHFR**
3′-In*DHFR*	5′-CCTGCGCAGCAGTTGATTTG-3′	To identify the deletion of loxP-*DHFR**
5′-InU5ldh1	5′-CTGTCCAGCGTAGCAATCAC-3′	PCR1 of *Δompdc Δldh1*
3′-In *DHFR**	5′-ACCACGCCAAAGTAGAAAGG-3′	PCR1 of *Δompdc Δldh1*
5′-In*DHFR**	5′-TGCTGGACTGTTGCTGTCTG-3′	PCR2 of *Δompdc Δldh1*
3′-InU3ldh1	5′-GTGGCCGACCTTTTCAGAGC-3′	PCR2 of *Δompdc Δldh1*
5′-UpgRNA ldh1	5′-GCTAGACGCGGAGAGTTGTG-3′	PCR3 of *Δompdc Δldh1*
3′-DngRNA ldh1	5′-AGCTGCTTCTCCGTGACTAC-3′	PCR3 of *Δompdc Δldh1*
RT-tubulin-F	5′-CACTGGTACACGGGTGAAGGT-3′	β-tubulin-based qPCR
RT-tubulin-R	5′-ATTCTCCCTCTTCCTCTGCG-3′	β-tubulin-based qPCR

TABLE 2 | Plasmids used in this study.

Plasmid name	Use	Source
pSAG1-Cas9-sgUPRT	Template for gene-specific CRISPR plasmid construction	Addgene plasmid #54467
pSAG1-Cas9-sgLDH1	LDH1-specific CRISPR plasmid	(28)
pSAG1-Cas9-sgOMPDC	OMPDC-specific CRISPR plasmid	This work
pOMPDC: loxp-*DHFR**-loxp	To replace OMPDC with loxp-*DHFR**-loxp	This work
pLDH1: loxp-*DHFR**-loxp	To replace LDH1 with loxp-*DHFR**-loxp	This work
pLDH1:*DHFR*	Template for *PUC19:LDH1-5UTR-3UTR* amplification	(28)
pDONR-G265-loxP-*DHFR**-loxp	Template for loxp-*DHFR**-loxp amplification	This work
pmin-Cre-eGFP	To remove the selection marker DHFR*	(38)

Gehan–Breslow–Wilcoxon test or one-way ANOVA with Bonferroni posttests as indicated in figure legends.

ETHICS STATEMENT

All animals were maintained under standard conditions according to the regulations specified by Administration of Affairs Concerning Experimental Animals. Animal experiments were approved by the ethical committee of Huazhong Agricultural University (permit #: HZAUMO2016049).

AUTHOR CONTRIBUTIONS

BS, NX, and TZ conceived and designed the experiments; NX, TZ, XL, SY, PZ, and JY performed the experiments; BS, NX, TZ, YZ, and JZ analyzed the data; BS and NX wrote the paper.

ACKNOWLEDGMENTS

The authors are grateful to Drs. Min Cui, Min Hu, Rui Fang, and Lan He from the college of veterinary medicine, Huazhong Agricultural University for their thoughtful suggestions during this study.

FUNDING

This work was supported the National Key Research and Development Program of China (Grant No. 2017YFD0501304), the National Natural Science Foundation of China (Grant No. 31572508), and the Natural Science Foundation of Hubei Province (Project 2017CFA020). The funders had no role in the study design, data collection and analysis, preparation of the manuscript, or decision to submit the work for publication.

REFERENCES

1. Elmore SA, Jones JL, Conrad PA, Patton S, Lindsay DS, Dubey JP. *Toxoplasma gondii*: epidemiology, feline clinical aspects, and prevention. *Trends Parasitol* (2010) 26(4):190–6. doi:10.1016/j.pt.2010.01.009
2. Montoya JG, Liesenfeld O. Toxoplasmosis. *Lancet* (2004) 363(9425):1965–76. doi:10.1016/S0140-6736(04)16412-X
3. Petersen E, Pollak A, Reiter-Owona I. Recent trends in research on congenital toxoplasmosis. *Int J Parasitol* (2001) 31(2):115–44. doi:10.1016/S0020-7519(00)00140-5
4. Dubey JP. Toxoplasmosis in pigs – the last 20 years. *Vet Parasitol* (2009) 164(2–4):89–103. doi:10.1016/j.vetpar.2009.05.018
5. Dubey JP, Hill DE, Jones JL, Hightower AW, Kirkland E, Roberts JM, et al. Prevalence of viable *Toxoplasma gondii* in beef, chicken, and pork from retail meat stores in the United States: risk assessment to consumers. *J Parasitol* (2005) 91(5):1082–93. doi:10.1645/GE-683.1
6. Alday PH, Doggett JS. Drugs in development for toxoplasmosis: advances, challenges, and current status. *Drug Des Devel Ther* (2017) 11:273–93. doi:10.2147/DDDT.S60973
7. Dubey JP. Advances in the life cycle of *Toxoplasma gondii*. *Int J Parasitol* (1998) 28(7):1019–24. doi:10.1016/S0020-7519(98)00023-X
8. Hunter CA, Sibley LD. Modulation of innate immunity by *Toxoplasma gondii* virulence effectors. *Nat Rev Microbiol* (2012) 10(11):766–78. doi:10.1038/nrmicro2858
9. VanWormer E, Fritz H, Shapiro K, Mazet JA, Conrad PA. Molecules to modeling: *Toxoplasma gondii* oocysts at the human-animal-environment interface. *Comp Immunol Microbiol Infect Dis* (2013) 36(3):217–31. doi:10.1016/j.cimid.2012.10.006
10. Howe DK, Sibley LD. *Toxoplasma gondii* comprises three clonal lineages: correlation of parasite genotype with human disease. *J Infect Dis* (1995) 172(6):1561–6. doi:10.1093/infdis/172.6.1561
11. Khan A, Dubey JP, Su C, Ajioka JW, Rosenthal BM, Sibley LD. Genetic analyses of atypical *Toxoplasma gondii* strains reveal a fourth clonal lineage in North America. *Int J Parasitol* (2011) 41(6):645–55. doi:10.1016/j.ijpara.2011.01.005
12. Lorenzi H, Khan A, Behnke MS, Namasivayam S, Swapna LS, Hadjithomas M, et al. Local admixture of amplified and diversified secreted pathogenesis determinants shapes mosaic *Toxoplasma gondii* genomes. *Nat Commun* (2016) 7:10147. doi:10.1038/ncomms10147
13. Behnke MS, Khan A, Lauron EJ, Jimah JR, Wang Q, Tolia NH, et al. Rhoptry proteins ROP5 and ROP18 are major murine virulence factors in genetically divergent South American strains of *Toxoplasma gondii*. *PLoS Genet* (2015) 11(8):e1005434. doi:10.1371/journal.pgen.1005434
14. Jensen KD, Camejo A, Melo MB, Cordeiro C, Julien L, Grotenbreg GM, et al. *Toxoplasma gondii* superinfection and virulence during secondary infection correlate with the exact ROP5/ROP18 allelic combination. *MBio* (2015) 6(2):e02280. doi:10.1128/mBio.02280-14
15. Ezz Eldin HM, Kamel HH, Badawy AF, Shash LS. A comparative study between excretory/secretory and autoclaved vaccines against RH strain of *Toxoplasma gondii* in murine models. *J Parasit Dis* (2015) 39(3):526–35. doi:10.1007/s12639-013-0390-6
16. Waldeland H, Frenkel JK. Live and killed vaccines against toxoplasmosis in mice. *J Parasitol* (1983) 69(1):60–5. doi:10.2307/3281275
17. Darcy F, Maes P, Gras-Masse H, Auriault C, Bossus M, Deslee D, et al. Protection of mice and nude rats against toxoplasmosis by a multiple antigenic peptide construction derived from *Toxoplasma gondii* P30 antigen. *J Immunol* (1992) 149(11):3636–41.
18. Petersen E, Nielsen HV, Christiansen L, Spenter J. Immunization with *E. coli* produced recombinant *T. gondii* SAG1 with alum as adjuvant protect mice against lethal infection with *Toxoplasma gondii*. *Vaccine* (1998) 16(13):1283–9. doi:10.1016/S0264-410X(98)00039-5
19. Dautu G, Munyaka B, Carmen G, Zhang G, Omata Y, Xuenan X, et al. *Toxoplasma gondii*: DNA vaccination with genes encoding antigens MIC2, M2AP, AMA1 and BAG1 and evaluation of their immunogenic potential. *Exp Parasitol* (2007) 116(3):273–82. doi:10.1016/j.exppara.2007.01.017
20. Beghetto E, Nielsen HV, Del Porto P, Buffolano W, Guglietta S, Felici F, et al. A combination of antigenic regions of *Toxoplasma gondii* microneme proteins induces protective immunity against oral infection with parasite cysts. *J Infect Dis* (2005) 191(4):637–45. doi:10.1086/427660
21. Pan M, Lyu C, Zhao J, Shen B. Sixty years (1957–2017) of research on toxoplasmosis in China-an overview. *Front Microbiol* (2017) 8:1825. doi:10.3389/fmicb.2017.01825

22. Zhang NZ, Chen J, Wang M, Petersen E, Zhu XQ. Vaccines against *Toxoplasma gondii*: new developments and perspectives. *Expert Rev Vaccines* (2013) 12(11):1287–99. doi:10.1586/14760584.2013.844652
23. Buxton D, Innes EA. A commercial vaccine for ovine toxoplasmosis. *Parasitology* (1995) 110(Suppl):S11–6. doi:10.1017/S003118200000144X
24. Buxton D, Thomson K, Maley S, Wright S, Bos HJ. Vaccination of sheep with a live incomplete strain (S48) of *Toxoplasma gondii* and their immunity to challenge when pregnant. *Vet Rec* (1991) 129(5):89–93. doi:10.1136/vr.129.5.89
25. Fox BA, Bzik DJ. Avirulent uracil auxotrophs based on disruption of orotidine-5'-monophosphate decarboxylase elicit protective immunity to *Toxoplasma gondii*. *Infect Immun* (2010) 78(9):3744–52. doi:10.1128/IAI.00287-10
26. Fox BA, Bzik DJ. De novo pyrimidine biosynthesis is required for virulence of *Toxoplasma gondii*. *Nature* (2002) 415(6874):926–9. doi:10.1038/415926a
27. Fox BA, Bzik DJ. Nonreplicating, cyst-defective type II *Toxoplasma gondii* vaccine strains stimulate protective immunity against acute and chronic infection. *Infect Immun* (2015) 83(5):2148–55. doi:10.1128/IAI.02756-14
28. Xia N, Yang J, Ye S, Zhang L, Zhou Y, Zhao J, et al. Functional analysis of *Toxoplasma* lactate dehydrogenases suggests critical roles of lactate fermentation for parasite growth in vivo. *Cell Microbiol* (2018) 20(1). doi:10.1111/cmi.12794
29. Cutchins EC, Warren J. Immunity patterns in the guinea pig following *Toxoplasma* infection and vaccination with killed *Toxoplasma*. *Am J Trop Med Hyg* (1956) 5(2):197–209. doi:10.4269/ajtmh.1956.5.197
30. Krahenbuhl JL, Ruskin J, Remington JS. The use of killed vaccines in immunization against an intracellular parasite: *Toxoplasma gondii*. *J Immunol* (1972) 108(2):425–31.
31. Zhang NZ, Wang M, Xu Y, Petersen E, Zhu XQ. Recent advances in developing vaccines against *Toxoplasma gondii*: an update. *Expert Rev Vaccines* (2015) 14(12):1609–21. doi:10.1586/14760584.2015.1098539
32. Innes EA, Panton WR, Thomson KM, Maley S, Buxton D. Kinetics of interferon gamma production in vivo during infection with the S48 vaccine strain of *Toxoplasma gondii*. *J Comp Pathol* (1995) 113(1):89–94. doi:10.1016/S0021-9975(05)80074-X
33. Saeij JP, Boyle JP, Grigg ME, Arrizabalaga G, Boothroyd JC. Bioluminescence imaging of *Toxoplasma gondii* infection in living mice reveals dramatic differences between strains. *Infect Immun* (2005) 73(2):695–702. doi:10.1128/IAI.73.2.695-702.2005
34. Huskinson-Mark J, Araujo FG, Remington JS. Evaluation of the effect of drugs on the cyst form of *Toxoplasma gondii*. *J Infect Dis* (1991) 164(1):170–1. doi:10.1093/infdis/164.1.170
35. Vercammen M, Scorza T, Huygen K, De Braekeleer J, Diet R, Jacobs D, et al. DNA vaccination with genes encoding *Toxoplasma gondii* antigens GRA1, GRA7, and ROP2 induces partially protective immunity against lethal challenge in mice. *Infect Immun* (2000) 68(1):38–45. doi:10.1128/IAI.68.1.38-45.2000
36. Shen B, Brown KM, Lee TD, Sibley LD. Efficient gene disruption in diverse strains of *Toxoplasma gondii* using CRISPR/CAS9. *MBio* (2014) 5(3):e1114–1114. doi:10.1128/mBio.01114-14
37. Shen B, Brown K, Long S, Sibley LD. Development of CRISPR/Cas9 for efficient genome editing in *Toxoplasma gondii*. *Methods Mol Biol* (2017) 1498:79–103. doi:10.1007/978-1-4939-6472-7_6
38. Heaslip AT, Nishi M, Stein B, Hu K. The motility of a human parasite, *Toxoplasma gondii*, is regulated by a novel lysine methyltransferase. *PLoS Pathog* (2011) 7(9):e1002201. doi:10.1371/journal.ppat.1002201

Conflict of Interest Statement: The authors declare that the research was conducted in the absence of any commercial or financial relationships that could be construed as a potential conflict of interest.

frontiers in Immunology

ORIGINAL RESEARCH
published: 29 June 2018
doi: 10.3389/fimmu.2018.01505

Immunization With a DNA Vaccine Cocktail Encoding TgPF, TgROP16, TgROP18, TgMIC6, and TgCDPK3 Genes Protects Mice Against Chronic Toxoplasmosis

Nian-Zhang Zhang[1], Qi Gao[1,2], Meng Wang[1], Hany M. Elsheikha[3], Bo Wang[4], Jin-Lei Wang[1], Fu-Kai Zhang[1], Ling-Ying Hu[1] and Xing-Quan Zhu[1,5]**

[1]State Key Laboratory of Veterinary Etiological Biology, Key Laboratory of Veterinary Parasitology of Gansu Province, Lanzhou Veterinary Research Institute, Chinese Academy of Agricultural Sciences, Lanzhou, China, [2]Hunan Entry-Exit Inspection and Quarantine Bureau, Changsha, China, [3]Faculty of Medicine and Health Sciences, School of Veterinary Medicine and Science, University of Nottingham, Loughborough, United Kingdom, [4]Department of Mathematics, University of Leicester, Leicester, United Kingdom, [5]Jiangsu Co-Innovation Center for the Prevention and Control of Important Animal Infectious Diseases and Zoonoses, Yangzhou University College of Veterinary Medicine, Yangzhou, China

OPEN ACCESS

Edited by:
Xun Suo, China Agricultural University, China

Reviewed by:
Dolores Correa, Instituto Nacional de Pediatria, Mexico
Dina Weilhammer, United States Department of Energy (DOE), United States

***Correspondence:**
Nian-Zhang Zhang
zhangnianzhang@caas.cn;
Xing-Quan Zhu
xingquanzhu1@hotmail.com

Specialty section:
This article was submitted to Microbial Immunology, a section of the journal Frontiers in Immunology

Received: *24 February 2018*
Accepted: *18 June 2018*
Published: *29 June 2018*

Citation:
Zhang N-Z, Gao Q, Wang M, Elsheikha HM, Wang B, Wang J-L, Zhang F-K, Hu L-Y and Zhu X-Q (2018) Immunization With a DNA Vaccine Cocktail Encoding TgPF, TgROP16, TgROP18, TgMIC6, and TgCDPK3 Genes Protects Mice Against Chronic Toxoplasmosis. Front. Immunol. 9:1505. doi: 10.3389/fimmu.2018.01505

Toxoplasmosis is a zoonotic disease caused by the intracellular protozoan *Toxoplasma gondii*; and a major source of infection in humans is *via* ingestion of *T. gondii* tissue cysts. Ultimately, the goal of anti-toxoplasmosis vaccines is to elicit a sustainable immune response, capable of preventing formation of the parasite tissue cysts—or, at least, to restrain its growth. In this study, we formulated a cocktail DNA vaccine and investigated its immunologic efficacy as a protection against the establishment of *T. gondii* cysts in the mouse brain. This multicomponent DNA vaccine, encoded the TgPF, TgROP16, TgROP18, TgMIC6, and TgCDPK3 genes, which play key roles in the pathogenesis of *T. gondii* infection. Results showed that mice immunized *via* intramuscular injection three times, at 2-week intervals with this multicomponent DNA vaccine, mounted a strong humoral and cellular immune response, indicated by significantly high levels of total IgG, $CD4^+$ and $CD8^+$ T lymphocytes, and antigen-specific lymphocyte proliferation when compared with non-immunized mice. Immunization also induced a mixed Th1/Th2 response, with a slightly elevated IgG2a to IgG1 ratio. The increased production of proinflammatory cytokines gamma-interferon, interleukin-2, and interleukin-12 ($p < 0.0001$) correlated with increased expression of p65/RelA and T-bet genes of the NF-κB pathway. However, no significant difference was detected in level of interleukin-4 ($p > 0.05$). The number of brain cysts in immunized mice was significantly less than those in non-immunized mice (643.33 ± 89.63 versus 3,244.33 ± 96.42, $p < 0.0001$), resulting in an 80.22% reduction in the parasite cyst burden. These findings indicate that a multicomponent DNA vaccine, encoding TgPF, TgROP16, TgROP18, TgMIC6, and TgCDPK3 genes, shows promise as an immunization strategy against chronic toxoplasmosis in mice, and calls for a further evaluation in food-producing animals.

Keywords: *Toxoplasma gondii*, chronic toxoplasmosis, cocktail DNA vaccine, multistage antigens, mixed Th1/Th2 immune response

INTRODUCTION

Toxoplasma gondii, the causative agent of toxoplasmosis, infects nearly all warm-blooded vertebrates, including birds and humans (1, 2). Toxoplasmosis in immunocompetent people usually manifests as a flu-like, self-limiting infection; however, in immunocompromised patients (cancer, AIDS, and organ transplant recipients), reactivation of chronic toxoplasmosis can cause fatal complications, such as toxoplasmic encephalitis (3, 4). The reactivation of tissue cysts is manifested by their rupture, followed by the conversion of released bradyzoites to tachyzoites, and a proliferation of tachyzoites. Therefore, the removal of *T. gondii* tissue cysts from infected individuals would prevent such reactivation. Tissue cysts of *T. gondii* in animals also present a potential threat to human health if they are consumed in raw or undercooked meat (5, 6). Currently, there are no available drugs to eliminate *T. gondii* tissue cysts (7, 8). It is therefore imperative that new approaches are developed for immunotherapy against this infection.

Development of vaccines to prevent *T. gondii* tissue cyst formation can be an effective approach to ensure the safety of meat products, originating from food-producing animals under backyard and free-ranging conditions (9, 10). Over the last two decades, various anti-*T. gondii* vaccine approaches have been evaluated in animal models. Previous studies have shown that DNA vaccine can induce, through enhanced humoral and cellular immune responses, immune protection against acute and chronic toxoplasmosis in animal models (11–15). Additional advantages of the DNA vaccination, when compared with using live-type vaccines, are their thermal stability, safety, and the low cost of production (12, 14). To date, no single DNA vaccine has provided full protection against *T. gondii* cyst formation (9, 16, 17).

Toxoplasma gondii-specific cytotoxic T lymphocytes (CTLs) induced by immunization can improve the protective immunity against parasite infection (9, 14). Previous studies have shown that a multicomponent vaccine may offer better protection than a single antigen (16–19) due to the elevated numbers of *T. gondii*-specific CTLs, and the subsequent increase in the production of antigen-specific cytokine gamma-interferon (IFN-γ) (19, 20). A combination of different antigens, in theory, contain more CTL epitopes and are considered superior to a single antigen for protecting the host against *T. gondii* infection (14, 21).

This study aimed to examine the protective efficacy of a DNA multicomponent vaccine against chronic *T. gondii* infection. Five well-characterized antigens play key roles in host–parasite interaction including host cell attachment (MIC6) (22), gliding motility and invasion (profilin) (23, 24), signal transduction and egress (calcium-dependent protein kinase 3; CDPK3) (25), intracellular proliferation (ROP18) (26), and modulation of host gene expression (ROP16) (27). These antigens were selected to formulate a cocktail DNA vaccine. We investigated the immunologic efficacy of this vaccine, in protecting Kunming mice against chronic *T. gondii* infection. In addition, we conducted a longitudinal immune analysis and evaluated several immunization strategies, in order to provide some guidance for optimal schedules of vaccine administration in future clinical trials. Utilization of the DNA vaccine with multi-antigens is a step forward in the development of commercial vaccine formulations against chronic toxoplasmosis for use in humans and food-producing animals.

MATERIALS AND METHODS

Ethics Statement

Animal experiments were reviewed and approved by the Animal Administration and Ethics Committee of Lanzhou Veterinary Research Institute, Chinese Academy of Agricultural Sciences. The study was performed in strict compliance with the recommendations set forth in the Animal Ethics Procedures and Guidelines of the People's Republic of China. All efforts were made to minimize animal suffering and to reduce the numbers of animals used in the experiments.

Mice and Parasite Strain

Specific pathogen-free female Kunming mice, aged 6–8 weeks, were purchased from the Center of Laboratory Animals, Lanzhou Institute of Biological Products, Lanzhou, China. They were housed, in pathogen-free conditions, at Lanzhou Veterinary Research Institute in controlled room under stable conditions (12-h/12-h dark/light cycle, 50–60% humidity, and ~22°C temperature). Mice had access to sterilized food and water *ad libitum* and were acclimated for 1 week before use. The avirulent *T. gondii* type II Prugniuad (Pru) was propagated in our laboratory, by oral passage of infected brain homogenates in Kunming mice (28). Bradyzoites of *T. gondii* Pru strain were used to prepare the *T. gondii* lysate antigen (TLA) as described previously (29, 30).

Preparation of Multicomponent DNA Vaccine

The pVAX1 plasmids encoding *T. gondii* profilin (pVAX1-PF), rhoptry protein 16 (pVAX1-ROP16), rhoptry protein ROP18 (pVAX1-ROP18), microneme protein 6 (pVAX1-MIC6), and calcium-dependent protein kinase 3 (pVAX1-CDPK3) were constructed as previously reported (31–35), with the fidelity of all plasmids confirmed by sequencing (Sangon, China). The five eukaryotic plasmids were each transformed into *E. coli* DH5α for propagation and were isolated by anion exchange chromatography (EndoFree Plasmid Giga Kit, Qiagen Sciences, MD, USA) following the manufacturer's instruction. Plasmid concentration and purity was determined by measuring the optical density ratio A_{260}/A_{280}. The purified plasmids were stored at −20°C until used in the mouse immunization protocols.

Immunization and Challenge

Mice ($n = 120$) were randomly allocated to six groups of 20 mice. Mice in groups G1, G2, and G3 were immunized using plasmids encoding either five genes, four genes, or one gene, respectively. Further details of the various vaccination regimens are listed in **Table 1**. Mice received intramuscular (i.m.) injections of 100 μg of plasmids in 100 μl phosphate-buffered saline (PBS), into the tibialis anterior muscles using a 1-ml insulin syringe with a 28-G needle. Three vaccinations at 2-week intervals were

TABLE 1 | Vaccination regimens used in this study.

Group	Immunization protocol	Content	Volume	Administration
G1	pVAX1 plasmids expressing ROP16 + ROP18 + MIC6 + CDPK3 + PF	20 μg/plasmid	100 μl	Intramuscular
G2	pVAX1 plasmids expressing ROP16 + ROP18 + MIC6 + CDPK3	25 μg/plasmid	100 μl	Intramuscular
G3	pVAX1-PF	100 μg	100 μl	Intramuscular
G4	pVAX1	100 μg	100 μl	Intramuscular
G5	Phosphate-buffered saline	–	100 μl	Intramuscular
G6	Healthy control	–	–	–

performed. Mice in G4 and G5 received empty pVAX1 vector and PBS, respectively. Mice in G6 were healthy untreated controls (non-immunized and uninfected). Following the primary immunization, mice in G1–G5 were provided with two booster immunizations at weeks 2 and 4. For the challenge, 2 weeks after the final immunization (6 weeks post initial immunization), 6 mice from each group were inoculated orally with 200 μl of PBS containing 10 tissue cysts of the avirulent *T. gondii* Pru strain. Control mice received 200 μl of PBS without cysts. Six weeks post challenge, the mouse brains were removed, homogenized in 1 ml of PBS and cysts were morphologically identified and counted under a microscope (40× objective) on three aliquots of 20 μl, without staining.

Multicomponent DNA Vaccine Induced a Systemic Humoral Immune Response

The blood samples from three mice in each group were collected from the tail vein pre-immunization, and 2 weeks after each of the three sequential immunizations (i.e., at 2, 4, and 6 weeks post immunization). The sera were separated by centrifugation of blood samples at 3,000 × *g* for 10 min. Levels of anti-*T. gondii*, total IgG, and IgG isotypes (IgG2a and IgG1 antibodies, as markers for Th1 and Th2 responses) were examined in mice in each group using the SBA Clonotyping System-HRP Kit according to the manufacture's instruction (Southern Biotech Co., Ltd., Birmingham, AL, USA). Wells of 96-well microtiter plates were coated with 100 μl (10 μg/ml) TLA diluted in PBS at 4°C overnight, and then washed with PBST (PBS with 0.05% Tween-20). Plates were then treated with PBS-T plus 1% low fat milk for 1 h at ambient temperature, in order to block non-specific binding sites. After washing the wells three times with PBS, mouse serum samples (1:10 diluted with PBS) were added to the wells, and incubated at 37°C for 1 h followed by washing three times with PBST. The serum from non-immunized mice was used as a negative control. Horse radish peroxidase (HRP) conjugated anti-mouse IgG (1:500 diluted with PBS) and anti-mouse IgG1 or IgG2a (1:1,000 diluted with PBS) were added to the wells and incubated for 1 h at 37°C. Wells were then washed five times with PBST, and streptavidin–horseradish peroxidase was added for 1 h at ambient temperature. TMB (3,3′,5,5′-tetramethyl benzidine) in 200 μl citrate-phosphate buffer (0.05 M Na_2HPO_4, 0.025 M citric acid, pH 4.0) and 2 mM H_2O_2 were added to monitor the peroxidase activity. The reaction was stopped after 30 min by adding 2 M H_2SO_4. Analysis of antibody responses was based on absorbance, measured at 450 nm using an ELISA plate reader (iMark microplate absorbance reader; Bio-Rad, Hercules, CA, USA). All measurements were performed in triplicate.

Lymphocyte Proliferation Assay

Spleens from five mice in each group were aseptically collected, 2 weeks after the final/third booster immunization and were pushed through a fine nylon mesh. After removal of red blood cells, using erythrocyte lysis buffer (Sangon, China), the purified splenocytes were re-suspended in RPMI medium, supplemented with 10% fetal calf serum and 100 U/ml penicillin/streptomycin. The number of purified splenic lymphocytes was determined, and cells were cultured at a concentration of 2×10^5 cells/well in 96-well flat-bottom microwell plates, in complete RPMI medium. Cell cultures were stimulated with TLA (10 or 5 μg/ml) in three wells. RPMI media only (no antigen) and Concanavalin A (ConA; 5 μg/ml; Sigma, St. Louis, MO, USA) were used as nonstimulated and positive controls, respectively. After 4 days at 37°C in a humidified 5% CO_2 incubator, the level of *in vitro* proliferative response was determined using the 3-(4,5-dimethylthiazol-2-yl)-5-(3-carboxymethoxyphenyl)-2-(4-sulfophenyl)-*2H*-tetrazolium, inner salt (MTS) assay (Promega, USA). The OD values were measured using a microplate reader (iMark microplate absorbance reader; Bio-Rad, Hercules, CA, USA) at 490 nm. Data were expressed as stimulation index (SI), which was calculated as the ratio of mean OD_{590} values in immunized and control groups.

Antigen-Specific T-Cell Proliferation

The percentages of $CD4^+$ and $CD8^+$ T lymphocytes in the purified splenocytes were determined by flow cytometry. The specific antigen epitope of each T subclass was stained with phycoerythrin-labeled anti-mouse CD3 (eBioscience), allophycocyanin-labeled anti-mouse CD4 (eBioscience), and fluorescein isothiocyanate-labeled anti-mouse CD8 (eBioscience) antibodies. The cell suspension was then fixed with FACScan buffer (PBS containing 1% BSA and 0.1% sodium azide) and 2% paraformaldehyde. All samples were analyzed for their fluorescence profiles on a FACScan flow cytometer (BD Biosciences) using System II software (Coulter).

Cytokines

Splenocytes at a density of 2×10^5 cells/well were co-cultured with TLA and medium only (negative control). Culture supernatants were harvested at 24 h for quantification of interleukin-2 (IL-2) and IL-4 and at 96 h for IFN-γ and interleukin-12 (IL-12). The level of each cytokine was determined using commercial ELISA

kits, according to the manufacturer's instructions (BioLegend, USA). The supernatants from each cell culture were pipetted into microplate wells followed by assay buffer A. Then, 100 µl of the detection solution was added into each well. After washing the plate four times, avidin-HRP A solution and the substrate solution E were added sequentially. The reaction was stopped by adding 100 µl of stop solution. The sensitivity limits for the assays were 4 pg/ml for IL-12 (p70), 20 pg/ml for IFN-γ, 10 pg/ml for IL-4, and 50 pg/ml for IL-2. Optical absorbance was read at 450 nm. This experiment was performed in triplicate.

We studied the expression of the two transcription factors, p65/RelA and T-bet of the NF-κB pathway, in an effort to establish their roles in mediating the increased production of T cell cytokine (e.g., IFN-γ and IL-12). Total RNA from 10^7 purified splenocytes of mice from G1 to G6 were extracted using Trizol reagent (Invitrogen, USA), as per the manufacturer's instructions. RNAs were dissolved in RNase-free ddH_2O (TaKaRa, China) and reverse transcribed first-strand cDNAs were used as templates for real-time (RT)-PCR. The primers for amplification of RelA/p65 and T-bet genes are listed in **Table 2**. β-Actin was used as a housekeeping reference gene. The SYBR Green qPCR SuperMix was purchased from Invitrogen (USA). RT-PCR was performed on ABI PRISM® 7500 Sequence Detection System (Applied Biosystems). The amplification reactions were performed under the following conditions: 50°C 2 min, 95°C 2 min, 40 cycles of 95°C for 15 s, and 60°C for 32 s. Melting curve analysis was carried out under the following conditions: 1 min at 95°C, 65°C for 2 min, and progressive increase from 65 to 95°C to ensure that a single product was amplified in each reaction. All measurements were run in triplicate.

Statistical Analysis

Two-way ANOVA with matched data at different weeks was used to compare the total IgG antibody responses between the mouse groups. Tukey's multiple comparisons test was then employed to test the differences between each of the three vaccination groups, and each of the three control groups at each week. One-way ANOVA and Tukey's multiple comparisons test were used for comparison in regards to the levels of IgG1 and IgG2a, and IgG2a/IgG1 ratio, proliferation of splenocytes, the numbers of $CD3^+$ $CD4^+$ $CD8^+$ and $CD3^+$ $CD8^+$ $CD4^+$ T cells, cytokine production, and the numbers of brain cysts. Welch's *t* test was used to compare the qPCR in the three genes (p65/RelA, T-bet, and β-actin) between the blank control group and mice in group 1. Data are presented as mean ± SD. All analyses and graphs were performed using GraphPad Prism version 7.04 (San Diego, CA, USA). The level of significance was defined as $^*p \leq 0.05$, $^{**}p \leq 0.01$, $^{***}p \leq 0.001$, and $^{****}p \leq 0.0001$.

TABLE 2 | Sequences of primers used for amplification of p65/RelA, T-bet, and β-actin genes.

Primer name	Sequence
T-bet-F	5′-GCCAGGGAACCGCTTATATG-3′
T-bet-R	5′-TGGAGAGACTGCAGGACGAT-3′
RelA-F	5′-GAACCAGGGTGTGTCCATGT-3′
RelA-R	5′-TCCGCAATGGAGGAGAAGTC-3′
β-Actin-F	5′-GCTTCTAGGCGGACTGTTAC-3′
β-Actin-R	5′-CCATGCCAATGTTGTCTCTT-3′

RESULTS

Identification of Plasmids

Five purified plasmids pVAX1-PF, pVAX1-ROP16, pVAX1-ROP18, pVAX1-MIC6, and pVAX1-CDPK3 were confirmed by sequencing prior to use in the immunization experiment. Sequence alignment analysis showed that no base deletion or change was detected after alignment with the corresponding sequences in GenBank: accession numbers AY937257.1, DQ116422, AM075204, EF102772, and AJ488146.2.

Kinetics of Humoral Immune Responses

We characterized temporal changes in the humoral immune responses following immunization. Sera were available pretreatment, and at weeks 2, 4, and 6 post sequential immunizations from mice in all groups. Levels of total IgG and its subclasses (IgG2a and IgG1) from these time points were determined using ELISA. As shown in **Figure 1**, the IgG responses tended to increase with the increased number of immunizations, and with the increased number of plasmids used in immunization. Levels of IgG in mice in G1, G2, and G3 increased proportionally with time following immunization, and peaked at 2 weeks after the third/final booster immunization. Statistical analyses of the results (for weeks 0, 2, 4, and 6 post immunization) were performed using a two-way ANOVA for matched data. Both time and group variables had significant effects ($p < 0.0001$ for time and $p = 0.0140$ for group). Tukey's multiple comparisons test showed no significant differences in all groups at week 0, 2, and 4 after immunization. At week 6 post immunization, the levels of IgG production in mice from G1 were significantly higher than those in the control groups G4, G5, and G6 ($p < 0.0001$, $p < 0.0001$, and $p < 0.0001$, respectively). The levels of IgG in G2 mice were significantly elevated compared with the control groups G4, G5, and G6 ($p = 0.0004$, $p = 0.0004$, and $p = 0.0003$, respectively). The levels of IgG in G3 mice were significantly high compared with the control groups G4, G5, and G6 ($p = 0.6142$, $p = 0.5803$, and $p = 0.5576$, respectively). The levels of IgG antibodies in mice from control groups (G4, G5, and G6) were not significantly different when compared with each other. Within G1, G2, and G3 groups, levels of IgG antibodies were not significantly different in G1 versus G2 ($p = 0.8977$), but were significantly different in G1 versus G3 ($p = 0.0023$) and in G2 versus G3 ($p = 0.0447$).

The levels of IgG1 and IgG2a were determined 2 weeks after the final immunization. One-way ANOVA and Tukey's multiple comparisons test were used for statistical analysis of IgG1 and IgG2a data. The results of IgG1 analysis showed that G1 versus G4, G5, and G6 were all significantly different; G2 versus G4 ($p = 0.0626$), G2 versus G5 ($p = 0.0504$), G2 versus G6 ($p = 0.0335$), whereas G3 versus G4, G5, and G6 were not significant (**Figure 2**). The levels of IgG2a showed that G1 versus G4, G5, and G6 were all significant; G2 versus G4, G5, and G6 were all significant; and G3 versus G4 ($p = 0.0765$), G3 versus G5 ($p = 0.0053$), and G3 versus G6 ($p = 0.0049$). These results suggest that both IgG1 and

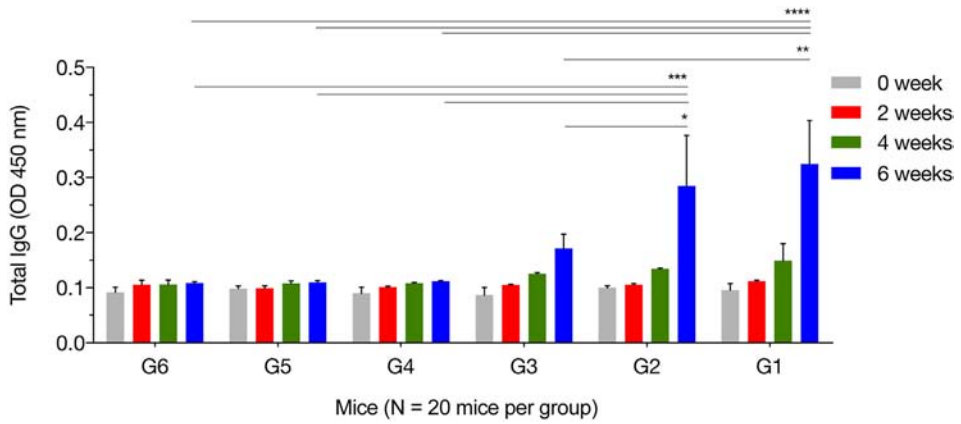

FIGURE 1 | Antigen-specific antibody response in immunized mice. Total IgG antibodies were determined in the sera of mice pre-immunization (0 week) and at 2, 4, and 6 weeks post three consecutive booster immunizations. Experimental groups include G1 mice received pVAX1 plasmids containing five antigens (ROP16, ROP18, MIC6, CDPK3, and PF); G2 mice received pVAX1 plasmids containing four antigens (ROP16, ROP18, MIC6, and CDPK3); G3 mice received pVAX1-PF; G4 mice received an empty pVAX1; G5 mice received phosphate-buffered saline alone; G6 healthy control mice. Data are mean ± SDs for three wells (representative of three independent experiments). *$p < 0.05$, **$p < 0.01$, ***$p < 0.001$, and ****$p < 0.0001$, compared with the control groups.

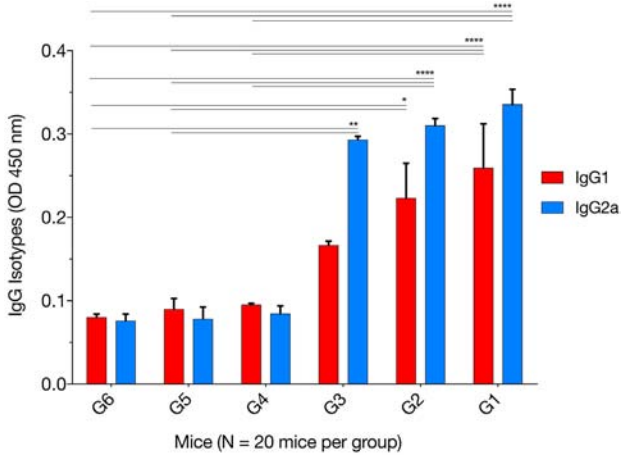

FIGURE 2 | Levels of IgG subclasses (IgG1 and IgG2a) in the sera of mice 2 weeks after the final booster immunization. The patterns of IgG2a to IgG1 post immunization using various immunization regimens suggest the induction of a mixed Th1/Th2 immune response. Experimental groups include G1: mice received pVAX1 plasmids containing five antigens (ROP16, ROP18, MIC6, CDPK3, and PF); G2: mice received pVAX1 plasmids containing four antigens (ROP16, ROP18, MIC6, and CDPK3); G3: mice received pVAX1-PF; G4: mice received an empty pVAX1; G5: mice received phosphate-buffered saline alone; G6: healthy control mice. Each bar represents the group OD_{450} ± SDs for three wells (representative of three experiments). *$p < 0.05$, **$p < 0.01$, and ****$p < 0.0001$, compared with the control groups.

IgG2a antibodies were higher in mice in G1, G2, and G3 than those in control groups at 2 weeks after the third immunization, suggesting a mixed Th1/Th2 immune response. To provide information on the dominant cellular immune type (Th1 or Th2) induced by immunization, ELISA was used to determine the ratio of IgG2a to IgG1 in the sera of all mouse groups. Results showed that immunized mouse groups, in particular, mice immunized with pVAX1-PF, had a slightly Th1-biased immune response as indicated by the higher IgG2a/IgG1 ratio (G1: 1.29; G2: 1.38; G3: 1.75) when compared with that of the control mouse groups (G4: 0.88; G5: 0.87; G6: 0.94; $p = 0.0877$).

Cellular Immune Responses

The MTS assay was used to assess the T lymphocyte's proliferative response following stimulation with TLA or ConA. As expected, there was no difference for the SIs between the immunized groups (G1, G2, and G3). However, *in vitro* lymphocyte proliferation assay revealed that splenic lymphocytes from immunized mice had a significantly higher SI than their counterparts from non-immunized controls, either in the presence of ConA or TLA extract. Exposure to 10 μg/ml TLA increased T-cell proliferation in G1, G2, and G3 compared with that obtained from control mice (**Figure 3**): G1 versus G6 ($p = 0.0010$), G2 versus G6 ($p = 0.0012$), and G3 versus G6 ($p = 0.0001$). Similar results for T lymphocyte proliferation were obtained from splenocytes sensitized with 5 μg/ml TLA in mice from G1, G2, and G3 (**Figure 3**). The results of this *ex vivo* splenic lymphocyte proliferation assay suggested that immunization has induced antigen-specific lymphocyte proliferation.

We further characterized the cellular immune response, using flow cytometry analysis, and found that the numbers of $CD3^+$ $CD4^+$ $CD8^-$ T cells in spleens of mice from G1, G2, and G3 were significantly higher than those from the controls (**Figure 4**). One-way ANOVA and Tukey's multiple comparisons test of the absolute numbers of $CD3^+$ $CD4^+$ $CD8^-$ T cells in spleens, showed that G1 versus G4 ($p = 0.0010$), G1 versus G5 ($p = 0.0003$), G1 versus G6 ($p = 0.0005$); G2 versus G4 ($p = 0.0359$), G2 versus G5 ($p = 0.0130$), G2 versus G6 ($p = 0.0187$); G3 versus G4 ($p = 0.0752$), G3 versus G5 ($p = 0.0287$), G3 versus G6 ($p = 0.0407$). After the third vaccination, mice immunized with various vaccines produced significantly higher $CD3^+$ $CD8^+$ $CD4^-$ T cells in splenic

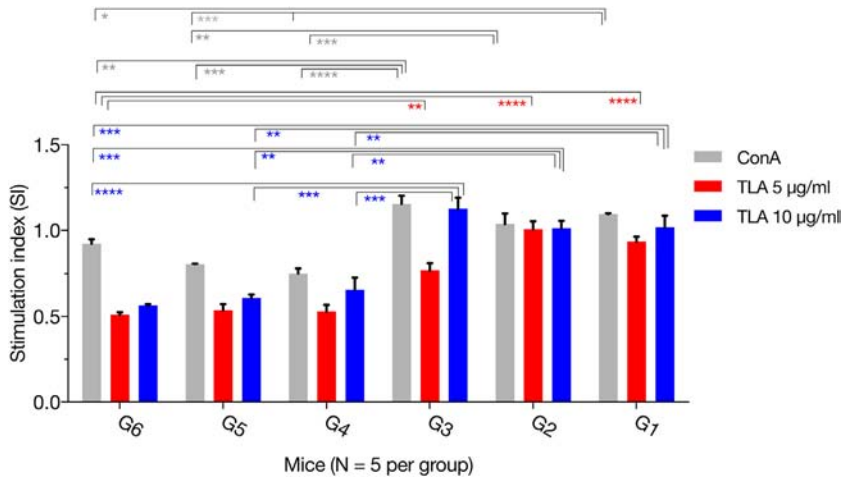

FIGURE 3 | *In vitro* lymphocyte proliferation induced by immunization. Splenocyte proliferation was assessed in mice 2 weeks after the final booster immunization. Exposure of splenocytes to 10 or 5 µg/ml *T. gondii* lysate antigen (TLA) significantly increased T cell proliferation in splenocytes obtained from mice in G1, G2, and G3, compared with proliferation in the control using antigen alone suggesting the induction of antigen-specific T-cell immune response after DNA immunization. Experimental groups include G1: mice received pVAX1 plasmids containing five antigens (ROP16, ROP18, MIC6, CDPK3, and PF); G2: mice received pVAX1 plasmids containing four antigens (ROP16, ROP18, MIC6, and CDPK3); G3: mice received pVAX1-PF; G4: mice received an empty pVAX1; G5: mice received phosphate-buffered saline alone; G6: healthy control mice. Each sample was assayed at least in triplicate. Data represent the mean ± SD (error bars) from the five mice. *$p < 0.05$, **$p < 0.01$, ***$p < 0.001$, and ****$p < 0.0001$, compared with the control groups.

lymphocytes as did the controls. The numbers of $CD3^+$ $CD8^+$ $CD4^-$ T cells in mice from G1, G2, and G3 were significantly increased compared with those from control mice (**Figure 4**). One-way ANOVA and Tukey's multiple comparisons test of the absolute numbers of $CD3^+$ $CD8^+$ $CD4^-$ showed that G1 versus G4 ($p = 0.0026$), G1 versus G5 ($p = 0.0038$), G1 versus G6 ($p = 0.0007$); G2 versus G4 ($p = 0.0381$), G2 versus G5 ($p = 0.0527$), G2 versus G6 ($p = 0.0111$); G3 versus G4 ($p = 0.0590$), G3 versus G5 ($p = 0.0804$), G3 versus G6 ($p = 0.0178$). These findings suggest that the frequency of $CD4^+$ $CD8^+$ T cells were augmented after DNA immunization.

Cytokine Production by Spleen Cells

Following stimulation with TLA, significantly high levels of IFN-γ, IL-2, and IL-12 were observed in splenocyte cultures from mice in G1, G2, and G3 when compared with those from control mouse groups (**Table 3**). In regard to IL-2, G1, G2, and G3 were all significantly higher than G4, G5, and G6 (all $p < 0.0001$). For IL-12, G1, G2, and G3 were all significantly higher than G4, G5, and G6 (all $p < 0.0001$), and for IFN-γ, G1, G2, and G3 are all significantly higher than G4, G5, and G6 (all $p < 0.001$). Levels of IL-4 in mice immunized with various DNA vaccines were not significantly different than those in mice from control groups ($p = 0.5028$). We analyzed the expression level of the transcription factors p65/RelA and T-bet using RT-PCR. We examined the difference between the expression of these two genes between control mice and mice in G1. Results showed that the expression of both p65/RelA and T-bet genes was significantly higher in G1 mice than in the control group ($p < 0.0001$ and $p = 0.0010$) (**Figure 5**). This result indicates that p65/RelA and T-bet are induced by immunization and are likely to increase the production of IFN-γ and IL-12 cytokines.

Assessment of Protective Activity

We evaluated which immunization regimen generated an immune response that was strong enough to protect against the formation of *T. gondii* brain cysts. Six mice from each group were challenged with 10 cysts of *T. gondii* Pru strain; and brain cyst loads were determined 6 weeks later. As shown in **Figure 6**, mice from G1, G2, and G3 had significantly lower numbers of brain cysts than those from control groups G4, G5, and G6 (all $p < 0.0001$). The lowest number of brain cysts was detected in immunized mice from G1 (643.33 ± 89.63), which represented a significant reduction (80.22%, $p < 0.0001$) when compared with the number of cysts found in control non-immunized + challenged mice (3,244.33 ± 96.42). The number of brain cysts in G1 mice was significantly lower than in G2 or G3 mice ($p < 0.0001$).

DISCUSSION

Despite significant research to develop and evaluate anti-*T. gondii* vaccines, there is little consensus on the "best" antigens to target and the optimal means of targeting them. The development of vaccines to prevent cerebral toxoplasmosis disease in high risk populations could reduce the enormous tragedy associated with brain infection with cystogenic (brain cyst-forming) strains of *T. gondii*. A substantially reduced parasite cyst load in the brains of immunized mice in our study, together with enhanced humoral and cell-mediated immune responses—compared with non-immunized infected mice demonstrate that immunization with a DNA cocktail vaccine of five antigens, provides considerable protection in mice against a primary oral challenge with the avirulent cystogenic *T. gondii* Pru strain. These elements are believed to be important in developing an effective therapeutic vaccine. Our results showed that immunization using

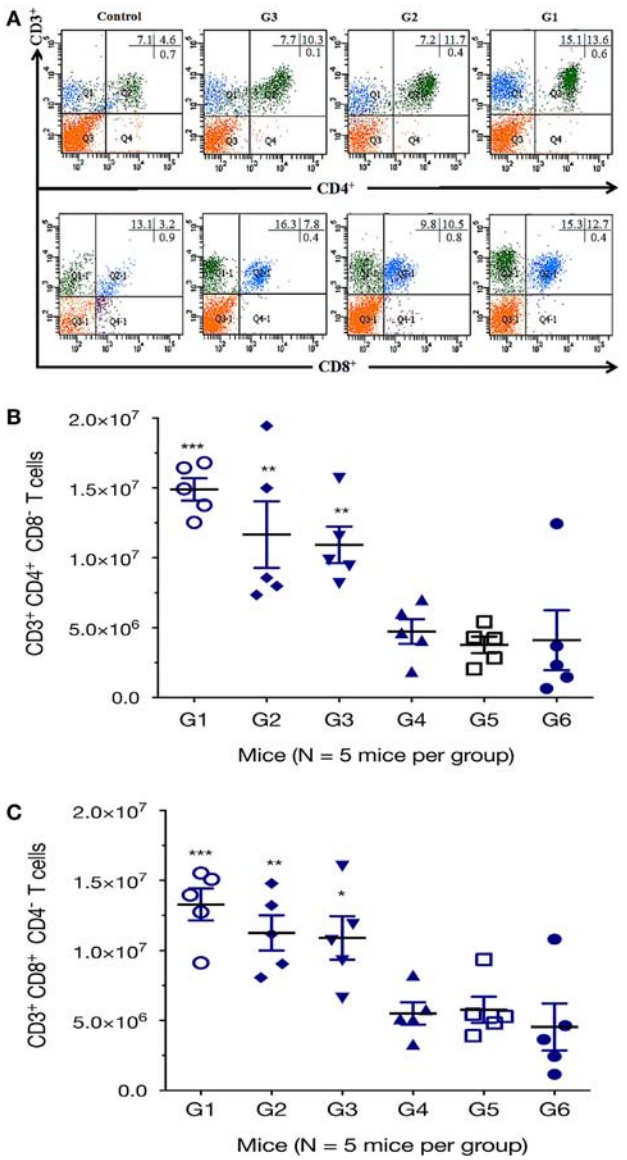

FIGURE 4 | DNA immunization augmented the frequency of antigen-specific T cells. Percentages of CD4+ and CD8+ T cells subsets were determined in the spleen of mice 2 weeks after the final immunization by flow cytometry analysis. **(A)** Representative dot plots showing the percentages of $CD3^+$ $CD4^+$ $CD8^-$ and $CD3^+$ $CD8^+$ $CD4^-$ T lymphocytes. **(B)** Total numbers of $CD3^+$ $CD4^+$ $CD8^-$ T lymphocytes per spleen. **(C)** Total numbers of $CD3^+$ $CD8^+$ $CD4^-$ T lymphocytes per spleen. Experimental groups include G1: mice received pVAX1 plasmids containing five antigens (ROP16, ROP18, MIC6, CDPK3, and PF); G2: mice received pVAX1 plasmids containing four antigens (ROP16, ROP18, MIC6, and CDPK3); G3: mice received pVAX1-PF; G4: mice received an empty pVAX1; G5: mice received phosphate-buffered saline alone; G6: healthy control mice. Data are mean ± SDs (representative of three experiments). $^*p < 0.05$, $^{**}p < 0.01$, and $^{***}p < 0.001$, compared with the control groups.

the cocktail DNA vaccine is a promising approach to control chronic toxoplasmosis, when compared with vaccination based on single antigens (31–35). In this study, cocktail DNA vaccine achieved an 80.22% reduction in the parasite cyst burden, compared with 50% obtained by DNA vaccine expressing *T. gondii* CDPK3 (34) and 39.08% by DNA vaccine (pVAX1-PF) encoding TgPF gene (35). Reduction in the brain cysts' load achieved in our study, was also greater than the 57.8% reduction achieved by vaccination using multiple antigenic peptides encapsulated by chitosan microspheres (36).

The cytokine Th1 immune response is crucial for the control of infection with this obligate intracellular pathogen (14, 37). In our study, immunized mice developed a high level of anti-*T. gondii* IgG antibodies, particularly after the third booster immunization. It is arguable that a high level of antibodies plays an important role in protection against subsequent infection with *T. gondii* tachyzoites, and in controlling *T. gondii* during chronic infection, by preventing cysts' reactivation. A requirement for B cells, in addition to cell-mediated immunity, has been reported for mice challenged with virulent *T. gondii* parasites after vaccination with attenuated tachyzoites—suggesting that antibody-mediated immunity is also critical for *T. gondii*-induced protection (38). Our previous studies have demonstrated that the individual protective immunity offered by pVAX1-PF, pVAX1-ROP16, pVAX1-ROP18, pVAX1-MIC6, or pVAX1-CDPK3 against *T. gondii* infection, elicited a mixed Th1/Th2 or Th1-biased immunity *via* the induction of lymphocyte proliferation, activation of $CD8^+$ T cells and increased IFN-γ production (31–35). In this study, a mixed Th1/Th2 immune response, with a slight bias toward the Th1-type response, was detected in mice in groups G1, G2, and G3, as indicated by a slightly increased lgG2a/IgG1 ratio (i.e., a higher level of IgG2a than IgG1). Vaccination using five antigens evoked an increase in $CD8^+$ T lymphocytes and IFN-γ production along with low levels of IL-4 in G1 mice compared with controls; all are characteristic features of a Th1-type cellular immune response. These findings indicate that a mixed Th1/Th2 protective immune response was elicited following immunization with the cocktail vaccine—consistent with the results of previous studies (14, 39).

A cellular immune response, including high levels of IFN-γ, $CD4^+$, and $CD8^+$ T lymphocytes, is required for protection against chronic *T. gondii* infection (39–43). Both cell types act synergistically to control *T. gondii* infection, and effective control of *T. gondii* infection requires $CD4^+$ for the generation of proficient $CD8^+$-mediated immunity (44). $CD8^+$ T cells possess anti-cyst activity, mediated by a perforin-dependent mechanism (45, 46) and high levels of $CD8^+$ T lymphocytes can contribute to a decrease of brain cyst loads (39, 43, 47–50). In our study, the significantly increased numbers of $CD8^+$ T cells in mice immunized with our cocktail vaccine may have contributed toward reducing the brain cyst burden.

Gamma-interferon, a crucial mediator of immune resistance to *T. gondii* infection, was detected in elevated levels in mice from G1, G2, and G3. IFN-γ can activate macrophages and the CTL response during infection (51). Significantly higher expression of the transcription factor T-bet ($p = 0.0010$) was observed in mice in G1, compared with mice from the control group. This finding indicates that increased IFN-γ production may have resulted from T-bet-mediated activation of $CD4^+$ T cells and natural killer (NK) cells (36). In marked contrast with IFN-γ, the level

TABLE 3 | Cytokine production by splenocytes of immunized Kunming mice after stimulation by *T. gondii* lysate antigen.

Group[b]	Cytokine production (pg/ml)[a]			
	Gamma-interferon	Interleukin-2 (IL-2)	IL-4	Interleukin-12 (IL-12)
G1	1,003.66 ± 311.02	294.24 ± 11.1	<10	411.96 ± 57.94
G2	644.94 ± 190	269.35 ± 19.17	11.1 ± 17.4	184.75 ± 39.95
G3	1,930.26 ± 5.46	277.14 ± 2.24	<10	400.14 ± 54.43
G4	169.29 ± 1.66	<50	<10	15.42 ± 2.01
G5	182.94 ± 33.64	<50	<10	<10
G6	177.75 ± 22.32	<50	<10	<10

[a]*No significant difference ($p > 0.05$) in the level of the four cytokines was observed between the immunized groups (G1, G2, and G3) nor between the control groups (G4, G5, and G6). Differences between immunized groups and control groups were significant for INF-γ ($p < 0.001$), and for IL-2 and IL-12 ($p < 0.0001$). Levels of IL-4 did not show any significant differences between the different mouse groups ($p > 0.05$).*

[b]*Experimental groups included G1: mice received pVAX1 plasmids containing five antigens (ROP16, ROP18, MIC6, CDPK3, and PF); G2: mice received pVAX1 plasmids containing four antigens (ROP16, ROP18, MIC6, and CDPK3); G3: mice received pVAX1-PF; G4: mice received an empty pVAX1; G5: mice received phosphate-buffered saline alone; G6: healthy control mice. Data are mean ± SDs for three wells (representative of three independent experiments).*

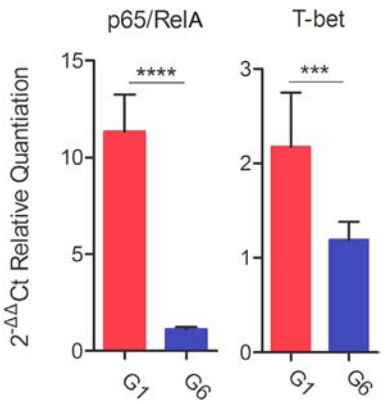

FIGURE 5 | Real-time-PCR expression analysis of the transcription factors p65/RelA and T-bet. β-Actin was used as a housekeeping reference gene. Experimental groups include G1: mice received pVAX1 plasmids containing five antigens (ROP16, ROP18, MIC6, CDPK3, and PF); G6: healthy control mice. Each sample was analyzed in triplicate. Data are mean ± SDs (error bars) from the two mice. ***$p < 0.001$ and ****$p < 0.0001$.

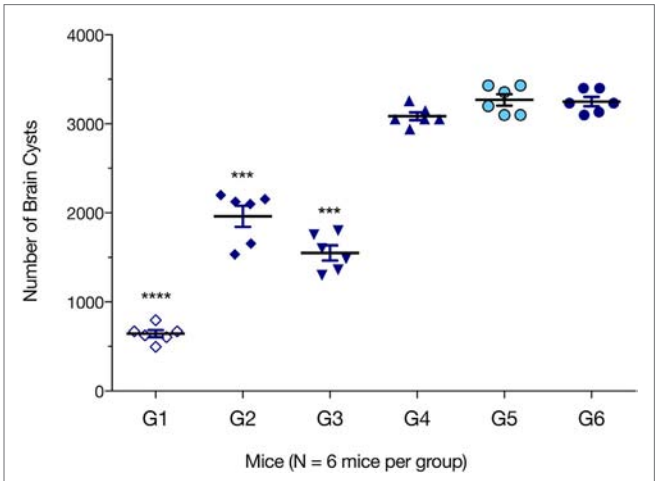

FIGURE 6 | Protection against chronic toxoplasmosis in immunized mice 2 weeks after the final booster immunization. Six mice per group were challenged orally with a dose of 10 cysts of the Pru strain (type II). Cyst load was counted from whole brain homogenates of mice 6 weeks after challenge. Experimental groups include G1: mice received pVAX1 plasmids containing five antigens (ROP16, ROP18, MIC6, CDPK3, and PF); G2: mice received pVAX1 plasmids containing four antigens (ROP16, ROP18, MIC6, and CDPK3); G3: mice received pVAX1-PF; G4: mice received an empty pVAX1; G5: mice received phosphate-buffered saline alone; G6: healthy control mice. Data are mean ± SDs (representative of three experiments). ***$p < 0.001$ and ****$p < 0.0001$, compared with the control groups.

of IL-4 was not statistically different between any mouse groups. IL-4 is a Th2-type cytokine, produced in response to receptor activation by Th2-type $CD4^+$ T cells, basophils, and mast cells, and possesses B-cell stimulatory and Th2-promoting properties (52). IL-4 functions are generally antagonistic to those of IFN-γ, in line with the increased IFN-γ and decreased IL-4 levels seen in our study. Elevated IFN-γ production, together with a low level of IL-4, was also detected in mice immunized with DNA vaccines encoding TgROP1 (15), TgROM5 (39), TgCDPK2 (53), TgSAG1 (54), or multi-antigens (17, 19). IL-4 also promotes isotype-switching in murine B cells to IgG1 and IgE, but inhibits switching to IgG2a, IgG2b, and IgG3. This is in agreement with the reduced IL-4 and a high IgG2a to IgG1 ratio, observed in our study—providing more evidence of a biased Th1 type immune response.

Previous studies have shown that high levels of $CD4^+$ and IL-2 production, increased mouse resistance to chronic toxoplasmosis (30, 41, 42, 55). We also found an increased production of $CD4^+$, IL-2, and IL-12, along with a reduction in the brain cyst load in mice vaccinated with various DNA vaccines. A major role of NF-κB in resistance to *T. gondii* is the induction of IL-12 secretion (56). IL-12, putatively *via* STAT4, is important for the optimal production of INF-γ, which in turn induces differentiation of Th1 T lymphocytes, and possibly $CD8^+$ and NK cells, to control *T. gondii* infection. Significantly increased expression of the transcription factor p65/RelA (a transcription factor of the NF-κB pathway) was observed in mice in G1, when compared with mice in the control group ($p < 0.0001$). This result, in addition to the increased level of IFN-γ, presents activation of NF-κB pathway as an additional mechanism for increased IFN-γ production to limit *T. gondii* infection. Suppressed

expression of IL-12 resulted in 100% mortality in mice infected with *T. gondii* (57). High levels of IL-12 contributed to brain cyst reduction in mice (54, 58). Toll-like receptor 11 (TLR11) signaling is an important pathway involved in the production of IL-12 (23, 59). *T. gondii* profilin (TgPF) can act as a ligand for TLR11 to mediate cytokine production (60–62) and has been exploited as a TLR-based vaccine adjuvant to enhance immune responses generated by vaccination (62–65). TgPF also plays an essential role in *T. gondii* gliding motility, invasion and egress from host cells (23, 24) and is an immunodominant antigen (35, 66). These key characteristics of TgPF prompted us to separately evaluate the protective efficacy of immunization with this gene against chronic toxoplasmosis. The specific finding that DNA vaccine encoding TgPF alone induced the production of high level of IL-12 is consistent with previous data (60) and, together with a higher IgG2a/IgG1 ratio and reduced brain cyst numbers may be of particular relevance. The enhanced protective immunity seen in mice from G1, compared with mice from group G2, suggests that TgPF may be necessary to augment the immune response induced by the multicomponent *T. gondii* DNA vaccine used in our study.

CONCLUSION

We have demonstrated that a strong humoral and cellular immune response, conferring significant protection against chronic *T. gondii* infection in mice—after immunization three times at 2-week intervals with a DNA vaccine encoding multiple antigens (TgPF, TgROP16, TgROP18, TgMIC6, and TgCDPK3). Several DNA immunizations were necessary to elicit the specific IgG antibody response. Immunization with several plasmids expressing more antigens produced a greater antibody response when compared with immunization using fewer plasmids expressing less number of antigens. These data support a call for further evaluation of multivalent synthetic plasmids as potential therapeutic *T. gondii* vaccines. Our findings are significant as they open up the possibility that chronic toxoplasmosis can be controlled by the combined action of multiple parasite-derived antigens. Although further studies and clinical evaluations are required, this study puts into place a "proof of concept" that tests the efficacy of the combination of a range of *T. gondii* antigens in preventing a chronic brain infection that is incurable with current therapeutics.

ETHICS STATEMENT

All animal protocols were reviewed and approved by the Animal Administration and Ethics Committee of Lanzhou Veterinary Research Institute, Chinese Academy of Agricultural Sciences. The study was performed in strict compliance with the recommendations set forth in the Animal Ethics Procedures and Guidelines of the People's Republic of China. All efforts were made to minimize animal suffering and to reduce the numbers of animals used in the experiments.

AUTHOR CONTRIBUTIONS

X-QZ, N-ZZ, and HE designed the experiments, interpreted the data, and critically revised the manuscript. N-ZZ, QG, MW, BW, and J-LW performed the experiments and analyzed the data. N-ZZ drafted the manuscript. F-KZ, MW, and L-YH helped in the implementation of the study. All the authors reviewed and approved the final version of the manuscript.

FUNDING

Project support was provided by the National Key Research and Development Program of China (Grant no. 2017YFD0501304), by the National Natural Science Foundation of China (Grant no. 31602045), by the Elite Program of Chinese Academy of Agricultural Sciences, and by the Agricultural Science and Technology Innovation Program (ASTIP) (Grant No. CAAS-ASTIP-2016-LVRI-03).

REFERENCES

1. Montoya JG, Liesenfeld O. Toxoplasmosis. *Lancet* (2004) 363:1965–76. doi:10.1016/S0140-6736(04)16412-X
2. Robert-Gangneux F, Darde ML. Epidemiology of and diagnostic strategies for toxoplasmosis. *Clin Microbiol Rev* (2012) 25:264–96. doi:10.1128/CMR.05013-11
3. Wohlfert EA, Blader IJ, Wilson EH. Brains and brawn: *Toxoplasma* infections of the central nervous system and skeletal muscle. *Trends Parasitol* (2017) 33:519–31. doi:10.1016/j.pt.2017.04.001
4. Wang ZD, Liu HH, Ma ZX, Ma HY, Li ZY, Yang ZB, et al. *Toxoplasma gondii* infection in immunocompromised patients: a systematic review and meta-analysis. *Front Microbiol* (2017) 8:389. doi:10.3389/fmicb.2017.00389
5. Hill DE, Dubey JP. *Toxoplasma gondii* as a parasite in food: analysis and control. *Microbiol Spectr* (2016) 4:PFS–0011–2015. doi:10.1128/microbiolspec.PFS-0011-2015
6. Belluco S, Simonato G, Mancin M, Pietrobelli M, Ricci A. *Toxoplasma gondii* infection and food consumption: a systematic review and meta-analysis of case-controlled studies. *Crit Rev Food Sci Nutr* (2017) 11:1–12. doi:10.1080/10408398.2017.1352563
7. Pan M, Lyu C, Zhao J, Shen B. Sixty years (1957-2017) of research on toxoplasmosis in China-an overview. *Front Microbiol* (2017) 8:1825. doi:10.3389/fmicb.2017.01825
8. Alday PH, Doggett JS. Drugs in development for toxoplasmosis: advances, challenges, and current status. *Drug Des Devel Ther* (2017) 11:273–93. doi:10.2147/DDDT.S60973
9. Zhang NZ, Chen J, Wang M, Petersen E, Zhu XQ. Vaccines against *Toxoplasma gondii*: new developments and perspectives. *Expert Rev Vaccines* (2013) 12:1287–99. doi:10.1586/14760584.2013.844652
10. Vercruysse J, Knox DP, Schetters TP, Willadsen P. Veterinary parasitic vaccines: pitfalls and future directions. *Trends Parasitol* (2004) 20:488–92. doi:10.1016/j.pt.2004.07.009
11. Robinson HL. DNA vaccines: basic mechanism and immune responses (review). *Int J Mol Med* (1999) 4:549–55.
12. Gurunathan S, Wu CY, Freidag BL, Seder RA. DNA vaccines: a key for inducing long-term cellular immunity. *Curr Opin Immunol* (2000) 12:442–7. doi:10.1016/S0952-7915(00)00118-7
13. Chen J, Huang SY, Li ZY, Yuan ZG, Zhou DH, Petersen E, et al. Protective immunity induced by a DNA vaccine expressing eIF4A of *Toxoplasma gondii* against acute toxoplasmosis in mice. *Vaccine* (2013) 31:1734–9. doi:10.1016/j.vaccine.2013.01.027
14. Zhang NZ, Wang M, Xu Y, Petersen E, Zhu XQ. Recent advances in developing vaccines against *Toxoplasma gondii*: an update. *Expert Rev Vaccines* (2015) 14:1609–21. doi:10.1586/14760584.2015.1098539
15. Sonaimuthu P, Ching XT, Fong MY, Kalyanasundaram R, Lau YL. Induction of protective immunity against toxoplasmosis in BALB/c mice vaccinated

with *Toxoplasma gondii* rhoptry-1. *Front Microbiol* (2016) 7:808. doi:10.3389/fmicb.2016.00808
16. Jongert E, Melkebeekd V, De Craeyeb S, Dewitc J, Verhelst D, Coxd E. An enhanced GRA1–GRA7 cocktail DNA vaccine primes anti-*Toxoplasma* immune responses in pigs. *Vaccine* (2008) 26:1025–31. doi:10.1016/j.vaccine.2007.11.058
17. Fang R, Feng H, Hu M, Khan MK, Wang L, Zhou Y, et al. Evaluation of immune responses induced by SAG1 and MIC3 vaccine cocktails against *Toxoplasma gondii*. *Vet Parasitol* (2012) 187:140–6. doi:10.1016/j.vetpar.2011.12.007
18. Mévélec MN, Bout D, Desolme B, Marchand H, Magné R, Bruneel O, et al. Evaluation of protective effect of DNA vaccination with genes encoding antigens GRA4 and SAG1 associated with GM-CSF plasmid, against acute, chronical and congenital toxoplasmosis in mice. *Vaccine* (2005) 23:4489–99. doi:10.1016/j.vaccine.2005.04.025
19. Hoseinian Khosroshahi K, Ghaffarifar F, D'Souza S, Sharifi Z, Dalimi A. Evaluation of the immune response induced by DNA vaccine cocktail expressing complete SAG1 and ROP2 genes against toxoplasmosis. *Vaccine* (2011) 29:778–83. doi:10.1016/j.vaccine.2010.11.012
20. Beghetto E, Nielsen HV, Del Porto P, Buffolano W, Guglietta S, Felici F, et al. A combination of antigenic regions of *Toxoplasma gondii* microneme proteins induces protective immunity against oral infection with parasite cysts. *J Infect Dis* (2005) 191:637–45. doi:10.1086/427660
21. Picchio MS, Sánchez VR, Arcon N, Soto AS, Perrone Sibilia M, Aldirico MLA, et al. Vaccine potential of antigen cocktails composed of recombinant *Toxoplasma gondii* TgPI-1, ROP2 and GRA4 proteins against chronic toxoplasmosis in C3H mice. *Exp Parasitol* (2018) 185:62–70. doi:10.1016/j.exppara.2018.01.006
22. Zheng B, He A, Gan M, Li Z, He H, Zhan X. MIC6 associates with aldolase in host cell invasion by *Toxoplasma gondii*. *Parasitol Res* (2009) 105:441–5. doi:10.1007/s00436-009-1401-5
23. Plattner F, Yarovinsky F, Romero S, Didry D, Carlier MF, Sher A, et al. *Toxoplasma* profilin is essential for host cell invasion and TLR11-dependent induction of an Interleukin-12 response. *Cell Host Microbe* (2008) 3:77–87. doi:10.1016/j.chom.2008.01.001
24. Koblansky AA, Jankovic D, Oh H, Hieny S, Sungnak W, Mathur R, et al. Recognition of profilin by toll-like receptor 12 is critical for host resistance to *Toxoplasma gondii*. *Immunity* (2013) 38:119–30. doi:10.1016/j.immuni.2012.09.016
25. McCoy JM, Whitehead L, van Dooren GG, Tonkin CJ. TgCDPK3 regulates calcium-dependent egress of *Toxoplasma gondii* from host cells. *PLoS Pathog* (2012) 8:1003066. doi:10.1371/journal.ppat.1003066
26. El Hajj H, Lebrun M, Arold ST, Vial H, Labesse G, Dubremetz JF. ROP18 is a rhoptry kinase controlling the intracellular proliferation of *Toxoplasma gondii*. *PLoS Pathog* (2007) 3:e14. doi:10.1371/journal.ppat.0030014
27. Jensen KD, Hu K, Whitmarsh RJ, Hassan MA, Julien L, Lu D, et al. *Toxoplasma gondii* rhoptry 16 kinase promotes host resistance to oral infection and intestinal inflammation only in the context of the dense granule protein GRA15. *Infect Immun* (2013) 81:2156–67. doi:10.1128/IAI.01185-12
28. Zhou CX, Zhou DH, Elsheikha HM, Zhao Y, Suo X, Zhu XQ. Metabolomic profiling of mice serum during toxoplasmosis progression using liquid chromatography-mass spectrometry. *Sci Rep* (2016) 6:19557. doi:10.1038/srep19557
29. Bastos LM, Macêdo AG Jr, Silva MV, Santiago FM, Ramos EL, Santos FA, et al. *Toxoplasma gondii*-derived synthetic peptides containing B- and T-cell epitopes from GRA2 protein are able to enhance mice survival in a model of experimental toxoplasmosis. *Front Cell Infect Microbiol* (2016) 6:59. doi:10.3389/fcimb.2016.00059
30. Wang JL, Elsheikha HM, Zhu WN, Chen K, Li TT, Yue DM, et al. Immunization with *Toxoplasma gondii* GRA17 deletion mutant induces partial protection and survival in challenged mice. *Front Immunol* (2017) 8:730. doi:10.3389/fimmu.2017.00730
31. Peng GH, Yuan ZG, Zhou DH, He XH, Liu MM, Yan C, et al. *Toxoplasma gondii* microneme protein 6 (MIC6) is a potential vaccine candidate against toxoplasmosis in mice. *Vaccine* (2009) 27:6570–4. doi:10.1016/j.vaccine.2009.08.043
32. Yuan ZG, Zhang XX, Lin RQ, Petersen E, He S, Yu M, et al. Protective effect against toxoplasmosis in mice induced by DNA immunization with gene encoding *Toxoplasma gondii* ROP18. *Vaccine* (2011) 29:6614–9. doi:10.1016/j.vaccine.2011.06.110
33. Yuan ZG, Zhang XX, He XH, Petersen E, Zhou DH, He Y, et al. Protective immunity induced by *Toxoplasma gondii* rhoptry protein 16 against toxoplasmosis in mice. *Clin Vaccine Immunol* (2011) 18:119–24. doi:10.1128/CVI.00312-10
34. Zhang NZ, Huang SY, Zhou DH, Chen J, Xu Y, Tian WP, et al. Protective immunity against *Toxoplasma gondii* induced by DNA immunization with the gene encoding a novel vaccine candidate: calcium-dependent protein kinase 3. *BMC Infect Dis* (2013) 13:512. doi:10.1186/1471-2334-13-512
35. Gao Q, Zhang NZ, Zhang FK, Wang M, Hu LY, Zhu XQ. Immune response and protective effect against chronic *Toxoplasma gondii* infection induced by vaccination with a DNA vaccine encoding profilin. *BMC Infect Dis* (2017) 18:117. doi:10.1186/s12879-018-3022-z
36. Guo J, Sun X, Yin H, Wang T, Li Y, Zhou C, et al. Chitosan microsphere used as an effective system to deliver a linked antigenic peptides vaccine protect mice against acute and chronic toxoplasmosis. *Front Cell Infect Microbiol* (2018) 8:163. doi:10.3389/fcimb.2018.00163
37. Ismael AB, Sekkai D, Collin C, Bout D, Mévélec MN. The MIC3 gene of *Toxoplasma gondii* is a novel potent vaccine candidate against toxoplasmosis. *Infect Immun* (2003) 71:6222–8. doi:10.1128/IAI.71.11.6222-6228.2003
38. Sayles PC, Gibson GW, Johnson LL. B cells are essential for vaccination-induced resistance to virulent *Toxoplasma gondii*. *Infect Immun* (2000) 68(3):1026–33. doi:10.1128/IAI.68.3.1026-1033.2000
39. Zhang NZ, Xu Y, Wang M, Petersen E, Chen J, Huang SY, et al. Protective efficacy of two novel DNA vaccines expressing *Toxoplasma gondii* rhomboid 4 and rhomboid 5 proteins against acute and chronic toxoplasmosis in mice. *Expert Rev Vaccines* (2015) 14:1289–97. doi:10.1586/14760584.2015.1061938
40. Gazzinelli RT, Hakim FT, Hieny S, Shearer GM, Sher A. Synergistic role of CD4+ and CD8+ T lymphocytes in IFN-gamma production and protective immunity induced by an attenuated *Toxoplasma gondii* vaccine. *J Immunol* (1991) 146:286–92.
41. Jordan KA, Hunter CA. Regulation of CD8+ T cell responses to infection with parasitic protozoa. *Exp Parasitol* (2010) 126:318–25. doi:10.1016/j.exppara.2010.05.008
42. Gazzinelli R, Xu Y, Hieny S, Cheever A, Sher A. Simultaneous depletion of CD4+ and CD8+ T lymphocytes is required to reactivate chronic infection with *Toxoplasma gondii*. *J Immunol* (1992) 149:175–80.
43. El Bissati K, Zhou Y, Paulillo SM, Raman SK, Karch CP, Roberts CW, et al. Protein nanovaccine confers robust immunity against *Toxoplasma*. *NPJ Vaccines* (2017) 2:24. doi:10.1038/s41541-017-0024-6
44. Casciotti C, Ely K, Williams M, Khan I. CD8+-T-cell immunity against *Toxoplasma gondii* can be induced but not maintained in mice lacking conventional CD4+ T cells. *Infect Immun* (2002) 70:434–43. doi:10.1128/IAI.70.2.434-443.2002
45. Hakim FT, Gazzinelli RT, Denkers E, Hieny S, Shearer GM, Sher A. CD8+ T cells from mice vaccinated against *Toxoplasma gondii* are cytotoxic for parasite-infected or antigen-pulsed host cells. *J Immunol* (1991) 147:2310–6.
46. Suzuki Y, Sa Q, Gehman M, Ochiai E. Interferon-gamma- and perforin-mediated immune responses for resistance against *Toxoplasma gondii* in the brain. *Expert Rev Mol Med* (2011) 13:e31. doi:10.1017/S1462399411002018
47. Xu Y, Zhang NZ, Tan QD, Chen J, Lu J, Xu QM, et al. Evaluation of immunoefficacy of a novel DNA vaccine encoding *Toxoplasma gondii* rhoptry protein 38 (TgROP38) against chronic toxoplasmosis in a murine model. *BMC Infect Dis* (2014) 14:525. doi:10.1186/1471-2334-14-525
48. Scorza T, D'Souza S, Laloup M, Dewit J, De Braekeleer J, Verschueren H, et al. A GRA1 DNA vaccine primes cytolytic CD8(+) T cells to control acute *Toxoplasma gondii* infection. *Infect Immun* (2003) 71:309–16. doi:10.1128/IAI.71.1.309-316.2003
49. Zhou J, Wang L. SAG4 DNA and peptide vaccination provides partial protection against *T. gondii* infection in BALB/c mice. *Front Microbiol* (2017) 8:1733. doi:10.3389/fmicb.2017.01733
50. Landrith TA, Sureshchandra S, Rivera A, Jang JC, Rais M, Nair MG, et al. CD103+ CD8 T cells in the *Toxoplasma*-infected brain exhibit a tissue-resident memory transcriptional profile. *Front Immunol* (2017) 8:335. doi:10.3389/fimmu.2017.00335
51. Bessieres MH, Swierczynski B, Cassaing S, Miedouge M, Olle P, Sequela JP, et al. Role of IFN-gamma, TNF-alpha, IL4 and IL10 in the regulation of experimental *Toxoplasma gondii* infection. *J Eukaryot Microbiol* (1997) 44:87S. doi:10.1111/j.1550-7408.1997.tb05800.x

52. Bao Y, Cao X. The immune potential and immunopathology of cytokine-producing B cell subsets: a comprehensive review. *J Autoimmun* (2014) 55: 10–23. doi:10.1016/j.jaut.2014.04.001
53. Chen K, Wang JL, Huang SY, Yang WB, Zhu WN, Zhu XQ. Immune responses and protection after DNA vaccination against *Toxoplasma gondii* calcium-dependent protein kinase 2 (TgCDPK2). *Parasite* (2017) 24:41. doi:10.1051/parasite/2017045
54. Meng M, He S, Zhao G, Bai Y, Zhou H, Cong H, et al. Evaluation of protective immune responses induced by DNA vaccines encoding *Toxoplasma gondii* surface antigen 1 (SAG1) and 14-3-3 protein in BALB/c mice. *Parasit Vectors* (2012) 5:273. doi:10.1186/1756-3305-5-273
55. Hwang S, Cobb DA, Bhadra R, Youngblood B, Khan IA. Blimp-1-mediated CD4 T cell exhaustion causes CD8 T cell dysfunction during chronic toxoplasmosis. *J Exp Med* (2016) 213:1799–818. doi:10.1084/jem.20151995
56. Mason NJ, Artis D, Hunter CA. New lessons from old pathogens: what parasitic infections have taught us about the role of nuclear factor-kappaB in the regulation of immunity. *Immunol Rev* (2004) 201:48–56. doi:10.1111/j.0105-2896.2004.00189.x
57. Gazzinelli RT, Wysocka M, Hayashi S, Denkers EY, Hieny S, Caspar P, et al. Parasite-induced IL-12 stimulates early IFN-gamma synthesis and resistance during acute infection with *Toxoplasma gondii*. *J Immunol* (1994) 153:2533–43.
58. Yang WB, Zhou DH, Zou Y, Chen K, Liu Q, Wang JL, et al. Vaccination with a DNA vaccine encoding *Toxoplasma gondii* ROP54 induces protective immunity against toxoplasmosis in mice. *Acta Trop* (2017) 176:427–42. doi:10.1016/j.actatropica.2017.09.007
59. Pifer R, Yarovinsky F. Innate responses to *Toxoplasma gondii* in mice and humans. *Trends Parasitol* (2011) 27:388–93. doi:10.1016/j.pt.2011.03.009
60. Yarovinsky F, Zhang D, Andersen JF, Bannenberg GL, Serhan CN, Hayden MS, et al. TLR11 activation of dendritic cells by a protozoan profilin-like protein. *Science* (2005) 308:1626–9. doi:10.1126/science.1109893
61. Denkers EY, Striepen B. Deploying parasite profilin on a mission of invasion and danger. *Cell Host Microbe* (2008) 3:61–3. doi:10.1016/j.chom.2008.01.003
62. Yarovinsky F, Hieny S, Sher A. Recognition of *Toxoplasma gondii* by TLR11 prevents parasite-induced immunopathology. *J Immunol* (2008) 181:8478–84. doi:10.4049/jimmunol.181.12.8478
63. Pyo KH, Lee YW, Lim SM, Shin EH. Immune adjuvant effect of a *Toxoplasma gondii* profilin-like protein in autologous whole-tumor-cell vaccination in mice. *Oncotarget* (2016) 7:74107–19. doi:10.18632/oncotarget.12316
64. Neal LM, Knoll LJ. *Toxoplasma gondii* profilin promotes recruitment of Ly6Chi CCR2+ inflammatory monocytes that can confer resistance to bacterial infection. *PLoS Pathog* (2014) 10:e1004203. doi:10.1371/journal.ppat.1004203
65. Hedhli D, Moiré N, Akbar H, Laurent F, Héraut B, Dimier-Poisson I, et al. The antigen-specific response to *Toxoplasma gondii* profilin, a TLR11/12 ligand, depends on its intrinsic adjuvant properties. *Med Microbiol Immunol* (2016) 205:345–52. doi:10.1007/s00430-016-0452-3
66. Tanaka S, Kuroda Y, Ihara F, Nishimura M, Hiasa J, Kojima N, et al. Vaccination with profilin encapsulated in oligomannose-coated liposomes induces significant protective immunity against *Toxoplasma gondii*. *Vaccine* (2014) 32:1781–5. doi:10.1016/j.vaccine.2014.01.095

Conflict of Interest Statement: The authors declare that the research was conducted in the absence of any commercial or financial relationships that could be construed as a potential conflict of interest.

frontiers in Immunology

ORIGINAL RESEARCH
published: 26 July 2018
doi: 10.3389/fimmu.2018.01566

Trichinella spiralis Infection Mitigates Collagen-Induced Arthritis *via* Programmed Death 1-Mediated Immunomodulation

*Yuli Cheng[1], Xing Zhu[1], Xiaohuan Wang[1], Qinghui Zhuang[1], Xu Huyan[1], Ximeng Sun[1], Jingjing Huang[1], Bin Zhan[2] and Xinping Zhu[1]**

[1] Department of Medical Microbiology and Parasitology, School of Basic Medical Sciences, Capital Medical University, Beijing, China, [2] Department of Pediatrics, National School of Tropical Medicine, Baylor College of Medicine, Houston, TX, United States

Helminth infection induces Th2-biased immune responses and inhibitory/regulatory pathways that minimize excessive inflammation to facilitate the chronic infection of helminth in the host and in the meantime, prevent host hypersensitivity from autoimmune or atopic diseases. However, the detailed molecular mechanisms behind modulation on inflammatory diseases are yet to be clarified. Programmed death 1 (PD-1) is one of the important inhibitory receptors involved in the balance of host immune responses during chronic infection. Here, we used the murine model to examine the role of PD-1 in $CD4^+$ T cells in the effects of *Trichinella spiralis* infection on collagen-induced arthritis (CIA). Mice infected with *T. spiralis* demonstrated higher expression of PD-1 in the spleen $CD4^+$ T cells than those without infection. Mice infected with *T. spiralis* 2 weeks prior to being immunized with type II collagen displayed lower arthritis incidence and significantly attenuated pathology of CIA compared with those of uninfected mice. The therapeutic effect of *T. spiralis* infection on CIA was reversed by blocking PD-1 with anti-PD-1 antibody, associated with enhanced Th1/Th17 pro-inflammatory responses and reduced Th2 responses. The role of PD-1 in regulating $CD4^+$ T cell differentiation and proliferation during *T. spiralis* infection was further examined in PD-1 knockout (PD-$1^{-/-}$) C57BL/6 J mice. Interestingly, *T. spiralis*-induced alteration of attenuated Th1 and enhanced Th2/regulatory T cell differentiation in wild-type (WT) mice was effectively diminished in PD-$1^{-/-}$ mice characterized by recovered Th1 cytokine levels, reduced levels of Th2 and regulatory cytokines and $CD4^+CD25^+Foxp3^+$ cells. Moreover, *T. spiralis*-induced $CD4^+$ T cell proliferation suppression in WT mice was partially restored in PD-$1^{-/-}$ mice. This study introduces the first evidence that PD-1 plays a critical role in helminth infection-attenuated CIA in a mouse model by regulating the $CD4^+$ T cell function, which may provide the new insights into the mechanisms of helminth-induced immunomodulation of host autoimmunity.

Keywords: ***Trichinella spiralis*, rheumatoid arthritis, programmed death 1, $CD4^+$ T cell, immunomodulation**

OPEN ACCESS

Edited by:
Xun Suo,
China Agricultural University, China

Reviewed by:
Sandip Chakraborty,
College of Veterinary Sciences and Animal Husbandry, India
Juan Li,
Rockefeller University, United States
Sara Lustigman,
New York Blood Center, United States

****Correspondence:***
Xinping Zhu
zhuxping@ccmu.edu.cn

Specialty section:
This article was submitted to Microbial Immunology, a section of the journal Frontiers in Immunology

Received: *30 January 2018*
Accepted: *25 June 2018*
Published: *26 July 2018*

Citation:
Cheng Y, Zhu X, Wang X, Zhuang Q, Huyan X, Sun X, Huang J, Zhan B and Zhu X (2018) Trichinella spiralis Infection Mitigates Collagen-Induced Arthritis via Programmed Death 1-Mediated Immunomodulation. Front. Immunol. 9:1566. doi: 10.3389/fimmu.2018.01566

INTRODUCTION

After co-evolution with their hosts over a long period of time, helminths have developed the ability to induce host immune tolerance to facilitate their survival in the hosts. This helminth-induced immunomodulation may also benefit hosts to reduce pathological lesions caused by aberrant inflammatory responses that may underline many autoimmune disorders (1, 2). Rheumatoid arthritis

(RA) is a chronic autoimmune disease characterized by synovial inflammation and bone erosion, which affects up to 1% of the population worldwide. There is strong evidence that abnormally activated Th1 and Th17 cells and impaired $CD4^+CD25^+Foxp3^+$ regulatory T cell (Treg) contribute to the pathogenesis of RA (3). Helminth infections skew host immune response from Th1 to Th2/Treg characterized by stimulating the secretion of Th2 cytokine IL-4, IL-5, IL-10, and IL-13 (4) and induction of Treg development (5, 6). Th2 polarization and Treg-released IL-10, TGF-β downregulate the Th1 cell subset (6–8) that promotes the establishment of chronic infection (9). Immunomodulation by helminth infection has inspired to the idea of using helminthic therapy for atopic and autoimmune diseases in animal models and human trials which have provided convincing evidences for effectively alleviating a number of autoimmune diseases up to date (1). It has also been reported that helminth infection or helminth-derived products effectively alleviated the inflammatory arthritis by inducing Th2 responses or inducing $Foxp3^+$ T regulatory cells (10, 11). However, the detailed molecular mechanisms behind the modulation of inflammatory diseases are yet to be clarified.

Programmed death 1 (PD-1) is a member of the B7 family on the surface of T cells that delivers inhibitory signals to promote self-tolerance by suppressing T cell inflammatory activity and reduce immune-mediated tissue damage (12). PD-1 is an important immune checkpoint to keep immune balance and exerts critical inhibitory functions in the setting of persistent antigenic stimulation such as during encounter of self-antigens, chronic infections, and tumors (13, 14). There is evidence supporting a distinct role of PD-1 and its ligands (PD-L1/B7-H1 and PD-L2/B7-DC) in regulating T cell tolerance and autoimmunity (15). In humans, a role for PD-1 in the regulation of self-tolerance and autoimmunity was suggested to be associated with autoimmune diseases such as systemic lupus erythematosus, RA, multiple sclerosis, and type 1 diabetes mellitus (16–19). In animal models of collagen-induced arthritis (CIA), defective expression of PD-1 has been confirmed to contribute to T cell hyperactivity within the inflamed joint (20). In human investigations, blockade of PD-1 with anti-PD-1 increases the risk of developing RA (21).

In recent years, many studies indicated that helminths may exploit the PD-1 pathway to modulate host immune system to minimize excessive inflammation and promote the chronicity of helminth infection (22–24). *Trichinella spiralis* is an intestine- and tissue-dwelled nematode that secretes molecules to modulate hosts' immune system. Infection of this nematode or *Trichinella*-secreted proteins have been used for treatment of many hyperimmune-associated disorders in experimental studies such as asthma and allergic disorders (25), inflammatory bowel diseases (26, 27), encephalomyelitis (28), and type 1 diabetes (29), and significant alleviation of these diseases has been achieved.

It is well established that $CD4^+$ T cells play a central role in the pathogenesis of RA (30). In this study, we aim to investigate whether *T. spiralis* infection affects the PD-1 expression in $CD4^+$ T cells and its role in alleviation of arthritis using a CIA mouse model. We demonstrated for the first time that *T. spiralis* infection significantly alleviated CIA through activating the expression of PD-1 on $CD4^+$ T cells. Moreover, this study highlights the importance of PD-1 as a checkpoint for *T. spiralis*-induced Th2 polarization and Treg generation which may provide new insights into the mechanisms of helminths' immunomodulation on host autoimmunity.

MATERIALS AND METHODS

Ethics Statement

This study was carried out in accordance with the recommendations of "IRB of Capital Medical University." All animal experimental procedures were approved by the Animal Care and Use Committee of Capital Medical University (AEEI-2016-008) and comply with the National Institutes of Health Guidelines for the Care and Use of Experimental Animals.

Mice

Male DBA/1 mice with 6–8 weeks old were purchased from the Laboratory Animal Services Center of Capital Medical University (Beijing, China) for induction of arthritis and related experiments. Wild-type (WT) and $PD\text{-}1^{-/-}$ mice bred on the C57BL/6 background were purchased from the Jackson Laboratory (Stock no. 021157, USA). All mice were maintained under pathogen-free conditions with suitable humidity and temperature at the Animal Center of Capital Medical University.

Helminth Infection Model

The *T. spiralis* (ISS 533) strain used in this study was maintained in female ICR mice. Mice were each infected with 400 infective *T. spiralis* muscle larvae by oral gavage.

Induction of CIA

Experimental arthritis was induced in DBA/1 mice based on the method previously described (31). Bovine type II collagen (CII) purchased from Chondrex (Redmond, WA, USA) was dissolved in 0.01 M acetic acid at concentration of 2 mg/ml by stirring over night at 4°C and emulsified with the equal volume of complete Freund's adjuvant. Male DBA/1 mice were immunized intradermally at the base of the tail with 0.1 ml emulsion containing 100 μg CII. The mice were boosted once with the same amount of CII emulsified with incomplete Freund's adjuvant (Chondrex) 21 days after the first immunization. Induced arthritic mice were clinically assessed for redness and swelling of all limbs every other day up to 50 days. The clinical scores were assigned as previously described to evaluate disease (32) as follows: 0 = no signs of arthritis: 1 = swelling and/or redness of the paw or one digit; 2 = two joints involved; 3 = more than two joints involved and 4 = severe arthritis of the entire paw and digits. Each limb was graded, resulting in a maximal clinical score of 16 per animal.

Histopathologic Analysis

The paws of the mice were removed after being euthanized and fixed overnight in 4% paraformaldehyde, decalcified in 20% EDTA for 6 weeks, and then dehydrated and embedded in paraffin. The tissue serial paraffin sections (2 mm) were cut along longitudinal axis, mounted and sections were stained with hematoxylin and eosin or toluidine blue (TB). The severity of

inflammatory cell infiltration in joint and cartilage destruction was scored using a semi-quantitative scale described previously (33, 34). The severity of inflammatory cell infiltration was scored 0–4 as follows: 0 = no infiltrate; 1 = minimal (few cells in perisynovial and synovial tissues); 2 = mild (infiltrating cells more numerous in perisynovial and synovial tissues, and/or in bone marrow beneath joints); 3 = moderate (inflammatory cell infiltrate more intense in perisynovial and synovial tissues, and often extending into adjacent periosseous tissues and/or in bone marrow beneath joints); and 4 = marked (increasing intensity of inflammatory cell infiltrate in synovial and perisynovial tissues, and extending into adjacent periosseous tissues and/or widely dispersed in bone marrow). Cartilage damage was scored 0–5 according to the following criteria: 0 = normal; 1 = minimal (loss of TB staining only); 2 = mild (loss of TB staining and mild cartilage thinning); 3 = moderate (moderate diffuse or multifocal cartilage loss); 4 = marked (marked diffuse or multifocal cartilage loss); and 5 = severe (severe diffuse or multifocal cartilage loss).

In Vivo Blockade of PD-1

In some experiments, the expression of PD-1 on immune cells in mice was blocked by injection of anti-mouse CD279 (PD-1) antibody (clone 29F.1A12, BioLegend, San Diego, CA, USA). Each mouse received 200 μg mAb intraperitoneally (i.p.) every 3 days, starting at 14 days post-infection until 3 days before the mice were sacrificed. For control mice, each was given the same amount of rat IgG2a isotype (clone RTK2758, BioLegend).

Isolation of Lymphocytes From Spleen and Lymph Nodes

Four weeks after second immunization, the draining inguinal lymph nodes (ILNs) and spleens were removed and minced through a 70-μm cell strainer. Lymphocytes were isolated using Ficoll density-gradient centrifugation for flow cytometry or released-cytokine measurement.

Spleen Cell Culture and Cytokine ELISA

Splenocytes were cultured in RPMI 1640 medium supplemented with 10% fetal bovine serum (FBS, Gibco, Grand Island, NY, USA), 100 U/ml penicillin, and 100 μg/ml streptomycin, at 2×10^6 cells/ml in 24-well culture plates. During culture, the cells were stimulated with anti-CD3 (1 μg/ml)/anti-CD28 (1 μg/ml) (Peprotech, NJ, USA). The supernatants were collected at 48 h and kept frozen at −80°C until used. Cytokines IFN-γ, IL-4, IL-5, IL-13, IL-10, IL-17A, and TNF-α in the culture supernatants were measured with Ready-Set Go! Kits or recombinant cytokine/antibody sets from eBioscience (San Diego, CA, USA) according to the manufacturer's instructions.

Anti-CII Antibody Measurement

Sera were collected from mice 4 weeks after the second immunization of CII and the anti-CII-specific IgG and subtype IgG1 and IgG2a were measured by using antibody assay kit according to the manufacturer's instructions (Chondrex, Redmond, WA, USA). Each sample was assayed in duplicate. OD values were measured at 490 nm using a Model 550 microplate reader and the results were analyzed using Microplate Manager III for Macintosh (Bio-Rad laboratories, Hercules, CA, USA).

$CD4^+$ T Cells Purification, CFSE Labeling, and Stimulation

$CD4^+$ T cells were isolated from spleen or ILNs by positive selection using a magnetic-activated cell sorting system with anti-CD4 mAb (Miltenyi Biotec, Bergisch Gladbach, Germany) according to the manufacturer's instructions. Isolated cells (5×10^6 cells) were suspended in 1 ml sterile PBS containing 3% FBS. Carboxyfluorescein succinimidyl amino ester (CFSE, Invitrogen, Carlsbad, CA, USA) was added into the culture up to 5 μM for 5 min to label the cells. Labeling reaction was stopped by diluting with 9 ml of PBS containing 3% FCS and cells were washed twice. The labeled $CD4^+$ T cells were used for the experiment of proliferation assessment and flow cytometry analysis. In experiment for determining non-specific T cell proliferation, the splenic $CD4^+$ T cells isolated from *T. spiralis*-infected mice were cultured in plates coated with anti-CD3 (5 μg/ml, BioLegend, San Diego, CA, USA) in the presence of anti-CD28 (5 μg/ml, BioLegend) for 72 h. In experiment for determining specific anti-CII T cell proliferation, mice were immunized with CII on day ≥35 after *T. spiralis* infection. Then $CD4^+$ T cells isolated from ILNs of mice on day 10 after CII immunization were cultured in the presence of CII for 72 h (20 μg/ml).

Flow Cytometry

To analyze PD-1 expression in $CD4^+$ T cells, the cells were stained with anti-mouse CD3-antigen-presenting cell (APC) (clone 17A2, eBioscience, Waltham, MA, USA), CD4-FITC (clone GK1.5, eBioscience), PD-1-PE (clone J43, eBioscience). To detect intracellular cytokine expression, T cells from each mouse were stimulated with 2 μl/ml. Cell Activation Cocktail (with Brefeldin) (BioLegend, San Diego, CA, USA) in complete RPMI 1640 medium for 6 h at 37°C in 5% CO_2, then collected and surface stained with CD3 and CD4. The cells were washed, fixed, and permeabilized with cytofix/cytoperm buffer (BD Pharmingen), then intracellularly stained with anti-IFN-γ PE-Cyanine7 (clone XMG1.2), IL-4 PE-Cyanine7 (clone 11B11), and IL-17A PE-Cyanine7 (clone eBio17B7), or rat IgG1 and IgG2a isotype antibody (clone eBRG1, all from eBioscience) as control, respectively. To determine Tregs, the $CD4^+$ cells were surface stained with anti-mouse CD3-PerCP (clone 17A2), CD4-FITC (clone RM4-5), and CD25-APC (clone PC61.5) in a Mouse Regulatory T cell Staining Kit (eBioscience). The cells were then permeabilized with cold Fix/Perm Buffer, and stained with anti-mouse Foxp3-PE (clone FJK-16s) or rat IgG2a isotype control antibody (clone eBR2a). Following immunofluorescence staining, samples were analyzed on a Flow cytometer (BD) using flowjo software (TreeStar). The cells were gated on $CD3^+$ $CD4^+$ T cells.

Statistical Analysis

Statistical analysis was performed using SPSS version 11.0. All data are expressed as mean ± SEM. To determine differences between multiple groups, analysis of variance was used with *post hoc* comparisons using Tukey's method. For comparison

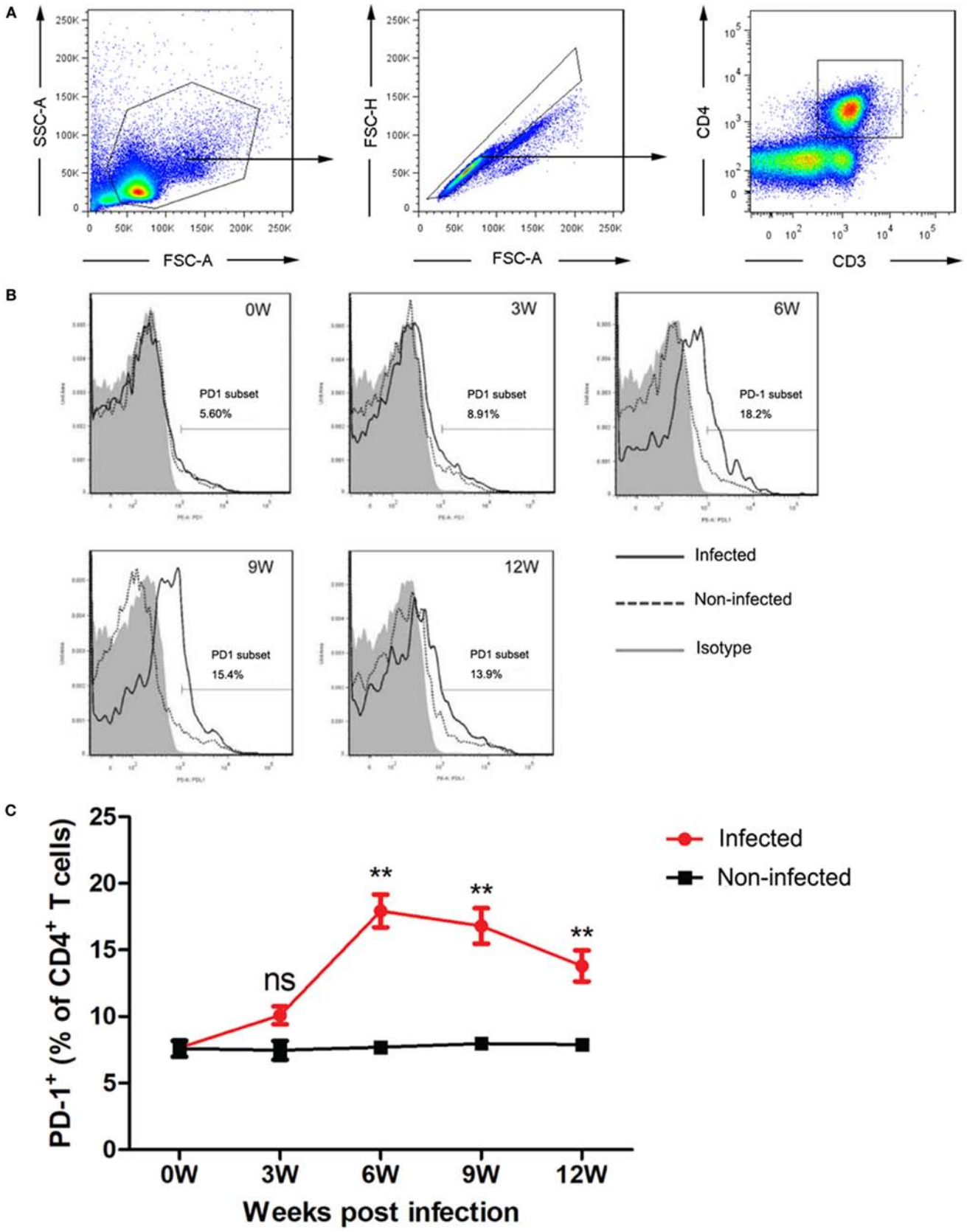

FIGURE 1 | Continued

FIGURE 1 | Dynamics of programmed death 1 (PD-1) expression in CD4+ T cells from *Trichinella spiralis*-infected mice. **(A)** FACS gating strategy for CD4+ T cells expressing PD-1. PD-1 gating was shown based on the PD-1 isotype control. **(B)** Flow cytometry showing the PD-1 subset in CD4+ T cells from spleen of infected mice compared with those from non-infected mice. Non-specific isotype antibody was used as control. The representative PD-1 expression is represented in solid line in *T. spiralis*-infected mice and in dotted line in non-infected mice. Isotype control is illustrated in gray. **(C)** The dynamic expression of PD-1 in CD4+ T cells of mice during *T. spiralis* infection. Data are expressed as mean ± SEM from three independent experiments ($n = 5$ mice per group).

between two groups, a Student's *t*-test was performed. A *P*-value <0.05 was considered significant.

RESULTS

T. spiralis Infection Upregulates PD-1 Expression in CD4+ T Cells

Programmed death 1 expression in spleen CD4+ T cells was upregulated in mice infected with *T. spiralis*. Increased expression of PD-1 in spleen CD4+ T cells was observed in the initial acute stage of infection, peaked at week 6, and followed by a slight decline thereafter (**Figure 1**) with significant difference to the baseline expression level in the CD4+ T cells of normal mice.

T. spiralis Infection Alleviates CIA Through PD-1 Pathway

To determine whether the infection of *T. spiralis* alleviates the severity of CIA in mice, mice were infected with *T. spiralis* 14 days prior to the first immunization of CII. The representative paw of mice with CIA was shown in **Figures 2A,B**. As shown in **Figures 2C,D**, *T. spiralis*-infected CIA mice displayed significant reduction in the incidence of induced CIA and alleviated arthritic score compared with uninfected CIA mice. PD-1 blockade with specific antibody significantly increased the incidence and severity of arthritis in *T. spiralis*-infected CIA mice (**Figures 2C,D**). Histologic analysis of the paws showed significantly decreased inflammation scores and cartilage destruction in *T. spiralis*-infected CIA mice compared with non-infected CIA mice. Similarly, the amelioration of inflammatory cell infiltration and cartilage destruction in *T. spiralis*-infected CIA mice was effectively reversed by the blockage of PD-1 with anti-PD-1 (**Figures 2E,F**). Isotype IgG2a control had no any effect on CIA (data not shown). These data suggested that PD-1 plays an important role in the inhibitory effect of *T. spiralis* infection on CIA in mouse.

Nematode-Induced Inhibition of Th1/Th17 Responses and Enhancement of Th2 Responses Were Abated by Blocking PD-1 in CIA Mice

To understand the mechanisms involved in the *T. spiralis* infection-attenuated CIA, the humoral and cellular immune responses were measured in the treated mice. It is well established that anti-CII antibody is involved in the pathogenesis of CIA (35). Serological levels of antigen-specific total IgG, and subtypes IgG2a and IgG1 were measured. As shown in **Figure 3A**, the anti-CII total IgG level in the sera of mice infected with *T. spiralis* was significantly lower than that in mice without infection. Subtype analysis demonstrated that the reduced IgG level mostly resulted from the reduction in the IgG2a (Th1) but not in IgG1 (Th2). The reduced levels of IgG and IgG2a in *T. spiralis*-infected mice were effectively restored when PD-1 was blocked using anti-PD-1 antibody. The cytokine profile of splenocytes stimulated by anti-CD3/anti-CD28 antibodies showed that *T. spiralis*-infected CIA mice produced significantly lower levels of pro-inflammatory cytokines including IFN-γ (Th1), IL-17 (Th17), and TNF-α, but higher level of Th2 cytokines IL-4, IL-5, IL-13, and regulatory cytokine IL-10 compared with CIA mice without infection (**Figure 3B**). However, the nematode-reduced pro-inflammatory cytokines and boosted Th2 cytokines in CIA mice were significantly abated when PD-1 was blocked using anti-PD-1 antibody. The above results indicate that alleviation of CIA by the infection of *T. spiralis* is associated with the reduced Th1/Th17, enhanced Th2 responses possibly through stimulating the expression of suppressive PD-1 in the immune cells.

PD-1 Knockout Offsets *T. spiralis*-Induced Anti-Inflammatory Modulation of CD4+ T Cells

To further investigate whether *T. spiralis* infection-induced immunomodulation is PD-1 mediated, we profiled cytokines secreted by splenocytes upon stimulation of anti-CD3/anti-CD28 in WT and PD-$1^{-/-}$ C57BL/6 J mice infected with or without *T. spiralis*. As shown in **Figure 4A**, the inhibited IFN-γ and IL-17 production following *T. spiralis* infection in WT mice was recovered in PD-$1^{-/-}$ mice. By contrast, *T. spiralis*-enhanced IL-4, IL-5, IL-13, and IL-10 production in WT mice was abated in PD-$1^{-/-}$ mice. This result further suggests that *T. spiralis* may activate PD-1 pathway to inhibit Th1- and Th17-associated pro-inflammatory cytokine production and to boost Th2-associated anti-inflammatory cytokine and regulatory cytokine production. Flow cytometry also showed that *T. spiralis* infection decreased IFN-γ+ (Th1), and increased IL-4+ (Th2) CD4+ T cells and CD25+Foxp3+ Tregs, but little effected on IL-17A+ (Th17) CD4+ T cells. However, these *T. spiralis*-induced attenuated Th1 and enhanced Th2/Treg differentiation in WT mice were effectively diminished in PD-$1^{-/-}$ mice (**Figures 4B–E**). These results with PD-$1^{-/-}$ mice further confirm that *T. spiralis*-induced differential control of CD4+ T cell subsets is PD-1 mediated, suggesting that PD-1 play a critical role in *T. spiralis*-induced immunomodulation.

To determine the responsiveness of T cell in *T. spiralis*-infected mice, we examined the CD4+ T cell proliferation upon non-specific (anti-CD3/anti-CD28) and antigen-specific stimulation in WT and PD-$1^{-/-}$ mice with or without infection. The proliferation of splenic CD4+ T cells upon non-specific stimulation (anti-CD3/anti-CD28) was significantly inhibited in cells from *T. spiralis*-infected mice compared to those from non-infected mice. The inhibited CD4+ T cell proliferation was partially restored in mice with PD-1 knockout (**Figure 5A**). We further analyzed the

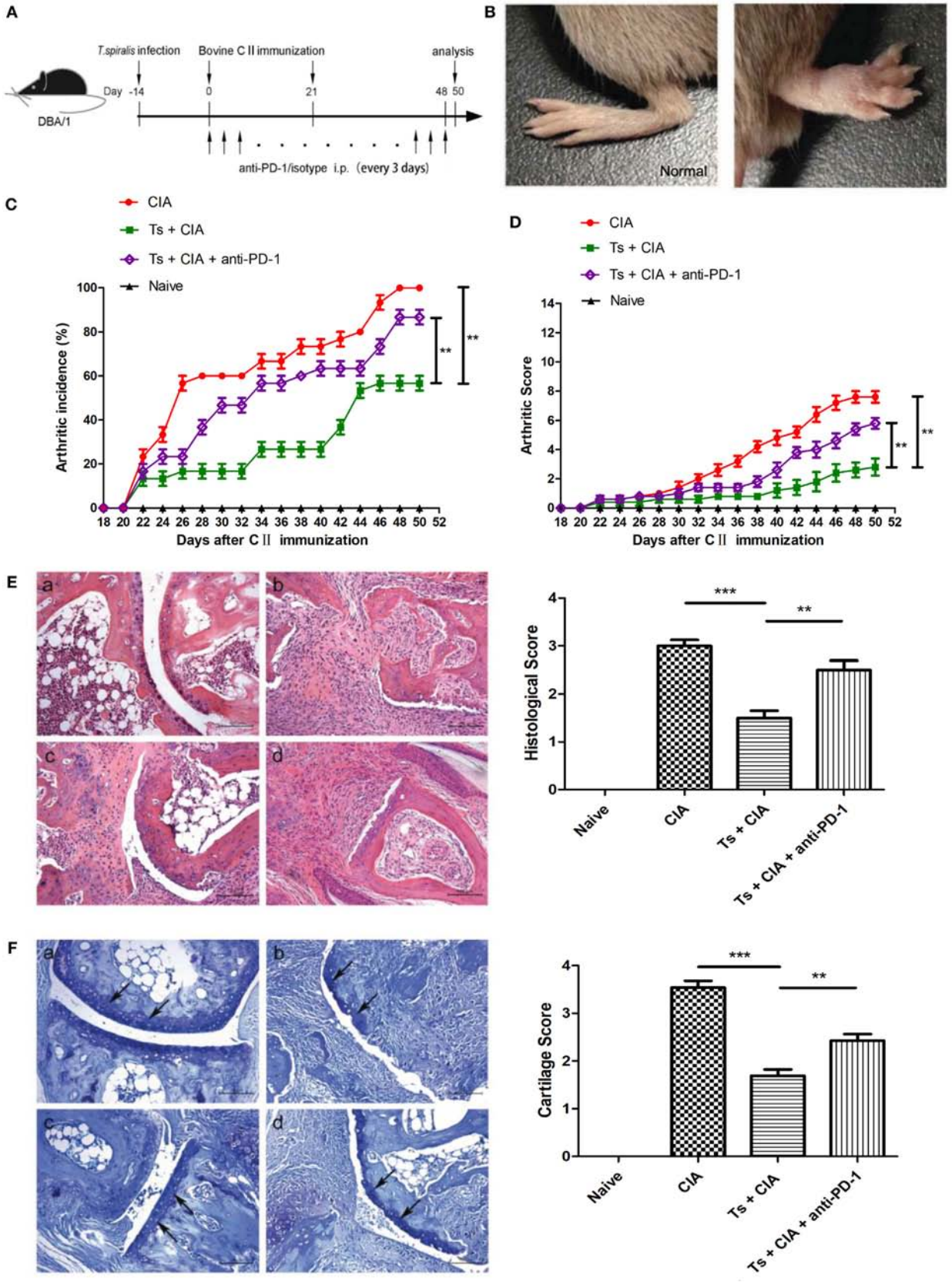

FIGURE 2 | Continued

FIGURE 2 | Programmed death 1 (PD-1) blockade abated *Trichinella spiralis* infection-induced attenuation of collagen-induced arthritis (CIA) in DBA/1 mice. **(A)** The regimen of study including the induction of CIA, treatment with infection of *T. spiralis* and anti-PD-1 antibody. **(B)** Hind paw of a mouse before and after induction of arthritis with bovine type II collagen (CII). Arthritic incidence **(C)** and total arthritic score **(D)** of mice from different groups ($n = 10$) at different time points. **(E)** Hematoxylin and eosin of the representative inflamed joints in the hind paw of mice from different groups at day 50 post first CII immunization, the histological score was shown on the right (mean ± SEM, $n = 6$). **(E)** The toluidine blue staining and cartilage score **(F)** of the representative inflamed joints in the hind paw of mice from different groups at day 50 post first CII immunization. (a) Naïve untreated control, (b) CIA, (c) Ts + CIA, (d) Ts + CIA + anti-PD-1. The bar graphs on the right side **(E,F)** show the histopathological scores for each group given as mean ± SEM ($n = 6$ mice per group). Statistical significance is determined by Student's *t*-test for single comparison. $^{**}P < 0.01$ and $^{***}P < 0.001$ (one-way analysis of variance).

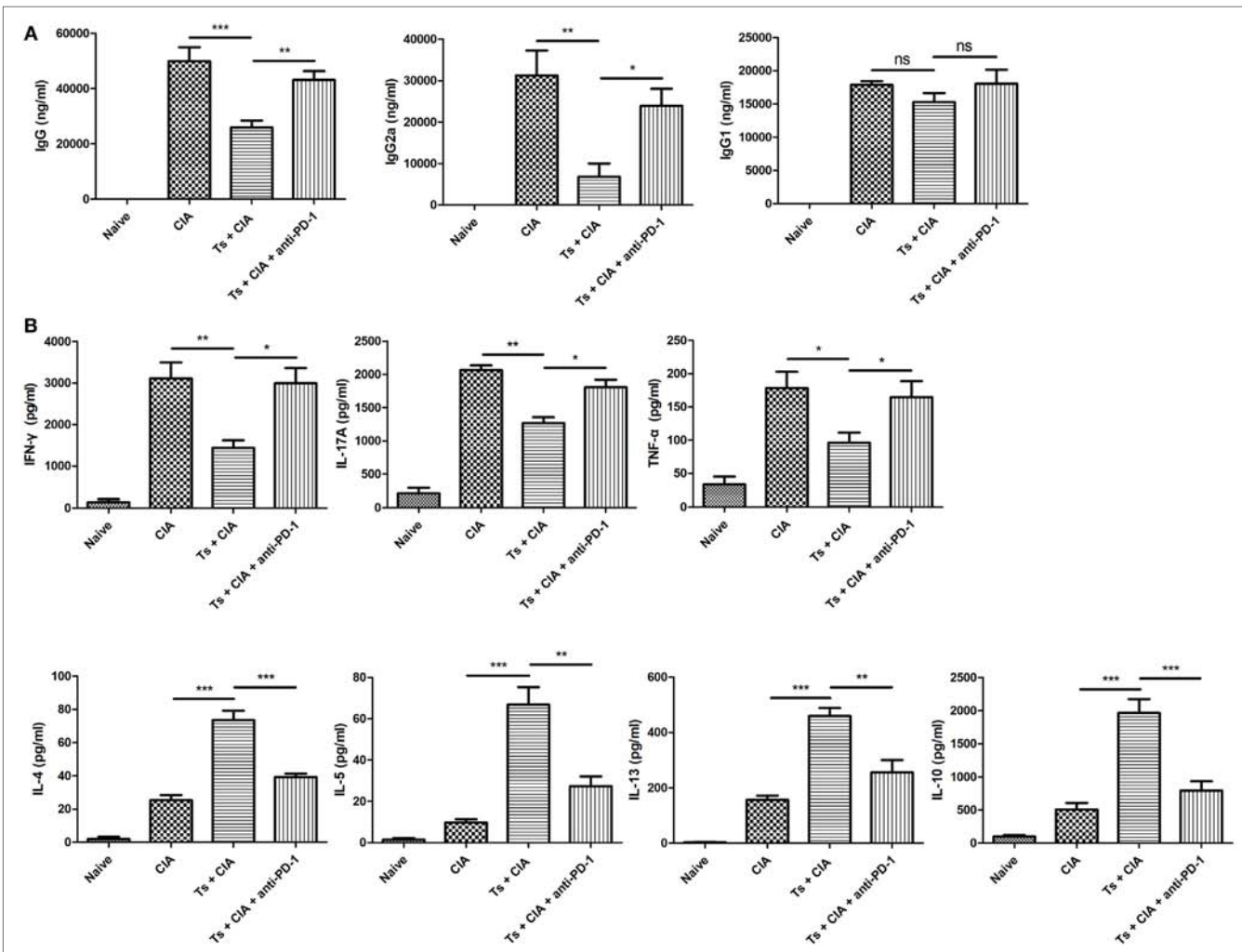

FIGURE 3 | Programmed death 1 (PD-1) blockade offsets the inhibited Th1/Th17 responses and enhanced Th2 responses induced by *Trichinella spiralis* infection in collagen-induced arthritis (CIA) mice. Anti-type II collagen (CII) antibody and cytokine profile were determined by ELISA on day 50 after immunization. **(A)** Serological titers of anti-CII total IgG and subtypes IgG1 and IgG2a in mice of different groups. **(B)** Cytokine profiles secreted by splenocytes stimulated with anti-CD3 (1 μg/ml)/anti-CD28 (1 μg/ml) for 48 h. Data are expressed as mean ± SEM for duplicate serum samples or cell cultures. Data are representative of results from two independent experiments ($n = 6$ mice per group). $^{*}P < 0.05$; $^{**}P < 0.01$; $^{***}P < 0.001$; ns, not significant (one-way analysis of variance).

antigen-specific T cell proliferation in $CD4^+$ T cells isolated from ILNs of CII-immunized mice upon CII stimulation. Similarly, the inhibition of $CD4^+$ T-cell proliferation upon re-stimulation of specific antigen CII in *T. spiralis*-infected mice was partially lifted in T cells from PD-$1^{-/-}$ mice (**Figure 5B**). These results suggest that PD-1 partially contributes to *T. spiralis*-induced hyposensitivity of $CD4^+$ T cells.

DISCUSSION

Immune responses are regulated by the balance of positive and negative regulatory pathways. Negative regulatory pathways are crucial for peripheral self-tolerance and preventing autoimmunity, and can function through signals delivered by cell surface inhibitory receptors, immunoregulatory cytokines, and Tregs (30).

Multiple co-inhibitory receptors such as lymphocyte activation gene 3 (LAG-3), B- and T-lymphocyte attenuator 4 (BTLA-4), cytotoxic T-lymphocyte antigen 4 (CTLA-4), and T cell membrane protein 3 (Tim-3), CD244, and CD160 are expressed in T cells to dampen immune activation and limit immune-mediated pathology (36, 37). Recent studies demonstrated that these inhibitory receptors also play an important role in the response to pathogens. It is reported that helminth infection drives the sustained expression of T cell inhibitory receptors, which may negatively regulate proliferation and the production of pro-inflammatory cytokines by helminth antigen-specific T cells (38–40). Because these molecules largely function to prevent over exuberant T cell activation, their essential role in preventing parasite-induced immunopathology have been confirmed in animal studies (38, 41). However, the impact of these parasite-induced inhibitory molecules on autoimmune pathology has not been clarified.

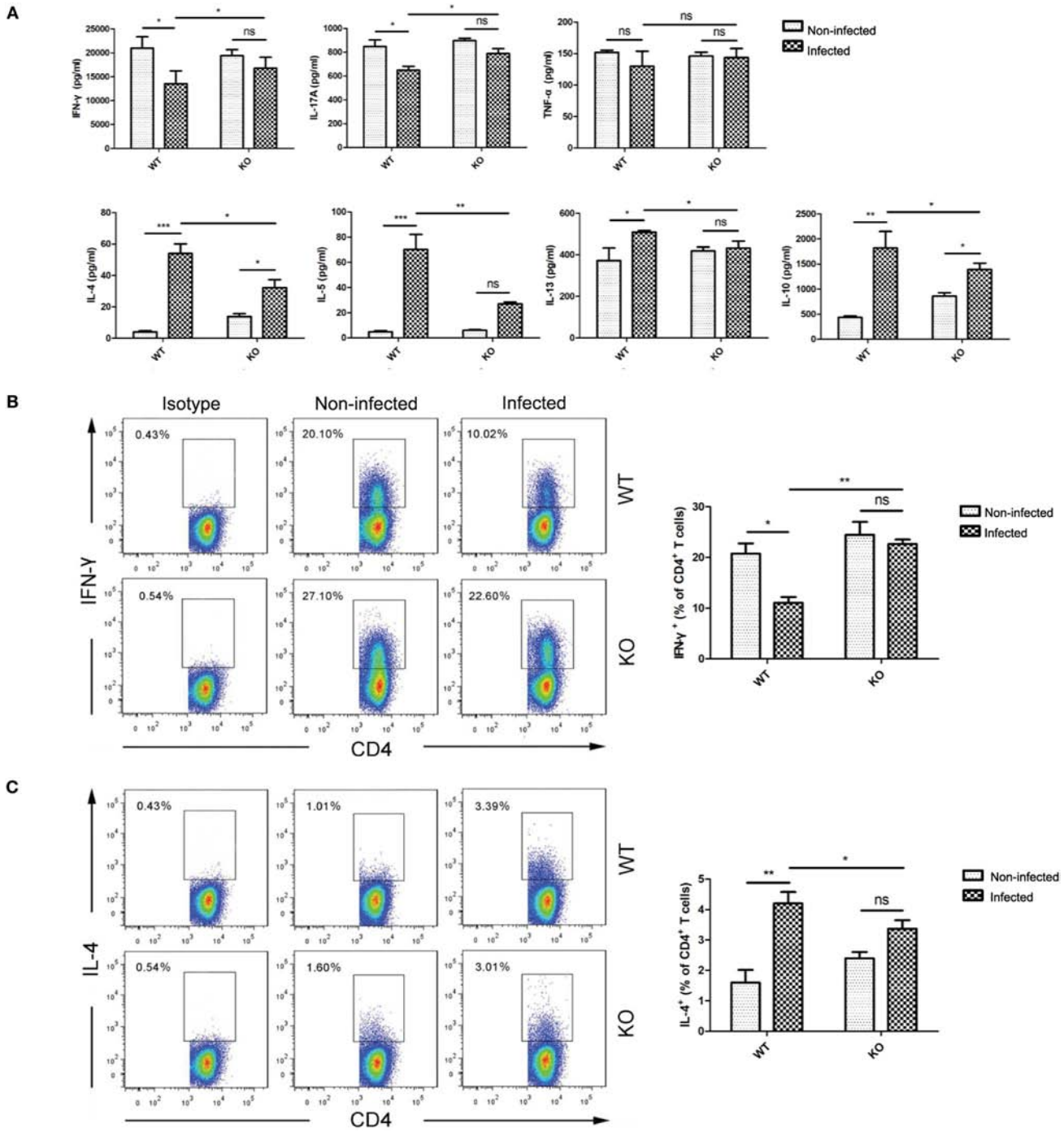

FIGURE 4 | Continued

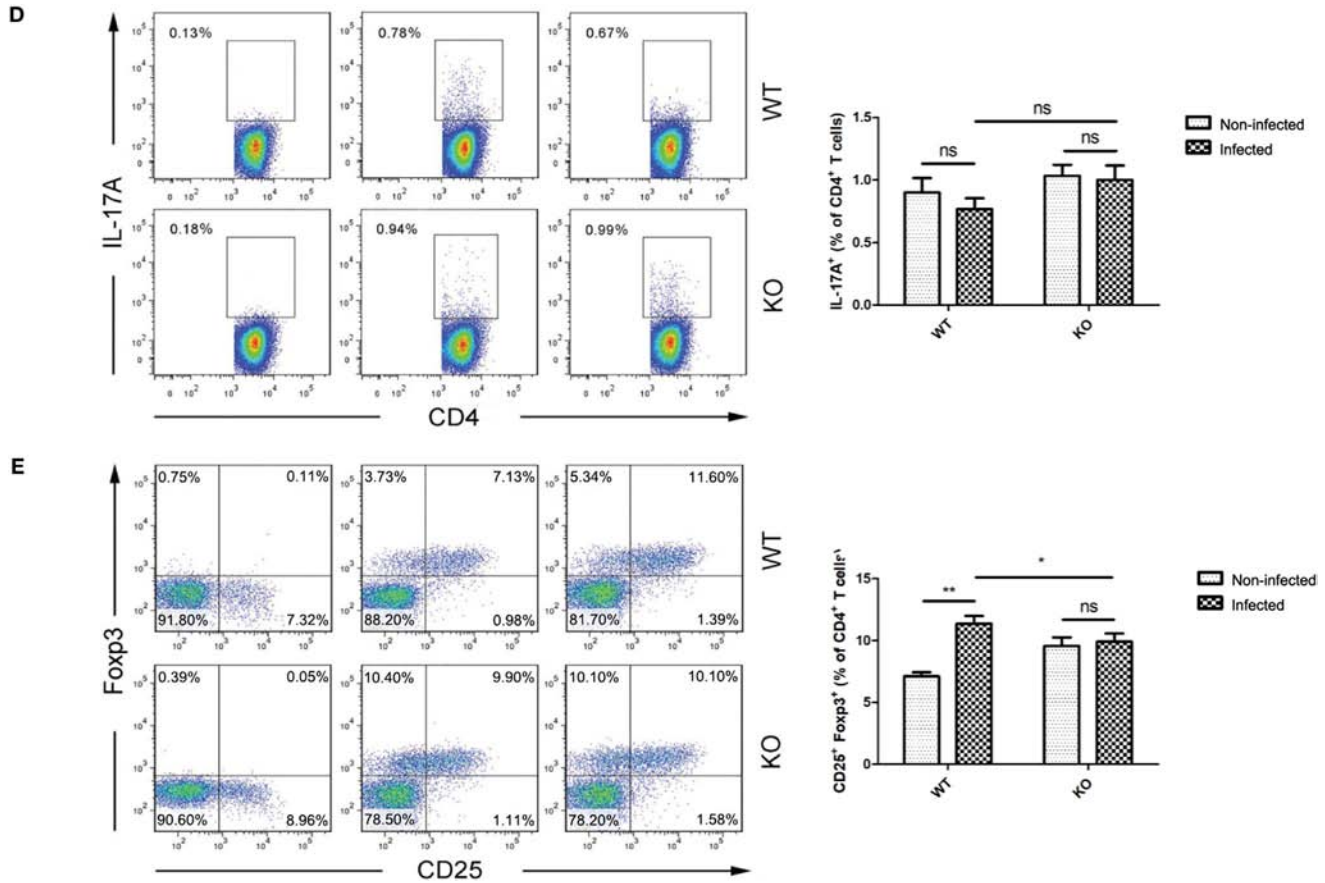

FIGURE 4 | Programmed death 1 (PD-1) knockout abated *Trichinella spiralis*-induced Th1/17 inhibition and Th2/regulatory T cell (Treg) enhancement. Single-cell suspensions of spleens from wild-type (WT) and PD-1$^{-/-}$ mice (KO) infected with or without *T. spiralis* were prepared. **(A)** Cytokine profiles secreted by splenocytes (IFN-γ, IL-17A, TNF-α, IL-10, IL-4, IL-5, and IL-13) upon stimulation with anti-CD3/CD28 for 48 h measured by ELISA. **(B–E)** Representative staining and percentages for IFN-γ-, IL-4-, IL-17-producing CD4$^+$ T cells and CD4$^+$ CD25$^+$ Foxp3$^+$ Treg cells by FACS. Data are expressed as mean ± SEM from three independent experiments (n = 5 mice per group). *P < 0.05; **P < 0.01; ns, not significant (paired Student's t-test).

Programmed death 1 plays a critical role in maintaining host immune homeostasis during chronic infection (42, 43). In this study, we observed upregulation of PD-1 in lymphocytes of mice infected with *T. spiralis*. The upregulation of PD-1 was also observed in the chronic infections of *Schistosoma japonicum* (24), *Fasciola hepatica* (44), *Taenia solium* (45), *Echinococcus multilocularis* (45) related to the survival of helminth in the host and reducing infection caused immunopathology.

To determine if the *T. spiralis* infection reduces the pathology of inflammatory arthritis, we established a collagen-induced mouse model (CIA). The CII-reactive CD4$^+$ T cells are the primary mediators of disease induction by driving autoantibody production in B cells and enhancing the chronic inflammatory response (46, 47). Our results demonstrated that *T. spiralis* infection significantly mitigated the pathology of CIA in mice mostly through reducing Th1/Th17 pro-inflammatory responses and boosting Th2 response. The results are in accordance with previous studies that showed increased Th1/Th17 cellular response played a key role in the CIA (48, 49). *T. spiralis* infection reduces these pro-inflammatory responses therefore alleviates pathology of CIA. It is well known that helminth chronic infection-induced Th2 polarization is also involved in the therapeutic effects on autoimmune diseases. *Nippostrongylus brasiliensi*-induced activation of Th2 axis effectively mitigates the course of inflammatory arthritis and this protective effect is dependent on IL-4/IL-13-induced STAT6 pathway (50). *F. hepatica* excretory–secretory products were reported to protect against experimental autoimmune encephalomyelitis *via* type 2 cytokines (51).

Given that the PD-1 expression is upregulated in the CD4$^+$ T cells of *T. spiralis*-infected mice and PD-1 is an important inhibitory and checkpoint receptor on immune cells, we postulated that *T. spiralis*-induced PD-1 expression may be involved in the alleviation of CIA by suppressing Th1 and Th17 responses and boosting Th2 response. Indeed, we observed that the reduced pathology of CIA in *T. spiralis*-infected mice was correlated with the increased expression of PD-1 in CD4$^+$ T cells. Blocking PD-1 with anti-PD-1 mAb seriously reversed the amelioration of CIA in *T. spiralis*-infected mice, correlating with recovered level of Th1/Th17 response and reduced Th2 response. PD-1 knockout also demonstrated its reversion to *T. spiralis* infection-involved Th1 and Th2 changes, however, it did not change much the frequency of Th17 within CD4$^+$ T cells at day 42 post-infection

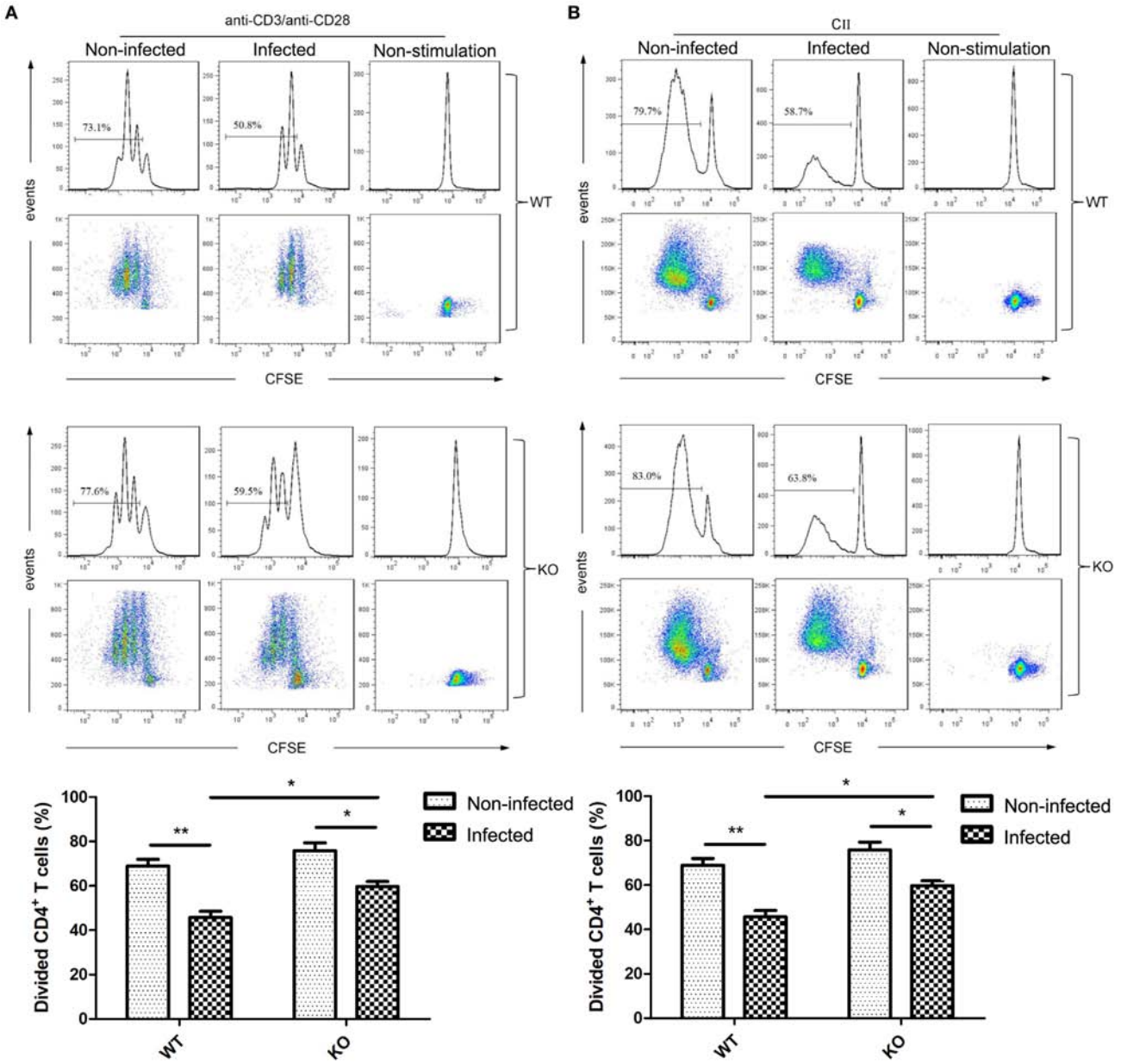

FIGURE 5 | Programmed death 1 (PD-1) knockout partially restored suppressed proliferation of CD4+ T cells in *Trichinella spiralis*-infected mice. CD4+ T cells were isolated from C57BL/6 wild-type (WT) and PD-1$^{-/-}$ mice and stained with CFSE. Decay of CFSE staining of CD4+ T cells was determined by flow cytometry. **(A)** FACS analysis of CD4+ T cell proliferation in response to non-specific stimulation. Purified CD4+ T cells from spleen of uninfected or *T. spiralis*-infected mice at day ≥35 of infection were stained with CFSE and incubated in the presence of anti-CD3/anti-CD28 for 72 h. **(B)** FACS analysis of CD4+ T cells proliferation in response to type II collagen (CII)-specific stimulation. Mice with or without *T. spiralis* infection (at day ≥35 of infection) were immunized with CII. CD4+ T cells were purified from LNCs of mice at day 10 post CII immunization and stained with CFSE, then incubated in the presence of CII (10 μg/ml) for 72 h. Irradiated naïve splenocytes were used as antigen-presenting cells (APCs). Data were expressed as mean ± SEM from two independent experiments ($n \geq 3$ mice per group). $^{**}P < 0.05$; $^{*}P < 0.01$ (paired Student's *t*-test).

(**Figure 4D**), possibly because the stage of chronic *T. spiralis* infection may not affect much on IL-17 expression (52). Th17 cells are known to be involved in the inflammatory immune responses and autoimmune diseases as shown in CIA induction in this study (**Figure 3B**). However, it is not well understood the role of Th17 cells in the helminth infections (53), even though it has been observed that *T. spiralis* infection really reduced the CIA-induced Th17 secretion (**Figure 3B**).

Our results provide strong evidences at the first time that PD-1 pathway is involved in immunomodulation induced by *T. spiralis* infection that attenuates autoimmune-related arthritis. We postulate that pre-infection with *T. spiralis* may induce an anti-inflammatory modulation ahead of the initiation of CIA *via* activating the PD-1 pathway.

The costimulatory pathway consists of the PD-1 and its ligands, PD-L1 and PD-L2, delivering inhibitory signals that

regulate the balance among T-cell activation and immune-mediated tissue damage to prevent autoimmunity (13, 54, 55). Manipulation of PD-1:PD-L1/2 pathway is considered a potential therapeutic approach for treating autoimmune diseases (15). Impact of PD-L:PD-1 axis on differentiation of $CD4^+$ T cell subsets has been reported in previous studies (32, 56, 57). In this study, we also observed that the increased expression of PD-1 in $CD4^+$ T cells in *T. spiralis*-infected mice and knockout of PD-1 resulted in the recovery of inhibited $CD4^+$ T cell proliferation caused by nematode infection, indicating PD-1 is involved in the nematode infection caused regulation of $CD4^+$ T cells. At the meantime, we identified that the Th2 polarization and Treg generation induced by *T. spiralis* infection were effectively diminished in PD-$1^{-/-}$ mice. The results imply a critical role of PD-1 in modulating the balance of Th1/Th2 and Treg responses upon infection of *T. spiralis* that may outline the molecular mechanism behind the helminth-induced immunomodulation. Activation of PD-L1:PD-1 pathway may result in the enhanced Foxp3 expression and suppressive function of established induced regulatory T (iTreg) cells (12). $CD4^+CD25^+FoxP3^+$ Tregs are highly involved in the regulation of immune responses and preventing autoimmunity (58–60). *Schistosoma mansoni* and *T. spiralis* derived antigens have been demonstrated to exert protective effect against adjuvant arthritis by upregulation of the $Foxp3^+$ Tregs (10). Here, we confirmed that *T. spiralis*-induced expression of Foxp3 is highly dependent on PD-1 expression on immune cells, which implies that PD-1-mediated generation of $Foxp3^+$ Tregs may contribute to the *T. spiralis*-attenuated CIA. However, different helminth infection may modulate host immune regulation through different PD-L/PD-1 pathway. The conditional deletion of PD-L1 impaired Th2 polarization and cytokine production in mice following *N. brasiliensis* infection (56). By contrast, blockade of PD-1 results in recovery of hyporesponsive Th2 cell function which was mediated through PD-L2 during chronic infection with *Litomosoides sigmodontis* (22). While the reasons for the discrepancies regarding the role of PD-1 in regulating Th2 cytokine production remain unclear, it seems to be related to the types of PD-L which interact with PD-1 expressed in the $CD4^+$ T cells to control the function of Th subsets. It has been demonstrated that PD-L1 and PD-L2 have distinct roles in regulating host Th cell differentiation in response to leishmaniasis (61). Moreover, PD-1 has been suggested to enhance Th2 responses under conditions of sub-optimal TCR stimulation, which might be associated with the type of antigen (62).

In addition to activating Th2 cell-biased responses, helminths have also developed multiple mechanisms to regulate the host immune system. Humans with chronic infectious diseases, including helminth infection, experience sustained immune activation that is often accompanied by T cell hyporesponsiveness. Recent studies revealed that helminth infection induced T cell hyporesposiveness might contribute to suppression of autoimmune diseases. For example, infection with *Schistosome* regulates lymphocyte function *in vivo* by suppressing T cell activation (63, 64). Since PD-1 is described as a co-inhibitory receptor which induces T cell exhaustion, we examined the role of PD-1 in regulating T cell proliferation in *T. spiralis*-infected mice. Our study demonstrated a decreased T cell proliferation in *T. spiralis*-infected mice in response to both non-specific and CII-specific stimulation. However, PD-1 deletion only partially restored *T. spiralis*-suppressed $CD4^+$ T cells proliferation. Although blockage of PD-1 can reverse the hyporesponsiveness to *S. japonicum* (24) and *L. sigmodontis* (22), many possible mechanisms may underlie the incomplete recovery of the suppressed T-cell proliferation induced by *T. spiralis* infection after PD-1 deletion observed in this study. Helminth infection modulates host T cell function through multiple factors including induction of Tregs, IL-10/TGF-β regulatory cytokines (23, 64), PD-1/PD-L, and other co-inhibitory molecules such as LAG-3, BTLA-4, CTLA-4, Tim-3, etc. (9, 65). We postulate that synergetic effects from different inhibitory pathways may contribute to *T. spiralis*-induced $CD4^+$ T cells hyporesponsiveness besides PD-1/PD-L. Therefore, blocking PD-1/PD-L inhibitory pathway may not take away the whole inhibitory effects induced by *T. spiralis* infection.

In summary, this study demonstrates that *T. spiralis* infection significantly reduced the pathology of CIA in mice by inhibiting Th1/Th17 pro-inflammatory responses and inducing Th2/Treg polarization. PD-1 plays a critical role within the helminth-involved immunomodulation of $CD4^+$ T cell subsets which are central mediators of RA. However, the detailed molecular interaction between PD-1/PD-L pathway and the helminth-iTreg cell and cytokine IL-10 and TGF-β still remains unknown. Further studies are needed to explore the mechanism of PD-1-mediated regulation of immune response during helminth infection and autoimmune diseases.

ETHICS STATEMENT

This study was carried out in accordance with the recommendations of "IRB of Capital Medical University." The protocol was approved by the Animal Care and Use Committee of Capital Medical University (AEEI-2016-008) and comply with the National Institutes of Health Guidelines for the Care and Use of Experimental Animals.

AUTHOR CONTRIBUTIONS

YC and XPZ conceived and designed the experiments. YC, XZ, XW, QZ, XH, and JH performed the experiments. YC, XPZ, BZ, and XS analyzed the data. XPZ, YC, and BZ wrote the paper. All authors reviewed the manuscript.

ACKNOWLEDGMENTS

We thank Xiaoxue Xu (Core facility center, Capital Medical University) for her assistance with flow cytometry analysis. We thank Wenming Zhao and Huihui Yuan (Department of immunology, School of Basic Medical Sciences, Capital Medical University) for their technical assistance with induction of CIA in mouse model.

FUNDING

This work was supported by grants from the National Natural Science Foundation of China (81572016, 81672042) and Beijing Natural Science Foundation (7162017).

REFERENCES

1. Smallwood TB, Giacomin PR, Loukas A, Mulvenna JP, Clark RJ, Miles JJ. Helminth immunomodulation in autoimmune disease. *Front Immunol* (2017) 8:453. doi:10.3389/fimmu.2017.00453
2. Gieseck RR, Wilson MS, Wynn TA. Type 2 immunity in tissue repair and fibrosis. *Nat Rev Immunol* (2018) 18:62–76. doi:10.1038/nri.2017.90
3. Cope AP, Schulze-Koops H, Aringer M. The central role of T cells in rheumatoid arthritis. *Clin Exp Rheumatol* (2007) 25:S4–11.
4. Pritchard DI, Brown A. Is *Necator americanus* approaching a mutualistic symbiotic relationship with humans? *Trends Parasitol* (2001) 17:169–72. doi:10.1016/S1471-4922(01)01941-9
5. McSorley HJ, Maizels RM. Helminth infections and host immune regulation. *Clin Microbiol Rev* (2012) 25:585–608. doi:10.1128/CMR.05040-11
6. Ricci ND, Fiuza JA, Bueno LL, Cancado GG, Gazzinelli-Guimaraes PH, Martins VG, et al. Induction of CD4(+)CD25(+)FOXP3(+) regulatory T cells during human hookworm infection modulates antigen-mediated lymphocyte proliferation. *PLoS Negl Trop Dis* (2011) 5:e1383. doi:10.1371/journal.pntd.0001383
7. Maizels RM, Yazdanbakhsh M. Immune regulation by helminth parasites: cellular and molecular mechanisms. *Nat Rev Immunol* (2003) 3:733–44. doi:10.1038/nri1183
8. MacDonald AS, Loke P, Martynoga R, Dransfield I, Allen JE. Cytokine-dependent inflammatory cell recruitment patterns in the peritoneal cavity of mice exposed to the parasitic nematode *Brugia malayi*. *Med Microbiol Immunol* (2003) 192:33–40. doi:10.1007/s00430-002-0156-8
9. Zander RA, Butler NS. Dysfunctional adaptive immunity during parasitic infections. *Curr Immunol Rev* (2013) 9:179–89. doi:10.2174/1573395509666131126230832
10. Eissa MM, Mostafa DK, Ghazy AA, El AM, Boulos LM, Younis LK. Anti-arthritic activity of *Schistosoma mansoni* and *Trichinella spiralis* derived-antigens in adjuvant arthritis in rats: role of FOXP3+ Treg cells. *PLoS One* (2016) 11:e165916. doi:10.1371/journal.pone.0165916
11. Bashi T, Bizzaro G, Ben-Ami SD, Blank M, Shoenfeld Y. The mechanisms behind helminth's immunomodulation in autoimmunity. *Autoimmun Rev* (2015) 14:98–104. doi:10.1016/j.autrev.2014.10.004
12. Francisco LM, Sage PT, Sharpe AH. The PD-1 pathway in tolerance and autoimmunity. *Immunol Rev* (2010) 236:219–42. doi:10.1111/j.1600-065X.2010.00923.x
13. Sharpe AH, Wherry EJ, Ahmed R, Freeman GJ. The function of programmed cell death 1 and its ligands in regulating autoimmunity and infection. *Nat Immunol* (2007) 8:239–45. doi:10.1038/ni1443
14. Keir ME, Butte MJ, Freeman GJ, Sharpe AH. PD-1 and its ligands in tolerance and immunity. *Annu Rev Immunol* (2008) 26:677–704. doi:10.1146/annurev.immunol.26.021607.090331
15. Zamani MR, Aslani S, Salmaninejad A, Javan MR, Rezaei N. PD-1/PD-L and autoimmunity: a growing relationship. *Cell Immunol* (2016) 310:27–41. doi:10.1016/j.cellimm.2016.09.009
16. Mahmoudi M, Rezaiemanesh A, Salmaninejad A, Harsini S, Poursani S, Bahrami T, et al. PDCD1 single nucleotide genes polymorphisms confer susceptibility to juvenile-onset systemic lupus erythematosus. *Autoimmunity* (2015) 48:488–93. doi:10.3109/08916934.2015.1058370
17. Zou Y, Zhang Z, Liu Y, Liu D, Xu W. Are programmed cell death 1 gene polymorphisms correlated with susceptibility to rheumatoid arthritis? A meta-analysis. *Medicine (Baltimore)* (2017) 96:e7805. doi:10.1097/MD.0000000000007805
18. Pawlak-Adamska E, Nowak O, Karabon L, Pokryszko-Dragan A, Partyka A, Tomkiewicz A, et al. PD-1 gene polymorphic variation is linked with first symptom of disease and severity of relapsing-remitting form of MS. *J Neuroimmunol* (2017) 305:115–27. doi:10.1016/j.jneuroim.2017.02.006
19. Momin S, Flores S, Angel BB, Codner DE, Carrasco PE, Perez-Bravo F. Interactions between programmed death 1 (PD-1) and cytotoxic T lymphocyte antigen 4 (CTLA-4) gene polymorphisms in type 1 diabetes. *Diabetes Res Clin Pract* (2009) 83:289–94. doi:10.1016/j.diabres.2008.12.003
20. Raptopoulou AP, Bertsias G, Makrygiannakis D, Verginis P, Kritikos I, Tzardi M, et al. The programmed death 1/programmed death ligand 1 inhibitory pathway is up-regulated in rheumatoid synovium and regulates peripheral T cell responses in human and murine arthritis. *Arthritis Rheum* (2010) 62:1870–80. doi:10.1002/art.27500
21. Belkhir R, Burel SL, Dunogeant L, Marabelle A, Hollebecque A, Besse B, et al. Rheumatoid arthritis and polymyalgia rheumatica occurring after immune checkpoint inhibitor treatment. *Ann Rheum Dis* (2017) 76:1747–50. doi:10.1136/annrheumdis-2017-211216
22. van der Werf N, Redpath SA, Azuma M, Yagita H, Taylor MD. Th2 cell-intrinsic hypo-responsiveness determines susceptibility to helminth infection. *PLoS Pathog* (2013) 9:e1003215. doi:10.1371/journal.ppat.1003215
23. Hartmann W, Schramm C, Breloer M. Litomosoides sigmodontis induces TGF-beta receptor responsive, IL-10-producing T cells that suppress bystander T-cell proliferation in mice. *Eur J Immunol* (2015) 45:2568–81. doi:10.1002/eji.201545503
24. Zhou S, Jin X, Li Y, Li W, Chen X, Xu L, et al. Blockade of PD-1 signaling enhances Th2 cell responses and aggravates liver immunopathology in mice with *Schistosomiasis japonica*. *PLoS Negl Trop Dis* (2016) 10:e5094. doi:10.1371/journal.pntd.0005094
25. Park HK, Cho MK, Choi SH, Kim YS, Yu HS. *Trichinella spiralis*: infection reduces airway allergic inflammation in mice. *Exp Parasitol* (2011) 127:539–44. doi:10.1016/j.exppara.2010.10.004
26. Khan WI, Blennerhasset PA, Varghese AK, Chowdhury SK, Omsted P, Deng Y, et al. Intestinal nematode infection ameliorates experimental colitis in mice. *Infect Immun* (2002) 70:5931–7. doi:10.1128/IAI.70.11.5931-5937.2002
27. Yang X, Yang Y, Wang Y, Zhan B, Gu Y, Cheng Y, et al. Excretory/secretory products from *Trichinella spiralis* adult worms ameliorate DSS-induced colitis in mice. *PLoS One* (2014) 9:e96454. doi:10.1371/journal.pone.0096454
28. Gruden-Movsesijan A, Ilic N, Mostarica-Stojkovic M, Stosic-Grujicic S, Milic M, Sofronic-Milosavljevic L. Mechanisms of modulation of experimental autoimmune encephalomyelitis by chronic *Trichinella spiralis* infection in Dark Agouti rats. *Parasite Immunol* (2010) 32:450–9. doi:10.1111/j.1365-3024.2010.01207.x
29. Saunders KA, Raine T, Cooke A, Lawrence CE. Inhibition of autoimmune type 1 diabetes by gastrointestinal helminth infection. *Infect Immun* (2007) 75:397–407. doi:10.1128/IAI.00664-06
30. Kondo Y, Yokosawa M, Kaneko S, Furuyama K, Segawa S, Tsuboi H, et al. Transcriptional regulation of CD4+ T cell differentiation in experimentally-induced arthritis and rheumatoid arthritis. *Arthritis Rheumatol* (2018) 70(5):653–61. doi:10.1002/art.40398
31. Yuan H, Qian H, Liu S, Zhang X, Li S, Wang W, et al. Therapeutic role of a vaccine targeting RANKL and TNF-alpha on collagen-induced arthritis. *Biomaterials* (2012) 33:8177–85. doi:10.1016/j.biomaterials.2012.07.047
32. Bratke K, Fritz L, Nokodian F, Geissler K, Garbe K, Lommatzsch M, et al. Differential regulation of PD-1 and its ligands in allergic asthma. *Clin Exp Allergy* (2017) 47:1417–25. doi:10.1111/cea.13017
33. Stolina M, Schett G, Dwyer D, Vonderfecht S, Middleton S, Duryea D, et al. RANKL inhibition by osteoprotegerin prevents bone loss without affecting local or systemic inflammation parameters in two rat arthritis models: comparison with anti-TNFalpha or anti-IL-1 therapies. *Arthritis Res Ther* (2009) 11:R187. doi:10.1186/ar2879
34. Romas E, Sims NA, Hards DK, Lindsay M, Quinn JW, Ryan PF, et al. Osteoprotegerin reduces osteoclast numbers and prevents bone erosion in collagen-induced arthritis. *Am J Pathol* (2002) 161:1419–27. doi:10.1016/S0002-9440(10)64417-3
35. Nandakumar KS, Svensson L, Holmdahl R. Collagen type II-specific monoclonal antibody-induced arthritis in mice: description of the disease and the influence of age, sex, and genes. *Am J Pathol* (2003) 163:1827–37. doi:10.1016/S0002-9440(10)63542-0
36. Brown KE, Freeman GJ, Wherry EJ, Sharpe AH. Role of PD-1 in regulating acute infections. *Curr Opin Immunol* (2010) 22:397–401. doi:10.1016/j.coi.2010.03.007
37. Blackburn SD, Shin H, Haining WN, Zou T, Workman CJ, Polley A, et al. Coregulation of CD8+ T cell exhaustion by multiple inhibitory receptors during chronic viral infection. *Nat Immunol* (2009) 10:29–37. doi:10.1038/ni.1679
38. Wammes LJ, Hamid F, Wiria AE, May L, Kaisar MM, Prasetyani-Gieseler MA, et al. Community deworming alleviates geohelminth-induced immune hyporesponsiveness. *Proc Natl Acad Sci U S A* (2016) 113:12526–31. doi:10.1073/pnas.1604570113
39. Gagliani N, Magnani CF, Huber S, Gianolini ME, Pala M, Licona-Limon P, et al. Coexpression of CD49b and LAG-3 identifies human and mouse T regulatory type 1 cells. *Nat Med* (2013) 19:739–46. doi:10.1038/nm.3179

40. Hou N, Piao X, Liu S, Wu C, Chen Q. Tim-3 induces Th2-biased immunity and alternative macrophage activation during *Schistosoma japonicum* infection. *Infect Immun* (2015) 83:3074–82. doi:10.1128/IAI.00517-15
41. Prodjinotho UF, von Horn C, Debrah AY, Batsa DL, Albers A, Layland LE, et al. Pathological manifestations in lymphatic filariasis correlate with lack of inhibitory properties of IgG4 antibodies on IgE-activated granulocytes. *PLoS Negl Trop Dis* (2017) 11:e5777. doi:10.1371/journal.pntd.0005777
42. Jiang TT, Martinov T, Xin L, Kinder JM, Spanier JA, Fife BT, et al. Programmed death-1 culls peripheral accumulation of high-affinity autoreactive CD4 T cells to protect against autoimmunity. *Cell Rep* (2016) 17:1783–94. doi:10.1016/j.celrep.2016.10.042
43. Rao DA, Gurish MF, Marshall JL, Slowikowski K, Fonseka CY, Liu Y, et al. Pathologically expanded peripheral T helper cell subset drives B cells in rheumatoid arthritis. *Nature* (2017) 542:110–4. doi:10.1038/nature20810
44. Stempin CC, Motran CC, Aoki MP, Falcon CR, Cerban FM, Cervi L. PD-L2 negatively regulates Th1-mediated immunopathology during *Fasciola hepatica* infection. *Oncotarget* (2016) 7:77721–31. doi:10.18632/oncotarget.12790
45. Arce-Sillas A, Alvarez-Luquin DD, Cardenas G, Casanova-Hernandez D, Fragoso G, Hernandez M, et al. Interleukin 10 and dendritic cells are the main suppression mediators of regulatory T cells in human neurocysticercosis. *Clin Exp Immunol* (2016) 183:271–9. doi:10.1111/cei.12709
46. Son HJ, Lee SH, Lee SY, Kim EK, Yang EJ, Kim JK, et al. Correction: oncostatin M suppresses activation of IL-17/Th17 via SOCS3 regulation in CD4+ T cells. *J Immunol* (2017) 198:4879. doi:10.4049/jimmunol.1502314
47. Williams RO. Collagen-induced arthritis in mice. *Methods Mol Med* (2007) 136:191–9. doi:10.1007/978-1-59745-402-5_14
48. Kotake S, Yago T, Kobashigawa T, Nanke Y. The plasticity of Th17 cells in the pathogenesis of rheumatoid arthritis. *J Clin Med* (2017) 6:E67. doi:10.3390/jcm6070067
49. McInnes IB, Schett G. The pathogenesis of rheumatoid arthritis. *N Engl J Med* (2011) 365:2205–19. doi:10.1056/NEJMra1004965
50. Chen Z, Andreev D, Oeser K, Krljanac B, Hueber A, Kleyer A, et al. Th2 and eosinophil responses suppress inflammatory arthritis. *Nat Commun* (2016) 7:11596. doi:10.1038/ncomms11596
51. Finlay CM, Stefanska AM, Walsh KP, Kelly PJ, Boon L, Lavelle EC, et al. Helminth products protect against autoimmunity via innate type 2 cytokines IL-5 and IL-33, which promote eosinophilia. *J Immunol* (2016) 196:703–14. doi:10.4049/jimmunol.1501820
52. Kang SA, Cho MK, Park MK, Kim DH, Hong YC, Lee YS, et al. Alteration of helper T-cell related cytokine production in splenocytes during *Trichinella spiralis* infection. *Vet Parasitol* (2012) 186:319–27. doi:10.1016/j.vetpar.2011.12.002
53. Larkin BM, Smith PM, Ponichtera HE, Shainheit MG, Rutitzky LI, Stadecker MJ. Induction and regulation of pathogenic Th17 cell responses in schistosomiasis. *Semin Immunopathol* (2012) 34:873–88. doi:10.1007/s00281-012-0341-9
54. Nishimura H, Okazaki T, Tanaka Y, Nakatani K, Hara M, Matsumori A, et al. Autoimmune dilated cardiomyopathy in PD-1 receptor-deficient mice. *Science* (2001) 291:319–22. doi:10.1126/science.291.5502.319
55. Sage PT, Schildberg FA, Sobel RA, Kuchroo VK, Freeman GJ, Sharpe AH. Dendritic cell PD-L1 limits autoimmunity and follicular T cell differentiation and function. *J Immunol* (2018) 200(8):2592–602. doi:10.4049/jimmunol.1701231
56. Schwartz C, Khan AR, Floudas A, Saunders SP, Hams E, Rodewald HR, et al. ILC2s regulate adaptive Th2 cell functions via PD-L1 checkpoint control. *J Exp Med* (2017) 214:2507–21. doi:10.1084/jem.20170051
57. Han R, Luo J, Shi Y, Yao Y, Hao J. PD-L1 (programmed death ligand 1) protects against experimental intracerebral hemorrhage-induced brain injury. *Stroke* (2017) 48:2255–62. doi:10.1161/STROKEAHA.117.016705
58. Read S, Malmstrom V, Powrie F. Cytotoxic T lymphocyte-associated antigen 4 plays an essential role in the function of CD25(+)CD4(+) regulatory cells that control intestinal inflammation. *J Exp Med* (2000) 192:295–302. doi:10.1084/jem.192.2.295
59. Viglietta V, Baecher-Allan C, Weiner HL, Hafler DA. Loss of functional suppression by CD4+CD25+ regulatory T cells in patients with multiple sclerosis. *J Exp Med* (2004) 199:971–9. doi:10.1084/jem.20031579
60. Kukreja A, Cost G, Marker J, Zhang C, Sun Z, Lin-Su K, et al. Multiple immuno-regulatory defects in type-1 diabetes. *J Clin Invest* (2002) 109:131–40. doi:10.1172/JCI0213605
61. Liang SC, Greenwald RJ, Latchman YE, Rosas L, Satoskar A, Freeman GJ, et al. PD-L1 and PD-L2 have distinct roles in regulating host immunity to cutaneous leishmaniasis. *Eur J Immunol* (2006) 36:58–64. doi:10.1002/eji.200535458
62. McAlees JW, Lajoie S, Dienger K, Sproles AA, Richgels PK, Yang Y, et al. Differential control of CD4(+) T-cell subsets by the PD-1/PD-L1 axis in a mouse model of allergic asthma. *Eur J Immunol* (2015) 45:1019–29. doi:10.1002/eji.201444778
63. Prendergast CT, Sanin DE, Mountford AP. CD4 T-cell hyporesponsiveness induced by schistosome larvae is not dependent upon eosinophils but may involve connective tissue mast cells. *Parasite Immunol* (2016) 38:81–92. doi:10.1111/pim.12300
64. Prendergast CT, Sanin DE, Cook PC, Mountford AP. CD4+ T cell hyporesponsiveness after repeated exposure to *Schistosoma mansoni* larvae is dependent upon interleukin-10. *Infect Immun* (2015) 83:1418–30. doi:10.1128/IAI.02831-14
65. Said EA, Dupuy FP, Trautmann L, Zhang Y, Shi Y, El-Far M, et al. Programmed death-1-induced interleukin-10 production by monocytes impairs CD4+ T cell activation during HIV infection. *Nat Med* (2010) 16:452–9. doi:10.1038/nm.2106

Conflict of Interest Statement: The authors declare that the research was conducted in the absence of any commercial or financial relationships that could be construed as a potential conflict of interest.

frontiers in Immunology

ORIGINAL RESEARCH
published: 16 July 2018
doi: 10.3389/fimmu.2018.01627

The Serine/Threonine-Protein Phosphatase 1 From *Haemonchus contortus* Is Actively Involved in Suppressive Regulatory Roles on Immune Functions of Goat Peripheral Blood Mononuclear Cells

*Muhammad Ehsan, WenJuan Wang, Javaid Ali Gadahi, Muhammad Waqqas Hasan, MingMin Lu, YuJian Wang, XinChao Liu, Muhammad Haseeb, RuoFeng Yan, LiXin Xu, XiaoKai Song and XiangRui Li**

Department of Preventive Veterinary Medicine, College of Veterinary Medicine, Nanjing Agricultural University, Nanjing, China

OPEN ACCESS

Edited by:
Xun Suo, China Agricultural University, China

Reviewed by:
Phileno Pinge-Filho, Universidade Estadual de Londrina, Brazil
Laura Noelia Cariddi, National University of Río Cuarto, Argentina

***Correspondence:**
XiangRui Li
lixiangrui@njau.edu.cn

Specialty section:
This article was submitted to Microbial Immunology, a section of the journal Frontiers in Immunology

Received: *25 January 2018*
Accepted: *02 July 2018*
Published: *16 July 2018*

Citation:
Ehsan M, Wang W, Gadahi JA, Hasan MW, Lu M, Wang Y, Liu X, Haseeb M, Yan R, Xu L, Song X and Li X (2018) The Serine/Threonine-Protein Phosphatase 1 From Haemonchus contortus Is Actively Involved in Suppressive Regulatory Roles on Immune Functions of Goat Peripheral Blood Mononuclear Cells. Front. Immunol. 9:1627. doi: 10.3389/fimmu.2018.01627

Serine/threonine-protein phosphatases (STPs), as integral constituents of parasitic excretory/secretory proteins, are assumed to be released during the host–parasite interactions. However, knowledge about these phosphatases and their immunoregulatory and immune protective efficiencies with host peripheral blood mononuclear cells (PBMCs) is scant. In this study, an open reading frame of STP from *Haemonchus contortus* designated as HcSTP-1 was amplified and cloned using reverse-transcription-polymerase chain reaction (RT-PCR) method. The 951-bp nucleotides sequence was encoded to a protein of 316 amino acid residues, conserved in characteristics motifs GDXHG, GDYVDRG, GNHE, HGG, RG, and H. The HcSTP-1 protein was detected at approximately 35 kDa as recombinant protein fused in an expression vector system and resolved on sodium dodecyl sulfate-polyacrylamide gel electrophoresis. Immunohistochemically, HcSTP-1 was found to be localized in both male and female adult worm sections. Using immunofluorescence assay, the binding activity of rHcSTP-1 was confirmed on surface of goat PBMCs, which resulted in expression of multiple cytokines and various immunoregulatory activities *in vitro*. The RT-PCR results showed that mRNA level of interleukin-2, TGF-β1, IFN-γ, and IL-17 (with 10 μg/ml) was upregulated and IL-10 was decreased. However, IL-6 showed no change after PBMCs incubated with rHcSTP-1 protein. Further functional analysis showed that migratory activity of cells, intracellular nitrite production (NO), and apoptotic efficiency of PBMCs were elevated at significant level, whereas the proliferation of goat PBMCs and monocytes-associated major histocompatibility complex (MHC)-I and MHC-II expressions were decreased significantly at concentration-dependent fashion. Our results showed that the HcSTP-1 protein engaged in vital suppressive regulatory roles on host immune cells, which might represent a potential molecular target for controlling *H. contortus* infection in future.

Keywords: *Haemonchus contortus*, serine/threonine phosphatase, peripheral blood mononuclear cells, cytokines, immune responses

INTRODUCTION

Among gastrointestinal nematodes, *Haemonchus contortus* (barber pole worm) is most important parasite, responsible for health and economic problems in livestock industry worldwide (1). In severely infected animals like sheep and goats, the adult parasite penetrates in abomasal mucosa to feed on blood, results in anemia, loss of body weight and growth, and even death of the animals (2). Existing approaches for control of nematode parasites including *H. contortus*, mainly through widespread antihelmintics have resulted in stern drug resistance in domestic livestock (3, 4). Hence, the emergence of drug resistance in *H. contortus* demands for discoveries of novel anti-parasite drugs, vaccines, and development of immunological control strategies against nematode infections. In this regard, a comprehensive insight into the developmental biology of *H. contortus* at the molecular level might pinpoint some key antigens as new drug targets for parasite control (5).

The serine/threonine-protein phosphatase 1 (STP-1) belong to phosphoprotein phosphatase (PPP) family, and protein phosphatases (PPs) is largest class which is divided functionally into two major groups: first serine/threonine phosphatases (commonly cytoplasmic structural component, concerned with transcriptional activity and signal transduction) and second tyrosine phosphatases (typically bound with membrane and implicated in receptor-arbitrated signal transduction) (6). PPs can also be divided into four subclasses, such as PP1, PP2A, PP2B, and PP2C, based on substrate and inhibitory specificities (7). Furthermore, it was reported that PPs have been implicated in range of biological functions, such as exocytosis and apoptosis, neuronal activity, ion channel electrophysiology, and cell cycle (8–12).

Previously, various STPs from number of parasites have been identified and characterized, including those of *Oesophagostomum dentatum*, *Trichostrongylus vitrinus*, *Toxoplasma gondii*, *Toxocara canis*, and *Plasmodium falciparum* (13–17), and also suggested that STP-1 from *H. contortus* play a key role in some biological processes, such as spermatogenesis (18). However, information regarding the functions of STPs in parasitic nematode *H. contortus* is scant.

In our previous comparative proteomics analysis of excretory/secretory proteins (ESPs) from *H. contortus* (HcESPs), 59 proteins were identified at early and late adult developmental stages of parasite and amongst all, serine/threonine-protein phosphatase (STPs) were recognized as vital interacting proteins bind to the goat peripheral blood mononuclear cells (PBMCs) *in vivo* (19). The main objectives of current study were to clone and characterize a stage-specific gene from *H. contortus* designated as HcSTP-1, to express its recombinant protein in an expression vector system, and to evaluate potential immune regulatory roles of this protein (rHcSTP-1) with goat PBMCs *in vitro*. Our findings will provide valuable bases to better understand the biology of this parasite and to develop effective drugs and useful vaccines, which could be helpful in the prevention and control of *H. contortus* infection.

MATERIALS AND METHODS

Ethics Statement

All animals and laboratory experiments were strictly performed in accordance with the recommendations of the Animal Ethics Committee, Nanjing Agricultural University, China. All experimental procedures used in this study were permitted by the science and Technology Agency of Jiangsu Province [ID: SYXK (SU) 2010-0005].

Animals, Parasites, and PBMC Isolation

The native crossbred goats (3–6 months old) were housed indoor, provided with hay and corn (whole shelled) and water *ad libitum*. The anti-parasitic drug, levamisole (8 mg/kg body weight) was used with 2 weeks interval to keep goats free from naturally acquired helminth infection. The fecal samples were checked twice per week, using standard parasitological techniques and goats with no sign of helminths infection were used in subsequent experiments.

Sprague-Dawley (SD) rats with average body weight of 150 g, were bought at Experimental Animal Center of Jiangsu, PR China (Certified: SCXK 2008-0004). The rats were raised in microbe free condition.

The *H. contortus* strain was maintained by serial passage in helminth-free goats, at laboratory of immunology and molecular parasitology, Nanjing Agricultural University. The parasite eggs, larvae, and adults worms were collected and preserved according to the methods stated previously (20). The blood samples were taken from jugular vein of dewormed goats and PBMCs were collected by gradient centrifugation method (21). The PBMCs were cultured as the procedure stated previously (22).

Cloning and Sequence Analysis *H. contortus* STP-1 Gene

The freshly adults *H. contortus* parasites were collected from abomasum of the infected goats and the extraction of RNA was carried out using Trizol method according to the previously described procedure (23), followed by cDNA synthesis as per the manufacturer's guidelines of cDNA synthesis Kit (TaKaRa Biotech), and was preserved at −20°C for down-stream applications.

The open reading frame of HcSTP-1 was amplified by reverse-transcription-polymerase chain reaction (RT-PCR), from conserved domain sequences of *H. contortus* STP-1 gene (GenBank: GQ280010.1). For the subsequent cloning, underlined *BamH* I and *Xho* I restriction enzyme were inserted at the 5′-end of forward primer: (5′-GGATCCATGGACCCTACTCAAT-3′), and reverse primer: (5′-CTCGAGTTATTGACAAGGTGGAGC-3′). The amplified PCR fragment was electrophoresed and eluted with Gel purification Kit (Omega, USA) in accordance with kit protocol. The eluted product was then inserted into pMD19-T cloning vector (TaKaRa Biotechnology, China). The recombinant plasmid pMD19-T/HcSTP-1 was inserted into DH5α competent strain of *Escherichia coli* and cultured in Luria–Bertini medium

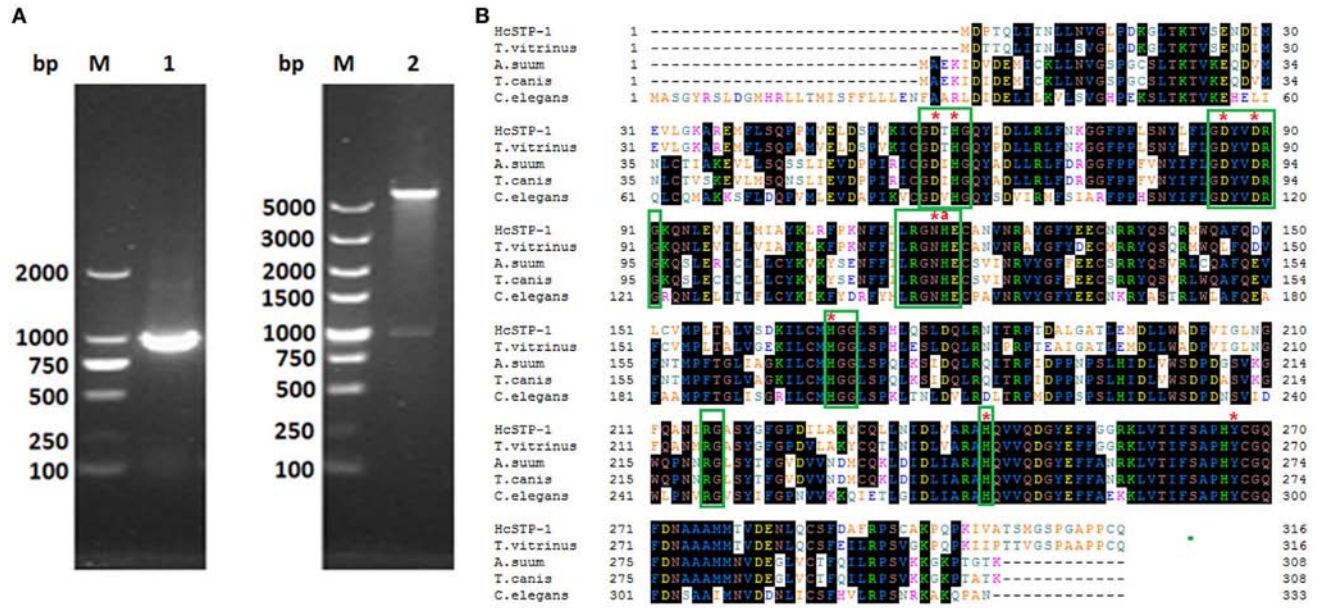

FIGURE 1 | Cloning and sequence analysis of HcSTP-1 gene. **(A)** Electrophoresis of PCR product of HcSTP-1 open reading frame (Lane 1). Restriction enzyme digestion of pET32a-HcSTP-1 with *BamH* I and *Xho* I (Lane 2) and molecular weight DNA marker (Lane M). **(B)** The comparison of amino acid sequence of *Haemonchus contortus* serine/threonine-protein phosphatase 1 (STP-1) and with predicted STPs from *Trichostrongylus vitrinus* (CAM84506.1), *A. suum* (CAJ98743.1), *Toxocara canis* (KHN86897.1), and *C. elegans* (NP_505086.2). Amino acids predicted to be involved in the catalytic metal binding are indicated by asterisks "*," and the histidine residue proposed for proton donation is indicated with "a." The conserved motifs found in all sequences including Prosite motif PS00125 (LRGNHE) are boxed in green color.

with ampicillin (100 μg/ml). The positive clones followed by sequencing (Invitrogen Biotech, Shanghai, China) were validated by sequence analysis online using Blast program.[1] The obtained nucleotide sequence was translated into amino acids sequence and aligned and compared with different nematode species using GENETYX Version 7.0.9 software. In addition, a number of online approaches/programs were used to detect N-terminal signal peptides/http://www.cbs.dtu.dk/services/SignalP/, Transmembrane protein prediction/http://www.cbs.dtu.dk/services/TMHMM/, T cell motifs/DNAstar: EditSeq, Protean, B cell epitopes/http://tools.immuneepitope.org/tools/bcell/iedb_input, and GPI modification Site Prediction/http://mendel.imp.ac.at/sat/gpi/gpi_server.html.

Expression and Purification of Recombinant HcSTP-1 Protein

The recognized recombinant pMD19-T/HcSTP-1 plasmid was digested with dual restriction enzymes *BamH* I and *Xho* I and ligated into prokaryotic expression vector pET32a (+) (Novagen, USA). Finally, the successful cloned STP-1 gene in a recombinant expression vector was sequenced to confirm its placement in the accurate reading frame. The recombinant plasmid pET32a (+)-HcSTP-1 was transferred into *E. coli* strain (BL21) and induced with 1 mM isopropyl-β-D-thiogalactopyranoside (IPTG; Sigma-Aldrich) after the OD_{600} of the culture reached 0.6 at 37°C. The cell pellet after centrifugation was lysed using 10 μg/ml of lysozyme (Sigma-Aldrich) followed by sonication, and was resolved on 12% (w/v) sodium dodecyl sulfate-polyacrylamide gel electrophoresis (SDS-PAGE). The purification of recombinant protein was carried out according to the manufacturer's instructions of Ni^{2+}-nitrilotriacetic acid (Ni-NTA) column (GE Healthcare, USA). The histidine-tagged protein (empty pET32a) used as control protein in multiple assays in this study was purified and expressed similar to the procedure described for rHcSTP-1 protein and determined at 12% SDS-PAGE after Coomassie blue staining and quantified by Bradford method (24).

Immuno-Blot Analysis

Polyclonal antibodies against recombinant protein were generated from SD rats by subcutaneous injection of 300 μg of rHcSTP-1 protein mixed equally with Freund's complete. After 2 weeks of first immunization, rats were injected three times at 1 week interval with same protein and Freund's incomplete mixture. The sera were collected after 10 days of last injection and preserved at −80°C for later use. The sera against *H. contortus* parasites were collected from naturally infected goats (25), and sera collected from normal goats or rats were used as negative control.

The SDS-PAGE products of recombinant HcSTP-1 and soluble/ES products from adult parasites, were shifted nitrocellulose membrane (Millipore, USA) for western blot analysis. After blocked with 5% (w/v) skimmed milk powder in TBST (TBS with 0.5% Tween-20) at 37°C for 2 h, the strips were incubated

[1]https://blast.ncbi.nlm.nih.gov/Blast.cgi.

with anti-*H. contortus* sera from goats or rat anti-sera against rHcSTP-1 (1:300 dilutions) as first antibody for treatment groups and normal goat serum or normal rat serum for control groups at 4°C overnight. Then, the membranes were incubated with the secondary antibody, HRP-conjugated goat anti-rat IgG (Santa Cruz, USA) in TBST (1:3,000 dilutions) at 37°C for 2 h. At end, the immunoreactions were visualized within 3–5 min, as per defined protocol of DAB Horseradish Peroxidase Color Development Kit (Beyotime Biotechnology).

Localization Assay

The mature parasites were suspended in TISSUE-TEK® O.C.T. compound (SAKURA, Torrance, CA, USA) and snap-frozen in liquid nitrogen. By using cryotome (CM1950, Wetzlar, Germany), worms were cut into sections with 10-μm thickness and fixed on poly-L-lysine hydrobromide glass slides. Non-specific bindings were confiscated by treating the slides with 10% normal goat serum, followed by incubation with rat-anti-STP-1 antiserum (1:300 dilutions) or normal rat serum as first antibody and Cy3-labeled Goat Anti-Rat IgG (1:3,000 dilutions) as second antibody (Beyotime, Shanghai, China) at 37°C for 2 h in each step. For DNA staining, the sections were marked with 1.5 μM 2-(4-amidinophenyl)-6-indolecarbamidine dihydrochloride (DAPI: Sigma, MO, USA) for 5 min. Finally, Anti-Fade Fluoromount Medium (Beyotime, Shanghai, China) was used and sections were examined under confocal microscope.

Binding of rHcSTP-1 on the Surface of Goat PBMCs

Freshly collected PBMCs, after washed with phosphate buffer saline (PBS: Ca^{2+}/Mg^{2+}-free, pH 7.4), were maintained at density of 1×10^5 cells/ml in cell culture medium (RPMI 1640), containing 10% fetal bovine serum (FBS), 100 U/ml penicillin and 100 mg/ml streptomycin (Gibco, Life Technology), and incubated with rHcSTP-1 or control protein pET32a or control buffer (PBS) at constant temperature (37°C) and humidity (5% CO_2) for 4 h. Protein binding at surface of goat PBMCs were confirmed by immunofluorescence assay (IFA). Briefly, PBMCs after being washed and stabled with 4% paraformaldehyde on poly-L-lysine-treated slides were then permeabilized using 1% TritonX-100 in PBS at normal temperature. The PBMCs were subjected to primary antibodies rat anti-rHcSTP-1-IgG (1:300 dilutions) or normal rat serum followed by Cy3-coupled goat anti-rat IgG (Beyotime, China) (1:3,000 dilutions) as second antibody for 1 h at 37°C temperature. At last, the slides were stained in darkness with DAPI (Sigma, USA) for 5 min, and subjected to Anti-Fade Fluoromount solution (Beyotime, China) before laser scanning confocal microscopic examination (LSM710, Zeiss, Jena, Germany) at 100× magnifications.

Detection of Cytokine Transcripts by RT-PCR

The PBMCs were stimulated with Concanavalin A (ConA/10 μg/ml), and treated with rHcSTP-1 (10, 20, and 40 μg/ml) or pET32a protein (10 μg/ml) and control buffer (PBS) in 24-well plate containing RPMI 1640 medium at 5% CO_2 and 37°C. The PBMCs were collected after 48 h of culture, by centrifugation and PrimeScript™ RT reagent kit (TaKaRa, CA, USA) was utilized to extract RNA from cells sediment as per the manufacturer's guidelines. The cDNA-based quantifications of cytokine transcriptions were evaluated as previously stated protocol of RT-PCR. The reaction conditions and set of primers used for cytokines [interleukin-2 (IL-2), IL-10, TGF-β1, IL-6, IFN-γ, and IL-17] and endogenous reference gene (β-actin), as well as their amplification efficiencies are mentioned in Tables S1–S3 in Supplementary Material. The data were analyzed based on Raw cycle thresholds (Ct), obtained from the ABI Prism 7500 software (Applied Biosystems, USA) by comparative Ct ($2^{-\Delta\Delta}$ Ct) method (26).

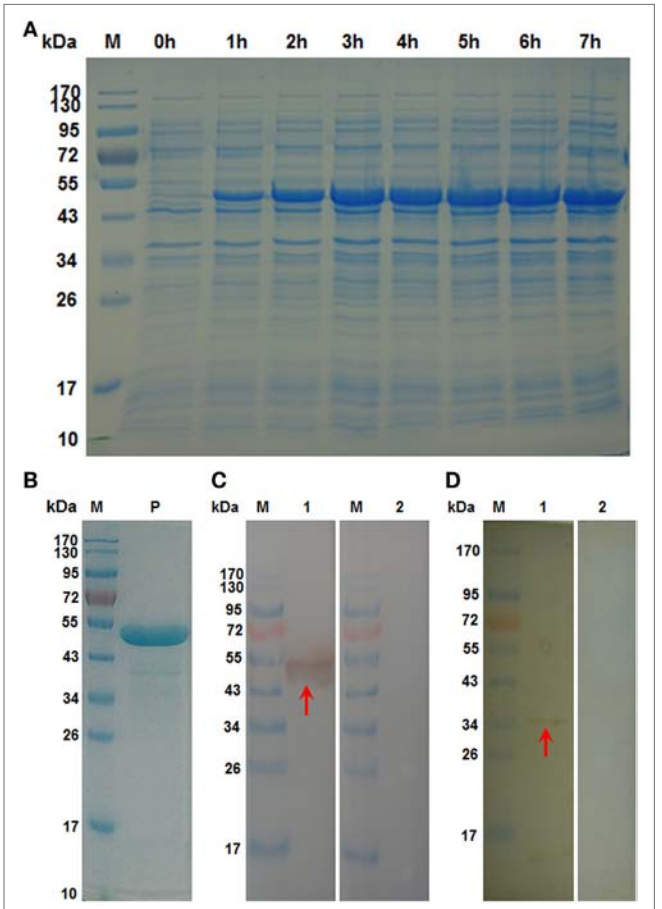

FIGURE 2 | Expression, purification and immuno reactivity of rHcSTP-1. **(A)** Recombinant expression vector before (Lane 0 h) and after 1 mM IPTG induction (Lane 1–7 h). Lane M: standard protein molecular weight marker. **(B)** Purified rHcSTP-1 protein resolved on sodium dodecyl sulfate-polyacrylamide gel electrophoresis (Lane P). **(C)** Western blot of rHcSTP-1 protein. (Lane 1) Purified recombinant protein was electrophoresed and transferred to a membrane probed with serum from goat infected with *Haemonchus contortus* and (Lane 2) with normal goat serum as negative control. **(D)** Western blot of total ES proteins of *H. contortus*. (Lane 1) ES proteins from *H. contortus* parasites were detected by rat antibodies against serine/threonine-protein phosphatase 1 (STP-1) protein and (Lane 2) with serum from normal rat as control.

Analysis of Major Histocompatibility Complex (MHC)-I and -II Molecule Expression

After separation of PBMCs by standard Ficoll-hypaque (GE Healthcare, USA) gradient centrifugation and two times washing with the PBS (Ca^{2+}/Mg^{2+}-free, pH 7.4), were poured into flat-bottom six well culture plates (Corning Inc., USA) containing RPMI 1640 medium (Invitrogen, USA) supplemented with 10% FBS and penicillin + streptomycin (Invitrogen, USA). The monocytes stick to the bottom of the plate, were collected (27) and adjusted at density of 1×10^6 cells/ml, whereas, Non-sticky cells were discarded by multiple washing steps. The purified monocytes were incubated in 24-well culture plates with different concentrations of rHcSTP-1 (treatment group) or pET32a protein and PBS (control group) at 37°C for 24 h. Subsequently, the monocytes were marked with monoclonal antibodies MHC-I (MCA2189A647, AbDserotec, Bio-Rad, USA) and MHC-II (MCA2225PE, AbDserotec), followed by flow cytometric analysis at FACS Calibur cytometer (BD Biosciences, San Jose, CA, USA) (**Figure 7A**).

Cell Proliferation Assay

The 100 µl of freshly isolated PBMCs at density of 1×10^6 cells/ml was poured into 96-well culture plate and stimulated with ConA (10 µg/ml). The PBMCs were incubated with serial concentrations of rHcSTP-1 protein (10, 20, and 40 µg/ml) in treatment group and pET32a empty protein or control vehicle (PBS) were added into control groups at 5% humidity and 37°C temperature for 72 h. Detection of PBMC proliferation was carried out according to the previously mentioned procedure of cell proliferation assay kit (28). 10 µl of CCK-8 solution (Beyotime China) was mixed in every well of plate 6 h prior to harvest and absorbance were checked by using spectrophotometer (Bio-Rad, USA) at wavelength 450 nm (OD_{450}). Result presented here are from three independent experiments.

Cell Migration Assay

The migration activity of cultured PBMCs was measured with 8.0-µm pores Millicell® insert (Merck-Millipore, USA) as stated previously. Briefly, in treatment group 200 µl of freshly separated cells were poured into the upper chamber with various concentrations of rHcSTP-1 (10, 20, and 40 µg/ml) and pET32a control protein or equal volume of control buffer (PBS) were added in control groups. Subsequently, 1,300 µl cell culture medium was filled in the lower chamber for 2 h incubation at 37°C and 5% CO_2. After that, columns were removed, and PBMC passed through polycarbonate layer were figure out by a Neubauer counting chamber. Data were resulted as percentage of seeded PBMCs. Three independent experiments were conducted.

Intracellular Nitrite Production by PBMCs

The goat PBMCs were separated and washed with Ca^{2+}/Mg^{2+}-free PBS (pH 7.4). 100 µl of cells containing DMEM medium was poured in 96-well plate with varying concentrations of rHcSTP-1 (10, 20, and 40 µg/ml), similarly the control groups were incubated with recombinant protein of pET32a or PBS (control buffer). NO production by cells was determined by Griess assay (29), by using Total Nitric Oxide Assay Kit (Beyotime, China) according to the manufacturer's instructions. The values in the

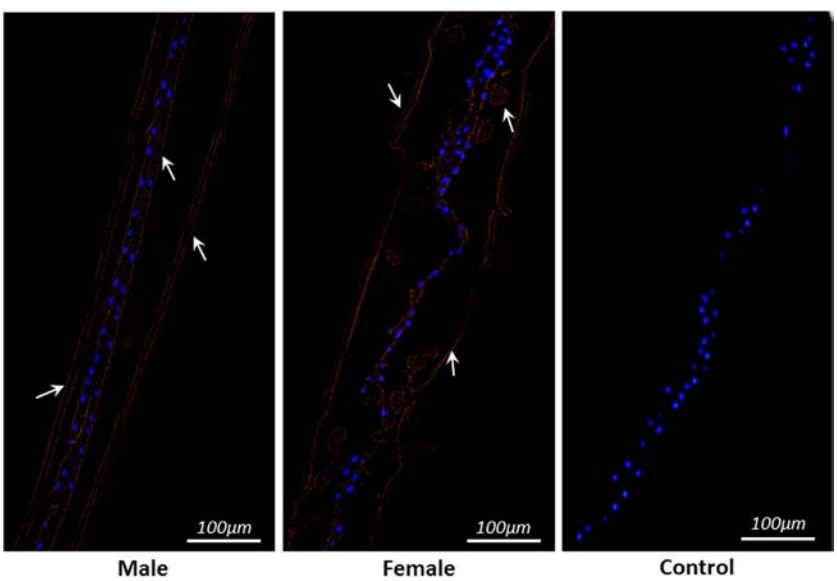

FIGURE 3 | Localization of serine/threonine-protein phosphatase 1 protein within parasite structure. Immunohistochemically STP-1 protein localizes inner and outer structure of *Haemonchus contortus* male and female adult worms. The red color indicates target protein stained with Cy3 and blue dots are localization of nuclei stained with DAPI. No red fluorescence was detected in control panel. Scale-bars: 100 µm.

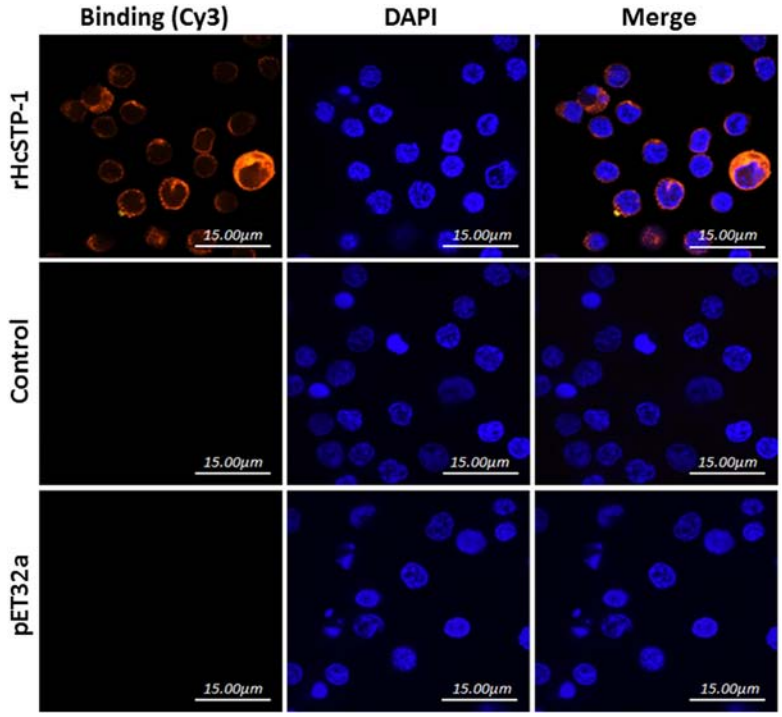

FIGURE 4 | Binding of rHcSTP-1 protein with goat peripheral blood mononuclear cells *in vitro*. The cells were incubated with rat sera anti-rHcSTP-1-O IgG, anti-HisTag protein (pET32a) or negative rat IgG as primary antibody followed by Cy3-labeled goat anti-rat IgG (red) as secondary antibody. Red fluorescence on surface of cells showed target protein staining (Cy3) and nuclei of cells were visualized by DAPI (blue). No red fluorescence was observed in control groups. The results were analyzed by using confocal laser scanning microscopy.

reaction mixture were measured at microplate spectrophotometer (Bio-Rad Laboratories, USA) at 540 nm (OD_{540}) wavelength. Data presented here are results of triplicate experiments.

Apoptotic Efficiency of rHcSTP-1 on PBMC

Efficiency of rHcSTP-1 to induce apoptosis of PBMC was assessed by flow cytometric analysis (BD Biosciences, USA). The PBMCs (1×10^7 cells/ml) treated with different rHcSTP-1 protein concentrations (5, 10, 20, and 40 µg/ml) and empty pET32a protein, were stained with Annexin V-FITC kit (Miltenyi Biotec, Germany) according to the manufacturer's protocols. The apoptosis rate was calculated by the percentage of early (Annexin V^+ PI−) and late (Annexin V^+ PI^+) PBMC apoptosis. Cells without any treatment were set as control. Data were analyzed using Flow Jo 7.6 software (Tree Star, USA).

Statistical Analysis

Data analysis regarding all experiments was performed by using the statistical package, GraphPad Premier 6.0 (GraphPad Prism, San Diego, CA, USA). Data are presented as mean ± SEM. The differences between groups were compared by one-way ANOVA, followed by a Tukey test and were considered statistically significant at $p < 0.05$.

RESULTS

Cloning and Protein Expression of *H. contortus* STP-1

The RT-PCR generated fragment of STP-1 gene with molecular size of 951 bp, was obtained from *H. contortus* cDNA and successfully cloned into an expression vector system, confirmed by enzymatic digestion with *BamH* I and *Xho* I (**Figure 1**). After that, cloned HcSTP-1 sequence was translated into 316 amino acids with predicted 35 kDa molecular mass and calculated pI of 6.328. The nucleotide and amino acid sequence identity HcSTP-1 using BLASTx and BLASTp revealed highly sequence resemblance with STPs from other parasite species, existing at NCBI database (see text footnote 1). In this study, characterization of HcSTP-1 cDNA showed 98% significant sequence identity to *H. contortus* (ADJ96628.1), 80% with *C. briggsae* (XM_002631635.1) (data not shown). Multiple sequence alignment showed that HcSTP-1 polypeptide shares a significant similarity of 91% with *T. vitrinus* (GenBank: CAM84506.1), 62% with *T. canis* (GenBank: KHN86897.1), 62% with *Ascaris suum* (GenBank: CAJ98743.1), and 58% with *Caenorhabditis elegans* (GenBank: NP_505086.2). The BLAST analysis predicted number of conserved metal ion-binding sites and histidine residue predicted to be involved in proton donation. The amino acids expressing STP protein motif LRGNHE was found during sequence analysis. The aligned STPs

sequences were highly similar in central regions, particularly in term of characteristics sequence motifs, such as GDXHG, GDYVDRG, GNHE, HGG, RG, and H (30), whereas there was a higher variation occurred regarding to N- and C-terminal regions among all align sequences (**Figure 1**). Further sequence analysis indicated lack of signal peptide, transmembrane domain, and GPI anchor site, whereas T and B cell motifs were predicted in deduced protein structure (Figures S1–S4 in Supplementary Material).

The recombinant product of HcSTP-1 gene inserted into *E. coli* was expressed after IPTG induction and detected after staining with Coomassie brilliant blue R-250 on SDS-PAGE. The rHcSTP-1 protein was expressed with molecular weight of about 53 kDa (**Figure 2**, Lane P) along with 18 kDa calculated mass of vector protein (pET32a). The target protein was confirmed at its original size of 35 kDa after reduction from vector protein. Polyclonal antibodies against rHcSTP-1 were identified by immuno-blot analysis, which revealed that rHcSTP-1 could be recognized by sera from goats infected with *H. contortus* and native STP-1 protein from *H. contortus* could be recognized by antibodies generated against rHcSTP-1 protein (**Figures 2C,D**, Lane 1). However, no protein was detected with normal sera taken from un-immunized goats/rats (**Figures 2C,D**, Lane 2).

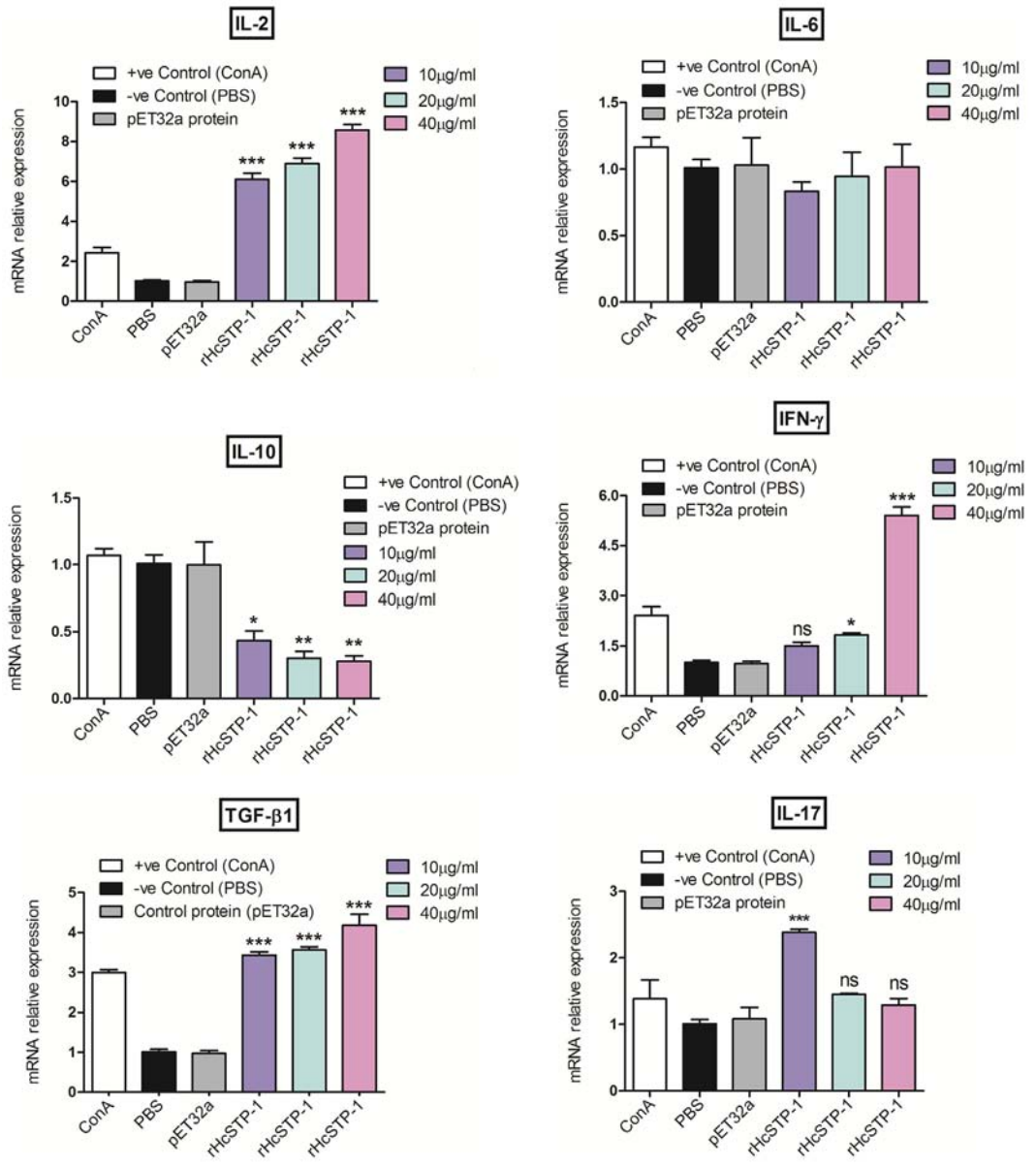

FIGURE 5 | Relative expression of multiple cytokines in goat peripheral blood mononuclear cells stimulated by the recombinant HcSTP-1. Cells were incubated with the recombinant serine/threonine-protein phosphatase 1 (STP-1) for 48 h, the mRNAs encoding interleukin-2 (IL-2), IL-6, IL-10, IFN-γ, TGF-β1, and IL-17 were quantified by reverse-transcription-polymerase chain reaction. The significant level was set at $^{*}p < 0.05$, $^{**}p < 0.01$, $^{***}p < 0.001$, and ns non-significant compared with the untreated group (control). Data are representative of three independent experiments.

HcSTP-1 Localized Outer and Inner Lining of *H. contortus* Worm Sections

The partial body sections of male and female adult worms are shown in **Figure 3**. Immunohistochemical analysis was performed to detect distribution of native STP-1 protein within the worms. The red lining at outer and inner layer of membranes and in gut region strongly indicated the presence of this protein within worms sections. However, no fluorescence was detected in the control section (**Figure 3**).

rHcSTP-1 Binding Confirmation on Surface of Goat PBMCs

The interaction of HcSTP-1 with PBMCs, which are key elements for immune responses, was investigated by using IFA. As shown in **Figure 4**, the Cy3-labeled target protein and the DAPI labeled nuclei displayed red and blue fluorescence, respectively. The red visualization on the surface of cells in treatment group (rHcSTP-1) indicated the binding of the protein whereas, no red labeling was detected in the control groups (pET32a or PBS), which clearly specified that rHcSTP-1 could bind on the surface of goat PBMCs and exerts its immune effects in a multiple manners (**Figure 4**).

rHcSTP-1 Decreased Anti-Inflammatory and Increased Pro-Inflammatory Cytokines Expression in a Balanced Th1-Th2 State *In Vitro*

The mRNA levels of cytokines produced by cultured goat immune cells (PBMCs) in response to STP-1 protein were tested at RT-PCR machine. As depicted in results of **Figure 5**, transcriptions level of IL-2 [ANOVA, $F_{(5,12)} = 198.9$, $p = 0.0001$] and transforming growth factor-β1 (TGF-β1) [ANOVA, $F_{(5,12)} = 108.0$, $p = 0.0001$] were increased significantly at dose-dependent manner to that of pET32a protein and PBS control group. However, the IL-10 transcription was decreased [ANOVA, $F_{(5,12)} = 19.04$, $p = 0.0001$] dose dependently to that of control groups. Here, we also noted that interferon gamma (IFN-γ) at protein concentration of 10 μg/ml showed no difference ($p = 0.337$); however, at 20 μg/ml ($p = 0.002$) and 40 μg/ml [ANOVA, $F_{(5,12)} = 105.6$, $p = 0.0001$] the transcription level was augmented significantly. After incubation with rHcSTP-1 protein, the expressions of IL-17 at 10 μg/ml reached at its significant level [ANOVA, $F_{(5,12)} = 11.76$, $p = 0.0003$], while at 20 and 40 μg/ml remained non-significant. However, IL-6 was not significantly different [ANOVA, $F_{(5,12)} = 0.604$, $p = 0.699$] when compared with control groups (**Figure 5**).

rHcSTP-1 Protein Affected PBMCs Proliferation

Antiproliferative effects of rHcSTP-1, compared to the negative control and control protein treated groups were evaluated by using cell counting kit (CCK8). The results demonstrated that, cells stimulated with ConA and incubated with rHcSTP-1 protein downregulated [ANOVA, $F_{(5,12)} = 67.38$, $p = 0.0001$] the multiplication efficiency dose dependently (**Figure 6**). However, no significant change was observed between control groups [ANOVA, $F_{(5,12)} = 67.38$, $p = 0.557$].

rHcSTP-1 Inhibited MHC-I and -II Expression on Goat Monocytes

In response to the rHcSTP-1, the expression of MHC-I and -II surface markers on monocytes were evaluated, and results showed that as compared to expression in control groups, rHcSTP-1 significantly decreased MHC-I (**Figures 7B,D**) molecule expression [$F_{(5,12)} = 780.3$] as well as MHC-II [$F_{(5,12)} = 157.2$] on the surface of the goat monocytes in a dose-dependent manner $p < 0.0001$ (**Figures 7C,E**).

PBMC Migration Assay

To investigate impact of the rHcSTP-1 on immune cell migration, the percentage of migrated cells through Millipore polycarbonate membrane into the lower chamber was calculated. Results showed that 16.67 ± 0.8819% cells with control and 16.33 ± 1.764% cells with control protein group (pET32a) were migrated into lower chamber ($p = 0.087$). At 10 μg/ml (27.00 ± 1.528%), 20 μg/ml (32.67 ± 2.603%), and 40 μg/ml (35.00 ± 2.309%) rHcSTP-1 protein concentrations, significant amount of cells were passed through membrane (**Figure 8**). However, no difference was found between control and 5 μg/ml (20.00 ± 1.155%) protein concentration ($p = 0.084$).

rHcSTP-1 Involved in Intra-PBMCs NO Production

Nitric oxide plays a crucial role in the host defense mechanism by preventing growth or killing the parasite directly during

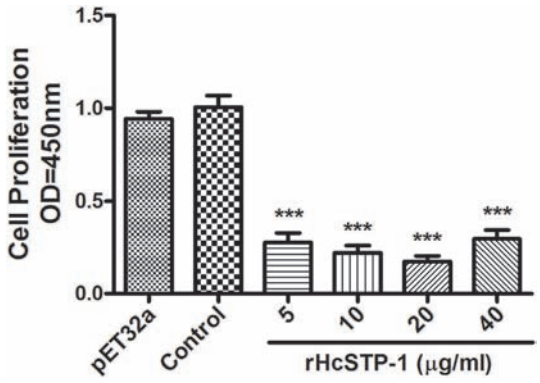

FIGURE 6 | Influences of different concentrations of rHcSTP-1 on peripheral blood mononuclear cells proliferation *in vitro*. Cells were simulated with ConA and treated with control buffer, His-Tag protein (pET32a), and various concentrations of recombinant serine/threonine-protein phosphatase 1 (STP-1) protein for 72 h. Proliferation test was conducted by CCK-8 and OD450 value was measured using microplate spectrophotometer. Cell proliferation index was calculated by considering the OD450 values in controls as 100%. The data are expressed as mean ± SEM of three independent experiments (***$p < 0.001$).

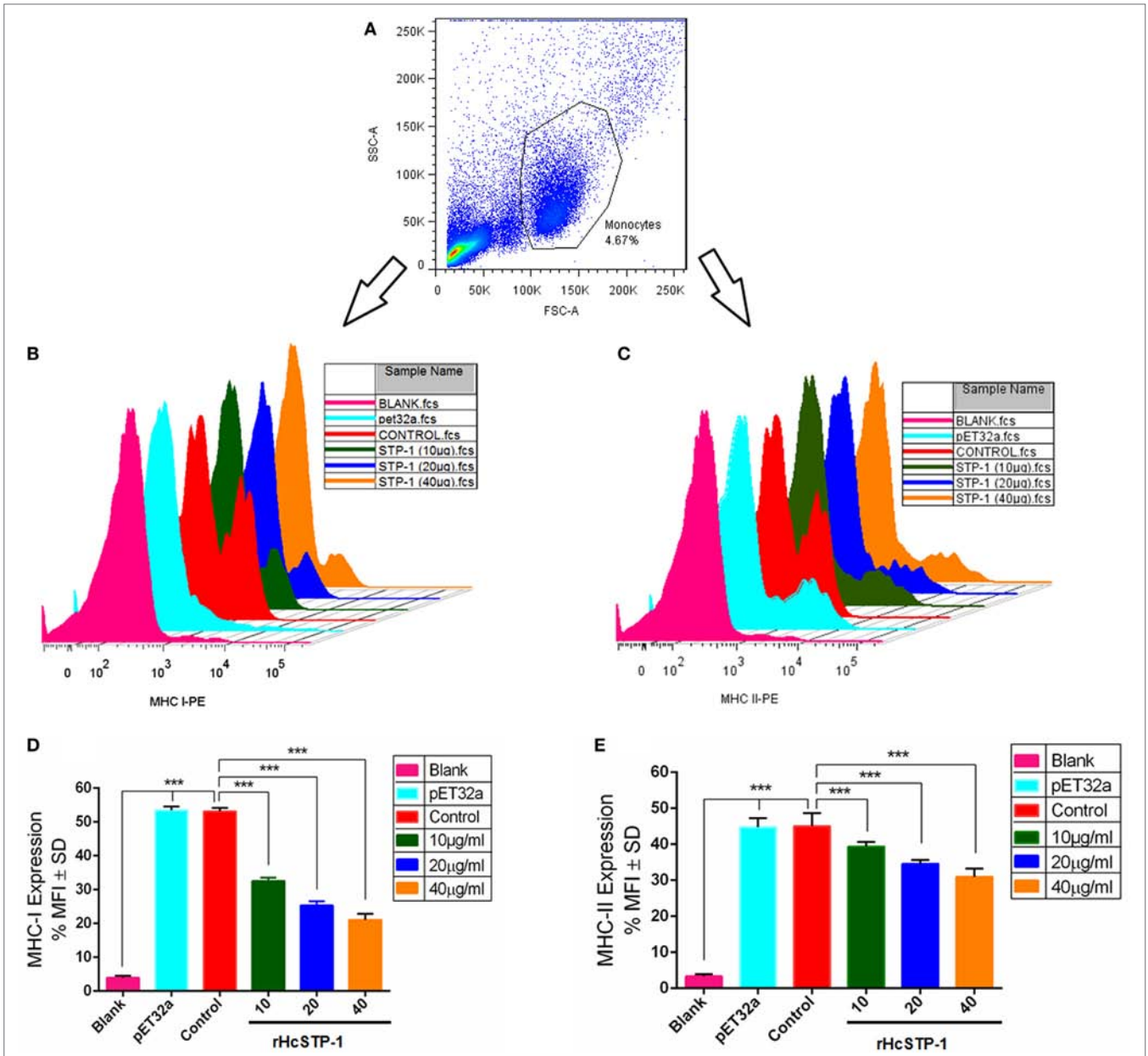

FIGURE 7 | rHcSTP-1 suppressed both major histocompatibility complex (MHC) class-I and II on goat monocytes. Monocytes were cultured in the presence of control buffer, HisTag protein (pET32a), and multiple concentrations of rHcSTP-1 for 24 h. MHC-II expression was measured by flow cytometric analysis and calculated as the percentage of mean fluorescence intensity (MFI). **(A)** Histogram corresponds to one representative of three independent experiments. **(B,C)** Stagger offset showing expression level of MHCs on monocytes. **(D,E)** Bar graphs represent the MFI ± SD of controls. The data are representative of three independent experiments (***$p < 0.001$).

infection. By using total nitric oxide kit, we found that no significant production was occurred [ANOVA, $F_{(5,12)} = 25.92$, $p = 0.504$] at 5 and 10 µg/ml compared with the groups treated as control. Here, we also observed that at 20 and 40 µg/ml, a significant level of NO was produced [ANOVA, $F_{(5,12)} = 25.92$, $p = 0.0001$]. However, production of NO between control (PBS) and pET32a group was also non-significant [ANOVA, $F_{(5,12)} = 25.92$, $p = 0.473$] (**Figure 9**).

rHcSTP-1 Dramatically Modulated Early and Late Apoptosis of PBMCs

It has been suggested that STPs obviously involved in various cellular processes including cell viability and cell death (10). The apoptotic activity of rHcSTP-1 on PBMCs was evaluated by using the externalization of membrane phospholipid phosphatidylserine (PS) as a marker of cell apoptosis. Flow cytometry assay revealed that cells incubated with different

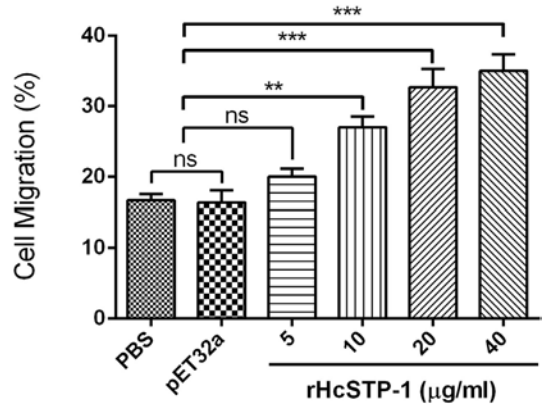

FIGURE 8 | Effects of the various concentrations of rHcSTP-1 on peripheral blood mononuclear cell migration *in vitro*. Cells were treated with control buffer, HisTag protein (pET32a), and multiple concentrations of rHcSTP-1. The migration percentage was determined randomly. The difference between the mean values was calculated using ANOVA. Data are representative of three independent experiments (**$p < 0.01$, ***$p < 0.001$, and ns non-significant versus the control).

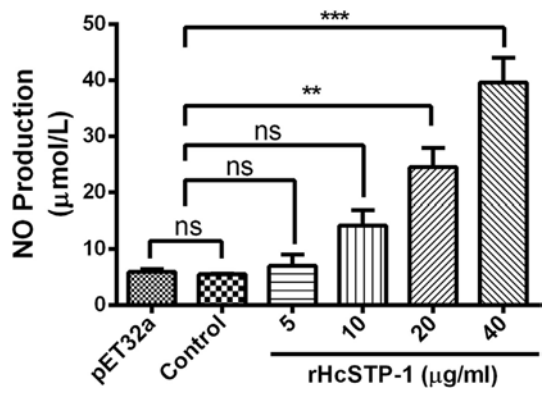

FIGURE 9 | Measurement of the intracellular nitric oxide production by goat peripheral blood mononuclear cells *in vitro*. Nitric oxide concentration in the supernatant of cell cultures was performed according to the instructions of Griess assay by Total Nitric Oxide Assay Kit. The data were presented here as mean ± SEM of three independent experiments (**$p < 0.01$ and ***$p < 0.001$).

protein concentrations (5, 10, 20, and 40 μg/ml) showed significantly increased frequency of apoptotic percentage in both early [ANOVA, $F_{(5,12)} = 69.08$, $p = 0.0001$] and late stage apoptosis [ANOVA, $F_{(5,12)} = 68.30$, $p = 0.0001$] compared with the control groups. Meanwhile, no significant change was observed [ANOVA, $F_{(5,12)} = 200.8$, $p = 0.0986$] between control and pET32a group (**Figure 10**).

DISCUSSION

Identification and development of novel drug targets are always a primacy in the biological study of socio-economically important parasites. Helminths ESPs including some antigens with unknown biological functions were characterized (31–33), and due to their sequences homology, these molecules have been proven as promising vaccine candidate against nematodes infections (34, 35). Among PPs, PP1 elaborate numerous biological activities, such as membrane receptors/channels regulations, protein synthesis, glycogen metabolism, transcription, cellular division, and apoptosis (36). In current investigation, an ES protein of *H. contortus* (STP-1) was characterized and localization of this protein through IFA confirmed its attachment with host immune cells for the first time, in shape of surface ligand complex (37), which is characteristic feature of ES proteins to suppress or modulate the immune functions of host PBMCs.

The PP1 is a major ubiquitously expressed STP, which shares a conserved catalytic domain with all other isotypes (PP2A, PP2B, PP4, PP5, PP6, and PP7) (38) and provides extensive information regarding their functions involved in numerous vital cellular mechanisms in all organisms (30, 39). In this study, highly significant amino acid identity of HcSTP-1 with presence of a conserved motif (LRGNHE) for STP protein pattern at positions 115–120 (18), involvement of amino acids for catalytic activity like metal ion-binding and proton donation were found (7). In the central regions of polypeptides, the amino acid sequences were highly conserved, particularly with the signature sequence motifs of the PPP family (GDXHG, GDXVDRG, GNHE, HGG, RG, and H) (30). However, the N- and C-terminal amino acids were variable, which suggested that it might be involved in protein binding and regulatory activity.

Previous studies suggested that STPs were associated with male reproductive processes of parasites, including sperm maturation, motility, and viability (40). In our previous proteomic analysis, STP-1 was found at adult and late adult developmental stages of *H. contortus in vivo* (19). In this study, immunohistochemically HcSTP-1 was localized in both male and female adult worms of *H. contortus*. Somehow, most PPs considered to be conserved during free-living as well as parasitic developmental stages; however, the biological pathways involved in the growth, development, survival, and/or reproduction reflects between invertebrates and vertebrates. Based on current information, a deep insight into the biochemical localization of STPs in *H. contortus* is required to understand the gender dependent immune stimulation by STPs during host–parasite interface.

The immune (Th1 and Th2) and inflammatory responses are deeply allied with secretion of various chemokines and cytokines by number of immune cell types (lymphocytes and monocytes), which perform crucial immunoregulatory functions (41), against parasitic infections like *H. contortus* (42). In this study, the levels of mRNA transcripts for IL-2, interleukin-10, transforming growth factor beta 1, interleukin-6, interferon-γ, and interleukin-17 in cultured PBMCs after treatment with rHcSTP-1 were detected for the first time. Schallig (43) suggested that sheep challenged with *H. contortus* infection responded cell mediate immune reaction (Th1), categorized by upregulation of IFN-γ and IL-2 mRNA expression. Similarly, in current research, goat PBMCs in response to rHcSTP-1 protein showed higher expression levels

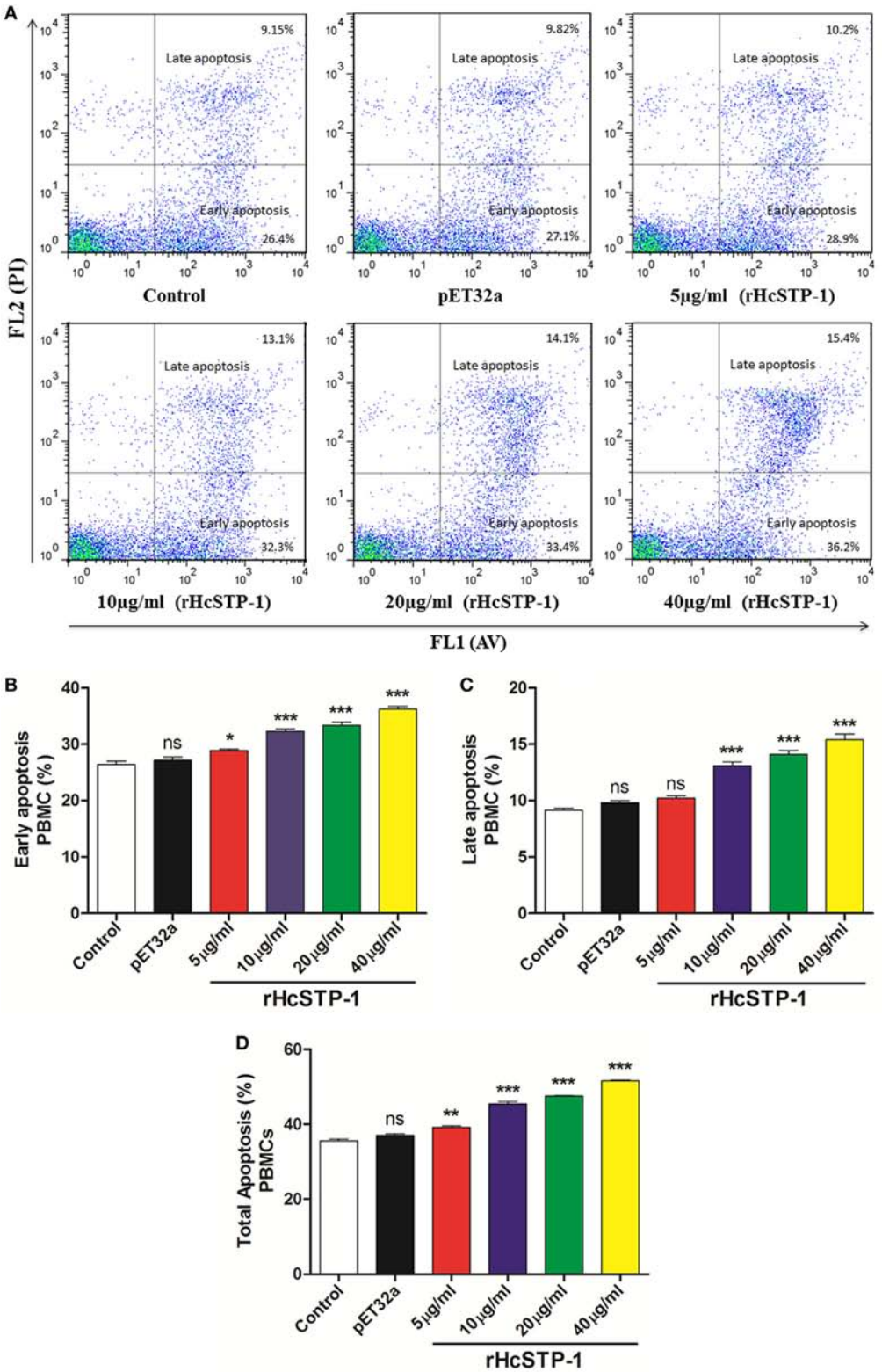

FIGURE 10 | Apoptotic analysis of peripheral blood mononuclear cells (PBMCs) by flow cytometry. **(A)** The dot plot showing percentages of PBMCs undergoing early and late stage apoptosis dually stained with Annexin V-FITC/PI. **(B)** Bar graph showing percentage of early stage apoptosis of PBMCs after rHcSTP-1 treatment. **(C)** Bar graph showing percentage of late stage apoptosis of PBMCs after rHcSTP-1 treatment. **(D)** The effect of the different protein treatments on total % (early + late) of apoptotic cells. Data are presented as the mean ± SEM ($n = 3$) from triplicate experiments. Asterisks designate treatment groups are significantly differ in respect to control one (*$p < 0.05$, **$p < 0.01$, ***$p < 0.001$, and ns non-significant).

of IL-2 and IFN-γ, suggesting that these cytokines might be in favor of non-protective Th responses against hemonchosis. The immunosuppressive cytokine IL-10 was responsible for inhibition of Th2 immune responses (44, 45). In this research, rHcSTP-1 protein showed a significant Th2 type immune response by decreased IL-10 cytokine in culture PBMCs, and thus exerts suppressive potential on differentiation of T_{reg} cells, which might be immune modulatory role of HcSTP-1 against parasite infection.

Previously, some researches demonstrated that IL-17 cytokine were involved in pathogenesis and inflammatory responses by numerous parasites (46–48). It was also elucidated that decreased level of IL-17 resulted favorable host protective responses (49). In our previous study, HcESPs were found to induce IL-17 cytokine by stimulation of the Th17 cells and resulted in inflammatory reaction favorable for worm survival in host. In this study, we found that rHcSTP-1 with concentration of 10 μg/ml significantly upregulated IL-17 cytokine. Our findings indicated that HcSTP-1 protein of *H. contortus* was adept in Th17 cells induction, which lead to inflammatory response. However, the resulted inflammatory reactions might be in favor of parasitic infection. TGF-β1 is functionally multidimensional cytokine that controls various immune system activities differentially on different cell types and potentially regulate various biological processes (50). It also plays vital roles to inhibit proliferation and to stimulate the apoptosis of various immune cells subset (51). In this investigation, the binding of recombinant protein HcSTP-1 to the goat PBMCs increased the production of TGF-β1, which could be a one of mechanism of rHcSTP-1 protein to facilitate immune evasion during host–parasite interactions.

Major histocompatibility complex is associated with many important immunological activities like: stimulation of antibody production and immune responses against microbial and parasitic pathogens (52, 53), although some cytokines especially IFN-γ and TGF-β (54) have been proven to upregulate MHC-I and -II gene expression in different immune cells. Here, we noted that STP-1 protein of *H. contortus* potentially suppress the MHC-I and -II molecules expression in goat monocytes. This indicated that STP-1 protein interferes with the MHC-I and -II antigen presentation pathway, which might be a key mechanism for evasion from the host's immune response.

The cellular processes such as cell migration part play an importance role in immune surveillance and tissue regeneration, by recruiting of immune cells into the surrounding tissue to destroy invading microorganisms. In addition, Type-1 as precise inhibitor of protein serine/threonine phosphatase (PHI-1) participated in regulatory events by modulating the migration of human endothelial and epithelial cells (55). Moreover, it was suggested that helminths actively induce migration of immune cell to infected sites (56). In this research, migration experiment concluded that rHcSTP-1 is an important binding protein to the goat PBMCs, which regulate the migration of immune cells to combat with invading *H. contortus* parasite and might be a contributor of HcESPs in the PBMCs migration.

Many proteins including ser/thr phosphatases were thought to be implicated in regulation of apoptosis (57). Till now, studies on cell death regulation by PPP subfamilies like PP2A and PP2B were well documented (10, 58); however, few studies highlighted the direct association and involvement of PP1, PP4, PP5, PP6, and PP7 members of phosphatase family in apoptosis (59–62). This study showed that rHcSTP-1 was involved in apoptosis as well as cell necrotic activity at dose-dependent manner.

In addition, cell proliferation is an indispensable process which is regulated or suppressed by both antigen-presenting cells (APCs) and T cells, thus modulate the host immune responses (63). In our earlier work, HcESPs significantly suppressed PBMCs multiplication at dose-dependent manner. In this study, PBMCs proliferation was decreased at significant level, which ultimately increased the pre- and post-apoptotic percentage in response to rHcSTP-1 treatment. Our study demonstrated that rHcSTP-1 as a constituent of HcESPs might interfere with modulatory activity on PBMCs proliferation and cell death regulation; however, the exact mechanism and pathways involved during host–parasite interaction upon HcSTP-1 protein involvement remains to be determined.

The immune cell-derived molecule, nitric oxide (NO) has been concerned with host non-specific defense against variety of infections such as hemonchosis, leishmaniasis, trypanosomiasis, malaria, toxoplasmosis, and schistosomiasis (64, 65). Previous studies provoked that PPs including P1 and P2A are involved in iNOS assertion in murine macrophages (66). Another study also witnessed that serine-threonine phosphatases post-transcriptionally regulate iNOS translation in rat hepatocytes (67). Furthermore, IFN-γ and TNF-α activated release of NO by macrophages was usually associated with killing functions on the helminths (68). In our previous study, the generation of NO was significantly suppressed by HcESPs due to decreased level of IFN-γ (69). In this study, intracellular nitrite production of goat PBMCs was significantly upregulated in a concentration-dependent fashion. These findings suggested that *H. contortus* STP-1 protein could induce the production of NO through increasing IFN-γ level which might mediate immunomodulatory functions on NO production and thus intensified the harmful effects of some chemical factors produced by the host cells on the helminths during host–parasite interface.

CONCLUSION

The current observations highlighted that *H. contortus* STP-1 as an important constituents of HcESPs localized in both gender, play pivotal stage-specific regulatory roles in interactions with host immune cells. This protein after being bind to host immune cells, regulate cytokines expression, cell proliferation, MHC expression, cell migration, NO production, and cell death regulation differentially. This study might be a powerful clue and would have major fundamental significant contribution in the discovery of novel therapeutic approaches to control hemonchosis. However, immune cells specific role of rHcSTP-1 and other related phosphatases subunits with PBMC sub-populations like T cell and B cell, NK cell, APCs, and macrophages involved in host–parasite relationship in

activating immune and cellular response are worthy for future research.

ETHICS STATEMENT

All experiments were conducted in accordance with the guidelines of the Animal Ethics Committee, Nanjing Agricultural University, China. All experimental protocols were approved by the science and Technology Agency of Jiangsu Province. The approval ID is SYXK (SU) 2010-0005.

AUTHOR CONTRIBUTIONS

XLi concerned with project designing, management, and coordination of this study. ME analyzed data and wrote the manuscript. WW, JG, ML, and YW provided technical support during experiments. MWH, MH, and XLiu participated in data analysis. LX, RY, and XS helped for providing all necessary materials during experiments.

FUNDING

This research work was financially supported by the "National Key Basic Research Program (973 Program) of P.R. China" (Grant No. 2015CB150300) and by the Priority Academic Program Development of Jiangsu Higher Education Institutions (PAPD).

SUPPLEMENTARY MATERIAL

The Supplementary Material for this article can be found online at https://www.frontiersin.org/articles/10.3389/fimmu.2018.01627/full#supplementary-material.

REFERENCES

1. Coles GC. The future of veterinary parasitology. *Vet Parasitol* (2001) 98:31–9. doi:10.1016/S0304-4017(01)00421-6
2. Jasmer DP, Lahmers KK, Brown WC. *Haemonchus contortus* intestine: a prominent source of mucosal antigens. *Parasite Immunol* (2007) 29:139–51. doi:10.1111/j.1365-3024.2006.00928.x
3. Kaplan RM, Vidyashankar AN. An inconvenient truth: global worming and anthelmintic resistance. *Vet Parasitol* (2012) 186:70–8. doi:10.1016/j.vetpar.2011.11.048
4. Kotze AC, Hunt PW, Skuce P, Von Samson-Himmelstjerna G, Martin RJ, Sager H, et al. Recent advances in candidate-gene and whole-genome approaches to the discovery of anthelmintic resistance markers and the description of drug/receptor interactions. *Int J Parasitol Drugs Drug Resist* (2014) 4:164–84. doi:10.1016/j.ijpddr.2014.07.007
5. Britton C, Roberts B, Marks ND. Functional genomics tools for *Haemonchus contortus* and lessons from other helminths. *Adv Parasitol* (2016) 93:599–623. doi:10.1016/bs.apar.2016.02.017
6. Sarmiento M, Zhao Y, Gordon SJ, Zhang ZY. Molecular basis for substrate specificity of protein-tyrosine phosphatase 1B. *J Biol Chem* (1998) 273:26368–74. doi:10.1074/jbc.273.41.26368
7. Barford D, Das AK, Egloff MP. The structure and mechanism of protein phosphatases: insights into catalysis and regulation. *Annu Rev Biophys Biomol Struct* (1998) 27:133–64. doi:10.1146/annurev.biophys.27.1.133
8. Cohen PT. Novel protein serine/threonine phosphatases: variety is the spice of life. *Trends Biochem Sci* (1997) 22:245–51. doi:10.1016/S0968-0004(97)01060-8
9. Herzig S, Neumann J. Effects of serine/threonine protein phosphatases on ion channels in excitable membranes. *Physiol Rev* (2000) 80:173–210. doi:10.1152/physrev.2000.80.1.173
10. Klumpp S, Krieglstein J. Serine/threonine protein phosphatases in apoptosis. *Curr Opin Pharmacol* (2002) 2:458–62. doi:10.1016/S1471-4892(02)00176-5
11. Berndt N. Roles and regulation of serine/threonine-specific protein phosphatases in the cell cycle. *Prog Cell Cycle Res* (2003) 5:497–510.
12. Sim AT, Baldwin ML, Rostas JA, Holst J, Ludowyke RI. The role of serine/threonine protein phosphatases in exocytosis. *Biochem J* (2003) 373:641–59. doi:10.1042/bj20030484
13. Delorme V, Garcia A, Cayla X, Tardieux I. A role for *Toxoplasma gondii* type 1 ser/thr protein phosphatase in host cell invasion. *Microbes Infect* (2002) 4:271–8. doi:10.1016/S1286-4579(02)01538-1
14. Boag PR, Ren P, Newton SE, Gasser RB. Molecular characterisation of a male-specific serine/threonine phosphatase from *Oesophagostomum dentatum* (Nematoda: Strongylida), and functional analysis of homologues in *Caenorhabditis elegans*. *Int J Parasitol* (2003) 33:313–25. doi:10.1016/S0020-7519(02)00263-1
15. Hu M, Abs EL-Osta YG, Campbell BE, Boag PR, Nisbet AJ, Beveridge I, et al. *Trichostrongylus vitrinus* (Nematoda: Strongylida): molecular characterization and transcriptional analysis of Tv-stp-1, a serine/threonine phosphatase gene. *Exp Parasitol* (2007) 117:22–34. doi:10.1016/j.exppara.2007.03.008
16. Kutuzov MA, Andreeva AV. Protein Ser/Thr phosphatases of parasitic protozoa. *Mol Biochem Parasitol* (2008) 161:81–90. doi:10.1016/j.molbiopara.2008.06.008
17. Ma GX, Zhou RQ, Hu SJ, Huang HC, Zhu T, Xia QY. Molecular characterization and functional analysis of serine/threonine protein phosphatase of *Toxocara canis*. *Exp Parasitol* (2014) 141:55–61. doi:10.1016/j.exppara.2014.03.019
18. Campbell BE, Rabelo EM, Hofmann A, Hu M, Gasser RB. Characterization of a *Caenorhabditis elegans* glc seven-like phosphatase (gsp) orthologue from *Haemonchus contortus* (Nematoda). *Mol Cell Probes* (2010) 24:178–89. doi:10.1016/j.mcp.2010.02.001
19. Gadahi JA, Wang S, Bo G, Ehsan M, Yan R, Song X, et al. Proteomic analysis of the excretory and secretory proteins of *Haemonchus contortus* (HcESP) binding to goat PBMCs In vivo revealed stage-specific binding profiles. *PLoS One* (2016) 11:e0159796. doi:10.1371/journal.pone.0159796
20. Ehsan M, Gao W, Gadahi JA, Lu M, Liu X, Wang Y, et al. Arginine kinase from *Haemonchus contortus* decreased the proliferation and increased the apoptosis of goat PBMCs in vitro. *Parasit Vectors* (2017) 10:311. doi:10.1186/s13071-017-2244-z
21. Nicholson IC, Mavrangelos C, Fung K, Ayhan M, Levichkin I, Johnston A, et al. Characterisation of the protein composition of peripheral blood mononuclear cell microsomes by SDS-PAGE and mass spectrometry. *J Immunol Methods* (2005) 305:84–93. doi:10.1016/j.jim.2005.07.005
22. Yuan C, Zhang H, Wang W, Li Y, Yan R, Xu L, et al. Transmembrane protein 63A is a partner protein of *Haemonchus contortus* galectin in the regulation of goat peripheral blood mononuclear cells. *Parasit Vectors* (2015) 8:211. doi:10.1186/s13071-015-0816-3
23. Gadahi JA, Ehsan M, Wang S, Zhang Z, Wang Y, Yan R, et al. Recombinant protein of *Haemonchus contortus* 14-3-3 isoform 2 (rHcftt-2) decreased the production of IL-4 and suppressed the proliferation of goat PBMCs in vitro. *Exp Parasitol* (2016) 171:57–66. doi:10.1016/j.exppara.2016.10.014
24. Bradford MM. A rapid and sensitive method for the quantitation of microgram quantities of protein utilizing the principle of protein-dye binding. *Anal Biochem* (1976) 72:248–54. doi:10.1016/0003-2697(76)90527-3
25. Yi D, Xu L, Yan R, Li X. *Haemonchus contortus*: cloning and characterization of serpin. *Exp Parasitol* (2010) 125:363–70. doi:10.1016/j.exppara.2010.03.002
26. Livak KJ, Schmittgen TD. Analysis of relative gene expression data using real-time quantitative PCR and the 2(-Delta Delta C(T)) Method. *Methods* (2001) 25:402–8. doi:10.1006/meth.2001.1262
27. Kaleab B, Ottenoff T, Converse P, Halapi E, Tadesse G, Rottenberg M, et al. Mycobacterial-induced cytotoxic T cells as well as nonspecific killer cells derived from healthy individuals and leprosy patients. *Eur J Immunol* (1990) 20:2651–9. doi:10.1002/eji.1830201219
28. Wang W, Wang S, Zhang H, Yuan C, Yan R, Song X, et al. Galectin Hco-gal-m from *Haemonchus contortus* modulates goat monocytes and T cell function

in different patterns. *Parasit Vectors* (2014) 7:342. doi:10.1186/1756-3305-7-342
29. Sun J, Zhang X, Broderick M, Fein H. Measurement of nitric oxide production in biological systems by using griess reaction assay. *Sensors* (2003) 3:276. doi:10.3390/s30800276
30. Shi Y. Serine/threonine phosphatases: mechanism through structure. *Cell* (2009) 139:468–84. doi:10.1016/j.cell.2009.10.006
31. García-Coiradas L, Angulo-Cubillán F, Méndez S, Larraga V, De La Fuente C, Cuquerella M, et al. Isolation and immunolocalization of a putative protective antigen (p26/23) from adult *Haemonchus contortus*. *Parasitol Res* (2008) 104:363. doi:10.1007/s00436-008-1204-0
32. Lejambre LF, Windon RG, Smith WD. Vaccination against *Haemonchus contortus*: performance of native parasite gut membrane glycoproteins in Merino lambs grazing contaminated pasture. *Vet Parasitol* (2008) 153:302–12. doi:10.1016/j.vetpar.2008.01.032
33. García-Coiradas L, Angulo-Cubillán F, Valladares B, Martínez E, De La Fuente C, Alunda JM, et al. Immunization against lamb haemonchosis with a recombinant somatic antigen of *Haemonchus contortus* (rHcp26/23). *Vet Med Int* (2010) 2010:8. doi:10.4061/2010/852146
34. Knox DP, Redmond DL, Skuce PJ, Newlands GFJ. The contribution of molecular biology to the development of vaccines against nematode and trematode parasites of domestic ruminants. *Vet Parasitol* (2001) 101:311–35. doi:10.1016/S0304-4017(01)00558-1
35. Knox DP, Smith WD. Vaccination against gastrointestinal nematode parasites of ruminants using gut-expressed antigens. *Vet Parasitol* (2001) 100:21–32. doi:10.1016/S0304-4017(01)00480-0
36. Ceulemans H, Bollen M. Functional diversity of protein phosphatase-1, a cellular economizer and reset button. *Physiol Rev* (2004) 84:1–39. doi:10.1152/physrev.00013.2003
37. Sun Y, Yan R, Muleke CI, Zhao G, Xu L, Li X. Recombinant galectins of *Haemonchus contortus* parasite induces apoptosis in the peripheral blood lymphocytes of goat. *Int J Pept Res Ther* (2007) 13:387–92. doi:10.1007/s10989-006-9045-0
38. Li BW, Rush AC, Crosby SD, Warren WC, Williams SA, Mitreva M, et al. Profiling of gender-regulated gene transcripts in the filarial nematode Brugia malayi by cDNA oligonucleotide array analysis. *Mol Biochem Parasitol* (2005) 143:49–57. doi:10.1016/j.molbiopara.2005.05.005
39. Ingebritsen TS, Cohen P. The protein phosphatases involved in cellular regulation. 1. Classification and substrate specificities. *Eur J Biochem* (1983) 132:255–61. doi:10.1111/j.1432-1033.1983.tb07357.x
40. Smith GD, Wolf DP, Trautman KC, Da Cruz E, Silva EF, Greengard P, et al. Primate sperm contain protein phosphatase 1, a biochemical mediator of motility. *Biol Reprod* (1996) 54:719–27. doi:10.1095/biolreprod54.3.719
41. Grencis RK. Cytokine regulation of resistance and susceptibility to intestinal nematode infection – from host to parasite. *Vet Parasitol* (2001) 100:45–50. doi:10.1016/S0304-4017(01)00482-4
42. Shakya KP, Miller JE, Horohov DW. A Th2 type of immune response is associated with increased resistance to *Haemonchus contortus* in naturally infected Gulf coast native lambs. *Vet Parasitol* (2009) 163:57–66. doi:10.1016/j.vetpar.2009.03.052
43. Schallig HD. Immunological responses of sheep to *Haemonchus contortus*. *Parasitology* (2000) 120(Suppl):S63–72. doi:10.1017/S003118209900579X
44. Taylor A, Verhagen J, Blaser K, Akdis M, Akdis CA. Mechanisms of immune suppression by interleukin-10 and transforming growth factor-beta: the role of T regulatory cells. *Immunology* (2006) 117:433–42. doi:10.1111/j.1365-2567.2006.02321.x
45. Grencis RK, Humphreys NE, Bancroft AJ. Immunity to gastrointestinal nematodes: mechanisms and myths. *Immunol Rev* (2014) 260:183–205. doi:10.1111/imr.12188
46. Larkin BM, Smith PM, Ponichtera HE, Shainheit MG, Rutitzky LI, Stadecker MJ. Induction and regulation of pathogenic Th17 cell responses in schistosomiasis. *Semin Immunopathol* (2012) 34:873–88. doi:10.1007/s00281-012-0341-9
47. Song X, Gao H, Qian Y. Th17 differentiation and their pro-inflammation function. *Adv Exp Med Biol* (2014) 841:99–151. doi:10.1007/978-94-017-9487-9_5
48. Katawa G, Layland LE, Debrah AY, Von Horn C, Batsa L, Kwarteng A, et al. Hyperreactive onchocerciasis is characterized by a combination of Th17-Th2 immune responses and reduced regulatory T cells. *PLoS Negl Trop Dis* (2015) 9:e3414. doi:10.1371/journal.pntd.0003414
49. Wen X, He L, Chi Y, Zhou S, Hoellwarth J, Zhang C, et al. Dynamics of Th17 cells and their role in *Schistosoma japonicum* infection in C57BL/6 Mice. *PLoS Negl Trop Dis* (2011) 5:e1399. doi:10.1371/journal.pntd.0001399
50. Li MO, Wan YY, Sanjabi S, Robertson AK, Flavell RA. Transforming growth factor-beta regulation of immune responses. *Annu Rev Immunol* (2006) 24:99–146. doi:10.1146/annurev.immunol.24.021605.090737
51. Lebman DA, Edmiston JS. The role of TGF-beta in growth, differentiation, and maturation of B lymphocytes. *Microbes Infect* (1999) 1:1297–304. doi:10.1016/S1286-4579(99)00254-3
52. Keskinen P, Ronni T, Matikainen S, Lehtonen A, Julkunen I. Regulation of HLA class I and II expression by interferons and influenza A virus in human peripheral blood mononuclear cells. *Immunology* (1997) 91:421–9. doi:10.1046/j.1365-2567.1997.00258.x
53. Lüder CGK, Lang T, Beuerle B, Gross U. Down-regulation of MHC class II molecules and inability to up-regulate class I molecules in murine macrophages after infection with *Toxoplasma gondii*. *Clin Exp Immunol* (1998) 112:308–16. doi:10.1046/j.1365-2249.1998.00594.x
54. Panek RB, Benveniste EN. Class II MHC gene expression in microglia. Regulation by the cytokines IFN-gamma, TNF-alpha, and TGF-beta. *J Immunol* (1995) 154:2846–54.
55. Tountas NA, Brautigan DL. Migration and retraction of endothelial and epithelial cells require PHI-1, a specific protein-phosphatase-1 inhibitor protein. *J Cell Sci* (2004) 117:5905–12. doi:10.1242/jcs.01506
56. Mcgovern KE, Wilson EH. Role of chemokines and trafficking of immune cells in parasitic infections. *Curr Immunol Rev* (2013) 9:157–68. doi:10.2174/1573395509666131217000000
57. Sun H, Wang Y. Novel Ser/Thr protein phosphatases in cell death regulation. *Physiology (Bethesda)* (2012) 27:43–52. doi:10.1152/physiol.00034.2011
58. Liu Q, Wilkins BJ, Lee YJ, Ichijo H, Molkentin JD. Direct interaction and reciprocal regulation between ASK1 and calcineurin-NFAT control cardiomyocyte death and growth. *Mol Cell Biol* (2006) 26:3785–97. doi:10.1128/MCB.26.10.3785-3797.2006
59. Cohen PT, Philp A, Vazquez-Martin C. Protein phosphatase 4 – from obscurity to vital functions. *FEBS Lett* (2005) 579:3278–86. doi:10.1016/j.febslet.2005.04.070
60. Festjens N, Vanden Berghe T, Cornelis S, Vandenabeele P. RIP1, a kinase on the crossroads of a cell's decision to live or die. *Cell Death Differ* (2007) 14:400–10. doi:10.1038/sj.cdd.4402085
61. Huang H-S, Lee EYC. Protein phosphatase-1 inhibitor-3 is an in vivo target of caspase-3 and participates in the apoptotic response. *J Biol Chem* (2008) 283:18135–46. doi:10.1074/jbc.M709735200
62. Kang Y, Lee JH, Hoan NN, Sohn HM, Chang IY, You HJ. Protein phosphatase 5 regulates the function of 53BP1 after neocarzinostatin-induced DNA damage. *J Biol Chem* (2009) 284:9845–53. doi:10.1074/jbc.M809272200
63. Loke PN, Macdonald AS, Robb A, Maizels RM, Allen JE. Alternatively activated macrophages induced by nematode infection inhibit proliferation via cell-to-cell contact. *Eur J Immunol* (2000) 30:2669–78. doi:10.1002/1521-4141(200009)30:9<2669::AID-IMMU2669>3.0.CO;2-1
64. Kotze AC, Mcclure SJ. *Haemonchus contortus* utilises catalase in defence against exogenous hydrogen peroxide in vitro. *Int J Parasitol* (2001) 31:1563–71. doi:10.1016/S0020-7519(01)00303-4
65. Wandurska-Nowak E. [The role of nitric oxide (NO) in parasitic infections]. *Wiad Parazytol* (2004) 50:665–78.
66. Dong Z, Yang X, Xie K, Juang SH, Llansa N, Fidler IJ. Activation of inducible nitric oxide synthase gene in murine macrophages requires protein phosphatases 1 and 2A activities. *J Leukoc Biol* (1995) 58:725–32. doi:10.1002/jlb.58.6.725
67. Taylor BS, Liu S, Villavicencio RT, Ganster RW, Geller DA. The role of protein phosphatases in the expression of inducible nitric oxide synthase in the rat hepatocyte. *Hepatology* (1999) 29:1199–207. doi:10.1002/hep.510290419
68. Gazzinelli RT, Oswald IP, James SL, Sher A. IL-10 inhibits parasite killing and nitrogen oxide production by IFN-gamma-activated macrophages. *J Immunol* (1992) 148:1792–6.

69. Gadahi JA, Yongqian B, Ehsan M, Zhang ZC, Wang S, Yan RF, et al. *Haemonchus contortus* excretory and secretory proteins (HcESPs) suppress functions of goat PBMCs in vitro. *Oncotarget* (2016) 7:35670–9. doi:10.18632/oncotarget.13487

Conflict of Interest Statement: The authors declare that the research was conducted in the absence of any commercial or financial relationships that could be construed as a potential conflict of interest.

frontiers in Immunology

ORIGINAL RESEARCH
published: 01 June 2018
doi: 10.3389/fimmu.2018.01222

Toxoplasma Chinese 1 Strain of WH3Δ*rop16*$_{I/III}$/*gra15*$_{II}$ Genetic Background Contributes to Abnormal Pregnant Outcomes in Murine Model

Cong Wang[1†], Weisheng Cheng[2†], Qian Yu[1], Tian Xing[1], Shoubin Chen[1], Lei Liu[1], Li Yu[1], Jian Du[1], Qingli Luo[1], Jilong Shen[1,3] and Yuanhong Xu[1,3]**

[1] Department of Pathogen Biology, Provincial Laboratories of Pathogen Biology and Zoonoses, School of Basic Medicine, Anhui Medical University, Hefei, China, [2] Department of Medical Genetics, Zhongshan School of Medicine, Sun Yat-sen University, The Key Laboratory of Tropical Disease Control, Ministry of Education, Guangzhou, China, [3] Department of Clinical Laboratory, The First Affiliated Hospital of Anhui Medical University, Hefei, China

OPEN ACCESS

Edited by:
Zhiguang Wu,
University of Edinburgh,
United Kingdom

Reviewed by:
Dolores Correa,
Instituto Nacional de Pediatria, Mexico
Hong-Juan Peng,
Southern Medical University, China
Yong Wang,
Nanjing Medical University, China

***Correspondence:**
Jilong Shen
shenjilong53@126.com;
Yuanhong Xu
xyhong1964@163.com

[†]These authors have contributed equally to this work.

Specialty section:
This article was submitted to Microbial Immunology, a section of the journal Frontiers in Immunology

Received: *24 January 2018*
Accepted: *15 May 2018*
Published: *01 June 2018*

Citation:
Wang C, Cheng W, Yu Q, Xing T, Chen S, Liu L, Yu L, Du J, Luo Q, Shen J and Xu Y (2018) Toxoplasma Chinese 1 Strain of WH3Δrop 16$_{I/III}$/gra15$_{II}$ Genetic Background Contributes to Abnormal Pregnant Outcomes in Murine Model. Front. Immunol. 9:1222. doi: 10.3389/fimmu.2018.01222

Toxoplasma gondii infection evokes a strong Th1-type response with interleukin (IL)-12 and interferon (IFN)-γ secretion. Recent studies suggest that the infection of pregnant mice with *T. gondii* may lead to adverse pregnancy results caused by subversion of physiological immune tolerance at maternofetal interface rather than direct invasion of the parasite. Genotype-associated dense granule protein GRA15$_{II}$ tends to induce classically activated macrophage (M1) differentiation and subsequently activating NK, Th1, and Th17 cells whereas rhoptry protein ROP16$_{I/III}$ drives macrophages to alternatively activated macrophage (M2) polarization and elicits Th2 immune response. Unlike the archetypal strains of types I, II, and III, type Chinese 1 strains possess both GRA15$_{II}$ and ROP16$_{I/III}$, suggesting a distinct pathogenesis of *Toxoplasma*-involved adverse pregnancies. We constructed *T. gondii* type Chinese 1 strain of WH3Δ*rop16* based on CRISPR/Cas9 technology to explore the ROP16$_{I/III}$-deficient/GRA15$_{II}$-dominant parasites in induction of trophoblast apoptosis *in vitro* and abnormal pregnant outcomes of mice *in vivo*. Our study showed that *Toxoplasma* WH3Δ*rop16* remarkably induced apoptosis of trophoblasts. C57BL/6 pregnant mice injected with the tachyzoites of WH3Δ*rop16* presented increased absorptivity of fetuses in comparison with the mice infected with WH3 wild type (WH3 WT) parasites although no remarkable difference of virulence to mice was seen between the two strains. Additionally, the mice inoculated with WH3Δ*rop16* tachyzoites exhibited a notable expression of both IL-17A and IFN-γ, while the percentage of $CD4^+CD25^+FoxP3$ [T regulatory cells (Tregs)] were diminished in splenocytes and placenta tissues compared to those infected with WH3 WT parasites. Accordingly, expressions of IL-4, IL-10, and transforming growth factor beta 1, the pivotal cytokines of Th2 and Tregs response, were significantly dampened whereas IFN-γ and IL-12 expressions were upregulated in WH3Δ*rop16*-infected mice, which gave rise to more prominent outcomes of abnormal pregnancies. Our results indicated that the WH3Δ*rop16* parasites with *gra15*$_{II}$ background of *T. gondii* type Chinese 1 strains may cause miscarriage and stillbirth due to subversion of the maternal immune tolerance and system immunity of the animals and the GRA15$_{II}$ effector contributes to the process of adverse pregnant consequences.

Keywords: *Toxoplasma gondii*, dense granule protein GRA15, rhoptry protein ROP16, CRISPR/Cas9, adverse pregnant outcome

INTRODUCTION

During normal pregnancy, allogeneic fetal cells invading the extraembryonic trophoblasts do not impair gestation by establishing tolerance at the maternal–fetal interface (1, 2). The physiological balance of Th1/Th2 is believed to play a crucial part in maintenance of normal pregnancy of mammals including humans (3). Previous studies showed that apoptosis is a normal physiological process of trophoblasts throughout gestation and is essential to normal placental development and fetal growth (4). Thus any unfavorable impact of immunological factors on the maternal–fetal interface and/or apoptosis of trophoblasts may lead to abnormal pregnancy outcomes.

It has been elucidated that T regulatory cells (Tregs) promote immune tolerance and successful pregnancy by secreting interleukin (IL)-10 and transforming growth factor beta 1 (TGF-β1) and dampen interferon (IFN)-γ and other inflammatory cytokines to maintain the normal development of embryos (5–8). The Tregs cells have been found to be insufficient in patients who experienced recurrent spontaneous abortions (9), while excessive secretion of IFN-γ and other Th1 type cytokines may give rise to adverse pregnancies (10). Therefore, Th2-dominant response in system immunity and at maternal–fetal interface is the prerequisite for normal pregnancy (3, 11–14).

Toxoplasma gondii is an extensive intracellular protozoan parasite that is capable of affecting almost all vertebrate animals including humans and leading to reproductive failure in its hosts (15, 16). Primary infection with *Toxoplasma* during pregnancy, particularly in the first trimester, may cause stillbirths, miscarriages, or fetal abnormalities (17). The apoptosis of trophoblasts might be induced by many stimuli. For example, apoptotic process of trophoblasts is notably increased in the case of spontaneous abortion when the cells were co-cultured with inflammatory macrophages that were infected with *T. gondii* (18). Glycosyl phosphatidylinositol on the membrane of *Toxoplasma* tachyzoites, similar to LPS of bacteria, could induce oxidative stress in several tissues, and it has been found to be a key molecule which is responsible for preterm labor in mice (19, 20). Despite the fact that *Toxoplasma* infection may cause abortion or congenital fetal infection *via* direct transmission of parasite to placentas and fetuses, some studies indicate that imbalance of immune tolerance at the maternal–fetal interface, rather than a direct action of the parasite, might be attributed to the abnormal pregnancies (21, 22), resulting in apoptosis of trophoblasts in the case of abortion with *T. gondii* infection. Further researches revealed that *Toxoplasma* infection in mice lead to adverse pregnant results with a mechanism of reduction of Tregs and elevation of Th17 cells (23).

Toxoplasma gondii invasion to the host cell is actually a series of parasite protein secretions. Secretory proteins of ROPs, GRAs, MICs, RONs, and other molecules are mainly generated by the organelles of dense granules, rhoptries, and micronemes. These parasite-derived polymorphic effectors are deeply involved in dictation of virulence and modulation of host signaling pathways (24–28). For instance, Jensen et al. found that ROP16$_{I/III}$ (of types I and III strains) kinase phosphorylates Stat6/Stat3 and induces alternatively activated macrophages (M2) at early phase of infection that is associated with promoted IL-4 and IL-10 expressions and Th2-polarized response, while GRA15$_{II}$ (of type II strains) activates NF-κB and elicits classically activated macrophages (M1) that is responsible for IL-12 generation and Th1-dominant immunity, subsequently activating NK and Th17 cells (19, 28–31), resulting in oxidative stress and further activation of the pro-apoptotic pathway (28, 32).

Studies reported that type Chinese 1 (ToxoDB #9) strains dominantly prevalent in China carry both GRA15$_{II}$ and ROP16$_{I/III}$ effectors that is different from the strains of archetypical types I, II, and III of *T. gondii* in Europe and North America (33, 34). The ROP16$_{I/III}$ with GRA15$_{II}$ background in Chinese 1 strains strongly suggests the distinct pathogenesis that differs from the strains of the other continents of the world. In the current study, we explored the impact of GRA15$_{II}$ with ROP16$_{I/III}$ deletion of Chinese 1 WH3 strain parasite on adverse pregnancy outcomes in murine model by making a *T. gondii* WH3Δ*rop16* strain based on CRISPR/Cas9 technology. We hypothesize that the Toxo-WH3Δ*rop16* strain with *gra15$_{II}$* background, similar to type II strains of *Toxoplasma*, might subvert the immune tolerance at the maternal–fetal interface and the systemic immunity, leading to adverse pregnancy, which is attributed to the M1/Th1/Th17 biased response. Moreover, this study would be helpful for better understanding of the genotype-associated mechanism of abnormal pregnancy caused by *Toxoplasma* predominantly circulating in China.

MATERIALS AND METHODS

Reagents

The following reagents were used in the experiment: Q5 mutagenesis kit (New England Biolabs, Ipswich, MA, USA) and ClonExpress MultiS One Step Cloning Kit (Vazyme Biotech, Nanjing, China). Phusion High-Fidelity PCR Kit (Thermo fisher, USA) was used for the PCR amplification. Percoll (GE Healthcare Life Sciences), pyrimethamine, penicillin, streptomycin, phorbol 12-myristate 13-acetate, ionomycin, HEPES, collagenase IV, and the Giemsa staining kit, were obtained from Sigma (St. Louis, MO, USA). Dulbecco's modified Eagle's medium, fetal bovine serum (FBS), and Roswell Park Memorial Institute 1640 medium (RPMI 1640) and D-Hanks solution were purchased from Wisent (Montreal, QC, Canada). Brefeldin A, FITC-labeled anti-mouse CD4, PE-labeled anti-mouse IL-17A, APC-labeled anti-mouse IL-4, Percp-cy5.5-labeled anti-mouse IFN-γ, APC-labeled anti-mouse CD25, PE-labeled anti-mouse Foxp3, FITC Annexin V Apoptosis Detection Kit, and Cytofix/Cytoperm kit were provided by BD Biosciences (New York, BD, USA). The nitrite was detected *via* Greiss Reagent System provided by Promega Biotech Company (Madison, WI, USA). The tumor necrosis factor (TNF-α), IL-17A enzyme-linked immunosorbent assay (ELISA) kit, and 1 × Fix/Perm buffer were purchased from eBioscience (San Diego CA, USA). IFN-γ, IL-12, IL-10, and TGF-β1 ELISA kit was obtained from R&D Systems (Minneapolis, MN, USA). The mouse trophoblasts (primary cells originated from C57BL/6 mice) were purchased from Wuhan Biofavor Biotechnology Company.

Propagation of *T. gondii*

Tachyzoites of *T. gondii* WH3 strain (type Chinese 1) were harvested from the continuous cell cultures in human foreskin fibroblasts (HFF, ATCC® SCRC-1041™) grown with Dulbecco's modified Eagle medium (DMEM) supplemented with 10% FBS, 100 μg/ml streptomycin, and 100 U/ml penicillin.

Generation of ROP16$_{I/III}$-Deficient Strain of Type Chinese 1

All the primers and plasmids used in the study are shown in **Table 1**. UPRT-targeting guide RNA (gRNA) in pSAG1:CAS9-U6:sgUPRT (Addgene plasmid #54467) was replaced with ROP16$_{I/III}$ targeting gRNA using Q5 mutagenesis kit. To make the homologous templates for gene replacements, homologous arms of ROP16$_{I/III}$ were amplified from the genomic DNA of type Chinese 1 WH3 WT strain as described in previous study (35). Subsequently, the homologous arms of ROP16 along with the selectable markers DHFR*-Ts were cloned into pUC19 using ClonExpress MultiS One Step Cloning Kit. The pSAG1:Cas9-U6:sgROP16$_{I/III}$ and donor DNA fragments were electroporated into *T. gondii* WH3 WT strain. After transfection, tachyzoites were immediately transferred into HFF cells. After culture for 48 h, parasites were selected with pyrimethamine for DHFR-TS. A single clone through limiting dilution in 96-well plate were seeded with HFF host cells and detected by PCR and Western blotting. Diagnostic PCRs (PCR1, PCR2, and PCR3) were used to screen individual clone. PCR reactions were performed using Taq DNA polymerase in a 25-μl reaction mixture containing 1 μl genomic DNA extracted from a single clone as templates. Subsequently, the products were examined by agarose gel electrophoresis. Rabbit polyclonal antibody against ROP18 and antibody against ROP16 was prepared in the laboratory. The invasion of WH3 WT or WH3Δ*rop16* strain in HFF cells were visualized after 48 h by Giemsa staining and the average number of tachyzoites per parasitophorous vacuole (PV) was obtained by counting 50 PVs in triplicate experiments. C57BL/6 mice were infected with 1×10^3 tachyzoites of WH3 WT or WH3Δ*rop16,* respectively. The animals were monitored daily for manifestations following infection and the survival rate was recorded.

Cells and Co-Culture System

Mouse peritoneal macrophages were acquired by washing the peritoneal cavity three times with ice-cold D-Hanks solution. Mouse peritoneal macrophages were cultured and suspension cells were washed off 24 h later. The transwell culture plates (Corning, Corning, NY, USA), were used to establish a co-culture system. Generally, the pore size of the bottom of the inserts is 0.4 μm, which allowed the passage of only small and soluble particles rather than cells and tachyzoites. Control macrophages (1×10^6) and WH3 WT (1×10^6) or WH3Δ*rop16* (1×10^6) tachyzoites infected macrophages were added to the upper well separately. The C57BL/6 primary placental trophoblasts (1×10^6) were co-cultured in the lower wells in 5% CO_2 at 37°C for 24 h. The co-culture system was kept in 1 ml of RPMI 1640 culture medium supplemented with 10% FBS and 1% penicillin/streptomycin. After co-culturing for 24 h, the macrophages were harvested for total RNA and culture supernatants were collected to analyze NO and TNF-α. The placental trophoblasts were collected for detection of apoptosis by flow cytometry (FCM). The apoptosis rates of trophoblasts cells were calculated as the sum of early and late apoptosis rates. The trophoblasts cells washed twice with cold PBS, and resuspended cells in 1 × binding buffer. The trophoblast cells were subjected to FITC annexin V and PI followed by gentle vortex, incubated for 15 min at 25°C in the dark and analyzed by FCM within 1 h.

Establishment of Animal Pregnant Model

The 6- to 8-week-old female and 8- to 10-week-old male C57BL/6 mice were purchased from the Animal Center of Anhui Medical University (AMU) and had free access to sterilized water and food under standard conditions, and permitted to adapt for 1 week before the experiment. The mice were treated in compliance with the Chinese National Institute of Health Guide for the Care and Use of Laboratory Animals.

TABLE 1 | Primers used in this study.

Primers	Sequence	Used for
5′-ROP16-guide RNA (gRNA)	GTGGCAGCGCGTTTTAGAGCTAGAAATAGCAAG	Q5 mutagenesis changing the gRNA in
3′-ROP16-gRNA	CGGTGCGTCCAACTTGACATCCCCATTTAC	pSAG1:CAS9-U6:sgUPRT to gRNA-ROP16
UpROP16 F	AAAACGACGGCCAGTGAATTCAGTTTGAATCTCTGGGTAGAACAGC	To produce UpROP16 PCR product for
UpROP16 R	GGGGGTGAAAATCGAATGACACTGCCCCTGAGTCGAGCCAC	making pROP16:DHFR-I
DHFR-TS F	TGTCATTCGATTTTCACCCCC	To produce DHFR PCR product for
DHFR-TS R	TCCTCCGCTCCTCTCTAGCAGGATCGATCCCCCCGGGCTGC	making pROP16:DHFR-I
DnROP16 F	GCAGCCCGGGGGGATCGATCCTGCTAGAGAGGAGCGGAGGA	To produce DnROP16 PCR product for
DnROP16 R	GACCATGATTACGCCAAGCTTGCTCCGCAGTCTCTGTAAGT	making pROP16:DHFR-I
5′-UpROP16	TGTGATGCTGAGTCTTGCGAGT	PCR1
5′-InDHFR	TACCAGTCATGGACGAGATCG	
3′-InDHFR	ACACGCATGTCTACACGAACC	PCR2
3′-DnROP16	TGGTGGTTGCGACTGGACTA	
5′-InROP16	ATGAAAGTGACCACGAAAGG	PCR3
3′-InROP16	CTACATCCGATGTGAAGAAAGTT	

All procedures were followed strictly according to the ethical standards formulated by Institutional Review Board of AMU Institute of Biomedicine AMU (permit No: AMU26-081108). After 1 week of adaptation to the new environment, females were housed overnight with males (2 females for 1 male). The presence of vaginal plugs on the second day was designated day 0 of gestation (GD 0). Briefly, all pregnant mice were divided into three equal groups randomly (WH3 WT group, WH3Δ*rop16* group, and control group) with five mice in each. On gestation GD8, pregnant mice were intraperitoneally injected with 4×10^2 WH3 WT and WH3Δ*rop16* tachyzoites in 200 μl sterile PBS, and the control was exposed to only 200 μl sterile PBS at the same time. All mice were sacrificed with euthanasia on GD14, the uteruses were moved away and implantation and resorption sites were recorded. The resorption sites were defined by their small sizes, necrotic, and hemorrhagic appearance of placentas and embryos. The ratio of resorption sites to total implantation sites was calculated as the percentage of fetal loss.

The experiments that are related to using viable parasites and animal infections were performed in the AMU Biosecurity II Laboratory licensed by the local health administrative department.

Preparation of Single Cell Suspension

The placentas, uterine tissues, and spleens of experimental mice were removed aseptically. The spleen tissues were placed in a sterile nylon mesh gently. The cells were harvested after mashing through sterile nylon gauze and lysed with erythrocyte lytic buffer and cultured in RPMI 1640 supplemented with 10% FBS. At the same time, the placentas and the uterus were placed in the dish and cut into pieces followed by washing thoroughly and the shredded tissue was moved to a 50 ml centrifuge tube. The tissues digested with 2.5 mg/ml collagenase IV, 10% FBS, and 10 mM HEPES sodium salt dissolved in RPMI 1640 and then incubated at 37°C for 30 min with gentle shaking. The suspension cells were filtered through sterile nylon mesh to take away undigested tissue. The mononuclear cells were collected by discontinuous 70%/40% Percoll (GE Healthcare Life Sciences) density gradient centrifugation.

FCM Analysis of Lymphocytes

Lymphocytes from spleens, placentas, and uterine tissues were regulated to the appropriate cell number (1×10^6/ml) and cultivated in 6-well plate in 2 ml of RPMI 1640 medium supplemented with 10% FBS. For intracellular cytokine staining, ionomycin (1 mg/ml) and PMA (20 ng/ml) were used to stimulate the cells for 5 h in the presence of brefeldin A (1 mg/ml). The cells were subjected to FITC-labeled anti-mouse CD4 for 30 min at 4°C to avoid the light and were washed twice, and fixed with the Cytofix/Cytoperm kit according to manufacturer's instructions. The cells were incubated for 1 h at 4°C in the dark and were washed twice, and PE-labeled anti-mouse IL-17A, APC-labeled anti-mouse IL-4, and Percp-cy5.5-labeled anti-mouse IFN-γ were used for staining of intracellular cytokines, respectively. Tregs were marked by the FITC-labeled anti-mouse CD4 and APC-labeled anti-mouse CD25 for 30 min at 4°C in the dark and were washed twice. After surface staining, the cells were fixed and permeabilized in 1 × Fix/Perm buffer at 4°C for 1 h in the dark and washed twice, followed by PE-labeled anti-mouse Foxp3 staining at 4°C for 30 min in protection from light. After washing, the cells were analyzed on FCM.

RNA Extraction and qRT-PCR

Total RNA from the co-cultured cells, spleens, and placentas were extracted using TRIzol (Invitrogen Life Technologies, Carlsbad, CA, USA) and transcribed into cDNA using Takara Kit (Takara, Japan) following the manufacturer's instructions. The quantitative analysis was performed by testing expression of iNOS, TNF-α, IFN-γ, IL-12, IL-17A, IL-10, and TGF-β1 using SYBR Premix Ex Taq kit (Takara, Japan) by the Light Cycler 480. The glyceraldehyde-3-phosphate dehydrogenase (GAPDH) was used to normalize the results. The relative mRNA expression was counted with the comparative ΔCt method using the formula $2^{-\Delta\Delta Ct}$. The qRT-PCR was conducted in technical triplicates by using the sense and antisense primers listed in **Table 2**.

Enzyme-Linked Immunosorbent Assay

The co-cultured supernatants were obtained for TNF-α detection by ELISA. To detect cytokines in splenocyte supernatants, we used the ionomycin (1 mg/ml) and PMA (20 ng/ml) to stimulate the splenocyte cells (2×10^6) in 6-well plate in 2 ml/well of RPMI 1640 medium supplemented with 10% FBS for 5 h. Splenocyte supernatants were collected and subjected to examination for IFN-γ, IL-12, IL-17A, IL-10, and TGF-β1 by ELISA. Accurately weighed placenta tissues were homogenized with a ratio of 1 mg of placental tissues to 10 μl of PBS and centrifuged at 12,000 *g* at 4°C for 30 min. The supernatants of the tissue lysates were gathered and equal volume of the supernatants was added to each well. The cytokines of IFN-γ, IL-12, IL-17A, IL-10, and TGF-β1 were detected by ELISA according to the manufacturer's protocols. Three duplicate wells were set up for each group. The absorbance was measured at 450 nm on the ELISA plate reader (Biotek, Winooski, VT, USA).

Nitrite Detection

The co-cultured supernatant was collected for examination of nitrite oxide (NO). It was detected using the Griess Reagent

TABLE 2 | The primers used for qRT-PCR.

Primers	Forward primer (5′–3′)	Reverse primer (5′–3′)
TNF-α	ACGGCATGGATCTCAAAGAC	GTGGGTGAGGAGCACGTAGT
iNOS	CACCTTGGAGTTCACCCAGT	ACCACTCGTACTTGGGATGC
IFN-γ	AGCAAGGCGAAAAAGGATGC	TCATTGAATGCTTGGCGCTG
IL-12	GATGTCACCTGCCCAACTG	TGGTTTGATGATGTCCCTGA
IL-10	GCTCCTAGAGCTGCGGACT	TGTTGTCCAGCTGGTCCTTT
TGF-β1	CTGGATACCAACTACT GCTTCAG	TTGGTTGTAGAGGGCAAGG ACCT
IL-17A	TCTCTGATGCTGTTGCTGCT	CGTGGAACGGTTGAGGTAGT
GAPDH	CAACTTTGGCATTGTGGAAGG	ACACATTGGGGGTAGGAACAC

GAPDH, glyceraldehyde-3-phosphate dehydrogenase; IFN, interferon; IL, interleukin; iNOS, inducible nitric synthase; TNF, tumor necrosis factor; TGF-β1, transforming growth factor beta 1.

system as previously described (36) following the manufacturer's instruction. The absorbance was measured at 550 nm on an ELISA plate reader.

Statistical Analysis

The experimental data acquired were subjected to statistical analyses using one-way ANOVA and paired *t*-test after precheck of the data for homogeneity of variances. Statistical significance was defined by using GraphPad Prism Software, and $P < 0.05$ was regarded as significant. The results were presented as mean ± SD, which gives a summary of the data from at least three times experiments.

RESULTS

The WH3Δ*rop16* Strain of *T. gondii* Type Chinese 1 Was Constructed Using CRISPR/Cas9 Technology

The CRISPR/Cas9 strategy was used to inactivate ROP16 by inserting pyrimethamine-resistant DHFR (DHFR*) followed by PCR identification of a single clone (**Figure 1A**). PCR identification proved that DHFR coding sequence was successfully inserted to the target position (**Figure 1B**). Western blotting analysis showed no expression of ROP16$_{I/III}$ protein by WH3Δ*rop16* strain (**Figure 1C**). Giemsa staining results indicated that less number of parasites (13 tachyzoites vs 22 tachyzoites) per PV in WH3Δ*rop16* infected cells compared to WH3 WT-infected cells, respectively ($p < 0.05$) (**Figure 1D**). Virulence examination indicated that all animals infected by both strains died on day 12 post-infection (**Figure 1E**) and no difference of the virulence to mice was noted between WH3 WT and WH3Δ*rop16* strains.

WH3Δ*rop16* Strain Infection Drove Macrophages to M1 and Lead to Trophoblast Apoptosis

Compared to the WH3 WT group, macrophages infected with WH3Δ*rop16* strain produced a higher level of NO, iNOS, and TNF-α (**Figures 2A,B**). To elucidate the placental trophoblasts apoptosis, we detected cell apoptosis of placental tissues by fluorescein isothiocyanate/propidium iodide (FITC/PI) staining assay. Compared to the WH3 WT group, the number of total, early, and late apoptotic cells of trophoblasts was elevated when co-cultured with WH3Δ*rop16* strain-infected macrophages for 24 h (**Figure 2C**). The remarkable apoptosis of trophoblasts caused by WH3Δ*rop16* strain was observed (**Figure 2D**).

WH3Δ*rop16* Strain Infection Induced Adverse Pregnancy

Most samples of the pregnant uteruses showed significant fetal resorption and placental hemorrhage in the mice

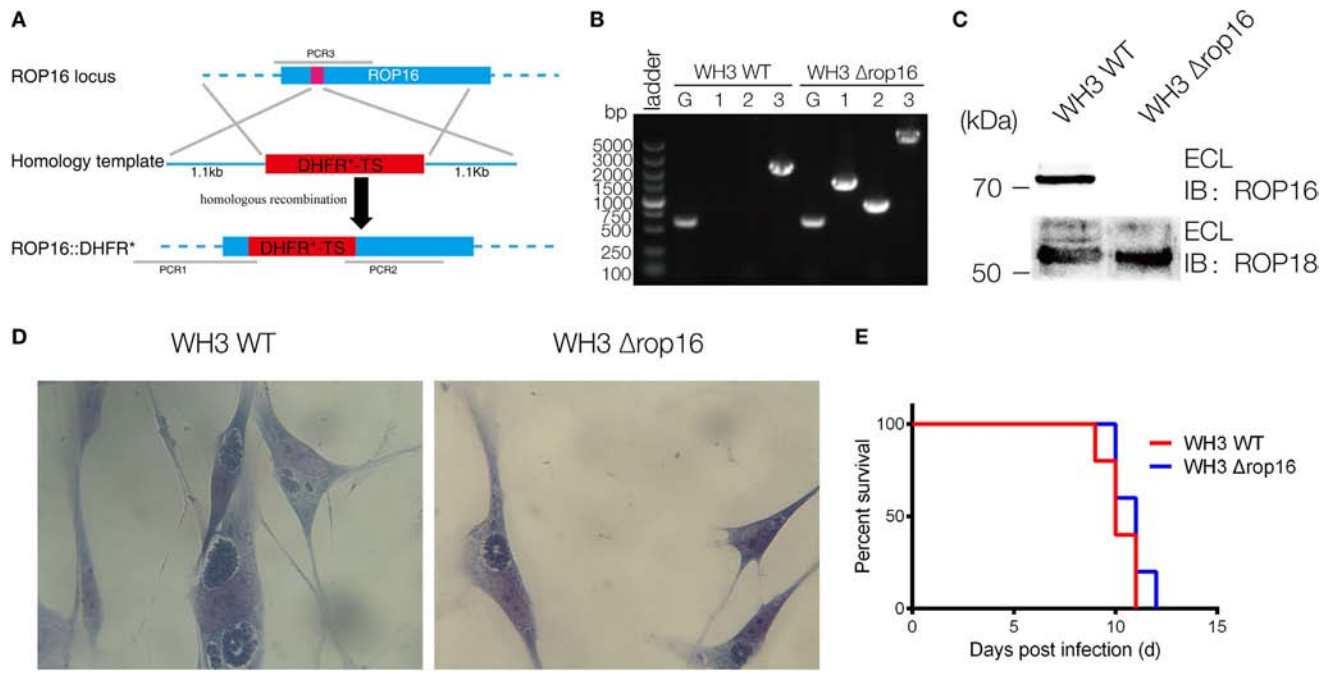

FIGURE 1 | Construction of the WH3Δ*rop16* strain of *Toxoplasma gondii* type Chinese 1 by using CRISPR-Cas9 technology. **(A)** Schematic of CRISPR/CAS9 strategy for inactivation of *rop16* by inserting pyrimethamine-resistant DHFR (DHFR*) and PCR identification of single clone. **(B)** PCR identification of WH3Δ*rop16 T. gondii* strain. G represents the GRA1 promoter positive control, as shown in **Figure 1A**. 1: PCR1 fragment; 2: PCR2 fragment, 3: PCR3 fragment. PCR1 and PCR2 examined the integration of DHFR-TS* into corresponding genes, and PCR3 checked the deletion of ROP16 sequences. **(C)** Western blotting for detection of ROP16 expression in WH3 WT and WH3Δ*rop16*. Rabbit polyclonal antibody against ROP18 was used as the control. **(D)** The number of parasites per parasitophorous vacuole of WH3Δ*rop16* or WH3 WT. **(E)** Mouse survival after inoculation with *T. gondii* tachyzoites.

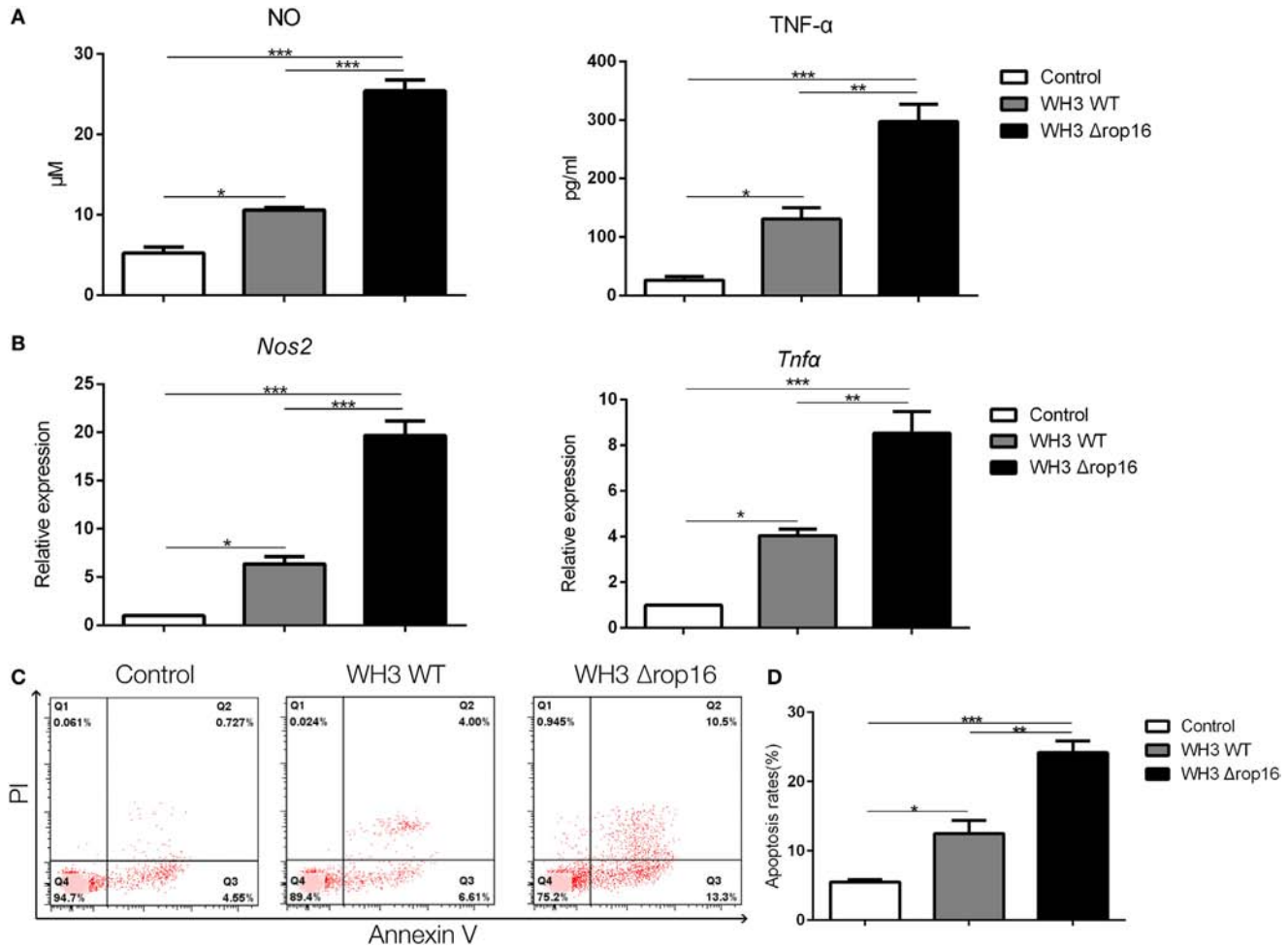

FIGURE 2 | The high production of nitrite oxide (NO), inducible nitric synthase (iNOS), and tumor necrosis factor (TNF)-α and apoptosis of trophoblasts co-cultured with macrophages infected with the WH3Δ*rop16* tachyzoites. **(A)** The culture supernatants were collected and analyzed for NO and TNF-α production. **(B)** The relative mRNA expressions of iNOS and TNF-α after co-culture. **(C)** Increased apoptosis of trophoblasts co-cultured with WH3Δ*rop16* infected macrophages. **(D)** Total, early, and late apoptosis of placental trophoblasts (*$p < 0.05$, **$p < 0.01$, ***$p < 0.001$).

infected with the tachyzoites of WH3Δ*rop16* in comparison with the WH3 WT group (**Figures 3A,B**). The weights of fetuses, placentas, and rate of fetal loss were determined at day 6 post infection. The weight loss of fetuses and placentas was observed and the rate of fetal loss significantly increased in mice infected with WH3Δ*rop16* strain compared to WH3 WT strain (**Figure 3C**).

WH3Δ*rop16* Strain Infection Induced Immune Bias to Th1 in the Spleens and Placentas of Pregnant Mice

We examined the IFN-γ in the lymphocytes of the spleen and placenta tissues using FCM to investigate the immune bias at maternal–fetal interface of the pregnant mice after *T. gondii* infection. The expression of IFN-γ and IL-12 were analyzed using qRT-PCR and ELISA in the spleens and placentas. Compared to WH3 WT group, Th1 subsets ($CD4^+IFN\gamma^+$) of WH3Δ*rop16* inoculated mice were remarkably elevated (**Figures 4A,B**). The data were further confirmed by using qRT-PCR and ELISA (**Figures 4C–F**). Consistent with the IFN-γ assay, the expression of IL-12 (**Figures 4C–F**) was synchronously increased in the mice of WH3Δ*rop16* infection.

Th17 Response Was Upregulated in the Spleens and Placentas of the Pregnant Mice Infected With WH3Δ*rop16* Strain

We examined the Th17 cytokine ($CD4^+IL\text{-}17A^+$) in the spleens and placentas in the three groups of mice by FCM and found that the mice infected with WH3Δ*rop16* strain exhibited a high expression of IL-17A (**Figures 5A,B**). The level of IL-17A mRNA expression in WH3Δ*rop16* group was significantly increased when compared to WH3 WT (**Figures 5C,D**), which is in parallel with the result of IL-17A detection in supernatants by ELISA (**Figures 5C,D**).

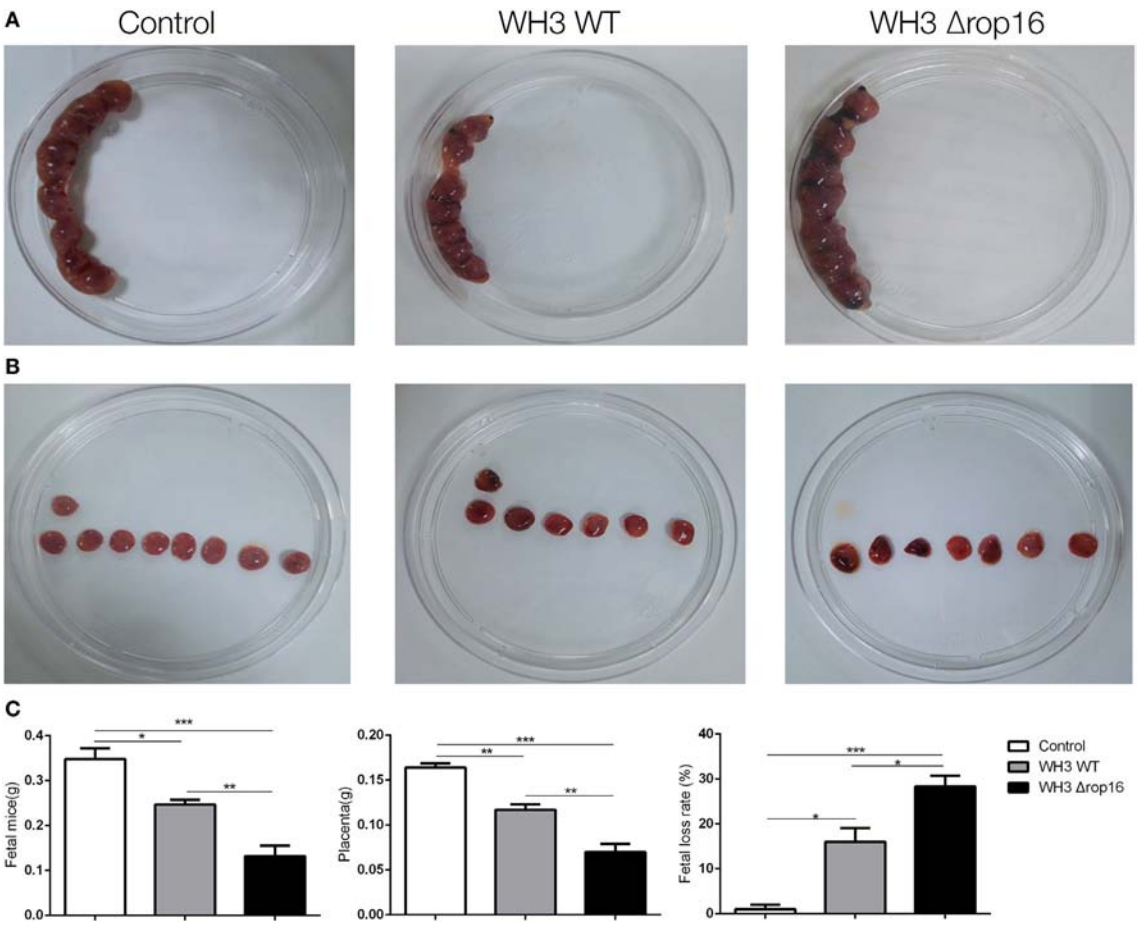

FIGURE 3 | *Toxoplasma gondii* infection induced adverse pregnancy outcomes in mice. **(A,B)** The uteruses of WH3Δ*rop16*-infected mice presented notable fetal resorption and placental bleeding in comparison with the WH3 WT group. **(C)** The weights of fetuses, placentas, and rate of fetal loss were measured at day 6 post infection. The fetal loss rate was calculated by ratio of resorption sites to the total number of implantation sites. (*$p < 0.05$, **$p < 0.01$, ***$p < 0.001$).

Percentage of Tregs Decreased in the Spleens and Placentas of the Pregnant Mice Following WH3Δ*rop16* Strain Infection

To clarify whether the mutant WH3Δ*rop16* strain infection can negatively affect the Tregs population, we detected the percentage of Tregs in the splenocytes and the cells isolated from the placentas of pregnant mice by FCM (**Figures 6A,B**). The results revealed that Tregs were significantly dampened in WH3Δ*rop16*-infected mice. Accordingly, relative mRNA expression of IL-10 and TGF-β1 in the spleens (**Figure 6C**) and placentas (**Figure 6D**) was synchronously reduced in WH3Δ*rop16* group compared to WH3 WT group. In addition, the levels of IL-10 and TGF-β1 in the spleens (**Figure 6E**) and placentas (**Figure 6F**) remarkably declined in the WH3Δ*rop16*-infected mice when compared to WH3 WT mice.

Compared to the WH3 WT-infected C57BL/6 pregnant mice, the animals inoculated with WH3Δ*rop16* tachyzoites presented a diminished expression of IL-4 determined by FCM (**Figures 7A,B**).

DISCUSSION

Toxoplasma gondii is one of the common causative agent of prenatal infections during pregnancy (15, 16). The parasite may be transmitted vertically by tachyzoites that are passed to the fetus *via* the placenta, leading to miscarriages, stillbirths, and other adverse pregnant outcomes depending on the stage of the pregnancy at which infection takes place (37). Most strains which infect humans in Europe are type II and a large proportion of cases of congenital toxoplasmosis are asymptomatic at birth if the mother acquired the infection after the second trimester of gestation (38). It has been well recognized that vertical transmission of the parasite, particularly type I virulent strain of *Toxoplasma* with superior migratory capacity, may directly cause abnormal pregnancy. However, the non-virulent strains such as PRU or ME49 may induce a decrease in the fertility if infection occurs during the later phase of gestation (39). Previous studies indicated that neither parasites nor their DNAs are detectable in the diseased tissue samples of some abnormal pregnancies and we attempted to examine the parasite by bioassay or its derived DNAs by PCR from placentas and tissues of aborted fetuses in the

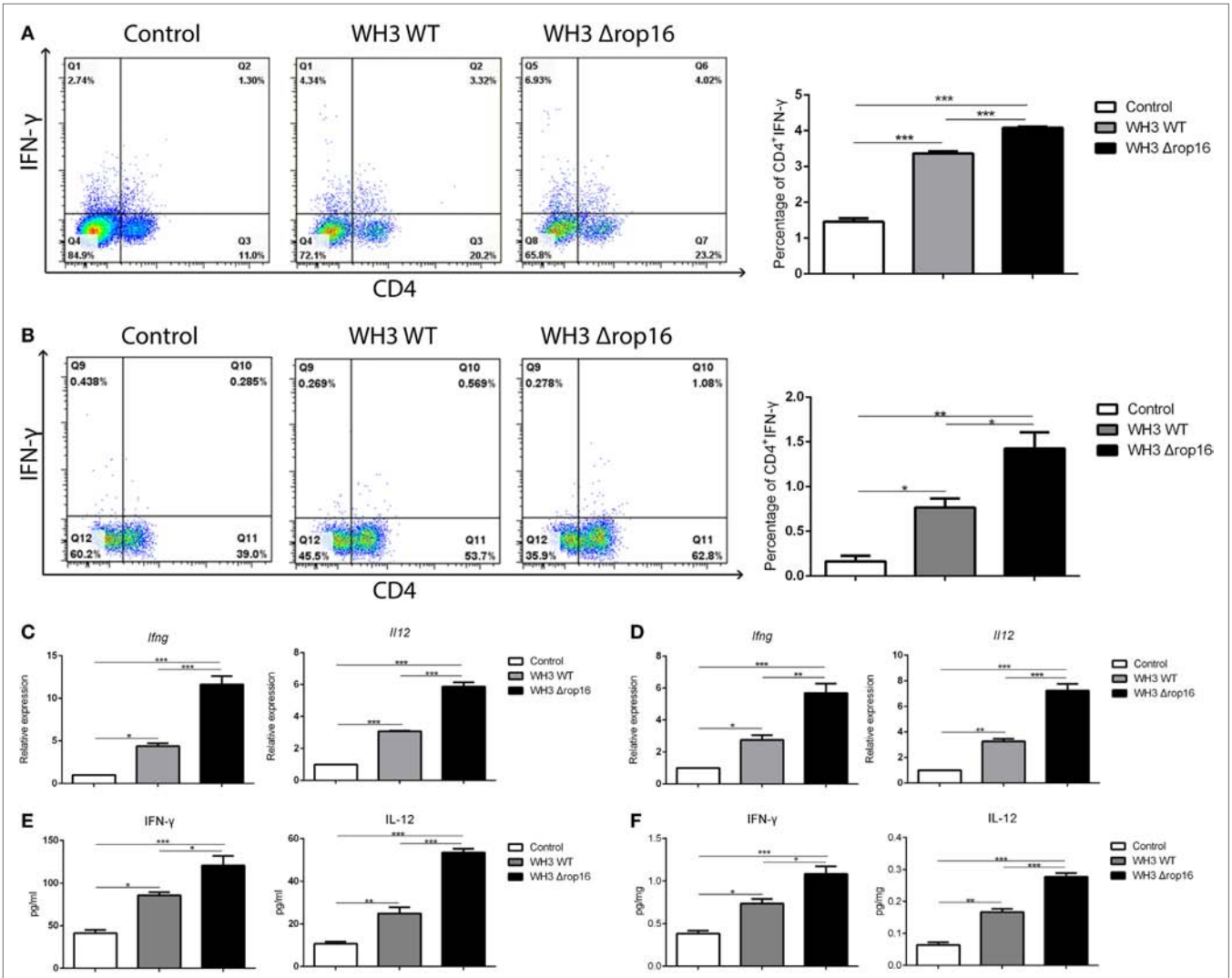

FIGURE 4 | WH3Δ*rop16* strain infection upregulated Th1 response of pregnant mice. Increased percentage of Th1 ($CD4^+IFN\gamma^+$) cell population in the spleens **(A)** and placentas **(B)** of WH3Δ*rop16* tachyzoites compared to the control. The relative mRNA expressions of interferon (IFN)-γ and interleukin (IL)-12 were sharply increased in the spleens **(C)** of WH3Δ*rop16*-infected mice and placentas **(D)**. The supernatants were tested for IFN-γ and IL-12 in the spleens (pg/ml) **(E)** and placentas (pg/mg) **(F)** by enzyme-linked immunosorbent assay (*$p < 0.05$, **$p < 0.01$, ***$p < 0.001$).

pregnant women, some of whom showing positive IgG antibodies against *Toxoplasma*, but no positive results were obtained (data not shown). Consistent results were also reported by Senegas in murine model (40). All of these data imply that the resorption, abortion, or fetal damage might be indirectly due to lesions of the placenta induced by maternal biased immunity such as Th1/IFN-γ polarized immune response (41) and that the maternal immunity-associated but not viable parasite-generated "sterile" pathology actually takes place in abnormal pregnant consequences caused by *Toxoplasma* infection. Herein, we focused on the maternal immunity associated rather than the mother-to-child vertical transmission causative adverse outcomes of pregnancy. Our results strongly suggest that the immunity subversion-related pathogenesis is involved in early gestation induced by *T. gondii* but not due to a direct invasion of the parasite in adverse pregnancies.

It has been reported that the consequences of congenital toxoplasmosis vary in genotypes of *Toxoplasma* strain (42). Strains of *T. gondii* from Europe and North America belong to three distinct clonal lineages (type I, type II, and type III) which differ phenotypically in virulence (43, 44). Recent studies revealed that polarization of alternatively activated macrophage (M2) or classically activated macrophage (M1) of host macrophages depends on the polymorphism of ROP16 or GRA15 of *Toxoplasma* at early stage of infection. One site mutation of ROP16 at 503L/S would determine the activity or inactivity of ROP16 in phosphorylation of Stat6/Stat3. Type I and type III strains carry $ROP16_{I/III}$, which strongly drives M2 bias but $ROP16_{II}$ is negligible (30, 45, 46), while type II strains infected macrophages are classically activated through bypassing TLRs and directly activating NF-κB by the dense granule protein $GRA15_{II}$ (28, 30). Interestingly, we found that type Chinese 1 (ToxoDB #9) strains carry both $ROP16_{I/III}$

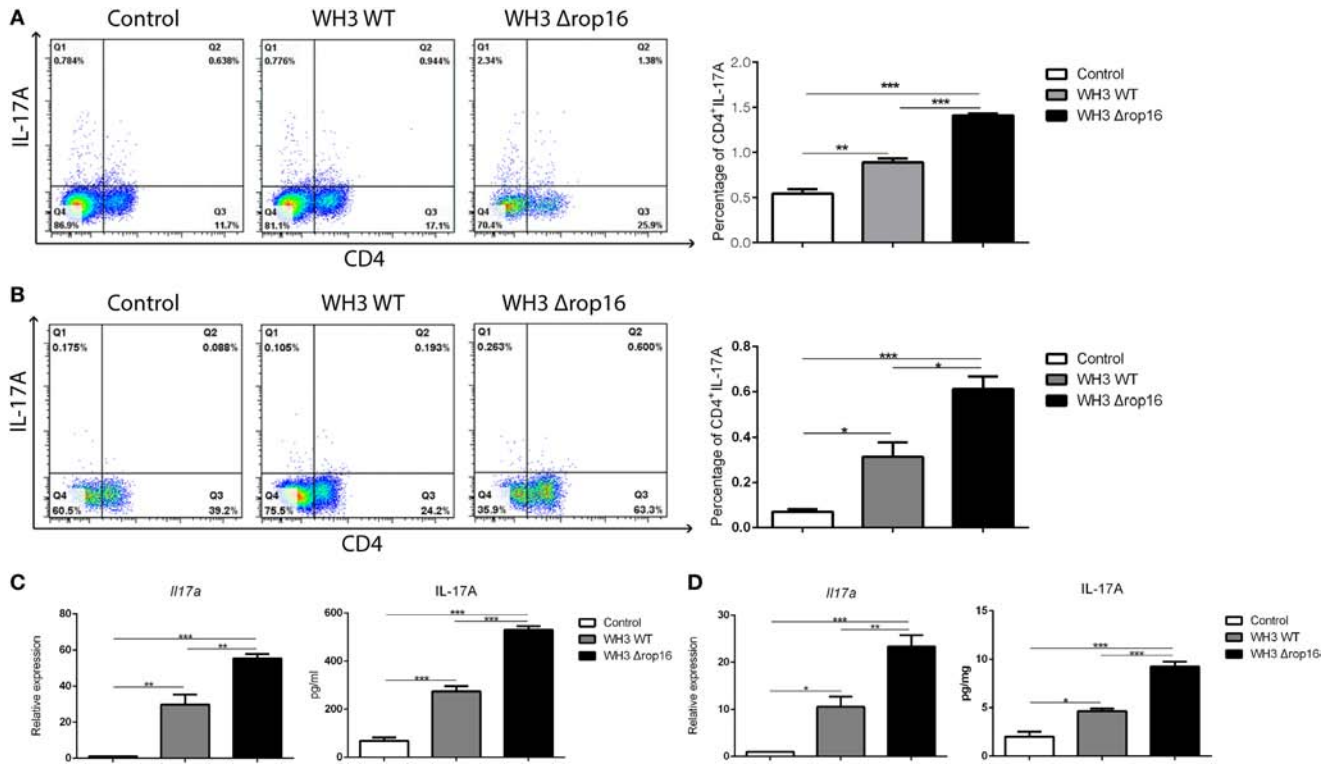

FIGURE 5 | WH3Δ*rop16* strain infection upregulated Th17 response in the spleens and placentas of the pregnant mice. The mice infected with WH3Δ*rop16* strain expressed a high level of interleukin (IL)-17A in the spleens **(A)** and placentas **(B)** determined by flow cytometry. IL-17A mRNA expression in the animals infected with WH3Δ*rop16* in the spleens **(C)** and placentas **(D)**. The IL-17A in the supernatants of spleens (pg/ml) **(C)** and placentas (pg/mg) **(D)** confirmed by enzyme-linked immunosorbent assay (*$p < 0.05$,**$p < 0.01$,***$p < 0.001$).

and GRA15$_{II}$ (33, 34). Thus, we postulated that Chinese 1 strains might have immunopathogenesis which is distinct from the archetypical strains circulating in the other parts of the world. Herewith, we constructed *T. gondii* WH3Δ*rop16* strain based on CRISPR/Cas9 strategy. The genetically manipulated parasite WH3 strain with *rop16$_{I/III}$*-deficient and *gra15$_{II}$*-dominant background (WH3Δ*rop16*/*gra15$_{II}$*), which resembles the archetypical type II of European/North American strains, may be prone to induce adverse pregnant outcomes *via* the mechanism of subverting maternal immunotolerance. We noted that WH3Δ*rop16*/*gra15$_{II}$* efficiently *in vitro* drove macrophage polarization toward M1 cells, producing NO, TNF-α, and iNOS, and gave rise to trophoblast cells apoptosis compared to WH3 WT strain. We also found that the WH3Δ*rop16*/*gra15$_{II}$* strain induced characteristic Th1-biased and Th17-involved inflammatory response *in vivo* at maternal–fetal interface featured by high expression of IFN-γ and IL-12, and resulted in more severe adverse pregnant consequences in murine model. These results suggest that ToxoGRA15$_{II}$ is one of the key factors involved in the imbalance of maternal immune tolerance during pregnancy which is associated with M1/Th1/Th17 skewed response. These results are in correspondence with the findings previously reported. Surely, in addition to GRA15$_{II}$, other *Toxoplasma*-derived effectors of type Chinese 1 strain may also contribute to the pathology of immunity imbalance in pregnant animals.

In the construction of the plasmids, insertion of the pyrimethamine resistance gene (dihydrofolate reductase-thymidylate synthase, DHFR-TS*) has been frequently used as the selectable marker for transformant screening of CRISPR/Cas9-based genetic deletion of *Toxoplasma* (35, 47). The DHFR-TS* is not believed to evoke the detectable phenotypical alterations in *Toxoplasma*-infected host, since it is a modified endogenous gene that exists in wild-type strains of the parasite. So far, no evidence has shown its immunogenicity which is able to induce undesirable immune response in its host cells. Moreover, we here did not use ROP16$_{II}$ insertion substituting ROP16$_{I/III}$ because, as stated above, ROP16$_{I/III}$, rather than ROP16$_{II}$, decides ROP16 kinase activity on Stat6/Stat3 and induces M2 polarization which is pivotal to M2 and subsequent Th2 response (45, 46). We deleted ROP16$_{I/III}$ in order to generate a GRA15$_{II}$ dominant transformant to explore the pathology of adverse pregnancy and the mechanisms of pathogenesis caused by the atypical strain of Chinese 1 epidemic in China.

Despite of expressing paternal antigens, the human allogenic fetus is histocompatible with the maternal immune system, presenting an immune down-modulation on CD8$^+$ T cells, Th1, and Th17 cells, which contributes to creation of an immune-privileged environment at the maternal–fetal interface. Previous investigations indicated that microbial endotoxin (LPS) administration to pregnant mice prior to delivery (16.5 day post

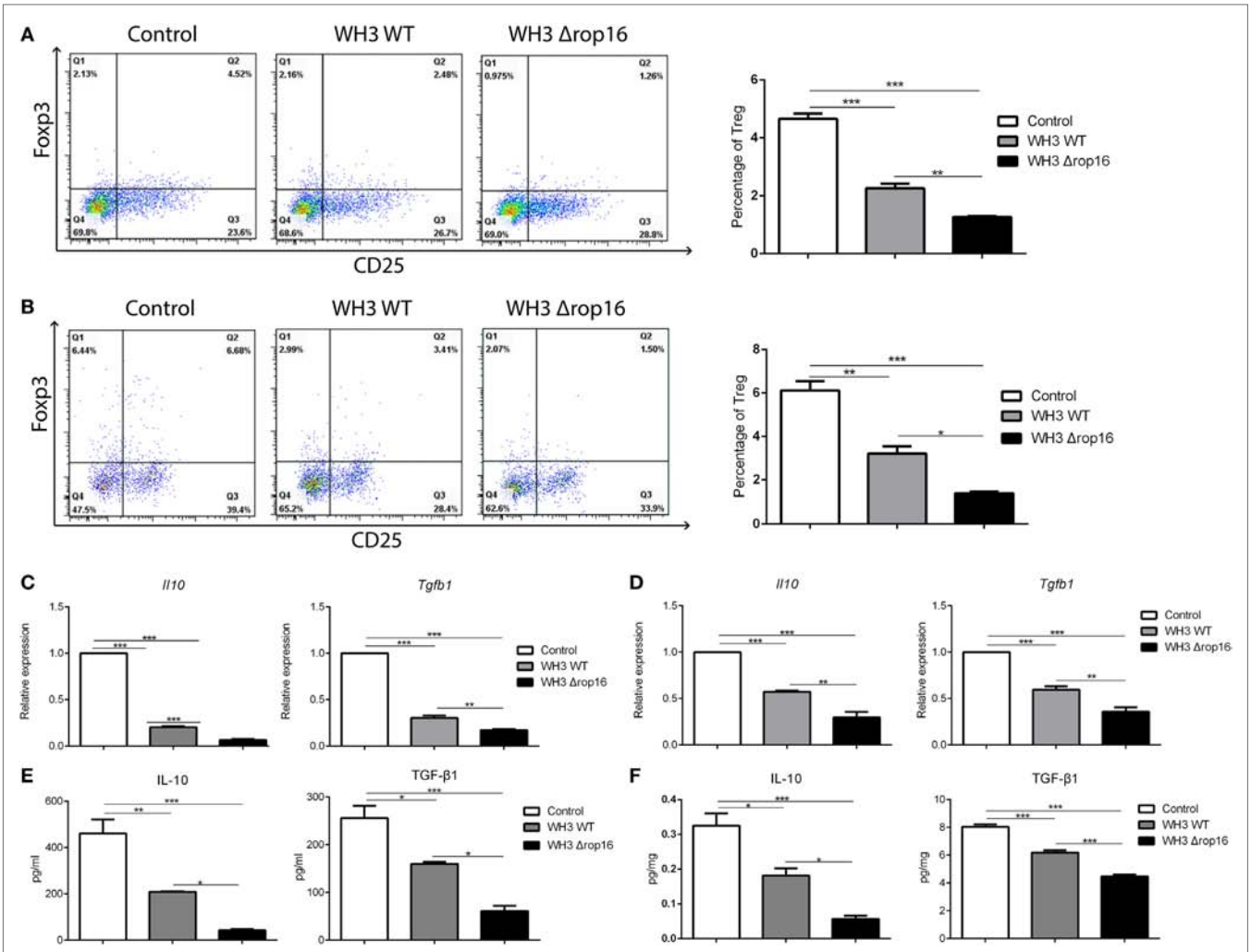

FIGURE 6 | *Toxoplasma* WH3Δ*rop16* strain infection induced impairments of T regulatory cells (Tregs). Tregs cell population in the spleens **(A)** and placentas **(B)** were detected by flow cytometry. Tregs number was significantly decreased in WH3Δ*rop16* infected group compared to control group. The relative mRNA expressions interleukin (IL)-10 and transforming growth factor beta 1 (TGF-β1) in the spleens **(C)** and placentas **(D)** were markedly reduced in WH3Δ*rop16* group. The levels of IL-10 and TGF-β1 in the spleens (pg/ml) **(E)** and placentas (pg/mg) **(F)** were significantly decreased in the group of WH3Δ*rop16* (*$p < 0.05$, **$p < 0.01$, ***$p < 0.001$).

coitum) causes a Tregs and Th17 cells involved imbalance at the maternal–fetal interface and in the spleen, inducing preterm labor (48). However, we found that mice infected with the WH3Δ*rop16/gra15II* strain at the early stage (seventh day of fertility) presented remarkable manifestations of adverse pregnant results, indicating that the mutant strain infection of *Toxoplasma* may lead to abnormal pregnant outcomes in which Tregs and Th17 cells are also involved. Various types of immune cells, such as Tregs, play a pivotal role in the maintenance of normal gestation (11, 49–52). Our study revealed that the percentage of Tregs and expression of IL-10 and TGF-β1 by Tregs as well as M2 cells were significantly diminished in the spleen and placenta tissues of early phase and metaphase of pregnancy of mice infected with the WH3Δ*rop16/gra15$_{II}$* strain, which is consistent with the previous reports of low expression of IL-10 and TGF-β1 cytokines in mice with a high incidence of fetal rejection (53). This result demonstrates that the impairment of Tregs takes place in *T. gondii*-infected pregnant mice, particularly in mice infected with the strain of WH3 Δ*rop16/gra15$_{II}$*.

A growing body of evidence indicates that Th17 cells are involved in infiltrative inflammation in patients with recurrent spontaneous abortions (54). The imbalance of Tregs/Th17 has also been seen in human abortions (54, 55). Our previous work revealed that *T. gondii* type II strain-derived molecule of ToxoGRA15$_{II}$ is responsible for inducing M1 polarization of RAW264.7 cells *via* NF-κB activation (29, 56) eliciting host innate immunity and Th1-dominant and Th17-involved inflammatory response, and adverse pregnancy outcomes in mice (data in manuscript). Here, we also noted that expression of Th1 cytokines and IL-17A in splenocytes and placenta tissues was observably elevated in the pregnant animals infected with WH3Δ*rop16/gra15$_{II}$* strain

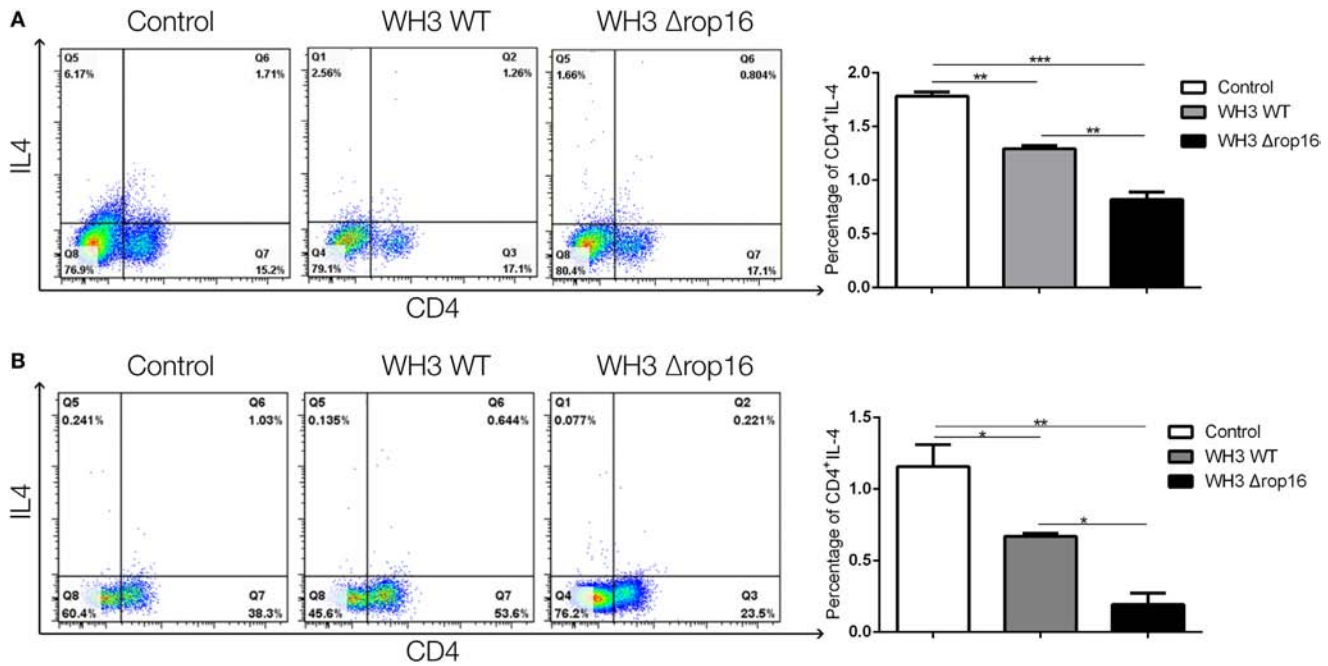

FIGURE 7 | *Toxoplasma* WH3Δ*rop16* strain infection downregulated Th2 response of pregnant mice. The expression of IL-4 in WH3Δ*rop16* group in the spleens **(A)** and placentas **(B)** compared to the control group determined with flow cytometry (*$p < 0.05$, **$p < 0.01$, ***$p < 0.001$).

of type Chinese 1 (**Figures 4** and **5**), implying a direct involvement of increased Th17 cells in fetal loss. Additional studies are on going to explore the IFN-γ/NK-involved mechanism at the maternal–fetal interface in abnormal pregnancies associated with *T. gondii* infection.

In summary, our data demonstrate that WH3Δ*rop16* strain with GRA15$_{II}$ background of *T. gondii* type Chinese 1 may cause subversion of immune tolerance at the maternal–fetus interface and in systemic immunity, leading to adverse pregnancy outcomes, which is associated with the Th1 and Th17 biased response. This study would provide an explanation for pregnancy failure caused by non/less virulent strains of type II and offer a deep insight into the pathogenesis of abnormal pregnancy caused by strains of *T. gondii* type Chinese 1 dominating in China.

ETHICS STATEMENT

The mice were treated in compliance with the Chinese National Institute of Health Guide for the Care and Use of Laboratory Animals. All procedures were followed strictly according to the ethical standards formulated by Institutional Review Board of Anhui Medical University Institute of Biomedicine (permit no: AMU26-081108).

AUTHOR CONTRIBUTIONS

JS and CW conceived and designed the experiments. CW, WC, QY, and TX performed the experiments. WC, CW, and JS drafted the manuscript. All authors contributed to discussion of the results followed by writing and reviewing the manuscript.

ACKNOWLEDGMENTS

The pSAG1:CAS9-U6:sgUPRT was gifted by David Sibley at Washington University School of Medicine, USA. The pDHFR-TS plasmid was a gift from Honglin Jia in Harbin Veterinary Research Institute of Chinese Academy of Agricultural Sciences, China.

FUNDING

The work was funded by the National Key R&D Program of China (No. 2017YFD0500400), the National Science Foundation of China (No. 81471983), the National Basic Research Program of China (No. 2010CB530001), and the Natural Science Foundation of China(NSFC funding NO.81572801).

REFERENCES

1. Sacks GP, Studena K, Sargent K, Redman CW. Normal pregnancy and preeclampsia both produce inflammatory changes in peripheral blood leukocytes akin to those of sepsis. *Am J Obstet Gynecol* (1998) 179(1):80–6. doi:10.1016/S0002-9378(98)70254-6
2. Trowsdale J, Betz AG. Mother's little helpers: mechanisms of maternal-fetal tolerance. *Nat Immunol* (2006) 7(3):241–6. doi:10.1038/ni1317
3. Saito S, Sakai M, Sasaki Y, Tanebe K, Tsuda H, Michimata T. Quantitative analysis of peripheral blood Th0, Th1, Th2 and the Th1: Th2 cell ratio during normal human pregnancy and preeclampsia. *Clin Exp Immunol* (1999) 117(3):550–5. doi:10.1046/j.1365-2249.1999.00997.x

4. Huppertz B, Kadyrov M, Kingdom JC. Apoptosis and its role in the trophoblast. *Am J Obstet Gynecol* (2006) 195(1):29–39. doi:10.1016/j.ajog.2005.07.039
5. Asseman C, Mauze S, Leach MW, Coffman RL, Powrie F. An essential role for interleukin 10 in the function of regulatory T cells that inhibit intestinal inflammation. *J Exp Med* (1999) 190(7):995–1004. doi:10.1084/jem.190.7.995
6. Santner-Nanan B, Straubinger K, Hsu P, Parnell G, Tang B, Xu B, et al. Fetal-maternal alignment of regulatory T cells correlates with IL-10 and Bcl-2 upregulation in pregnancy. *J Immunol* (2013) 191(1):145–53. doi:10.4049/jimmunol.1203165
7. Zenclussen AC, Gerlof K, Zenclussen ML, Ritschel S, Zambon Bertoja A, Fest S, et al. Regulatory T cells induce a privileged tolerant microenvironment at the fetal-maternal interface. *Eur J Immunol* (2006) 36(1):82–94. doi:10.1002/eji.200535428
8. Maloy KJ, Salaun L, Cahill R, Dougan G, Saunders NJ, Powrie F. CD4+CD25+ T(R) cells suppress innate immune pathology through cytokine-dependent mechanisms. *J Exp Med* (2003) 197(1):111–9. doi:10.1084/jem.20021345
9. Darrasse-Jeze G, Klatzmann D, Charlotte F, Salomon BL, Cohen JL. CD4+CD25+ regulatory/suppressor T cells prevent allogeneic fetus rejection in mice. *Immunol Lett* (2006) 102(1):106–9. doi:10.1016/j.imlet.2005.07.002
10. Lash GE, Otun HA, Innes BA, Kirkley M, De Oliveira L, Searle RF, et al. Interferon-gamma inhibits extravillous trophoblast cell invasion by a mechanism that involves both changes in apoptosis and protease levels. *FASEB J* (2006) 20(14):2512–8. doi:10.1096/fj.06-6616com
11. Piccinni MP, Beloni L, Livi C, Maggi E, Scarselli G, Romagnani S. Defective production of both leukemia inhibitory factor and type 2 T-helper cytokines by decidual T cells in unexplained recurrent abortions. *Nat Med* (1998) 4(9):1020–4. doi:10.1038/2006
12. Mjosberg J, Berg G, Jenmalm MC, Ernerudh J. FOXP3+ regulatory T cells and T helper 1, T helper 2, and T helper 17 cells in human early pregnancy decidua. *Biol Reprod* (2010) 82(4):698–705. doi:10.1095/biolreprod.109.081208
13. Lin H, Mosmann TR, Guilbert L, Tuntipopipat S, Wegmann TG. Synthesis of T helper 2-type cytokines at the maternal-fetal interface. *J Immunol* (1993) 151(9):4562–73.
14. Xu C, Mao D, Holers VM, Palanca B, Cheng AM, Molina H. A critical role for murine complement regulator crry in fetomaternal tolerance. *Science* (2000) 287(5452):498–501. doi:10.1126/science.287.5452.498
15. Montoya JG, Liesenfeld O. Toxoplasmosis. *Lancet* (2004) 363(9425):1965–76. doi:10.1016/S0140-6736(04)16412-X
16. Wong SY, Remington JS. Toxoplasmosis in pregnancy. *Clin Infect Dis* (1994) 18(6):853–61; quiz 862. doi:10.1093/clinids/18.6.853
17. Robbins JR, Zeldovich VB, Poukchanski A, Boothroyd JC, Bakardjiev AI. Tissue barriers of the human placenta to infection with *Toxoplasma gondii*. *Infect Immun* (2012) 80(1):418–28. doi:10.1128/IAI.05899-11
18. Xu X, He L, Zhang A, Li Q, Hu W, Chen H, et al. *Toxoplasma gondii* isolate with genotype Chinese 1 triggers trophoblast apoptosis through oxidative stress and mitochondrial dysfunction in mice. *Exp Parasitol* (2015) 154:51–61. doi:10.1016/j.exppara.2015.04.008
19. Hunter CA, Sibley LD. Modulation of innate immunity by *Toxoplasma gondii* virulence effectors. *Nat Rev Microbiol* (2012) 10(11):766–78. doi:10.1038/nrmicro2858
20. Wang H, Hirsch E. Bacterially-induced preterm labor and regulation of prostaglandin-metabolizing enzyme expression in mice: the role of toll-like receptor 4. *Biol Reprod* (2003) 69(6):1957–63. doi:10.1095/biolreprod.103.019620
21. Fu B, Li X, Sun R, Tong X, Ling B, Tian Z, et al. Natural killer cells promote immune tolerance by regulating inflammatory TH17 cells at the human maternal-fetal interface. *Proc Natl Acad Sci U S A* (2013) 110(3):E231–40. doi:10.1073/pnas.1206322110
22. Zhang H, Hu X, Liu X, Zhang R, Fu Q, Xu X. The Treg/Th17 imbalance in *Toxoplasma gondii*-infected pregnant mice. *Am J Reprod Immunol* (2012) 67(2):112–21. doi:10.1111/j.1600-0897.2011.01065.x
23. Lee SK, Kim JY, Lee M, Gilman-Sachs A, Kwak-Kim J. Th17 and regulatory T cells in women with recurrent pregnancy loss. *Am J Reprod Immunol* (2012) 67(4):311–8. doi:10.1111/j.1600-0897.2012.01116.x
24. Saeij JP, Boyle JP, Coller S, Taylor S, Sibley LD, Brooke-Powell ET, et al. Polymorphic secreted kinases are key virulence factors in toxoplasmosis. *Science* (2006) 314(5806):1780–3. doi:10.1126/science.1133690
25. Taylor S, Barragan A, Su C, Fux B, Fentress SJ, Tang K, et al. A secreted serine-threonine kinase determines virulence in the eukaryotic pathogen *Toxoplasma gondii*. *Science* (2006) 314(5806):1776–80. doi:10.1126/science.1133643
26. Saeij JP, Coller S, Boyle JP, Jerome ME, White MW, Boothroyd JC. *Toxoplasma* co-opts host gene expression by injection of a polymorphic kinase homologue. *Nature* (2007) 445(7125):324–7. doi:10.1038/nature05395
27. Reese ML, Zeiner GM, Saeij JP, Boothroyd JC, Boyle JP. Polymorphic family of injected pseudokinases is paramount in *Toxoplasma* virulence. *Proc Natl Acad Sci U S A* (2011) 108(23):9625–30. doi:10.1073/pnas.1015980108
28. Rosowski EE, Lu D, Julien L, Rodda L, Gaiser RA, Jensen KD, et al. Strain-specific activation of the NF-kappaB pathway by GRA15, a novel *Toxoplasma gondii* dense granule protein. *J Exp Med* (2011) 208(1):195–212. doi:10.1084/jem.20100717
29. Xie Y, Wen H, Yan K, Wang S, Wang X, Chen J, et al. *Toxoplasma gondii* GRA15II effector-induced M1 cells ameliorate liver fibrosis in mice infected with *Schistosomiasis japonica*. *Cell Mol Immunol* (2016) 15(2):120–34. doi:10.1038/cmi.2016.21
30. Jensen KD, Wang Y, Wojno ED, Shastri AJ, Hu K, Cornel L, et al. *Toxoplasma* polymorphic effectors determine macrophage polarization and intestinal inflammation. *Cell Host Microbe* (2011) 9(6):472–83. doi:10.1016/j.chom.2011.04.015
31. Loke P, Allison JP. PD-L1 and PD-L2 are differentially regulated by Th1 and Th2 cells. *Proc Natl Acad Sci U S A* (2003) 100(9):5336–41. doi:10.1073/pnas.0931259100
32. Melo MB, Jensen KD, Saeij JP. *Toxoplasma gondii* effectors are master regulators of the inflammatory response. *Trends Parasitol* (2011) 27(11):487–95. doi:10.1016/j.pt.2011.08.001
33. Cheng W, Liu F, Li M, Hu X, Chen H, Pappoe F, et al. Variation detection based on next-generation sequencing of type Chinese 1 strains of *Toxoplasma gondii* with different virulence from China. *BMC Genomics* (2015) 16:888. doi:10.1186/s12864-015-2106-z
34. Cai Y, Chen H, Mo X, Tang Y, Xu X, Zhang A, et al. *Toxoplasma gondii* inhibits apoptosis via a novel STAT3-miR-17-92-Bim pathway in macrophages. *Cell Signal* (2014) 26(6):1204–12. doi:10.1016/j.cellsig.2014.02.013
35. Shen B, Brown KM, Lee TD, Sibley LD. Efficient gene disruption in diverse strains of *Toxoplasma gondii* using CRISPR/CAS9. *MBio* (2014) 5(3):e01114–01114. doi:10.1128/mBio.01114-14
36. Ding AH, Nathan CF, Stuehr DJ. Release of reactive nitrogen intermediates and reactive oxygen intermediates from mouse peritoneal macrophages. Comparison of activating cytokines and evidence for independent production. *J Immunol* (1988) 141(7):2407–12.
37. Remington JS, McLeod R, Desmonts G. Toxoplasmosis. 4th ed. In: Remington JS, Klein JO, editors. *Infectious Diseases of the Fetus and Newborn Infant*. Philadelphia: WB Saunders (1995). p. 140–267.
38. Dunn D, Wallon M, Peyron F, Petersen E, Peckham C, Gilbert R. Mother-to-child transmission of toxoplasmosis: risk estimates for clinical counselling. *Lancet* (1999) 353(9167):1829–33. doi:10.1016/S0140-6736(98)08220-8
39. Vargas-Villavicencio JA, Cedillo-Pelaez C, Rico-Torres CP, Besne-Merida A, Garcia-Vazquez F, Saldana JI, et al. Mouse model of congenital infection with a non-virulent *Toxoplasma gondii* strain: vertical transmission, "sterile" fetal damage, or both? *Exp Parasitol* (2016) 166:116–23. doi:10.1016/j.exppara.2016.04.002
40. Senegas A, Villard O, Neuville A, Marcellin L, Pfaff AW, Steinmetz T, et al. *Toxoplasma gondii*-induced foetal resorption in mice involves interferon-gamma-induced apoptosis and spiral artery dilation at the maternofoetal interface. *Int J Parasitol* (2009) 39(4):481–7. doi:10.1016/j.ijpara.2008.08.009
41. Pfaff AW, Abou-Bacar A, Letscher-Bru V, Villard O, Senegas A, Mousli M, et al. Cellular and molecular physiopathology of congenital toxoplasmosis: the dual role of IFN-gamma. *Parasitology* (2007) 134(Pt 13):1895–902. doi:10.1017/S0031182007000200
42. Rico-Torres CP, Vargas-Villavicencio JA, Correa D. Is *Toxoplasma gondii* type related to clinical outcome in human congenital infection? Systematic and critical review. *Eur J Clin Microbiol Infect Dis* (2016) 35(7):1079–88. doi:10.1007/s10096-016-2656-2

43. Howe DK, Sibley LD. *Toxoplasma gondii* comprises three clonal lineages: correlation of parasite genotype with human disease. *J Infect Dis* (1995) 172(6):1561–6. doi:10.1093/infdis/172.6.1561
44. Sibley LD, Boothroyd JC. Virulent strains of *Toxoplasma gondii* comprise a single clonal lineage. *Nature* (1992) 359(6390):82–5. doi:10.1038/359082a0
45. Murray PJ. Macrophages as a battleground for *Toxoplasma* pathogenesis. *Cell Host Microbe* (2011) 9(6):445–7. doi:10.1016/j.chom.2011.05.010
46. Yamamoto M, Standley DM, Takashima S, Saiga H, Okuyama M, Kayama H, et al. A single polymorphic amino acid on *Toxoplasma gondii* kinase ROP16 determines the direct and strain-specific activation of Stat3. *J Exp Med* (2009) 206(12):2747–60. doi:10.1084/jem.20091703
47. Shen B, Brown K, Long S, Sibley LD. Chapter 6. Development of CRISPR/Cas9 for efficient genome editing in *Toxoplasma gondii*. In: Reeves A, editor. *In Vitro Mutagenesis Methods and Protocols*. Warrenville, IL: Coskata, Inc. (2017) 79–106.
48. Arenas-Hernandez M, Romero R, St Louis D, Hassan SS, Kaye EB, Gomez-Lopez N. An imbalance between innate and adaptive immune cells at the maternal-fetal interface occurs prior to endotoxin-induced preterm birth. *Cell Mol Immunol* (2016) 13(4):462–73. doi:10.1038/cmi.2015.22
49. Somerset DA, Zheng Y, Kilby MD, Sansom DM, Drayson MT. Normal human pregnancy is associated with an elevation in the immune suppressive CD25+ CD4+ regulatory T-cell subset. *Immunology* (2004) 112(1):38–43. doi:10.1111/j.1365-2567.2004.01869.x
50. Tilburgs T, Scherjon SA, van der Mast BJ, Haasnoot GW, Versteeg VDV-MM, Roelen DL, et al. Fetal-maternal HLA-C mismatch is associated with decidual T cell activation and induction of functional T regulatory cells. *J Reprod Immunol* (2009) 82(2):148–57. doi:10.1016/j.jri.2009.05.003
51. Tilburgs T, Roelen DL, van der Mast BJ, de Groot-Swings GM, Kleijburg C, Scherjon SA, et al. Evidence for a selective migration of fetus-specific CD4+CD25bright regulatory T cells from the peripheral blood to the decidua in human pregnancy. *J Immunol* (2008) 180(8):5737–45. doi:10.4049/jimmunol.180.8.5737
52. Quinn KH, Lacoursiere DY, Cui L, Bui J, Parast MM. The unique pathophysiology of early-onset severe preeclampsia: role of decidual T regulatory cells. *J Reprod Immunol* (2011) 91(1–2):76–82. doi:10.1016/j.jri.2011.05.006
53. Blois S, Tometten M, Kandil J, Hagen E, Klapp BF, Margni RA, et al. Intercellular adhesion molecule-1/LFA-1 cross talk is a proximate mediator capable of disrupting immune integration and tolerance mechanism at the feto-maternal interface in murine pregnancies. *J Immunol* (2005) 174(4):1820–9. doi:10.4049/jimmunol.174.4.1820
54. Wang WJ, Hao CF, Yi L, Yin GJ, Bao SH, Qiu LH, et al. Increased prevalence of T helper 17 (Th17) cells in peripheral blood and decidua in unexplained recurrent spontaneous abortion patients. *J Reprod Immunol* (2010) 84(2):164–70. doi:10.1016/j.jri.2009.12.003
55. Liu YS, Wu L, Tong XH, Wu LM, He GP, Zhou GX, et al. Study on the relationship between Th17 cells and unexplained recurrent spontaneous abortion. *Am J Reprod Immunol* (2011) 65(5):503–11. doi:10.1111/j.1600-0897.2010.00921.x
56. Li Y, Poppoe F, Chen J, Yu L, Deng F, Luo Q, et al. Macrophages polarized by expression of ToxoGRA15II inhibit growth of hepatic carcinoma. *Front Immunol* (2017) 8:137. doi:10.3389/fimmu.2017.00137

Conflict of Interest Statement: The authors declare that the research was conducted in the absence of any commercial or financial relationships that could be construed as a potential conflict of interest.

frontiers in Immunology

ORIGINAL RESEARCH
published: 31 July 2018
doi: 10.3389/fimmu.2018.01648

Galectin-3 and Galectin-9 May Differently Regulate the Expressions of Microglial M1/M2 Markers and T Helper 1/Th2 Cytokines in the Brains of Genetically Susceptible C57BL/6 and Resistant BALB/c Mice Following Peroral Infection With *Toxoplasma gondii*

Jinfeng Liu[1,2], Shiguang Huang[3] and Fangli Lu[1,2]**

[1] Department of Parasitology, Zhongshan School of Medicine, Sun Yat-sen University, Guangzhou, China, [2] Key Laboratory of Tropical Disease Control of Ministry of Education, Sun Yat-sen University, Guangzhou, China, [3] School of Stomatology, Jinan University, Guangzhou, China

OPEN ACCESS

Edited by:
Xun Suo, China Agricultural University, China

Reviewed by:
Hridayesh Prakash, All India Institute of Medical Sciences, India
Marisa Mariel Fernandez, Instituto de Estudios de la Inmunidad Humoral (IDEHU), Argentina

***Correspondence:**
Shiguang Huang
thshg@126.com;
Fangli Lu
fanglilu@yahoo.com

Specialty section:
This article was submitted to Microbial Immunology, a section of the journal Frontiers in Immunology

Received: *07 January 2018*
Accepted: *04 July 2018*
Published: *31 July 2018*

Citation:
Liu J, Huang S and Lu F (2018) Galectin-3 and Galectin-9 May Differently Regulate the Expressions of Microglial M1/M2 Markers and T Helper 1/Th2 Cytokines in the Brains of Genetically Susceptible C57BL/6 and Resistant BALB/c Mice Following Peroral Infection With Toxoplasma gondii. Front. Immunol. 9:1648. doi: 10.3389/fimmu.2018.01648

Toxoplasmic encephalitis (TE), an opportunistic infection, is a severe health problem in immunocompromised patients. Previous studies have revealed that C57BL/6 mice are susceptible and BALB/c mice are resistant to TE. To investigate the mechanisms involved in the immunopathogenesis of TE in susceptible C57BL/6 and resistant BALB/c mice, both strains of mice were perorally infected with the Prugniuad (Pru) strain of *Toxoplasma gondii*. Our results showed that compared with BALB/c mice, C57BL/6 mice infected with *T. gondii* Pru strain had more severe brain histopathological damage, and higher mRNA expression levels of tachyzoite-specific surface antigen 1, bradyzoite-specific antigen 1, interferon gamma (IFNγ), interleukin (IL)-10, arginase1 (Arg1) (M2 marker), galectin (Gal)-3, Gal-9, *T. gondii* microneme protein 1 (TgMIC1), TgMIC4, and TgMIC6 during the course of infection by using quantitative real-time reverse transcription-polymerase chain reaction. Further analysis displayed that BALB/c mice showed higher numbers of microglial cells and higher levels of IL-1β, inducible nitric oxide synthase (iNOS) (M1 marker), and chitinase-3-like protein 3 (Ym1) (M2 marker) in the early infective stage [at day 14 or 35 post infection (p.i.)] compared with C57BL/6 mice, whereas C57BL/6 mice showed higher numbers of microglial cells and higher levels of IL-10, iNOS (M1 marker), and Ym1 (M2 marker) at days 35, 50, or 70 p.i. compared with BALB/c mice. Correlation analysis showed that significant positive correlations existed between Gal-3 and IL-4/IL-10/iNOS/Ym1 and between Gal-9 and IL-4/Ym1 in C57BL/6 mice; between Gal-3 and IFNγ/Arg1 and between Gal-9 and IFNγ/Arg1 in BALB/c mice. Together, our data demonstrated that different Gal-3 and Gal-9 expressions as well as different positive correlations were found between Gal-3 and T helper 1 (Th1)/Th2/M1/M2 cytokines or between Gal-9 and Th1/Th2/M2 cytokines in the brains of *T. gondii* Pru strain-infected C57BL/6 and BALB/c mice.

Keywords: toxoplasmic encephalitis, galectins, microglial M1/M2 markers, *T. gondii* microneme proteins, mice

INTRODUCTION

Toxoplasma gondii, a pathogen of medical and veterinary importance, is an obligate intracellular protozoan parasite that has a global distribution and can infect almost any warm-blooded vertebrate (1). *T. gondii* infection in the immunocompetent individual is effectively controlled by a vigorous immune response (2); however, the infection can cause toxoplasmic encephalitis (TE), a life-threatening disease in immunocompromised patients (3). Although all mice lineages develop a strong T helper 1 (Th1) immune response to *T. gondii* infection (4), the immune response to the parasite infection in the brains can be drastically different between genetically resistant mice (e.g., BALB/c mice) and that of susceptible mice (e.g., C57BL/6 mice) (5). During the late stage of infection, resistant mouse strain establishes a latent chronic infection, while susceptible strain spontaneously develops necrotizing TE (6). So far, the mechanisms behind the differences between the two strains of mice during the development of TE are not fully understood.

It has been proposed that *T. gondii* utilizes innate immune cells such as macrophages to migrate to immunoprivileged sites such as the central nervous system (CNS) to establish chronic infection (7). Macrophages are generally categorized into two distinct subsets as either classically activated (M1) or alternatively activated (M2). M1 type macrophages, characterized by CD86 expression, can release high levels of pro-inflammatory markers such as monocyte chemotactic protein-1β, inducible nitric oxide synthase (iNOS), interleukin (IL)-6, and tumor necrosis factor alpha (TNFα) (8). M2 macrophages can produce a large amount of IL-10, chitinase-3-like protein 3 (Ym1), macrophage and granulocyte inducer-form 1, and arginase1 (Arg1) and play important roles in the protection of the host by decreasing inflammation and promoting tissue repair (9, 10). During *T. gondii* infection, Th1 cells produce cytokines such as interferon gamma (IFNγ) to activate macrophages and cytotoxic T lymphocytes, while Th2 cells secrete cytokines such as IL-4 to induce humoral type immune responses (11, 12). IFNγ-activated microglial cells significantly upregulate iNOS and produce nitric oxide (NO), which can inhibit intracellular *T. gondii* replication (13).

Galectins belong to the family of β-galactoside-binding lectins, which are known to regulate a number of pathways that involve in apoptosis (14), immune tolerance, inflammation (15), and cell adhesion (16). Currently, 15 members of the galectin family have been identified in mammals; some members are widely distributed in different cells and tissue types, while others are more selectively expressed (17). The major galectins expressed in the CNS are galectin (Gal)-1, Gal-3, Gal-4, Gal-8, and Gal-9 (18). Under normal physiological conditions, galectins maintain CNS homeostasis, while in neuronal diseases and experimental neuroinflammatory disease models, galectins may serve as extracellular mediators or intracellular regulators in controlling the inflammatory response or conferring the remodeling capacity in damaged CNS tissues (18). So far, the roles of galectins in TE remains poorly understood.

Apicomplexan parasites such as *T. gondii* and *Plasmodium* spp. utilize apical complex organelles consisting of dense granules, rhoptries, and micronemes to deploy for the release (egress), attachment, and invasion of host cells, as well as the establishment of the parasitophorous vacuole (19). *T. gondii* microneme proteins (TgMICs) are secreted by micronemes upon contact with host cells and play important roles in *T. gondii* motility, invasion, intracellular survival, and egress from host cells (20). TgMIC6 and TgMIC8 genes are expressed in the rapidly dividing tachyzoites, whereas TgMIC7 and TgMIC9 genes are predominantly expressed in the slowly dividing encysted bradyzoites (21). TgMIC1 and TgMIC4 can bind to host cells, while TgMIC6 serves as an escorter for two soluble adhesins TgMIC1 and TgMIC4 and along with adhesins can establish a molecular bridge between the host and parasites (22). So far, limited data are available about the role of TgMICs in the immune response to *T. gondii* infection.

Based on the relationship between galectins and brain diseases, this study was designed to compare the expressions of galectins, microglial activation markers (M1 and M2 phenotypes), TgMICs, and Th1 and Th2 cytokines between C57BL/6 and BALB/c mice infected with *T. gondii* Pru strain. We found that significant positive correlations existed between Gal-3 and Th1/Th2/M1/M2 cytokines as well as between Gal-9 and Th1/Th2/M2 cytokines in C57BL/6 or BALB/c mice after *T. gondii* Pru strain infection.

MATERIALS AND METHODS

Mice, Parasites, and Experimental Infections

This experimental study and all administrations were reviewed and approved by the Ethical Committee of Animal Experiments at Sun Yat-sen University.

Female 6- to 8-week-old C57BL/6 and BALB/c mice were purchased from the Experimental Animal Center at Sun Yat-sen University (Guangzhou, China), and 20 mice were used per each group. All animals were housed under specific-pathogen-free conditions in the animal facility at Sun Yat-sen University. Mice were infected *via* oral route with eight cysts of *T. gondii* Pru strain prepared from the brain of chronically infected mice. To establish a chronic infection by controlling the proliferation of tachyzoites during acute stage, mice were treated with sulfadiazine (Sigma-Aldrich, Shanghai, China) in the drinking water as described previously (23).

Histopathology

Mice infected with *T. gondii* Pru strain were euthanatized by CO_2 asphyxiation at 14, 35, 50, and 70 days post infection (p.i.), and their brains were harvested and immediately fixed in 10% buffered natural formaldehyde (Guangzhou Chemical Reagent Factory, China) for over 48 h. The paraffin-embedded tissues from each mouse were sectioned at 5 μm and prepared for hematoxylin and eosin (Sigma-Aldrich, Shanghai, China) staining. The histopathological changes of brains from each group were determined under 200× magnification in three noncontiguous sections from four mice, and histopathological scores were given based on previously described criteria (23) with some modifications. In brief, the histological changes were scored semi-quantitatively as 1, 2, 3, and 4 (e.g., normal, mild inflammation, moderate inflammation and necrosis, and severe inflammation and necrosis, respectively).

Immunohistochemical Staining

The paraffin-embedded brain sections (6-μm) were deparaffinized and rehydrated in distilled water. Heat-induced antigen retrieval was carried out in an 800-W microwave oven for 30 min. Sections were treated with 3% hydrogen peroxide in methanol for 10 min at 37°C, and then incubated in 10% normal goat serum with 1% bovine serum albumin (Sigma-Aldrich, Shanghai, China) in PBS (pH 7.4) for 10 min at room temperature to block nonspecific binding. After washing with PBS, sections were incubated with rabbit anti-Iba1 (1:200 dilutions) (Wako Pure Chemical Industries, Osaka, Japan), rabbit anti-Gal-9 (1:200 dilutions) (Boster Biological Technology, Wuhan, China), and mouse anti-Gal-3 (1:200 dilutions) (R&D Systems, Minneapolis, MN, USA) overnight at 4°C. Those sections incubated with secondary antibodies alone were used as isotype controls. Immunohistochemical staining was then performed with a streptavidin–biotin–peroxidase complex kit and developed with diaminobenzidine tetrahydrochloride (Zhongshan Golden Bridge Technology, Beijing, China). The sections were counterstained with hematoxylin and positive cells were identified by dark-brown staining under light microscopy.

Morphometric Analysis

Serial sections from the brains were immunostained with anti-Iba1. A total of three mice were analyzed in each time point, and four sections per animal were selected for counting of positive cells. In every brain section, the microglial cells expressing Iba1 markers were captured with a digital microscopy under 400× magnification and the numbers of Iba1-positive cells in the brains (0.015066 mm^2 tissue section) were determined by Image-Pro Plus (Image Z1 software, Media Cybernetics, MD, USA), and the density of positive cells was expressed as the number of cells per square millimeter.

Selection of Galectins

Gal-1, Gal-3, Gal-7, Gal-8, and Gal-9 are known to be relevant to brain diseases (18). Therefore, in this study, the specific expression pattern of these five galectins was examined.

Determination of mRNA Expression Using Quantitative Real-Time Reverse Transcription-Polymerase Chain Reaction (qRT-PCR)

Total RNA was extracted from about 100 mg of mouse brain tissues from each group using a RNA Extraction Kit (TaKaRa, Shiga, Japan) as per the manufacturer's protocol. RNA amount was determined by measuring the ratio of absorbance at 260 and 280 nm using a NanoDrop ND-1000 spectrophotometer (NanoDrop Technologies). First-strand cDNA was constructed from 1.0 μg of total RNA with oligo (dT) as primers using a PrimeScript 1st Strand cDNA Synthesis Kit (TaKaRa, Shiga, Japan). To determine tissue mRNA levels of cytokines (IL-1β, IFNγ, IL-4, IL-10, iNOS, Arg1, and Ym-1), galectins (Gal-1, Gal-3, Gal-4, Gal-8, and Gal-9), TgMICs (TgMIC1, TgMIC4, TgMIC6, TgMIC3, and TgMIC8), β-actin, actin of the ME49 strain of *T. gondii*, *T. gondii* tachyzoite-specific surface antigen 1 (SAG1), and *T. gondii* bradyzoite-specific antigen 1 (BAG1), qRT-PCR measurements were performed using SYBR Green QPCR Master Mix (TaKaRa, Shiga, Japan). Primers are listed in **Table 1**. Briefly, a total of 10 μl reaction mixture contained 5.0 μl of SYBR® Premix Ex TaqTM (2×), 0.5 μl of each primer (10 pM), 3.0 μl of dH_2O, and 1.0 μl of cDNA (0.2 μg/μl). Amplification was pre-denaturized for 30 s at 95°C, followed by 43 cycles of 5 s at 95°C and 20 s at 60°C with a LightCycler® 480 instrument (Roche Diagnostics, USA). The mRNA expression levels of cytokines, SAG1, and BAG1 were normalized to that of mouse housekeeping gene, β-actin, and the mRNA levels of TgMICs were normalized to that of *T. gondii* housekeeping gene (actin of *T. gondii* ME49 strain). The results were expressed as fold change compared with uninfected controls.

Statistical Analysis

Results of experimental studies were reported as mean ± SD. Statistical analysis of the data was performed by the Wilcoxon

TABLE 1 | Primer sequences of genes used for quantitative real-time reverse transcription-polymerase chain reaction assays.

Genes	Forward primer (5′→3′)	Reverse primer (5′→3′)	Reference/accession
IL-1β	AATGACCTGTTCTTTGAAGTTGA	TGATGTGCTGCTGCGAGATTTGAAG	(24)
IFNγ	GGAACTGGCAAAAGGATGGTGAC	GCTGGACCTGTGGGTTGTTGAC	(25)
IL-4	ACAGGAGAAGGGACGCCAT	GAAGCCCTACAGACGAGCTCA	(26)
IL-10	AGCCGGGAAGACAATAACTG	CATTTCCGATAAGGCTTGG	(25)
iNOS	GTTCTCAGCCCAACAATACAAGA	GTGGACGGGTCGATGTCAC	(27)
Arg1	CTCCAAGCCAAAGTCCTTAGAG	AGGAGCTATCATTAGGGACATC	(27)
Ym1	AGAAGGGAGTTTCAA ACCTGGT	GTCTTGCTCATGTGTGTAAGTGA	(27)
Gal-1	CGCCAGCAACCTGAATC	GTCCCATCTTCCTTGGTGTTA	(28)
Gal-3	GCTACTGGCCCCTTTGGT	CCAGGCAAGGGCATATCGTA	(29)
Gal-4	CAACCCTCCACAGATGAACACCTT	TCCAGCGTGTCTACCATTTGGAAT	(30)
Gal-8	GGGTGGTGGGTGGAACTG	GCCTTTGAGCCCCCAATATC	(31)
Gal-9	GAGCTTTGCTTCCTGGTACAGA	CGGTGTGAGTACTGTACAAAGAAGT	(29)
β-actin	TGGAATCCTGTGGCATCCATGAAAC	TAAAACGCAGCTCAGTAACAGTCCG	(25)
TgMIC1	GCGAATTTCCTTGATGGATT	GTAGTCGAGGACAACAGCGA	XM_002368490.1
TgMIC3	AGCCATCACACACACACCTT	ATGCACAGAAACGCACTCTC	XM_002369792.1
TgMIC4	CCTGCAAGGCTTCACTGATA	CTATTGTGGGAGCCCTTGAT	XM_002369565.1
TgMIC6	CGCCAGATGCAGTACAGAGT	GCGTCGATTGTCGCTATAAA	XM_002370595.1
TgMIC8	GTAAAGGCGAGGTCGAAGAC	GTACTGCGGGAAAGGATGAT	XM_002366938.1
T. gondii ME49 actin	ATTATGAAGTGCGACGTGGA	TGATCTTCATGGTGGAAGGA	XM_002369622.1

rank sum test and one-way ANOVA followed by Bonferroni's multiple comparison tests using SPSS software for windows (version 19.0; SPSS, Inc., IL, USA). Pearson's correlation coefficient was used to analyze correlations between the levels of cytokines and galectins. All graphs were performed using GraphPad Prism software (version 5.0). A value of $P < 0.01$ was considered significant for correlation analysis, while a value of $P < 0.05$ was considered significant for other statistical analysis.

RESULTS

Comparison of Histopathology and Parasite Burdens in the Brains of *T. gondii*-Susceptible C57BL/6 and *T. gondii*-Resistant BALB/c Mice

Histological observation showed that control sections of the brains from uninfected C57BL/6 and BALB/c mice had no obvious inflammations or structural abnormalities. The brains of *T. gondii* Pru strain-infected C57BL/6 mice showed moderate-to-severe inflammation, diffuse inflammatory cellular infiltration, necrotic focus, and tissue structural damages at days 14, 35, 50, and 70 p.i., while the brains of infected BALB/c mice showed limited infiltration of inflammatory cells at the aforementioned times (**Figure 1A**). Semi-quantitative analysis of the severity of inflammation and necrosis in the brain sections of the two strains of mice were performed. Compared with uninfected controls, the pathological severity scores of brains were significantly increased in both C57BL/6 and BALB/c mice at days 14, 35, 50, and 70 p.i. Compared with BALB/c mice, the histopathological scores in the brains of C57BL/6 mice were significantly higher at days 35 ($P < 0.05$), 50 ($P < 0.01$), and 70 ($P < 0.01$) p.i. (**Figure 1B**).

Stage conversion between tachyzoite and bradyzoite forms is associated with stage specific antigen expression. In this study, the mRNA expression levels of tachyzoite-specific SAG1 and bradyzoite-specific BAG1 in the brains of C57BL/6 and BALB/c mice infected with *T. gondii* Pru strain were detected by using qRT-PCR and the transcript. Levels of SAG1 and BAG1 were relative to day 14 p.i. (e.g., the relative transcript level at day 14 p.i. = 1.0). Compared with day 14 p.i., the SAG1 levels in the brains of both C57BL/6 and BALB/c mice were significantly decreased at days 35, 50, and 70 p.i. The BAG1 levels in the brains of C57BL/6 mice were significantly elevated at days 35 and 70 p.i., while the BAG1 level in BALB/c mice was significantly reduced at day 70 p.i. Compared with BALB/c mice, both SAG1 and BAG1 levels were significantly higher in the brains of C57BL/6 mice at days 35, 50, and 70 p.i. ($P < 0.01$ and $P < 0.05$, respectively) (**Figure 1C**).

Comparison of Microglial Cells in the Brains of *T. gondii*-Susceptible C57BL/6 and *T. gondii*-Resistant BALB/c Mice

A few Iba1-positive microglial cells were observed in the sections of brains of uninfected C57BL/6 and BALB/c mice. However, a large number of activated microglial cells were observed in the brains of both *T. gondii* Pru strain-infected C57BL/6 and BALB/c mice; the majority of activated microglial cells were ameboid shape with thickened and retracted branches (**Figure 2A**). Quantitative analysis of Iba1 staining showed that, compared with uninfected controls, the numbers of Iba1-positive microglial cells in the brains of both C57BL/6 and BALB/c mice were significantly increased at days 14, 35, 50, and 70 p.i. However, compared with BALB/c mice, the microglial cell numbers in the brains of C57BL/6 mice were significantly higher at days 35 ($P < 0.001$), 50 ($P < 0.001$), and 70 ($P < 0.01$) p.i. (**Figure 2B**).

Comparison of mRNA Levels of M1/M2 Markers in the Brains of *T. gondii*-Susceptible C57BL/6 and *T. gondii*-Resistant BALB/c Mice

The mRNA levels of M1 marker (iNOS) and M2 marker (Arg1 and Ym1) in the brains of *T. gondii* Pru strain-infected C57BL/6 and BALB/c mice were examined. Compared with uninfected controls, iNOS levels were significantly increased in the brains of both C57BL/6 and BALB/c mice at days 14, 35, 50, and 70 p.i.; Arg1 and Ym1 levels were significantly increased in C57BL/6 mice at days 14, 35, 50, and 70 p.i., and significantly increased in BALB/c mice at days 14 and 35 p.i. (**Figure 3A**). Compared with BALB/c mice, there were significantly lower iNOS levels at days 14 and 35 p.i. ($P < 0.01$); while there were significantly higher iNOS levels at days 50 and 70 p.i. ($P < 0.001$), significantly higher Arg1 levels at days 14 ($P < 0.05$), 35 ($P < 0.01$), 50 ($P < 0.001$), and 70 ($P < 0.01$) p.i., and significantly lower Ym1 level at day 14 p.i. ($P < 0.001$) and significantly higher Ym1 levels at days 35 ($P < 0.01$), 50 ($P < 0.001$), and 70 ($P < 0.001$) p.i. in the brains of C57BL/6 mice (**Figure 3B**).

Comparison of mRNA Levels of Th1/Th2 Cytokines in the Brains of *T. gondii*-Susceptible C57BL/6 and *T. gondii*-Resistant BALB/c Mice

Compared with uninfected controls, the levels of IL-1β, IFNγ, and IL-10 were significantly increased in the brains of both C57BL/6 and BALB/c mice at days 14, 35, 50, and 70 p.i.; IL-4 levels were significantly increased in both *T. gondii* Pru strain-infected C57BL/6 and BALB/c mice at days 35, 50, and 70 p.i. (**Figure 4A**). Compared with BALB/c mice, significantly lower IL-1β level at day 35 p.i. ($P < 0.05$), significantly higher IL-10 level at day 50 p.i. ($P < 0.01$), and significantly higher IFNγ levels at days 14 ($P < 0.05$), 35 ($P < 0.05$), 50 ($P < 0.01$), and 70 ($P < 0.01$) p.i. were detected in the brains of C57BL/6 mice (**Figure 4B**).

Comparison of mRNA Levels of Galectins in the Brains of *T. gondii*-Susceptible C57BL/6 and *T. gondii*-Resistant BALB/c Mice

Compared with uninfected controls, Gal-3 expression levels were significantly increased in the brains of both *T. gondii* Pru strain-infected C57BL/6 and BALB/c mice at days 14, 35, 50, and 70 p.i.; Gal-9 levels were significantly increased in both C57BL/6 and BALB/c mice at days 14, 35, and 50 p.i., and significantly increased in C57BL/6 mice at day 70 p.i. (**Figure 5A**). Compared

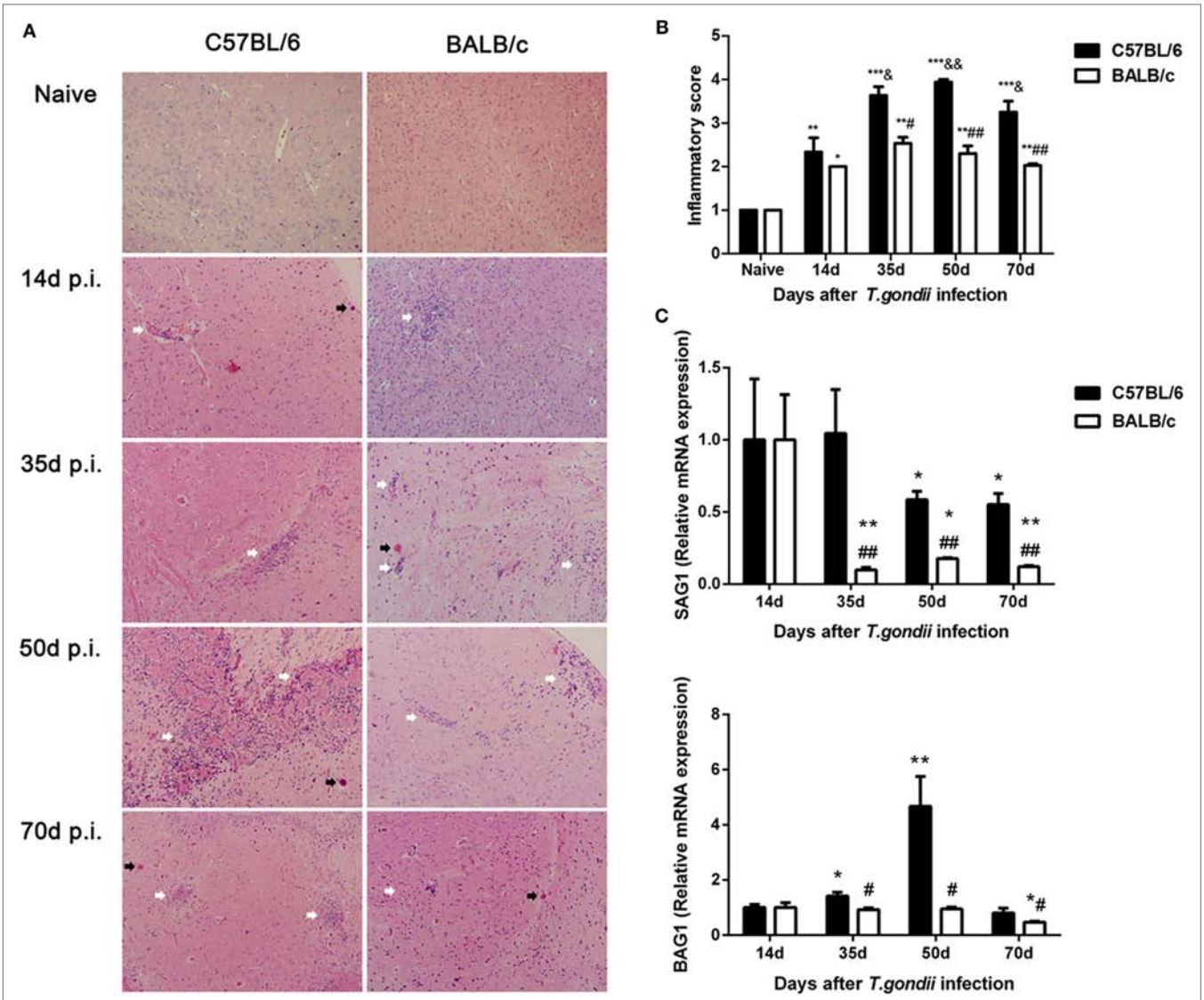

FIGURE 1 | Histopathological changes and parasite burdens in the brains of *Toxoplasma gondii* Pru strain-infected C57BL/6 and BALB/c mice. **(A)** Histopathological changes in the brains at days 14, 35, 50, and 70 post infection (p.i.). Cysts were indicated with black arrow heads and inflammatory cell infiltrates were indicated with white arrow heads. Original magnification 200×; hematoxylin and eosin stain. **(B)** Histopathological score analysis at days 14, 35, 50, and 70 p.i. Data are represented as mean ± SEM. Significant differences between groups are analyzed by the Wilcoxon rank sum test. $^{*}P < 0.05$, $^{**}P < 0.01$, and $^{***}P < 0.001$ vs naive; $^{\&}P < 0.05$ and $^{\&\&}P < 0.01$ vs 14 days p.i.; $^{\#}P < 0.05$ and $^{\#\#}P < 0.01$ vs C57BL/6 mice. **(C)** Parasite burdens in the brains at days 14, 35, 50, and 70 p.i. Relative mRNA expressions of surface antigen 1 (SAG1) and bradyzoite-specific antigen 1 (BAG1) were detected by using quantitative real-time reverse transcription-polymerase chain reaction. Transcript level at day 14 p.i. was taken as 1. Values are means from triplicate measurements, and data are presented as mean ± SD. $^{*}P < 0.05$ and $^{**}P < 0.01$ vs naive; $^{\#}P < 0.05$ and $^{\#\#}P < 0.01$ vs C57BL/6 mice. There were four mice per group. The data shown are representative of those from two different experiments.

with BALB/c mice, there were significantly higher levels of Gal-3 and Gal-9 in the brains of C57BL/6 mice at days 35 ($P < 0.05$), 50 ($P < 0.01$ and $P < 0.05$, respectively), and 70 ($P < 0.01$) p.i. (**Figure 5B**).

Comparison of mRNA Levels of TgMICs in the Brains of *T. gondii*-Susceptible C57BL/6 and *T. gondii*-Resistant BALB/c Mice

Compared with day 14 p.i., TgMIC1 levels were significantly decreased in the brains of both *T. gondii* Pru strain-infected C57BL/6 and BALB/c mice at days 35, 50, and 70 p.i.; TgMIC3 levels were significantly increased in C57BL/6 mice at days 35, 50, and 70 p.i.; TgMIC4 levels were significantly increased in C57BL/6 mice at days 50 and 70 p.i. and significantly increased in BALB/c mice at day 70 p.i. TgMIC6 levels were significantly decreased in BALB/c mice at days 35, 50, and 70 p.i., and TgMIC8 levels were significantly decreased in both C57BL/6 and BALB/c mice at days 35, 50, and 70 p.i. (**Figure 6A**). Compared with BALB/c mice, there were significantly higher levels of TgMIC1 at days 35 and 70 p.i. ($P < 0.05$) and significantly higher levels of TgMIC4 and TgMIC6 at days

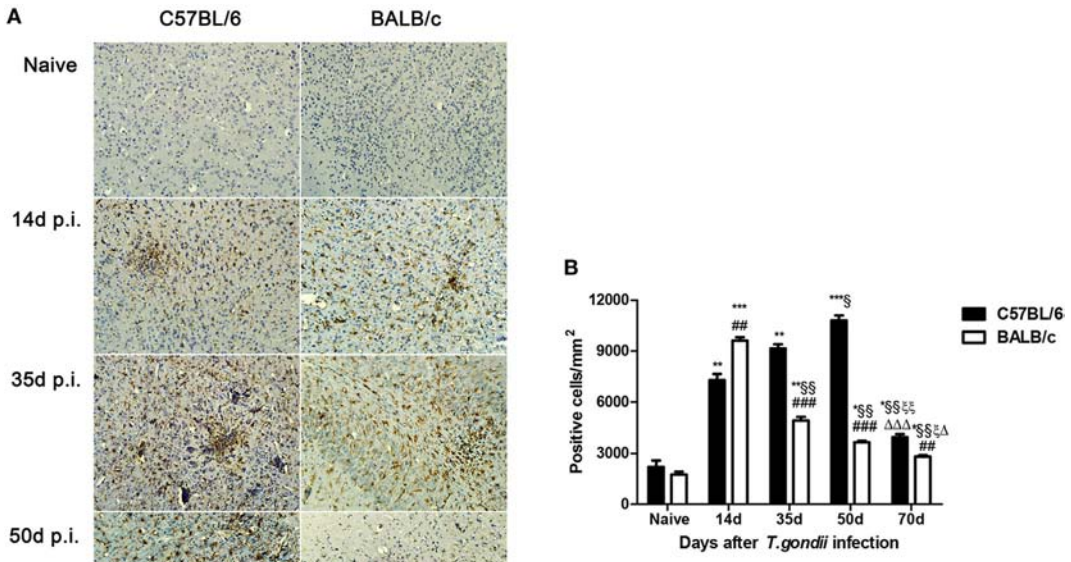

FIGURE 2 | Expression of activated microglial marker Iba1 in the brains of *Toxoplasma gondii* Pru strain-infected C57BL/6 and BALB/c mice. **(A)** Immunohistochemistry for Iba1 in the brains of uninfected mice, and mice infected with *T. gondii* Pru strain at days 14, 35, 50, and 70 post infection (p.i.). Original magnification 200×. **(B)** Quantitative analysis of Iba1-positive microglia. The density of positive cells was expressed as the number of cells per square millimeter. Data are presented as means ± SD; experiments were performed with three mice per group. $^{*}P < 0.05$, $^{**}P < 0.01$, and $^{***}P < 0.001$ vs Naive; $^{\S}P < 0.05$ and $^{\S\S}P < 0.01$ vs 14 days p.i.; $^{\xi}P < 0.05$ and $^{\xi\xi}P < 0.01$ vs 35 days p.i.; $^{\Delta}P < 0.05$ and $^{\Delta\Delta\Delta}P < 0.001$ vs 50 days p.i.; $^{\#\#}P < 0.01$ and $^{\#\#\#}P < 0.001$ vs C57BL/6 mice.

35, 50, and 70 p.i. in the brains of C57BL/6 mice ($P < 0.05$) (**Figure 6B**).

Correlations Between Gal-3/Ga-9 and Th1/Th2/M1/M2 Cytokines in the Brains of *T. gondii*-Resistant BALB/c and *T. gondii*-Susceptible C57BL/6 Mice

The correlations between mRNA levels of Gal-3/Gal-9 and Th1/Th2/M1/M2 in the brains of *T. gondii* Pru strain-infected C57BL/6 and BALB/c mice were evaluated, herein only significant correlations were shown. There were significant correlations between the mRNA levels of Gal-3 and IL-4 ($r = 0.8424$, $P = 0.0002$), Gal-3 and IL-10 ($r = 0.6996$, $P = 0.0037$), Gal-3 and iNOS ($r = 0.7344$, $P = 0.0018$), Gal-3 and Ym1 ($r = 0.6866$, $P = 0.0047$), Gal-9 and IL-4 ($r = 0.8293$, $P = 0.0002$), and Gal-9 and Ym1 ($r = 0.6714$, $P = 0.0061$) in *T. gondii* Pru strain-infected C57BL/6 mice (**Figure 7A**). However, there were significant correlations between the mRNA levels of Gal-3 and IFNγ ($r = 0.6993$, $P = 0.0078$), Gal-3 and Arg1 ($r = 0.8099$, $P = 0.0004$), Gal-9 and IFNγ ($r = 0.7378$, $P = 0.0040$), and Gal-9 and Arg1 ($r = 0.7963$, $P = 0.0007$) in *T. gondii* Pru strain-infected BALB/c mice (**Figure 7B**). Taken together, in C57BL/6 mice, significant positive correlations existed between Gal-3 and IL-4/IL-10/iNOS/Ym1 as well as between Gal-9 and IL-4/Ym1; whereas in BALB/c mice, significant positive correlations existed between Gal-3 and IFNγ/Arg1 as well as between Gal-9 and IFNγ/Arg1.

DISCUSSION

When *T. gondii* parasites infect the host, the cysts can exist predominantly in the brain tissue for lifetime, and an immunocompetent host will establish a strong and persistent Th1-biased cell-mediated immunity to resist cyst reactivation and the consequences of TE (4). However, there is a remarkable difference in susceptibility to the infection of *T. gondii* among inbred strains of mice. After peroral infection with *T. gondii* ME49 strain, C57BL/6 mice all died whereas BALB/c mice all survived (32). So far, the immune responses differing between TE-resistant and TE-susceptible hosts are not fully understood. In this study, genetically susceptible C57BL/6 and resistant BALB/c mice were perorally infected with *T. gondii* Pru strain, and significantly more severe histopathological damage (inflammation and necrosis) were found in the brains of C57BL/6 mice

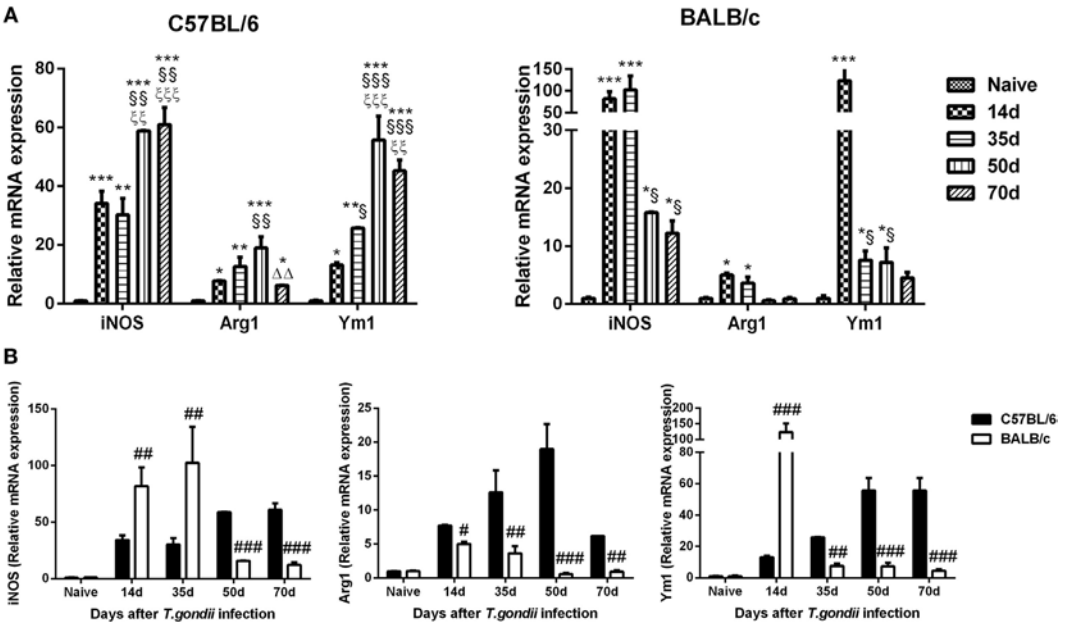

FIGURE 3 | Relative mRNA expressions of inducible nitric oxide synthase (iNOS), arginase1 (Arg1), and Ym1 in the brain tissues of *Toxoplasma gondii* Pru strain-infected C57BL/6 and BALB/c mice were detected by using quantitative real-time reverse transcription-polymerase chain reaction. **(A)** iNOS, Arg1, and Ym1 expressions in the brains of C57BL/6 and BALB/c mice. **(B)** Comparison of iNOS, Arg1, and Ym1 levels in the brains of C57BL/6 and BALB/c mice. Values are means from triplicate measurements, and data are presented as mean ± SD. There were four mice per group. The data shown are representative of those from two different experiments. $^{*}P < 0.05$, $^{**}P < 0.01$, and $^{***}P < 0.001$ vs naive; $^{§}P < 0.05$; $^{§§}P < 0.01$, and $^{§§§}P < 0.001$ vs 14 days post infection (p.i.); $^{ξξ}P < 0.01$ and $^{ξξξ}P < 0.001$ vs 35 days p.i.; $^{ΔΔ}P < 0.01$ vs 50 days p.i.; $^{#}P < 0.05$, $^{##}P < 0.01$, and $^{###}P < 0.001$ vs C57BL/6 mice.

in comparison of those of BALB/c mice at all the times during the observations (e.g., at days 14, 35, 50, and 70 p.i.). The levels of mRNA transcripts of both tachyzoite-specific SAG1 and bradyzoite-specific BAG1 genes were significantly higher in the brains of C57BL/6 mice than those of BALB/c mice at days 35, 50, and 70 p.i. It has been reported that following *T. gondii* ME49 strain infection, C57BL/6 mice showed an intense and progressive inflammatory alteration in the CNS, while BALB/c mice showed slight inflammatory reaction in the CNS (33). After infection with low virulent *T. gondii* DX strain, C57BL/6 mice presented higher tachyzoite and bradyzoite loads than those of BALB/c mice (34). Our data were in accordance with the previous studies.

Microglia activation is recognized as the hallmark of neuroinflammation. Microglial cells are the primary source for inflammatory mediators. Resident microglial cells play a critical role in TE, producing essential pro- and anti-inflammatory cytokines such as IL-1β, IL-10, TNFα, IL-12, and IL-15 (35–37). In this study, we found that microglial cell numbers in the brains of C57BL/6 mice were significantly higher than those of BALB/c mice at days 35, 50, and 70 p.i.; however, the number of microglial cells was significantly higher in BALB/c mice than that of C57BL/6 mice at day 14 p.i. Our data suggest that resident microglia are activated earlier in BALB/c mice, which may be essential for control of the parasite in the early infective stage in *T. gondii*-resistant BALB/c mice; whereas increased microglial activation remains longer in C57BL/6 mice, which may be required for establishing chronic TE in *T. gondii*-susceptible C57BL/6 mice.

It has been reported that activated microglial cells range from the pro-inflammatory M1 phenotype to the alternative/M2 phenotype and play neuroprotective or neurodetrimental roles (38). Therefore, identifying microglia phenotypes is critical for understanding the role of microglia in the pathogenesis of TE. In this study, we found that alterations in M1 and M2 phenotypes differed between the two models. In *T. gondii* Pru strain-infected BALB/c mice, both M1 (iNOS) and M2 (Ym1) phenotypic markers were significantly increased in the early infective stage (at day 14 or 35 p.i.); while in C57BL/6 mice, both M1 (iNOS) and M2 (Ym1) phenotypic markers were significantly increased in the late infective stage (at days 50 and 70 p.i.) and M2 marker (Arg1) was significantly increased at all the times during the study. M1 macrophages are critical for host defense against intracellular pathogens and have roles in antitumor immunity and autoimmune inflammation, whereas M2 macrophages are protective against helminth parasites and are important regulators of the wound healing response, tissue homeostasis, and adiposity (39). Inhibition of iNOS exacerbates chronic TE in *T. gondii*-susceptible C57BL/6 mice but does not lead to reactivation of latent TE in *T. gondii*-resistant BALB/c mice (34). CBA/Ca mice are susceptible to the development of TE. An *in vitro* study demonstrated that microglia from CBA/Ca mice show decreased production of NO and decreased inhibition of *T. gondii* replication after stimulation with lipopolysaccharide or IFNγ plus TNFα compared with microglia from BALB/c mice (40). Our data demonstrated that both M1 (iNOS) and M2 (Ym1 and Arg1) responses may play a role during chronic TE in *T. gondii*-susceptible C57BL/6 mice.

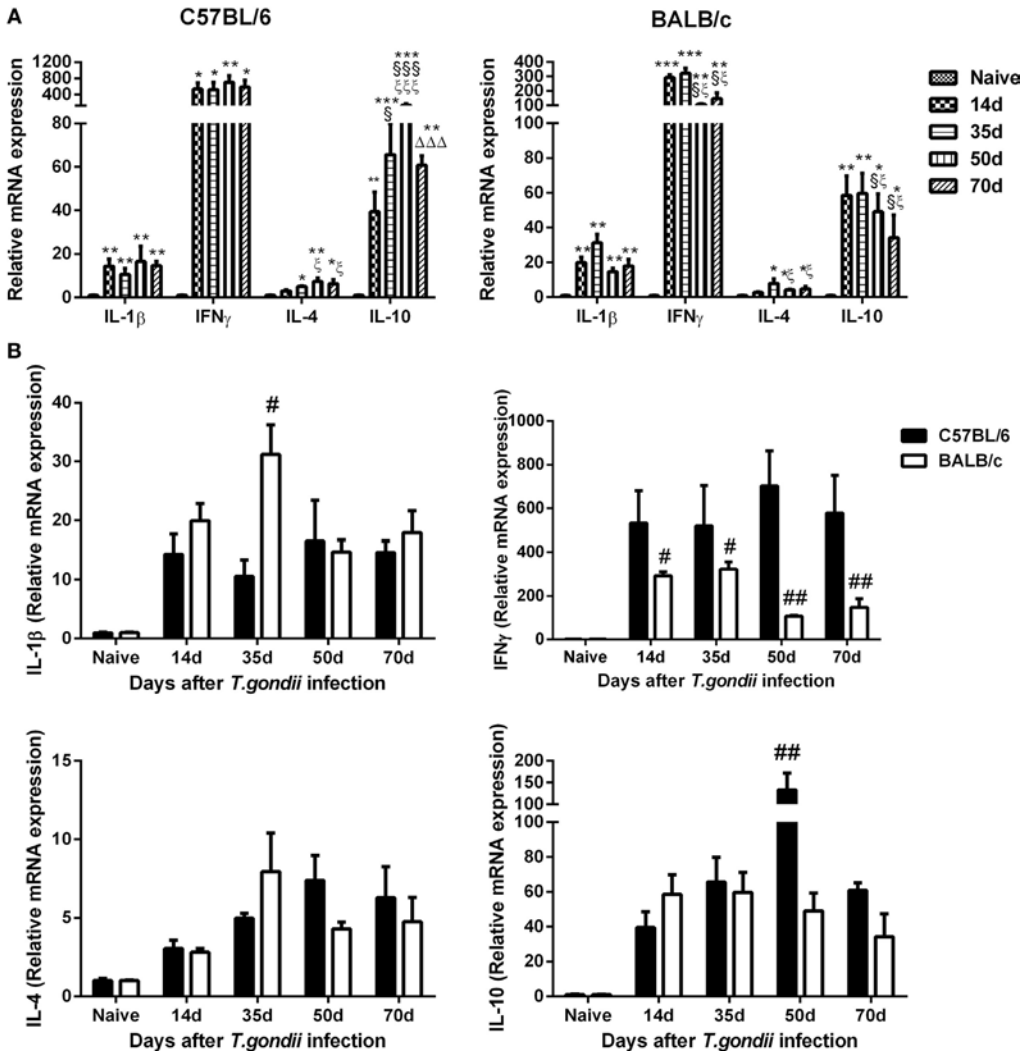

FIGURE 4 | Relative mRNA expressions of interleukin (IL)-1β, interferon gamma (IFNγ), IL-4, and IL-10 in the brain tissues of *Toxoplasma gondii* Pru strain-infected C57BL/6 and BALB/c mice were detected by using quantitative real-time reverse transcription-polymerase chain reaction. **(A)** IL-1β, IFNγ, IL-4, and IL-10 expressions in the brains of C57BL/6 and BALB/c mice. **(B)** Comparison of IL-1β, IFNγ, IL-4, and IL-10 levels in the brains of C57BL/6 and BALB/c mice. Values are means from triplicate measurements, and data are presented as mean ± SD. There were four mice per group. The data shown are representative of those from two different experiments. $^{*}P < 0.05$, $^{**}P < 0.01$, and $^{***}P < 0.001$ vs naive; $^{§}P < 0.05$ and $^{§§§}P < 0.001$ vs 14 days post infection (p.i.); $^{ξ}P < 0.05$ and $^{ξξξ}P < 0.001$ vs 35 days p.i.; $^{ΔΔΔ}P < 0.001$ vs 50 days p.i.; $^{#}P < 0.05$ and $^{##}P < 0.01$ vs C57BL/6 mice.

Toxoplasma gondii infection induces Th1-biased immune response, which is critical for the prevention of reactivation of TE (41). In this study, although the mRNA levels of Th1-associated cytokines (IFNγ and IL-1β) and Th2-associated cytokines (IL-4 and IL-10) were increased in the brain tissues of both C57BL/6 and BALB/c mice infected with *T. gondii* Pru strain, susceptible C57BL/6 mice presented a dominant Th1 response characterized by high expression of IFNγ at all the times after infection, accompanied by stronger neuroinflammatory outcomes. Our data suggested that the delayed M1 and M2 microglial activation and increased IFNγ expression in C57BL/6 mice after *T. gondii* Pru strain infection may be a part of the reason that C57BL/6 mice are more susceptible than BALB/c mice during TE.

Galectins have recently been demonstrated to play vital roles in host–pathogen interaction (42). Galectins are important modulators participating in homeostasis of the CNS and neuroinflammation; the major galectins expressed in the CNS are Gal-1, Gal-3, Gal-4, Gal-8, and Gal-9 (18). In this study, we compared the dynamic gene expressions of Gal-1, Gal-3, Gal-4, Gal-8, and Gal-9 in the brains between C57BL/6 and BALB/c mice infected with *T. gondii* Pru strain, only Gal-3 and Gal-9 were highly expressed in the brains of both C57BL/6 and BALB/c mice. C57BL/6 mice presented significantly higher mRNA expressions of Gal-3 and Gal-9 than those of BALB/c mice at days 35, 50, and 70 p.i. Gal-3 and Gal-9 are known pro-inflammatory mediators and regulators of apoptosis (29). Gal-9 is produced by activated

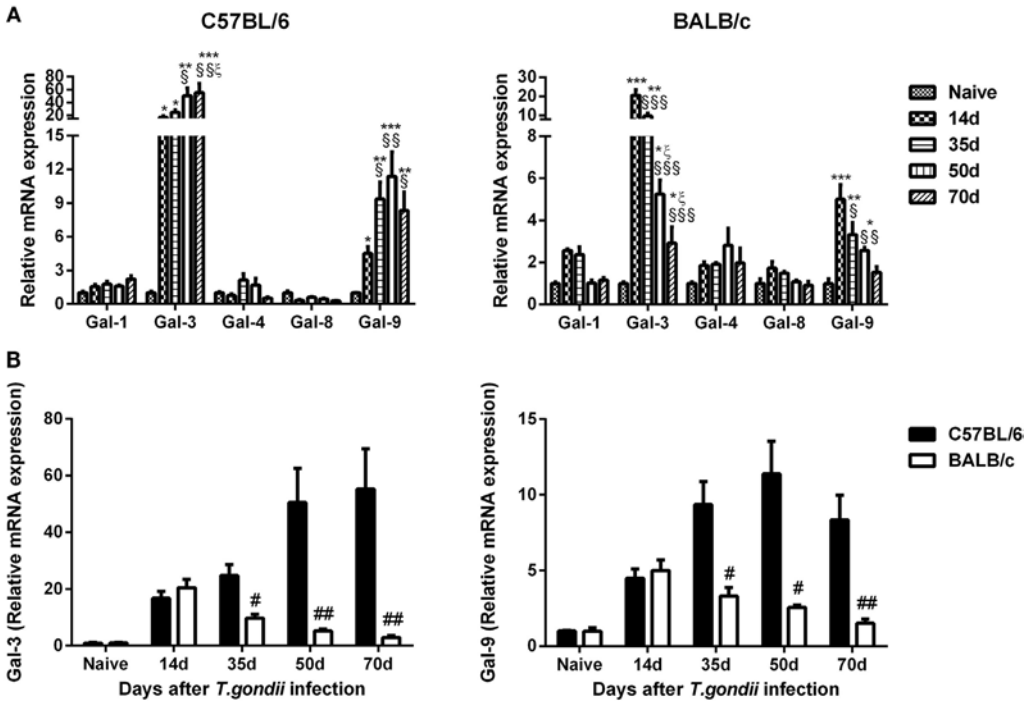

FIGURE 5 | Relative mRNA expressions of Gal-1, Gal-3, Gal-4, Gal-8, and Gal-9 in the brain tissues of *Toxoplasma gondii* Pru strain-infected C57BL/6 and BALB/c mice were detected by using quantitative real-time reverse transcription-polymerase chain reaction. **(A)** Galectin expressions in the brains of C57BL/6 and BALB/c mice. **(B)** Comparison of Gal-3 and Gal-9 levels in the brains of C57BL/6 and BALB/c mice. Values are means from triplicate measurements, and data are presented as mean ± SD. There were four mice per group. The data shown are representative of those from two different experiments. $^{*}P < 0.05$, $^{**}P < 0.01$, and $^{***}P < 0.001$ vs naive; $^{§}P < 0.05$, $^{§§}P < 0.01$, and $^{§§§}P < 0.001$ vs 14 days post infection (p.i.); $^{ξ}P < 0.05$ vs 35 days p.i.; $^{\#}P < 0.05$ and $^{\#\#}P < 0.01$ vs C57BL/6 mice.

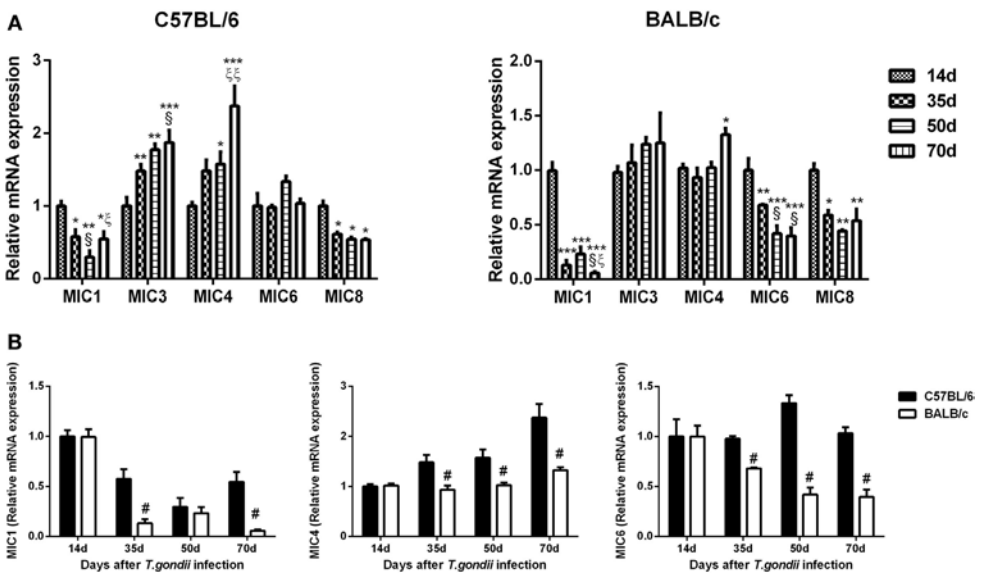

FIGURE 6 | Relative mRNA expressions of TgMIC1, TgMIC4, TgMIC6, TgMIC3, and TgMIC8 in the brain tissues of *Toxoplasma gondii* Pru strain-infected C57BL/6 and BALB/c mice were detected by using quantitative real-time reverse transcription-polymerase chain reaction. **(A)** TgMICs expressions in the brains of C57BL/6 and BALB/c mice. **(B)** Comparison of TgMIC1, TgMIC4, and TgMIC6 levels in the brains of C57BL/6 and BALB/c mice. Transcript level at day 14 post infection (p.i.) was taken as 1. Values are means from triplicate measurements, and data are presented as mean ± SD. There were four mice per group, and data are representative of those from two different experiments. $^{*}P < 0.05$, $^{**}P < 0.01$, and $^{***}P < 0.001$ vs 14 days p.i.; $^{§}P < 0.05$ vs 35 days p.i.; $^{ξ}P < 0.05$ and $^{§§}P < 0.05$ vs 50 days p.i.; $^{\#}P < 0.05$ vs C57BL/6 mice.

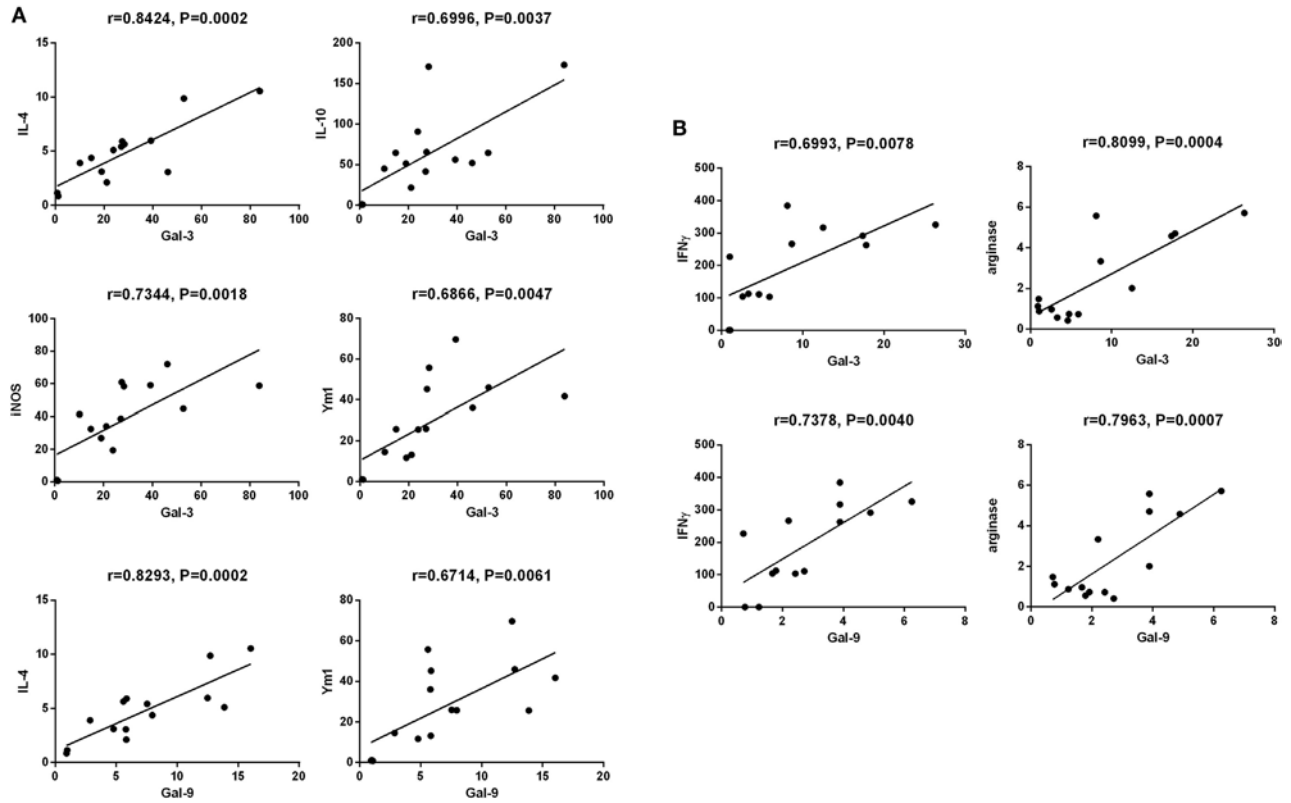

FIGURE 7 | Correlation analysis between Gal-3 and T helper 1 (Th1)/Th2/M1/M2 cytokines as well as between Gal-9 and Th1/Th2/M2 cytokines in the brain tissues of *Toxoplasma gondii* Pru strain-infected C57BL/6 and BALB/c mice ($n = 16$). **(A)** Significant correlations between Gal-3 and IL-4/IL-10/iNOS/Ym1 as well as between Gal-9 and IL-4/Ym1 existed in the brains of *T. gondii*-infected C57BL/6 mice. **(B)** Significant correlations between Gal-3 and IFNγ/Arg1 as well as between Gal-9 and IFNγ/Arg1 existed in the brains of *T. gondii*-infected BALB/c mice. The *r* value generates for the theoretical line of best fit, and the *P* value indicates the significance of the correlation.

astrocytes (43), functions as an astrocyte–microglia communication signal and promotes cytokine production, such as TNF, from microglia (44). After infection with ME49 strain of *T. gondii*, gal3$^{-/-}$ mice exhibits a higher parasite burden, delayed inflammatory response in the CNS, and significantly higher concentrations of IL-12p40 and IFNγ in the sera compared with those of gal3$^{+/+}$ mice (45). Gal-3 is required for resident microglia activation and proliferation in response to ischemic injury in a mouse model (46). Our data demonstrated that both Gal-3 and Gal-9 are important factors in TE-susceptible C57BL/6 and TE-resistant BALB/c mice infected with *T. gondii* Pru strain. In addition, the inflammatory response is more pronounced in the brains of C57BL/6 mice, which are corresponded well with the increased numbers of Iba1-positive resident microglia as well as increased Gal-3 and Gal-9 expressions in C57BL/6 mice. Furthermore, we evaluated the correlations between the gene expressions of Gal-3/Gal-9 and the levels of Th1 and Th2 cytokines, and M1- and M2-associated cytokines in the brains after *T. gondii* Pru strain infection. Positive correlations were found in the mRNA levels between Gal-3 and IL-4/IL-10/iNOS/Ym1 as well as between Gal-9 and IL-4/Ym1 in C57BL/6 mice; whereas positive correlations were found between Gal-3 and IFNγ/Arg1 as well as between Gal-9 and IFNγ/Arg1 in BALB/c mice. These data suggest that Gal-3 is related to Th2 and M1/M2 immune responses while Gal-9 is related to Th2 and M2 immune responses in *T. gondii*-infected C57BL/6 mice. Indeed, both Gal-3 and Gal-9 are related to Th1 and M2 immunity in BALB/c mice with chronic *T. gondii* infection. Our data suggested that Gal-3 and Gal-9 may involve in different immune responses to *T. gondii* Pru strain infection in the two lineages of mice.

Proteins secreted from apicomplexan MICs play important roles in the parasite adhesion and invasion of the host cells (47). MICs, which have been identified with lectin domains, support several key cellular processes including gliding motility, active cell invasion and migration through cells, biological barriers, and tissues (47). Our data showed that C57BL/6 mice expressed significantly higher levels of TgMIC1, TgMIC4, and TgMIC6 at days 35, 50, or 70 p.i. than those of BALB/c mice after *T. gondii* Pru strain infection. Therefore, TgMICs may be expressed differently in the two strains of mice with different genetic background. TgMIC1–4–6 complex contributes to host cell recognition and attachment *via* the action of TgMIC1 as well as contributes to the virulence of *T. gondii* in mice (48). Our data indicate that the different expression levels of TgMIC1, TgMIC4, and TgMIC6 in the two strains of mice may be associated with the different outcomes in *T. gondii* Pru strain-infected C57BL/6 and BALB/c mice.

In conclusion, this study has provided evidences that Gal-3 and Gal-9 may play a critical role in the regulation of M1, M2, Th1, and Th2 cytokines in the hosts with TE. Our data demonstrated

that significant different mRNA expressions of Gal-3 and Gal-9 as well as microglial activation markers, cytokines, and TgMICs were found between C57BL/6 and BALB/c mice after *T. gondii* Pru strain infection. Whether these differences are related to the phenomenon that C57BL/6 mice are susceptible while BALB/c mice are resistant to the development of TE needs to be further investigated.

ETHICS STATEMENT

This study was carried out in accordance with the recommendations of the requirements of the Animal Ethics Committee at Sun Yat-sen University. The protocol was approved by the Animal Ethics Committee at Sun Yat-sen University.

AUTHOR CONTRIBUTIONS

FL designed experiments, wrote, and edited the manuscript. JL conducted experiments, analyzed data, and wrote the manuscript draft. SH revised and edited the manuscript.

FUNDING

This work was supported by the Natural Science Foundation of China (no. 81471973) and the 2016 Medical Education Research Project of Chinese Medical Association Medical Education Branch and China Higher Education Society of Medical Education Professional Committee (2016B-KY013).

REFERENCES

1. Dubey JP. The history of *Toxoplasma gondii* – the first 100 years. *J Eukaryot Microbiol* (2008) 55(6):467–75. doi:10.1111/j.1550-7408.2008.00345.x
2. Weiss LM, Dubey JP. Toxoplasmosis: a history of clinical observations. *Int J Parasitol* (2009) 39(8):895–901. doi:10.1016/j.ijpara.2009.02.004
3. Connolly MP, Goodwin E, Schey C, Zummo J. Toxoplasmic encephalitis relapse rates with pyrimethamine-based therapy: systematic review and meta-analysis. *Pathog Glob Health* (2017) 111(1):31–44. doi:10.1080/20477724.2016.1273597
4. Denkers EY, Gazzinelli RT. Regulation and function of T-cell-mediated immunity during *Toxoplasma gondii* infection. *Clin Microbiol Rev* (1998) 11(4):569–88.
5. Suzuki Y, Kang H, Parmley S, Lim S, Park D. Induction of tumor necrosis factor-alpha and inducible nitric oxide synthase fails to prevent toxoplasmic encephalitis in the absence of interferon-gamma in genetically resistant BALB/c mice. *Microbes Infect* (2000) 2(5):455–62. doi:10.1016/S1286-4579(00)00318-X
6. Suzuki Y. Immunopathogenesis of cerebral toxoplasmosis. *J Infect Dis* (2002) 186(Suppl 2):S234–40. doi:10.1086/344276
7. Da Gama LM, Ribeiro-Gomes FL, Guimaraes U Jr, Arnholdt AC. Reduction in adhesiveness to extracellular matrix components, modulation of adhesion molecules and in vivo migration of murine macrophages infected with *Toxoplasma gondii*. *Microbes Infect* (2004) 6(14):1287–96. doi:10.1016/j.micinf.2004.07.008
8. Sica A, Mantovani A. Macrophage plasticity and polarization: in vivo veritas. *J Clin Invest* (2012) 122(3):787–95. doi:10.1172/JCI59643
9. Galvan-Pena S, O'Neill LA. Metabolic reprograming in macrophage polarization. *Front Immunol* (2014) 5:420. doi:10.3389/fimmu.2014.00420
10. Martinez FO, Helming L, Gordon S. Alternative activation of macrophages: an immunologic functional perspective. *Annu Rev Immunol* (2009) 27:451–83. doi:10.1146/annurev.immunol.021908.132532
11. Constant SL, Bottomly K. Induction of Th1 and Th2 $CD4^+$ T cell responses: the alternative approaches. *Annu Rev Immunol* (1997) 15:297–322. doi:10.1146/annurev.immunol.15.1.297
12. Kalinski P, Moser M. Consensual immunity: success-driven development of T-helper-1 and T-helper-2 responses. *Nat Rev Immunol* (2005) 5(3):251–60. doi:10.1038/nri1569
13. Chao CC, Anderson WR, Hu S, Gekker G, Martella A, Peterson PK. Activated microglia inhibit multiplication of *Toxoplasma gondii* via a nitric oxide mechanism. *Clin Immunol Immunopathol* (1993) 67(2):178–83. doi:10.1006/clin.1993.1062
14. Hernandez JD, Baum LG. Ah, sweet mystery of death! Galectins and control of cell fate. *Glycobiology* (2002) 12(10):127r–36r. doi:10.1093/glycob/cwf081
15. Rabinovich GA, Toscano MA. Turning "sweet" on immunity: galectin-glycan interactions in immune tolerance and inflammation. *Nat Rev Immunol* (2009) 9(5):338–52. doi:10.1038/nri2536
16. Perillo NL, Marcus ME, Baum LG. Galectins: versatile modulators of cell adhesion, cell proliferation, and cell death. *J Mol Med (Berl)* (1998) 76(6):402–12. doi:10.1007/s001090050232
17. Liu FT, Rabinovich GA. Galectins: regulators of acute and chronic inflammation. *Ann N Y Acad Sci* (2010) 1183:158–82. doi:10.1111/j.1749-6632.2009.05131.x
18. Chen HL, Liao F, Lin TN, Liu FT. Galectins and neuroinflammation. *Adv Neurobiol* (2014) 9:517–42. doi:10.1007/978-1-4939-1154-7_24
19. Child MA, Garland M, Foe I, Madzelan P, Treeck M, van der Linden WA, et al. *Toxoplasma* DJ-1 regulates organelle secretion by a direct interaction with calcium-dependent protein kinase 1. *MBio* (2017) 8(1):e02189-16. doi:10.1128/mBio.02189-16
20. Liu Q, Li FC, Zhou CX, Zhu XQ. Research advances in interactions related to *Toxoplasma gondii* microneme proteins. *Exp Parasitol* (2017) 176:89–98. doi:10.1016/j.exppara.2017.03.001
21. Meissner M, Reiss M, Viebig N, Carruthers VB, Toursel C, Tomavo S, et al. A family of transmembrane microneme proteins of *Toxoplasma gondii* contain EGF-like domains and function as escorters. *J Cell Sci* (2002) 115(Pt 3):563–74.
22. Reiss M, Viebig N, Brecht S, Fourmaux MN, Soete M, Di Cristina M, et al. Identification and characterization of an escorter for two secretory adhesins in *Toxoplasma gondii*. *J Cell Biol* (2001) 152(3):563–78. doi:10.1083/jcb.152.3.563
23. Dunay IR, Heimesaat MM, Bushrab FN, Muller RH, Stocker H, Arasteh K, et al. Atovaquone maintenance therapy prevents reactivation of toxoplasmic encephalitis in a murine model of reactivated toxoplasmosis. *Antimicrob Agents Chemother* (2004) 48(12):4848–54. doi:10.1128/AAC.48.12.4848-4854.2004
24. Dang Y, Xu Y, Wu W, Li W, Sun Y, Yang J, et al. Tetrandrine suppresses lipopolysaccharide-induced microglial activation by inhibiting NF-kappaB and ERK signaling pathways in BV2 cells. *PLoS One* (2014) 9(8):e102522. doi:10.1371/journal.pone.0102522
25. Jones LA, Roberts F, Nickdel MB, Brombacher F, McKenzie AN, Henriquez FL, et al. IL-33 receptor (T1/ST2) signalling is necessary to prevent the development of encephalitis in mice infected with *Toxoplasma gondii*. *Eur J Immunol* (2010) 40(2):426–36. doi:10.1002/eji.200939705
26. Jash A, Kwon HK, Sahoo A, Lee CG, So JS, Kim J, et al. Topical application of porcine placenta extract inhibits the progression of experimental contact hypersensitivity. *J Ethnopharmacol* (2011) 133(2):654–62. doi:10.1016/j.jep.2010.10.054
27. Zhang AM, Shen Q, Li M, Xu XC, Chen H, Cai YH, et al. Comparative studies of macrophage-biased responses in mice to infection with *Toxoplasma gondii* ToxoDB #9 strains of different virulence isolated from China. *Parasit Vectors* (2013) 6(1):308. doi:10.1186/1756-3305-6-308
28. Zhou X, Xu Y, Yang G, Li F. Increased galectin-1 expression in muscle of *Astragalus* polysaccharide-treated type 1 diabetic mice. *J Nat Med* (2011) 65(3–4):500–7. doi:10.1007/s11418-011-0527-9
29. Bellac CL, Coimbra RS, Simon F, Imboden H, Leib SL. Gene and protein expression of galectin-3 and galectin-9 in experimental pneumococcal meningitis. *Neurobiol Dis* (2007) 28(2):175–83. doi:10.1016/j.nbd.2007.07.005
30. Markova V, Smetana K Jr, Jenikova G, Lachova J, Krejcirikova V, Poplstein M, et al. Role of the carbohydrate recognition domains of mouse galectin-4 in oligosaccharide binding and epitope recognition and expression of galectin-4 and galectin-6 in mouse cells and tissues. *Int J Mol Med* (2006) 18(1):65–76. doi:10.3892/ijmm.18.1.65

31. Tribulatti MV, Mucci J, Cattaneo V, Aguero F, Gilmartin T, Head SR, et al. Galectin-8 induces apoptosis in the $CD4^{high}CD8^{high}$ thymocyte subpopulation. *Glycobiology* (2007) 17(12):1404–12. doi:10.1093/glycob/cwm104
32. Liesenfeld O, Kosek J, Remington JS, Suzuki Y. Association of $CD4^+$ T cell-dependent, interferon-gamma-mediated necrosis of the small intestine with genetic susceptibility of mice to peroral infection with *Toxoplasma gondii*. *J Exp Med* (1996) 184(2):597–607. doi:10.1084/jem.184.2.597
33. Silva NM, Manzan RM, Carneiro WP, Milanezi CM, Silva JS, Ferro EA, et al. *Toxoplasma gondii*: the severity of toxoplasmic encephalitis in C57BL/6 mice is associated with increased ALCAM and VCAM-1 expression in the central nervous system and higher blood-brain barrier permeability. *Exp Parasitol* (2010) 126(2):167–77. doi:10.1016/j.exppara.2010.04.019
34. Schluter D, Deckert-Schluter M, Lorenz E, Meyer T, Rollinghoff M, Bogdan C. Inhibition of inducible nitric oxide synthase exacerbates chronic cerebral toxoplasmosis in *Toxoplasma gondii*-susceptible C57BL/6 mice but does not reactivate the latent disease in *T. gondii*-resistant BALB/c mice. *J Immunol* (1999) 162(6):3512–8.
35. Schluter D, Kaefer N, Hof H, Wiestler OD, Deckert-Schluter M. Expression pattern and cellular origin of cytokines in the normal and *Toxoplasma gondii*-infected murine brain. *Am J Pathol* (1997) 150(3):1021–35.
36. Schluter D, Meyer T, Strack A, Reiter S, Kretschmar M, Wiestler OD, et al. Regulation of microglia by $CD4^+$ and $CD8^+$ T cells: selective analysis in CD45-congenic normal and *Toxoplasma gondii*-infected bone marrow chimeras. *Brain Pathol* (2001) 11(1):44–55. doi:10.1111/j.1750-3639.2001.tb00380.x
37. Fischer HG, Nitzgen B, Reichmann G, Hadding U. Cytokine responses induced by *Toxoplasma gondii* in astrocytes and microglial cells. *Eur J Immunol* (1997) 27(6):1539–48. doi:10.1002/eji.1830270633
38. Jones RS, Lynch MA. How dependent is synaptic plasticity on microglial phenotype? *Neuropharmacology* (2015) 96(Pt A):3–10. doi:10.1016/j.neuropharm.2014.08.012
39. Murray PJ, Wynn TA. Protective and pathogenic functions of macrophage subsets. *Nat Rev Immunol* (2011) 11(11):723–37. doi:10.1038/nri3073
40. Freund YR, Zaveri NT, Javitz HS. In vitro investigation of host resistance to *Toxoplasma gondii* infection in microglia of BALB/c and CBA/Ca mice. *Infect Immun* (2001) 69(2):765–72. doi:10.1128/IAI.69.2.765-772.2001
41. Suzuki Y, Remington JS. The effect of anti-IFN-gamma antibody on the protective effect of Lyt-2^+ immune T cells against toxoplasmosis in mice. *J Immunol* (1990) 144(5):1954–6.
42. Shi W, Xue C, Su XZ, Lu F. The roles of galectins in parasitic infections. *Acta Trop* (2018) 177:97–104. doi:10.1016/j.actatropica.2017.09.027
43. Burman J, Svenningsson A. Cerebrospinal fluid concentration of galectin-9 is increased in secondary progressive multiple sclerosis. *J Neuroimmunol* (2016) 292:40–4. doi:10.1016/j.jneuroim.2016.01.008
44. Steelman AJ, Li J. Astrocyte galectin-9 potentiates microglial TNF secretion. *J Neuroinflammation* (2014) 11:144. doi:10.1186/s12974-014-0144-0
45. Bernardes ES, Silva NM, Ruas LP, Mineo JR, Loyola AM, Hsu DK, et al. *Toxoplasma gondii* infection reveals a novel regulatory role for galectin-3 in the interface of innate and adaptive immunity. *Am J Pathol* (2006) 168(6):1910–20. doi:10.2353/ajpath.2006.050636
46. Lalancette-Hebert M, Swarup V, Beaulieu JM, Bohacek I, Abdelhamid E, Weng YC, et al. Galectin-3 is required for resident microglia activation and proliferation in response to ischemic injury. *J Neurosci* (2012) 32(30):10383–95. doi:10.1523/JNEUROSCI.1498-12.2012
47. Carruthers VB, Tomley FM. Microneme proteins in apicomplexans. *Subcell Biochem* (2008) 47:33–45. doi:10.1007/978-0-387-78267-6_2
48. Cerede O, Dubremetz JF, Soete M, Deslee D, Vial H, Bout D, et al. Synergistic role of micronemal proteins in *Toxoplasma gondii* virulence. *J Exp Med* (2005) 201(3):453–63. doi:10.1084/jem.20041672

Conflict of Interest Statement: The authors declare that the research was conducted in the absence of any commercial or financial relationships that could be construed as a potential conflict of interest.

frontiers in Immunology

ORIGINAL RESEARCH
published: 28 May 2018
doi: 10.3389/fimmu.2018.01164

Allocation of Interferon Gamma mRNA Positive Cells in Caecum Hallmarks a Protective Trait Against Histomonosis

*Fana Alem Kidane[1], Taniya Mitra[1], Patricia Wernsdorf[1], Michael Hess[1,2] and Dieter Liebhart[1]**

[1] Clinic for Poultry and Fish Medicine, Department for Farm Animals and Veterinary Public Health, University of Veterinary Medicine Vienna, Vienna, Austria, [2] Christian Doppler Laboratory for Innovative Poultry Vaccines, University of Veterinary Medicine Vienna, Vienna, Austria

Histomonosis is a parasitic disease of gallinaceous birds characterized by necrotic lesions in cacum and liver that usually turns fatal in turkeys while it is less severe in chickens. Vaccination using *in vitro* attenuated *Histomonas meleagridis* has been experimentally shown to confer protection against histomonosis. The protective mechanisms that underpin the vaccine-induced immune response are not resolved so far. Therefore, the actual study aimed to evaluate the location and quantitative distribution patterns of signature cytokines of type 1 [interferon gamma (IFN-γ)] or type 2 [interleukin (IL)-13] immune responses in vaccinated or infected hosts. An intergroup and interspecies difference in the spatial and temporal distribution patterns of cytokine mRNA positive cells was evident. Quantification of cells showed a significantly decreased percentage of IFN-γ mRNA positive cells at 4 days post-inoculation (DPI) in caeca of turkeys inoculated exclusively with the attenuated or the virulent inocula, compared to control birds. The decrement was followed by a surge of cells expressing mRNA for IFN-γ or IL-13, reaching a peak of increment at 10 DPI. By contrast, turkeys challenged following vaccination showed a slight increment of cecal IFN-γ mRNA positive cells at 4 DPI after which positive cell counts became comparable to control birds. The increase in infected birds was accompanied by an extensive distribution of positively stained cells up to the muscularis layer of cecal tissue whereas the vaccine group maintained an intact mucosal structure. In chickens, the level of changes of positive cells was generally lower compared to turkeys. However, control chickens were found with a higher percentage of IFN-γ mRNA positive cells in cecum compared to their turkey counterparts indicating a higher resistance to histomonosis, similar to the observation in immunized turkeys. In chickens, it could be shown that the changes of cytokine-positive cells were related to variations of mononuclear cells quantified by immunofluorescence. Furthermore, gene expression measured by reverse transcription quantitative real time PCR confirmed variations in organs between the different groups of both bird species. Overall, it can be concluded that a proportionally increased, yet controlled, allocation of IFN-γ mRNA positive cells in caeca hallmarks a protective trait against histomonosis.

Keywords: *Histomonas meleagridis*, histomonosis, vaccination, interferon gamma, interleukin-13, *in situ* hybridization, immunofluorescence, image analysis

OPEN ACCESS

Edited by:
Zhiguang Wu,
University of Edinburgh,
United Kingdom

Reviewed by:
Yongxiu Yao,
Pirbright Institute (BBSRC),
United Kingdom
Xun Suo,
China Agricultural University, China
Jean-Remy Sadeyen,
Pirbright Institute (BBSRC),
United Kingdom

****Correspondence:***
Dieter Liebhart
dieter.liebhart@vetmeduni.ac.at

Specialty section:
This article was submitted to Microbial Immunology, a section of the journal Frontiers in Immunology

Received: *12 December 2017*
Accepted: *09 May 2018*
Published: *28 May 2018*

Citation:
Kidane FA, Mitra T, Wernsdorf P, Hess M and Liebhart D (2018) Allocation of Interferon Gamma mRNA Positive Cells in Caecum Hallmarks a Protective Trait Against Histomonosis. Front. Immunol. 9:1164. doi: 10.3389/fimmu.2018.01164

INTRODUCTION

Histomonosis (syn.: blackhead disease, enzootic typhlohepatitis) is a parasitic disease of gallinaceous birds caused by the flagellate *Histomonas meleagridis* (1). The disease can cause high mortality rates in turkeys (*Meleagris gallopavo*) while in chickens (*Gallus gallus*) clinical signs are less severe, however, the infection entails an impaired performance in chickens leading to severe economic losses (2, 3). In both species, the parasite is able to infiltrate the cecum and triggers severe inflammation, thickening of the cecal wall and formation of fibrinous exudates. Histomonads can then migrate to the liver leading to multifocal areas of inflammation and necrosis, which is commonly observed in infected turkeys (4). Recently, a live vaccine prepared from an *in vitro* passaged clonal culture of *H. meleagridis* has been experimentally shown as safe and capable of providing protection from the disease (5–7). However, investigations on the immune response against histomonosis are rare and relevant protective mechanisms are so far not identified.

Only a few studies investigated the immune system of poultry in response to virulent *H. meleagridis* (8). It could be demonstrated that the level of serum antibody in turkeys may not be a key component in the protection against the parasite as passive immunization using immune sera or active immunization with killed vaccines failed to protect turkeys during challenge (5, 9, 10). However, local antibodies were measured in different parts of the intestine of infected chickens, a host species more resistant to fatal histomonosis, leading to the speculation that mucosal antibodies might be components that contribute toward protection (11). In a different study, an early onset of cytokine expression in cecal tonsils of infected chickens compared to infected turkeys was demonstrated and it was hypothesized to induce a timely immune response in order to prevent the parasite from migrating to the liver (12). Recently, flow cytometry was applied and changes in various immune cell populations in cecum, liver, spleen and blood of vaccinated and/or infected turkeys and chickens were determined showing a less pronounced changes in the frequency of immune cells in vaccinated hosts compared to an exacerbated influx in infected hosts (13).

Successful immunization depends on the ability to induce response selectively and reliably, and for this type 1/type 2 classes of immunity have been characterized in mammals in association with protection following infection or vaccination (14). Type 1/type 2 immunity has also been shown in chickens (15, 16) and can serves as a model for characterizing and optimizing immune responses in poultry for a better conferment of resistance through rational vaccine design (17). Previous studies on type 1/type 2 immunity following histomonosis, however, yielded inconclusive results. Powell et al. (12) found indications for a type 2 response with a persistently enhanced expression of interleukin (IL)-13 mRNA in infected chickens and turkeys, whereas a type 1 driven response with an augmented expression of interferon gamma (IFN-γ) mRNA was described when chickens were co-infected with histomonads and the intestinal worm *Heterakis gallinarum* (18). However, these studies utilized different infection protocols and applied undefined inocula for infection and the relevant pathway elicited during vaccination with attenuated live histomonads has never been investigated.

Moreover, in characterizing the expression patterns of cytokines of type 1/type 2 immunity, the widely utilized method has been reverse transcription quantitative real time PCR (RT-qPCR). While the technique delivered valuable information on the overall changes of transcription levels in homogenized samples, parameters such as the location and quantity of the expressing cells in tissues remained unlocked. Thus, to localize avian cells expressing T helper (Th)1/Th2 signature cytokines, respectively, INF-γ and IL-13, this study employed an *in situ* hybridization (ISH) approach to localize the cells in cecum, liver and spleen of vaccinated and/or infected turkeys and chickens. For verification of variations of the cytokines between the groups and species, RT-qPCR was employed to measure transcripts of IFN-γ and IL-13 mRNA on selected samples of turkeys and chickens, considering the different approach of both techniques. Furthermore, identification of immune cells recruited during vaccination or infection was conducted using immunofluorescence (IF) to reveal changes in populations of B cells, T cells and macrophage/monocytes in selected samples from chickens.

Abbreviations: CC, control chickens; CT, control turkeys; DIG, digoxigenin; DPI, days post-inoculation; IC, infected chickens; IF, immunofluorescence; IFN-γ, interferon gamma; IL, interleukin; ISH, *in situ* hybridization; IT, infected turkeys; MLS, mean lesion score; Th, T helper; VC, vaccinated chickens; VIC, vaccinated and infected chickens; VIT, vaccinated and infected turkeys; VT, vaccinated turkeys.

MATERIALS AND METHODS

Animal Trial

Inoculum for Vaccination and Infection

The inocula used for vaccination or infection originated from a clonal culture of *H. meleagridis*/Turkey/Austria/2922-C6/04, established from cecal contents of a diseased turkey (19). The clonal culture was propagated for a short period of time (21 passages) to preserve virulence, hence used for challenge, or for 295 passages to achieve attenuation, according to previous protocols (5, 20). The parasites were kept as cryopreserved cultures (stored at −150°C) were then thawing and incubated at 40°C in a culture medium consisting of Medium 199 supplemented with Earle's salts, L-glutamine, 25 mM HEPES and L-amino acids (Gibco™, Invitrogen, Lofer, Austria), 15% of fetal calf serum (Gibco™) and 0.66 mg of rice starch (Sigma–Aldrich, Vienna, Austria). Before administration, the number of viable cells was determined using a Neubauer cell counting chamber (Reichert, Buffalo, NY, USA) after staining with 0.4% trypan blue solution and adjusted to 1×10^6 histomonads per ml of medium.

Birds

A total of 60 turkeys (B.U.T. 6™; Aviagen Turkeys Ltd., Tattenhall, UK) and the same number of specific pathogen-free chickens (VALO Biomedia, Osterholz-Scharmbeck, Germany) were used. The birds were numerically labeled with a subcutaneously attached tag and housed on deep litter. Unmedicated commercial turkey, respectively, chicken starter feed and water were provided *ad libitum,* except for a 5 h abstinence from feed directly after

inoculation. The animal trials were approved by the institutional ethics committee and the national authority according to §26 of the Law for Animal Experiments, Tierversuchsgesetz—TVG (license number bmwf GZ 68.205/0147-II/3b/2013).

Experimental Design and Inoculation

In the main experiment (trial 1, **Table 1**), four groups of turkeys, as well as the same number of chicken groups, were arranged in separate groups ($n = 15$ per group). The groups comprised of only vaccinated turkeys or chickens (VT and VC), only IT and IC, vaccinated and infected turkeys or chickens (VIT and VIC) and control turkeys or chickens (CT and CC). Birds in group VIT and VIC were vaccinated at their first day of life. The challenge of the VIT and VIC was given on their 28th day of life, together with the infection or vaccination of the other groups.

Each bird received a dosage of 6×10^5 attenuated or virulent histomonads in 0.6 ml of medium, equally split *via* oral and cloacal application. Control birds were sham inoculated with equal volumes of pure culture media only. The oral and cloacal administration was performed using crop tubes attached to a sterile syringe, respectively, pipette tips on a 1 ml pipette. The feed was withdrawn for 5 h following inoculation to promote an adequate colonization of the parasite in the gut. To confirm successful inoculation, cloacal swabs were taken from every bird in intervals of 2–3 days and parasites were incubated for 3 days at 40°C in a culture medium mentioned above. Growth was controlled by microscopical examination of viable parasites.

In a similar setting, an additional experiment (trial 2) was conducted for generating additional cecum, liver and spleen samples for IF labeling of B cells, T cells and monocytes/macrophages in the above-described organs of chickens. For that, three groups of chickens were used: IC, VC, and control chickens (CC). Each infected, respectively, vaccinated bird received 1×10^4 histomonads orally and cloacally.

Clinical Monitoring and Postmortem Lesion Scoring

The birds were monitored daily for clinical signs of histomonosis such as ruffled feathers, depression and yellowish diarrhea. Birds showing clinical signs of the disease were euthanized.

At 4, 7, 10, 14 and 21 days post-inoculation (DPI), three predefined birds per group were killed according to their tag-numbers by bleeding after intravenous injection of sodium thiopental (Sandoz, Kundl, Austria). Postmortem examination and grading of lesions in cecum and liver were performed according to a previous scheme that used scores from 0 (no lesion) to 4 (severe lesions) (11, 21).

Histological Techniques

ISH for Localization of *H. meleagridis*

Pieces of mid-cecum, liver and spleen samples intended for ISH were fixed in 4% neutral buffered formaldehyde (SAV liquid production, Flintsbach, Germany) for at least 48 h at room temperature. The tissues were then trimmed and rinsed in running tap water for an hour before proceeding to routine histological processing. The processing involved dehydration in serially graded alcohols (80, 96 and 100%), clearing in Neo-Clear® (Merck, Darmstadt, Germany) and paraffin infiltration. Finally, the tissues were embedded in paraffin wax and stored until use. For the scheduled ISH, serial sections of 4 µm were prepared using Microme HM360 rotary microtome (Microme, Walldorf, Germany) and mounted on Superfrost Plus slides (Menzel-Gläser, Braunschweig, Germany). To further ensure adhesion of sections on the slides, an overnight treatment of the slides was allowed at 37°C. The ISH with *H. meleagridis* specific digoxigenin (DIG)-labeled oligonucleotide probes was performed according to a published protocol (22).

ISH for Localization of IFN-γ or IL-13 mRNA

Generation of RNA Probes

The use of *in vitro* transcribed DIG-labeled RNA probes for detection of chicken IFN-γ and IL-13 mRNA in liver and spleen paraffin sections has been established earlier. The same approach was followed to establish turkey's staining antisense IFN-γ or IL-13 RNA probes together with negative control sense probes as previously described (23). Briefly, gene-specific primers were designed to amplify the mRNA of turkey IFN-γ and IL-13 (**Table 2**). The targets were amplified from total RNA extracted from the spleen of a non-infected turkey by RT-PCR using QIAGEN OneStep RT-PCR kit (Qiagen, Hilden, Germany). The PCR products were then separated on 1.5% Agarose gel and purified using QIAquick® Gel Extraction Kit (Qiagen). The respective cDNAs were ligated into pCR®4-TOPO® vector for cloning in One Shot® TOP10 Chemically Competent *E. coli*, according to the manufacturer's instructions (Invitrogen, Carlsbad, CA, USA). The nucleotide

TABLE 1 | Experimental scheme and sampling strategy for different groups of turkeys and chickens inoculated with attenuated and/or virulent histomonads.

	Age of birds in days/days post-inoculation						
Group	**1**	**28**	**32/4**	**35/7**	**38/10**	**42/14**	**49/21**
Vaccinated turkeys (VT)		Vaccination	x[a]	x	X	X	x
Vaccinated chickens (VC)		Vaccination	x	x	X	X	x
Infected turkeys (IT)		Infection	x	x	X	N/A[b]	N/A
Infected chickens (IC)		Infection	x	x	X	X	x
Vaccinated and infected turkeys (VIT)	Vaccination	Infection	x	x	X	X	x
Vaccinated and infected chickens (VIC)	Vaccination	Infection	x	x	X	X	x
Control turkeys (CT)		Mock infection	x	x	X	X	x
Control chickens (CC)		Mock infection	x	x	X	X	x

[a]*Necropsy and sampling of three birds.*

[b]*Not applicable due to death caused by virulent histomonads at earlier time points.*

TABLE 2 | Primers, Genbank accession number and the size of the PCR product used for RNA probe generation for *in situ* hybridization of interferon gamma (IFN-γ) and interleukin (IL)-13 mRNA.

Target	Primer sequence	Accession number	Product size (bp)
Turkey-IFN-γ	F: CACCAAGAAGATGACTTACCAG R: TGAGGATGGCTCCTTTTCC	XM_003202048	486
Turkey-IL-13	F: GCTCCATGCCCAAGATGAAG R: AGCGTTGGCAAGAAGTTCC	AM493431	289

sequence and insertion of the cloned products were verified by sequencing (LGC Genomics, Augsburg, Germany).

Plasmids validated to contain the cDNA of the cytokines were linearized with *Spe*I or *Not*I restriction enzymes (Thermo Scientific, Dreieich, Germany). Depending on the insertion, T7 or T3 RNA polymerases were used separately to generate sense or antisense DIG-labeled RNA probes using DIG RNA Labeling Kit (SP6/T7) (Roche Diagnostics, Mannheim, Germany) according to the manufacturer's protocol. The probe yield was quantified using NanoDrop spectrophotometer (Thermo Scientific) and the size of the transcribed probes was verified by gel electrophoresis. Furthermore, the efficiency of the DIG-labeling was assessed by immunoblotting dilution series of DIG-labeled RNA probes according to the manufacturer's recommended protocol given in the DIG RNA Labeling Kit (SP6/T7) (Roche Diagnostics) with some modifications mentioned in the previous work (23).

RNA ISH

The ISH protocol for staining cytokine mRNA positive cells was described in an earlier study (23). Briefly, paraffin sections were deparaffinized with Neo-Clear® (Merck) and rehydrated in a series of graded alcohols (100, 96 and 70%) and diethyl pyrocarbonate (DEPC) treated distilled water. The sections were then digested with 2.8 µg/ml of proteinase K (Invitrogen, Carlsbad, CA, USA) in 0.05 M Tris–HCl (pH 7.5), at 40°C for 30 min. Afterwards, rinsing and dehydration were performed in DEPC-treated water and increasing concentrations of ethanol. Following a short period of air drying, the sections were covered with a hybridization mix composed of 50% formamide, 4× standard saline citrate buffer (SSC), Herring's Sperm DNA (500 ng/ml), 1× Denhardt's solution, 10% dextran sulfate, and the optimal concentration of the respective DIG-labeled RNA probe. A concentration of probes that ranged from 10 to 1,000 ng/ml of hybridization buffer was tested initially to find a defined concentration for further use. Hybridization of the probe with the target RNA was performed in a humidified chamber for overnight at 40°C.

On the next day, stringency washes were made with 2× SSC at room temperature for 30 min, followed by RNase A (20 ng/ml) (Roche Diagnostics) treatment in a solution mix of 0.5 M NaCl, 5 mM Tris–HCl (pH 7.5) and 1 mM EDTA, at 40°C for 30 min. Further washing steps were done two times in 1× and 0.1× SSC at room temperature for 10 min each.

For conjugating the DIG-labeled hybrid-complexes with an enzyme to be used for the color reaction, the sections were first incubated in a blocking solution (50% of Buffer I, 0.3% TRITON®-X and 5% normal goat serum in distilled water) for 30 min in a humidified chamber. The blocking solution was replaced by anti-DIG-AP-antibody diluted 1:100 in the blocking solution mix and incubated for 1 h at room temperature. Afterward, washing and equilibration were performed in three steps. First, unbound antibody was removed by washing the slides in a 1 to 1 dilution of Buffer I (100 mM Tris–HCl pH 7.5, 150 mM NaCl) in distilled water for 15 min. Second, the washing mentioned before was repeated and finally, equilibration in Buffer II (100 mM Tris–HCl pH 7.5, 100 mM NaCl, 50 mM $MgCl_2$, final pH 9.5) was made for 10 min.

For visualizing the target molecules, color reaction was developed using a substrate mix of an equilibration buffer (Buffer II), NBT (4-nitro blue tetrazolium chloride) (0.45 mg/ml), BCIP (5-bromo-4-chloro-3-indolyl-phosphate) (0.175 mg/ml) (Roche Diagnostics) and Levamisole (240 µg/ml) (Sigma, Deisenhofen, Germany). The color reaction was performed in a humidified chamber under dark conditions for overnight. On the next day, the reaction was terminated by immersing the sections in Tris-EDTA (pH 8.0) for at least 10 min. Finally, the sections were counterstained with Gill's hematoxylin (Merck) and mounted under coverslips (Menzel-Gläser) with Aquatex® aqueous mounting medium (Merck). For controlling the specificity of the technique, ISH was performed using the respective sense probes. Moreover, a slide from sections incubated with DEPC-water instead of the probes was used in parallel as negative control.

Immunofluorescence

Cecum, liver and spleen of one bird per group obtained from trial 2 were cryopreserved after embedding in Tissue-Tek® (Sakura Finetek Europe B.V., Flemingweg, the Netherlands) on aluminum foils. Liquid nitrogen was used to freeze the embedded tissue samples. The frozen samples were then stored at −80°C until they were cut into 5 µm slices by a cryostat (CM1800, Leica Mikrosysteme GmbH, Vienna, Austria) and directly processed for IF.

A multicolor staining protocol was employed using mouse anti-chicken Bu-1-Biotin for the detection of B cells, unlabeled mouse anti-chicken CD3 for the detection of T cells and mouse anti-chicken KUL01-PE for the detection of monocytes/macrophages (all SouthernBiotech, Birmingham, AL, USA). For labeling, the cryosections were first fixed in pre-cooled acetone at −20°C. After drying and rehydration in PBS, they were treated with blocking solution (PBS, 2% bovine serum albumin and 10% goat serum) and then incubated overnight with the CD3 antibody at 4°C in a humidified chamber.

On the next day, slides were repeatedly washed with PBS and covered with the secondary antibody goat anti-mouse Alexa 488 (Invitrogen, Vienna, Austria). Following extensive washing and treatment with the blocking solution mentioned above, the other two primary antibodies (biotin-labeled anti-chicken Bu-1 and anti-chicken KUL01 directly labeled with r-phycoerythrin) were applied on the tissues and incubated overnight in a humidified chamber in the same way as mentioned before.

On the third day, streptavidin-Alexa 647 (Life Technologies, Vienna, Austria) was used for conjugation with the Bu-1

antibody. Cell nucleus staining was performed with 4, 6-diamidine-2-phenylindole dihydrochloride (DAPI) (Boehringer Mannheim GmbH, Germany). An isotype control for IgG1k (eBioscience, Vienna, Austria) together with the goat anti-mouse Alexa 488 antibody and samples without primary antibodies were included as controls to confirm the specificity of primary antibody binding.

Microscopy and Analysis of Images for Quantification of Stained Cells

Tissue sections processed by chromogenic ISH for staining cytokine mRNA expressing cells were examined using light transmission microscopy under Zeiss Axio Imager Z1 (Carl Zeiss Microscopy GmbH, Germany). Sections were examined for the location of the stained cells in context of the histological architecture of the respective tissues. Afterward, digital images of the sections were made using a USB camera and the TissueFAXs image acquisition software (TissueGnostics GmbH, Vienna, Austria). The digital images were analyzed for quantification of cells by HistoQuest (version 4.04.0150, TissueGnostics GmbH). For cell quantification, a region of interest (ROI) was selected randomly excluding artifacts, major blood vessels and edges of the sections. The ROI for each sample was a total tissue area of 2 mm^2 divided among equal sizes of eight rectangular ROI. Then, a total number of cells within those 2 mm^2 of the ROI were counted based on their blue nuclei staining after using hematoxylin as a master channel. Valid cells were gated by hematoxylin area versus hematoxylin mean intensity. By applying the software integrated color separation method named single reference shade, a second color detection was performed to automatically separate the hematoxylin (blue) nuclei staining from NBT-BCIP (dark violet) staining based on their optical density. Cutoff values for discriminating NBT-BCIP positive cells from negative cells were set interactively based on the background signal measured in the negative controls (sections treated with sense probes or no probe). In addition, backward viewing was performed to verify the correct discrimination of NBT-BCIP stained cells from negative cells by the source image, shades and color overlay. The percentage of NBT-BCIP stained cells out of the total quantified cells in each tissue section was then exported to SPSS (SPSS 21.0, IBM, Armonk, NY, USA) for statistical analysis.

The procedure for quantification of cells in triple stained IF sections were described earlier (24). Briefly, a multichannel acquisition was made using a Zeiss Axio Imager Z1 fitted with a PCO USB camera and eight regions of interest were selected in digital images of each tissue sample covering an area of 2 mm^2. The identification of each cell was achieved by TissueQuest software using the fluorescence of DAPI (master channel). Valid cells were gated by DAPI area versus DAPI mean intensity. From this population of cells, T cells, B cells and monocytes/macrophages with their respective fluorescence signals were subsequently gated. According to the setup of the respective gates, T cells, B cells and monocytes/macrophages were quantified by the software.

RT-qPCR

Stabilization of RNA in pieces of cecum, liver and spleen samples was performed by immersing the tissues in RNAlater® solution (Qiagen) according to the manufacturer's instruction. Total RNA was then extracted using RNeasy® mini kit (Qiagen) after homogenizing the tissues with QIAshredders (Qiagen) according to manufacturer's instructions. Every RNA sample was assessed for purity, quantity and integrity by using NanoDrop 2000 (ThermoFisher Scientific, Vienna, Austria) and 4200 TapeStation (Agilent Technologies, Waldbronn, Germany), respectively. The RNA samples were stored at −80°C until used.

The expression level of IFN-γ or IL-13 mRNA was quantified by applying TaqMan one-step real-time RT-qPCR using Brilliant III Ultra-Fast QRT-PCR master mix kit (Agilent Technologies, Waldbronn, Germany). Previously published primers and probes for reference genes TFRC (transferring receptor protein 1) and RPL13 (ribosomal protein L13) for turkeys or RPL13 and TBP (TATA box binding protein) for chickens, as well as for the mentioned cytokines were applied (**Table 3**) (12, 25). Amplification of the primary transcripts and quantification of their specific products were performed using AriaMx real-time PCR system (Agilent Technologies, Waldbronn, Germany) together with the Agilent AriaMx1.0 software (Agilent Technologies, Waldbronn, Germany). The thermal cycle profile was as follows: 1 cycle of RT at 50°C for 10 min followed by 95°C for 3 min to hot start, 40 cycles of amplification at 95°C for 5 s and 60°C for 10 s. Different types of controls such as non-reverse transcriptase and non-template control were run to check for genomic DNA contamination and overall PCR contamination.

The cytokines' average cycle threshold (Ct) values for every organ were normalized using geometric mean Ct of the reference genes, to exclude technical variations during sampling and processes of RT-qPCR. Fold change of cytokines was then calculated from the normalized mean Ct value of cytokines from each group by applying the formula $2^{(-\Delta\Delta Ct)}$ (26).

TABLE 3 | Reverse transcription-qPCR primers and probes.

Target	Primer and probe sequences	Reference
Turkey IFN-γ	F: AACCTTCCTGATGGCGTGAA R: CTTGCGCTGGATTCTCAAGTC P:HEX-AAAGATATCATGGACCTGGCCAAGCTTCA-BHQ1	(12)
Turkey IL-13	F: CCTGCACGGCCAGATGA R: GGCAAGAAGTTCCGCAGGTA P: CY5-TGCCAGCTGAGCACCGACAACG-BHQ1	
Chicken IFN-γ	F: GTGAAGAAGGTGAAAGATATCATGGA R: GCTTTGCGCTGGATTCTCA P: HEX-TGGCCAAGCTCCCGATGAACGA-BHQ1	
Chicken IL-13	F: CACCCAGGGCATCCAGAA R: TCCGATCCTTGAAAGCCACTT P: CY5-CATTGCAAGGGACCTGCACTCCTCTG-BHQ1	
RPL13	F: GGAGGAGAAGAACTTCAAGGC R: CCAAAGAGACGAGCGTTTG P: HEX-CTTTGCCAGCCTGCGCATG-BHQ1	(24)
TBP	F: CTGGGATAGTGCCACAGCTA R: GCACGAAGTGCAATGGTTT P: ROX-TGCAACCAAGATTCACCGTGGA-BHQ2	
TFRC	F: AGCTGTGGGTGCTACTGAA R: GGCAGAAATCTTGACATGG P: ROX-CTCTGCCATGCTGCATGCCA-BHQ2	

Statistical Analysis

The statistical package SPSS (SPSS 21.0, IBM, Armonk, NY, USA) was used to execute the descriptive and non-descriptive statistics. Mean lesion scores of cecum or liver were calculated for each group of turkeys or chickens necropsied at the specified DPI. Similarly, total mean lesion scores (MLSs) of cecum or liver were calculated for each group of turkeys or chickens by pooling the total lesion scores of each group and divided by the total number of birds in the group. For comparing differences in the mean percentage of cytokine mRNA positive cells, first normality of the data distribution obtained from percentages of quantified ISH-positive cells for each cytokine was tested using Kolmogorov–Smirnov test according to the tissue and host species. Then, since the data generated from quantification of turkey IFN-γ and IL-13 mRNA positive cells were normally distributed, mean values obtained from the different groups necropsied at different days were compared with the control using independent samples *t*-test. By contrast, due to lack of normality of data distribution in chicken tissues, Mann–Whitney *U* test was used to test the significance of mean differences. Furthermore, *t*-test was used to compare mean of normalized Ct values of the RT-qPCR data. Mean value differences were considered significant when the *P*-value was less than 0.05 ($^*P < 0.05$).

RESULTS

Animal Trial

Turkeys inoculated with virulent histomonads without prior vaccination (IT) exhibited typical signs of histomonosis such as a ruffled feather, depression and sulfur-colored diarrhea starting from 7 DPI. Consequently, two birds had to be euthanized due to severe suffering at 11 DPI while the remaining animals were found dead at 12 and 13 DPI. There were not any overt clinical signs in the rest of the turkeys' as well as all of the chickens' groups until the experiment was terminated at 21 DPI. Microscopical investigation of cultured cloacal swabs, however, confirmed the presence of the flagellate in the gut of birds of every group except the controls (data not shown).

Necropsy findings are given by MLS of every group on each sampling day. Total mean lesions scores differed according to the given inoculum, respectively, were found to be reduced in birds that received the vaccination (**Figure 1**). In turkeys (**Figure 1A**), the global MLS was 0.8 in cecum and 0.5 in the liver of VT. Turkeys in group IT had a total MLS of 3.2 and 2.8 in cecum and liver, respectively. In VIT, a total MLS of 2.7 in cecum and MLS of 1.3 in liver were observed. In chickens (**Figure 1B**), the highest total MLS recorded was in cecum and liver of IC (2 and 1.6, respectively). Chickens in group VC and VIC displayed a global MLS below 0.5 in both cecum and liver. None of the control birds in group CT or CC showed lesions at any sampling day.

Localization of *H. meleagridis* in Tissue Sections

Detailed results on frequencies of *H. meleagridis* localized by ISH in cecum and liver of the birds are given in **Table 4**. In cecum, histomonads could be localized in the majority of the turkeys that were inoculated either with the attenuated and/or virulent histomonads. Groups of chickens inoculated with histomonads showed the parasite localized in the cecal sections yet with less frequency than the turkeys inoculated with the same histomonads.

The presence of histomonads was generally uncommon in livers except in IT in which the parasite was detected throughout the sampling days. The protozoa could be found in only one VT collected at 21 DPI and few liver samples (3 out of 15 birds) taken from VIT. In chickens, only three liver samples taken from IC were positive for histomonads.

The spleen of all turkey and chicken samples, independent of the group they belong to, were without parasite infestation and the control groups confirmed the status of non-inoculated birds. Localization and distribution of virulent or attenuated histomonads in cecum and liver are comparatively shown in turkeys of the respective groups (**Figure 2**).

Evaluation of IFN-γ and IL-13 RNA Probes

The DIG-labeled RNA probes generated to hybridize to turkey IFN-γ or IL-13 mRNA in paraffin sections of cecum, liver and spleen could label cells containing the mRNA of the cytokines at a probe concentration of 600 or 300 ng/ml of hybridization buffer for IFN-γ or IL-13, respectively. Similarly, probes against chicken IFN-γ or IL-13 mRNA resulted in distinct coloration of target cells at a concentration of 400 or 100 ng/ml of hybridization buffer, respectively. Positive cells could be recognized by their dark purple color developing from the enzymatic reaction of NBT-BCIP. A higher or lower concentration of probes than the ones mentioned resulted in fainting or over staining of sections, hindering identification of individual cells (data not shown).

Localization and Quantitative Distribution Patterns of IFN-γ or IL-13 mRNA Positive Cells Following Vaccination or Infection

Spatial and Temporal Distribution Differences of Quantified IFN-γ mRNA Positive Cells

The spatial distribution patterns of stained cells in cecum and liver of turkeys inoculated with the tentative vaccine or the virulent inoculum are shown in **Figure 3**. In cecum, IFN-γ mRNA positive cells in VT were exclusively localized as individual cells studded to the intraepithelial region and as small aggregates of cells in the lamina propria as seen in control birds throughout the study period. Quantification of these cells (**Figure 4A**), however, revealed a significantly lower percentage of positive cells at 4 DPI. The early decrement in VT was followed by an abrupt increment characterized by a statistically significant change at 10 DPI. Relative numbers of IFN-γ mRNA positive cells gradually decreased on 14 DPI until the experiment ended at 21 DPI, although being still higher than in the control birds. In IT, the distribution pattern of positive cells at 4 DPI was similar to VT and significantly lower compared to the control group. At 7 and 10 DPI, positive cells showed an extensive spread within the lamina propria and muscularis, along with a total loss of the mucosal structure. Coincidentally, the relative number of these cells was significantly higher at 10 DPI. There were no surviving birds left in group IT from 14 DPI onward. In VIT, the distribution

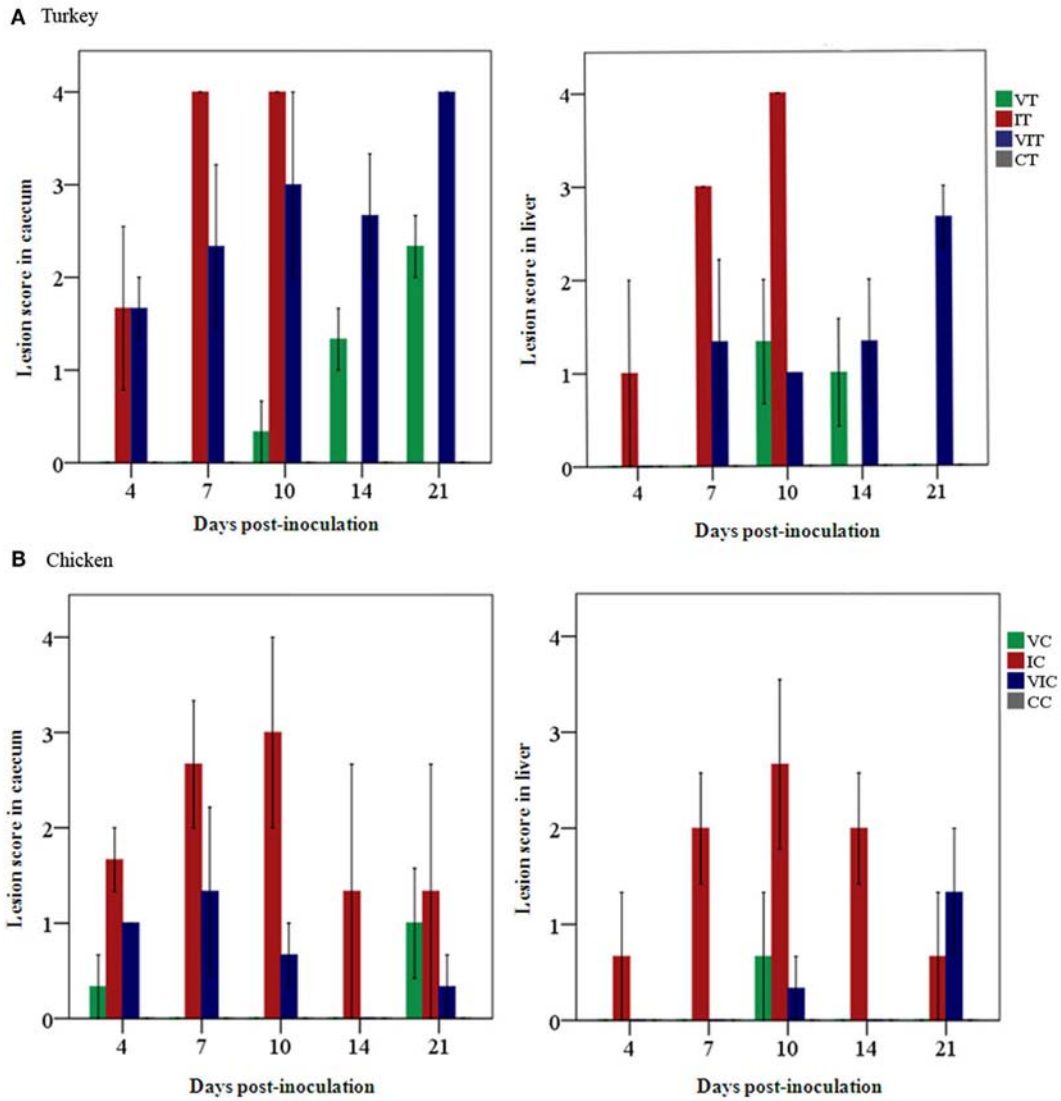

FIGURE 1 | Mean lesion scores (n = 3 birds/day) recorded in cecum and liver. Scores were graded from 0 to 4, indicating no lesion to severe lesion in **(A)** groups of vaccinated turkeys (VT), infected turkeys (IT) and vaccinated and infected turkeys (VIT) and in **(B)** groups of vaccinated chickens (VC), infected chickens (IC), or vaccinated and infected chickens (VIC) necropsied at different days post-inoculation. There were no lesions observed in control turkeys or chickens (CT or CC) throughout the time points.

of positive cells started out like mentioned above for the other groups. However, at 4 DPI, the percentage of cells was slightly higher than in the control, albeit statistically not significant. From 7 DPI onward, the cecal wall had infiltrated mononuclear cells with IFN-γ mRNA positive cells sporadically distributed among them. Calculation of positive cells, however, was more or less similar to birds from the control group.

In the liver of VT and CT, stained cells could be found as lymphoid aggregates and sporadically between hepatocytes. There was no change in the spatial distribution until 21 DPI when two liver samples of VT showed a restricted yet ectopic lymphoid alteration in one area with few positive cells interspersed within. Despite the similarity in the spatial distributions of stained cells in these groups, relative numbers of cells (**Figure 4A**) were higher in VT from 7 DPI onward with significant changes observed at 10 and 14 DPI. In IT, changes, both in the location and percentage of positive cells, were different at and after 7 DPI when positive cells were observed within the inflammatory infiltrates between the parenchyma and periphery of necrotized regions. The percentage of these cells was also significantly higher at 10 DPI. Positive cells in livers of VIT were similar to CT, both in location and abundance.

In spleen, positive cells had a wider spatial distribution ranging from aggregates in the periarteriolar lymphatic sheath to solitary cells in the rest of white and red pulp, regardless of the experimental treatment. Percentages of positive cells (**Figure 4A**), however, significantly decreased in VIT at 14 DPI, whereas the changes in the other groups were not statistically supported.

The location of positive cells in cecum, liver and spleen of control and affected tissues described in turkeys also applies to chickens and differences among the groups of chickens were mostly marginal. In VC, however, there was neither a location nor a percentage change in the relative numbers of positive cells in caeca throughout the experiment (**Figure 4B**). In caeca of IC, positive cells extensively spread to the lamina propria as the disease progressed at and after 7 DPI. Similarly, in VIC, a localized yet infiltrated area with positive cells was observed only at 7 DPI. Livers of VC and VIC were similar to control birds throughout the experiment, whereas positive cells were observed in infiltrates of leukocytes of affected livers of IC collected at 14 and 21 DPI. In spleen, the only noticeable changes were the significantly decreased percentage of positive cells in the spleens of IC and VIC at 21 DPI.

TABLE 4 | Number of samples positive for *Histomonas meleagridis* detected by *in situ* hybridization (n = 3 birds/day).

		Vaccinated DPI					Infected DPI					Vaccinated and infected DPI				
		4	7	10	14	21	4	7	10	14	21	4	7	10	14	21
Turkey	Cecum	0	3	3	2	2	3	3	3	N/A	N/A	3	3	3	2	2
	Liver	0	0	0	0	1	3	3	3	N/A	N/A	0	1	1	0	1
Chicken	Cecum	0	1	2	0	0	1	2	2	1	1	2	1	1	2	0
	Liver	0	0	0	0	0	0	1	2	0	0	0	0	0	0	0

DPI, days post-inoculation.

Spatial and Temporal Distribution Differences of Quantified IL-13 mRNA Positive Cells

The localization of IL-13 mRNA positive cells in turkeys and chickens was similar to the distributional localization of IFN-γ mRNA positive cells described for each group and DPI. The percentage of positive cells, however, varied at different DPI.

In turkeys (**Figure 5A**), the percentage of IL-13 mRNA positive cells increased in the cecum of VT from 7DPI onward; the only significant change, however, was the higher percentage at 10 DPI. Positive cells also increased in caeca of IT at 7 and 10 DPI; these changes nevertheless were not statistically significant. By contrast, the percentage of positive cells showed no change or was lower in VIT throughout the trial when positive cells significantly decreased at 10 and 14 DPI. In livers, the percentage of positive cells significantly increased in VT as well as IT at 10 DPI. In spleens, even though the percentages increased variably in VT and IT at and after 7 DPI, the changes were not statistically significant. By contrast, the percentage significantly decreased in spleens of VIT at 10 and 14 DPI.

In chickens, changes in the percentage of IL-13 mRNA positive cells (**Figure 5B**) were not significant, but slight changes could be noticed at 4 DPI when positive cells increased in the cecum of VC and VIC as well as in spleens of VC.

Comparison of Quantified IFN-γ or IL-13 mRNA Positive Cells

Comparison of percentages of cytokine mRNA positive cells highlighted a varying magnitude in the abundance of cells expressing

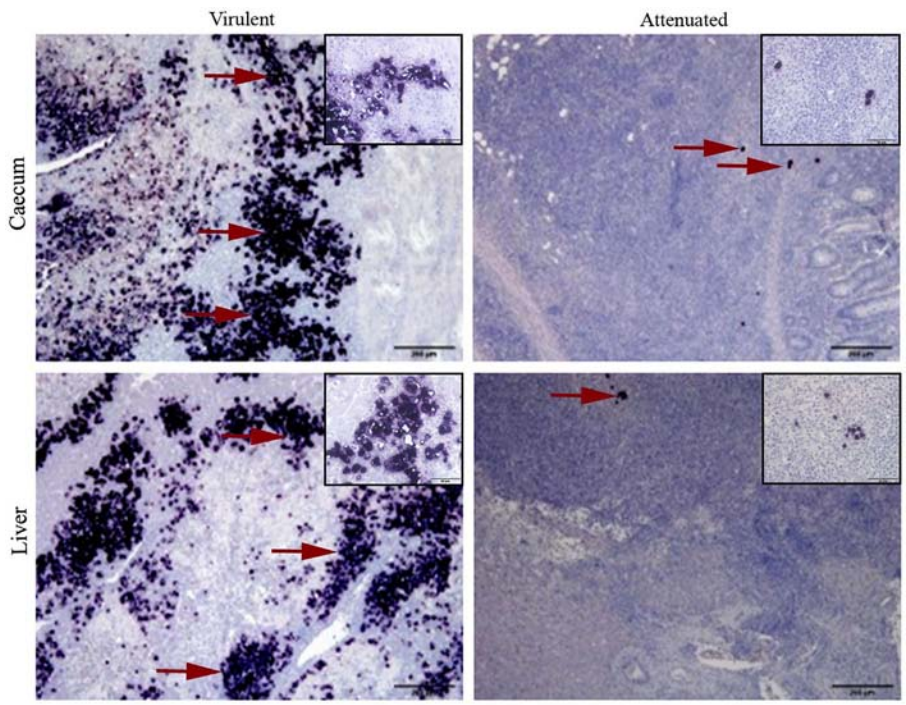

FIGURE 2 | Virulent and attenuated histomonads localized in cecum and liver by *in situ* hybridization. Stained histomonads could be seen in dark purple (examples shown in red arrow). Virulent histomonads could be seen in larger number, whereas only a few attenuated histomonads could be detected surrounded by an influx of mononuclear cells. Samples are representatives for tissues collected from turkeys inoculated with virulent histomonads (group infected turkey) necropsied on 10 days post-inoculation (DPI) and turkeys inoculated with only attenuated histomonads (group vaccinated turkeys) necropsied on 21 DPI. Insets show higher magnifications of histomonads and the surrounding cells in the respective tissue sample.

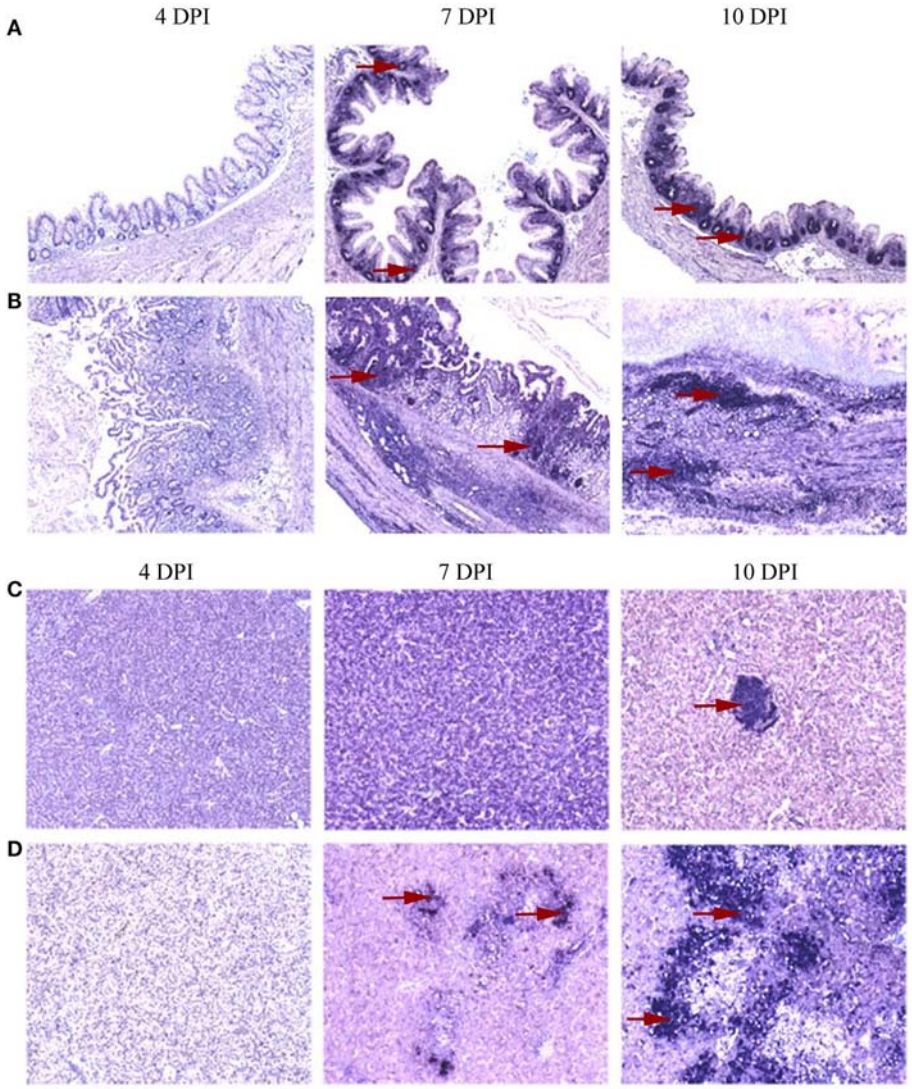

FIGURE 3 | Distribution of interferon gamma (IFN-γ) mRNA positive cells localized by *in situ* hybridization in cecum and liver. A distinct distribution pattern of cytokine mRNA positive cells in the primarily affected organs was evident between groups of turkeys that received only attenuated parasites and those inoculated with virulent *Histomonas meleagridis*. Representative distribution patterns are given using IFN-γ mRNA positive cells with areas of positive cells indicated by red arrows. At 4 days post-inoculation (DPI), positive cells were rarely distributed in caeca which then became abundant at 7 and 10 DPI with accumulation of positive cells being restricted to the lamina propria of birds that receive the attenuated culture **(A)**, whereas virulent histomonads triggered further distribution of positive cells to the muscularis layer with losing of the mucosal fold at 10 DPI **(B)**. In livers, positive cells were occasionally found as sporadic cells studded between hepatocytes and lymphoid aggregates **(C)** or in more expansive distribution comprising mononuclear infiltrates when affected by virulent histomonads **(D)**.

mRNA of IFN-γ or IL-13 pertinent to the inoculum, tissue type and host species. In turkeys (**Figure 6A**), there was a comparable level of IFN-γ and IL-13 mRNA positive cells within each type of tissue independent of the treatment group. Generally, spleen had the highest percentage of IFN-γ and IL-13 mRNA positive cells, followed by cecum whereas liver had the least percentage.

In contrast to turkeys, chicken tissues showed a divergent percentage of IFN-γ and IL-13 mRNA positive cells. Chicken IFN-γ mRNA positive cells were found to be more abundant than IL-13 mRNA positive cells in cecum and spleen of all the experimental groups (**Figure 6B**). Both tissues had more IFN-γ and IL-13 mRNA positive cells than liver. In contrast to cecum and spleen, a balanced percentage of IFN-γ and IL-13 mRNA positive cells was detected in livers of chickens, with an exception of the slight increment IFN-γ mRNA positive cells at 10 DPI in livers of VC.

Comparing percentages of cytokine mRNA positive cells between tissues of turkeys and chickens also revealed variations in the percentages of positive cells. The most obvious differences were observed in IFN-γ mRNA positive cells in the cecum and spleen of VIC and CC when compared with their counterpart turkey groups (VIT and CT).

Changes in Immune Cell Population in Chickens During Vaccination or Infection

B cells, T cells and monocytes/macrophages stained by IF in the cecum, liver and spleen cryosections of chickens from trial

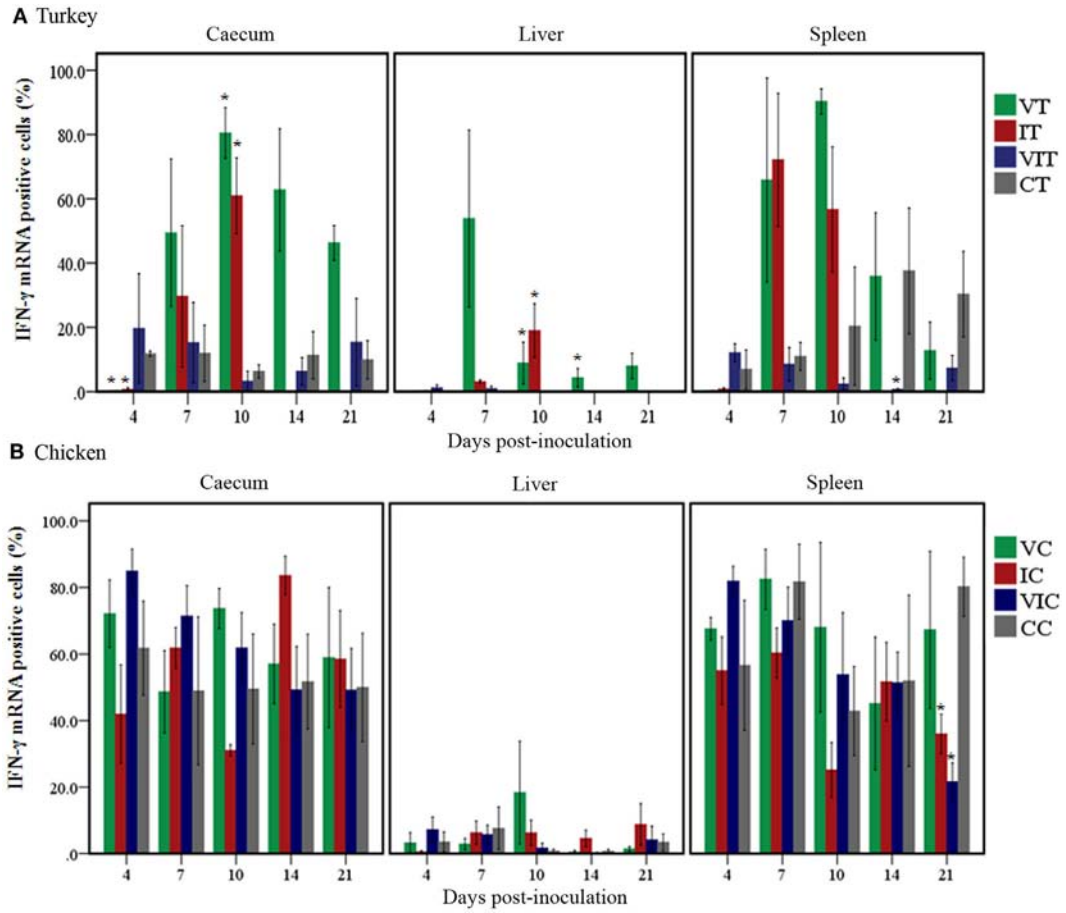

FIGURE 4 | Quantity of interferon gamma (IFN-γ) mRNA positive cells. Positive cells were quantified by TissueFAXS and its accompanying software HistoQuest in cecum, liver and spleen of turkeys **(A)** and chickens **(B)** inoculated with attenuated and/or virulent *Histomonas meleagridis*. Mean values of percentages of mRNA positive cells in each treatment group were compared with the age-matched control at the respective days post-inoculation. $n = 3$ birds/day, $^*P < 0.05$.

2 inoculated with either virulent or attenuated histomonads revealed changes in the population of these cells at different days post-inoculation (**Figure 7**). Quantification of the stained cells (**Figure 8**) showed distinct changes in IC which had an increased percentage of B cells, T cells and monocytes/macrophages in cecum at 4, 7 and 10 DPI as wall as in the liver at 10 and 14 DPI. By contrast, spleens of the same group showed decrement of B cells at 7 and 14 DPI and T cells from 4 DPI until 21 DPI. The levels in VCs were very similar to the control.

Fold Changes in the Expression Levels of IFN-γ and IL-13 mRNA Measured by RT-qPCR

Expression levels of IFN-γ and IL-13 mRNA were measured from samples collected at 10 and 21 DPI to supplement results obtained by quantification of the expressing cells. In most cases, results of RT-qPCR harmonized with quantification of cells.

In turkeys, cecal IFN-γ mRNA (**Figure 9A**) was upregulated in all of the inoculated groups sampled at 10 and 21 DPI although the only statistically significant change was noticed in caeca of VIT at 10 DPI. Similarly, a significant fold change was found at 10 DPI in liver and spleen of IT. By contrast, the expression was significantly downregulated at 21 DPI in spleens of VIT. In chickens (**Figure 9B**), cecal IFN-γ mRNA was significantly upregulated in IC at 10 DPI and in all groups at 21 DPI. Livers of IC also had a significantly enhanced expression at 10 DPI, whereas the changes in the other groups were lower. The expression was significantly downregulated in spleens of VC and VIC at 10 and 21 DPI.

Turkey IL-13 mRNA (**Figure 9C**) transcripts were significantly upregulated in the cecum of IT and VIT at 10 DPI. Similarly, an enhanced expression was found at 21 DPI in VT and VIT. In livers, a significant increment of expression was found in IT sampled at 10 DPI. In spleens, IL-13 transcripts showed increased fold changes at 10 DPI in IC and at 21 DPI in VT and VIT. In chickens, IL-13 expression (**Figure 9D**) was downregulated at 10 DPI in all caeca samples drawn from inoculated groups although the changes were not significant. The downregulation projected into a significant upregulation of the transcript at 21 DPI in all the groups with significant changes observed in VC and VIC. In livers, a significantly enhanced expression was observed at 10 DPI

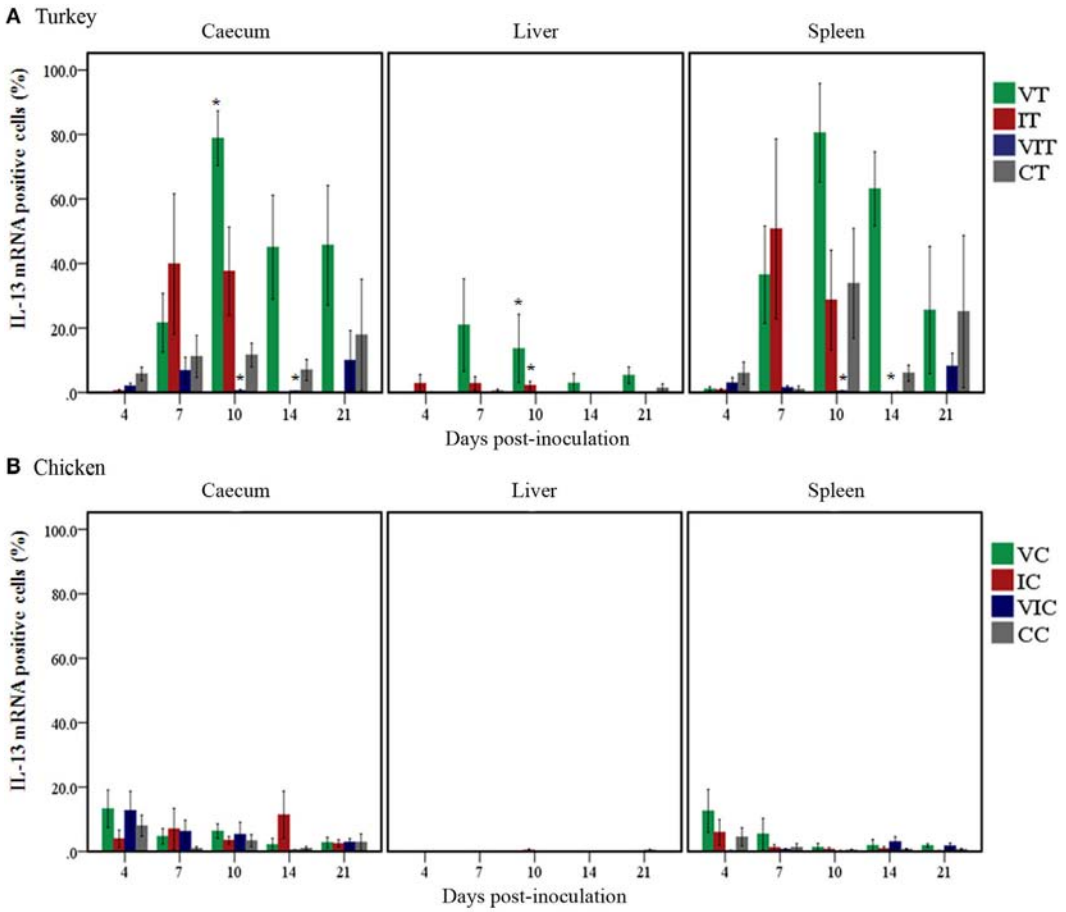

FIGURE 5 | Quantity of interleukin (IL)-13 mRNA positive cells. Positive cells were quantified in caeca, livers and spleens of groups of turkeys **(A)** and chickens **(B)** inoculated with attenuated and/or virulent *Histomonas meleagridis*. Mean percentage obtained from each treatment group was compared with the age-matched control. $n = 3$ birds/day, $^*P < 0.05$.

in VC. In spleen, the transcript was significantly downregulated in VIC at 21 DPI.

DISCUSSION

The present study quantified cells that express the mRNA of representative cytokines of type 1 and type 2 immune responses, IFN-γ, respectively, IL-13 in cecum, liver and spleen samples for elucidating cytokine expression patterns that could be attributed to vaccination or infection of turkeys and chickens with clonal cultures of *H. meleagridis*. Groups of birds were inoculated with virulent or attenuated histomonads and necropsied at different time points post-inoculation. The time points were selected based on a previous study in which cecal lesions in affected chicken reached the maximum on days 7–14 after infection and then regresses at 21 DPI (21).

Previously, the safety of the vaccine has been tested by administering 10^4 cultured histomonads exclusively *via* the oral route for turkeys and with an additional dose of 10^4 parasites cloacally to chickens. Challenges were tested in turkeys with 10^4 parasites administered by the cloaca route only (5–7). The birds in the main experiment of this study were inoculated with a 3×10^5 histomonads administrated both orally and cloacally which proved the tentative vaccine safe as noticed in vaccinated hosts together with the capability of inducing a potent immunity during challenge.

The distribution of attenuated histomonads was confined to the cecum in the majority of the samples investigated by ISH, which was in agreement with previous findings (6). On the other hand, virulent histomonads migrated further to the livers of all unprotected turkeys were a much more pronounced invasion as compared to livers of unprotected chickens. The differential kinetics in dissemination patterns of virulent histomonads in livers of turkeys and chickens was comparable to a previous study (12). However, the absence of histomonads in the spleen of all experimental birds was in contrast to a previous finding that demonstrated virulent parasites by ISH in a few spleen sections (27). This could be due to the higher dose of histomonads used in the past study which was 19 times higher per bird than in the present study.

This study employed a simultaneous assessment of localization of cytokine mRNA expressing cells and their quantitative differences in response to attenuated and virulent histomonads.

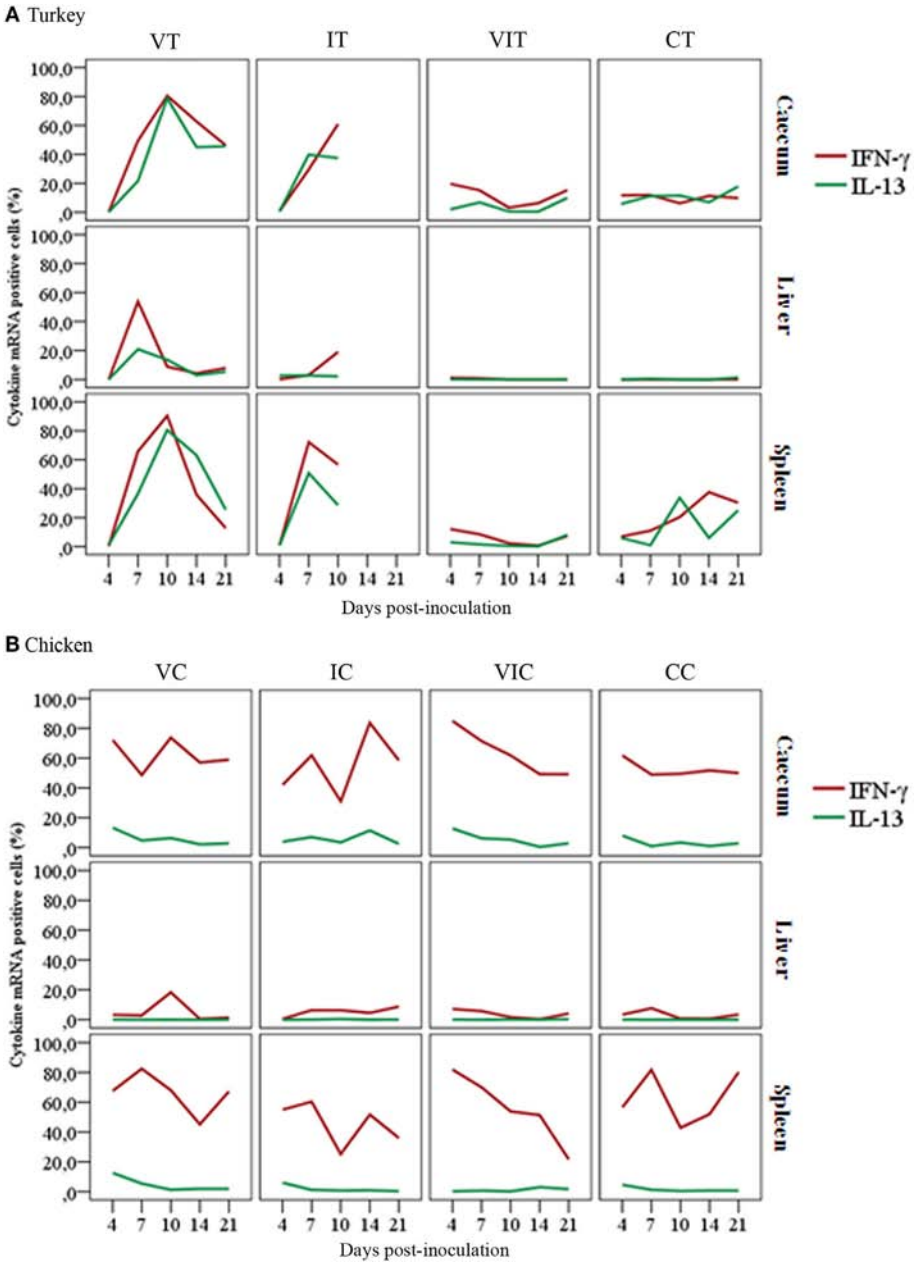

FIGURE 6 | Comparison of cytokine mRNA positive cells show a varying magnitude in the abundance of cells expressing mRNA of interferon gamma (IFN-γ) or interleukin (IL)-13. Panel **(A)** shows the percentage of turkey IFN-γ mRNA positive cells was comparable with IL-13 mRNA positive cells within the respective tissue types, regardless of their treatment condition with slight variations at different days post-inoculation. As indicated in panel **(B)**, the overall percentage of chicken IFN-γ mRNA positive cells was higher compared to the percentage of IL-13 mRNA positive cells in cecum and spleen of the respective groups throughout the trial. Remarkable differences can also be seen in the relative number of IFN-γ mRNA positive cells between cecum of control birds, turkeys (CT) and chickens (CC), with $n = 3$ birds/day.

Results showed that IFN-γ mRNA positive cells increased in the cecum of vaccinated turkeys without compromising the integrity of the tissue. By contrast, virulent histomonads caused tissue destruction along with the exacerbated increment of positive cells after a decrement of positive cells at 4 DPI. The low percentage of positive cells at this early stages in IT was in agreement with the downregulation observed by Powell et al. (12) who measured the transcript via RT-qPCR. In the present study, no data on RT-qPCR of cytokine expression were determined which limits the direct comparison. However, the authors of the last mentioned study observed a delay in cytokine response of ITs at 3 DPI which later increased to a storm of cytokines after the parasite could migrate to the liver leading to destruction of cecum and liver tissues. In concordance with this, findings of the present work showed that

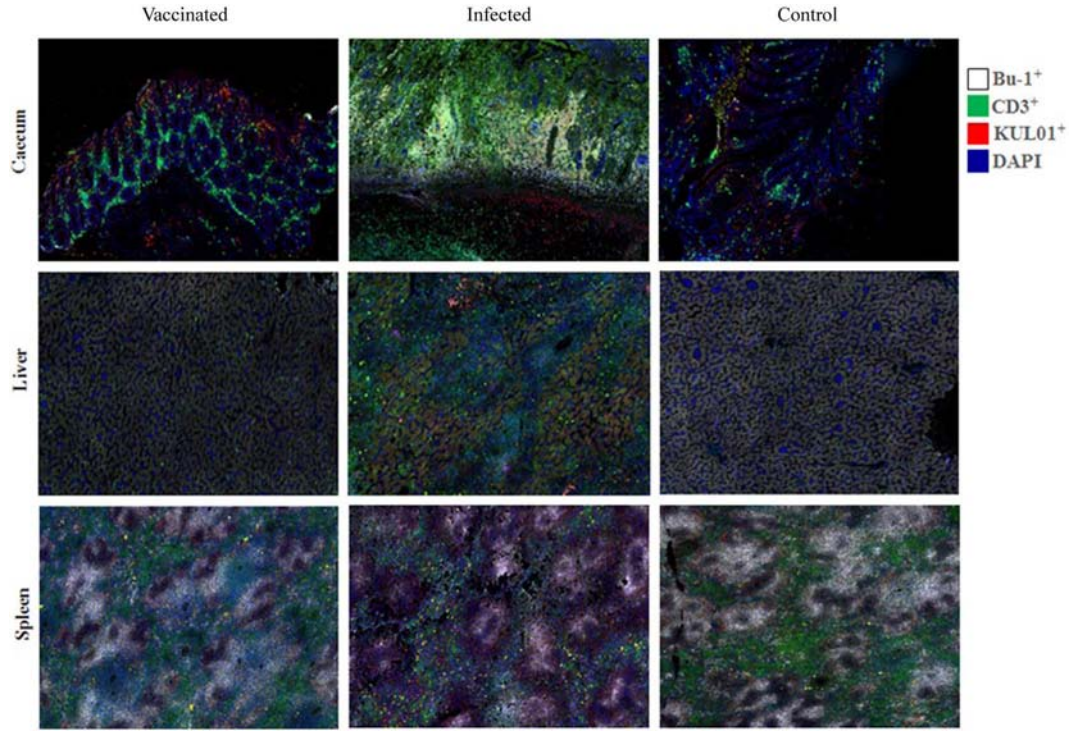

FIGURE 7 | B cells (Bu-1+), T cells (CD3+) and monocytes/macrophages (KUL01+) detected by immunofluorescence in tissues of chickens. An increase of B and T cells in the mucosa of the cecum [4 days post-inoculation (DPI)] and the liver (14 DPI) of infected chickens (inoculated with only virulent histomonads) is indicated by a higher intensity of the respective fluorochromes. By contrast, fluorescent signals of the lymphocytes in the spleen (14 DPI) are comparatively reduced in the same group.

the attenuation of the protozoa allowed the host to project the appropriate immune response without inducing tissue damage. Hence, an effective stimulation of cytokine expression that does not result in tissue damage can be considered as a desirable trait of vaccination with *in vitro* attenuated *H. meleagridis*.

In general, vaccination induces a restricted immune response to develop appropriate local and/or systemic immunity. In the present experiment, vaccinated and challenged turkeys showed a slight increment of IFN-γ mRNA positive cells in the caeca at 4 DPI. This finding indicates that the vaccine provided priming of the immune system against invading virulent histomonads. The fact that the response was shortly activated at the site of infection argues for the presence of effector memory T cells as this cell population is known to counteract re-infection by secreting antimicrobial cytokines such as IFN-γ and TNF-α (28).

The absence of any distinct separation in the relative levels of IFN-γ and IL-13 mRNA expressing cells in turkeys suggests that both type 1 and type 2 immune responses have been elicited during vaccination or infection. This could be due to the protozoa's mixed host-cellular niche. Even though it is known as an extracellular protozoan, immunohistochemical localization of the parasite in turkey liver revealed that it could occasionally be detected within host cells, mostly phagocytized by macrophages and giant cells (29). Previously, a strict intracellular pathogen (Newcastle disease virus) and extracellular helminth, *Ascaridia galli*, have been shown to cause a polarized type of cytokine expression in chickens (30).

In contrast to turkeys, a higher percentage of IFN-γ mRNA positive cells than IL-13 mRNA were noticed in chickens, regardless of the treatment conditions. Past studies on infection with virulent *H. meleagridis* or dual infection with the cecal nematode, *Heterakis gallinarum*, delivered inconclusive results in regards to type 1/type 2 responses in chicken cecal tonsils or cecum. Quantification of IFN-γ or IL-13 mRNA by RT-qPCR in cecal tonsils of turkeys and chickens infected with *H. meleagridis* inoculum prepared from an infected tissue homogenate showed a development of type 2 response with IL-13 expression although other cytokines including IFN-γ were also enhanced (12). By contrast, a dominance of type 1 response with augmented expression of IFN-γ was noticed in chicken cecum dually infected with *H. meleagridis* and *H. gallinarum* (18). Our data on the predominance of IFN-γ in chicken tissues in response to clonal cultures of histomonads was in agreement with the gene expression studies of dual infections by Schwarz et al. (18), highlighting a type 1 response in this species. Chickens probably enhance IL-13 expression only upon the encounter of the relevant pathogen. Expression of IL-13 in this species, compared to the turkeys, could be stricter, particularly in non-lymphoid tissues (31, 32). Thus, factors such as mRNA decay rate and an inter species difference in the regulation of both cytokines should be considered and explored further for defining a threshold of measurement.

In mammals, the balance between Th1/Th2 lymphocytes subsets, the main sources of signature cytokines of type 1/type 2

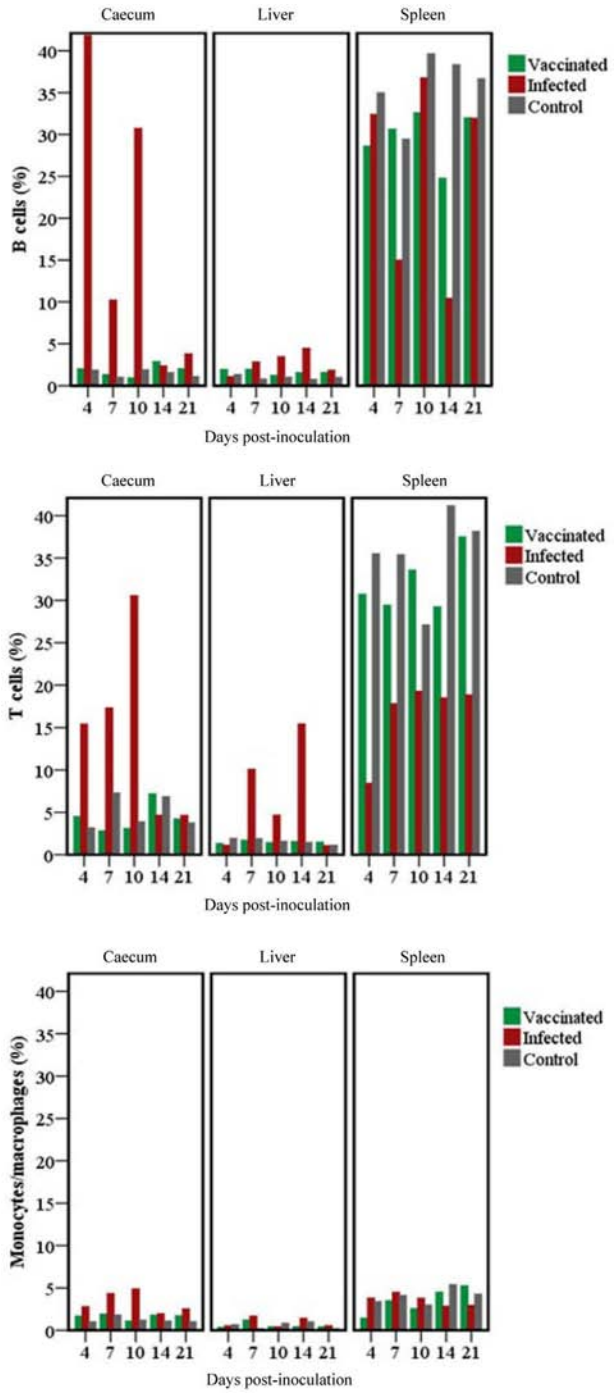

FIGURE 8 | Changes in B cells, T cells and monocytes/macrophages stained in cecum, livers and spleens of chickens. Analysis of the relative number of target cells was performed using TissueQuest after an automated image acquisition with TissueFAXS in tissues of groups of chickens inoculated with only attenuated (vaccinated) or virulent (infected) *Histomonas meleagridis*. Samples were drawn from a single chicken per group for the different days post-inoculation.

immunity, determines susceptibility to some disease states (16). In this context, the presence of a higher percentage of IFN-γ mRNA positive cells in the avian cecum seems to correlate with protection against histomonosis as noticed in chickens and vaccinated turkeys. In a study focusing on an extracellular intestinal protozoan parasite of humans, *Entameba histolytica*, it was demonstrated that asymptomatic carriers of the pathogen had higher levels of IFN-γ, reflecting a Th1 response, while patients showing disease displayed higher levels of IL-4, resembling that of a Th2 response (33). The study further revealed that re-infection in vaccinated mice was mediated by IFN-γ-producing $CD4^+$ T cells and IL-17 secreting $CD8^+$ T cells. Overall, in the mentioned study, IFN-γ was shown to enhance anti-parasitic activity in macrophages, which might be as well an important mechanism in the immune response against histomonosis of poultry. It is worth mentioning here that the mammalian key type 2 cytokine, IL-4, has been shown in the avian immune system to be less expressed compared to IL-13 in several extracellular infection models (12, 18, 23, 30, 34), hence measuring IL-13 was opted in the current study.

An important observation in the actual study was the difference in the percentage of IFN-γ mRNA positive cells in CC compared to CT. Reasons to this could be diverse and would demand research based verification. It can, however, be speculated that growth-selected turkey lines might have a trade-off between immune function and growth. Previous metanalysis on various poultry lines selected for increased growth showed a strong and significant decrease in immune function (35). In this regard, the higher surface-area abundance of these cells in the chicken cecum might be one of the reasons why this species is less susceptible to histomonosis. Their well-equipped caeca might make them immunologically competent to ward-off the protozoa at the port of entry. With this observation, it can be assumed that the presence of IFN-γ in cecum is supportive in the defense against histomonads as was shown enhancing resistance against coccidiosis (36) and *E. coli* (37) challenge. Even though further studies are needed to elucidate the specific effector function of this enhanced percentage of cells during vaccination or infection with histomonads, several effects of the cytokine might play a role in the immune response against the parasite. IFN-γ is known to promote cell-mediated immunity through activation of macrophages for phagocytosis (17). Moreover, it has been shown to stimulate secondary IgG response and enhance the expression of the genes for MHC class II in chickens (38). These traits can endow the hosts with an immune response that can better present histomonad antigens as well as efficiently fight infection.

Avian IFN-γ can be presumably be produced by macrophages, dendritic cells, $CD4^+$ and $CD8^+$ T cells, like in mammals (39–42). Recently, IFN-γ producing innate B lymphocytes have also been characterized in mice that produce high levels of IFN-γ that promotes macrophage activation, facilitating the innate immune response during early stages of infection (43). Likewise, various innate and adaptive stages of immune cells can synthesize IL-13. Hematopoietic cells of the innate immune system such as eosinophils, basophils and mast cells have been shown to produce IL-13 in mice (44). In addition, Th2 ($CD4^+$) cells are described as the main source of IL-13 during the effector phase of type 2 immune responses in worm-infested mice (45). In this study, the cellular background of the cytokine mRNAs could not be directly demonstrated due to the lack of immune cell markers for turkeys

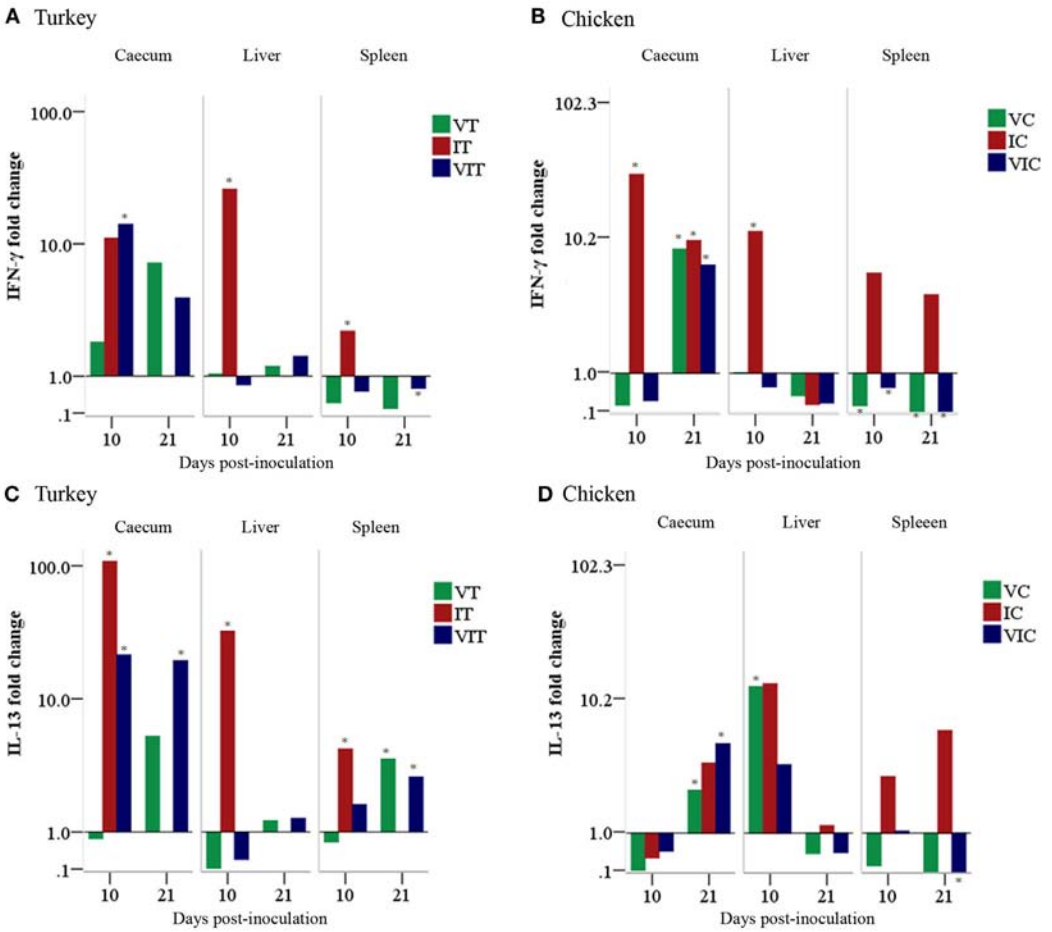

FIGURE 9 | Cytokine mRNA expression levels measured by reverse transcription-qPCR. The expression level of interferon gamma (IFN-γ) in tissues of turkeys **(A)** and chickens **(B)** as well as the expression level of interleukin (IL)-13 in tissues of turkeys **(C)** and chickens **(D)** are shown as a fold change of mRNA expression levels relative to age-matched controls. $n = 3$ birds/day, $^*P < 0.05$.

and the incompatibility of the staining techniques. However, interpretation of the IF results in context of the cytokine ISH results in chickens indicate that more cell types than B cells, T cells and macrophages could be involved in producing the cytokines as the percentages of cytokine-expressing cells were higher than the immune cells quantified by IF. Nevertheless, this indication needs to be verified in prospective studies by establishing a technique enabling co-staining of cytokines and cell markers.

This study employed RT-qPCR on samples taken from selected days to observe the congruence of mRNA quantification results with that of quantification of ISH stained cells. The high percentage of IFN-γ mRNA positive cells in the cecum of VT and IT coinciding with an enhanced expression of IFN-γ mRNA at 10 DPI demonstrated the agreement of the results. By contrast, some discrepancies were observed for instance with the increased percentages of IFN-γ mRNA positive cells in liver and spleen of VT in comparison to the RT-qPCR results of both tissues at 10 DPI. The discrepancies may arise from the difference in the detection system of both techniques. ISH labels mRNA positive cells and a higher percentage indicates a wider distribution of positive cells in a given area, whereas PCR amplifies a pooled mRNA extracted from a myriad of cells which may have more or no expressed transcript. Hence, a result of a high percentage of positive cells with a low or moderate amount of the transcript might be underestimated by fewer numbers containing a higher quantity of the transcript and *vice versa* (46).

In conclusion, immunization of turkeys using *in vitro* attenuated *H. meleagridis* causes an increased percentage of IFN-γ and IL-13 mRNA positive cells in the cecum of turkeys without compromising the integrity of the tissue. Infection in non-immunized turkeys also induced an increased presence of cytokine mRNA positive cells in cecum following an early decrement but with severe destruction of the mucosa, as well as infiltration of cytokine-expressing cells up to the muscularis layer with similar destruction and cytokine distribution in livers. Overall, the cytokine expression pattern in turkeys followed both type 1 and type 2 cytokine response with attenuated and virulent histomonads. The higher percentage of IFN-γ mRNA positive cells in chicken cecum than turkeys might also be implicated in the differential survival of this species during histomonosis.

Consequently, since a higher percentage of IFN-γ mRNA positive cells have been observed in chickens as well as in immunized turkeys capable to defend histomonosis with early expression of IFN-γ mRNA, it can be concluded that increased presence of IFN-γ mRNA positive cells indicates a protective trait against histomonosis.

ETHICS STATEMENT

The animal trials were discussed and approved by the institutional ethics committee and the national authority according to §26 of the Law for Animal Experiments, Tierversuchsgesetz 2012—TVG 2012, license number: bmwf GZ 68.205/0147-II/3b/2013.

AUTHOR CONTRIBUTIONS

DL, MH and FK conceived and designed the work. FK, TM, DL and PW performed the animal trial and collection of samples. FK and PW performed ISH and IF experiments. FK and DL performed image acquisition and analysis. TM performed and analyzed the RT-qPCR. FK and DL interpreted the data and drafted the manuscript. MH revised the manuscript critically for important intellectual content. All authors read and approved the final manuscript.

ACKNOWLEDGMENTS

The authors are thankful to Prof. Erika Jensen-Jarolim and Sarah Meitz from Department of Comparative Medicine, Messerli Research Institute, University of Veterinary Medicine Vienna, for providing access and assistance to use their TissueFAXS platform. The authors also acknowledge the VetCore Facility for research, University of Veterinary Medicine Vienna, for providing 4200 TapeStation (Agilent) to control the quality of the RNA samples used in this study.

FUNDING

This research was supported by Austrian Science Fund (FWF): P 25054.

SUPPLEMENTARY MATERIAL

The Supplementary Material for this article can be found online at https://www.frontiersin.org/articles/10.3389/fimmu.2018.01164/full#supplementary-material.

FIGURE S1 | Quantification strategy for cytokine mRNA positive cells detected by bright field microscopy and TissueFAXS image acquisition. The image is given exemplary from a single region of interest in cecum, liver and spleen tissue sections after *in situ* hybridization (ISH) staining with turkey interferon gamma antisense probe. Original bright field microscopy images **(A)**, setting a cutoff value to discriminate ISH (NBT-BCIP) positive cells **(B)** and backward viewing **(C)** to verify the correct discrimination of ISH positive (red mask) and negative cells (green mask) of the source image.

FIGURE S2 | Attenuated histomonads localized by *in situ* hybridization in the cecum of turkeys necropsied at 10 days post-inoculation showing the parasites restricted to the lumen of the cecum.

REFERENCES

1. Smith T. An infectious disease among turkeys caused by protozoa (infectious entero-hepatitis). *US Dep Agric Bur Anim Ind Bull* (1895) 8:1–38.
2. McDougald LR. Blackhead disease (histomoniasis) in poultry: a critical review. *Avian Dis* (2005) 49:462–76. doi:10.1637/7420-081005R.1
3. Hess M, Liebhart D, Bilic I, Ganas P. *Histomonas meleagridis*—new insights into an old pathogen. *Vet Parasitol* (2015) 208:67–76. doi:10.1016/j.vetpar.2014.12.018
4. Tyzzer EE. The flagellate character and reclassification of the parasite producing "blackhead" in Turkeys: *Histomonas* (Gen. nov.) *meleagridis* (Smith). *J Parasitol* (1920) 6:124. doi:10.2307/3271065
5. Hess M, Liebhart D, Grabensteiner E, Singh A. Cloned *Histomonas meleagridis* passaged *in vitro* resulted in reduced pathogenicity and is capable of protecting turkeys from histomonosis. *Vaccine* (2008) 26:4187–93. doi:10.1016/j.vaccine.2008.05.071
6. Liebhart D, Zahoor MA, Prokofieva I, Hess M. Safety of avirulent histomonads to be used as a vaccine determined in turkeys and chickens. *Poult Sci* (2011) 90:996–1003. doi:10.3382/ps.2010-01255
7. Sulejmanovic T, Liebhart D, Hess M. *In vitro* attenuated *Histomonas meleagridis* does not revert to virulence, following serial *in vivo* passages in turkeys or chickens. *Vaccine* (2013) 31:5443–50. doi:10.1016/j.vaccine.2013.08.098
8. Liebhart D, Ganas P, Sulejmanovic T, Hess M. Histomonosis in poultry: previous and current strategies for prevention and therapy. *Avian Pathol* (2017) 46:1–18. doi:10.1080/03079457.2016.1229458
9. Bleyen N, Ons E, De Gussem M, Goddeeris BM. Passive immunization against *Histomonas meleagridis* does not protect turkeys from an experimental infection. *Avian Pathol* (2009) 38:71–6. doi:10.1080/03079450802641255
10. Clarkson MJ. Immunological responses to *Histomonas meleagridis* in the Turkey and Fowl. *Immunology* (1963) 6:156–68.
11. Windisch M, Hess M. Experimental infection of chickens with *Histomonas meleagridis* confirms the presence of antibodies in different parts of the intestine. *Parasite Immunol* (2010) 32:29–35. doi:10.1111/j.1365-3024.2009.01159.x
12. Powell FL, Rothwell L, Clarkson MJ, Kaiser P. The turkey, compared to the chicken, fails to mount an effective early immune response to *Histomonas meleagridis* in the gut. *Parasite Immunol* (2009) 31:312–27. doi:10.1111/j.1365-3024.2009.01113.x
13. Mitra T, Gerner W, Kidane FA, Wernsdorf P, Hess M, Saalmüller A, et al. Vaccination against histomonosis limits pronounced changes of B cells and T-cell subsets in turkeys and chickens. *Vaccine* (2017) 35:4184–96. doi:10.1016/j.vaccine.2017.06.035
14. Yip HC, Karulin AY, Tary-Lehmann M, Hesse MD, Radeke H, Heeger PS, et al. Adjuvant-guided type-1 and type-2 immunity: infectious/noninfectious dichotomy defines the class of response Hualin. *J Immunol* (1999) 162:3942–9.
15. Kaiser P, Stäheli P. Avian cytokines and chemokines. In: Schat KA, Kaspers B, Kaiser P, editors. *Avian Immunology*. San Diego, CA: Elsevier Science Publishing (2013). p. 189–204.
16. Kidd P. Th1/Th2 balance: the hypothesis, its limitations, and implications for health and disease. *Altern Med Rev* (2003) 8:223–46.
17. Schijns VEJC, van de Zande S, Lupiani B, Reddy SM. Practical aspects of poultry vaccination. In: Schat KA, Kaspers B, Kaiser P, editors. *Avian Immunology*. San Diego, CA: Elsevier Science Publishing (2013). p. 345–62.
18. Schwarz A, Gauly M, Abel H, Daş G, Humburg J, Weiss ATA, et al. Pathobiology of *Heterakis gallinarum* mono-infection and co-infection with *Histomonas meleagridis* in layer chickens. *Avian Pathol* (2011) 40:277–87. doi:10.1080/03079457.2011.561280
19. Hess M, Kolbe T, Grabensteiner E, Prosl H. Clonal cultures of *Histomonas meleagridis*, *Tetratrichomonas gallinarum* and a *Blastocystis* sp. established through micromanipulation. *Parasitology* (2006) 133:547–54. doi:10.1017/S0031182006000758
20. Liebhart D, Grabensteiner E, Hess MA. A virulent mono-eukaryotic culture of *Histomonas meleagridis* is capable of inducing fatal histomonosis in different aged turkeys of both sexes, regardless of the infective dose. *Avian Dis* (2008) 52:168–72. doi:10.1637/8107-090707-ResNote
21. Zahoor MA, Liebhart D, Hess M. Progression of histomonosis in commercial chickens following experimental infection with an *in vitro* propagated clonal

culture of *Histomonas meleagridis*. *Avian Dis* (2011) 55:29–34. doi:10.1637/9508-082110-Reg.1
22. Liebhart D, Weissenböck H, Hess M. *In-situ* hybridization for the detection and identification of *Histomonas meleagridis* in tissues. *J Comp Pathol* (2006) 135:237–42. doi:10.1016/j.jcpa.2006.08.002
23. Kidane FA, Bilic I, Mitra T, Wernsdorf P, Hess M, Liebhart D. *In situ* hybridization to detect and localize signature cytokines of T-helper (Th) 1 and Th2 immune responses in chicken tissues. *Vet Immunol Immunopathol* (2016) 175:51–6. doi:10.1016/j.vetimm.2016.05.007
24. Paudel S, Hess C, Wernsdorf P, Käser T, Meitz S, Jensen-Jarolim E, et al. The systemic multiplication of *Gallibacterium anatis* in experimentally infected chickens is promoted by immunosuppressive drugs which have a less specific effect on the depletion of leukocytes. *Vet Immunol Immunopathol* (2015) 166:22–32. doi:10.1016/j.vetimm.2015.05.001
25. Mitra T, Bilic I, Hess M, Liebhart D. The 60S ribosomal protein L13 is the most preferable reference gene to investigate gene expression in selected organs from turkeys and chickens, in context of different infection models. *Vet Res* (2016) 47:105. doi:10.1186/s13567-016-0388-z
26. Livak KJ, Schmittgen TD. Analysis of relative gene expression data using real-time quantitative PCR and the 2(-Delta Delta C(T)) method. *Methods* (2001) 25:402–8. doi:10.1006/meth.2001.1262
27. Grabensteiner E, Liebhart D, Weissenböck H, Hess M. Broad dissemination of *Histomonas meleagridis* determined by the detection of nucleic acid in different organs after experimental infection of turkeys and specified pathogen-free chickens using a mono-eukaryotic culture of the parasite. *Parasitol Int* (2006) 55:317–22. doi:10.1016/j.parint.2006.07.004
28. Esser MT, Marchese RD, Kierstead LS, Tussey LG, Wang F, Chirmule N, et al. Memory T cells and vaccines. *Vaccine* (2003) 21:419–30. doi:10.1016/S0264-410X(02)00407-3
29. Singh A, Weissenböck H, Hess M. *Histomonas meleagridis*: immunohistochemical localization of parasitic cells in formalin-fixed, paraffin-embedded tissue sections of experimentally infected turkeys demonstrates the wide spread of the parasite in its host. *Exp Parasitol* (2008) 118:505–13. doi:10.1016/j.exppara.2007.11.004
30. Degen WGJ, Daal Nv, Rothwell L, Kaiser P, Schijns VE. Th1/Th2 polarization by viral and helminth infection in birds. *Vet Microbiol* (2005) 105:163–7. doi:10.1016/j.vetmic.2004.12.001
31. Avery S, Rothwell L, Degen WDJ, Schijns VEJC, Young J, Kaufman J, et al. Characterization of the first nonmammalian T2 cytokine gene cluster: the cluster contains functional single-copy genes for IL-3, IL-4, IL-13, and GM-CSF, a gene for IL-5 that appears to be a pseudogene, and a gene encoding another cytokinelike transcript. *J Interf Cytokine Res* (2004) 24:600–10. doi:10.1089/jir.2004.24.600
32. Powell F, Rothwell L, Clarkson M, Kaiser P. Development of reagents to study the turkey's immune response: cloning and characterisation of two turkey cytokines, interleukin (IL)-10 and IL-13. *Vet Immunol Immunopathol* (2012) 147:97–103. doi:10.1016/j.vetimm.2012.03.013
33. Quach J, St-Pierre J, Chadee K. The future for vaccine development against *Entamoeba histolytica*. *Hum Vaccin Immunother* (2014) 10:1514–21. doi:10.4161/hv.27796
34. Schwarz A, Gauly M, Abel H, Daş G, Humburg J, Rohn K, et al. Immunopathogenesis of *Ascaridia galli* infection in layer chicken. *Dev Comp Immunol* (2011) 35:774–84. doi:10.1016/j.dci.2011.02.012
35. Van Der Most PJ, De Jong B, Parmentier HK, Verhulst S. Trade-off between growth and immune function: a meta-analysis of selection experiments. *Funct Ecol* (2011) 25:74–80. doi:10.1111/j.1365-2435.2010.01800.x
36. Lowenthal JW, York JJ, O'neil TE, Rhodes S, Prowse SJ, David A, et al. In vivo effects of chicken interferon-γ during infection with *Eimeria*. *J Interf Cytokine Res* (1997) 17:551–8. doi:10.1089/jir.1997.17.551
37. Janardhana V, Ford ME, Bruce MP, Broadway MM, O'Neil TE, Karpala AJ, et al. IFN-γ enhances immune responses to *E. coli* infection in the chicken. *J Interf Cytokine Res* (2007) 27:937–46. doi:10.1089/jir.2007.0020
38. Lowenthal JW, York JJ, O'Neil TE, Steven RA, Strom DG, Digby MR. Potential use of cytokine therapy in poultry. *Vet Immunol Immunopathol* (1998) 63:191–8. doi:10.1016/S0165-2427(98)00095-6
39. Munder M, Mallo M, Eichmann K, Modolell M. Murine macrophages secrete interferon gamma upon combined stimulation with interleukin (IL)-12 and IL-18: a novel pathway of autocrine macrophage activation. *J Exp Med* (1998) 187:2103–8. doi:10.1084/jem.187.12.2103
40. Fukao T, Frucht DM, Yap G, Gadina M, O'Shea JJ, Koyasu S. Inducible expression of Stat4 in dendritic cells and macrophages and its critical role in innate and adaptive immune responses. *J Immunol* (2001) 166:4446–55. doi:10.4049/jimmunol.166.7.4446
41. Kohno K, Kataoka J, Ohtsuki T, Suemoto Y, Okamoto I, Usui M, et al. IFN-gamma-inducing factor (IGIF) is a costimulatory factor on the activation of Th1 but not Th2 cells and exerts its effect independently of IL-12. *J Immunol* (1997) 158:1541–50.
42. Tomura M, Maruo S, Mu J, Zhou XY, Ahn HJ, Hamaoka T, et al. Differential capacities of CD4+, CD8+, and CD4-CD8- T cell subsets to express IL-18 receptor and produce IFN-gamma in response to IL-18. *J Immunol* (1998) 160:3759–65.
43. Bao Y, Liu X, Han C, Xu S, Xie B, Zhang Q, et al. Identification of IFN-γ-producing innate B cells. *Cell Res* (2014) 24:161–76. doi:10.1038/cr.2013.155
44. Voehringer D, Reese TA, Huang X, Shinkai K, Locksley RM. Type 2 immunity is controlled by IL-4/IL-13 expression in hematopoietic non-eosinophil cells of the innate immune system. *J Exp Med* (2006) 203:1435–46. doi:10.1084/jem.20052448
45. Morimoto M, Morimoto M, Whitmire J, Xiao S, Anthony RM, Mirakami H, et al. Peripheral CD4 T cells rapidly accumulate at the host:parasite interface during an inflammatory Th2 memory response. *J Immunol* (2004) 172:2424–30. doi:10.4049/jimmunol.172.4.2424
46. Rosa FE, Santos RM, Rogatto SR, Domingues MAC. Chromogenic *in situ* hybridization compared with other approaches to evaluate HER2/neu status in breast carcinomas. *Braz J Med Biol Res* (2013) 46:207–16. doi:10.1590/1414-431X20132483

Conflict of Interest Statement: The authors declare that the research was conducted in the absence of any commercial or financial relationships that could be construed as a potential conflict of interest.

frontiers in Immunology

ORIGINAL RESEARCH
published: 23 April 2018
doi: 10.3389/fimmu.2018.00859

Trypanosoma cruzi Exploits Wnt Signaling Pathway to Promote Its Intracellular Replication in Macrophages

*Ximena Volpini[1,2], Laura F. Ambrosio[1,2], Laura Fozzatti[1,2], Constanza Insfran[1,2], Cinthia C. Stempin[1,2], Laura Cervi[1,2] and Claudia Cristina Motran[1,2]**

[1] Departamento de Bioquímica Clínica, Facultad de Ciencias Químicas, Universidad Nacional de Córdoba, Córdoba, Argentina, [2] Centro de Investigaciones en Bioquímica Clínica e Inmunología (CIBICI), CONICET, Haya de la Torre y Medina Allende, Ciudad Universitaria, Córdoba, Argentina

During the acute phase of *Trypanosoma cruzi* infection, macrophages can act as host cells for the parasites as well as effector cells in the early anti-parasitic immune response. Thus, the targeting of specific signaling pathways could modulate macrophages response to restrict parasite replication and instruct an appropriate adaptive response. Recently, it has become evident that Wnt signaling has immunomodulatory functions during inflammation and infection. Here, we tested the hypothesis that during *T. cruzi* infection, the activation of Wnt signaling pathway in macrophages plays a role in modulating the inflammatory/tolerogenic response and therefore regulating the control of parasite replication. In this report, we show that early after *T. cruzi* infection of bone marrow-derived macrophages (BMM), β-catenin was activated and Wnt3a, Wnt5a, and some Frizzled receptors as well as Wnt/β-catenin pathway's target genes were upregulated, with Wnt proteins signaling sustaining the activation of Wnt/β-catenin pathway and then activating the Wnt/Ca^{+2} pathway. Wnt signaling pathway activation was critical to sustain the parasite's replication in BMM; since the treatments with specific inhibitors of β-catenin transcriptional activation or Wnt proteins secretion limited the parasite replication. Mechanistically, inhibition of Wnt signaling pathway armed BMM to fight against *T. cruzi* by inducing the production of pro-inflammatory cytokines and indoleamine 2,3-dioxygenase activity and by downregulating arginase activity. Likewise, *in vivo* pharmacological inhibition of the Wnts' interaction with its receptors controlled the parasite replication and improved the survival of lethally infected mice. It is well established that *T. cruzi* infection activates a plethora of signaling pathways that ultimately regulate immune mediators to determine the modulation of a defined set of effector functions in macrophages. In this study, we have revealed a new signaling pathway that is activated by the interaction between protozoan parasites and host innate immunity, establishing a new conceptual framework for the development of new therapies.

Keywords: ***Trypanosoma cruzi*** **infection, Wnt proteins, beta-catenin, macrophages, cytokines, indoleamine 2,3-dioxygenase**

OPEN ACCESS

Edited by:
Xun Suo,
China Agricultural University, China

Reviewed by:
Debora Decote-Ricardo,
Universidade Federal Rural do Rio de Janeiro, Brazil
Thomas Jacobs,
Bernhard-Nocht-Institut für Tropenmedizin (BMITM), Germany

***Correspondence:**
Claudia Cristina Motran
cmotran@fcq.unc.edu.ar

Specialty section:
This article was submitted to Microbial Immunology, a section of the journal Frontiers in Immunology

Received: *24 November 2017*
Accepted: *06 April 2018*
Published: *23 April 2018*

Citation:
Volpini X, Ambrosio LF, Fozzatti L, Insfran C, Stempin CC, Cervi L and Motran CC (2018) Trypanosoma cruzi Exploits Wnt Signaling Pathway to Promote Its Intracellular Replication in Macrophages. Front. Immunol. 9:859. doi: 10.3389/fimmu.2018.00859

INTRODUCTION

Chagas' disease, caused by the protozoan parasite *Trypanosoma cruzi*, represents a major cause of heart disease and cardiovascular-related deaths in endemic areas and causes a significant economic burden on the affected countries. Approximately 8 million people are infected with *T. cruzi* in Central and South America, and at least 120 million are at risk of infection (1). Currently, there are no vaccines available to prevent Chagas disease, and treatment options are limited to anti-parasitic drugs that are expensive, not well tolerated, and effective only during short periods of the acute phase (2).

The entry of metacyclic trypomastigotes (Tps) of *T. cruzi* into the mammalian host initiates the invasion by these parasites of several host cell types where they are converted into amastigotes, which are the replicative form of this parasite (3). During the acute phase of the infection macrophages represent an important target of *Trypanosoma cruzi* and therefore, these cells are central for the control of this pathogen. Within macrophages, the replication of *T. cruzi* can be either inhibited or favored leading to the dissemination of the parasite (4). Thus, it has been reported that during the early phase of infection, the control *T. cruzi* parasitism is dependent on macrophage activation through toll-like receptors (TLRs) and their subsequent activation by pro-inflammatory cytokines. Activated macrophages upregulate inducible nitric oxide synthase (iNOS) and indoleamine 2,3-dioxygenase (IDO) enzymes, leading to the production of nitric oxide (NO) and kynurenines, with both being important effector molecules that induce death of the amastigotes (5–9). The protective mechanisms of cell-mediated immunity (Th1 cells) are required for the resistance during this infection; nevertheless, unbalanced Th1 cells can also orchestrate a deleterious response that can cause tissue damage and fibrosis, since high levels of NO, IFN-γ, and tumor necrosis factor (TNF) have been associated with the pathogenesis of chronic Chagas disease (10–14). Therefore, a better understanding of the cellular and molecular mechanisms that orchestrate the different signals that promote the effective macrophage activation (able to restrict parasite replication) followed by its opportune contraction to prevent immunopathology is mandatory to design improved therapeutic strategies.

The Wnt pathway is an evolutionarily highly conserved signaling system that plays a critical role in cellular development, motility, polarization, survival, and proliferation (15, 16). In the last years, emerging studies have highlighted that the Wnt signaling pathway, particularly in dendritic cells (DC) and macrophages, plays a major role in regulating tolerance versus immunity. Members of the Wnt family are lipid-modified glycoproteins secreted by different cell types that bind to G-protein-coupled receptors of the Frizzled (Fzd) family and different coreceptors to activate a signaling cascade involved in complex mechanisms of gene regulation. In mice and human, 19 ligands secreted glycoproteins of the Wnt family, 10 seven-transmembrane receptors of the Fzd family, as well as several coreceptors or alternative receptors are known (16, 17). Depending on the composition of the Wnt–Fzd-coreceptor complex and the cellular context, Wnt proteins can initiate at least three different intracellular signaling cascades that regulate many cellular events: the Wnt/β-catenin called canonical pathway, the Wnt/Planar cell polarity pathway, and the Wnt/Ca^{+2} pathway (18, 19). In resting state, cytosolic/nuclear β-catenin is maintained at a very low level through rapid turnover of free β-catenin. This turnover is executed through a multi-protein complex, termed the β-catenin destruction complex, integrated by AXIN1/2, adenomatous polyposis coli, casein kinase I-alpha, and glycogen synthase kinase 3 beta (GSK-3β). GSK-3β sequentially phosphorylates β-catenin with β-catenin hyperphosphorylated subjected to ubiquitination and proteasomal degradation. Activation of Wnt/β-catenin signaling pathway results in the inhibition of the activity of GSK-3β, which leads to the accumulation of β-catenin in the cytoplasm and its translocation to the nucleus, where it interacts with T-cell factor/lymphoid enhancer factor family members and regulates the transcription of several target genes (16, 17). While canonical Wnt signaling has been extensively studied from the view point of innate and adaptive immune response, the non-canonical Wnt/Ca^{+2} signaling cascade has been less focused on. The binding of Wnt ligand to cognate Fzd receptor leads to the activation of calcium/calmodulin-dependent kinase II (CaMKII) and protein kinase C (PKC). Both CaMKII and PKC activate many nuclear transcription factors as NF-κB and CREB. Similarly, calcium ions can activate widely expressed protein phosphatase calcineurin that can activate cytoplasmic protein nuclear factor associated with T cells (NFAT) *via* dephosphorylation. This event results in accumulation, nuclear translocation and transcription of several NFAT target genes, including pro-inflammatory genes in lymphocytes (20).

Human and murine DC and macrophages express various receptors and Wnt proteins and are susceptible to both canonical and non-canonical signaling, and recently, several studies have emphasized the important role of DC and macrophages Wnt/β-catenin pathway in regulating inflammatory responses to microbial infections (21, 22). In DC, the activation of canonical and Wnt/Ca^{+2} pathways is associated with the development of a tolerogenic profile, secretion of anti-inflammatory cytokines, induction of Treg cells, and the inhibition of the adaptive immune response (23–28). However, Wnt pathways activation in macrophages may have both pro- and anti-inflammatory consequences, and different Wnt proteins may effectively cross-regulate each other in macrophages [reviewed in Ref. (21, 29)]. Wnt proteins and Fzd receptors are induced by STAT3-, TLR2-, TLR4-, and NF-κB-mediated signaling and, in addition to direct activation of β-catenin by Wnt proteins, TLR-mediated signals can also directly activate β-catenin (21, 26, 28, 30–37). Considering that TLR2 and TLR4 are involved in the recognition of different *T. cruzi* components (38–40), here we tested the hypothesis that during *T. cruzi* infection, the activation of Wnt signaling pathway in macrophages plays a role modulating the inflammatory/tolerogenic response and therefore regulating the control of intracellular parasite replication.

MATERIALS AND METHODS

Mice and Parasites

All animal experiments were approved by and conducted in accordance with guidelines of the Animal Care and Use Committee of the Facultad de Ciencias Químicas, Universidad

Nacional de Córdoba (Approval Number HCD 831/15). C57BL/6 (B6) was obtained from School of Veterinary, La Plata National University (La Plata, Argentina). All animals were housed in the Animal Facility of the Facultad de Ciencias Químicas, Universidad Nacional de Córdoba (OLAW Assurance number A5802-01). The Tulahuen strain of *T. cruzi* was used, which was maintained by weekly i.p. inoculations in mice.

Reagents

Macrophages were cultured in complete medium: RPMI 1640 (Gibco, ThermoFisher Scientific) supplemented with 2 mM GlutaMAX (Gibco, ThermoFisher Scientific), 10% heat-inactivated fetal calf serum (Gibco, Thermo Fisher), and 50 µg/mL Gentamicin (Gibco, ThermoFisher Scientific). PBS was purchased from Gibco (ThermoFisher Scientific); bovine serum albumin and DMSO were obtained from Sigma-Aldrich.

Cells

Bone marrow-derived macrophages (BMM) were generated as described previously (41). Peritoneal macrophages (PM) were obtained as described previously (42). J774 murine macrophages and the human monocytic THP-1 cell lines were obtained from the American Type Culture Collection (Manassas, VA, USA). THP-1 cell line was differentiated into macrophages by culture in complete medium supplemented with of 50 nM phorbol 12-myristate 13-acetate (Sigma-Aldrich) for 24 h followed by 24 h of incubation in complete medium.

In Vitro Infections and Treatments

Mo were incubated with LiCl (10 mM, #746460 Sigma-Aldrich), BIO (5 µM, #3194 TOCRIS), iCRT14 (50 µM, #4299, TOCRIS), CCT036477 (20 µM, #BML-WN114, ENZO), IWP-L6 (20 µM, #504819, Calbiochem), IFN-γ (10 ng/mL, Sigma-Aldrich) plus LPS (10 µg/mL, from *Escherichia coli* serotype 0111:B4, Sigma-Aldrich), 1-methyl-D-tryptophan (1-MT, #860646, Sigma-Aldrich) or complete medium before being infected with *T. cruzi* Tps (Mo:Tps = 1:3). Culture medium with PBS or DMSO was used as vehicle control for LiCl and 1-MT or iCRT14, CCT036477, and IWP-L6, respectively. MeBIO (5 µM, #3873, TOCRIS) was used as control of BIO.

In Vitro Trypanocidal Activity Assay

The growth of parasites in Mos was evaluated by counting the intracellular amastigotes by immunofluorescence assay using serum of patient with chronic Chagas disease as described previously (8). The number of intracellular amastigotes was calculated by dividing intracellular parasites (*n*/200 cells) in differentially treated cultures by number of intracellular parasites (*n*/200 cells) in the corresponding vehicle-treated cultures, and expressed as relative units.

Western Blotting

Spleen cells or BMM treated with RIPA buffer were analyzed by 10% SDS-PAGE and transferred to a nitrocellulose membrane. After blocking with 5% milk the membranes were incubated with the following antibodies: anti-β-catenin (15B8, eBioscience), anti-p-Ser552-β-catenin (D8E11, Cell Signaling), anti-NFATc1 (7A6, Santa Cruz Biotechnology), anti-p-Thr286-CaMKII (D21E4, Cell Signaling), anti-p-Ser9-GSK-3β (37F11, Cell Signaling), anti-Wnt3a (ab19925-100 polyclonal, Abcam), anti-Wnt5a (ab72583 polyclonal, Abcam), anti-IDO antibody (Santa Cruz Biotechnology) followed by anti-rabbit or -mouse fluor-coupled secondary antibody. Anti-β-actin (mAbcam8226, Abcam) was used as loading control. The blots were revealed by incubation with corresponding IRD Fluor 800-labeled IgG or IRD Fluor 680-labeled IgG secondary antibody (LI-COR Inc., Lincoln, NE, USA) for 1 h at room temperature. After washing, the membranes were scanned with the Odyssey infrared imaging system (LI-COR, Lincoln, NE, USA) at a wavelength of 700–800 nm. Densitometric analysis was performed using ImageJ software.

β-Catenin and NFATc1 Immunofluorescence

The cells were fixed in 4% formaldehyde and perm with 10% TritonX-100 for 15 min, washed three times with 0.01 M PBS, and incubated with 5% bovine serum albumin (Sigma-Aldrich) for 1 h for blocking. The sections were then incubated overnight at 4°C with anti-β-catenin (15B8, eBioscience) or anti-NFATc1 (7A6, Santa Cruz Biotechnology) primary antibodies. Next, the cells were washed three times with 0.01 M PBS, incubated with secondary antibody Alexa Fluor 488-conjugated Goat anti-Mouse IgG (#A11001, Invitrogen) for 4 h and washed three times with 0.01 M PBS. For nuclear counterstaining, the cells were incubated with 4′,6-diamidino-2-phenylindone (Cell Signaling Technology, #4083) for 10 min, washed in 1× PBS, and the slides were set with FluorSave™ reagent (EMD Millipore). Expression and localization of beta-catenin were observed with an Olympus FV1200 laser scanning confocal microscope (Olympus Corporation) with fixed exposure time for all samples. Colocalization was quantified as a ratio of overlapping pixels to the total number of pixels by Threshold Mander's coefficient and expressed as nuclear percentage (% nuclear). The preparations were visualized using confocal microscopy (Olympus FV1200), and the analyses of images were carried out using FIJI/ImageJ.

Measurement of Cytokine Production

Cytokines were measured in culture supernatants of BMM 24 h post-infection (pi) by capture ELISA using antibodies and protocols suggested by the manufacturer (eBioscience). The cytokine concentration was expressed as index of cytokine release (Index) obtained by dividing the cytokine release of inhibitors/activators-treated BMM by the cytokine release of vehicle-treated BMM.

Quantitative Real-Time-PCR (q-PCR)

RNA was extracted from BMM by the Trizol reagent (Invitrogen, ThermoFisher Scientific) and reverse-transcribed into cDNA by using Revert Aid First Strand cDNA Synthesis (Fermentas). Transcripts were quantified by real-time quantitative PCR on an StepOnePlus™ Real-Time System (ThermoFisher Scientific) using SYBR Green (ThermoFisher Scientific) with the following primers (all primers listed in the 5′ to 3′ orientation): *Wnt3a* TTC TTA CTT GAG GGC GGA GA (forward) and CTG TCG GGT CAA GAG AGG AG (reverse); *Wnt5a* GCA GGA CTT TCT CAA

GGA CA (forward) and CCC TGC CAA AGA CAG AAG TA (reverse); *Ctnnb1* AGC CGA GAT GGC CCA GAA T (forward) and AAG GGC AAG GTT TCG AAT CAA (reverse); *Ccnd1* AGT GCG TGC AGA AGG AGA TT (forward) and CAC AAC TTC TCG GCA GTC AA (reverse); *Axin1* CTG GGC TTG TAT CCC ACT GT (forward) and ACC AAG CTG GTG GCT AGA GA (reverse); *Wisp1* CTG GAC AGA AAA GGG CAT GT (forward) and AGG AAG GAG GGG AAA TCT CA (reverse); *Fzd4* CTG CAG CAT GCC TAA TGA GA (forward) and CGT CTG CCT AGA TGC AAT CA (reverse); *Fzd6* TCC GAC GCT TGA AGA AAA CT (forward) and CAA CCC CAG GTC CTC AAG TA (reverse); *Fzd8* GCA GCA TGT TCG CTA TGA AA (forward) and AGT AGC CTG CTA TGG CCT CA (reverse); *Fzd9* AGA GCC TGT GCT ACC GAA AA (forward) and CAA GGA GGG AGC AAC CAT AA (reverse); *Actb* CGC CAC CAG TTC GCC ATG GA (forward) and TAC AGC CCG GGG AGC ATC GT (reverse). Relative expression was normalized to β-actin (*Actb*) and expressed as mRNA relative levels. The cycling conditions included a hot start at 95°C for 10 min, followed by 40 cycles at 95°C for 15 s and 60°C for 1 min. Specificity was verified by melting curve analysis and agarose gel electrophoresis.

Arginase and IDO Activity

Arginase and IDO assays were performed as described previously (8, 43) with cell lysates that had been cultured in different conditions as indicated in the figure legends.

NO Assay

The production of NO was measured indirectly by assaying nitrites in the culture supernatant using the Griess reaction as described previously (8).

Lactate Dehydrogenase (LDH) Assay

Lactate dehydrogenase release was measured in the supernatant of BMM using LDH colorimetric assay kit (Wiener Lab) following the manufacturer's protocol and expressed as international units (I/U).

IWP-L6 Treatment

Groups of 6 mice (6–8 weeks old) maintained under standard conditions were infected with 5,000 bloodstream *T. cruzi* Tps by the i.p. route. On days 5, 8, 11, and 14 pi, mice were treated with IWP-L6 (7.5 mg/kg/dose) by the i.p. route. We resuspended IWP-L6 in DMSO (10 mg/mL) and then injected diluted in PBS, with this vehicle also being employed as a negative control. The levels of parasitemia were monitored every 2 days as described earlier, and the number of deaths was recorded daily. Determination of tissue parasitism was assessed in heart and liver obtained from 180-day-infected IWP-L6 or control mice as described previously (7).

Statistical Analysis

Statistical analyses were performed using Student's *t*-test, and two-way ANOVA followed by Bonferroni's post-test for comparing more than two groups. The Kaplan–Meier analysis test was used for comparing survival of control and treated mice. Percent survival at each time was also compared by using the log-rank and Gehan–Breslow–Wilcoxon tests. The results were considered significantly different when $P < 0.05$.

RESULTS

T. cruzi Infection Promotes Wnt Signaling Pathway Activation in Spleen Cells

Trypanosoma cruzi-infected B6 mice have great difficulty in controlling inflammatory response, resulting in the premature death of these animals by liver failure. Interestingly, we have observed that B6, unlike BALB/c mice, did not expand the population of Treg cells in parallel with the large expansion undergone by the T cell compartment resulting in an increased ratio of T effector/Treg cells (not shown). These results suggest that, as observed in patients with severe chronic Chagas disease cardiomyopathy (12, 44), the fatal outcome in B6 mice may be linked to an unbalanced inflammatory response. For that, although in *T. cruzi*-infected B6 mice the main target organ of pathological inflammatory response is the liver, and not the heart as in infected human patients, we performed the experiments in B6 mice to evaluate both parasite replication and inflammatory pathology.

To study whether experimental infection with *T. cruzi* induces the production of Wnt pathway proteins, the expression of the most common inflammation-linked Wnt proteins such as Wnt3a and Wnt5a, and β-catenin was evaluated in spleen cells from infected B6 mice at different times pi. **Figure 1** shows that, as *T. cruzi* infection progresses, the expression of Wnt3a, Wnt5a, and β-catenin is positively regulated in spleen cells. These results suggest that *T. cruzi* recognition induces in spleen cells the expression of Wnt proteins that could signal for the activation of the Wnt/β catenin canonical pathway, taking into account the accumulation of β-catenin.

T. cruzi Infection Induces Expression of Wnt Proteins and Fzd Receptors in Macrophages

To evaluate whether *T. cruzi* experimental infection induces the expression of proteins involved in Wnt signaling in macrophages, BMM were *in vitro* infected with *T. cruzi* Tps and the expression of Wnt3a and Wnt5a transcripts and proteins determined by q-PCR and Western blot. **Figures 2A,B** show that *in vitro* infection of BMM with *T. cruzi* induced the expression of Wnt5a and Wnt3a transcripts and proteins. The evaluation by means of q-PCR of the transcripts corresponding to Fzd receptors that most strongly interact with Wnt3a and Wnt5a, such as Fzd4, Fzd6, Fzd8, and Fzd9 (45), revealed that as early as 5 min pi, there is an increase in the transcription of these genes (**Figure 2C**), suggesting that after the recognition of *T. cruzi* by innate immune receptors start the transcription of Wnt proteins that could signal through Fzd receptors to activate the Wnt signaling pathways.

T. cruzi Infection Induces First β-Catenin Activation and Then Activates Wnt/Ca^{+2} Pathway in Macrophages

To evaluate whether *T. cruzi* infection activates β-catenin in BMM, the kinetics of expression of β-catenin (mRNA and protein) and

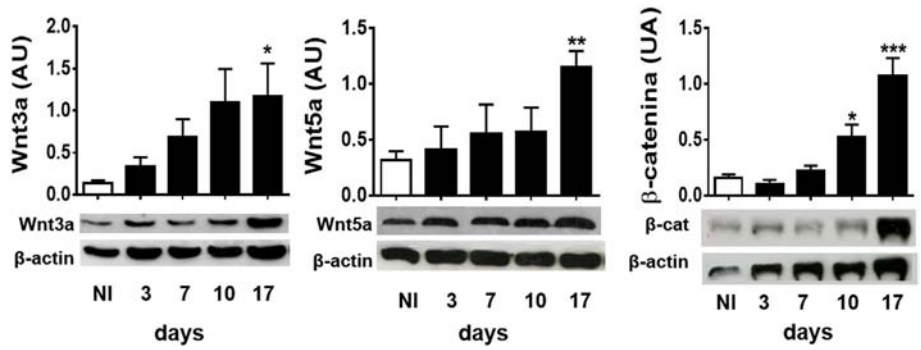

FIGURE 1 | Experimental *Trypanosoma cruzi* infection induces the expression of Wnt pathway proteins. Western blot analysis of Wnt3a, Wnt5a, and β-catenin expression in spleen mononuclear cell homogenates derived from uninfected (NI) or *T. cruzi*-infected B6 mice at different times post-infection. Images show one representative NI and one infected mice by time point. Each bar represents the mean ± SEM of protein relative expression levels quantified by scanning the intensity of bands areas in the homogenates normalized to β-actin (n = 5 mice per time point) (*P < 0.05; **P < 0.01; and ***P < 0.001).

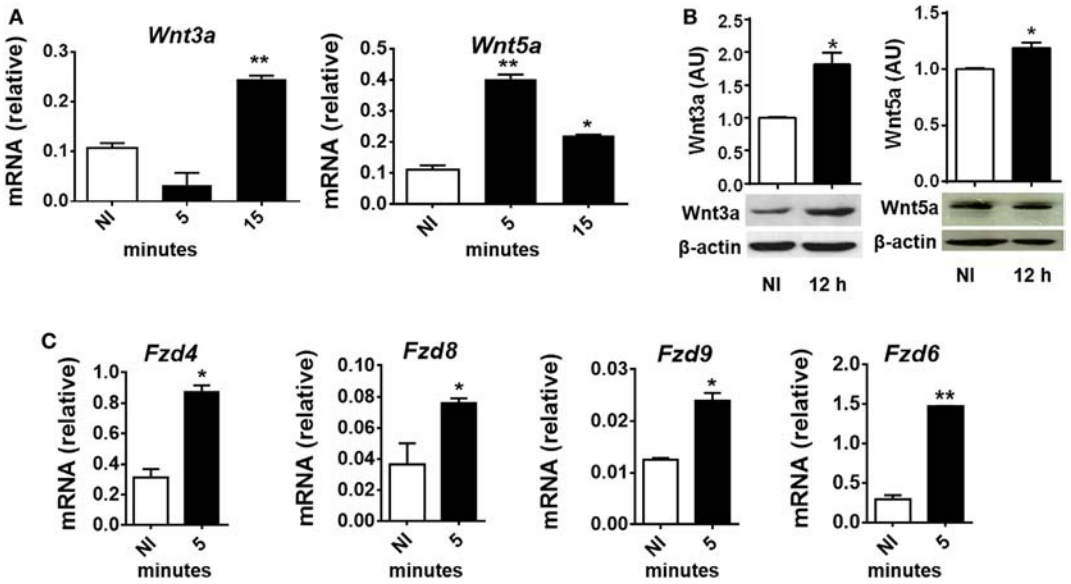

FIGURE 2 | *In vitro Trypanosoma cruzi* infection induces expression of Wnt proteins, Frizzled (Fzd) receptors, and β-catenin macrophages. Bone marrow-derived macrophages were *in vitro* infected with *T. cruzi* trypomastigotes or left uninfected (NI) and then evaluated for expression of Wnt proteins and Fzd receptors at different times post-infection (pi). **(A)** Expression of Wnt3a and Wnt5a mRNA (relative to β-actin) was determined by quantitative real-time-PCR. **(B)** The relative abundance of Wnt3, Wnt5a, and β-actin in the cell lysates were determined by Western blot and densitometry at 12 h pi. Representative Western blot and the ratio of Wnt3a or Wnt5a to β-actin are shown. **(C)** Expression of Fzd4, Fzd8, Fzd9, and Fzd6 mRNA (relative to β-actin) was determined by q-PCR. The results are expressed as the average of three independent experiments ± SEM. Abbreviation: AU, arbitrary units (*P < 0.05 and **P < 0.01).

its translocation to the nucleus were evaluated in *in vitro*-infected BMM at different times pi. At very short times after the infection (5 min), a significant increase in the transcription of the gene coding for β-catenin (*Ctnnb1*) was detected (**Figure 3A**), while the protein expression and translocation to the nucleus began at 2 h pi and reached the maximum between 8 and 12 h pi (**Figures 3A,B**). Moreover, the upregulation of Wnt/β-catenin pathway-target genes transcription, such as *Wisp1*, *Axin1*, and *Ccnd1*, correlates with β-catenin accumulation and nucleus translocation (**Figure 3C**). In addition, accumulation of β-catenin was observed in PM from B6-infected mice obtained at 24 h pi (**Figure 3D**). Taken together, our results showed that *in vitro* and *in vivo T. cruzi* infection was associated with significant activation of the genes and proteins involved in the canonical Wnt signaling pathway in macrophages.

Next, we tested whether *T. cruzi* infection is also able to activate Wnt/Ca^{+2} pathway by analyzing the expression of CaMKII phosphorylated at Thr286 [phosphorylated CAMKII (p-CAMKII)] and the activation and nuclear translocation of NFATc1. As shown in **Figure 4A**, *T. cruzi* infection led to an increase in the phosphorylation of CaMKII at Thr286 from 12 h pi. We also detected an induced NFATc1 activation after 18 h pi as measured

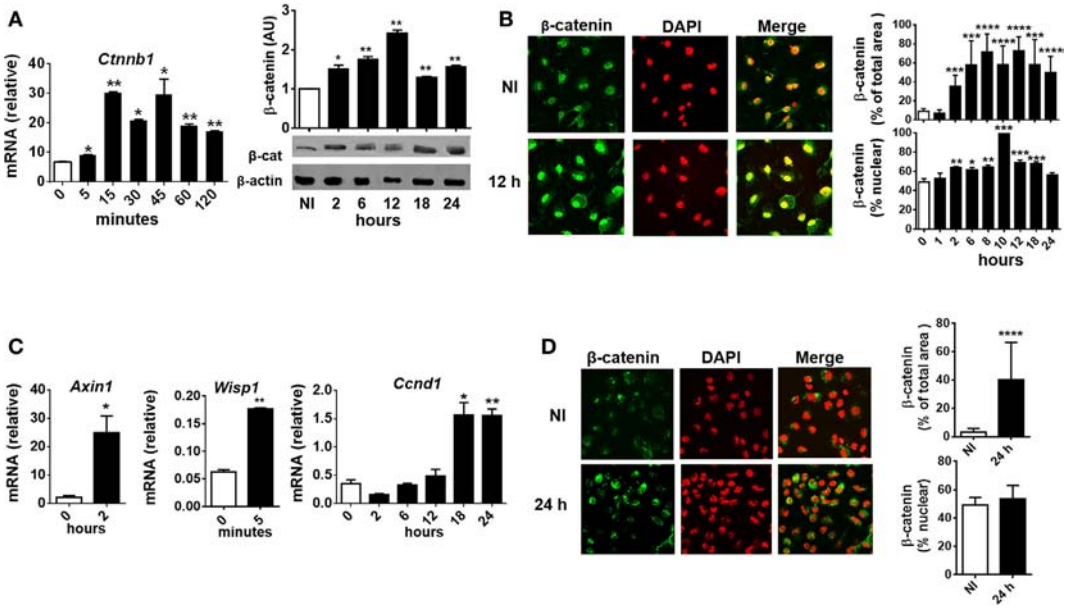

FIGURE 3 | *Trypanosoma cruzi* infection induces early β-catenin activation in macrophages. Bone marrow-derived macrophages were *in vitro* infected with trypomastigotes of *T. cruzi* or left uninfected (NI) and then evaluated for β-catenin activation. **(A)** mRNA and protein expression levels of β-catenin by q-PCR and Western blot at different times post-infection (pi). β-Catenin mRNA relative to β-actin is shown. A representative Western blot and the ratio of β-catenin to β-actin are shown. The results are expressed as the average of three independent experiments ± SEM. Abbreviation: AU, arbitrary units. **(B)** Expression and localization of β-catenin by immunofluorescence and confocal microscopy. **(C)** mRNA relative expression of β-catenin target genes Axin1, Wisp1, and Ccnd1 by q-PCR. mRNA expression levels normalized over the expression of β-actin are expressed as the average of three independent experiments ± SEM. **(D)** Peritoneal macrophages were obtained from uninfected or infected mice at 24 h pi, and the levels of expression and localization of β-catenin were evaluated by immunofluorescence and confocal microscopy. In panels **(B,D)**, a representative field for each group is shown [**(B,D)**, 1,200×]. Nuclear staining was detected with 4′,6-diamidino-2-phenylindone (DAPI), and the levels of expression of β-catenin (% of total area) and the threshold Mander's colocalization (% nuclear) coefficients calculated using FIJI/ImageJ program as described in Section "Materials and Methods." Green, β-catenin; red, DAPI (*$P < 0.05$; **$P < 0.01$; ***$P < 0.001$; and ****$P < 0.0001$).

by faster migrating, dephosphorylated, active NFATc1 bands on Western blot (arrows; **Figure 4B**) and the increased expression and nuclear translocation of NFATc1 detected by immunofluorescence (**Figure 4C**). Interestingly, the upregulation of p-CaMKII and activation of NFATc1 were dependent on the secretion of Wnt proteins; since the use of IWP-L6, a porcupine inhibitor that is the *O*-acetyltransferase membrane involved in the palmitoylation of Wnt proteins, a critical modification for its secretion, was able to inhibit both p-CaMKII upregulation and NFATc1 activation (**Figures 4D,E**). Treatment of BMM with the calcium ionophore ionomycin was used as positive control of Ca^{+2} pathway activation (46). Moreover, we were unable to detect NFATc1 upregulation or translocation to the nucleus in PM obtained at 24 h pi (Figure S1 in Supplementary Material), even though it's upregulation was evident in PM obtained from infected mice at 18 days pi (Figure S2 in Supplementary Material).

The Inhibition of Wnt/β-Catenin Signaling Pathway Limits the Replication of *T. cruzi* in Macrophages

To evaluate the role of the Wnt/β-catenin pathway activation in the control of *T. cruzi* intracellular replication, BMM were pretreated with LiCl or BIO, both inhibitors of GSK-3β activity which mimics activation of Wnt/β catenin signaling, or specific inhibitors of β-catenin-responsive transcription such as iCRT14 and CCT036477 for 24 h before being infected. Then, the intracellular amastigotes were counted by IF assay, with the results shown in **Figures 5A,B**. Treatment of BMM with IFN-γ plus LPS was used to activate BMM to control *T. cruzi* replication as described previously (8). β-Catenin-responsive transcription blockade with iCRT14 and CCT036477 was shown to result in a strong inhibitory effect on intracellular parasite growth. Similar results were obtained by inhibiting the secretion of Wnt proteins with IWP-L6 (**Figures 5A,B**). The inhibition of parasite replication observed by β-catenin transcription blockade was even more significant than those observed after the activation of BMM with IFN-γ plus LPS, and these results were not due to drugs-induced cytotoxicity, as revealed by using LDH release assay to determine cell membrane integrity (**Figure 5C**). In addition, the treatment with IWP-L6 inhibited both β-catenin accumulation and nucleus translocation at 12 h pi (**Figure 5D**). Similar results were obtained when the drugs were added to the culture at the same time as the parasites (not shown). Likewise, inhibition of Wnt/β-catenin pathway or Wnt protein secretion in human monocyte-derived THP-1 macrophages and J774 cell line (macrophages derived from BALB/c mice) resulted in the suppression of intracellular parasite replication (Figure S3 in Supplementary Material). On the other hand, treatments with β-catenin activators (LiCl and BIO) were unable to significantly increase the intracellular parasite growth (**Figures 5A,B**).

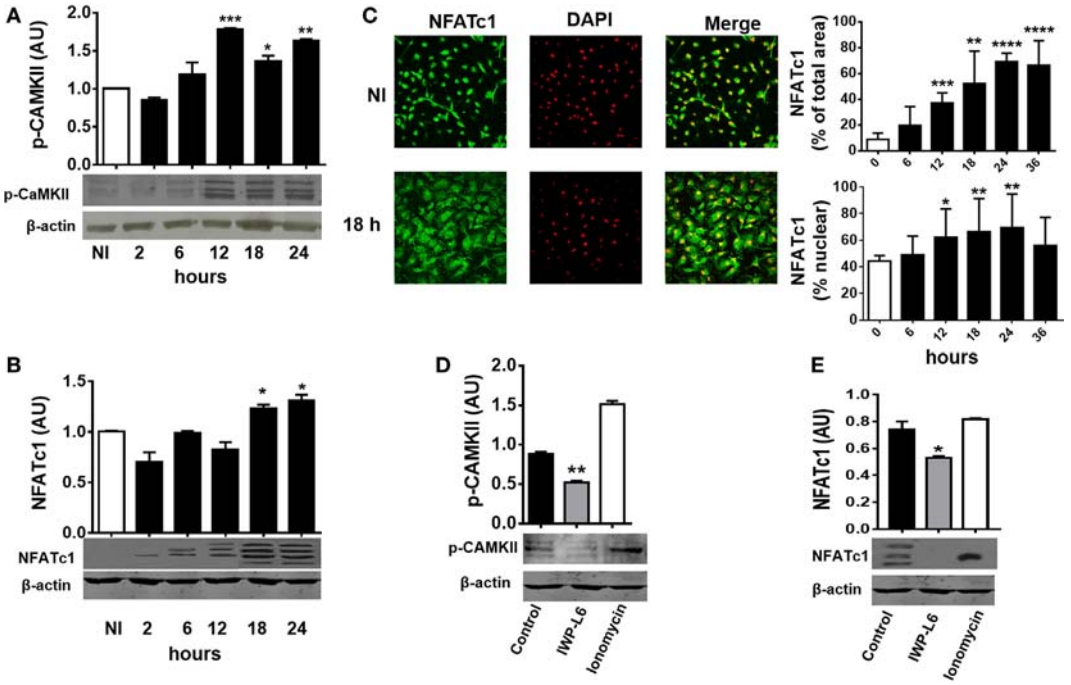

FIGURE 4 | *Trypanosoma cruzi* infection induces late Wnt/Ca^{+2} pathway activation in macrophages. Bone marrow-derived macrophages were *in vitro* infected with trypomastigotes (Tps) of *T. cruzi* or left uninfected (NI) and then evaluated for calcium/calmodulin-dependent kinase II (CaMKII) phosphorylated at Thr286 expression and NFATc1 expression and localization at different times post-infection (pi). Phosphorylated CAMKII (p-CAMKII) expression **(A)** and NFATc1 expression **(B)** were assessed by Western blot and normalized to β-actin. **(C)** Expression and localization of β-catenin by immunofluorescence and confocal microscopy. A representative field for each group is shown (1,200×). Nuclear staining was detected with 4′,6-diamidino-2-phenylindone (DAPI), and the levels of expression of NFATc1 (% of total area) and the threshold Mander's colocalization (% nuclear) coefficients calculated using FIJI/ImageJ program as described in Section "Materials and Methods." Green, NFATc1; red, DAPI. **(D,E)** Bone marrow-derived macrophages (BMM) were treated for 24 h with the PORCN inhibitor (IWP-L6) or left untreated (control), infected with *T. cruzi* Tps and assayed for p-CaMKII and NFATc1 expression at 24 h pi. Ionomycin-activated BMM (20 min, 1 μM) were used as a positive control. In panels **(A,B,D,E)**, a representative Western blot and the ratio of protein expression to β-actin are shown. The results are expressed as the average of three independent experiments ± SEM. Abbreviation: AU, arbitrary units (*$P < 0.05$; **$P < 0.01$; ***$P < 0.001$; and ****$P < 0.0001$).

Then, we studied whether the inhibition of canonical Wnt signaling regulates macrophages function by modulating the secretion of pro-inflammatory and anti-inflammatory cytokines. **Figure 6A** shows that inhibition of Wnt/β-catenin signaling induced the secretion of the pro-inflammatory cytokines IFN-γ, IL-12, IL-6, and TNF while inhibited the production of TGF-β (**Figure 6A**; Table S1 in Supplementary Material), an effect that correlates with the control of parasite replication observed in iCRT14-, CCT036477-, or IWP-L6-treated BMM (**Figures 5A,B**). In addition, canonical signaling activation using LiCl or BIO induced a slightly upregulation of TGF-β while only LiCl increased IL-10 production by *T. cruzi*-infected BMM (**Figure 6A**).

Nitric oxide production is counteracted by the expression of arginase, an enzyme that competes with iNOS for L-arginine that leads to L-ornithine and urea production (47). *T. cruzi* antigens can upregulate arginase activity with this type of activation profile associated with the ability to promote the intracellular growth of *T. cruzi* (48). Interestingly, although the pharmacological inhibition of Wnt/β-catenin pathway did not affect NO production (**Figure 6B**), the treatments with CCT036477 and IWP-L6 significantly downregulated arginase activity in infected BMM (**Figure 6C**).

Because IDO activity is also critical for the control of *T. cruzi* amastigote growth in macrophages (7–9), we analyzed the effect of the inhibition of Wnt/β-catenin signaling on the activity and expression of IDO and their role in the intracellular parasite replication control. The inhibition of both β-catenin-responsive gene transcription as well as Wnt secretion induced upregulation of IDO expression and activity in infected BMM (**Figures 6C,D**). Remarkably, the inhibitory effect of intracellular amastigote growth induced by pharmacological inhibitors of the Wnt/β-catenin pathway was reversed when IDO activity was blocked using 1-MT (**Figure 6E**). In addition, as it was previously demonstrated, 1-MT exacerbated the intracellular parasite replication in untreated BMM (**Figure 6E**). Taken together, these results demonstrated that pharmacological inhibition of Wnt/β-catenin pathway activates macrophages to fight against *T. cruzi*.

In Vivo Inhibition of Wnt Signaling Improves the Resistance to *T. cruzi* Infection

Next, we evaluated whether the inhibition of Wnt proteins secretion *in vivo* would result in the control of the parasite load. Five

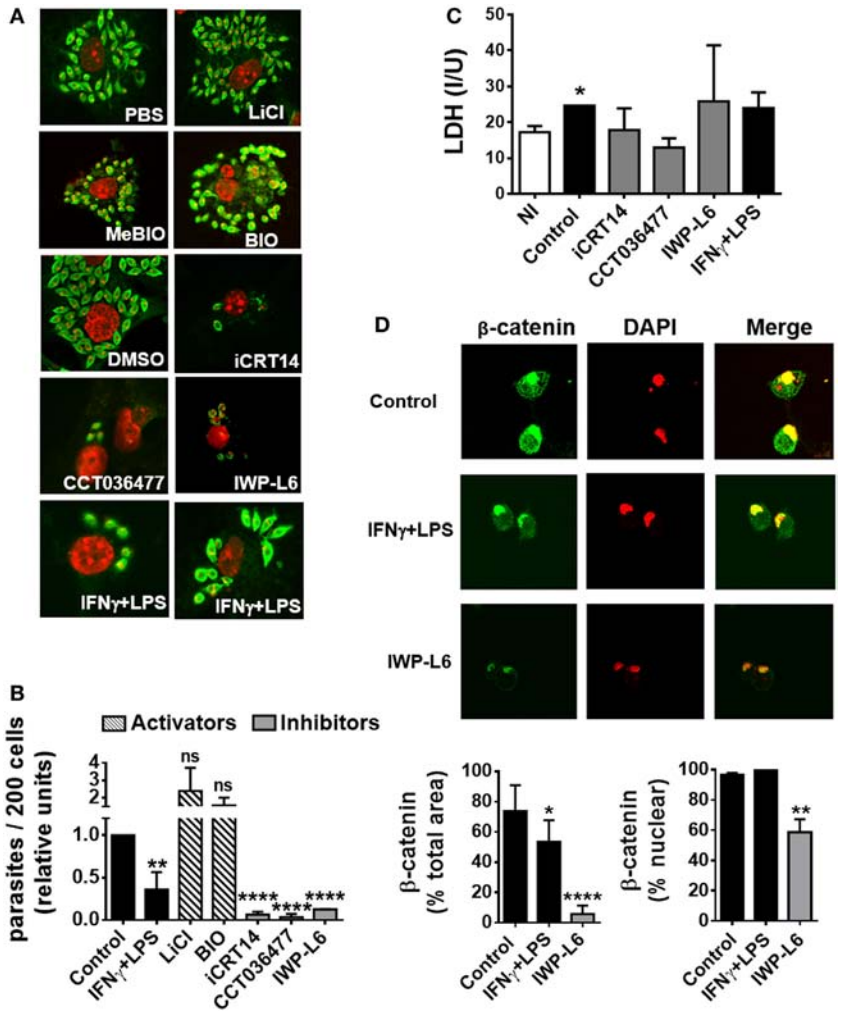

FIGURE 5 | The activation of Wnt signaling pathway promotes the replication of *Trypanosoma cruzi* in macrophages. Bone marrow-derived macrophages (BMM) were treated for 24 h with β-catenin activators (LiCl or BIO), specific β-catenin transcriptional inhibitors (iCRT14 and CCT036477), PORCN inhibitor (IWP-L6), or IFNγ plus LPS as BMM activation control. Then, the cells were infected with trypomastigotes of *T. cruzi*, and intracellular parasites were counted by immunofluorescence assay. **(A)** A representative field for each group is shown (2,000×). PBS or DMSO was used as vehicle for LiCl or iCRT14, CCT036477, and IWP-L6, respectively. MeBIO was used as control of BIO treatment. **(B)** The number of intracellular amastigotes was determined by confocal microscopy. Bars represent relative units, calculated by dividing number of intracellular parasites (*n*/200 cells) in differentially treated cultures by number of intracellular parasites (*n*/200 cells) in the corresponding vehicle-treated cultures. **(C)** Lactate dehydrogenase (LDH) levels were determined in the culture supernatant of uninfected (NI) or differentially treated infected BMM at 24 h post-infection. **(D)** Effect of IWP-L6 treatment on β-catenin activation. Accumulation and nuclear translocation of β-catenin in untreated (control), IFNγ plus LPS- or IWP-L6-treated *T. cruzi*-infected BMM was calculated as described in Section "Materials and Methods." A representative field for each group is shown (1,200×). Bars in panels **(B–D)** represent averages ± SEM from three **(C)** or four **(B,D)** independent experiments (**P* < 0.05; ***P* < 0.01; ****P* < 0.001; and *****P* < 0.0001).

days after *T. cruzi* infection with a lethal dose 50 (DL50) of Tps, the mice were treated every 3 days with IWP-L6 (**Figure 7A**). The dose of IWP-L6 used has been previously assayed to examine the effect of Wnt proteins in an experimental model of cancer (49). As expected, *in vivo* IWP-L6 treatment could maintain inhibited both Wnt/β-catenin as well as Wnt/Ca^{+2} signaling pathways until 18 days pi, as denoted by the lack of β-catenin or NFATc1 accumulation in PM from treated versus control mice (Figure S2 in Supplementary Material). Mice infected with *T. cruzi* and injected with vehicle presented high levels of parasitemia, causing death of ~50% of mice between 18 and 30 days pi (**Figure 7B**). By contrast, although only four doses of IWP-L6 were given, 100% of treated mice survived to acute infection and displayed lower parasitemia than control mice during the acute phase of the infection (**Figure 7C**). In addition, IWP-L6-treated mice showed significantly lower parasite load in liver and heart than control mice during the chronic phase of the disease (**Figure 7D**).

DISCUSSION

Given that during the acute phase of *T. cruzi* infection macrophages can act as host cells for the parasites as well as effector cells in the early anti-parasitic immune response, the targeting of specific signaling pathways in macrophages could modulate its response

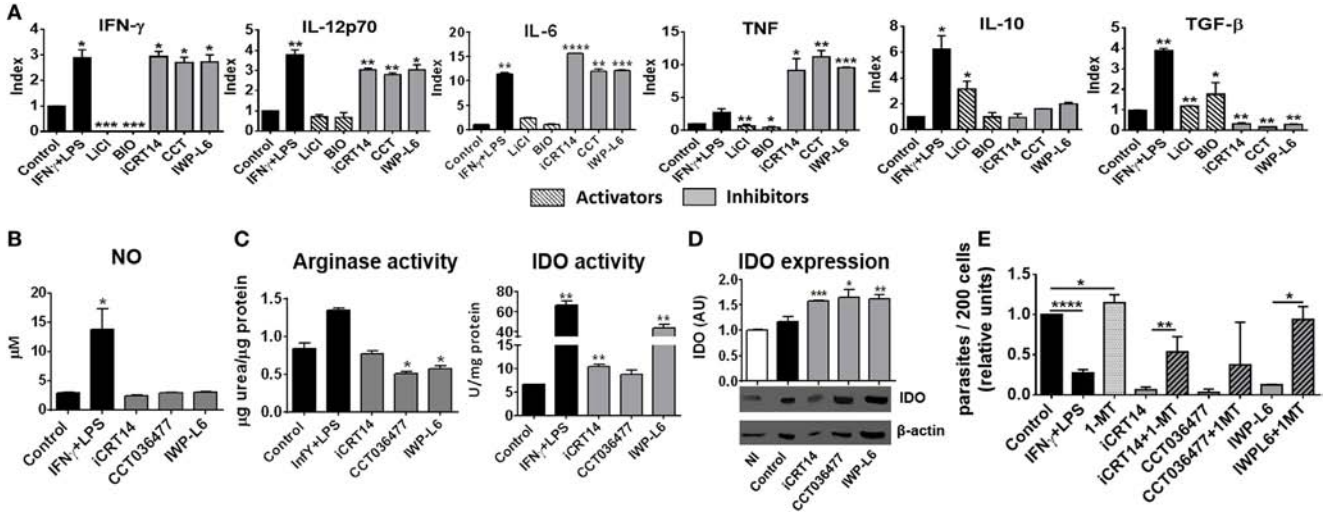

FIGURE 6 | Pharmacological inhibition of Wnt pathway enhances anti-*Trypanosoma cruzi* activity of macrophages. Bone marrow-derived macrophages (BMM) were treated for 24 h with β-catenin activators (LiCl or BIO), specific β-catenin transcriptional inhibitors (iCRT14 and CCT036477), IWP-L6, 1-MT, IFNγ plus LPS or vehicle before being infected with *T. cruzi* trypomastigotes. **(A)** Cytokine levels assayed in 24 h post-infection (pi)-supernatants represented as Index obtained by dividing the cytokine release of inhibitors/activators-treated BMM for the cytokine release of the corresponding vehicle-treated BMM. The bars represent averages ± SEM from three independent experiments. **(B)** Nitrite concentration in 24 h pi-supernatant. **(C)** Arginase and indoleamine 2,3-dioxygenase (IDO) activity assayed in 24 h pi-cell **(D)** IDO expression. One representative experiment out of three performed for each condition is shown. The ratio of protein expression to β-actin is shown, and the results are expressed as the average of three independent experiments ± SEM. Abbreviation: AU, arbitrary units. Data points of nitric oxide (NO) concentrations, arginase, and IDO activity represent means ± SEM of data pooled from three cultures of the same experiment. All data are from one experiment representative of three in total. **(E)** Number of intracellular amastigotes determined by confocal microscopy at 72 h pi. The bars represent relative units, calculated as described in **Figure 5B** (*$P < 0.05$; **$P < 0.01$; ***$P < 0.001$; and ****$P < 0.0001$).

to restrict parasite replication and instruct an appropriate adaptive immune response. In recent years, it has become apparent that Wnt signaling pathway, known for its essential participation in embryonic development and tissue homeostasis, exerts immunomodulatory functions during inflammation and infection.

In this study, we have demonstrated that early after the recognition of *T. cruzi* by innate immune receptors in BMM, β-catenin was activated and Wnt3a, Wnt5a, some Fzd receptors as well as target genes of Wnt/β-catenin pathway as *Axin1*, *Wisp1*, and *Ccnd1* were upregulated. Subsequently to canonical pathway activation, Wnt/Ca^{+2} pathway was activated; since we have demonstrated an Wnt proteins-dependent upregulated of p-CaMKII-Thr286 and activated NFATc1 expression after infection. Many studies have demonstrated that *T. cruzi* utilize the host Ca^{+2} signaling to establish the infection (50) and several mechanisms have been proposed to explain the intracellular Ca^{+2} influx that occurs during *T. cruzi* infection (51). In addition, Kayama et al. (52) have reported that NFATc1 is activated in response to *T. cruzi* infection in a TLR-independent manner, but the critical molecules and signaling pathways that lead to NFATc1 activation during *T. cruzi* infection have not yet been identified. Wnt3a and Wnt5a are more commonly associated with canonical and non-canonical Wnt signaling, respectively (19). However, Wnt5a can also activate discrete β-catenin signaling (53, 54), and recent reports have suggested that the activity of Wnt ligands and their binding to Fzd receptors depend on the cellular context; therefore, Wnt and Fzd proteins cannot be rigorously subdivided according to the pathways they induce (55). Thus, considering that we found that *T. cruzi* infection-induced β-catenin, p-CaMKII-Thr286, and activated NFATc1 upregulation were suppressed by IWP-L6 treatment, these results suggest that both Wnt3a and Wnt5a proteins, and others Wnt proteins not evaluated in this paper, could be the responsible for the activation and maintenance of both canonical and non-canonical signaling pathways during *T. cruzi* infection which allows the parasite to spread in the host.

Resistance to *T. cruzi* infection has been associated with the capacity of NK cells and T lymphocytes to generate IFN-γ which can, in turn, activate macrophages to kill the obligate intracellular amastigote form of *T. cruzi*. The trypanocidal activity of pro-inflammatory cytokines-activated macrophages is mediated at least by the upregulation of the enzymes iNOS and IDO which lead to the production of NO and kynurenines, respectively (5–9, 56). On the other hand, susceptibility to infection is associated with the production of IL-10 and transforming growth factor beta (TGF-β) (5, 56). Here, we have demonstrated that while the activation of Wnt/β-catenin pathway did not promote the intracellular parasite replication, the treatments of macrophages with specific inhibitors of β-catenin transcriptional activity or the inhibition of Wnt proteins secretion were able to inhibit the parasite replication by modifying macrophages activity. Inhibition of Wnt signaling pathway enhanced production of the pro-inflammatory cytokines IFN-γ, IL-12, TNF and IL-6 and suppressed production of TGF-β, results that are in agreement

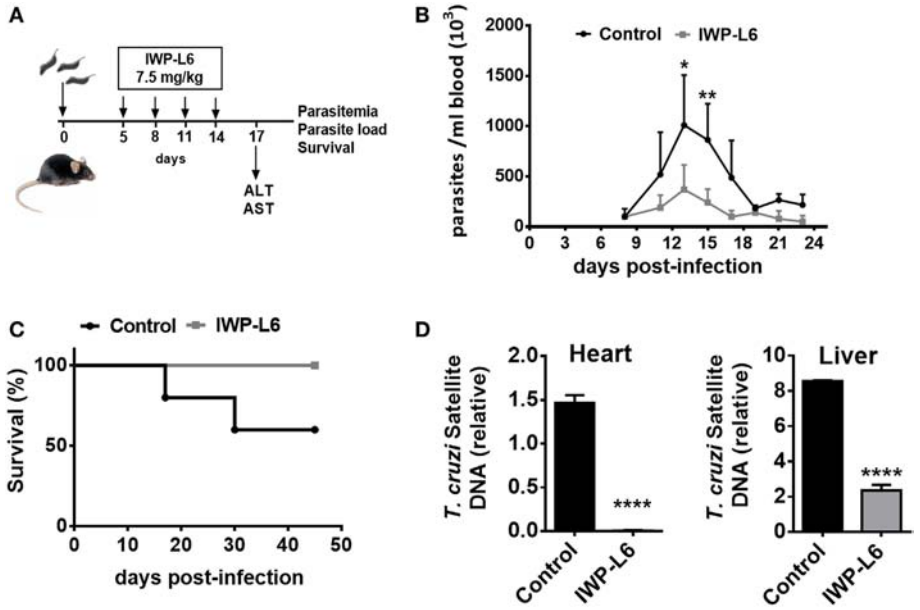

FIGURE 7 | *In vivo* inhibition of Wnt signaling improves the resistance to *Trypanosoma cruzi* infection. **(A)** B6 mice infected with 5,000 *T. cruzi* trypomastigotes were treated with IWP-L6. Vehicle-treated mice were used as control. **(B)** Parasitemia. Results are means ± SD of 5–6 animals/group and are representative of three independent experiments. **(C)** Survival rate. Data are representative of one of three independent experiments. **(D)** Relative amount of *T. cruzi* satellite DNA in heart and liver from 180-day *T. cruzi*-infected IWP-L6 and control mice. Murine GAPDH was used for normalization. Data are shown as mean ± SD of triplicates (control, $n = 4$; IWP-L6, $n = 6$) mice per group (*$P < 0.05$; **$P < 0.001$; and ****$P < 0.0001$).

with previous reports showing that the activation of the canonical pathway in macrophages and DC controls the inflammatory response (28). In addition, these treatments induced downregulation of arginase activity, an enzyme that counteracts iNOS activity, but failed to upregulate iNOS activity, suggesting that the resulting treated-macrophages do not fully fit in the classically activated/inflammatory macrophage phenotype. Interestingly, and despite the fact that there is a close relationship between the activation of the Wnt/β-catenin pathway and the induction of IDO and *vice versa* (27, 57, 58), in our experimental model the inhibition of β-catenin-induced transcription or Wnt proteins secretion upregulated IDO expression and activity. In addition, IDO activity proved to be critical for the control of *T. cruzi* replication in BMM, as denoted by the recovery of *T. cruzi* replication observed in cultures where the inhibitors were combined with 1-MT. Expression of IDO and activation of β-catenin within macrophages and DC under tolerogenic conditions are particularly important mechanisms that limits inflammation within the gastrointestinal tract and tumor cell microenvironment (28, 59). The IDO promoter has been shown to exhibit LEF-1 binding sites, and kynurenine and quinolinic acid, produced by IDO activity, can activate the Wnt/β-catenin pathway (60, 61). However, as IDO gene expression is induced not only in tolerogenic conditions but also by IFNs and TNF during inflammatory conditions (62, 63), in our experimental settings the upregulation of IDO could be induced by the milieu of pro-inflammatory cytokines generated in inhibitors-treated *T. cruzi*-infected macrophages. Thus, our results suggest that the anti-*T. cruzi* activity of inhibitor-treated macrophages is due to the production of pro-inflammatory cytokines-inducible antimicrobial molecules, with IDO being one of the most important.

In summary, in this study, we have revealed a new signaling pathway that is activated by the interaction between protozoan parasites and host innate immunity. In this context, it is well founded that *T. cruzi* infection activates a plethora of signaling pathways that ultimately regulate the immune mediators to determine the modulation of a defined set of effector functions in macrophages and thus establishes a conceptual framework for the development of novel therapeutics.

ETHICS STATEMENT

All animal experiments were approved by and conducted in accordance with guidelines of the Animal Care and Use Committee of the Facultad de Ciencias Químicas, Universidad Nacional de Córdoba (Approval Number HCD 831/15).

AUTHOR CONTRIBUTIONS

XV, LF, and CM designed the experiments. XV, LA, LF, and CI performed the experiments. XV, LF, LC, CS, and CM analyzed the data. XV, LC, and CM wrote the manuscript.

ACKNOWLEDGMENTS

XV, LA, and CI thank Consejo Nacional de Investigaciones Científicas y Técnicas from Argentina for the fellowships granted.

CM, LF, CS, and LC are members of the Scientific Career of Consejo Nacional de Investigaciones Científicas y Técnicas from Argentina. We thank Eva Acosta Rodriguez for providing us with various reagents and technical support and David Rojas Marquez for their skillful technical assistance. We thank F. Navarro, D. Lutti, V. Blanco, and C. Florit for animal care.

FUNDING

This work was supported by grants from Consejo Nacional de Investigaciones Científicas y Técnicas from Argentina (CONICET), Agencia Nacional de Promoción Científica y Técnica (PICT 2016-0415, PICT 2015-2488), and Secretaría de Ciencia y Técnica, Universidad Nacional de Córdoba (grants to CM). The funding bodies had no role in the study design, data collection and analysis, decision to publish, or preparation of the manuscript.

SUPPLEMENTARY MATERIAL

The Supplementary Material for this article can be found online at https://www.frontiersin.org/articles/10.3389/fimmu.2018.00859/full#supplementary-material.

REFERENCES

1. Salvatella R, Irabedra P, Sánchez D, Castellanos LG, Espinal M. South-south cooperation for Chagas disease. *Lancet* (2013) 382(9890):395–6. doi:10.1016/S0140-6736(13)61671-2
2. Le Loup G, Pialoux G, Lescure FX. Update in treatment of Chagas disease. *Curr Opin Infect Dis* (2011) 24(5):428–34. doi:10.1097/QCO.0b013e32834a667f
3. Sosa-Estani S, Segura E. Etiological treatment in patients infected by *Trypanosoma cruzi*: experiences in Argentina. *Curr Opin Infect Dis* (2006) 19(6):583–7. doi:10.1097/01.qco.0000247592.21295.a5
4. Tanowitz HB, Kirchhoff LV, Simon D, Morris SA, Weiss LM, Wittner M. Chagas' disease. *Clin Microbiol Rev* (1992) 5(4):400–19. doi:10.1128/CMR.5.4.400
5. Gazzinelli RT, Oswald IP, Hieny S, James SL, Sher A. The microbicidal activity of interferon-gamma-treated macrophages against *Trypanosoma cruzi* involves an L-arginine-dependent, nitrogen oxide-mediated mechanism inhibitable by interleukin-10 and transforming growth factor-beta. *Eur J Immunol* (1992) 22(10):2501–6. doi:10.1002/eji.1830221006
6. Silva JS, Vespa GN, Cardoso MA, Aliberti JC, Cunha FQ. Tumor necrosis factor alpha mediates resistance to *Trypanosoma cruzi* infection in mice by inducing nitric oxide production in infected gamma interferon-activated macrophages. *Infect Immun* (1995) 63(12):4862–7.
7. Knubel CP, Martinez FF, Acosta Rodriguez EV, Altamirano A, Rivarola HW, Diaz Lujan C, et al. 3-Hydroxy kynurenine treatment controls *T. cruzi* replication and the inflammatory pathology preventing the clinical symptoms of chronic Chagas disease. *PLoS One* (2011) 6(10):e26550. doi:10.1371/journal.pone.0026550
8. Knubel CP, Martinez FF, Fretes RE, Lujan CD, Theumer MG, Cervi L, et al. Indoleamine 2,3-dioxygenase (IDO) is critical for host resistance against *Trypanosoma cruzi*. *FASEB J* (2010) 24(8):2689–701. doi:10.1096/fj.09-150920
9. Knubel CP, Insfran C, Martinez FF, Diaz Lujan C, Fretes RE, Theumer MG, et al. 3-hydroxykynurenine, a tryptophan metabolite generated during the infection, is active against *Trypanosoma cruzi*. *ACS Med Chem Lett* (2017) 8(7):757–61. doi:10.1021/acsmedchemlett.7b00169
10. Martin D, Tarleton R. Generation, specificity, and function of CD8+ T cells in *Trypanosoma cruzi* infection. *Immunol Rev* (2004) 201(1):304–17. doi:10.1111/j.0105-2896.2004.00183.x
11. Lúcia CJA, Luiz VR, Bárbara I, Fabiana A, Fernando B, Dirceu C, et al. Chronic Chagas' disease cardiomyopathy patients display an increased IFN-γ response to *Trypanosoma cruzi* infection. *J Autoimmun* (2001) 17(1):99–107. doi:10.1006/jaut.2001.0523
12. Gomes JAS, Bahia-Oliveira LMG, Rocha MOC, Martins-Filho OA, Gazzinelli G, Correa-Oliveira R. Evidence that development of severe cardiomyopathy in human Chagas' disease is due to a Th1-specific immune response. *Infect Immun* (2003) 71(3):1185–93. doi:10.1128/IAI.71.3.1185-1193.2003
13. Jacqueline Araújo F, Ricardo Toshio F, Juliana Assis Silva G, Manoel Otávio das Costa R, Ana Thereza C, Fernanda Fortes de A, et al. Profile of central and effector memory T cells in the progression of chronic human Chagas disease. *PLoS Negl Trop Dis* (2009) 3(9):e512. doi:10.1371/journal.pntd.0000512
14. Gomes JAS, Bahia-Oliveira LMG, Rocha MOC, Busek SCU, Teixeira MM, Silva JS, et al. Type 1 chemokine receptor expression in Chagas' disease correlates with morbidity in cardiac patients. *Infect Immun* (2005) 73(12):7960–6. doi:10.1128/IAI.73.12.7960-7966.2005
15. van Amerongen R, Nusse R. Towards an integrated view of Wnt signaling in development. *Development* (2009) 136(19):3205–14. doi:10.1242/dev.033910
16. Clevers H, Nusse R. Wnt/β-catenin signaling and disease. *Cell* (2012) 149(6):1192–205. doi:10.1016/j.cell.2012.05.012
17. Staal FJ, Luis TC, Tiemessen MM. WNT signalling in the immune system: WNT is spreading its wings. *Nat Rev Immunol* (2008) 8(8):581–93. doi:10.1038/nri2360
18. Angers S, Moon RT. Proximal events in Wnt signal transduction. *Nat Rev Mol Cell Biol* (2009) 10(7):468–77. doi:10.1038/nrm2717
19. Kikuchi A, Yamamoto H, Sato A, Matsumoto S. Chapter 2 – new insights into the mechanism of Wnt signaling pathway activation. In: Kwang WJ, editor. *International Review of Cell and Molecular Biology*. (Vol. 291), Netherlands: Academic Press (2011). p. 21–71.
20. Feske S, Okamura H, Hogan PG, Rao A. Ca 2+/calcineurin signalling in cells of the immune system. *Biochem Biophys Res Commun* (2003) 311(4):1117–32. doi:10.1016/j.bbrc.2003.09.174
21. Schaale K, Neumann J, Schneider D, Ehlers S, Reiling N. Wnt signaling in macrophages: augmenting and inhibiting mycobacteria-induced inflammatory responses. *Eur J Cell Biol* (2011) 90(6–7):553–9. doi:10.1016/j.ejcb.2010.11.004
22. Silva-Garcia O, Valdez-Alarcon JJ, Baizabal-Aguirre VM. The Wnt/beta-catenin signaling pathway controls the inflammatory response in infections caused by pathogenic bacteria. *Mediators Inflamm* (2014) 2014:310183. doi:10.1155/2014/310183
23. Jiang A, Bloom O, Ono S, Cui W, Unternaehrer J, Jiang S, et al. Disruption of E-cadherin-mediated adhesion induces a functionally distinct pathway of dendritic cell maturation. *Immunity* (2007) 27(4):610–24. doi:10.1016/j.immuni.2007.08.015
24. Oderup C, LaJevic M, Butcher EC. Canonical and noncanonical Wnt proteins program dendritic cell responses for tolerance. *J Immunol* (2013) 190(12):6126–34. doi:10.4049/jimmunol.1203002
25. Reuter S, Martin H, Beckert H, Bros M, Montermann E, Belz C, et al. The Wnt/beta-catenin pathway attenuates experimental allergic airway disease. *J Immunol* (2014) 193(2):485–95. doi:10.4049/jimmunol.1400013
26. Valencia J, Hernández-López C, Martínez V, Hidalgo L, Zapata A, Vicente Á, et al. Wnt5a skews dendritic cell differentiation to an unconventional phenotype with tolerogenic features. *J Immunol* (2011) 187(8):4129–39. doi:10.4049/jimmunol.1101243
27. Holtzhausen A, Zhao F, Evans KS, Tsutsui M, Orabona C, Tyler DS, et al. Melanoma-derived Wnt5a promotes local dendritic-cell expression of IDO and immunotolerance: opportunities for pharmacologic enhancement of immunotherapy. *Cancer Immunol Res* (2015) 3(9):1082–95. doi:10.1158/2326-6066.CIR-14-0167
28. Manicassamy S, Reizis B, Ravindran R, Nakaya H, Salazar-Gonzalez R, Wang Y-C, et al. Activation of beta-catenin in dendritic cells regulates immunity versus tolerance in the intestine. *Science* (2010) 329(5993):849–53. doi:10.1126/science.1188510
29. Sen M, Ghosh G. Transcriptional outcome of Wnt-frizzled signal transduction in inflammation: evolving concepts. *J Immunol* (2008) 181(7):4441–5. doi:10.4049/jimmunol.181.7.4441
30. Katoh M, Katoh M. STAT3-induced WNT5A signaling loop in embryonic stem cells, adult normal tissues, chronic persistent inflammation, rheumatoid arthritis and cancer (Review). *Int J Mol Med* (2007) 19(2):273–8. doi:10.3892/ijmm.19.2.273

31. Manoharan I, Hong Y, Suryawanshi A, Angus-Hill ML, Sun Z, Mellor AL, et al. TLR2-dependent activation of beta-catenin pathway in dendritic cells induces regulatory responses and attenuates autoimmune inflammation. *J Immunol* (2014) 193(8):4203–13. doi:10.4049/jimmunol.1400614
32. Brown JB, Cheresh P, Goretsky T, Managlia E, Grimm GR, Ryu H, et al. Epithelial phosphatidylinositol-3-kinase signaling is required for beta-catenin activation and host defense against *Citrobacter rodentium* infection. *Infect Immun* (2011) 79(5):1863–72. doi:10.1128/IAI.01025-10
33. Bansal K, Trinath J, Chakravortty D, Patil SA, Balaji KN. Pathogen-specific TLR2 protein activation programs macrophages to induce Wnt-β-catenin signaling. *J Biol Chem* (2011) 286(42):37032–44. doi:10.1074/jbc.M111.260414
34. Bergenfelz C, Medrek C, Ekström E, Jirström K, Janols H, Wullt M, et al. Wnt5a induces a tolerogenic phenotype of macrophages in sepsis and breast cancer patients. *J Immunol* (2012) 188(11):5448–58. doi:10.4049/jimmunol.1103378
35. Neumann J, Schaale K, Farhat K, Endermann T, Ulmer AJ, Ehlers S, et al. Frizzled1 is a marker of inflammatory macrophages, and its ligand Wnt3a is involved in reprogramming *Mycobacterium tuberculosis*-infected macrophages. *FASEB J* (2010) 24(11):4599–612. doi:10.1096/fj.10-160994
36. Blumenthal A, Ehlers S, Lauber J, Buer J, Lange C, Goldmann T, et al. The Wingless homolog WNT5A and its receptor frizzled-5 regulate inflammatory responses of human mononuclear cells induced by microbial stimulation. *Blood* (2006) 108(3):965–73. doi:10.1182/blood-2005-12-5046
37. Pereira C, Schaer DJ, Bachli EB, Kurrer MO, Schoedon G. Wnt5A/CaMKII signaling contributes to the inflammatory response of macrophages and is a target for the antiinflammatory action of activated protein C and interleukin-10. *Arterioscler Thromb Vasc Biol* (2008) 28(3):504–10. doi:10.1161/ATVBAHA.107.157438
38. Ouaissi A, Guilvard E, Delneste Y, Caron G, Magistrelli G, Herbault N, et al. The *Trypanosoma cruzi* Tc52-released protein induces human dendritic cell maturation, signals via toll-like receptor 2, and confers protection against lethal infection. *J Immunol* (2002) 168(12):6366–74. doi:10.4049/jimmunol.168.12.6366
39. Oliveira AC, Peixoto JR, de Arruda LB, Campos MA, Gazzinelli RT, Golenbock DT, et al. Expression of functional TLR4 confers proinflammatory responsiveness to *Trypanosoma cruzi* glycoinositolphospholipids and higher resistance to infection with *T. cruzi*. *J Immunol* (2004) 173(9):5688–96. doi:10.4049/jimmunol.173.9.5688
40. Oliveira AC, de Alencar BC, Tzelepis F, Klezewsky W, da Silva RN, Neves FS, et al. Impaired innate immunity in Tlr4(-/-) mice but preserved CD8+ T cell responses against *Trypanosoma cruzi* in Tlr4-, Tlr2-, Tlr9- or Myd88-deficient mice. *PLoS Pathog* (2010) 6(4):e1000870. doi:10.1371/journal.ppat.1000870
41. Hsu YM, Zhang Y, You Y, Wang D, Li H, Duramad O, et al. The adaptor protein CARD9 is required for innate immune responses to intracellular pathogens. *Nat Immunol* (2007) 8(2):198–205. doi:10.1038/ni1426
42. Motran CC, Diaz FL, Montes CL, Bocco JL, Gruppi A. In vivo expression of recombinant pregnancy-specific glycoprotein 1a induces alternative activation of monocytes and enhances Th2-type immune response. *Eur J Immunol* (2003) 33(11):3007–16. doi:10.1002/eji.200323993
43. Motran CC, Diaz FL, Gruppi A, Slavin D, Chatton B, Bocco JL. Human pregnancy-specific glycoprotein 1a (PSG1a) induces alternative activation in human and mouse monocytes and suppresses the accessory cell-dependent T cell proliferation. *J Leukoc Biol* (2002) 72(3):512–21. doi:10.1189/jlb.72.3.512
44. Araujo F, Vitelli-Avelar D, Teixeira-Carvalho A, Antas P, Gomes J, Sathler-Avelar R, et al. Regulatory T cells phenotype in different clinical forms of Chagas' disease. *PLoS Negl Trop Dis* (2011) 5(5):e992. doi:10.1371/journal.pntd.0000992
45. Dijksterhuis JP, Baljinnyam B, Stanger K, Sercan HO, Ji Y, Andres O, et al. Systematic mapping of WNT-FZD protein interactions reveals functional selectivity by distinct WNT-FZD pairs. *J Biol Chem* (2015) 290(11):6789–98. doi:10.1074/jbc.M114.612648
46. Dejmek J, Safholm A, Kamp Nielsen C, Andersson T, Leandersson K. Wnt-5a/Ca2+-induced NFAT activity is counteracted by Wnt-5a/Yes-Cdc42-casein kinase 1alpha signaling in human mammary epithelial cells. *Mol Cell Biol* (2006) 26(16):6024–36. doi:10.1128/MCB.02354-05
47. Munder M, Eichmann K, Modolell M. Alternative metabolic states in murine macrophages reflected by the nitric oxide synthase/arginase balance: competitive regulation by CD4+ T cells correlates with Th1/Th2 phenotype. *J Immunol* (1998) 160(11):5347–54.
48. Stempin C, Giordanengo L, Gea S, Cerban F. Alternative activation and increase of *Trypanosoma cruzi* survival in murine macrophages stimulated by cruzipain, a parasite antigen. *J Leukoc Biol* (2002) 72(4):727–34. doi:10.1189/jlb.72.4.727
49. Hong Y, Manoharan I, Suryawanshi A, Shanmugam A, Swafford D, Ahmad S, et al. Deletion of LRP5 and LRP6 in dendritic cells enhances anti-tumor immunity. *Oncoimmunology* (2015) 5(4):e1115941. doi:10.1080/21624 02X.2015.1115941
50. Yoshida N. Molecular basis of mammalian cell invasion by *Trypanosoma cruzi*. *An Acad Bras Cienc* (2006) 78(1):87–111. doi:10.1590/S0001-37652006000100010
51. Burleigh BA, Andrews NW. The mechanisms of *Trypanosoma cruzi* invasion of mammalian cells. *Annu Rev Microbiol* (1995) 49:175–200. doi:10.1146/annurev.mi.49.100195.001135
52. Kayama H, Koga R, Atarashi K, Okuyama M, Kimura T, Mak TW, et al. NFATc1 mediates toll-like receptor-independent innate immune responses during *Trypanosoma cruzi* infection. *PLoS Pathog* (2009) 5(7):e1000514. doi:10.1371/journal.ppat.1000514
53. Mikels AJ, Nusse R. Purified Wnt5a protein activates or inhibits beta-catenin-TCF signaling depending on receptor context. *PLoS Biol* (2006) 4(4):e115. doi:10.1371/journal.pbio.0040115
54. Pukrop T, Binder C. The complex pathways of Wnt 5a in cancer progression. *J Mol Med (Berl)* (2008) 86(3):259–66. doi:10.1007/s00109-007-0266-2
55. Niehrs C. The complex world of WNT receptor signalling. *Nat Rev Mol Cell Biol* (2012) 13(12):767–79. doi:10.1038/nrm3470
56. Silva JS, Morrissey PJ, Grabstein KH, Mohler KM, Anderson D, Reed SG. Interleukin 10 and interferon gamma regulation of experimental *Trypanosoma cruzi* infection. *J Exp Med* (1992) 175(1):169–74. doi:10.1084/jem.175.1.169
57. Thomas SR, Mohr D, Stocker R. Nitric oxide inhibits indoleamine 2,3-dioxygenase activity in interferon-gamma primed mononuclear phagocytes. *J Biol Chem* (1994) 269(20):14457–64.
58. von Bergwelt-Baildon MS, Popov A, Saric T, Chemnitz J, Classen S, Stoffel MS, et al. CD25 and indoleamine 2,3-dioxygenase are up-regulated by prostaglandin E2 and expressed by tumor-associated dendritic cells in vivo: additional mechanisms of T-cell inhibition. *Blood* (2006) 108(1):228–37. doi:10.1182/blood-2005-08-3507
59. Munn DH, Mellor AL. IDO and tolerance to tumors. *Trends Mol Med* (2004) 10(1):15–8. doi:10.1016/j.molmed.2003.11.003
60. Soichot M, Hennart B, Al Saabi A, Leloire A, Froguel P, Levy-Marchal C, et al. Identification of a variable number of tandem repeats polymorphism and characterization of LEF-1 response elements in the promoter of the IDO1 gene. *PLoS One* (2011) 6(9):e25470. doi:10.1371/journal.pone.0025470
61. Thaker AI, Rao MS, Bishnupuri KS, Kerr TA, Foster L, Marinshaw JM, et al. IDO1 metabolites activate β-catenin signaling to promote cancer cell proliferation and colon tumorigenesis in mice. *Gastroenterology* (2013) 145(2):416–25.e4. doi:10.1053/j.gastro.2013.05.002
62. Hassanain HH, Chon SY, Gupta SL. Differential regulation of human indoleamine 2,3-dioxygenase gene expression by interferons-gamma and -alpha. Analysis of the regulatory region of the gene and identification of an interferon-gamma-inducible DNA-binding factor. *J Biol Chem* (1993) 268(7):5077–84.
63. Robinson CM, Hale PT, Carlin JM. The role of IFN-gamma and TNF-alpha-responsive regulatory elements in the synergistic induction of indoleamine dioxygenase. *J Interferon Cytokine Res* (2005) 25(1):20–30. doi:10.1089/jir.2005.25.20

Conflict of Interest Statement: The authors declare that the research was conducted in the absence of any commercial or financial relationships that could be construed as a potential conflict of interest.

frontiers in Immunology

ORIGINAL RESEARCH
published: 05 February 2018
doi: 10.3389/fimmu.2018.00158

Characteristics of Infection Immunity Regulated by *Toxoplasma gondii* to Maintain Chronic Infection in the Brain

*Young Sang Hwang[1†], Ji-Hun Shin[1†], Jung-Pyo Yang[1], Bong-Kwang Jung[1,2], Sang Hyung Lee[3] and Eun-Hee Shin[1,4]**

[1] Department of Parasitology and Tropical Medicine, Seoul National University College of Medicine, and Institute of Endemic Diseases, Seoul National University, Seoul, South Korea, [2] Institute of Parasitic Diseases, Korea Association of Health Promotion, Seoul, South Korea, [3] Department of Neurosurgery, Seoul National University College of Medicine, SMG-SNU Boramae Medical Center, Seoul, South Korea, [4] Seoul National University Bundang Hospital, Seongnam, South Korea

To examine the immune environment of chronic *Toxoplasma gondii* infection in the brain, the characteristics of infection-immunity (premunition) in infection with *T. gondii* strain ME49 were investigated for 12 weeks postinfection (PI). The results showed that neuronal cell death, microglia infiltration and activation, inflammatory and anti-inflammatory cytokine expression, Stat1 phosphorylation, and microglia activation and inflammatory gene transcripts related to M1 polarization in the brain were increased during the acute infection (AI) stage (within 6 weeks PI), suggesting that innate and cellular inflammatory response activation and neurodegeneration contributed to excessive inflammatory responses. However, these immune responses decreased during the chronic infection (CI) stage (over 6 weeks PI) with reductions in phosphorylated STAT1 (pSTAT1) and eosinophilic neurons. Notably, increases were observed in transcripts of T-cell exhaustion markers (TIM3, LAG3, KLRG1, etc.), suppressor of cytokines signaling 1 protein (SOCS1), inhibitory checkpoint molecules (PD-1 and PD-L1), and Arg1 from the AI stage (3 weeks PI), implying active immune intervention under the immune environment of M1 polarization of microglia and increases in inflammatory cytokine levels. However, when BV-2 microglia were stimulated with *T. gondii* lysate antigens (strain RH or ME49) *in vitro*, nitrite production increased and urea production decreased. Furthermore, when BV-2 cells were infected by *T. gondii* tachyzoites (strain RH or ME49) *in vitro*, nitric oxide synthase and COX-2 levels decreased, whereas Arg1 levels significantly increased. Moreover, Arg1 expression was higher in ME49 infection than in RH infection, whereas nitrite production was lower in ME49 infection than in RH infection. Accordingly, these results strongly suggest that immune triggering of *T. gondii* antigens induces M1 polarization and activation of microglia as well as increase NO production, whereas *T. gondii* infection induces the inhibition of harmful inflammatory responses, even with M1 polarization and activation of microglia and Th1 inflammatory responses, suggesting a host–parasite relationship through immune regulation during CI. This is a characteristic of infection immunity in infection with *T. gondii* in the central nervous system, and SOCS1, a negative regulator of toxoplasmic encephalitis, may play a role in the increase in Arg1 levels to suppress NO production.

Keywords: *Toxoplasma gondii*, brain, chronic infection, microglial polarization, infection immunity

OPEN ACCESS

Edited by:
Xun Suo, China Agricultural University, China

Reviewed by:
M. Victoria Delpino, National Scientific and Technical Research Council (CONICET), Argentina
Robin Stephens, University of Texas Medical Branch, United States

***Correspondence:**
Eun-Hee Shin
ehshin@snu.ac.kr

†These authors have contributed equally to this work.

Specialty section:
This article was submitted to Microbial Immunology, a section of the journal Frontiers in Immunology

Received: *05 November 2017*
Accepted: *18 January 2018*
Published: *05 February 2018*

Citation:
Hwang YS, Shin J-H, Yang J-P, Jung B-K, Lee SH and Shin E-H (2018) Characteristics of Infection Immunity Regulated by Toxoplasma gondii to Maintain Chronic Infection in the Brain. Front. Immunol. 9:158. doi: 10.3389/fimmu.2018.00158

INTRODUCTION

Toxoplasma gondii is an Apicomplexan pathogen of the central nervous system (CNS) (1). Human *T. gondii* infection generally occurs *via* ingestion of oocysts (an environmentally resistant form) released in cat feces or undercooked meat containing tissue cysts (1). Following ingestion, bradyzoites and sporozoites released from cysts and oocysts invade intestinal cells, where they are converted to tachyzoites, which can then be disseminated *via* the blood or lymphatic system to remote organs and can induce an acute infection (AI) or chronic infection (CI) (1). In general, the brain is the most commonly affected site *via* congenital transmission and subsequent CI, which elicits lifelong immunity against toxoplasmosis (1). Immune responses to *T. gondii* infection differ during the proliferative (acute) and dormant (chronic and latent) stages and are dependent on differences in phenotype, virulence, and clinical sequelae of the strains of the clonal lineages, such as the highly virulent strain RH (type I) and the avirulent strain ME49 (type II) (1–3). CI of a type II parasite is maintained by the conversion of tachyzoites into bradyzoites, which produce intracellular tissue cysts. The onset and progression of *T. gondii* encystation result from both intrinsic preprogramming within the parasite and the immune response of the host, which eventually help to maintain a CI (1).

The AI stage of the RH strain is characterized by marked elevations in serum Th1 cytokine levels, such as interferon (IFN)-γ, tumor necrosis factor (TNF)-α, interleukin (IL)-12, and IL-18, and is followed by a lethal outcome in mice at 8 days postinfection (PI) (2). In contrast, non-lethal infection (ME49 strain) is characterized by modest elevations in Th1 cytokines that lead to control of *T. gondii* infection and minimal damage to the host (2). More specifically, in the CNS, IFN-γ plays a critical role in the prevention of toxoplasmic encephalitis (TE) during the late stage of infection in mice *via* inhibition of tachyzoite proliferation. However, simultaneous IFN-γ activation of microglia may cause tissue injury *via* the production of toxic metabolites, such as nitric oxide (NO) (4, 5). However, neurodegeneration does not commonly occur during CI of *T. gondii*, despite potential NO toxicity (4), possibly to control parasitic proliferation and avoid tissue damage in the infected brain *via* regulation of the appropriate induction between the cytokines IFN-γ, IL-10, and transforming growth factor beta (TGF-β), and the toxic mediator NO (4, 6–8).

Microglia, which are a type of glial cell and account for 10–15% of all cells within the brain parenchyma, are macrophages that reside in the brain and spinal cord, and have plasticity due to the CNS immune environment and consequently play a key role the regulation of CNS inflammatory reactions, tissue injury, and tissue homeostasis (9). During *T. gondii* infection, microglia are major effector cells that prevent NO-mediated pathogen proliferation (5). During the immune response of the host, *T. gondii* infection progresses from an acute stage, where tachyzoites replicates for 2 months PI, to the chronic stage, which is characterized by the formation of dormant cysts after 2 months PI (4, 10, 11). Simultaneously, life-threatening toxoplasmosis characterized by encephalitis is gradually decreased in the latent stage of *T. gondii* infection (7). However, the underlying switching mechanisms from the prevention of pathogen proliferation to the inhibition of cellular toxic immune response in the CNS remain unclear, although previous *in vitro* studies have reported a fractional infection period (1–8, 12–15). For example, the cytokines IL-2, IL-12, IFN-γ, and TNF-α, which inhibit the growth of *T. gondii*, and IL-4, IL-10, and TGF-β, which are involved in the downregulation of the intracerebral immune response, favor the growth of *T. gondii* and have been implicated in TE (7). Besides, several reports insisted that the decrease in the expression levels of the effector molecules IFN-γ and NO is important for latent infection of *T. gondii* (4, 5, 8, 15, 16). Hence, active intervention may be a good strategy for prolonged parasitic survival and establishment of a host–parasite relationship without expulsion of the parasites by the host cells.

Our previous study found that a decrease in NO in Tg2576 mice caused Alzheimer's disease even with inflammation of the brain due to TE (8). In particular, because brain tissue is susceptible to the noxious effects of NO, such as wide-spread neurodegeneration, NO production in *T. gondii* infection has been widely studied as an important regulator and indicator of both protective effects and tissue damage (4, 5, 8, 15, 16). In the CNS, microglial cells lead to broad range of immunoregulatory functions with regulation of NO production to prevent further *T. gondii* proliferation (1, 5, 8, 15). However, despite numerous investigations, the time-specific kinetics of microglia activation in chronically infected normal mice have not been defined. Hence, further studies are needed because *T. gondii* infection is very chronic in immunocompetent hosts and can recur with time. Unfortunately, no previous study has investigated the immunomodulation in the brain during long-term CI of *T. gondii* and the key events in the regulation of CI, immunity, and parasite proliferation must be addressed to reduce the harmful effects of CI to brain tissues. As previously revealed, IFN-γ, TNF-α, and IL-12 were found to inhibit parasitic growth both *in vivo* and *in vitro*, and IL-10 and TGF-β are important to reduce the excessive inflammatory response of the brain to CI of *T. gondii* (2–7, 12, 15). The interactions of these cytokines inhibit NO production and promote the conversion of M1-type microglial cells to the M2-type *via* alternative activation accompanying arginase 1 (Arg1) activity and expression of the mannose receptor type C (CD206) (3, 5, 7, 12, 15, 16). The effector molecules of *T. gondii* that induce the polarization of macrophages include *Toxoplasma* rhoptry kinase ROP16 in the alternative activation pathway and *Toxoplasma* dense granule protein GRA15 in the classical activation pathway, which activate STAT6 and NF-κB, respectively (3). However, immune modulation may not be limited by the molecular actions

Abbreviations: *T. gondii*, *Toxoplasma gondii*; PI, postinfection; CI, chronic infection; (), acute infection; NO, nitric oxide; TGF-β, transforming growth factor-β; GM-CSF, granulocyte-macrophage colony-stimulating factor; IL-12, interleukin-12; STAT1, signal transducer and activator of transcription1; SOCS1, suppressor of cytokines signaling 1 protein; MHCII, major histocompatibility complex II; TLA, *T. gondii* lysate antigen; CNS, central nervous system; TE, toxoplasmic encephalitis; iNOS, nitric oxide synthase; PAMPs, pathogen-associated molecular pattern molecules; DG, hippocampal dentate gyrus; MFI, mean fluorescence intensity; IHC, immunohistochemistry; ME-TLA, lysate antigen of *T. gondii* ME49 strain tachyzoites; (RH-TLA), (COX-2) (Arg1), lysate antigen of *T. gondii* RH strain tachyzoites.

of *T. gondii*, but rather may be the result of interactions between the host and parasite to continually change the overall immune response during the latent infection stage due to changes in the immune characteristics and the course of infection. For example, several studies have investigated immune characteristics *via* genetic manipulation, such as the dense granule protein GRA15-KO-T of transgenic *T. gondii* (*Toxoplasma*-Cre) in IL-10$^{-/-}$ mice, but neglected to specify the time-varying infectious immunity during CI in regard to the host–parasite interactions (14, 17–19).

The characteristics of infectious immunity in the *T. gondii*-infected brain have been mainly investigated in TE with a focus on the AI stage (20). The most important effector molecules of TE and protection against *T. gondii* include the IL-12/IFN-γ axis, as well as IFN-γ through signal transducer and activator of transcription 1 (STAT1) and inducible nitric oxide synthase (iNOS) (5, 12, 17). Nevertheless, prolonged *T. gondii* infection results in decreased neurodegeneration and inflammatory immune responses, thus we previously identified components of basic and integrative infection immunity (8). In this respect, we aimed to investigate the processes underlying changes in infection immunity from the AI stage to the CI stage, and identified key responses in the immune regulation between a harmful inflammatory response and restoring neurodegeneration in the brain. To this end, we investigated the changes underlying neurodegeneration during *T. gondii* infection, as well as the activation and polarization of microglial cells as effector cells against *T. gondii* infection. Also, inflammatory and anti-inflammatory responses, changes in transcript expression patterns during the infection period, induction of NO and Arg1, an arginine hydrolytic enzyme, and finally *in vitro* infection of *T. gondii* tachyzoites (RH− or ME49 strain) as well as *in vitro* stimulation of *T. gondii* lysate antigen (TLA) (RH− or ME-TLA) were investigated to reveal the differences in immune-triggering events between *T. gondii* infection in the host–parasite relationship and immune characteristics of TLA as pathogen-associated molecular pattern molecules (PAMPs). The results of the present study are very important and interesting in regard to characterizing the infection immunity processes regulated by the host–parasite relationship through proper control of the protective inflammatory immune response, while reducing the harmful effects of neurodegeneration.

MATERIALS AND METHODS

Experimental Animals

Male, 7-week-old, C57BL/6 mice were purchased from the ORIENT BIO Animal Center (Seongnam, South Korea) and housed at room temperature (20–23°C) on a 12-h light/dark cycle with *ad libitum* access to sterilized (irradiated and autoclaved) food and water. All animal experiments were conducted in accordance with the ethical standards of the Institutional Animal Care and Use Committee of Seoul National University (SNU-110315-5).

Ethics Statement

This study protocol was approved by the Ethics Committee of Seoul National University and conducted in strict accordance with the Guidelines for Animal Experiments (SNUIBC-R110302-1). All surgeries were performed under anesthesia and all efforts were made to ensure minimal animal suffering.

T. gondii Infection

C57BL/6 mice (Orient Bio) at the age of 7 weeks were intraperitoneally injected with *T. gondii* strain ME49 (infection dose of 10 cysts) isolated from *T. gondii*-infected brains harvested at 3 months PI and housed in the animal facility of Seoul National University College of Medicine. Most experiments were conducted at 3 months PI. Six mice were randomly sacrificed at 0, 3, 6, 9, and 12 weeks PI, and brain tissues were collected for histological examinations, cytokine analysis, and microarray analysis.

Neuronal Degeneration in the Hippocampal Dentate Gyrus (DG) Detected by Hematoxylin and Eosin (H&E) Staining

Brain tissues were embedded in paraffin and coronal-sectioned at thickness of 10 μm through the hippocampus, mounted, and stained with H&E. Then, the tissue specimens were dehydrated with a graded alcohol series, cleared in xylene, fixed with Canadian balsam (Caedax; Merck, Darmstadt, Germany), and mounted on cover slips. Neuronal degeneration in the hippocampal DG was determined by the detection of eosinophilic neurons under a light microscope (Olympus PM-20; Olympus Corporation, Tokyo, Japan). The number of degenerative cells were counted in photomicrographs obtained with a digital camera (Leica DFC 280, Leica Microsystems, Wetzlar, Germany) attached to a microscope (BX-51; Olympus Corporation) using Image J software ver. 1.46.[1]

Detection of *T. gondii* Cyst in the Brain by Reverse Transcription Polymerase Chain Reaction (RT-PCR)

Total RNA was isolated from *T. gondii*-infected mouse brain tissue using the RNeasy Mini kit (Qiagen, Hilden, Germany) according to the manufacturer's protocol. All samples were subjected to RT-PCR using the RT premix reverse transcription kit (Elpis Biotech Inc., Daejeon, South Korea) and MG Taq DNA polymerase (Macrogen, Seoul, South Korea) with the following primer pairs: GAPDH (Primer Bank ID 6679937a1): forward 5′-AGG TCG GTG TGA ACG GAT TTG-3′ and reverse 5′-TGT AGA CCA TGT AGT TGA GGT CA-3′ (123 bp); *T. gondii* B1 gene: forward 5′-TCC CCT CTG CTG GCG AAA AGT-3′ and reverse 5′-AGC GTT CGT GGT CAA CTA TCG ATT G-3′ (98 bp). RT-PCR was performed for 35 cycles with an annealing temperature of 54–55°C and the products were analyzed by 1% agarose gel electrophoresis.

Real-time PCR

Total RNA was isolated from Total RNA was isolated from T. gondii-infected mouse brain tissue using the RNeasy Mini kit (Qiagen, Hilden, Germany) according to the manufacturer's protocol. All samples were reverse transcribed using RT premix

[1]http://pga.mgh.harvard.edu/primerbank/.

(Elpis Biotech Inc.). Real-time PCR was performed using the CFX96 (Bio-Rad) and SYBR green (Enzynomics™, Daejeon, Korea) was used to detect amplification products. The reaction conditions used were; initial denaturation at 95°C for 15 min, 40 amplification cycles [denaturation at 95°C for 10 s, annealing at 60°C for 20 s, and extension at 72°C for 30 s], followed by melting curve analysis. Data analysis was performed using CFX96 software (Bio-Rad). The following primer sequences were used for real-time PCR: GAPDH: forward 5′-GGT GAA GGT CGG TGT GAA CG-3′ and reverse 5′-CTC GCT CCT GGA AGA TGG TG-3′ (578 bp); and Socs1: forward 5′-CTG CGG CTT CTA TTG GGG AC-3′ and reverse 5′-AAA AGG CAG TCG AAG GTC TCG-3′ (217 bp); and Nos2 (iNOS): forward 5′-CAG CAC AGA ATG TTC CAG AAT CC-3′ and reverse 5′-TGT CAT GCA AAA TCT CTC CAC TGC-3′ (105 bp); and Arg1: forward 5′-CTT TAA CCT TGG CTT GCT TCG GAA-3′ and reverse 5′-CTT AGT TCT GTC TGC TTT GCT GTG-3′ (140 bp).

Immunostaining of *T. gondii*-Infected Mouse Brain Tissues

Mice were sacrificed by CO_2 asphyxiation at the pre-determined times and brain tissues were collected, then fixed in formalin and embedded in paraffin using the Leica TP1020 Tissue Processor (Leica Microsystems GmbH, Wetzlar, Germany). For specific immunostaining, samples were immunostained using the ChromoMap Kit and the Discovery XT automated staining instrument (Ventana Medical Systems, Inc., Tucson, AZ, USA). Briefly, 4 μm-thick tissue sections were fixed on Probe-On-Plus Slides (Thermo Fisher Scientific, Swedesboro, NJ, USA), deparaffinized in xylene, rehydrated in a graded series of alcohol (100, 95, 80, and 70), and finally rinsed with distilled water. After antigen retrieval, the endogenous peroxidase activity of the samples was blocked by treatment of H_2O_2 with blocking buffer [1% fetal bovine serum in phosphate-buffered saline (PBS)] for 30 min. Then, the samples were incubated for 60 min at room temperature with either rabbit anti-mouse Iba-1 (1:2000, Wako Chemicals, Richmond, VA, USA) or anti-phospho-STAT1 (Tyr701) (58D6, rabbit mAb) (1:500, Cell Signaling Technology, Beverly, MA, USA) primary antibodies, washed thrice with Tris-buffered saline, and incubated with secondary antibodies in UltraMap anti-Rb horseradish peroxidase (HRP) (Ventana Medical Systems, Inc.). Streptavidin-biotin-HRP complex (sABC/HRP) was detected with the ChromoMap DAB detection kit (Ventana Medical System, Inc.). The immunostained sections were then counterstained with hematoxylin (Ventana Medical System, Inc.) and plated on cover slips using Canadian balsam solution (Polysciences Inc., Warrington, PA, USA). Reactions were observed using a light microscope (PM-20; Olympus Corporation) and photomicrographs were acquired with a BX-51 microscope (Olympus Corporation) equipped with a color digital camera (DFC280; Leica Microsystems).

Levels of Inflammatory and Anti-inflammatory Cytokines in *T. gondii*-Infected Brain Tissue

Cytokine levels of IL-6, IL-12 (p70), IFN-γ, TNF-α, granulocyte-macrophage colony-stimulating factor (GM-CSF), IL-10, IL-4, and TGF-β in *T. gondii*-infected mouse brains were examined using the Bio-Plex mouse cytokine assay kit (Bio-Rad Laboratories, Hercules, CA, USA) and enzyme-linked immunosorbent assay (ELISA) kits (R&D Systems, Inc., Minneapolis, MN, USA). Brain tissues of C57BL/6 mice were obtained at 0, 3, 6, 9, and 12 weeks PI, and lysed using the MicroRotofor Cell Lysis Kit (Bio-Rad Laboratories) ($n = 3$). The soluble homogenate proteins were quantified using a bicinchoninic acid (BCA) assay kit (Pierce Biotechnology, Inc., Rockford, IL, USA). The Bio-Plex assay was performed according to the manufacturer's instructions and the raw data [mean fluorescent intensities (MFI)] were analyzed with Bio-Plex Manager Software (Bio-Rad Laboratories) to obtain concentration values. The one-way analysis of variance (ANOVA) was used for statistical analysis, and the results were analyzed using Bio-Plex Data Pro™ software. Cytokine analysis was performed using ELISA kits (R&D Systems, Inc.) according to the manufacturer's protocol. The reaction was measured at 450 nm using an Epoch microplate reader (BioTek Instruments, Inc., Winooski, VT, USA) and cytokine concentrations were calculated using a standard curve of the corresponding cytokine provided with the ELISA kit.

Microarray Analysis of *T. gondii*-Infected Brain

Total RNA of *T. gondii*-infected brain tissues was separately extracted at 0, 3, 6, 9, and 12 weeks PI, and pooled for microarray analysis ($n = 3$), which was performed by Macrogen Inc. (Seoul, South Korea) using an Illumina MouseRef-8 v2 Expression BeadChip array (Illumina, Inc., San Diego, CA, USA). Briefly, 0.55 μg of total RNA was amplified using the Illumina TotalPrep RNA Amplification Kit (Ambion, Austin, TX, USA) and purified using the Ambion Illumina RNA amplification kit (Ambion) to yield biotinylated cRNA. Following fragmentation, 0.75 μg of cRNA were hybridized to the Mouse Expression BeadChip (Illumina, Inc.) according to the manufacturer's protocol. Arrays were scanned with the Illumina Bead Array Reader Confocal Scanner. Array data export processing and analysis was performed using Illumina GenomeStudio v2011.1 (Gene Expression Module v1.9.0), and the data were analyzed with R v. 2.15.1 statistical software. Hierarchical cluster analysis was performed using Permute Matrix EN software. All heat maps were generated using Excel Spreadsheet Software (Microsoft Corporation, Redmond, WA, USA) with conditional formatting. The expression rates of each gene at 3, 6, 9 and 12 weeks PI were compared to baseline (week 0 PI). Positive correlations are depicted in yellow (increased expression) and negative correlations (decreased expression) are depicted in blue. Heat maps of inflammatory and anti-inflammatory cytokines, microglia phenotype markers, and immune regulatory markers are represented by color scales. Each row represents cytokines and immune markers, and each column represents infection times from 0 to 12 weeks PI. The color scale of the heat map corresponds the relative minimum (−3) and maximum (+3) values of each cytokine.

TLAs Prepared from Tachyzoites of *T. gondii* Strains RH and ME49

Toxoplasma gondii lysate antigens of strain RH or ME49 were prepared as previously described with slight modifications (8, 11).

Briefly, peritoneal exudates of infected mice at day 4 PI were passed twice through a 25-gauge needle and then through a 5-μm Millex filter membrane (Merck Millipore, Tullagreen, Ireland) to remove debris and host cells. Then, tachyzoites of *T. gondii* strain RH were recovered and washed with sterilized PBS (pH 7.2). Parasites were then washed and suspended in PBS (pH 7.2) for further antigen preparation. To prepare ME49 tachyzoite antigens, 20 cysts of strain ME49 were intraperitoneally injected to BALB/c mice to obtain ME49 tachyzoites converted from cysts. At 6 to 8 days PI, the tachyzoites were harvested by washing the peritoneal cavity with PBS. Tachyzoites of both *T. gondii* strains RH and ME49 were cultured in Vero cells (monkey kidney cells, KCLB cell line; no. 10081) grown in complete Roswell Park Memorial Institute 1640 media (WelGENE Inc., Daegu, Korea) supplemented with 100 μg/mL of penicillin (Gibco/BRL, Grand Island, NY, USA), 100 μg/mL of streptomycin (Gibco/BRL), and 5% fetal calf serum (Lonza, Walkersville, MD, USA) at 37°C under an atmosphere of 5% CO_2. After culturing in Vero cells, tachyzoites of strains ME49 and RH were passed through a 25-gauge needle twice, and then debris and cells were removed by passing through 5-μm filter membranes. After washing, the tachyzoites were re-suspended in PBS, sonicated on ice, and then centrifuged. Supernatants, containing the TLA fractions (respectively named as RH-TLA and ME-TLA) were filtered through 0.22-μm filter membranes (Millipore Corp., Bedford, MA, USA). Proteins in the TLA fraction were quantified using a BCA commercial reagent (Pierce Biotechnology, Inc.) and stored at −80°C until used.

Flow Cytometry Analysis to Determine the Microglia Phenotype of BV-2 Cells after Treatment of the *T. gondii* Antigen

Antigens against *T. gondii* strain RH or ME49 tachyzoites (40 μg/mL) and/or recombinant IFN-γ (100 ng/mL; PeproTech, Rocky Hill, NJ, USA) were used for *in vitro* activation of BV-2 cells, a murine microglial cell line. BV-2 cells were cultured in Dulbecco's modified essential medium (Applied Scientific, San Francisco, CA, USA) supplemented with 10% heat-inactivated fetal calf serum (Hyclone, Ogden, UT, USA), 4 mM L-glutamine, 0.2 mM penicillin, 0.05 mM streptomycin, and 20 mM HEPES (Sigma-Aldrich Corporation, St. Louis, MO, USA) at 37°C under an atmosphere of 5% CO_2 (8). After incubation for 24 h, BV-2 cells were harvested for further fluorescence-activated cell sorting (FACS) analysis. The following anti-mouse antibodies were used for flow cytometry analysis of the cultured BV-2 microglial cells: fluorescein isothiocyanate (FITC)-conjugated anti-CD80 (eBioscience, Inc., San Diego, CA, USA), phycoerythrin (PE)-conjugated anti-CD86 (eBioscience, Inc.), FITC-conjugated anti-CD274 (PD-L1) (B7-H1; eBioscience, Inc.), PE-conjugated anti-CD273 (PD-L2) (B7-DC; eBioscience, Inc.), allophycocyanin (APC)-conjugated anti-major histocompatibility complex (MHC) II (CD74, eBioscience), PE-conjugated anti-CD40 (eBioscience, Inc.), and FITC-conjugated anti-CD206 (BioLegend, San Diego, CA, USA). All staining processes for FACS analysis were conducted in accordance with the manufacturer's protocols with FACS staining buffer (PBS containing 1% bovine serum albumin and 0.1% sodium azide). Samples were analyzed using a FACSCalibur flow cytometer (BD Immunocytometry Systems, San Jose, CA, USA) with forward/side scatter gates to exclude nonviable cells and the data were analyzed using FlowJo software (Tree Star, Inc., Ashland, OR, USA). Data are presented as the mean (±SD) fluorescence intensity (MFI). In this study, *in vitro* experiment of BV-2 cell culture was data obtained after conducting three individual experiments.

Western Blot Analysis

Total proteins were extracted from uninfected and infected whole mouse brains using the PRO-PREP™ Protein Extraction Kit (iNtRON Biotechnology, Seongnam-Si, Korea) and quantified with a NanoDrop spectrophotometer (NanoDrop Technologies, Oxfordshire, UK). Proteins were separated by sodium dodecyl sulfate-10% polyacrylamide gel electrophoresis at 100 V for 110 min and then transferred to a nitrocellulose membrane (Bio-Rad Laboratories) using the Mini Trans-Blot® Electrophoretic Transfer Cell (Bio-Rad Laboratories) at 80 V for 100 min. The membranes were then incubated with the primary antibodies goat anti-SOCS1 (ab9870; Abcam, Cambridge, UK) (1:200) and mouse anti-β-actin (sc-47778; dilution, 1:500; Santa Cruz Biotechnology, Dallas, TX, USA), followed by the secondary antibodies donkey anti-goat immunoglobulin (Ig)G-HRP (sc-2020; dilution, 1:2,000; Santa Cruz Biotechnology) and goat anti-mouse IgG-HRP (sc-2005; dilution, 1:4,000; Santa Cruz Biotechnology). Signals were detected by exposing the membrane to chemiluminescence HRP substrate (Thermo Fisher Scientific) using a Fuji LAS1000 Lumino Image Analyzer (Fujifilm Corporation, Tokyo, Japan).

Nitrite and Urea Production by BV-2 Cells Stimulated by Various Cytokines and Strain-Specific Tachyzoite Antigens (RH-TLA and ME-TLA)

BV-2 cells were incubated for 24 h in 6-well culture plates (SPL Lifesciences Co., Ltd., Pocheon, South Korea) with either 100 ng/mL of IFN-γ (PeproTech), 20 ng/mL of IL-4 (Prospec-Tany Technogene Ltd., Rehovot, Israel), and/or one of the *T. gondii* antigens (RH-TLA or ME-TLA) at a concentration of 20 or 40 μg/mL. Culture supernatants were collected and assayed to determine contents of nitrite and urea, which reflect NO production and Arg1 levels, respectively. NO production was determined using Griess reagent (Sigma-Aldrich Corporation). After 50 μL of culture supernatant was reacted with 50 μL of Griess reagent in each well of a 96-well plate (SPL Lifesciences Co., Ltd.), the reaction was measured using a microplate reader at an optical density (OD) of 540 nm (Biotech, VT, USA). Urea concentration was determined using a commercial urea kit (Abnova Corporation, Taipei, Taiwan) according to the manufacturer's protocol. In brief, 50 μL of culture supernatant was mixed with 50 μL of distilled water and the solution was reacted with 200 μL of a working reagent for 20 min. Then, the OD value of the sample was measured at 520 nm and the concentrations of nitrite and urea were calculated using standard curves. *In vitro* experiment of BV-2 cell culture was data obtained after conducting three individual experiments.

mRNA Levels of iNOS, COX-2, and Arg1 in *T. gondii*-Infected BV-2 Cells

BV-2 cells were infected with tachyzoites of *T. gondii* strain RH or ME49 *in vitro* at an effector to target ratio (E:T ratio; *T. gondii*:BV-2 cell) of 1:5 for 24 h. Total RNA of the cultured cells was extracted using the RNeasy kit (Qiagen). All samples were reverse transcribed using RT premix (Elpis Biotech Inc.) and the iQ5 real-time PCR detection system (Bio-Rad Laboratories) with SYBR green master mix (Enzynomics, Cheongju, South Korea) under the following condition: initial denaturation at 50°C for 5 min and 95°C for 10 min, followed by 40 amplification cycles of denaturation at 95°C for 10 s and annealing at 60°C for 30 s, with a final extension cycle at 72°C for 5 min. Specific amplification was verified by analysis of the melting curve and separation of the RT-PCR products on a 3% agarose gel. Data analysis was performed using iQ™5 optical system software (Bio-Rad Laboratories). The following primer sequences and amplicon sizes were retrieved from the PrimerBank database[2]: GAPDH (PrimerBank ID 6679937a1) forward 5′-AGG TCG GTG TGA ACG GAT TTG-3′ and reverse 5′-TGT AGA CCA TGT AGT TGA GGT CA-3′ (123 bp); Arg1 (PrimerBank ID7106255a1) forward 5′-CTC CAA GCC AAA GTC CTT AGA G-3′ and reverse 5′-AGG AGC TGT CAT TAG GGA CAT C-3′ (185 bp); Nos2 (iNOS) forward 5′-GTT CTC AGC CCA ACA ATA CAA GA-3′and reverse 5′-GTG GAC GGG TCG ATG TCA C-3′(127 bp); and Ptgs2 (COX-2) forward 5′-TGT GAC TGT ACC CGG ACT GG-3′ and reverse 5′-TGC ACA TTG TAA GTA GGT GGA C-3′(233 bp).

Statistical Analysis

All statistical analyses were performed using Microsoft Excel and GraphPad Prism 5 software (GraphPad Software, Inc., La Jolla, CA, USA). Data are presented as the mean ± SD. One-way ANOVA followed by the Bonferroni multiple-comparison test were used to assess differences between experimental groups. A probability (p) values of <0.05 was considered statistically significant. * indicates significant difference by one-way ANOVA compared with the control. # indicates significant difference between the experimental groups.

RESULTS

Histopathological Changes and Microglia Activation in the Hippocampal DG during the AI to CI Stage of *T. gondii*

To observe the neuronal cell damage caused by *T. gondii* infection, histopathologic changes in the hippocampal region were examined by H&E staining. As shown in **Figure 1A**, purple-colored normal and un-injured neurons were observed with a light microscopic throughout most of the hippocampal DG (**Figure 1A**, week 0), whereas *T. gondii* infection resulted in an increase the proportion of eosinophilic neurons, which were characterized by cell body shrinkage, intensely stained eosinophilic cytoplasm, and small/shrunken darkly stained nuclei (**Figure 1A**, at 3 and 6 weeks PI). The appearance of eosinophilic neurons was increased during the AI stage and then significantly decreased during the CI stage from 6.7 ± 3.88% at week 0 to 83.8 ± 0.57% at week 3, 80.8 ± 2.38% at week 6, 50.1 ± 9.66 at week 9, and 28.5 ± 6.13% at week 12 PI (**Figure 1C**, $p < 0.05$). At this time, activation and infiltration of microglial cells in the DG were evaluated by immunohistochemical analysis with antibody against Iba-1, an activation marker of microglia (**Figure 1B**). The infiltration of Iba-1-positive cells (colored in brown) during hippocampal formation had increased from 3 weeks PI and was sustained during the 12-week experimental period (**Figure 1B**). These histopathological changes appeared after infection of *T. gondii*, which were detected by monitoring of the B1 gene (**Figure 1D**). Importantly, this result suggests that

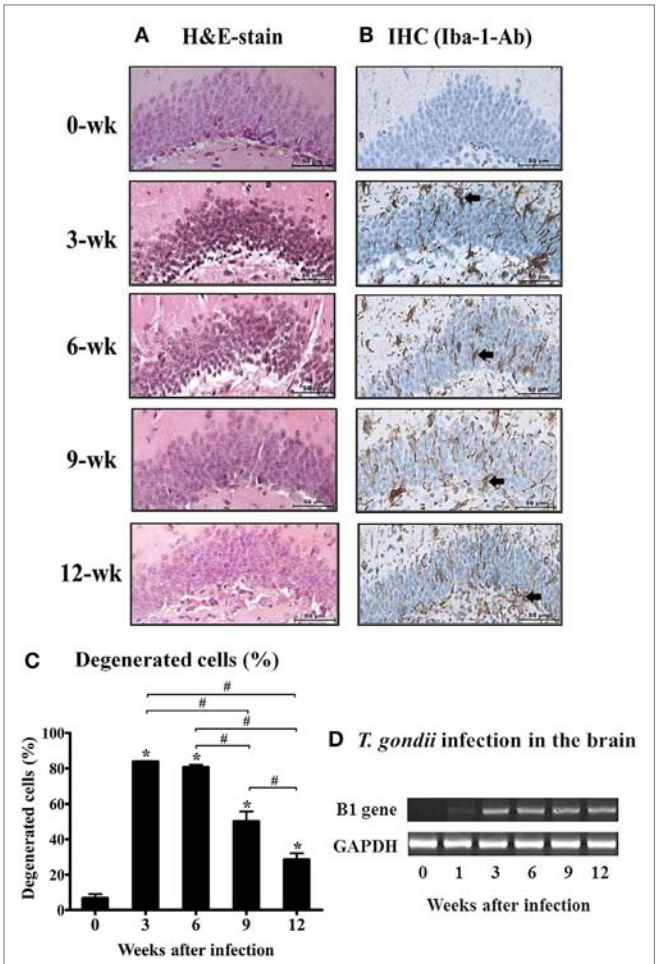

FIGURE 1 | Changes in neuronal degeneration and proliferation of microglial cells in the hippocampal dentate gyrus during *T. gondii* infection. The brain tissues were harvested at 0, 3, 6, 9, and 12 weeks postinfection, and subjected to histological staining. **(A)** hematoxylin and eosin staining, 400×. **(B)** Immunohistochemistry (IHC) results of the brain tissue stained with Iba-1-antibody (brown color), 400×. Scale bar = 50 μm. **(C)** Degenerated cells in the brain tissues after *T. gondii* infection were counted and are expressed by percentage (%).* indicates significant difference compared with the control. # indicates significant difference between the experimental groups. **(D)** *T. gondii*-specific B1 gene expression and RT-PCR products were loaded into 1% agarose gels (98 bp).

[2]http://pga.mgh.harvard.edu/primerbank/.

neurodegeneration increases during the AI stage and decreases in the CI stage (9 weeks PI), despite the presence of harmful signs in the brain tissue, such as activation of inflammatory microglia and continuity of *T. gondii* infection. Accordingly, further analysis showed that neurodegeneration accompanying *T. gondii* infection had decreased during the CI stage.

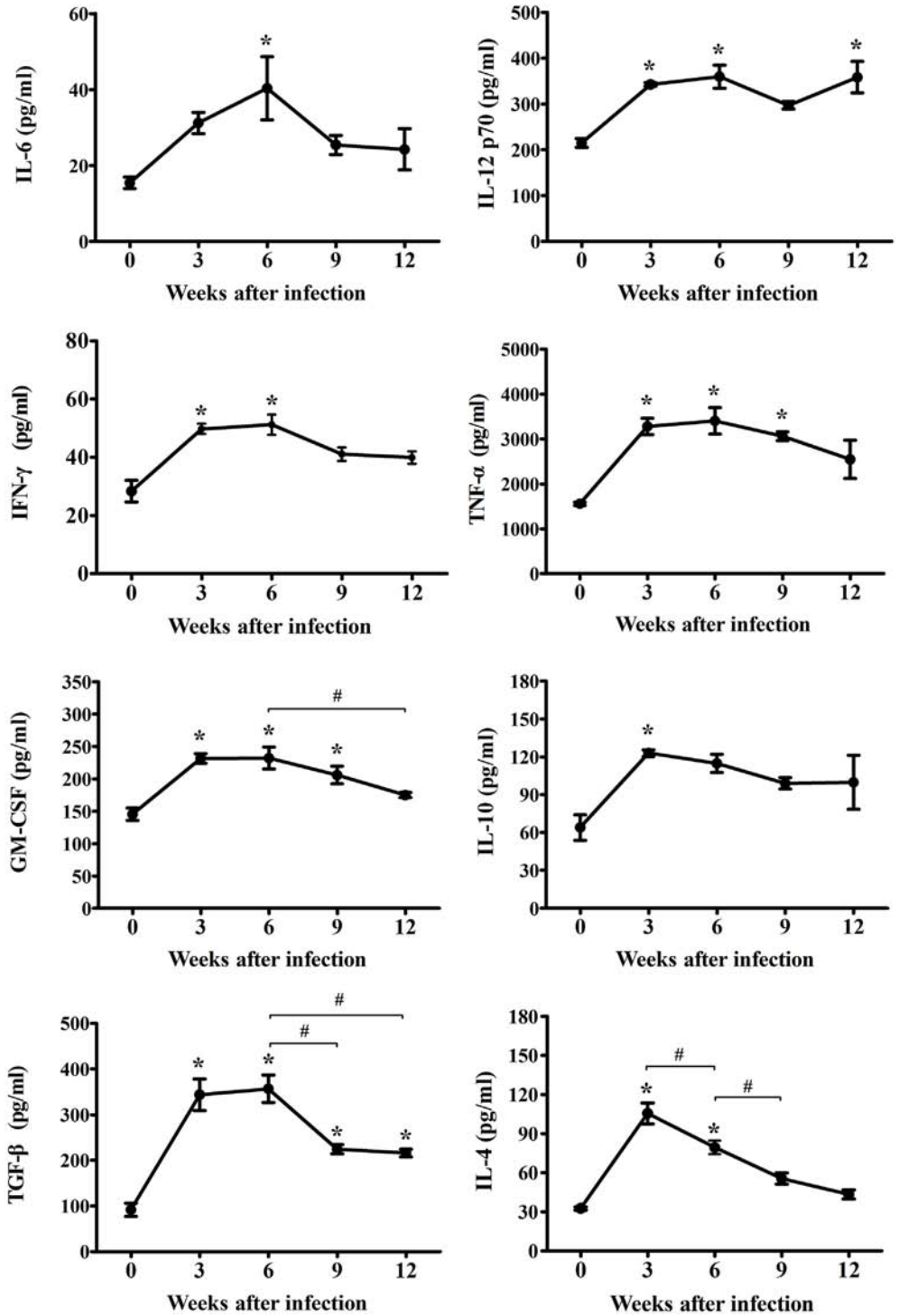

FIGURE 2 | Expression changes of cytokines in cerebral *Toxoplasma gondii* infection from the acute infection stage to the chronic infection stage. Brain tissues were harvested at 0, 3, 6, 9, and 12 weeks postinfection and analyzed for changes in cytokine levels due to infection. Levels of inflammatory cytokines [IL-6, IL-12p70, IFN-γ, tumor necrosis factor (TNF)-α, and granulocyte-macrophage colony-stimulating factor (GM-CSF)] and anti-inflammatory cytokines [IL-4, IL-10, and transforming growth factor-β (TGF-β)]. Cytokine levels are presented as the mean ± SD at each infection stage. *$p < 0.05$ (one-way analysis of variance). * indicates significant difference compared with the control. # indicates significant difference between the experimental groups.

Profiles of Inflammatory and Anti-inflammatory Cytokines in the Mouse Brain According to the Time of *T. gondii* Infection

To reveal the characteristics of the inflammatory mechanisms underlying microglia activation after *T. gondii* infection, inflammatory, and anti-inflammatory cytokines (IL-6, IL-12p70, IFN-γ, TNF-α, GM-CSF, IL-4, IL-10, and TGF-β) were examined at 0, 3, 6, 9, and 12 weeks PI. As show in **Figure 2**, the concentrations of inflammatory- (IL-6, IL-12p70, IFN-γ, TNF-α, and GM-CSF) and anti-inflammatory-cytokines (IL-4, IL-10, and TGF-β) had gradually and statistically increased during the AI stage (3–6 weeks PI, * $p < 0.05$ at every time point compared, as compared to week 0). Furthermore, the levels of inflammatory cytokines (IL-6, IL-12p70, IFN-γ, TNF-α, and GM-CSF) had peaked at 6 weeks PI, while those of the anti-inflammatory cytokines (IL-4 and IL-10) had peaked at 3 weeks PI, suggesting that levels of the anti-inflammatory cytokines had decreased immediately after the rapid increase during the early stage of infection (**Figure 2**). At this time, TGF-β, which is known to be associated with neuroprotection, continued to increase until 6 weeks PI. The peak level of each cytokine is shown in **Figure 2**. The abundance of the inflammatory cytokines IL-6, IL-12p70, IFN-γ, TNF-α, and GM-CSF had increased from baseline (week 0) to 6 weeks PI by 262, 167, 180, 218, and 160%, respectively, whereas the abundance of the anti-inflammatory cytokines IL-4 and IL-10 had increased by 324 and 192% at 3-weeks PI, respectively, and that of TGF-β had increased by 389% at 6 weeks PI. The cytokine IFN-γ, which produces a noxious cellular effect on the CNS and simultaneously activates the inflammatory cellular responses, had decreased at 6 weeks PI, whereas the levels of IL-12, which activates microglia, were sustained with no remarkable decrease during the experimental period. Moreover, levels of the cytokine TGF-β, which induces neuroprotective anti-inflammatory responses, were mostly sustained during the experimental period, but had decreased slightly. The levels of the anti-inflammatory cytokines IL-4 and IL-10 had decreased significantly during the CI stage (9–12 weeks). The results of the present study showed that levels of the inflammatory cytokines had continually increased to 6 weeks PI and were maintain at high levels even during the CI stage, although there were slight decreases, whereas levels of the anti-inflammatory cytokines had remarkably increased during the AI stage (3 weeks PI) and then decreased immediately thereafter during the CI stage. The most important finding was the significant increase and maintenance of IL-12 and TGF-β levels during the CI stage for 12 weeks PI (**Figure 2**, * $p < 0.05$).

Relative Cytokine mRNA Levels and Microglia Phenotype Markers for *T. gondii*-Infected Mouse Brain

Changes in gene expression levels of inflammatory and anti-inflammatory cytokines after *T. gondii* infection are shown in **Figure 3**. Gene expression levels of each cytokine at each time point of infection were compared to those of normal brain tissues (onefold at week 0 PI, a faint khaki color). Data are presented as heat maps (**Figure 3**), which depict the most commonly up- and downregulated transcripts from microarray analysis. The data presented in blue and yellow indicate reduced and increased cytokine expression levels. The present study analyzed gene expression patterns of inflammatory and anti-inflammatory cytokines (**Figure 3A**), as well as the microglia phenotype markers of the M1 and M2 types (**Figure 3B**). As compared with the anti-inflammatory cytokines (IL-4, IL-10 and TGF-β; 1.0- to 1.6-fold), transcript levels of the inflammatory cytokines (IL-12, IFN-γ, and TNF-α) had increased by 1.5- to 3.3-fold, as compared to $\log_2$-values (onefold) of the transcript levels of control mice. Especially, IFN-γ was remarkably increased by 3.3-fold at 3 weeks PI and was constantly maintained at 2.2-fold at 12 weeks PI. Likewise, the inflammatory cytokine TNF-α and the anti-inflammatory cytokine TGF-β were relatively increased by 1.5- to 1.8-fold during the 12-week experimental period. Expression levels of the phenotype markers M1-type and M2-type were found to be polarized in the M1-type microglia (**Figure 3B**). Most importantly, Arg1 levels among M2-markers were consistently increased for 12 weeks PI at 1.7- to 3.4-fold, even though the increase in IFN-γ levels was 2.2- to 3.3-fold. Further examining of the 12 polarization markers in each type of microglial cell phenotype showed that nine markers of the M1-type (IL-1β, IL-12, TNF-α, IFN-γ, CCL5, CXCL1, CXCL10, CD16, and CD86) and four markers of the M2-type (IL-1Rα, TGF-β, Arg1, and YM1) were consistently expressed for the entire 12-week period after infection (**Figure 3B**). Most notably, there was no increase in iNOS, while Arg1 was remarkably increased even if polarization and activation of M1-type microglia were distinct during the CI stage (**Figure 3B**).

Kinetics of Microglia Activation and Phosphorylation of Stat1 in *T. gondii*-Infected Mouse Brain Tissues

The above results showed that the expression levels of the inflammatory cytokines (IL-12, IFN-γ, and TNF-α) had continuously increased during the CI stage. Among these cytokines, mRNA and protein levels of IL-12, a key cytokine of microglial cells activation, and IFN-γ, a key cytokine of Th1-helper T-cell activation, were maintained steadily with high levels during the CI stage (**Figures 2** and **3**). To comprehensively link changes between gene and protein expression levels, brain tissues were immunohistologically stained with Iba-1- and phosphorylated STAT-1 (pStat1) antibodies for microglial activation and to determine whether these molecules participate in the IFN-γ-mediated pathway, respectively (**Figures 4A,B**). Because IFN-γ plays a role in adaptive cellular immunity against *T. gondii* infection and STAT-1 is important for intracellular downregulation of IFN-γ, the increase in pStat1-stained cells in the brain indicates an increase in IFN-γ-mediated Th1-T-cell immune responses. However, pStat1-stained cells were observed around the cyst (red arrow) over a relatively short period of time at 6 weeks PI and, thereafter, were undetectably in the brain tissues (**Figure 4B**). At this time, the proportion of microglial cells had remarkably increased around the *T. gondii* cysts (red arrow) during the AI stage and

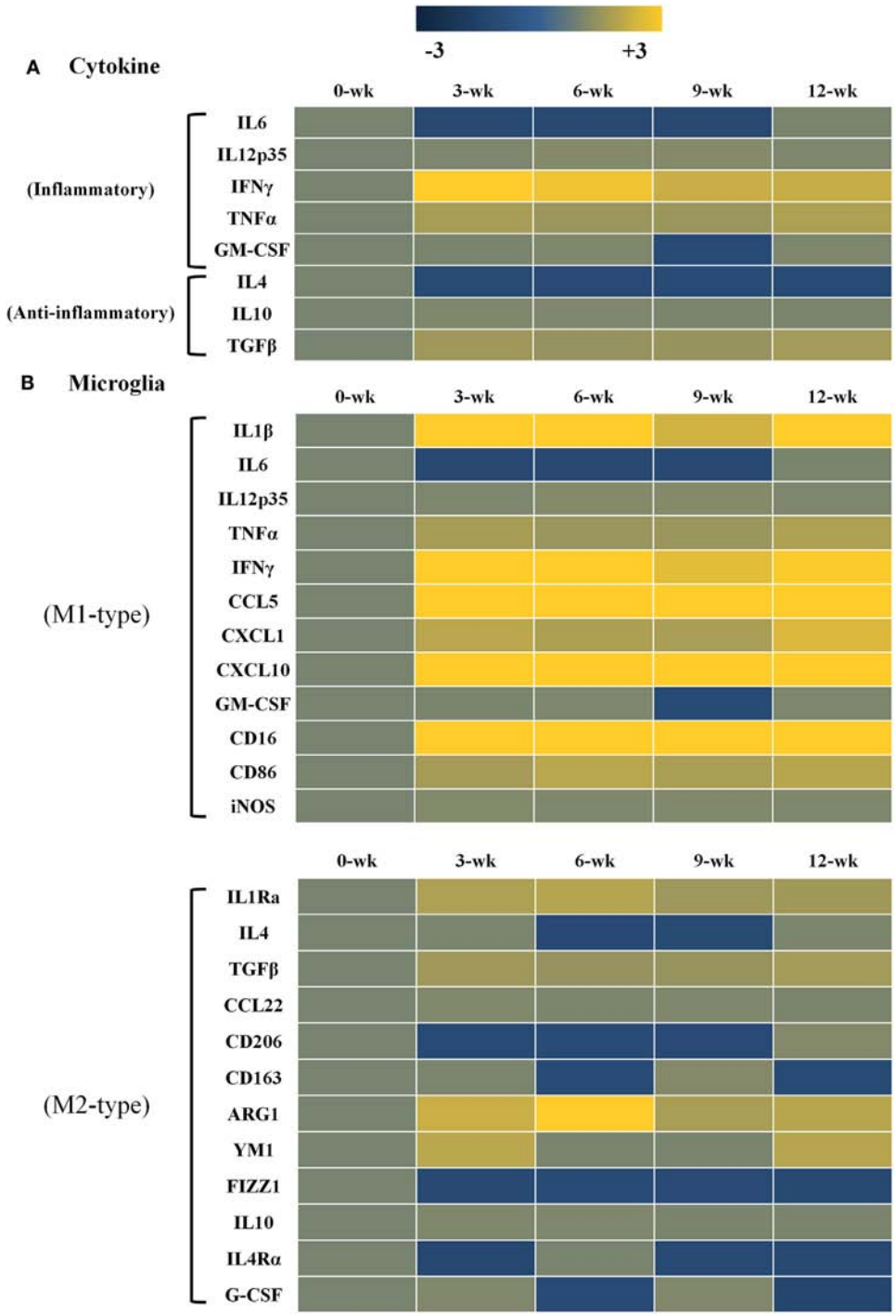

FIGURE 3 | Heat maps representing cytokine and chemokine concentrations in the inflammatory immune response and microglia phenotypes. Transcript levels of inflammatory and anti-inflammatory cytokines as well as microglia phenotype markers were measured in *Toxoplasma gondii*-infected mouse brains using microarray analysis. Each row of the heat map represents cytokines related with inflammatory and anti-inflammatory responses **(A)** as well as microglia phenotype markers related with the M1-type and M2-type **(B)**. Each column represents infection times from week 0 to 12 postinfection. The color scale corresponds to the relative expression of the cytokine for the minimum (−3) and maximum (+3) of all values.

was activated continuously during the CI stage (**Figure 4A**). This activation of microglial cells can be explained by morphological characteristics, such as hyper-ramification and long, thin processes extending from the cell body into the surrounding milieu (**Figure 4A**, colored in brown). The increase in activated microglia was greatest at 6–9 weeks PI and then had decreased

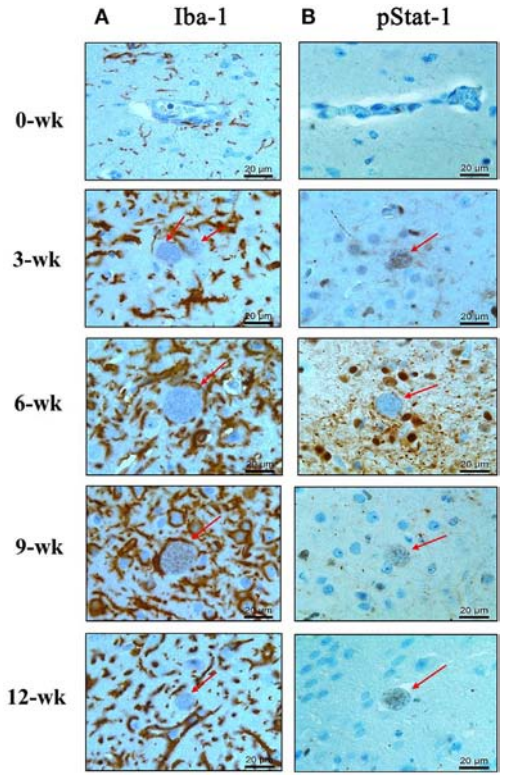

FIGURE 4 | Phosphorylation of Stat1 (pStat1) and Iba-1-stained microglia infiltrated and activated around *Toxoplasma gondii* cysts. *T. gondii*-infected mouse brains were harvested at 0, 3, 6, 9, and 12 weeks postinfection, embedded in paraffin, and immunostained with Iba-1- **(A)** and phosphorylated Stat-1 antibodies **(B)**. *T. gondii* cysts (arrow). Activated microglia [**(A)** brown color]. pStat1 immunoreactivity [**(B)** brown color]. Magnification, 400×. Scale bar = 20 μm.

slightly at 12 weeks PI (CI stage). These results strongly suggest microglia are activated throughout the infection period, whereas STAT1 phosphorylation was limited and no longer maintained during the CI stage.

Effects of TLA (RH- or ME-TLA) on the Polarization and Activation of Microglial Cells

Infection immunity in *T. gondii*-infected brain tissues can be explained by the immune characteristics regulated by the host–parasite relationship. Infectious immunity shown in the present study was characterized by an increase in microglial cells and the limited IFN-γ-mediated immune response. However, it remains unclear whether these immune responses were induced by immune regulation *via* the host–parasite relationship or by immunological triggering of *T. gondii* antigens as a PAMP. For this purpose, TLAs were prepared from RH- or ME49 tachyzoites to investigate the effects of TLA on the activation and polarization of microglia, which were further compared with transcript levels in the brain (**Figures 5A,B**). TLAs contain many PAMPs and stimulate toll-like receptor (TLR)-based immune responses. Moreover, because *T. gondii* strains (RH and ME49) have different modes of infectious immunity, the comparison of *T. gondii* antigens (RH-TLA or ME-TLA) on microglia activation is important to evaluate difference in immune responses between the AI and CI stages. As shown by the results, the MFI (FACS analysis) of the activation markers of BV-2 microglial cells [i.e., major histocompatibility complex II (MHCII), CD40, CD80, and CD86] had increased in response to IFN-γ stimulation (**Figure 5A**). Such an increase in MFI indicates an increase in target molecules in FACS. IFN-γ stimulation of BV-2 cells had increased the expression levels of these activation markers, which was accelerated by the presence of TLA (**Figure 5A**). At this time, ME-TLA had a greater effect on the increase in activation markers than RH-TLA. In contrast, expression of the M2 polarization marker CD206 was lower in ME-TLA than RH-TLA (**Figure 5A**). These results are consistent with the microarray results (**Figure 5B**). Subunit transcripts of MHC class II molecules (H2-Eb1, -Aa, and -Ab1), *Cd40*, *Cd80*, and *Cd86* were increased (16). In contrast, *Cd206* was decreased, as compared to the control (khaki) (**Figure 5B**). The M1 markers *Cd40*, *H2-EB1 (-Aa, -Ab1)* (MHCII), and *Cd86* (B7-2) were upregulated in activated microglial cell and acted as co-stimulatory molecules for further T- and B-cell immune responses. Both mRNA and protein levels of the representative M2 marker CD206 were decreased simultaneously in cells infected with *T. gondii* strain ME49, as well as by antigen treatment (ME-TLA) as PAMPs. Accordingly, our results showed that both *TLA* treatment and *T. gondii* infection induced the activation and M1 polarization of microglial cells compared with the control (no-treatment of IFN-γ and lysate antigens *in vitro* study as well as 0-week PI *in vivo* study).

Changes in Transcripts for T-Cell Differentiation- and T-Cell Exhaustion-Markers in the Brain during *T. gondii* Infection

CI of *T. gondii* in the brain may induce T-cell exhaustion and dysfunction. The results of this study showed a decrease in the IFN-γ-mediated immune response during CI even if microglial cell activation was maintained. To arrive at a possible explanation, markers of T-cell differentiation and dysfunction were examined, which showed that Th1 cell-specific transcription factor TBX21 that controls the expression of IFN-γ was mainly increased during CI, as compared to the Th2 cell-secreted cytokines *Gata3* and *Foxp3*, which promote the functions of regulatory T cells (**Figure 6A**). Nevertheless, markers of T-cell exhaustion, including *Tim3* and *Lag3*, were also increased simultaneously from the AI stage at 3 weeks PI (**Figure 6B**). *Tim3* and *Lag3* are known to negatively regulate T-cell proliferation, homeostasis, and Th1 immunity, and act as immune checkpoints. This result means that *T. gondii* infection actively influences the induction of the host immune response against infection. In other words, although these findings were limited to transcript profiles, *T. gondii* infection of the brain simultaneously induces both T-cell differentiation and exhaustion from the AI stage at 3 weeks PI, and maintains the immune environment during the entire the CI stage (**Figure 6**).

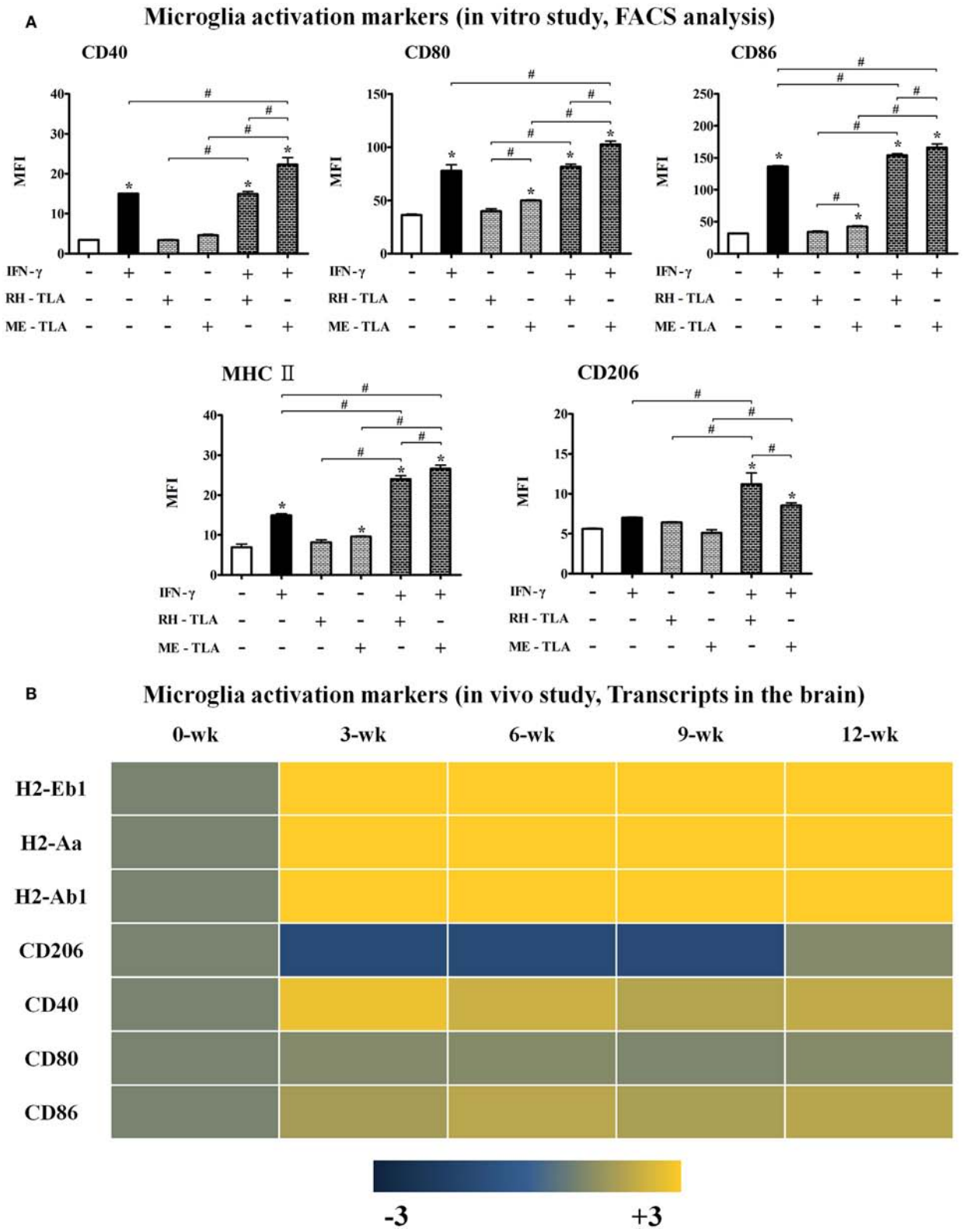

FIGURE 5 | Microglia activation in *Toxoplasma gondii*-infected brain and BV-2 cells stimulated with *T. gondii* lysate antigens (TLAs) (RH-TLA and ME-TLA). Expression levels of major histocompatibility complex II antigens (H2-Eb1, H2-Aa, and H2-Ab1), CD40, and CD86 by FACS analysis. **(A)** Heat map expression of cell surface markers related with microglia activation in *T. gondii*-infected brains, **(B)** results are expressed as the mean ± SD of the mean fluorescence intensity. *$p < 0.05$ (one-way analysis of variance). * indicates significant difference compared with the control. # indicates significant difference between the experimental groups.

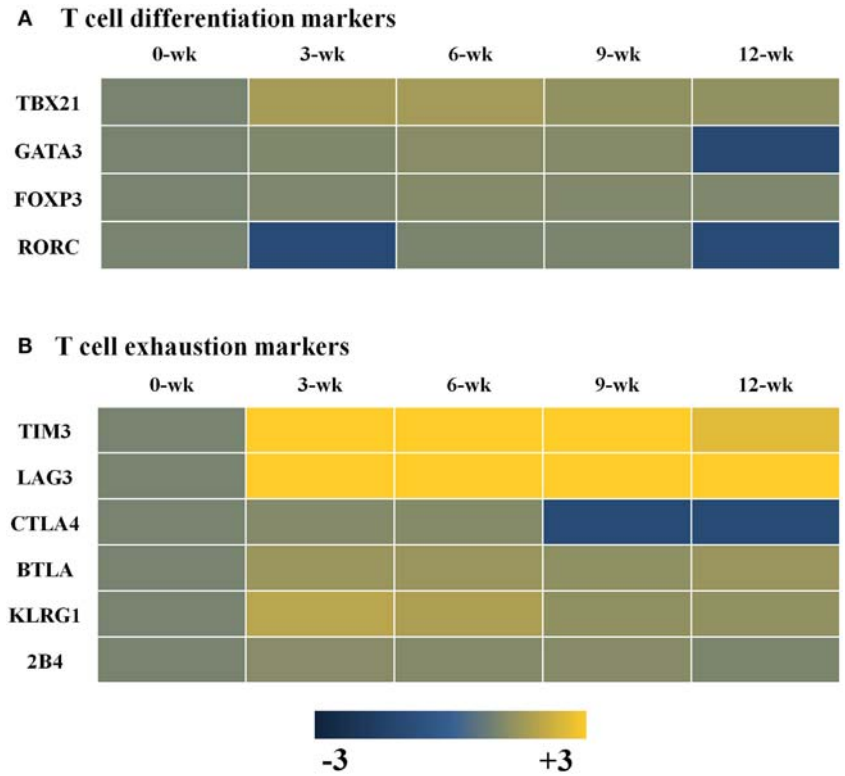

FIGURE 6 | Changes in T-cell differentiation **(A)** and exhaustion **(B)** markers in *Toxoplasma gondii*-infected brain tissues. Expression values represent the intensity of gene expression varying from −3 to +3 colored with blue or yellow.

Changes in mRNA Levels of Immune Effector and Checkpoint Molecules in *T. gondii*-Infected Brain Tissues

To investigate the expression of effector molecules associated with both inflammatory and anti-inflammatory responses, changes in transcripts and quantitative gene levels of Socs1, iNos, and Arg1 during the 12-week experimental period were compared to those at baseline (week 0 PI) (**Figure 7A**). Transcript levels of Socs1, which is thought to be an important immune regulatory factor in this study, was increased by 1.5-fold at 3-weeks PI and maintained during the CI stage (**Figure 7A**). Likewise, quantitative gene expression levels of Socs1 was the highest at 3 weeks PI (2.63-fold) with statistical significance and, thereafter, had slightly decreased during the CI stage. Similarly, the results of western blot analysis showed an increase in SOCS1 expression during the infection period. In contrast, there was no significant increase in iNOS mRNA levels, and quantitative gene expression levels of iNOS/Arg1 were decreased even during the AI stage (3 and 6 weeks PI). This result is also supported by transcript level of Arg1 (2.2- and 3.4-fold at 3 and 6 weeks PI, respectively) (**Figure 7A**). Expression levels of the of the immune inhibitory checkpoint molecules PD-1, PD-L1, and PD-L2, as related with T-cell dysfunction, were examined at the transcript level and by FACS analysis. As shown in **Figure 7B**, transcript levels of PD-1, an inhibitory receptor of T cells, were slightly increased by 1.1- to 1.4-fold at week 12 PI, whereas levels of PD-L1 were remarkably increased by 19.5-, 21.4-, 18.9-, and 23.0-fold at 3, 6, 9, and 12 weeks PI, respectively. This result was also strongly supported by the FACS results expressed as the MFI, suggesting strong activation of the M1-type microglia. When RH- or ME-TLA as PAMPs of *T. gondii* stimulate BV-2 microglial cells, the increase in the MFI of PD-L1 was greater than that of PD-L2 and the degree of increase was greater *via* stimulation of ME-TLA than RH-TLA. Accordingly, it is expected that the immune-triggering effect of *T. gondii* strain ME49 during CI seems to limit the expression of inflammatory effector molecules such as iNOS, even with activation of innate immunity by microglial cells.

Effects of *T. gondii* Antigens (RH- and ME-TLA) on Nitrite and Urea Production according to Microglia Polarization

For 12 weeks PI, iNOS production was decreased and Arg1 production was increased. As well, when BV-2 cells were treated with *T. gondii* antigens as a PAMPs, expression levels of the activation markers were increased. In this regard, an aim of this study was to investigate whether treatment of BV-2 microglial cells with *T. gondii* antigens (RH-TLA or ME-TLA) can induce changes in NO and urea production, as with *T. gondii*-infected brain tissues. In general, nitrite production is mainly increased as a result of M1-type activation, whereas urea production is increased by M2-type microglia activation. The results of the present study showed that the production of nitrite was increased by stimulation

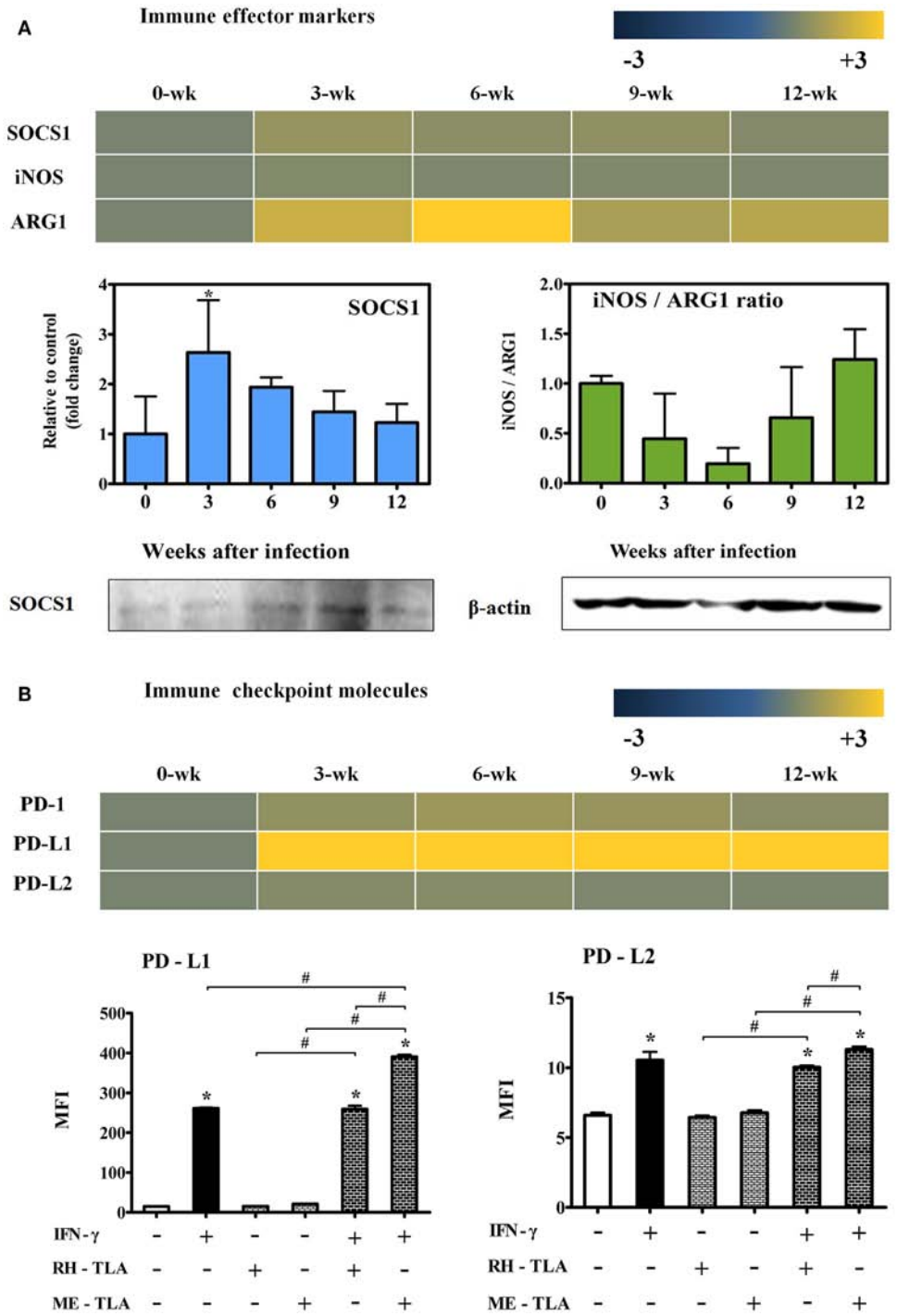

FIGURE 7 | Changes in immune effector and checkpoint molecules. Transcripts of immune effector markers [nitric oxide synthase (iNos) and Arg1] **(A)**, immune control marker (Socs1) **(A)** and immune checkpoint markers (PD-1, PD-L1 and PD-L2) **(B)**. RT-PCR results (SOCS1 and the iNos/Arg1 ratio) and western blot (SOCS1 and β-actin) **(A)**. Transcript expressions(PD-1, PD-L1, and PD-L2) and FACS analysis (PD-L1 and PD-L2) **(B)**. Results are expressed as the mean ± SD of the mean fluorescence intensity (MFI). *$p < 0.05$ (one-way analysis of variance). * indicates significant difference compared with the control. # indicates significant difference between the experimental groups.

of IFN-γ alone (9.5 ± 0.3 μM) or IFN-γ with *T. gondii* antigen (6.6 ± 0.2 μM with RH-TLA and 17.1 ± 0.7 μM with ME-TLA), as compared to the control (4.3 ± 0.4 μM) (**Figure 8A**). At this time, nitrite concentration had significantly increased *via* stimulation with ME-TLA, as compared to RH-TLA, suggesting that ME-TLA itself is more preferable for the induction of M1-type

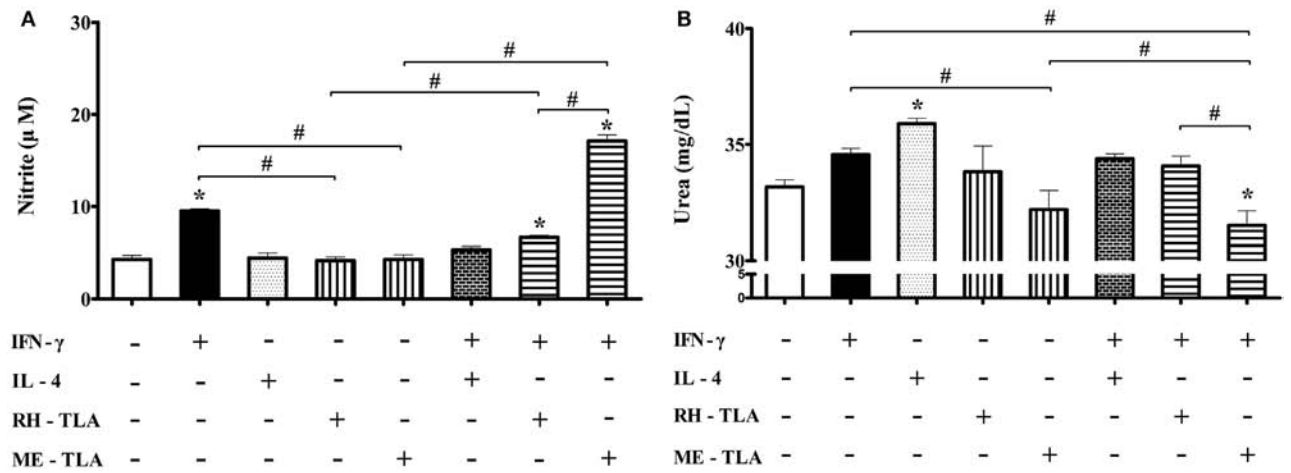

FIGURE 8 | Nitrite and urea production in BV-2 microglia stimulated with recombinant cytokines affecting microglia polarization (IFN-γ and IL-4) or *Toxoplasma gondii* antigens (RH-TLA or ME-TLA). Nitrite (μM) **(A)** and urea (mg/dL) concentrations **(B)**. Data are presented as the mean ± SD. *$p < 0.05$ (one-way analysis of variance). * indicates significant difference compared with the control. # indicates significant difference between the experimental groups.

microglial activation (*$p < 0.05$). In contrast, urea concentration was increased significantly by stimulation of IL-4, as compared to the control (36.0 ± 0.2 vs. 33.2 ± 0.3, respectively) (**Figure 8B**). As well, urea production was more decreased by ME-TLA than RH-TLA (32.2 ± 0.8 vs. 33.8 ± 1.1 mg/dL, respectively). Notably, treatment with IFN-γ + ME-TLA had decreased urea production even further than with treatment of IFN-γ + RH-TLA (31.5 ± 0.6 and 34.1 ± 0.4, respectively, *$p < 0.05$). These results clearly show that treatment of BV-2 cells with ME-TLA induced M1 polarization and M1-activation, which subsequently remarkably increased nitrite production and decreased urea production, suggesting that the immune induction of ME-TLA acts as a PAMP. However, this result is in contrast to the transcript results of the *T. gondii*-infected brain tissues. To clarify this difference, infection of BV-2 cells was performed *in vitro* (**Figure 9**).

Effects of *In Vitro T. gondii* Infection (RH- and ME-Strain) on mRNA Expression (iNOS, Cox-2, and Arg1) and Nitrite Production

To elucidate the differences in inflammatory responses and NO production between *T. gondii* infection in the brain and *in vitro* experiments with the *T. gondii* antigens (RH-TLA and ME-TLA), BV-2 cells were infected with *T. gondii* tachyzoites *in vitro*. As shown in **Figure 9**, the expression levels of the inflammatory response markers iNos and Cox-2 were significantly decreased after *T. gondii* infection *in vitro*, whereas that of Arg1 was significantly increased. Notably, Arg1 expression levels at 24 h after *in vitro* RH and ME49 infection were increased by 2.0 ± 0.3- and 2.9 ± 0.1-fold, respectively, as compared to control (*$p < 0.05$). Likewise, Arg1 induction was significantly greater after infection with strain ME49, as compared to strain RH. At this time, nitrite production was the highest with treatment of IFN-γ alone (39.6 ± 2.0 μM) and decreased significantly with IFN-γ + *T. gondii* infection (RH and ME49) (28.9 ± 1.4 and 24.0 ± 0.9 μM, respectively, *$p < 0.05$). As compared to IFN-γ alone, nitrite levels were 27% lower with IFN-γ + *T. gondii* strain RH infection and 39.4% lower with IFN-γ + *T. gondii* strain ME49 infection. Accordingly, these results emphasize that *in vitro T. gondii* infection induces polarization of microglial cells into the M1-type. However, simultaneous inhibition of harmful inflammatory factors, such as NO, had increased Arg1 expression for further immune regulation. This is an important result showing that *in vivo* and *in vitro* infection was consistent. In other words, TLAs acting as PAMPs had strongly induced polarization of M1-type microglial cells and inflammatory responses, while infection of *T. gondii* (*in vivo* and *in vitro*) induced polarization of M1-type microglial cells. However, it simultaneously inhibited a detrimental inflammatory response, such as NO production, *via* Arg1 induction. This host–parasite relationship seems to be a strategy of *T. gondii* to maintain a CI in the brain.

DISCUSSION

The results of our previous study demonstrated that *T. gondii* infection decreased the neurodegeneration in a Tg2576 mouse model of Alzheimer's disease (8). In that study, *T. gondii* infection of the brain inhibited neuronal degeneration, as well as learning and memory impairments in Tg2576 mice. As a possible reason, we proposed that the increase in the expression levels of the anti-inflammatory cytokines IL-10 and TGF-β, as well as decreased NO production had favorable effects of *T. gondii* infection and the pathogenesis and progression of Alzheimer's disease in mice (8). However, because inflammatory responses induced by IFN-γ and NO are essential for the control of *T. gondii* infection, NO regulation in the CNS is very important to control both parasitic proliferation and damage to the host tissues. As an extension of the above results, the aim of the present study was to address the progression of infection immunity to identify the appropriate timing to induce an anti-inflammatory response during CI. In

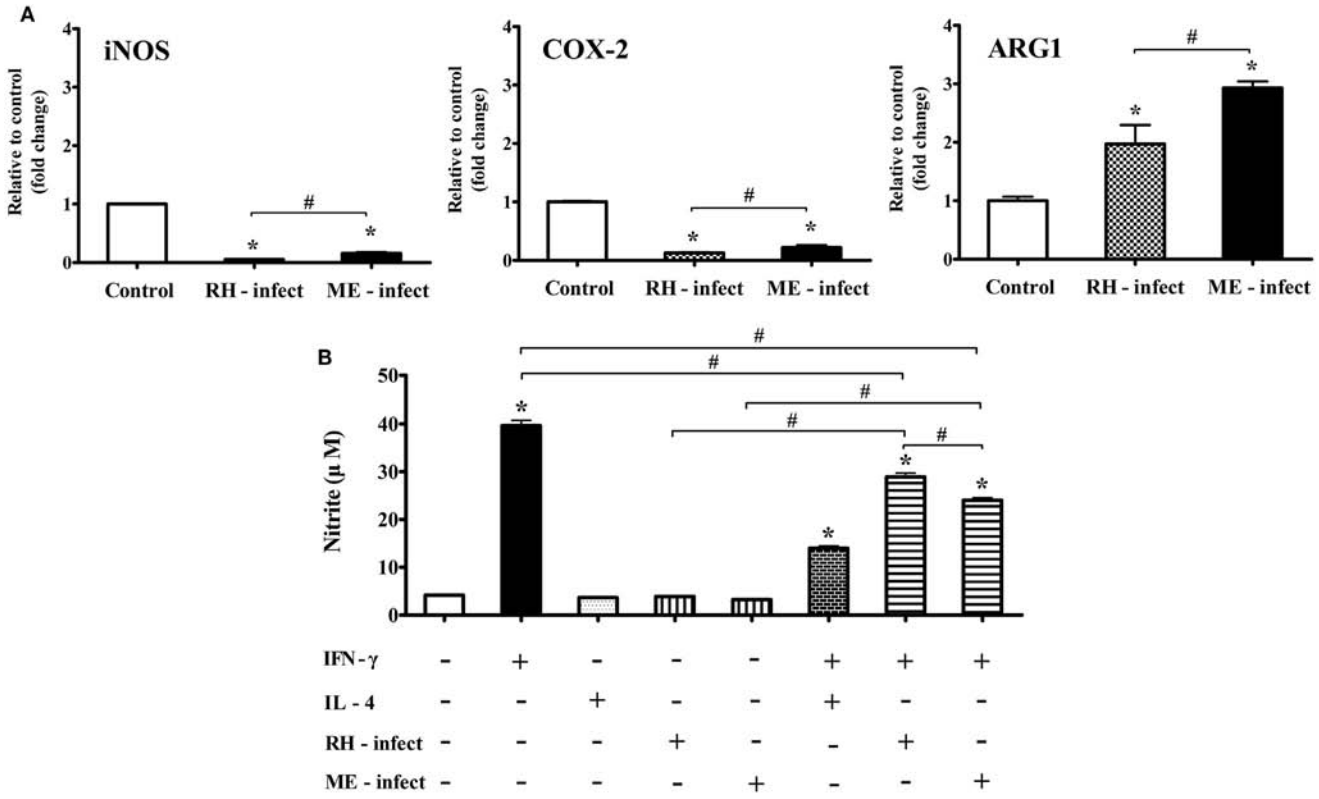

FIGURE 9 | mRNA levels of nitric oxide synthase (iNos), Cox-2, and Arg1, and nitrite production in *Toxoplasma gondii*-infected BV-2 microglial cells. **(A)** RT-PCR analysis of iNos, Cox-2, and Arg1 in *T. gondii* tachyzoites (strains RH and ME49)-infected BV-2 cells. **(B)** Nitrite concentration (μM) in culture supernatant treated with recombinant IFN-γ and/or IL-4, and/or *T. gondii* tachyzoites. Data are presented as the mean ± SD. *$p < 0.05$ (one-way analysis of variance). * indicates significant difference compared with the control. # indicates significant difference between the experimental groups.

particular, because *T. gondii* is a pathogen that can lead to CI of the host, as well as induce encephalitis and neurodegeneration, it is very important to understand the infection immunity related with microglia polarization and harmful inflammatory responses.

Encephalitis is an important symptom of *T. gondii* infection, although the neuronal degeneration associated with neuroinflammation is not a common finding because immune modulation by *T. gondii* infection has been the focus of numerous previous studies (1–5, 8, 9). In the present study, neuronal cell death caused by *T. gondii* infection in the DG region of the hippocampus was increased in the AI stage at 3–6 weeks PI, which then decreased in the CI stage accompanied with slight decreases in the expression levels of the inflammatory cytokines IL-6, IFN-γ, TNF-α, and GM-CSF. Even in this case, the Iba-1 staining intensity of microglial cells was not significantly decreased during the entire 12-week experimental period. In fact, the microarray results of the *T. gondii*-infected brain and FACS analysis of *in vitro* cultured BV-2 microglial cells with lysate antigens (RH-TLA and ME-TLA) prepared from tachyzoites of *T. gondii* strains RH and ME49, showed M1 polarization of microglial cells both *in vivo* and *in vitro*. However, high levels of the inflammatory and anti-inflammatory cytokines remained during the 12-week experimental, even though the levels had slightly decreased from 6 weeks PI. Thus, it is necessary to consider why neuronal cell death was highest at 3 weeks PI and then decreased. Clearly, *T. gondii* infection induces a mixed immune response characterized by an increase in the expression levels of inflammatory cytokines and the activation and proliferation of microglial cells, as well as increases in the expression levels of the anti-inflammatory cytokines and Arg1 and decreased expression of iNOS and COX-2 accompanied with NO production.

The strategy of *T. gondii* intracellular parasitism involves the manipulation of an excessive response of immune cells and alterations in macrophage phenotypes to suppress inflammatory response and reduce damage to the host. According to the results of an earlier study, *T. gondii* infection is generally controlled by a strong Th1-type immune response *via* the cytokines IL-12p70, TNF-α, and IFN-γ. However, the recruited monocyte population is converted to an anti-inflammatory phenotype in order to restrain excessive immune responses during infection of *T. gondii* strain RH (3–6, 12, 14, 21, 22). On the other hand, the time of infection for the change in microglial cells and inflammatory responses as a cause of CI of the brain infected with strain ME49 it is not well defined. Some studies have provided important clues to prevent excessive activation of macrophages after *T. gondii* infection (3, 14). For example, *Toxoplasma* rhoptry and dense granule proteins play roles in the modulation of pro-inflammatory responses

through the regulation in IFN-γ and NF-kB by GRA15 in addition to STAT3/6 activation by ROP16 (3, 14). ROP16 induces STAT1 tyrosine phosphorylation as well as *Socs1 via* STAT3 or 6 (23). As a result, the authors insisted that the infected hosts are able to induce a proper resistance against *T. gondii* infection as well as protection against excessive inflammatory immunity (3, 14, 23). However, these studies were limited by the failure to explain the promotion of immune modulation during *T. gondii* infection because the experiments employed Raw264.7, J447, DC2.4, or human foreskin fibroblast cells for *in vitro T. gondii* infection and *T. gondii*-infected peritoneal exudate cells for *in vivo* infection (3, 14). So, these studies do not reflect the entire infection process. On the contrary, the present study addressed the changes in the infection immunity during the CI stage. For example, the immune regulation for the control of parasitic proliferation without inducing harmful immunopathological events in the brain. Moreover, the present study provides some evidence of the immune regulation against *T. gondii* infection and protective immunity to prevent damage to host cells by an excessive inflammatory response.

The IFN-γ-mediated type 1 immune response with upregulation of the anti-parasitic factor NO is required to prevent the reactivation of *T. gondii* and TE in the brain (1). In the brain, microglia and infiltrating CD4 and CD8 T cells are the primary sources of IFN-γ, a cytokine leading noxious cellular effects in the CNS (1, 4). On the contrary, our earlier research also highlighted the importance of TGF-β in neuroprotection after *T. gondii* infection (8). In addition, the results of the present study suggest the importance of the interactions of various immunological factors between protective immunity and immunopathological effects by tracking of the immune response during the CI stage. First of all, changes in the immune response after *T. gondii* infection can be confirmed by microarray analysis of mRNA expression patterns, which can also predict the immunological phenotype. In the present study, there were increases in the mRNA levels of the T-cell exhaustion markers TIM3, LAG3, and KLRG1 without distinct increases in the mRNA levels of the T-cell differentiation markers TBX21, GATA3, FOXP3, and RORC during the AI stage, even though microglia activation was maintained in the M1-type. T-cell exhaustion markers are highly expressed by chronic antigen stimulation, but yet diminish the effector function of CD8 T cells (24). Accordingly, these results suggest that the inhibition of immune extension of adaptive T-cell immunity can accelerate neuronal cell death by expanding inflammatory cellular responses, although it is helpful for protective immunity of the host against *T. gondii* infection. Actually, pStat1, which is activated by IFN-γ and induces iNOS (25), was remarkably decreased at 6 weeks PI although the increase in IFN-γ expression was maintained for 12 weeks PI. Although IFN-γ-mediated activation of macrophages is critical for resistance against AI with *T. gondii*, *T. gondii* infection inhibits STAT1 transcriptional activity to allow the parasite to establish a CI (5, 23). Additionally, SOCS proteins, which can downregulate phosphorylation of JAK and STAT1, are actually induced by *T. gondii* infection (26). To understand the importance of microglia activation and further T-cell immune responses against *T. gondii* infection, transcript data of markers related to microglial cell polarization and T-cell-mediated adaptive immune responses were investigated. In particular, PD-L1 (B7-H1) was highly expressed in inflammatory macrophages, while PD-L2 (B7-DC) can be induced by alternative activation *via* IL-4 (27). Furthermore, PD-L1 might play a role in the downregulation of activated T cells and the expression of PD-L1 in a non-Stat1-dependent manner (27). Likewise, our results showed that PD-L1 expression was increased, as compared to PD-L2, at both transcript levels *in vivo* and *in vitro* ME-TLA stimulation (19.0–23.0- and 1.1–1.2-fold changes, respectively). At this time, M1-type activation of microglia and increases in the expression levels of the inflammatory cytokines IFN-γ, IL-12, and TNF-α were observed. However, these changes did not result in an increase in Stat-1 phosphorylation. This result provides a subtle balance for the control of parasitic proliferation and simultaneous inhibition of the increase in inflammatory cellular immune responses, which induce tissue damage during CI by altering the mRNA expression levels of PD-L1 and PD-1 because PD-1/PD-L1 interactions are required for the maturation of microglial cells and expansion of protective T-cell responses in *T. gondii* infection. However, excessive PD-1-mediated CD8 T-cell dysfunction plays a central role in immune tolerance, as well as *T. gondii* differentiation and reactivation (28–30). This is an important mechanism for the control of parasite expansion, even with the inhibition of iNOS, as in the present study.

The induction of iNOS, a M1-marker that leads to NO production, is generally elevated in the AI stage of *T. gondii* infection and in M1-like microglia (26, 31). Surprisingly, the results of the present showed that ME-TLA, a lysate antigen of *T. gondii* strain ME49, strongly induces the polarization of M1-type microglial cells and NO production. In other words, ME-TLA treatment of BV-2 microglial cells induced greater M1 polarization and NO production than treatment with IFN-γ. Simultaneously, urea production was decreased by treatment with the *T. gondii* antigens (RH and ME49) *in vitro*. TLA includes a variety of antigen pools, including TLR-based immune-triggering PAMPs (32). When soluble parasite TLA, as in the present study, stimulates dendritic cells and macrophages, the immune response resulted in TLR-signaling dependent production of IL-12 and NO (32). Accordingly, it is evident that the treatment of TLA as a PAMPs and parasite infection induce different immune triggering both *in vivo* and *in vitro*. To confirm this finding, NO production was compared between an *in vitro* infection model using *T. gondii* tachyzoites (strains RH and ME49) and an *in vitro* model using BV-2 microglial cell culture with TLA. As expected, the results were consistent with the *in vivo* infection study. NO production was decreased and mRNA expression levels of iNOS and COX-2 were lowered, while mRNA expression of Arg1 was increased by 2.9-fold. Based on these results, the authors insist that the host–parasite relationship in the regulation parasite control and host tissue damage by an excessive inflammatory response induces the control of effector molecules, which differs from the immune-triggering effect of TLA shown by the *in vitro* stimulation study. As a possible mechanism, increases in transcripts of SOCS and Arg1 during the CI stage are focused because of their immune regulatory functions.

Suppressor of cytokines signaling 1 protein is a known feedback inhibitor of IFN-γ receptor signaling and is induced directly by viable *T. gondii* parasites (26). In general, the SOCS proteins, especially SOCS1, are expressed by immune cells and cells of the CNS, and have the potential to impact immune processes within the CNS, including inflammatory cytokine and chemokine production, as well as activation of microglia (33). In this study, transcripts of SOCS1 were steadily expressed during the CI stage. It is known that SOCS induces a high Arg1:iNOS activity ratio and suppresses T-cell proliferation (34). Moreover, SOCS1 contributes to the inhibition of IFN-γ signaling and NO production without the dependency of TLR stimulation (35). In other words, due to upregulation of SOCS1 by IL-4-dependent M2 macrophage activation (34), the role of SOCS1 in the present study is sufficiently predictable for the direct increase in the Arg1:iNOS activity ratio, the decrease in transcripts of T-cell differentiation markers and Stat1 phosphorylation, and the increase in transcripts of T-cell exhaustion markers, suggesting modulations of the host–parasite relationship between parasite control and tissue damage in the brain.

Taken together, these results highlight the critical importance of M1-type microglia for the control of *T. gondii* as well as the limitation of STAT1 phosphorylation and the induction of SOCS1 to reduce detrimental inflammatory immune responses. Moreover, these results provide new insights into the characteristics of infection immunity through the host–parasite relationship during CI of *T. gondii*. In other words, *T. gondii* infection basically induces M1-type polarization of microglial cells, the limitation of IFN-γ-mediated inflammatory responses, including T-cell differentiation and Stat1 phosphorylation, and the reduction of iNOS/Arg1 ratio mediated by Socs1 induction. These phenomena are only expected by infection immunity due to the difference in the levels of effector molecules *via* the *in vitro* cellular response with TLA. In particular, this study revealed the characteristics of immune regulation in infection immunity by observing the persistent changes in the immune environment during a CI rather than at any one time.

ETHICS STATEMENT

This study protocol was approved by the Ethics Committee of Seoul National University and conducted in strict accordance with the Guidelines for Animal Experiments (SNUIBC-R110302-1). All surgeries were performed under anesthesia and all efforts were made to ensure minimal animal suffering.

AUTHOR CONTRIBUTIONS

YH and E-HS conceived and designed the experiments. J-HS and YH performed the experiments. J-HS, J-PY, and E-HS analyzed the data. B-KJ, SL, and E-HS contributed reagents/materials/analysis tools. E-HS wrote the paper.

FUNDING

This work was supported by the Basic Science Research Program of the National Research Foundation of Korea funded by the Ministry of Education, Science and Technology (grant no. NRF-2015R1D1A1A01058902) and the Seoul National University Bundang Hospital Research Fund (grant no. 02-2012-040).

REFERENCES

1. Wohlfert EA, Blader IJ, Wilson EH. Brains and Brawn: *Toxoplasma* infections of the central nervous system and skeletal muscle. *Trends Parasitol* (2017) 33:519–31. doi:10.1016/j.pt.2017.04.001
2. Mordue DG, Monroy F, La Regina M, Dinarello CA, Sibley LD. Acute toxoplasmosis leads to lethal overproduction of Th1 cytokines. *J Immunol* (2001) 167:4574–84. doi:10.4049/jimmunol.167.8.4574
3. Jensen KD, Wang Y, Wojno ED, Shastri AJ, Hu K, Cornel L, et al. *Toxoplasma* polymorphic effectors determine macrophage polarization and intestinal inflammation. *Cell Host Microbe* (2011) 9:472–83. doi:10.1016/j.chom.2011.04.015
4. Rozenfeld C, Martinez R, Seabra S, Sant'anna C, Goncalves JG, Bozza M, et al. *Toxoplasma gondii* prevents neuron degeneration by interferon-gamma-activated microglia in a mechanism involving inhibition of inducible nitric oxide synthase and transforming growth factor-beta1 production by infected microglia. *Am J Pathol* (2005) 167:1021–31. doi:10.1016/S0002-9440(10)61191-1
5. Suzuki Y. Host resistance in the brain against *Toxoplasma gondii*. *J Infect Dis* (2002) 185(Suppl 1):S58–65. doi:10.1086/337999
6. Jankovic D, Kugler DG, Sher A. IL-10 production by CD4+ effector T cells: a mechanism for self-regulation. *Mucosal Immunol* (2010) 3:239–46. doi:10.1038/mi.2010.8
7. Sarciron ME, Gherardi A. Cytokines involved in Toxoplasmic encephalitis. *Scand J Immunol* (2000) 52:534–43. doi:10.1046/j.1365-3083.2000.00817.x
8. Jung BK, Pyo KH, Shin KY, Hwang YS, Lim H, Lee SJ, et al. *Toxoplasma gondii* infection in the brain inhibits neuronal degeneration and learning and memory impairments in a murine model of Alzheimer's disease. *PLoS One* (2012) 7:e33312. doi:10.1371/journal.pone.0033312
9. Orihuela R, McPherson CA, Harry GJ. Microglial M1/M2 polarization and metabolic states. *Br J Pharmacol* (2016) 173:649–65. doi:10.1111/bph.13139
10. Nguyen TD, Bigaignon G, Van Broeck J, Vercammen M, Nguyen TN, Delmee M, et al. Acute and chronic phases of *Toxoplasma gondii* infection in mice modulate the host immune responses. *Infect Immun* (1998) 66:2991–5.
11. Hester J, Mullins J, Sa Q, Payne L, Mercier C, Cesbron-Delauw MF, et al. *Toxoplasma gondii* antigens recognized by IgG antibodies differ between mice with and without active proliferation of tachyzoites in the brain during the chronic stage of infection. *Infect Immun* (2012) 80:3611–20. doi:10.1128/IAI.00604-12
12. El Kasmi KC, Qualls JE, Pesce JT, Smith AM, Thompson RW, Henao-Tamayo M, et al. Toll-like receptor-induced arginase 1 in macrophages thwarts effective immunity against intracellular pathogens. *Nat Immunol* (2008) 9:1399–406. doi:10.1038/ni.1671
13. Guillemin GJ, Brew BJ. Microglia, macrophages, perivascular macrophages, and pericytes: a review of function and identification. *J Leukoc Biol* (2004) 75:388–97. doi:10.1189/jlb.0303114
14. Rosowski EE, Lu D, Julien L, Rodda L, Gaiser RA, Jensen KD, et al. Strain-specific activation of the NF-kappaB pathway by GRA15, a novel *Toxoplasma gondii* dense granule protein. *J Exp Med* (2011) 208:195–212. doi:10.1084/jem.20100717
15. Harris TH, Wilson EH, Tait ED, Buckley M, Shapira S, Caamano J, et al. NF-kappaB1 contributes to T cell-mediated control of *Toxoplasma gondii* in the CNS. *J Neuroimmunol* (2010) 222:19–28. doi:10.1016/j.jneuroim.2009.12.009
16. Rozenfeld C, Martinez R, Figueiredo RT, Bozza MT, Lima FR, Pires AL, et al. Soluble factors released by *Toxoplasma gondii*-infected astrocytes down-modulate nitric oxide production by gamma interferon-activated

microglia and prevent neuronal degeneration. *Infect Immun* (2003) 71:2047–57. doi:10.1128/IAI.71.4.2047-2057.2003
17. Tait ED, Hunter CA. Advances in understanding immunity to *Toxoplasma gondii*. *Mem Inst Oswaldo Cruz* (2009) 104:201–10. doi:10.1590/S0074-02762009000200013
18. Christian DA, Koshy AA, Reuter MA, Betts MR, Boothroyd JC, Hunter CA. Use of transgenic parasites and host reporters to dissect events that promote interleukin-12 production during toxoplasmosis. *Infect Immun* (2014) 82:4056–67. doi:10.1128/IAI.01643-14
19. Lu F, Huang S, Kasper LH. Interleukin-10 and pathogenesis of murine ocular toxoplasmosis. *Infect Immun* (2003) 71:7159–63. doi:10.1128/IAI.71.12.7159-7163.2003
20. Kamerkar S, Davis PH. *Toxoplasma* on the brain: understanding host-pathogen interactions in chronic CNS infection. *J Parasitol Res* (2012) 2012:589295. doi:10.1155/2012/589295
21. Pyo KH, Jung BK, Xin CF, Lee YW, Chai JY, Shin EH. Prominent IL-12 production and tumor reduction in athymic nude mice after *Toxoplasma gondii* lysate antigen treatment. *Korean J Parasitol* (2014) 52:605–12. doi:10.3347/kjp.2014.52.6.605
22. Pyo KH, Lee YW, Lim SM, Shin EH. Immune adjuvant effect of a *Toxoplasma gondii* profilin-like protein in autologous whole-tumor-cell vaccination in mice. *Oncotarget* (2016) 7:74107–19. doi:10.18632/oncotarget.12316
23. Rosowski EE, Saeij JP. *Toxoplasma gondii* clonal strains all inhibit STAT1 transcriptional activity but polymorphic effectors differentially modulate IFNgamma induced gene expression and STAT1 phosphorylation. *PLoS One* (2012) 7:e51448. doi:10.1371/journal.pone.0051448
24. Legat A, Speiser DE, Pircher H, Zehn D, Fuertes Marraco SA. Inhibitory receptor expression depends more dominantly on differentiation and activation than "exhaustion" of human CD8 T cells. *Front Immunol* (2013) 4:455. doi:10.3389/fimmu.2013.00455
25. Gavrilescu LC, Butcher BA, Del Rio L, Taylor GA, Denkers EY. STAT1 is essential for antimicrobial effector function but dispensable for gamma interferon production during *Toxoplasma gondii* infection. *Infect Immun* (2004) 72:1257–64. doi:10.1128/IAI.72.3.1257-1264.2004
26. Zimmermann S, Murray PJ, Heeg K, Dalpke AH. Induction of suppressor of cytokine signaling-1 by *Toxoplasma gondii* contributes to immune evasion in macrophages by blocking IFN-gamma signaling. *J Immunol* (2006) 176:1840–7. doi:10.4049/jimmunol.176.3.1840
27. Loke P, Allison JP. PD-L1 and PD-L2 are differentially regulated by Th1 and Th2 cells. *Proc Natl Acad Sci U S A* (2003) 100:5336–41. doi:10.1073/pnas.0931259100
28. Bhadra R, Gigley JP, Weiss LM, Khan IA. Control of *Toxoplasma* reactivation by rescue of dysfunctional CD8+ T-cell response via PD-1-PDL-1 blockade. *Proc Natl Acad Sci U S A* (2011) 108:9196–201. doi:10.1073/pnas.1015298108
29. McBerry C, Dias A, Shryock N, Lampe K, Gutierrez FR, Boon L, et al. PD-1 modulates steady-state and infection-induced IL-10 production in vivo. *Eur J Immunol* (2014) 44:469–79. doi:10.1002/eji.201343658
30. Bhadra R, Gigley JP, Khan IA. PD-1-mediated attrition of polyfunctional memory CD8+ T cells in chronic toxoplasma infection. *J Infect Dis* (2012) 206:125–34. doi:10.1093/infdis/jis304
31. Lan X, Han X, Li Q, Yang QW, Wang J. Modulators of microglial activation and polarization after intracerebral haemorrhage. *Nat Rev Neurol* (2017) 13:420–33. doi:10.1038/nrneurol.2017.69
32. Denkers EY. From cells to signaling cascades: manipulation of innate immunity by *Toxoplasma gondii*. *FEMS Immunol Med Microbiol* (2003) 39:193–203. doi:10.1016/S0928-8244(03)00279-7
33. Baker BJ, Akhtar LN, Benveniste EN. SOCS1 and SOCS3 in the control of CNS immunity. *Trends Immunol* (2009) 30:392–400. doi:10.1016/j.it.2009.07.001
34. Whyte CS, Bishop ET, Ruckerl D, Gaspar-Pereira S, Barker RN, Allen JE, et al. Suppressor of cytokine signaling (SOCS)1 is a key determinant of differential macrophage activation and function. *J Leukoc Biol* (2011) 90:845–54. doi:10.1189/jlb.1110644
35. Stutz A, Kessler H, Kaschel ME, Meissner M, Dalpke AH. Cell invasion and strain dependent induction of suppressor of cytokine signaling-1 by *Toxoplasma gondii*. *Immunobiology* (2012) 217:28–36. doi:10.1016/j.imbio.2011.08.008

Conflict of Interest Statement: The authors declare that the research was conducted in the absence of any commercial or financial relationships that could be construed as a potential conflict of interest.

frontiers in Immunology

ORIGINAL RESEARCH
published: 05 February 2018
doi: 10.3389/fimmu.2018.00061

Genome-Wide Bimolecular Fluorescence Complementation-Based Proteomic Analysis of *Toxoplasma gondii* ROP18's Human Interactome Shows Its Key Role in Regulation of Cell Immunity and Apoptosis

*Jing Xia[1], Ling Kong[1†], Li-Juan Zhou[1†], Shui-Zhen Wu[1†], Li-Jie Yao[1†], Cheng He[1], Cynthia Y. He[2] and Hong-Juan Peng[1]**

[1] Department of Pathogen Biology, Guangdong Provincial Key Laboratory of Tropical Disease Research, School of Public Health, Southern Medical University, Guangzhou, China, [2] Department of Biological Sciences, National University of Singapore, Singapore, Singapore

OPEN ACCESS

Edited by:
Xun Suo,
China Agricultural University, China

Reviewed by:
Tiago W. P. Mineo,
Federal University of Uberlandia, Brazil
Wai-Hong Tham,
Walter and Eliza Hall Institute of Medical Research, Australia
Dirk Schlüter,
Otto-von-Guericke-Universität Magdeburg, Germany

***Correspondence:**
Hong-Juan Peng
hongjuan@smu.edu.cn

†These authors have contributed equally to this work.

Specialty section:
This article was submitted to Microbial Immunology, a section of the journal Frontiers in Immunology

Received: 22 October 2017
Accepted: 10 January 2018
Published: 05 February 2018

Citation:
Xia J, Kong L, Zhou L-J, Wu S-Z, Yao L-J, He C, He CY and Peng H-J (2018) Genome-Wide Bimolecular Fluorescence Complementation-Based Proteomic Analysis of Toxoplasma gondii ROP18's Human Interactome Shows Its Key Role in Regulation of Cell Immunity and Apoptosis. Front. Immunol. 9:61. doi: 10.3389/fimmu.2018.00061

Toxoplasma gondii rhoptry protein ROP18 (*Tg*ROP18) is a key virulence factor secreted into the host cell during invasion, where it modulates the host cell response by interacting with its host targets. However, only a few *Tg*ROP18 targets have been identified. In this study, we applied a high-throughput protein–protein interaction (PPI) screening in human cells using bimolecular fluorescence complementation (BiFC) to identify the targets of Type I strain ROP18 ($ROP18_I$) and Type II strain ROP18 ($ROP18_{II}$). From a pool of more than 18,000 human proteins, 492 and 141 proteins were identified as the targets of $ROP18_I$ and $ROP18_{II}$, respectively. Gene ontology, search tool for the retrieval of interacting genes/proteins PPI network, and Ingenuity pathway analyses revealed that the majority of these proteins were associated with immune response and apoptosis. This indicates a key role of *Tg*ROP18 in manipulating host's immunity and cell apoptosis, which might contribute to the immune escape and successful parasitism of the parasite. Among the proteins identified, the immunity-related proteins N-myc and STAT interactor, IL20RB, IL21, ubiquitin C, and vimentin and the apoptosis-related protein P2RX1 were further verified as $ROP18_I$ targets by sensitized emission-fluorescence resonance energy transfer (SE-FRET) and co-immunoprecipitation. Our study substantially contributes to the current limited knowledge on human targets of *Tg*ROP18 and provides a novel tool to investigate the function of parasite effectors in human cells.

Keywords: *Toxoplasma gondii*, ROP18, human interactome, bimolecular fluorescence complementation, genome-wide

INTRODUCTION

Toxoplasma gondii is an obligate intracellular protozoon that causes zoonotic toxoplasmosis. It is estimated that one third of the world's population is chronically infected with this parasite (1). *T. gondii* belongs to the phylum of Apicomplexa, characterized by the presence of an apical complex containing secretory organelles, including rhoptries, micronemes, and dense granules (2). Rhoptry

discharges a family of proteins termed rhoptry proteins (ROPs) that are of importance for host cell invasion, intracellular survival, and interference with host functions (3, 4).

T. gondii isolates collected from North America and Europe primarily fall into one of the three distinct clonal lineages, types I, II, and III (5), which present a number of different phenotypes, such as growth, migration, and transmigration (6). The best characterized phenotype is their virulence in laboratory mice (7, 8): Type I strains exhibit acute lethal virulence [lethal dose (LD_{100}) ≈ 1], whereas types II and III strains are much less virulent [median $LD_{50} \geq 10^5$] (9, 10). According to previous forward genetic mapping studies, in which Types I, II, or III were intercrossed to identify the virulence determinant genes, the highly polymorphic *rop18* gene was identified as a key virulence determinant (11, 12). *Tg*ROP18 is a serine/threonine kinase secreted from the rhoptry into the parasitophorous vacuole membrane (PVM) and host cytosol during parasite invasion (13), of which the Type I strain ($ROP18_I$) (RH strain, GenBank accession NO: AFO54817.1) and the Type II strain ($ROP18_{II}$) (ME49, GenBank accession NO: XP_002367757.1) are different at 28 amino acid sites.

In murine cells, $ROP18_I$ can target and inactivate the immunity-related GTPases (IRGs) Irga6 and Irgb6 by phosphorylating a critical threonine residue in the switch loop 1 of the IRGs, thereby disrupting their accumulation on the PVM and protecting the parasites from destruction (14, 15). Although the precise molecular functions of *Tg*ROP18 in human cells remain obscure, it is known that it regulates parasite's multiplication in human cells and host cell apoptosis. It has been reported that a Type III strain (CEP) expressing $ROP18_I$ showed a dramatic increase in replication rate in human foreskin fibroblasts (HFFs) in comparison to the wild-type CEP strain without *Tg*ROP18 expression (13). It has also been shown that $ROP18_I$ inhibits cell apoptosis *via* the mitochondrial apoptosis pathway in human embryonic kidney 293 T cells (16). *Tg*ROP18 exerts its regulation on some important host cell signaling by interacting with its host targets. For instance, $ROP18_I$ phosphorylates and mediates the degradation of the host endoplasmic reticulum (c)-bound transcription factor ATF6β, which is expressed in both human and murine cells, resulting in compromised $CD8^+$ T cell-mediated host defense against *T. gondii* infection (17). $ROP18_I$ has also been shown to associate with p65, a member of the human NF-κB family of transcription factors, and targets this protein for ubiquitin-dependent degradation to suppress the human NF-κB pathway (18). Despite the important roles of the virulence factor *Tg*ROP18 in disrupting host cell functions and preserving survival of parasites in human cells, only a few binding partners of $ROP18_I$ have been determined, and the complex regulatory network of protein–protein interactions (PPIs) between $ROP18_I$ and host cell proteins remains to be elucidated. Moreover, very little is known regarding the host targets of $ROP18_{II}$, even though it is functionally expressed in Type II strains and is capable of conferring virulence to a Type III strain (11, 19).

A previous study has identified eight *Tg*ROP18-interacting proteins with a yeast two-hybrid (YTH) system (20). However, YTH generates a high occurrence of false positives and requires that the interacting proteins accumulate in the yeast nucleus (21). More recently, by using a protein array approach, Yang et al. have identified 68 substrates of the *Tg*ROP18 kinase, and four of them have been validated as the host targets (22). Although protein array is useful for comprehensive screens of protein functions, it requires pure functional proteins that are difficult to obtain because of the difficulties in expressing the proteins in a soluble form with correct folding (23). The bimolecular fluorescence complementation (BiFC) technique has been proven to be a useful and efficient tool to study PPIs. The BiFC assay is based on the principle that two non-fluorescent fragments [e.g., amino-yellow fluorescence protein, NYFP, or carboxyl-yellow fluorescence protein, C-terminal fragment of YFP (CYFP)] of a fluorescent reporter protein (e.g., yellow fluorescence protein, YFP) can refold together and reconstitute the functional fluorescent entity when they are in close proximity, for example by fusing to a pair of interacting proteins (**Figure 1A**) (24). Thus, the fluorescence intensity is proportional to the amount of formed dimer and can be detected by microscopy or flow cytometry (25). Here, we applied a high-throughput PPI screening based on BiFC (HT-BiFC) combined with a Gateway cloning system (26) to identify the potential *Tg*ROP18 ($ROP18_I$ and $ROP18_{II}$) interaction partners within a human ORFeome library containing more than 18,000 human cDNA clones (27). This screening helped us gain insights into the biological functions of *Tg*ROP18 in human cells.

MATERIALS AND METHODS

Parasites and Cell Lines

The RH and PRU strains of *T. gondii* were maintained by serial passage in HFFs, as described previously (28). The HFFs (#ATCC SCRC-1041), Phoenix (#ATCC CRL-3213), and COS-7 (#ATCC CRL-1651) cell lines were purchased from the American Type Culture Collection (Manassas, VA, USA). The HTC75 cell line was kindly provided by Professor Wenbin Ma (Sun Yat-Sen University, Guangzhou, China). Parasites and cells were cultured in Dulbecco's Modified Eagle Medium (DMEM, Gibco, #11995065) supplemented with 10% fetal bovine serum (Gibco, #16000044) and 1% penicillin/streptomycin (Gibco, #15070063) at 37°C in a 5% CO_2 incubator.

Antibodies

Anti-NMI rabbit monoclonal antibody (#183724) was obtained from Abcam (Cambridge, MA, USA). Anti-FLAG mouse monoclonal antibody (#AE005) was obtained from Abclonal (Woburn, MA, USA). Anti-HA rabbit monoclonal (#3724) and anti-β-Actin rabbit monoclonal (#4970) antibodies were obtained from Cell Signaling Technology (Danvers, MA, USA). Normal rabbit control IgG (#AB-105-C) was obtained from R&D Systems (Minneapolis, MN, USA). Anti-P2RX1 goat polyclonal (#sc-31491) and normal goat IgG (#sc-2028) antibodies were obtained from Santa Cruz Biotechnology (Dallas, TX, USA). Normal mouse IgG (#12-371) was obtained from Sigma-Aldrich (Billerica, MA, USA). Mono- and polyubiquitinylated conjugates monoclonal (FK2) antibody (#BML-PW8810) was obtained from Enzo Life Sciences (Farmingdale, NY, USA).

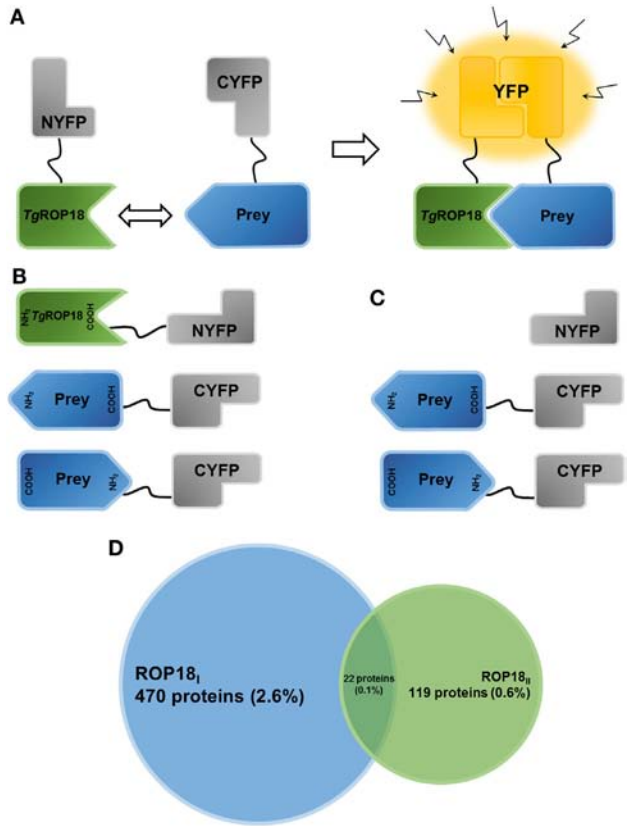

FIGURE 1 | Establishment of the HT-BiFC screening system and *Tg*ROP18-interacting proteins. **(A)** Principle of the bimolecular fluorescence complementation (BiFC) assay. The non-fluorescent fragments of a fluorescent reporter protein are fused with the proteins of interest and expressed in human cells. If the interaction between the proteins of interest takes place, the split fragments will be pulled close enough to refold together and reconstitute the functional fluorescent entity. **(B)** Schematic representation illustrating the *Tg*ROP18/prey BiFC constructs generated in the present study. *Tg*ROP18 is fused with the N-terminal fragment of YFP (NYFP) at the C-terminus, and the prey protein is tethered with the C-terminal fragment of YFP (CYFP) at either the N- or C-terminus. **(C)** Schematic representation illustrating the control screening. Non-fused NYFP is mated with each CYFP-prey/prey-CYFP constructs. **(D)** Venn diagram depicting the number (percentage) of $ROP18_I$-specific targets (blue), $ROP18_{II}$-specific targets (green), and $ROP18_I$/$ROP18_{II}$ targets (in the middle).

Plasmid Construction

Total RNA of *T. gondii* RH and PRU tachyzoites was extracted using the RNeasy Plus Mini Kit (#74034, Qiagen, Germantown, MD, USA) following manufacturer's instructions. The cDNA fragments of $ROP18_I$ (ToxoDB #TGGT1_205250) and $ROP18_{II}$ (ToxoDB #TGME49_205250) were amplified by RT-PCR from the total RNA of the RH and PRU tachyzoites with the forward primer 5′-ATAGCGGCCGCAATGTTTTCGGTACAGCG-3′ and the reverse primer 5′-GGCGCGCCCTTCTGTGTGGAGATG-3′. The cDNAs of $ROP18_I$ and $ROP18_{II}$ were then fused with the N-terminal fragment (residues 1–155) of yellow fluorescent protein (NYFP) at the C-terminus to construct the bait vectors, pBabe-CMV-$ROP18_I$-NYFP-neo and pBabe-CMV-$ROP18_{II}$-NYFP-neo, respectively (**Figure 1B**). The cDNAs of N-myc and STAT interactor (NMI), interleukin 20 receptor-β (IL20RB), purinergic receptor P2X1 (P2RX1), interleukin 21 (IL21), ubiquitin C (UBC), and vimentin were individually amplified by PCR from the human ORFeome v3.1 (Open Biosystems) and subcloned into pcDNA3.1 for eukaryotic expression, or into pEYFP-C1 for expression fused with enhanced yellow fluorescent protein. In addition, $ROP18_I$ and $ROP18_{II}$ cDNAs were, respectively, subcloned into pcDNA3.1 for eukaryotic expression, and into pECFP-N1 for expression fused with enhanced cyan fluorescent protein. All constructs were verified by DNA sequencing.

HT-BiFC Assay

The HT-BiFC screening was conducted by Longjie Biotechnology Co., Ltd. (Foshan, Guangdong, China). Bait vectors were transfected into the packaging cell lines, Phoenix cells, to generate the retrovirus, and the harvested retroviruses were used to infect HTC75 cells. Stable bait cell lines expressing $ROP18_I$-NYFP or $ROP18_{II}$-NYFP were obtained after 10 days of selection with 300 μg/mL G418. Meanwhile, a pool of prey vectors were constructed from the human ORFeome v7.1 library, containing 18,414 human open reading frames (ORFs), using the Gateway recombination system. At the end of the process, 17,076 colonies with a coverage of 93% of all human ORFs were successfully obtained (27). The prey collections were tethered to the C-terminal fragment (residues 156–239) of YFP (CYFP) at either the N- or C-terminus (pCL-CMV-prey-CYFP-puro and pCL-CMV-CYFP-prey-puro) (**Figure 1B**). CYFP-tagged prey retroviruses were produced as mentioned above and used to infect the stable NYFP tagged $ROP18_I$ (or $ROP18_{II}$) bait cells. Two days after infection, the infected cells were subjected to 5–10 days of selection with 1 μg/mL puromycin to obtain the stable cell lines co-expressing NYFP-tagged $ROP18_I$ (or $ROP18_{II}$) and CYFP-tagged prey. All procedures were performed in 96-well plates, using the Biomek 3000 Laboratory Automation Workstation (Beckman Coulter, Brea, CA, USA). The resulting diploid cells were then harvested, and the fluorescent cells were sorted out using the LSRII flow cytometer equipped with a high-throughput sampler (BD Biosciences, San Jose, CA, USA), along with the HTC75 cells infected with only CYFP-EV retroviruses as the negative control group. The positive fluorescent cells were harvested and subjected to another round of sorting until the desired positive rate (more than 90%) was reached (Figure S1 in Supplementary Material). mRNAs of the final positive cells were extracted and reverse-transcribed into cDNA by RT-PCR amplification and were then identified through Illumina/Solexa sequencing (29).

To determine the false-positive BiFC signals resulting from the self-assembly of the two YFP fragments, a control screening was performed, in which a stable bait cell line was generated to express NYFP without fusion to $ROP18_I$ or $ROP18_{II}$. The expressed NYFP was then mated with each CYFP-prey/prey-CYFP in the prey library (**Figure 1C**). The Original Total Reads of each prey was calculated through the high-throughput sequencing analysis of the whole prey library, and the NYFP Total Reads were calculated through the sequencing analysis of the positive cells obtained

from the control screening. A Bias Ratio was then defined as the tendency of the NYFP fragment to associate with the CYFP-prey/prey-CYFP, by comparing the NYFP Total Reads to the Original Total Reads for each prey. The higher the Bias Ratio, the higher risk of identifying the prey as a positive signal. The preys with a Bias Ratio of more than 1% were regarded as false-positives and discarded.

SE-FRET Assay

The day before transfection, a total of 1×10^5 COS-7 cells were seeded in each well of a 12-well plate with 1 mL DMEM growth medium (no antibiotics). When the cells were about 60% to 80% confluent, 1 μg of pEYFPC1-NMI (pEYFPC1-IL20RB, pEYFPC1-P2RX1, pEYFPC1-IL21, pEYFPC1-UBC, or pEYFPC1-vimentin) and/or 1 μg of pECFPN1-ROP18$_I$ plasmids were transfected into COS-7 cells for the experimental groups, using Lipofectamine 2000 transfection reagent (#11668-019, Invitrogen, Waltham, MA, USA). For the negative control group, pECFPN1 and pEYFPC1 empty vectors were transfected into the cells, while for the positive control group, pECFPN1-EYFP was transfected into the cells. At 6 h post-transfection, the medium was replaced with fresh complete growth medium.

For the SE-FRET assay, prior to the testing of co-transfection samples, the images of the donor (CFP-ROP18$_I$ only) and acceptor (YFP-prey only) channels were collected to determine the spectral bleed-through. The images of the donor, acceptor, and FRET channels were simultaneously collected for selection of the region of interest during detection of the samples co-transfected with CFP-ROP18$_I$ and YFP-prey. The adjusted fluorescence density was obtained by subtraction of the background light density from the fluorescence density of the protein signal. The fluorescence signal, FRET efficiency, and distance between donor and acceptor were analyzed and calculated using the Olympus FluoView FV1000 viewer software (Olympus, Tokyo, Japan).

Co-immunoprecipitation (Co-IP) Assay

COS-7 cells overexpressing ROP18$_I$ and/or NMI (IL20RB, P2RX1, IL21, or vimentin) were prepared as mentioned previously in the FRET assay. Cell extracts were prepared by lysing the cells in cell lysis buffer (#P0013, Beyotime, Shanghai, China) with 1 mM phenylmethanesulfonyl fluoride (#WB-0181, Beijing Dingguo Changsheng Biotechnology, Beijing, China). Cell lysates were incubated with the primary antibody (anti-NMI rabbit monoclonal antibody anti-HA rabbit monoclonal antibody, anti-P2RX1 goat polyclonal antibody, or anti-FLAG mouse monoclonal antibody) with gentle rotation for 1 h at 4°C. Protein A-Agarose (#sc-2001, Santa Cruz Biotechnology, Santa Cruz, CA, USA) was then added to the immunoprecipitation reaction with incubation overnight at 4°C. The immunoprecipitates were washed four times with phosphate-buffered saline and then eluted by boiling with SDS-PAGE loading buffer (#9173, TAKARA, Kusatsu, Japan). The eluates were analyzed by western blotting with the indicated antibodies, as described previously (28). For the UBC experiment, cells were treated with 10 μM proteasome inhibitor MG132 (#S1748, Beyotime, Shanghai, China) for 12 h before harvesting.

Data Analysis

Each protein sequence and functional information was obtained from the UniProt Database (http://www.uniprot.org/). To further define the biological functions of the *Tg*ROP18 interactome, the *Tg*ROP18-interacting proteins were analyzed using DAVID Bioinformatics Resources 6.8 (30, 31) for gene ontology (GO) annotation and enrichment analysis. Pathway analyses were done using Ingenuity Pathway Analysis (IPA, Ingenuity® Systems, www.ingenuity.com) by importing the Entrez GeneID of the *Tg*ROP18-interacting proteins into online servers. Additionally, a combination of the search tool for the retrieval of interacting genes/proteins (STRING) version 10.0 database (32) and Cytoscape version 3.4.0 (33) was used to explore and build the PPI network. Statistical analysis data are presented as mean ± SD. Student's *t*-test was utilized for statistical analysis to evaluate the significant difference between different groups using IBM SPSS Statistics 20.0 (34). Statistical significance was accepted if $p < 0.05$.

RESULTS

Characterization of the *Tg*ROP18 Interactome

After multiple rounds of flow cytometric sorting, the final positive sorting rate of the HTC75 cells co-expressing ROP18$_I$-NYFP and CYFP-tagged prey and the HTC75 cells co-expressing ROP18$_{II}$-NYFP and CYFP-tagged prey were 93.2 and 98.6%, respectively (Figure S1 in Supplementary Material). After background noises in sequencing were filtered out using a cutoff value of five in total reads, 492 ROP18$_I$ (2.88%) and 141 ROP18$_{II}$ (0.83%) interacting proteins were identified, compared to control cells (**Figure 1D**). Tables S1 and S2 in Supplementary Material present the list of ROP18$_I$- and ROP18$_{II}$-interacting proteins with their total reads, respectively. Based on the specificity of the interaction, we classified the interacting proteins into three groups: A. 470 ROP18$_I$-specific targets; B. 119 ROP18$_{II}$-specific targets; and C. 22 targets for both ROP18$_I$ and ROP18$_{II}$ (**Figure 1D**). Regarding the ROP18$_I$ specific targets, many were ribosomal proteins (e.g., RPL23, RPL11, RPL37A, RPS14, and RPS6), GTPases (e.g., SAR1B, ARL17B, and RND2), and receptors (e.g., PTPRF, FPR1, IL9R, IL20RB, and KLRD1), whereas for the ROP18$_{II}$ specific targets, many were transmembrane proteins (e.g., TM4SF20, CMTM3, TMEM147, and TMBIM4) and zinc finger proteins (e.g., ZNF232, ZSCAN2, ZSCAN32, and ZNF273). Interestingly, we found that some humoral regulating factors (e.g., UTS2, CST2, and DEFB129) and some enzymes (e.g., DEGS1 and TPO) were targeted by both ROP18$_I$ and ROP18$_{II}$.

Among the ROP18$_I$-interacting proteins, CNBP, DCTD, NUP160, and PRAC, which had been previously confirmed as ROP18$_I$-interacting proteins by a previous human proteome array (22), were also identified in our HT-BiFC assay, indicating the reliability and quality of our results. In addition to these known interactions, 488 interactions of ROP18$_I$ with human proteins were newly defined in our study. Notably, to our knowledge, our findings provided the first report of ROP18$_{II}$-interacting proteins in human cells and specifically identified 141 ROP18$_{II}$-interacting human proteins.

Validation of the *Tg*ROP18-Interacting Proteins

To further validate the interactions identified by the HT-BiFC assay, six ROP18$_I$-interacting proteins (NMI, IL20RB, P2RX1, IL21, UBC, and vimentin) with a broad range of total reads (169793, 30861, 25144, 2214, 116, and 6, respectively) were selected for two independent assays, the SE-FRET assay and the Co-IP assay.

In the SE-FRET assay (**Figure 2A**), the donor and acceptor channels show the co-localizations of ROP18$_I$ with NMI, IL20RB, P2RX1, IL21, or UBC in the cytoplasm, suggesting the potential PPIs and their cytoplasmic localization. In addition, positive FRET signals were observed in the positive control cells and the COS-7 cells co-expressing ROP18$_I$ and NMI, IL20RB, P2RX1, IL21, or UBC (**Figure 2A**), yielding significantly higher FRET efficiency and less intermolecular distance than negative control cells ($p < 0.05$, see **Figure 2B**). The SE-FRET results of ROP18$_I$ and vimentin have been published recently in a study from our laboratory (35). These findings demonstrate the stable interactions of ROP18$_I$ with NMI, IL20RB, P2RX1, IL21, UBC, and vimentin in the cytoplasm and are consistent with the HT-BiFC results, despite slight differences between the FRET efficiency values and total reads.

The interactions were also confirmed by our three replicates of Co-IP assays (**Figure 3**). The results show that in the dually transfected cells, ROP18$_I$ could be readily detected in the immunoprecipitates by using the specific antibodies anti-NMI, HA, P2RX1, and FLAG, but not with the control IgG. The Co-IP result of ROP18$_I$ and vimentin has been published recently in a study from our laboratory (35). These results confirmed the consistency between the two assays, suggesting the robustness and reliability of the HT-BiFC results.

Bioinformatic Analysis of the *Tg*ROP18-Interacting Proteins

To obtain a comprehensive view of the *Tg*ROP18 interactome, we performed a GO analysis to identify significantly enriched functional terms of *Tg*ROP18-interacting proteins. The top

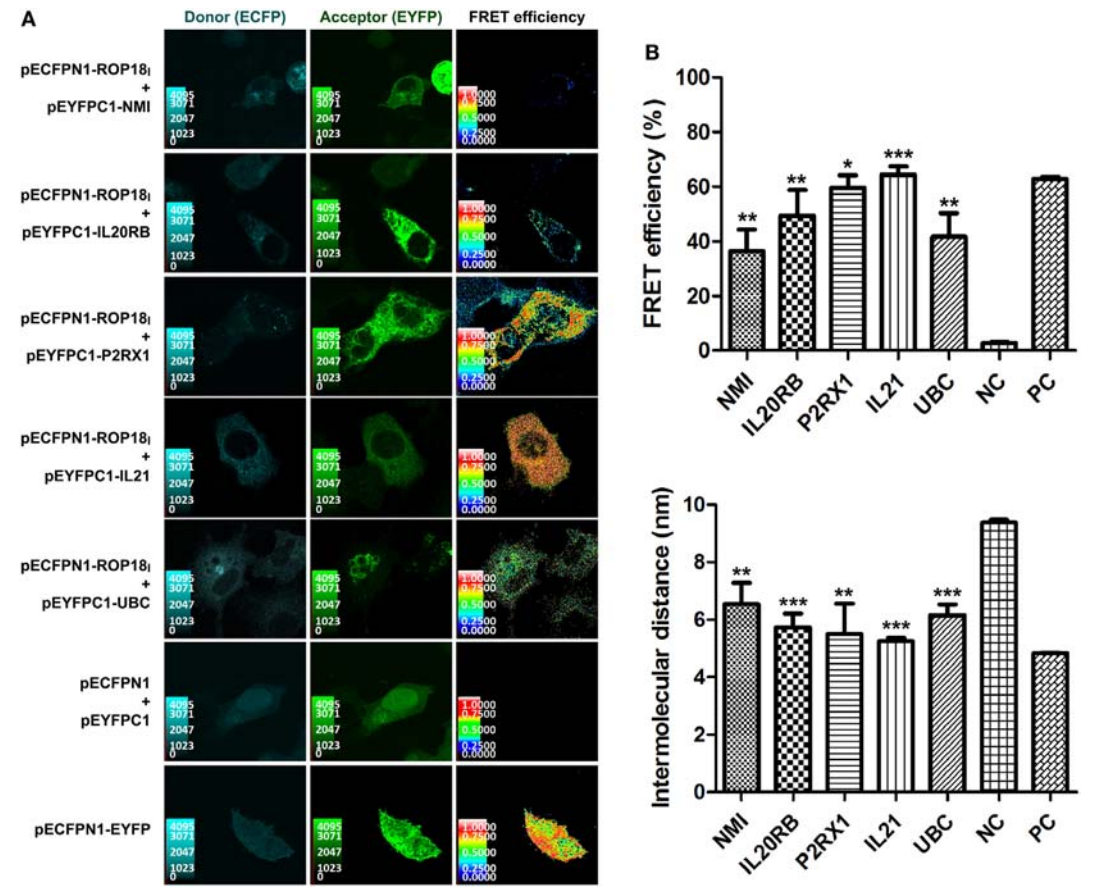

FIGURE 2 | Validation of the *Tg*ROP18-interacting proteins by SE-FRET assay. **(A)** Co-localization and FRET interaction of ROP18$_I$ with NMI, IL20RB, P2RX1, IL21, and UBC. Localization and co-localization of ROP18$_I$ and the five indicated candidates are shown in the donor channel (column 1) and the acceptor channel (column 2), respectively. The FRET efficiency is shown in column 3, in which a thermal pseudo color-matched FRET signal intensity scale is indicated for each image. **(B)** Quantitative analysis of FRET efficiency and intermolecular distance between ROP18$_I$ and the five indicated candidates. Error bars represent the means ± SD of triplicates. Student's *t*-tests results are between the six experimental groups and NC, $^*p < 0.05$; $^{**}p < 0.01$; $^{***}p < 0.001$. Abbreviations: NC, negative control; PC, positive control.

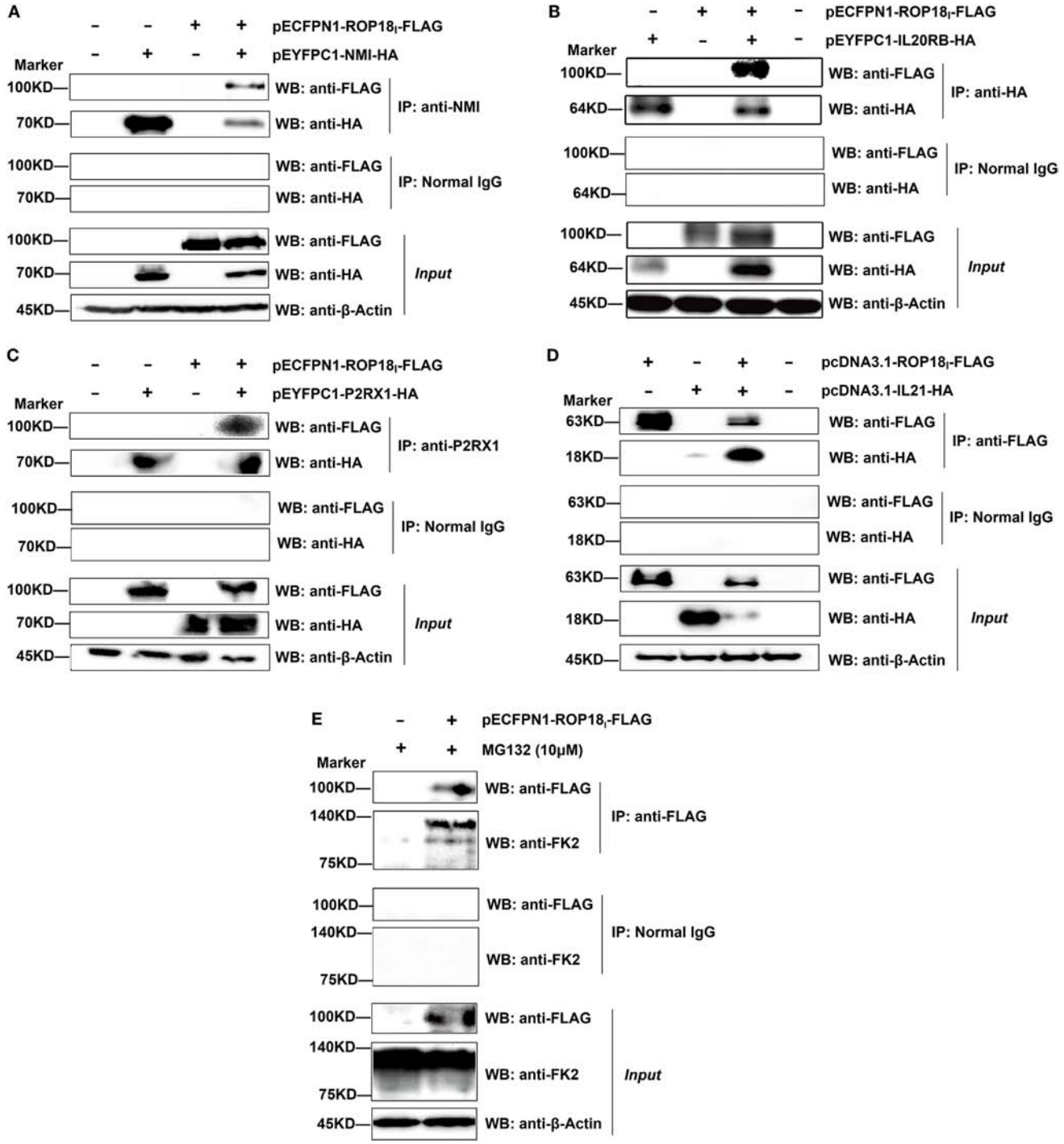

FIGURE 3 | Validation of the *Tg*ROP18-interacting proteins by co-immunoprecipitation (Co-IP) assay. **(A–D)** Lysates of COS-7 cells co-overexpressing $ROP18_I$ and the indicated interacting proteins were immunoprecipitated with the indicated antibodies. Rabbit, mouse, or goat normal control IgG were used as negative controls. The immunoprecipitates were detected by SDS-PAGE and western blotting using the antibodies indicated. **(E)** Lysates of COS-7 cells overexpressing $ROP18_I$ in the presence of MG132 (10 μM) for 12 h were immunoprecipitated with the anti-FLAG antibody. Endogenous UBC (a smear of bands) was detected in the immunoprecipitates through western blotting with anti-FK2 antibody, which recognizes mono- and polyubiquitinylated conjugates.

five enriched terms within the "Biological Process" ontology category, together with their protein counts and *p*-values, are shown in **Figure 4**. The results reveal that both $ROP18_I$ and $ROP18_{II}$-interacting proteins were significantly enriched in a variety of biological processes ($p < 0.05$). As expected, $ROP18_I$-interacting proteins were significantly overrepresented in the

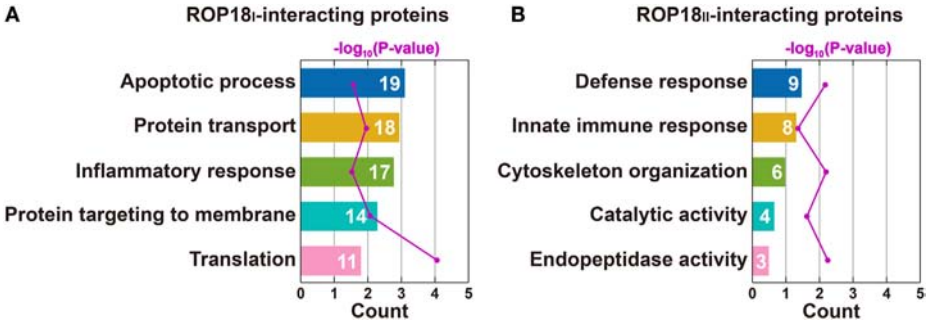

FIGURE 4 | Top five enriched biological processes for ROP18$_I$ **(A)** and ROP18$_{II}$-interacting proteins **(B)** identified by GO analysis. **(A)** ROP18$_I$-interacting proteins were significantly overrepresented in the biological processes of apoptotic process, protein transport, inflammatory response, protein targeting to membrane, and translation. **(B)** ROP18$_{II}$-interacting proteins were significantly overrepresented in the biological processes of defense response, innate immune response, cytoskeleton organization, catalytic activity, and endopeptidase activity.

biological processes of apoptotic process ($p = 2.7 \times 10^{-2}$), inflammatory response ($p = 1.1 \times 10^{-2}$), and protein targeting to membrane ($p = 8.7 \times 10^{-5}$), and for ROP18$_{II}$, we also added host targets to the expected biological processes, including defense response ($p = 7.8 \times 10^{-3}$) and innate immune response ($p = 4.0 \times 10^{-2}$). In addition to the roles of *Tg*ROP18 in the expected biological processes mentioned above, interesting roles of ROP18$_I$ in protein transport ($p = 3.0 \times 10^{-2}$) and translation ($p = 8.5 \times 10^{-5}$), and ROP18$_{II}$ in cytoskeleton organization ($p = 6.9 \times 10^{-3}$), catalytic activity ($p = 2.2 \times 10^{-2}$), and endopeptidase activity ($p = 6.1 \times 10^{-3}$) were also identified with great significance.

To elucidate whether the *Tg*ROP18-interacting proteins were functionally related, we conducted a deeper exploration of the PPI networks by using the STRING 10.0 database. By applying a medium confidence ($p > 0.4$), 353 (71.7%) of the ROP18$_I$-interacting proteins were tied to a single large network with a PPI enrichment p-value < 0.001; whereas for the ROP18$_{II}$-interacting proteins, 55 (39.0%) were enriched in a large PPI network, with a PPI enrichment p-value of 0.009 (**Figure 5**), which indicated that each one of the two sets of interacting proteins were biologically connected as a network with a significantly greater number of interactions, rather than as a random set of proteins. As shown in **Figure 5A**, 785 edges (PPIs) were observed among the 353 ROP18$_I$-interacting proteins, and seven protein–protein-interacting clusters were evident in the network, such as a cluster of ribosomal proteins containing RPS4X, RPL35, RPL23, RPL37A, and RPS6; a cluster of chemokines containing CXCL6, CXCL5, CCL19, CXCL11, and CXCL10; and a cluster of interleukins containing IL2, IL9, IL21, and IL24. Notably, UBC was observed as a main hub situated in the core of the network with 211 edges. Among the 55 ROP18$_{II}$-interacting proteins, 44 edges and four protein–protein-interacting clusters were determined by STRING analysis (**Figure 5B**). The cytoskeleton proteins ACTL7B, TUBB6, and TBCB were in close proximity and formed a cluster; TNS3 and UTS2 tensins were closely clustered with a tachykinin, TAC1; several functional regulators, such as TBRG4, PPIA, S100A1, and FKBP4 were tied together as a cluster; and several disease-related proteins, such as SNCG, STMN1, SSSCA1, and S100A16, were identified to be clustered.

By using the IPA database, we carried out an Ingenuity pathway analysis to further investigate the significant human signaling pathways influenced by ROP18$_I$/ROP18$_{II}$. Among the 492 ROP18$_I$-interacting proteins, 71 (14.4%) were mapped to 34 pathways, and 13 (9.2%) out of the 141 ROP18$_{II}$-interacting proteins were mapped to 16 pathways in total. All the involved significant pathways with their p-values and associated molecules are listed in Table S3 in Supplementary Material. The top five enriched pathways for the ROP18$_I$ and ROP18$_{II}$-interacting proteins shown in **Figure 6** were closely related to cell growth, cytokine signaling, and cellular immune response. For the ROP18$_I$-interacting proteins, MRAS was involved in the higher number of pathways, followed by ATM; whereas for the ROP18$_{II}$-interacting proteins, human leukocyte antigen (HLA)-DRB5 was involved in the higher number of pathways, followed by HLA-DQA1.

DISCUSSION

Protein–protein interaction plays indispensable roles in structuring and regulating biological processes in all biological systems. The "protein-protein interactome" refers to the whole union of all PPIs in a particular cell or organism (36). In addition to serving as a foundation for more detailed studies on the prediction of protein functions or disease associated genes (37, 38), interactome mapping has become a critical and powerful postgenomic research tool that facilitates a better understanding of genotype-to-phenotype relationship and biological systems (39). *Tg*ROP18, which is a key virulence determinant of *T. gondii*, modulates the host cell and mediates the parasite virulence by interacting with host proteins. However, only a few host targets of ROP18$_I$ have been identified, and knowledge about the host targets of ROP18$_{II}$ is still very limited.

The BiFC technique is an effective and robust tool for studying PPIs, as it enables not only the direct visualization of the occurrence and subcellular localization of PPIs in live cells (40, 41) but also the detection of weak or transient interactions due to the strong signal and high stability of the reconstituted fluorescent complex (25, 42). In the present study, we used a genome-wide BiFC-based proteomic approach to profile the *Tg*ROP18 (ROP18$_I$ and ROP18$_{II}$) interactome in human cells.

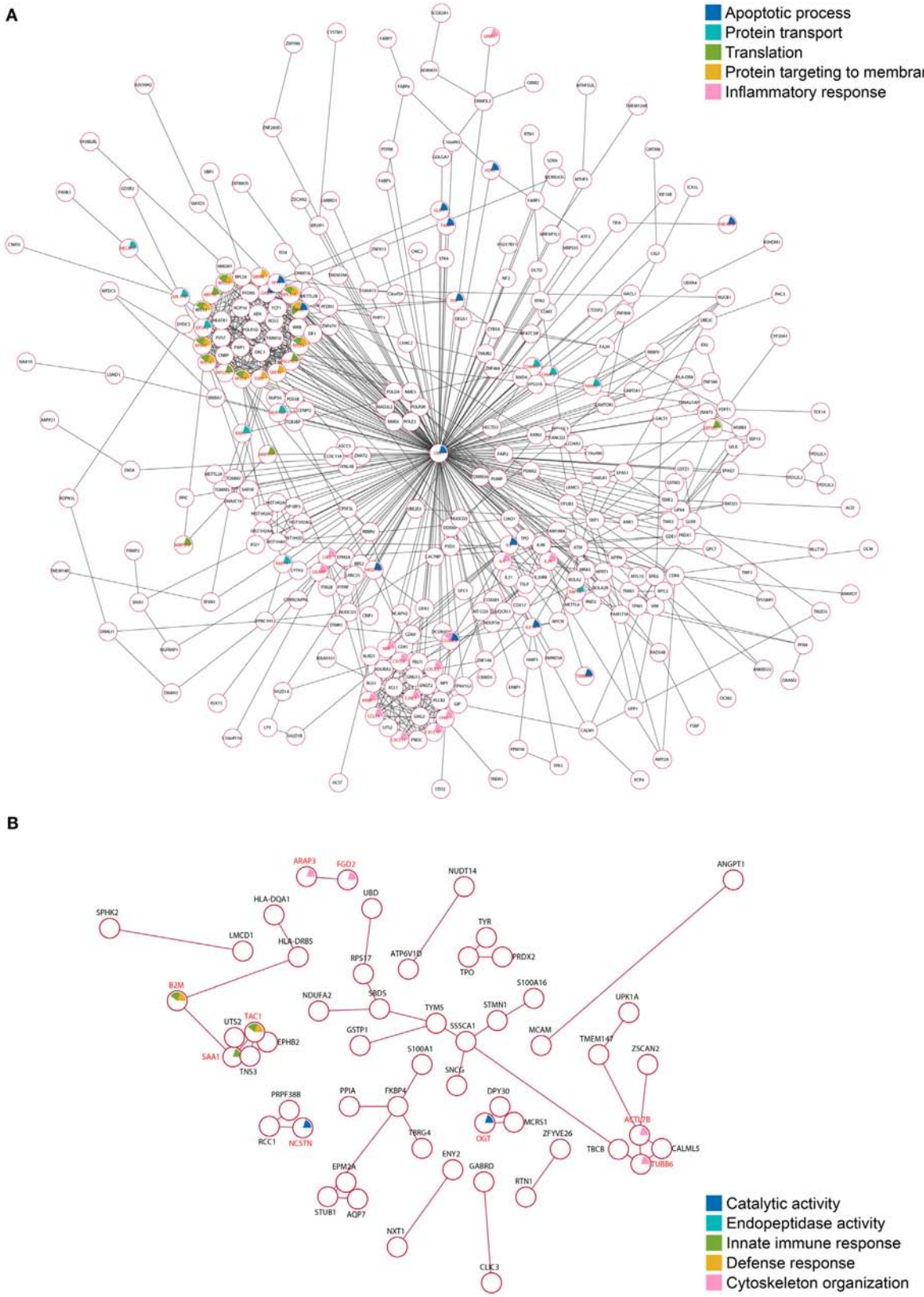

FIGURE 5 | Protein–protein interaction (PPI) networks of the *Tg*ROP18-interacting proteins. **(A)** Among the ROP18$_{I}$-interacting proteins, 353 (71.7%) are tied to a single large network with 785 edges. **(B)** Among the ROP18$_{II}$-interacting proteins, 55 (39.0%) are enriched in a PPI network with 44 edges.

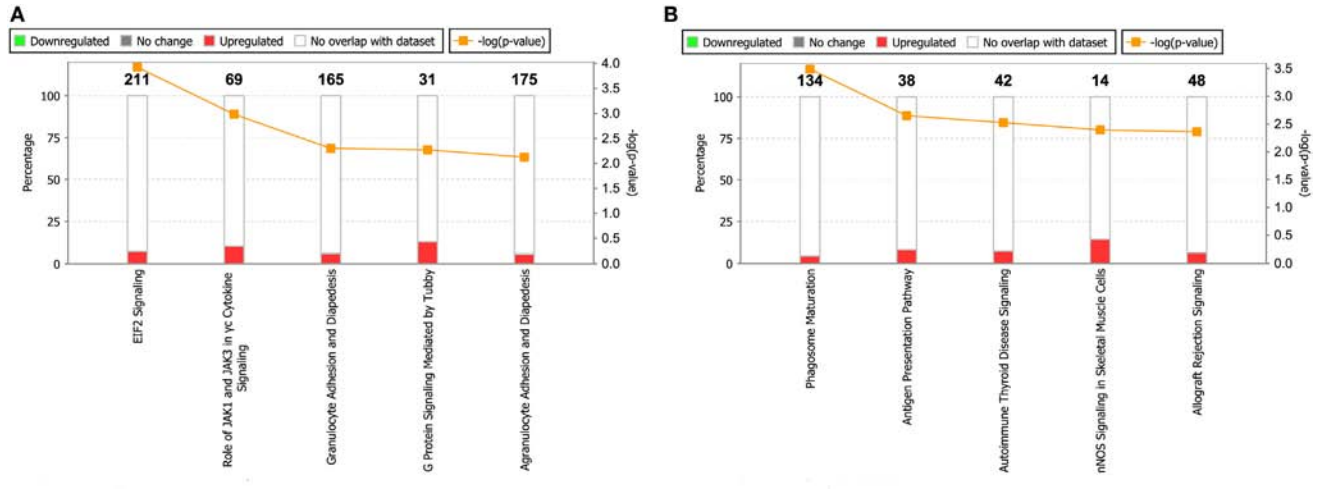

FIGURE 6 | Top five enriched pathways for ROP18$_I$ **(A)** and ROP18$_{II}$ **(B)** interacting proteins. The stacked bar chart indicates the number of proteins overlapped with the database, and the connected orange points represent the logarithm of the *p*-values.

Compared with control cells, a total of 492 ROP18$_I$ and 141 ROP18$_{II}$-interacting proteins were identified. Among these proteins, six of them, NMI, IL20RB, P2RX1, IL21, UBC, and vimentin, were further confirmed as authentic ROP18$_I$ targets by our SE-FRET and Co-IP assays and, furthermore, four of them, CNBP, DCTD, NUP160, and PRAC, had been previously reported as *Tg*ROP18 substrates by a human protein array (22). All of these results confirming the *Tg*ROP18 targets have strongly supported the power of our HT-BiFC assay. In this HT-BiFC assay, the NYFP- or CYFP-tagged prey collections covered 93% of all human ORFs, facilitating a much more complete and previously unavailable description of the *Tg*ROP18 interactome. We also newly identified 488 ROP18$_I$-interacting proteins when compared to the two previous screenings for ROP18$_I$ targets (20, 22). Such findings have demonstrated the significant advantages of the BiFC system to detect not only strong binding, but also transient or weak PPIs that would often be missed by using YTH and protein arrays (20, 22). The discovery of the novel *Tg*ROP18-interacting proteins have also shown the differences between the experimental methods used in the present study and in previous studies using YTH (20) and protein array methods (22), which analyzed the PPIs in yeast or *in vitro*. To our knowledge, ours is the first study to report the *Tg*ROP18 interactome in the natural cellular context. Our data appears to be highly complementary to the existing information about *Tg*ROP18, and the newly identified *Tg*ROP18-interacting proteins will be potential candidates for further investigations into the regulatory roles of *Tg*ROP18 in human cells.

*Tg*ROP18 and Immune Response

During *T. gondii* infection, immune defense against the parasite is strongly induced in its mammalian hosts, and T cell-mediated immune response plays a key role in this defense (43, 44). In our results, most *Tg*ROP18-interacting proteins were associated to the processes of immune response, including innate immune response, antigen presentation, activation and chemotaxis of naïve T lymphocytes, and cytotoxic reaction of effector T lymphocytes (**Figure 7**).

Innate immune response provides a first line of defense against *T. gondii* infection and is essential for the activation of the adaptive immune response (45). Following the infection of *T. gondii*, innate cells, including macrophages, dendritic cells, and neutrophils, are recruited to the sites of infection, producing proinflammatory cytokines, phagocytizing the parasites, or generating reactive chemical substances in order to inhibit the replication and dissemination of the parasites (46–49). Human NPY, LGALS1, S100A12, SAA1, and TREM1 have been reported as regulators of innate immunity, modulating the innate immune functions by controlling the innate cells physiology and cytokines release (50–55). In this study, NPY, LGALS1, and TREM1 were found as targets of ROP18$_I$, and S100A12, SAA1, and TREM1 were targets of ROP18$_{II}$. These results indicate a potential role of *Tg*ROP18 in manipulating and disarming the host innate immune response, which may contribute to the increase in parasites' survival in infected cells.

Antigen presentation is the first step for induction of T cell-mediated response (56). Infection with *T. gondii* provides a strong stimulus for antigen-specific CD4$^+$ and CD8$^+$ T cells, which suggests that the parasite antigens are efficiently acquired by APCs and presented to antigen-specific T lymphocytes during infection. It has been reported that intermediate filament protein vimentin plays a key role in antigen presentation, and disruption of vimentin in Langerhans cells results in failed antigen presentation of these cells (57). HLA molecules have also been known to carry out an indispensable role in antigen processing and presentation, by binding the pathogen antigens and displaying them on the cell surface for recognition by T lymphocytes (56). In this study, we found an interaction between ROP18$_I$ and vimentin, and this interaction was confirmed by FRET and Co-IP assays (35). Moreover, HLA-DQA1 and HLA-DRB5 were identified as the targets of ROP18$_{II}$. These results suggest that *Tg*ROP18 may confer the virulence to the parasite and exert its influence on

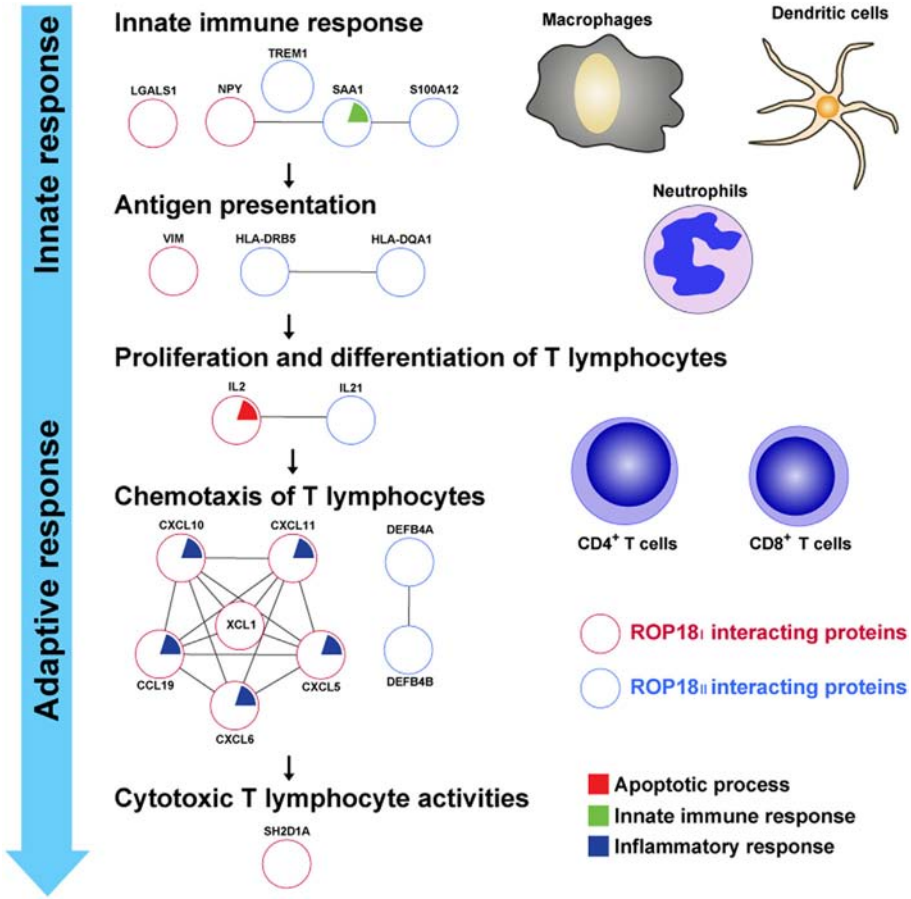

FIGURE 7 | *Tg*ROP18-interacting proteins involved in the immune response. Numerous $ROP18_I$ (red circles) and $ROP18_{II}$ (blue circles) identified interacting proteins related to the processes of immune response. During *T. gondii* infection, innate immune response acts rapidly to provide the first line of defense and activate the adaptive immune response, with release of proinflammatory cytokines by macrophages, dendritic cells, and neutrophils. In the milieu of proinflammatory cytokines, T cell-mediated immune response is initiated when naïve $CD4^+$ or $CD8^+$ T cells encounter the parasite antigens presented by antigen presenting cells (APCs). Once the antigen-specific T lymphocytes are activated, they proliferate, differentiate, and traffic to the sites of infection, protecting the host by exhibiting cytotoxic T lymphocyte (CTL) activities toward infected cells.

human cellular immunity by forming PPIs with the key proteins involved in antigen processing and presentation.

Once the T lymphocytes are specifically sensitized by exposure to the parasite antigens, they undergo proliferation and differentiation, which is regulated by inflammatory cytokines (58). Proinflammatory cytokines, such as IL-2 and IL-21, are pivotal mediators in triggering development of T cell populations and effector functions against *T. gondii* infection mediated by T lymphocytes. Though the IL-2 response is not potently induced during *T. gondii* infection (59), $IL\text{-}2^{-/-}$ mice have a defect in production of IFN-γ and exhibit poor $CD8^+$ T cell responses against the parasite (60). In addition, Khan et al. have reported that in mice lacking functional IL-21, expression of co-stimulatory molecules on $CD8^+$ T cells is strongly downregulated by *T. gondii* infection, and in the absence of IL-21 receptors, the functions of $CD8^+$ T cells are significantly affected (61). In the present study, we identified IL-2 and IL-21 as the host targets of $ROP18_I$. In particular, IL-21 was further confirmed as the $ROP18_I$-interacting protein by FRET and Co-IP assays (**Figures 2** and **3**). These data suggest that $ROP18_I$ may inhibit the activation and development of host T lymphocytes by targeting the key cytokines, resulting in the dysregulation of T cell-mediated immunity.

During *T. gondii* infection, multiple chemokines are upregulated, contributing to T cells entry into the sites of infection and targeting of parasites (62). In murine ocular and cerebral toxoplasmosis, there is a significant increase in the expression levels of CXCL10 and CXCL11 over the course of infection (63, 64). CCL19 is a vital chemokine in multiple immunological processes, including generation of thymocytes, promotion of regulatory T cells activity, and homing of leukocytes (65–67). The family of β-defensins (DEFB) consists of a number of cationic host defense peptides, such as DEFB4A and DEFB4B, which play a dual role in both innate and adaptive immune response (68). In this study, chemokines CXCL5, CXCL6, CXCL10, CXCL11, CCL19, and XCL1 were identified as the $ROP18_I$-interacting proteins, and DEFB4A and DEFB4B were identified as the $ROP18_{II}$ targets, which indicate a regulatory role of *Tg*ROP18 in human chemokines, enabling the parasite to

interfere with the host immune responses and finally promote parasite's survival.

After being attracted to the sites of infection, the antigen-specific effector T lymphocytes display strong effector functions toward infected cells for host protection (69). SH2D1A (or signaling lymphocytic activation molecule-associated protein, SAP) is an adaptor protein that regulates signaling through signaling lymphocytic activation molecule family receptors expressed on T lymphocytes and NK cells (70). Mutations in the *sh2d1a* gene or lack of SH1D2A protein show a significant decrease in the production of IFN-γ, resulting in disruption of cytotoxic T lymphocyte (CTL) function and defective lytic activity against EBV-positive target cells (71). In our study, we identified SH2D1A as a host target of $ROP18_I$. Given the importance of SH2D1A in CTL activities, being targeted by $ROP18_I$ may lead to impaired function of SH2D1A, thereby decreasing cytotoxic activity against *T. gondii* infection.

*Tg*ROP18 and Apoptosis

Apoptosis is a programmed, regulated form of cell death that permits the active and safe self-destruction of the cell (72). It plays a major role in cell development, tissue homeostasis, immune defense, and protection against tumorigenesis (73). *T. gondii* appears to use various strategies to interfere with host cell apoptosis through both pro-apoptotic and anti-apoptotic activities. Such complex dual activities of the parasite may be crucial for stable host-parasite interaction and sustained toxoplasmosis (74, 75). After acute infection, increased apoptosis of immune cells induced by *T. gondii* may suppress the immune responses against the parasite, thereby leading to immune evasion. On the other hand, inhibition of host cell apoptosis may serve as a mechanism for preserving intracellular replication and long-term survival of the parasite (76).

*Tg*ROP18 has been shown to use a variety of mechanisms, including the mitochondrial pathway, to modulate the host cell apoptosis (16). As a mitochondrial inner membrane protein, HIGD1A inhibits cytochrome c release and reduces caspases activities, thus suppressing the mitochondrial pathway of apoptosis (77). IGF1R, which is a tyrosine kinase, acts as an anti-apoptotic agent by upregulating the expression of anti-apoptotic members of the BCL2 family. Inhibition of IGF1R not just leads to reduced anti-apoptotic BCL2 proteins, but also increases expression of proapoptotic Bax/Bak-like BCL2 proteins and cleavage of caspase 3 (78). In our research, we found that HIGD1A and IGFIR were targeted by $ROP18_I$, suggesting that these host proteins might be significant for $ROP18_I$ to manipulate human cell apoptosis through the mitochondrial pathway.

The death receptor pathway is another major pathway of apoptosis. Fas apoptotic inhibitory molecule (FAIM) is a death receptor antagonist that protects the cell from Fas-induced apoptosis by inhibiting auto-ubiquitinylation and proteasome-dependent degradation of the apoptotic suppressor protein XIAP (79). Cells overexpressing FAIM show increased resistance to apoptosis triggered by the death receptor, and suppression of FAIM expression protects the cell against death receptor-induced apoptotic cell death (80). We found an interaction between $ROP18_I$ and FAIM in this study, which suggested that the parasite might interfere with the death receptor pathway of host cell apoptosis through targeting the key component in this pathway by *Tg*ROP18.

The ER is a central cellular organelle responsible for several crucial biological processes, and ER stress condition can trigger cell apoptosis when the stress is prolonged and severe (81). It has been reported that *T. gondii* can induce apoptosis of host cells *via* the ER stress pathway by upregulating the expression of C/EBP homologous protein, c-JUN NH2-terminal kinase, and activated caspase 12 (82, 83). Furthermore, $ROP18_I$ exerts a facilitated effect on the ER stress-induced apoptosis of the host cell by increasing the expression levels of the key molecules involved in the pathway (84). Consistent with this, two human proteins, PPT1 and PSMD10, which were involved in the ER stress-induced apoptosis, were identified as the $ROP18_{II}$-interacting proteins in our HT-BiFC assay. PPT1 is a lysosomal enzyme that is associated with the depalmitoylation and degradation of S-acylated proteins. PSMD10, also named as p28, suppresses ER stress-induced apoptosis by upregulating the expression of GRP78 and promoting the recovery of the cell from ER stress (85). Considering the significant roles of PPT1 and PSMD10 in ER stress-induced apoptosis, disruption of PPT1 and PSMD10 by $ROP18_{II}$ may facilitate the ER stress-induced apoptosis of host cells, leading to restricted immune responses and high parasite burden. Our study suggests a pleiotropic role of *Tg*ROP18 in altering the host cell apoptosis through multiple targets and pathways, providing a new and better understanding of this pathological process.

CONCLUSION

Identification of the host targets of *T. gondii* effectors is important to reveal host-parasite interaction. We used high-throughput PPI screening based on BiFC for the first time to identify the human host proteins targeted by the *T. gondii* key virulence factor *Tg*ROP18. In total, 492 and 141 human proteins were identified as the targets of $ROP18_I$ and $ROP18_{II}$, respectively. These *Tg*ROP18-interacting proteins were involved in crucial pathways related to immune response and apoptosis. Our findings characterized an interactome of *Tg*ROP18 in human cells and described novel regulatory roles of *Tg*ROP18 on host cell functions. The analysis of the $ROP18_I$ and $ROP18_{II}$ PPIs networks would be useful to reveal the strategies of *T. gondii* virulence elicitation and the regulatory mechanisms of human responses to *T. gondii* infection.

ETHICS STATEMENT

This article does not contain any experiments with human participants or animal subjects performed by any of the authors.

AUTHOR CONTRIBUTIONS

JX designed and performed experiments, analyzed data, and drafted manuscript. LK performed FRET and Co-IP assays of IL20RB, and graphed data. L-JZ performed FRET and Co-IP assays of P2RX1. S-ZW performed FRET and Co-IP assays of IL21. L-JY performed FRET assay of UBC. CH performed

FRET and Co-IP assays of vimentin. CYH revised manuscript. H-JP designed experiments, revised manuscript, and submitted manuscript. All the authors read and approved the final version of the manuscript.

FUNDING

This research is supported by the funding of National key R&D program of China (2017YFD0500400), the National Natural Science Foundation of China (81572012, 81772217), the Guangdong Provincial Natural Science Foundation (2016A030311025, 2017A030313694), and Guangzhou health and medical collaborative innovation major special project (201604020011) to H-JP.

SUPPLEMENTARY MATERIAL

The Supplementary Material for this article can be found online at http://www.frontiersin.org/articles/10.3389/fimmu.2018.00061/full#supplementary-material.

FIGURE S1 | Flow cytometry histograms of HTC75 cells co-expressing $ROP18_{I}$- (upper panel) or $ROP18_{II}$-NYFP (lower panel) and Prey-CYFP, or expressing control constructs CYFP-EV, showing the ultimate positive sorting rate was more than 90%. EV, empty vector.

TABLE S1 | List of $ROP18_{I}$-interacting proteins identified by HT-BiFC assay.

TABLE S2 | List of $ROP18_{II}$-interacting proteins identified by HT-BiFC assay.

TABLE S3 | List of significant pathways related to $ROP18_{I}$ or $ROP18_{II}$-interacting proteins.

REFERENCES

1. Moncada PA, Montoya JG. Toxoplasmosis in the fetus and newborn: an update on prevalence, diagnosis and treatment. *Expert Rev Anti Infect Ther* (2012) 10:815–28. doi:10.1586/eri.12.58
2. Morrison DA. Evolution of the apicomplexa: where are we now? *Trends Parasitol* (2009) 25:375–82. doi:10.1016/j.pt.2009.05.010
3. Nichols BA, Chiappino ML, O'Connor GR. Secretion from the rhoptries of *Toxoplasma gondii* during host-cell invasion. *J Ultrastruct Res* (1983) 83:85–98. doi:10.1016/S0022-5320(83)90067-9
4. Boothroyd JC, Dubremetz JF. Kiss and spit: the dual roles of *Toxoplasma* rhoptries. *Nat Rev Microbiol* (2008) 6:79–88. doi:10.1038/nrmicro1800
5. Howe DK, Sibley LD. *Toxoplasma gondii* comprises three clonal lineages: correlation of parasite genotype with human disease. *J Infect Dis* (1995) 172:1561–6. doi:10.1093/infdis/172.6.1561
6. Barragan A, Sibley LD. Migration of *Toxoplasma gondii* across biological barriers. *Trends Microbiol* (2003) 11:426–30. doi:10.1016/S0966-842X(03)00205-1
7. Howe DK, Summers BC, Sibley LD. Acute virulence in mice is associated with markers on chromosome VIII in *Toxoplasma gondii*. *Infect Immun* (1996) 64:5193–8.
8. Mordue DG, Monroy F, La Regina M, Dinarello CA, Sibley LD. Acute toxoplasmosis leads to lethal overproduction of Th1 cytokines. *J Immunol* (1950) 2001(167):4574–84.
9. Sibley LD, Ajioka JW. Population structure of *Toxoplasma gondii*: clonal expansion driven by infrequent recombination and selective sweeps. *Annu Rev Microbiol* (2008) 62:329–51. doi:10.1146/annurev.micro.62.081307.162925
10. Sibley LD, Boothroyd JC. Virulent strains of *Toxoplasma gondii* comprise a single clonal lineage. *Nature* (1992) 359:82–5. doi:10.1038/359082a0
11. Saeij JP, Boyle JP, Coller S, Taylor S, Sibley LD, Brooke-Powell ET, et al. Polymorphic secreted kinases are key virulence factors in toxoplasmosis. *Science* (2006) 314:1780–3. doi:10.1126/science.1133690
12. Taylor S, Barragan A, Su C, Fux B, Fentress SJ, Tang K, et al. A secreted serine-threonine kinase determines virulence in the eukaryotic pathogen *Toxoplasma gondii*. *Science* (2006) 314:1776–80. doi:10.1126/science.1133643
13. El Hajj H, Lebrun M, Arold ST, Vial H, Labesse G, Dubremetz JF. ROP18 is a rhoptry kinase controlling the intracellular proliferation of *Toxoplasma gondii*. *PLoS Pathog* (2007) 3:e14. doi:10.1371/journal.ppat.0030014
14. Fentress SJ, Behnke MS, Dunay IR, Mashayekhi M, Rommereim LM, Fox BA, et al. Phosphorylation of immunity-related GTPases by a *Toxoplasma gondii*-secreted kinase promotes macrophage survival and virulence. *Cell Host Microbe* (2010) 8:484–95. doi:10.1016/j.chom.2010.11.005
15. Steinfeldt T, Konen-Waisman S, Tong L, Pawlowski N, Lamkemeyer T, Sibley LD, et al. Phosphorylation of mouse immunity-related GTPase (IRG) resistance proteins is an evasion strategy for virulent *Toxoplasma gondii*. *PLoS Biol* (2010) 8:e1000576. doi:10.1371/journal.pbio.1000576
16. Wu L, Wang X, Li Y, Liu Y, Su D, Fu T, et al. *Toxoplasma gondii* ROP18: potential to manipulate host cell mitochondrial apoptosis. *Parasitol Res* (2016) 115:2415–22. doi:10.1007/s00436-016-4993-6
17. Yamamoto M, Ma JS, Mueller C, Kamiyama N, Saiga H, Kubo E, et al. ATF6beta is a host cellular target of the *Toxoplasma gondii* virulence factor ROP18. *J Exp Med* (2011) 208:1533–46. doi:10.1084/jem.20101660
18. Du J, An R, Chen L, Shen Y, Chen Y, Cheng L, et al. *Toxoplasma gondii* virulence factor ROP18 inhibits the host NF-kappaB pathway by promoting p65 degradation. *J Biol Chem* (2014) 289:12578–92. doi:10.1074/jbc.M113.544718
19. Niedelman W, Gold DA, Rosowski EE, Sprokholt JK, Lim D, Farid Arenas A, et al. The rhoptry proteins ROP18 and ROP5 mediate *Toxoplasma gondii* evasion of the murine, but not the human, interferon-gamma response. *PLoS Pathog* (2012) 8:e1002784. doi:10.1371/journal.ppat.1002784
20. Cheng L, Chen Y, Chen L, Shen Y, Shen J, An R, et al. Interactions between the ROP18 kinase and host cell proteins that aid in the parasitism of *Toxoplasma gondii*. *Acta Trop* (2012) 122:255–60. doi:10.1016/j.actatropica.2012.02.065
21. Fields S, Song O. A novel genetic system to detect protein-protein interactions. *Nature* (1989) 340:245–6. doi:10.1038/340245a0
22. Yang Z, Hou Y, Hao T, Rho HS, Wan J, Luan Y, et al. A human proteome array approach to identifying key host proteins targeted by *Toxoplasma* kinase ROP18. *Mol Cell Proteomics* (2017) 16(3):469–84. doi:10.1074/mcp.M116.063602
23. Howell JM, Winstone TL, Coorssen JR, Turner RJ. An evaluation of in vitro protein-protein interaction techniques: assessing contaminating background proteins. *Proteomics* (2006) 6:2050–69. doi:10.1002/pmic.200500517
24. Kerppola TK. Design and implementation of bimolecular fluorescence complementation (BiFC) assays for the visualization of protein interactions in living cells. *Nat Protoc* (2006) 1:1278–86. doi:10.1038/nprot.2006.201
25. Kodama Y, Hu CD. Bimolecular fluorescence complementation (BiFC): a 5-year update and future perspectives. *Biotechniques* (2012) 53:285–98. doi:10.2144/000113943
26. Lee OH, Kim H, He Q, Baek HJ, Yang D, Chen LY, et al. Genome-wide YFP fluorescence complementation screen identifies new regulators for telomere signaling in human cells. *Mol Cell Proteomics* (2011) 10:M110.001628. doi:10.1074/mcp.M110.001628
27. Yang X, Boehm JS, Yang X, Salehi-Ashtiani K, Hao T, Shen Y, et al. A public genome-scale lentiviral expression library of human ORFs. *Nat Methods* (2011) 8:659–61. doi:10.1038/nmeth.1638
28. Na RH, Zhu GH, Luo JX, Meng XJ, Cui L, Peng HJ, et al. Enzymatically active Rho and Rac small-GTPases are involved in the establishment of the vacuolar membrane after *Toxoplasma gondii* invasion of host cells. *BMC Microbiol* (2013) 13:125. doi:10.1186/1471-2180-13-125
29. Balasubramanian S. Solexa sequencing: decoding genomes on a population scale. *Clin Chem* (2015) 61:21–4. doi:10.1373/clinchem.2014.221747
30. Huang da W, Sherman BT, Lempicki RA. Bioinformatics enrichment tools: paths toward the comprehensive functional analysis of large gene lists. *Nucleic Acids Res* (2009) 37:1–13. doi:10.1093/nar/gkn923
31. Huang da W, Sherman BT, Lempicki RA. Systematic and integrative analysis of large gene lists using DAVID bioinformatics resources. *Nat Protoc* (2009) 4:44–57. doi:10.1038/nprot.2008.211

32. Szklarczyk D, Franceschini A, Wyder S, Forslund K, Heller D, Huerta-Cepas J, et al. STRING v10: protein-protein interaction networks, integrated over the tree of life. *Nucleic Acids Res* (2015) 43:D447–52. doi:10.1093/nar/gku1003
33. Shannon P, Markiel A, Ozier O, Baliga NS, Wang JT, Ramage D, et al. Cytoscape: a software environment for integrated models of biomolecular interaction networks. *Genome Res* (2003) 13:2498–504. doi:10.1101/gr.1239303
34. *IBM SPSS Statistics for Windows. Version 20.0 ed*. Armonk, New York: IBM Corporation (2011).
35. He C, Kong L, Zhou L, Xia J, Wei H, Liu M, et al. Host cell vimentin restrains *Toxoplasma gondii* invasion and phosphorylation of vimentin is partially regulated by interaction with TgROP18. *Int J Biol Sci* (2017) 13:1126–37. doi:10.7150/ijbs.21247
36. Vidal M, Cusick ME, Barabasi AL. Interactome networks and human disease. *Cell* (2011) 144:986–98. doi:10.1016/j.cell.2011.02.016
37. Mostafavi S, Ray D, Warde-Farley D, Grouios C, Morris Q. GeneMANIA: a real-time multiple association network integration algorithm for predicting gene function. *Genome Biol* (2008) 9(Suppl 1):S4. doi:10.1186/gb-2008-9-s1-s4
38. Vanunu O, Magger O, Ruppin E, Shlomi T, Sharan R. Associating genes and protein complexes with disease via network propagation. *PLoS Comput Biol* (2010) 6:e1000641. doi:10.1371/journal.pcbi.1000641
39. Barabasi AL, Gulbahce N, Loscalzo J. Network medicine: a network-based approach to human disease. *Nat Rev Genet* (2011) 12:56–68. doi:10.1038/nrg2918
40. Hu CD, Chinenov Y, Kerppola TK. Visualization of interactions among bZIP and Rel family proteins in living cells using bimolecular fluorescence complementation. *Mol Cell* (2002) 9:789–98. doi:10.1016/S1097-2765(02)00496-3
41. Citovsky V, Lee LY, Vyas S, Glick E, Chen MH, Vainstein A, et al. Subcellular localization of interacting proteins by bimolecular fluorescence complementation in planta. *J Mol Biol* (2006) 362:1120–31. doi:10.1016/j.jmb.2006.08.017
42. Morell M, Espargaro A, Aviles FX, Ventura S. Detection of transient protein-protein interactions by bimolecular fluorescence complementation: the Abl-SH3 case. *Proteomics* (2007) 7:1023–36. doi:10.1002/pmic.200600966
43. Silva NM, Vieira JC, Carneiro CM, Tafuri WL. *Toxoplasma gondii*: the role of IFN-gamma, TNFRp55 and iNOS in inflammatory changes during infection. *Exp Parasitol* (2009) 123:65–72. doi:10.1016/j.exppara.2009.05.011
44. Suzuki Y, Conley FK, Remington JS. Importance of endogenous IFN-gamma for prevention of toxoplasmic encephalitis in mice. *J Immunol* (1950) 1989(143):2045–50.
45. Yarovinsky F. Innate immunity to *Toxoplasma gondii* infection. *Nat Rev Immunol* (2014) 14:109–21. doi:10.1038/nri3598
46. Mordue DG, Sibley LD. A novel population of Gr-1+-activated macrophages induced during acute toxoplasmosis. *J Leukoc Biol* (2003) 74:1015–25. doi:10.1189/jlb.0403164
47. Bliss SK, Butcher BA, Denkers EY. Rapid recruitment of neutrophils containing prestored IL-12 during microbial infection. *J Immunol* (1950) 2000(165):4515–21.
48. Del Rio L, Bennouna S, Salinas J, Denkers EY. CXCR2 deficiency confers impaired neutrophil recruitment and increased susceptibility during *Toxoplasma gondii* infection. *J Immunol* (1950) 2001(167):6503–9.
49. Liu CH, Fan YT, Dias A, Esper L, Corn RA, Bafica A, et al. Cutting edge: dendritic cells are essential for in vivo IL-12 production and development of resistance against *Toxoplasma gondii* infection in mice. *J Immunol* (1950) 2006(177):31–5.
50. Wheway J, Herzog H, Mackay F. NPY and receptors in immune and inflammatory diseases. *Curr Top Med Chem* (2007) 7:1743–52. doi:10.2174/156802607782341046
51. Barrionuevo P, Beigier-Bompadre M, Ilarregui JM, Toscano MA, Bianco GA, Isturiz MA, et al. A novel function for galectin-1 at the crossroad of innate and adaptive immunity: galectin-1 regulates monocyte/macrophage physiology through a nonapoptotic ERK-dependent pathway. *J Immunol* (1950) 2007(178):436–45.
52. Levroney EL, Aguilar HC, Fulcher JA, Kohatsu L, Pace KE, Pang M, et al. Novel innate immune functions for galectin-1: galectin-1 inhibits cell fusion by Nipah virus envelope glycoproteins and augments dendritic cell secretion of proinflammatory cytokines. *J Immunol* (1950) 2005(175):413–20.
53. Foell D, Wittkowski H, Kessel C, Luken A, Weinhage T, Varga G, et al. Proinflammatory S100A12 can activate human monocytes via toll-like receptor 4. *Am J Respir Crit Care Med* (2013) 187:1324–34. doi:10.1164/rccm.201209-1602OC
54. Chen M, Zhou H, Cheng N, Qian F, Ye RD. Serum amyloid A1 isoforms display different efficacy at toll-like receptor 2 and formyl peptide receptor 2. *Immunobiology* (2014) 219:916–23. doi:10.1016/j.imbio.2014.08.002
55. Zhong J, Huang W, Deng Q, Wu M, Jiang H, Lin X, et al. Inhibition of TREM-1 and dectin-1 alleviates the severity of fungal keratitis by modulating innate immune responses. *PLoS One* (2016) 11:e0150114. doi:10.1371/journal.pone.0150114
56. Janeway CA Jr, Travers P, Shlomchik MJ, Walport M. *Immunobiology: The Immune System in Health and Disease*. 5th ed. New York: Garland Science (2001).
57. Bacci S, Nakamura T, Streilein JW. Failed antigen presentation after UVB radiation correlates with modifications of Langerhans cell cytoskeleton. *J Invest Dermatol* (1996) 107:838–43. doi:10.1111/1523-1747.ep12330994
58. Kim MT, Harty JT. Impact of inflammatory cytokines on effector and memory CD8+ T cells. *Front Immunol* (2014) 5:295. doi:10.3389/fimmu.2014.00295
59. Haque S, Khan I, Haque A, Kasper L. Impairment of the cellular immune response in acute murine toxoplasmosis: regulation of interleukin 2 production and macrophage-mediated inhibitory effects. *Infect Immun* (1994) 62:2908–16.
60. Villegas EN, Lieberman LA, Carding SR, Hunter CA. Susceptibility of interleukin-2-deficient mice to *Toxoplasma gondii* is associated with a defect in the production of gamma interferon. *Infect Immun* (2002) 70:4757–61. doi:10.1128/IAI.70.9.4757-4761.2002
61. Hwang S, Khan IA. CD8+ T cell immunity in an encephalitis model of *Toxoplasma gondii* infection. *Semin Immunopathol* (2015) 37:271–9. doi:10.1007/s00281-015-0483-7
62. Strack A, Asensio VC, Campbell IL, Schluter D, Deckert M. Chemokines are differentially expressed by astrocytes, microglia and inflammatory leukocytes in *Toxoplasma* encephalitis and critically regulated by interferon-gamma. *Acta Neuropathol* (2002) 103:458–68. doi:10.1007/s00401-001-0491-7
63. Kikumura A, Ishikawa T, Norose K. Kinetic analysis of cytokines, chemokines, chemokine receptors and adhesion molecules in murine ocular toxoplasmosis. *Br J Ophthalmol* (2012) 96:1259–67. doi:10.1136/bjophthalmol-2012-301490
64. Wen X, Kudo T, Payne L, Wang X, Rodgers L, Suzuki Y. Predominant interferon-gamma-mediated expression of CXCL9, CXCL10, and CCL5 proteins in the brain during chronic infection with Toxoplasma gondii in BALB/c mice resistant to development of toxoplasmic encephalitis. *J Interferon Cytokine Res* (2010) 30:653–60. doi:10.1089/jir.2009.0119
65. Davalos-Misslitz AC, Rieckenberg J, Willenzon S, Worbs T, Kremmer E, Bernhardt G, et al. Generalized multi-organ autoimmunity in CCR7-deficient mice. *Eur J Immunol* (2007) 37:613–22. doi:10.1002/eji.200636656
66. Menning A, Hopken UE, Siegmund K, Lipp M, Hamann A, Huehn J. Distinctive role of CCR7 in migration and functional activity of naive- and effector/memory-like Treg subsets. *Eur J Immunol* (2007) 37:1575–83. doi:10.1002/eji.200737201
67. MartIn-Fontecha A, Sebastiani S, Hopken UE, Uguccioni M, Lipp M, Lanzavecchia A, et al. Regulation of dendritic cell migration to the draining lymph node: impact on T lymphocyte traffic and priming. *J Exp Med* (2003) 198:615–21. doi:10.1084/jem.20030448
68. Semple F, Dorin JR. beta-Defensins: multifunctional modulators of infection, inflammation and more? *J Innate Immun* (2012) 4:337–48. doi:10.1159/000336619
69. Denkers EY, Gazzinelli RT. Regulation and function of T-cell-mediated immunity during *Toxoplasma gondii* infection. *Clin Microbiol Rev* (1998) 11:569–88.
70. Sayos J, Wu C, Morra M, Wang N, Zhang X, Allen D, et al. The X-linked lymphoproliferative-disease gene product SAP regulates signals induced through the co-receptor SLAM. *Nature* (1998) 395:462–9. doi:10.1038/26683
71. Sharifi R, Sinclair JC, Gilmour KC, Arkwright PD, Kinnon C, Thrasher AJ, et al. SAP mediates specific cytotoxic T-cell functions in X-linked lymphoproliferative disease. *Blood* (2004) 103:3821–7. doi:10.1182/blood-2003-09-3359

72. Fleisher TA. Apoptosis. *Ann Allergy Asthma Immunol* (1997) 78:245–9; quiz 9–50. doi:10.1016/S1081-1206(10)63176-6
73. Elmore S. Apoptosis: a review of programmed cell death. *Toxicol Pathol* (2007) 35:495–516. doi:10.1080/01926230701320337
74. Schaumburg F, Hippe D, Vutova P, Luder CG. Pro- and anti-apoptotic activities of protozoan parasites. *Parasitology* (2006) 132(Suppl):S69–85. doi:10.1017/S0031182006000874
75. Luder CG, Gross U, Lopes MF. Intracellular protozoan parasites and apoptosis: diverse strategies to modulate parasite-host interactions. *Trends Parasitol* (2001) 17:480–6. doi:10.1016/S1471-4922(01)02016-5
76. Luder CG, Gross U. Apoptosis and its modulation during infection with *Toxoplasma gondii*: molecular mechanisms and role in pathogenesis. *Curr Top Microbiol Immunol* (2005) 289:219–37. doi:10.1007/3-540-27320-4_10
77. An HJ, Shin H, Jo SG, Kim YJ, Lee JO, Paik SG, et al. The survival effect of mitochondrial Higd-1a is associated with suppression of cytochrome C release and prevention of caspase activation. *Biochim Biophys Acta* (2011) 1813:2088–98. doi:10.1016/j.bbamcr.2011.07.017
78. Hou C, Zhu M, Sun M, Lin Y. MicroRNA let-7i induced autophagy to protect T cell from apoptosis by targeting IGF1R. *Biochem Biophys Res Commun* (2014) 453:728–34. doi:10.1016/j.bbrc.2014.10.002
79. Moubarak RS, Planells-Ferrer L, Urresti J, Reix S, Segura MF, Carriba P, et al. FAIM-L is an IAP-binding protein that inhibits XIAP ubiquitinylation and protects from Fas-induced apoptosis. *J Neurosci* (2013) 33:19262–75. doi:10.1523/JNEUROSCI.2479-13.2013
80. Segura MF, Sole C, Pascual M, Moubarak RS, Perez-Garcia MJ, Gozzelino R, et al. The long form of Fas apoptotic inhibitory molecule is expressed specifically in neurons and protects them against death receptor-triggered apoptosis. *J Neurosci* (2007) 27:11228–41. doi:10.1523/JNEUROSCI.3462-07.2007
81. Ron D, Walter P. Signal integration in the endoplasmic reticulum unfolded protein response. *Nat Rev Mol Cell Biol* (2007) 8:519–29. doi:10.1038/nrm2199
82. Wang T, Zhou J, Gan X, Wang H, Ding X, Chen L, et al. *Toxoplasma gondii* induce apoptosis of neural stem cells via endoplasmic reticulum stress pathway. *Parasitology* (2014) 141:988–95. doi:10.1017/S0031182014000183
83. Zhou J, Gan X, Wang Y, Zhang X, Ding X, Chen L, et al. *Toxoplasma gondii* prevalent in China induce weaker apoptosis of neural stem cells C17.2 via endoplasmic reticulum stress (ERS) signaling pathways. *Parasit Vectors* (2015) 8:73. doi:10.1186/s13071-015-0670-3
84. Wan L, Gong L, Wang W, An R, Zheng M, Jiang Z, et al. T. gondii rhoptry protein ROP18 induces apoptosis of neural cells via endoplasmic reticulum stress pathway. *Parasit Vectors* (2015) 8:554. doi:10.1186/s13071-015-1103-z
85. Dai RY, Chen Y, Fu J, Dong LW, Ren YB, Yang GZ, et al. p28GANK inhibits endoplasmic reticulum stress-induced cell death via enhancement of the endoplasmic reticulum adaptive capacity. *Cell Res* (2009) 19:1243–57. doi:10.1038/cr.2009.104

Conflict of Interest Statement: The authors declare that the research was conducted in the absence of any commercial or financial relationships that could be construed as a potential conflict of interest.

frontiers in Immunology

ORIGINAL RESEARCH
published: 09 February 2018
doi: 10.3389/fimmu.2018.00207

Elevated Systemic Levels of Eosinophil, Neutrophil, and Mast Cell Granular Proteins in *Strongyloides Stercoralis* Infection that Diminish following Treatment

Anuradha Rajamanickam[1], Saravanan Munisankar[1], Yukthi Bhootra[1], Chandra Kumar Dolla[2], Thomas B. Nutman[3] and Subash Babu[1,3]*

[1] National Institutes of Health – National Institute of Research in Tuberculosis (ICMR) – International Center for Excellence in Research, Chennai, India, [2] National Institute of Research in Tuberculosis (ICMR), Chennai, India, [3] Laboratory of Parasitic Diseases, National Institute of Allergy and Infectious Diseases, National Institutes of Health, Bethesda, MD, United States

OPEN ACCESS

Edited by:
Hyun Soon Lillehoj, Beltsville Agricultural Research Center (USDA-ARS), United States

Reviewed by:
William Horsnell, University of Cape Town, South Africa
Woo Hyun Kim, Beltsville Agricultural Research Center (USDA-ARS), United States
Atul Chaudhari, Alabama State University, United States

***Correspondence:**
Anuradha Rajamanickam
anuradha@nirt.res.in

Specialty section:
This article was submitted to Microbial Immunology, a section of the journal Frontiers in Immunology

Received: *13 October 2017*
Accepted: *24 January 2018*
Published: *09 February 2018*

Citation:
Rajamanickam A, Munisankar S, Bhootra Y, Dolla CK, Nutman TB and Babu S (2018) Elevated Systemic Levels of Eosinophil, Neutrophil, and Mast Cell Granular Proteins in Strongyloides Stercoralis Infection that Diminish following Treatment. Front. Immunol. 9:207. doi: 10.3389/fimmu.2018.00207

Infection with the helminth parasite *Strongyloides stercoralis* (*Ss*) is commonly clinically asymptomatic that is often accompanied by peripheral eosinophilia. Granulocytes are activated during helminth infection and can act as immune effector cells. Plasma levels of eosinophil and neutrophil granular proteins convey an indirect measure of granulocyte degranulation and are prominently augmented in numerous helminth-infected patients. In this study, we sought to examine the levels of eosinophil, neutrophil, and mast cell activation-associated granule proteins in asymptomatic *Ss* infection and to understand their kinetics following anthelmintic therapy. To this end, we measured the plasma levels of eosinophil cationic protein, eosinophil-derived neurotoxin, eosinophil peroxidase, eosinophil major basic protein, neutrophil elastase, myeloperoxidase, neutrophil proteinase-3, mast cell tryptase, leukotriene C4, and mast cell carboxypeptidase-A3 in individuals with asymptomatic *Ss* infection or without *Ss* infection [uninfected (UN)]. We also estimated the levels of all of these analytes in infected individuals following definitive treatment of *Ss* infection. We demonstrated that those infected individuals have significantly enhanced plasma levels of eosinophil cationic protein, eosinophil-derived neurotoxin, eosinophil peroxidase, eosinophil major basic protein, elastase, myeloperoxidase, mast cell tryptase, leukotriene C4, and carboxypeptidase-A3 compared to UN individuals. Following the treatment of *Ss* infection, each of these granulocyte-associated proteins drops significantly. Our data suggest that eosinophil, neutrophil, and mast cell activation may play a role in the response to *Ss* infection.

Keywords: eosinophils, neutrophils, mast cells, granular proteins, helminths, *Strongyloides stercoralis*

INTRODUCTION

Strongyloides stercoralis (Ss), an intestinal parasitic nematode, infects 30–100 million people worldwide (1). The clinical manifestation of *Ss* can range from clinically asymptomatic to, at its most severe, a potentially fatal disseminated infection. Granulocytes are activated during helminth infection and act as immune effector cells. *In vitro* granulocyte mediated immunity against helminths can be

attained through antibody-dependent cell-mediated cytotoxicity, and antibody attaches to the parasite's cell surface and triggers degranulation and extrusion of toxic granule contents against the parasite (2).

In healthy people, eosinophils normally constitute only 2–5% of peripheral leukocytes. However, during active helminth infection, the eosinophils fraction in the blood can increase to more than 40% (3). Eosinophils have eosinophil-specific toxic proteins stored in their secondary granules. These include eosinophil cationic protein (ECP), eosinophil peroxidase (EPX), eosinophil-derived neurotoxin (EDN), and eosinophil major basic protein (MBP). ECP, EPX, and MBP are potent helminth toxins (4). MBP can provoke histamine release from mast cells; however, EDN and ECP can act as ribonucleases (4, 5). Experimental helminth infection studies revealed that eosinophils accumulate in the gastrointestinal tract, where it is believed that they assist to eliminate parasites (6). Interestingly, evidence suggests that there could be dissimilarities in the mechanisms of eosinophil-mediated killing among different life cycle stages of the same parasite (7).

Among granulocytes, neutrophils are effective at phagocytosis, and they can engulf and execute microorganisms by producing reactive oxygen intermediates in phagolysosomes. Conversely, helminths are very large to be phagocytosed, and as a outcome, the function of neutrophils in helminth-driven effector responses has been ignored till now (2). Neutrophils can be defensive against nematode parasites, and this has been exhibited conclusively in the *Strongyloides sp.* model (8). Like neutrophils, granulocytes are also critical in controlling *Streptococcus ratti* in mice (9). Myeloperoxidase (MPO) purified from human neutrophils is toxic to *Trichinella spiralis* and *Schistosoma mansoni* (10, 11) and functions in killing *S. stercoralis* larvae (12). Neutrophil elastase (NE) secreted following contact with *S. mansoni* is potentially toxic to a number of stages of this parasite (13).

Mast cells also play an important role in parasitic infections and have been implicated in the regulation of innate and adaptive immune responses following infection (14). Helminth infections are associated with elevations in tissue mast cell numbers (15). In the presence of helminth antigens, FcεRI receptor provokes mast cell degranulation, which results in the release of mast cell tryptase (MCT), carboxypeptidase-A3 (CPA-3), and leukotriene C4 (LTC4), which has direct cytotoxic effect on helminths (15, 16). During helminth infection, studies have revealed that mast cells are crucial in the expulsion of several helminth species from the gastrointestinal tract (17) including *T. spiralis*, *Nippostrongylus brasiliensis*, and *S. ratti* in rodent models (18, 19).

In this study, we wanted to characterize the presence and persistence of eosinophil, neutrophil, and mast cell degranulation proteins in *Ss* infection before and after treatment. We hypothesized that the plasma levels of granular proteins would reflect the activation profile of these important granulocyte subsets and its association to *Ss* infection. To this end, we measured the plasma levels of eosinophil granular proteins (ECP, EDN, EPX, and MBP), neutrophil granular proteins [NE, MPO, and proteinase-3 (PTN-3)], and mast cell granular proteins and mediators (MCT, LTC4, and CPA-3) in *Ss*-infected (INF) and *Ss*-uninfected (UN) individuals. Plasma levels of ECP, EPX, EDN, MBP, NE, MPO, MCT, LTC4, and CPA-3 levels were all significantly increased in *Ss* infection compared to those without *Ss* infection. These levels decreased significantly after anthelmintic treatment.

MATERIALS AND METHODS

Ethics Statement

All participants were examined as a part of a natural history study protocol (12-I-073) approved by Institutional Review Boards of the National Institute of Allergy and Infectious Diseases (USA) and the National Institute for Research in Tuberculosis (India), and informed written consent was obtained from all participants.

Study Population

We studied a total of 118 individuals including of 60 clinically asymptomatic, INF individuals and 58 UNF, endemic healthy individuals in Tamil Nadu, South India (**Table 1**). These individuals were all enrolled from a rural population. None had previous anthelmintic treatment, a history of helminth infections, or HIV. The INF individuals were followed up after 6 months of anthelmintic treatment.

Strongyloides stercoralis infection was detected by measuring IgG antibodies to the recombinant NIE antigen, as explained elsewhere (20, 21). Further confirmation was done using specialized stool examination with nutrient agar plate cultures (22). None of the study population had lymphatic filariasis (based on ELISA) or other intestinal helminths (based on the stool microscopy). All INF individuals were treated with single doses of ivermectin and albendazole, and follow-up blood draws were collected after 6 months. Treated individuals were *Ss* infection negative by stool microscopy at 6 months posttreatment (post-T). All UN individuals were negative for anti-*Ss*-NIE and for filarial and other intestinal helminths.

Measurement of Hematological Parameters

Hematological parameters were measured from fresh venous EDTA blood samples on all individuals using an ACT 5 Diff. hematology analyzer (Beckman Coulter, Brea, CA, USA).

Measurement of Eosinophils, Neutrophils, and Mast Cell Granular Proteins

Plasma levels of ECP, EDN, EPX, MBP (MyBiosource, Inc., San Diego, CA, USA), MPO, PTN-3 (R&D Systems, Minneapolis, MN, USA), NE (Cell Sciences Hycult Biotech, Canton, MA, USA), MCT, LTC4, and CPA-3 were measured using the Mybiosource ELISA kits (MyBiosource, Inc., San Diego, CA, USA), followed

TABLE 1 | Baseline demographics of the study population.

Study demographics	*Ss* infected (INF)	Ss uninfected (UN)
Number	60	58
Gender (male/female)	33/27	35/23
Median age (range)	36 (20–65)	39 (20–60)
NIE ELISA	Positive	Negative

the manufacturer's protocol. The detection limits were as follows: ECP, 1.56–100 ng/ml; EDN, 0.625–40 ng/ml; EPX, 78–5,000 pg/ml; MBP, 0.468–30 ng/ml; MPO, 62.50–4,000 pg/ml; PTN-3, 15.6–1,000 pg/ml; NE, 0.4–25 ng/ml; MCT, 3.12–100 ng/ml; LTC4, 78–5,000 pg/ml; and CPA-3, 0.78–50 ng/ml. We have assigned the lowest standard value to the samples that were below the threshold of detection.

Statistical Analysis

Data analyses were done using GraphPad PRISM 7 (GraphPad Software, Inc., San Diego, CA, USA). Central tendency was calculated using geometric mean (GM). Nonparametric Mann–Whitney *U* test and Wilcoxon matched pair test were used to calculate the statistical significant difference. Multiple comparisons were corrected using the Holm's correction. JMP 13 (SAS) software was used to perform Spearman rank correlation matrix.

RESULTS

Ss Infection Is Associated with Elevated Absolute Neutrophil and Eosinophil Counts and Reversal following Treatment

As shown in **Table 1**, there was no significant difference in age or gender between the two groups. We measured the hematological parameters in the two groups. As shown in **Figure 1A**, INF had significantly enhanced levels of neutrophils (GM of 6,566/μl in INF Vs GM of 4,848/μl in UN; $p = 0.0001$) and eosinophils (GM of 550/μl in INF vs GM of 281/μl in UN; $p < 0.0001$) in comparison with UN individuals. The other hematological parameters did not show any significant difference between the two groups. Upon anthelminthic treatment, the absolute numbers were significantly reversed. As shown in **Figure 1B**, absolute counts of neutrophils [GM of 6,566/μl in pretreatment (pre-T) vs GM of 6,000/μl in post-T; $p < 0.0001$] and eosinophils (GM of 550/μl in pre-T Vs GM of 483/μl in post-T; $p < 0.0001$) were significantly decreased. Other hematological parameters did not show any significant changes following treatment.

Ss Infection Is Associated with Elevated Levels of Eosinophils, Neutrophils, and Mast Cell Granular Proteins

To characterize the role of eosinophils, neutrophils, mast cell granular proteins, and lipid mediators in *Ss* infection, we measured the plasma levels of eosinophil granular proteins (ECP, EDN, EPX, and MBP), neutrophil granular proteins (NE, MPO, and PTN-3), mast cell granular proteins, and lipid mediator (MCT, LTC4, and CPA-3) in INF and UN individuals. As shown in **Figure 2A**, INF had significantly higher levels of ECP (GM of 71.18 ng/ml in INF vs. 48.59 ng/ml in UN; $p = 0.0007$), EDN (GM of 1.811 ng/ml in INF vs. 1.014 ng/ml in UN; $p = 0.0072$), EPX (GM of 1,1945 ng/ml in INF vs. 7,407 ng/ml in UN; $p = 0.0065$), and MBP (GM of 288.4 ng/ml in INF vs. 223.7 ng/ml in UN; $p = 0.0464$) in comparison to UN individuals. As shown in **Figure 2B**, INF had significantly enhanced levels of NE (GM of 8,456 ng/ml in INF vs. 6,422 ng/ml in UN; $p = 0.0363$) and MPO (GM of 45.12 pg/ml in INF vs. 37.26 pg/ml in UN; $p = 0.0340$) in comparison to UN individuals. As shown in **Figure 2C**, INF had significantly increased levels of MCT (GM of 8,456 ng/ml in INF vs. 6,422 ng/ml in UN; $p = 0.0363$), LTC4 (GM of 45.12 pg/ml in INF vs. 37.26 pg/ml in UN; $p = 0.0340$), and CPA-3 (GM of

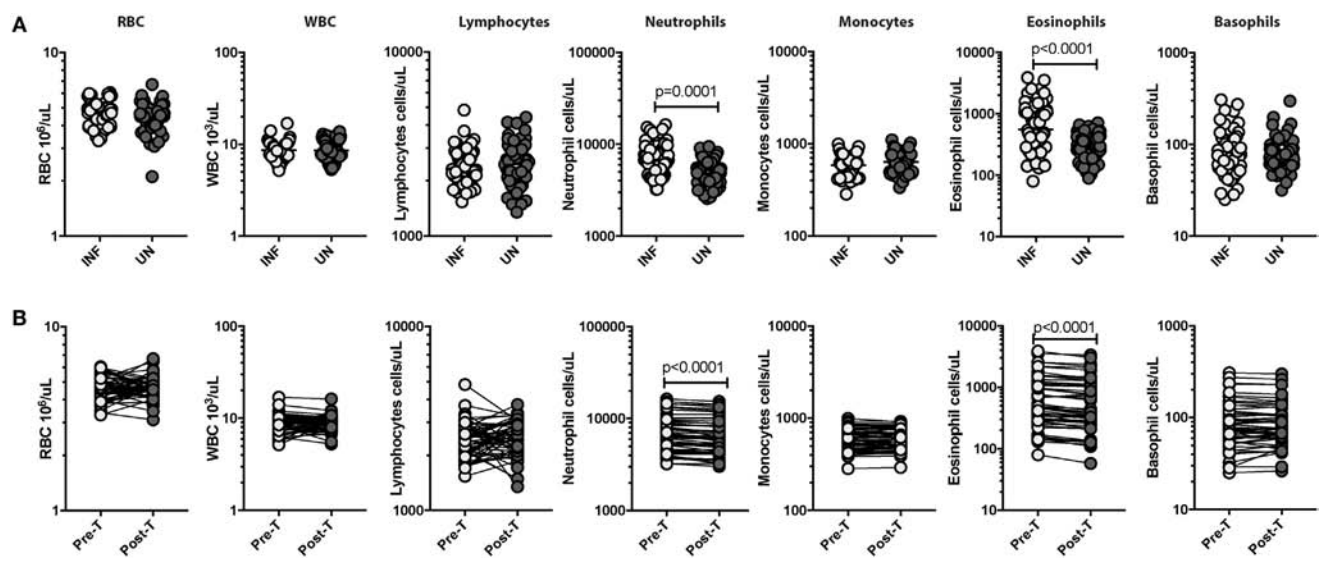

FIGURE 1 | *Strongyloides stercoralis* (*Ss*) infection is associated with elevated absolute neutrophil and eosinophil counts and reversal following treatment. **(A)** Absolute counts of hematological parameters from Ss-infected (INF; $n = 60$) or uninfected (UN; $n = 58$) individuals were measured. Data are shown as scatter plots with the bar representing the geometric mean. *p* Values were calculated using the Mann–Whitney test with Holm's correction for multiple comparisons. **(B)** Absolute counts of hematological parameters from Ss-infected pretreatment (pre-T; $n = 60$) and 6 months after treatment posttreatment (post-T) individuals were measured. *p* Values were calculated using the Wilcoxon matched pair test with Holm's correction for multiple comparisons.

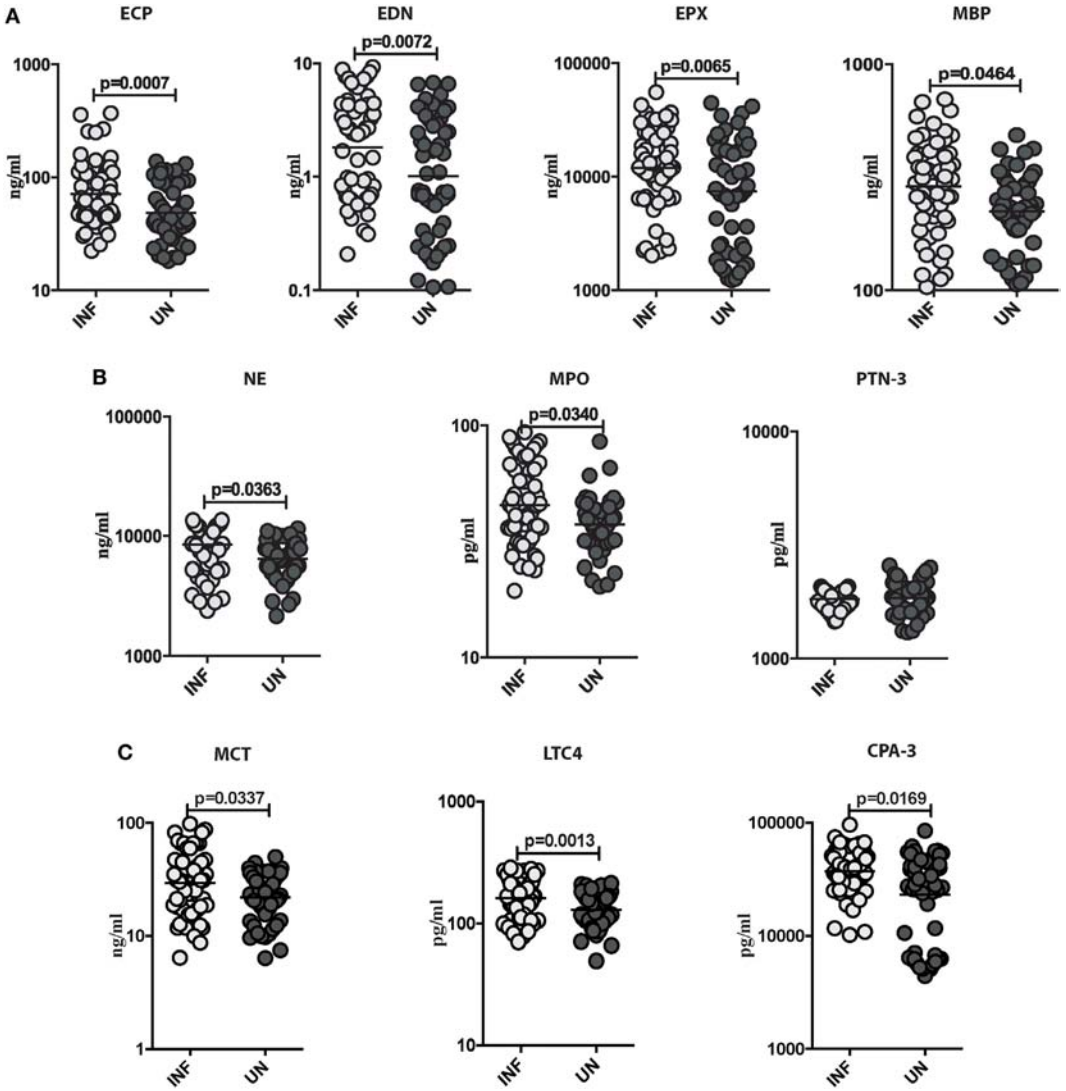

FIGURE 2 | *Strongyloides stercoralis* (*Ss*) infection is associated with elevated levels of eosinophils, neutrophils, and mast cell granular proteins. **(A)** Plasma levels of eosinophil cationic protein (ECP), eosinophil-derived neurotoxin (EDN), eosinophil peroxidase (EPX), and major basic protein (MBP), from *Ss*-infected (INF; $n = 60$) or *Ss*-uninfected (UN; $n = 58$) individuals were measured by ELISA. Data are shown as scatter plots with the bar representing the geometric mean. p Values were calculated using the Mann–Whitney test. **(B)** Plasma levels of plasma levels of neutrophil elastase (NE), myeloperoxidase (MPO), and proteinase-3 (PTN-3) from (INF; $n = 60$) or (UN; $n = 58$) individuals were measured by ELISA. Data are shown as scatter plots with the bar representing the geometric mean. p Values were calculated using the Mann–Whitney test. **(C)** Plasma levels of plasma levels of mast cell tryptase (MCT), leukotriene C4 (LTC4), and carboxypeptidase A-3 (CPA-3) from INF ($n = 60$) or UN ($n = 58$) individuals were measured by ELISA. Data are shown as scatter plots with the bar representing the geometric mean. p Values were calculated using the Mann–Whitney test with Holm's correction for multiple comparisons.

45.12 pg/ml in INF vs. 37.26 pg/ml in UN; $p = 0.0340$) in comparison to UN individuals.

Ss Infection Is Associated with Decreased Levels of Eosinophils, Neutrophils, and Mast Cell Granular Proteins following Anthelminthic Treatment

To determine the outcome of treatment on the levels of these granulocyte-associated proteins in those with *Ss* infection, all INF individuals were treated, and the levels of eosinophil granular proteins (ECP, EDN, EPX, and MBP), neutrophil granular proteins (NE, MPO, and PTN-3), and mast cell products (MCT, LTC4, and CPA-3) were measured in INF individuals before and after anthelminthic treatment. As shown in **Figure 3A**, the systemic levels of ECP (GM of 71.18 ng/ml in pre-T vs. 57.78 ng/ml in post-T; $p = 0.0007$), EDN (GM of 1.811 ng/ml in pre-T vs. 1.365 ng/ml in post-T; $p = 0.0006$), EPX (GM of 1,1945 ng/ml in pre-T vs. 1,1146 ng/ml in post-T; $p = 0.0005$), and MBP (GM of 288.4 ng/ml in pre-T vs. 167 ng/ml in post-T; $p = 0.0084$) were significantly decreased in INF individuals following anthelmintic treatment. For the neutrophil-associated

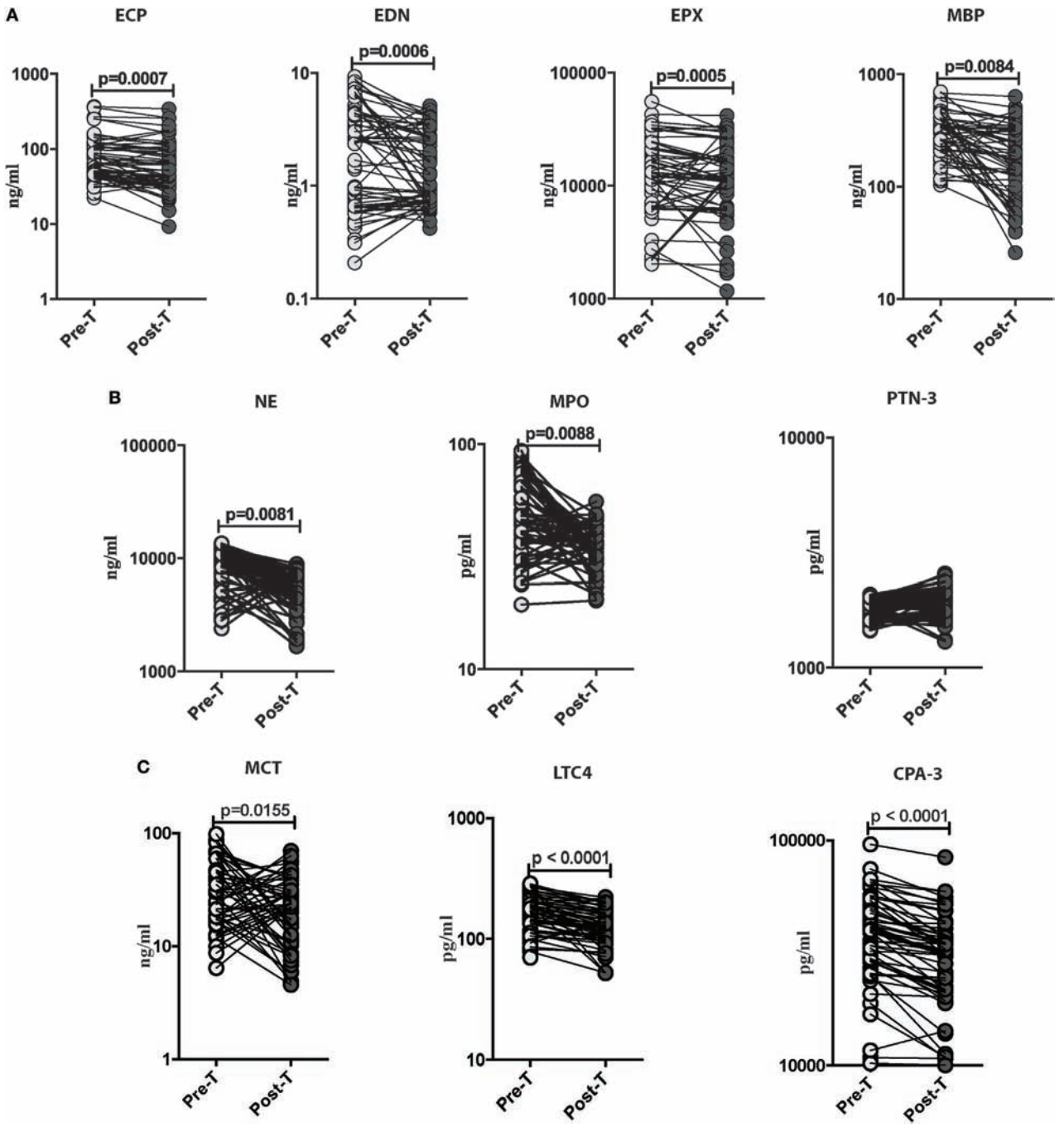

FIGURE 3 | *Strongyloides stercoralis* (*Ss*) infection is associated with decreased levels of eosinophils, neutrophils, and mast cell granular proteins following anthelminthic treatment. **(A)** Plasma levels of eosinophil cationic protein (ECP), eosinophil-derived neurotoxin (EDN), eosinophil peroxidase (EPX), and major basic protein (MBP), from *Ss*-infected pre treatment (pre-T; $n = 60$) and 6 months following treatment from posttreatment (post-T) individuals were measured by ELISA. *p* Values were calculated using the Wilcoxon matched pair test. **(B)** Plasma levels of neutrophil elastase (NE), myeloperoxidase (MPO), and proteinase-3 (PTN-3) from *Ss* infected (pre-T; $n = 60$) and 6 months following treatment from post-T individuals were measured by ELISA. *p* Values were calculated using the Wilcoxon matched pair test. **(C)** Plasma levels of mast cell tryptase (MCT), leukotriene C4 (LTC4), and carboxypeptidase A3 (CPA-3) from *Ss*-infected (pre-T; $n = 60$) and 6 months following treatment from post-T individuals were measured by ELISA. *p* Values were calculated using the Wilcoxon matched pair test with Holm's correction for multiple comparisons.

proteins, as shown in **Figure 3B**, the systemic levels of NE (GM of 8,456 ng/ml in pre-T vs. 4,491 ng/ml in post-T; $p = 0.0081$) and MPO (GM of 45.12 pg/ml in pre-T vs. 36.58 pg/ml in post-T; $p = 0.0088$) were significantly decreased in INF individuals following anthelmintic treatment. Furthermore, the systemic levels of MCT (GM of 8,456 ng/ml in pre-T vs. 4,491 ng/ml in post-T;

$p = 0.0081$), LTC4 (GM of 45.12 pg/ml in pre-T vs. 36.58 pg/ml in post-T; $p = 0.0088$), and CPA-3 (GM of 45.12 pg/ml in pre-T vs. 36.58 pg/ml in post-T; $p = 0.0088$) were also significantly diminished in INF individuals following anthelmintic treatment (**Figure 3C**).

Relationship between Eosinophils, Neutrophils, and Mast Cell Granular Protein Levels and Absolute Numbers of Eosinophils, Neutrophils, and Basophils in INF Individuals

The relationships between the levels of eosinophils, neutrophils, and mast cell granular proteins and the absolute numbers of eosinophils, neutrophils, and basophils were next assessed (**Figure 4A**). There was a significant positive correlation between absolute eosinophil count (AEC) and the levels of ECP ($r = 0.2413$; $p = 0.0085$), EPX ($r = 0.2196$; $p = 0.0169$), and MBP ($r = 0.1918$; $p = 0.0375$). There was also a significant positive correlation between levels of NE ($r = 0.2637$; $p = 0.0039$) and MPO ($r = 0.2006$; $p = 0.0294$) and the absolute neutrophil count (ANC). Finally, there was also a significant positive correlation between the levels of MCT ($r = 0.2637$; $p = 0.0039$) and the absolute basophil count. Next, we assessed the correlation between the post anthelmintic treatment levels of eosinophils, neutrophils, and mast cell granular proteins and the absolute numbers of eosinophils, neutrophils, and basophils. We did not find any significant correlation between granular proteins and the absolute numbers of eosinophils, neutrophils, and basophils at the post-T time point (**Figure 4B**).

DISCUSSION

Eosinophils are one of the foremost components of the immune system, which play a prominent role in parasitic infections. Eosinophilia is a hallmark of helminth infections, and in some host–parasite interactions, eosinophils have been witnessed to kill worms and mediate protective immunity (6, 23, 24). Eosinophils are also presumed to play a role as APCs for the initiation of the primary and secondary Th2 immune responses to *S. stercoralis* (25), indicating an elemental role for eosinophils at the boundary between innate and adaptive immune responses. Eosinophils have secondary granules, which contain MBP, ECP, EDN, and EPO, and which are directly toxic to the larvae of *S. stercoralis* (26, 27).

Eosinophils and antibodies play a crucial function in defense mechanisms against *S. stercoralis* larvae in innate (28) and adaptive immune responses (29). Previous studies have shown that mice deficient in MBP and (30) and EPO (31) are more susceptible to Strongyloides infection. O'Connell et al. have shown that MBP involved in eosinophil-mediated larval killing (12). ECP and EDN possess ribonuclease activity that form pores into the membrane of target cells, facilitating the entry of other toxic molecules into the cells with subsequent degeneration (26). Plasma levels of eosinophil granule proteins deliver an indirect measure of degranulation in the tissues and

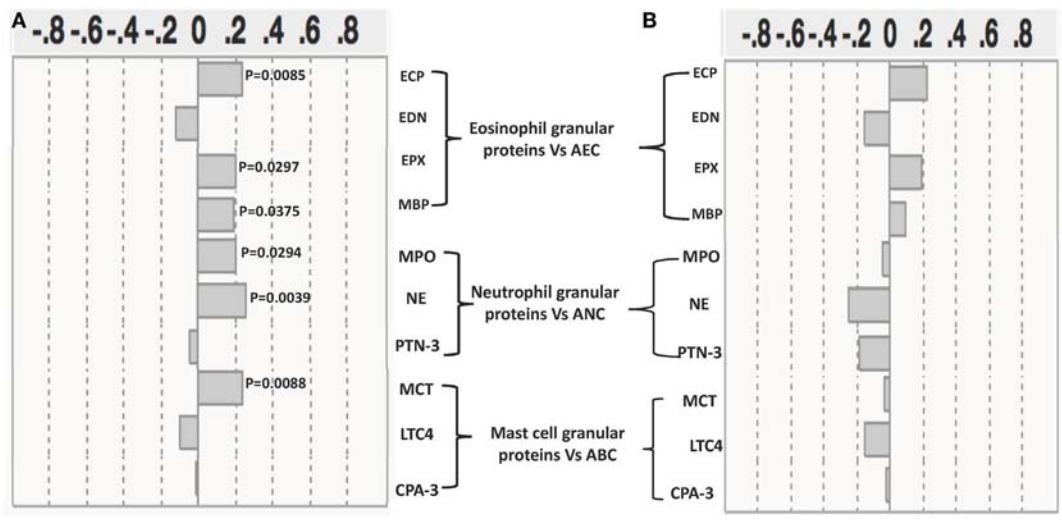

FIGURE 4 | Relationship between eosinophil, neutrophil, and mast cell granular protein levels and absolute numbers of eosinophils, neutrophils, and basophils in *Strongyloides stercoralis* (*Ss*)-infected individuals and following anthelminthic treatment. **(A)** The absolute count of eosinophils was correlated with plasma levels of eosinophil cationic protein (ECP), eosinophil-derived neurotoxin (EDN), eosinophil peroxidase (EPX), and major basic protein (MBP); the absolute count of neutrophils was correlated with plasma levels of neutrophil elastase (NE), myeloperoxidase (MPO), and proteinase-3 (PTN-3), and the absolute count of neutrophils were correlated with plasma levels of mast cell tryptase (MCT), leukotriene C4 (LTC4), and carboxypeptidase A-3 in *Ss*-infected individuals ($n = 60$). **(B)** The absolute count of eosinophils correlation with plasma levels of ECP, EDN, EPX, and MBP; the absolute count of neutrophils correlation with plasma levels of NE, MPO, and PTN-3; and the absolute count of neutrophils correlation with plasma levels of MCT, LTC4, and carboxypeptidase A-3 (CPA-3) in *Ss*-infected following anthelmintic treated individuals ($n = 60$). *p* and *r* values were calculated using the Spearman rank correlation test using JMP software.

are prominently augmented in many helminth-infected patients (32). Our data also show that eosinophil granular protein levels were increased in INF individuals. Earlier studies on onchocerciasis, lymphatic filarisis, schistosomiasis, and loiasis showed that ECP and EDN/EPX levels were elevated (32, 33). The serum concentrations of these proteins emerge consequently to reflect the functional activity of the corresponding granulocyte effector system in the host. In our study, we observed that there was a positive correlation between plasma levels of ECP, EPX and MBP, and the AEC, a finding similar to that seen in loiasis (32, 33). Thus, eosinophil granular proteins appear to reflect eosinophil activation.

Neutrophils are involved in the activation, regulation, and effector functions of innate and adaptive immune cells (34). NE and PTN-3 are directly involved in intracellular killing of phagocytosed bacteria in phagolysosomes, in conjunction with MPO and reactive oxygen species (35). During certain helminth infections, as with non-helminth induced inflammation, neutrophils are often the first cells to be recruited; these can mediate a degree of protective immunity against nematode parasites, as has been revealed most conclusively in the *Strongyloides sp.* model (9, 36, 37). Maximum killing happened by neutrophils when EPO from eosinophils attached to the surface of *S. mansoni* (38). In other mouse models, purified neutrophils have been shown to independently kill Strongyloides larvae (39). In addition, neutrophils are known to mediate adult worm killing through an MPO-dependent mechanism (12, 40). In our study, NE and MPO levels were significantly increased in INF individuals, and the levels were significantly associated with ANCs. This is similar to an earlier study on *Onchocerca volvulus* infection that showed that the plasma level of MPO was correlated with ANC (32, 41). Changes in the PTN-3 levels may be due to increased production during inflammatory activity and neutrophil or mononuclear cell leakage/degranulation. PTN-3 has antimicrobial properties and is known to efficiently kill bacteria (41). However, in our study, PTN-3 did not show any significant alterations in Ss infection. Thus, neutrophil granular proteins, similar to their eosinophil counterparts, appear to reflect neutrophil-mediated activation in *Ss* infection.

Mast cell tryptase, CPA-3, and arachidonic acid-derived lipid mediators such as LTC4 are produced during mast cell activation (42, 43). MCT is a major protein product of human mast cells (44). During the activation of mast cells, MCT levels have been shown to be elevated in anaphylaxis (45) and systemic mastocytosis (46). Infection with *T. spiralis* has shown increased numbers of gastrointestinal tract mast cells and associated levels of LTC4, that was felt to be involved in rapid worm expulsion (47). In line with these data, INF individuals showed significantly increased levels of MCT, CPA-3, and LTC4 when compared with UN individuals.

Earlier studies have demonstrated that eosinophils and neutrophils are the key players mediating microfilarial killing following anthelmintic treatment (48). Destruction of parasites occurs through eosinophil degranulation after anthelmintic treatment with DEC or ivermectin (49, 50). Cooper et al. showed that plasma levels of MCT increased following treatment for onchocerciasis (51). In this study, we show that the augmented levels of eosinophils, neutrophils, and mast cell granular proteins are significantly diminished at 6 months following treatment. This indicates that the release of these granular proteins is intimately related to the presence of active helminth infection and that elimination of the parasite removes the stimulus for increased release of these factors.

Our study adds to the growing body of literature showing the importance of granulocytes and their activation in helminth infections. While the roles of neutrophils in animal models of helminth infections are well studied (36), very scant data exist on the role of these important innate mediators in human helminth infection. Thus, our study derives strength from the fairly large sample size and the homogeneity of the population studied. Further studies exploring the exact role of these granular proteins should provide valuable insight into the regulation of the protective or pathogenic immune response in helminth infections at large.

ETHICS STATEMENT

All individuals were examined as part of a natural history study protocol approved by Institutional Review Boards of the National Institute of Allergy and Infectious Diseases (USA) and the National Institute for Research in Tuberculosis (India), and informed written consent was obtained from all participants.

AUTHOR CONTRIBUTIONS

Conceived and designed the experiments: AR and SB. Performed the experiments: AR, SM, and YB. Analyzed the data: AR and SB. Contributed reagents/materials/analysis tools: CD and TN. Wrote the paper: AR, TN, and SB.

ACKNOWLEDGMENTS

We thank Dr. M. Satiswaran and Prabbu Balakrishnan for valuable assistance in collecting the clinical data for this study. We thank the staff of the Department of Epidemiology, NIRT, for valuable assistance in recruiting the patients for this study.

FUNDING

This work was funded by the Division of Intramural Research, NIAID, NIH.

REFERENCES

1. Puthiyakunnon S, Boddu S, Li Y, Zhou X, Wang C, Li J, et al. Strongyloidiasis – an insight into its global prevalence and management. *PLoS Negl Trop Dis* (2014) 8:e3018. doi:10.1371/journal.pntd.0003018
2. Oppenheim JJ, Yang D. Alarmins: chemotactic activators of immune responses. *Curr Opin Immunol* (2005) 17:359–65. doi:10.1016/j.coi.2005.06.002
3. Reimert CM, Fitzsimmons CM, Joseph S, Mwatha JK, Jones FM, Kimani G, et al. Eosinophil activity in *Schistosoma mansoni* infections in vivo and in vitro in relation to plasma cytokine profile pre- and posttreatment

with praziquantel. *Clin Vaccine Immunol* (2006) 13:584–93. doi:10.1128/CVI.13.5.584-593.2006
4. Gessner A, Mohrs K, Mohrs M. Mast cells, basophils, and eosinophils acquire constitutive IL-4 and IL-13 transcripts during lineage differentiation that are sufficient for rapid cytokine production. *J Immunol* (2005) 174:1063–72. doi:10.4049/jimmunol.174.2.1063
5. Walsh GM. Eosinophil granule proteins and their role in disease. *Curr Opin Hematol* (2001) 8:28–33. doi:10.1097/00062752-200101000-00006
6. Klion AD, Nutman TB. The role of eosinophils in host defense against helminth parasites. *J Allergy Clin Immunol* (2004) 113:30–7. doi:10.1016/j.jaci.2003.10.050
7. Brattig NW, Tischendorf FW, Strote G, Medina-De La Garza CE. Eosinophil-larval-interaction in onchocerciasis: heterogeneity of in vitro adherence of eosinophils to infective third and fourth stage larvae and microfilariae of *Onchocerca volvulus*. *Parasite Immunol* (1991) 13:13–22. doi:10.1111/j.1365-3024.1991.tb00259.x
8. Herbert DR, Nolan TJ, Schad GA, Abraham D. The role of B cells in immunity against larval *Strongyloides stercoralis* in mice. *Parasite Immunol* (2002) 24:95–101. doi:10.1046/j.0141-9838.2001.00441.x
9. Watanabe K, Noda K, Hamano S, Koga M, Kishihara K, Nomoto K, et al. The crucial role of granulocytes in the early host defense against *Strongyloides ratti* infection in mice. *Parasitol Res* (2000) 86:188–93. doi:10.1007/s004360050030
10. Jong EC, Mahmoud AA, Klebanoff SJ. Peroxidase-mediated toxicity to schistosomula of *Schistosoma mansoni*. *J Immunol* (1981) 126:468–71.
11. Buys J, Wever R, Ruitenberg EJ. Myeloperoxidase is more efficient than eosinophil peroxidase in the in vitro killing of newborn larvae of *Trichinella spiralis*. *Immunology* (1984) 51:601–7.
12. O'Connell AE, Hess JA, Santiago GA, Nolan TJ, Lok JB, Lee JJ, et al. Major basic protein from eosinophils and myeloperoxidase from neutrophils are required for protective immunity to *Strongyloides stercoralis* in mice. *Infect Immun* (2011) 79:2770–8. doi:10.1128/IAI.00931-10
13. Freudenstein-Dan A, Gold D, Fishelson Z. Killing of schistosomes by elastase and hydrogen peroxide: implications for leukocyte-mediated schistosome killing. *J Parasitol* (2003) 89:1129–35. doi:10.1645/GE-96R
14. Bulfone-Paus S, Bahri R. Mast cells as regulators of T cell responses. *Front Immunol* (2015) 6:394. doi:10.3389/fimmu.2015.00394
15. Weller CL, Collington SJ, Williams T, Lamb JR. Mast cells in health and disease. *Clin Sci (Lond)* (2011) 120:473–84. doi:10.1042/CS20100459
16. Melendez AJ, Harnett MM, Pushparaj PN, Wong WS, Tay HK, Mcsharry CP, et al. Inhibition of Fc epsilon RI-mediated mast cell responses by ES-62, a product of parasitic filarial nematodes. *Nat Med* (2007) 13:1375–81. doi:10.1038/nm1654
17. Pennock JL, Grencis RK. The mast cell and gut nematodes: damage and defence. *Chem Immunol Allergy* (2006) 90:128–40. doi:10.1159/000088885
18. Abe T, Nawa Y. Worm expulsion and mucosal mast cell response induced by repetitive IL-3 administration in *Strongyloides ratti*-infected nude mice. *Immunology* (1988) 63:181–5.
19. Marshall JS. Mast-cell responses to pathogens. *Nat Rev Immunol* (2004) 4:787–99. doi:10.1038/nri1460
20. Bisoffi Z, Buonfrate D, Sequi M, Mejia R, Cimino RO, Krolewiecki AJ, et al. Diagnostic accuracy of five serologic tests for *Strongyloides stercoralis* infection. *PLoS Negl Trop Dis* (2014) 8:e2640. doi:10.1371/journal.pntd.0002640
21. Buonfrate D, Sequi M, Mejia R, Cimino RO, Krolewiecki AJ, Albonico M, et al. Accuracy of five serologic tests for the follow up of *Strongyloides stercoralis* infection. *PLoS Negl Trop Dis* (2015) 9:e0003491. doi:10.1371/journal.pntd.0003491
22. Sato Y, Kobayashi J, Toma H, Shiroma Y. Efficacy of stool examination for detection of *Strongyloides* infection. *Am J Trop Med Hyg* (1995) 53:248–50. doi:10.4269/ajtmh.1995.53.248
23. Huang L, Appleton JA. Eosinophils in helminth infection: defenders and dupes. *Trends Parasitol* (2016) 32:798–807. doi:10.1016/j.pt.2016.05.004
24. Huang L, Gebreselassie NG, Gagliardo LF, Ruyechan MC, Luber KL, Lee NA, et al. Eosinophils mediate protective immunity against secondary nematode infection. *J Immunol* (2015) 194:283–90. doi:10.4049/jimmunol.1402219
25. Padigel UM, Lee JJ, Nolan TJ, Schad GA, Abraham D. Eosinophils can function as antigen-presenting cells to induce primary and secondary immune responses to *Strongyloides stercoralis*. *Infect Immun* (2006) 74:3232–8. doi:10.1128/IAI.02067-05
26. Weller PF. The immunobiology of eosinophils. *N Engl J Med* (1991) 324:1110–8. doi:10.1056/NEJM199104183241607
27. Zuo L, Rothenberg ME. Gastrointestinal eosinophilia. *Immunol Allergy Clin North Am* (2007) 27:443–55. doi:10.1016/j.iac.2007.06.002
28. Satoh M, Toma H, Sato Y, Kikuchi M, Takara M, Shiroma Y, et al. Production of a high level of specific IgG4 antibody associated with resistance to albendazole treatment in HLA-DRB1*0901-positive patients with strongyloidiasis. *Am J Trop Med Hyg* (1999) 61:668–71. doi:10.4269/ajtmh.1999.61.668
29. Mir A, Benahmed D, Igual R, Borras R, O'Connor JE, Moreno MJ, et al. Eosinophil-selective mediators in human strongyloidiasis. *Parasite Immunol* (2006) 28:397–400. doi:10.1111/j.1365-3024.2006.00826.x
30. Denzler KL, Farmer SC, Crosby JR, Borchers M, Cieslewicz G, Larson KA, et al. Eosinophil major basic protein-1 does not contribute to allergen-induced airway pathologies in mouse models of asthma. *J Immunol* (2000) 165:5509–17. doi:10.4049/jimmunol.165.10.5509
31. Denzler KL, Borchers MT, Crosby JR, Cieslewicz G, Hines EM, Justice JP, et al. Extensive eosinophil degranulation and peroxidase-mediated oxidation of airway proteins do not occur in a mouse ovalbumin-challenge model of pulmonary inflammation. *J Immunol* (2001) 167:1672–82. doi:10.4049/jimmunol.167.3.1672
32. Tischendorf FW, Brattig NW, Burchard GD, Kubica T, Kreuzpaintner G, Lintzel M. Eosinophils, eosinophil cationic protein and eosinophil-derived neurotoxin in serum and urine of patients with onchocerciasis coinfected with intestinal nematodes and in urinary schistosomiasis. *Acta Trop* (1999) 72:157–73. doi:10.1016/S0001-706X(98)00088-6
33. Herrick JA, Metenou S, Makiya MA, Taylar-Williams CA, Law MA, Klion AD, et al. Eosinophil-associated processes underlie differences in clinical presentation of loiasis between temporary residents and those indigenous to Loa-endemic areas. *Clin Infect Dis* (2015) 60:55–63. doi:10.1093/cid/ciu723
34. Mantovani A, Cassatella MA, Costantini C, Jaillon S. Neutrophils in the activation and regulation of innate and adaptive immunity. *Nat Rev Immunol* (2011) 11:519–31. doi:10.1038/nri3024
35. Kobayashi SD, Voyich JM, Burlak C, DeLeo FR. Neutrophils in the innate immune response. *Arch Immunol Ther Exp (Warsz)* (2005) 53(6):505–17.
36. Bonne-Annee S, Kerepesi LA, Hess JA, O'Connell AE, Lok JB, Nolan TJ, et al. Human and mouse macrophages collaborate with neutrophils to kill larval *Strongyloides stercoralis*. *Infect Immun* (2013) 81:3346–55. doi:10.1128/IAI.00625-13
37. Bonne-Annee S, Hess JA, Abraham D. Innate and adaptive immunity to the nematode *Strongyloides stercoralis* in a mouse model. *Immunol Res* (2011) 51:205–14. doi:10.1007/s12026-011-8258-2
38. Jong EC, Chi EY, Klebanoff SJ. Human neutrophil-mediated killing of schistosomula of *Schistosoma mansoni*: augmentation by schistosomal binding of eosinophil peroxidase. *Am J Trop Med Hyg* (1984) 33:104–15. doi:10.4269/ajtmh.1984.33.104
39. Galioto AM, Hess JA, Nolan TJ, Schad GA, Lee JJ, Abraham D. Role of eosinophils and neutrophils in innate and adaptive protective immunity to larval *Strongyloides stercoralis* in mice. *Infect Immun* (2006) 74:5730–8. doi:10.1128/IAI.01958-05
40. Doyle AD, Jacobsen EA, Ochkur SI, Mcgarry MP, Shim KG, Nguyen DT, et al. Expression of the secondary granule proteins major basic protein 1 (MBP-1) and eosinophil peroxidase (EPX) is required for eosinophilopoiesis in mice. *Blood* (2013) 122:781–90. doi:10.1182/blood-2013-01-473405
41. Sørensen OE, Follin P, Johnsen AH, Calafat J, Tjabringa GS, Hiemstra PS, et al. Human cathelicidin, hCAP-18, is processed to the antimicrobial peptide LL-37 by extracellular cleavage with proteinase 3. *Blood* (2001) 97:3951–9. doi:10.1182/blood.V97.12.3951.
42. Goldstein SM, Kaempfer CE, Proud D, Schwartz LB, Irani AM, Wintroub BU. Detection and partial characterization of a human mast cell carboxypeptidase. *J Immunol* (1987) 139:2724–9.
43. Schechter NM, Irani AM, Sprows JL, Abernethy J, Wintroub B, Schwartz LB. Identification of a cathepsin G-like proteinase in the MCTC type of human mast cell. *J Immunol* (1990) 145:2652–61.
44. Schwartz LB. Diagnostic value of tryptase in anaphylaxis and mastocytosis. *Immunol Allergy Clin North Am* (2006) 26:451–63. doi:10.1016/j.iac.2006.05.010

45. Vliagoftis H, Lacy P, Luy B, Adamko D, Hollenberg M, Befus D, et al. Mast cell tryptase activates peripheral blood eosinophils to release granule-associated enzymes. *Int Arch Allergy Immunol* (2004) 135:196–204. doi:10.1159/000081304
46. Stone KD, Prussin C, Metcalfe DD. IgE, mast cells, basophils, and eosinophils. *J Allergy Clin Immunol* (2010) 125:S73–80. doi:10.1016/j.jaci.2009.11.017
47. Knight PA, Brown JK, Pemberton AD. Innate immune response mechanisms in the intestinal epithelium: potential roles for mast cells and goblet cells in the expulsion of adult *Trichinella spiralis*. *Parasitology* (2008) 135:655–70. doi:10.1017/S0031182008004319
48. Tischendorf FW, Brattig NW, Hoyer A, Medina-De La Garza CE, Geisinger F. Modulatory effects of antifilarial drugs ivermectin, CGP 6140 and CGP 20376 on the oxidative burst of eosinophilic granulocytes. *Acta Trop* (1993) 53:27–37. doi:10.1016/0001-706X(93)90003-T
49. Racz P, Tenner-Racz K, Luther B, Buttner DW, Albiez EJ. Immunopathologic aspects in human onchocercal lymphadenitis. *Bull Soc Pathol Exot Filiales* (1983) 76:676–80.
50. Wildenburg G, Darge K, Knab J, Tischendorf FW, Bonow I, Buttner DW. Lymph nodes of onchocerciasis patients after treatment with ivermectin: reaction of eosinophil granulocytes and their cationic granule proteins. *Trop Med Parasitol* (1994) 45:87–96.
51. Cooper PJ, Schwartz LB, Irani AM, Awadzi K, Guderian RH, Nutman TB. Association of transient dermal mastocytosis and elevated plasma tryptase levels with development of adverse reactions after treatment of onchocerciasis with ivermectin. *J Infect Dis* (2002) 186:1307–13. doi:10.1086/344318

Conflict of Interest Statement: The authors declare that the research was conducted in the absence of any commercial or financial relationships that could be construed as a potential conflict of interest.

The reviewer WK and handling Editor declared their shared affiliation.

frontiers in Microbiology

ORIGINAL RESEARCH
published: 05 June 2018
doi: 10.3389/fmicb.2018.01177

CD100/Sema4D Increases Macrophage Infection by *Leishmania (Leishmania) amazonensis* in a CD72 Dependent Manner

*Mariana K. Galuppo[1], Eloiza de Rezende[1], Fabio L. Forti[2], Mauro Cortez[1], Mario C. Cruz[3], Andre A. Teixeira[2], Ricardo J. Giordano[2] and Beatriz S. Stolf[1]**

[1] Department of Parasitology, Institute of Biomedical Sciences, University of São Paulo, São Paulo, Brazil, [2] Department of Biochemistry, Institute of Chemistry, University of São Paulo, São Paulo, Brazil, [3] Department of Immunology, Institute of Biomedical Sciences, University of São Paulo, São Paulo, Brazil

Leishmaniasis is caused by trypanosomatid protozoa of the genus *Leishmania*, which infect preferentially macrophages. The disease affects 12 million people worldwide, who may present cutaneous, mucocutaneous or visceral forms. Several factors influence the form and severity of the disease, and the main ones are the *Leishmania* species and the host immune response. CD100 is a membrane bound protein that can also be shed. It was first identified in T lymphocytes and latter shown to be induced in macrophages by inflammatory stimuli. The soluble CD100 (sCD100) reduces migration and expression of inflammatory cytokines in human monocytes and dendritic cells, as well as the intake of oxidized low-density lipoprotein (oxLDL) by human macrophages. Considering the importance of macrophages in *Leishmania* infection and the potential role of sCD100 in the modulation of macrophage phagocytosis and activation, we analyzed the expression and distribution of CD100 in murine macrophages and the effects of sCD100 on macrophage infection by *Leishmania (Leishmania) amazonensis.* Here we show that CD100 expression in murine macrophages increases after infection with *Leishmania*. sCD100 augments infection and phagocytosis of *Leishmania (L.) amazonensis* promastigotes by macrophages, an effect dependent on macrophage CD72 receptor. Besides, sCD100 enhances phagocytosis of zymosan particles and infection by *Trypanosoma cruzi*.

Keywords: CD100, *Leishmania amazonensis*, macrophages, phagocytosis, infection index, CD72

OPEN ACCESS

Edited by:
Juarez Antonio Simões Quaresma, Instituto Evandro Chagas, Brazil

Reviewed by:
Debora Decote-Ricardo, Universidade Federal Rural do Rio de Janeiro, Brazil
Wenbin Tuo, Agricultural Research Service (USDA), United States

****Correspondence:***
Beatriz S. Stolf
bstolf@usp.br

Specialty section:
This article was submitted to Microbial Immunology, a section of the journal Frontiers in Microbiology

Received: *27 September 2017*
Accepted: *15 May 2018*
Published: *05 June 2018*

Citation:
Galuppo MK, de Rezende E, Forti FL, Cortez M, Cruz MC, Teixeira AA, Giordano RJ and Stolf BS (2018) CD100/Sema4D Increases Macrophage Infection by Leishmania (Leishmania) amazonensis in a CD72 Dependent Manner. Front. Microbiol. 9:1177. doi: 10.3389/fmicb.2018.01177

INTRODUCTION

Leishmaniasis is a complex of diseases caused by trypanosomatid protozoa of the genus *Leishmania,* which can be grouped into cutaneous or visceral forms (Alvar et al., 2012). Due to their considerable impact on global health, leishmaniasis are listed among the priority endemic diseases of the World Health Organization (WHO). It is estimated that 12 million people in the world are infected, and about 1.5 million new cases are reported every year (Alvar et al., 2012). The disease currently affects 98 countries, and in Brazil it has been observed an increase in the number of cases in recent years, accompanied by their geographical spread (WHO, 2015). Many species of *Leishmania* cause leishmaniasis in humans. The parasite species as well as the host immune response are the main determinants of the clinical form and the course of the disease (McMahon-Pratt and Alexander, 2004). The available treatment options for many *Leishmania*

species and clinical forms are toxic and not always effective (McGwire and Satoskar, 2014). Thus, understanding the molecular basis of infection may be an important step toward the development of novel therapeutic approaches for this disease.

Leishmania is an intracellular parasite that infects mononuclear phagocytic cells of vertebrates. Macrophages are the main parasite host cells and their activation is crucial for the resolution of the infection (Iniesta et al., 2002, 2005). The general process of phagocytosis is an essential mechanism of the innate immune response by which phagocytes such as macrophages internalize microorganisms, dead or dying cells, and debris. It is an actin-dependent process triggered by the interaction between phagocyte's receptors and ligands of the particle to be engulfed (May and Machesky, 2001; Underhill and Goodridge, 2012).

The receptors most frequently involved in the phagocytosis of *Leishmania* are complement receptors 3 (CR3) and 1 (CR1), mannose receptor (MR), fibronectin receptor (FnR) and receptors Fc gamma (FcγRs) (Blackwell et al., 1985; Mosser and Edelson, 1985; Wyler et al., 1985; Da Silva et al., 1989; Guy and Belosevic, 1993). The receptors and internalization pathways may vary depending on the parasite stage (Ueno and Wilson, 2012). The actin cytoskeleton also plays important role in *Leishmania* binding and internalization, and was studied in more detail in *L. (Leishmania) donovani* (May et al., 2000; Roy et al., 2014; Podinovskaia and Descoteaux, 2015). The association of polymerized F-actin and parasite binding was also shown for *L. (Viannia) braziliensis* (Azevedo et al., 2012), *L.* (*L.*) *amazonensis,* and *L. (Leishmania) major* (Courret et al., 2002).

CD100, also known as Sema4D, belongs to class IV of semaphorins and was the first semaphorin described in the immune system (Bougeret et al., 1992; Mizui et al., 2009; Ch'ng and Kumanogoh, 2010). It exists as a membrane bound dimer or as a soluble protein originated by proteolytic cleavage (Elhabazi et al., 2003; Basile et al., 2007) that interacts with specific receptors, mainly plexin B1 (Basile et al., 2004; Conrotto et al., 2005; Nkyimbeng-Takwi and Chapoval, 2011) and CD72 (Kumanogoh et al., 2000; Ishida et al., 2003; Smith et al., 2011).

CD100 is expressed by the majority of the cells of the hematopoietic system, including B and T lymphocytes, natural killer and myeloid cells, and its expression usually increases upon activation (Elhabazi et al., 2003). Membrane CD100 is cleaved from the cell surface in an activation-dependent manner (Kikutani and Kumanogoh, 2003). In fact, sCD100 is shed by activated T and B cells, and sCD100 can be detected in sera of mice immunized with T-cell–dependent antigens or in sera of MRL/lpr mice with autoimmune disease (Wang et al., 2001). In mice, sCD100 increases proliferation, differentiation and IgG1 production by stimulated B cells (Kumanogoh et al., 2000; Shi et al., 2000). CD100 mediates DC-T cell interaction increasing activation, proliferation and differentiation of T cells (Shi et al., 2000; Kumanogoh et al., 2002; Mizui et al., 2009), and inducing DC maturation (Kumanogoh et al., 2002). In humans, sCD100 inhibits migration of B cells (Delaire et al., 2001), monocytes and immature DCs (Chabbert-de Ponnat et al., 2005). It also increases IL-10 secretion and reduces IL-6, IL-8 and TNF-α in monocytes and DCs (Chabbert-de Ponnat et al., 2005).

Although it is known that CD100 is expressed in macrophages (Kikutani and Kumanogoh, 2003; Nkyimbeng-Takwi and Chapoval, 2011), few studies have reported its effects on these cells. One of them analyzed the role of macrophage shed sCD100 in tumor angiogenesis (Sierra et al., 2008). Other showed that CD100 is also important in glomerular nephritis, enhancing T and B cell activation and the recruitment of macrophages (Li et al., 2009). We have shown that macrophages from human atherosclerotic plaques express CD100, and that sCD100 inhibits internalization of oxidized LDL (Luque et al., 2013). We have also shown that CD100 participates on the interaction between human monocyte and endothelial cell by binding to plexins B1 and B2 (Luque et al., 2015).

The effect of sCD100 on oxLDL phagocytosis by macrophage, the main *Leishmania* host cells, prompted us to study the expression of this molecule and its effects on the phagocytosis of this parasite. *Leishmania* lesions are characterized by intense inflammatory infiltrates, and thus sCD100 is probably shed by activated T and B cells near infected and non-infected macrophages. Here we show that sCD100 increases macrophage phagocytosis of *L.* (*L.*) *amazonensis* promastigotes, *Trypanosoma cruzi* trypomastigotes and zymosan particles. In addition, we demonstrated that sCD100 effects depend on macrophage CD72, a receptor for CD100. This is the first report of CD100 effect on a parasitic infection, and further studies should address the role of this molecule in animal models of leishmaniasis.

MATERIALS AND METHODS

Leishmania (*Leishmania*) *amazonensis* Promastigotes

Promastigotes of *L.* (*L.*) *amazonensis* LV79 strain (MPRO/BR/72/M1841) were cultured at 24°C in M199 medium supplemented with 10% fetal calf serum (FCS). Parasites were subcultured every 7 days at an initial inoculum of 2×10^6/mL.

When indicated, promastigotes were incubated for 2 h with 200 ng/ml sCD100 in M199 at 24°C, centrifuged at 2,500 × *g* for 10 min and resuspended in RPMI 1640 medium supplemented with 10% FBS for subsequent infection of peritoneal macrophages.

Ethics Statement

All animals were used according to the Brazilian College of Animal Experimentation guidelines, and the protocols were approved by the Institutional Animal Care and Use Committee (CEUA) of the University of São Paulo (protocol number 001/2009).

Recombinant sCD100 Production

sCD100 protein fused to Fc portion of IgG was produced in HEK (human embryonic kidney) 293T cells transfected with CD100-Fc plasmid, kindly given byKumanogoh et al. (2000). Briefly, $7{,}5 \times 10^6$ HEK cells were plated in DMEM with 5% serum "low-IgG" (Life Technologies) supplemented with 2 mM L-glutamine, 1 mM sodium pyruvate and 1× antibiotic-antimycotic solution (Life Technologies). Ten micrograms of

CD100-Fc plasmid were mixed with 1 mL of a 150 mM NaCl solution and then with 100 μL of a polyethylenimine solution (PEI, Sigma) at 0.45 mg/mL. The total volume was added slowly to each dish, which was then incubated at 37°C with 5% CO2 for 7 days. After this period, supernatants of cell cultures were collected, filtered through a 0.22 μm membrane and centrifuged at 7,500 × *g* for 10 min. PMSF to 100 μM was added to the supernatant and proteins were precipitated with 60% w/v ammonium sulfate under slow stirring at 4°C for 24 h. Two successive centrifugations at 10,000 × *g* for 45 min were performed, precipitates were resuspended in PBS and centrifuged. The supernatant was incubated with protein G beads (1 mL Protein G Sepharose 4FF GE beads/50 mL supernatant) under rotation at 4°C for 24 h. The suspension was then centrifuged at 800 × *g* for 5 min and the beads were transferred to a chromatography column (Bio-Rad). The column was washed twice with 5 mL ice cold PBS and protein was eluted in aliquots of 500 μL using 0.1 M glycine buffer, pH 3.0, neutralized by 50 μl 1 M Tris buffer pH 8.0. Protein concentrations were determined by Bradford (Bio-Rad) and sCD100 was analyzed by SDS–PAGE and Western blot.

Macrophage Infection With *Leishmania* and Phagocytosis of Zymosan

Peritoneal macrophages were isolated as previously described (Velasquez et al., 2016). We then transferred 8×10^5 cells in RPMI 1640 pH 7.2 to each well of 24 well plates laid with 13 mm circular coverslips. After 2 h of incubation at 37°C in 5% CO_2, the medium was changed to RPMI with 10% FCS with or without 100 or 200 ng/mL sCD100 and cells were incubated until the next day. Infection was performed with *L. (L.) amazonensis* promastigotes at the beginning of stationary phase (day four) using a multiplicity of infection (MOI) of 5:1 for 4 h. After removing the non-internalized parasites, cells were further incubated for 24, 48, and 72 h with or without (control) sCD100. Control experiments for the effect of sCD100 Fc portion on *Leishmania* infection were performed using recombinant IgG1 and FcR blocker, and are described latter. Zymosan particles were incubated with macrophages at a ratio of 1:1 for 1 h to analyze the phagocytosis index. In *Leishmania* and zymosan experiments cells were fixed with methanol, stained with Giemsa and mounted with Entellan (Merck). One hundred macrophages were analyzed per glass slide to determine the proportion of infected cells (IM), the total number of amastigotes (AMA), amastigotes/infected macrophage and Infection Index or Phagocytosis Index (II = IM x AMA). Three coverslips were prepared for each condition.

Cell Infection by *Trypanosoma cruzi*

Experimental procedures were carried as previously described (Teixeira A. A. et al., 2015). Briefly, peritoneal macrophages were seeded in 24 well plates laid with 13 mm circular coverslips as described above, with or without 200 ng/mL sCD100. Cells were then infected with tissue culture-derived trypomastigotes (Y strain) at MOI = 10 with or without 200 ng/mL CD100 ($N = 3$ for each condition) for 2 h at 37°C. The cells were then washed 10 times with PBS and further cultivated for 24 h to allow parasite differentiation. Macrophages were fixed with 4% paraformaldehyde, stained with anti-*T. cruzi* polyclonal antibody and propidium iodide and photographed with an epifluorescence microscope. Quantification was performed by counting the number of total and infected cells in at least 4 different fields (20 × magnification) for each replicate.

Macrophage Infections With sCD100 and Fc Receptor Blocker, Human Recombinant IgG1, or Anti-CD72

To monitor the effect of sCD100 Fc portion on *Leishmania* infection, incubations with *L. (L.) amazonensis* were performed in the presence of sCD100 and FcR blocker, and in the presence of human recombinant Fc portion of IgG1. To evaluate the role of CD72 in sCD100 effects, infections were done in the presence of anti-CD72. For FcR blocking: macrophages were plated and incubated with Fc receptor blockers (CD16 and CD32-BD Biosciences) at 0.1 ug/mL for 10 min, and then 200 ng/mL of sCD100 was added. *Leishmania* was added in the following day in the presence of FcR blocker and sCD100 for 4 and 24 h. For IgG1, macrophages were plated and incubated with 70 ng/mL of human recombinant IgG1 Fc (R&D Systems) and 200 ng/mL sCD100, and infected in the following day in the presence of the same proteins. For anti-CD72, plated macrophages were incubated with 10 μg/mL of anti-CD72 H-96 (Santa Cruz Biotechnology) and 1 h later sCD100 was added to 200 ng/mL. Infection was performed in the following day in the presence of both proteins. Control conditions included incubation only with sCD100 and with each treatment (Fc blocker or Fc-IgG1) separately, as well as untreated infected macrophages. The analysis and comparisons were based on infection rates.

Immunofluorescence for Phagocytosis and for F-Actin, CD100, and CD72 Labeling

Resident peritoneal macrophages from BALB/c mice were plated on glass slides as described and incubated with no stimulus or with 100 or 200 ng/mL of sCD100, or 100 or 200 ng/mL of BSA overnight.

For phagocytosis and for F-actin and CD100 labeling: Promastigotes of *L.* (*L.*) *amazonensis* were added in the proportion of 10 parasites per cell in the presence or absence of sCD100 or BSA and the plate was kept on ice for 2 h, and at 33°C with 5% CO_2 for different periods. After washing, macrophages were fixed with 4% paraformaldehyde for 10 min, washed with PBS 1X with 2% FBS, incubated for 30 min in 50 mM ammonium chloride and washed in PBS 1X with 2% FBS.

For labeling of CD100 and actin, cells were permeabilized with TBS containing 1% BSA and 0.1% Triton for 10 min. Slides were washed and incubated overnight with anti-CD100 (eBioscience) at 1:50 dilution, and after washing were incubated with anti-Rat IgG Alexa Fluor 568 (Thermo Scientific) diluted 1: 1000 and DAPI 1: 600 for 1 h. Alternatively, cells were incubated with phalloidin Texas Red (Molecular Probes) 1: 500 and DAPI 1: 600 for 1 h. In both cases, coverslips were washed five times with PBS and mounted in ProLong (Molecular Probes).

For analysis of phagocytosis glass slides were incubated overnight with anti-*Leishmania* serum diluted 1:75 in PBS 1X, washed five times with PBS and incubated for 1 h with a mix containing anti-mouse IgG Alexa Fluor 488 (Thermo Scientific) 1: 1000. After washing, permeabilization with TBS containing 1% BSA and 0.1% Triton for 10 min and further washing, phalloidin Texas Red (Molecular Probes) 1: 500 and DAPI 1: 600 were added for 1 h. After five washes, cells were mounted in ProLong (Molecular Probes). For calculation of the phagocytosis index, 500 macrophages were analyzed and promastigotes were quantified as attached (labeled in green and blue) or internalized (labeled only with blue-DAPI).

For CD72 labeling, slides containing non-infected macrophages were fixed as described. After washing they were incubated with anti-CD72 antibody M-96 (Santa Cruz Biotechnologies) 1:75 overnight, washed and incubated for 2 h with DAPI at 1: 600 and anti-rabbit Alexa Fluor 488 (Thermo Scientific) 1: 100. After labeling, coverslips were washed three times in PBS 1X with 2% FBS and cells were mounted in ProLong (Molecular Probes).

For CD100 quantification, images were acquired in a DMI6000B/AF6000 (Leica) fluorescence microscope coupled to a digital camera system (DFC 365 FX) and analyzed with the Image J program.

For actin and CD72 labeling and for the phagocytosis assay, images were captured using a Zeiss LSM 780 confocal laser scanning inverted microscope (Carl Zeiss, Germany) in a 1024 × 1024 pixel format. Image stacks comprised 8 images captured with a Plan-Apochromat 63×/1.4 DIC Oil M27 objective (Zeiss), applying a zoom factor of 1.0. Step intervals along the Z-axis ranged from 450 nm. Image acquisition and processing were performed using the Zen 2011 software (Zeiss, version 11.00.190).

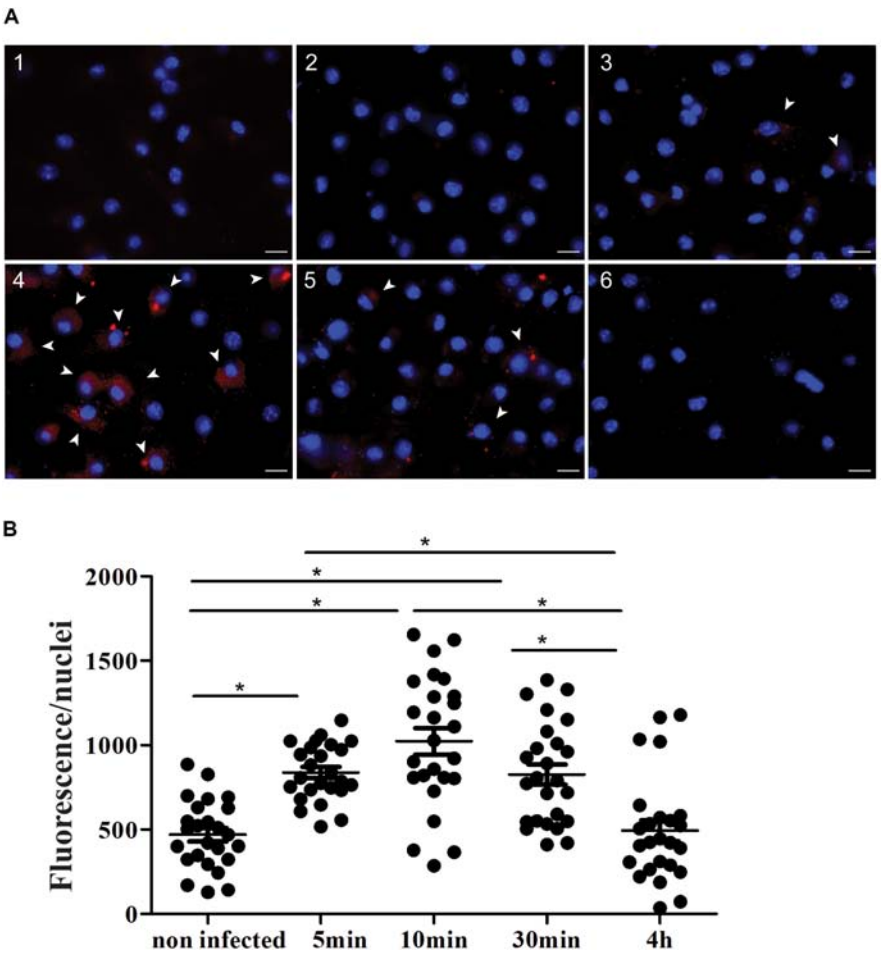

FIGURE 1 | Expression of CD100 in peritoneal macrophages infected or not with promastigotes of *L. (L.) amazonensis*. **(A)** Immunofluorescence staining for CD100 on infected and non-infected macrophages. Peritoneal macrophages from BALB/c mice non-infected (1 and 2), infected with promastigotes of *L. (L.) amazonensis* at MOI of 10:1 for 5 min (3), 10 min (4), 30 min (5), and 4 h (6). Staining with anti-CD100 antibody and secondary anti-rat Alexa Fluor 568 (red) and DAPI (blue nucleus). Control: DAPI (1) and secondary anti-rat Alexa Fluor 568 + DAPI (2). Images were captured in a DMI6000B/AF6000 (Leica) fluorescence microscope coupled to a digital camera system (DFC 365 FX). White bars correspond to 10 μm. **(B)** Quantification of red fluorescence/nuclei in 25 fields for each condition. Statistical analysis by ANOVA with Tukey's post-test, significant differences are labeled as $^*p \leq 0.05$.

SDS–PAGE and Western Blot

SDS–PAGE (running gels with 10% acrylamide: bisacrylamide) and Western blots were performed as we previously described (Teixeira P. C. et al., 2015), using the following antibodies and incubation conditions: anti β-actin (Imuny, Brazil) 1: 1000 overnight and anti-rabbit IgG (H + L) (Imuny, Brazil) 1: 2000 for 1 h; anti-CD72 H-96 (Santa Cruz Biotechnology) 1: 200 overnight and anti-rabbit HRP (Imuny) 1: 1000 for 1 h, anti-GAPDH (Sigma-Aldrich) 1: 10000 overnight and anti-rabbit HRP (Imuny) 1: 1000 for 1 h. Normalizations for CD72 were done using anti-GAPDH while actin polymerization was estimated by F/G ratio.

Statistical Analysis

Statistical analyses were done using *t*-test or one-way ANOVA followed by Tukey's multiple comparison test, depending on the number of samples. Data were considered statistically different (*) when $p < 0.05$.

RESULTS

CD100 Expression Increases in Macrophages During Infection With *Leishmania* (*L.*) *amazonensis*

Although CD100 expression in macrophages has already been documented (Kikutani and Kumanogoh, 2003; Nkyimbeng-Takwi and Chapoval, 2011), its expression and effects during parasitic infection were never explored. Thus, we have performed labeling and quantification of CD100 protein in peritoneal BALB/c macrophages under controlled conditions and at different time points following infection with *L.* (*L.*) *amazonensis* promastigotes at a MOI (multiplicity of infection) of 10 parasites per macrophage. We observed that CD100 protein levels are altered following infection in a time dependent manner (**Figure 1A**): intracellular CD100 increases between 5 and 30 min after infection and then returns to basal levels within 4 h (**Figure 1B**).

Soluble CD100 Increases Infection of Macrophages by *Leishmania (L.) amazonensis*

After demonstrating that *Leishmania* infection increases macrophage CD100 endogenous levels, we evaluated whether the host cell infection by the parasite was affected by soluble CD100 (sCD100) added to the media. In the *Leishmania* lesion environment, sCD100 may be shed by macrophages, which express low levels of the protein (Sierra et al., 2008; Li et al., 2009; Luque et al., 2013), or by other cells, mainly activated T cells, which are known to release sCD100 (Wang et al., 2001). We thus analyzed the role of exogenous sCD100 on macrophage infection by *Leishmania*. We produced sCD100-Fc recombinant protein (from now on named as sCD100) in HEK293T and incubated macrophages with sCD100 before and together with *L. (L.) amazonensis* for different times.

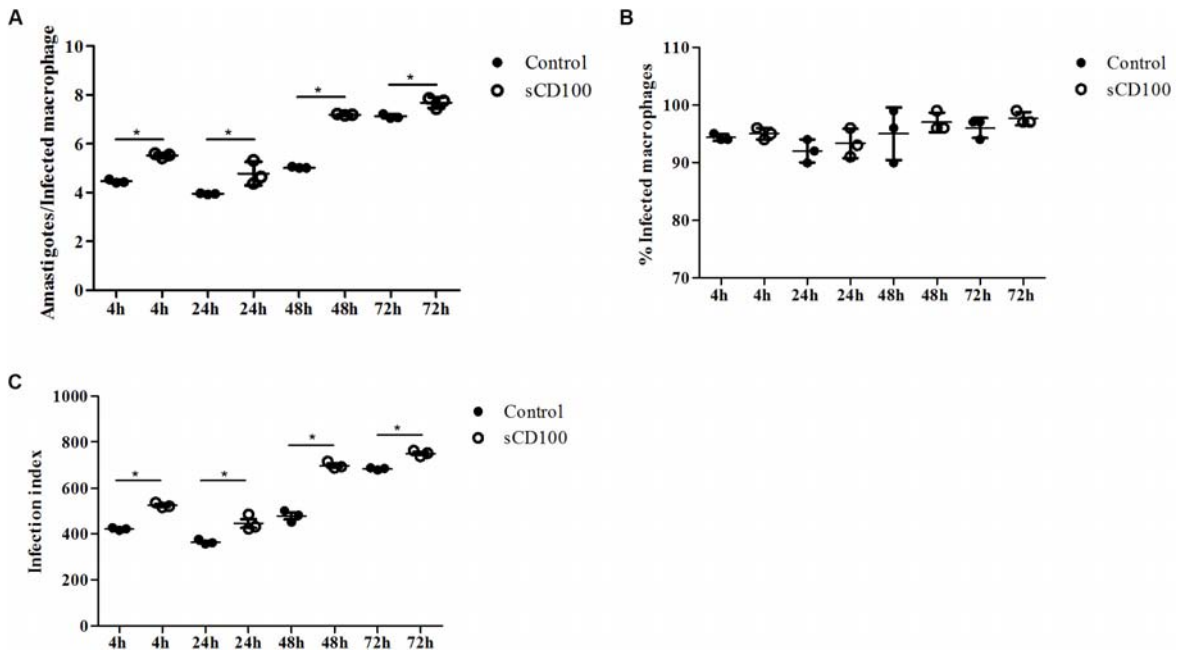

FIGURE 2 | Effects of sCD100 on infection of macrophages. Macrophages from BALB/c mice were infected with *L. (L.) amazonensis* promastigotes at a MOI of 5 per 4, 24, 48, or 72 h in the presence or not of 100 ng/mL sCD100. **(A)** Amastigotes per infected cell. **(B)** Percentage of infected macrophages. **(C)** Infection index. Statistical analysis was performed by ANOVA with Tukey's post-test, and significant differences are labeled as $*p \leq 0.05$. Results of a representative experiment of three with similar profiles.

Our results show that the number of amastigotes per cell (**Figure 2A**), and consequently infection rates (calculated as a product of the proportion of infected cells and the number of amastigotes) (**Figure 2C**), increase significantly in the presence of sCD100 in 4, 24, 48, and 72 h of infection. On the other hand, the percentages of infected macrophages (**Figure 2B**) do not change significantly over time with or without sCD100.

Pre-incubation of Promastigotes With sCD100 Does Not Increase Infection of Macrophages

A possible explanation for the increase of infection by *L.* (*L.*) *amazonensis* induced by sCD100 could be the binding of this molecule to the parasite, promoting its adhesion to a CD100 receptor present on the macrophage or to Fc receptors, as sCD100 protein is fused to human Fc region of IgG1 (Kumanogoh et al., 2000). To verify the first hypothesis, we pre-incubated promastigotes with sCD100 prior to macrophage infection. Again, infection was performed for 4, 24, 28, and 72 h. No significant difference in the number of macrophages infected with *L.* (*L.*) *amazonensis* or in the number of amastigote forms inside individual infected cells was observed by pre-incubation with sCD100 relative to controls at all time points (**Figure 3**). These data indicate that sCD100 does not increase infection by direct contact/interaction with the parasite. On the other hand, when macrophages are pre-incubated with sCD100, the infection rate increases significantly (**Figures 3A–D**, control vs. sCD100).

Because the recombinant sCD100 that we used is produced as fusion between sCD100 and the Fc portion of IgG1, we next analyzed whether its effect on phagocytosis could be due to an interaction of the Fc IgG1 portion with the macrophage Fc receptor (FcR). To evaluate this possibility, macrophage infection assays were repeated in the presence of recombinant Fc region of human IgG1. The same control protein has been used in different studies, including one with *Leishmania* infection (Cortez et al., 2011). As expected, sCD100 alone increased macrophage infection by *L.* (*L.*) *amazonensis* while soluble IgG1 had no effect (**Figure 4**). Similar results were obtained when we blocked Fc receptor using the commercial blockers CD16 and CD32 (Supplementary Figure 1). Taken together, these results demonstrate that the increase in infection is directly mediated by sCD100.

CD72 Is Expressed in Macrophages and Mediates sCD100 Effects on Infection

CD72 is considered the main receptor for CD100 in macrophages (Kumanogoh et al., 2000; Ishida et al., 2003; Smith et al., 2011),

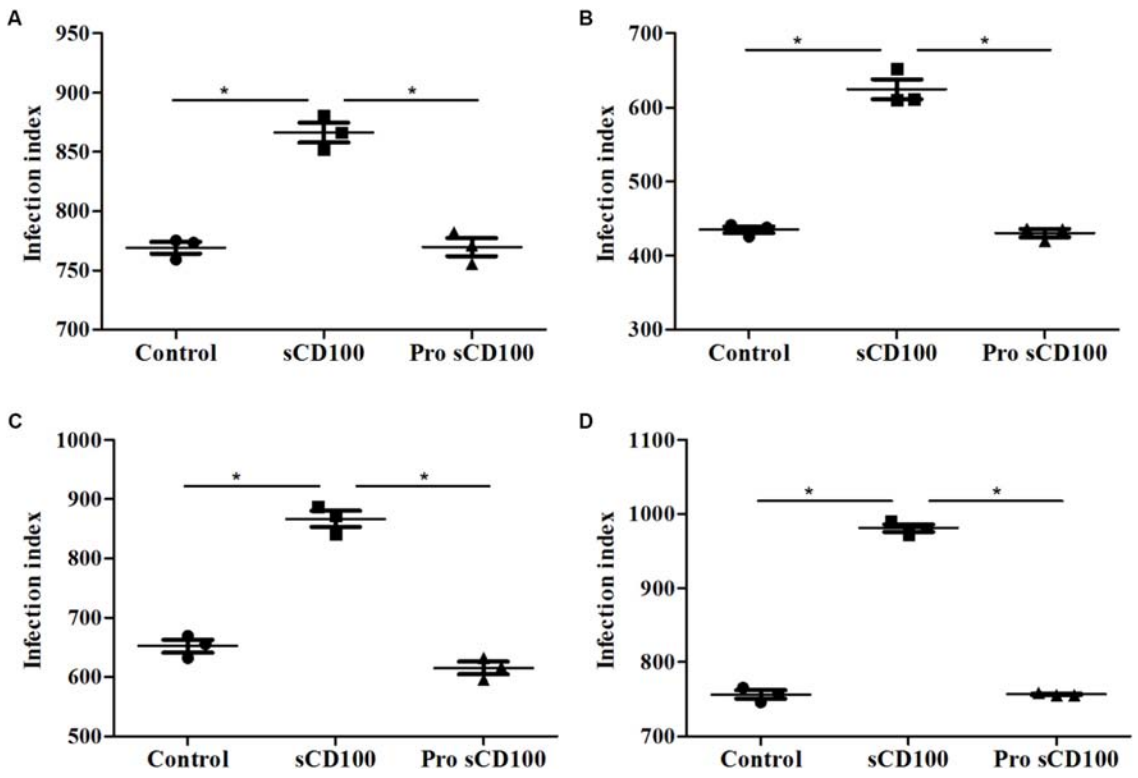

FIGURE 3 | Effects of preincubation of promastigotes with sCD100 on infection index. Peritoneal macrophages from BALB/c mice were infected with *L. (L.) amazonensis* at a MOI of 5 for 4 **(A)**, 24 **(B)**, 48 **(C)**, or 72 **(D)** hours at different conditions: macrophages and parasites without sCD100 (control), promastigotes preincubated with sCD100 at a concentration of 200 ng/mL (promastigote+sCD100), macrophages and promastigotes in the continuous presence of sCD100 at a concentration of 200 ng/mL (sCD100). Statistical analysis was performed by ANOVA with Tukey's post-test, and significant differences are labeled as $^*p \leq 0.05$. Results of a representative experiment of three.

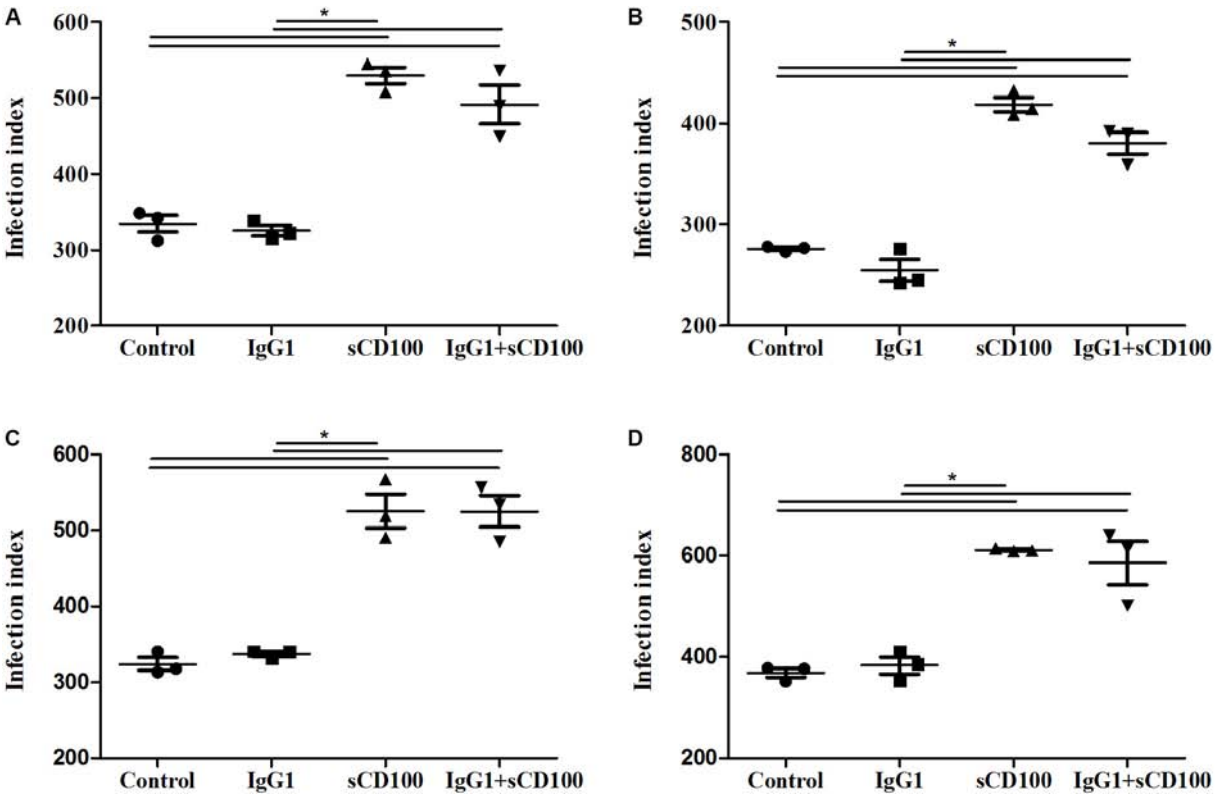

FIGURE 4 | Effects of IgG1 competition on infection index. Peritoneal macrophages from BALB/c mice were infected with *L. (L.) amazonensis* at a MOI of 5 for 4 **(A)**, 24 **(B)**, 48 **(C)**, and 72 **(D)** hours in the absence of stimulus (control), in the presence of 200 ng/mL of sCD100, 70 ng/mL of human IgG1 or IgG1+sCD100. Statistical analysis was performed by ANOVA with Tukey's post-test, and significant differences are labeled as $*p \leq 0.05$. Results of a representative experiment of three.

but its expression has not been analyzed in murine peritoneal macrophages. We thus verified the expression of this receptor in these cells. By Western blot we observed the reactivity of CD72 immunospecific antibodies with a 45 kDa protein, the expected molecular weight for this receptor (**Figure 5A**, lane 1). Its expression is not altered upon incubation of the macrophages with sCD100, since we observed similar levels (ratios of CD72/GAPDH, the endogenous control used) in macrophages plated in the presence or not of sCD100 (**Figure 5A**, lane 2). An unrelated cell line (L929 fibroblast), which does not express CD72, was used as negative control (**Figure 5A**, lane 3). By immunofluorescence, we observed CD72 labeling in peritoneal macrophages (**Figure 5B**), confirming the presence of the receptor in these cells.

Next, we evaluated whether blockage of CD72 would affect sCD100-induced increase in macrophage infection. Macrophages were preincubated with anti-CD72 antibodies and infected with *Leishmania*. We observed that anti-CD72 antibodies alone have no effect on macrophage infection (**Figure 5C**, lane 2), as the number of infected cells is similar to control, and that sCD100 increases macrophage infection, as expected. However, when anti-CD72 antibody is added before sCD100, infection levels returned to basal levels (**Figure 5C**). These results indicate that sCD100 increases *L. (L.) amazonensis* infection in a CD72 dependent manner.

sCD100 Increases Phagocytosis of *L.* (*L.*) *amazonensis* and Zymosan Particles

We have shown that sCD100 increases infection of macrophages after 4 h of incubation with *Leishmania*, suggesting that the molecule could participate in the initial steps of phagocytosis. To test this hypothesis, we performed a phagocytosis assay in which macrophages were plated (overnight) in the presence or absence of sCD100 and then incubated with promastigotes in the presence or abscence of sCD100 for only 5 min. Promastigotes attached to the host cell were visualized by fluorescent microscopy in green and blue (anti-*Leishmania* and DAPI, respectively), while internalized parasites were labeled only in blue (DAPI) (Supplementary Figure 2). Phagocytosis of *Leishmania* was assessed quantitatively by the percentage of infected macrophages and the total number of promastigotes phagocytosed. Phagocytosis of zymosan was also analyzed. An increase in infected macrophages and internalized promastigotes (**Figures 6A,B**) was observed in the presence of sCD100, indicating that it affects the initial steps of phagocytosis. Besides, there was a significant increase in the phagocytosis of zymosan (represented by the phagocytosis index) at both sCD100 concentrations tested (**Figure 6C**), indicating that this protein augments phagocytosis in general and not specifically of *Leishmania* parasites.

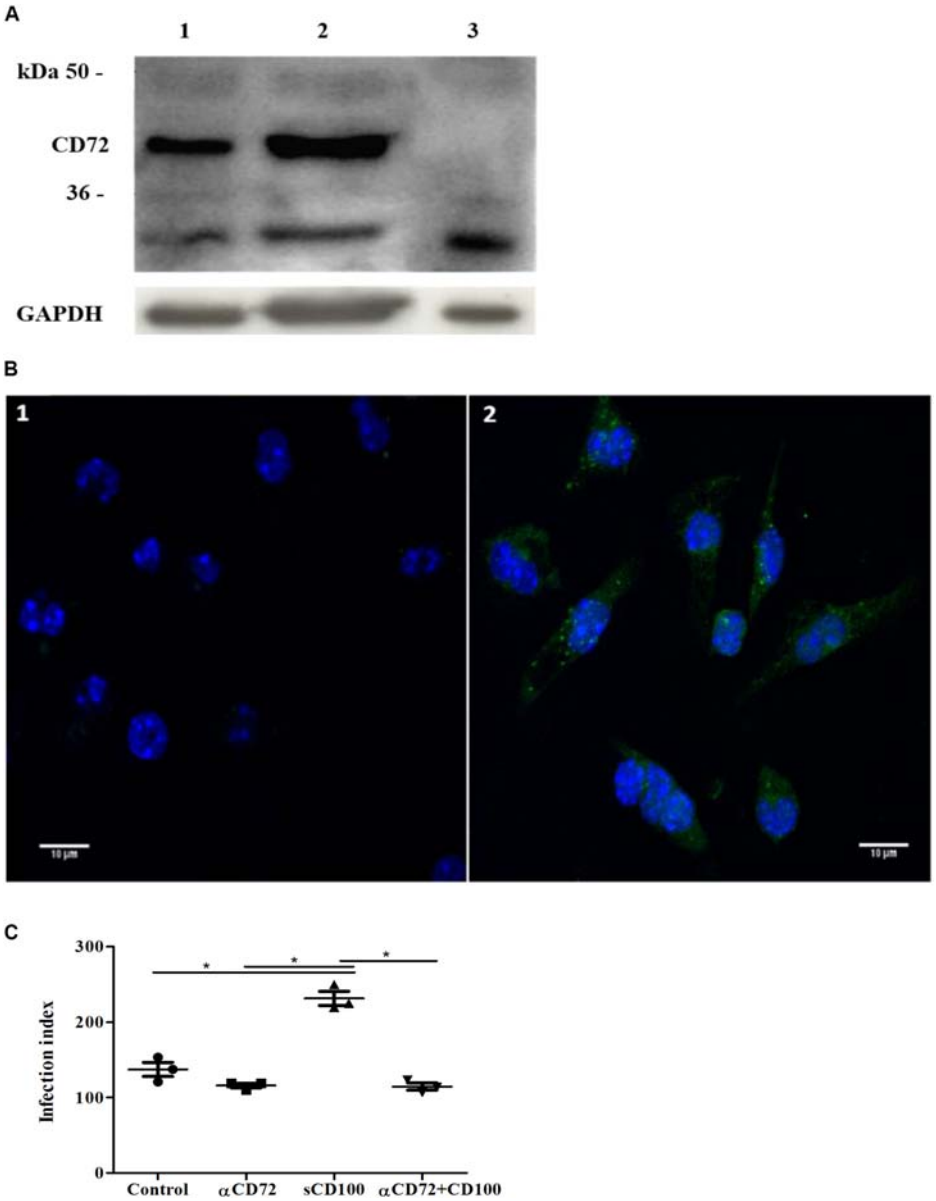

FIGURE 5 | Expression of CD72 and its role in sCD100 effects on macrophages. **(A)** Western blot showing expression of CD72 and GAPDH in peritoneal macrophages from BALB/c mice (lane 1), macrophage incubated with 200 ng/mL of sCD100 for 48 h (lane 2) and L929 cells (negative control - lane 3). Thirty micrograms of protein extracts were analyzed in 10% SDS–PAGE. **(B)** Immunofluorescence staining for CD72 in peritoneal macrophages from BALB/c mice: control incubated with anti-rabbit Alexa Fluor 488 secondary antibody and DAPI (image 1), macrophages incubated with anti-CD72, anti-rabbit Alexa Fluor 488 secondary antibody and DAPI (image 2). Images were captured in Zeiss LSM 780-NLO confocal microscope, magnifying 63 ×, 1.0 zoom. **(C)** Infection index of macrophages from BALB/c mice in the presence or absence of sCD100, preincubated or not with anti-CD72 for 48 h. Data represent means and standard deviations of one experiment with triplicates. Statistical analysis was performed by ANOVA followed by Tukey's post-test, and significant differences are labeled as $^*p \leq 0.05$.

sCD100 Does Not Affect Actin Polymerization

Since *Leishmania* is internalized in an actin-dependent process, we analyzed whether sCD100 modulated actin polymerization. Actin was analyzed in macrophages plated in the presence or abscence of sCD100 and infected with promastigotes in the presence or abscence of sCD100 for different periods. **Figure 7A** shows representative confocal images of immunofluorescence of macrophages incubated with sCD100 and infected for 30 min and 4 h, as well as the same conditions with no sCD100. The analysis of multiple fields at 4 h of infection showed that F-actin (polymerized actin, labeled with Texas Red Phalloidin) has a different organization in macrophages stimulated with sCD100. In fact, while a cortical distribution (arrowhead) of F-actin is shown in the absence of sCD100 (**Figure 7A**, image 3), the presence of sCD100 leads to a more heterogeneous

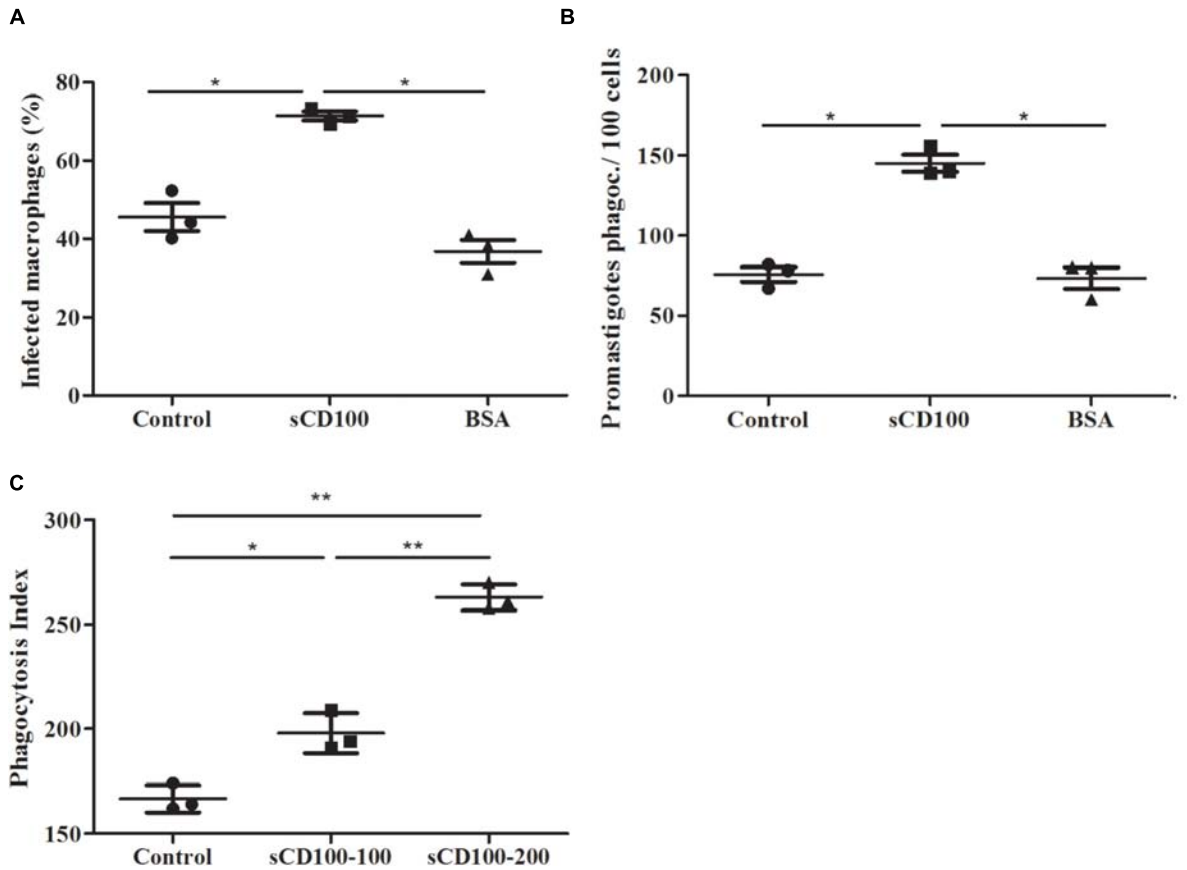

FIGURE 6 | Effect of sCD100 on phagocytosis of *Leishmania* and zymosan by peritoneal macrophages from BALB/c. **(A)** Percentage of infected macrophages and **(B)** promastigotes phagocytosed by 100 macrophages in the continuous presence of 100 ng/mL sCD100 or BSA or with no stimulus (control), analyzed by immunofluorescence. Data represent means and standard deviations of three independent experiments. **(C)** Phagocytosis index of zymosan using 1 particle per macrophage for 1 h in the continuous presence of 100 or 200 ng/mL sCD100 or with no stimulus (control). Results of a representative experiment out of three with similar values. Statistical analysis was performed by ANOVA followed by Tukey's post-test, and significant differences are labeled as $*p \leq 0.05$.

and cytoplasmic distribution of polymerized actin (**Figure 7A**, image 4). A cytoplasmic pattern of F-actin was also visualized at 30 min of infection, in both conditions (**Figure 7A**, images 1, 2). Confirming our previous results, the presence of sCD100 at 4 h of infection increased the number of promastigotes attached (arrows) and internalized by macrophages (**Figure 7A**, images 6,5, respectively), suggesting a correlation between the effect of sCD100 on F-actin dynamics and *Leishmania* infection.

Since small differences in F-actin polymerization may not be perceived by immunofluorescence, we evaluated actin polymerization in control macrophages and in macrophages treated with sCD100, infected or not with *L. (L.) amazonensis* by Western blot (**Figure 7B**). The experiment was based on the separation of F-actin (insoluble) and G-actin (soluble) by ultracentrifugation, followed by blotting for actin in the two fractions. As a technical control, we employed extracts of macrophages treated with Latrunculin A, which blocks actin polymerization (Oliveira et al., 1996). Under all conditions F-actin band is about two times more intense than G-actin band, irrespective of sCD100 stimulus or infection by *L.* (*L.*) *amazonensis* (**Figure 7B**, representative experiment). Thus, no clear correlation between sCD100 and actin polymerization can be drawn. The control with Latrunculin A shows a clear decrease in the F-actin band, indicating that the separation of soluble and insoluble actin was efficient using this method.

Soluble CD100 Increases Infection of Macrophages by *Trypanosoma cruzi*

We have here shown that sCD100 binds to macrophage CD72 and increases *Leishmania* phagocytosis. We have also shown that treatment of macrophages with sCD100 increases phagocytosis of zymosan, indicating that this effect is not specific for *Leishmania*. Therefore, we decided to investigate whether cCD100 could modulate infection of macrophage by other parasites.

Trypanosoma cruzi has several developmental stages, and the infective trypomastigotes can enter almost all nucleated cells of the vertebrate host, phagocytic or non-phagocytic. Tissue resident macrophages are importante targets for early infection, and parasite entry into these cells can occur by a phagocytic-like or a non-phagocytic mechanism (Epting et al., 2010; Barrias et al., 2013). We thus analyzed whether sCD100 could

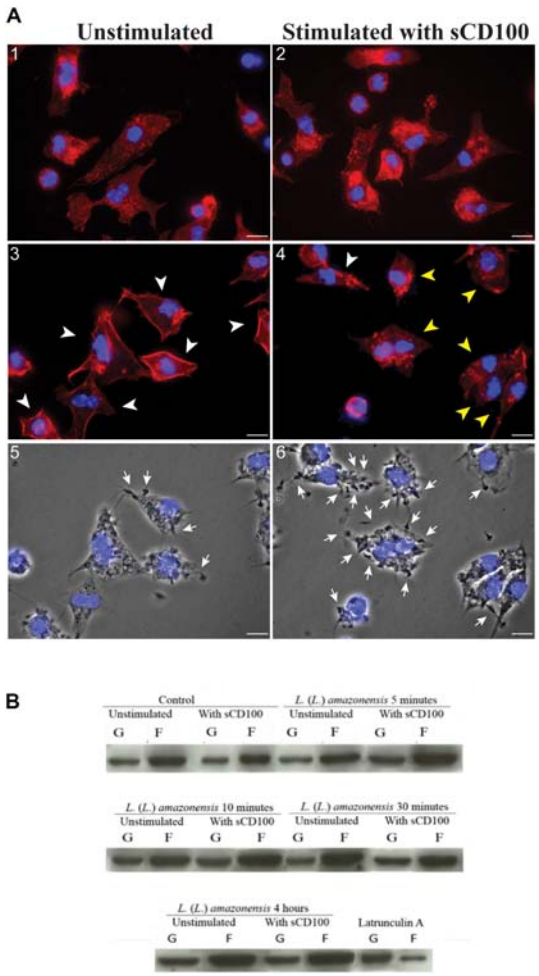

FIGURE 7 | Effect of sCD100 on actin polymerization in infected and non-infected macrophages. **(A)** Peritoneal macrophages from BALB/c mice unstimulated (1, 3, 5) or stimulated with 200 ng/mL of sCD100 (2, 4, 6) were infected with *L. (L.) amazonensis* at MOI of 10 for 30 min (1, 2) or 4 h (3, 4), followed by staining with phalloidin Red: Actin (labeled with phalloidin-Texas Red), Blue: nuclear DNA and kinetoplast (DAPI). Images were captured in DMI6000B/AF6000 (Leica) fluorescence microscope coupled to a digital camera system (DFC 365 FX). White bars correspond to 10 μm. The arrowheads point to macrophages presenting cortical (white) or cytoplasmic (yellow) organization of F-actin. Contrast phase of the samples at 4 h from unstimulated and stimulated with sCD100 (5, 6). The arrows point to parasites attached to macrophages. The images are representative of two independent experiments. **(B)** Western blot for actin in soluble and insoluble fractions of bone marrow macrophages incubated with or without sCD100, infected or not for 5, 10, 30 min or 4 h. This representative image shows soluble actin (supernatant, G-actin), and polymerized actin (pellet, F-actin) bands, and the graph shows F/G actin ratio after densitometry. Results of a representative experiment of three with the same profile.

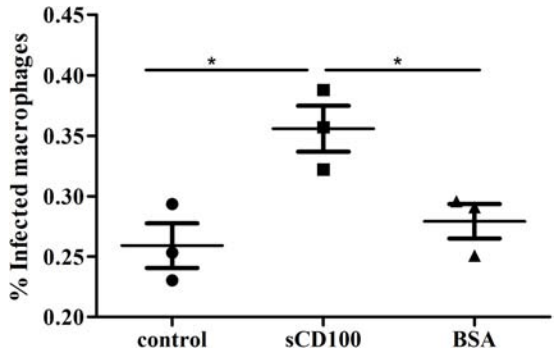

FIGURE 8 | Effects of sCD100 on infection of macrophages by Trypanosoma cruzi. Macrophages from BALB/c mice were infected with *T. cruzi* trypomastigotes at a MOI of 10 for 24 h in the presence or not of 200 ng/mL sCD100. Statistical analysis was performed by ANOVA with Tukey's post-test, and significant differences are labeled as $*p \leq 0.05$. Results of one experiment representative of two with similar profile.

also affect macrophage infection by *T. cruzi* trypomastigotes. Trypomastigotes were incubated with macrophages in the presence or absence of sCD100 and the percentage of infected cells was quantified. Similar to *Leishmania*, we observed that sCD100 promoted a significant increase in cell infection by *T. cruzi* (**Figure 8**). These results suggest that CD100 may play an important role in macrophage infection by different trypanosomatid parasites.

DISCUSSION

Monocytes and the mature macrophage cells are key elements in immunity, and their role in parasitic infection has been clearly demonstrated for trypanosomatids (Dos-Santos et al., 2016). Understanding the molecular mechanisms of parasite phagocytosis by these cells is an important step toward the development of novel therapeutic options for infected patients, in particular for visceral leishmaniasis, for which treatment is necessary but therapeutic options are usually toxic and with poor efficacy (McGwire and Satoskar, 2014). CD100 is an important molecule involved in the communication between immune cells (Kumanogoh et al., 2000; Shi et al., 2000; Mizui et al., 2009), but its role in macrophage functions has been poorly studied. In fact, the only report concerning CD100 and phagocytosis by these cells is a previous paper from our group showing that soluble CD100 (sCD100) decreases internalization of oxidized LDL by human macrophages by inhibiting the expression of the scavenger receptor CD36 (Luque et al., 2015).

Apart from their role in immune response, macrophages are the main host cells for *Leishmania*. We here showed that these cells respond to sCD100 by increasing phagocytosis of *Leishmania*, *Trypanosoma cruzi* and zymosan. Zymosan is a β-glucan rich particle derived from the yeast *Saccharomyces cerevisiae*, frequently used as a model for phagocytosis. Non-opsonized zymosan is mainly recognized by macrophage dectin-1 receptor (Brown et al., 2002), which is not involved in *Leishmania* phagocytosis. *T. cruzi* is internalized by host cells via multiple endocytic pathways. Entry into macrophages occurs mainly but not only by phagocytosis (Epting et al., 2010; Barrias et al., 2013), and involves several macrophage receptors, some of them different from the ones used for *Leishmania* internalization. Thus, the effect of sCD100 on phagocytosis

probably does not depend on a specific phagocytic receptor of macrophages.

The increase in *Leishmania* infection promoted by sCD100 depends on its interaction with CD72 receptor. The effects of sCD100 on phagocytosis may differ in murine and human macrophages. In fact, CD72 is the main CD100 receptor in murine macrophages (Tamagnone et al., 1999; Kumanogoh et al., 2000), while we have shown that plexin B2 is an effective CD100 receptor in human monocytes and macrophages (Luque et al., 2015). CD72 was shown to be expressed in bronchial epithelial cells, alveolar macrophages, B cells, dendritic cells, fibroblasts, basophils (Kikutani and Kumanogoh, 2003; Mizui et al., 2009; Smith et al., 2011), and we here show its expression also in murine resident peritoneal macrophages. CD72 belongs to the superfamily of C-type lectins, which contain a cytoplasmic domain with two tyrosine inhibitory motifs (ITIMs) that when phosphorylated bind to the protein tyrosine phosphatase 1 (SHP-1) and the adapter protein Grb2 (Wu and Bondada, 2009; Nkyimbeng-Takwi and Chapoval, 2011). No study has ever analyzed CD72 signaling in macrophages, but most studies show that binding of CD100 to CD72 in B cell reverse the inhibitory potential of CD72 to cause dephosphorylation ITIM and release of SHP-1 (Wu and Bondada, 2009). It will be interesting to analyze whether sCD100 binding to macrophage affects not only parasite entry, as we demonstrated here, but also further signaling events such as ITIM phosphorylation and SHP1 release from the CD72 cytoplasmic tail. Infection in the presence of sCD100 led to changes in F-actin organization. Indeed, the cortical distribution of F-actin observed in macrophages at 4 h of infection changed to a heterogeneous and cytoplasmic pattern in the presence of sCD100. Similar changes in actin organization have already been reported in medullary macrophages when infected with *Leishmania amazonensis* (de Menezes et al., 2017) and in cultured chromaffin cells compared to cells in adrenomedullary tissue (Gimenez-Molina et al., 2017).

This work is the first to report the role of CD100 in parasitic infection. Further studies must be performed to unravel how CD100 binding to macrophage CD72 increases phagocytosis of zymosan, *Leishmania* and *T. cruzi*, which interact with different surface receptors. Further studies should also address the role of sCD100 in *in vivo* models of leishmaniasis, and on *Leishmania* phagocytosis by human macrophages.

AUTHOR CONTRIBUTIONS

MG was the student responsible for the project, who performed most experiments, wrote the paper, and prepared most figures. ER performed immunofluorescence for CD100, prepared the corresponding figure, and revised the paper. FF helped in experimental design and phosphatase experiment (not included) and revised the paper. MC contributed with actin separation and immunofluorescence experiments and revised the paper. MCC performed confocal microscopy. AT and RG designed and performed *T. cruzi* infection experiments and revised the paper. BS designed and supervised the project, wrote the paper, and was responsible for the funding.

FUNDING

This work was supported by FAPESP- Fundação de Amparo à Pesquisa do Estado de São Paulo (Grant No. 2011/12634-9) to BS.

ACKNOWLEDGMENTS

We thank Atsushi Kumanogoh for CD100-Fc plasmid, Silvia Boscardin for help with protein production, Ana Paula Lepique for FcR blocker, and Silvia Uliana for important discussions during this project. We also thank CEFAP (Centro de Facilidades de Apoio a Pesquisa) -USP for confocal microscopy facility.

SUPPLEMENTARY MATERIAL

The Supplementary Material for this article can be found online at: https://www.frontiersin.org/articles/10.3389/fmicb.2018.01177/full#supplementary-material

REFERENCES

Alvar, J., Velez, I. D., Bern, C., Herrero, M., Desjeux, P., Cano, J., et al. (2012). Leishmaniasis worldwide and global estimates of its incidence. *PLoS One* 7:e35671. doi: 10.1371/journal.pone.0035671

Azevedo, E., Oliveira, L. T., Castro Lima, A. K., Terra, R., Dutra, P. M., and Salerno, V. P. (2012). Interactions between *Leishmania braziliensis* and macrophages are dependent on the cytoskeleton and Myosin Va. *J. Parasitol. Res.* 2012:275436. doi: 10.1155/2012/275436

Barrias, E. S., de Carvalho, T. M., and De Souza, W. (2013). *Trypanosoma cruzi*: entry into Mammalian host cells and parasitophorous vacuole formation. *Front. Immunol.* 4:186. doi: 10.3389/fimmu.2013.00186

Basile, J. R., Barac, A., Zhu, T., Guan, K. L., and Gutkind, J. S. (2004). Class IV semaphorins promote angiogenesis by stimulating Rho-initiated pathways through plexin-B. *Cancer Res.* 64, 5212–5224. doi: 10.1158/0008-5472.CAN-04-0126

Basile, J. R., Holmbeck, K., Bugge, T. H., and Gutkind, J. S. (2007). MT1-MMP controls tumor-induced angiogenesis through the release of semaphorin 4D. *J. Biol. Chem.* 282, 6899–6905. doi: 10.1074/jbc.M609570200

Blackwell, J. M., Ezekowitz, R. A., Roberts, M. B., Channon, J. Y., Sim, R. B., and Gordon, S. (1985). Macrophage complement and lectin-like receptors bind *Leishmania* in the absence of serum. *J. Exp. Med.* 162, 324–331. doi: 10.1084/jem.162.1.324

Bougeret, C., Mansur, I. G., Dastot, H., Schmid, M., Mahouy, G., Bensussan, A., et al. (1992). Increased surface expression of a newly identified 150-kDa dimer early after human T lymphocyte activation. *J. Immunol.* 148, 318–323.

Brown, G. D., Taylor, P. R., Reid, D. M., Willment, J. A., Williams, D. L., Martinez-Pomares, L., et al. (2002). Dectin-1 is a major beta-glucan receptor on macrophages. *J. Exp. Med.* 196, 407–412. doi: 10.1084/jem.20020470

Chabbert-de Ponnat, I., Marie-Cardine, A., Pasterkamp, R. J., Schiavon, V., Tamagnone, L., Thomasset, N., et al. (2005). Soluble CD100 functions on human monocytes and immature dendritic cells require plexin C1 and plexin B1, respectively. *Int. Immunol.* 17, 439–447. doi: 10.1093/intimm/dxh224

Ch'ng, E. S., and Kumanogoh, A. (2010). Roles of Sema4D and Plexin-B1 in tumor progression. *Mol. Cancer* 9:251. doi: 10.1186/1476-4598-9-251

Conrotto, P., Valdembri, D., Corso, S., Serini, G., Tamagnone, L., Comoglio, P. M., et al. (2005). Sema4D induces angiogenesis through Met recruitment by Plexin B1. *Blood* 105, 4321–4329. doi: 10.1182/blood-2004-07-2885

Cortez, M., Huynh, C., Fernandes, M. C., Kennedy, K. A., Aderem, A., and Andrews, N. W. (2011). *Leishmania* promotes its own virulence by inducing expression of the host immune inhibitory ligand CD200. *Cell Host Microbe* 9, 463–471. doi: 10.1016/j.chom.2011.04.014

Courret, N., Frehel, C., Gouhier, N., Pouchelet, M., Prina, E., Roux, P., et al. (2002). Biogenesis of *Leishmania*-harbouring parasitophorous vacuoles following phagocytosis of the metacyclic promastigote or amastigote stages of the parasites. *J. Cell Sci.* 115(Pt 11), 2303–2316.

Da Silva, R. P., Hall, B. F., Joiner, K. A., and Sacks, D. L. (1989). CR1, the C3b receptor, mediates binding of infective Leishmania major metacyclic promastigotes to human macrophages. *J. Immunol.* 143, 617–622.

de Menezes, J. P., Koushik, A., Das, S., Guven, C., Siegel, A., Laranjeira-Silva, M. F., et al. (2017). *Leishmania* infection inhibits macrophage motility by altering F-actin dynamics and the expression of adhesion complex proteins. *Cell Microbiol.* 19:3. doi: 10.1111/cmi.12668

Delaire, S., Billard, C., Tordjman, R., Chedotal, A., Elhabazi, A., Bensussan, A., et al. (2001). Biological activity of soluble CD100. II. Soluble CD100, similarly to H-SemaIII, inhibits immune cell migration. *J. Immunol.* 166, 4348–4354. doi: 10.4049/jimmunol.166.7.4348

Dos-Santos, A. L., Carvalho-Kelly, L. F., Dick, C. F., and Meyer-Fernandes, J. R. (2016). Innate immunomodulation to trypanosomatid parasite infections. *Exp. Parasitol.* 167, 67–75. doi: 10.1016/j.exppara.2016.05.005

Elhabazi, A., Marie-Cardine, A., Chabbert-de Ponnat, I., Bensussan, A., and Boumsell, L. (2003). Structure and function of the immune semaphorin CD100/SEMA4D. *Crit. Rev. Immunol.* 23, 65–81. doi: 10.1615/CritRevImmunol.v23.i12.40

Epting, C. L., Coates, B. M., and Engman, D. M. (2010). Molecular mechanisms of host cell invasion by *Trypanosoma cruzi*. *Exp. Parasitol.* 126, 283–291. doi: 10.1016/j.exppara.2010.06.023

Gimenez-Molina, Y., Villanueva, J., Nanclares, C., Lopez-Font, I., Viniegra, S., Frances, M. D. M., et al. (2017). The differential organization of f-actin alters the distribution of organelles in cultured when compared to native Chromaffin cells. *Front. Cell. Neurosci.* 11:135. doi: 10.3389/fncel.2017.00135

Guy, R. A., and Belosevic, M. (1993). Comparison of receptors required for entry of *Leishmania* major amastigotes into macrophages. *Infect Immun.* 61, 1553–1558.

Iniesta, V., Carcelen, J., Molano, I., Peixoto, P. M., Redondo, E., Parra, P., et al. (2005). Arginase I induction during *Leishmania* major infection mediates the development of disease. *Infect Immun.* 73, 6085–6090. doi: 10.1128/IAI.73.9.6085-6090.2005

Iniesta, V., Gomez-Nieto, L. C., Molano, I., Mohedano, A., Carcelen, J., Miron, C., et al. (2002). Arginase I induction in macrophages, triggered by Th2-type cytokines, supports the growth of intracellular *Leishmania* parasites. *Parasite Immunol.* 24, 113–118. doi: 10.1046/j.1365-3024.2002.00444.x

Ishida, I., Kumanogoh, A., Suzuki, K., Akahani, S., Noda, K., and Kikutani, H. (2003). Involvement of CD100, a lymphocyte semaphorin, in the activation of the human immune system via CD72: implications for the regulation of immune and inflammatory responses. *Int. Immunol.* 15, 1027–1034. doi: 10.1093/intimm/dxg098

Kikutani, H., and Kumanogoh, A. (2003). Semaphorins in interactions between T cells and antigen-presenting cells. *Nat. Rev. Immunol.* 3, 159–167. doi: 10.1038/nri1003

Kumanogoh, A., Suzuki, K., Ch'ng, E., Watanabe, C., Marukawa, S., Takegahara, N., et al. (2002). Requirement for the lymphocyte semaphorin, CD100, in the induction of antigen-specific T cells and the maturation of dendritic cells. *J. Immunol.* 169, 1175–1181. doi: 10.4049/jimmunol.169.3.1175

Kumanogoh, A., Watanabe, C., Lee, I., Wang, X., Shi, W., Araki, H., et al. (2000). Identification of CD72 as a lymphocyte receptor for the class IV semaphorin CD100: a novel mechanism for regulating B cell signaling. *Immunity* 13, 621–631. doi: 10.1016/S1074-7613(00)00062-5

Li, M., O'Sullivan, K. M., Jones, L. K., Lo, C., Semple, T., Kumanogoh, A., et al. (2009). Endogenous CD100 promotes glomerular injury and macrophage recruitment in experimental crescentic glomerulonephritis. *Immunology* 128, 114–122. doi: 10.1111/j.1365-2567.2009.03098.x

Luque, M. C., Gutierrez, P. S., Debbas, V., Kalil, J., and Stolf, B. S. (2015). CD100 and plexins B2 and B1 mediate monocyte-endothelial cell adhesion and might take part in atherogenesis. *Mol. Immunol.* 67, 559–567. doi: 10.1016/j.molimm.2015.07.028

Luque, M. C., Gutierrez, P. S., Debbas, V., Martins, W. K., Puech-Leao, P., Porto, G., et al. (2013). Phage display identification of CD100 in Human atherosclerotic plaque macrophages and foam cells. *PLoS One* 8:e75772. doi: 10.1371/journal.pone.0075772

May, R. C., Caron, E., Hall, A., and Machesky, L. M. (2000). Involvement of the Arp2/3 complex in phagocytosis mediated by FcgammaR or CR3. *Nat. Cell Biol.* 2, 246–248. doi: 10.1038/35008673

May, R. C., and Machesky, L. M. (2001). Phagocytosis and the actin cytoskeleton. *J. Cell Sci.* 114(Pt 6), 1061–1077.

McGwire, B. S., and Satoskar, A. R. (2014). Leishmaniasis: clinical syndromes and treatment. *QJM* 107, 7–14. doi: 10.1093/qjmed/hct116

McMahon-Pratt, D., and Alexander, J. (2004). Does the *Leishmania* major paradigm of pathogenesis and protection hold for New World cutaneous Leishmaniases or the visceral disease? *Immunol. Rev.* 201, 206–224.

Mizui, M., Kumanogoh, A., and Kikutani, H. (2009). Immune semaphorins: novel features of neural guidance molecules. *J. Clin. Immunol.* 29, 1–11. doi: 10.1007/s10875-008-9263-7

Mosser, D. M., and Edelson, P. J. (1985). The mouse macrophage receptor for C3bi (CR3) is a major mechanism in the phagocytosis of Leishmania promastigotes. *J. Immunol.* 135, 2785–2789.

Nkyimbeng-Takwi, E., and Chapoval, S. P. (2011). Biology and function of neuroimmune semaphorins 4A and 4D. *Immunol. Res.* 50, 10–21. doi: 10.1007/s12026-010-8201-y

Oliveira, C. A., Kashman, Y., and Mantovani, B. (1996). Effects of latrunculin A on immunological phagocytosis and macrophage spreading-associated changes in the F-actin/G-actin content of the cells. *Chem. Biol. Interact.* 100, 141–153. doi: 10.1016/0009-2797(96)03695-2

Podinovskaia, M., and Descoteaux, A. (2015). *Leishmania* and the macrophage: a multifaceted interaction. *Fut. Microbiol.* 10, 111–129. doi: 10.2217/fmb.14.103

Roy, S., Kumar, G. A., Jafurulla, M., Mandal, C., and Chattopadhyay, A. (2014). Integrity of the actin cytoskeleton of host macrophages is essential for *Leishmania donovani* infection. *Biochim. Biophys. Acta* 1838, 2011–2018. doi: 10.1016/j.bbamem.2014.04.017

Shi, W., Kumanogoh, A., Watanabe, C., Uchida, J., Wang, X., Yasui, T., et al. (2000). The class IV semaphorin CD100 plays nonredundant roles in the immune system: defective B and T cell activation in CD100-deficient mice. *Immunity* 13, 633–642. doi: 10.1016/S1074-7613(00)00063-7

Sierra, J. R., Corso, S., Caione, L., Cepero, V., Conrotto, P., Cignetti, A., et al. (2008). Tumor angiogenesis and progression are enhanced by Sema4D produced by tumor-associated macrophages. *J. Exp. Med.* 205, 1673–1685. doi: 10.1084/jem.20072602

Smith, E. P., Shanks, K., Lipsky, M. M., DeTolla, L. J., Keegan, A. D., and Chapoval, S. P. (2011). Expression of neuroimmune semaphorins 4A and 4D and their receptors in the lung is enhanced by allergen and vascular endothelial growth factor. *BMC Immunol.* 12:30. doi: 10.1186/1471-2172-12-30

Tamagnone, L., Artigiani, S., Chen, H., He, Z., Ming, G. I., Song, H., et al. (1999). Plexins are a large family of receptors for transmembrane, secreted, and GPI-anchored semaphorins in vertebrates. *Cell* 99, 71–80. doi: 10.1016/S0092-8674(00)80063-X

Teixeira, A. A., de Vasconcelos Vde, C., Colli, W., Alves, M. J., and Giordano, R. J. (2015). *Trypanosoma cruzi* binds to Cytokeratin through conserved peptide motifs found in the laminin-G-like domain of the gp85/Trans-sialidase proteins. *PLoS Negl. Trop. Dis.* 9:e0004099. doi: 10.1371/journal.pntd.0004099

Teixeira, P. C., Velasquez, L. G., Lepique, A. P., de Rezende, E., Bonatto, J. M., Barcinski, M. A., et al. (2015). Regulation of *Leishmania* (L.) amazonensis protein expression by host T cell dependent responses: differential expression of oligopeptidase B, tryparedoxin peroxidase and HSP70 isoforms in amastigotes isolated from BALB/c and BALB/c nude mice. *PLoS Negl. Trop. Dis.* 9:e0003411. doi: 10.1371/journal.pntd.0003411

Ueno, N., and Wilson, M. E. (2012). Receptor-mediated phagocytosis of *Leishmania*: implications for intracellular survival. *Trends Parasitol.* 28, 335–344. doi: 10.1016/j.pt.2012.05.002

Underhill, D. M., and Goodridge, H. S. (2012). Information processing during phagocytosis. *Nat. Rev. Immunol.* 12, 492–502. doi: 10.1038/nri3244

Velasquez, L. G., Galuppo, M. K., De Rezende, E., Brandao, W. N., Peron, J. P., Uliana, S. R., et al. (2016). Distinct courses of infection with Leishmania (L.) amazonensis are observed in BALB/c, BALB/c nude and C57BL/6 mice. *Parasitology* 143, 692–703. doi: 10.1017/S003118201600024X

Wang, X., Kumanogoh, A., Watanabe, C., Shi, W., Yoshida, K., and Kikutani, H. (2001). Functional soluble CD100/Sema4D released from activated lymphocytes: possible role in normal and pathologic immune responses. *Blood* 97, 3498–3504. doi: 10.1182/blood.V97.11.3498

Wu, H. J., and Bondada, S. (2009). CD72, a coreceptor with both positive and negative effects on B lymphocyte development and function. *J. Clin. Immunol.* 29, 12–21. doi: 10.1007/s10875-008-9264-6

WHO (2015). *World Health Statistics*. Available at: http://www.who.int/gho/publications/world_health_statistics/2015/en/

Wyler, D. J., Sypek, J. P., and McDonald, J. A. (1985). In vitro parasite-monocyte interactions in human Leishmaniasis: possible role of fibronectin in parasite attachment. *Infect Immun.* 49, 305–311.

Conflict of Interest Statement: The authors declare that the research was conducted in the absence of any commercial or financial relationships that could be construed as a potential conflict of interest.

Advantages of publishing in Frontiers

OPEN ACCESS
Articles are free to read for greatest visibility and readership

FAST PUBLICATION
Around 90 days from submission to decision

HIGH QUALITY PEER-REVIEW
Rigorous, collaborative, and constructive peer-review

TRANSPARENT PEER-REVIEW
Editors and reviewers acknowledged by name on published articles

Frontiers
Avenue du Tribunal-Fédéral 34
1005 Lausanne | Switzerland

Visit us: www.frontiersin.org
Contact us: info@frontiersin.org | +41 21 510 17 00

REPRODUCIBILITY OF RESEARCH
Support open data and methods to enhance research reproducibility

DIGITAL PUBLISHING
Articles designed for optimal readership across devices

FOLLOW US
@frontiersin

IMPACT METRICS
Advanced article metrics track visibility across digital media

EXTENSIVE PROMOTION
Marketing and promotion of impactful research

LOOP RESEARCH NETWORK
Our network increases your article's readership